frontiers | Research Topics

Current challenges in complement diagnostics

Edited by
Erik J. M. Toonen, Per Nilsson and
Lillemor Skattum

Published in
Frontiers in Immunology
Frontiers in Physiology

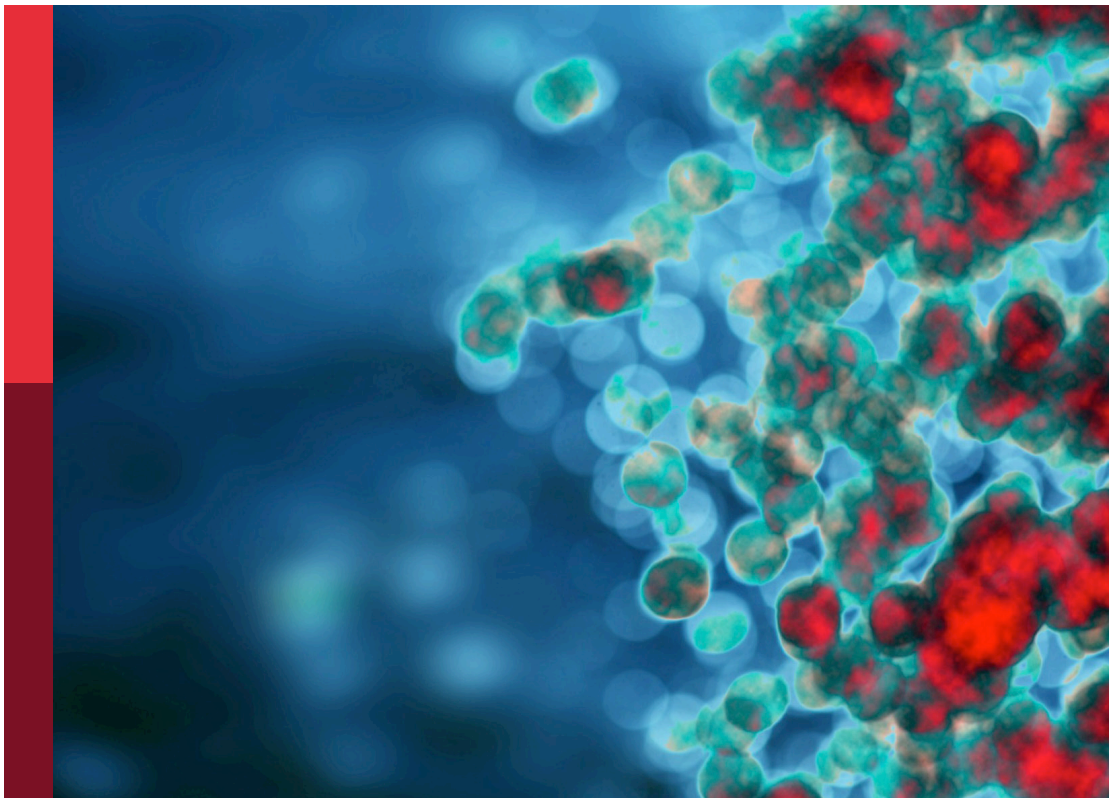

FRONTIERS EBOOK COPYRIGHT STATEMENT

The copyright in the text of individual articles in this ebook is the property of their respective authors or their respective institutions or funders. The copyright in graphics and images within each article may be subject to copyright of other parties. In both cases this is subject to a license granted to Frontiers.

The compilation of articles constituting this ebook is the property of Frontiers.

Each article within this ebook, and the ebook itself, are published under the most recent version of the Creative Commons CC-BY licence. The version current at the date of publication of this ebook is CC-BY 4.0. If the CC-BY licence is updated, the licence granted by Frontiers is automatically updated to the new version.

When exercising any right under the CC-BY licence, Frontiers must be attributed as the original publisher of the article or ebook, as applicable.

Authors have the responsibility of ensuring that any graphics or other materials which are the property of others may be included in the CC-BY licence, but this should be checked before relying on the CC-BY licence to reproduce those materials. Any copyright notices relating to those materials must be complied with.

Copyright and source acknowledgement notices may not be removed and must be displayed in any copy, derivative work or partial copy which includes the elements in question.

All copyright, and all rights therein, are protected by national and international copyright laws. The above represents a summary only. For further information please read Frontiers' Conditions for Website Use and Copyright Statement, and the applicable CC-BY licence.

ISSN 1664-8714
ISBN 978-2-8325-4088-6
DOI 10.3389/978-2-8325-4088-6

About Frontiers

Frontiers is more than just an open access publisher of scholarly articles: it is a pioneering approach to the world of academia, radically improving the way scholarly research is managed. The grand vision of Frontiers is a world where all people have an equal opportunity to seek, share and generate knowledge. Frontiers provides immediate and permanent online open access to all its publications, but this alone is not enough to realize our grand goals.

Frontiers journal series

The Frontiers journal series is a multi-tier and interdisciplinary set of open-access, online journals, promising a paradigm shift from the current review, selection and dissemination processes in academic publishing. All Frontiers journals are driven by researchers for researchers; therefore, they constitute a service to the scholarly community. At the same time, the *Frontiers journal series* operates on a revolutionary invention, the tiered publishing system, initially addressing specific communities of scholars, and gradually climbing up to broader public understanding, thus serving the interests of the lay society, too.

Dedication to quality

Each Frontiers article is a landmark of the highest quality, thanks to genuinely collaborative interactions between authors and review editors, who include some of the world's best academicians. Research must be certified by peers before entering a stream of knowledge that may eventually reach the public - and shape society; therefore, Frontiers only applies the most rigorous and unbiased reviews. Frontiers revolutionizes research publishing by freely delivering the most outstanding research, evaluated with no bias from both the academic and social point of view. By applying the most advanced information technologies, Frontiers is catapulting scholarly publishing into a new generation.

What are Frontiers Research Topics?

Frontiers Research Topics are very popular trademarks of the *Frontiers journals series*: they are collections of at least ten articles, all centered on a particular subject. With their unique mix of varied contributions from Original Research to Review Articles, Frontiers Research Topics unify the most influential researchers, the latest key findings and historical advances in a hot research area.

Find out more on how to host your own Frontiers Research Topic or contribute to one as an author by contacting the Frontiers editorial office: frontiersin.org/about/contact

Current challenges in complement diagnostics

Topic editors
Erik J. M. Toonen — Hycult Biotech, Netherlands
Per Nilsson — Linnaeus University, Sweden
Lillemor Skattum — Lund University, Sweden

Citation
Toonen, E. J. M., Nilsson, P., Skattum, L., eds. (2023). *Current challenges in complement diagnostics*. Lausanne: Frontiers Media SA.
doi: 10.3389/978-2-8325-4088-6

Table of contents

06 Editorial: Current challenges in complement diagnostics
Per H. Nilsson, Lillemor Skattum and Erik J. M. Toonen

09 Circulating Levels of Anti-C1q and Anti-Factor H Autoantibodies and Their Targets in Normal Pregnancy and Preeclampsia
Douwe Jan Dijkstra, A. Inkeri Lokki, Lobke Marijn Gierman, Nicole Veronique Borggreven, Carin van der Keur, Michael Eikmans, Kyra Andrea Gelderman, Hannele Laivuori, The FINNPEC Core Investigator Group , Ann-Charlotte Iversen, Marie-Louise P. van der Hoorn and Leendert Adrianus Trouw

20 *Ex Vivo* Test for Measuring Complement Attack on Endothelial Cells: From Research to Bedside
Marie-Sophie Meuleman, Anna Duval, Véronique Fremeaux-Bacchi, Lubka T. Roumenina and Sophie Chauvet

35 Complement Factor I Variants in Complement-Mediated Renal Diseases
Yuzhou Zhang, Renee X. Goodfellow, Nicolo Ghiringhelli Borsa, Hannah C. Dunlop, Stephen A. Presti, Nicole C. Meyer, Dingwu Shao, Sarah M. Roberts, Michael B. Jones, Gabriella R. Pitcher, Amanda O. Taylor, Carla M. Nester and Richard J. H. Smith

46 Complement and endothelial cell activation in COVID-19 patients compared to controls with suspected SARS-CoV-2 infection: A prospective cohort study
Flavio Bruni, Panteleimon Charitos, Maurin Lampart, Stephan Moser, Martin Siegemund, Roland Bingisser, Stefan Osswald, Stefano Bassetti, Raphael Twerenbold, Marten Trendelenburg, Katharina M. Rentsch and Michael Osthoff

56 A catalog of the genetic causes of hereditary angioedema in the Canary Islands (Spain)
Alejandro Mendoza-Alvarez, Eva Tosco-Herrera, Adrian Muñoz-Barrera, Luis A. Rubio-Rodríguez, Aitana Alonso-Gonzalez, Almudena Corrales, Antonio Iñigo-Campos, Lourdes Almeida-Quintana, Elena Martin-Fernandez, Dara Martinez-Beltran, Eva Perez-Rodriguez, Ariel Callero, Jose C. Garcia-Robaina, Rafaela González-Montelongo, Itahisa Marcelino-Rodriguez, Jose M. Lorenzo-Salazar and Carlos Flores

67 The OSE complotype and its clinical potential
Lejla Alic, Christoph J. Binder and Nikolina Papac-Milicevic

78 Complement C1s as a diagnostic marker and therapeutic target: Progress and propective
Jun Ye, Peng Yang, Yili Yang and Sheng Xia

88 The C1q-ApoE complex: A new hallmark pathology of viral hepatitis and nonalcoholic fatty liver disease
Livia K. L. Habenicht, Zhihua Wang, Xi Zhang, Yuanfang Li, Carolin Mogler, Julia Slotta Huspenina, Roland M. Schmid, Christian Weber, Sarajo K. Mohanta, Zhe Ma and Changjun Yin

101 Levels of soluble complement regulators predict severity of COVID-19 symptoms
Anna L. Tierney, Wajd Mohammed Alali, Thomas Scott, Karen S. Rees-Unwin, CITIID-NIHR BioResource COVID-19 Collaboration , Simon J. Clark and Richard D. Unwin

113 Pitfalls in complement analysis: A systematic literature review of assessing complement activation
Ricardo J. M. G. E. Brandwijk, Marloes A. H. M. Michels, Mara van Rossum, Aline H. de Nooijer, Per H. Nilsson, Wieke C. C. de Bruin and Erik J. M. Toonen

139 Distinction of early complement classical and lectin pathway activation *via* quantification of C1s/C1-INH and MASP-1/C1-INH complexes using novel ELISAs
Lisa Hurler, Erik J. M. Toonen, Erika Kajdácsi, Bregje van Bree, Ricardo J. M. G. E. Brandwijk, Wieke de Bruin, Paul A. Lyons, Laura Bergamaschi, Cambridge Institute of Therapeutic Immunology and Infectious Disease-National Institute of Health Research (CITIID-NIHR) COVID BioResource Collaboration , György Sinkovits, László Cervenak, Reinhard Würzner and Zoltán Prohászka

161 Challenges in diagnostic testing of nephritic factors
Marloes A. H. M. Michels, Elena B. Volokhina, Nicole C. A. J. van de Kar and Lambertus P.W. J. van den Heuvel and on behalf of the COMBAT consortium

174 Case report: Novel FHR2 variants in atypical Hemolytic Uremic Syndrome: A case study of a translational medicine approach in renal transplantation
Emma Diletta Stea, Christine Skerka, Matteo Accetturo, Francesco Pesce, Thorsten Wiech, Andrea Hartman, Paola Pontrelli, Francesca Conserva, Giuseppe Castellano, Peter F. Zipfel and Loreto Gesualdo

183 C1QBP regulates mitochondrial plasticity to impact tumor progression and antitumor immune response
Qiping Wang, Dafei Chai, Navid Sobhani, Nan Sun, Praveen Neeli, Junnian Zheng and Hui Tian

194 High MBL-expressing genotypes are associated with deterioration in renal function in type 2 diabetes
G. H. Dørflinger, P. H. Høyem, E. Laugesen, J. A. Østergaard, K. L. Funck, R. Steffensen, P. L. Poulsen, T. K. Hansen and M. Bjerre

206 Association of low ficolin-2 concentration in cord serum with respiratory distress syndrome in preterm newborns
Gabriela Gajek, Anna S. Świerzko, Dariusz Jarych, Damian Mikulski, Paulina Kobiela, Karolina Chojnacka, Maja Kufelnicka-Babout, Agnieszka Szala-Poździej, Jędrzej Chrzanowski, Katarzyna Sobczuk, Wojciech Fendler, Misao Matsushita, Iwona Domżalska-Popadiuk, Jan Mazela, Jarosław Kalinka, Hideharu Sekine and Maciej Cedzyński

216 Free complement and complement containing extracellular vesicles as potential biomarkers for neuroinflammatory and neurodegenerative disorders
Marlies Burgelman, Pieter Dujardin, Charysse Vandendriessche and Roosmarijn E. Vandenbroucke

243 Quantitative fluorescence resonance energy transfer-based immunoassay for activated complement C1s
Jun Ye, Jie Xu, Chuanmeng Zhang, Li Zhu and Sheng Xia

254 Three different pathways of IgM-antibody-dependent hemolysis are mainly regulated by complement
Thilo Bartolmäs, Axel Pruß and Beate Mayer

261 An *ex vivo* test to investigate genetic factors conferring susceptibility to atypical haemolytic uremic syndrome
Sara Gastoldi, Sistiana Aiello, Miriam Galbusera, Matteo Breno, Marta Alberti, Elena Bresin, Caterina Mele, Rossella Piras, Lucia Liguori, Donata Santarsiero, Ariela Benigni, Giuseppe Remuzzi and Marina Noris

280 Proteomics profiling of vitreous humor reveals complement and coagulation components, adhesion factors, and neurodegeneration markers as discriminatory biomarkers of vitreoretinal eye diseases
Fátima M. Santos, Sergio Ciordia, Joana Mesquita, Carla Cruz, João Paulo Castro e Sousa, Luís A. Passarinha, Cândida T. Tomaz and Alberto Paradela

299 Autoantibodies against complement factor B in rheumatoid arthritis
Alexandra T. Matola, Angéla Fülöp, Bernadette Rojkovich, György Nagy, Gabriella Sármay, Mihály Józsi and Barbara Uzonyi

311 C9 immunostaining as a tissue biomarker for periprosthetic joint infection diagnosis
Ann-Kathrin Meinshausen, Jacqueline Färber, Sebastian Illiger, Paolo Macor, Christoph H. Lohmann and Jessica Bertrand

322 Decreased mannan-binding lectin level in adults with hypopituitarism; dependence on appropriate hormone replacement therapies
Aleksandra E. Matusiak, Jan Stępniak, Andrzej Lewiński and Małgorzata Karbownik-Lewińska

341 Modeling complement activation on human glomerular microvascular endothelial cells
Kes H. Stevens, Laura M. Baas, Thea J. A. M. van der Velden, Romy N. Bouwmeester, Niels van Dillen, Eiske M. Dorresteijn, Arjan D. van Zuilen, Jack F. M. Wetzels, Marloes A. H. M. Michels, Nicole C. A. J. van de Kar and Lambertus P. van den Heuvel

353 Functional evaluation of complement factor I variants by immunoassays and SDS-PAGE
Alexandra Gerogianni, Laura M. Baas, Dick J. Sjöström, Nicole C. A. J. van de Kar, Marit Pullen, Siem J. van de Peppel, Per H. Nilsson and Lambertus P. van den Heuvel

frontiers | Frontiers in Immunology

TYPE Editorial
PUBLISHED 24 November 2023
DOI 10.3389/fimmu.2023.1334050

Check for updates

OPEN ACCESS

EDITED AND REVIEWED BY
Francesca Granucci,
University of Milano-Bicocca, Italy

*CORRESPONDENCE
Erik J. M. Toonen
e.toonen@hycultbiotech.com

RECEIVED 06 November 2023
ACCEPTED 13 November 2023
PUBLISHED 24 November 2023

CITATION
Nilsson PH, Skattum L and Toonen EJM (2023) Editorial: Current challenges in complement diagnostics.
Front. Immunol. 14:1334050.
doi: 10.3389/fimmu.2023.1334050

COPYRIGHT
© 2023 Nilsson, Skattum and Toonen. This is an open-access article distributed under the terms of the Creative Commons Attribution License (CC BY). The use, distribution or reproduction in other forums is permitted, provided the original author(s) and the copyright owner(s) are credited and that the original publication in this journal is cited, in accordance with accepted academic practice. No use, distribution or reproduction is permitted which does not comply with these terms.

Editorial: Current challenges in complement diagnostics

Per H. Nilsson[1,2], Lillemor Skattum[3,4] and Erik J. M. Toonen[5]*

[1]Linnaeus Centre for Biomaterials Chemistry, Linnaeus University, Kalmar, Sweden, [2]Department of Chemistry and Biomedical Sciences, Linnaeus University, Kalmar, Sweden, [3]Clinical Immunology and Transfusion Medicine, Region Skåne, Lund, Sweden, [4]Department of Laboratory Medicine, Section of Microbiology, Immunology and Glycobiology, Lund University, Lund, Sweden, [5]Research & Development Department, Hycult Biotech, Uden, Netherlands

KEYWORDS

complement diagnostics, complement system, assessment of complement components, diagnostic techniques and procedures, complement-mediated disease

Editorial on the Research Topic
Current challenges in complement diagnostics

The complement system is an essential innate immune surveillance network that plays a crucial role in safeguarding the host against various threats, including invading microorganisms, dying or malignant cells, and immune complexes. It is a highly intricate system, comprising about 50 soluble and cell surface-bound proteins that interact with each other to eliminate danger, regulate cell activity, and retain homeostasis. To prevent uncontrolled activation, the complement system needs tight regulation. Dysregulation or inadequate functioning is associated with a myriad of diseases, including autoimmune and acute or chronic inflammatory diseases, infection susceptibility, and cancer. Uncontrolled or exaggerated activation can lead to life-threatening conditions such as systemic inflammation, shock, and, in the worst cases, organ failure and death (1).

In recent years, the complement system has been the subject of significant research interest as a target for therapeutic intervention. Eculizumab, the first approved complement inhibitor, has been highly effective in treating diseases associated with complement dysregulation such as atypical hemolytic uremic syndrome (aHUS) and paroxysmal nocturnal hemoglobinuria (PNH), and many more drug candidates targeting various complement components are currently undergoing evaluation in clinical trials (2). As a result, complement diagnostics has become increasingly important in the clinic. Accurate and comprehensive analysis of complement activity is crucial to diagnose, manage, and treat complement-related disorders. However, accurate determination of complement status has proven to be challenging, particularly within the constraints of routine clinical practice. Some of the challenges currently encountered include:

- Pathway complexity: The complement system consists of multiple components and three activation pathways that also interconnect with other immune pathways. Most diagnostic methods focus on a limited set of complement components, only providing a partial view of the cascade (Hurler et al.).
- Heterogeneity of complement-mediated diseases: The diversity of complement-related disorders makes it difficult to accurately identify and diagnose specific complement deficiencies, excesses, or abnormalities (3, 4).
- Patient heterogeneity: Patients with complement disorders exhibit substantial clinical diversity and variations in complement profiles. In addition, complement activation is highly dynamic and can change rapidly in response to stimuli (4). A snapshot measurement may not capture the full extent of complement activation. These variations not only complicate diagnostic accuracy but also affect treatment decisions, as a one-size-fits-all approach is often inadequate.
- Lack of sensitivity: Complement assays may lack the sensitivity to detect subtle changes in complement activity, especially in cases with partial complement deficiency or subtle dysregulation (4).
- Sample sensitivity: Many of the complement proteins are heat-labile and sensitive to post-sampling *in vitro* activation, which necessitates strict requirements for pre-analytical sample handling (5, 6).
- Lack of standardization: The absence of standardized methods, assays and reference materials, and uniform protocols for pre-analytical sample handling (collection, processing, and storage) can lead to inconsistent results obtained from different laboratories, hindering reliable comparisons (5–7).

This Research Topic provides a platform to critically discuss recent advancements in complement diagnostics and strategies for overcoming its challenges, offering recommendations for future research. This topic includes studies dedicated to unraveling the mechanisms underlying complement dysregulation and explores novel biomarkers relevant to complement-mediated diseases.

With regard to new biomarkers, Burgelman et al. summarize in their review article the current knowledge and explore future opportunities regarding complement proteins as biomarkers for neurodegenerative disorders such as Alzheimer's disease (AD) and multiple sclerosis (MS). They suggest that assessing complement protein levels in biofluids could potentially serve as biomarkers for disease progression, severity, or responses to treatment in these diseases. The authors indicate that measuring 'free' complement components in blood/biofluids has several drawbacks, e.g. that the cellular origin of these free components is lost. In that light, they suggest measuring extracellular vesicles (EVs) offers an additional platform to enhance the diagnostic utility of complement markers. EVs can contain complement proteins, while the cellular origin can be identified through the presence of EV surface markers. This opens new directions for future research, as EVs are not (yet) thoroughly investigated as biomarkers for complement-mediated diseases.

Other studies on this topic investigated complement components as potential biomarkers for diseases such as COVID-19 (Bruni et al., Tierney et al.), rheumatoid arthritis (RA) (Matola et al.), kidney diseases (Zhang et al., Stea et al., Gastoldi et al.), type 2 diabetes and nonalcoholic fatty liver disease (NAFLD) (Habenicht et al., Dorflinger et al.), and cancer (Wang et al.).

The topic also includes studies presenting new methods or assays to improve the sensitivity and quality of the measurements (Meuleman et al., Hurler et al., Ye et al., Meinshausen et al., Stevens et al., Gastoldi et al.) and discusses the lack of standardization (Brandwijk et al., Michels et al.). Regarding new methods, Meuleman et al. and coworkers argue in their review for assays capable of analyzing complement deposits on cultured endothelial cells incubated with pathologic human serum. They propose this *ex vivo* test as a promising method for assessing complement activation, as it resembles the physiological context. This assay has been used to study complement activation in various diseases, and in some cases, to adjust treatment with complement inhibitory drugs. However, the authors also mention that there is no international standard for these assays and that the mechanisms for activation are not fully understood. Moreover, primary cell culture is challenging and hampers the development of a standardized commercial assay. The lack of standardized assays and reference materials not only holds true for assays using primary cells but is a challenge for complement diagnostics in general. This concern is also discussed by (Michels et al.). Their review focuses on C3 nephritic factor (NeF), a well-established biomarker for rare complement-mediated kidney disorders, but measuring NeFs for diagnostic purposes remains difficult. The authors discuss the diseases linked to NeFs, the diverse mechanisms of action seen in various NeF types, a number of laboratory techniques, and initiatives to establish standardized approaches.

Advances in complement diagnostics have the potential to improve the diagnosis and treatment of complement-mediated diseases, and it is a battle on two fronts. First, a continuous strive for novel achievements in the scientific forefront using advanced methodology and unraveling novel biomarkers. Second, and equally important, is to make complementary diagnostics accessible for everyday use in clinical and research settings. Addressing these challenges will require increased collaboration between researchers, clinicians, and industry partners.

Author contributions

PN: Conceptualization, Investigation, Writing – review & editing. LS: Conceptualization, Investigation, Writing – review & editing. ET: Conceptualization, Investigation, Supervision, Writing – original draft.

Funding

The author(s) declare financial support was received for the research, authorship, and/or publication of this article. PN was supported by the Swedish Research Council (Project 2018-04087), the Crafoord Foundation (Project 20210961), and the Health Research Council in the South East of Sweden, FORSS (Project 940971). ET received funding from the European Union's Horizon 2020 research and innovation programme under grant agreement No. 899163 "Screening of inFlammation to enable personalized Medicine" (SciFiMed, https://scifimed.eu/).

Acknowledgments

We would like to thank all the authors for their contributions to this Research Topic. We are also grateful to all reviewers for their insightful evaluation of all manuscripts submitted to this topic.

Conflict of interest

ET is an employee of Hycult Biotech.

The remaining authors declare that the research was conducted in the absence of any commercial or financial relationships that could be construed as a potential conflict of interest.

Publisher's note

All claims expressed in this article are solely those of the authors and do not necessarily represent those of their affiliated organizations, or those of the publisher, the editors and the reviewers. Any product that may be evaluated in this article, or claim that may be made by its manufacturer, is not guaranteed or endorsed by the publisher.

References

1. Ricklin D, Reis ES, Lambris JD. Complement in disease: a defence system turning offensive. *Nat Rev Nephrol.* (2016) 12(7):383–401. doi: 10.1038/nrneph.2016.70

2. Mastellos DC, Ricklin D, Lambris JD. Clinical promise of next-generation complement therapeutics. *Nat Rev Drug Discov* (2019) 18(9):707–29. doi: 10.1038/s41573-019-0031-6

3. Pouw RB, Ricklin D. Tipping the balance: intricate roles of the complement system in disease and therapy. *Semin Immunopathol* (2021) 43(6):757–71. doi: 10.1007/s00281-021-00892-7

4. Nilsson B, Ekdahl KN. Complement diagnostics: concepts, indications, and practical guidelines. *Clin Dev Immunol* (2012) 2012:962702. doi: 10.1155/2012/962702

5. Brandwijk R, Michels M, van Rossum M, de Nooijer AH, Nilsson PH, de Bruin WCC, et al. Pitfalls in complement analysis: A systematic literature review of assessing complement activation. *Front Immunol* (2022) 13:1007102. doi: 10.3389/fimmu.2022.1007102

6. Prohaszka Z, Nilsson B, Frazer-Abel A, Kirschfink M. Complement analysis 2016: Clinical indications, laboratory diagnostics and quality control. *Immunobiology* (2016) 221(11):1247–58. doi: 10.1016/j.imbio.2016.06.008

7. Poppelaars F, Goicoechea de Jorge E, Jongerius I, Baeumner AJ, Steiner MS, Jozsi M, et al. A family affair: addressing the challenges of factor H and the related proteins. *Front Immunol* (2021) 12:660194. doi: 10.3389/fimmu.2021.660194

frontiers in Immunology

ORIGINAL RESEARCH
published: 31 March 2022
doi: 10.3389/fimmu.2022.842451

Circulating Levels of Anti-C1q and Anti-Factor H Autoantibodies and Their Targets in Normal Pregnancy and Preeclampsia

Douwe Jan Dijkstra[1], A. Inkeri Lokki[2,3], Lobke Marijn Gierman[4], Nicole Veronique Borggreven[1], Carin van der Keur[1], Michael Eikmans[1], Kyra Andrea Gelderman[5], Hannele Laivuori[3,6,7], The FINNPEC Core Investigator Group, Ann-Charlotte Iversen[4], Marie-Louise P. van der Hoorn[8] and Leendert Adrianus Trouw[1*]*

[1] Department of Immunology, Leiden University Medical Center, Leiden, Netherlands, [2] Department of Bacteriology and Immunology, University of Helsinki and Helsinki University Hospital, Helsinki, Finland, [3] Medical and Clinical Genetics, University of Helsinki and Helsinki University Hospital, Helsinki, Finland, [4] Centre of Molecular Inflammation Research, Department of Clinical and Molecular Medicine, Norwegian University of Science and Technology, Trondheim, Norway, [5] Department of Immunopathology and Haemostasis, Sanquin Diagnostic Services, Amsterdam, Netherlands, [6] Institute for Molecular Medicine Finland, Helsinki Institute of Life Science, University of Helsinki, Helsinki, Finland, [7] Department of Obstetrics and Gynecology, Tampere University Hospital and Tampere University, Faculty of Medicine and Health Technology, Tampere Center for Child, Adolescent, and Maternal Health Research, Tampere, Finland, [8] Department of Obstetrics and Gynecology, Leiden University Medical Center, Leiden, Netherlands

OPEN ACCESS

Edited by:
Erik J.M. Toonen,
Hycult Biotech, Netherlands

Reviewed by:
Rohan Willis,
University of Texas Medical Branch at Galveston, United States
Chiara Agostinis,
Institute for Maternal and Child Health Burlo Garofolo (IRCCS), Italy

***Correspondence:**
Douwe Jan Dijkstra
d.j.dijkstra@lumc.nl
Leendert Adrianus Trouw
L.A.Trouw@lumc.nl

Specialty section:
This article was submitted to Molecular Innate Immunity, a section of the journal Frontiers in Immunology

Received: 23 December 2021
Accepted: 07 March 2022
Published: 31 March 2022

Citation:
Dijkstra DJ, Lokki AI, Gierman LM, Borggreven NV, van der Keur C, Eikmans M, Gelderman KA, Laivuori H, The FINNPEC Core Investigator Group, Iversen A-C, van der Hoorn M-LP and Trouw LA (2022) Circulating Levels of Anti-C1q and Anti-Factor H Autoantibodies and Their Targets in Normal Pregnancy and Preeclampsia. Front. Immunol. 13:842451. doi: 10.3389/fimmu.2022.842451

Preeclampsia (PE) generally manifests in the second half of pregnancy with hypertension and proteinuria. The understanding of the origin and mechanism behind PE is incomplete, although there is clearly an immune component to this disorder. The placenta constitutes a complicated immune interface between fetal and maternal cells, where regulation and tolerance are key. Stress factors from placental dysfunction in PE are released to the maternal circulation evoking the maternal response. Several complement factors play a role within this intricate landscape, including C1q in vascular remodeling and Factor H (FH) as the key regulator of alternative pathway complement activation. We hypothesize that decreased levels of C1q or FH, or disturbance of their function by autoantibodies, may be associated with PE. Autoantibodies against C1q and FH and the concentrations of C1q and FH were measured by ELISA in maternal sera from women with preeclamptic and normal pregnancies. Samples originated from cohorts collected in the Netherlands (n=63 PE; n=174 control pregnancies, n=51 nonpregnant), Finland (n=181 PE; n=63 control pregnancies) and Norway (n=59 PE; n=27 control pregnancies). Serum C1q and FH concentrations were higher in control pregnancy than in nonpregnant women. No significant differences were observed for serum C1q between preeclamptic and control pregnancy in any of the three cohorts. Serum levels of FH were lower in preeclamptic pregnancies compared to control pregnancies in two of the cohorts, this effect was driven by the early onset PE cases. Neither anti-C1q autoantibodies nor anti-FH autoantibodies

levels differed between women with PE and normal pregnancies. In conclusion, levels of anti-C1q and anti-FH autoantibodies are not increased in PE. C1q and FH are increased in pregnancy, but importantly, a decrease in FH concentration is associated with PE.

Keywords: C1q, complement, factor H, autoantibodies, preeclampsia, pregnancy

INTRODUCTION

Preeclampsia (PE) is a vascular complication presenting in the second half of pregnancy. PE occurs in about 3% of pregnancies and is an important cause of both fetal and maternal morbidity (1). The disease is characterized by newly developed hypertension and proteinuria, or new-onset PE-associated signs in the absence of proteinuria, and can progress systemically to include organ dysfunction. Onset of PE is unpredictable, with the only cure being delivery of the placenta (2). Although the mechanism behind the development of PE is incompletely understood, its origin may involve improper placentation with incomplete remodeling of the uterine spiral arteries and development of a dysfunctional placenta with vascular malperfusion (3). As the pregnancy progresses and the fetus demands a fully functional placenta, the placenta releases increasing amounts of stress signals to the maternal circulation and the mother may eventually develop endothelial dysfunction and the clinical manifestation of PE.

In the context of healthy pregnancy, a well-functioning and regulated complement system is key. The complement system is an important component of the innate immune system, consisting of more than 30 protein factors that form three converging activation pathways (classical, lectin and alternative pathways) with their accessory regulators (4). Although classically known in the defense against infections, the complement system is also involved in clearance of immune complexes and dying cells, tissue regeneration and angiogenesis (5). Additionally, complement forms a bridge towards cellular immune responses, attracting and activating immune cells locally with activation fragments that act as anaphylatoxins and opsonins.

The initiator of the classical pathway of the complement system, C1q, binds directly to apoptotic cells and debris that results from tissue remodeling, labeling it for clearance (6). The relevance of C1q for a healthy pregnancy was highlighted by the observation of impaired labyrinth development and vessel remodeling in pregnant C1q-deficient mice compared to wildtype mice (7). Additionally, C1q-deficient mice are predisposed to present with PE-like symptoms and higher fetal loss (8). In human pregnancy, C1q is found throughout the maternal side of the placenta and is also locally produced by invading trophoblasts, the fetal cell type directly interacting with maternal cells at the maternal-fetal interface (7). In healthy pregnancy the local presence of C1q in the placenta does not result in overt complement activation (9). Human C1q deficiency is very rare and although it is studied in great detail because of its association with development of Systemic Lupus Erythematosus (SLE) and infections (10), no information is currently available on pregnancy outcomes.

Factor H (FH) is a key regulator of the alternative pathway because of its ability to block C3 convertase formation and its function as a cofactor for Factor I. In this way, FH plays an important role in the steady state protection of host cells throughout the body, especially circulating cells and endothelial cells. In addition, FH provides protection against excessive complement activation on apoptotic cells, which downregulate membrane-bound complement inhibitors (11). FH is abundantly present in the placenta, but the observed irregular distribution of FH in the PE placenta may suggest a disturbed balance between complement activation and regulation in PE (12). FH was even observed intracellularly in syncytiotrophoblast, although this FH may actually be of fetal rather than maternal origin (13).

Autoantibodies may target multiple complement proteins, including C1q and FH (14). Anti-C1q autoantibodies are typically present in diseases like SLE, Hypocomplementemic Urticarial Vasculitis Syndrome and Rheumatoid Vasculitis, but are also present in a fraction of healthy individuals (15). Importantly, anti-C1q autoantibodies do not deplete circulating C1q, but may amplify classical pathway driven complement activation (16) and dysregulate other processes driven by C1q (17). Autoantibodies to FH have been described in atypical Hemolytic Uremic Syndrome and C3-glomerulopathy as well as in antiphospholipid syndrome and other autoimmune diseases (18, 19). Anti-FH autoantibodies may have different functional consequences, as some form immune complexes leading to (partial) FH depletion, while other anti-FH autoantibodies affect the functional properties of FH (19). Consequences of these autoantibodies are often associated with autoimmune diseases, where they may drive or enhance pathogenesis. Several previous studies showed a relationship between anti-C1q autoantibodies and negative pregnancy outcomes in miscarriage, ectopic pregnancy and autoimmune thyroid disorders, but not for PE (20–22). A study focusing on pregnancy in lupus nephritis patients found that anti-C1q was not a predictor of PE (23).

We hypothesize that a balance between complement activation, needed for tissue remodeling and clearance of apoptotic cells in the placenta, and regulation is critical for a healthy pregnancy. This balance may be disturbed in PE, which could contribute to the underlying pathogenesis. Autoantibodies against complement factors may further hamper their proper function or incite unwanted immune activation. In this study, we therefore compared the serum levels of C1q and FH, and autoantibodies against these factors, in women with healthy or preeclamptic pregnancies.

MATERIALS AND METHODS

Patients and Samples

Serum samples of women with preeclamptic and control pregnancies were derived from three cohorts collected in the Netherlands, Finland and Norway. PE was defined as hypertension (systolic blood pressure ≥140 mmHg or diastolic blood pressure ≥90 mmHg) and proteinuria (≥0.3 g/24h or ≥0.3 g/L), or newly developed PE-associated signs in the absence of proteinuria, with onset beyond 20 weeks of gestation. Women with normal pregnancies and no previous history of PE were included as controls.

The cohort from the Netherlands was collected at the Leiden University Medical Center (LUMC) and comprised 63 women with PE and 174 women with control pregnancies. Serum samples from these women were collected on the day of delivery, although it varied whether this was performed before or after the actual delivery. Additionally, a group of 51 nonpregnant women with a similar age profile as the pregnancy cohorts (median age 31 years, range 20-46), was included.

The cohort from Finland comprises samples of 181 preeclamptic and 63 control pregnancies from the Finnish Genetics of Pre-eclampsia Consortium (FINNPEC) that has been described before (24). In this cohort proteinuria could additionally be diagnosed based on two ≥1 readings on a dipstick in a random urine determination with no evidence of a urinary tract infection. Samples were collected at recruitment, 74% were taken prior to the day of delivery (range 1 to 31 days before delivery), while 25% of samples were taken on the day of delivery, one sample in the control pregnancy group was taken on the second day after delivery.

The Norwegian cohort was collected at St. Olavs and Haukeland University Hospitals and comprises sera from 59 women with PE and 27 women with control pregnancies. All samples in this cohort were collected before delivery on the day of delivery by caesarean section, without signs of being in labor. Caesarean sections for the control group were indicated due to breech position, suspected birth defects, previous obstetric history, or birth anxiety. Serum samples from Finland and Norway were stored frozen and were transported to LUMC for analysis. Ethical approval for the three cohorts was obtained at the individual centers (the Netherlands: P08.229/228, Finland: 149/EO/2007, Norway: REC 2012/1040).

Anti-C1q Antibody ELISA

Antibodies against C1q were measured by QUANTA Lite Anti-C1q ELISA (Inova Diagnostics) according to the manufacturer's protocol. Briefly, 100 µl of 1:101 diluted sera in Samples Diluent were incubated in ELISA plate wells for 30 minutes at room temperature. Wells were washed 3 times with wash buffer, incubated with 100 µl horseradish peroxidase (HRP) conjugated anti-IgG and incubated for 30 minutes at room temperature. After washing 3 times, wells were incubated with 100 µl TMB Chromogen for 30 minutes at room temperature, followed by addition of 100 µl acidic HRP Stop Solution. Absorbance values were read at 450 nm and used to calculate anti-C1q units based positive control samples included in the kit. The cut-off for positivity was 20 units, as recommended by the manufacturer.

Anti-FH Antibody ELISA

Measurement of antibodies against FH was performed using an in-house developed ELISA. Nunc MaxiSorp ELISA plates (ThermoScientific) were coated with 50 µl of 10 µg/ml FH (Complement Technology) in 0.1M bicarbonate coating buffer (pH 9.6) and incubated overnight at 4°C. Wells were washed 3 times with PBS/0.05% Tween, blocked with 100 µl PBS/1% BSA for 1 hour at 37°C and washed 3 times. Serum samples were diluted 1:50 in PBS/0.05% Tween/1% BSA (PTB) and 50 µl sample was incubated in wells for 1 hour at 37°C. After washing 3 times, 50 µl 0.11 µg/ml Goat anti-human IgG-biotin (Invitrogen) was added, followed by incubation for 1 hour at 37°C and washing 3 times. Secondary detection consisted of 50 µl 0.5 µg/ml streptavidin-HRP (ThermoScientific), incubated for 1 hour at 37°C. After the final washing sequence, 50 µl 2,2'-azino-bis(3-ethylbenzothiazoline-6-sulfonic acid (ABTS)/0.015% H_2O_2 was added. Absorbance was read at 415 nm. Anti-FH units (U) were determined based on standard curve of anti-FH standard (180kU; Sanquin Diagnostics, Amsterdam, the Netherlands) by an Excel-based logit calculation. Cut-off for positivity was set at 95th percentile of all control pregnancy samples combined.

C1q ELISA

To measure the concentration of C1q in serum samples, an in-house ELISA was performed as described before (25). Nunc MaxiSorp ELISA plates (ThermoScientific) were coated with 50 µl 2.5 µg/ml mouse anti-human C1q monoclonal antibody (mAb) 2204 (kind gift Prof. C. van Kooten, Dept Nephrology, LUMC) in 0.1M bicarbonate coating buffer (pH 9.6) and incubated overnight at room temperature. Wells were washed 3 times with PBS/0.05% Tween and blocked with 100 µl PBS/1% BSA and incubated for 1 hour at 37°C. After washing, 50 µl of serially diluted serum samples in PTB, as well as a standard curve from a pool of normal human serum were added to the wells, followed by incubation for 1 hour at 37°C and washing 3 times. Wells were then incubated with 50 µl 1:2000 diluted rabbit anti-human C1q (DAKO) for 1 hour at 37°C. After washing, 50 µl 1:2000 goat anti-rabbit-HRP (DAKO) was added for detection and wells were incubated for 1 hour at 37°C. Following the final washing sequence, wells were incubated with 50 µl ABTS/0.015% H_2O_2 and absorbance was read at 415 nm. C1q concentrations were calculated based on the standard curve of a reference serum.

FH ELISA

Concentration of FH in serum was determined by an in-house ELISA on Nunc MaxiSorp ELISA plates (ThermoScientific). Wells were coated with 50 µl 0.5 µg/ml mouse anti-FH (clone FH.16; Sanquin) in bicarbonate coating buffer (pH 9.6) and incubated overnight at room temperature. After washing 3 times with PBS/0.05% Tween, wells were blocked with 100 µl PBS/1%

BSA for 1 hour at 37°C. Samples were diluted 1:2000 and 1:4000 in PTB, and 50 µl was added to the wells. For calculation of FH concentration, a standard curve of a reference serum with known FH concentration was added on each plate. Wells were incubated for 1 hour at 37°C and washed, then incubated with 50 µl 0.25 µg/ml biotinylated mouse anti-human FH mAb OX-23 for 1 hour at 37°C. After washing, detection was performed by incubating the wells with 50 µl 0.5 µg/ml streptavidin-HRP (ThermoScientific) for 1 hour at 37°C. Following the final wash, wells were stained with 50 µl ABTS/0.015% H_2O_2 and absorbance was read at 415 nm. FH concentrations were calculated based on the standard curve of a reference serum.

Statistical Analysis

All statistical analyses were performed using GraphPad Prism 8 for Windows (GraphPad Software, San Diego, CA, USA). Normal distribution of data was examined by D'Agostino & Pearson normality test. Comparisons of numerical data were performed by Mann-Whitney U test, whereas categorical data was analyzed with Fisher's exact test. Analysis of samples matched for gestational age (in the cohort from Finland) was performed by forming pairs with maximum 2 days difference in gestational age, C1q and Factor H concentrations were then compared between pairs by paired t test. Correlation between data was analyzed by Spearman's rank correlation.

RESULTS

Patient Characteristics

To study the relationship between the presence of anti-complement autoantibodies and complement protein levels and PE we analyzed serum samples obtained from cohorts from the Netherlands, Finland and Norway, comprising a total of 289 preeclamptic pregnancies and 264 control pregnancies. Three cohorts from different countries were investigated to provide a robust basis for conclusions. Overall, the three cohorts displayed the expected clinical characteristics associated with PE, such as increased diastolic blood pressure, proteinuria and lower gestational age in the PE-complicated pregnancies as compared to the control pregnancies (**Table 1**). Both gravidity and parity were in general lower in the PE group than in controls although some differences existed between the cohorts. The proportion of deliveries performed through Caesarean section was not significantly different between the groups in any of the cohorts. Maternal body mass index (BMI) was higher in the Finnish PE group as compared to the control group, no difference in BMI was present in Norway, while BMI data from the Netherlands was not available. When comparing the three cohorts of PE cases, the cohort from Finland stands out with a higher median gestational age and fetal birthweight, (**Table 2**). Moreover, among both PE cases and controls, a

TABLE 1 | Clinical characteristics of the included subjects.

The Netherlands	**Preeclampsia (n = 63)**	**Control (n = 174)**	**p-value**
Maternal age (years)	31 (18-46)	33 (23-42)	**0.0117**[#]
Gestational age (days)	220 (170-283)	275 (266-297)	**<0.0001**[#]
Fetal birthweight (g)	1246 (380-4030)	3598 (2445-5100)	**<0.0001**[#]
Blood pressure (mmHg)	104 (90-160)	75 (55-90)	**<0.0001**[#]
Proteinuria (mg/24hr)	2300 (310-14000) [(16)]	N/A	N/A
Gravidity	2 (1-9)	3 (1-9)	**<0.0001**[#]
Parity	0 (0-5)	1 (0-6)	**<0.0001**[#]
Caesarean section (%)	49 (78%)	113 (65%)	0.0814[$]
Finland	**Preeclampsia (n = 181)**	**Control (n = 63)**	**p-value**
Maternal age (years)	32 (18-47)	31 (21-43)	**<0.0001**[#]
Gestational age (days)	246 (165-286) [(1)]	280 (167-297) [(1)]	**<0.0001**[#]
Fetal birthweight (g)	2775 (310-5110)	3470 (330-4748)	**<0.0001**[#]
Blood pressure (mmHg)	111 (91-173)	84 (67-130) [(1)]	**<0.0001**[#]
Proteinuria (mg/L)	3200 (300-19100) [(3)]	200-270 [(60)]	**<0.0001**[#]
Gravidity	1 (1-18)	2 (1-5) [(1)]	**<0.0001**[#]
Parity	0 (0-12)	1 (1-2) [(1)]	0.4621[#]
Caesarean section (%)	90 (50%)	25 (40%) [(1)]	0.2389[$]
BMI (start of pregnancy)	23.90 (18.20-48.40)	22.90 (18.20-39.10) [(1)]	**<0.0001**[#]
Norway	**Preeclampsia (n = 45)**	**Control (n = 27)**	**p-value**
Maternal age (years)	30 (20-45)	33 (23-41)	**0.0447**[#]
Gestational age (days)	223 (178-275)	274 (265-294)	**<0.0001**[#]
Fetal birthweight (g)	1286 (550-5010)	3510 (2800-4330)	**<0.0001**[#]
Blood pressure (mmHg)	100 (80-130)	75 (60-99)	**<0.0001**[#]
Proteinuria (Yes/No)	Yes: 45	No: 26 [(1)]	**<0.0001**[$]
Gravidity	2 (1-13)	2 (1-5)	0.0743[#]
Parity	0 (0-3)	1 (0-3)	**0.0095**[#]
Caesarean section (%)	45 (100%)	27 (100%)	>0.9999[$]
BMI (start of pregnancy)	24.4 (18.2-38.4) [(4)]	24.6 (16.4-33.8) [(2)]	0.522

For patient characteristics, median and range are indicated. For blood pressure, the highest diastolic blood pressure is used. Where information was not available for all subjects, the number of missing data points is indicated in superscript. N/A, not applicable. Statistical significance calculated by Mann Whitney U test (#) or Fisher's exact test ($).
P-values <0.05 are indicated in bold.

lower frequency of Caesarean sections is present in the Finnish cohort.

Anti-C1q Autoantibodies and C1q

Anti-C1q antibodies were absent in maternal serum of preeclamptic pregnancies in the cohort from the Netherlands, while 10.3% of control pregnancy sera and 17.6% of sera from nonpregnant women were positive for anti-C1q (**Figure 1A**). However, no significant differences between control and preeclamptic pregnancies were observed for anti-C1q levels in the other cohorts (**Figures 1B, C, G**).

For serum C1q concentration, no significant differences were observed between the PE and control pregnancies in any of the cohorts (**Figures 1D–F**). Analysis of pooled data from all cohorts and gestational age-matched samples confirmed the lack of association between C1q concentration and PE (**Figures 1H, I**). Interestingly, the serum C1q concentration was higher for both control and preeclamptic pregnancies than for nonpregnant women (**Figure 1D**).

Anti-FH Autoantibodies and FH

We tested whether dysregulation of FH by the presence of autoantibodies is associated with PE, but no significant differences were observed regarding the levels of anti-FH autoantibodies between PE and control pregnancies (**Figures 2A–C, G**). However, importantly we observed significantly decreased levels of FH comparing the preeclamptic pregnancies to healthy pregnancies. In the cohorts from the Netherlands and Norway, the FH concentration was significantly lower in the PE group compared to controls pregnancies (**Figures 2D, F**). In samples from Finland, a similar trend of lower FH concentration in the PE group was observed (p=0.067) (**Figure 2E**). When pooled data from all cohorts were analyzed, the lower FH concentration remained significant (**Figure 2H**). Additionally, an analysis of samples matched for gestational age in the cohort from Finland shows the same result, excluding the possibility of data skewing by lower gestational ages in PE (**Figure 2I**). Similar to what was observed for C1q, women with control pregnancies showed higher FH concentration than nonpregnant controls (**Figure 2D**).

Study of the Association of Complement and Autoantibodies With Clinical Parameters and Subgroups of PE Patients

To further investigate the relationship between PE and C1q, FH or autoantibodies targeting these proteins, Spearman correlations with clinical parameters associated with PE were explored for all PE patients (**Table 3**). The clinical parameters included proteinuria and diastolic blood pressure, fetal birthweight and gestational age at delivery, (**Table 1**). Interestingly, a positive correlation was found between the mother's BMI and serum FH concentration in the cohorts from Finland and Norway (Spearman r=0.288; p=8.6e-5 and r=0.351; p=0.024 respectively). However, no other consistent significant correlations were found relating to PE symptoms or other relevant clinical parameters.

Further analyses were performed on subgroups of PE patients based on time of disease onset or presence of fetal growth restriction (FGR) (**Table 4**). Early onset of PE (gestational age below 34 weeks) was associated with decreased FH concentration compared to late onset, this difference was significant in cohorts from Finland and Norway, while a similar trend was observed in the cohort from the Netherlands. PE with FGR was associated to higher serum levels of anti-FH antibodies compared to preeclampsia with normal fetal growth, but this difference was only statistically significant in the cohort from the Netherlands.

TABLE 2 | Comparison of clinical characteristics between the three independent cohorts in control pregnancies and in PE cases.

	Control pregnancies			
Parameter	**The Netherlands (n=174)**	**Finland (n=63)**	**Norway (n=27)**	**p-value**
Maternal age (years)	33 (23-42)	31 (21-43)	33 (23-41)	0.032
Gestational age (days)	275 (266-297)	280 (167-297)[1]	274 (265-294)	0.205
Fetal birthweight (g)	3598 (2445-5100)	3470 (330-4748)	3510 (2800-4330)	0.089
Blood pressure (mmHg)	75 (55-90)	84 (67-130)[1]	75 (60-99)	**<0.0001**
Gravidity	3 (1-9)	2 (1-5)[1]	2 (1-5)	**0.0006**
Parity	1 (0-6)	1 (1-2)[1]	1 (0-3)	**<0.0001**
Caesarean section (%)	113 (65%)	25 (40%)[1]	27 (100%)	**<0.0001**
	Preeclampsia			
Parameter	**The Netherlands (n = 63)**	**Finland (n = 181)**	**Norway (n = 45)**	**p-value**
Maternal age (years)	31 (18-46)	32 (18-47)	30 (20-45)	0.409
Gestational age (days)	220 (170-283)	246 (165-286)[1]	223 (178-275)	**<0.0001**
Fetal birthweight (g)	1246 (380-4030)	2775 (310-5110)	1286 (550-5010)	**<0.0001**
Blood pressure (mmHg)	104 (90-160)	111 (91-173)	100 (80-130)	**<0.0001**
Gravidity	2 (1-9)	1 (1-18)	2 (1-13)	0.532
Parity	0 (0-5)	0 (0-12)	0 (0-3)	0.038
Caesarean section (%)	49 (78%)	90 (50%)	45 (100%)	**<0.0001**

Where information was not available for all subjects, the number of missing data points is indicated in superscript. All comparisons were performed with Kruskal-Wallis test, except for the mode of delivery, which was analyzed by Chi-square test.
P-values <0.05 are indicated in bold.

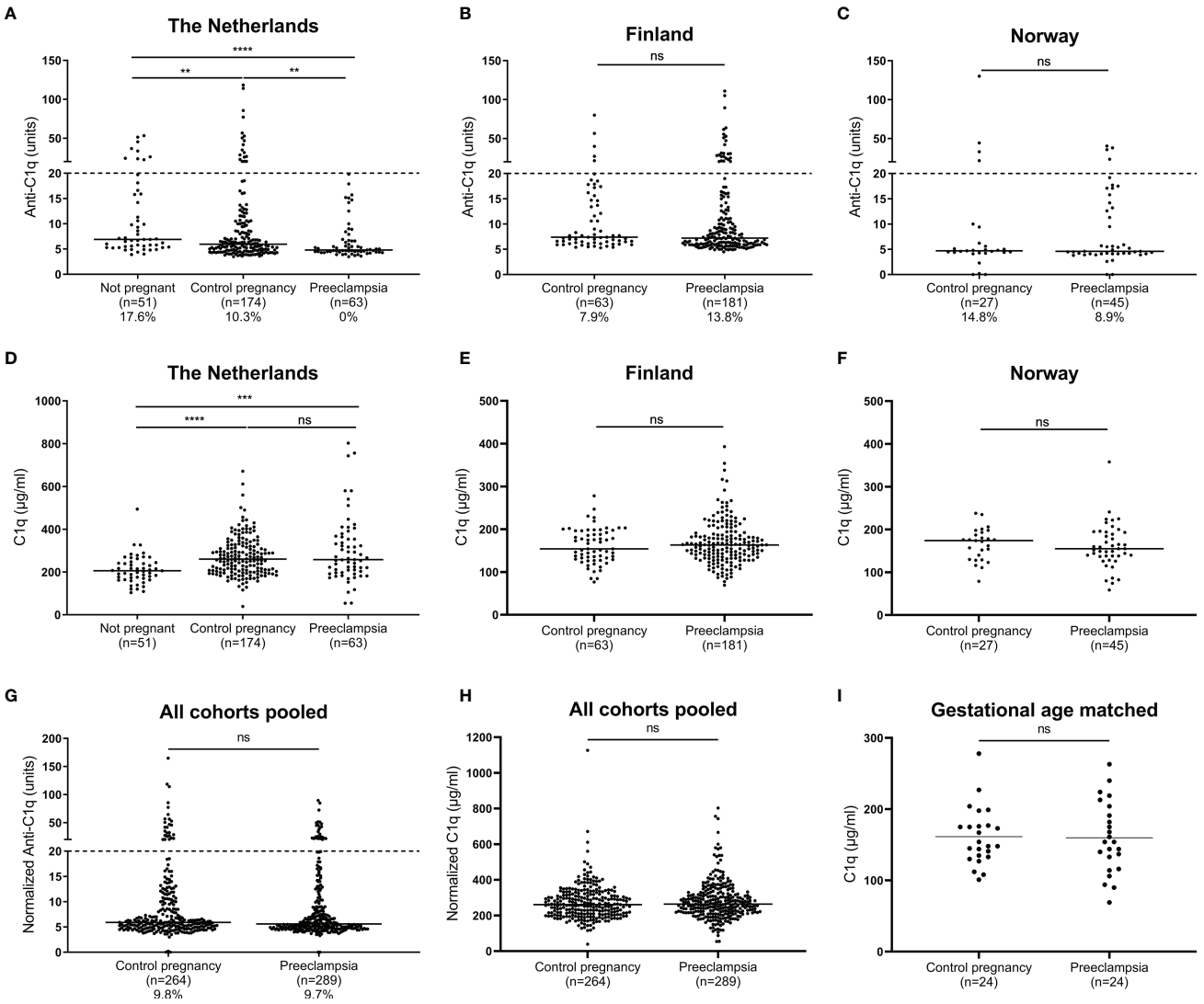

FIGURE 1 | Anti-C1q antibodies and C1q in healthy or PE pregnancy. Anti-C1q antibodies measured in maternal serum in cohorts from the Netherlands **(A)**, Finland **(B)** and Norway **(C)**, with percentages under the graph indicating the proportion samples deemed anti-C1q positive (>20 units, also indicated by dashed line). C1q concentration measured in maternal serum in cohorts from the Netherlands **(D)**, Finland **(E)** and Norway **(F)**. Data from different cohorts was normalized and pooled for anti-C1q **(G)** and C1q **(H)**. For the cohort from Finland, a subanalysis with samples matched for gestational age was additionally performed **(I)**. Comparisons tested by Mann-Whitney, or paired t test for panel I; ns, not significant ($p > 0.05$); **, $0.001 < p < 0.01$; ***, $0.0001 < p < 0.001$; ****, $p < 0.0001$.

DISCUSSION

In the current study, we investigated the relation between the pregnancy complication PE and the circulating levels of complement factors C1q and FH, as well as autoantibodies against these factors. We observed that the presence of autoantibodies against C1q or FH is not associated with PE. Circulating C1q and FH levels were higher in pregnant than in nonpregnant women. Decreased serum concentrations of FH were associated with PE, while this was not the case for serum C1q concentrations. Serum FH levels were lower in the subset of PE cases with earlier onset, compared to late onset cases.

Although the etiology of PE remains unclear, multiple immune mechanisms have been proposed to play a role, as the placenta constitutes a unique immune environment. Differentially expressed levels of fetal Human Leukocyte Antigen (HLA), especially HLA-G (26–28), immune cell influx (29) and cytokine expression (30) have been reported in preeclamptic placentas. Complement has also been implicated in the development of PE. Our data now add to this understanding that the circulating levels of the endogenous complement inhibitor FH are decreased in PE. Several studies linked anti-C1q autoantibodies to various negative pregnancy outcomes, but not to PE (20–23). The current study reinforces

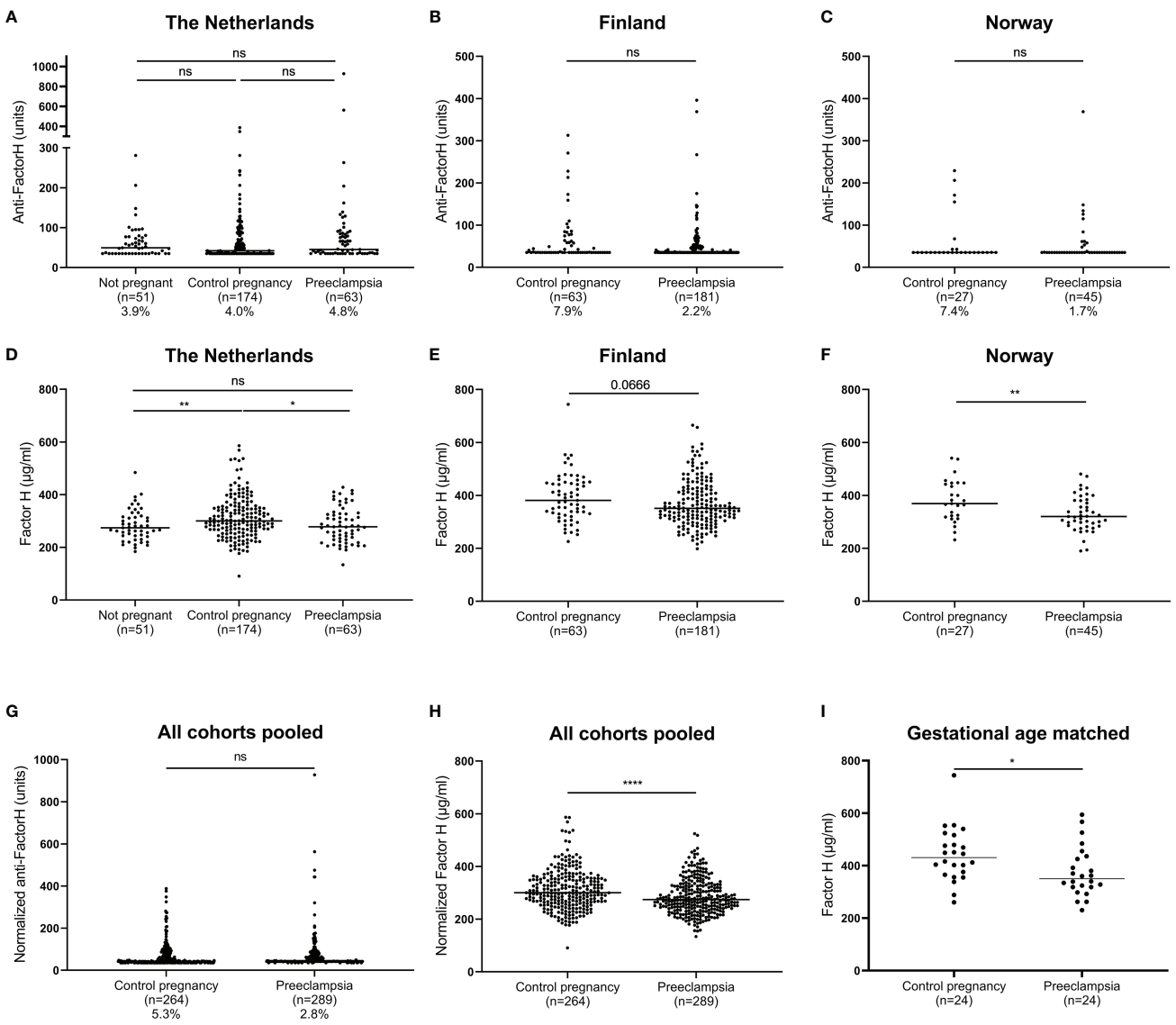

FIGURE 2 | Anti-Factor H antibodies and Factor H in healthy or PE pregnancy. Anti-Factor H antibodies measured in maternal serum in cohorts from the Netherlands **(A)**, Finland **(B)** and Norway **(C)**, dotted line indicates the detection limit at 35.2 units. Factor H concentration measured in maternal serum in cohorts from the Netherlands **(D)**, Finland **(E)** and Norway **(F)**. Data from different cohorts was normalized and pooled for anti-FH **(G)** and FH **(H)**. For the cohort from Finland, a subanalysis with samples matched for gestational age was additionally performed **(I)**. Comparisons tested by Mann-Whitney, or paired t test for panel I; ns, not significant ($p > 0.05$); *, $0.05 < p < 0.01$; **, $0.001 < p < 0.01$; ****, $p < 0.0001$.

that the presence of anti-C1q does not associate with PE. Likewise, no evidence for a link between anti-FH and PE was observed. These results contradict the hypothesis of a contribution by complement dysregulation by autoantibodies to development of PE.

C1q has multiple functions during pregnancy, e.g. in angiogenesis, tissue remodeling and clearance of cellular debris. These functions are supported by the ability of C1q to recognize exposed or altered self-structures, facilitating clearance without overt inflammation (31). Next to observations in human pregnancy, data from experiments in mice indicate a key role for C1q in placentation as the litter size in C1q deficient mice is smaller as compared to wild-type mice (7). The notion that C1q plays an important role in pregnancy fits with our finding of increased C1q levels in pregnant women, both complicated and control, as compared to nonpregnant women. Especially the role C1q plays in the clearance of apoptotic cells and debris is postulated to be important in the case of PE. Fragments of apoptotic syncytiotrophoblast from the placenta may enter the maternal circulation and the complement system assists in clearing these fragments by labelling them for phagocytosis. One previous study showed decreased C1q in severe PE cases

TABLE 3 | Correlation between clinical parameters and C1q, FH and autoantibodies in preeclamptic pregnancies.

Parameter	The Netherlands (n = 63)							
	Anti-C1q		C1q		Anti-FH		FH	
	Spearman r	p-value	Spearman r	p-value	Spearman r	p-value	Spearman r	p-value
Gestational age	-0.199	0.118	0.050	0.696	-0.248	0.050	0.023	0.861
Proteinuria	-0.243	0.100	-0.200	0.178	0.146	0.326	0.090	0.549
Highest diastole	0.078	0.541	-0.088	0.495	0.179	0.160	0.101	0.430
Fetal birthweight	-0.150	0.241	-0.074	0.566	**-0.291**	**0.021**	0.031	0.806
	Finland (n = 181)							
	Anti-C1q		C1q		Anti-FH		FH	
	Spearman r	p-value	Spearman r	p-value	Spearman r	p-value	Spearman r	p-value
Gestational age	-0.044	0.562	0.026	0.734	0.082	0.271	0.090	0.227
Proteinuria	-0.017	0.826	-0.069	0.360	0.008	0.911	**-0.157**	**0.037**
Highest diastole	-0.145	0.051	-0.073	0.330	**-0.198**	**0.007**	0.100	0.180
Fetal birthweight	-0.117	0.118	-0.023	0.756	0.005	0.948	0.135	0.071
BMI	-0.111	0.135	0.004	0.958	0.034	0.649	**0.288**	**8.57e-5**
	Norway (n = 45)							
	Anti-C1q		C1q		Anti-FH		FH	
	Spearman r	p-value	Spearman r	p-value	Spearman r	p-value	Spearman r	p-value
Gestational age	0.016	0.920	-0.125	0.412	0.042	0.785	**0.327**	**0.029**
Highest diastole	0.006	0.967	-0.155	0.311	-0.194	0.203	0.071	0.644
Fetal birthweight	0.061	0.691	-0.257	0.089	-0.025	0.873	0.250	0.098
BMI	0.025	0.877	0.306	0.052	0.008	0.961	**0.351**	**0.024**

P-values <0.05 are indicated in bold.

(32), however this is contradicted by our finding that there was no difference in C1q levels between PE patients and controls.

In a prospective study increased FH and C1q levels were reported in maternal plasma of later PE patients relative to controls at 6 to 13 weeks of pregnancy (33). However, these differences were not observed in the second and third trimesters. The current study investigated only third trimester samples and will therefore have missed differences in complement protein levels in the first trimester. However, the current study does find a difference in third trimester serum FH level, which was not observed in the previous study by He and colleagues.

The balance between complement activation and regulation is key in a healthy pregnancy, which is substantiated by findings that FH levels increase during pregnancy (32, 34). This conclusion is corroborated by our results where women with control pregnancies had higher serum FH concentration than nonpregnant women. Abnormalities in activating and regulating components of the alternative complement pathway have been reported in PE. Multiple investigations found increased levels of

TABLE 4 | Analysis of complement factors C1q, FH and autoantibodies in subgroups based on early onset of disease or presence of fetal growth restriction.

	The Netherlands		Finland		Norway	
	Early (n=50) vs late (n=13) onset PE	p-value	Early (n=36) vs late (n=145) onset PE	p-value	Early (n=33) vs late (n=12) onset PE	p-value
Anti-C1q	4.75 – 5.00	0.407	7.95 – 7.10	0.198	4.60 – 4.90	0.854
C1q	265 – 225	0.753	165 – 162.6	0.881	155 – 150	0.608
Anti-FH	56.7 – 37.3	0.122	35.2 – 35.2	0.194	35.2 – 35.2	0.392
FH	276 – 306	0.537	**322.5 – 354**	**0.019**	**306 – 381**	**0.001**
	The Netherlands		**Finland**		**Norway**	
	PE with (n = 17) vs without (n = 46) FGR	p-value	PE with (n = 84) vs without (n = 97) FGR	p-value	PE with (n = 33) vs without (n = 12) FGR	p-value
Anti-C1q	4.60 – 4.95	0.715	7.40 – 7.10	0.294	4.50 – 5.70	0.391
C1q	257 – 256	0.772	166.8 – 155.9	0.119	159 – 146	0.377
Anti-FH	**79.0 – 41.9**	**0.029**	35.2 – 35.2	0.369	35.2 – 35.2	0.253
FH	282 – 277	0.936	344.5 – 354	0.222	318 – 363	0.255

Medians of each groups are indicated, together with significance as determined with Mann-Whitney test. Early onset was defined as gestational age at delivery below 34 weeks; fetal growth restriction (FGR) was defined as gestational age-adjusted birthweight up to percentile 10 (of growth curve for respective country).
P-values <0.05 are indicated in bold.

activation fragment Bb in PE cases, indicating higher than normal alternative pathway activation (35, 36). Another study found increased Bb as well as decreased FH levels in PE patients, although this study was limited by relatively small samples size and a focus on only severe PE cases (32). Additionally, genetic variants in genes encoding the regulators Factor I and membrane cofactor protein, but not FH, were linked to PE (37). This trend of disbalance of the alternative pathway in PE is supported by our finding that FH concentration is decreased in PE patients. As the main fluid-phase complement regulator FH is conceivably of key importance in preventing or limiting C1q driven complement activation in the placenta. Aberrant FH levels or disturbed FH function would then result in the increased levels of complement activation as reported for PE.

Early onset PE cases showed lower FH concentration than late onset cases, implying that early onset cases were driving the lower FH concentration found in the general PE group compared to control pregnancies. This may also explain why FH concentration was not significantly lower in the cohort from Finland, as there were relatively fewer early onset cases in this cohort than in cohorts from the Netherlands and Norway. The larger variety in sampling timepoints in the Finnish cohort could also be involved. This study also investigated relations between the experimental data and relevant clinical parameters related to PE. No consistent significant correlations were found, indicating that within the PE pregnancies FH is not correlated with more severe disease. The observed correlation between BMI and FH is in line with earlier links found between FH and BMI (38, 39).

The strengths of the current analysis include the side-by-side comparison of three independent well-documented European cohorts, together comprising sizable numbers of cases and controls. In addition, all measurements were performed in the same lab with the same assays. Moreover, the current study also investigated correlations with several clinical parameters that could indicate severity of PE. The weaknesses of the study include the not completely identical sampling time points in the cohorts as samples in the Netherlands and Norway were collected on the day of delivery, while samples in Finland were mainly (74%) collected before the day of delivery, with an interval up to 31 days. Sample collection and processing may possibly have led to some *in vitro* complement activation. Importantly, such pre-analytical steps may impact on hemolytic activity of complement activity of samples or on complement activation fragments but does typically not impact on complement protein levels as measured by sandwich ELISA. If such effect may be present in a subset of the samples, then this is at least partially mitigated by the fact that samples for PE and controls were handled similarly. Furthermore, the focus on systemic levels in this investigation may not be fully representative of local effects in the placenta, leaving the question of cause and consequence in the etiology of PE open.

In conclusion, circulating levels of anti-FH and anti-C1q are not associated with the occurrence of PE. Circulating levels of C1q and FH are increased in healthy pregnancies as compared to nonpregnant controls. Importantly, circulating levels of FH are decreased in PE as compared to control pregnancy. Exactly how C1q is involved in the processes of placentation and pregnancy as a whole is still under investigation, but a key aspect appears to be that C1q is mediating its effect in the absence of clear complement activation (9). C1q deficiency is strongly associated with autoimmune disease SLE, as a result of insufficient cellular waste clearance (40). The increased C1q levels found during pregnancy could be a way to avoid accumulation of waste from placental remodeling. Upregulation of FH during healthy pregnancy could be a way to counteract excess complement activation, but FH has also been shown to promote a tolerogenic phenotype in dendritic cells, hinting at a noncanonical function for FH (41). Failure to increase FH level during pregnancy may therefore result in insufficient immune regulation contributing to development of PE. Further research will have to disclose what share of PE etiology can be ascribed to a disrupted equilibrium of complement activation and regulation.

DATA AVAILABILITY STATEMENT

The raw data supporting the conclusions of this article will be made available by the authors, without undue reservation.

ETHICS STATEMENT

Ethical approval for the three cohorts was obtained locally, from the Medical Research Ethics Committee of Leiden University Medical Center, the Coordinating Ethics Committee, Hospital District of Helsinki and Uusimaa or the Regional Committee for Medical Research Ethics Central Norway, respectively. The patients/participants provided their written informed consent to participate in this study.

THE FINNISH GENETICS OF PRE-ECLAMPSIA CONSORTIUM (FINNPEC) CORE INVESTIGATOR GROUP

The FINNPEC core investigator group consists of the following persons:

Hannele Laivuori, principal investigator

Seppo Heinonen

Obstetrics and Gynecology, University of Helsinki and Helsinki University Hospital, Helsinki, Finland

Eero Kajantie

PEDEGO Research Unit, Medical Research Center Oulu, Oulu University Hospital and University of Oulu, Oulu, Finland

Public Health Promotion Unit, National Institute for Health and Welfare, Helsinki and Oulu, Finland

Children's Hospital, University of Helsinki and Helsinki University Hospital, Helsinki, Finland

Department of Clinical and Molecular Medicine, Norwegian University of Health and Technology, Trondheim, Norway

Juha Kere

Department of Biosciences and Nutrition, Karolinska Institutet, Huddinge, Sweden

Folkhälsan Research Center and Stem Cells and Metabolism Research Program, University of Helsinki, Helsinki, Finland

Katja Kivinen

Institute for Molecular Medicine Finland, Helsinki Institute of Life Science, University of Helsinki, Helsinki, Finland

Anneli Pouta

Department of Government Services, National Institute for Health and Welfare, Helsinki, Finland

AUTHOR CONTRIBUTIONS

ME, M-LvdH, and LT designed the study. DD, NB, and CvdK performed the laboratory work. DD, AL, and LG analyzed the data. DD wrote the draft manuscript. All authors provided feedback to the manuscript and approved it.

FUNDING

LT has received funding from the European Research Council (ERC) under the European Union's Horizon 2020 research and innovation program (grant agreement No 724517).

REFERENCES

1. Lisonkova S, Joseph KS. Incidence of Preeclampsia: Risk Factors and Outcomes Associated With Early- Versus Late-Onset Disease. *Am J Obstet Gynecol* (2013) 209(6):544.e1–.e12. doi: 10.1016/j.ajog.2013.08.019
2. Redman CW, Sargent IL. Latest Advances in Understanding Preeclampsia. *Science* (2005) 308(5728):1592–4. doi: 10.1126/science.1111726
3. Steegers EA, von Dadelszen P, Duvekot JJ, Pijnenborg R. Pre-Eclampsia. *Lancet* (2010) 376(9741):631–44. doi: 10.1016/S0140-6736(10)60279-6
4. Walport MJ. Complement. First of Two Parts. *N Engl J Med* (2001) 344 (14):1058–66. doi: 10.1056/NEJM200104053441406
5. Ricklin D, Hajishengallis G, Yang K, Lambris JD. Complement: A Key System for Immune Surveillance and Homeostasis. *Nat Immunol* (2010) 11(9):785. doi: 10.1038/ni.1923
6. Nauta AJ, Trouw LA, Daha MR, Tijsma O, Nieuwland R, Schwaeble WJ, et al. Direct Binding of C1q to Apoptotic Cells and Cell Blebs Induces Complement Activation. *Eur J Immunol* (2002) 32(6):1726–36. doi: 10.1002/1521-4141(200206)32:6<1726::AID-IMMU1726>3.0.CO;2-R
7. Agostinis C, Bulla R, Tripodo C, Gismondi A, Stabile H, Bossi F, et al. An Alternative Role of C1q in Cell Migration and Tissue Remodeling: Contribution to Trophoblast Invasion and Placental Development. *J Immunol* (2010) 185(7):4420–9. doi: 10.4049/jimmunol.0903215
8. Singh J, Ahmed A, Girardi G. Role of Complement Component C1q in the Onset of Preeclampsia in Mice. *Hypertension* (2011) 58(4):716–24. doi: 10.1161/HYPERTENSIONAHA.111.175919
9. Agostinis C, Tedesco F, Bulla R. Alternative Functions of the Complement Protein C1q at Embryo Implantation Site. *J Reprod Immunol* (2017) 119:74–80. doi: 10.1016/j.jri.2016.09.001
10. van Schaarenburg RA, Magro-Checa C, Bakker JA, Teng YK, Bajema IM, Huizinga TW, et al. C1q Deficiency and Neuropsychiatric Systemic Lupus Erythematosus. *Front Immunol* (2016) 7:647. doi: 10.3389/fimmu.2016.00647
11. Trouw LA, Bengtsson AA, Gelderman KA, Dahlbäck B, Sturfelt G, Blom AM. C4b-Binding Protein and Factor H Compensate for the Loss of Membrane-Bound Complement Inhibitors to Protect Apoptotic Cells Against Excessive Complement Attack. *J Biol Chem* (2007) 282(39):28540–8. doi: 10.1074/jbc.M704354200
12. Lokki AI, Heikkinen-Eloranta J, Jarva H, Saisto T, Lokki ML, Laivuori H, et al. Complement Activation and Regulation in Preeclamptic Placenta. *Front Immunol* (2014) 5:312. doi: 10.3389/fimmu.2014.00312
13. Lokki AI, Heikkinen-Eloranta J. Pregnancy Induced TMA in Severe Preeclampsia Results From Complement-Mediated Thromboinflammation. *Hum Immunol* (2021) 82(5):371–8. doi: 10.1016/j.humimm.2021.03.006
14. Dragon-Durey MA, Blanc C, Marinozzi MC, van Schaarenburg RA, Trouw LA. Autoantibodies Against Complement Components and Functional Consequences. *Mol Immunol* (2013) 56(3):213–21. doi: 10.1016/j.molimm.2013.05.009
15. Seelen MA, Trouw LA, Daha MR. Diagnostic and Prognostic Significance of Anti-C1q Antibodies in Systemic Lupus Erythematosus. *Curr Opin Nephrol Hypertens* (2003) 12(6):619–24. doi: 10.1097/00041552-200311000-00008
16. Trouw LA, Groeneveld TW, Seelen MA, Duijs JM, Bajema IM, Prins FA, et al. Anti-C1q Autoantibodies Deposit in Glomeruli But Are Only Pathogenic in Combination With Glomerular C1q-Containing Immune Complexes. *J Clin Invest* (2004) 114(5):679–88. doi: 10.1172/JCI200421075
17. van de Bovenkamp FS, Dijkstra DJ, van Kooten C, Gelderman KA, Trouw LA. Circulating C1q Levels in Health and Disease, More Than Just a Biomarker. *Mol Immunol* (2021) 140:206–16. doi: 10.1016/j.molimm.2021.10.010
18. Foltyn Zadura A, Memon AA, Stojanovich L, Perricone C, Conti F, Valesini G, et al. Factor H Autoantibodies in Patients With Antiphospholipid Syndrome and Thrombosis. *J Rheumatol* (2015) 42(10):1786–93. doi: 10.3899/jrheum.150185
19. Blanc C, Togarsimalemath SK, Chauvet S, Le Quintrec M, Moulin B, Buchler M, et al. Anti-Factor H Autoantibodies in C3 Glomerulopathies and in Atypical Hemolytic Uremic Syndrome: One Target, Two Diseases. *J Immunol* (2015) 194(11):5129–38. doi: 10.4049/jimmunol.1402770
20. Vitkova H, Jiskra J, Springer D, Limanova Z, Telicka Z, Bartakova J, et al. Anti-C1q Autoantibodies Are Linked to Autoimmune Thyroid Disorders in Pregnant Women. *Clin Exp Immunol* (2016) 186(1):10–7. doi: 10.1111/cei.12813
21. Menzhinskaya IV, Van'ko LV, Kashentseva MM, Kiryushchenkov PA, Sukhikh GT. Incidence of Autoantibodies to C1Q Complement Component in Women With Miscarriages and Autoantibodies to Phospholipids and Chorionic Gonadotropin. *Bull Exp Biol Med* (2015) 160(2):260–3. doi: 10.1007/s10517-015-3144-x
22. Daponte A, Deligeoroglou E, Pournaras S, Hadjichristodoulou C, Garas A, Anastasiadou F, et al. Interleukin-15 (IL-15) and Anti-C1q Antibodies as Serum Biomarkers for Ectopic Pregnancy and Missed Abortion. *Clin Dev Immunol* (2013) 2013:637513. doi: 10.1155/2013/637513
23. Moroni G, Doria A, Giglio E, Imbasciati E, Tani C, Zen M, et al. Maternal Outcome in Pregnant Women With Lupus Nephritis. A Prospective Multicenter Study. *J Autoimmun* (2016) 74:194–200. doi: 10.1016/j.jaut.2016.06.012
24. Jääskeläinen T, Heinonen S, Kajantie E, Kere J, Kivinen K, Pouta A, et al. Cohort Profile: The Finnish Genetics of Pre-Eclampsia Consortium (FINNPEC). *BMJ Open* (2016) 6(11):e013148. doi: 10.1136/bmjopen-2016-013148
25. Lubbers R, Sutherland JS, Goletti D, de Paus RA, van Moorsel CHM, Veltkamp M, et al. Complement Component C1q as Serum Biomarker to Detect Active Tuberculosis. *Front Immunol* (2018) 9:2427. doi: 10.3389/fimmu.2018.02427
26. Yie SM, Taylor RN, Librach C. Low Plasma HLA-G Protein Concentrations in Early Gestation Indicate the Development of Preeclampsia Later in Pregnancy. *Am J Obstet Gynecol* (2005) 193(1):204–8. doi: 10.1016/j.ajog.2004.11.062
27. Hackmon R, Koifman A, Hyodo H, Glickman H, Sheiner E, Geraghty DE. Reduced Third-Trimester Levels of Soluble Human Leukocyte Antigen G Protein in Severe Preeclampsia. *Am J Obstet Gynecol* (2007) 197(3):255.e1–5. doi: 10.1016/j.ajog.2007.06.033
28. Marozio L, Garofalo A, Berchialla P, Tavella AM, Salton L, Cavallo F, et al. Low Expression of Soluble Human Leukocyte Antigen G in Early Gestation and Subsequent Placenta-Mediated Complications of Pregnancy. *J Obstet Gynaecol Res* (2017) 43(9):1391–6. doi: 10.1111/jog.13377
29. Ghaebi M, Nouri M, Ghasemzadeh A, Farzadi L, Jadidi-Niaragh F, Ahmadi M, et al. Immune Regulatory Network in Successful Pregnancy and

Reproductive Failures. *BioMed Pharmacother* (2017) 88:61–73. doi: 10.1016/j.biopha.2017.01.016
30. Wedenoja S, Yoshihara M, Teder H, Sariola H, Gissler M, Katayama S, et al. Fetal HLA-G Mediated Immune Tolerance and Interferon Response in Preeclampsia. *EBioMedicine* (2020) 59:102872. doi: 10.1016/j.ebiom.2020.102872
31. Benoit ME, Clarke EV, Morgado P, Fraser DA, Tenner AJ. Complement Protein C1q Directs Macrophage Polarization and Limits Inflammasome Activity During the Uptake of Apoptotic Cells. *J Immunol* (2012) 188 (11):5682–93. doi: 10.4049/jimmunol.1103760
32. Jia K, Ma L, Wu S, Yang W. Serum Levels of Complement Factors C1q, Bb, and H in Normal Pregnancy and Severe Pre-Eclampsia. *Med Sci Monit* (2019) 25:7087–93. doi: 10.12659/MSM.915777
33. He YD, Xu BN, Wang ML, Wang YQ, Yu F, Chen Q, et al. Dysregulation of Complement System During Pregnancy in Patients With Preeclampsia: A Prospective Study. *Mol Immunol* (2020) 122:69–79. doi: 10.1016/j.molimm.2020.03.021
34. Derzsy Z, Prohászka Z, Rigó JJr., Füst G, Molvarec A. Activation of the Complement System in Normal Pregnancy and Preeclampsia. *Mol Immunol* (2010) 47(7-8):1500–6. doi: 10.1016/j.molimm.2010.01.021
35. Hoffman MC, Rumer KK, Kramer A, Lynch AM, Winn VD. Maternal and Fetal Alternative Complement Pathway Activation in Early Severe Preeclampsia. *Am J Reprod Immunol* (2014) 71(1):55–60. doi: 10.1111/aji.12162
36. Lynch AM, Murphy JR, Byers T, Gibbs RS, Neville MC, Giclas PC, et al. Alternative Complement Pathway Activation Fragment Bb in Early Pregnancy as a Predictor of Preeclampsia. *Am J Obstet Gynecol* (2008) 198 (4):385.e1–9. doi: 10.1016/j.ajog.2007.10.793
37. Salmon JE, Heuser C, Triebwasser M, Liszewski MK, Kavanagh D, Roumenina L, et al. Mutations in Complement Regulatory Proteins Predispose to Preeclampsia: A Genetic Analysis of the PROMISSE Cohort. *PloS Med* (2011) 8(3):e1001013. doi: 10.1371/journal.pmed.1001013
38. Xin Y, Hertle E, van der Kallen CJH, Schalkwijk CG, Stehouwer CDA, van Greevenbroek MMJ. Longitudinal Associations of the Alternative and Terminal Pathways of Complement Activation With Adiposity: The CODAM Study. *Obes Res Clin Pract* (2018) 12(3):286–92. doi: 10.1016/j.orcp.2017.11.002
39. Moreno-Navarrete JM, Martínez-Barricarte R, Catalán V, Sabater M, Gómez-Ambrosi J, Ortega FJ, et al. Complement Factor H Is Expressed in Adipose Tissue in Association With Insulin Resistance. *Diabetes* (2010) 59(1):200–9. doi: 10.2337/db09-0700
40. Tsokos GC, Lo MS, Costa Reis P, Sullivan KE. New Insights Into the Immunopathogenesis of Systemic Lupus Erythematosus. *Nat Rev Rheumatol* (2016) 12(12):716–30. doi: 10.1038/nrrheum.2016.186
41. Olivar R, Luque A, Cárdenas-Brito S, Naranjo-Gómez M, Blom AM, Borràs FE, et al. The Complement Inhibitor Factor H Generates an Anti-Inflammatory and Tolerogenic State in Monocyte-Derived Dendritic Cells. *J Immunol* (2016) 196(10):4274–90. doi: 10.4049/jimmunol.1500455

Conflict of Interest: The authors declare that the research was conducted in the absence of any commercial or financial relationships that could be construed as a potential conflict of interest.

Publisher's Note: All claims expressed in this article are solely those of the authors and do not necessarily represent those of their affiliated organizations, or those of the publisher, the editors and the reviewers. Any product that may be evaluated in this article, or claim that may be made by its manufacturer, is not guaranteed or endorsed by the publisher.

Copyright © 2022 Dijkstra, Lokki, Gierman, Borggreven, van der Keur, Eikmans, Gelderman, Laivuori, The FINNPEC Core Investigator Group, Iversen, van der Hoorn and Trouw. This is an open-access article distributed under the terms of the Creative Commons Attribution License (CC BY). The use, distribution or reproduction in other forums is permitted, provided the original author(s) and the copyright owner(s) are credited and that the original publication in this journal is cited, in accordance with accepted academic practice. No use, distribution or reproduction is permitted which does not comply with these terms.

frontiers | Frontiers in Immunology

REVIEW
published: 12 April 2022
doi: 10.3389/fimmu.2022.860689

Ex Vivo Test for Measuring Complement Attack on Endothelial Cells: From Research to Bedside

Marie-Sophie Meuleman, Anna Duval, Véronique Fremeaux-Bacchi, Lubka T. Roumenina and Sophie Chauvet*

Centre de Recherche des Cordeliers, INSERM, Sorbonne Université, Université de Paris, Paris, France

As part of the innate immune system, the complement system plays a key role in defense against pathogens and in host cell homeostasis. This enzymatic cascade is rapidly triggered in the presence of activating surfaces. Physiologically, it is tightly regulated on host cells to avoid uncontrolled activation and self-damage. In cases of abnormal complement dysregulation/overactivation, the endothelium is one of the primary targets. Complement has gained momentum as a research interest in the last decade because its dysregulation has been implicated in the pathophysiology of many human diseases. Thus, it appears to be a promising candidate for therapeutic intervention. However, detecting abnormal complement activation is challenging. In many pathological conditions, complement activation occurs locally in tissues. Standard routine exploration of the plasma concentration of the complement components shows values in the normal range. The available tests to demonstrate such dysregulation with diagnostic, prognostic, and therapeutic implications are limited. There is a real need to develop tools to demonstrate the implications of complement in diseases and to explore the complex interplay between complement activation and regulation on human cells. The analysis of complement deposits on cultured endothelial cells incubated with pathologic human serum holds promise as a reference assay. This *ex vivo* assay most closely resembles the physiological context. It has been used to explore complement activation from sera of patients with atypical hemolytic uremic syndrome, malignant hypertension, elevated liver enzymes low platelet syndrome, sickle cell disease, pre-eclampsia, and others. In some cases, it is used to adjust the therapeutic regimen with a complement-blocking drug. Nevertheless, an international standard is lacking, and the mechanism by which complement is activated in this assay is not fully understood. Moreover, primary cell culture remains difficult to perform, which probably explains why no standardized or commercialized assay has been proposed. Here, we review the diseases for which endothelial assays have been applied. We also compare this test with others currently available to explore complement overactivation. Finally, we discuss the unanswered questions and challenges to overcome for validating the assays as a tool in routine clinical practice.

Keywords: complement, endothelial cells, diagnostics, prognostics, therapeutics, kidney injury, nephrology, explorations

OPEN ACCESS

Edited by:
Erik J. M. Toonen, Hycult Biotech, Netherlands

Reviewed by:
Jeffrey Laurence, Cornell University, United States
Daniel Ricklin, University of Basel, Switzerland

****Correspondence:***
Marie-Sophie Meuleman
marie-sophie.meuleman@inserm.fr

Specialty section:
This article was submitted to Molecular Innate Immunity, a section of the journal Frontiers in Immunology

Received: *23 January 2022*
Accepted: *21 March 2022*
Published: *12 April 2022*

Citation:
Meuleman M-S, Duval A, Fremeaux-Bacchi V, Roumenina LT and Chauvet S (2022) Ex Vivo Test for Measuring Complement Attack on Endothelial Cells: From Research to Bedside. Front. Immunol. 13:860689. doi: 10.3389/fimmu.2022.860689

INTRODUCTION

As part of the complex innate immune surveillance system, the complement system plays a key role in defense against pathogens and in host homeostasis. This enzymatic cascade is rapidly triggered in the presence of activating surfaces, such as bacteria or apoptotic necrotic cells. However, the cascade is highly physiologically regulated on host cells to avoid self-aggression. The endothelium is one of the primary targets of complement dysregulation. There is increasing evidence of complement implications in the pathophysiology of many human diseases. Many complement-blocking therapeutics are under development, and some are already available in clinical practice. Nevertheless, detection of abnormal functioning complement is challenging, because in many pathological conditions C3 and C4 plasma levels, the two main biomarkers of complement activation, remain within normal ranges. The available tests to demonstrate such overactivation with diagnostic, prognostic, and therapeutic implications are limited. Methods are poorly standardized, and only a few have functional value. Therefore, there is a need to develop a robust and standardized tool for identifying infraclinical complement activation.

The final objective is to allow better pathophysiologically based therapeutic management of patients. The analysis of complement deposits on cultured endothelial cells (EC) incubated with patient serum holds promise as a reference assay. This approach has been used to explore complement activation in the sera of patients with atypical hemolytic uremic syndrome (aHUS), malignant hypertension, hemolysis, elevated liver enzymes, and low platelet (HELLP) syndrome, sickle cell disease (SCD), and pre-eclampsia. In some cases, adjusting the complement-blocking drugs has been considered. Nevertheless, the international standard for this test is lacking, and the mechanism by which complement is activated in this assay is not fully understood.

After a brief summary of the complement cascade, we present the mechanisms of complement activation and how they contribute to cell damage in several human diseases. We then provide an overview of the tests currently available to explore complement overactivation in routine practice. Finally, through a comparative analysis of the available endothelial assays for complement exploration, we discuss the unanswered questions and challenges to overcome to validate the study of complement deposition on cultured EC as a tool in routine clinical practice.

THE COMPLEMENT SYSTEM IN HEALTH AND DISEASE

The complement system plays a key role in cell homeostasis, inflammation, and defense against pathogens. It is the first line of defense. The system comprises more than 30 soluble and membrane-bound proteins. Three different pathways lead to complement activation: the classical (CP), lectin (LP), and alternative (AP) pathways. When activated, these serine protease cascades converge to the formation of two enzymes, C3 convertase and C5 convertase, allowing the generation of the main effectors of this system: anaphylatoxins (C3a and C5a), opsonin (C3b/iC3b), and the membrane attack complex (MAC) (C5b-9). CP and LP are initiated by the recognition of pathogen-associated molecular patterns or damage-associated molecular patterns by pattern-recognition molecules (C1q and mannose-binding lectin). Conversely, AP is constantly activated at a low level in the fluid phase, generating a small quantity of C3b. In the presence of an activating surface (apopto-necrotic or bacterial), C3b covalently binds to the surface, and thus, initiates cell surface C3 convertase formation (C3bBb) and the AP amplification loop. To avoid self-aggression, AP is highly regulated in the fluid phase and on the host cell surface by soluble (factor H (FH), factor I (FI)) and membrane-bound regulators (membrane cofactor protein (MCP) or CD46, complement receptor 1 (CR1) or CD35, decay accelerating factor or CD55, and CD59). In humans, deficiencies in complement regulatory proteins are associated with rare diseases, such as aHUS, C3 glomerulopathy (C3G), and paroxysmal nocturnal hemoglobinuria (PNH). However, complement activation triggered by different pathophysiological processes that overwhelm the capacity of regulation has been increasingly described in a wide spectrum of diseases.

COMPLEMENT IMPLICATION IN DISEASES

While AP overactivation is the central mechanism of cell and tissue injury in complementopathies (aHUS, C3G, and PNH), complement is crucial to tissue injury in a wide variety of diseases. These include age-related macular degeneration (AMD), antibody-mediated rejection (ABMR), cryoglobulinemic vasculitis (CV), IgA nephropathy (IgAN), systemic lupus erythematosus (SLE), anti-phospholipid syndrome (APS), ANCA-associated vasculitis (AAV), rheumatoid arthritis (RA), HELLP syndrome, pre-eclampsia, myasthenia gravis (MG), neuromyelitis optica spectrum disorder (NMOSD), SCD, and rhabdomyolysis-induced acute kidney injury (RIAKI). To a lesser extent, complement seems to be involved in an increasing spectrum of human pathological conditions, such as inflammatory disorders, ischemia/reperfusion, cancer, degenerative disorders (e.g., Alzheimer's disease, atherosclerosis), and more recently, viral infections that include COVID-19 (1) (**Figure 1**).

Complementopathies are characterized by a specific cell target of AP-mediated damage. In aHUS and PNH, AP dysregulation occurs on the cell membrane, EC surface or platelets (2) and erythrocyte surface (3). In C3G, overactivation of C3 and C5 convertases may occur in the fluid phase or locally within the glomeruli, where the targeted surface remains to be determined (suggestions include glomerular EC and mesangial cells). AP dysregulation is a central pathophysiological mechanism in these diseases. It can be related to innate or acquired abnormalities in complement components, mainly regulators (FH, FI, or MCP) or C3 convertase components (C3 or FB) (4–15).

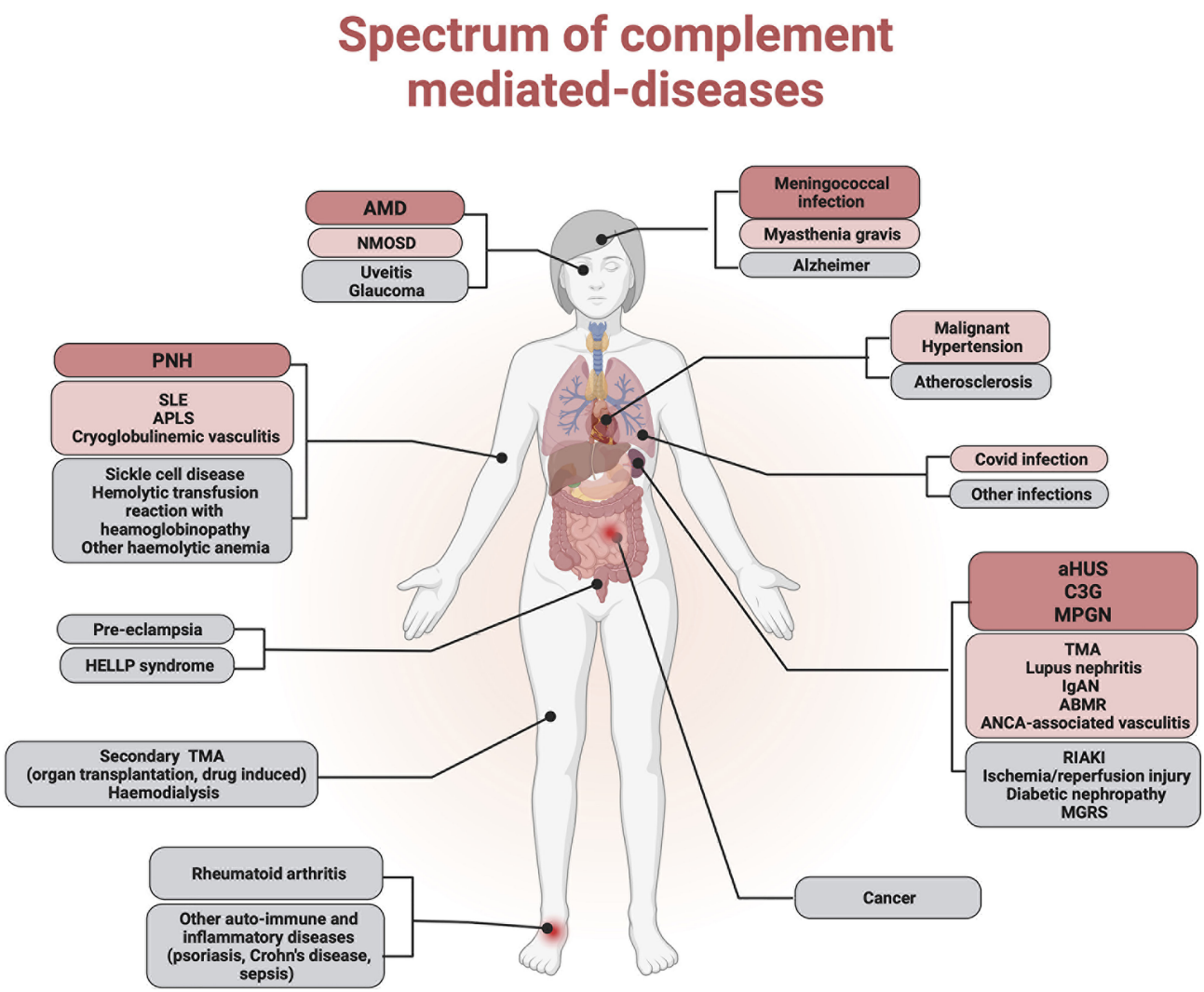

FIGURE 1 | Complement implication in human diseases. Complement dysregulation has been implicated in the pathophysiology of several human diseases. Complementopathies in which alternative pathway dysregulation is the central mechanism of cell and tissue injury are represented in red. Conditions in which the complement system has been demonstrated to contribute significantly to tissue injury are represented in pink. Other diseases in which complement plays an accessory role are represented in gray.

In diseases with major complement contributions, complement activation can be triggered by one or another pathway. In CV (16) and ABMR (17), activation occurs through CP in the presence of immune complexes (IC). In cryoglobulinemia (type II), IC are composed of IgM with rheumatoid factor activity associated with polyclonal IgG. In ABMR, IC are composed of IgG and donor HLA molecules. Conversely, despite the disease being triggered by the presence of IC, AP appears to be essential for disease development in mouse models of RA (18, 19) and SLE (20–22). This activation can be enhanced by apoptotic and necrotic cells due to prior damage (23) or by proteins of the extracellular matrix (ECM) from damaged cartilage in RA (24). In IgAN, AP (25), and LP (26) activation is mediated by polymeric IgA. *In vitro*, a correlation was found between C3 cleavage products (iC3b, C3c, C3dg) and IgA-A-IgG IC levels, suggesting that IC-containing IgA may act as a surface for soluble AP activation (27). In AAV, AP may be activated by neutrophil extracellular traps, thus amplifying complement activation and damage of EC (28). Finally, a disease-specific soluble factor has been implicated in complement activation. Free heme renders EC more sensitive to complement activation in SCD (29), aHUS (30), and RIAKI (31). *In vitro*, thrombin induces C5 cleavage in C5a in APS (32).

Complement activation does not arise from a unique mechanism but can be triggered in several ways according to the disease pathophysiology. Identification of the precise mechanisms of complement activation will help determine different potential therapeutic targets within the cascade.

Complement activation contributes to cell and tissue injuries in different ways. First, it promotes inflammatory cell

recruitment mainly in CV (33), ABMR (34), AMD (35), SLE (36) and RA. C5a and its receptor C5aR are involved in neutrophil recruitment (37–39) and endothelial activation (40) in AAV. Complement activation can promote specific disease processes. Thus, MAC can directly affect collagenase production by synovial fibroblasts in RA (41). In IgAN, mesangial cells exposed to complement activation and C3 deposition promote phenotypic conversion to a more synthetic and proliferative state (42). In AMD, C3a and C5a promote choroidal and C5a induces vascular endothelial growth factor secretion by retinal pigment epithelium (35). In pre-eclampsia, it has been suggested that the binding of C5a to C5aR expressed on trophoblasts contributes to the acquisition of their anti-angiogenic phenotype (43).

The complement system can also act as an amplifier for other molecules involved in injury. The C5a/C5aR axis participates in neutrophil recruitment and activation, which in turn can induce complement activation in AAV (38). C5a induces tissue factor expression by neutrophils, leading to factor X activation and thrombin generation, which in turn cleaves C5 into C5a in APS (32).

Ultimately, several triggers of complement activation and effectors may contribute to cell and tissue damage in heterogeneous human diseases. The identification of specific triggers of complement activation and fine pathophysiological mechanisms resulting in cell and tissue complement-mediated injury is needed to determine the best therapeutic target within the cascade. Complement inhibitor anti-C5 monoclonal antibody (eculizumab, and more recently its long-acting form, ravulizumab) is the gold standard in two complementopathies, aHUS and PNH, and has obtained Food and Drug Administration (FDA) approval for MG and NMOSD. Avacopan is a C5aR1 antagonist that has also been approved by the FDA for patients with AAV, another disease with a major complement contribution. Understanding the detailed mechanisms of complement activation and complement-mediated damage is necessary to guide the prescription of new complement inhibitors.

OVERVIEW OF THE TESTS EXPLORING COMPLEMENT ACTIVATION

Quantification of Complement Components

Currently available tests mainly consist in quantification of individual complement components or activation products.

- For the quantification of individual complement proteins in plasma, various types of immunoassays are used to determine the concentration of individual complement components. The most common is nephelometry. Polyclonal antibodies to component are added in excess of the sample and bind to their target. Quantification is performed by passing a light beam through the sample, which is distorted by the IC that have formed (44).
- Quantification of complement activation products corresponding to cleavage fragments or complement protein complexes (C3a, C3dg, C4a, C4d, Ba, Bb, C5a, C3bBbP, MASP2, and sC5b-9) is possible. Several assays have been described, mostly based on the recognition of a neoepitope of the complement component in an enzyme-linked immunosorbent assay (ELISA) format. Thus, C4a and C4d reflect CP/LP activation, Ba, Bb, and C3bBbP reflect AP activation, MASP2 is a key enzyme in LP activation (45) and increasing soluble C5b-9 reflects TP activation (46). C3a and C5a are common to the three activation pathways.
- Detection of auto-Abs (anti-FH, FB, C3b, C3bBb, and C1q) targeting complement proteins can be performed using ELISA (14).

Functional Assays

- Quantification of complement function is used to explore the activity of a pathway or the entire cascade.
  - In hemolytic assays, CP activation can be assessed by incubating patient sera with sheep erythrocytes coated with rabbit anti-sheep red blood cell antibodies (47). In this assay, termed the CH50 assay, C1q binds to immunoglobulins, initiates the formation of CP C3 convertase, and leads to MAC assembly and erythrocyte lysis. Hemoglobin release is determined to calculate the number of hemolytic sites per cell. Activation through AP can be assessed using rabbit or guinea pig erythrocytes, which are activators of human AP, incubated with patient serum added to ethylene glycol-bis (β-aminoethyl ether) (EGTA), which chelates Ca2+ and inhibits activation *via* CP and LP (48). This hemolytic assay is termed the AP50 assay.
  - Liposomes coated with an activator can be used in a similar manner to CH50 assays (49). The main difference is the readout, which consists of the unquenching of a fluorescent dye and not the lysis of erythrocytes.
  - Assays based on ELISA method can also be used to explore the function of the three pathways. Microtiter plate wells are coated with recognition structures specific to each pathway (IgM for CP, mannan or acetylated bovine serum albumin for LP, and LPS for AP). Patient serum is added and incubated under conditions in which only one pathway is operative at any given time; the other two pathways are blocked. Finally, activation capacity is detected through the formation of the C5b-9 complex by monoclonal antibodies targeting a neo-epitope in complex-bound C9 (50).
- Different hemolytic assays have been developed to explore specific steps of the AP.
  - Sanchez-Corral et al. (51) developed a hemolytic assay to study FH functional defects in aHUS. The assay relies on the knowledge that sheep erythrocytes are highly sialylated and favor FH binding, whereas their membrane complement regulators are incompatible with human complement proteins. Therefore, they are protected from complement lysis due to the binding of human FH to their surface. In the assay, sheep erythrocytes are incubated with human plasma in Mg-EGTA buffer, allowing activation of AP only.

Normal plasma does not induce lysis, whereas aHUS plasma with FH functional defects (mutations or autoantibodies) induces lysis under these conditions (51).

- Hemolytic assays can also be used to study the stabilization of cell-bound AP convertases (52). This assay has been used to detect C3Nef in C3G cells. Sheep erythrocytes bearing C3 convertase C3bBb (generated by exposure of sheep erythrocytes bearing C3b to FB and FD) were incubated with patient IgG. C3Nef activity correlates with residual C3bBb hemolytic sites, and lysis is developed by the addition of rat serum.
- Staining of tissue sections for the deposition of complement activation products can provide information about local complement activation in tissue. This can be performed by immunohistochemistry or immunofluorescence (53). For example, this technique has been used to study C5b-9 deposition in the skin of patients with aHUS (54).

These tests allow only the characterization of a specific molecule or step of the complement cascade. To reproduce human pathological conditions and their complexity, several authors have proposed the use of an *ex vivo* endothelial assay. The assay detects and quantifies complement component deposition on the EC surface after incubation with human serum. The EC surface is used as the regulating surface. The objective is to detect abnormal complement deposition that could result from either complement overactivation exceeding the capacity of regulation, or from a defect in complement regulation in fluid or on the EC surface. The *ex vivo* endothelial assay is presented in **Figure 2**.

We next discuss the advantages and limits of this functional approach.

STUDY OF COMPLEMENT DEPOSITION ON CULTURED ENDOTHELIAL CELLS

Heterogeneity of Endothelial Cells Populations and Their Complement Regulation

EC line blood vessels and constitute an active regulatory organ that has been implicated in vascular homeostasis, permeability regulation, vasomotor tone, angiogenesis, and diapedesis of immune cells (55). As first barrier between the blood and interstitium it is in constant equilibrium with the environment. Thus, heterogeneity in the structure and function of EC is a core property of the endothelium, allowing diverse vascular functions and regional specificity (56, 57). This diversity can be partially explained by a distinct transcriptional profile (58) in relation to neighboring cells (59). Hence, EC from different blood vessels have distinct and dynamic expression profiles of complement components and regulators, which may explain the different susceptibility and specific organ tropism observed in some complement-mediated diseases (60).

At a steady state, EC can produce most complement components and express high levels of complement regulators on their membranes (**Table S1**). Under inflammatory conditions, complement component production and regulatory protein expression are modified (**Table 1**). In addition to the steady state, the modulation of complement protein expression under inflammatory conditions differs according to the EC type and probably contributes to a specific damage mediated by AP and the different organ tropisms observed in complement-mediated diseases. Sartain et al. demonstrated that resting or tumor necrosis factor (TNF)-stimulated brain microvascular EC expressed higher levels of regulatory molecules (FH, FI, CD46, CD55, and THBD), generated lower levels of C3a and C4a, and enhanced lower degree AP activation (measured by lower Ba generation) than human renal glomerular EC (HRGEC) (61). The authors also demonstrated a slight increase in CD46 expression, decrease in thrombomoduline (TM), and increase in C3 and FB transcription in HRGEC exposed to TNF (62). These results agree with the prior demonstrations of an increase in C3 and FB production by human umbilical vein EC (HUVEC) exposed to TNF (63), increased FH transcription and production by HUVEC exposed to interferon (INF) gamma (64), increased C2, FH, FB, and C1inh transcription, and decreased C3 production by HUVEC exposed to INF gamma (65). May et al. compared the properties of four EC types (HRGEC, glomerular EC (GEnC), human microvascular EC (HMEC), and HUVEC) in the resting state and after overnight exposure to heme (66). While there was no difference in expression of regulatory factors (MCP, CD55, TM) at resting state, after overnight heme exposure, C3 deposits on glomerular EC were greater than on other EC. This was associated with, and possibly explained by, weaker FH binding and TM upregulation and lower upregulation of heme-oxygenase 1 (cytoprotective heme-degrading enzyme) compared to HUVEC. Moreover, HUVEC, but not EC, of glomerular origin were protected from complement deposition after re-challenge with heme (**Table S2**).

EC used for *ex vivo* experiments comprise two types: conditionally immortalized EC (CI-EC) and primary EC (**Table 2**). Primary EC can be difficult to isolate and maintain in culture, and have a limited lifespan. Moreover, differences in the genetic background of individual donors can lead to interexperimental variability. In particular, inter-individual heterogeneity in complement regulator expression at the EC surface cannot be excluded. CI-EC has been developed to overcome these difficulties. HMEC-1 and CI-GEnC are HMEC and GEnCs, respectively, that have been transfected with SV40 large T antigen (67, 68). EA.hy926 cells were obtained by fusing HUVEC with A549 cells obtained from human lung carcinoma (69). The EA.hy926 cells were used to generate glycosylphosphatidylinositol-anchored complement regulatory protein-deficient cells when treated with phosphatidylinositol-specific phospholipase C. These cells have been used along with the PIGA-mutant TF-1 to study complement deposits by confocal microscopy and flow cytometry after incubation with serum from patients with thrombotic microangiopathy (TMA), this test was called the modified Ham test (70). After incubation with serum from aHUS patients, cell surface C5b-9 deposits were reportedly higher than after incubation with thrombotic thrombocytopenic purpura (TTP) serum.

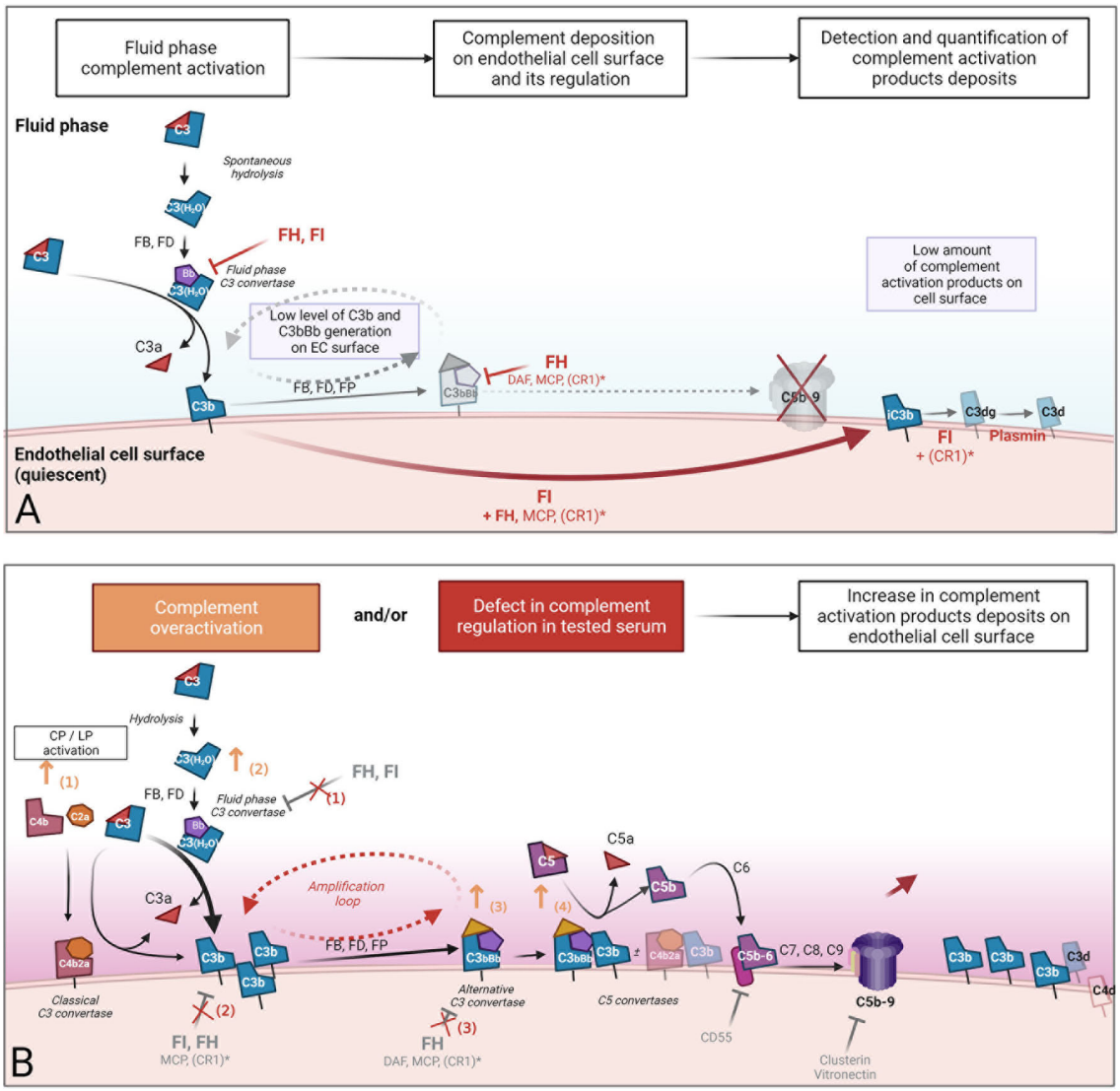

FIGURE 2 | Concept of *ex vivo* complement deposition on endothelial cells. An *ex vivo* endothelial assay was developed to reproduce human pathological conditions and their complexity. The assay consists of the detection and quantification of complement component deposition on the cultured endothelial cells (EC) surface after incubation with human serum. The EC surface was used as the regulatory surface. **(A)** In serum from healthy individuals, the alternative pathway is active at low levels but tightly regulated in the fluid phase by regulators, resulting in a very low level of complement activation product deposition on the EC surface. The detection of an increased complement deposition when incubation is performed with pathological serum **(B)** could result in either i) complement overactivation that overwhelms EC capacity of regulation (orange) or ii) defect in complement regulation in fluid or solid phase. Both are induced by tested human serum incubated with EC. Orange arrows represent some mechanisms involved in complement overactivation in serum (1): the participation of a coactivation of classical/alternative pathway due to pathological immunoglobins, immune complexes, or lectin pathway activation by polymeric IgA in IgA nephropathy (2), an increase in the formation of fluid phase C3 convertases in the presence of heme or fluid phase activating surface, and the stabilization of C3 (3) or C5 (4) convertases by pathological immunoglobulins, such as C3 and C5 nephritic factors. Red crosses represent potential defects in alternative complement pathway regulation in the fluid phase (1) and on the cell surface (2, 3). These defects in complement regulation could be the consequence of inhibition of the main alternative pathway regulator FH due to anti-factor H antibodies (such as in aHUS), a lack of function, or a quantitative deficiency of FH and FI due to pathological genetic variants. *CR1: weak expression of CR1 on endothelial cells. CR1, complement receptor 1 (CD35); FB, factor B; FD, factor D; FH, factor H; FI, factor I; FP, properdin; MCP, membrane cofactor protein.

Therefore, this test has been considered a tool to distinguish aHUS from TTP. It is important to note that sC5b-9, reflecting terminal pathway activation and regulation, is elevated under both aHUS and TTP plasma conditions (71, 72). One possibility is that both conditions are associated with complement activation. However, in aHUS, complement overactivation exceeds alternative and terminal pathway regulation, leading to C5b-9 deposits. In contrast, in TTP, complement activation is counterbalanced by complement regulation, leading to sC5b-9 release, but not C5b-9 deposits in the modified Ham test.

TABLE 1 | Production of distinct complement components and expression of regulators according to endothelial cell type after stimulation.

		TNF	INF gamma	IL1 beta	Heme
HRGEC	C3	↑	↑	→*	
	C4	→*	↑	→*	
	C5	→*		→*	
	FB	↑		→*	
	FD	→*		→*	
	Properdin	↓*		→*	
	FH	→		→*	
	FI			→*	
	TM	↓		↑	
	CD46	↑		→	↓
	CD55	→		→	↓
	CD59	→		→	
	E-selectine	↑	→		
	C3aR	↑			
	C5aR				
BMVEC	C3	↑			
	C4	→*			
	C5	→*			
	FB	↑			
	FD	→*			
	Properdin	↓*			
	FH	→			
	CD46	↑			
	CD55	→			
	C3aR	↑			
	C5aR				
HMEC	E-selectine	↑	→		
	C3		→		
	C4		↑		
	CD46				↓
	CD55				→
HUVEC	C2		↑		
	C3	↑	→/↓	↑	
	C4			→*	
	C5			→*	
	FB	↑	↑	↑*	
	FD			→*	
	Properdin			→*	
	FH		↑	↓	
	FI			→*	
	TM	↓		→	
	CD46	↑		→	↓
	CD55	↑		↑	↓
	CD59	→		→	→
	E-selectin	↑	→		
	P-selectin				↑
	C1-inh		↑		

The data presented here are mainly concerned with protein expression.
↑, increase in protein production; ↓, decrease and →, no change.
Denotes transcriptomic data. For details, please refer to **Table S2. BMVEC, brain microvascular endothelial cells; HMEC, human microvascular endothelial cells; HRGEC, human renal glomerular endothelial cells; HUVEC, human umbilical vein endothelial cells.*

Micro- or macrovascular origin of the EC tissue lineages also needs to be considered. Complement-mediated EC injury demonstrates specific cell tropism according to pathophysiological processes. In HUS and TTP, microvascular EC of dermal, renal, and cerebral origin are more sensitive to apoptosis, whereas microvascular EC of pulmonary and hepatic origin and macrovascular EC are resistant (73). Distinct sensitivity of EC to complement attack has also been explored in aHUS and heme exposure. The demonstration of a distinct EC response in terms of complement regulator expression after a trigger (here heme) was proposed to partially explain the kidney tropism in this disease (66).

HUVEC are primary macrovascular EC isolated from human umbilical cords. These are the most frequently used cells for *ex vivo* assays (74). If tissue specificity is required, HRGEC (75) or GEnCs (76), which are both isolated from human glomeruli, can be used. More recently, the use of blood outgrowth EC obtained from the differentiation of circulating marrow-derived endothelial progenitor cells isolated from peripheral blood has been proposed (77).

Comparative Analysis of the Available Endothelial Assays

These tests consist of the quantification of complement activation products (C3 activation fragments and C5b-9) deposits on EC by immunofluorescence (IF) measured by confocal microscopy or flow cytometry (fluorescence-activated cell sorting, FACS) after incubation with a serum sample of interest. Different protocols have been proposed to study complement activation on the EC surface in several pathological conditions, including aHUS (30, 78–88), TMA of other etiologies (89, 90), HELLP syndrome and pre-eclampsia (91), C3G (14, 92), lupus nephritis (LN) (93, 94), APS (95, 96), SCD (29), hemolytic anemia (97) and hyperhemolytic transfusion reaction without hemoglobinopathy (98).

The general procedure of the *ex vivo* assay and the different protocols are presented in **Figure 3**.

To Pre-Activate or Not Pre-Activate EC?

Resting EC or EC pre-activated by cytokines, ADP, or heme can be used (**Table S3**) to provide additional information.

When resting HUVEC were incubated with aHUS FB mutants added to FB-depleted normal human serum (NHS), enhanced C3b/iC3b-fragment deposition as measured by an anti-C3c-reacting antibody was observed (78). The same result was obtained for some cases when aHUS patient serum was incubated with resting HUVEC (30, 79). Nevertheless, incubation with NHS depleted in FB and reconstituted with other aHUS FB variants (80) or incubation with aHUS serum from patients carrying some C3 or FH variants (30, 79) may be insufficient to induce C3 or C5b-9 deposits. When quiescent HMEC-1 were incubated with aHUS serum from patients carrying mutations in FH, FI, C3, or FH/CFHR1 hybrid, enhanced C3c or C5b-9 deposition was reported only if serum was collected during the acute phases of the disease and not after reaching remission (82, 89). Furthermore, deposits on quiescent HMEC-1 are better correlated with relapse risk during the tapering or discontinuation of eculizumab (85).

TABLE 2 | Endothelial cells used for *ex vivo* experiments.

	Conditionally immortalized	Primary
Macrovascular		HUVEC
Microvascular	CI-GEnC	BMVEC
	HMEC-1	HRGEC
		BOEC

BMVEC, brain microvascular endothelial cells; BOEC, blood outgrowth endothelial cells; CI-GEnC, conditionally immortalized human glomerular endothelial cells; HMEC, human microvascular endothelial cells; HRGEC, human renal glomerular endothelial cells; HUVEC, human umbilical vein endothelial cells.

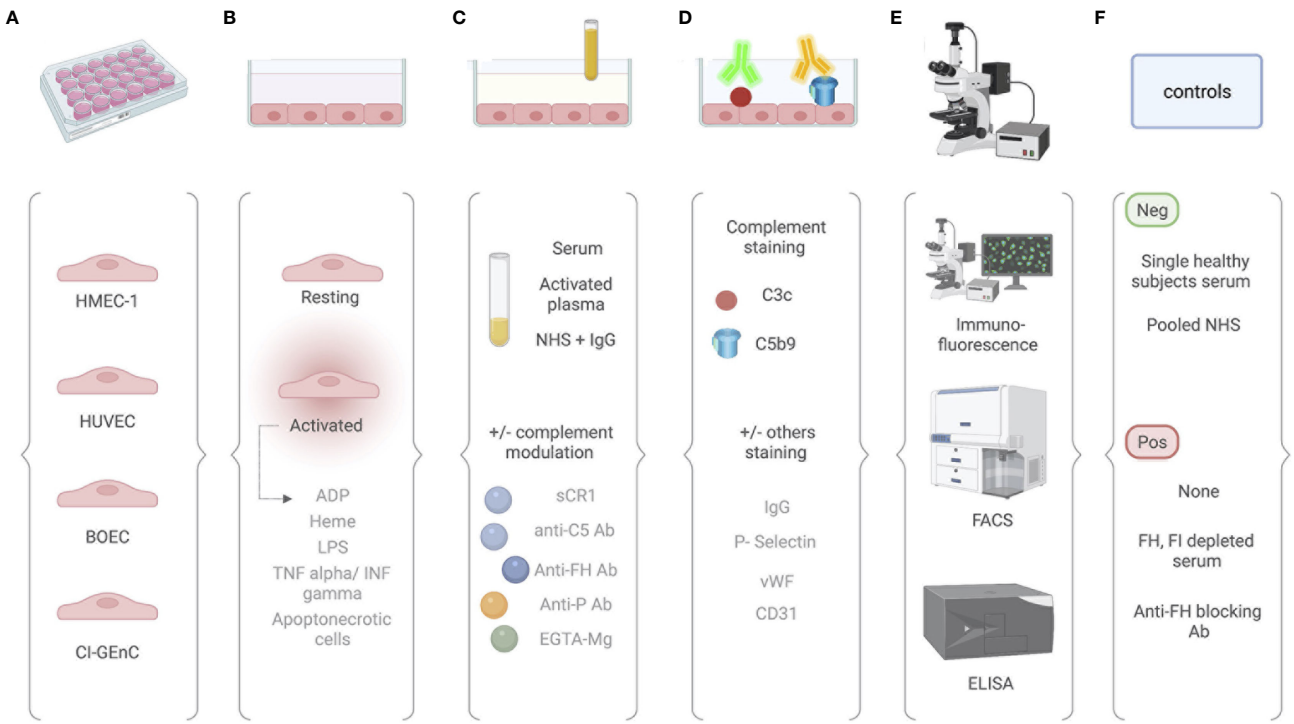

FIGURE 3 | Comparative analysis of different protocols used for the *ex vivo* complement activation test with endothelial cells. **(A)** The *ex vivo* test for measuring complement attack on endothelial cells can be performed on different endothelial cells, including human dermal microvascular endothelial cells (HMEC-1), human umbilical vein endothelial cells (HUVEC), blood outgrowth endothelial cells (BOEC), and glomerular endothelial cells (GEnC). **(B)** Cultured EC are then used at their resting state or after an activation by either ADP, heme, LPS, TNF/INF gamma, or apoptonecrotic cells. **(C)** EC are incubated with sample of interest. Either serum or activated plasma (consisting of patient citrated plasma mixed 1:1 with control serum pool) or normal human serum with addition of the protein of interest (e.g., IgG). Complement activation can be modulated in by addition of sCR1, anti-C5 antibody, anti-FH antibody, anti-properdin antibody, or EGTA-Mg buffer. **(D)** Complement activation products are then revealed by fluorescent tagged antibody. Antibody directed again C3c or C5b9 can be used. According to the context, staining for other molecules have been proposed and include IgG, P-selectin, vWF, and CD31. **(E)** Quantification is then performed using immunofluorescence scanning, flow cytometry, or ELISA. **(F)** Controls are required and vary according to the protocols.

To increase test sensitivity, the authors proposed pre-activating EC. Modifications in surface-bound protein expression enable complement activation. This was achieved in the case of P-selectin expression on HMEC-1 pre-activated with ADP, LPS, or thrombin (82) or P-selectin expression on HUVEC or GEnC pre-activated with heme (30, 80, 99), which could allow C3b binding and C3 convertase formation. Enhanced formation of C3 fragments by TNF/IFN pre-activation and C5b-9 deposition by ADP pre-activation on HUVEC or HMEC-1 cells was described after incubation of these cells with serum from asymptomatic carriers of mutations in AP regulatory proteins or C3 (79, 82). The normal range was established when pre-activated EC were incubated with sera from healthy donors. In addition, serum from healthy family members without the mutation was within the normal range in this assay (79).

What Kind of Blood Samples Might Be Incubated With EC?

Serum has been used as the source of complement proteins in the vast majority of the tests described above. One limitation of these tests, particularly when deposits are detected by IF, is the variation in the results, reportedly from 30% to 52% when

activated HMEC-1 were incubated with serum collected at the acute phase of aHUS (91). To reduce this variation, Palomo et al. proposed the use of activated plasma, which refers to citrated plasma mixed 1:1 with a control serum pool. Using this approach, the authors derived a coefficient of variation of 9% to 18% (91). C3 consumption by the patient or loss of C3 activity during the pre-analytical phase are also potential factors responsible for this variation (4). Finally, for all complement assays and to avoid *in vitro* complement activation, proper blood collection and processing must be achieved (100). Processing of plasma or serum sample must be performed within a few hours of collection, with storage at −80°C and defrosting immediately before use to avoid repeated freezing and thawing.

To explore the functional consequences of autoantibodies against C3 and properdin in SLE, Vasilev et al. and Radanova et al. incubated HUVEC with NHS supplemented with purified IgG from patients positive for such autoantibodies (93, 94). Using this strategy, complement deposition on EC can be directly ascribed to the addition of autoantibodies to NHS. The same approach was applied for anti-C3b/FB autoantibodies in patients with C3G (14). To understand the mechanism behind complement deposits on EC from patients with SCD, microvesicles from normal or patient-derived erythrocytes were added to normal serum to model the disease condition. Enhanced binding of the C3 activation products was demonstrated (29, 101).

Which Controls Are Relevant?

Most often, NHS is used as a negative control (14, 29, 30, 78–83) (**Table S4**). An important aspect to consider is the inter-individual variability in deposits induced by normal sera. FACS analysis has revealed that this variability was relatively low when sera from 50 healthy donors were tested (79). However, this is a concern, particularly when deposits are detected by IF. This has not been directly reported, but has been suggested by the use of pooled sera in more recent papers (85, 91) and our own experience. Aiello et al. reported that C3 and C5b-9 deposits obtained after a single healthy subject serum (N=12) incubation range from 0.5 to 1.5 fold increase of stained surface area compared to pooled serum (from 10 healthy donors) run in parallel (87).

Several authors did not use any positive controls for their experiments (82, 83, 85, 90, 91). The comparison was only made with the deposits obtained with negative controls. It might be interesting to position the results on a scale. Positive controls with published data are FH or FI depleted NHS (14, 79, 81) or normal serum supplemented with blocking anti-FH antibodies targeting the N-terminus or C-terminus (30, 80) or with FH19-20, corresponding to the two last domains of FH, able to compete with the full FH protein for cell surface binding (97).

The main issues with this type of assay are the lack of validated international standards as well as standardized positive and negative controls. The variability of the results in samples from healthy donors needs to be studied extensively to determine the appropriate cutoff. In addition, the impact of C3 or other complement protein consumption in the patient and the influence of the pre-analytical phase must be determined to avoid false positive and false negative results.

Which Deposits Should Be Measured?

The objective of these tests is to demonstrate and explore complement overactivation or dysregulation on the EC surface after incubation with blood samples of interest. This is enabled by quantification of the deposition of complement component products resulting from activation or regulation. C3c (a common epitope to C3, C3(H2O), C3b, and iC3b) (which reflects C3 convertase activity and the early phase of the complement cascade) can be detected by polyclonal anti-C3c antibody. Antibody targeting C5b-9 reveals the final step of the cascade. When a signal is detected on the cell membrane, it can be assumed that the detected fragment is C3b or iC3b covalently attached to the surface. Nevertheless, heme-activated EC and likely ADP-activated EC (102, 103) express P-selectin, which recruits C3b, C3(H2O), and a C3(H2O)-like form of C3 generated after contact with heme (30, 99). Properdin also binds to heme-exposed or stressed EC, promoting complement activation in a similar manner without covalent C3b binding (97). This is an additional mechanism for amplification of complement activation on the EC surface. C5b-9 deposits may be more relevant in identifying dysregulation at any step. Nevertheless, early dysregulation can induce C3 activation fragment deposits without C5b-9 formation because of TP regulation. C5b-9 is readily detectable by IF but is much more difficult to detect by FACS because of the weak shifts of the peaks. To test for CP participation, the presence of C4d-positive deposits was also investigated (82, 89). Staining can also be performed under the same conditions for von Willebrand Factor, C5aR1, P-selectin, and others (87).

Evaluation of Activated Pathways

The test can be modified to assess which complement pathway is activated in given pathological settings. The test can be performed under different conditions to avoid CP and LP contributions, which include C2 (30) or C1q (104) depleted NHS, addition of SCR1 (87) or Mg-EGTA buffer (30, 78, 93, 94). EGTA chelates Ca2+, which is crucial for CP and LP activation, whereas AP depends on Mg2+. If AP has to be inhibited, FB-depleted NHS can be used. These reagents are applicable for test conditions, where the activating factor is added externally to the serum (i.e., IgG, heme, microvesicles, etc.). When patient samples are used directly, the same effect can be achieved by inhibiting C1q, C4, FB, or properdin with blocking antibodies, protein constructs, or small molecules, if available (97). Quantification of complement activation products (split fragments generated by cleavage of complement components or protein complexes when activated components bind their target (i.e., C3a, C4a, Ba, Bb, C5a, and sC5b-9) in the supernatant might be an additional element to study complement cascade activation.

Which Techniques Are Used for Detection and Quantification?

The two main detection techniques commonly used are FACS and IF. HUVEC pre-activated with heme and then incubated with NHS or aHUS serum showed results similar by FACS or IF detection (30). IF directly analyzes deposits on EC grown on slides. FACS requires a cell detachment step before staining, with

the potential risk of losing a part of the deposit signal. In contrast, as mentioned by Gavriilaki et al., obtaining quantitative data by IF requires confocal microscopy and further analysis using specialized software (70). When IF is used, the area occupied by fluorescent staining in fields systematically digitized along the surface is quantified. The quantified results expressed as the mean of the square number of pixels per field are compared with the negative control (82, 83, 85, 89, 91). Considering the number of EC on which fluorescence has been measured and the staining intensity might appear relevant. In contrast, FACS allows the rapid and objective quantification of deposits.

What Are the Functional Consequences of Such Deposits?

If enhancement of complement fragment deposits on EC is interpreted as pathogenic, the functional consequences of such deposits must be questioned. Lactate dehydrogenase release from EC reflects cell damage. This release can be measured in the cell culture supernatant (104). Analysis of complement deposits can also be associated with a cell viability assay, corresponding to a colorimetric assay based on cleavage of the WST-1 tetrazolium salt by mitochondrial dehydrogenases in viable cells (70). Cellular integrity can be verified by May-Grunwald Giemsa staining (88). Direct cell death rarely occurs under these experimental conditions. Experiments testing cell activation status by complement overactivation have not been reported in the literature and are needed to further understand the impact of complement on endothelial injury. Analysis of transcriptomic modifications in EC exposed to complement deposits under several conditions could also be of interest.

Clinical and Therapeutic Relevance of the Obtained Results

The *ex vivo* EC assay, consisting in the quantification of complement activation products (C3 activation fragments or C5b-9) deposits on EC (by IF measured on confocal microscopy or FACS), after incubation with a serum sample of interest, was first used for specific characterization of complement component abnormalities (78–81, 83) or exploration of mechanisms implicated in EC injury (30) in the main complementopathy, aHUS. The assay was then used to demonstrate and explore complement activation and participation in the pathophysiology of several diseases, including C3G (14, 92), HELLP syndrome and pre-eclampsia (91, 105), TMA associated with severe hypertension (89, 106), drug-induced TMA (90), SCD (29), hemolytic anemia (97, 98), SLE (93, 94), and APS (96). Demonstration of increasing complement deposits on EC incubated with pathological sera is not sufficient to determine what is responsible for complement activation at the EC surface. Modulation of the test conditions can help in detailing complement activation. This was the case when complement activation was inhibited by the addition of hemopexin to the sera of patients with SCD (29).

Noris et al. and Galbusera et al. also proposed the use of this *ex vivo* EC test to monitor eculizumab therapy in patients with aHUS (82, 85). During eculizumab tapering or discontinuation, disease relapse preceded or was associated with an increase in C5b-9 deposits on resting HMEC-1 in all patients. In contrast, only one patient without relapse showed increased deposits (85). In clinical practice, CH50 is the only routine test used to monitor eculizumab therapy. CH50 is reportedly strongly suppressed in patients receiving eculizumab according to the standard protocol. However, CH50 does not allow monitoring of eculizumab dosage tapering or discontinuation, as it is not well correlated with relapse risk (82, 85). Eculizumab therapy monitoring using the Wieslab® complement system screen (107) or the modified Ham test (108) has also been proposed. Thus, the *ex vivo* EC assay could represent a test of interest to a better personalized complement-blocking therapy, but first needs to be more standardized.

This test can also be used to better classify and assess the prognosis of specific diseases. This is the case for hypertensive TMA, as Timmermans et al. demonstrated in a cohort of hypertension emergencies associated with TMA (106). The authors demonstrated a statistical association between increased C5b-9 deposition in the EC *ex vivo* test and kidney survival. Moreover, they reported an improvement in renal function for those with increased deposits treated with eculizumab. The authors proposed a classification of TMA-hypertensive emergency based on the EC *ex vivo* test (106).

Finally, many new anti-complement drugs targeting specific steps of the cascade have been under development in recent years (109). A standardized and validated assay to study complement activation could be a useful tool in their development.

DISCUSSION AND CONCLUSION

The increasing demonstration of complement involvement in the pathophysiology of many human diseases has mandated the development of tools to finely explore complement activation. Complement is a complex enzymatic cascade that is highly regulated in constant interplay with its environment. The current arsenal for complement exploration does not provide functional characterization and does not report on the complex interplay between complement and its environment, particularly the cell surface.

The development of tests with these capabilities could allow for a deeper exploration of the mechanisms of complement activation in several diseases. This information could inform the development of a complement blocking therapeutic strategy based on pathophysiological mechanisms.

Ex vivo complement activation on EC represents a promising tool for demonstrating and exploring complement activation (**Figure 4**). It not only recapitulates complex complement cascade regulation *in vivo*, but also allows modification of several steps of the experimental procedure to characterize complement activation mechanisms.

However, there are still unanswered questions hindering broad used. The first is the variability in the results and the inter-individual variability in deposits induced by normal sera. Comprehension of the precise mechanism responsible for complement deposition in this assay would improve its better use. The second issue is to standardize the main steps of the procedure to improve the interexperimental comparison.

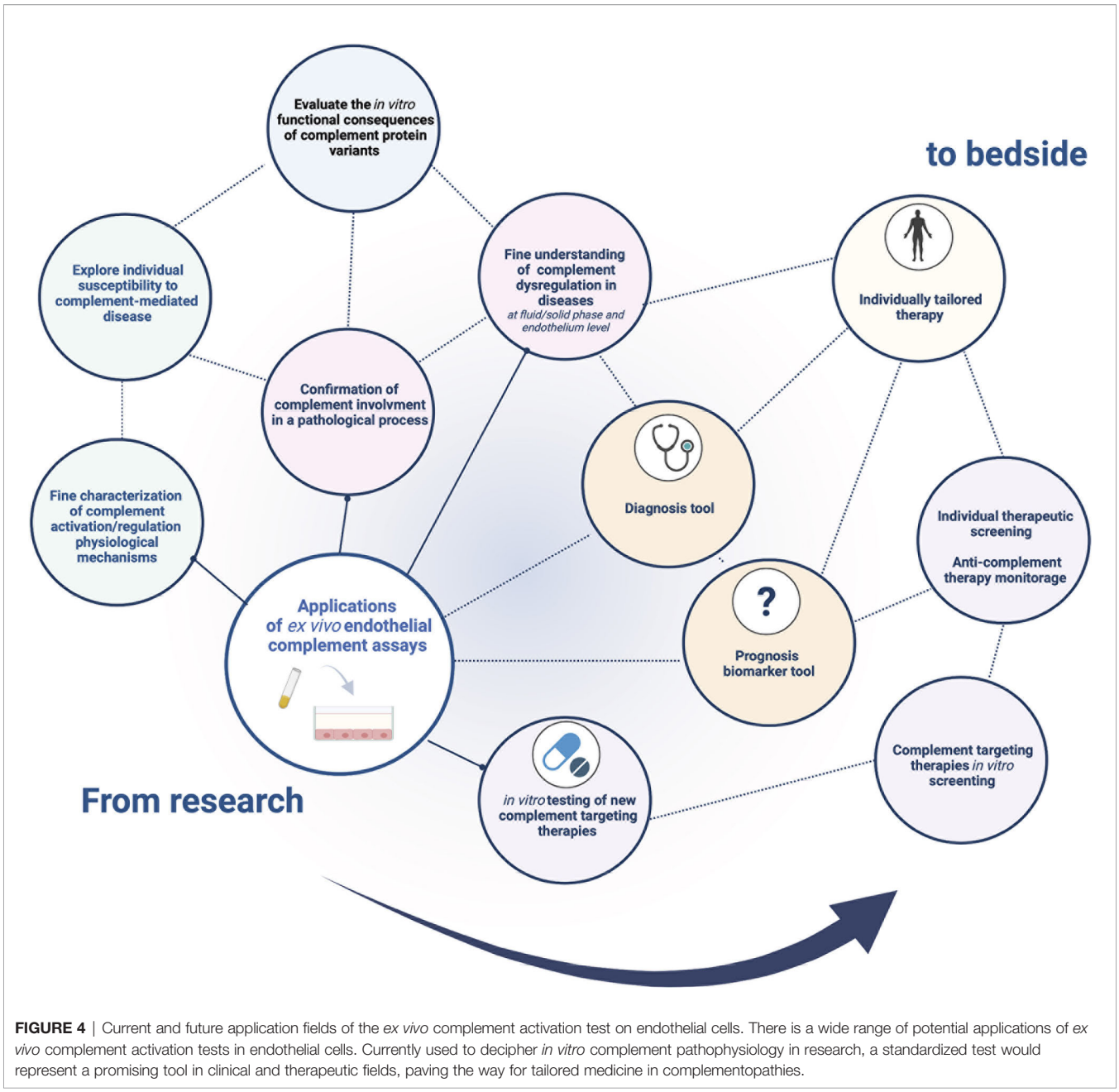

FIGURE 4 | Current and future application fields of the *ex vivo* complement activation test on endothelial cells. There is a wide range of potential applications of *ex vivo* complement activation tests in endothelial cells. Currently used to decipher *in vitro* complement pathophysiology in research, a standardized test would represent a promising tool in clinical and therapeutic fields, paving the way for tailored medicine in complementopathies.

The use of such a test could be multiple, including molecular functional characterization, disease pathophysiology exploration, prognosis classification, complement targeting drug development, and complement therapeutic monitoring. The use of standardized conditions will expand the field of this promising tool.

AUTHOR CONTRIBUTIONS

M-SM, SC, and LR conceptualized and conceived the manuscript. M-SM drafted the manuscript, including the literature search, reading, and writing. SC, VF-B, AD, and LR edited and critically evaluated the manuscript. All authors have contributed to the manuscript and approved the submitted version.

FUNDING

This research was funded by ANR JCJC 2020 COMSIGN.

SUPPLEMENTARY MATERIAL

The Supplementary Material for this article can be found online at: https://www.frontiersin.org/articles/10.3389/fimmu.2022.860689/full#supplementary-material

REFERENCES

1. Magro C, Mulvey JJ, Laurence J, Seshan S, Crowson AN, Dannenberg AJ, et al. Docked SARS CoV-2 Proteins Within the Cutaneous and Subcutaneous Microvasculature and Their Role in the Pathogenesis of Severe COVID-19. *Hum Pathol* (2020) 106:106–16. doi: 10.1016/j.humpath.2020.10.002
2. Fakhouri F, Zuber J, Frémeaux-Bacchi V, Loirat C. Haemolytic Uraemic Syndrome. *Lancet* (2017) 390:681–96. doi: 10.1016/S0140-6736(17)30062-4
3. Brodsky RA. Paroxysmal Nocturnal Hemoglobinuria. *Blood* (2014) 124:2804–11. doi: 10.1182/blood-2014-02-522128
4. Roumenina LT, Loirat C, Dragon-Durey M-A, Halbwachs-Mecarelli L, Sautes-Fridman C, Fremeaux-Bacchi V. Alternative Complement Pathway Assessment in Patients With Atypical HUS. *J Immunol Methods* (2011) 365:8–26. doi: 10.1016/j.jim.2010.12.020
5. Heinen S, Józsi M, Hartmann A, Noris M, Remuzzi G, Skerka C, et al. Hemolytic Uremic Syndrome: A Factor H Mutation (E1172Stop) Causes Defective Complement Control at the Surface of Endothelial Cells. *J Am Soc Nephrol* (2007) 18:506–14. doi: 10.1681/ASN.2006091069
6. Dragon-Durey M-A. Heterozygous and Homozygous Factor H Deficiencies Associated With Hemolytic Uremic Syndrome or Membranoproliferative Glomerulonephritis: Report and Genetic Analysis of 16 Cases. *J Am Soc Nephrol* (2004) 15:787–95. doi: 10.1097/01.ASN.0000115702.28859.A7
7. Lehtinen MJ, Rops AL, Isenman DE, van der Vlag J, Jokiranta TS. Mutations of Factor H Impair Regulation of Surface-Bound C3b by Three Mechanisms in Atypical Hemolytic Uremic Syndrome. *J Biol Chem* (2009) 284:15650–8. doi: 10.1074/jbc.M900814200
8. Manuelian T, Hellwage J, Meri S, Caprioli J, Noris M, Heinen S, et al. Mutations in Factor H Reduce Binding Affinity to C3b and Heparin and Surface Attachment to Endothelial Cells in Hemolytic Uremic Syndrome. *J Clin Invest* (2003) 111:1181–90. doi: 10.1172/JCI16651
9. Kavanagh D, Richards A, Noris M, Hauhart R, Liszewski MK, Karpman D, et al. Characterization of Mutations in Complement Factor I (CFI) Associated With Hemolytic Uremic Syndrome. *Mol Immunol* (2008) 45:95–105. doi: 10.1016/j.molimm.2007.05.004
10. Bienaime F, Dragon-Durey M-A, Regnier CH, Nilsson SC, Kwan WH, Blouin J, et al. Mutations in Components of Complement Influence the Outcome of Factor I-Associated Atypical Hemolytic Uremic Syndrome. *Kidney Int* (2010) 77:339–49. doi: 10.1038/ki.2009.472
11. Fremeaux-Bacchi V, Moulton EA, Kavanagh D, Dragon-Durey M-A, Blouin J, Caudy A, et al. Genetic and Functional Analyses of Membrane Cofactor Protein (CD46) Mutations in Atypical Hemolytic Uremic Syndrome. *J Am Soc Nephrol* (2006) 17:2017–25. doi: 10.1681/ASN.2005101051
12. Dragon-Durey M-A, Loirat C, Cloarec S, Macher M-A, Blouin J, Nivet H, et al. Anti–Factor H Autoantibodies Associated With Atypical Hemolytic Uremic Syndrome. *J Am Soc Nephrol* (2005) 16:555–63. doi: 10.1681/ASN.2004050380
13. Blanc C, Togarsimalemath SK, Chauvet S, Le Quintrec M, Moulin B, Buchler M, et al. Anti–Factor H Autoantibodies in C3 Glomerulopathies and in Atypical Hemolytic Uremic Syndrome: One Target, Two Diseases. *J Immunol* (2015) 194:5129–38. doi: 10.4049/jimmunol.1402770
14. Marinozzi MC, Roumenina LT, Chauvet S, Hertig A, Bertrand D, Olagne J, et al. Anti-Factor B and Anti-C3b Autoantibodies in C3 Glomerulopathy and Ig-Associated Membranoproliferative Gn. *J Am Soc Nephrol* (2017) 28:1603–13. doi: 10.1681/ASN.2016030343
15. Iatropoulos P, Noris M, Mele C, Piras R, Valoti E, Bresin E, et al. Complement Gene Variants Determine the Risk of Immunoglobulin-Associated MPGN and C3 Glomerulopathy and Predict Long-Term Renal Outcome. *Mol Immunol* (2016) 71:131–42. doi: 10.1016/j.molimm.2016.01.010
16. Sansonno D, Gesualdo L, Manno C, Schena FP, Dammacco F. Hepatitis C Virus-Related Proteins in Kidney Tissue From Hepatitis C Virus-Infected Patients With Cryoglobulinemic Membranoproliferative Glomerulonephritis. *Hepatology* (1997) 25:1237–44. doi: 10.1002/hep.510250529
17. Stegall MD, Chedid MF, Cornell LD. The Role of Complement in Antibody-Mediated Rejection in Kidney Transplantation. *Nat Rev Nephrol* (2012) 8:670–8. doi: 10.1038/nrneph.2012.212
18. Banda NK, Takahashi K, Wood AK, Holers VM, Arend WP. Pathogenic Complement Activation in Collagen Antibody- Induced Arthritis in Mice Requires Amplification by the Alternative Pathway. *J Immunol* (2007) 179:4101–9. doi: 10.4049/jimmunol.179.6.4101
19. Banda NK, Thurman JM, Kraus D, Wood A, Carroll MC, Arend WP, et al. Alternative Complement Pathway Activation Is Essential for Inflammation and Joint Destruction in the Passive Transfer Model of Collagen-Induced Arthritis. *J Immunol* (2006) 177:1904–12. doi: 10.4049/jimmunol.177.3.1904
20. Watanabe H, Garnier G, Circolo A, Wetsel RA, Ruiz P, Holers VM, et al. Modulation of Renal Disease in MRL/ *Lpr* Mice Genetically Deficient in the Alternative Complement Pathway Factor B. *J Immunol* (2000) 164:786–94. doi: 10.4049/jimmunol.164.2.786
21. Elliott MK, Jarmi T, Ruiz P, Xu Y, Holers VM, Gilkeson GS. Effects of Complement Factor D Deficiency on the Renal Disease of MRL/lpr Mice. *Kidney Int* (2004) 65:129–38. doi: 10.1111/j.1523-1755.2004.00371.x
22. Sekine H, Kinser TTH, Qiao F, Martinez E, Paulling E, Ruiz P, et al. The Benefit of Targeted and Selective Inhibition of the Alternative Complement Pathway for Modulating Autoimmunity and Renal Disease in MRL/lpr Mice. *Arthritis Rheum* (2011) 63:1076–85. doi: 10.1002/art.30222
23. Nauta AJ, Trouw LA, Daha MR, Tijsma O, Nieuwland R, Schwaeble WJ, et al. Direct Binding of C1q to Apoptotic Cells and Cell Blebs Induces Complement Activation. *Eur J Immunol* (2002) 32:1726. doi: 10.1002/1521-4141(200206)32:6<1726::AID-IMMU1726>3.0.CO;2-R
24. Sjöberg AP, Manderson GA, Mörgelin M, Day AJ, Heinegård D, Blom AM. Short Leucine-Rich Glycoproteins of the Extracellular Matrix Display Diverse Patterns of Complement Interaction and Activation. *Mol Immunol* (2009) 46:830–9. doi: 10.1016/j.molimm.2008.09.018
25. Russell MW, Mansa B. Complement-Fixing Properties of Human IgA Antibodies Alternative Pathway Complement Activation by Plastic-Bound, But Not Specific Antigen-Bound, IgA. *Scand J Immunol* (1989) 30:175–83. doi: 10.1111/j.1365-3083.1989.tb01199.x
26. Roos A, Bouwman LH, van Gijlswijk-Janssen DJ, Faber-Krol MC, Stahl GL, Daha MR. Human IgA Activates the Complement System *Via* the Mannan-Binding Lectin Pathway. *J Immunol* (2001) 167:2861–8. doi: 10.4049/jimmunol.167.5.2861
27. Maillard N, Boerma LJ, Hall S, Huang ZQ, Mrug M, Moldoveanu Z, et al. L'analyse Protéomique De Complexes Immuns Artificiels IgA1-IgG Révèle Une Association Avec Des Formes Activées De C3. *Néphrologie Thérapeutique* (2014) 10:279. doi: 10.1016/j.nephro.2014.07.347
28. Schreiber A, Rousselle A, Becker JU, von Mässenhausen A, Linkermann A, Kettritz R. Necroptosis Controls NET Generation and Mediates Complement Activation, Endothelial Damage, and Autoimmune Vasculitis. *Proc Natl Acad Sci* (2017) 114:E9618–25. doi: 10.1073/pnas.1708247114
29. Roumenina LT, Chadebech P, Bodivit G, Vieira-Martins P, Grunenwald A, Boudhabhay I, et al. Complement Activation in Sickle Cell Disease: Dependence on Cell Density, Hemolysis and Modulation by Hydroxyurea Therapy. *Am J Hematol* (2020) 95:456–64. doi: 10.1002/ajh.25742
30. Frimat M, Tabarin F, Dimitrov JD, Poitou C, Halbwachs-Mecarelli L, Fremeaux-Bacchi V, et al. Complement Activation by Heme as a Secondary Hit for Atypical Hemolytic Uremic Syndrome. *Blood* (2013) 122:282–92. doi: 10.1182/blood-2013-03-489245
31. Boudhabhay I, Poillerat V, Grunenwald A, Torset C, Leon J, Daugan MV, et al. Complement Activation is a Crucial Driver of Acute Kidney Injury in Rhabdomyolysis. *Kidney Int* (2020) 99(3):581–97. doi: 10.1016/j.kint.2020.09.033
32. Ritis K, Doumas M, Mastellos D, Micheli A, Giaglis S, Magotti P, et al. A Novel C5a Receptor-Tissue Factor Cross-Talk in Neutrophils Links Innate Immunity to Coagulation Pathways. *J Immunol* (2006) 177:4794–802. doi: 10.4049/jimmunol.177.7.4794
33. Sansonno D, Dammacco F. Hepatitis C Virus, Cryoglobulinaemia, and Vasculitis: Immune Complex Relations. *Lancet Infect Dis* (2005) 5:227–36. doi: 10.1016/S1473-3099(05)70053-0
34. Loupy A, Lefaucheur C. Antibody-Mediated Rejection of Solid-Organ Allografts. *N Engl J Med* (2018) 379:1150–60. doi: 10.1056/NEJMra1802677
35. Nozaki M, Raisler BJ, Sakurai E, Sarma JV, Barnum SR, Lambris JD, et al. Drusen Complement Components C3a and C5a Promote Choroidal Neovascularization. *Proc Natl Acad Sci* (2006) 103:2328–33. doi: 10.1073/pnas.0408835103
36. Botto M, Dell' Agnola C, Bygrave AE, Thompson EM, Cook HT, Petry F, et al. Homozygous C1q Deficiency Causes Glomerulonephritis Associated With Multiple Apoptotic Bodies. *Nat Genet* (1998) 19:56–9. doi: 10.1038/ng0598-56

37. Dick J, Gan P-Y, Ford SL, Odobasic D, Alikhan MA, Loosen SH, et al. C5a Receptor 1 Promotes Autoimmunity, Neutrophil Dysfunction and Injury in Experimental Anti-Myeloperoxidase Glomerulonephritis. *Kidney Int* (2018) 93:615–25. doi: 10.1016/j.kint.2017.09.018
38. Schreiber A, Xiao H, Jennette JC, Schneider W, Luft FC, Kettritz R. C5a Receptor Mediates Neutrophil Activation and ANCA-Induced Glomerulonephritis. *J Am Soc Nephrol* (2009) 20:289–98. doi: 10.1681/ASN.2008050497
39. Camous L, Roumenina L, Bigot S, Brachemi S, Frémeaux-Bacchi V, Lesavre P, et al. Complement Alternative Pathway Acts as a Positive Feedback Amplification of Neutrophil Activation. *Blood* (2011) 117:1340–9. doi: 10.1182/blood-2010-05-283564
40. Foreman KE, Vaporciyan AA, Bonish BK, Jones ML, Johnson KJ, Glovsky MM, et al. C5a-Induced Expression of P-Selectin in Endothelial Cells. *J Clin Invest* (1994) 94:1147–55. doi: 10.1172/JCI117430
41. Jahn B, Von Kempis J, Krämer KL, Filsinger S, Hänsch GM. Interaction of the Terminal Complement Components C5b-9 With Synovial Fibroblasts: Binding to the Membrane Surface Leads to Increased Levels in Collagenase-Specific mRNA. *Immunology* (1993) 78:329–34.
42. Wan J-X, Fukuda N, Endo M, Tahira Y, Yao E-H, Matsuda H, et al. Complement 3 is Involved in Changing the Phenotype of Human Glomerular Mesangial Cells. *J Cell Physiol* (2007) 213:495–501. doi: 10.1002/jcp.21129
43. Ma Y, Kong L-R, Ge Q, Lu Y-Y, Hong M-N, Zhang Y, et al. Complement 5a-Mediated Trophoblasts Dysfunction is Involved in the Development of Pre-Eclampsia. *J Cell Mol Med* (2017) 22(2):1034–46. doi: 10.1111/jcmm.13466
44. Ekdahl KN, Persson B, Mohlin C, Sandholm K, Skattum L, Nilsson B. Interpretation of Serological Complement Biomarkers in Disease. *Front Immunol* (2018) 9:2237. doi: 10.3389/fimmu.2018.02237
45. Elhadad S, Chapin J, Copertino D, Van Besien K, Ahamed J, Laurence J. MASP2 Levels Are Elevated in Thrombotic Microangiopathies: Association With Microvascular Endothelial Cell Injury and Suppression by Anti-MASP2 Antibody Narsoplimab. *Clin Exp Immunol* (2021) 203:96–104. doi: 10.1111/cei.13497
46. Mollnes TE, Lea T, Froland SS, Harboe M. Quantification of the Terminal Complement Complex in Human Plasma by an Enzyme-Linked Immunosorbent Assay Based on Monoclonal Antibodies Against a Neoantigen of the Complex. *Scand J Immunol* (1985) 22:197–202. doi: 10.1111/j.1365-3083.1985.tb01871.x
47. Mayer MM. On the Destruction of Erythrocytes and Other Cells by Antibody and Complement. *Cancer Res* (1961) 21:1262–9.
48. Platts-Mills TA, Ishizaka K. Activation of the Alternate Pathway of Human Complements by Rabbit Cells. *J Immunol Baltim Md 1950* (1974) 113:348–58.
49. Yamamoto S, Kubotsu K, Kida M, Kondo K, Matsuura S, Uchiyama S, et al. Automated Homogeneous Liposome-Based Assay System for Total Complement Activity. *Clin Chem* (1995) 41:586–90. doi: 10.1093/clinchem/41.4.586
50. Seelen MA, Roos A, Wieslander J, Mollnes TE, Sjöholm AG, Wurzner R, et al. Functional Analysis of the Classical, Alternative, and MBL Pathways of the Complement System: Standardization and Validation of a Simple ELISA. *J Immunol Methods* (2005) 296:187–98. doi: 10.1016/j.jim.2004.11.016
51. Sanchezcorral P. Functional Analysis in Serum From Atypical Hemolytic Uremic Syndrome Patients Reveals Impaired Protection of Host Cells Associated With Mutations in Factor H. *Mol Immunol* (2004) 41:81–4. doi: 10.1016/j.molimm.2004.01.003
52. Daha MR, Fearon DT, Austen KF. C3 Nephritic Factor (C3NeF): Stabilization of Fluid Phase and Cell-Bound Alternative Pathway Convertase. *J Immunol Baltim Md 1950* (1976) 116:1–7.
53. Mori H, Cardiff RD. "Methods of Immunohistochemistry and Immunofluorescence: Converting Invisible to Visible.,". In: J Ursini-Siegel and N Beauchemin, editors. *The Tumor Microenvironment*. New York, NY: Springer (2016). p. 1–12. doi: 10.1007/978-1-4939-3801-8_1
54. Magro CM, Momtahen S, Mulvey JJ, Yassin AH, Kaplan RB, Laurence JC. Role of the Skin Biopsy in the Diagnosis of Atypical Hemolytic Uremic Syndrome. *Am J Dermatopathol* (2015) 37:349–56. doi: 10.1097/DAD.0000000000000234
55. Sturtzel C. "Endothelial Cells". In: S Sattler and T Kennedy-Lydon, editors. *The Immunology of Cardiovascular Homeostasis and Pathology*. Cham: Springer International Publishing (2017). p. 71–91. doi: 10.1007/978-3-319-57613-8_4
56. Aird WC. Endothelial Cell Heterogeneity. *Cold Spring Harb Perspect Med* (2012) 2:a006429–a006429. doi: 10.1101/cshperspect.a006429
57. Dumas SJ, Meta E, Borri M, Luo Y, Li X, Rabelink TJ, et al. Phenotypic Diversity and Metabolic Specialization of Renal Endothelial Cells. *Nat Rev Nephrol* (2021) 17:441–64. doi: 10.1038/s41581-021-00411-9
58. Chi J-T, Chang HY, Haraldsen G, Jahnsen FL, Troyanskaya OG, Chang DS, et al. Endothelial Cell Diversity Revealed by Global Expression Profiling. *Proc Natl Acad Sci* (2003) 100:10623–8. doi: 10.1073/pnas.1434429100
59. Jambusaria A, Hong Z, Zhang L, Srivastava S, Jana A, Toth PT, et al. Endothelial Heterogeneity Across Distinct Vascular Beds During Homeostasis and Inflammation. *eLife* (2020) 9:e51413. doi: 10.7554/eLife.51413
60. Roumenina LT, Rayes J, Frimat M, Fremeaux-Bacchi V. Endothelial Cells: Source, Barrier, and Target of Defensive Mediators. *Immunol Rev* (2016) 274:307–29. doi: 10.1111/imr.12479
61. Sartain SE, Turner NA, Moake JL. Brain Microvascular Endothelial Cells Exhibit Lower Activation of the Alternative Complement Pathway Than Glomerular Microvascular Endothelial Cells. *J Biol Chem* (2018) 293:7195–208. doi: 10.1074/jbc.RA118.002639
62. Sartain SE, Turner NA, Moake JL. TNF Regulates Essential Alternative Complement Pathway Components and Impairs Activation of Protein C in Human Glomerular Endothelial Cells. *J Immunol* (2016) 196:832–45. doi: 10.4049/jimmunol.1500960
63. Kawakami Y, Watanabe Y, Yamaguchi M, Sakaguchi H, Kono I, Ueki A. TNF-α Stimulates the Biosynthesis of Complement C3 and Factor B by Human Umbilical Cord Vein Endothelial Cells. *Cancer Lett* (1997) 116:21–6. doi: 10.1016/S0304-3835(97)04737-X
64. Brooimans RA, van der Ark AA, Buurman WA, van Es LA, Daha MR. Differential Regulation of Complement Factor H and C3 Production in Human Umbilical Vein Endothelial Cells by IFN-Gamma and IL-1. *J Immunol Baltim Md 1950* (1990) 144:3835–40.
65. Lappin DF, Guc D, Hill A, McShane T, Whaley K. Effect of Interferon-γ on Complement Gene Expression in Different Cell Types. *Biochem J* (1992) 281:437–42. doi: 10.1042/bj2810437
66. May O, Merle NS, Grunenwald A, Gnemmi V, Leon J, Payet C, et al. Heme Drives Susceptibility of Glomerular Endothelium to Complement Overactivation Due to Inefficient Upregulation of Heme Oxygenase-1. *Front Immunol* (2018) 9:3008. doi: 10.3389/fimmu.2018.03008
67. Ades EW, Candal FJ, Swerlick RA, George VG, Susan S, DC B, et al. HMEC-1: Establishment of an Immortalized Human Microvascular Endothelial Cell Line. *J Invest Dermatol* (1992) 99:683–90. doi: 10.1111/1523-1747.ep12613748
68. Satchell SC, Tasman CH, Singh A, Ni L, Geelen J, von Ruhland CJ, et al. Conditionally Immortalized Human Glomerular Endothelial Cells Expressing Fenestrations in Response to VEGF. *Kidney Int* (2006) 69:1633–40. doi: 10.1038/sj.ki.5000277
69. Edgell CJ, McDonald CC, Graham JB. Permanent Cell Line Expressing Human Factor VIII-Related Antigen Established by Hybridization. *Proc Natl Acad Sci* (1983) 80:3734–7. doi: 10.1073/pnas.80.12.3734
70. Gavriilaki E, Yuan X, Ye Z, Ambinder AJ, Shanbhag SP, Streiff MB, et al. Modified Ham Test for Atypical Hemolytic Uremic Syndrome. *Blood* (2015) 125:3637–46. doi: 10.1182/blood-2015-02-629683
71. Réti M, Farkas P, Csuka D, Rázsó K, Schlammadinger Á, Udvardy ML, et al. Complement Activation in Thrombotic Thrombocytopenic Purpura. *J Thromb Haemost JTH* (2012) 10:791–8. doi: 10.1111/j.1538-7836.2012.04674.x
72. Bettoni S, Galbusera M, Gastoldi S, Donadelli R, Tentori C, Spartà G, et al. Interaction Between Multimeric Von Willebrand Factor and Complement: A Fresh Look to the Pathophysiology of Microvascular Thrombosis. *J Immunol* (2017) 199:1021–40. doi: 10.4049/jimmunol.1601121
73. Mitra D, Jaffe EA, Weksler B, Hajjar KA, Soderland C, Laurence J. Thrombotic Thrombocytopenic Purpura and Sporadic Hemolytic-Uremic Syndrome Plasmas Induce Apoptosis in Restricted Lineages of Human Microvascular Endothelial Cells. *Blood* (1997) 89:1224–34. doi: 10.1182/blood.V89.4.1224
74. Jaffe EA, Nachman RL, Becker CG, Minick CR. Culture of Human Endothelial Cells Derived From Umbilical Veins. Identification By

Morphologic And Immunologic Criteria. *J Clin Invest* (1973) 52:2745–56. doi: 10.1172/JCI107470
75. Mcginn S, Poronnik P, Gallery ED, Pollock CA. A Method for the Isolation of Glomerular and Tubulointerstitial Endothelial Cells and a Comparison of Characteristics With the Human Umbilical Vein Endothelial Cell Model. *Nephrology* (2004) 9:229–37. doi: 10.1111/j.1440-1797.2004.00254.x
76. van Setten PA, van Hinsbergh VWM, van der Velden TJAN, van de Kar NCAJ, Vermeer M, Mahan JD, et al. Effects of Tnfα on Verocytotoxin Cytotoxicity in Purified Human Glomerular Microvascular Endothelial Cells. *Kidney Int* (1997) 51:1245–56. doi: 10.1038/ki.1997.170
77. Martin-Ramirez J, Hofman M, van den Biggelaar M, Hebbel RP, Voorberg J. Establishment of Outgrowth Endothelial Cells From Peripheral Blood. *Nat Protoc* (2012) 7:1709–15. doi: 10.1038/nprot.2012.093
78. Roumenina LT, Jablonski M, Hue C, Blouin J, Dimitrov JD, Dragon-Durey M-A, et al. Hyperfunctional C3 Convertase Leads to Complement Deposition on Endothelial Cells and Contributes to Atypical Hemolytic Uremic Syndrome. *Blood* (2009) 114:2837–45. doi: 10.1182/blood-2009-01-197640
79. Roumenina LT, Frimat M, Miller EC, Provot F, Dragon-Durey M-A, Bordereau P, et al. A Prevalent C3 Mutation in aHUS Patients Causes a Direct C3 Convertase Gain of Function. *Blood* (2012) 119:4182–91. doi: 10.1182/blood-2011-10-383281
80. Marinozzi MC, Vergoz L, Rybkine T, Ngo S, Bettoni S, Pashov A, et al. Complement Factor B Mutations in Atypical Hemolytic Uremic Syndrome —Disease-Relevant or Benign? *J Am Soc Nephrol* (2014) 25:2053–65. doi: 10.1681/ASN.2013070796
81. Schramm EC, Roumenina LT, Rybkine T, Chauvet S, Vieira-Martins P, Hue C, et al. Mapping Interactions Between Complement C3 and Regulators Using Mutations in Atypical Hemolytic Uremic Syndrome. *Blood* (2015) 125:2359–69. doi: 10.1182/blood-2014-10-609073
82. Noris M, Galbusera M, Gastoldi S, Macor P, Banterla F, Bresin E, et al. Dynamics of Complement Activation in aHUS and How to Monitor Eculizumab Therapy. *Blood* (2014) 124:1715–26. doi: 10.1182/blood-2014-02-558296
83. Valoti E, Alberti M, Tortajada A, Garcia-Fernandez J, Gastoldi S, Besso L, et al. A Novel Atypical Hemolytic Uremic Syndrome–Associated Hybrid *CFHR1/CFH* Gene Encoding a Fusion Protein That Antagonizes Factor H–Dependent Complement Regulation. *J Am Soc Nephrol* (2015) 26:209–19. doi: 10.1681/ASN.2013121339
84. Rigothier C, Delmas Y, Roumenina LT, Contin-Bordes C, Lepreux S, Bridoux F, et al. Distal Angiopathy and Atypical Hemolytic Uremic Syndrome: Clinical and Functional Properties of an Anti–Factor H Igaλ Antibody. *Am J Kidney Dis* (2015) 66:331–6. doi: 10.1053/j.ajkd.2015.03.039
85. Galbusera M, Noris M, Gastoldi S, Bresin E, Mele C, Breno M, et al. An Ex Vivo Test of Complement Activation on Endothelium for Individualized Eculizumab Therapy in Hemolytic Uremic Syndrome. *Am J Kidney Dis* (2019) 74:56–72. doi: 10.1053/j.ajkd.2018.11.012
86. Madden I, Roumenina LT, Langlois-Meurinne H, Guichoux J, Llanas B, Frémeaux-Bacchi V, et al. Hemolytic Uremic Syndrome Associated With Bordetella Pertussis Infection in a 2-Month-Old Infant Carrying a Pathogenic Variant in Complement Factor H. *Pediatr Nephrol* (2019) 34:533–7. doi: 10.1007/s00467-018-4174-1
87. Aiello S, Gastoldi S, Galbusera M, Ruggenenti PL, Portalupi V, Rota S, et al. C5a and C5aR1 are Key Drivers of Microvascular Platelet Aggregation in Clinical Entities Spanning From aHUS to COVID-19. *Blood Adv* (2021) 6 (3):866–81. doi: 10.1182/bloodadvances.2021005246
88. Piras R, Iatropoulos P, Bresin E, Todeschini M, Gastoldi S, Valoti E, et al. Molecular Studies and an Ex Vivo Complement Assay on Endothelium Highlight the Genetic Complexity of Atypical Hemolytic Uremic Syndrome: The Case of a Pedigree With a Null CD46 Variant. *Front Med* (2020) 7:579418. doi: 10.3389/fmed.2020.579418
89. Timmermans SAMEG, Abdul-Hamid MA, Potjewijd J, Theunissen ROMFIH, Damoiseaux JGMC, Reutelingsperger CP, et al. C5b9 Formation on Endothelial Cells Reflects Complement Defects Among Patients With Renal Thrombotic Microangiopathy and Severe Hypertension. *J Am Soc Nephrol* (2018) 29:2234–43. doi: 10.1681/ASN.2018020184
90. Blasco M, Martínez-Roca A, Rodríguez-Lobato LG, Garcia-Herrera A, Rosiñol L, Castro P, et al. Complement as the Enabler of Carfilzomib-Induced Thrombotic Microangiopathy. *Br J Haematol* (2020) 193(1):181–7. doi: 10.1111/bjh.16796
91. Palomo M, Blasco M, Molina P, Lozano M, Praga M, Torramade-Moix S, et al. Complement Activation and Thrombotic Microangiopathies. *Clin J Am Soc Nephrol* (2019) 14:1719–32. doi: 10.2215/CJN.05830519
92. Chauvet S, Roumenina LT, Bruneau S, Marinozzi MC, Rybkine T, Schramm EC, et al. A Familial C3GN Secondary to Defective C3 Regulation by Complement Receptor 1 and Complement Factor H. *J Am Soc Nephrol* (2016) 27:1665–77. doi: 10.1681/ASN.2015040348
93. Vasilev VV, Noe R, Dragon-Durey M-A, Chauvet S, Lazarov VJ, Deliyska BP, et al. Functional Characterization of Autoantibodies Against Complement Component C3 in Patients With Lupus Nephritis. *J Biol Chem* (2015) 290:25343–55. doi: 10.1074/jbc.M115.647008
94. Radanova M, Mihaylova G, Ivanova D, Daugan M, Lazarov V, Roumenina L, et al. Clinical and Functional Consequences of Anti-Properdin Autoantibodies in Patients With Lupus Nephritis. *Clin Exp Immunol* (2020) 201(2):135–44. doi: 10.1111/cei.13443
95. Chaturvedi S, Braunstein EM, Yuan X, Yu J, Alexander A, Chen H, et al. Complement Activity and Complement Regulatory Gene Mutations are Associated With Thrombosis in APS and CAPS. *Blood* (2020) 135:239–51. doi: 10.1182/blood.2019003863
96. Timmermans S, Damoiseaux J, Reutelingsperger C, van Paassen P. More About Complement in the Antiphospholipid Syndrome. *Blood* (2020) 136 (12):1456–9. doi: 10.1182/blood.2020005171
97. Chen JY, Galwankar NS, Emch HN, Menon SS, Cortes C, Thurman JM, et al. Properdin Is a Key Player in Lysis of Red Blood Cells and Complement Activation on Endothelial Cells in Hemolytic Anemias Caused by Complement Dysregulation. *Front Immunol* (2020) 11:1460. doi: 10.3389/fimmu.2020.01460
98. Cid J, Fernández J, Palomo M, Blasco M, Bailó N, Diaz-Ricart M, et al. Hyperhemolytic Transfusion Reaction in Non-Hemoglobinopathy Patients and Terminal Complement Pathway Activation: Case Series and Review of the Literature. *Transfus Med Rev* (2020) 34(3):172–7. doi: 10.1016/j.tmrv.2020.06.002
99. Merle NS, Paule R, Leon J, Daugan M, Robe-Rybkine T, Poillerat V, et al. P-Selectin Drives Complement Attack on Endothelium During Intravascular Hemolysis in TLR-4/Heme-Dependent Manner. *Proc Natl Acad Sci* (2019) 116:6280–5. doi: 10.1073/pnas.1814797116
100. Mollnes TE, Garred P, Bergseth G. Effect of Time, Temperature and Anticoagulants on *In Vitro* Complement Activation: Consequences for Collection and Preservation of Samples to be Examined for Complement Activation. *Clin Exp Immunol* (1988) 73:484–8.
101. Merle NS, Grunenwald A, Rajaratnam H, Gnemmi V, Frimat M, Figueres M-L, et al. Intravascular Hemolysis Activates Complement *via* Cell-Free Heme and Heme-Loaded Microvesicles. *JCI Insight* (2018) 3:e96910. doi: 10.1172/jci.insight.96910
102. del Conde I, Crúz MA, Zhang H, López JA, Afshar-Kharghan V. Platelet Activation Leads to Activation and Propagation of the Complement System. *J Exp Med* (2005) 201:871–9. doi: 10.1084/jem.20041497
103. Morigi M, Galbusera M, Gastoldi S, Locatelli M, Buelli S, Pezzotta A, et al. Alternative Pathway Activation of Complement by Shiga Toxin Promotes Exuberant C3a Formation That Triggers Microvascular Thrombosis. *J Immunol* (2011) 187:172–80. doi: 10.4049/jimmunol.1100491
104. Noone DG, Riedl M, Pluthero FG, Bowman ML, Liszewski MK, Lu L, et al. Von Willebrand Factor Regulates Complement on Endothelial Cells. *Kidney Int* (2016) 90:123–34. doi: 10.1016/j.kint.2016.03.023
105. Youssef L, Miranda J, Blasco M, Paules C, Crovetto F, Palomo M, et al. Complement and Coagulation Cascades Activation Is the Main Pathophysiological Pathway in Early-Onset Severe Preeclampsia Revealed by Maternal Proteomics. *Sci Rep* (2021) 11:3048. doi: 10.1038/s41598-021-82733-z
106. Timmermans SAMEG, Wérion A, Damoiseaux JGMC, Morelle J, Reutelingsperger CP, van Paassen P. Diagnostic and Risk Factors for Complement Defects in Hypertensive Emergency and Thrombotic Microangiopathy. *Hypertension* (2020) 75:422–30. doi: 10.1161/HYPERTENSIONAHA.119.13714
107. Volokhina EB, van de Kar NCAJ, Bergseth G, van der Velden TJAM, Westra D, Wetzels JFM, et al. Sensitive, Reliable and Easy-Performed Laboratory

Monitoring of Eculizumab Therapy in Atypical Hemolytic Uremic Syndrome. *Clin Immunol Orlando Fla* (2015) 160:237–43. doi: 10.1016/j.clim.2015.05.018
108. Merrill SA, Brittingham ZD, Yuan X, Moliterno AR, Sperati CJ, Brodsky RA. Eculizumab Cessation in Atypical Hemolytic Uremic Syndrome. *Blood* (2017) 130:368–72. doi: 10.1182/blood-2017-02-770214
109. Mastellos DC, Ricklin D, Lambris JD. Clinical Promise of Next-Generation Complement Therapeutics. *Nat Rev Drug Discov* (2019) 18:707–29. doi: 10.1038/s41573-019-0031-6

Conflict of Interest: The authors declare that the research was conducted in the absence of any commercial or financial relationships that could be construed as a potential conflict of interest.

Publisher's Note: All claims expressed in this article are solely those of the authors and do not necessarily represent those of their affiliated organizations, or those of the publisher, the editors and the reviewers. Any product that may be evaluated in this article, or claim that may be made by its manufacturer, is not guaranteed or endorsed by the publisher.

Copyright © 2022 Meuleman, Duval, Fremeaux-Bacchi, Roumenina and Chauvet. This is an open-access article distributed under the terms of the Creative Commons Attribution License (CC BY). The use, distribution or reproduction in other forums is permitted, provided the original author(s) and the copyright owner(s) are credited and that the original publication in this journal is cited, in accordance with accepted academic practice. No use, distribution or reproduction is permitted which does not comply with these terms.

frontiers | Frontiers in Immunology

ORIGINAL RESEARCH
published: 10 May 2022
doi: 10.3389/fimmu.2022.866330

Complement Factor I Variants in Complement-Mediated Renal Diseases

*Yuzhou Zhang, Renee X. Goodfellow, Nicolo Ghiringhelli Borsa, Hannah C. Dunlop, Stephen A. Presti, Nicole C. Meyer, Dingwu Shao, Sarah M. Roberts, Michael B. Jones, Gabriella R. Pitcher, Amanda O. Taylor, Carla M. Nester and Richard J. H. Smith**

Molecular Otolaryngology and Renal Research Laboratories, University of Iowa, Iowa City, IA, United States

OPEN ACCESS

Edited by:
Erik J. M. Toonen, Hycult Biotech, Netherlands

Reviewed by:
Elisabetta Valoti, Mario Negri Pharmacological Research Institute (IRCCS), Italy
Richard Benjamin Pouw, Sanquin Research, Netherlands

***Correspondence:**
Richard J. H. Smith
Richard-smith@uiowa.edu

Specialty section:
This article was submitted to Molecular Innate Immunity, a section of the journal Frontiers in Immunology

Received: *31 January 2022*
Accepted: *08 March 2022*
Published: *10 May 2022*

Citation:
Zhang Y, Goodfellow RX, Ghiringhelli Borsa N, Dunlop HC, Presti SA, Meyer NC, Shao D, Roberts SM, Jones MB, Pitcher GR, Taylor AO, Nester CM and Smith RJH (2022) Complement Factor I Variants in Complement-Mediated Renal Diseases. Front. Immunol. 13:866330. doi: 10.3389/fimmu.2022.866330

C3 glomerulopathy (C3G) and atypical hemolytic uremic syndrome (aHUS) are two rare diseases caused by dysregulated activity of the alternative pathway of complement secondary to the presence of genetic and/or acquired factors. Complement factor I (FI) is a serine protease that downregulates complement activity in the fluid phase and/or on cell surfaces in conjunction with one of its cofactors, factor H (FH), complement receptor 1 (CR1/CD35), C4 binding protein (C4BP) or membrane cofactor protein (MCP/CD46). Because altered FI activity is causally related to the pathogenesis of C3G and aHUS, we sought to test functional activity of select *CFI* missense variants in these two patient cohorts. We identified 65 patients (16, C3G; 48, aHUS; 1 with both) with at least one rare variant in *CFI* (defined as a MAF < 0.1%). Eight C3G and eleven aHUS patients also carried rare variants in either another complement gene, *ADAMTS13* or *THBD*. We performed comprehensive complement analyses including biomarker profiling, pathway activity and autoantibody testing, and developed a novel FI functional assay, which we completed on 40 patients. Seventy-eight percent of rare *CFI* variants (31/40) were associated with FI protein levels below the 25th percentile; in 22 cases, FI levels were below the lower limit of normal (type 1 variants). Of the remaining nine variants, which associated with normal FI levels, two variants reduced FI activity (type 2 variants). No patients carried currently known autoantibodies (including FH autoantibodies and nephritic factors). We noted that while rare variants in *CFI* predispose to complement-mediated diseases, phenotypes are strongly contingent on the associated genetic background. As a general rule, in isolation, a rare *CFI* variant most frequently leads to aHUS, with the co-inheritance of a *CD46* loss-of-function variant driving the onset of aHUS to the younger age group. In comparison, co-inheritance of a gain-of-function variant in *C3* alters the phenotype to C3G. Defects in *CFH* (variants or fusion genes) are seen with both C3G and aHUS. This variability underscores the complexity and multifactorial nature of these two complement-mediated renal diseases.

Keywords: complement, factor I, C3 glomerulopathy, atypical hemolytic uremic syndrome, C3 glomerulonephritis, dense deposit disease

INTRODUCTION

The complement cascade is the cornerstone of the innate defense system. It is the first line of defense against foreign and altered host cells, it activates and potentiates adaptive immunity, and it provides integrated crosstalk with other pathways including the coagulation pathway (1). Activation of complement is triggered *via* one of three pathways–the classical (CP), lectin (LP) and alternative (AP)–all of which converge on C3bBb, a C3 convertase that cleaves C3 to C3b, to amplify the complement response and initiate the terminal pathway with ultimate formation of the membrane-bound lytic unit membrane attack complex (C5b-9). The entire cascade is tightly regulated by several mechanisms involving soluble and membrane-bound regulators such as factor H (FH), factor I (FI) and membrane cofactor protein (MCP/CD46) (2).

The primary function of FI is to downregulate complement activity by proteolytic inactivation of C3b to iC3b and C4b to iC4b in the presence of one of its four co-factors, FH, CR1, C4BP and MCP. FI-mediated regulation is especially important in controlling activity of the AP as this pathway is constitutively active. FI is synthesized by the liver as a 66 kDa single chain peptide that undergoes posttranslational glycosylation (adding 22 kDa of glycans) and protein cleavage to remove the signal sequence and four internal amino acids (RRKR, residues 336 to 339) to generate a mature protein with a heavy chain (50 kDa, Lys19–Ile335) and a light chain (38 kDa, Ile340–Val583) linked by a single disulfide bond (Cys255-Cys471) (3, 4). The five recognizable domains include a membrane-attack complex (FIMAC) domain, scavenger receptor cysteine-rich (SRCR) domain, two low-density lipoprotein receptor domains (LDLR1 and LDLR2) and, after a C-terminal linker on the heavy chain, the catalytic or serine protease (SP) domain with its catalytic triad His380-Asp429-Ser525 on the light chain (**Figure 1**) (5).

Deficiency of FI leads to unchecked AP amplification and consumptive deficiency of complement components, such as C3, with various phenotypic consequences (6). Complete absence of FI, which is rare, results in severe and recurrent infections, glomerulonephritis and/or autoimmune disease (7–11). Partial FI deficiencies, which are much more common, lead to dysregulated C3 convertase activity and predispose to several complement-mediated diseases such as atypical hemolytic uremic syndrome (aHUS) (12–15), age-related macular degeneration (AMD) (16–18), and occasionally, C3 glomerulopathy (C3G) (19–22).

C3G and aHUS are rare renal diseases caused by dysregulated complement activity of the AP typically driven by genetic and/or acquired factors. In C3G, uncontrolled complement activity in the fluid phase and glomerular microenvironment leads to a characteristic pattern of glomerular injury defined by the predominant deposition of C3 fragments for which the disease is named (23–25). Based on electron microscopy, two major subclasses of C3G are recognized–C3 glomerulonephritis (C3GN) and dense deposit disease (DDD). Classic clinical findings of both subtypes are hematuria and proteinuria (26). aHUS is a form of complement-mediated thrombotic microangiopathy (TMA) characterized by microangiopathic hemolytic anemia, consumptive thrombocytopenia, and multisystem end organ involvement primarily affecting the kidney (27). In aHUS, dysregulated complement activity primarily occurs on cell surfaces, leading to local prothrombotic states, especially in the kidney.

Here, we reported 45 variants in *CFI* (MAF < 0.1%) identified in 65 patients with either C3G or aHUS. We completed detailed studies in 40 patients that included a novel FI functional assay and identified both type 1 and type 2 *CFI* variants.

METHODS

Patients

Our C3G and TMA registry (C3G, n = 1048; TMA, n = 1468) was searched for patients who were evaluated between 2009-'21 and carried a *CFI* variant with a minor allele frequency (MAF) < 0.1%. Biomaterials included DNA (all patients) isolated from peripheral blood using established methods (28), and serum and plasma (most patients) collected at the time of disease onset (acute flare) in patients with aHUS or during ongoing disease (chronic period) in patients with C3G using a standard protocol (29) and stored as one-time-use aliquots at -80°C. The study was approved by the Institutional Review Board of Carver College of Medicine at the University of Iowa.

Genetic and Biomarker Analyses

Genetic analysis was performed using a targeted sequencing panel, which captures relevant complement genes as well as *THBD*, *ADAMTS13* and *DGKE* as we have described (30). In addition, the *CFH-CFHR* and *CFI* genomic regions were screened for copy number variation by multiplex ligation-dependent probe amplification (MLPA) using the MRC Holland SALSA kit and in-house designed probes.

Biomarker/functional testing was performed using a customized panel that includes ELISAs, radial immunodiffusion (RID), immunofixation electrophoresis (IFE), and hemolytic-based assays (29). Specifically, CP and AP activities were assessed using Quidel (San Diego, CA) and Wieslab kits (SVAR, Malmö, Sweden). Fluid-phase activity was also tested using IFE on a SPIFE machine (Helena Laboratories, Beaumont, TX). Serum levels of C3, C5, properdin, FH, FI and complement activation products C3c, Ba, Bb, sC5b-9 were measured using ELISA kits (Hycult Biotech, Wayne, PA or Quidel, San Diego, CA). C4, FB and FI were run by RID (The Binding Site, San Diego, CA). FH and FB autoantibody assays were done by ELISA against purified proteins FH and FB, respectively (Complement Tech, Tyler, TX). C3-, C4-, and C5-nephritic factors were detected by cell-based hemolytic methods (31).

Factor I Co-Factor Activity

To assess FI co-factor activity, we developed a novel FI functional assay using C3b-decorated sheep erythrocytes (C3b-ShE) prepared as previously described (32). To minimize the effect of endogenous FH, patient serum or plasma was diluted 1:32 in GVB-Mg^{2+} buffer (16). To assess FI function, 50 μL of diluted

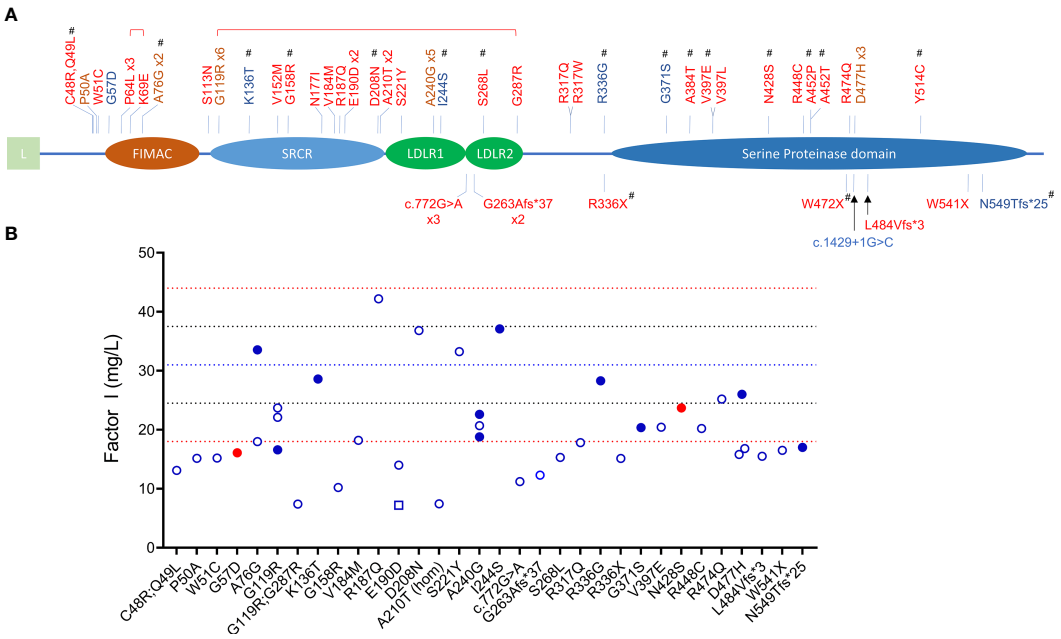

FIGURE 1 | *CFI* variants identified in patients with C3G and aHUS. **(A)** Schematic view of factor I and the 45 rare variants (MAF < 0.1%) identified in 65 patients (red, aHUS; blue, C3G; brown, both C3G and aHUS). All variants were identified in heterozygosis except one homozygote (p.Ala210Thr) and two compound heterozygotes (brackets above variants indicate compound heterozygosity). Novel variants are marker with #. (L, leading sequence; FIMAC, Factor I Membrane Attack Complex; SRCR, Scavenger Receptor Cysteine-Rich; LDLR, Low-Density Lipoprotein Receptor). **(B)** FI levels in 40 patients (open circles, aHUS; filled blue circles, C3GN; filled red circles, DDD; open square, C3G/aHUS; dashed lines, reference values: red, upper and lower limits of normal; blue, percentile lines).

serum/plasma, 50 µL of C3b-ShE ($1x10^9$/mL) and 100 µL of co-factors were added to 200 µL of GVB-EDTA buffer. The co-factors [FH (Complement Tech, Tyler, TX), sCR1 (Celldex Therapeutics, New Haven, CT) or sMCP (Alexion Pharmaceuticals, Boston, MA)] were assayed at final concentrations of 50nM, 25nM and 50nM, respectively. The resulting mixture was incubated at 37°C for 15 minutes. After 3 washes, cells were resuspended in 50 µL of GVB-Mg^{2+} buffer and remaining C3b on ShE was titrated out by excess FB (5x of the amount at Z = 1) and FD (0.3 µg) in GVB-Mg^{2+} buffer to form C3 convertase at 30°C over a 5-minute period; the reaction was stopped by adding 300 µL of GVB-EDTA buffer. 50 µL of the mixture was transferred to an empty 96-well plate and hemolysis was induced by adding 50 µL of rat EDTA serum diluted (1:10) in GVB-EDTA buffer (as a source of C5-C9). After centrifugation at 1000 x g, cell-free supernatant was transferred to a flat bottom 96-well plate and absorbance was read at OD415. The percentage of hemolysis in each well was calculated using hypotonic lysis induced by water as 100%.

Western Blot

Serum or plasma (1:80 diluted) in Laemmli buffer with or without reducing reagent was separated on 4-15% polyacrylamide gels (Bio-Rad, Hercules, CA). After transferring, FI was visualized using rabbit monoclonal antibody to FI (ab278524, Abcam, Waltham, MA) followed by a secondary incubation and chemiluminescence.

Statistics

Statistical analysis was performed using the Student's *t*-test for two group comparisons, Fisher's exact test for contingency tables, and Pearson correlation to measure linear relationships between variables using GraphPad Prism 8.2 (GraphPad Software, San Diego, CA). Error bars represent means ± SD. The number of samples and number of experimental repetitions are indicated in the figure legends. $P < 0.05$ was considered significant.

RESULTS

Patient Cohorts and Rare Variants in *CFI*

Sixty-five unrelated patients (sixteen C3G [ten, C3GN; six, DDD]; 48 aHUS; one C3G/aHUS) with rare variants in *CFI* were identified in our registry (**Figure 1**), which represents significant enrichment in our aHUS cohort as compared to the prevalence of rare variants with MAF < 0.1% reported in gnomAD (1.77% of 141433 individuals in gnomAD vs 1.62% of 1048 C3G patients ($P > 0.05$) and vs 3.34% of 1468 TMA patients ($P < 0.0001$)) (33). In addition, the prevalence of rare variants is significantly higher in aHUS as compared to C3G ($P = 0.0078$). Disease occurred at any age in both cohorts (median age, 27.5 vs 37, respectively), although more aHUS patients were diagnosed in early childhood (age < 5, six aHUS vs one C3G). In the aHUS cohort, there were also more females (female/male, 35/13), while in the C3G cohort, both

genders were equally affected (male/female, 9/8) (**Figure 2A**). Demographic data and basic clinical information are shown in **Table 1**.

Null alleles were found in nine of 48 (19%) patients with aHUS and two of 15 (13%) patients with C3G (**Tables 2**, **3**). Three aHUS patients (#27, #28, #29) carried the same splice-region variant (c.772G>A, p.Ala258Thr; the last nucleotide of exon 5), which results in exon 5 skipping (34). Three patients (#35, #46, #48) carried nonsense mutations (p.Arg336Ter, p.Trp472Ter and p.Trp541Ter) and three patients (#31, #32, #47) had micro-deletions that result in frame shifts (two with c.786delA and one with c.1450_1454del). In the C3G cohort, two null alleles were identified–a microdeletion (c.1646delA; #58, C3GN) and a splice site variant (c.1429+1G>C; #64, DDD). Western blot confirmed the absence of detectable circulating truncated proteins in all patients with null alleles, suggesting that the transcribed mutant message undergoes nonsense-mediated decay. We also confirmed non-expression of the c.1429+1G>C allele on a western blot in a homozygote patient we are following for recurrent infections.

Most variants (64/65) were found in heterozygosis, although we identified one aHUS patient homozygous for p.Ala210Thr (#21) and two who were compound heterozygotes (p.Pro64Leu/p.Lys69Glu, #6; p.Gly119Arg/p.Gly287Arg, #10). One aHUS

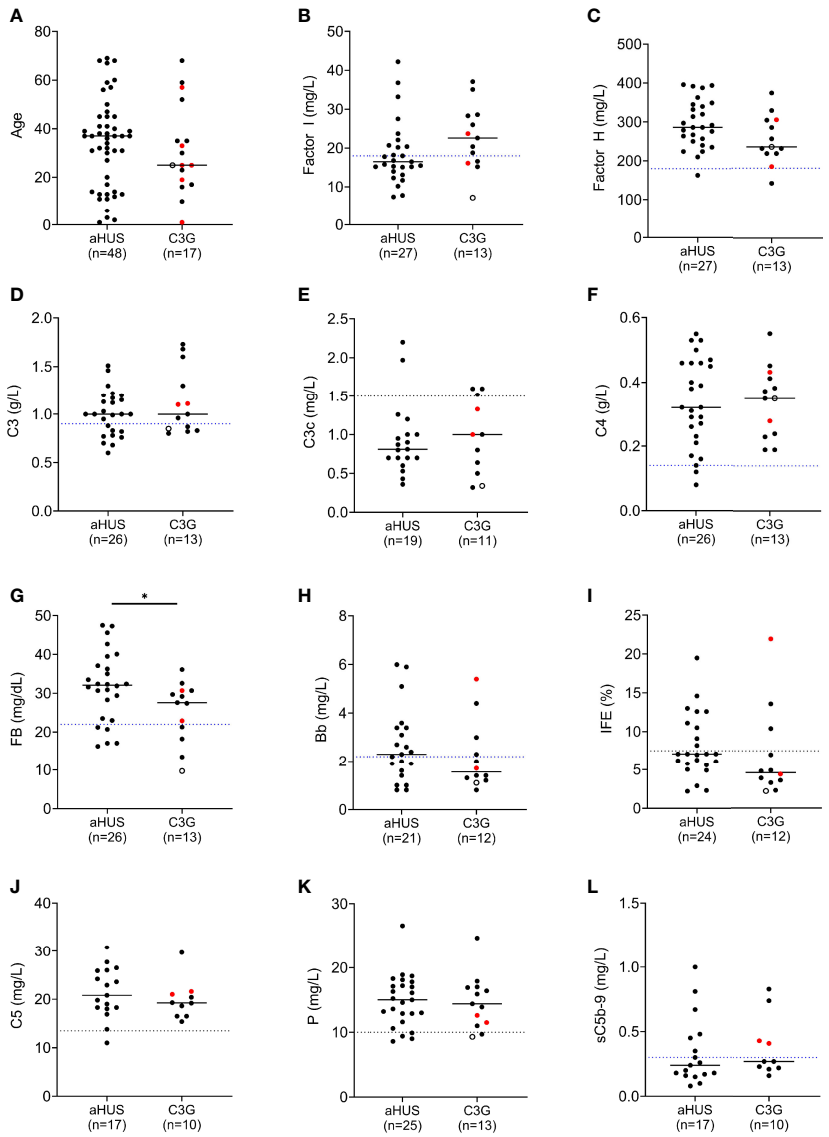

FIGURE 2 | Complement biomarker profiling in aHUS and C3G patients. **(A)** Age distribution. **(B)** Factor I levels. **(C)** Factor H levels. **(D–H)** Biomarkers for alternative pathway (AP) activity including C3 and factor B, and associated activation products C3c and Bb. **(I)** AP fluid-phase activity by immunofixation eletrophoresis. **(J–L)** Biomarkers for terminal pathway activity including C5, properdin and soluble terminal complement complex (sC5b-9). (left column, aHUS; right column-red dots, DDD patients; black dots, C3GN patients; open circle, C3GN/aHUS patient; dashed line, lower limit of normal value for each assay; patients on eculizumab excluded from **(J, L)**; $^*P < 0.05$).

TABLE 1 | Patient demographics.

Characteristics	C3G		aHUS
	C3GN	DDD	
Patients, n	11	6	48
Sex (Male/Female)	7/4	2/4	13/35
Age, yr (median, quartile range)	30, 20-42	25, 21-31	37, 16-45
Onset, median age (yr, quartile range)	25, 14-37	17, 12-23	30, 10-38
Ethnicity			
Caucasian (n, %)	9 (82%)	6 (100%)	36 (75%)
Non-Caucasian (n, %)	2 (18%)	0 (0%)	12 (25%)
Proteinuria (n/data avail, %)	11/11 (100%)	6/6 (100%)	11/14 (79%)
Hematuria (n/data avail, %)	8/11 (73%)	2/2 (100%)	13/20 (65%)
Outcome and treatments			
ESRD, n	3	2	24
Transplantation, n	1	0	7
Failed transplant, n	1	0	2
complement C5 inhibition, n	4	0	15

patient carried two variants on the same allele (p.Cys48Arg/p.Gln49Leu, #1) (**Table 2**). No C3G patients carried a second rare variant in *CFI* and no large genomic deletions in the *CFI* region were identified (**Tables 3**).

Additional Genetic and Acquired Drivers

Genetic variants (pathogenic or likely pathogenic, MAF < 0.1%) in other complement or TMA genes were identified in ten patients with aHUS and eight with C3G. One aHUS patient (#46) carried a *CFH-CFHR1* fusion gene identified by MLPA (**Table 2**). In addition, two DDD patients carried a null allele in a terminal pathway gene (#63, #64) (**Table 3**).

Homozygous deletions of *CFHR3-CHR1* were found in 3/60 (5%) patients, however none was positive for factor H autoantibodies (FHAAs). All patients were also negative for FBAAs and all C3G patients were negative for C3-, C4- and C5-nephritic factors.

Factor I Levels and Complement Dysregulation

FI levels were measured in 40 patients (12 C3G; 27 aHUS and 1 C3G/aHUS) (**Figure 2B** and **Supplementary Tables 1**, **2**). In 31 of 40 (78%) patients, these levels were in the lowest quartile of the normal reference range (24.5 mg/L, normal reference mean = 31, standard deviation = 6.5). The lowest FI levels were found in two aHUS patients with biallelic variants. Excluding these two patients, FI levels were higher in C3G patients as compared to aHUS patients, however the difference was not statistically significant (median C3G vs aHUS, 24 vs 19.4, P = 0.09). FH levels showed the reverse trend and tended to be lower in C3G patients, although this comparison also did not reach statistical significance (**Figure 2C**, P = 0.08).

Several serum complement biomarkers were abnormal, including C3, which was low in four of twelve (33%) C3G and nine of 27 (33%) aHUS patients (**Figure 2D**), consistent with increased C3 convertase activity. In both cohorts, elevation in C3c occurred in a few patients while C4 was normal in most patients (**Figures 2E, F**). FB was low in three of twelve (25%) patients with C3G and five of 26 (19%) aHUS patients (**Figure 2G**), while Bb was high in four of eleven (36%) C3G and twelve of 21 (57%) aHUS patients (**Figure 2H**). Overall, the levels of FI showed moderate correlation with plasma C3 and factor B levels (Pearson's r correlation = 0.39 and 0.36; P = 0.014 and 0.026, respectively). These findings also reflect increased convertase activity associated with a decrease in FI. Ba was elevated in most patients (**Supplementary Tables 1**, **2**) however this biomarker does not accurately reflect complement dysregulation but rather the degree of renal injury (35, 36). The positive IFE in three of eleven (27%) C3G and nine of 24 (38%) aHUS patients recapitulated dysregulated upstream complement activity (**Figure 2I**). Of terminal pathway biomarkers (**Figures 2J–L**), sC5b-9 was elevated in six of seventeen (35%) aHUS and four of ten (40%) C3G patients not on Eculizumab (**Figure 2L**).

Cell-Based FI Functional Assay

In nine patients [four aHUS patients (p.Arg187Gln, p.Asp208Asn, p.Ser221Tyr, p.Arg474Gln); five C3G patients (p.Ala76Gly, p.Lys136Thr, p.Ile244Ser, p.Arg336Gly, p.Asp477His)], FI levels were above the lowest quartile and in these patients, we evaluated FI co-factor activity. Two type 2 variants were identified–p.Arg474Gln and p.Arg336Gly–both of which reduced C3b cleavage activity with all three cofactors (FH, sCR1 and MCP) (**Figures 3A–C**). Western blotting showed that p.Arg336Gly circulates as unprocessed single chain (**Figure 3D**). No functional impairment of FI activity was detectable with the other variants.

DISCUSSION

Sixty-five unrelated patients [sixteen C3G (ten, C3GN; six, DDD); 48 aHUS; one C3G/aHUS] with rare variants in *CFI* were identified in our registry, which represents significant enrichment in our aHUS cohort as compared to the prevalence of rare *CFI* variants reported in gnomAD (1.77% of 141433 individuals in gnomAD vs 1.62% of 1048 C3G patients (P > 0.05) and vs 3.34% of 1468 TMA patients (P < 0.0001)) (33). Eighteen of these variants are novel and three (p.Val184Met, p.Arg448Cys,

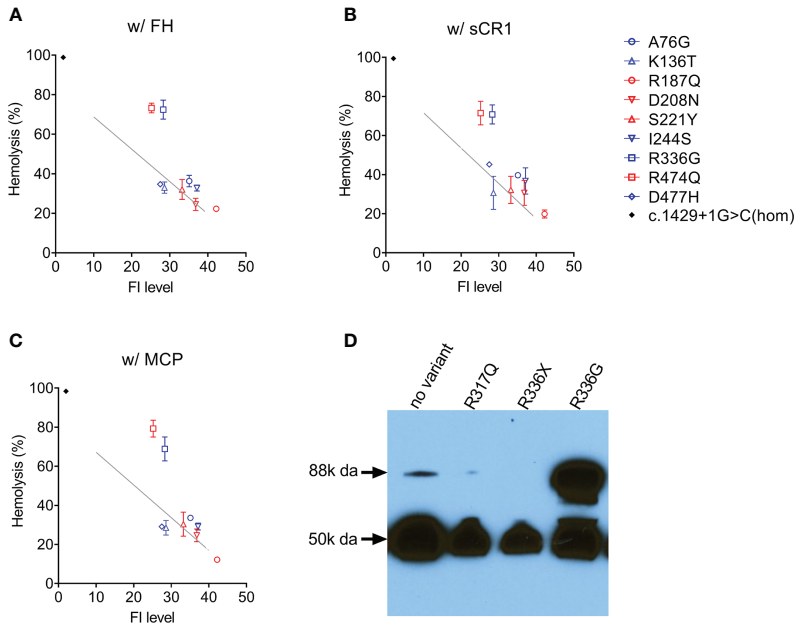

FIGURE 3 | Assessing FI function. In the presence of a cofactor **(A)** FH 50 nM; **(B)** sCR1 25nM; **(C)** MCP 50nM, C3b cleavage activity by FI in patient serum (diluted 1:32) is measured using C3b-decorated sheep erythrocytes. Non-cleaved C3b is developed by the addition of both FB/FD to form C3 convertase and rat-EDTA serum as a source of C5-C9. Percent hemolysis is calculated and plotted as a function of FI concentration determined by ELISA. The grey line in each figure serves as a normal reference line calculated from a normal sample (FI concentration, 40 mg/L) with serial dilutions. Serum from a *CFI* c.1429+1G>C homozygote (FI is undetectable) serves as a positive control (black dot). **(D)** Circulating FI by a Western blot. Patient sample (1:80 diluted in PBS) with reducing reagent separated on a 4-15% polyacrylamide gel and transferred. FI was visualized by an antibody specific to the heavy chain (50k Da). *CFI* p.Arg336Gly results in an unprocessed single chain (88k Da).

p.Trp541Ter) are reported for the first time in an aHUS cohort [previously associated only with AMD (18, 37–39)]. In 40 patients, we completed serological and functional studies to facilitate the classification of these variants based on ACMG guidelines.

Low FI levels have a variety of phenotypic consequences with the most extreme, complete CFI deficiency, leading to uncontrolled AP activity and C3 consumption (7). As a consequence of C3 consumption, severe and recurrent pyogenic infections with encapsulated organisms such as *Streptococcus pneumoniae*, *Haemophilus influenzae* and *Neisseria meningitidis* develop, driven by defective opsonization, immune adherence and phagocytosis (40). Whilst we have not seen complete FI deficiency in our C3G and aHUS cohorts, we have identified several patients with low or borderline low FI levels (16-24.5 mg/L, normal range 18 – 44) with the presenting phenotype typically driven by other acquired or genetic factors. For example, in isolation a rare *CFI* variant most frequently leads to aHUS, however the co-inheritance of a *CD46* loss-of-function pathogenic variant drives the onset of aHUS to the younger age group (#4, #7, #9, #30, #45) while a gain-of-function pathogenic variant in *C3* alters the phenotype to C3G (4 of 15 *vs* 1 of 48, C3G *vs* aHUS, $P = 0.0097$). Defects in *CFH* (variants or fusion genes) are seen with both C3G and aHUS (3 of 15 *vs* 2 of 48, C3G *vs* aHUS, $P = 0.0828$).

Autoantibodies to complement components (such as FHAAs, FBAAs, C3-, C4-, C5-nephritic factors) also play an important role in the pathogenesis of C3G and aHUS (23, 41), and while none of the patients in this study was co-positive for autoantibodies, we did not consider this finding surprising. With respect to aHUS, the prevalence of FHAAs is generally low, and when identified, they are typically seen in the pre-teenage years in children who are homozygous for the deletion of *CFHR3-CFHR1*. This genotype was identified only three times in our aHUS cohort, all in adults. With respect to C3G, about 60% of patients are positive for genetic mutations and/or autoantibodies as drivers of disease (19, 29). Of this 60%, ~10% are co-positive for both genetic drivers and autoantibodies, ~70% have only autoantibodies, and ~20% have only genetic variants. In our C3G cohort, half had additional genetic variants contributing to the complement dysregulation.

In 27 patients in our aHUS cohort, we measured FI levels and identified 18 type 1 variants (low expression) and five variants with limited expression (within 1st quartile, **Figure 1B**). The remaining 4 variants–p.Arg187Gln, p.Asp208Asn, p.Ser221Tyr and p.Arg474Gln–were associated with normal FI levels (above the lowest quartile). Of these, p.Asp208Asn is a novel variant, while p.Arg187Gln, p.Ser221Tyr and p.Arg474Gln have been reported. Although no data are provided for p.Arg187Gln, p.Ser221Tyr was associated with normal FI levels in two AMD studies (16, 18). p.Arg474Gln has also been reported in AMD cohorts with normal FI levels (18, 42, 43) and in an aHUS cohort with low FI levels, although the aHUS patient also carried another type 1 variant p.Ala258Thr (44). Our functional data show that p.Arg474Gln affects FI cofactor activity with all three cofactors (FH, MCP,

TABLE 2 | Demographic and genetic data in patients with aHUS.

ID	Age	Onset	Sex	DNA	Protein	Domain	MAF (gnomAD)	CADD	Other genes (including *ADAMTS13*, *THBD*, terminal pathway genes)	*CFHR3-1-4-2-5*
1	37	36	M	c.142T>C;	p.Cys48Arg;		Novel	26.4		wildtype
				c.146A>T**	p.Gln49Leu**			24.1		
2	67	65	F	c.148C>G	p.Pro50Ala		9.6E-05	24.8		wildtype
3	41	32	F	c.153G>T	p.Trp51Cys		Novel	28		del(*CFHR3-1*)
4	6	3	F	c.191C>T	p.Pro64Leu	FIMAC	2.3E-04	27.2	*CFH* c.3553G>C, p.A1185P	wildtype
									CD46 c.191G>A, p.C64Y	
5	13	5	F	c.191C>T	p.Pro64Leu	FIMAC	2.3E-04	27.2		wildtype
6	50	43	F	c.191C>T;	p.Pro64Leu;	FIMAC	2.3E-04	27.2		del(*CFHR3-1*)
				c.205A>G^	p.Lys69Glu^		2.4E-05	25.4		
7	11	3	F	c.227C>G	p.Ala76Gly	FIMAC	Novel	15.5	*CD46* c.350_351dupAC#	wildtype
8	37	31	M	c.338G>A	p.Ser113Asn		2.1E-05	8.8		del(*CFHR3-1*)
9	1	1	F	c.355G>A	p.Gly119Arg	SRCR	4.2E-04	23	*CD46* c.565T>G, p.Y189D	wildtype
10	34	22	F	c.355G>A;	p.Gly119Arg;	SRCR	4.2E-04;	23;		wildtype
				c.859G>A^	p.Gly287Arg^		4.6E-05	23.2		
11	45	35	F	c.355G>A	p.Gly119Arg	SRCR	4.2E-04	23		Not done
12	47	40	F	c.355G>A	p.Gly119Arg	SRCR	4.2E-04	23		wildtype
13	45	38	F	c.355G>A	p.Gly119Arg	SRCR	4.2E-04	23		del(*CFHR3-1*)
14	32	20	F	c.454G>A	p.Val152Met	SRCR	4.2E-05	27.8		wildtype
15	13	5	M	c.472G>A	p.Gly158Arg	SRCR	Novel	28.2		Not done
16	27	20	F	c.530A>T	p.Asn177Ile	SRCR	6.0E-05	16.8		del(*CFHR3-1*)
17	31	31	F	c.550G>A	p.Val184Met	SRCR	Novel	22	*ADAMTS13* c.2753T>C, p.L918P	del(*CFHR3-1*)
18	60	52	F	c.560G>A	p.Arg187Gln	SRCR	7.8E-05	16.5		del(*CFHR3-1*)
19	37	37	F	c.570G>T	p.Glu190Asp	SRCR	8.0E-06	24.1		wildtype
20	2	1	F	c.622G>A	p.Asp208Asn	SRCR	4.0E-06	8.4		wildtype
21	30	27	F	c.628G>A#	p.Ala210Thr#	SRCR	1.2E-05	23.7		del(*CFHR3-1*)#
22	45	38	M	c.628G>A	p.Ala210Thr	SRCR	1.2E-05	23.7		del(*CFHR3-1*)#
23	68	62	M	c.662C>A	p.Ser221Tyr	LDLR1	4.0E-06	9.3		del(*CFHR3-1*)
24	31	22	F	c.719C>G	p.Ala240Gly	LDLR1	2.5E-04	23.8		wildtype
25	20	11	F	c.719C>G	p.Ala240Gly	LDLR1	2.5E-04	23.8		del(*CFHR3-1*)
26	39	33	M	c.719C>G	p.Ala240Gly	LDLR1	2.5E-04	23.8		wildtype
27	56	55	F	c.772G>A	p.Ala258Thr	LDLR2	1.2E-04	34		Not done
28	38	30	M	c.772G>A	p.Ala258Thr	LDLR2	1.2E-04	34		wildtype
29	39	32	F	c.772G>A	p.Ala258Thr	LDLR2	1.2E-04	34		wildtype
30	14	6	F	c.803C>T	p.Ser268Leu	LDLR2	Novel	26.4	*CD46* c.768C>A, p.C256X#	wildtype
31	57	45	M	c.786delA	p.Gly263Alafs*37	LDLR2	2.0E-05		*C9* c.1030A>G, p.T344A	wildtype
32	13	4	F	c.786delA	p.Gly263Alafs*37	LDLR2	2.0E-05			del(*CFHR3-1*)
33	31	26	M	c.950G>A	p.Arg317Gln		2.1E-05	18.6		wildtype
34	37	34	F	c.949C>T	p.Arg317Trp		8.5E-05	14.9		wildtype
35	37	29	F	c.1006C>T	p.Arg336Ter		Novel	35		wildtype
36	12	1	M	c.1150G>A	p.Ala384Thr	SP	7.8E-05	3.7		Not done
37	59	51	M	c.1190T>A	p.Val397Glu	SP	Novel	17.1		wildtype
38	36	30	F	c.1189G>T	p.Val397Leu	SP	Novel	0.001	*CFH* c.575G>A, p.C192Y	wildtype
39	68	60	F	c.1342C>T	p.Arg448Cys	SP	7.2E-05	11.1		del(*CFHR3-1*)
40	11	8	F	c.1354G>C	p.Ala452Pro	SP	3.2E-05	25.7	*THBD* c.1465G>T, p.D489Y	wildtype
41	38	36	F	c.1354G>A	p.Ala452Thr	SP	1.2E-05	25.1		wildtype
42	41	33	F	c.1421G>A	p.Arg474Gln	SP	4.8E-05	22.1		del(*CFHR3-1*)
43	14	5	F	c.1429G>C	p.Asp477His	SP	2.0E-05	35		del(*CFHR3-1*)
44	3	2	F	c.1429G>C	p.Asp477His	SP	2.0E-05	35		wildtype
45	17	11	M	c.1541A>G	p.Tyr514Cys	SP	4.0E-06	15.8	*CD46* c.350_351dupAC	Not done
46	32	24	M	c.1415G>A	p.Trp472Ter	SP	Novel	41		*CFH-CFHR1* fusion
47	69	69	F	c.1450_1454del	p.Leu484Valfs*3	SP	2.8E-05		*C3* c.1898A>G, p.K633R	del(*CFHR3-1*)#
48	40	40	F	c.1622G>A	p.Trp541Ter	SP	Novel	42		wildtype

All variants (including MLPA results) identified are heterozygotes except:
#homozygote.
^compound heterozygote.
***on same allele.*

sCR1) (**Figure 3**), making p.Arg474Gln a type 2 pathogenic variant. No functional defects were observed with p.Arg187Gln, p.Asp208Asn and p.Ser221Tyr, and based on these data, these three variants should be classified as likely benign.

Low FI levels (< 25%) were found in six C3GN patients and one DDD patient (#60). Of the six C3GN patients, two *CFI* variants were identified in each of two patients (p.Gly119Arg, #50 and #62; p.Ala240Gly, #52 and #53), with the remaining two

patients carrying truncating variants (p.Asn549Thrfs*25, #58; c.1429+1G>C, #64). Interestingly, p.Gly119Arg and p.Ala240Gly were also identified in aHUS patients (p.Gly119Arg, #9, #10, #11, #12, #13; p.Ala240Gly, #24, #25, #26) and are well-documented type 1 variants (18, 21, 45–48). p.Gly119Arg and p.Ala240Gly are also present in the general population with the highest minor allele frequencies in Europeans (MAF = 0.000852 and 0.000093, respectively). These data suggest that carrying p.Gly119Arg or p.Ala240Gly is a risk factor for complement-mediated disease depending, in part, on the expressivity of the other *CFI* allele and/or the presence of mutations in other genes. For example, one aHUS patient (#10) had extremely low FI levels as a result of compound heterozygosis (p.Gly119Arg and p.Gly287Arg on opposite alleles), while all C3G patients carrying either the p.Gly119Arg allele or the p.Ala240Gly allele had a second pathogenic or likely pathogenic variant in *CFH* or *C3* (#50, #52, #53, #62; **Table 3**).

Similarly, p.Pro64Leu, a variant that has been documented in AMD patients with low FI expression (16, 18), was identified in three aHUS patients (one *CFI* compound het) and one DDD patient (#4, #5, #6 and #61). The DDD patient also carried a gain-of-functions variant in *C3*, p.Arg161Trp, which has been shown to increase C3b affinity for factor B and reduce binding to MCP, although FH-mediated regulation is unchanged (14, 49, 50).

With two other variants [p.Ala76Gly (novel), p.Asp477His] identified in both C3GN and aHUS patients (#49 *vs* #7 and #57 *vs* #43 and #44, C3G *vs* aHUS), we noticed much higher FI levels in C3G as compared to aHUS patients. In these five patients, all FI results were confirmed by another technique (RID) and Western blotting, and large genomic deletions were ruled out by MLPA. In addition, FI functional assays showed normal C3b cleavage in all patients. Further research is required to understand this variability. We classified both variants as VUSs (variant of unknown significance).

We completed functional studies on all C3G patients with normal FI levels (p.Lys136Thr, p.Ile244Ser, p.Arg336Gly, p.Asn428Ser) and observed significantly impaired FI function (C3b cleavage) with all cofactors (FH, MCP, sCR1) for only p.Arg336Gly (**Figures 3A–C**). Because maturation of FI requires a proteolytic process that removes four amino acids (Arg-Arg-Lys-Arg) at residues 336-339, FI p.Gly336 circulates as an unprocessed pro-peptide without functional activity (**Figure 3D**). This finding has also been reported for p.Arg339Lys and p.Arg339Glu in aHUS patients (21, 44) and p.Arg339Gln in AMD patients (18, 38, 43). Common to all these mutations is the removal of a positive charged residue from the consensus sequence R-x-K/R-R. Therefore, we would expect individuals carrying these variants to have an identifiable circulating unprocessed single peptide and these variants should be classified as likely pathogenic.

Finally, when measuring FI levels, it should be remembered that as an acute-phase protein its serum concentration increases non-specifically in response to many cytokines (17). In our experience, in the acute phase, FI levels can be elevated ~25% above baseline, however this increase does not occur in isolation but rather in conjunction with an increase in other complement biomarkers, especially FB, C4 and FH (**Figure 4**). To ensure that the impact of a rare hypomorphic allele variant is not masked by the normal allele, serial testing of complement biomarkers is advisable. Anti-C5 therapy with eculizumab does not impact FI levels although it does elevate plasma C5, suppress sC5b-9, and

TABLE 3 | Demographic and genetic data in patients with C3G.

ID	Age	Onset	Sex	DNA	Protein	Domain	MAF (gnomAD)	CADD	Other genes (including *ADAMTS13*, *THBD*, terminal pathway genes)	*CFHR3-1-4-2-5*
C3GN										
49	30	25	F	c.227C>G	p.Ala76Gly	FIMAC	Novel	15.5	*C3* c.2203C>T, p.R735W	wildtype
50	68	67	M	c.355G>A	p.Gly119Arg	SRCR	4.2E-04	23	*CFH* c.3628C>T, R1210C	wildtype
51	35	28	F	c. 407A>C	p.Lys136Thr	SRCR	Novel	4.9		wildtype
52	59	47	M	c.719C>G	p.Ala240Gly	LDLR1	2.5E-04	23.8	*CFH* c.790+1 G>A	del(*CFHR3-1*)
53	16	13	F	c.719C>G	p.Ala240Gly	LDLR1	2.5E-04	23.8	*C3* c.2203C>T, p.R735W	wildtype
54	23	15	F	c.731T>G	p.Ile244Ser	LDLR1	3.6E-05	23		wildtype
55	10	7	M	c.1006C>G	p.Arg336Gly		5.2E-05	22.9		wildtype
56	35	28	M	c.1111G>A	p.Gly371Ser	SP	Novel	31		wildtype
57	52	46	M	c.1429G>C	p.Asp477His	SP	2.0E-05	35		Not done
58	17	12	M	c.1646delA	p.Asn549Thrfs*25	SP	Novel			del(*CFHR3-1*)
DDD										
59	25	12	F	c.148C>G	p.Pro50Ala		9.6E-05	24.8		wildtype
60	25	23	F	c.170G>A	p.Gly57Asp	FIMAC	4.0E-06	23.1		wildtype
61	1	1	M	c.191C>T	p.Pro64Leu	FIMAC	2.3E-04	27.2	*C3* c.481C>T, p.R161W	del(*CFHR3-1*)
62	19	12	F	c.355G>A	p.Gly119Arg	SRCR	4.2E-04	23	*C3* c.4594C>T, p.R1532W	del(*CFHR3-1*)
63	57	57	F	c.1283A>G	p.Asn428Ser	SP	Novel	23.4	*CFH* c.1056T>A, p.Y352X *C6* c.1375A>T, p.K459X	wildtype
64	33	22	M	c.1429+1G>C	Exon skipping	SP	2.8E-05	33	*C9* c.1042delA	wildtype
C3GN/aHUS										
65	25	19	M	c.570G>T	p.Glu190Asp	SRCR	8.0E-06	24.1		del(*CFHR3-1*)

All variants (including MLPA results) identified are heterozygotes.

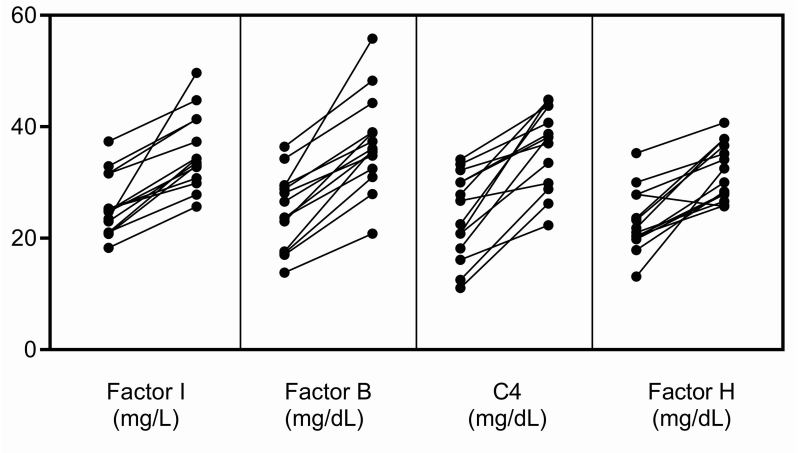

FIGURE 4 | Increases in FI, FB, C4 and FH in the acute phase. These complement proteins are positive acute-phase reactants, and their levels were significantly increased in the acute phase in fourteen patients in our C3G and aHUS registries. The increase in FI does not occur in isolation but rather in conjunction with increases in other complement biomarkers, especially FB, C4 and FH. This pattern of increase was not observed in the patients described in this study (left, complement levels in remission; right, complement levels in the acute phase).

abolish activity of the classical and alternative pathways. And finally, we found that the prevalence of rare *CFI* variants is significantly higher in aHUS as compared to C3G ($P = 0.0078$). While this finding suggests that partial FI deficiency might have less impact on C3G, precisely how a relative deficiency in FI contributes to the underlying pathophysiology of these two diseases requires further study.

In summary, rare variants in *CFI* play a causal role in C3G and aHUS although the clinically observed phenotype is strongly contingent on the associated genetic background. Functional testing should be considered to assess FI activity if a rare *CFI* variant is identified. Our results suggest that the majority of *CFI* missense variants with a MAF < 0.1% will be type 1 variants (~80%), although a small of type 2 variants (~5%) will also be identified.

DATA AVAILABILITY STATEMENT

The original contributions presented in the study are included in the article/**Supplementary Material**. Further inquiries can be directed to the corresponding author.

ETHICS STATEMENT

The studies involving human participants were reviewed and approved by Institutional Review Board of Carver College of Medicine at the University of Iowa. Written informed consent to participate in this study was provided by the participants' legal guardian/next of kin.

AUTHOR CONTRIBUTIONS

YZ and RS conceived of the study, designed experiments, and wrote the manuscript. RG, NGB, HD, SP, NM, DS, SR, MJ, GP, and AT performed the experiments. CN provided crucial conceptual input. All authors reviewed and approved the manuscript.

FUNDING

This work was supported in part by National Institute of Health R01 DK110023.

ACKNOWLEDGMENTS

We are grateful to all patients whose participation made this research possible.

SUPPLEMENTARY MATERIAL

The Supplementary Material for this article can be found online at: https://www.frontiersin.org/articles/10.3389/fimmu.2022.866330/full#supplementary-material

Supplementary Table 1 | Biomarker data in patients with aHUS.

Supplementary Table 2 | Biomarker data in patients with C3G.

REFERENCES

1. Markiewski MM, Lambris JD. The Role of Complement in Inflammatory Diseases From Behind the Scenes Into the Spotlight. *Am J Pathol* (2007) 171 (3):715–27. doi: 10.2353/ajpath.2007.070166
2. Merle NS, Church SE, Fremeaux-Bacchi V, Roumenina LT. Complement System Part I - Molecular Mechanisms of Activation and Regulation. *Front Immunol* (2015) 6:262. doi: 10.3389/fimmu.2015.00262
3. Tsiftsoglou SA, Arnold JN, Roversi P, Crispin MD, Radcliffe C, Lea SM, et al. Human Complement Factor I Glycosylation: Structural and Functional Characterisation of the N-Linked Oligosaccharides. *Biochim Biophys Acta* (2006) 1764(11):1757–66. doi: 10.1016/j.bbapap.2006.09.007
4. Goldberger G, Arnaout MA, Aden D, Kay R, Rits M, Colten HR. Biosynthesis and Postsynthetic Processing of Human C3b/C4b Inactivator (Factor I) in Three Hepatoma Cell Lines. *J Biol Chem* (1984) 259(10):6492–7. doi: 10.1016/S0021-9258(20)82168-1
5. Roversi P, Johnson S, Caesar JJ, McLean F, Leath KJ, Tsiftsoglou SA, et al. Structural Basis for Complement Factor I Control and Its Disease-Associated Sequence Polymorphisms. *Proc Natl Acad Sci USA* (2011) 108(31):12839–44. doi: 10.1073/pnas.1102167108
6. Nilsson SC, Sim RB, Lea SM, Fremeaux-Bacchi V, Blom AM. Complement Factor I in Health and Disease. *Mol Immunol* (2011) 48(14):1611–20. doi: 10.1016/j.molimm.2011.04.004
7. Naesens L, Smet J, Tavernier SJ, Schelstraete P, Hoste L, Lambrecht S, et al. Plasma C3d Levels as a Diagnostic Marker for Complete Complement Factor I Deficiency. *J Allergy Clin Immunol* (2021) 147(2):749–53 e2. doi: 10.1016/j.jaci.2020.08.014
8. Haerynck F, Stordeur P, Vandewalle J, Van Coster R, Bordon V, De Baets F, et al. Complete Factor I Deficiency Due to Dysfunctional Factor I With Recurrent Aseptic Meningo-Encephalitis. *J Clin Immunol* (2013) 33(8):1293–301. doi: 10.1007/s10875-013-9944-8
9. Nita IM, Genel F, Nilsson SC, Smart J, Truedsson L, Choo S, et al. Molecular Characterization of Two Novel Cases of Complete Complement Inhibitor Factor I Deficiency. *Mol Immunol* (2011) 48(8):1068–72. doi: 10.1016/j.molimm.2011.01.012
10. Nielsen HE, Christensen KC, Koch C, Thomsen BS, Heegaard NH, Tranum-Jensen J. Hereditary, Complete Deficiency of Complement Factor H Associated With Recurrent Meningococcal Disease. *Scand J Immunol* (1989) 30(6):711–8. doi: 10.1111/j.1365-3083.1989.tb02480.x
11. Nilsson SC, Trouw LA, Renault N, Miteva MA, Genel F, Zelazko M, et al. Genetic, Molecular and Functional Analyses of Complement Factor I Deficiency. *Eur J Immunol* (2009) 39(1):310–23. doi: 10.1002/eji.200838702
12. Bu F, Maga T, Meyer NC, Wang K, Thomas CP, Nester CM, et al. Comprehensive Genetic Analysis of Complement and Coagulation Genes in Atypical Hemolytic Uremic Syndrome. *J Am Soc Nephrol* (2014) 25(1):55–64. doi: 10.1681/ASN.2013050453
13. Fremeaux-Bacchi V, Fakhouri F, Garnier A, Bienaime F, Dragon-Durey MA, Ngo S, et al. Genetics and Outcome of Atypical Hemolytic Uremic Syndrome: A Nationwide French Series Comparing Children and Adults. *Clin J Am Soc Nephrol* (2013) 8(4):554–62. doi: 10.2215/CJN.04760512
14. Bresin E, Rurali E, Caprioli J, Sanchez-Corral P, Fremeaux-Bacchi V, Rodriguez de Cordoba S, et al. Combined Complement Gene Mutations in Atypical Hemolytic Uremic Syndrome Influence Clinical Phenotype. *J Am Soc Nephrol* (2013) 24(3):475–86. doi: 10.1681/ASN.2012090884
15. Westra D, Vernon KA, Volokhina EB, Pickering MC, van de Kar NC, van den Heuvel LP. Atypical Hemolytic Uremic Syndrome and Genetic Aberrations in the Complement Factor H-Related 5 Gene. *J Hum Genet* (2012) 57(7):459–64. doi: 10.1038/jhg.2012.57
16. Java A, Baciu P, Widjajahakim R, Sung YJ, Yang J, Kavanagh D, et al. Functional Analysis of Rare Genetic Variants in Complement Factor I (Cfi) Using a Serum-Based Assay in Advanced Age-Related Macular Degeneration. *Transl Vis Sci Technol* (2020) 9(9):37. doi: 10.1167/tvst.9.9.37
17. Hallam TM, Marchbank KJ, Harris CL, Osmond C, Shuttleworth VG, Griffiths H, et al. Rare Genetic Variants in Complement Factor I Lead to Low Fi Plasma Levels Resulting in Increased Risk of Age-Related Macular Degeneration. *Invest Ophthalmol Vis Sci* (2020) 61(6):18. doi: 10.1167/iovs.61.6.18
18. Kavanagh D, Yu Y, Schramm EC, Triebwasser M, Wagner EK, Raychaudhuri S, et al. Rare Genetic Variants in the Cfi Gene Are Associated With Advanced Age-Related Macular Degeneration and Commonly Result in Reduced Serum Factor I Levels. *Hum Mol Genet* (2015) 24(13):3861–70. doi: 10.1093/hmg/ddv091
19. Iatropoulos P, Noris M, Mele C, Piras R, Valoti E, Bresin E, et al. Complement Gene Variants Determine the Risk of Immunoglobulin-Associated Mpgn and C3 Glomerulopathy and Predict Long-Term Renal Outcome. *Mol Immunol* (2016) 71:131–42. doi: 10.1016/j.molimm.2016.01.010
20. Zhao W, Ding Y, Lu J, Zhang T, Chen D, Zhang H, et al. Genetic Analysis of the Complement Pathway in C3 Glomerulopathy. *Nephrol Dial Transplant* (2018) 33(11):1919–27. doi: 10.1093/ndt/gfy033
21. Osborne AJ, Breno M, Borsa NG, Bu F, Fremeaux-Bacchi V, Gale DP, et al. Statistical Validation of Rare Complement Variants Provides Insights Into the Molecular Basis of Atypical Hemolytic Uremic Syndrome and C3 Glomerulopathy. *J Immunol* (2018) 200(7):2464–78. doi: 10.4049/jimmunol.1701695
22. Servais A, Noel LH, Roumenina LT, Le Quintrec M, Ngo S, Dragon-Durey MA, et al. Acquired and Genetic Complement Abnormalities Play a Critical Role in Dense Deposit Disease and Other C3 Glomerulopathies. *Kidney Int* (2012) 82(4):454–64. doi: 10.1038/ki.2012.63
23. Smith RJH, Appel GB, Blom AM, Cook HT, D'Agati VD, Fakhouri F, et al. C3 Glomerulopathy - Understanding a Rare Complement-Driven Renal Disease. *Nat Rev Nephrol* (2019) 15(3):129–43. doi: 10.1038/s41581-018-0107-2
24. Sethi S, Gamez JD, Vrana JA, Theis JD, Bergen HR3rd, Zipfel PF, et al. Glomeruli of Dense Deposit Disease Contain Components of the Alternative and Terminal Complement Pathway. *Kidney Int* (2009) 75(9):952–60. doi: 10.1038/ki.2008.657
25. Hou J, Markowitz GS, Bomback AS, Appel GB, Herlitz LC, Barry Stokes M, et al. Toward a Working Definition of C3 Glomerulopathy by Immunofluorescence. *Kidney Int* (2014) 85(2):450–6. doi: 10.1038/ki.2013.340
26. Bomback AS, Appel GB. Pathogenesis of the C3 Glomerulopathies and Reclassification of PGNn. *Nat Rev Nephrol* (2012) 8(11):634–42. doi: 10.1038/nrneph.2012.213
27. Berger BE. Atypical Hemolytic Uremic Syndrome: A Syndrome in Need of Clarity. *Clin Kidney J* (2019) 12(3):338–47. doi: 10.1093/ckj/sfy066
28. Bu F, Borsa NG, Jones MB, Takanami E, Nishimura C, Hauer JJ, et al. High-Throughput Genetic Testing for Thrombotic Microangiopathies and C3 Glomerulopathies. *J Am Soc Nephrol* (2016) 27(4):1245–53. doi: 10.1681/ASN.2015040385
29. Zhang Y, Nester CM, Martin B, Skjoedt MO, Meyer NC, Shao D, et al. Defining the Complement Biomarker Profile of C3 Glomerulopathy. *Clin J Am Soc Nephrol* (2014) 9(11):1876–82. doi: 10.2215/CJN.01820214
30. Bu F, Zhang Y, Wang K, Borsa NG, Jones MB, Taylor AO, et al. Genetic Analysis of 400 Patients Refines Understanding and Implicates a New Gene in Atypical Hemolytic Uremic Syndrome. *J Am Soc Nephrol* (2018) 29(12):2809–19. doi: 10.1681/ASN.2018070759
31. Zhang Y, Meyer NC, Wang K, Nishimura C, Frees K, Jones M, et al. Causes of Alternative Pathway Dysregulation in Dense Deposit Disease. *Clin J Am Soc Nephrol* (2012) 7(2):265–74. doi: 10.2215/CJN.07900811
32. Martin Merinero H, Zhang Y, Arjona E, Del Angel G, Goodfellow R, Gomez-Rubio E, et al. Functional Characterization of 105 Factor H Variants Associated With Atypical Hus: Lessons for Variant Classification. *Blood* (2021) 138(22):2185–201. doi: 10.1182/blood.2021012037
33. Karczewski KJ, Francioli LC, Tiao G, Cummings BB, Alfoldi J, Wang Q, et al. The Mutational Constraint Spectrum Quantified From Variation in 141,456 Humans. *Nature* (2020) 581(7809):434–43. doi: 10.1038/s41586-020-2308-7
34. Ponce-Castro IM, Gonzalez-Rubio C, Delgado-Cervino EM, Abarrategui-Garrido C, Fontan G, Sanchez-Corral P, et al. Molecular Characterization of Complement Factor I Deficiency in Two Spanish Families. *Mol Immunol* (2008) 45(10):2764–71. doi: 10.1016/j.molimm.2008.02.008
35. Kaiser JP, Oppermann M, Gotze O, Deppisch R, Gohl H, Asmus G, et al. Significant Reduction of Factor D and Immunosuppressive Complement Fragment Ba by Hemofiltration. *Blood Purif* (1995) 13(6):314–21. doi: 10.1159/000170215
36. Zhang Y, Keenan A, Dai DF, May KS, Anderson EE, Lindorfer MA, et al. C3 (H2O) Prevents Rescue of Complement-Mediated C3 Glomerulopathy in Cfh-/- Cfd-/- Mice. *JCI Insight* (2020) 5(9):e135758. doi: 10.1172/jci.insight.135758

37. Tan PL, Garrett ME, Willer JR, Campochiaro PA, Campochiaro B, Zack DJ, et al. Systematic Functional Testing of Rare Variants: Contributions of Cfi to Age-Related Macular Degeneration. *Invest Ophthalmol Vis Sci* (2017) 58 (3):1570–6. doi: 10.1167/iovs.16-20867
38. Geerlings MJ, Volokhina EB, de Jong EK, van de Kar N, Pauper M, Hoyng CB, et al. Genotype-Phenotype Correlations of Low-Frequency Variants in the Complement System in Renal Disease and Age-Related Macular Degeneration. *Clin Genet* (2018) 94(3-4):330–8. doi: 10.1111/cge.13392
39. Seddon JM, Yu Y, Miller EC, Reynolds R, Tan PL, Gowrisankar S, et al. Rare Variants in Cfi, C3 and C9 Are Associated With High Risk of Advanced Age-Related Macular Degeneration. *Nat Genet* (2013) 45(11):1366–70. doi: 10.1038/ng.2741
40. Lambris JD. The Multifunctional Role of C3, the Third Component of Complement. *Immunol Today* (1988) 9(12):387–93. doi: 10.1016/0167-5699(88)91240-6
41. Zhang Y, Ghiringhelli Borsa N, Shao D, Dopler A, Jones MB, Meyer NC, et al. Factor H Autoantibodies and Complement-Mediated Diseases. *Front Immunol* (2020) 11:607211. doi: 10.3389/fimmu.2020.607211
42. de Jong S, Volokhina EB, de Breuk A, Nilsson SC, de Jong EK, van der Kar N, et al. Effect of Rare Coding Variants in the Cfi Gene on Factor I Expression Levels. *Hum Mol Genet* (2020) 29(14):2313–24. doi: 10.1093/hmg/ddaa114
43. Fritsche LG, Igl W, Bailey JN, Grassmann F, Sengupta S, Bragg-Gresham JL, et al. A Large Genome-Wide Association Study of Age-Related Macular Degeneration Highlights Contributions of Rare and Common Variants. *Nat Genet* (2016) 48(2):134–43. doi: 10.1038/ng.3448
44. Szarvas N, Szilagyi A, Csuka D, Takacs B, Rusai K, Muller T, et al. Genetic Analysis and Functional Characterization of Novel Mutations in a Series of Patients With Atypical Hemolytic Uremic Syndrome. *Mol Immunol* (2016) 71:10–22. doi: 10.1016/j.molimm.2016.01.003
45. Bienaime F, Dragon-Durey MA, Regnier CH, Nilsson SC, Kwan WH, Blouin J, et al. Mutations in Components of Complement Influence the Outcome of Factor I-Associated Atypical Hemolytic Uremic Syndrome. *Kidney Int* (2010) 77(4):339–49. doi: 10.1038/ki.2009.472
46. Maga TK, Nishimura CJ, Weaver AE, Frees KL, Smith RJ. Mutations in Alternative Pathway Complement Proteins in American Patients With Atypical Hemolytic Uremic Syndrome. *Hum Mutat* (2010) 31(6):E1445–60. doi: 10.1002/humu.21256
47. Fakhouri F, Roumenina L, Provot F, Sallee M, Caillard S, Couzi L, et al. Pregnancy-Associated Hemolytic Uremic Syndrome Revisited in the Era of Complement Gene Mutations. *J Am Soc Nephrol* (2010) 21(5):859–67. doi: 10.1681/ASN.2009070706
48. Garg N, Zhang Y, Nicholson-Weller A, Khankin EV, Borsa NG, Meyer NC, et al. C3 Glomerulonephritis Secondary to Mutations in Factors H and I: Rapid Recurrence in Deceased Donor Kidney Transplant Effectively Treated With Eculizumab. *Nephrol Dial Transplant* (2018) 33(12):2260–5. doi: 10.1093/ndt/gfx369
49. Martinez-Barricarte R, Heurich M, Lopez-Perrote A, Tortajada A, Pinto S, Lopez-Trascasa M, et al. The Molecular and Structural Bases for the Association of Complement C3 Mutations With Atypical Hemolytic Uremic Syndrome. *Mol Immunol* (2015) 66(2):263–73. doi: 10.1016/j.molimm.2015.03.248
50. Roumenina LT, Frimat M, Miller EC, Provot F, Dragon-Durey MA, Bordereau P, et al. A Prevalent C3 Mutation in Ahus Patients Causes a Direct C3 Convertase Gain of Function. *Blood* (2012) 119(18):4182–91. doi: 10.1182/blood-2011-10-383281

Conflict of Interest: The authors declare that the research was conducted in the absence of any commercial or financial relationships that could be construed as a potential conflict of interest.

Publisher's Note: All claims expressed in this article are solely those of the authors and do not necessarily represent those of their affiliated organizations, or those of the publisher, the editors and the reviewers. Any product that may be evaluated in this article, or claim that may be made by its manufacturer, is not guaranteed or endorsed by the publisher.

Copyright © 2022 Zhang, Goodfellow, Ghiringhelli Borsa, Dunlop, Presti, Meyer, Shao, Roberts, Jones, Pitcher, Taylor, Nester and Smith. This is an open-access article distributed under the terms of the Creative Commons Attribution License (CC BY). The use, distribution or reproduction in other forums is permitted, provided the original author(s) and the copyright owner(s) are credited and that the original publication in this journal is cited, in accordance with accepted academic practice. No use, distribution or reproduction is permitted which does not comply with these terms.

frontiers | Frontiers in Immunology

TYPE Original Research
PUBLISHED 20 September 2022
DOI 10.3389/fimmu.2022.941742

Check for updates

OPEN ACCESS

EDITED BY
Per Nilsson,
Linnaeus University, Sweden

REVIEWED BY
Marina Noris,
Mario Negri Pharmacological Research Institute (IRCCS), Italy
Kavitha Mukund,
University of California, San Diego, United States

*CORRESPONDENCE
Michael Osthoff
michael.osthoff@usb.ch

†These authors have contributed equally to this work and share last authorship

SPECIALTY SECTION
This article was submitted to Molecular Innate Immunity, a section of the journal Frontiers in Immunology

RECEIVED 11 May 2022
ACCEPTED 29 August 2022
PUBLISHED 20 September 2022

CITATION
Bruni F, Charitos P, Lampart M, Moser S, Siegemund M, Bingisser R, Osswald S, Bassetti S, Twerenbold R, Trendelenburg M, Rentsch KM and Osthoff M (2022) Complement and endothelial cell activation in COVID-19 patients compared to controls with suspected SARS-CoV-2 infection: A prospective cohort study. *Front. Immunol.* 13:941742. doi: 10.3389/fimmu.2022.941742

COPYRIGHT
© 2022 Bruni, Charitos, Lampart, Moser, Siegemund, Bingisser, Osswald, Bassetti, Twerenbold, Trendelenburg, Rentsch and Osthoff. This is an open-access article distributed under the terms of the Creative Commons Attribution License (CC BY). The use, distribution or reproduction in other forums is permitted, provided the original author(s) and the copyright owner(s) are credited and that the original publication in this journal is cited, in accordance with accepted academic practice. No use, distribution or reproduction is permitted which does not comply with these terms.

Complement and endothelial cell activation in COVID-19 patients compared to controls with suspected SARS-CoV-2 infection: A prospective cohort study

Flavio Bruni[1], Panteleimon Charitos[1], Maurin Lampart[2], Stephan Moser[1], Martin Siegemund[3], Roland Bingisser[4], Stefan Osswald[2], Stefano Bassetti[1], Raphael Twerenbold[2,5], Marten Trendelenburg[1], Katharina M. Rentsch[6†] and Michael Osthoff[1*†]

[1]Division of Internal Medicine, Department of Biomedicine and Department of Clinical Research, University Hospital Basel, University of Basel, Basel, Switzerland, [2]Department of Cardiology and Cardiovascular Research Institute Basel (CRIB), University Hospital Basel, University of Basel, Basel, Switzerland, [3]Intensive Care Unit, University Hospital Basel, Basel, Switzerland, [4]Emergency Department, University Hospital Basel, Basel, Switzerland, [5]University Center of Cardiovascular Science & Department of Cardiology, University Heart and Vascular Center Hamburg, University Medical Center Hamburg-Eppendorf, Hamburg, Germany, [6]Laboratory Medicine, University Hospital Basel, Basel, Switzerland

Background: Thromboinflammation may influence disease outcome in COVID-19. We aimed to evaluate complement and endothelial cell activation in patients with confirmed COVID-19 compared to controls with clinically suspected but excluded SARS-CoV-2 infection.

Methods: In a prospective, observational, single-center study, patients presenting with clinically suspected COVID-19 were recruited in the emergency department. Blood samples on presentation were obtained for analysis of C5a, sC5b-9, E-selectin, Galectin-3, ICAM-1 and VCAM-1.

Results: 153 cases and 166 controls (suffering mainly from non-SARS-CoV-2 respiratory viral infections, non-infectious inflammatory conditions and bacterial pneumonia) were included. Hospital admission occurred in 62% and 45% of cases and controls, respectively. C5a and VCAM-1 concentrations were significantly elevated and E-selectin concentrations decreased in COVID-19 out- and inpatients compared to the respective controls. However, relative differences in outpatients vs. inpatients in most biomarkers were comparable between cases and controls. Elevated concentrations of C5a, Galectin-3, ICAM-1 and VCAM-1 on presentation were associated with the composite outcome of ICU- admission or 30-day mortality in COVID-19 and controls, yet more pronounced in COVID-19. C5a and sC5b-9 concentrations were

significantly higher in COVID-19 males vs. females, which was not observed in the control group.

Conclusions: Our data indicate an activation of the complement cascade and endothelium in COVID-19 beyond a nonspecific inflammatory trigger as observed in controls (i.e., "over"-activation).

KEYWORDS

COVID-19, complement system, endothelial cells, SARS-CoV-2, ICAM-1, VCAM-1, E-Selectin, galectin-3

Introduction

Coronavirus disease 2019 (COVID-19) includes a variety of clinical pictures ranging from oligosymptomatic upper airway disease to severe disease presenting with a hyperinflammatory state and leading to acute respiratory distress syndrome in up to 31% of the patients (1). Thromboinflammation is a hallmark of COVID-19 and has a major impact on COVID-19 morbidity and mortality (2). Both, activation of the complement system and endothelial cell dysfunction after SARS-CoV-2 infection have been identified as important contributors (3).

The complement system is a central part of the innate immune response. Its activation has been demonstrated upon viral infections and its importance in the immune defense is underscored by strategies of viruses to disable and exploit complemental activation (4). SARS-CoV-2 was shown to directly activate both, the alternative and the lectin pathway of the complement system (5–7), and also the classical pathway *via* SARS-CoV-2 antibodies (8). Besides its beneficial effects, overactivation of complement may result in host damage. Improved outcome and reduced pulmonary tissue damage was demonstrated in murine models upon coronavirus infection, when complement system activation was blocked (9). Histopathology findings revealed extensive deposits of complement components C5b-9, C4d, and mannose-binding lectin serine protease 2 (MASP-2) in COVID-19 patients who died of respiratory failure (10). A subset of clinical studies reported elevated complement activation products in sera of COVID-19 patients that positively correlated with disease severity and were associated with adverse outcomes (11), but comparative data in disease controls are scarce.

Various pathways are involved in endothelial cell activation in COVID-19. Complement components C5a and C5b-9 were shown to induce downstream thromboinflammatory responses, resulting in endothelial activation and damage (12, 13). SARS-CoV-2 tropism for endothelial cells is suggested to further contribute to endothelial activation and dysfunction (14, 15) causing thromboembolism, tissue ischemia and impaired barrier function (10, 16). Upon infection and activation, endothelial surface adhesion molecules E-selectin, intercellular cell adhesion molecule-1 (ICAM-1) and vascular cell adhesion molecule-1 (VCAM-1) are upregulated. E-selectin mediates rolling of leucocytes while ICAM-1 and VCAM-1 are further involved in firm leucocyte adhesion (17, 18) initiating their transendothelial migration to the site of inflammation. Soluble forms of ICAM-1, VCAM-1 and E-selectin are used as biomarkers for endothelial cell activation, and several studies demonstrate increased concentrations of these proteins in COVID-19 patients related to the disease severity (19–21).

A prothrombotic state is the result of an inflammatory feedback loop secondary to complement activation, endothelial cell injury and hypercoagulability (4). Therefore, the interaction between complement and endothelial cell activation is of interest, considering possible therapeutic options in COVID-19 (16, 22, 23). Male sex is a relevant risk factor for mortality in COVID-19 (24) and higher levels of chemokines and cytokines that firmly interact with the complement system (25, 26) were found in male COVID-19 patients vs females (27). Thus, therapeutic options may differ between males and females, respectively.

Another regulator of the inflammatory-associated immune response is Galectin-3, a member of the beta-galactoside binding-protein family with pleiotropic effects, including cell-proliferation, apoptotic regulation and fibrosis (28). Preliminary evidence implies a role for galectin-3 as biomarker and target in COVID-19 due to its upregulation in severe COVID-19 (29, 30) and potential mediator for viral adhesion (31).

Although elevated markers of complement and endothelial activation as well as elevated Galectin-3 concentrations were demonstrated in COVID-19 patients, most studies compared

cases with healthy controls, and therefore may overestimate the specificity of the innate immune response upon SARS-CoV-2 infection.

In this prospective cohort study, we primarily evaluated specificity and possible interactions of complement activation and markers of endothelial cell activation in COVID-19 patients by comparing cases to a control population with symptoms suggestive of COVID-19 but tested negative for SARS-CoV-2 infection. Secondarily we analyzed associations of markers with adverse outcomes and investigated patterns of marker activation as well as sex differences in cases and controls.

Materials and methods

Patient inclusion, sample collection and data extraction

The COVIVA study was a prospective, observational cohort study that recruited unselected patients aged 18 years and older presenting with symptoms consistent with COVID-19 to the emergency department (ED) of the University Hospital Basel, Switzerland, from March 2020 to June 2020. Patients were considered SARS-CoV-2 infected if at least one SARS-CoV-2 PCR from a nasopharyngeal swab performed at ED presentation or within 14 days prior to or after was positive in combination with consistent clinical signs and symptoms. Patients that were tested negative for SARS-CoV-2 infection by PCR were considered as controls. Adjudication of the final (non-COVID-19) diagnosis was performed by five board-certified physicians that reviewed all medical data available including 30 days post-discharge follow-up information.

All patients underwent a clinical assessment by the treating ED physician according to local standard operating procedures. We obtained blood samples within 24 hours after presentation to the ED. Samples were transferred to the laboratory immediately after sampling, centrifuged, aliquoted and stored at −80°C until measurement.

Patients were contacted by telephone or in written form 30 days after discharge for follow-up. Records of hospitals and primary care physicians as well as national death registries were screened, if applicable.

For the present analysis, blood samples with sufficient residual volume to determine the investigational biomarkers were available from 153/191 COVID-19 patients, which served as cases. Subsequently samples from 166/890 SARS-CoV-2 negative patients were randomly selected to serve as controls. Overall, the numbers of available samples for C5a, sC5b-9, E-selectin, Galectin-3, ICAM-1 and VCAM-1 were 302, 302, 290, 289, 290 and 290, respectively.

Laboratory assessment

Concentrations of ICAM-1, VCAM-1, Galectin-3 and E-selectin in serum samples were determined by a multiplexed enzyme-linked immunosorbent assay according to the manufacturer's instruction (proteinsimple, Bio-techne, Minneapolis, MN, U.S.A.). C5a and sC5b-9 concentrations were quantified using enzyme-linked immunosorbent assay (ELISA) kits according to the manufacturer's instruction (sC5b-9: BD Biosciences Pharmingen, San Diego, CA, U.S.A.; C5a: ThermoFisher Scientific, Waltham, MA, U.S.A.).

Primary and secondary endpoints

Primary endpoint of this study was the comparison of the systemic concentration of complement activation products (C5a, C5b-9), endothelial activation markers (ICAM-1, VCAM-1, E-selectin) and Galectin-3 in COVID-19 patients and in patients with suspected but excluded SARS-CoV-2 infection, in the out- and inpatient setting.

Secondary endpoints included the association of markers with the composite endpoint of admission to the intensive care unit (ICU) or death within a 30-day follow-up period and with thromboembolic events. Correlations with other laboratory inflammatory markers and sex differences were also analyzed.

Statistical analysis

Statistical analyses were performed using SPSS software, version 25 (IBM, USA), and data were visualized with GraphPad Prism 7 software (GraphPadSoftwares Inc., La Jolla, Ca, USA). Data are expressed as medians and interquartile range (IQR) for continuous variables, and as numbers and percentages (%) for categorical variables. Continuous variables showed mostly skewed distributions and were compared by Mann-Whitney U test, and Spearman's rank test was used to evaluate correlations. For nominal variables Chi-squared test and Fisher's exact test was used.

Ethics statement

All participating patients or their legally authorized representatives consented by signing a local general consent form. This study was conducted according to the principles of the Declaration of Helsinki and approved by the Ethics Committee of Northwestern and Central Switzerland (EKNZ 2020-00566).

10.3389/fimmu.2022.941742

Results

Baseline characteristics in COVID-19 cases and controls

Overall, 1086 patients were recruited presenting with symptoms suspicious for COVID-19 from March 2020 to June 2020, and 153/191 COVID-19 and 166/890 randomly selected controls were included in the present analysis. Hospital admission was required in 95 (62%) and 75 (45%) of COVID-19 patients and controls, respectively. Admission to the ICU or death at day 30 occurred in 41 (43%) inpatient cases and 27 (36%) inpatient controls. COVID-19 inpatients were younger than inpatient controls (median age 64 [52, 75] vs. 71 [59, 80] years, p=0.02) and stayed longer in the hospital (8 [5.0, 15.0] vs. 5 [2.0, 11.0] days, p=0.01). Controls suffered mainly from viral infections other than COVID-19 (n = 67, 40%), non-infectious inflammatory conditions (n=40, 25%) and bacterial pneumonia (n = 24, 14%). The demographic and clinical characteristics of the two groups are shown in Table 1.

TABLE 1 Baseline characteristics.

Variables	Outpatients			Inpatients		
	COVID-19 (n = 58)	Controls (n = 91)	P value	COVID-19 (n = 95)	Controls (n = 75)	P value
	Demographics					
Age, years	47 (35 - 59)	46 (32 - 59)	0.661	64 (52 - 75)	71 (59 - 80)	**0.020**
Male gender	31 (53)	53 (58)	0.565	61 (64)	42 (56)	0.277
	Comorbidities					
Cardiac disease	5 (9)	12 (13)	0.393	29 (31)	37 (49)	**0.012**
Hypertension	13 (22)	30 (33)	0.166	54 (57)	45 (60)	0.678
Pulmonary disease	11 (19)	29 (32)	0.083	19 (20)	22 (29)	0.158
- Asthma	10 (17)	20 (22)	0.482	8 (8)	5 (7)	0.669
- COPD	0 (0)	6 (7)	0.082	8 (8)	11 (15)	0.199
Active or previous smoker	16 (28)	36 (40)	0.135	36 (38)	31 (41)	0.649
Chronic kidney disease	0 (0)	2 (2)	0.521	24 (25)	28 (37)	0.090
Diabetes mellitus	3 (5)	7 (8)	0.741	28 (30)	17 (23)	0.318
Immunodeficiency	2 (3)	6 (7)	0.484	6 (6)	7 (9)	0.462
Cancer	4 (7)	1 (1)	0.076	10 (11)	10 (13)	0.573
	Symptoms and scores at ED					
Cough	41 (71)	63 (69)	0.850	60 (63)	36 (48)	**0.048**
Dyspnea	23 (40)	53 (58)	**0.027**	40 (42)	41 (55)	0.103
Blood oxygen saturation, %	98 (97-99)	98 (97 - 99)	0.378	95 (93 - 97)	96 (95 - 98)	**0.007**
NEWS score	1 (0 - 3)	1 (0 - 2)	0.079	4 (2 - 6)	3 (3 - 6)	0.347
Time from first symptom to ED presentation, days	7 (3 - 14)	5 (2 - 10)	**0.021**	7 (3 - 11)	6 (1-6)	**<0.001**
	Laboratory findings					
CRP, mg/L	2.1 (0.9 – 11.0)	1.2 (0.5 - 6.8)	**0.049**	70.1 (32.8 – 145.7)	49.8 (8.2 – 114.9)	0.053
D-Dimer, mg/L	0.38 (0.29 - 0.65)	0.29 (0.29 - 0.39)	**<0.001**	0.87 (0.51 - 2.00)	1.21 (0.63 - 3.46)	0.134
Ferritin, µg/L	205 (99 – 395)	137 (76 – 248)	**0.020**	720 (374 – 1238)	273 (114 – 667)	**<0.001**
Leukocytes, G/L	5.8 (4.5 - 7.0)	8.1 (6.3 - 10)	**<0.001**	6.7 (5.1 - 8.9)	11.1 (8.3 - 14.8)	**<0.001**
Lymphocytes, G/L	1.37 (0.96 - 1.97)	1.80 (1.45 - 2.54)	**<0.001**	0.95 (0.61 - 1.26)	1.02 (0.76 - 1.42)	0.084
LDH, U/L	206 (178 – 236)	199 (179 – 227)	0.453	325 (257 – 447)	236 (190 – 362)	**<0.001**
eGFR, mL/min/1.73m^2	99 (89 – 111)	99 (83 – 113)	0.962	78 (49 – 97)	69 (41 – 96)	0.591
	Patient management and outcomes					
Length of hospital stay, days	0	0		8.0 (5.0 – 15.0)	5.0 (2.0 – 11.0)	**0.010**
ICU admission or death within 30 days	0	0		41 (43)	27 (36)	0.327
Intubation	0	0		29 (31)	18 (24)	0.345
Intubation, days	0	0		9.0 (5.5 – 12.5)	3.0 (1.0 – 7.3)	0.088

Data are expressed in numbers (percentage) or median (interquartile range). Values are shown in bold in case of significant difference.
COPD, chronic obstructive pulmonary disease; NEWS score, National Early Warning Score; ED, emergency department; CRP, C-reactive protein; LDH, lactate dehydrogenase; eGFR, estimated glomerular filtration rate; ICU, intensive care unit.

Serum levels of Galectin-3, complement and endothelial cell activation markers in COVID-19 cases and controls

Overall, C5a and VCAM-1 concentrations were elevated and E-selectin concentrations decreased in COVID-19 cases compared to controls (p<0.001 for all markers, Table 2) with a borderline difference in sC5b-9 levels (p=0.037). These differences were also evident when outpatients and inpatients were separately analyzed with the exception of sC5b-9 in the outpatient group (Table 2). Similarly, control patients with a diagnosis of bacterial pneumonia or other respiratory viral infections showed lower C5a and VCAM-1 concentrations compared to COVID-19 cases despite a slightly higher CRP concentration, whereas an increase in E-selectin concentrations was mainly observed in patients with bacterial pneumonia and was less pronounced in patients with other respiratory viral infections (Supplementary Tables 1, 2). No significant differences in ICAM-1 and Galectin-3 levels were observed in any analyses.

Almost all markers were significantly elevated in inpatients vs. outpatients in both groups, and relative increases in inpatients vs. outpatients were comparable in cases and controls (Table 3).

Association of Galectin-3, complement and endothelial cell activation markers with outcomes

Overall, elevated concentrations of C5a, Galectin-3, ICAM-1 and VCAM-1 levels on presentation were associated with the composite outcome of ICU admission or 30-day mortality in cases and controls (Table 4), as were concentrations of D-Dimer and the inflammatory markers C-reactive protein (CRP) and ferritin. However, when focusing only on inpatients (the composite outcome did not occur in outpatients), elevated concentrations of these activation markers were only predictive of the composite outcome in cases, but not in controls (Supplementary Table 3).

In patients with the composite outcome, concentrations of most markers were significantly higher in COVID-19 cases compared to controls with the exception of D-Dimer levels. In particular, median C5a and ferritin concentrations were markedly elevated (C5a, 4.46 ng/ml in COVID-19 cases vs 1.46 ng/mL in controls, p<0.001; ferritin, 1200 µg/L vs. 256 µg/L, p<0.001).

The analysis of thromboembolic events was limited by the low number of events (n=13). Increased median Galectin-3 and ICAM-1 levels were associated with thromboembolic events in both, cases and controls (Supplementary Table 4), whereas associations of increased median C5a and E-selectin concentrations with thromboembolic events were only observed in controls.

Correlations of Galectin-3, markers of complement and endothelial cell activation and inflammation

C5a levels correlated moderately with markers of endothelial cell activation and Galectin-3 in both, COVID-19 cases and controls, whereas the correlation was weaker for sC5b-9 (Figures 1A, B). C5a, ICAM-1, VCAM-1 and Galectin-3 correlated moderately to strongly with CRP and D-Dimer concentrations in cases and controls, whereas correlation with ferritin and LDH was much weaker in controls. E-selectin correlated strongly with ICAM-1 and VCAM-1 in controls

TABLE 2 Concentrations of markers of complement and endothelial cell activation on admission.

Variable	Overall			Outpatients			Inpatients		
	COVID-19 (n=153)	Controls (n=166)	P value	COVID-19 (n=58)	Controls (n=91)	P value	COVID-19 (n=95)	Controls (n=75)	P value
C5a, ng/ml	3.23 (1.46 – 5.95)	0.91 (0.41 – 1.93)	**<0.001**	1.69 (0.93 - 3.61)	0.57 (0.11 – 1.28)	**<0.001**	4.20 (2.31 – 7.05)	1.46 (0.78 – 2.75)	**<0.001**
sC5b-9, ng/ml	1139 (720 – 1679)	992 (744 – 1315)	**0.037**	1001 (642 - 1364)	954 (719 – 1277)	0.922	1268 (783 – 1905)	1019 (792 – 1391)	**0.026**
E-selectin, ng/ml	25.1 (17.6 – 34.6)	30.5 (22.4 -42.4)	**<0.001**	22.0 (14.5 – 32.1)	28.1 (19.8 -39.9)	**0.005**	26.6 (19.2 – 37.9)	36.8 (25.3 – 51.1)	**0.001**
Galectin-3, ng/ml	9.3 (7.1 – 12.3)	8.5 (6.9 – 10.8)	0.100	7.3 (6.0 – 8.2)	7.5 (6.4 – 9.5)	0.239	11.5 (8.4 – 14.2)	10.6 (8.2 – 12.6)	0.174
ICAM-1, ng/ml	386 (319 -497)	374 (292 – 500)	0.340	330 (279 – 403)	321 (281 – 421)	0.866	442 (353 – 544)	456 (366 – 590)	0.387
VCAM-1, ng/ml	961 (675 – 1434)	625 (493 – 853)	**<0.001**	677 (556 – 862)	532 (445 – 654)	**<0.001**	1276 (908 – 1566)	840 (662 – 1229)	**<0.001**

Median (interquartile range), values are shown in bold in case of significant difference.

10.3389/fimmu.2022.941742

TABLE 3 Relative differences in inpatients vs. outpatients.

Variable	Relative difference COVID-19*	P value	Relative difference Controls*	P value	Δ relative differences cases vs. controls in %
C5a	↑ 2.5	<0.001	↑ 2.6	**<0.001**	-3
C5b-9	↑ 1.3	0.003	↔ 1.1	0.343	19
E-Selectin	↑ 1.2	0.016	↑ 1.3	**0.003**	-8
Galectin-3	↑ 1,6	<0.001	↑ 1.4	**<0.001**	12
ICAM-1	↑ 1.3	<0.001	↑ 1.4	**<0.001**	-6
VCAM-1	↑ 1.9	<0.001	↑ 1.6	**<0.001**	19

*Arrows indicate direction, numbers indicate factor of elevation in in- vs. outpatients. Values are shown in bold in case of significant difference.

(r= 0.602 and r = 0.468, p<0.01), while a weaker correlation was found in cases (r = 0.477 and r = 0.258, p<0.01).

Higher levels of complement and inflammatory markers in males vs. females (inpatients)

Both, median C5a and sC5b-9 concentrations were higher in COVID-19 males vs. females (C5a, 4.62 vs. 3.46 ng/ml, p=0.019; sCb5-9, 1476 ng/ml vs 859 ng/mL, p=0.008) which was not observed in the control group. Ferritin was significantly higher in males vs. females in both, COVID 19 cases and controls, whereas significantly higher CRP levels in males vs. females were only observed in COVID-19 cases (Table 5). Endothelial cell activation markers were similarly distributed with the exception of higher VCAM-1 levels in COVID-19 males vs. females (data not shown).

Discussion

Thromboinflammation has been shown to contribute substantially to the pathogenesis and disease severity in COVID-19 (2). The present study is the largest study to date to assess complement activation markers C5a, C5b-9 as well as endothelial cell activation markers E-selectin, ICAM-1 and VCAM-1 and Galectin-3, an immunoregulatory protein, in COVID-19 cases and SARS-CoV-2 negative controls with similar symptoms and presentation. With few exceptions (32, 33), most previous studies had chosen healthy individuals as controls, thereby potentially overestimating the specificity of those biomarkers for COVID-19.

Indeed, while concentrations of C5a and VCAM-1 were higher and E-selectin concentrations lower in COVID-19 cases vs. the respective controls, the relative difference when comparing inpatients vs. outpatients was comparable in cases and controls. Moreover, these markers correlated equally well with other inflammatory proteins such as CRP or D-Dimer. This is consistent with an unspecific increase of complement and endothelial cell activation depending on severity. As such the increase in complement and endothelial cell activation may be regarded as nonspecific for SARS-CoV-2 and rather reflect the clinical picture it causes.

However, despite a similar degree of inflammation (as assessed by CRP and D-Dimer levels), C5a and VCAM-1 concentrations were significantly higher and E-selectin concentrations significantly lower in COVID-19 cases

TABLE 4 Concentrations of markers of complement and endothelial cell activation and inflammation on admission according to the composite outcome of admission to the intensive care unit or death at 30 days in cases and controls.

	COVID-19, composite outcome			Controls, composite outcome		
Variables	Yes (n=41)	No (n=112)	P value	Yes (n=27)	No (n=139)	P value
C5a, ng/ml	4.46 (3.31 – 7.61)	2.52 (1.38 – 5.55)	**0.001**	1.46 (0.80 – 2.16)	0.82 (0.27 – 1.76)	**0.024**
sC5b-9, ng/ml	1244 (767 – 1929)	1110 (709 – 1533)	0.119	955 (783 – 1131)	1000 (733 – 1333)	0.79
E-selectin, ng/ml	30.9 (19.7 – 47.9)	24.0 (17.4 – 34.1)	0.059	36.8 (25.5 – 59.2)	29.8 (21.9 – 41.6)	0.064
Galectin-3, ng/ml	12.1 (10.3 – 15.9)	8.1 (6.5 – 11.3)	**<0.001**	10.9 (8.3 – 14.2)	8.0 (6.7 – 10.5)	**0.005**
ICAM-1, ng/ml	486 (377 – 662)	366 (301 – 472)	**<0.001**	452 (380 – 614)	358 (289 – 478)	**0.003**
VCAM-1, ng/ml	1323 (1029 – 1699)	835 (654 – 1329)	**<0.001**	863 (678 – 1340)	591 (483 – 797)	**0.001**
CRP, mg/L	112 (48 – 163)	16.9 (1.5 – 52.3)	**<0.001**	57.3 (30.4 – 127.4)	3.2 (0.6 – 33.0)	**<0.001**
D-Dimer, mg/L	1.16 (0.53 – 2.84)	0.52 (0.34 – 1.08)	**0.002**	1.41 (0.56 – 4.89)	0.37 (0.29 – 0.89)	**<0.001**
Ferritin, µg/L	1200 (445 – 2055)	351 (151 – 633)	**<0.001**	256 (115 – 865)	161 (80 – 310)	**0.039**

Median (interquartile range), values are shown in bold in case of significant difference.
CRP, C-reactive protein.

A

	C5a	sC5b-9	E-selectin	Galectin-3	ICAM-1	VCAM-1	CRP	Ferritin	D-Dimer	Leuko-cytes	Lympho-cytes	LDH
C5a	1	0.738*	0.140	0.451*	0.409*	0.367*	0.516*	0.515*	0.434*	0.237*	-0.279*	0.516*
sC5b-9	0.738*	1	0.131	0.275*	0.342*	0.165	0.327*	0.336*	0.259*	0.217*	-0.067	0.355*
E-selectin	0.140	0.131	1	0.251*	0.477*	0.258*	0.312*	0.278*	0.070	0.357*	-0.072	0.289*
Galectin-3	0.451*	0.275*	0.251*	1	0.527*	0.401*	0.587*	0.535*	0.588*	0.386*	-0.190*	0.676*
ICAM-1	0.409*	0.342*	0.477*	0.527*	1	0.508*	0.616*	0.511*	0.451*	0.322*	-0.225*	0.507*
VCAM-1	0.367*	0.165	0.258*	0.401*	0.508*	1	0.723*	0.596*	0.435*	0.105	-0.589*	0.607*
CRP	0.516*	0.327*	0.312*	0.587*	0.616*	0.723*	1	0.703*	0.558*	0.300*	-0.491*	0.721*
Ferritin	0.515*	0.336*	0.278*	0.535*	0.511*	0.596*	0.703*	1	0.483*	0.288*	-0.371*	0.639*
D-Dimer	0.434*	0.259*	0.070	0.588*	0.451*	0.435*	0.558*	0.483*	1	0.240*	-0.324*	0.595*
Leuko-cytes	0.237*	0.217*	0.357*	0.386*	0.322*	0.105	0.300*	0.288*	0.240*	1	0.121	0.328
Lympho-cytes	-0.279*	-0.067	-0.072	-0.190*	-0.225*	-0.589*	-0.491*	-0.371*	-0.324*	0.121	1	-0.365*
LDH	0.516*	0.355*	0.289*	0.676*	0.507*	0.607*	0.721*	0.639*	0.595*	0.328	-0.365*	1

B

	C5a	sC5b-9	E-selectin	Galectin-3	ICAM-1	VCAM-1	CRP	Ferritin	D-Dimer	Leuko-cytes	Lympho-cytes	LDH
C5a	1	0.464*	0.302*	0.340*	0.414*	0.437*	0.637*	0.290*	0.435*	0.207*	-0.311*	0.197*
sC5b-9	0.464*	1	0.214*	0.090	0.201*	0.164*	0.325*	0.215*	0.177*	0.029	-0.026	-0.050
E-selectin	0.302*	0.214*	1	0.400*	0.602*	0.468*	0.446*	0.155	0.263*	0.272*	0.036	0.164
Galectin-3	0.340*	0.090	0.400*	1	0.536*	0.474*	0.508*	0.062	0.459*	0.210*	-0.297*	0.412*
ICAM-1	0.414*	0.201*	0.602*	0.536*	1	0.704*	0.607*	0.184*	0.545*	0.202*	-0.223*	0.338*
VCAM-1	0.437*	0.164*	0.468*	0.474*	0.704*	1	0.588*	0.322*	0.563*	0.172*	-0.383*	0.342*
CRP	0.637*	0.325*	0.446*	0.508*	0.607*	0.588*	1	0.402*	0.668*	0.457*	-0.308*	0.378*
Ferritin	0.290*	0.215*	0.155	0.062	0.184*	0.322*	0.402*	1	0.425*	0.145	-0.106	0.223*
D-Dimer	0.435*	0.177*	0.263*	0.459*	0.545*	0.563*	0.668*	0.425*	1	0.381*	-0.396*	0.328*
Leuko-cytes	0.207*	0.029	0.272*	0.210*	0.202*	0.172*	0.457*	0.145	0.381*	1	-0.079	0.293*
Lympho cytes	-0.311*	-0.026	0.036	-0.297*	-0.223*	-0.383*	-0.308*	-0.106	-0.396*	-0.079	1	-0.220*
LDH	0.197*	-0.050	0.164	0.412*	0.338*	0.342*	0.378*	0.223*	0.328*	0.293*	-0.220*	1

FIGURE 1
(A) Correlation coefficients in COVID-19 patients. *p<0.01 (Spearman correlation coefficient), CRP, C-reactive protein; LDH, lactate dehydrogenase. **(B)** Correlation coefficients in controls. *p<0.01 (Spearman correlation coefficient), CRP, C-reactive protein; LDH, lactate dehydrogenase.

compared to control patients with bacterial pneumonia pointing towards a differential response in COVID-19 patients. Hence, increased complement and endothelial cell activation seems to be a distinctive feature of COVID-19 that cannot be solely explained by a higher inflammatory response. Interestingly, their correlation with ferritin, a protein that has been identified as a promising outcome predictor in severe COVID-19 (34), was stronger in COVID-19 patients compared to controls again arguing for a specific response of the analyzed markers in SARS-CoV-2 infection.

Recently, Ma et al. (33) showed elevated sC5b-9 in severe COVID-19 compared to those hospitalized with influenza or other forms of acute respiratory failure. Here we demonstrated elevated levels of C5a and sC5b-9 in COVID-19 patients compared to a broad control population in an inpatient and outpatient setting, consisting mostly of patients with viral respiratory infection other than COVID-19, bacterial pneumonia but also with systemic inflammatory response syndromes secondary to non-infectious etiologies. Notably, sC5b-9 was markedly elevated in inpatient cases vs controls (1268 vs 1019 ng/mL, p=0.026) while no relevant difference was found in outpatients. These findings may reflect increasing involvement of sC5b-9 in COVID-19 in severe disease. Histopathologic findings support the hypothesis of C5b-9-mediated endotheliopathy in COVID-19, induced by C5b-9 pore formation on endothelial membrane (35). Our findings underscore the growing evidence (36) of the involvement of the cytolytic complement system in severe COVID-19 and the assumption that the membrane attack complex is a major contributor to observed endotheliopathy.

TABLE 5 Sex differences of complement activation and inflammatory markers in COVID-19 inpatients vs. controls on admission.

	COVID-19			Controls		
Variables	**Male (n = 61)**	**Female (n=34)**	**P value**	**Male (n=42)**	**Female (n=33)**	**P value**
C5a, ng/ml	4.62 (2.67 – 9.15)	3.46 (1.47 – 5.59)	**0.019**	1.91 (0.99 – 4.02)	1.27 (0.43 – 2.06)	0.054
sC5b-9, ng/ml	1476 (816 – 2023)	859 (718 – 1486)	**0.008**	1044 (802 – 1384)	986 (591 – 1449)	0.852
CRP, mg/L	86.7 (35.3 – 169.4)	56.9 (25.3 – 81.5)	**0.025**	56.4 (28.6 – 151)	39.7 (3.7 – 92.2)	0.180
Ferritin, µg/L	930 (511 – 1397)	392 (199 -728)	**<0.001**	463 (174 – 856)	148 (67 – 468)	**0.004**

Median (interquartile range), values are shown in bold in case of significant differences.
CRP, C-reactive protein.

Bauer et al. showed elevated VCAM-1 concentrations, while ICAM-1 and E-selectin did not differ in cases vs. disease controls. In line with these findings, Cugno and Yao (19, 37) showed no difference in E-selectin concentrations between mild to moderate COVID-19 cases and healthy controls. Our results regarding the cellular adhesion molecules are in line with these studies, but we demonstrate markedly lower E-selectin concentrations in cases vs. controls, mostly driven by control patients with bacterial pneumonia. Previous studies reported substantially higher E-selectin concentrations in patients with bacterial sepsis (18). Still, E-selectin concentrations were also higher in outpatient controls with viral respiratory infections compared to COVID-19 cases, and thus a lower degree of E-selectin production may be regarded as specific feature of COVID-19.

Previous studies showed increased Galectin-3 plasma levels in patients with COVID-19 compared to healthy controls (29, 30). In the present study, we did not observe a difference in Galectin-3 concentrations in cases and disease controls. We assume that previous findings of elevated Galectin-3 in patients with COVID-19 compared to healthy controls are not specific for COVID-19 but reflects a nonspecific inflammatory response. However, Galectin-3 binding protein was recently identified as elevated in critically ill COVID-19 patients only (and not in disease controls) and to correlate with complement proteins and regulators (38). Hence, Galectin-3 may be considered as a therapeutic target upon SARS-CoV-2 infection due to its possible role in viral adhesion, and its association with disease severity and adverse outcome as demonstrated in the present study.

Associations of elevated complement and endothelial activation markers with COVID-19 outcome or adverse events were previously described (20, 21, 33, 39–41). At first sight, the association of elevated C5a, ICAM-1 and VCAM-1 concentration on admission with ICU admission or 30-day mortality did not point towards a specific feature of COVID-19, as it was observed in cases and controls in the present study. However, the association was not evident in controls anymore, when focusing on inpatients only. Likewise, the magnitude of C5a elevation was more pronounced in COVID-19 cases progressing towards the composite outcome compared to disease controls. Hence, our data are consistent with an additional activation of the complement system and endothelial cells in COVID-19 beyond a nonspecific baseline inflammatory activation of these systems (i.e., "over"-activation) in COVID-19. This has also been described (and confirmed in the present study) for ferritin levels (42). Although complement activation may serve as predictive marker for adverse outcomes, indicators such as CRP, ferritin or D-Dimer are more convenient, as they are equally associated with adverse outcomes (43) and correlate at least moderately with complement activation.

A relevant risk factor for mortality in COVID-19 is male sex which is not completely explained by a higher prevalence of comorbidities in men (24). Differences in sex chromosome genes (immune response X-linked genes and disease susceptibility genes), sex hormones and expression of ACE2 receptors are discussed as underlying cause of different outcomes in COVID-19 (44). Takahashi et al. found that levels of pro-inflammatory innate immunity chemokines and cytokines, such as IL-8, IL-18 and CCL5 were higher in male patients (27). C5a strongly amplifies IL-8 expression (26) and complement was shown to elicit secretion of IL-18 (25). Mussini et al. suggested that C-reactive protein explains 85% of the different incidence in invasive mechanical ventilation or death between male and females, which was to a lesser extent the case for ferritin and LDH. They proposed a differential activation of the innate immune response, mediated by CRP, to explain the observed sex difference in COVID-19 (45). CRP is known to aggravate the inflammatory response by activating the classical complement pathway culminating in the cleavage of C3 and C5 generating anaphylatoxins such as C5a. We observed higher CRP, C5a and sC5b-9 levels on admission in COVID-19 males compared to females, which was not evident in the control population. These results suggest a different level of activation of the complement system in males vs. females upon SARS-CoV-2 infection. Future studies are required to elucidate if differences in alternative pathway activation in males vs. females, as observed in healthy individuals (46), may drive the observed excessive activation in males and may explain sex difference in clinical outcomes in COVID-19. Of note, an overactivated alternative pathway has recently been implicated in critically ill COVID-19 patients (47).

Our study has several limitations. First, the single-center design limits external validity. Second, COVID-19 cases and controls were not matched, hence some differences were significant suggesting that COVID-19 inpatients may have had less comorbidities. Third, only one sample was drawn on admission for most patients limiting the analysis of the time course of the investigated parameters. As an example, E-selectin concentrations are known to decrease shorty after induction. A major strength of this study is the prospective design with enrolment of consecutive patients presenting to the ED with suspicion of COVID-19 and adjudication of the final diagnosis by five board-certified physicians.

In conclusion, the present study confirms increased complement and endothelial cell activity in COVID-19 patients compared to disease controls. Our data are consistent with an additional activation of the complement cascade and endothelial cells in COVID-19 exceeding a rather nonspecific baseline inflammatory trigger as observed in disease controls

(i.e., "over"-activation). The observed increase in complement activation markers in male vs. female COVID-19 patients requires further studies.

Data availability statement

The raw data supporting the conclusions of this article will be made available by the authors, without undue reservation.

Ethics statement

The studies involving human participants were reviewed and approved by the Ethics Committee of Northwestern and Central Switzerland. The patients/participants provided their written informed consent to participate in this study.

Author contributions

FB and MO had full access to all of the data in the study and take responsibility for the integrity of the data and the accuracy of the data analysis. All authors contributed substantially to the study design and interpretation. FB, ML, and RT collected the data. FB and MO analyzed the data. FB and MO prepared a first manuscript draft. All authors contributed substantially to the writing of the manuscript, critically revised the manuscript for important intellectual content and approved the final version.

Funding

The COVIVA study was supported by the Swiss Heart Foundation, the Cardiovascular Research Foundation Basel, and an unrestricted research grant by Roche Diagnostics. The presented analysis was however funded by departmental funds of the corresponding author.

Conflict of interest

MO reports research support from the Swiss National Science Foundation (Grant No 32003B_197880) and Pharming Biotechnologies B.V. outside the submitted work. RT reports research support from the Swiss National Science Foundation (Grant No P300PB_167803), the Swiss Heart Foundation, the Swiss Society of Cardiology, the Cardiovascular Research Foundation Basel, the University of Basel and the University Hospital Basel and speaker honoraria/consulting honoraria from Abbott, Amgen, Astra Zeneca, Roche, Siemens, Singulex, and Thermo Scientific BRAHMS.

The remaining authors declare that the research was conducted in the absence of any commercial or financial relationships that could be construed as a potential conflict of interest.

The handling editor (PN) declared a shared committee with the author (MT) at the time of review.

Publisher's note

All claims expressed in this article are solely those of the authors and do not necessarily represent those of their affiliated organizations, or those of the publisher, the editors and the reviewers. Any product that may be evaluated in this article, or claim that may be made by its manufacturer, is not guaranteed or endorsed by the publisher.

Supplementary material

The Supplementary Material for this article can be found online at: https://www.frontiersin.org/articles/10.3389/fimmu.2022.941742/full#supplementary-material

References

1. Zhou F, Yu T, Du R, Fan G, Liu Y, Liu Z, et al. Clinical course and risk factors for mortality of adult inpatients with COVID-19 in wuhan, China: a retrospective cohort study. *Lancet* (2020) 395(10229):1054–62. doi: 10.1016/S0140-6736(20)30566-3

2. Gu SX, Tyagi T, Jain K, Gu VW, Lee SH, Hwa JM, et al. Thrombocytopathy and endotheliopathy: crucial contributors to COVID-19 thromboinflammation. *Nat Rev Cardiol* (2021) 18(3):194–209. doi: 10.1038/s41569-020-00469-1

3. Haslbauer JD, Zinner C, Stalder AK, Schneeberger J, Menter T, Bassetti S, et al. Vascular damage, thromboinflammation, plasmablast activation, T-cell dysregulation and pathological histiocytic response in pulmonary draining lymph nodes of COVID-19. *Front Immunol* (2021) 12:763098. doi: 10.3389/fimmu.2021.763098

4. Java A, Apicelli AJ, Liszewski MK, Coler-Reilly A, Atkinson JP, Kim AH, et al. The complement system in COVID-19: friend and foe? *JCI Insight* (2020) 5(15). doi: 10.1172/jci.insight.140711

5. Gao T, Hu M, Zhang X, Li H, Zhu L, Liu H, et al. Highly pathogenic coronavirus n protein aggravates lung injury by MASP-2-mediated complement over-activation. *medRxiv* (2020) 2020:03.29.20041962. doi: 10.1101/2020.03.29.20041962

6. Yu J, Yuan X, Chen H, Chaturvedi S, Braunstein EM, Brodsky RA. Direct activation of the alternative complement pathway by SARS-CoV-2 spike proteins is blocked by factor d inhibition. *Blood* (2020) 136(18):2080–9. doi: 10.1182/blood.20200082487

7. Ali YM, Ferrari M, Lynch NJ, Yaseen S, Dudler T, Gragerov S, et al. Lectin pathway mediates complement activation by SARS-CoV-2 proteins. *Front Immunol* (2021) 12(2645). doi: 10.3389/fimmu.2021.7145118

8. Jarlhelt I, Nielsen SK, Jahn CXH, Hansen CB, Pérez-Alós L, Rosbjerg A, et al. SARS-CoV-2 antibodies mediate complement and cellular driven inflammation. *Front Immunol* (2021) 12(4612). doi: 10.3389/fimmu.2021.7679819

9. Gralinski LE, Sheahan TP, Morrison TE, Menachery VD, Jensen K, Leist SR, et al. Complement activation contributes to severe acute respiratory syndrome coronavirus pathogenesis. *mBio* (2018) 9(5). doi: 10.1128/mBio.01753-1810

10. Magro C, Mulvey JJ, Berlin D, Nuovo G, Salvatore S, Harp J, et al. Complement associated microvascular injury and thrombosis in the

pathogenesis of severe COVID-19 infection: A report of five cases. *Transl Res* (2020) 220:1–13. doi: 10.1016/j.trsl.2020.04.00736

11. Kurtovic L, Beeson JG. Complement factors in COVID-19 therapeutics and vaccines. *Trends Immunol* (2021) 42(2):94–103. doi: 10.1016/j.it.2020.12.002

12. Ng N, Powell CA. Targeting the complement cascade in the pathophysiology of COVID-19 disease. *J Clin Med* (2021) 10(10). doi: 10.3390/jcm10102188

13. Fletcher-Sandersjoo A, Bellander BM. Is COVID-19 associated thrombosis caused by overactivation of the complement cascade? a literature review. *Thromb Res* (2020) 194:36–41. doi: 10.1016/j.thromres.2020.06.027

14. Ou X, Liu Y, Lei X, Li P, Mi D, Ren L, et al. Characterization of spike glycoprotein of SARS-CoV-2 on virus entry and its immune cross-reactivity with SARS-CoV. *Nat Commun* (2020) 11(1):1620. doi: 10.1038/s41467-020-15562-9

15. Perico L, Benigni A, Casiraghi F, Ng LFP, Renia L, Remuzzi G. Immunity, endothelial injury and complement-induced coagulopathy in COVID-19. *Nat Rev Nephrol* (2021) 17(1):46–64. doi: 10.1038/s41581-020-00357-4

16. Libby P, Luscher T. COVID-19 is, in the end, an endothelial disease. *Eur Heart J* (2020) 41(32):3038–44. doi: 10.1093/eurheartj/ehaa623

17. Schmidt EP, Yang Y, Janssen WJ, Gandjeva A, Perez MJ, Barthel L, et al. The pulmonary endothelial glycocalyx regulates neutrophil adhesion and lung injury during experimental sepsis. *Nat Med* (2012) 18(8):1217–23. doi: 10.1038/nm.2843

18. Zonneveld R, Martinelli R, Shapiro NI, Kuijpers TW, Plötz FB, Carman CV. Soluble adhesion molecules as markers for sepsis and the potential pathophysiological discrepancy in neonates, children and adults. *Crit Care* (2014) 18(1):204. doi: 10.1186/cc13733

19. Cugno M, Meroni PL, Gualtierotti R, Griffini S, Grovetti E, Torri A, et al. Complement activation and endothelial perturbation parallel COVID-19 severity and activity. *J Autoimmun* (2021) 116:102560. doi: 10.1016/j.jaut.2020.102560

20. Spadaro S, Fogagnolo A, Campo G, Zucchetti O, Verri M, Ottaviani I, et al. Markers of endothelial and epithelial pulmonary injury in mechanically ventilated COVID-19 ICU patients. *Crit Care* (2021) 25(1):74. doi: 10.1186/s13054-021-03499-4

21. Vassiliou AG, Keskinidou C, Jahaj E, Gallos P, Dimopoulou I, Kotanidou A, et al. ICU Admission levels of endothelial biomarkers as predictors of mortality in critically ill COVID-19 patients. *Cells* (2021) 10(1). doi: 10.3390/cells10010186

22. Cugno M, Meroni PL, Gualtierotti R, Griffini S, Grovetti E, Torri A, et al. Complement activation in patients with COVID-19: A novel therapeutic target. *J Allergy Clin Immunol* (2020) 146(1):215–7. doi: 10.1016/j.jaci.2020.05.006

23. Cai S, Dole VS, Bergmeier W, Scafidi J, Feng H, Wagner DD, et al. A direct role for C1 inhibitor in regulation of leukocyte adhesion. *J Immunol* (2005) 174 (10):6462–6. doi: 10.4049/jimmunol.174.10.6462

24. Alkhouli M, Nanjundappa A, Annie F, Bates MC, Bhatt DL. Sex differences in case fatality rate of COVID-19: Insights from a multinational registry. *Mayo Clin Proc* (2020) 95(8):1613–20. doi: 10.1016/j.mayocp.2020.05.014

25. Laudisi F, Spreafico R, Evrard M, Hughes TR, Mandriani B, Kandasamy M, et al. Cutting edge: the NLRP3 inflammasome links complement-mediated inflammation and IL-1β release. *J Immunol* (2013) 191(3):1006–10. doi: 10.4049/jimmunol.1300489

26. Wang L, Han G, Wang R, Chen G, Xu R, Xiao H, et al. Regulation of IL-8 production by complement-activated product, C5a, *in vitro* and *in vivo* during sepsis. *Clin Immunol* (2010) 137(1):157–65. doi: 10.1016/j.clim.2010.05.012

27. Takahashi T, Ellingson MK, Wong P, Israelow B, Lucas C, Klein J, et al. Sex differences in immune responses that underlie COVID-19 disease outcomes. *Nature* (2020) 588(7837):315–20. doi: 10.1038/s41586-020-2700-3

28. Hara A, Niwa M, Noguchi K, Kanayama T, Niwa A, Matsuo M, et al. Galectin-3 as a next-generation biomarker for detecting early stage of various diseases. *Biomolecules* (2020) 10(3). doi: 10.3390/biom10030389

29. De Biasi S, Meschiari M, Gibellini L, Bellinazzi C, Borella R, Fidanza L, et al. Marked T cell activation, senescence, exhaustion and skewing towards TH17 in patients with COVID-19 pneumonia. *Nat Commun* (2020) 11(1):3434. doi: 10.1038/s41467-020-17292-4

30. Kazancioglu S, Yilmaz FM, Bastug A, Ozbay BO, Aydos O, Yucel C, et al. Assessment of galectin-1, galectin-3, and PGE2 levels in patients with COVID-19. *Jpn J Infect Dis* (2021). doi: 10.7883/yoken.JJID.2021.020

31. Garcia-Revilla J, Deierborg T, Venero JL, Boza-Serrano A. Hyperinflammation and fibrosis in severe COVID-19 patients: Galectin-3, a target molecule to consider. *Front Immunol* (2020) 11:2069. doi: 10.3389/fimmu.2020.02069

32. Bauer W, Ulke J, Galtung N, Strasser-Marsik LC, Neuwinger N, Tauber R, et al. Role of cell adhesion molecules for prognosis of disease development of patients with and without COVID-19 in the emergency department. *J Infect Dis* (2021) 223(8):1497–9. doi: 10.1093/infdis/jiab042

33. Ma L, Sahu SK, Cano M, Kuppuswamy V, Bajwa J, McPhatter JN, et al. Increased complement activation is a distinctive feature of severe SARS-CoV-2 infection. *Sci Immunol* (2021) 6(59):eabh2259. doi: 10.1126/sciimmunol.abh2259

34. Kaushal K, Kaur H, Sarma P, Bhattacharyya A, Sharma DJ, Prajapat M, et al. Serum ferritin as a predictive biomarker in COVID-19. a systematic review, meta-analysis and meta-regression analysis. *J Crit Care* (2022) 67:172–81. doi: 10.1016/j.jcrc.2021.09.023

35. Farkas I, Baranyi L, Ishikawa Y, Okada N, Bohata C, Budai D, et al. CD59 blocks not only the insertion of C9 into MAC but inhibits ion channel formation by homologous C5b-8 as well as C5b-9. *J Physiol* (2002) 539(Pt 2):537–45. doi: 10.1113/jphysiol.2001.013381

36. Shen B, Yi X, Sun Y, Bi X, Du J, Zhang C, et al. Proteomic and metabolomic characterization of COVID-19 patient sera. *Cell* (2020) 182(1):59–72.e15. doi: 10.1016/j.cell.2020.05.03241

37. Yao S, Luo N, Liu J, Zha H, Ai Y, Luo J, et al. Elevated serum levels of progranulin and soluble vascular cell adhesion molecule-1 in patients with COVID-19. *J Inflammation Res* (2021) 14:4785–94. doi: 10.2147/JIR.S330356

38. Gutmann C, Takov K, Burnap SA, Singh B, Ali H, Theofilatos K, et al. SARS-CoV-2 RNAemia and proteomic trajectories inform prognostication in COVID-19 patients admitted to intensive care. *Nat Commun* (2021) 12(1):3406. doi: 10.1038/s41467-021-23494-1

39. Holter JC, Pischke SE, de Boer E, Lind A, Jenum S, Holten AR, et al. Systemic complement activation is associated with respiratory failure in COVID-19 hospitalized patients. *Proc Natl Acad Sci U.S.A.* (2020) 117(40):25018–25. doi: 10.1073/pnas.2010540117

40. de Nooijer AH, Grondman I, Janssen NAF, Netea MG, Willems L, van de Veerdonk FL, et al. Complement activation in the disease course of coronavirus disease 2019 and its effects on clinical outcomes. *J Infect Dis* (2021) 223(2):214–24. doi: 10.1093/infdis/jiaa646

41. Kristensen MK, Plovsing RR, Berg RMG, Madsen RK, Ronit A. Cell adhesion molecules and vascular endothelial growth factor at the systemic and alveolar level in COVID-19 ARDS. *J Infect Dis* (2021). doi: 10.1093/infdis/jiab34742

42. Colafrancesco S, Alessandri C, Conti F, Priori R. COVID-19 gone bad: A new character in the spectrum of the hyperferritinemic syndrome? *Autoimmun Rev* (2020) 19(7):102573. doi: 10.1016/j.autrev.2020.10257343

43. Petrilli CM, Jones SA, Yang J, Rajagopalan H, O'Donnell L, Chernyak Y, et al. Factors associated with hospital admission and critical illness among 5279 people with coronavirus disease 2019 in new York city: prospective cohort study. *BMJ* (2020) 369:m1966. doi: 10.1136/bmj.m196644

44. Sharma G, Volgman AS, Michos ED. Sex differences in mortality from COVID-19 pandemic: Are men vulnerable and women protected? *JACC Case Rep* (2020) 2(9):1407–10. doi: 10.1016/j.jaccas.2020.04.02745

45. Mussini C, Cozzi-Lepri A, Menozzi M, Meschiari M, Franceschini E, Rogati C, et al. Better prognosis in females with severe COVID-19 pneumonia: possible role of inflammation as potential mediator. *Clin Microbiol Infect* (2021) 27 (8):1137–44. doi: 10.1016/j.cmi.2020.12.010

46. Gaya da Costa M, Poppelaars F, van Kooten C, Mollnes TE, Tedesco F, Würzner R, et al. Age and sex-associated changes of complement activity and complement levels in a healthy Caucasian population. *Front Immunol* (2018) 9:2664–. doi: 10.3389/fimmu.2018.02664

47. Charitos P, Heijnen IAFM, Egli A, Bassetti S, Trendelenburg M, Osthoff M. Functional activity of the complement system in hospitalized COVID-19 patients: A prospective cohort study. *Front Immunol* (2021) 12:765330–. doi: 10.3389/fimmu.2021.765330

frontiers | Frontiers in Immunology

TYPE Original Research
PUBLISHED 20 September 2022
DOI 10.3389/fimmu.2022.997148

Check for updates

OPEN ACCESS

EDITED BY
Erik J. M. Toonen,
Hycult Biotech, Netherlands

REVIEWED BY
Yang Cao,
Peking Union Medical College Hospital (CAMS), China
Chiara Suffritti,
IRCCS Ca 'Granda Foundation Maggiore Policlinico Hospital, Italy

*CORRESPONDENCE
Carlos Flores
cflores@ull.edu.es

SPECIALTY SECTION
This article was submitted to Molecular Innate Immunity, a section of the journal Frontiers in Immunology

RECEIVED 18 July 2022
ACCEPTED 23 August 2022
PUBLISHED 20 September 2022

CITATION
Mendoza-Alvarez A, Tosco-Herrera E, Muñoz-Barrera A, Rubio-Rodríguez LA, Alonso-Gonzalez A, Corrales A, Iñigo-Campos A, Almeida-Quintana L, Martin-Fernandez E, Martinez-Beltran D, Perez-Rodriguez E, Callero A, Garcia-Robaina JC, González-Montelongo R, Marcelino-Rodriguez I, Lorenzo-Salazar JM and Flores C (2022) A catalog of the genetic causes of hereditary angioedema in the Canary Islands (Spain). *Front. Immunol.* 13:997148. doi: 10.3389/fimmu.2022.997148

COPYRIGHT
© 2022 Mendoza-Alvarez, Tosco-Herrera, Muñoz-Barrera, Rubio-Rodríguez, Alonso-Gonzalez, Corrales, Iñigo-Campos, Almeida-Quintana, Martin-Fernandez, Martinez-Beltran, Perez-Rodriguez, Callero, Garcia-Robaina, González-Montelongo, Marcelino-Rodriguez, Lorenzo-Salazar and Flores. This is an open-access article distributed under the terms of the Creative Commons Attribution License (CC BY). The use, distribution or reproduction in other forums is permitted, provided the original author(s) and the copyright owner(s) are credited and that the original publication in this journal is cited, in accordance with accepted academic practice. No use, distribution or reproduction is permitted which does not comply with these terms.

A catalog of the genetic causes of hereditary angioedema in the Canary Islands (Spain)

Alejandro Mendoza-Alvarez[1], Eva Tosco-Herrera[1], Adrian Muñoz-Barrera[2], Luis A. Rubio-Rodríguez[2], Aitana Alonso-Gonzalez[1,3], Almudena Corrales[1,4], Antonio Iñigo-Campos[2], Lourdes Almeida-Quintana[5], Elena Martin-Fernandez[6], Dara Martinez-Beltran[7], Eva Perez-Rodriguez[8], Ariel Callero[8], Jose C. Garcia-Robaina[8], Rafaela González-Montelongo[2], Itahisa Marcelino-Rodriguez[1,9], Jose M. Lorenzo-Salazar[2] and Carlos Flores[1,2,4,10]*

[1]Research Unit, Hospital Universitario Nuestra Señora de Candelaria, Santa Cruz de Tenerife, Spain, [2]Genomics Division, Instituto Tecnológico y de Energías Renovables, Santa Cruz de Tenerife, Spain, [3]Universidad de Santiago de Compostela, Santiago de Compostela, Spain, [4]CIBER de Enfermedades Respiratorias, Instituto de Salud Carlos III, Madrid, Spain, [5]Allergy Service, Hospital Universitario de Gran Canaria Dr. Negrín, Las Palmas de Gran Canaria, Spain, [6]Allergy Service, Hospital Universitario Dr. Molina Orosa, Las Palmas de Gran Canaria, Spain, [7]Allergy Service, Hospital Universitario Insular-Materno Infantil, Las Palmas de Gran Canaria, Spain, [8]Allergy Service, Hospital Universitario Nuestra Señora de Candelaria, Santa Cruz de Tenerife, Spain, [9]Public Health and Preventive Medicine Area, Universidad de La Laguna, Santa Cruz de Tenerife, Spain, [10]Facultad de Ciencias de la Salud, Universidad Fernando Pessoa Canarias, Las Palmas de Gran Canaria, Spain

Hereditary angioedema (HAE) is a rare disease where known causes involve C1 inhibitor dysfunction or dysregulation of the kinin cascade. The updated HAE management guidelines recommend performing genetic tests to reach a precise diagnosis. Unfortunately, genetic tests are still uncommon in the diagnosis routine. Here, we characterized for the first time the genetic causes of HAE in affected families from the Canary Islands (Spain). Whole-exome sequencing data was obtained from 41 affected patients and unaffected relatives from 29 unrelated families identified in the archipelago. The Hereditary Angioedema Database Annotation (HADA) tool was used for pathogenicity classification and causal variant prioritization among the genes known to cause HAE. Manual reclassification of prioritized variants was used in those families lacking known causal variants. We detected a total of eight different variants causing HAE in this patient series, affecting essentially *SERPING1* and *F12* genes, one of them being a novel *SERPING1* variant (c.686-12A>G) with a predicted splicing effect which was reclassified as likely pathogenic in one family. Altogether, the diagnostic yield by assessing previously reported causal genes and considering variant reclassifications according to the American College of Medical Genetics guidelines reached 66.7% (95% Confidence Interval [CI]: 30.1-91.0) in families with more than one affected member and 10.0% (95% CI: 1.8-33.1) among cases without family information for the disease. Despite the

genetic causes of many patients remain to be identified, our results reinforce the need of genetic tests as first-tier diagnostic tool in this disease, as recommended by the international WAO/EAACI guidelines for the management of HAE.

KEYWORDS

hereditary angioedema, genetic cause, rare disease, variant interpretation, precision medicine

Introduction

Hereditary angioedema (HAE) is a rare genetic dominant condition with incomplete penetrance characterized by recurrent swellings (edema) affecting the skin, internal organs, mucosa or the upper airways (1, 2). Where genetic pathogenesis is known, symptoms are caused by dysfunction of the C1 esterase inhibitor (C1-INH) or dysregulation of the kinin cascade, leading to bradykinin release and resulting in inflammation episodes. Bradykinin is a vasoactive peptide and the main activator of the bradikinin receptor B2 expressed in endothelial cells (3) whose activation leads to increased vascular permeability and edema, causing the HAE symptoms (4). HAE attacks can turn into a life-threatening episode if the edema develops in the laryngeal track, which leads to the obstruction of the upper respiratory airways (5). HAE attacks are unpredictable and often develop in response to triggering factors such as mental stress (6), use of contraception hormones (7), infections (8), injuries or surgery interventions (9), and weather changes (6), among others. HAE prevalence has been estimated in over 1:50,000 worldwide (10) and has been reported in all ethnic groups (11).

This genetic condition is typically divided in two main groups attending to the C1-INH plasmatic levels. The most frequent form (85% of the cases described) is caused by decreased levels of C1-INH (11, 12), also known as HAE-C1-INH of type I. The rest of cases are found either with normal levels of non-functional C1-INH protein (also known as HAE-C1-INH of type II) or with normal levels of a functional C1-INH protein (HAE-nC1-INH). At the moment, more than 450 disease causing variants have been reported in *SERPING1* gene leading to HAE-C1-INH forms (11, 13–15). However, causal variants affecting other genes of the bradykinin pathway underlie HAE-nC1-INH cases (11).

The first genetic study in HAE families with normal levels of C1-INH detected a mutation in the exon nine of *F12* (16). FXII activation increases the bradykinin accumulation, driving to increased vascular permeability. Surprisingly, only 20% of patients with HAE-nC1-INH in Europe carry causal variants in the *F12* gene (17). Until 2018, only *SERPING1* and *F12* were known to cause HAE, which explains why HAE diagnosis has been mostly based on plasmatic determinations of complement proteins or the activity. The decreasing costs of Next Generation Sequencing (NGS) prompted the first whole-exome sequencing (WES) which allowed to detect variants affecting function in HAE-nC1-INH patients in angiopoietin (*ANGPT1*) and plasminogen (*PLG*) genes (18, 19). Using the same approach, Bork et al. also identified variants in the kininogen 1 (*KNG1*) gene as another cause of HAE (20). Most recently, two other causal genes were found by applying WES in HAE-nC1-INH families, encoding the heparan sulfate 3-O-sulfotransferase 6 (*HS3ST6*), and myoferlin (*MYOF*) (21, 22). The latter being causal strongly suggests a key role of VEGF-mediated signaling in HAE pathophysiology, although the mechanism triggering the symptoms remains unclear.

Because of the nonspecific signs, HAE remains a poorly recognized clinical entity, resulting in delayed diagnoses and deficient treatment conditions for long periods. In fact, a reported mean diagnosis delay of 7.9 years, ranging from months to 50 years, has been recently exposed in the HAE cases from the Canary Islands (23). Those patients lacking a diagnosis have an increased risk for morbidities and mortality compared to those that had been diagnosed, especially if attacks affect the airways (24). Advances in testing procedures and disease recognition have not improved HAE diagnosis, still representing a challenge for professionals (25). Currently, genetic testing is not part of the clinical diagnosis of HAE routine in many health care systems despite the updated HAE management guidelines recommend a genetic-based diagnosis in order to increase the diagnostic yield and reduce the diagnosis odyssey (11, 26, 27). Furthermore, the debilitating nature of HAE attacks makes early and precise diagnosis critical to rapidly establish the actions and treatments for short and long-term prophylaxis (28). Because of the importance of establishing an accurate diagnosis and to prescribe the optimal treatment, many countries have developed their own HAE patient registry. This has fostered the development of standards and specialized facilities to help managing and diagnosing patients while reducing the diagnosis delay. Here we present the first genetic characterization of HAE patients from the Canary Islands (Spain).

10.3389/fimmu.2022.997148

Material and methods

Patient population and setting

The study was approved by the Hospital Universitario Nuestra Señora de Candelaria (HUNSC; PI 57–17) Ethics Committee and written informed consent was obtained from all patients and relatives. The patient cohort is composed by affected individuals that had compatible clinical history of angioedema attacks without urticaria, and a differential diagnosis by blood molecular assays. We excluded patients using medication that were known to trigger angioedema attacks (i.e., angiotensin-converting enzyme inhibitors) and patients suffering other pathologies that can potentially cause angioedema attacks (i.e., hepatitis, HIV, hepatic/renal disorders, immunological deficiencies, and infections due to *Helicobacter pylori*).

HAE diagnosis was based on plasmatic determination of C1-INH and C4, and C1-INH activity, according to the international WAO/EAACI guidelines for the management of HAE (29).

Whole-exome sequencing and variant calling

DNA was extracted from 4 mL of peripheral blood with Illustra™ blood genomicPrep kit (GE Healthcare; Chicago, IL). Alternatively, for pediatric patients and adults where blood sample extraction was not available, DNA from saliva samples were obtained with the OG-250 kit (DNA Genotek, Ontario, CA) following manufacturer's instructions. DNA concentration was evaluated using the dsDNA BroadRange Assay Kit for the Qubit® 3.0 Fluorometer (Termo Fisher Scientific, Waltham, MA).

Libraries were prepared using the TruSeq Rapid Exome Library Prep Kit (Illumina, San Francisco, CA). Library sizes and concentrations were assesed on a TapeStation 4200 (Agilent Technologies, Santa Clara, CA) and sequences were obtained with a HiSeq 4000 Sequencing System (Illumina, San Francisco, CA) with paired-end 75-base reads. PhiX was loaded and sequenced at 1% as an internal control of the experiments (Figure 1).

Sequencing reads were preprocessed with bcl2fastq v2.18 and mapped to hg19/GRCh37 with Burrows-Wheeler Aligner v0.7.15 (30), and BAM files were processed with Qualimap v2.2.1 (31), SAMtools v1.3 (32), BEDTools (33), and Picard v2.10.10 (http://broadinstitute.github.io/picard) for quality control steps. Variant calling of germline variants was performed using an in-house bioinformatics pipeline based on the Genome Analysis Toolkit (GATK) v.3.8 (34). The pipeline has been designed for the detection of nucleotide substitutions (SNVs) and small indels (<50 bp) following the GATK best practices (35) and its description is publicly available (https://github.com/genomicsITER/benchmarking/tree/master/WES).

Subsequently, the identified variation was filtered by means of SAMtools and VCFtools (36) based on "PASS" filter, depth of coverage per position (≥ 20×), genotype quality (≥ 100), and mapping quality (≥ 50).

The analysis was carried out at the Teide-HPC Supercomputing facility (http://teidehpc.iter.es/en).

Variant annotation and causal variant prioritization

The resulting variant calls were annotated with available information (Figure 1). For that, ANNOVAR (37) was used to include the allele frequency in reference populations, gene

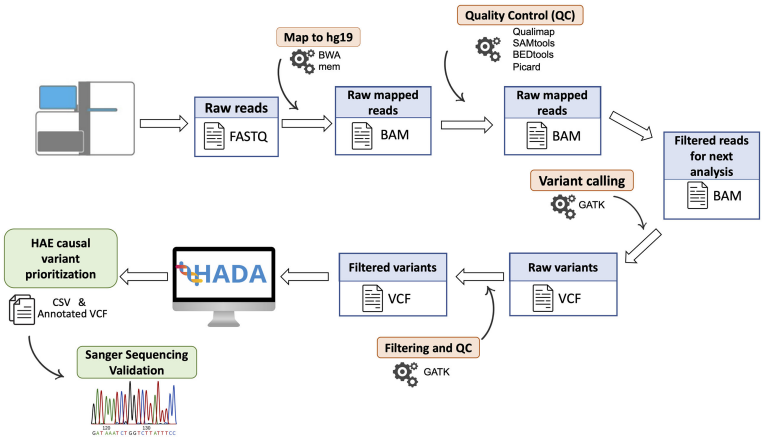

FIGURE 1
Schematic representation of the steps followed for patient DNA sequencing data. Algorithms are shown in orange and processed files in blue. The HAE causal variants prioritized by HADA and the Sanger validation step are shown in green.

location, known functional consequences, links with disease based on ClinVar (38) and The Human Gene Mutation Database (39), and several pathogenicity scores including the Combined Annotation-Dependent Depletion (CADD, 40), among others. The classification of pathogenic potential of variants was obtained and annotated using InterVar software (41) following the American College of Medical Genetics and Genomics (ACMG) guidelines (42).

The annotated variant calls were individually processed for each patient by Hereditary Angioedema Database Annotation tool (HADA, http://hada.hpc.iter.es/), an in-house designed variant prioritization server of HAE genes to facilitate the identification of the variants affecting function as well as other accompanying information from the literature (13). In those patients where causal variants were not detected by HADA, Exomiser v12.1 was used to aim to identify the variants affecting function causing HAE (43). SQUIRLs v1.3.0 was used to specifically analyze candidate splicing variants and their predicted effect, prioritizing them by the internal pathogenicity score (44).

Finally, the variants that were classified as Variants of Uncertain Significance (VUS) that could be reclassified as Pathogenic/Likely Pathogenic variants based on complimentary information were validated by direct Sanger sequencing of PCR amplicons from the two strands. This assessment was performed by Macrogen Spain sequencing services with a customized design of primers (Supplementary Table 1).

Assessment of potential structural variants in sequencing data

ExomeDepth v1.1.15 was used to identify putative structural variants (SVs) that could constitute possible variants affecting function causing HAE (45). Candidate variants obtained from BAM files were filtered to remove false positives calls by Bayes factor (BF) higher than 20.

To provide a clinical interpretation of the candidate SVs, filtered calls were processed with ClassifyCNV (46), based on the ACMG guidelines to determine pathogenicity potential. Complementarily, StrVCTURE (47) was used to distinguish pathogenic SVs from benign SVs that overlap exons based on CADD scores. The classification was carried out with the consensus of both algorithms.

Screening for mobile elements in sequencing data

At least 17 *Alu* elements which are in *SERPING1* gene have been reported in the scientific literature. As such, pathogenic rearrangements associated with this repetitive element have been estimated to be responsible for approximately 15% of HAE cases (48). Because of that, the Soft Clipped Read Alignment Mapper v1.0.1 (SCRAMble) (49) was used to screen for mobile element insertions (MEIs) in the exome data, with a particular emphasis on *SERPING1*.

Results

Patient population and sequencing summary

Forty-one patients and nine healthy relatives from 29 unrelated families with HAE diagnoses residing in the Canary Islands were included in the study. Thirty-seven patients self-declared European ancestry, two declared ancestry from Colombia (family 3), and two from Israel (family 5). The study sample included eight males (19.5%) and 33 females (80.5%). The protective role of male hormones and the well-known influence of estrogens as one of the main triggers of HAE attacks could explain this sexual disbalance (50–52). The patients were aged between four and 72 years (mean: 36.8 ± 16.9 years) and a positive family history for HAE attacks was reported for 23 (56.1%) of them. Based on biochemical analysis, all HAE types are present in the study sample, where HAE-C1-INH was predominant, with 23 patients diagnosed for HAE type I (56.1%) and four patients for HAE type II (9.8%). The rest of patients (14, 34.1%) were diagnosed as HAE-nC1-INH, and most of them were females (92.8%).

WES of this case series yielded an average of 8.36 Gb per patient, with an average of 100% of on-target reads and a median depth of 57×, and a transition/transversion ratio in the range of 3.1 to 3.3.

Causal variant identification and concordance between clinical and genetic assessments

Using HADA, we detected a total of six variants affecting function linked to different HAE types in the study (Table 1 and Figure 2). *SERPING1* was the most commonly affected gene (n=5). Two unrelated families clinically classified as HAE type I were carriers of the synonymous variant affecting function c.751C>T; p.Leu251= (families 4 and 11), which was previously reported in Spain (53). The missense variant c.613T>C; p.Cys205Arg, previously described in Spanish cases, was also found in another family with HAE type I (family 8). We detected a likely pathogenic frameshift variant affecting function located in exon 3 of *SERPING1* gene, c.143_144delCA; p.Thr48SerfsTer9, which was associated with decreased C1-INH plasmatic levels and leading to HAE type I (family 9). We also detected the causative missense variant c.1396C>T; p.Arg466Ser in the index patient of family 1. In this family, the

TABLE 1 Detected causal variants affecting function of HAE in this study.

Family ID	Individual ID	Gene	Chr	Position start-end	HGVS	Aminoacid change	HAE type	ACMG class
1	1, 4	*SERPING1*	11	57381947- 57381947	c.1396C>T	p.Arg466Cys	II	Pathogenic
2	5, 6	*F12*	5	176831232- 176831232	c.983G>T	p.Thr328Lys	HAE-nC1-INH	Likely pathogenic
3	1, 2, 3	*SERPING1*	11	57373471- 57373471	c.686-12A>G	None	I	Likely pathogenic[†]
4	1, 2	*SERPING1*	11	57373548- 57373548	c.751C>T	p.Leu251=	I	Benign
5	1	*SERPING1*	11	57369570- 57369570	c.613T>C	p.Cys205Arg	I	Likely pathogenic
9	1, 2	*SERPING1*	11	57367442- 57367442	c.143_144delCA	p.Thr48SerfsTer9	I	Likely pathogenic
10	1	*SERPING1*	11	57378700-57378700	c.1100T>C	p.Leu367Pro	I	Likely pathogenic[†]
11	1	*SERPING1*	11	57373548- 57373548	c.751C>T	p.Leu251=	I	Benign

[†]Validated previously VUS reclassified according to publicly available genomic information.

index patient [with normal levels of C1-INH (47 mg/dL), reduced C1-INH activity (10%) and low C4 levels (1.8 mg/dL) had similar biochemical findings as his asymptomatic sister (with normal) levels of C1-INH (65 mg/dl); reduced C1-INH activity (< 10%), and low C4 levels (7.6 mg/dl)]. Sequence analysis of this asymptomatic relative also releveled the missense variant c.1396C>T; p.Arg466Ser. This variant has been widely reported in Spanish patients in the literature, although linked to HAE type II instead (54).

Furthermore, a well-known causal variant of *F12* (c.983G>T; p.Thr328Lys) was detected in members of the family 2 with HAE-nC1-INH (Figure 2). This variant affecting function has not been previously reported in Spanish patients and is absent from ExAC (55) and gnomAD (56).

We also identified a missense variant affecting function in *SERPING1* gene that was previously classified as a VUS. The variant c.1100T>C; p.Leu367Pro was detected in one patient for which information from relatives was lacking (Figure 3). Although this variant was described in previous genetic studies with HAE patients, it lacks population frequency data or prediction scores which could supporta a damaging effect, including individual predictions (SIFT, PolyPhen2, CADD, M-CAP, among others) and meta scores (MetaLR, MetaSVM, MetaRNN and REVEL). Despite that, we reclassified it as a likely pathogenic variant according to the ACMG guidelines using VarSome (57) based on the classification criteria PM1 (moderate), PM2 (moderate), PM5 (moderate), PP2 (supporting), and PP3 (supporting).

The manual inspection of sequencing data in the positions with candidate calls for SVs and MEIs revealed that all the prioritized findings were false positives due to low depth of coverage in the inspected regions, therefore, offering insufficient support to declare variants.

Splicing defects detected

The splicing variant defect c.686-12A>G in *SERPING1* was identified in all the affected patients of family 3 (Figure 4). This variant was previously reported in two unrelated Italian patients

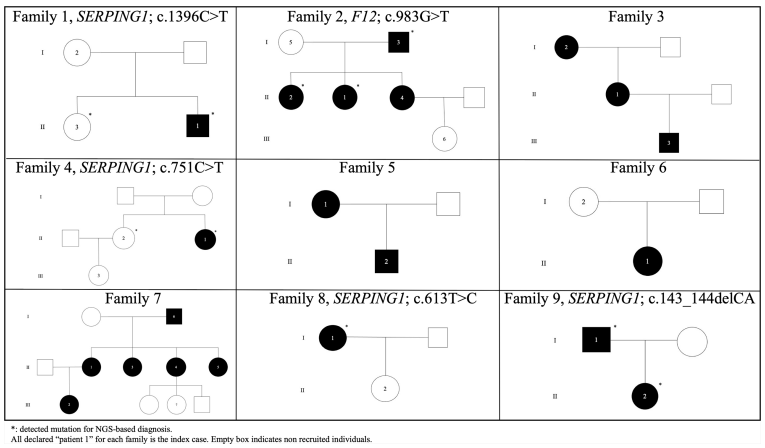

FIGURE 2
Pedigrees of unrelated HAE families in the Canary Islands.

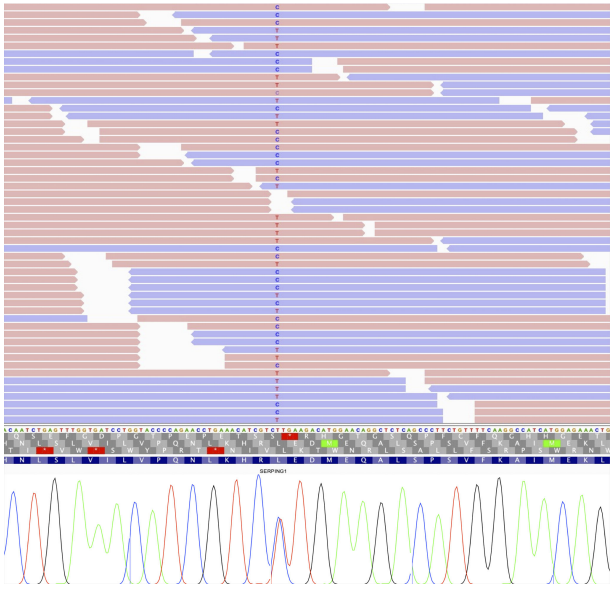

FIGURE 3
IGV view of sequencing reads supporting each allele of *SERPING1* variant (up), and Sanger sequencing validation showing both alleles (down).

(58) and in one case of a Serbian HAE type I family (59). However, despite the authors did not assess the pathogenicity of the variant, its function was assessed using a minigene *in vitro* model (60). According to that study, the c.686-12A>G variant was found to provoke an aberrant splicing effect possibly triggering transcript degradation as deduced by the minimal amount of the transcript detected in the patient's blood. Based on this extended information, we then scored this variant with the following ACMG criteria: BP4 (supporting), PS2 (strong), PM2 (moderate), PP1 (supporting), PP3 (supporting), and PP4 (supporting). As a result, VarSome reclassified the c.686-12A>G variant from VUS to Likely Pathogenic.

Diagnostic yield

Aggregating all the described evidence for the variants affecting function detected across study patients from families with different affected members, we obtained a genetic diagnostic yield of 66.7% (95% Confidence Interval [CI]: 30.1-91.0%; 6/9 families) when considering only the previously known causal variants (Figure 2). However, the genetic diagnosis yield among proband-only cases decreased to 10.0% (95% CI: 1.8-33.1%; 2/20 cases). This finding supports the recommendation of the WAO/EAACI current guidelines for HAE management to recruit unaffected family members for causal variant screening.

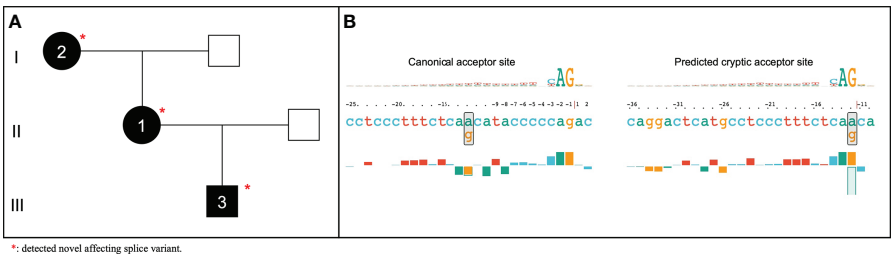

FIGURE 4
Pedigree of HAE affected family without previously reported causal variant **(A)** and representation generated by SQUIRLs of predicted acceptor site for the novel *SERPING1* c.686-12A>G affecting splice variant **(B)**.

Discussion

In recent years, the widely use of NGS in the clinical field has significantly contributed to the achievement of early and accurate diagnosis. In this context, we aimed to characterize for the first time the underlying genetic causes of HAE in the Canary Islands, where clinical studies have estimated a prevalence of around 1.90:100,000 (23). This prevalence is higher than the that reported for overall Spain and is closer to that observed in other European studies, estimated in 2:100,000 (53). The isolation and the recent demographic history of the Canary Islands population could explain the HAE prevalence in the archipelago. Genetic studies have highlighted that the genes from the regulation of inflammatory response and the complement cascade are significantly enriched in the genomic regions that harbor distinctive genetic variation of this population (61). These findings, together with the estimated higher prevalence of HAE in the Canary Islands, may add to the underlying genetic factors involved in angioedema that have not been identified so far. In this context, NGS-based studies with HAE affected individuals and families are being constantly implemented in several countries with the aim of increasing the diagnostic yield, such as Denmark (62), Saudi Arabia (63), Turkey (64), Japan (65), Portugal (66), Greece (67), Norway (68), Switzerland (69), Croatia (70), China (71), Romania (72), Austria (73), and Puerto Rico (74), among others. However, NGS-based genetic studies have not been common in HAE studies until recently (17). Part of the explanation may reside in the fact that only two causal genes were identified until 2018 and that clinical diagnosis was essentially based on clinical symptoms and biochemical measurements of C4 and C1-INH levels/C1-INH activity in plasma (11). In certain cases, the clinicians could not refine the diagnosis in HAE borderline patients. In these cases, WES brings new and efficient opportunities to clearly identify the underlaying causes, especially in those without C1-INH deficiency (11). Besides, obtaining WES from all patients offers the possibility to unravel novel disease genes, as well as to identify the underlying causes in the known HAE genes in a single test. In this context, this study describes the first step in the genetic characterization of HAE patients from the Canary Islands. Subsequent studies based on phenotype-driven prioritizations of causal variants from the whole-exome and genome-wide studies will aim to identify novel genetic factors involved in HAE in this population.

Following the international WAO/EAACI guidelines for the management of HAE (26), we have obtained two remarkable results in one of the families. First, we amended the initial diagnosis based on the clinical and biochemical studies, which supported a HAE type I in family 1. However, the prioritization of genetic variants revealed a well-known variant of HAE type II (*SERPING1*; c.1396C>T). Secondly, this variant was also detected in one asymptomatic relative, allowing a diagnostic anticipation to the manifestation of symptoms in this family member. The development of bioinformatics tools focused on variant interpretation in the context of rare diseases accelerates diagnosis accuracy, which translates into a great benefit for patients and their families. However, we face a global problem with the high proportion of VUS detected in NGS-based studies, since it complicates an accurate clinical diagnosis identifying the genetic causes, as recommended by current international guidelines for HAE patient management. In addition, there is also a widespread conflict in the pathogenic classification rules for genetic variants. In family 4, we identified the synonymous variant *SERPING1*; c.751C>T, which has been classified as benign according to the ACMG guidelines. However, this variant has been declared as causal of the disease in Spanish patients with HAE (53). Synonymous variants can contribute to diseases, affecting gene function by splicing (75), binding of transcription factors (76), or mRNA stability (77), among others. They are common in the human genome, but their role in diseases have often been underestimated (78). It is well-known that variants affecting splicing are significant contributors to human diseases and are often missed in standard variant filtering approaches, which tend to focus on protein coding regions (79). In this study, we detected the *SERPING1* c.686-12A>G variant in all affected members of a recruited HAE type I family, previously reported as VUS and here reclassified as likely pathogenic. As indicated before, the increased number of sequencing studies in rare disorders have overcome the main limitations to the interpretation of the pathogenic potential of detected variants and their association with the disease (80, 81). In this context, the diagnostic yield of NGS-based solutions has improved to 35-60% nowadays (44). However, the genetic cause of most cases of this study is lacking (21/29 independent cases, 72.4%, 95% CI: 52.5-86.6). The diagnostic process of HAE is also a stressful period due to confusing signs with histaminergic angioedema attacks, which could be delayed for many years. To reduce the clinical odyssey, we previously designed HADA, a variant prioritization tool for DNA sequencing studies focused on HAE diagnosis (13). HADA retrieves previously reported causal variants in HAE patients in a few minutes, integrating extended genetic variant information from public updated databases used for pathogenic classification according to ACMG guidelines. Taken all prioritized variants by HADA in our study, we have estimated a NGS diagnostic yield of 66.7% (6/9 families). Unfortunately, the diagnosis yield decreases to 10.0% in proband-only analyses (2/20 cases). Remarkably, despite the capabilities of using a WES approach, we did not find variants affecting function in *PLG*, *ANGPT1*, *KNG1*, *MYOF*, and *HS3ST6* genes (involved in HAE-nC1-INH) in any of the studied families.

Our study has some strengths and limitations. Among limitations, we acknowledge that the number of patients where a causal variant was identified is limited, precluding for now a robust study of the relationships between phenotypes and genotypes, as well as the links with drug responses or the

patient management. We also acknowledge a relatively low breath of coverage of some exons of the *F12* gene compared with that of *SERPING1* gene (66.49% of bases covered at least 10× in *F12* compared with 88.33% for *SERPING1*), which may hinder the identification of causal genetic variants in patients with clinical suspicion of HAE-nC1-INH. Another limitation was the low genetic diagnosis yield obtained among proband-only cases, which could be increased with the recruitment of family members for genetic causative variant identification and determining its origin (inherited vs *de novo*), as is recommended by WAO/EAACI guidelines. Although WES is not the optimal approach, we have aimed to identify and prioritize candidate SVs and MEIs. However, the results did not support the possibility that the cases could be caused by SVs in the known HAE genes. Even though HADA assist in the genetic testing of HAE patients, the tool was designed to prioritize genetic variants within the literature identified genes of HAE, thus lacking the function to identify novel HAE genes. To fill this gap, complementary studies relying on phenotype-driven approaches and genomic scans, among others, are needed to allow the identification of novel genetic factors of HAE, especially in those affected patients who remain without genetic diagnosis. Among the strengths of our study, we highlight the widespread recruitment of HAE patients and their relatives in the archipelago by the Allergy Services of the main hospitals from each island, allowing us to carry out an early detection of new cases of HAE and study the genetic causes through DNA sequencing. The detection of the *SERPING1* c.1396C>T; p.Arg466Ser variant led to a diagnosis anticipation in an asymptomatic relative considering both genetic results and the biochemical findings, allowing to achieve a precise diagnosis of HAE type II. Our study highlights the benefits of a first-tier genetic testing for HAE diagnosis and reinforces the need to clearly identify underlying genetic causes, as recommended by the international WAO/EAACI guidelines for the management of HAE and enhance the benefits of NGS as first-tier genetic testing tool for its diagnosis (26).

Conclusions

To characterize the underlying genetic causes of HAE in the Canary Islands, we have performed the first genomic study of affected families from the region. A rapid detection of the causal variants in sequencing data from whole-exome was carried out based on HADA, providing in some families a refined diagnosis, and revealing the genetic affectation in asymptomatic members. Our results reinforce the necessity of NGS based studies on HAE patients to identify and characterize novel genetic factors involved in this disease. Complementary and more exhaustive analysis are required to identify the genetic cause in all the families.

Data availability statement

The data presented in the study are deposited in the EGA repository (https://ega-archive.org/datasets/EGAD00001009318). Further inquiries can be directed to the corresponding author.

Ethics statement

The studies involving human participants were reviewed and approved by Hospital Universitario Nuestra Señora de Candelaria Ethics Committee (HUNSC; PI 57–17). Written informed consent to participate in this study was provided by the participants' legal guardian/next of kin.

Author contributions

Conceptualization, CF and ACa; methodology, AM-A, ET-H and IM-R; patient and sample recruitment, LA-Q, EM-F, DM-B, EP-R, JG-R, and ACa; sample preparation and DNA sequencing, ACo, AI-C, and RG-M; formal analysis, AM-A, AM-B, LR-R, AA-G and JL-S; writing—original draft preparation, AM-A and CF; writing—review and editing, AM-A, IM-R, JL-S, ACa and CF; supervision, CF; funding acquisition, ACa, IM-R and CF. All authors have read and agreed to the published version of the manuscript. All authors contributed to the article and approved the submitted version.

Funding

This work was supported by the Ministerio de Ciencia e Innovación (RTC-2017-6471-1; AEI/FEDER, UE) and the Instituto de Salud Carlos III (CD19/00231), which were co-financed by the European Regional Development Funds 'A way of making Europe' from the European Union; Cabildo Insular de Tenerife (CGIEU0000219140); Agreement OA17/008 with the Instituto Tecnológico y de Energías Renovables (ITER) to strengthen scientific and technological education, training, research, development, and innovation in genomics, personalized medicine, and biotechnology; Fundación Canaria Instituto de Investigación Sanitaria de Canarias (PIFIISC19/48); and SEAIC Foundation (18_A01). A.M.-A. and E.T.-H. were supported by a fellowship from Agencia Canaria De Investigación Innovación Y Sociedad De La Información Gobierno De Canarias (TESIS2020010002 and TESIS2021010046, respectively) co-funded by European Social Fund. AAG was supported by Ministerio de Universidades (modality Margarita Salas). The content of this publication is solely the responsibility of the authors and does not necessarily reflect the views or policies of the funding agencies.

Acknowledgments

We would like to thank the patients and nurses involved in the design of this study. AM-A, ET-H, AM-B, and LR-R. acknowledge the University of La Laguna for the training support during their PhD studies.

Conflict of interest

The authors declare that the research was conducted in the absence of any commercial or financial relationships that could be construed as a potential conflict of interest.

Publisher's note

All claims expressed in this article are solely those of the authors and do not necessarily represent those of their affiliated organizations, or those of the publisher, the editors and the reviewers. Any product that may be evaluated in this article, or claim that may be made by its manufacturer, is not guaranteed or endorsed by the publisher.

Supplementary material

The Supplementary Material for this article can be found online at: https://www.frontiersin.org/articles/10.3389/fimmu.2022.997148/full#supplementary-material

References

1. Nzeako UC, Frigas E, Tremaine WJ. Hereditary angioedema: a broad review for clinicians. *Arch Intern Med* (2001) 161:2417–29. doi: 10.1001/archinte.161.20.2417

2. Agostoni A, Aygören-Pürsün E, Binkley KE, Blanch A, Bork K, Bouillet L, et al. Hereditary and acquired angioedema: problems and progress: proceedings of the third C1 esterase inhibitor deficiency workshop and beyond. *J Allergy Clin Immunol* (2004) 114:S51–131. doi: 10.1016/j.jaci.2004.06.047

3. Kaplan AP, Joseph K, Silverberg M. Pathways for bradykinin formation and inflammatory disease. *J Allergy Clin Immunol* (2002) 109:195–209. doi: 10.1067/mai.2002.121316

4. Banday AZ, Kaur A, Jindal AK, Rawat A, Singh S. An update on the genetics and pathogenesis of hereditary angioedema. *Genes Dis* (2019) 7:75–83. doi: 10.1016/j.gendis.2019.07.002

5. Caballero T, Cabañas R, Campos A, Cimbollek S, Gómez-Traseira C, González-Quevedo T, et al. Consensus statement on the diagnosis, management, and treatment of angioedema mediated by bradykinin. part i. classification, epidemiology, pathophysiology, genetics, clinical symptoms, and diagnosis. *J Investig Allergol Clin Immunol* (2011) 21:333–47.

6. Zotter Z, Csuka D, Szabó E, Czaller I, Nébenführer Z, Temesszentandrási G, et al. The influence of trigger factors on hereditary angioedema due to C1-inhibitor deficiency. *Orphanet J Rare Dis* (2014) 9:44. doi: 10.1186/1750-1172-9-44

7. Gompel A, Fain O, Boccon-Gibod I, Gobert D, Bouillet L. Exogenous hormones and hereditary angioedema. *Int Immunopharmacol* (2019) 78:106080. doi: 10.1016/j.intimp.2019.106080

8. Campos R de A, Valle SOR, Toledo EC. Hereditary angioedema: a disease seldom diagnosed by pediatricians. *J Pediatr* (2021) 97(Suppl 1):S10–6. doi: 10.1016/j.jped.2020.10.011

9. Campos RA, Valle SOR, Toledo EC. Hereditary angioedema: a disease seldom diagnosed by pediatricians. *J Pediatr* (2021) 97:S10–16. doi: 10.1016/j.jped.2020.10.011

10. Zuraw BL. Clinical practice. hereditary angioedema. *N Engl J Med* (2008) 359:1027–36. doi: 10.1056/NEJMcp0803977

11. Marcelino I, Callero A, Mendoza-Alvarez A, Pérez-Rodríguez E, Barrios-Recio J, García-Robaina J, et al. Bradykinin-mediated angioedema: an update of the genetic causes and the impact of genomics. *Front Genet* (2019) 10:900. doi: 10.3389/fgene.2019.00900

12. Caballero T, Farkas H, Bouillet L, Bowen T, Gompel A, Fagerberg C, et al. International consensus and practical guidelines on the gynecologic and obstetric management of female patients with hereditary angioedema caused by C1 inhibitor deficiency. *J Allergy Clin Immunol* (2012) 129:308–20. doi: 10.1016/j.jaci.2011.11.025

13. Mendoza-Alvarez A, Muñoz-Barrera A, Rubio-Rodríguez LA, Marcelino-Rodriguez I, Corrales A, Iñigo-Campos A, et al. Interactive web-based resource for annotation of genetic variants causing hereditary angioedema (HADA): Database development, implementation, and validation. *J Med Internet Res* (2020) 22: e19040. doi: 10.2196/19040

14. Patel G, Pongracic JA. Hereditary and acquired angioedema. *Allergy Asthma Proc* (2019) 40:441–5. doi: 10.2500/aap.2019.40.4267

15. Ponard D, Gaboriaud C, Charignon D, Ghannam A, Wagenaar-Bos IGA, Roem D, et al. SERPING1 mutation update: Mutation spectrum and C1 inhibitor phenotypes. *Hum Mutat* (2019) 41:38– 57. doi: 10.1002/humu.23917

16. Dewald G, Bork K. Missense mutations in the coagulation factor XII (Hageman factor) gene in hereditary angioedema with normal C1 inhibitor. *Biochem Biophys Res Commun* (2006) 343:1286–9. doi: 10.1016/j.bbrc.2006.03.092

17. Zuraw BL. Hereditary angioedema with normal C1 inhibitor: Four types and counting. *J Allergy Clin Immunol* (2018) 141:884–5. doi: 10.1016/j.jaci.2018.01.015

18. Bafunno V, Firinu D, D'Apolito M, Cordisco G, Loffredo S, Leccese A, et al. Mutation of the angiopoietin-1 gene (ANGPT1) associates with a new type of hereditary angioedema. *J Allergy Clin Immunol* (2018) 141:1009–17. doi: 10.1016/j.jaci.2017.05.020

19. Bork K, Wulff K, Steinmüller-Magin L, Braenne I, Staubach-Renz P, Witzke G, et al. Hereditary angioedema with a mutation in the plasminogen gene. *Allergy* (2018) 73:442–50. doi: 10.1111/all.13270

20. Bork K, Wulff K, Rossmann H, Steinmüller-Magin L, Braenne I, Witzke G, et al. Hereditary angioedema cosegregating with a novel kininogen 1 gene mutation changing the n-terminal cleavage site of bradykinin. *Allergy* (2019) 74:2479–81. doi: 10.1111/all.13869

21. Ariano A, D'Apolito M, Bova M, Bellanti F, Loffredo S, D'Andrea G, et al. A myoferlin gain-of-function variant associates with a new type of hereditary angioedema. *Allergy* (2020) 75:2989–92. doi: 10.1111/all.14454

22. Bork K, Wulff K, Möhl BS, Steinmüller-Magin L, Witzke G, Hardt J, et al. Novel hereditary angioedema linked with a heparan sulfate 3-o-sulfotransferase 6 gene mutation. *J Allergy Clin Immunol* (2021) 148:1041–8. doi: 10.1016/j.jaci.2021.01.011

23. Mendoza-Alvarez A, Marcelino-Rodriguez I, Almeida-Quintana L, Martin-Fernandez E, Martinez-Beltran D, Almeida-Sanchez Z, et al. First census of patients with hereditary angioedema in the canary islands. *J Clin Med Res* (2021) 10:4711. doi: 10.3390/jcm10204711

24. Bork K, Hardt J, Witzke G. Fatal laryngeal attacks and mortality in hereditary angioedema due to C1-INH deficiency. *J Allergy Clin Immunol* (2012) 130:692–7. doi: 10.1016/j.jaci.2012.05.055

25. Bernstein JA. Severity of hereditary angioedema, prevalence, and diagnostic considerations. *Am J Manage Care* (2018) 24:S292–8.

26. Maurer M, Magerl M, Ansotegui I, Aygören-Pürsün E, Betschel S, Bork K, et al. The international WAO/EAACI guideline for the management of hereditary angioedema – the 2017 revision and update. *World Allergy Organ J* (2018) 11:5. doi: 10.1186/s40413-017-0180-1

27. Germenis AE, Cicardi M. Driving towards precision medicine for angioedema without wheals. *J Autoimmun* (2019) 104:102312. doi: 10.1016/j.jaut.2019.102312

28. Henry Li H, Zuraw B, Longhurst HJ, Cicardi M, Bork K, Baker J, et al. Subcutaneous C1 inhibitor for prevention of attacks of hereditary angioedema: additional outcomes and subgroup analysis of a placebo-controlled randomized study. *Allergy Asthma Clin Immunol* (2019) 15:1–8. doi: 10.1186/s13223-019-0362-1

29. Maurer M, Magerl M, Betschel S, Aberer W, Ansotegui IJ, Aygören-Pürsün E, et al. The international WAO/EAACI guideline for the management of hereditary angioedema – the 2021 revision and update. *World Allergy Organ J* (2022) 15:100627. doi: 10.1016/j.waojou.2022.100627

30. Li H, Durbin R. Fast and accurate short read alignment with burrows-wheeler transform. *Bioinformatics* (2009) 25:1754–60. doi: 10.1093/bioinformatics/btp324

31. García-Alcalde F, Okonechnikov K, Carbonell J, Cruz LM, Götz S, Tarazona S, et al. Qualimap: evaluating next-generation sequencing alignment data. *Bioinformatics* (2012) 28:2678–9. doi: 10.1093/bioinformatics/bts503

32. Li H, Handsaker B, Wysoker A, Fennell T, Ruan J, Homer N, et al. The sequence Alignment/Map format and SAMtools. *Bioinformatics* (2009) 25:2078–9. doi: 10.1093/bioinformatics/btp352

33. Quinlan AR, Hall IM. BEDTools: a flexible suite of utilities for comparing genomic features. *Bioinformatics* (2010) 26:841–2. doi: 10.1093/bioinformatics/btq033

34. McKenna A, Hanna M, Banks E, Sivachenko A, Cibulskis K, Kernytsky A, et al. The genome analysis toolkit: a MapReduce framework for analyzing next-generation DNA sequencing data. *Genome Res* (2010) 20:1297–303. doi: 10.1101/gr.107524.110

35. DePristo MA, Banks E, Poplin R, Garimella KV, Maguire JR, Hartl C, et al. A framework for variation discovery and genotyping using next-generation DNA sequencing data. *Nat Genet* (2011) 43:491–8. doi: 10.1038/ng.806

36. Danecek P, Auton A, Abecasis G, Albers CA, Banks E, DePristo MA, et al. The variant call format and VCFtools. *Bioinformatics* (2011) 27:2156–8. doi: 10.1093/bioinformatics/btr330

37. Wang K, Li M, Hakonarson H. ANNOVAR: functional annotation of genetic variants from high-throughput sequencing data. *Nucleic Acids Res* (2010) 38:e164. doi: 10.1093/nar/gkq603

38. Landrum MJ, Lee JM, Riley GR, Jang W, Rubinstein WS, Church DM, et al. ClinVar: public archive of relationships among sequence variation and human phenotype. *Nucleic Acids Res* (2014) 42:D980–5, 42. doi: 10.1093/nar/gkt1113

39. Stenson PD, Mort M, Ball EV, Evans K, Hayden M, Heywood S, et al. The human gene mutation database: towards a comprehensive repository of inherited mutation data for medical research, genetic diagnosis and next-generation sequencing studies. *Hum Genet* (2017) 136:665–77. doi: 10.1007/s00439-017-1779-6

40. Kircher M, Witten DM, Jain P, O'Roak BJ, Cooper GM, Shendure J. A general framework for estimating the relative pathogenicity of human genetic variants. *Nat Genet* (2014) 46:310–5. doi: 10.1038/ng.2892

41. Li Q, Wang K. InterVar: Clinical interpretation of genetic variants by the 2015 ACMG-AMP guidelines. *Am J Hum Genet* (2017) 100:267–80. doi: 10.1016/j.ajhg.2017.01.004

42. Richards S, Aziz N, Bale S, Bick D, Das S, Gastier-Foster J, et al. Standards and guidelines for the interpretation of sequence variants: a joint consensus recommendation of the American college of medical genetics and genomics and the association for molecular pathology. *Genet Med* (2015) 17:405–24. doi: 10.1038/gim.2015.30

43. Robinson PN, Köhler S, Oellrich ASanger Mouse Genetics Project, , Wang K, Mungall CJ, et al. Improved exome prioritization of disease genes through cross-species phenotype comparison. *Genome Res* (2014) 24:340–8. doi: 10.1101/gr.160325.113

44. Danis D, Jacobsen JOB, Carmody L, Gargano M, McMurry JA, Hegde A, et al. Interpretable prioritization of splice variants in diagnostic next-generation sequencing. *Cold Spring Harbor Lab* (2021) 108:1564–77. doi: 10.1101/2021.01.28.428499. 2021.01.28.428499.

45. Plagnol V, Curtis J, Epstein M, Mok KY, Stebbings E, Grigoriadou S, et al. A robust model for read count data in exome sequencing experiments and implications for copy number variant calling. *Bioinformatics* (2012) 28:2747–54. doi: 10.1093/bioinformatics/bts526

46. Gurbich TA, Ilinsky VV. ClassifyCNV: a tool for clinical annotation of copy-number variants. *Sci Rep* (2020) 10:20375. doi: 10.1038/s41598-020-76425-3

47. Sharo AG, Hu Z, Sunyaev SR, Brenner SE. StrVCTVRE: A supervised learning method to predict the pathogenicity of human genome structural variants. *Am J Hum Genet* (2022) 109:195–209. doi: 10.1016/j.ajhg.2021.12.007. 2020.05.15.097048.

48. Carter PE, Duponchel C, Tosi M, Fothergill JE. Complete nucleotide sequence of the gene for human C1 inhibitor with an unusually high density of alu elements. *Eur J Biochem* (1991) 197:301–8. doi: 10.1111/j.1432-1033.1991.tb15911.x

49. Torene RI, Galens K, Liu S, Arvai K, Borroto C, Scuffins J, et al. Mobile element insertion detection in 89,874 clinical exomes. *Genet Med* (2020) 22:974–8. doi: 10.1038/s41436-020-0749-x

50. Bygum A, Aygören-Pürsün E, Caballero T, Beusterien K, Gholizadeh S, Musingarimi P, et al. The hereditary angioedema burden of illness study in Europe (HAE-BOIS-Europe): background and methodology. *BMC Dermatol* (2012) 12:4. doi: 10.1186/1471-5945-12-4

51. Craig T. Triggers and short-term prophylaxis in patients with hereditary angioedema. *Allergy Asthma Proc* (2020) 41:S30–4. doi: 10.2500/aap.2020.41.200058

52. Kulkarni M, Travers JB, Rohan C. High Estrogen States in Hereditary Angioedema: a Spectrum. *Clin Rev Allergy Immunol* (2021) 60:396–403. doi: 10.1007/s12016-021-08863-4

53. Roche O, Blanch A, Duponchel C, Fontán G, Tosi M, López-Trascasa M. Hereditary angioedema: the mutation spectrum of SERPING1/C1NH in a large Spanish cohort. *Hum Mutat* (2005) 26:135–44. doi: 10.1002/humu.20197

54. López-Lera A, Garrido S, Roche O, López-Trascasa M. SERPING1 mutations in 59 families with hereditary angioedema. *Mol Immunol* (2011) 49:18–27. doi: 10.1016/j.molimm.2011.07.010

55. Lek M, Karczewski KJ, Minikel EV, Samocha KE, Banks E, Fennell T, et al. Analysis of protein-coding genetic variation in 60,706 humans. *Nature* (2016) 536:285–91. doi: 10.1038/nature19057

56. Karczewski KJ, Francioli LC, Tiao G, Cummings BB, Alföldi J, Wang Q, et al. The mutational constraint spectrum quantified from variation in 141,456 humans. *Nature* (2020) 581:434–43. doi: 10.1038/s41586-020-2308-7

57. Kopanos C, Tsiolkas V, Kouris A, Chapple CE, Albarca Aguilera M, Meyer R, et al. VarSome: The human genomic variant search engine. *Bioinformatics* (2018) 35:1978–80. doi: 10.1093/bioinformatics/bty897

58. Pappalardo E, Caccia S, Suffritti C, Tordai A, Zingale LC, Cicardi M. Mutation screening of C1 inhibitor gene in 108 unrelated families with hereditary angioedema: functional and structural correlates. *Mol Immunol* (2008) 45:3536–44. doi: 10.1016/j.molimm.2008.05.007

59. Andrejević S, Korošec P, Šilar M, Košnik M, Mijanović R, Bonači-Nikolić B, et al. Hereditary Angioedema Due to C1 Inhibitor Deficiency in Serbia: Two Novel Mutations and Evidence of Genotype-Phenotype Association. *PloS One* (2015) 10:e0142174. doi: 10.1371/journal.pone.0142174

60. Grodecká L, Hujová P, Kramárek M, Kršjaková T, Kováčová T, Vondrášková K, et al. Systematic analysis of splicing defects in selected primary immunodeficiencies-related genes. *Clin Immunol* (2017) 180:33–44. doi: 10.1016/j.clim.2017.03.010

61. Guillen-Guio B, Lorenzo-Salazar JM, González-Montelongo R, Díaz-de Usera A, Marcelino-Rodríguez I, Corrales A, et al. Genomic analyses of human European diversity at the southwestern edge: Isolation, African influence and disease associations in the canary islands. *Mol Biol Evol* (2018) 35:3010–26. doi: 10.1093/molbev/msy190

62. Bygum A. Hereditary angio-oedema in Denmark: a nationwide survey. *Br J Dermatol* (2009) 161:1153–8. doi: 10.1111/j.1365-2133.2009.09366.x

63. Faiyaz-Ul-Haque M, Al-Gazlan S, Abalkhail HA, Al-Abdulatif A, Toulimat M, Peltekova I, et al. Novel and recurrent mutations in the C1NH gene of Arab patients affected with hereditary angioedema. *Int Arch Allergy Immunol* (2010) 151:149–54. doi: 10.1159/000236005

64. Kesim B, Uyguner ZO, Gelincik A, Mete Gökmen N, Sin AZ, Karakaya G, et al. The Turkish hereditary angioedema pilot study (TURHAPS): the first Turkish series of hereditary angioedema. *Int Arch Allergy Immunol* (2011) 156:443–50. doi: 10.1159/000323915

65. Iwamoto K, Tanaka A, Hiragun M, Kawai M, Mihara S, Takenaka M, et al. Novel and recurrent C1 inhibitor gene mutations in nine Japanese patients with hereditary angioedema. *J Dermatol Sci* (2012) 68:68–70. doi: 10.1016/j.jdermsci.2012.06.012

66. Martinho A, Mendes J, Simões O, Nunes R, Gomes J, Dias Castro E, et al. Mutations analysis of C1 inhibitor coding sequence gene among Portuguese patients with hereditary angioedema. *Mol Immunol* (2013) 53:431–4. doi: 10.1016/j.molimm.2012.09.003

67. Psarros F, Koutsostathis N, Farmaki E, Speletas MG, Germenis AE. Hereditary angioedema in Greece: the first results of the greek hereditary angioedema registry. *Int Arch Allergy Immunol* (2014) 164:326–32. doi: 10.1159/000366276

68. Johnsrud I, Kulseth MA, Rødningen OK, Landrø L, Helsing P, Waage Nielsen E, et al. A nationwide study of Norwegian patients with hereditary angioedema with C1 inhibitor deficiency identified six novel mutations in SERPING1. *PloS One* (2015) 10:e0131637. doi: 10.1371/journal.pone.0131637

69. Steiner UC, Keller M, Schmid P, Cichon S, Wuillemin WA. Mutational spectrum of the SERPING1 gene in Swiss patients with hereditary angioedema. *Clin Exp Immunol* (2017) 188:430–6. doi: 10.1111/cei.12941

70. Karadža-Lapić L, Barešić M, Vrsalović R, Ivković-Jureković I, Sršen S, Prkačin I, et al. Hereditary angioedema due to C1-inhibitor deficiency in pediatric patients in croatia. first national study, diagnostic and prophylactic challenges. *Acta Clin Croat.* (2019) 58:139–46. doi: 10.20471/acc.2019.58.01.18

71. Liu S, Xu Y, Liu Y, Zhi Y. Hereditary angioedema: a Chinese perspective. *Eur J Dermatol* (2019) 29:14–20. doi: 10.1684/ejd.2018.3487

72. Gábos G, Moldovan D, Dobru D, Mihály E, Bara N, Nădăşan V, et al. Mutational spectrum and genotype-phenotype relationships in a cohort of Romanian hereditary angioedema patients caused by C1 inhibitor deficiency. *Rev Română Medicină Laborator* (2019) 27:255–68. doi: 10.2478/rrlm-2019-0029

73. Schöffl C, Wiednig M, Koch L, Blagojevic D, Duschet P, Hawranek T, et al. Hereditary angioedema in Austria: prevalence and regional peculiarities. *J Dtsch Dermatol Ges* (2019) 17:416–23. doi: 10.1111/ddg.13815

74. Arce-Ayala YM, Diaz-Algorri Y, Craig T, Ramos-Romey C. Clinical profile and quality of life of Puerto ricans with hereditary angioedema. *Allergy Asthma Proc* (2019) 40:103–10. doi: 10.2500/aap.2019.40.4200

75. Pagani F, Raponi M, Baralle FE. Synonymous mutations in CFTR exon 12 affect splicing and are not neutral in evolution. *Proc Natl Acad Sci U S A* (2005) 102:6368–72. doi: 10.1073/pnas.0502288102

76. Stergachis AB, Haugen E, Shafer A, Fu W, Vernot B, Reynolds A, et al. Exonic transcription factor binding directs codon choice and affects protein evolution. *Science* (2013) 342:1367–72. doi: 10.1126/science.1243490

77. Duan J, Shi J, Ge X, Dölken L, Moy W, He D, et al. Genome-wide survey of interindividual differences of RNA stability in human lymphoblastoid cell lines. *Sci Rep* (2013) 3:1318. doi: 10.1038/srep01318

78. Zeng Z, Aptekmann AA, Bromberg Y. Decoding the effects of synonymous variants. *Nucleic Acids Res* (2021) 49:12673–91. doi: 10.1093/nar/gkab1159

79. Lord J, Baralle D. Splicing in the diagnosis of rare disease: Advances and challenges. *Front Genet* (2021) 12:689892. doi: 10.3389/fgene.2021.689892

80. Tomar S, Sethi R, Lai PS. Specific phenotype semantics facilitate gene prioritization in clinical exome sequencing. *Eur J Hum Genet* (2019) 27:1389–97. doi: 10.1038/s41431-019-0412-7

81. Walsh R, Lahrouchi N, Tadros R, Kyndt F, Glinge C, Postema PG, et al. Enhancing rare variant interpretation in inherited arrhythmias through quantitative analysis of consortium disease cohorts and population controls. *Genet Med* (2020) 23:47–58. doi: 10.1038/s41436-020-00946-5

frontiers | Frontiers in Immunology

TYPE Mini Review
PUBLISHED 30 September 2022
DOI 10.3389/fimmu.2022.1010893

Check for updates

OPEN ACCESS

EDITED BY
Per Nilsson,
Linnaeus University, Sweden

REVIEWED BY
Xuchu Que,
University of California, San Diego,
United States

*CORRESPONDENCE
Nikolina Papac-Milicevic
nikolina.papac@meduniwien.ac.at

SPECIALTY SECTION
This article was submitted to
Molecular Innate Immunity,
a section of the journal
Frontiers in Immunology

RECEIVED 03 August 2022
ACCEPTED 12 September 2022
PUBLISHED 30 September 2022

CITATION
Alic L, Binder CJ and Papac-Milicevic N
(2022) The OSE complotype
and its clinical potential.
Front. Immunol. 13:1010893.
doi: 10.3389/fimmu.2022.1010893

COPYRIGHT
© 2022 Alic, Binder and Papac-Milicevic.
This is an open-access article distributed
under the terms of the Creative
Commons Attribution License (CC BY).
The use, distribution or reproduction
in other forums is permitted, provided
the original author(s) and the
copyright owner(s) are credited and
that the original publication in this
journal is cited, in accordance with
accepted academic practice. No use,
distribution or reproduction is
permitted which does not comply with
these terms.

The OSE complotype and its clinical potential

Lejla Alic[1], Christoph J. Binder[2] and Nikolina Papac-Milicevic[2]*

[1]Department of Medical Biochemistry, Faculty of Medicine, University of Sarajevo, Sarajevo, Bosnia and Herzegovina, [2]Department of Laboratory Medicine, Medical University of Vienna, Vienna, Austria

Cellular death, aging, and tissue damage trigger inflammation that leads to enzymatic and non-enzymatic lipid peroxidation of polyunsaturated fatty acids present on cellular membranes and lipoproteins. This results in the generation of highly reactive degradation products, such as malondialdehyde (MDA) and 4-hydroxynonenal (4-HNE), that covalently modify free amino groups of proteins and lipids in their vicinity. These newly generated neoepitopes represent a unique set of damage-associated molecular patterns (DAMPs) associated with oxidative stress termed oxidation-specific epitopes (OSEs). OSEs are enriched on oxidized lipoproteins, microvesicles, and dying cells, and can trigger sterile inflammation. Therefore, prompt recognition and removal of OSEs is required to maintain the homeostatic balance. This is partially achieved by various humoral components of the innate immune system, such as natural IgM antibodies, pentraxins and complement components that not only bind OSEs but in some cases modulate their pro-inflammatory potential. Natural IgM antibodies are potent complement activators, and 30% of them recognize OSEs such as oxidized phosphocholine (OxPC-), 4-HNE-, and MDA-epitopes. Furthermore, OxPC-epitopes can bind the complement-activating pentraxin C-reactive protein, while MDA-epitopes are bound by C1q, C3a, complement factor H (CFH), and complement factor H-related proteins 1, 3, 5 (FHR-1, FHR-3, FHR-5). In addition, CFH and FHR-3 are recruited to 2-(ω-carboxyethyl) pyrrole (CEP), and full-length CFH also possesses the ability to attenuate 4-HNE-induced oxidative stress. Consequently, alterations in the innate humoral defense against OSEs predispose to the development of diseases associated with oxidative stress, as shown for the prototypical OSE, MDA-epitopes. In this mini-review, we focus on the mechanisms of the accumulation of OSEs, the pathophysiological consequences, and the interactions between different OSEs and complement components. Additionally, we will discuss the clinical potential of genetic variants in OSE-recognizing complement proteins – the OSE complotype - in the risk estimation of diseases associated with oxidative stress.

KEYWORDS

oxidation-specific epitopes, oxidative stress, DAMPs (damage-associated molecular patterns), complement - immunological terms, natural antibodies (NAbs), pentraxins, immune recognition

10.3389/fimmu.2022.1010893

1 Introduction

1.1 Generation of OSE

Increased oxidative stress, characterized by exalted levels of reactive oxygen species, leads to lipid peroxidation of polyunsaturated fatty acids localized in cellular membranes. Lipid peroxidation can be initiated by enzymatic or non-enzymatic mechanisms, resulting in the generation of reactive lipid mediators. Adduction of reactive lipid degradation products to free amino-groups on macromolecules generates novel neo-epitopes, termed oxidation-specific epitopes (OSEs) (1). Once adducted, OSEs have the capacity to alter the function of the affected biomolecule and tag their carrier as "altered-self". Although there is a large amount of different lipid degradation byproducts that can create OSEs, the best studied examples are malondialdehyde and the more advanced malondialdehydeacetaldehyde, which we are collectively calling MDA (as umbrella term for different MDA-epitopes), 4-hydroxynonenal (4-HNE), 2-(ω-carboxyethyl)-pyrrole (CEP), oxidized cardiolipin (OxCL) and the phosphocholine head group-containing oxidized phospholipids (OxPC).

Within tissues or in the circulation, OSE-decorated structures are considered to be markers of oxidative stress and are found in many pathological conditions such as chronic inflammation, autoimmunity, infections, cancer, and neurological disorders (1–7).

1.2 Biological carriers and function of OSEs

The ubiquitous presence of lipids in living cells enables OSEs formation on versatile biological carriers. Major carriers are free biomolecules, oxidized lipoproteins, microvesicles, and apoptotic cells (1).

1.2.1 Free biomolecules

1.2.1.1 Proteins

On proteins, OSEs are attached to the amino groups of lysine and arginine side chains, but modifications of other amino acids have been shown (8–12). This irreversible adduction can alter protein carrier function, lead to aggregation, and increase its immunogenicity (13, 14). The ultimate fate of OSE-modified proteins in homeostasis is proteolytic degradation or clearance by immune responses.

1.2.1.2 Nucleic acids

Nuclear and mitochondrial DNA modifications by MDA and 4-HNE are mutagenic and cancerogenic by causing nucleotide exchange or forming cross-links (11, 15).

1.2.1.3 Phospholipids

Amino group-containing phospholipids, such as phosphatidylethanolamine (PE) and phosphatidylserine (PS), can be modified by MDA, 4-HNE, and CEP (16–21). OSEs on phospholipids alter their recognition by pattern recognition receptors (PRR) and their ability to serve as phospholipase substrates (22–24).

1.2.2 Lipoproteins

1.2.2.1 Low-density lipoprotein

Oxidized LDL has been discovered as the initial carrier of OSEs, where they are considered to be major drivers of atherosclerosis development (25, 26). Following the retention of plasma LDL in the intima of the arterial wall, both the lipid and protein components of LDL can become oxidized (OxLDL). Newly oxidized LDL is pro-inflammatory, chemotactic, and pro-coagulatory (2, 27). Upon OxLDL clearance, engulfing macrophages are converted into foam cells - hallmark cells of atherosclerotic plaques (28–30). Additionally, MDA-, 4-HNE-, OxPC-, and OxCL-epitopes have been documented in atherosclerotic plaques of mice and humans (25, 31–36).

1.2.2.2 High-density lipoprotein

Once modified by OSEs, HDL loses its function to remove cholesterol from cells *via* the ATP-binding cassette transporter A1 (ABCA1) pathway and, *via* CD36, promotes platelet aggregation (37–41).

1.2.3 Microvesicles

Microvesicles are extracellular vesicles (0,1 - 1 μm) with a phospholipid bilayer enriched in phosphatidylserine. They are generated by cellular activation or apoptosis and are pro-coagulatory and pro-inflammatory (2, 42, 43). As carriers of parental cells' biological cargo, they play a role in inter-organ communication, and alterations in their numbers and content are associated with many pathologies (43, 44). The presence of OSEs, namely MDA- and OxPC-epitopes, has been demonstrated on a subset of circulating MVs and MVs from *in vitro* stimulated cells (45–47).

1.2.4 Dying cells

The presence of OSEs on dying cells and apoptotic blebs seems to be independent of the mechanism of apoptosis induction and the cell types undergoing apoptosis (33, 34, 48–52). Early experiments already proposed that the presence of OSEs on cells undergoing programmed cell death (apoptosis and necrosis) plays a role in their clearance by enhancing their ability to be recognized by phagocytic cells (48, 53).

1.3 The function of OSEs as danger-associated molecular pattern molecules

Among well-established DAMPs, like histones, cholesterol crystals, DNA, and others, OSEs represent a distinct group (1, 54). Exposure of OSEs mediates the recognition by innate immunity sensors and can trigger sterile inflammation (51, 52, 55–60). The main cellular innate sensors of OSEs are scavenger receptors and - typically in cooperation - toll-like receptors (TLRs), which are responsible not only for recognition but also for the initiation of downstream signaling events (1).

In vitro, treatment with MDA-modified proteins and MDA+ MVs induces cytokine secretion (e.g., interleukin-8 (IL-8), or its murine functional homologues chemokine ligand 1(CXCL1) and CXCL2) in various human or murine cell types and cell lines (47, 51, 52, 61). Moreover, *in vivo*, intravitreal injection of MDA-modified bovine serum albumin (BSA) led to an increase in CXCL1 expression in retinal pigment epithelial (RPE) cells (52). Similarly, in a mouse peritonitis model, injection of MDA-BSA resulted in secretion of CXCL1 and CXCL2 and recruitment of neutrophils and monocytes. Moreover, treatment with the anti-MDA IgM antibody (LR04) attenuated hepatic pro-inflammatory cytokine secretion and leukocyte infiltration induced by the western diet (51). Scavenger receptor A1 (SRA1), CD36, lectin-like OxLDL receptor (LOX1), and CD16 on monocytes and macrophages have been shown to act as sensors for MDA (51, 62–64).

4-HNE increased cytokine secretion, e.g., IL-8, recruitment of neutrophils and macrophages *via* TLR4/NFκB in animal models of atherosclerosis and chronic obstructive pulmonary disease (59, 60). Also, it stimulated the release of pro-coagulatory tissue factor-positive MVs from perivascular cells (65). LOX1 has been identified as the scavenger receptor for 4-HNE (66).

OxPC or OxPC-rich MVs have been reported to induce endothelial cell activation, monocyte recruitment, cytokine secretion (e.g., IL-6) by macrophages, and apoptosis in smooth muscle cells (3, 45, 49, 67). Furthermore, OxPC drives hypercholesterolemia-induced inflammation and atherogenesis and restrains bone formation *in vivo* (4, 35). SRB1, TLR2, and CD36-TLR4-TLR6 heterotrimeric signaling complex are required to recognize Ox-PC (68–70).

CEP has been shown to activate the NLRP3 inflammasome and stimulate the production of IL-1β (71). Moreover, injection of CEP into the mouse eye increased Th1 response and enhanced angiogenesis (72–74). Additionally, in a peritonitis model, CEP generated by neutrophils promotes infiltration of monocytes and macrophages by binding to β2 integrins on their surfaces (75). For CEP binding and clearance, the coordinated action of CD36 and TLR2 is required (76).

2 Recognition of OSEs by innate humoral immunity

Both innate and adaptive immune responses against OSEs have been demonstrated, and their functional implications are being elucidated. Thus, in this mini-review we will focus solely on representatives of soluble innate immune responses to OSEs: natural IgM antibodies, pentraxins, and several components of the complement cascade because their levels and genetic variants have been implicated in the development of diseases associated with increased oxidative stress (Table 1).

2.1 Natural antibodies

Natural IgM antibodies are pre-existing antibodies that typically contain unmutated variable regions encoded by germline gene sequences. In mice, natural antibodies are

TABLE 1 Plasma proteins recognizing OSEs and their reported biological effects.

Complement component	OSEs	The biological effect of OSE binding	Reference
Natural antibodies	MDA-, OxLDL	Clearance and neutralization of OxLDL-, MV-, and apoptotic cells-induced inflammation; protection against atherosclerosis and CVDs; inhibition of MV-mediated coagulation	(42, 45, 47, 77–92)
CRP	OxPC-	Binding to apoptotic cells and in atherosclerotic lesions; activation of CCC	(49, 93, 94)
PTX3	OxLDL	Promoting OxLDL uptake by macrophages	(95, 96)
C1q	MDA-, OxLDL	CCC activation; clearance of oxLDL in an anti-inflammatory manner	(97–100)
C3a	MDA-	OxLDL facilitates clearance of C3a by macrophages	(101, 102)
CFH	MDA-[a], OxLDL (OxPC-)[b], 4-HNE-[c], CEP-[d]	Decreasing inflammation[a], inhibition of complement activation[b,d], protection from cell death[c]	(52, 103–109)
FHR-1	MDA-	Propagation of inflammation and deregulation of CFH function	(105, 110, 111)
FHR-3	MDA-, CEP-	Propagation of inflammation	(105, 112)
FHR-5	MDA-	Reducing CFH cofactor activity and increasing C3 deposition	(113)

The superscript letter in the second column designates the reported biological function in the third column.

secreted by B1 cells, but marginal zone B cells may also contribute to their production. Natural antibodies arise in newborns without infections or exposure to exogenous antigens and thus can be found in gnotobiotic mice. Thirty percent of all natural IgM antibodies have specificity for OSEs, such as MDA, OxPC, and 4-HNE, among which MDA is the predominant antigen (50). A series of OSE-specific natural IgM antibodies have been cloned, of which the best characterized are LR04, NA17, and E014 (recognizing MDA), T15/E06 (recognizing OxPC), and LR01 (recognizing OxCL) (25, 33, 34, 48, 50, 114). They bind to microbial antigens and altered-self structures, which allows them to mediate important functions in host defense, but also makes them essential in homeostasis maintenance, respectively (115). Natural IgM antibodies neutralize the pro-inflammatory effects of oxidized lipids and MVs, mediate apoptotic cell clearance, and are anti-atherogenic by blocking OxLDL uptake and foam cell formation (45, 47, 77–79). Additionally, we have shown that anti-MDA IgM hinders the binding of coagulation factors X/Xa on MVs, attenuating the propagation of coagulation and protecting from pulmonary thrombosis in mice (42). Moreover, MDA-targeted passive and active immunization strategies that increase the levels of MDA-specific IgM protect from atherosclerosis and hepatic inflammation (80–82). Furthermore, mice unable to secrete natural IgM antibodies display impaired clearance of apoptotic cells and develop arthritis and lupus-like disease, which can be in part explained by the lack of OSE-specific IgMs (83–85). Finally, studies in various human cohorts demonstrated that low levels of IgMs against OSEs are associated with an elevated risk of developing cardiovascular diseases (CVDs), confirming the beneficial role of anti-OSE IgMs (86–92).

2.2 Pentraxins

Pentraxins are acute-phase proteins and represent soluble innate pattern recognition proteins. As such, they facilitate the removal of invading microorganisms and damaged host cells. There are two types of pentraxins, short (C-reactive protein (CRP) and serum amyloid P (SAP)) and long ones (pentraxin 3 (PTX3)) (116). CRP has been shown to bind to OxPC on OxLDL, and they colocalize on the surface of apoptotic cells and in human atherosclerotic lesions (49, 93). When CRP is complexed with OxPC-epitopes, it recruits C1q and activates the C1 complex of the classical complement cascade (CCC) (94). In contrast to CRP, SAP and PTX3 do not bind to OSEs, although SAP competes out the binding of plasma IgM and CRP on late apoptotic cells (93). Interestingly, OxLDL enhanced the expression of PTX3, which promoted OxLDL uptake by macrophages and blocked cholesterol efflux (95, 96). Furthermore, PTX3 protects against 4-HNE-induced complement activation by recruiting CFH to the basal RPE and inner Bruch's membrane in AMD (117).

2.3 Complement components

The complement cascade protects and orchestrates the removal of invading pathogens and altered self- or foreign-structures by employing three pathways. Its activity is steered by complement activators and regulators that prevent collateral damage to host tissues.

2.3.1 C1q

C1q is a multimeric protein, a part of the initiator complex of the CCC. With its globular head, it can recognize pathogen-associated molecular patterns (PAMPs), DAMPs, and immune complexes, and once bound, it activates the CCC with the collagen-like domain. It binds to OxLDL, which leads to the complement activation and deposition of C3b, facilitating OxLDL uptake by monocytes and macrophages (97, 98). Additionally, the engulfment of OxLDL with C1q suppresses macrophage NFκB and NLRP3 activation, resulting in an enhancement of IL-10 and a reduction in IL-1β secretion (99). The initial notion that the binding of C1q to oxidized lipoproteins is mediated through OSEs came from the finding that MDA-LDL binds C1q, resulting in the deposition of C4b and activation of the CCC, which can be inhibited by ApoE (100). Furthermore, C1q is found both on circulating MVs, and apoptotic cells; however, if this binding is (in part) OSE-dependent has not been investigated so far (118–120). Due to the impairment of apoptotic cell clearance, C1q deficiency in mice and men predisposes to the development of systemic lupus erythematosus (SLE) (118, 121).

2.3.2 C3a

Complement anaphylatoxin C3a is a small degradation product of C3 generated by C3 convertase. It is a chemotactic molecule of the immune system, and although classically considered a pro-inflammatory molecule, C3a has been shown to have some anti-inflammatory functions (122, 123). MDA-epitopes are ligands for C3a on OxLDL and apoptotic cells. Furthermore, this OxLDL-C3a interaction results in increased internalization of C3a by macrophages, thus making OxLDL a platform enhancing uptake of C3a (101). Myeloperoxidase-rich MVs can also be the carriers of C3a; however, if recruitment of C3a to MVs is mediated by OSEs has to be elucidated (124).

2.3.3 Complement factor H

Complement factor H is the regulator of the alternative complement pathway. It comprises 20 short consensus repeat (SCR) domains and acts as a sensor of PAMPs and DAMPs. Additionally, a splice variant of CFH exists – factor H-like protein 1 (FHL-1). Impairment of CFH functions contributes to the development of many diseases, with AMD and atypical hemolytic uremic syndrome as the most prominent examples (125, 126). Weismann et al. demonstrated that CFH and FHL-1

recognize MDA-epitopes and colocalize within the retina and atherosclerotic lesions. MDA recognition is achieved by SCR7 and SCR19-20, where SCR7 is the most critical, but SCR19-20 also matter (103–106). CFH protects from MDA-induced IL-8 secretion and inactivates C3b into iC3b on MDA-carrying surfaces (52). Furthermore, the CFH variant Tyr402His (rs1061170) within SCR7 that predisposes to AMD results in decreased binding to MDA-epitopes in healthy individuals and AMD patients (52, 105). Similarly, transgenic mice with human SCR6-8 402His inserted into a mouse CFH display an AMD-like phenotype (103). In addition, CFH binds CEP-decorated surfaces and this binding is attenuated in the presence of complement factor H-related protein 3 (FHR-3) (112). The observation that CFH binds to OxPC-epitopes requires further validation (52, 107, 108). Although CFH does not directly interact with 4-HNE-epitopes, it protects ARPE-19 cells from 4-HNE-induced cell death by attenuating apoptotic and necroptotic cell death pathways (52, 109). Next to OSEs, CFH binds many other DAMPs on the surface of dying cells, apoptotic blebs, and MVs (52, 110, 127, 128). There, CFH compensates for the loss of membrane-bound complement inhibitors by protecting cells from excessive complement activation and limiting inflammatory potential (127, 128).

2.3.4 Complement factor H-related proteins

FHRs are five plasma proteins that share high structural and functional similarities with CFH, among other recognition of OSEs by FHR-1, 3-, and -5. Interestingly, FHRs do not have potent complement regulatory activity like CFH. Their competition with CFH in recruitment to various ligands labels them as "deregulators of CFH activity" (129, 130).

Using a genome-wide association study, we identified FHR-1 as the main competitor to CFH for binding MDA-epitopes in a cohort of healthy individuals. Once bound to MDA-epitopes, FHR-1 blocks CFH-mediated C3b inactivation, allowing C3b and Bb deposition and propagation of the alternative complement pathway. MDA-epitopes on necrotic cells are recognized by FHR-1 *via* SCR1-2 (105, 110, 111). This activates monocytes in the vicinity *via* EMR2 receptors and NLRP3 pathway (111). Consequently, in necrotic cores of atherosclerotic lesions, FHR-1 colocalizes with macrophages and stimulates IL-1β and IL-8 secretion (110). Considering its property to bind MDA-epitopes, deletion of the gene encoding for FHR-1 (CFHR1) is assumed to be beneficial in chronic inflammation. Indeed, carriers of this deletion have a reduced risk of atherosclerotic CVDs and anti-neutrophil cytoplasmic antibody-associated vasculitis and display lower levels of inflammatory markers (110, 111). Therefore, on MDA-carrying host surfaces, FHR-1 is pro-inflammatory. Of note, FHR-1 does not bind any other OSEs (105).

The deletion of CFHR3&CFHR1 genes was shown to enhance CFH binding to MDA-epitopes because, as FHR-1, FHR-3 competes for them. Compared to FHR-1 and CFH, it displays the lowest affinity towards MDA-epitopes. Once bound to MDA-epitopes, FHR-3 does not cause deregulation of CFH function (105). Moreover, FHR-3 has been shown to also bind to CEP-epitopes but does not interact with OxPC- and 4-HNE-modifications (105, 112). Interestingly, when attached to the surface of polarized senescent ARPE-19 cells, FHR-3 is internalized. Engulfed FHR-3 drives pro-inflammatory responses of RPE cells by upregulating C3 and factor B expression and translocating newly generated C3a from the cytoplasm to the membrane (112). Although the relation between OSE-binding and FHR-3 has not been investigated in diseases associated with a high level of oxidative stress, in many of them, e.g., rheumatoid arthritis and SLE, FHR-3 serum levels are increased, and the lack of CFHR3 gene is protective (131).

Complement factor H-related protein 5, one of the largest members of the FHR family, attaches itself to apoptotic and necrotic cells through SCR5-7 domains. MDA-epitopes were shown to be the predominant ligands responsible for this recruitment, as demonstrated by the fact that the density of these epitopes determines the amount of FHR-5 bound. Like FHR-1 and FHR-3, when attached to MDA-epitopes, FHR-5 reduces CFH cofactor activity and enhances C3 deposition. Additionally, a hybrid protein FHR-21-2-FHR-5 obtained from the serum of a patient with C3 glomerulopathy binds to MDA-epitopes (113). When adhered to apoptotic and necrotic cells' surfaces, FHR-5 and FHR-1 recruit CRP and PTX3 and activate classical and alternative complement pathways, facilitating opsonization (132).

2.4 The connection between natural IgM antibodies, pentraxins, and complement proteins

Although OSE-recognizing IgM antibodies and pentraxins have been shown to instruct phagocytic cells for clearance of damaged structures individually, they can also employ the complement cascade to ensure even more efficient and potent removal machinery (1, 49, 114, 133).

Natural IgM antibodies, CRP, and SAP have been shown to recruit early components of the CCC, such as C1q, mannose-binding lectin, and ficolins in efferocytosis (49, 84, 93, 134–137). Additionally, on the surface of apoptotic cells, regulators of complement activity - C4-binding protein (C4BP) and CFH - can attach directly to DAMPs or indirectly, e.g., through CRP (108, 138, 139). Recruitment of these complement regulators prevents the assembly of the membrane attack complex and lysis, keeping efferocytosis immunosilent. After engulfment of apoptotic cells opsonized with CRP and complement, macrophages maintain an anti-inflammatory status (136, 140, 141). In contrast to other complement components, FHR-1, -3, and -5 have been shown to bind to the surface of necrotic cells *via* OSEs, CRP, or other DAMPs to enhance opsonization by

complement activation and act pro-inflammatory (111, 113, 132, 142).

Importantly, it has to be kept in mind that the combined recognition of MDA and any other co-expose OSE by various humoral immune responses as well as the cellular receptors binding them and/or the cellular receptors binding OSE directly will ultimately determine the net biological effect. The elucidation of these functional responses will provide insights into the pathophysiological relevance of OSE recognition by humoral immunity.

3 OSEs, recognition of OSEs and its clinical potential

Structures modified by OSEs have been detected practically everywhere, in various tissues and body fluids (4, 10).

As markers of enhanced oxidative stress, OSEs occur early, contribute to disease development, and have strong biomarker potential that has not been explored enough. The most commonly used assay for lipid peroxidation, thiobarbituric acid reactive substances assay (TBARS), is not specific, while mass spectrometry, immunological, chromatography, and imaging techniques are much more specific and reliable but costly. Still, even today, TBA-based assays are used in many clinical studies (143, 144). In contrast, studies that monitor immune responses against OSEs and their effects have not been broadly performed. Many such investigations have been conducted for atherosclerosis as a prototypical OSE-driven pathology with a vital contribution of the immune system. Evidence obtained from this research supports the observation that IgG antibodies to OxLDL are pro-atherogenic and increase the risk of developing CVDs – though this association may be more complex and depend on the IgG isotype. In contrast, IgM antibodies to OxLDL have largely shown to be associated with atheroprotection (145, 146). An even more precise prediction for CVD events was observed in a prospective 15-year-long study when the multivariable prediction models, including levels of oxidized phospholipids (OxPL)/apolipoprotein B (apoB) as OSEs, OSE-specific IgM and IgG antibodies, and CRP were used (88). It is known that the levels of CRP correlate with the levels of OSEs (MDA and 4-HNE), but if this association depends on CRP genetic variants influencing CRP levels and/or recruitment to damaged surfaces have not been investigated so far (147).

Furthermore, OSE-recognizing complement components have been associated with the development of autoimmunity,

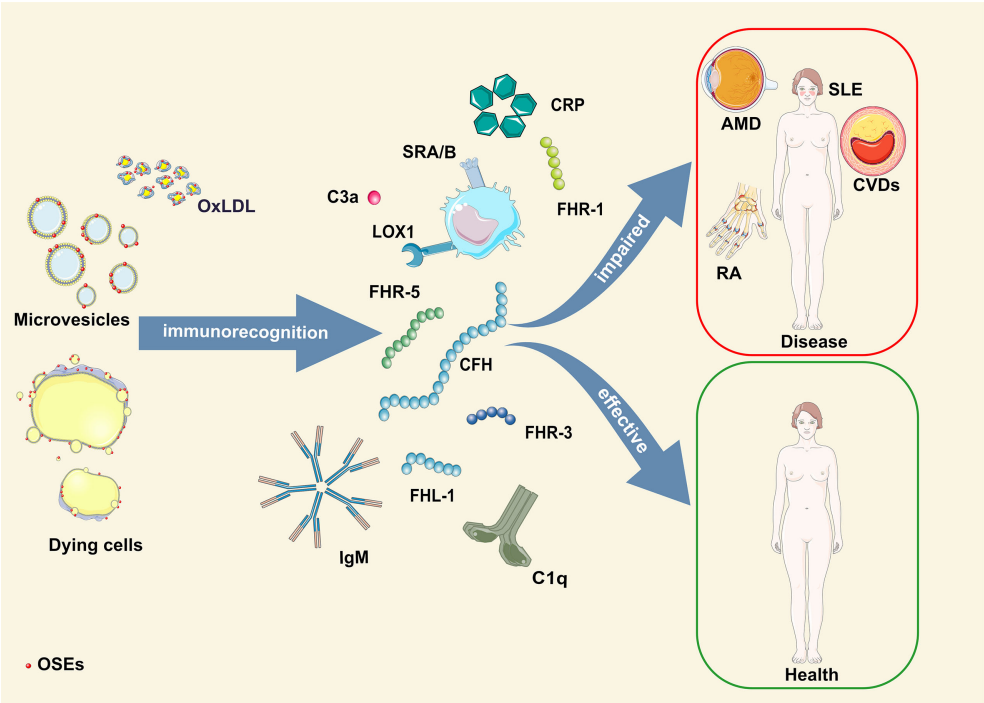

FIGURE 1
Schematic illustration of OSE humoral immunorecognition and consequences thereof. AMD, age-related macular degeneration; CFH, complement factor H-related protein; CRP, C-reactive protein; CVDs, cardiovascular diseases; FHL-1, factor H-like protein 1; FHR-1, -3, -5, complement factor H-related protein 1, 3, 5; OSE, oxidation-specific epitopes; OxLDL, oxidized low-density lipoprotein; RA, rheumatoid arthritis; SLE, systemic lupus erythematosus.

emphasizing the importance of these proteins in the clearance of damaged cells and prevention of autoantigen spill-over. So far, the interaction between C1q and MDA has not been characterized; therefore, no polymorphisms in C1q were shown to influence MDA-binding or levels. However, congenital C1q deficiency is associated with the development of lupus-like autoimmunity due to the impaired clearance of apoptotic cells (118, 148). Interestingly, in SLE, the OSE levels (MDA, 4-HNE, and OxPC) and OSE-specific IgM and IgG antibodies are altered (149–151).

The most important modulators of CFH binding to MDA-epitopes – the CFH variant Tyr402His and the deletion of CFHR3&CFHR1 genes – are frequent in the population and affect the development of the two most common diseases, atherosclerosis and AMD (52, 105). Although these diseases affect different organs, they have a similar underlying pathology linked with increased oxidative stress. Deletion of CFHR3&CFHR1 genes offers protection in both of them, while Tyr402His is deleterious in AMD and possibly atherosclerosis, highlighting CFH's importance in homeostatic responses (110, 152–155). Since CFH is a crucial player in regulating complement activation, variants affecting its activity have been used in combined genetic risk scores/haplotypes for some complementopathies (153).

Based on the available literature, it is evident that the early appearance of OSEs and innate humoral immune responses are critical players in the development and progression of pathologies caused by oxidative stress (Figure 1). Therefore, using individual genetic variants or levels of OSE-recognizing proteins in disease prediction models generates less accurate prediction scores. To obtain a more precise, personalized risk prediction score for the ability of the host to deal with increased oxidative stress, we suggest using integrative analysis that considers all individual OSE-related parameters combined (levels of OSE and OSE-recognizing proteins and genetic variant within OSE-recognizing proteins). A strong argument for such an approach comes from a study in which combining CEP levels with AMD risk alleles in ARMS2, HtrA serine peptidase 1 (HTRA1), CFH or C3 showed a twofold to threefold increased risk score compared to a genotype-based score alone (156).

Thus, we propose a novel concept – the OSE complotype. The OSE complotype would include levels of specific OSEs, immune responses involved in their detection and clearance, and a repertoire of inherited genetic variants that modulate properties of OSE-recognizing proteins. This integrative method would allow for a more precision medicine-directed approach to evaluate the individual risk, progression, and therapeutic responses in oxidative stress-related diseases.

Author contributions

All authors listed have made a substantial, direct, and intellectual contribution to the work and approved it for publication.

Funding

CJB was supported by grants of the Austrian Science Fund (SFB F54) and the Leducq Foundation (TNE-20CVD03). NPM was supported by the Vienna Science and Technology Fund (WWTF LS20-081).

Acknowledgments

The figure was created using Servier Medical Art (https://servier.com/en/brochure/servier-medical-art/).

Conflict of interest

The authors declare that the research was conducted in the absence of any commercial or financial relationships that could be construed as a potential conflict of interest.

Publisher's note

All claims expressed in this article are solely those of the authors and do not necessarily represent those of their affiliated organizations, or those of the publisher, the editors and the reviewers. Any product that may be evaluated in this article, or claim that may be made by its manufacturer, is not guaranteed or endorsed by the publisher.

References

1. Binder CJ, Papac-Milicevic N, Witztum JL. Innate sensing of oxidation-specific epitopes in health and disease. *Nat Rev Immunol* (2016) 16(8):485–97. doi: 10.1038/nri.2016.63

2. Obermayer G, Afonyushkin T, Binder CJ. Oxidized low-density lipoprotein in inflammation-driven thrombosis. *J Thromb Haemost* (2018) 16(3):418–28. doi: 10.1111/jth.13925

3. Imai Y, Kuba K, Neely GG, Yaghubian-Malhami R, Perkmann T, van Loo G, et al. Identification of oxidative stress and toll-like receptor 4 signaling as a key pathway of acute lung injury. *Cell* (2008) 133(2):235–49. doi: 10.1016/j.cell.2008.02.043

4. Ambrogini E, Que X, Wang S, Yamaguchi F, Weinstein RS, Tsimikas S, et al. Oxidation-specific epitopes restrain bone formation. *Nat Commun* (2018) 9(1):1–11. doi: 10.1038/s41467-018-04047-5

5. Maes M, Mihaylova I, Kubera M, Leunis JC, Geffard M. IgM-mediated autoimmune responses directed against multiple neoepitopes in depression: New pathways that underpin the inflammatory and neuroprogressive pathophysiology. *J Affect Disord* (2011) 135(1–3):414–8. doi: 10.1016/j.jad.2011.08.023

6. Furnkranz A, Schober A, Bochkov VN, Bashtrykov P, Kronke G, Kadl A, et al. Oxidized phospholipids trigger atherogenic inflammation in murine arteries. *Arterioscler Thromb Vasc Biol* (2005) 25(3):633–8. doi: 10.1161/01.ATV.0000153106.03644.a0

7. Palmieri M, Kim H, Gomez-Acevedo H, Que X, Tsimikas S, Jilka RL, et al. A neutralizing antibody targeting oxidized phospholipids promotes bone anabolism in chow-fed young adult mice. *J Bone Miner Res* (2021) 36(1):170–85. doi: 10.1002/jbmr.4173

8. Esterbauer H, Schaur RJ, Zollner H. Chemistry and biochemistry of 4-hydroxynonenal, malonaldehyde and related aldehydes. *Free Radic Biol Med* (1991) 11(1):81–128. doi: 10.1016/0891-5849(91)90192-6

9. Papac-Milicevic N, Busch CJL, Binder CJ. Malondialdehyde epitopes as targets of immunity and the implications for atherosclerosis. In: *Advances in immunology*, *1st ed*. Cambridge, MA, USA: Elsevier Inc (2016). p. 1–59. doi: 10.1016/bs.ai.2016.02.001

10. Lesgards JF, Frayne IR, Comte B, Busseuil D, Rhéaume É, Tardif JC, et al. Differential distribution of 4-hydroxynonenal adducts to sulfur and nitrogen residues in blood proteins as revealed using raney nickel and gas chromatography-mass spectrometry. *Free Radic Biol Med* (2009) 47(10):1375–85. doi: 10.1016/j.freeradbiomed.2009.08.002

11. Salomon RG. Carboxyethylpyrroles: From hypothesis to the discovery of biologically active natural products. *Chem Res Toxicol* (2017) 30(1):105–13. doi: 10.1021/acs.chemrestox.6b00304

12. Reis A, Domingues P, Ferrer-Correia AJV, Domingues MRM. Peptide-phospholipid cross-linking reactions: Identification of leucine enkephalin-Alka(e)nal-Glycerophosphatidylcholine adducts by tandem mass spectrometry. *J Am Soc Mass Spectrom* (2006) 17(5):657–60. doi: 10.1016/j.jasms.2006.01.006

13. Domingues RM, Domingues P, Melo T, Pérez-Sala D, Reis A, Spickett CM. Lipoxidation adducts with peptides and proteins: Deleterious modifications or signaling mechanisms? *J Proteomics* (2013) 92:110–31. doi: 10.1016/j.jprot.2013.06.004

14. Nakashima I, Liu W, Akhand AA, Takeda K, Kawamoto Y, Kato M, et al. 4-hydroxynonenal triggers multistep signal transduction cascades for suppression of cellular functions. *Mol Aspects Med* (2003) 24(4–5):231–8. doi: 10.1016/S0098-2997(03)00018-9

15. Xu J, Zhong Y, Jing D, Wu Z. Preoperative enteral immunonutrition improves postoperative outcome in patients with gastrointestinal cancer. *World J Surg* (2006) 30(7):1284–9. doi: 10.1007/s00268-005-0756-8

16. Bhuyan DK, Master RWP, Bhuyan KC. Crosslinking of aminophospholipids in cellular membranes of lens by oxidative stress in vitro. *Biochim Biophys Acta - Biomembr* (1996) 1285(1):21–8. doi: 10.1016/S0005-2736(96)00142-3

17. Guo L, Chen Z, Amarnath V, Davies SS. Identification of novel bioactive aldehyde-modified phosphatidylethanolamines formed by lipid peroxidation. *Free Radic Biol Med* (2012) 53(6):1226–38. doi: 10.1016/j.freeradbiomed.2012.07.077

18. Xiao M, Zhong H, Xia L, Tao Y, Yin H. Pathophysiology of mitochondrial lipid oxidation: Role of 4-hydroxynonenal (4-HNE) and other bioactive lipids in mitochondria. *Free Radic Biol Med* (2017) 111:316–27. doi: 10.1016/j.freeradbiomed.2017.04.363

19. Guo J, Wang H, Hrinczenko B, Salomon RG. Efficient quantitative analysis of carboxyalkylpyrrole ethanolamine phospholipids: Elevated levels in sickle cell disease blood. *Chem Res Toxicol* (2016) 29(7):1187–97. doi: 10.1021/acs.chemrestox.6b00152

20. Wang H, Guo J, West XZ, Bid HK, Lu L, Hong L, et al. Detection and biological activities of carboxyethylpyrrole ethanolamine phospholipids (CEP-EPs). *Chem Res Toxicol* (2014) 27(12):2015–22. doi: 10.1021/tx500216a

21. Biswas S, Xin L, Panigrahi S, Zimman A, Wang H, Yakubenko VP, et al. Novel phosphatidylethanolamine derivatives accumulate in circulation in hyperlipidemic ApoE-/- mice and activate platelets *via* TLR2. *Blood* (2016) 127(21):2618–29. doi: 10.1182/blood-2015-08-664300

22. Borisenko GG, Iverson SL, Ahlberg S, Kagan VE, Fadeel B. Milk fat globule epidermal growth factor 8 (MFG-E8) binds to oxidized phosphatidylserine: Implications for macrophage clearance of apoptotic cells. *Cell Death Differ* (2004) 11(8):943–5. doi: 10.1038/sj.cdd.4401421

23. Guichardant M, Bernoud-Hubac N, Chantegrel B, Deshayes C, Lagarde M. Aldehydes from n-6 fatty acid peroxidation. effects on aminophospholipids. *Prostaglandins Leukot Essent Fat Acids* (2002) 67(2–3):147–9. doi: 10.1054/plef.2002.0412

24. Uderhardt S, Herrmann M, Oskolkova OV, Aschermann S, Bicker W, Ipseiz N, et al. 12/15-lipoxygenase orchestrates the clearance of apoptotic cells and maintains immunologic tolerance. *Immunity* (2012) 36(5):834–46. doi: 10.1016/j.immuni.2012.03.010

25. Palinski W, Hörkkö S, Miller E, Steinbrecher UP, Powell HC, Curtiss LK, et al. Cloning of monoclonal autoantibodies to epitopes of oxidized lipoproteins from apolipoprotein e-deficient mice: Demonstration of epitopes of oxidized low density lipoprotein in human plasma. *J Clin Invest* (1996) 98:800–14. doi: 10.1172/JCI118853

26. Steinberg D, Witztum JL. History of discovery: Oxidized low-density lipoprotein and atherosclerosis. *Arterioscler Thromb Vasc Biol* (2010) 30(12):2311–6. doi: 10.1161/ATVBAHA.108.179697

27. Roy P, Orecchioni M, Ley K. How the immune system shapes atherosclerosis: roles of innate and adaptive immunity. *Nat Rev Immunol* (2022) 22(4):251–65. doi: 10.1038/s41577-021-00584-1

28. Quinn MT, Parthasarathy S, Fong LG, Steinberg D. Oxidatively modified low density lipoproteins: A potential role in recruitment and retention of monocyte/macrophages during atherogenesis. *Proc Natl Acad Sci USA* (1987) 84(9):2995–8. doi: 10.1073/pnas.84.9.2995

29. Glass CK, Witztum JL. Atherosclerosis. *Cell* (2001) 104(4):503–16. doi: 10.1016/S0092-8674(01)00238-0

30. Leibundgut G, Witztum JL, Tsimikas S. Oxidation-specific epitopes and immunological responses: Translational biotheranostic implications for atherosclerosis. *Curr Opin Pharmacol* (2013) 13(2):168–79. doi: 10.1016/j.coph.2013.02.005

31. Hörkkö S, Bird DA, Miller E, Itabe H, Leitinger N, Subbanagounder G, et al. Monoclonal autoantibodies specific for oxidized phospholipids or oxidized phospholipid-protein adducts inhibit macrophage uptake of oxidized low-density lipoproteins. *J Clin Invest* (1999) 103(1):117–28. doi: 10.1172/JCI4533

32. Jurgens G, Chen Q, Esterbauer H, Mair S, Ledinski G, Dinges HP. Immunostaining of human autopsy aortas with antibodies to modified apolipoprotein b and apoprotein(a). *Arterioscler Thromb* (1993) 13(11):1689–99. doi: 10.1161/01.atv.13.11.1689

33. Tuominen A, Miller YI, Hansen LF, Kesäniemi YA, Witztum JL, Hörkkö S. A natural antibody to oxidized cardiolipin binds to oxidized low-density lipoprotein, apoptotic cells, and atherosclerotic lesions. *Arterioscler Thromb Vasc Biol* (2006) 26(9):2096–102. doi: 10.1161/01.ATV.0000233333.07991.4a

34. Amir S, Hartvigsen K, Gonen A, Leibundgut G, Que X, Jensen-Jarolim E, et al. Peptide mimotopes of malondialdehyde epitopes for clinical applications in cardiovascular disease. *J Lipid Res* (2012) 53(7):1316–26. doi: 10.1194/jlr.M025445

35. Que X, Hung MY, Yeang C, Gonen A, Prohaska TA, Sun X, et al. Oxidized phospholipids are proinflammatory and proatherogenic in hypercholesterolaemic mice. *Nature* (2018) 558(7709):301–6. doi: 10.1038/s41586-018-0198-8

36. Sawada N, Obama T, Mizuno M, Fukuhara K, Iwamoto S, Aiuchi T, et al. Transfer and enzyme-mediated metabolism of oxidized phosphatidylcholine and lysophosphatidylcholine between low-and high-density lipoproteins. *Antioxidants* (2020) 9(11):1–13. doi: 10.3390/antiox9111045

37. Shao B, Tang C, Heinecke JW, Oram JF. Oxidation of apolipoprotein a-I by myeloperoxidase impairs the initial interactions with ABCA1 required for signaling and cholesterol export. *J Lipid Res* (2010) 51(7):1849–58. doi: 10.1194/jlr.M004085

38. Salmon S, Maziére C, Auclair M, Theron L, Santus R, Maziére JC. Malondialdehyde modification and copper-induced autooxidation of high-density lipoprotein decrease cholesterol efflux from human cultured fibroblasts. *Biochim Biophys Acta (BBA)/Lipids Lipid Metab* (1992) 1125(2):230–5. doi: 10.1016/0005-2760(92)90050-6

39. Florens N, Calzada C, Lemoine S, Boulet MM, Guillot N, Barba C, et al. CKD increases carbonylation of HDL and is associated with impaired antiaggregant properties. *J Am Soc Nephrol* (2020) 31(7):1462–77. doi: 10.1681/ASN.2019111205

40. Lê QH, El Alaoui M, Véricel E, Ségrestin B, Soulère L, Guichardant M, et al. HDL enriched with oxidized phospholipids and HDL from diabetic patients inhibit platelet function. *J Clin Endocrinol Metab* (2015) 100(5):2006–14. doi: 10.1210/jc.2014-4214

41. Assinger A, Koller F, Schmid W, Zellner M, Babeluk R, Koller E, et al. Specific binding of hypochlorite-oxidized HDL to platelet CD36 triggers proinflammatory and procoagulant effects. *Atherosclerosis* (2010) 212(1):153–60. doi: 10.1016/j.atherosclerosis.2010.05.010

42. Obermayer G, Afonyushkin T, Göderle L, Puhm F, Schrottmaier WC, Taqi S, et al. Natural IgM antibodies inhibit microvesicle-driven coagulation and thrombosis. *Blood* (2020) 137(10):1406–15. doi: 10.1182/blood.2020007155

43. Van Niel G, D'Angelo G, Raposo G. Shedding light on the cell biology of extracellular vesicles. *Nat Rev Mol Cell Biol* (2018) 19(4):213–28. doi: 10.1038/nrm.2017.125

44. Witwer KW, Buzás EI, Bemis LT, Bora A, Lässer C, Lötvall J, et al. Standardization of sample collection, isolation and analysis methods in extracellular vesicle research. *J Extracell Vesicles* (2013) 2(1):20360. doi: 10.3402/jev.v2i0.20360

45. Huber J, Vales A, Mitulovic G, Blumer M, Schmid R, Witztum JL, et al. Oxidized membrane vesicles and blebs from apoptotic cells contain biologically

active oxidized phospholipids that induce monocyte-endothelial interactions. *Arterioscler Thromb Vasc Biol* (2002) 22(1):101–7. doi: 10.1161/hq0102.101525

46. Liu ML, Scalia R, Mehta JL, Williams KJ. Cholesterol-induced membrane microvesicles as novel carriers of damage-associated molecular patterns: Mechanisms of formation, action, and detoxification. *Arterioscler Thromb Vasc Biol* (2012) 32(9):2113–21. doi: 10.1161/ATVBAHA.112.255471

47. Tsiantoulas D, Perkmann T, Afonyushkin T, Mangold A, Prohaska TA, Papac-Milicevic N, et al. Circulating microparticles carry oxidation-specific epitopes and are recognized by natural IgM antibodies. *J Lipid Res* (2015) 56 (2):440–8. doi: 10.1194/jlr.P054569

48. Chang MK, Bergmark C, Laurila A, Hörkkö S, Han KH, Friedman P, et al. Monoclonal antibodies against oxidized low-density lipoprotein bind to apoptotic cells and inhibit their phagocytosis by elicited macrophages: Evidence that oxidation-specific epitopes mediate macrophage recognition. *P Natl Acad Sci USA* (1999) 96(May):6353–8. doi: 10.1073/pnas.96.11.6353

49. Chang MK, Binder CJ, Torzewski M. Witztum JL. c-reactive protein binds to both oxidized LDL and apoptotic cells through recognition of a common ligand: Phosphorylcholine of oxidized phospholipids. *Proc Natl Acad Sci USA* (2002) 99 (20):13043–8. doi: 10.1073/pnas.192399699

50. Chou MY, Fogelstrand L, Hartvigsen K, Hansen LF, Woelkers D, Shaw PX, et al. Oxidation-specific epitopes are dominant targets of innate natural antibodies in mice and humans. *J Clin Invest* (2009) 119(5):1335–49. doi: 10.1172/JCI36800

51. Busch CJL, Hendrikx T, Weismann D, Jäckel S, Walenbergh SMA, Rendeiro AF, et al. Malondialdehyde epitopes are sterile mediators of hepatic inflammation in hypercholesterolemic mice. *Hepatology* (2017) 65(4):1181–95. doi: 10.1002/hep.28970

52. Weismann D, Hartvigsen K, Lauer N, Bennett KL, Scholl HPN, Issa PC, et al. Complement factor h binds malondialdehyde epitopes and protects from oxidative stress. *Nature* (2011) 478(7367):76–81. doi: 10.1038/nature10449

53. Terpstra V, Bird DA, Steinberg D. Evidence that the lipid moiety of oxidized low density lipoprotein plays a role in its interaction with macrophage receptors. *Proc Natl Acad Sci USA* (1998) 95(4):1806–11. doi: 10.1073/pnas.95.4.1806

54. Chen GY, Nuñez G. Sterile inflammation: sensing and reacting to damage. *Nat Rev Immunol* (2010) 10(12):826–37. doi: 10.1038/nri2873

55. Palinski W, Rosenfeld ME, Ylä-Herttuala S, Gurtner GC, Socher SS, Butler SW, et al. Low density lipoprotein undergoes oxidative modification *in vivo*. *Proc Natl Acad Sci USA* (1989) 86(4):1372–6. doi: 10.1073/pnas.86.4.1372

56. Thiele GM, Duryee MJ, Anderson DR, Klassen LW, Mohring SM, Young KA, et al. Malondialdehyde-acetaldehyde adducts and anti-Malondialdehyde-Acetaldehyde antibodies in rheumatoid arthritis. *Arthritis Rheumatol* (2015) 67 (3):645–55. doi: 10.1002/art.38969

57. Moretto N, Facchinetti F, Southworth T, Civelli M, Singh D, Patacchini R. α,β-unsaturated aldehydes contained in cigarette smoke elicit IL-8 release in pulmonary cells through mitogen-activated protein kinases. *Am J Physiol - Lung Cell Mol Physiol* (2009) 296(5):839–49. doi: 10.1152/ajplung.90570.2008

58. Facchinetti F, Amadei F, Geppetti P, Tarantini F, Di Serio C, Dragotto A, et al. A,B-unsaturated aldehydes in cigarette smoke release inflammatory mediators from human macrophages. *Am J Respir Cell Mol Biol* (2007) 37(5):617–23. doi: 10.1165/rcmb.2007-0130OC

59. Gargiulo S, Gamba P, Testa G, Rossin D, Biasi F, Poli G, et al. Relation between TLR4/NF-κB signaling pathway activation by 27-hydroxycholesterol and 4-hydroxynonenal, and atherosclerotic plaque instability. *Aging Cell* (2015) 14 (4):569–81. doi: 10.1111/acel.12322

60. Takimoto T, Yoshida M, Hirata H, Kashiwa Y, Takeda Y, Goya S, et al. 4-Hydroxy-2-nonenal induces chronic obstructive pulmonary disease-like histopathologic changes in mice. *Biochem Biophys Res Commun* (2012) 420 (1):84–90. doi: 10.1016/j.bbrc.2012.02.119

61. Duryee MJ, Klassen LW, Freeman TL, Willis MS, Tuma DJ, Thiele GM. Lipopolysaccharide is a cofactor for malondialdehyde-acetaldehyde adduct-mediated cytokine/chemokine release by rat sinusoidal liver endothelial and kupffer cells. *Alcohol Clin Exp Res* (2004) 28(12):1931–8. doi: 10.1097/01.ALC.0000148115.90045.C5

62. Shechter I, Fogelman AM, Haberland ME, Seager J, Hokom M, Edwards PA. The metabolism of native and malondialdehyde-altered low density lipoproteins by human monocyte-macrophages. *J Lipid Res* (1981) 22(1):63–71. doi: 10.1016/s0022-2275(20)34741-6

63. Miller YI, Choi SH, Wiesner P, Fang L, Harkewicz R, Hartvigsen K, et al. Oxidation-specific epitopes are danger-associated molecular patterns recognized by pattern recognition receptors of innate immunity. *Circ Res* (2011) 108(2):235–48. doi: 10.1161/CIRCRESAHA.110.223875

64. Zhu X, Ng HP, Lai YC, Craigo JK, Nagilla PS, Raghani P, et al. Scavenger receptor function of mouse fcγ receptor III contributes to progression of atherosclerosis in apolipoprotein e hyperlipidemic mice. *J Immunol* (2014) 193 (5):2483–95. doi: 10.4049/jimmunol.1303075

65. Ansari SA, Keshava S, Pendurthi UR, Rao LVM. Oxidative stress product, 4-Hydroxy-2-Nonenal, induces the release of tissue factor-positive microvesicles from perivascular cells into circulation. *Arterioscler Thromb Vasc Biol* (2021) 41 (1):250–65. doi: 10.1161/ATVBAHA.120.315187

66. Kumano-Kuramochi M, Xie Q, Kajiwara S, Komba S, Minowa T, Machida S. Lectin-like oxidized LDL receptor-1 is palmitoylated and internalizes ligands *via* caveolae/raft-dependent endocytosis. *Biochem Biophys Res Commun* (2013) 434 (3):594–9. doi: 10.1016/j.bbrc.2013.03.120

67. Loidl A, Sevcsik E, Riesenhuber G, Deigner HP, Hermetter A. Oxidized phospholipids in minimally modified low density lipoprotein induce apoptotic signaling *via* activation of acid sphingomyelinase in arterial smooth muscle cells. *J Biol Chem* (2003) 278(35):32921–8. doi: 10.1074/jbc.M306088200

68. Gao D, Ashraf MZ, Kar NS, Lin D, Sayre LM, Podrez EA. Structural basis for the recognition of oxidized phospholipids in oxidized low density lipoproteins by class b scavenger receptors CD36 and SR-BI. *J Biol Chem* (2010) 285(7):4447–54. doi: 10.1074/jbc.M109.082800

69. Kadl A, Sharma PR, Chen W, Agrawal R, Meher AK, Rudraiah S, et al. Oxidized phospholipid-induced inflammation is mediated by toll-like receptor 2. *Free Radic Biol Med* (2011) 51(10):1903–9. doi: 10.1016/j.freeradbiomed.2011.08.026

70. Stewart CR, Stuart LM, Wilkinson K, Van Gils JM, Deng J, Halle A, et al. CD36 ligands promote sterile inflammation through assembly of a toll-like receptor 4 and 6 heterodimer. *Nat Immunol* (2010) 11(2):155–61. doi: 10.1038/ni.1836

71. Doyle SL, Campbell M, Ozaki E, Salomon RG, Mori A, Kenna PF, et al. NLRP3 has a protective role in age-related macular degeneration through the induction of IL-18 by drusen components. *Nat Med* (2012) 18(5):791–8. doi: 10.1038/nm.2717

72. Cruz-Guilloty F, Saeed AM, Echegaray JJ, Duffort S, Ballmick A, Tan Y, et al. Infiltration of proinflammatory m1 macrophages into the outer retina precedes damage in a mouse model of age-related macular degeneration. *Int J Inflam* (2013) 2013:1–12. doi: 10.1155/2013/503725

73. West XZ, Malinin NL, Merkulova AA, Tischenko M, Kerr BA, Borden EC, et al. Oxidative stress induces angiogenesis by activating TLR2 with novel endogenous ligands. *Nature* (2010) 467(7318):972–6. doi: 10.1038/nature09421.Oxidative

74. Salomon RG, Hong L, Hollyfield JG. Discovery of carboxyethylpyrroles (CEPs): Critical insights into AMD, autism, cancer, and wound healing from basic research on the chemistry of oxidized phospholipids. *Chem Res Toxicol* (2011) 24 (11):1803–16. doi: 10.1021/tx200206v

75. Yakubenko VP, Cui K, Ardell CL, Brown KE, West XZ, Gao D, et al. Oxidative modifications of extracellular matrix promote the second wave of inflammation *via* b2 integrins. *Blood* (2018) 132(1):78–88. doi: 10.1182/blood-2017-10-810176

76. Kim YW, Yakubenko VP, West XZ, Gugiu GB, Renganathan K, Biswas S, et al. Receptor-mediated mechanism controlling tissue levels of bioactive lipid oxidation products. *Circ Res* (2015) 117(4):321–32. doi: 10.1161/CIRCRESAHA.117.305925

77. Boullier A, Gillotte KL, Hörkkö S, Green SR, Friedman P, Dennis EA, et al. The binding of oxidized low density lipoprotein to mouse CD36 is mediated in part by oxidized phospholipids that are associated with both the lipid and protein moieties of the lipoprotein. *J Biol Chem* (2000) 275(13):9163–9. doi: 10.1074/jbc.275.13.9163

78. Chang MK, Binder CJ, Miller YI, Subbanagounder G, Silverman GJ, Berliner JA, et al. Apoptotic cells with oxidation-specific epitopes are immunogenic and proinflammatory. *J Exp Med* (2004) 200(11):1359–70. doi: 10.1084/jem.20031763

79. Gruber S, Hendrikx T, Tsiantoulas D, Ozsvar-Kozma M, Göderle L, Mallat Z, et al. Sialic acid-binding immunoglobulin-like lectin G promotes atherosclerosis and liver inflammation by suppressing the protective functions of b-1 cells. *Cell Rep* (2016) 14(10):2348–61. doi: 10.1016/j.celrep.2016.02.027

80. Faria-Neto JR, Chyu KY, Li X, Dimayuga PC, Ferreira C, Yano J, et al. Passive immunization with monoclonal IgM antibodies against phosphorylcholine reduces accelerated vein graft atherosclerosis in apolipoprotein e-null mice. *Atherosclerosis* (2006) 189(1):83–90. doi: 10.1016/j.atherosclerosis.2005.11.033

81. Gonen A, Hansen LF, Turner WW, Montano EN, Que X, Rafia A, et al. Atheroprotective immunization with malondialdehyde modified LDL is hapten-specific and dependant on advanced MDA-adducts: Implication for development of an atheroprotective vaccine. *J Lipid Res* (2014) 55(10):2137–55. doi: 10.1194/jlr.M053256

82. Freigang S, Hörkkö S, Miller E, Witztum JL, Palinski W. Immunization of LDL receptor-deficient mice with homologous malondialdehyde-modified and native LDL reduces progression of atherosclerosis by mechanisms other than induction of high titers of antibodies to oxidative neoepitopes. *Arterioscler Thromb Vasc Biol* (1998) 18(12):1972–82. doi: 10.1161/01.ATV.18.12.1972

83. Notley CA, Brown MA, Wright GP, Ehrenstein MR. Natural IgM is required for suppression of inflammatory arthritis by apoptotic cells. *J Immunol* (2011) 186 (8):4967–72. doi: 10.4049/jimmunol.1003021

84. Chen Y, Khanna S, Goodyear CS, Park YB, Raz E, Thiel S, et al. Regulation of dendritic cells and macrophages by an anti-apoptotic cell natural antibody that suppresses TLR responses and inhibits inflammatory arthritis. *J Immunol* (2009) 183(2):1346–59. doi: 10.4049/jimmunol.0900948

85. Boes M, Schmidt T, Linkemann K, Beaudette BC, Marshak-Rothstein A, Chen J. Accelerated development of IgG autoantibodies and autoimmune disease in the absence of secreted IgM. *Proc Natl Acad Sci USA* (2000) 97(3):1184–9. doi: 10.1073/pnas.97.3.1184

86. Karvonen J, Päivänsalo M, Kesäniemi YA, Hörkkö S. Immunoglobulin m type of autoantibodies to oxidized low-density lipoprotein has an inverse relation to carotid artery atherosclerosis. *Circulation* (2003) 108:2107–12. doi: 10.1161/01.CIR.0000092891.55157.A7

87. Tsimikas S, Brilakis ES, Lennon RJ, Miller ER, Witztum JL, McConnell JP, et al. Relationship of IgG and IgM autoantibodies to oxidized low density lipoprotein with coronary artery disease and cardiovascular events. *J Lipid Res* (2007) 48(2):425–33. doi: 10.1194/jlr.M600361-JLR200

88. Tsimikas S, Willeit P, Willeit J, Santer P, Mayr M, Xu Q, et al. Oxidation-specific biomarkers, prospective 15-year cardiovascular and stroke outcomes, and net reclassification of cardiovascular events. *J Am Coll Cardiol* (2012) 60(21):2218–29. doi: 10.1016/j.jacc.2012.08.979

89. Khamis RY, Hughes AD, Caga-anan M, Chang CL, Boyle JJ, Kojima C, et al. High serum immunoglobulin G and m levels predict freedom from adverse cardiovascular events in Hypertension : A nested case-control substudy of the Anglo-Scandinavian cardiac outcomes trial. *EBioMedicine* (2016) 9:372–80. doi: 10.1016/j.ebiom.2016.06.012

90. Eichinger S, Kyrle PA, Kammer M, Eischer L, Ozsvar-Kozma M, Binder CJ. Natural antibodies to oxidation-specific epitopes: Innate immune response and venous thromboembolic disease. *JTH* (2016) 38(1):42–9. doi: 10.1111/ijlh.12426

91. Frostegård J, Su J, Sing S, Hua X, Vikström M, Leander K, et al. IgM antibodies to oxidized phosphatidylserine as protection markers in cardiovascular disease among 60-year olds. *PloS One* (2017) 12(4):1–13. doi: 10.1371/journal.pone.0171195

92. van den Berg VJ, Haskard DO, Fedorowski A, Hartley A, Kardys I, Caga-Anan M, et al. IgM anti-malondialdehyde low density lipoprotein antibody levels indicate coronary heart disease and necrotic core characteristics in the Nordic diltiazem (NORDIL) study and the integrated imaging and biomarker study 3 (IBIS-3). *EBioMedicine* (2018) 36:63–72. doi: 10.1016/j.ebiom.2018.08.023

93. Ciurana CLF, Hack CE. Competitive binding of pentraxins and IgM to newly exposed epitopes on late apoptotic cells. *Cell Immunol* (2006) 239:14–21. doi: 10.1016/j.cellimm.2006.02.006

94. Bíró A, Rovó Z, Papp D, Cervenak L, Varga L, Füst G, et al. Studies on the interactions between c-reactive protein and complement proteins. *Immunology* (2007) 121(1):40–50. doi: 10.1111/j.1365-2567.2007.02535.x

95. Gustin C, Delaive E, Dieu M, Calay D, Raes M. Upregulation of pentraxin-3 in human endothelial cells after lysophosphatidic acid exposure. *Arterioscler Thromb Vasc Biol* (2008) 28(3):491–7. doi: 10.1161/ATVBAHA.107.158642

96. Liu W, Jiang J, Yan D, Li D, Li W, Ma Y, et al. Pentraxin 3 promotes oxLDL uptake and inhibits cholesterol efflux from macrophage-derived foam cells. *Exp Mol Pathol* (2014) 96(3):292–9. doi: 10.1016/j.yexmp.2014.03.007

97. Biró A, Thielens NM, Cervenák L, Prohászka Z, Füst G, Arlaud GJ. Modified low density lipoproteins differentially bind and activate the C1 complex of complement. *Mol Immunol* (2007) 44(6):1169–77. doi: 10.1016/j.molimm.2006.06.013

98. Fraser DA, Tenner AJ. Innate immune proteins C1q and mannan-binding lectin enhance clearance of atherogenic lipoproteins by human monocytes and macrophages. *J Immunol* (2010) 185(7):3932–9. doi: 10.4049/jimmunol.1002080

99. Spivia W, Magno PS, Le P, Fraser DA. Complement protein C1q promotes macrophage anti-inflammatory M2-like polarization during the clearance of atherogenic lipoproteins. *Inflammation Res* (2014) 63(10):885–93. doi: 10.1007/s00011-014-0762-0

100. Yin C, Ackermann S, Ma Z, Mohanta SK, Zhang C, Li Y, et al. ApoE attenuates unresolvable inflammation by complex formation with activated C1q. *Nat Med* (2019) 25(3):496–506. doi: 10.1038/s41591-018-0336-8

101. Veneskoski M, Turunen SP, Kummu O, Nissinen A, Rannikko S, Levonen AL, et al. Specific recognition of malondialdehyde and malondialdehyde acetaldehyde adducts on oxidized LDL and apoptotic cells by complement anaphylatoxin C3a. *Free Radic Biol Med* (2011) 51(4):834–43. doi: 10.1016/j.freeradbiomed.2011.05.029

102. Mogilenko DA, Kudriavtsev IV, Trulioff AS, Shavva VS, Dizhe EB, Missyul BV, et al. Modified low density lipoprotein stimulates complement C3 expression and secretion *via* liver X receptor and toll-like receptor 4 activation in human macrophages. *J Biol Chem* (2012) 287(8):5954–68. doi: 10.1074/jbc.M111.289322

103. Aredo B, Li T, Chen X, Zhang K, Wang CXZZ, Gou D, et al. A chimeric cfh transgene leads to increased retinal oxidative stress, inflammation, and accumulation of activated subretinal microglia in mice. *Investig Opthalmol Vis Sci* (2015) 56(6):3427. doi: 10.1167/iovs.14-16089

104. Hebecker M, Alba-Dominguez M, Roumenina LT, Reuter S, Hyvarinen S, Dragon-Durey MA, et al. An engineered construct combining complement regulatory and surface-recognition domains represents a minimal-size functional factor h. *J Immunol* (2013) 191:912–21. doi: 10.4049/jimmunol.1300269

105. Alic L, Papac-Milicevic N, Czamara D, Rudnick RB, Ozsvar-Kozma M, Hartmann A, et al. A genome-wide association study identifies key modulators of complement factor h binding to malondialdehyde-epitopes. *Proc Natl Acad Sci USA* (2020) 117(18):9942–51. doi: 10.1073/pnas.1913970117

106. Hyvärinen S, Uchida K, Varjosalo M, Jokela R, Jokiranta TS. Recognition of malondialdehyde-modified proteins by the c terminus of complement factor h is mediated *via* the polyanion binding site and impaired by mutations found in atypical hemolytic uremic syndrome. *J Biol Chem* (2014) 289(7):4295–306. doi: 10.1074/jbc.M113.527416

107. Shaw PX, Zhang L, Zhang M, Du H, Zhao L, Lee C, et al. Complement factor h genotypes impact risk of age-related macular degeneration by interaction with oxidized phospholipids. *Proc Natl Acad Sci USA* (2012) 109(34):13757–62. doi: 10.1073/pnas.1121309109

108. Sjöberg AP, Trouw LA, Clark SJ, Sjölander J, Heinegård D, Sim RB, et al. The factor h variant associated with age-related macular degeneration (His-384) and the non-disease-associated form bind differentially to c-reactive protein, fibromodulin, DNA, and necrotic cells. *J Biol Chem* (2007) 282(15):10894–900. doi: 10.1074/jbc.M610256200

109. Borras C, Canonica J, Jorieux S, Abache T, El Sanharawi M, Klein C, et al. CFH exerts anti-oxidant effects on retinal pigment epithelial cells independently from protecting against membrane attack complex. *Sci Rep* (2019) 9(1):1–12. doi: 10.1038/s41598-019-50420-9

110. Irmscher S, Zipfel SLH, Halder LD, Ivanov L, Gonzalez-Delgado A, Waldeyer C, et al. Factor h-related protein 1 (FHR-1) is associated with atherosclerotic cardiovascular disease. *Sci Rep* (2021) 11(1):1–15. doi: 10.1038/s41598-021-02011-w

111. Irmscher S, Brix SR, Zipfel SLH, Halder LD, Mutlutürk S, Wulf S, et al. Serum FHR1 binding to necrotic-type cells activates monocytic inflammasome and marks necrotic sites in vasculopathies. *Nat Commun* (2019) 10(1):1–14. doi: 10.1038/s41467-019-10766-0

112. Schäfer N, Rasras A, Ormenisan DM, Amslinger S, Enzmann V, Jägle H, et al. Complement factor h-related 3 enhanced inflammation and complement activation in human RPE cells. *Front Immunol* (2021) 12:769242(November). doi: 10.3389/fimmu.2021.769242

113. Rudnick RB, Chen Q, Stea ED, Hartmann A, Papac-Milicevic N, Person F, et al. FHR5 binds to laminins, uses separate C3b and surface-binding sites, and activates complement on malondialdehyde-acetaldehyde surfaces. *J Immunol* (2018) 200(7):2280–90. doi: 10.4049/jimmunol.1701641

114. Shaw PX, Hörkkö S, Chang M kyung K, Curtiss LK, Palinski W, Silverman GJ, et al. Natural antibodies with the T15 idiotype may act in atherosclerosis, apoptotic clearance, and protective immunity. *J Clin Invest* (2000) 105(12):1731–40. doi: 10.1172/JCI8472

115. Binder CJ. Natural IgM antibodies against oxidation-specific epitopes. *J Clin Immunol* (2010) 30(April):56–60. doi: 10.1007/s10875-010-9396-3

116. Haapasalo K, Meri S. Regulation of the complement system by pentraxins. *Front Immunol* (2019) 10:1750(August). doi: 10.3389/fimmu.2019.01750

117. Wang L, Cano M, Datta S, Wei H, Ebrahimi KB, Gorashi Y, et al. Pentraxin 3 recruits complement factor h to protect against oxidative stress-induced complement and inflammasome overactivation. *J Pathol* (2016) 240(4):495–506. doi: 10.1002/path.4811

118. Botto M, Dell' Agnola C, Bygrave AE, Thompson EM, Cook HT, Petry F, et al. Homozygous C1q deficiency causes glomerulonephritis associated with multiple apoptotic bodies. *Nat Genet* (1998) 19(1):56–9. doi: 10.1038/ng0598-56

119. Nauta AJ, Trouw LA, Daha MR, Tijsma O, Nieuwland R, Schwaeble WJ, et al. Direct binding of C1q to apoptotic cells and cell blebs induces complement activation. *Eur J Immunol* (2002) 32(6):1726–36. doi: 10.1002/1521-4141(200206)32:6<1726::AID-IMMU1726>3.0.CO;2-R

120. Gasser O, Hess C, Miot S, Deon C, Sanchez JC, Schifferli JA. Characterisation and properties of ectosomes released by human polymorphonuclear neutrophils. *Exp Cell Res* (2003) 285(2):243–57. doi: 10.1016/S0014-4827(03)00055-7

121. Stegert M, Bock M, Trendelenburg M. Clinical presentation of human C1q deficiency: How much of a lupus? *Mol Immunol* (2015) 67(1):3–11. doi: 10.1016/j.molimm.2015.03.007

122. Merle NS, Noe R, Halbwachs-Mecarelli L, Fremeaux-Bacchi V, Roumenina LT. Complement system part II: Role in immunity. *Front Immunol* (2015) 6:257. doi: 10.3389/fimmu.2015.00257

123. Coulthard LG, Woodruff TM. Is the complement activation product C3a a proinflammatory molecule? re-evaluating the evidence and the myth. *J Immunol* (2015) 194(8):3542–8. doi: 10.4049/jimmunol.1403068

124. Antovic A, Mobarrez F, Manojlovic M, Soutari N, De Porta Baggemar V, Nordin A, et al. Microparticles expressing myeloperoxidase and complement C3a and C5a as markers of renal involvement in antineutrophil cytoplasmic antibody-associated vasculitis. *J Rheumatol* (2020) 47(5):714–21. doi: 10.3899/jrheum.181347

125. Ferreira V, Pangburn M, Cortés C. Complement control protein factor h: the good, the bad, and the inadequate. *Mol Immunol* (2010) 47(13):2187–97. doi: 10.1016/j.molimm.2010.05.007.Complement

126. Meri S, Haapasalo K. Function and dysfunction of complement factor h during formation of lipid-rich deposits. *Front Immunol* (2020) 11:611830 (December). doi: 10.3389/fimmu.2020.611830

127. Trouw LA, Bengtsson AA, Gelderman KA, Dahlbäck B, Sturfelt G, Blom AM. C4b-binding protein and factor h compensate for the loss of membrane-bound complement inhibitors to protect apoptotic cells against excessive complement attack. *J Biol Chem* (2007) 282(39):28540–8. doi: 10.1074/jbc.M704354200

128. Martin M, Leffler J, Smolag KI, Mytych J, Björk A, Chaves LD, et al. Factor H uptake regulates intracellular C3 activation during apoptosis and decreases the inflammatory potential of nucleosomes. *Cell Death Differ* (2016) 23(5):903–11. doi: 10.1038/cdd.2015.164

129. Skerka C, Chen Q, Fremeaux-Bacchi V, Roumenina LT. Complement factor h related proteins (CFHRs). *Mol Immunol* (2013) 56(3):170–80. doi: 10.1016/j.molimm.2013.06.001

130. Jozsi M, Tortajada A, Uzonyi B, Goicoechea de Jorge E, Rodriguez de Cordoba S. Factor h-related proteins determine complement-activating surfaces. *Trends Immunol* (2015) 36(6):374–84. doi: 10.1016/j.it.2015.04.008

131. Schäfer N, Grosche A, Reinders J, Hauck SM, Pouw RB, Kuijpers TW, et al. Complement regulator FHR-3 is elevated either locally or systemically in a selection of autoimmune diseases. *Front Immunol* (2016) 7:542(November). doi: 10.3389/fimmu.2016.00542

132. Kárpáti É, Papp A, Schneider AE, Hajnal D, Cserhalmi M, Csincsi ÁI, et al. Interaction of the factor h family proteins FHR-1 and FHR-5 with DNA and dead cells: Implications for the regulation of complement activation and opsonization. *Front Immunol* (2020) 11:1297(July). doi: 10.3389/fimmu.2020.01297

133. Nauta AJ, Daha MR, Van Kooten C, Roos A. Recognition and clearance of apoptotic cells: A role for complement and pentraxins. *Trends Immunol* (2003) 24 (3):148–54. doi: 10.1016/S1471-4906(03)00030-9

134. Chen Y, Park YB, Patel E, Silverman GJ. IgM antibodies to apoptosis-associated determinants recruit C1q and enhance dendritic cell phagocytosis of apoptotic cells. *J Immunol* (2009) 182(10):6031–43. doi: 10.4049/jimmunol.0804191.IgM

135. Ogden CA, Kowalewski R, Peng Y, Montenegro V, Elkon KB. IGM is required for efficient complement mediated phagocytosis of apoptotic cells in vivo. *Autoimmunity* (2005) 38(4):259–64. doi: 10.1080/08916930500124452

136. Gershov D, Kim SJ, Brot N, Elkon KB. C-reactive protein binds to apoptotic cells, protects the cells from assembly of the terminal complement components, and sustains an antiinflammatory innate immune response: Implications for systemic autoimmunity. *J Exp Med* (2000) 192(9):1353–63. doi: 10.1084/jem.192.9.1353

137. Joseph K, Kulik L, Coughlin B, Kunchithapautham K, Bandyopadhyay M, Thiel S, et al. Oxidative stress sensitizes retinal pigmented epithelial (RPE) cells to complement-mediated injury in a natural antibody-, lectin pathway-, and phospholipid epitope-dependent manner. *J Biol Chem* (2013) 288(18):12753–65. doi: 10.1074/jbc.M112.421891

138. Laine M, Jarva H, Seitsonen S, Haapasalo K, Lehtinen MJ, Lindeman N, et al. Y402H polymorphism of complement factor h affects binding affinity to c-reactive protein. *J Immunol* (2007) 178(6):3831–6. doi: 10.4049/jimmunol.178.6.3831

139. Swinkels M, Zhang JH, Tilakaratna V, Black G, Mcharg S, Inforzato A, et al. C-reactive protein and pentraxin-3 binding of factor h-like protein 1 differs from complement factor H : implications for retinal inflammation. *Sci Rep* (2018) 8:1–12. doi: 10.1038/s41598-017-18395-7

140. Trouw LA, Bengtsson AA, Gelderman KA, Dahlbäck B, Sturfelt G, Blom AM. C4b-binding protein and factor h compensate for the loss of membrane-bound complement inhibitors to protect apoptotic cells against excessive complement attack. *J Biol Chem* (2007) 282(39):28540–8. doi: 10.1074/jbc.M704354200

141. Merle NS, Church SE, Fremeaux-Bacchi V, Roumenina LT. Complement system part I – molecular mechanisms of activation and regulation. *Front Immunol* (2015) 6:262(June). doi: 10.3389/fimmu.2015.00262

142. Csincsi ÁI, Szabó Z, Bánlaki Z, Uzonyi B, Cserhalmi M, Kárpáti É, et al. FHR-1 binds to c-reactive protein and enhances rather than inhibits complement activation. *J Immunol* (2017) 199(1):292–303. doi: 10.4049/jimmunol.1600483

143. Tsikas D. Assessment of lipid peroxidation by measuring malondialdehyde (MDA) and relatives in biological samples: Analytical and biological challenges. *Anal Biochem* (2017) 524:13–30. doi: 10.1016/j.ab.2016.10.021

144. Briley-Saebo K, Yeang C, Witztum JL, Tsimikas S. Imaging of oxidation-specific epitopes with targeted nanoparticles to detect high-risk atherosclerotic lesions: Progress and future directions. *J Cardiovasc Transl Res* (2014) 7(8):719–36. doi: 10.1007/s12265-014-9590-4

145. Ravandi A, Boekholdt SM, Mallat Z, Talmud PJ, Kastelein JJP, Wareham NJ, et al. Relationship of IgG and IgM autoantibodies and immune complexes to oxidized LDL with markers of oxidation and inflammation and cardiovascular events: results from the EPIC-Norfolk study. *J Lipid Res* (2011) 52:1829–36. doi: 10.1194/jlr.M015776

146. Gounopoulos P, Merki E, Hansen LF, Choi SH, Tsimikas S. Antibodies to oxidized low density lipoprotein: Epidemiological studies and potential clinical applications in cardiovascular disease. *Minerva Cardioangiol* (2007) 55(6):821–37.

147. Atik N, Putri Pratiwi S, Hamijoyo L. Correlation between c-reactive protein with malondialdehyde in systemic lupus erythematosus patients. *Int J Rheumatol* (2020) 2020:1–5. doi: 10.1155/2020/8078412

148. Botto M, Walport MJ. C1q, autoimmunity and apoptosis. *Immunobiology* (2002) 205(4–5):395–406. doi: 10.1078/0171-2985-00141

149. Svenungsson E, Jensen-Urstad K, Heimburger M, Silveira A, Hamsten A, de Faire U, et al. Risk factors for cardiovascular disease in systemic lupus erythematosus. *Circulation* (2001) 104(16):1887–93. doi: 10.1161/hc4101.097518

150. Wu R, Svenungsson E, Gunnarsson I, Haegerstrand-Gillis C, Andersson B, Lundberg I, et al. Antibodies to adult human endothelial cells cross-react with oxidized low-density lipoprotein and beta 2-glycoprotein I (beta 2-GPI) in systemic lupus erythematosus. *Clin Exp Immunol* (1999) 115:561–6. doi: 10.1046/j.1365-2249.1999.00830.x

151. Thiagarajan D, Oparina N, Lundström S, Zubarev R, Sun J, Beretta L, et al. IgM antibodies against malondialdehyde and phosphorylcholine in different systemic rheumatic diseases. *Sci Rep* (2020) 10(1):1–13. doi: 10.1038/s41598-020-66981-z

152. Hughes AE, Orr N, Esfandiary H, Diaz-Torres M, Goodship T, Chakravarthy U. A common CFH haplotype, with deletion of CFHR1 and CFHR3, is associated with lower risk of age-related macular degeneration. *Nat Genet* (2006) 38(10):1173–7. doi: 10.1038/ng1890

153. Hageman GS, Hancox LS, Taiber AJ, Gehrs KM, Anderson DH, Johnson LV, et al. Extended haplotypes in the complement factor h (CFH) and CFH-related (CFHR) family of genes protect against age-related macular degeneration: characterization, ethnic distribution and evolutionary implications. *Ann Med* (2006) 38(8):592–604. doi: 10.1080/07853890601097030

154. Kiss MG, Binder CJ. The multifaceted impact of complement on atherosclerosis. *Atherosclerosis* (2022) 351:29–40. doi: 10.1016/j.atherosclerosis.2022.03.014

155. Kardys I, Klaver CCW, Despriet DDG, Bergen AAB, Uitterlinden AG, Hofman A, et al. A common polymorphism in the complement factor h gene is associated with increased risk of myocardial infarction. *Rotterdam Study J Am Coll Cardiol* (2006) 47(8):1568–75. doi: 10.1016/j.jacc.2005.11.076

156. Gu J, Pauer GJT, Yue X, Narendra U, Sturgill GM, Bena J, et al. Assessing susceptibility to age-related macular degeneration with proteomic and genomic biomarkers. *Mol Cell Proteomics* (2009) 8(6):1338–49. doi: 10.1074/mcp.M800453-MCP200

frontiers | Frontiers in Immunology

TYPE Review
PUBLISHED 06 October 2022
DOI 10.3389/fimmu.2022.1015128

Check for updates

OPEN ACCESS

EDITED BY
Lillemor Skattum,
Lund University, Sweden

REVIEWED BY
Lubka T. Roumenina,
INSERM U1138 Centre de Recherche des Cordeliers (CRC), France
Hui Liu,
Dalian Medical University, China
Christine Gaboriaud,
UMR5075 Institut de Biologie Structurale (IBS), France

*CORRESPONDENCE
Sheng Xia
xiasheng1519@163.com

SPECIALTY SECTION
This article was submitted to Molecular Innate Immunity, a section of the journal Frontiers in Immunology

RECEIVED 09 August 2022
ACCEPTED 21 September 2022
PUBLISHED 06 October 2022

CITATION
Ye J, Yang P, Yang Y and Xia S (2022) Complement C1s as a diagnostic marker and therapeutic target: Progress and propective. *Front. Immunol.* 13:1015128. doi: 10.3389/fimmu.2022.1015128

COPYRIGHT
© 2022 Ye, Yang, Yang and Xia. This is an open-access article distributed under the terms of the Creative Commons Attribution License (CC BY). The use, distribution or reproduction in other forums is permitted, provided the original author(s) and the copyright owner(s) are credited and that the original publication in this journal is cited, in accordance with accepted academic practice. No use, distribution or reproduction is permitted which does not comply with these terms.

Complement C1s as a diagnostic marker and therapeutic target: Progress and propective

Jun Ye[1,2], Peng Yang[3], Yili Yang[4] and Sheng Xia[1*]

[1]Department of Immunology, School of Medicine, Jiangsu University, Zhenjiang, China, [2]Center for Translational Medicine, The Affiliated Taizhou People's Hospital of Nanjing Medical University, Taizhou, China, [3]Department of Emergency Medicine, The First Affiliated Hospital of Soochow University, Suzhou, China, [4]China Regional Research Centre, International Centre of Genetic Engineering and Biotechnology, Taizhou, China

The molecules of the complement system connect the effectors of innate and adaptive immunity and play critical roles in maintaining homeostasis. Among them, the C1 complex, composed of C1q, C1r, and C1s ($C1qr_2s_2$), is the initiator of the classical complement activation pathway. While deficiency of C1s is associated with early-onset systemic lupus erythematosus and increased susceptibility to bacteria infections, the gain-of- function variants of C1r and C1s may lead to periodontal Ehlers Danlos syndrome. As C1s is activated under various pathological conditions and associated with inflammation, autoimmunity, and cancer development, it is becoming an informative biomarker for the diagnosis and treatment of a variety of diseases. Thus, more sensitive and convenient methods for assessing the level as well as activity of C1s in clinic samples are highly desirable. Meanwhile, a number of small molecules, peptides, and monoclonal antibodies targeting C1s have been developed. Some of them are being evaluated in clinical trials and one of the antibodies has been approved by US FDA for the treatment of cold agglutinin disease, an autoimmune hemolytic anemia. In this review, we will summarize the biological properties of C1s, its association with development and diagnosis of diseases, and recent progress in developing drugs targeting C1s. These progress illustrate that the C1s molecule is an effective biomarker and promising drug target.

KEYWORDS

complement, C1s, biomarker, protein, immunity

Introduction

The complement system consists of more than 30 proteins found in soluble form or attached to cell membranes. Their biological functions include cell lysis, opsonization, degranulation of mast cells and basophils, activation of B lymphocytes, and clearance of immune complex and apoptotic cells. With its components mostly existing as precursor zymogens in the plasma, the system can be activated through the classical pathway (CP), alternative pathway (AP), and the lectin pathway (LP). Of note, the CP is typically activated by the immune complex formed by specific antibodies and antigens such as microbes, allo- and auto-antigens. Through the activation, the antibodies promote the formation of membrane attack complex that often lyses target cell directly, generate complement component-mediated opsonization, and augment inflammatory response. Thus, the classical pathway activation of the complement is involved in the initiation, progression, and prognosis of many bacterial and viral infections-induced responses, autoimmune diseases, and cancers (1–5). Conversely, inherited deficiency and hypofunction of the complement system are associated with primary immunodeficiencies as well as systematic lupus erythematosis and hereditary angioedema (6–8).

At molecular level, C1 is a complex composed of one C1q, two C1r, and two C1s subunits ($C1qr_2s_2$). In the classical pathway, antibodies complexed with antigens bind C1q and change its conformation, leading to activation of the protease activity of C1r, which in turn cleaves and activates C1s. C1q can also be activated through binding to C-reactive protein and the surface of pathogens (9, 10). The activated C1s subsequently cleaves substrates C4 and C2, resulting in the formation of C3-convertase (a complex of C4b and C2b) that splits C3 into C3a and C3b, which then cleaves C5 and triggers the formation of so-called membrane attack complex (MAC) consisting of C5b, C6, C7, C8, and polymeric C9 (Figure 1-1). Thus, monitoring C1s activity and targeting C1s with small molecular inhibitors and monoclonal antibodies have been the focus of many studies in recent years (11–14).

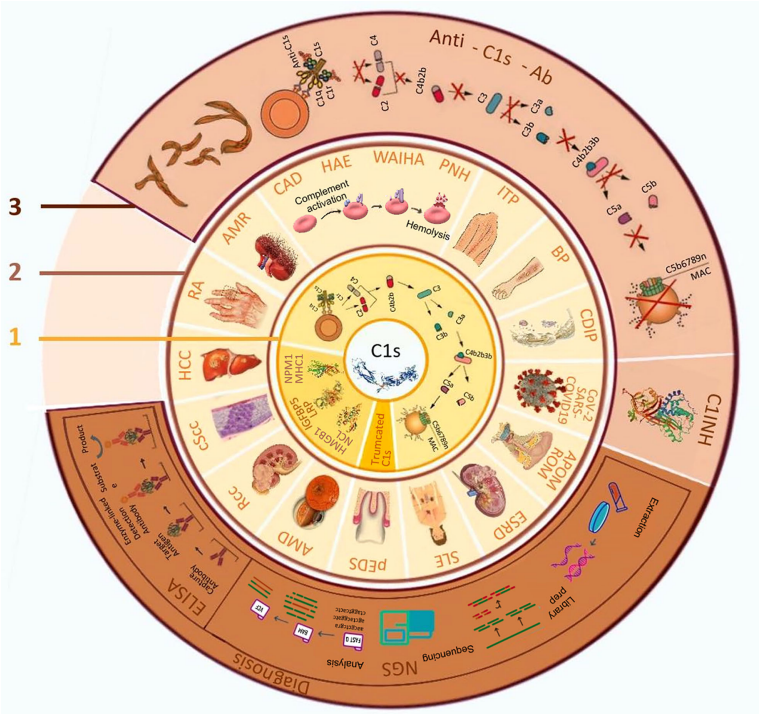

FIGURE 1
The biological function of C1s, related diseases and its application in diagnosis and treatment. 1. Biological functions of C1s; 2. C1s related diseases; 3. Application of C1s as a target in disease diagnosis and treatment. AMD: age-related macular degeneration; AMR: antibody-mediated rejection; APOM: acute pneumococcal otitis media; BP: bullous pemphigoid; CAD: cold agglutinin disease; CDIP: chronic inflammatory demyelinating polyradiculoneuropathy; COVID-19, coronavirus disease 2019; cScc: cutaneous squamous cell carcinoma cells; C1INH: C1 esterase inhibitors; ELISA, enzyme-linked immunosorbent assay; ESRD: end-stage renal disease; SLE: systemic lupus erythematosus; HAE: hereditary angioedema; HCC: hepatocellular carcinoma; HMGB1:high-mobility group box 1; IGFBP5: insulin-like growth factor binding protein-5; ITP: idiopathic thrombocytopenic purpura; LRP: low-density lipoprotein receptor-related protein; MAC: membrane attacking complex; MHC1: Major histocompatibility complex 1; NCL: nucleolin; NGS, next-generation sequencing; NPM1: nucleophosmin 1; pEDS: periodontal ehlers-danlos syndrome; PNH: paroxysmal nocturnal haemoglobinuria; RA: rheumatoid arthritis; Rcc: renal cell carcinoma; ROM: recurrent otitis media; SARS-CoV-2, severe acute respiratory syndrome coronavirus 2; WAIHA: warm autoimmune hemolytic anemia.

The *C1s* gene, located on the short arm of chromosome 12 (12p13.31), contains 12 exons and encodes a precursor C1s protein of 688 amino acids (15, 16). At its N-terminal region, the protein harbors CUB2 and CUB1 domains connected through an epidermal growth factor (EGF)-like domain, which are followed by complement control protein (CCP) modules CCP1 and CCP2. The C-terminal region of C1s has a serine protease (SP) domain (residues 423-688) that contains an activation peptide-like fragment (residues 423-437). During its activation, C1s is cleaved into a heavy chain of 422 amino acids (A-chain) and a light chain of 251 amino acids (B-chain). Of note, C1s is glycosylated at a number of sites and its serine protease activity shows trypsin-like specificity and cleaves arginyl bonds in substrate proteins.

Interestingly, besides C4 and C2, activated C1s also acts on many cellular proteins and exerts multiple regulatory actions. It has been found that activated C1s cleaves major histocompatibility complex I (MHC I) from the cell surface and hydrolyzes 2 microglobin, affecting T cell-mediated immune response (17, 18). It also cleaves insulin-like growth factor binding protein 5 (IGFBP5) from cultured fibroblast, whereas C1q activates the Wnt signaling pathway (17–20), which may affect cell growth as well as neuronal connectivity (21, 22). In addition, low-density lipoprotein receptor-related protein (LRP6), nucleophosmin 1 (NPM1) and nucleolin (NCL) are all substrates of C1s (20, 23). Interestingly, C1s can cleave high-mobility group box 1 (HMGB1) protein, a notable auto-antigen in autoimmune diseases (24). Although these proteolytic activities are far less efficient than the canonical C4 and C2 cleavages leading to complement activation, it is conceivable that they take part in tissue renewal process that reduces the immunogenicity of tissue debris and decreases the likelihood of autoimmunity induced by auto-antigens and danger associated molecular patterns (DAMPs). Thus, C1 activation affects physiological and pathological processes through multiple mechanisms (Figure 1-1).

C1s and human diseases

The critical roles of the complement system and C1s in maintaining homeostasis make their dysfunction associating with a variety of disease. While mutation of C1s is associated with rare genetic diseases and susceptibility to infections and autoimmune disorders, ongoing studies have indicated that the aberrant activation of C1s contributes to the development of autoimmune and infectious diseases and cancer, and serves as an informative biomarker and therapeutic target (Figure 1-2).

Loss and gain function mutation of C1s

It has been shown that deficiency of the classical pathway proteins of the complement system is strongly associated with the development of early-onset systemic lupus erythematosus (SLE), an autoimmune disease characterized by auto-antibody against multiple tissues and organs (3). The likely mechanisms include the lack of activated proteases, such as C1r and C1s, to digest the potential auto-antigens form dying cells and immune complexes and lack of modulation of the immune response set-point by activated complement components. Of note, studies in mouse model indicated that C1r/C1s deficiency alone is insufficient in inducing SLE (25), suggesting that the development of the disease is affected by multiple factors. Further analyses found that the appearance of stop codon (Y204X) in exon 6 that leads to premature protein translation termination is a commonly identified C1s mutation in SLE patients (26). It has also been reported in a family study that the propositus contains homozygous nonsense mutation R534X, and both parents and 4 family members in 2 generations are heterozygous of the mutation (27). Interestingly, it was found in an extended Japanese family that C1s deficiency may result from heterozygous combination of different mutations, including a 4-bp TTTG deletion in exon 10 that results in a frame shift mutation (28), a stop codon mutation (E597X) in exon 12 that encodes a C1s missing 80 amino acids at the C-terminal (29), and a missense mutation G630Q (30).

Periodontal Ehlers Danlos syndrome (pEDS) is a rare disorder characterized mostly by early-onset periodontitis. It has been shown that this subtype of Ehlers Danlos syndrome is caused by mutations in the genes of C1r and C1s (31). The mutations include heterozygous missense, in frame insertion, and deletion in C1r (15 families) or C1s (2 families). A recent study also identified multiple heterozygous C1s mutations (G962C, T961G, and T961A in an extended family as pathogenic variants (32). Interestingly, it was shown that the mutated C1s Val316del and Cys294Arg were produced in the cells as truncated proteins that lost their N-terminal domain (33). It is evident that these mutations led to constitutive activation of C1r and C1s and the development of pEDS. Structural analyses showed that C1r and C1s interact *via* an extensive interface encompassing the N-terminal regions of both proteins (34). Therefore, these mutations might disrupt the binding between C1r and C1s and facilitate aberrant C1s activation (Figure 1-1). It is also conceivable that the mutation break the interaction of C1r-C1s and C1q, uncoupling C1s activation from C1 complex binding.

Autoimmune diseases

As an important system involved both in innate and adaptive immunity, the aberrant activation of the complement is present in many autoimmune diseases, including cold agglutinin disease (CAD), rheumatoid arthritis (RA), and systemic lupus erythematosus (SLE) (13, 35). CAD is a rare autoimmune hemolytic anemia due to the production of IgM auto-antibody (cold agglutinin) against surface antigens of red blood cells (RBCs). The auto-antibodies bound to RBCs activate the complement CP, leading to formation of MAC and hemolysis that manifested as anemia, severe hemolytic crisis, and even death (36, 37). The success of anti-C1s mAbs in the treatment of CAD further demonstrated the critical role of C1 activation in the pathogenesis (38). Additionally, neuromyelitis optica spectrum disorder, characterized by central nervous system inflammation and demyelination, is mediated by anti-aquaporin-4 (anti-AQP4) auto-antibodies targeting astrocytes and subsequent complement activation (39). Clinical studies revealed that anti-C5 antibody eculizumab effectively prevented the disease development (40). It is interesting to further determine whether blocking C1 activation can also alleviate the tissue damage and the autoimmune disease.

Rheumatoid arthritis (RA) is an autoimmune disease of the joints, which results in inflammation and thickening of the joint capsule, and loss of underlying cartilage and bone. C1s activation has been found in the degenerative osteoarthrotic cartilage, but not in normal articular cartilage. The activated C1s was mostly restricted to the severely degraded part of cartilage in osteoarthritis, indicating the participation of C1s in the inflammation and the destroy of cartilage and bone (41). It has also been found that tumour necrosis factor alpha (TNF-α) increased the production of C1s in cultured chondrocytes, suggesting that the inflammatory and destructive roles of C1s may be amplified in the inflammatory joint.

Paradoxically, the roles of C1s in SLE is complicated. While C1r and C1s deficiency predisposes to lupus (42–44), C1s levels in plasma from SLE patients are significantly higher than that in normal subjects, likely reflecting that the increased auto-antibodies activate C1 (45). It has been shown that auto-antibodies against C1s were detected in 7 out of 15 patients with SLE, and may activate C1 and enhance C4 and C2 cleavage (46). However, the positive rate of anti-C1s auto-antibody was markedly lower (6.9%) in a study of a larger group of patients with lupus nephritis, and the presence of anti-C1s and anti-C1r auto-antibodies did not correlate with the clinical parameters of the disease (47). It is worth noting that C1q is frequently targeted by auto-antibodies (anti-C1q), which correlates best with active renal disease in SLE patients (48). It is interesting to further explore how the anti-C1q auto-antibodies affect the complement system and the disease progress. Further,the auto-antibody against C1q could be induced by antigen-derived from Epstein-Barr virus, a well-known trigger of SLE (49). Thus, there are complicated interactions between C1 activation and the development and progress of SLE. It is worth to further explore whether the C1 components may be utilized as diagnostic markers for disease initiation and progress, and as targets of therapeutic intervention at different stages of the disease.

Cancer

Given the close association of complement with immunity, it is not unexpected that activation of C1 is associated with the development, progression, metastasis, and treatment of a variety of cancers (50, 51). In clear cell renal cell carcinoma, local production and activation of C1s drove tumor progression and was associated with poor prognosis (52). Further explorations suggested that C1s facilitates the cancer progression by triggering complement activation, and by modulating the tumor cell phenotype and tumor microenvironment in a complement cascade independent manner (53). One of the cascade independent function may be mediated by the C1 receptor on monocytes, whose engagement drives the cells to migrate into tissues, differentiate into macrophages or dendritic cells (DCs), and initiate adaptive immunity (54). It has also been found that macrophage produced C1q and tumor cell-derived C1r, C1s were assembled in clear cell renal cell carcinoma and resulted in an immunosuppressive microenvironment that promotes tumor progress (55). Therefore, C1s and CP of the complement system can act as an effector of anti-tumor immunity as well as an promoter of the tumorigenic microenvironment in tumor.

Infectious diseases

It is well-known that complement can be activated through CP, LP, and AP on the surface of microbes, leading to the generation of MAC that kills bacteria and parasites *via* forming transmembrane pores (56). The complement may also mark bacteria for phagocytosis and processing by antigen-presenting cells to stimulate adaptive immune cells. While bacteria may utilize a variety of strategies to evade the action of complement, deficiency in the complement system results in susceptibility to infections of various microbes, especially encapsulated bacteria (57). Therefore, activation of complement is a hallmark of bacterial infection. For example, it has been reported that the level of C1s was increased in children with acute pneumococcal otitis media (58). Further, the elevated complement complexes detected in the sera of children with recurrent otitis media contained C1r and C1s, and were able to kill the bacteria (58). Complement activation is also involved in virus infection. Of

note, it was shown that up-regulation of C1s led to host cell damage *via* the classical pathway in a model of SARS-CoV-2 infection (59). Clinical investigation found that the mean 50% hemolytic complement (CH50) level in COVID-19 patients was significantly lower compared to that in healthy individuals, likely due to sustained CP activation in these SARS-CoV-2 infected patients (60). Further studies found that antibody-mediated increase of CP activation was highly associated to COVID-19 disease severity (61), although the downstream effects of this activation may differ depending the disease status of the individual and on the specific antigen targeted (62). Interestingly, the C1 esterase inhibitor (C1INH), which inhibits C1r and C1s activation, significantly reduced fever and inflammation in patients with COVID-19 (63). Due to the large inhibiting spectrum of C1INH, these findings suggest, but did not prove that activated C1s is an effector, biomarker, and potential therapeutic target of various infectious diseases.

C1s as a therapeutic target

The critical role of the complement system in innate and acquired immunity and various diseases prompted various efforts to develop specific therapeutic agents (Figure 1-3). C1s is an attractive target since its inhibition blocks the system at an early stage of the complement cascade. While peptide that binds C1q and blocks C1r and C1s activation have been developed (64), finding selective small molecular inhibitors for the serine protease is challenging. A number of reported molecules did not exhibit high specificity and adequate pharmacokinetics yet (65). A large machine learning-based virtual screening was carried out and found a series of potential valuable inhibitors (66). Further combination of *in silico* and *in vitro* approaches identified hit compounds with new chemo-types and high potency in inhibiting C1s (67). It is interesting to determine whether these inhibitors can interfere the activity of C1s under physiological and pathological conditions.

C1INH is a natural plasma protein whose level is further increased upon stress and inflammation. It has a characteristic serpin domain and irreversibly binds to and inactivates C1r and C1s proteases (68). Of note, C1INH also prevents complement activation through the lectin pathway and exhibits inhibition on multiple proteases, notably kallikrein, fXIa, and fXIIa (69), and therefore modulating the kinin, coagulation, and fibrinolytic systems. It has been proposed that the protein may be utilized in a variety of diseases, including septic shock, reperfusion injury, hyperacute transplant rejection, traumatic and hemorrhagic shock. Currently, C1INH prepared from human plasma (Cinryze™) has been approved for the treatment of hereditary angioedema, a rare autosomal dominant disease manifested by recurrent acute attacks of edema that results from C1INH deficiency (70).

Monoclonal and engineered antibodies have been the most advanced agents for blocking complement activation, including antibodies against C1s (Table 1) and C5 (79). In particular, anti-C1s antibody sutimlimab significantly inhibited Ig-induced activation of B cells derived from patients with rheumatoid arthritis, indicating that targeting C1s may not only block complement-mediated tissue damage, but also suppress the activation of autoimmune B cells, which is a critical pathogenic factor in many autoimmune diseases (13). For example, bullous pemphigoid (BP) is a potentially life-threatening skin disease characterized by blister formation resulted from auto-antibody-mediated complement action and subsequently inflammation and tissue damage. In an *ex vivo* human skin cryosection assay, anti-C1s antibody TNT003 effectively prevented complement activation induced by the bullous pemphigoid auto-antibodies (80, 81). In patients with thrombocytopenic purpura, auto-antibody against platelet membrane protein leads to activation of complement and destruction and reduction of platelet. Sutimlimab inhibited the CP of complement activation and significantly decreased plasma deposition of C3b and C5b-9 in these patients. Meanwhile, the direct damaging and reticuloendothelial system clearance of platelets were markedly reduced (14). Similar studies found

TABLE 1 Registered clinic trials with C1s targeted mAbs.

Disease	Medicine	Clinical staging	NCT NO
Bullous Pemphigoid Cold Agglutinin Disease Warm Antibody Type Autoimmune Hemolytic Anemia End stage renal disease	BIV009	1	NCT02502903 (71)
Cold Agglutinin Disease	sutimlimab (BIVV009)	3	NCT03347422 (72)
Cold Agglutinin Disease	Sutimlimab	3	NCT03347396 (73)
Idiopathic Thrombocytopenic Purpura	sutimlimab (BIVV009)	1	NCT03275454 (74)
Idiopathic Thrombocytopenic Purpura	BIVV020	2	NCT04669600 (75)
Autoimmune hemolytic anemia	BIVV020	1	NCT04802057 (76)
Autoimmune hemolytic anemia	BIVV020	1	NCT04269551 (77)
Chronic Inflammatory Demyelinating Polyradiculoneuropathy	BIVV020	2	NCT04658472 (78)

that anti-C1s antibodies were effective in blocking complement activation induced by auto-antibodies from patients with several types of autoimmune hemolytic anemia, such as paroxysmal nocturnal hemoglobinuria and CAD (14).

Antibody-mediated rejection (AMR) in solid organ transplantation is caused by donor-specific antibodies. It is characterized by the activation of the complement system and infiltration of macrophages ($CD4^+$ and $CD68^+$). In a study with aortic endothelial cells, it was demonstrated that the activation of the complement by anti-MHC antibodies facilitated the recruitment of monocytes. The anti-C1s antibodies TNT003 and TNT009 inhibited the antibody-induced complement activation and blocked C3d deposition (82), which are critical for the microvascular inflammation during AMR (83). The inhibitory effects of these antibodies on CP activation have also been demonstrated in patients (84). Whether they can reduce the microvascular inflammation during AMR and prolong the survival of transplants remain to be further explored. Interestingly, it was found that C1s-specific monoclonal antibody TNT005 did not abolish the therapeutic effects of anti-*Neisseria meningitidis* and *Streptococcus pneumoniae* antibodies, whereas simultaneous inhibition of CP and AP blocked the killing function of the anti-bacterial antibodies (85). Thus, targeting C1s may specifically prevent CP activation without abating the alternative and lectin pathways of complement activation and their associated immunological effector functions, and might also reduce the production of auto-antibodies.

There have been a number of registered clinical trials that target C1s with mAbs for the treatment of hereditary angioedema (HAE), chronic inflammatory demyelinating polyradiculoneuropathy (CIDP), cold agglutinin disease (CAD), thrombocytopenic purpura, and autoimmune hemolysis (Table 1). Sutimlimab (also known as TNT003, BIVV-009) is an humanized IgG4 mAb against C1s. It was reported that 7 of 10 CAD patients treated with sutimlimab achieved remission, and all 6 patients with a history of blood transfusion became transfusion-free during treatment (11). In a named patient program, 7 CAD patients responded to re-treatment, and sutimlimab increased hemoglobin from a median initial level of 7.7 g/dL to a median peak of 12.5 g/dL (P = 0.016). All patients remained transfusion free while receiving sutimlimab, and there were no treatment-related serious adverse events. In another trial with sutimlimab, 13 out of 24 (54%) CAD patients reached the primary end point. Of the 11 patients that did not meet the predefined criteria, 6 of them showed a therapeutic response (12). These and further clinical trials led the recent approval of sutimlimab for the treatment of CAD by the US FDA (86). Of note, another anti-C1s antibody BIVV020, whose tolerability safety study has been completed in patients with CAD, is being actively tried in clinic for the treatment of CAD, immune thrombocytopenia, and antibody-medediated transplant rejection (Table 1). It is conceivable that these antibodies may be proved as an effective therapeutics for additional forms of autoimmune hemolytic anemia in not-so-distant future.

C1s determination in biological samples

Various methods have been developed to detect the complement in clinical samples.Traditionally, the total complement activity of CP is quantified by hemolysis assay in serum, based on the dilution achieving 50% of hemolysis (CH50). Functional ELISAs using coated IgM and colorimetric substrate have also been developed to detect the activity of CP in serum (87, 88). However, these assays only evaluate the overall CP complement activity, but not the levels of individual complement components. The C1 assay through capture of C1q in serum may represent a better measurement of C1s (89). It has also been shown that the analyses of CP components, such as C1q and C1r could be achieved quantitatively or semi-quantitatively by immunodiffusion, ELISA, and nephelometry assays (90). However, these methods only detect the immuno- reactivities of target complement components, and do not necessarily reflect their activity states. For the studies of congenital complement deficiency or for the study of genetic polymorphisms in populations, next-generation sequencing (NGS) and qPCR are often deployed to analyze particular components (91). Therefore, there are no validated C1s quantification assays available in clinical practice currently, and the quantification of C1s in research is also difficult due to limited reliable antibodies and lack of standardized assays.

The level of the total C1s protein can be detected by bilateral diffusion (92), ELISA (27), gelatin zymography (45), and LC-MS/MS (93) (Table 2). As the protein is normally present in blood and tissues, it is important and highly desirable to assess activated C1s to understand its exact roles under physiological and pathological conditions. It has been shown that the activity of C1s can be measured by the cleavage C2 and C4 (94). However, the assay is only semi-quantitative, and C2 and C4 can also be cleaved by other serum proteases such as MASP2. Interestingly, antibodies recognized activated C1s have been reported, which make it possible to determine the protein through western blot. It has been shown that such antibodies detected activated C1s in degenerative cartilage matrix of RA through immunohistochemistry (96). To investigate the effects of C1INH on C1s (97), a synthetic chromogenic tripeptide-p-nitroanilide substrate S-2314 (DTNB) was utilized to determine the level of active C1s. However, the substrate can also be cleaved by activated C1r and other enzymes, such as granzyme H, which prevented its use in clinic for measuring active C1s in blood (95). Thus, it is conceivable that the ideal novel assay should be highly specific and convenient by combining the specific antibody,

TABLE 2 Methodology, advantages, and disadvantages of complement C1s detection.

Detection content	Methods	Clinical blood, body fluid or other samples	Quantitative or not	Advantages and disadvantages
C1s gene	PCR	Adaptive	Used to detect gene mutation and cannot be quantified	Low-flux
	NGS	Adaptive	Used to detect gene mutation and cannot be quantified	High flux, but special equipment is required
C1s protein concentration	ELISA	Adaptive	Quantitative	Low sensitivity
	Bilateral diffusion (92)	Adaptive	Semiquantitative	Low sensitivity
	Gelatin zymography (45)	Not adaptive	Semiquantitative	Operation complex
	LC-MS/MS (93)	Adaptive	Quantitative	Special equipment is required
C1s activation	Cut C2、C4 active test (94)	Not adaptive	Semiquantitative	Operation complex MASP1 and MASP2 interference
	DTNB chromogenic substrate (95)	Not adaptive, Only suitable for quantitative analysis of recombinant expression	Quantitative	Interference of granzyme H and other proteases
	S-2314 chromogenic substrate (97)	Not adaptive	Quantitative	C1r and other protease interference

catalytic and C2/C4 binding specificity of C1s and making use of labeling technologies, such as the fluorescence labeling.

Conclusions and future directions

The critical roles of the complement system in innate and acquired immunity make the activation of C1s an informative biomarker for a variety of diseases, particularly the inflammatory, autoimmune diseases and cancers. With the success of specific antibody preparation, C1s has been validated as an effective target of therapeutic intervention. It is conceivable that more small molecular, peptide/protein, and antibodies targeting C1s for the treatment of caner, autoimmune, and infectious diseases will be developed. Thus, the complement component is a unique target for both diagnostic and therapeutic actions. Further, ongoing clinical trials and the emerging of novel therapeutics against C1s will likely bring new and better drugs into clinic in the not-so-distant future.

It has been shown recently that the expression of C1s and another two other genes is associated with Age-related macular degeneration (AMD), a progressive neurodegenerative disease of the central retina and a leading cause of vision loss in older adults worldwide (98). Mechanistically, it is likely due to their correlation with NK cell infiltration, CD4 memory T cell activation, and macrophage polarization in AMD. Thus, the expression level of the C1s gene might be utilized as a prognostic biomarker for early diagnosis and treatment of AMD. While measuring the level of C1s molecule and its activation states in clinical specimen are of great value, it remains a significant challenge to develop convenient, specific, and sensitive assays to fulfill the need, particularly determining the the kinetics of activated C1s and C1s-mediated enzymatic reaction in the serum/plasma. It is conceivable that the successful and practical clinical evaluation of C1s will enable wide applications of the biomarker in pathogenesis, diagnosis, prognosis of diseases, and for individualized therapies targeting C1s.

Author contributions

JY and SX designed the project, JY wrote and SX revised the manuscript, PY and YY participated in the project and revised the manuscript. All authors contributed to the article and approved the submitted version.

Funding

This work was supported by the Medical Innovation Team Foundation of Taizhou People's Hospital (No. CXTDB201904), Research fund of the "333 project" of Jiangsu Province (No. BRA2020190), 2020 Taizhou People's Hospital Mandatory Project (No. ZL202022) and the National Natural Science Foundation of China (No. 81871234; No. 82172763).

Acknowledgments

We apologize for those colleagues whose important works were not cited due to limited space.

Conflict of interest

The authors declare that the research was conducted in the absence of any commercial or financial relationships that could be construed as a potential conflict of interest.

Publisher's note

All claims expressed in this article are solely those of the authors and do not necessarily represent those of their affiliated organizations, or those of the publisher, the editors and the reviewers. Any product that may be evaluated in this article, or claim that may be made by its manufacturer, is not guaranteed or endorsed by the publisher.

References

1. Campbell CM, Kahwash R. Will complement inhibition be the new target in treating COVID-19-Related systemic thrombosis? *Circulation* (2020) 22:1739–41. doi: 10.1161/CIRCULATIONAHA.120.047419

2. Risitano AM, Mastellos DC, Huber-Lang M, Yancopoulou D, Garlanda C, Ciceri F, et al. Complement as a target in COVID-19? *Nat Rev Immunol* (2020) 20:343–4. doi: 10.1038/s41577-020-0320-7

3. Manderson AP, Botto M, Walport MJ. The role of complement in the development of systemic lupus erythematosus. *Annu Rev Immunol* (2004) 22:431–56. doi: 10.1146/annurev.immunol.22.012703.104549

4. Berentsen S. Complement activation and inhibition in autoimmune hemolytic anemia: Focus on cold agglutinin disease. *Semin Hematol* (2018) 55:141–9. doi: 10.1053/j.seminhematol.2018.04.002

5. Chimenti MS, Ballanti E, Triggianese P, Perricone R. Vasculitides and the complement system: a comprehensive review. *Clin Rev Allergy Immunol* (2015) 49:333–46. doi: 10.1007/s12016-014-8453-8

6. Skattum L, van Deuren M, van der Poll T, Truedsson L. Complement deficiency states and associated infections. *Mol Immunol* (2011) 48:1643–55. doi: 10.1016/j.molimm.2011.05.001

7. Grumach AS, Kirschfink M. Are complement deficiencies really rare? overview on prevalence, clinical importance and modern diagnostic approach. *Mol Immunol* (2014) 61:110–7. doi: 10.1016/j.molimm.2014.06.030

8. Frazer-Abel A, Sepiashvili L, Mbughuni MM, Willrich MA. Overview of laboratory testing and clinical presentations of complement deficiencies and dysregulation. *Adv Clin Chem* (2016) 77:1–75. doi: 10.1016/bs.acc.2016.06.001

9. Gaboriaud C, Ling WL, Thielens NM, Bally I, Rossi V. Deciphering the fine details of c1 assembly and activation mechanisms: "mission impossible"? *Front Immunol* (2014) 5:565. doi: 10.3389/fimmu.2014.00565

10. Wallis R, Mitchell DA, Schmid R, Schwaeble WJ, Keeble AH. Paths reunited: Initiation of the classical and lectin pathways of complement activation. *Immunobiology* (2010) 215:1–11. doi: 10.1016/j.imbio.2009.08.006

11. Jager U, D'Sa S, Schorgenhofer C, Bartko J, Derhaschnig U, Sillaber C, et al. Inhibition of complement C1s improves severe hemolytic anemia in cold agglutinin disease: a first-in-human trial. *Blood* (2019) 133:893–901. doi: 10.1182/blood-2018-06-856930

12. Roth A, Barcellini W, D'Sa S, Miyakawa Y, Broome CM, Michel M, et al. Sutimlimab in cold agglutinin disease. *N Engl J Med* (2021) 384:1323–34. doi: 10.1056/NEJMoa2027760

13. Nikitin PA, Rose EL, Byun TS, Parry GC, Panicker S. C1s inhibition by BIVV009 (Sutimlimab) prevents complement-enhanced activation of autoimmune human b cells *In vitro*. *J Immunol* (2019) 202:1200–9. doi: 10.4049/jimmunol.1800998

14. Peerschke EI, Panicker S, Bussel J. Classical complement pathway activation in immune thrombocytopenia purpura: inhibition by a novel C1s inhibitor. *Br J Haematol* (2016) 173:942–5. doi: 10.1111/bjh.13648

15. Tosi M, Duponchel C, Meo T, Julier C. Complete cDNA sequence of human complement cls and close physical linkage of the homologous genes cls and clr. *Biochemistry-US* (1987) 26:8516–24. doi: 10.1021/bi00400a004

16. Nguyen VC, Tosi M, Gross MS, Cohen-Haguenauer O, Jegou-Foubert C, de Tand MF, et al. Assignment of the complement serine protease genes C1r and C1s to chromosome 12 region 12p13. *Hum Genet* (1988) 78:363–8. doi: 10.1007/BF00291737

17. Eriksson H, Nissen MH. Proteolysis of the heavy chain of major histocompatibility complex class I antigens by complement component C1s. *Biochim Biophys Acta* (1990) 1037:209–15. doi: 10.1016/0167-4838(90)90169-G

18. Nissen MH, Roepstorff P, Thim L, Dunbar B, Fothergill JE. Limited proteolysis of beta 2-microglobulin at lys-58 by complement component C1s. *Eur J Biochem* (1990) 189:423–9. doi: 10.1111/j.1432-1033.1990.tb15505.x

19. Busby WJ, Nam TJ, Moralez A, Smith C, Jennings M, Clemmons DR. The complement component C1s is the protease that accounts for cleavage of insulin-like growth factor-binding protein-5 in fibroblast medium. *J Biol Chem* (2000) 275:37638–44. doi: 10.1074/jbc.M006107200

20. Naito AT, Sumida T, Nomura S, Liu ML, Higo T, Nakagawa A, et al. Complement C1q activates canonical wnt signaling and promotes aging-related phenotypes. *CELL* (2012) 149:1298–313. doi: 10.1016/j.cell.2012.03.047

21. Stevens B, Allen NJ, Vazquez LE, Howell GR, Christopherson KS, Nouri N, et al. The classical complement cascade mediates CNS synapse elimination. *Cell* (2007) 131:1164–78. doi: 10.1016/j.cell.2007.10.036

22. Chu Y, Jin X, Parada I, Pesic A, Stevens B, Barres B, et al. Enhanced synaptic connectivity and epilepsy in C1q knockout mice. *Proc Natl Acad Sci U.S.A.* (2010) 107:7975–80. doi: 10.1073/pnas.0913449107

23. Cai Y, Teo BH, Yeo JG, Lu J. C1q protein binds to the apoptotic nucleolus and causes C1 protease degradation of nucleolar proteins. *J Biol Chem* (2015) 290:22570–80. doi: 10.1074/jbc.M115.670661

24. Yeo JG, Leong J, Arkachaisri T, Cai Y, Teo BH, Tan JH, et al. Proteolytic inactivation of nuclear alarmin high-mobility group box 1 by complement protease C1s during apoptosis. *Cell Death Discovery* (2016) 2:16069. doi: 10.1038/cddiscovery.2016.69

25. Uchio-Yamada K, Tanaka M, Manabe N. C1r/C1s deficiency is insufficient to induce murine systemic lupus erythematosus. *Genes Immun* (2019) 20:121–30. doi: 10.1038/s41435-018-0020-5

26. Amano MT, Ferriani VP, Florido MP, Reis ES, Delcolli MI, Azzolini AE, et al. Genetic analysis of complement C1s deficiency associated with systemic lupus erythematosus highlights alternative splicing of normal C1s gene. *Mol Immunol* (2008) 45:1693–702. doi: 10.1016/j.molimm.2007.09.034

27. Dragon-Durey MA, Quartier P, Fremeaux-Bacchi V, Blouin J, de Barace C, Prieur AM, et al. Molecular basis of a selective C1s deficiency associated with early onset multiple autoimmune diseases. *J Immunol* (2001) 166:7612–6. doi: 10.4049/jimmunol.166.12.7612

28. Inoue N, Saito T, Masuda R, Suzuki Y, Ohtomi M, Sakiyama H. Selective complement C1s deficiency caused by homozygous four-base deletion in the C1s gene. *Hum Genet* (1998) 103:415–8. doi: 10.1007/s004390050843

29. Endo Y, Kanno K, Takahashi M, Yamaguchi K, Kohno Y, Fujita T. Molecular basis of human complement C1s deficiency. *J Immunol* (1999) 162:2180–3.

30. Abe K, Endo Y, Nakazawa N, Kanno K, Okubo M, Hoshino T, et al. Unique phenotypes of C1s deficiency and abnormality caused by two compound heterozygosities in a Japanese family. *J Immunol* (2009) 182:1681–8. doi: 10.4049/jimmunol.182.3.1681

31. Kapferer-Seebacher I, Pepin M, Werner R, Aitman TJ, Nordgren A, Stoiber H, et al. Periodontal ehlers-danlos syndrome is caused by mutations in C1R and C1S, which encode subcomponents C1r and C1s of complement. *Am J Hum Genet* (2016) 99:1005–14. doi: 10.1016/j.ajhg.2016.08.019

32. El CS, Legrand A, Stoetzel C, Geoffroy V, Billon C, Adham S, et al. Periodontal (formerly type VIII) ehlers-danlos syndrome: Description of 13 novel cases and expansion of the clinical phenotype. *Clin Genet* (2021) 100:206–12. doi: 10.1111/cge.13972

33. Bally I, Dalonneau F, Chouquet A, Grobner R, Amberger A, Kapferer-Seebacher I, et al. Two different missense C1S mutations, associated to periodontal ehlers-danlos syndrome, lead to identical molecular outcomes. *Front Immunol* (2019) 10:2962. doi: 10.3389/fimmu.2019.02962

34. Almitairi J, Venkatraman GU, Furze CM, Simpson-Gray X, Badakshi F, Marshall JE, et al. Structure of the C1r-C1s interaction of the C1 complex of complement activation. *Proc Natl Acad Sci U.S.A.* (2018) 115:768–73. doi: 10.1073/pnas.1718709115

35. Ozen A, Comrie WA, Ardy RC, Dominguez CC, Dalgic B, Beser OF, et al. CD55 deficiency, early-onset protein-losing enteropathy, and thrombosis. *N Engl J Med* (2017) 377:52–61. doi: 10.1056/NEJMoa1615887

36. Berentsen S, Malecka A, Randen U, Tjonnfjord GE. Cold agglutinin disease: where do we stand, and where are we going? *Clin Adv Hematol Oncol* (2020) 18:35–44.

37. Gabbard AP, Booth GS. Cold agglutinin disease. *Clin Hematol Int* (2020) 2:95–100. doi: 10.2991/chi.k.200706.001

38. Berentsen S, Hill A, Hill QA, Tvedt T, Michel M. Novel insights into the treatment of complement-mediated hemolytic anemias. *Ther Adv Hematol* (2019) 10:153165097. doi: 10.1177/2040620719873321

39. Asavapanumas N, Tradtrantip L, Verkman AS. Targeting the complement system in neuromyelitis optica spectrum disorder. *Expert Opin Biol Ther* (2021) 21:1073–86. doi: 10.1080/14712598.2021.1884223

40. Pittock SJ, Zekeridou A, Weinshenker BG. Hope for patients with neuromyelitis optica spectrum disorders - from mechanisms to trials. *Nat Rev Neurol* (2021) 17:759–73. doi: 10.1038/s41582-021-00568-8

41. Nakagawa K, Sakiyama H, Tsuchida T, Yamaguchi K, Toyoguchi T, Masuda R, et al. Complement C1s activation in degenerating articular cartilage of rheumatoid arthritis patients: immunohistochemical studies with an active form specific antibody. *Ann Rheum Dis* (1999) 58:175–81. doi: 10.1136/ard.58.3.175

42. Pickering RJ, Naff GB, Stroud RM, Good RA, Gewurz H. Deficiency of C1r in human serum. effects on the structure and function of macromolecular C1. *J Exp Med* (1970) 131:803–15. doi: 10.1084/jem.131.4.803

43. Moncada B, Day NK, Good RA, Windhorst DB. Lupus-erythematosus-like syndrome with a familial defect of complement. *N Engl J Med* (1972) 286:689–93. doi: 10.1056/NEJM197203302861304

44. Day NK, Geiger H, Stroud R, DeBracco M, Mancaido B, Windhorst D, et al. C1r deficiency: an inborn error associated with cutaneous and renal disease. *J Clin Invest* (1972) 51:1102–8. doi: 10.1172/JCI106902

45. Ugarte-Berzal E, Martens E, Boon L, Vandooren J, Blockmans D, Proost P, et al. EDTA/gelatin zymography method to identify C1s versus activated MMP-9 in plasma and immune complexes of patients with systemic lupus erythematosus. *J Cell Mol Med* (2019) 23:576–85. doi: 10.1111/jcmm.13962

46. He S, Lin YL. *In vitro* stimulation of C1s proteolytic activities by C1s-presenting autoantibodies from patients with systemic lupus erythematosus. *J Immunol* (1998) 160:4641–7.

47. Radanova M, Vasilev V, Mihaylova G, Kosturkova M, Kishore U, Roumenina L. Autoantibodies against complement classical pathway components C1q, C1r, C1s and C1-inh in patients with lupus nephritis. *Int J Mol Sci* (2022) 23:9281. doi: 10.3390/ijms23169281

48. Kleer JS, Rabatscher PA, Weiss J, Leonardi J, Vogt SB, Kieninger-Grafitsch A, et al. Epitope-specific anti-C1q autoantibodies in systemic lupus erythematosus. *Front Immunol* (2021) 12:761395. doi: 10.3389/fimmu.2021.761395

49. Csorba K, Schirmbeck LA, Tuncer E, Ribi C, Roux-Lombard P, Chizzolini C, et al. Anti-C1q antibodies as occurring in systemic lupus erythematosus could be induced by an Epstein-Barr virus-derived antigenic site. *Front Immunol* (2019) 10:2619. doi: 10.3389/fimmu.2019.02619

50. Kim MK, Breitbach CJ, Moon A, Heo J, Lee YK, Cho M, et al. Oncolytic and immunotherapeutic vaccinia induces antibody-mediated complement-dependent cancer cell lysis in humans. *Sci Transl Med* (2013) 5:163r–85r. doi: 10.1126/scitranslmed.3005361

51. Riihila P, Viiklepp K, Nissinen L, Farshchian M, Kallajoki M, Kivisaari A, et al. Tumour-cell-derived complement components C1r and C1s promote growth of cutaneous squamous cell carcinoma. *Br J Dermatol* (2020) 182:658–70. doi: 10.1111/bjd.18095

52. Liu L, Du X, Fang J, Zhao J, Guo Y, Zhao Y, et al. Development of an interferon gamma response-related signature for prediction of survival in clear cell renal cell carcinoma. *J Inflammation Res* (2021) 14:4969–85. doi: 10.2147/JIR.S334041

53. Daugan MV, Revel M, Russick J, Dragon-Durey MA, Gaboriaud C, Robe-Rybkine T, et al. Complement C1s and C4d as prognostic biomarkers in renal cancer: Emergence of noncanonical functions of C1s. *Cancer Immunol Res* (2021) 9:891–908. doi: 10.1158/2326-6066.CIR-20-0532

54. Ghebrehiwet B, Ji Y, Valentino A, Pednekar L, Ramadass M, Habiel D, et al. Soluble gC1qR is an autocrine signal that induces B1R expression on endothelial cells. *J Immunol* (2014) 192:377–84. doi: 10.4049/jimmunol.1302031

55. Roumenina LT, Daugan MV, Noe R, Petitprez F, Vano YA, Sanchez-Salas R, et al. Tumor cells hijack macrophage-produced complement C1q to promote tumor growth. *Cancer Immunol Res* (2019) 7:1091–105. doi: 10.1158/2326-6066.CIR-18-0891

56. Heesterbeek D, Angelier ML, Harrison RA, Rooijakkers S. Complement and bacterial infections: From molecular mechanisms to therapeutic applications. *J Innate Immun* (2018) 10:455–64. doi: 10.1159/000491439

57. Syed I, Wooten RM. Interactions between pathogenic burkholderia and the complement system: A review of potential immune evasion mechanisms. *Front Cell Infect Microbiol* (2021) 11:701362. doi: 10.3389/fcimb.2021.701362

58. Johnson U, Kamme C, Laurell AB, Nilsson NI. C1 subcomponents in acute pneumococcal otitis media in children. *Acta Pathol Microbiol Scand C* (1977) 85:10–6. doi: 10.1111/j.1699-0463.1977.tb03604.x

59. Messner CB, Demichev V, Wendisch D, Michalick L, White M, Freiwald A, et al. Ultra-High-Throughput clinical proteomics reveals classifiers of COVID-19 infection. *Cell Syst* (2020) 11:11–24. doi: 10.1016/j.cels.2020.05.012

60. Keshavarz F, Ghalamfarsa F, Javdansirat S, Hasanzadeh S, Azizi A, Sabz G, et al. Patients with covid 19 have significantly reduced CH50 activity. *Virusdisease* (2021) 32:1–9. doi: 10.1007/s13337-021-00710-6

61. Jarlhelt I, Nielsen SK, Jahn CXH, Hansen CB, Perez-Alos L, Rosbjerg A, et al. SARS-CoV-2 antibodies mediate complement and cellular driven inflammation. *Front Immunol* (2020) 12:767981. doi: 10.3389/fimmu.2021.767981

62. Lamerton RE, Marcial-Juarez E, Faustini SE, Perez-Toledo M, Goodall M, Jossi SE, et al. SARS-CoV-2 spike- and nucleoprotein-specific antibodies induced after vaccination or infection promote classical complement activation. *Front Immunol* (2022) 13:838780. doi: 10.3389/fimmu.2022.838780

63. Urwyler P, Moser S, Charitos P, Heijnen I, Rudin M, Sommer G, et al. Treatment of COVID-19 with conestat Alfa, a regulator of the complement, contact activation and kallikrein-kinin system. *Front Immunol* (2020) 11:2072. doi: 10.3389/fimmu.2020.02072

64. Sharp JA, Whitley PH, Cunnion KM, Krishna NK. Peptide inhibitor of complement c1, a novel suppressor of classical pathway activation: mechanistic studies and clinical potential. *Front Immunol* (2014) 5:406. doi: 10.3389/fimmu.2014.00406

65. Travins JM, Ali F, Huang H, Ballentine SK, Khalil E, Hufnagel HR, et al. Biphenylsulfonyl-thiophene-carboxamidine inhibitors of the complement component C1s. *Bioorg Med Chem Lett* (2008) 18:1603–6. doi: 10.1016/j.bmcl.2008.01.064

66. Chen JJ, Schmucker LN, Visco DP. Pharmaceutical machine learning: Virtual high-throughput screens identifying promising and economical small molecule inhibitors of complement factor C1s. *Biomolecules* (2018) 8:24. doi: 10.3390/biom8020024

67. Szilagyi K, Hajdu I, Flachner B, Lorincz Z, Balczer J, Gal P, et al. Design and selection of novel C1s inhibitors by *in silico* and *in vitro* approaches. *Molecules* (2019) 24:3641. doi: 10.3390/molecules24203641

68. Karnaukhova E. C1-inhibitor: Structure, functional diversity and therapeutic development. *Curr Med Chem* (2022) 29:467–88. doi: 10.2174/0929867328666210804085636

69. Davis AR. Biological effects of C1 inhibitor. *Drug News Perspect* (2004) 17:439–46. doi: 10.1358/dnp.2004.17.7.863703

70. Lunn M, Santos C, Craig T. Cinryze as the first approved C1 inhibitor in the USA for the treatment of hereditary angioedema: approval, efficacy and safety. *J Blood Med* (2010) 1:163–70. doi: 10.2147/JBM.S9576

71. US National Library Of Medicine. *ClinicalTrials.gov* (2021). Available at: https://www.clinicaltrials.gov/show/NCT02502903.

72. US National Library Of Medicine. *ClinicalTrials.gov* (2021). Available at: https://www.clinicaltrials.gov/show/NCT03347422.

73. US National Library Of Medicine. *ClinicalTrials.gov* (2021). Available at: https://www.clinicaltrials.gov/show/NCT03347396.

74. US National Library Of Medicine. *ClinicalTrials.gov* (2021). Available at: https://www.clinicaltrials.gov/show/NCT03275454.

75. US National Library Of Medicine. *ClinicalTrials.gov* (2021). Available at: https://www.clinicaltrials.gov/show/NCT04669600.

76. US National Library Of Medicine. *ClinicalTrials.gov* (2021). Available at: https://www.clinicaltrials.gov/show/NCT04802057.

77. US National Library Of Medicine. *ClinicalTrials.gov* (2021). Available at: https://www.clinicaltrials.gov/show/NCT04269551.

78. US National Library Of Medicine. *ClinicalTrials.gov* (2021). Available at: https://www.clinicaltrials.gov/show/NCT04658472.

79. Gavriilaki E, de Latour RP, Risitano AM. Advancing therapeutic complement inhibition in hematologic diseases: PNH and beyond. *Blood* (2022) 139:3571–82. doi: 10.1182/blood.2021012860

80. Kushner CJ, Payne AS. Increasing the complement of therapeutic options in bullous pemphigoid. *J Invest Dermatol* (2018) 138:246–8. doi: 10.1016/j.jid.2017.09.026

81. Kasprick A, Holtsche MM, Rose EL, Hussain S, Schmidt E, Petersen F, et al. The anti-C1s antibody TNT003 prevents complement activation in the skin induced by bullous pemphigoid autoantibodies. *J Invest Dermatol* (2018) 138:458–61. doi: 10.1016/j.jid.2017.08.030

82. Thomas KA, Valenzuela NM, Gjertson D, Mulder A, Fishbein MC, Parry GC, et al. An anti-C1s monoclonal, TNT003, inhibits complement activation induced by antibodies against HLA. *Am J Transplant* (2015) 15:2037–49. doi: 10.1111/ajt.13273

83. Valenzuela NM, Thomas KA, Mulder A, Parry GC, Panicker S, Reed EF. Complement-mediated enhancement of monocyte adhesion to endothelial cells by HLA antibodies, and blockade by a specific inhibitor of the classical complement cascade, TNT003. *Transplantation* (2017) 101:1559–72. doi: 10.1097/TP.0000000000001486

84. Muhlbacher J, Jilma B, Wahrmann M, Bartko J, Eskandary F, Schorgenhofer C, et al. Blockade of HLA antibody-triggered classical complement activation in sera from subjects dosed with the anti-C1s monoclonal antibody TNT009-results

from a randomized first-in-Human phase 1 trial. *Transplantation* (2017) 101:2410–8. doi: 10.1097/TP.0000000000001804

85. Lewis LA, Panicker S, DeOliveira RB, Parry GC, Ram S. Effect of a C1s inhibitor on the efficacy of anti-capsular antibodies against neisseria meningitidis and streptococcus pneumoniae. *Immunohorizons* (2019) 3:519–30. doi: 10.4049/immunohorizons.1900031

86. Dhillon S. Sutimlimab: First approval. *Drugs* (2022) 82:817–23. doi: 10.1007/s40265-022-01711-5

87. Roos A, Wieslander J. Evaluation of complement function by ELISA. *Methods Mol Biol* (2014) 1100:11–23. doi: 10.1007/978-1-62703-724-2_2

88. Seelen MA, Roos A, Wieslander J, Mollnes TE, Sjoholm AG, Wurzner R, et al. Functional analysis of the classical, alternative, and MBL pathways of the complement system: standardization and validation of a simple ELISA. *J Immunol Methods* (2005) 296:187–98. doi: 10.1016/j.jim.2004.11.016

89. Roumenina LT, Sene D, Radanova M, Blouin J, Halbwachs-Mecarelli L, Dragon-Durey MA, et al. Functional complement C1q abnormality leads to impaired immune complexes and apoptotic cell clearance. *J Immunol* (2011) 187:4369–73. doi: 10.4049/jimmunol.1101749

90. Mollnes TE, Jokiranta TS, Truedsson L, Nilsson B, Rodriguez DCS, Kirschfink M. Complement analysis in the 21st century. *Mol Immunol* (2007) 44:3838–49. doi: 10.1016/j.molimm.2007.06.150

91. Dasdemir S, Yildiz M, Celebi D, Sahin S, Aliyeva N, Haslak F, et al. Genetic screening of early-onset patients with systemic lupus erythematosus by a targeted next-generation sequencing gene panel. *Lupus* (2022) 31:330–7. doi: 10.1177/09612033221076733

92. Ziccardi RJ, Cooper NR. Demonstration and quantitation of activation of the first component of complement in human serum. *J Exp Med* (1978) 147:385–95. doi: 10.1084/jem.147.2.385

93. Kodeboyina SK, Lee TJ, Bollinger K, Ulrich L, Bogorad D, Estes A, et al. Aqueous humor proteomic alterations associated with visual field index parameters in glaucoma patients: A pilot study. *J Clin Med* (2021) 10:1180. doi: 10.3390/jcm10061180

94. Matsumoto M, Nagaki K, Kitamura H, Kuramitsu S, Nagasawa S, Seya T. Probing the C4-binding site on C1s with monoclonal antibodies. evidence for a C4/C4b-binding site on the gamma-domain. *J Immunol* (1989) 142:2743–50.

95. Edwards KM, Kam CM, Powers JC, Trapani JA. The human cytotoxic T cell granule serine protease granzyme h has chymotrypsin-like (chymase) activity and is taken up into cytoplasmic vesicles reminiscent of granzyme b-containing endosomes. *J Biol Chem* (1999) 274:30468–73. doi: 10.1074/jbc.274.43.30468

96. Nakagawa K, Sakiyama H, Tsuchida T, Yamaguchi K, Toyoguchi T, Masuda R, et al. Complement C1s activation in degenerating articular cartilage of rheumatoid arthritis patients: immunohistochemical studies with an active form specific antibody. *Ann Rheum Dis* (1999) 58:175–81. doi: 10.1136/ard.58.3.175

97. Nilsson T, Wiman B. Kinetics of the reaction between human C1-esterase inhibitor and C1r or C1s. *Eur J Biochem* (1983) 129:663–7. doi: 10.1111/j.1432-1033.1983.tb07100.x

98. Zeng Y, Yin X, Chen C, Xing Y. Identification of diagnostic biomarkers and their correlation with immune infiltration in age-related macular degeneration. *Diagnostics* (2021) 11:1079. doi: 10.3390/diagnostics11061079

frontiers | Frontiers in Immunology

TYPE Original Research
PUBLISHED 06 October 2022
DOI 10.3389/fimmu.2022.970938

Check for updates

OPEN ACCESS

EDITED BY
Erik J.M. Toonen,
Hycult Biotech, Netherlands

REVIEWED BY
Matteo Stravalaci,
Humanitas University, Italy
Jamie Lynn Sturgill,
University of Kentucky, United States

*CORRESPONDENCE
Livia K. L. Habenicht
livia.habenicht@icloud.com
Changjun Yin
yinchj3@mail.sysu.edu.cn

†These authors have contributed equally to this work

SPECIALTY SECTION
This article was submitted to Molecular Innate Immunity, a section of the journal Frontiers in Immunology

RECEIVED 16 June 2022
ACCEPTED 31 August 2022
PUBLISHED 06 October 2022

CITATION
Habenicht LKL, Wang Z, Zhang X, Li Y, Mogler C, Huspenina JS, Schmid RM, Weber C, Mohanta SK, Ma Z and Yin C (2022) The C1q-ApoE complex: A new hallmark pathology of viral hepatitis and nonalcoholic fatty liver disease. *Front. Immunol.* 13:970938. doi: 10.3389/fimmu.2022.970938

COPYRIGHT
© 2022 Habenicht, Wang, Zhang, Li, Mogler, Huspenina, Schmid, Weber, Mohanta, Ma and Yin. This is an open-access article distributed under the terms of the Creative Commons Attribution License (CC BY). The use, distribution or reproduction in other forums is permitted, provided the original author(s) and the copyright owner(s) are credited and that the original publication in this journal is cited, in accordance with accepted academic practice. No use, distribution or reproduction is permitted which does not comply with these terms.

The C1q-ApoE complex: A new hallmark pathology of viral hepatitis and nonalcoholic fatty liver disease

Livia K. L. Habenicht[1,2*†], Zhihua Wang[2], Xi Zhang[2], Yuanfang Li[2], Carolin Mogler[3], Julia Slotta Huspenina[3,4], Roland M. Schmid[1], Christian Weber[2,5,6,7], Sarajo K. Mohanta[2,5], Zhe Ma[2†] and Changjun Yin[2,8*†]

[1]Klinik und Poliklinik für Innere Medizin II, Klinikum rechts der Isar, Technical University of Munich, Munich, Germany, [2]Institute for Cardiovascular Prevention (IPEK), Ludwig-Maximilians-University, Munich, Germany, [3]Institute of Pathology, Klinikum rechts der Isar, Technical University of Munich, Munich, Germany, [4]Tissue biobank of the Klinikum rechts der Isar, Technical University of Munich, Munich, Germany, [5]DZHK (German Centre for Cardiovascular Research), partner site Munich Heart Alliance, Munich, Germany, [6]Department of Biochemistry, Cardiovascular Research Institute Maastricht (CARIM), Maastricht University Medical Centre, Maastricht, Netherlands, [7]Munich Cluster for Systems Neurology (SyNergy), Munich, Germany, [8]Institute of Precision Medicine, The First Affiliated Hospital of Sun Yat-sen University, Guangzhou, China

We recently identified a high-affinity C1q-ApoE complex in human artery atherosclerotic intima lesions and in human amyloid plaques of Alzheimer's Disease brains defining a common pathogenetic pathway of two diverse diseases, i.e. atherosclerosis and dementia. C1q is the initiating and controlling protein of the classical complement cascade (CCC), which occupies a key role in multiple acute and chronic inflammatory tissue responses. C1q is largely produced by myeloid cells including Kupffer cells (KCs) and subsequently secreted into the circulation as an inactive preprotein. Its binding partner, Apolipoprotein E (ApoE), is produced by KCs and hepatocytes and it is also secreted into the circulation, where it regulates essential steps of lipid transport. In addition to its major source, ApoE can be produced by non-liver cells including immune cells and multiple other cells depending on local tissue contexts. To initiate the CCC cascade, C1q must be activated by molecules as varied as oxidized lipids, amyloid fibrils, and immune complexes. However, ApoE is mute towards inactive C1q but binds at high-affinity to its activated form. Specifically, our studies revealed that ApoE is a CCC-specific checkpoint inhibitor *via* the formation of the C1q-ApoE complex. We proposed that it may arise in multiple if not all CCC-associated diseases and that its presence indicates ongoing CCC activity. Here, we turned to the liver to examine C1q-ApoE complexes in human B- and C-viral hepatitis and nonalcoholic fatty liver disease (NAFLD). In addition, we used multidrug-resistance-2 gene-knockout (Mdr2-KO) mice as a model for inflammatory liver disease and hepatocellular carcinoma (HCC) pathogenesis. In normal murine and human livers, KCs were the major C1q-producing cell type while hepatocytes were the primary ApoE-forming cell type though the C1q-ApoE

complex was rare or nonexistent. However, significant numbers of C1q-ApoE complexes formed in both Mdr2-KO, human viral hepatitis, and NAFLD around portal triads where immune cells had infiltrated the liver. Additionally, high numbers of C1q-ApoE complexes emerged in human livers in areas of extracellular lipid droplets across the entire liver parenchyma in NAFLD-affected patients. Thus, the C1q-ApoE complex is a new pathological hallmark of viral hepatitis B and C and NAFLD.

KEYWORDS

C1q-ApoE complex, viral hepatitis, hepatocellular carcinoma (HCC), nonalcoholic fatty liver disease (NAFLD), classical complement cascade (CCC)

Introduction

Our previous observation of C1q-ApoE complexes in atherosclerosis and Alzheimer's Disease and the characterization of ApoE as a potent checkpoint inhibitor of the CCC (1, 2) raised an important question: does the C1q-ApoE complex represent a common universal pathology of all diseases in which the CCC is active (3, 4)? C1q-ApoE complex formation requires prior activation of inactive native C1q (1) illustrating that its detection is largely restricted to diseased tissues. The ability of ApoE to directly inhibit the CCC *in vitro* and *in vivo* at high affinity provided a molecular link between previously unrelated proteins in two major clinically significant diseases and possibly beyond. As C1q is the CCC-initiating and activity-controlling protein, these data revealed that ApoE directly affects a major pathway of innate immune responses by containing the activity of the CCC and restricting it from overactivation (3, 5). Moreover, recent studies on the CCC indicate that it is involved in adaptive immune responses in a variety of physiological and disease conditions (3). We also observed that treatment of mice with a liver-specific small interfering RNA directed against C5, i.e. a key downstream mediator of the CCC and the other two complement pathways (5, 6), attenuated atherosclerosis progression in arteries and reduced the microglia response around Alzheimer plaques in brains (1). These studies deserve attention as both C1q and ApoE have been shown to be related to multiple chronic inflammatory diseases in separate genome-wide association studies (GWAS) though the molecular mechanisms of the association of C1q and ApoE with distinct disease entities had remained unclear (7, 8).

We proposed that the formation of the C1q-ApoE complex in atherosclerosis and Alzheimer's Disease may indicate a universal common self-regulating mechanism of CCC-dependent inflammation in a wide range of inflammation-related diseases to control CCC activity´s *via* a feedback inhibition of its initiating protein (1). Here, we begin to address this issue by directing our attention towards the liver for several reasons: viral hepatitis ranges among the top four infectious diseases worldwide despite the progress in prevention medicine using vaccines as well as anti-viral treatments (9). Furthermore, some estimates show that nonalcoholic fatty liver disease (NAFLD) affect more than a quarter of the world population with still no available therapy (10, 11). Notably, NAFLD is associated with chronic liver inflammation, connective tissue accumulation and is the leading cause of liver cirrhosis and HCC (4). Similar to atherosclerosis (12) and Alzheimer's Disease (13), various clinically important liver diseases are associated with acute, subacute and chronic inflammation in which immune cells accumulate around portal triads (4, 14). The inflammatory component of viral hepatitis and of NAFLD is believed to be the most important driver of the reorganization of liver structure in chronic hepatitis, the subsequent emergence of liver fibrosis, the development of liver cirrhosis and the promotion of HCC (4, 15). While effective treatment regimens are available for both chronic B and C viral hepatitis (16, 17), no similar clinically applicable treatments are available for NAFLD. Indeed, obesity and its associated liver disease, i.e. NAFLD, is now viewed as a global epidemic with billions of people affected as of 2016 (15). Therefore, there is a major and urgent, increasing and unmet medical need to understand the underlying mechanisms of the detrimental mechanisms underlying NAFLD. As an experimental model for inflammatory liver disease and HCC, we used multidrug resistance protein 2 knockout (Mdr2-KO) mice. The Mdr2 gene encodes P-glycoprotein which transports phosphorylcholine across the canalicular membrane into the bile (18). In Mdr2-KO mice, the absence of phospholipids in bile damages tight junctions and basement membranes of bile ducts, leading to leakage of bile acid into the extracellular space with subsequent portal inflammation (19). Mdr2-KO mice develop cholangitis with portal inflammation peaking at 3 months of age, and mice develop HCC at 16 months of age (20).

Here, we sought to examine whether the C1q-ApoE complex develops in several forms of murine and human hepatitis and to define its localization within the liver lobule during disease

progression. Of particular interest was NAFLD in human livers whose initial pathology is characterized by intracellular and extracellular lipid droplets across the entire liver lobule (14). The accumulation of intra- and extracellular lipid droplets resembles intraplaque accumulation of oxidized lipids in atherosclerosis. In this regard it is of interest to note that oxidized low density lipoproteins are strong activators of C1q, i.e. an activity which is not shared by native low density lipoproteins. In addition to KCs as a source of circulating C1q and ApoE, activated immune cells and particularly macrophages and other cells of myeloid origin are known to produce both C1q and ApoE upon activation (21, 22) at sites of acute or chronic tissue inflammation (23). While the source of the large majority of circulating ApoE is derived from liver hepatocytes (22, 24), myeloid cells may also be a major source of both C1q and ApoE locally as shown by bone marrow transplantation studies in mice (21).

Materials and methods

Mice

FVB/NJ WT and FVB.129P2-Abcb4tm1Bor/J were purchased from Charles River Laboratories and housed in the animal facilities of Munich University. A total number of 6 FVB/NJ WT (3 female/3 male) and 6 FVB.129P2-Abcb4tm1Bor/J (3 female/3 male) have been used in this study. Mice were fed a standard rodent chow diet under pathogen free conditions. At 3 month of age liver tissue was dissected and embedded in Tissue-Tec (Sakura Finetek) and stored at -80°C. Animal procedures were approved by the Animal Care and Use Committee of Regierung of Oberbayern.

Human tissues

All human liver tissues were collected and provided by the biobank of the Technical University of Munich, Klinikum rechts der Isar. Samples were collected within the first 30 minutes after resection. They were macroscopically dissected by an experienced pathologist, snap frozen and stored in liquid nitrogen until further usage. A summary of the human tissues is available in Supplementary Table 1. The protocols applied to human samples were approved by the ethics committee of the Faculty of Medicine, Munich University.

Histology and immunofluorescent microscopy

All stainings were performed on 10 µm fresh-frozen sections. Oil red O (ORO) staining as well as hematoxylin and eosin (HE) staining of liver sections was performed to define liver histopathologies. Immunoflorescent (IF) stainings of mouse liver sections were performed using the following primary antibodies: anti-mouse/human ApoE (ab52607; Abcam); anti-mouse C1q (ab182451; Abcam); anti-mouse CLEC4F (ab2608299; Invitrogen); anti-mouse CD68 (FA11; Serotec); anti-mouse CD31 (ab553370; BD PharMingen); anti-human C3 (A213; ComplementTech); anti-mouse C4 (HM1046; Hycult Biotech); anti-mouse C5 (ab11898, Abcam). We had previously established the specificity of IF microscopy in mouse and human tissues including no primary antibody negative controls, isotype antibody controls, ApoE knockout mouse tissue (i.e., anti-ApoE antibodies) (1). IF stainings of human sections were performed using the following antibodies: anti-mouse/human ApoE (ab52607; Abcam); anti-human C1q (ab71089; Abcam); anti-human CD68 (EMB11; DAKO); anti-human C5 (A220; ComplementTech). Hepatitis sections as well as the appropriate control tissues were fixated with Delaunay solution prior to IF staining. Stained sections were analyzed using a Leica confocal microscope (SP8, Leica, Germany) using Leica Application Suite (Leica) and ImageJ software.

Proximity ligation assay

Protein-protein interaction *ex vivo* in mouse and human tissues *in situ* were performed using the Duolink® PLA kit (DUO92101 SIGMA) as previously described in (1): briefly, sections were stained with rabbit anti mouse ApoE (ab183597, Abcam) and mouse anti-C1q (HM1096BT, Hycult) for mouse liver tissues and with rabbit anti-human ApoE (ab52607, Abcam) and mouse anti-human C1q (ab71089, Abcam) for human livers. No or only one primary antibody were used as controls. PLA signals were detected according to the manufacturer's protocol. A Leica confocal microscope (SP8, Leica, Germany) equipped with a 96x or 100x oil objective (NA 1.4) was used for imaging.

Analyses of single cell transcriptome data

Single cell data analyses were performed using publicly available databases (https://www.livercellatlas.org/download.php) (25). The databases contain 147 samples obtained from mice and human livers with various single cell-based technologies, such as CITE-Seq, Single-nucleus RNA sequencing (Nuc-Seq), and scRNA-Seq. Data were loaded into Rstudio and processed with the Seurat package (version 4.1.0), respectively. The annotation data for each cell was downloaded to define each cell (25). Mice fed with standard diet (SD) were considered healthy controls, mice fed with Western diet (WD): 58% fat, 1% cholesterol, and drinking water with 23.1 g/L fructose and 18.9 g/L sucrose were

considered diseased mice (25). Human liver biopsies were collected from patients undergoing cholecystectomy or gastric bypass, and healthy adjacent liver tissue removed during liver resection from colorectal cancer metastasis patients (25). Patients with less than 10% steatosis are regarded as healthy controls; patients with more than 10% steatosis were considered diseased (25, 26). For human studies, a total of 125.844 cells were used, 8.383 hepatocytes (nucSeq) and 1.287 KCs (citeSeq). In mouse studies a total of 56.407 ($CD45^+$) and 33.241 ($CD45^-$) were used out of which 9.190 were hepatocytes and 5.265 KCs. Violin plots visualized the normalized expression of the selected genes by using *Seurat*. To evaluate the difference of gene expression between different groups, data were analyzed using *Wilcoxon rank sum test* in two groups or *Kruskal-Walli's test with Dunn's non-parametric all-pairs comparison test* in multiple groups. The p values were adjusted using *Benjamini Hochberg correction*. * p values <0.05; ** p values <0.01; *** p values <0.001.

Results

Cellular expression patterns of C1q and ApoE in Mdr2-KO livers

We used Mdr2-KO mice as a widely used model for human chronic hepatitis and HCC pathogenesis (18). A combination of ORO and HE staining at the peak of liver inflammation in Mdr2-KO mice at 3 months of age vs their sex- and age-matched controls, showed patches of inflammatory cells that were associated with lipid deposits. These areas were pronounced in the portal triads in Mdr2-KO liver lobules but not in healthy livers (Figure 1A). Antisera against CD31 delineated blood vessels, Clec4f stained KCs, and DAPI indicated nuclei. Radiating from the $CD31^+$ central vein (CV) of each lobule towards the portal triads, $Clec4f^+$ KCs were located along the sinusoids throughout the concentric centrolobular, midzonal and periportal parts of WT livers (27) as expected (Figure 1B). In Mdr2-KO livers, a similar localization for KCs was apparent (Figure 1B) but $CD31^+$ blood vessels were more abundant and sinusoids were enlarged, distended and more packed indicating neoangiogenesis in the Mdr2-KO lobules (27, 28). We next used antisera to stain C1q and ApoE in livers of WT and Mdr2-KO mice. In WT mice, C1q positivity located along the sinusoids similar to Clec4f but C1q was not observed in hepatocytes (Figure 1C), whereas ApoE signals were strong in hepatocytes (Figure 1C). In Mdr2-KO mice, C1q positivity was seen along the sinusoids (Figure 1C) similar to WT livers. However, unlike WT livers, Mdr2-KO livers revealed very strong C1q signals in the portal triads (Figure 1C). These data indicate that portal triad-infiltrating immune cells highly express C1q in Mdr2-KO livers in addition to KCs. In Mdr2-KO livers, ApoE signals were largely restricted to hepatocytes and - to a lesser degree - in cells of the portal triads (Figure 1C).

C1q- and ApoE-expressing cells in murine WT and Mdr2-KO livers

To distinguish KCs from monocyte-derived macrophages (27), we used Clec4f as a specific marker for mouse KCs together with CD68 as a distinct marker combination for KCs, i.e. KCs stain $Clec4f^+/CD68^+$ whereas macrophages are Clec4f negative but CD68 positive and thus stain $Clec4f^-/CD68^+$. In WT liver sinusoids, most $C1q^+$ cells stained double positive for Clec4f and CD68 indicating that KCs are the major C1q-expressing cell type in healthy livers (Figure 2A). In addition to KCs, however, $Clec4f^-/CD68^+$ liver parenchymal macrophages were also readily detected but their number was low when compared to KCs though WT liver parenchymal macrophages also stained positive for C1q (Figure 2A) indicating that the healthy liver contains two types of C1q-expressing cells, i.e. the majority are KCs and CD68 single positive parenchymal macrophages. In the parenchyma of Mdr2-KO lobules, the staining pattern of C1q in KCs versus parenchymal macrophages was similar to WT livers with most KCs staining positive for Clec4f and CD68 with some single $CD68^+$ macrophages also staining positive for C1q (Figure 2A). We note, however, that the morphology of KCs in Mdr2-KO mice differed from KCs of WT KCs in that they appeared to have a more elaborate and elongated network of cell extensions (Figure 2). Moreover, large macrophage infiltrates were observed in Mdr2-KO livers around portal triads (Figure 2A). The portal triad-associated macrophages stained strongly for C1q, indicating that these macrophages are a second major source of C1q protein in Mdr2-KO livers (Figure 2A). We next co-stained ApoE with Clec4f and CD68. ApoE was strongly expressed ubiquitously by hepatocytes throughout the lobules both in WT and Mdr2-KO livers (Figure 2B). In addition, hepatocytes, $Clec4f^+/CD68^+$ KCs and $Clec4f^-CD68^+$ macrophages in the parenchyma stained positive for ApoE (Figure 2B). In Mdr2-KO livers, ApoE was widely expressed by hepatocytes, KCs and parenchymal macrophages in non-inflamed liver parenchyma (Figure 2B). However, ApoE stained positive in portal triad macrophages though somewhat weaker compared to hepatocytes (Figure 2B).

Complement components in WT and Mdr2-KO livers

We next examined complement proteins in WT and Mdr2-KO livers. Complement component C4 was rather weak in WT KCs and hepatocytes (Figure 3A) when compared to KCs of Mdr2-KO livers (Figure 3A). These data indicated that KCs up-regulate C4 in Mdr2-KO livers. In addition, a subpopulation of Mdr2-KO portal triad macrophages stained strongly positive for C4 (Figure 3A). We next examined complement C5. Similar to C4, complement component C5 stained weakly in KCs of WT mice (Figure 3B). However, unlike C4, hepatocytes were strongly C5 positive in the WT and Mdr2-KO livers (Figure 3B). Similar to C4, C5 appeared to be upregulated in Mdr2-KO KCs and in a subpopulation of portal

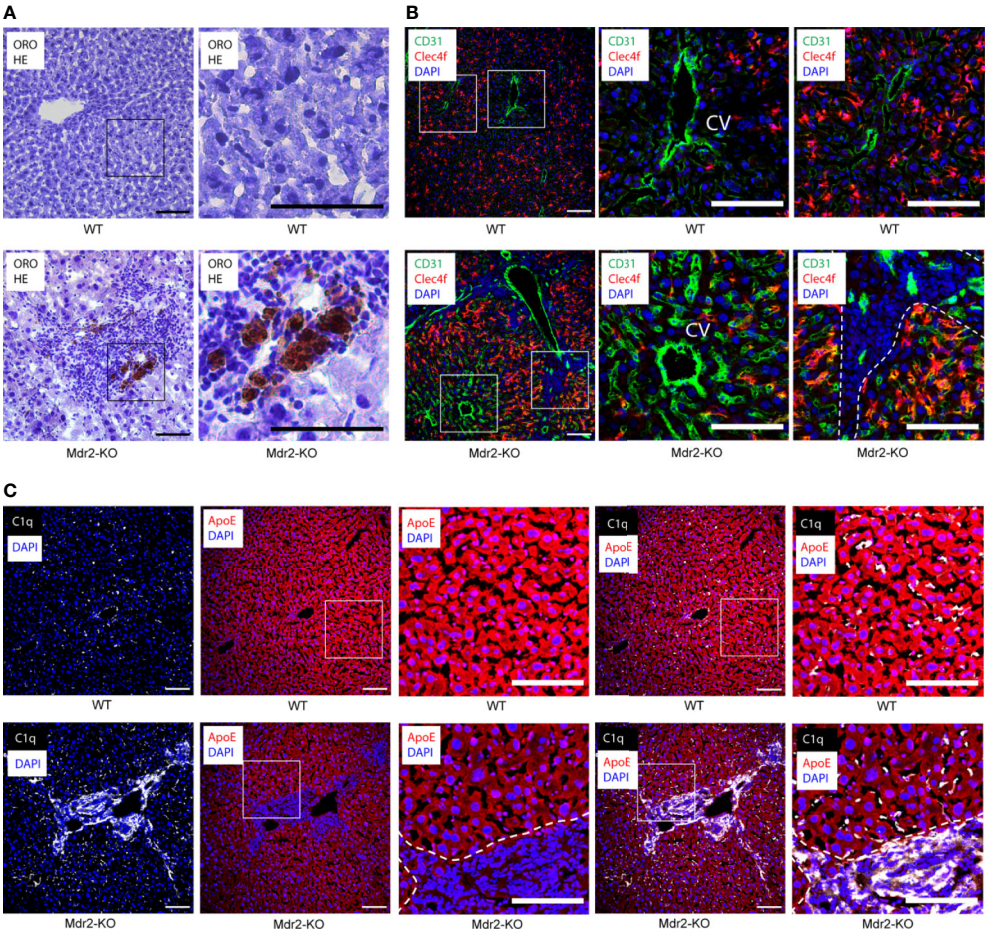

FIGURE 1
Localization of C1q and ApoE proteins in 3 month old WT and Mdr2-KO mouse livers. **(A)** Liver sections were stained with ORO for lipid (red) and HE for nuclei (blue). In Mdr2-KO immune cell infiltrates form primarily in the portal tract areas as well as in the interlobular space. Lipid droplets were observed within the infiltration sites. Black squares represent high magnification images below. **(B)** Sections were stained with CD31 for vascular structures (green), Clec4f for KCs (red) and DAPI for nuclei (blue). CV stands for central vein. Dotted lines demarcate immune cell infiltrates in the portal tract areas from surrounding liver tissue. An increase of CD31 expression in Mdr2-KO livers suggests ongoing angiogenesis. White squares represent high magnification images shown separately. **(C)** Liver sections were stained with ApoE (red), C1q (white) and DAPI for nuclei (blue). White squares represent high magnification images shown separately. Representative images of WT livers (n=6); Mdr2-KO livers (n=6) are shown. Scale bars 100 µm in images of low and high magnification.

triad macrophages (Figure 3B). We next examined complement component C3 expression in WT and Mdr2-KO mice. C3 protein was highly expressed by hepatocytes in WT mice as well as in Mdr2-KO mice (Figure 3C). These data indicate differential expression of C4, C5, and C3 in WT livers and an induction of both C4 and C5 in Mdr2-KO KCs as well as significant expression of C4 and C5 in a subpopulation of portal triad macrophages, while, C3 was widely expressed by hepatocytes in both mice.

C1q-ApoE complex formation in WT and Mdr2-KO livers

To identify the C1q-ApoE complex *in situ*, we used the proximity ligation assay (PLA) as previously described (1). Low levels of C1q-ApoE complexes were observed in WT livers (Figure 4, Supplementary Video 1). However, C1q-ApoE complexes were readily observed in the portal triads that were infiltrated by immune cells of Mdr2-KO livers (Figure 4, Supplementary Video 2).

ScRNAseq analyses of murine healthy and western diet-induced liver steatosis

To examine the expression of complement-related transcripts in KCs and hepatocytes in healthy and diseased mice, we mined single cell transcriptomes as reported by others (GSE156059, https://www.livercellatlas.org/download.

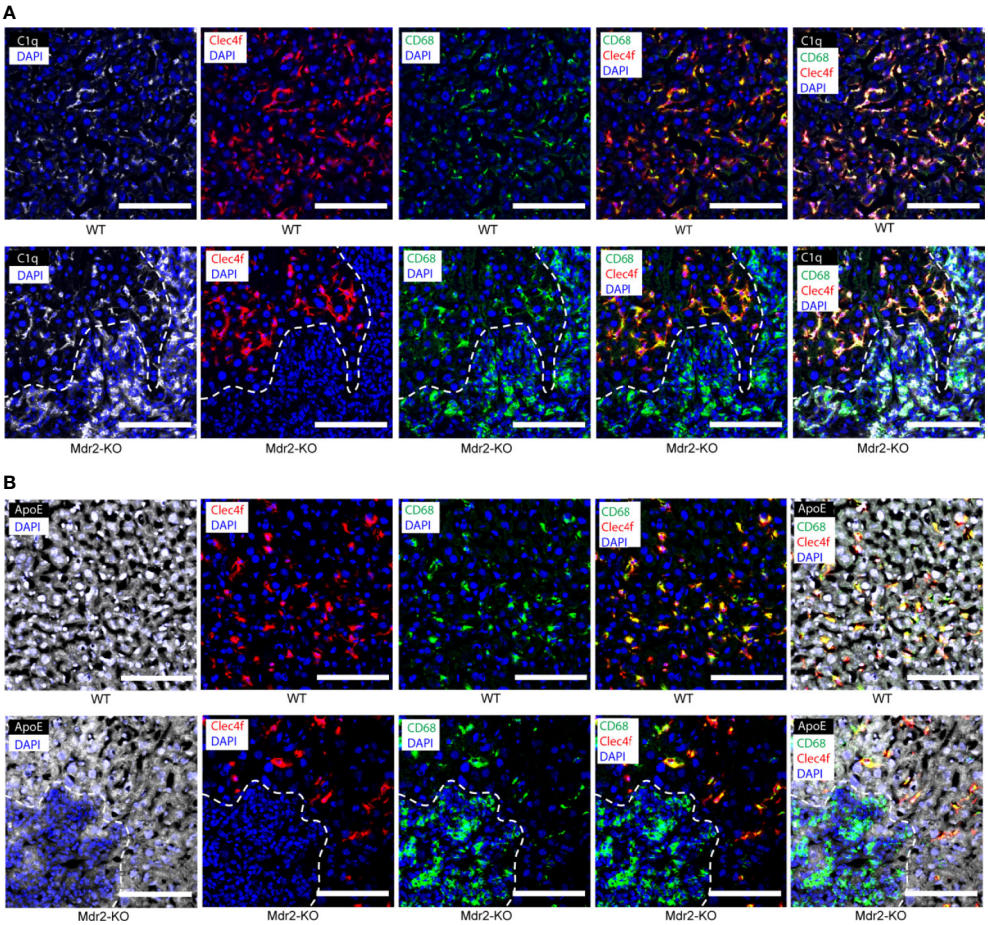

FIGURE 2
C1q- and ApoE-expressing cells in 3 month old WT and Mdr2-KO mouse livers. **(A)** Liver sections were stained with C1q (white), Clec4f (red) for KCs, CD68 (green) for macrophages and DAPI (blue) for nuclei. Dotted lines demarcate immune cell infiltrates in the portal tract areas from surrounding liver tissue. KCs are known to stain $CD68^{+}/Clec4f^{+}$. **(B)** Liver sections were stained with ApoE (white), Clec4f (red) for KCs, CD68 (green) for macrophages and DAPI (blue) for nuclei. Dotted lines demarcate immune cell infiltrates in the portal tract areas from surrounding liver tissue. Representative images of WT livers (n=6); Mdr2-KO livers (n=6) are shown. Scale bars 100 µm.

php) (25, 26). Specifically, C57BL/6 mice fed with a Western diet (WD) high in fat, sucrose and cholesterol for 24 weeks or 36 weeks developed liver pathologies resembling human NAFLD or non-alcoholic steatohepatitis (NASH) (26). Data banks were mined for transcripts of C1qa, C1qb, C1qc, ApoE, C4b, C3, and C5 in KCs of WD-fed mice aged 24 weeks and 36 weeks, as well as their sex- and age-matched healthy control mice. KCs in healthy and diseased mice highly expressed C1qa, C1qb, C1qc, and ApoE transcripts (Figure 5A). KCs in diseased mice expressed higher levels of ApoE when compared to healthy controls (Figure 5B). We next examined expression of C4b, C3, and C5 in KCs. KCs highly expressed C4b transcripts, but few KCs expressed C3 and C5 transcripts (Figure 5B). Hepatocytes in healthy and diseased mice did not express C1q transcripts, but highly expressed ApoE, C4b, C3, and C5 transcripts (Figures 5C, D). We next examined the expression of complement receptor CD55, and anaphylatoxin C5a receptors (C5aR1, C5aR2) in KCs and hepatocytes (Figures 5E, F). A low percentage of KCs and hepatocytes expressed CD55 and C5aR1/2 transcripts. These data indicate that KCs are the major source of C1q in the liver, and that KCs and hepatocytes are the major source of ApoE in both healthy and diseased livers.

C1q-ApoE complex formation in human livers with NAFLD and viral hepatitis B and C

To examine whether C1q-ApoE complexes form in human livers with acute and chronic inflammatory diseases,

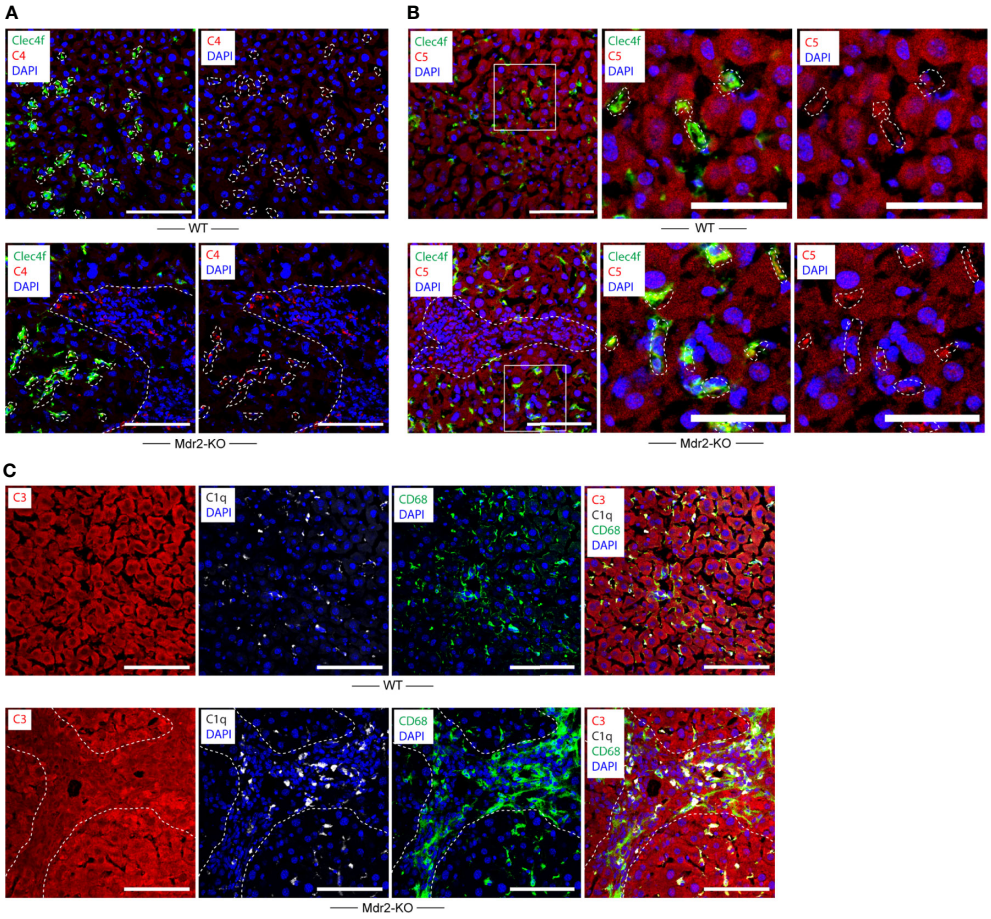

FIGURE 3
Complement component C4 and C5 expression in WT and Mdr2-KO mouse livers. **(A)** Liver sections were stained with Clec4f (green) for KCs, C4 (red), and DAPI for nuclei (blue). Dotted lines demarcate Clecf^{+} cells as well as immune cell infiltrates in portal triads from adjacent liver parenchyma. **(B)** Liver sections were stained with Clec4f (green) for KCs, C5 (red), and DAPI (blue) for nuclei. **(C)** Complement component C3, C1q, CD68 expression in WT and Mdr2-KO livers. Liver sections were stained with C3 (red), C1q (white), and CD68 (green) for macrophages/KCs and DAPI for nuclei (blue). Dotted lines demarcate immune cell infiltration sites from adjacent liver parenchyma. White squares represent high magnification images shown separately. Representative images of WT livers (n=6); Mdr2-KO livers (n=6) are shown. Scale bars 100 µm in images of low and high magnification.

we examined human liver biopsies obtained from patients who were diagnosed with NAFLD or hepatitis C and hepatitis B/C coinfection (Supplementary Table 1). We stained human livers with ORO for lipid droplets. We did not observe significant lipid droplets or immune cell aggregates in areas of healthy human livers (Figure 6A). We noticed intracellular and extracellular lipid droplets of various sizes and apparent immune cells throughout the parenchyma of NAFLD livers as expected (14) (Figure 6A). Of note, marked immune cell infiltrates were observed in portal triads whereas lipid droplets in the liver parenchyma in Hep-B/C livers were apparent to a lesser degree (Figure 6A). We next examined C1q and ApoE proteins in human livers. ApoE stained positive in all cells in the liver parenchyma and C1q was selectively stained in few cells consistent with KCs in healthy livers (Figure 6B). These data indicated that, similar to mouse livers, hepatocytes and KCs stained positive for ApoE, and KCs stained positive for C1q protein in healthy human livers. NAFLD liver parenchyma was interspersed with empty spaces, i.e. lipid droplets. Similar to controls, ApoE positive signals were detected in hepatocytes, and C1q positive signals stained scattered cells, i.e. KCs, in NAFLD livers (Figure 6B). In Hep-B/C livers, ApoE stained hepatocytes, C1q stained scattered cells, i.e. KCs in the parenchyma and in infiltration sites (Figure 6B). We next stained complement C5 protein in human liver tissues. Complement C5 protein stained positive in healthy-, NAFLD-, and Hep-B/C-liver tissues (Figure 6C). These data indicated that complement activation may represent a shared pathology for both NAFLD and viral hepatitis livers.

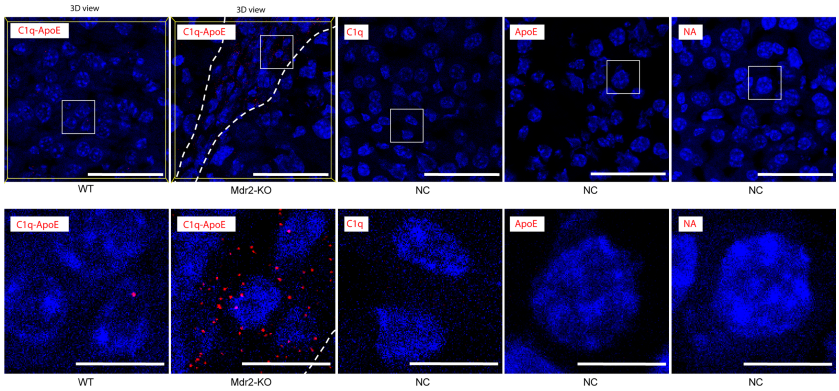

FIGURE 4
C1q-ApoE complex formation in WT and Mdr2-KO mouse livers. WT mouse liver sections were stained with C1q and ApoE by PLA. Anti-ApoE alone, Anti-C1q alone or no primary antibodies were used as negative controls. Dotted lines demarcate immune cell infiltrations from adjacent liver parenchyma. White square areas represent high magnification images below. 3Dview images are available as mp4 videos in supplements. Representative images of WT livers (n=6); Mdr2-KO livers (n=6) are shown. Scale bar 50 µm in low magnification images and 10 µm in images of high magnification.

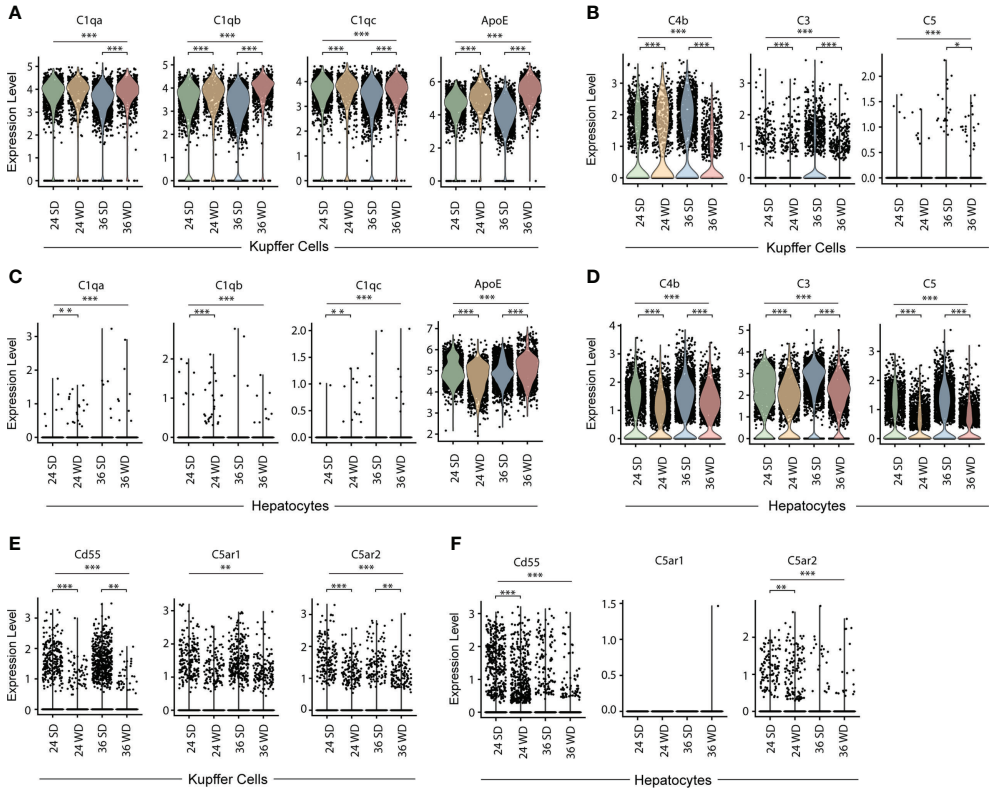

FIGURE 5
Transcript expression of C1q, ApoE and complement components in KCs and hepatocytes in healthy and diseased mouse livers. **(A, B)** Violin plots show C1qa, C1qb, C1qc, ApoE **(A)** and C4b, C3, and C5 **(B)** transcripts in KCs in standard diet-fed or WD-fed mice for 24 and 36 weeks. **(C, D)** Violin plots show C1qa, C1qb, C1qc, ApoE **(C)** and C4b, C3, and C5 **(D)** transcripts in hepatocytes in healthy and diseased mice. **(E, F)** Violin plots show CD55, C5AR1 and C5AR2 transcripts in KCs **(E)** and hepatocytes **(F)** in healthy and diseased mice. Each point represents one cell. Kruskal–Walli's test with Dunn's non-parametric all-pairs comparison test was adjusted by Benjamini Hochberg correction. *P < 0.05; **P < 0.01; ***P < 0.001.

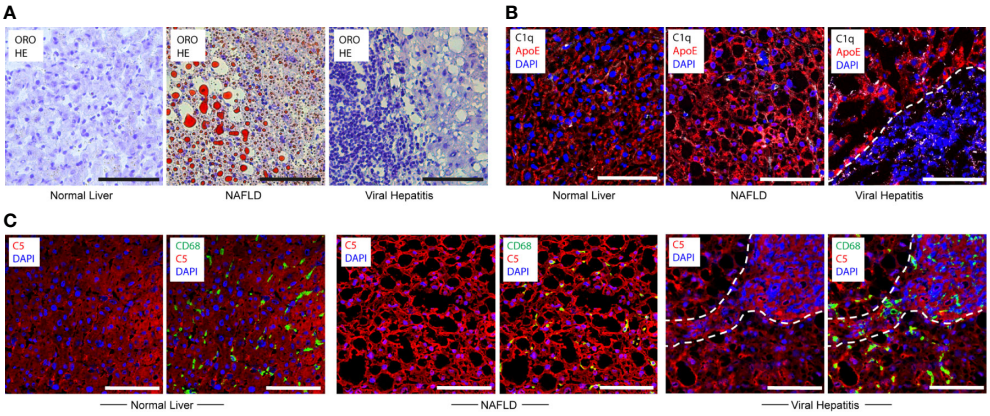

FIGURE 6
Translational studies in healthy and diseased human livers. **(A)** Normal liver sample Nr. 5 (Supplementary Table 1), NAFLD sample Nr. 9 (Supplementary Table 1) and viral hepatitis sample Nr. 7 (Supplementary Table 1) tissues were stained with ORO for lipid (red) and HE for nuclei (blue). **(B)** Human livers - as described in Figure 6A - were stained with ApoE (red), C1q (white), and DAPI (blue) showing similar staining patterns vs mouse livers. Dotted lines demarcate immune cell infiltration sites from adjacent liver parenchyma. **(C)** Human livers – as described in Figure 6A - were stained with C5 (red), CD68 (green) and DAPI (blue) indicating nuclei. Representative images of human samples (Supplementary Table 1) are shown. Dotted lines demarcate immune cell infiltration sites from adjacent liver parenchyma. Scale bars 100 µm.

We next searched for C1q-ApoE complexes *in situ* in human livers using the PLA. No or low levels of C1q-ApoE complexes were observed in control tissues (Figures 7A, B). C1q-ApoE complexes were abundantly detected in liver parenchyma obtained from NAFLD patients and in liver parenchyma and in portal infiltration sites of viral hepatitis (Figures 7A, B). These data indicated that the C1q-ApoE complex is a new pathological hallmark of NAFLD and viral Hep-B/C-infected livers. The human samples were used as proof-of-principle type experiments to confirm our findings in mice by showing the existence of the C1q-ApoE complex formation within different clinically important human liver diseases. Further studies to be performed in a larger cohort of human livers need to be conducted in future studies including cohorts of sex- and aged matched controls.

To examine complement-related transcript expression in human livers, we searched for C1q, ApoE, C2, C3 and C5 gene expression in published databanks (25). Patients with less than 10% liver steatosis are regarded as healthy controls; patients with more than 10% steatosis were considered diseased (25). KCs in healthy and steatosis patients highly expressed C1qa, C1qb, C1qc, and ApoE transcripts (Figure 8A). In healthy human livers there is evidence that specifically C1qc (but not C1qa or C1qb) is differentially expressed in two types of KCs, that i.e. one population with low and another population with high transcript expression per cell (Figure 8A). KCs expressed C2 transcripts, but few KCs expressed C3 and C5 transcripts (Figure 8B). The expression of C1qa, C1qb, C1qc, and C2 in KCs was significantly higher in patients with severe steatosis when compared to healthy controls (Figures 8A, B). Similar to murine hepatocytes, human hepatocytes did not express C1q transcripts (Figure 8C) but highly expressed ApoE, C3, and C5 transcripts (Figures 8C, D). Similar to mice, these data indicate that KCs are the major source of C1q while KCs and hepatocytes are the major source of ApoE in human livers. We also examined the expression of complement receptor transcript expression in KCs and hepatocytes, including CD55, C5aR1, and C5aR2 (Figures 8E, F). The expression of CD55 by KCs is almost undetectable in patients with severe steatosis when compared to healthy controls (Figure 8E). The expression of C5aR1 is higher is KCs when compared to hepatocytes, and the expression of C5aR2 is only detectable in few KCs and hepatocytes in both healthy and diseased livers (Figure 8F). These data demonstrate in a large number of human versus a large number of mouse single cell transcript analyses of hepatocytes and KCs the striking similarities between mouse and human livers. Moreover, they show that the expression of CCC components as proteins as revealed by IF analyses are analogous. As the mouse versus human transcript versus CCC protein data are comparable, we have also reason to believe that data on a limited number of IF analyses of human livers are tangible.

Discussion

Data reported above support the following conclusions: in healthy murine and human livers the number of C1q-ApoE complexes is low or absent; C1q-ApoE complexes form around portal triads in which activated myeloid cell aggregates emerge and to a lesser degree in the liver parenchyma; C1q-ApoE complexes are abundant in both portal triads and the liver parenchyma in NAFLD livers; numerous C1q-ApoE complexes

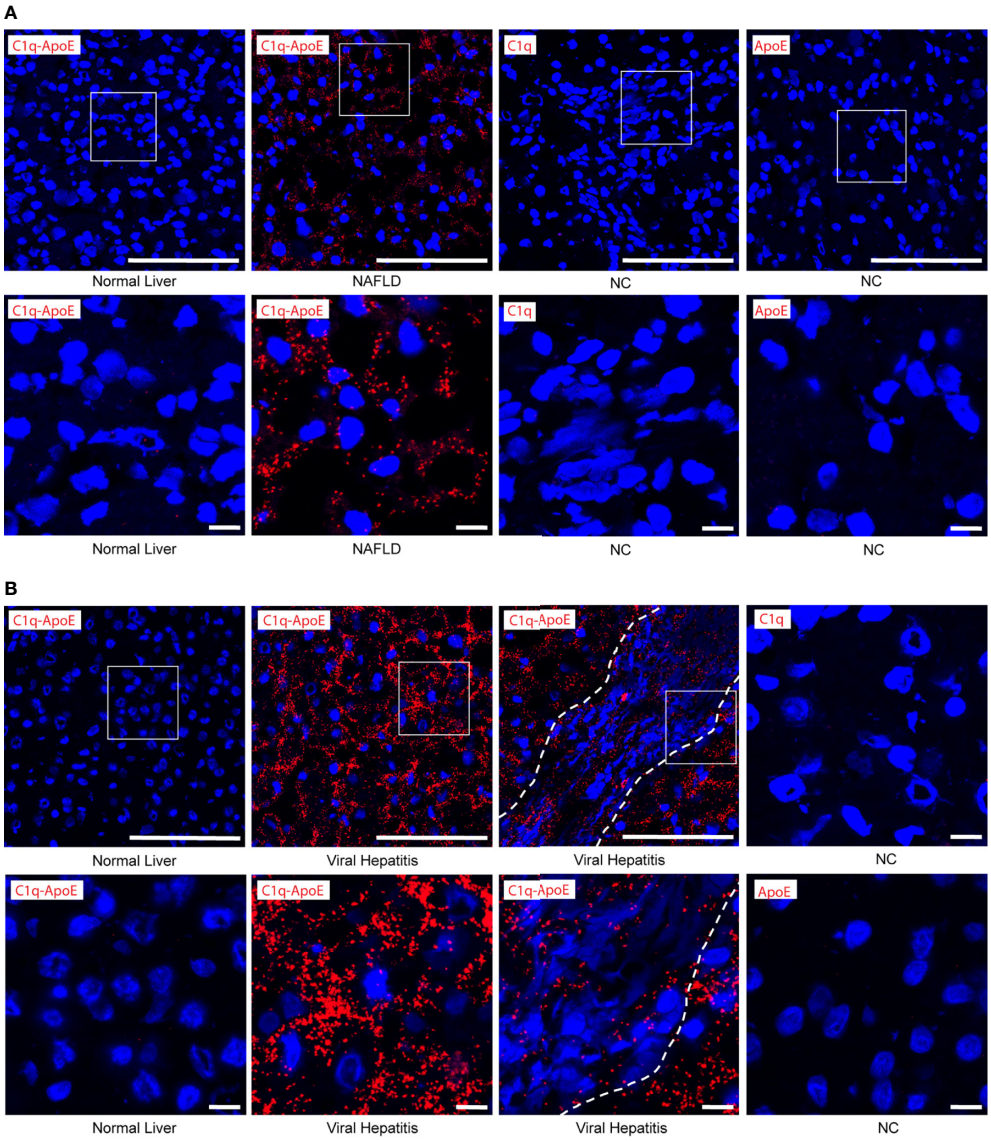

FIGURE 7
C1q-ApoE complex formation in human livers. **(A, B)** Human liver sections were stained with C1q and ApoE by PLA. Anti-C1q alone or Anti-ApoE alone were used as negative controls. Dotted lines demarcate immune cell infiltrates from adjacent liver parenchyma. White squares represent high magnification images shown separately. Scale bar 100 µm in low magnification images and 10 µm in images of high magnification. Representative images of human samples (Supplementary Table 1) are shown. **(A)** Normal liver sample Nr. 2 (Supplementary Table 1); NAFLD sample Nr. 9 (Supplementary Table 1). **(B)** Normal liver sample Nr. 3 (Supplementary Table 1); viral hepatitis sample Nr. 7 (Supplementary Table 1).

arise in HepC and HepB/C-infected livers with prominent expression in both portal triads and the liver parenchyma. We conclude that the formation of the C1q-ApoE complex represents a new common pathological hallmark of major forms of human hepatitis including NAFLD (Figure 9).

The following sequence of reactions are worth considering: the unique blood flow of the liver combines blood originating from the portal vein and the portal artery with the distinct structure of the liver sinusoids with their KC linings. This results in production and secretion of inactive C1q and ApoE in sinusoidal blood flowing towards the central vein without detectable formation of C1q-ApoE complexes. By contrast, portal inflammation in Mdr2-KO mice, human NAFLD livers and viral hepatitis results in marked formation of the C1q-ApoE complex in portal triads with inflammatory cells. Striking numbers of C1q-ApoE complexes form in both portal triads

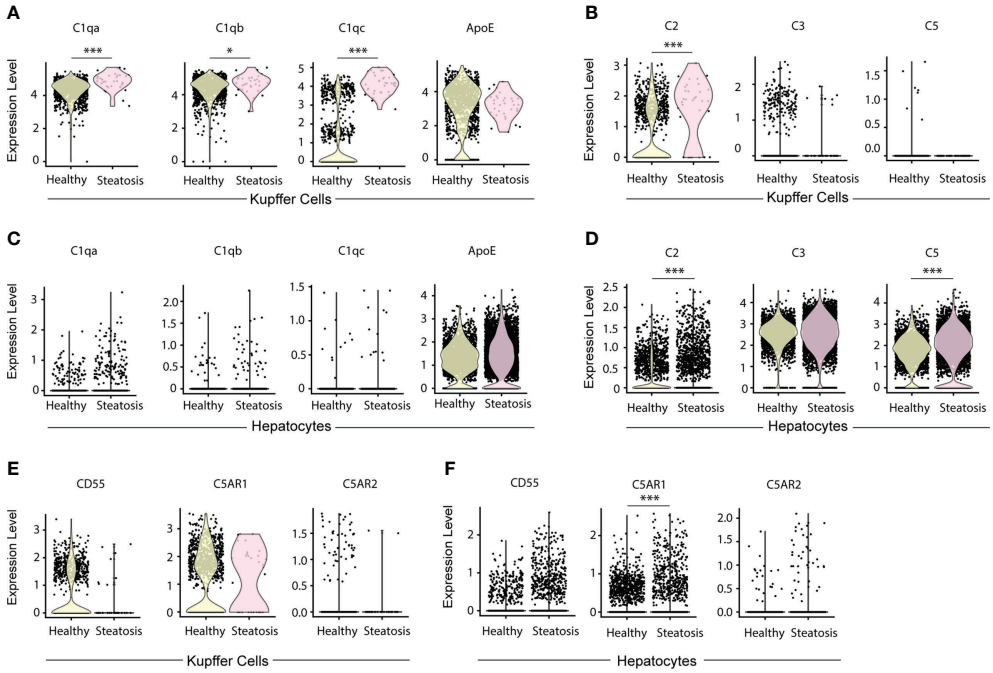

FIGURE 8
Expression of C1q, ApoE, and complement components in KCs and hepatocytes in human livers. **(A, B)** Violin plots show C1qa, C1qb, C1qc, and ApoE transcripts **(A)** and C2, C3, and C5 transcripts in KCs **(B)** in human livers. **(C, D)** Violin plots show C1qa, C1qb, C1qc, and ApoE transcripts **(C)** and C2, C3, and C5 transcripts in hepatocytes **(D)** in healthy and diseased livers. **(E, F)** Violin plots show CD55, C5AR1 and C5AR2 transcripts in KCs **(E)** and hepatocytes **(F)** in healthy and diseased human livers. Each point represents one cell. Data were analyzed by Wilcoxon rank sum test. P values were adjusted by Benjamini Hochberg correction. *P < 0.05, ***P < 0.001.

and the parenchyma of NAFLD and HepB/C-infected livers. These data are consistent with the possibility that there are multiple activators of C1q in the diseased human livers including activators produced in the inflammatory environment of portal triads and extracellular lipid droplets throughout the liver parenchyma. To identify the precise nature of C1q-activating agents in human liver diseases - in particular in NAFLD - requires further work. The purpose of such future studies should correlate the C1q-ApoE complexes with virus particles, immune complexes, lipid droplets, and oxidized lipids as C1q activators may turn out to be new pharmacological targets of CCC activity. These studies may lead to a better understanding of the culprits of C1q activation for potential therapeutic targeting these activators before the CCC is activated with the ultimate goal to prevent liver inflammation as it relates to the CCC. Such strategies may be beneficial particular for patients afflicted with NAFLD and turn out to be effective in the prevention of HCC.

Our observation of the C1q-ApoE complex in acute and chronic hepatitis opens the way for another therapeutic strategy involving ApoE itself. ApoE is a multidomain polymorphic protein with multiple binding sites. The identification of ApoE amino acid sequence that binds to C1q will be important to develop small ApoE peptides that are capable of binding to C1q and concomitantly attenuate its activity to limit detrimental CCC overactivation and HCC.

Several caveats of our study should be considered: The number of clinical samples in this study is rather limited. A clinical study should be performed in which the onset of liver inflammation in NAFLD should be more stringently defined to determine the time course of C1q-ApoE complex formation during subacute NAFLD hepatitis and the various stages of NAFLD including HCC. Furthermore, the C1q-ApoE complex is particularly pronounced in the portal triad where C1q and ApoE seem to be up-regulated in myeloid cells. Indeed, the portal triad-related inflammation may be rich in elusive C1q activators. We further suggest that preclinical studies of fatty liver diseases may yield information whether the course of fatty liver disease is attenuated by pharmaceuticals targeting not only the various components of the three complement pathways but also the C1q-ApoE complex itself and whether liver fibrosis, its development into liver cirrhosis and HCC may be halted by such

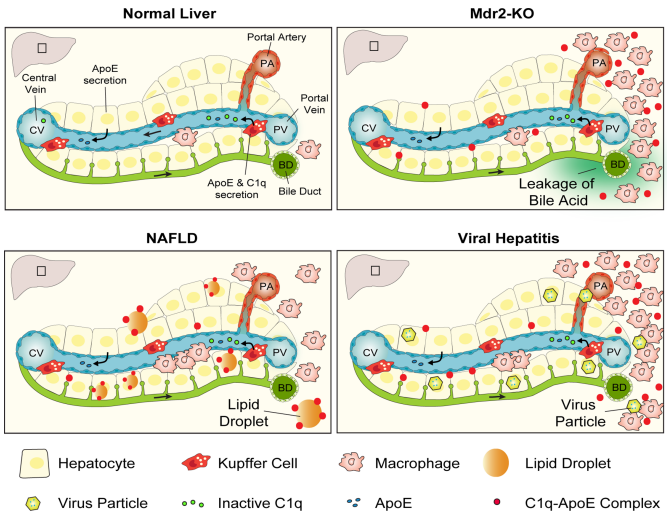

FIGURE 9
Graphical representation of the C1q-ApoE complex as a new hallmark pathology of diseased liver tissue. In normal liver tissue C1q is secreted into the circulation as an inactive preprotein by KCs as well as monocyte-derived macrophages. ApoE is secreted into the circulation by KCs and hepatocytes. Due to the leakage of bile acid in the portal tract areas of Mdr2-KO mice immune cell infiltrates develop and C1q gets activated and formation of the C1q-ApoE complex is initiated. In NAFLD, C1q is likely to be activated by lipid and in viral hepatitis by virus particles or secondary activators leading to the formation of the C1q-ApoE complex. Schematic Figure modified from (29) with the permission of the authors.

treatment regimens. ApoE-related replacement therapeutics including ApoE-derived peptides have been developed to treat Alzheimer's Disease (1, 30, 31). Such approaches may be considered to treat late stages of NAFLD in progressive liver cirrhosis which are associated with major dysfunction of ApoE homeostasis in both the liver and the circulation. Such strategies would be expected to be anti-inflammatory by replacing the bona fide checkpoint inhibitor of activated C1q.

Data availability statement

Publicly available datasets were analyzed in this study. This data can be found in the GEO repository under accession numbers GSE156059 and GSE192742. All data can be found here: https://www.livercellatlas.org/download.php.

Ethics statement

The animal study was reviewed and approved by the state of Bavaria, all animal procedures were conducted according to guidelines of the local Animal Use and Care Committees and the National Animal Welfare Laws. The use of human tissue was reviewed and approved by the ethics committee of the Ludwig-Maximilians-University, approval number [21-0095]. Written informed consent for participation was not required for this study in accordance with the national legislation and the institutional requirements.

Author contributions

LH, ZM and CY designed the experiments, performed experiments, and wrote the manuscript. All authors contributed to the article and approved the submitted version.

Funding

This study was supported by the Deutsche Forschungsgemeinschaft (DFG) grant YI 133/3-5, and an excellence grant (LMUexcellent 867949-0) of the Ludwig-Maximilians-University Munich to CY.

Acknowledgments

We thank Shalev Itzkovitz, Department of Cell Biology, Weizmann Institute of Science, Rehovot, Israel, for his permission to use the graphical design of Figure 1 published in Nat Rev Gastroenterol Hepatol. 2019 Jul; 16(7):395-410.

Conflict of interest

The authors declare that the research was conducted in the absence of any commercial or financial relationships that could be construed as a potential conflict of interest.

Publisher's note

All claims expressed in this article are solely those of the authors and do not necessarily represent those of their affiliated organizations, or those of the publisher, the editors and the reviewers. Any product that may be evaluated in this article, or claim that may be made by its manufacturer, is not guaranteed or endorsed by the publisher.

Supplementary material

The Supplementary Material for this article can be found online at: https://www.frontiersin.org/articles/10.3389/fimmu.2022.970938/full#supplementary-material

References

1. Yin C, Ackermann S, Ma Z, Mohanta SK, Zhang C, Li Y, et al. ApoE attenuates unresolvable inflammation by complex formation with activated C1q. *Nat Med* (2019) 25(3):496–506. doi: 10.1038/s41591-018-0336-8

2. Vogt LM, Kwasniewicz E, Talens S, Scavenius C, Bielecka E, Ekdahl KN, et al. Apolipoprotein e triggers complement activation in joint synovial fluid of rheumatoid arthritis patients by binding C1q. *J Immunol* (2020) 204(10):2779–90. doi: 10.4049/jimmunol.1900372

3. Kolev M, Friec GL, Kemper C. Complement - tapping into new sites and effector systems. *Nat Rev Immunol* (2014) 14(12):811–20. doi: 10.1038/nri3761

4. Ringelhan M, Pfister D, O'Connor T, Pikarsky E, Heikenwalder M. The immunology of hepatocellular carcinoma. *Nat Immunol* (2018) 19(3):222–32. doi: 10.1038/s41590-018-0044-z

5. Hajishengallis G, Reis ES, Mastellos DC, Ricklin D, Lambris JD. Novel mechanisms and functions of complement. *Nat Immunol* (2017) 18(12):1288–98. doi: 10.1038/ni.3858

6. Holers VM. Complement and its receptors: New insights into human disease. *Annu Rev Immunol* (2014) 32(1):433–59. doi: 10.1146/annurev-immunol-032713-120154

7. Wightman DP, Jansen IE, Savage JE, Shadrin AA, Bahrami S, Holland D, et al. A genome-wide association study with 1,126,563 individuals identifies new risk loci for alzheimer's disease. *Nat Genet* (2021) 53(9):1276–82. doi: 10.1038/s41588-021-00921-z

8. Trouw LA, Daha N, Kurreeman FA, Böhringer S, Goulielmos GN, Westra HJ, et al. Genetic variants in the region of the C1q genes are associated with rheumatoid arthritis. *Clin Exp Immunol* (2013) 173(1):76–83. doi: 10.1111/cei.12097

9. Cheung O, Sanyal AJ. Hepatitis c infection and nonalcoholic fatty liver disease. *Clinics liver Dis* (2008) 12(3):573–85. doi: 10.1016/j.cld.2008.03.005

10. Eslam M, Sanyal AJ, George J. MAFLD: A consensus-driven proposed nomenclature for metabolic associated fatty liver disease. *Gastroenterology* (2020) 158(7):1999–2014.e1. doi: 10.1053/j.gastro.2019.11.312

11. Katzenellenbogen M, Pappo O, Barash H, Klopstock N, Mizrahi L, Olam D, et al. Multiple adaptive mechanisms to chronic liver disease revealed at early stages of liver carcinogenesis in the Mdr2-knockout mice. *Cancer Res* (2006) 66(8):4001–10. doi: 10.1158/0008-5472.CAN-05-2937

12. Libby P. The changing landscape of atherosclerosis. *Nature* (2021) 592 (7855):524–33. doi: 10.1038/s41586-021-03392-8

13. Bettcher BM, Tansey MG, Dorothée G, Heneka MT. Peripheral and central immune system crosstalk in Alzheimer disease - a research prospectus. *Nat Rev Neurol* (2021) 17(11):689–701. doi: 10.1038/s41582-021-00549-x

14. Torbenson M, Washington K. Pathology of liver disease: advances in the last 50 years. *Hum Pathol* (2020) 95:78–98. doi: 10.1016/j.humpath.2019.08.023

15. Anstee QM, Reeves HL, Kotsiliti E, Govaere O, Heikenwalder M. From NASH to HCC: current concepts and future challenges. *Nat Rev Gastroenterol Hepatol* (2019) 16(7):411–28. doi: 10.1038/s41575-019-0145-7

16. Manns MP, Maasoumy B. Breakthroughs in hepatitis c research: From discovery to cure. *Nat Rev Gastroenterol Hepatol* (2022) 19(8):533–50. doi: 10.1038/s41575-022-00608-8

17. Cox AL, El-Sayed MH, Kao J-H, Lazarus JV, Lemoine M, Lok AS, et al. Progress towards elimination goals for viral hepatitis. *Nat Rev Gastroenterol Hepatol* (2020) 17(9):533–42. doi: 10.1038/s41575-020-0332-6

18. Mauad TH, van Nieuwkerk CM, Dingemans KP, Smit JJ, Schinkel AH, Notenboom RG, et al. Mice with homozygous disruption of the mdr2 p-glycoprotein gene. a novel animal model for studies of nonsuppurative inflammatory cholangitis and hepatocarcinogenesis. *Am J Pathol* (1994) 145 (5):1237–45.

19. Fickert P, Fuchsbichler A, Wagner M, Zollner G, Kaser A, Tilg H, et al. Regurgitation of bile acids from leaky bile ducts causes sclerosing cholangitis in Mdr2 (Abcb4) knockout mice. *Gastroenterology* (2004) 127(1):261–74. doi: 10.1053/j.gastro.2004.04.009

20. Katzenellenbogen M, Mizrahi L, Pappo O, Klopstock N, Olam D, Jacob-Hirsch J, et al. Molecular mechanisms of liver carcinogenesis in the mdr2-knockout mice. *Mol Cancer Res MCR* (2007) 5(11):1159–70. doi: 10.1158/1541-7786.MCR-07-0172

21. van de Bovenkamp FS, Dijkstra DJ, van Kooten C, Gelderman KA, Trouw LA. Circulating C1q levels in health and disease, more than just a biomarker. *Mol Immunol* (2021) 140:206–16. doi: 10.1016/j.molimm.2021.10.010

22. Mahley RW, Huang Y. Apolipoprotein e sets the stage: Response to injury triggers neuropathology. *Neuron* (2012) 76(5):871–85. doi: 10.1016/j.neuron.2012.11.020

23. Deczkowska A, Keren-Shaul H, Weiner A, Colonna M, Schwartz M, Amit I. Disease-associated microglia: A universal immune sensor of neurodegeneration. *Cell* (2018) 173(5):1073–81. doi: 10.1016/j.cell.2018.05.003

24. Liu C-C, Kanekiyo T, Xu H, Bu G. Apolipoprotein e and Alzheimer disease: risk, mechanisms and therapy. *Nat Rev Neurol* (2013) 9(2):106–18. doi: 10.1038/nrneurol.2012.263

25. Guilliams M, Bonnardel J, Haest B, Vanderborght B, Wagner C, Remmerie A, et al. Spatial proteogenomics reveals distinct and evolutionarily conserved hepatic macrophage niches. *Cell* (2022) 185(2):379–96.e38. doi: 10.1016/j.cell.2021.12.018

26. Remmerie A, Martens L, Thoné T, Castoldi A, Seurinck R, Pavie B, et al. Osteopontin expression identifies a subset of recruited macrophages distinct from kupffer cells in the fatty liver. *Immunity* (2020) 53(3):641–57.e14. doi: 10.1016/j.immuni.2020.08.004

27. Krenkel O, Tacke F. Liver macrophages in tissue homeostasis and disease. *Nat Rev Immunol* (2017) 17(5):306–21. doi: 10.1038/nri.2017.11

28. Zhou T, Kyritsi K, Wu N, Francis H, Yang Z, Chen L, et al. Knockdown of vimentin reduces mesenchymal phenotype of cholangiocytes in the Mdr2(-/-) mouse model of primary sclerosing cholangitis (PSC). *EBioMedicine* (2019) 48:130–42. doi: 10.1016/j.ebiom.2019.09.013

29. Ben-Moshe S, Itzkovitz S. Spatial heterogeneity in the mammalian liver. *Nat Rev Gastroenterol Hepatol* (2019) 16(7):395–410. doi: 10.1038/s41575-019-0134-x

30. Yamazaki Y, Zhao N, Caulfield TR, Liu CC, Bu G. Apolipoprotein e and Alzheimer disease: pathobiology and targeting strategies. *Nat Rev Neurol* (2019) 15 (9):501–18. doi: 10.1038/s41582-019-0228-7

31. Wang C, Najm R, Xu Q, Jeong DE, Walker D, Balestra ME, et al. Gain of toxic apolipoprotein E4 effects in human iPSC-derived neurons is ameliorated by a small-molecule structure corrector. *Nat Med* (2018) 24(5):647–57. doi: 10.1038/s41591-018-0004-z

frontiers | Frontiers in Immunology

TYPE Original Research
PUBLISHED 18 October 2022
DOI 10.3389/fimmu.2022.1032331

Check for updates

OPEN ACCESS

EDITED BY
Per Nilsson,
Linnaeus University, Sweden

REVIEWED BY
Abhishek Shastri,
Central and North West London NHS Foundation Trust, United Kingdom
Michael Osthoff,
University Hospital of Basel, Switzerland

*CORRESPONDENCE
Richard D. Unwin
r.unwin@manchester.ac.uk

†These authors have contributed equally to this work

SPECIALTY SECTION
This article was submitted to Molecular Innate Immunity, a section of the journal Frontiers in Immunology

RECEIVED 30 August 2022
ACCEPTED 26 September 2022
PUBLISHED 18 October 2022

CITATION
Tierney AL, Alali WM, Scott T, Rees-Unwin KS, CITIID-NIHR BioResource COVID-19 Collaboration, Clark SJ and Unwin RD (2022) Levels of soluble complement regulators predict severity of COVID-19 symptoms.
Front. Immunol. 13:1032331.
doi: 10.3389/fimmu.2022.1032331

COPYRIGHT
© 2022 Tierney, Alali, Scott, Rees-Unwin, CITIID-NIHR BioResource COVID-19 Collaboration, Clark and Unwin. This is an open-access article distributed under the terms of the Creative Commons Attribution License (CC BY). The use, distribution or reproduction in other forums is permitted, provided the original author(s) and the copyright owner(s) are credited and that the original publication in this journal is cited, in accordance with accepted academic practice. No use, distribution or reproduction is permitted which does not comply with these terms.

Levels of soluble complement regulators predict severity of COVID-19 symptoms

Anna L. Tierney[1,2], Wajd Mohammed Alali[2†], Thomas Scott[2†], Karen S. Rees-Unwin[2], CITIID-NIHR BioResource COVID-19 Collaboration[3], Simon J. Clark[4,5,6] and Richard D. Unwin[2*]

[1]Division of Cardiovascular Sciences, School of Medicine, Faculty of Biology Medicine and Health, The University of Manchester, Manchester, United Kingdom, [2]Stoller Biomarker Discovery Centre and Division of Cancer Sciences, School of Medicine, Faculty of Biology Medicine and Health, The University of Manchester, Manchester, United Kingdom, [3]NIHR BioResource, Cambridge University Hospitals NHS Foundation Trust, Cambridge Biomedical Campus, Cambridge, United Kingdom, [4]Institute for Opthalmic Research is based at Eberhard Karls University of Tubingen, Tubingen, BW, Germany, [5]University Eye Clinic, Eberhard Karls University of Tubingen, Tubingen, BW, Germany, [6]Lydia Becker Institute of Immunology and Inflammation, Faculty of Biology, Medicine, and Health, University of Manchester, Manchester, United Kingdom

The SARS-CoV-2 virus continues to cause significant morbidity and mortality worldwide from COVID-19. One of the major challenges of patient management is the broad range of symptoms observed. While the majority of individuals experience relatively mild disease, a significant minority of patients require hospitalisation, with COVID-19 still proving fatal for some. As such, there remains a desperate need to better understand what drives this severe disease, both in terms of the underlying biology, but also to potentially predict at diagnosis which patients are likely to require further interventions, thus enabling better outcomes for both patients and healthcare systems. Several lines of evidence have pointed to dysregulation of the complement cascade as a major factor in severe COVID-19 outcomes. How this is underpinned mechanistically is not known. Here, we have focussed on the role of the soluble complement regulators Complement Factor H (FH), its splice variant Factor H-like 1 (FHL-1) and five Factor H-Related proteins (FHR1-5). Using a targeted mass spectrometry approach, we quantified these proteins in a cohort of 188 plasma samples from controls and SARS-CoV-2 patients taken at diagnosis. This analysis revealed significant elevations in all FHR proteins, but not FH, in patients with more severe disease, particularly FHR2 and FHR5 (FHR2: 1.97-fold, $p<0.0001$; FHR5: 2.4-fold, $p<0.0001$). Furthermore, for a subset of 77 SARS-CoV-2 +ve patients we also analysed time course samples taken approximately 28 days post-diagnosis. Here, we see complement regulator levels drop in all individuals with asymptomatic or mild disease, but regulators remain high in those with more severe outcomes, with elevations in FHR2 over baseline levels in this group. These data support the hypothesis that elevation of circulating levels of the FHR family of proteins could predict disease severity in COVID-19 patients, and that the duration of elevation (or lack of immune activation resolution) may be partly responsible for driving poor outcomes in COVID-19.

KEYWORDS

COVID-19, SARS-CoV-2, complement, factor H, factor H-related proteins, biomarkers, mass spectrometry

Introduction

The outbreak of the severe acute respiratory syndrome coronavirus 2 (SARS-CoV-2), which causes coronavirus disease 2019 (COVID-19), has caused an unprecedented global health emergency. As of August 2022, there have been more than 590 million cases of COVID-19 worldwide and more than 6.4 million deaths have been confirmed (https://covid19.who.int/). The clinical manifestation of COVID-19 infection presents with variable severity, ranging from asymptomatic infection, severe viral pneumonia, and even death.

SARS-CoV-2 is transmitted *via* respiratory droplets into the respiratory tract, where it infects host cells through the binding of angiotensin-converting enzyme 2 (ACE-2). ACE-2 is highly expressed on alveolar epithelial cells in the lungs, and other organs in the cardiovascular and renal systems. It is believed that direct damage to the former from the cytopathic replication of SARS-CoV-2 is a prime driver of COVID-19 pathology (1). Most individuals (~80%) experience mild symptoms that commonly include a fever, cough, fatigue, dyspnoea, myalgia, intestinal symptoms, and anosmia, which resolve after a short period (1). In a minority of patients (~15%), dyspnoea deteriorates, requiring hospital treatment. Within approximately six days this can intensify into viral pneumonia and acute respiratory distress syndrome (ARDS). Intensive efforts by the medical and scientific research community have resulted in the identification of life-saving treatments like dexamethasone and the rapid generation of several highly effective COVID-19 vaccines (2, 3). However, patients continue to be hospitalised with severe COVID-19 – especially in populations with low vaccine penetrance (4). As such, there remains a pressing need to identify prognostic biomarkers for COVID-19, to inform treatment decisions and allow more effective use of overstretched clinical resources.

A promising method for the discovery of disease prognostic biomarkers is liquid chromatography-mass spectrometry (LC-MS). This enables the relative levels of hundreds of plasma or serum proteins to be compared within clinically-derived samples, and provides candidate biomarkers whose levels differ between experimental groups. These differences may subsequently have predictive power in respect of diagnosis, disease stratification and prognosis. To date, a number of proteomics screening studies have been performed in various COVID-19 cohorts (5–13). While these differ in respect of cohort, study aim and method, a common finding between these is dysregulation of proteins in the complement cascade, albeit represented by different individual proteins in different studies.

This finding fits with other data where complement activation is known to contribute to ARDS in other viral diseases (14). In COVID-19, gene variants in the complement pathway, specifically *CD59*, *CFH* and *C4BPa* are associated with poorer outcomes (15) and targeted studies have demonstrated elevations of C5a and C5b-9 in plasma from individuals with moderate and severe disease (16). Together, these observations have led to suggestions that the complement cascade is a strong candidate target for therapies which may protect against severe outcomes (17).

The complement cascade can be activated *via* three pathways, the lectin, classical or alternative pathways, and it is likely that SARS-CoV-2 can activate several of these. The viral spike protein can activate complement *via* MASP1 binding (18), while several studies have shown increased classical pathway receptors e.g. C1q in severe disease (19, 20). However, all of these pathways converge onto a central amplification loop, where C3 is activated *via* cleavage to C3a and C3b. C3a acts as a powerful anaphylatoxin, while C3b is both an opsonin and forms complexes which subsequently result in the cleavage of C5 to produce C5a (a second anaphylatoxin) and C5b, initiating the formation of the C5b-9 membrane attack complex. The activation loop is regulated by inactivation of C3b by Factor I (FI) and one of its necessary co-factors (such as Factor H (FH)). The effects of COVID-19 on different aspects of this pathway are reviewed in (17).

In recent years, a series of five additional FH-related regulators have been identified (FHR1-5) and, along with a shorter splice isoform of FH called Factor H-Like 1 (FHL-1), have been shown to further modulate complement cascade activity. While FHL-1 retains the same function as its larger FH counterpart, the FHR proteins are FH/FHL-1 antagonists and drive complement activation instead of inhibition (21). Altered levels of these proteins play a key role in several complement-related diseases, including renal diseases such as atypical haemolytic uremic syndrome (aHUS), C3 glomerulopathy (C3G) (22, 23) and Age-Related Macular Degeneration (AMD) (24). FHRs 2 and 5 have also been identified as potentially differentially expressed in association with severe COVID-19 in global proteomics studies (12, 25).

Here, we hypothesised that complement dysregulation associated with COVID-19 could be a result of altered regulation of the amplification loop by FHR levels. Because FHRs are closely related in terms of sequence – indeed FHL-1 is identical to the first third of FH with the exception of a unique 4 amino acid C-terminal tail – they have not been measured together previously in COVID-19 cohorts. In this study, we measured the levels of all seven fluid-phase cofactors (FH, FHL-1 and FHR1-5) using a bespoke targeted mass spectrometry approach which can confidently and specifically identify and quantify these proteins in COVID-19 cohorts, both in baseline samples and a subset of longitudinal samples.

Materials and methods

Plasma samples and patient details

Ethical approval for this study was granted by the Cambridge Central Research Ethics Committee (17/EE/0025). All plasma samples were procured from the National Institute for Health and Care Research (NIHR) Bioresource. Participants attended

10.3389/fimmu.2022.1032331

multiple hospitals across the South-East of England with COVID-19 symptoms during the first wave of the pandemic in 2020 and recruited prospectively for inclusion within this study. A positive viral status was confirmed for all participants using PCR testing for SARS-CoV-2 RNA either in isolation or in combination with positive serology tests for anti-SARS-CoV-2 immunoglobulins. Participant status was stratified according to their clinical presentation, as shown in Table 1, with the approximate corresponding World Health Organisation (WHO) minimal common outcome scale given for comparison (26). Blood was collected in EDTA tubes (4ml). Samples were processed at a central BioResource service laboratory on the same day as receipt. EDTA blood tubes were centrifuged at 2500 rcf for 10 minutes with no brake. Plasma was then manually removed, and plasma stock aliquots were stored at -80°C until sub-aliquots were prepared for export for the research study.

Preparation of FH, FHL-1 and FHR1-5 standard peptides

Proteins of interest were measured using a targeted mass spectrometry approach as described in Cipriani et al. (24). Briefly, heavy isotope labelled peptide standards were obtained from Cambridge Research Biochemicals, Cambridge, UK. The peptide sequences for FH, FHL-1, FHR-1, FHR-2b, FHR-3, FHR-4 and FHR-5 were VTY**K**cFE, NGWSPTP**R**cIRVSFTL, ATFcD**F**PKINHGILYDEE, AM**F**cDFPKINHGILYDEE, VAcHPG**Y**GLP**K**AQTTVTcTE, **Y**QcQSYYE, and **R**GWSTPPIcSFT**K**GE, respectively. A bold type denotes those residues that contained isotopically heavy amino acid, where K (+8), R (+10), F (+10) and Y (+10). A standard peptide stock was made in 105 µL in 0.1% TFA. The final concentration was 47.6 ng/µL for FH; 0.95 ng/µL for FHL-1; 7.14 ng/µL for FHR-1; 19 ng/µL for FHR-2b; and 4.76 ng/µL for FHR-3, FHR-4 and FHR-5. This concentrated standard mixture was subsequently aliquoted into 5 µL and stored at -80°C.

Plasma sample preparation for LC-MS/MS analysis

Frozen plasma samples were thawed to room temperature, vortexed for 5 min and centrifuged for 30 min at 13,300 g and 5 µL aliquoted to be processed. To each sample 90 µL, 1 µL, and 2 µL of 50 mM ammonium bicarbonate (pH 7.8), 500 mM dithiothreitol (prepared in 50 mM ammonium bicarbonate), and 1% w/v ProteaseMAX™ solution (Promega, Southampton, UK), prepared in 50 mM ammonium bicarbonate, were added, respectively and incubated for 25 min at 56°C. The samples were allowed to cool at room temperature, followed by the addition of 3 µL 500 mM iodoacetamide in 50 mM ammonium bicarbonate and incubated in the dark at room temperature for 15 mins. Proteins were then digested by addition of 43 µL and 1 µL of 50 mM ammonium bicarbonate (pH 7.8), and 1% w/v ProteaseMAX™ solution in 50 mM ammonium bicarbonate, respectively, with 2.5 µL endoproteinase Glu-C (1µg/µL), followed by incubation at 25°C for 16 h with shaking at 400 rpm.

Peptide standards were diluted by adding 195 µL of 50:50 acetonitrile:water to the 5 µL of concentrated standard mixture, and 2 µL of this diluted standard was added to each sample alongside 6 µL of 10% v/v TFA. By this point, the standard peptides are at the final concentration of 500 nM, 5 nM, 32.75 nM, 86.75 nM, 21.68 nM, 41.5 nM and 27.5 nM, for FH, FHL-1 and FHR-1–FHR-5, respectively. The samples were dried in a centrifugal evaporator (Eppendorf), and reconstituted in 50 µL of 0.1% v/v TFA and transferred to LC autosampler vials for analysis by LC-MS/MS.

Liquid chromatography-mass spectrometry analysis

The analysis was conducted in two parts. First, baseline samples were randomized into batches, with each batch containing 20 experimental samples with roughly equal

TABLE 1 Patient cohort details and classification.

Group Nomenclature	Clinical Presentation	WHO Minimal Common Outcome Scale	# Individuals (Baseline)	# Individuals (Timecourse)
Control	Healthy Individuals	–	30	
NA Non-COVID	Symptomatic COVID-ve by PCR	–	46	
A 'Asymptomatic'	Screening: no current symptoms	1	11	11
B 'Mildly Symptomatic'	Screening: symptomatic, but not hospitalised	2-3	15	23
C 'Moderate'	Hospitalised: oxygen not required	4	25	14
D 'Severe'	Hospitalised: low-flow oxygen required	5-6	28	17
E 'Critical	Hospitalised: Assisted ventilation required	7-9	33	12
Total			188	77

numbers from each group and a set of quality control (QC) samples. These QC samples were duplicates of a commercial, standard human serum sample (Sigma), a duplicate of one of the samples in the batch, and a replicate from a previously run duplicate sample. Subsequently, paired samples where a 28d sample was available were analysed, including a repeat of the baseline sample along with its 28d paired sample. Randomisation and batch structure were the same across both studies.

All samples were analysed by Liquid Chromatography-Selected Reaction Monitoring-Mass Spectrometry (LC-SRM-MS) using the method described in (24). Using a 6495 triple-quadrupole mass spectrometer with an electrospray ion source (Agilent), connected to an Agilent Infinity 1200 Series liquid chromatography system, 4 µL of each sample was injected directly onto a C18 column (250 mm × 2.1 mm I.D., Thermo Scientific Acclaim 120, 3 µm particle size) held at 50°C. Peptides were eluted at a 250 µL/min flow rate using the previously described gradient (24). Six acquisition windows were used for the eluting peptides, where one window was acquired for both FHL-1 and FHR-2.

Data analysis

Selected Reaction Monitoring (SRM) data were processed using Skyline (v19.1.0.193) (27). The retention time and heavy peptide peak area were visually checked for all samples to verify that the peaks were allocated and integrated appropriately. Peak-area data was extracted from Skyline into Microsoft Excel where the peak areas of heavy and light transitions were compared. The largest signal was used to quantify on-column loading of the endogenous peptide, whereas the other two transitions were used as a qualification signal to ensure the specificity and agreement in quantitation. Finally, concentration per unit volume was calculated based on each sample injection containing the equivalent of 0.8 µL plasma. All further statistical analysis was performed in GraphPad Prism (version 9.2.0). Initial normality testing was carried out on all datasets using a Kolmogorov-Smirnov test, with the most appropriate test then being used for regression analyses as described in the text.

Results

Measurement of FH, FHL-1 and FHR1-5 in baseline samples

Baseline samples were collected from 188 individuals and categorised according to COVID-19 diagnosis and severity. Key among these patients are those who were non-symptomatic and SARS-Cov-2 negative (control, n=30), and those who attended for SARS-Cov-2 testing and were therefore displaying symptoms, but were tested as SARS-Cov-2 negative (NA, n=46). Demographic data for these individuals is shown in Table 2.

Samples were randomised into 11 analytical batches, with each batch containing 2 types of quality control samples, one being a duplicate analysis of a single quality control sample in every batch, the second being a duplicate of an experimental sample which was analysed a third time in the subsequent batch. Analysis of the common quality control sample showed a batch effect for measurement of FH in batches 2, 3 and 5, for FHR-2 in the 3rd batch and for FHR4 in batches 1 and 2. Data for these proteins from these batches were subsequently excluded from further analysis. The variability of the QC in remaining batches was plotted on Levey-Jennings plots (Supplementary Figure 1) and percent coefficient of variance (%CV) measured across all batches was FH = 17.0%, FHL-1 = 14.3%, FHR1 = 14.7%, FHR2 = 17.8%, FHR3 = 10.3%, FHR4 = 23.5% and FHR5 = 13.0%. Evaluation of triplicate COVID-19 samples across adjacent batches, demonstrated that 93.4% of the measurements have a %CV less than 25% (Supplementary Table 1), indicating high assay reproducibility.

To compare levels of circulating FH, FHL-1 and FHR between groups, we confirmed normality of distribution in most groups using a Kolmogorov-Smirnov test and data were analysed *via* a one-way ANOVA. Differences in circulating proteins associated with COVID-19 severity were identified for FHL-1 ($p<0.0001$), FHR1 ($p=0.0007$), FHR2 ($p<0.0001$), FHR3 ($p<0.0001$), FHR4 ($p=0.0006$) and FHR5 ($p<0.0001$). FH concentrations did not correlate with severity ($p=0.126$). Pairwise comparisons between groups were subsequently carried out using a Tukey's multiple comparison test. All associations with adj. $p<0.01$ are described in Figure 1. Notably there were significant elevations in circulating levels of all proteins comparing controls and severe disease groups. These differences were greatest for FHR2 and FHR5 in particular, both of which saw a greater than 2-fold increase in protein levels across these groups, and indeed significant differences between almost all other groups and the most severe patients. These data suggest that FHL-1 and FHR levels are related to disease severity.

To test this further we calculated individual ROC curves for all proteins to demonstrate the predictive power of the FHR proteins with respect of severe disease (Figure 2). As expected FHR2 and FHR5 demonstrated the greatest power to predict the most severe disease vs controls, with AUROC values of 0.877 and 0.943 respectively.

In this baseline cohort, we noted that age was significantly different, with groups A and B being generally younger than other groups. This is demonstrated in Supplementary Figure 2A, where age distributions can be seen (although age ranges are similar). To rule this out as a factor driving the observed differences, we studied the relationships between age and FH,

10.3389/fimmu.2022.1032331

TABLE 2 Demographic data for patients enrolled in baseline measurement study.

Patient Classification	Total	Age (yrs) Mean (range) s.d (n)[a]	BMI Mean (range) s.d (n)[a]	% Male[a]
Ctrl	30	42.0 (20-73) 16.8 (n=30)	26.3 (23-30.1) 3.0 (n=4)	60% (12/20)
NA	46	57.4 (18-89) 18.13 (n=46)	28.0 (18.3-53.9) 8.1 (n=42)	43.5% (20/46)
A	11	39.4 (20-72) 15.6 (n=11)	25.4 (20.9-31.8) 3.8 (n=8)	18.2% (2/11)
B	15	36.47 (23-58) 12.0 (n=15)	27.0 (19.6-43.4) 6.8 (n=13)	13.3% (2/15)
C	25	59.4 (18-87) 16.5 (n=24)	29.3 (20-47.9) 7.2 (n=22)	41.6% (10/24)
D	28	66.2 (39-87) 14.3 (n=26)	29.0 (15-42.4) 5.6 (n=24)	69.2% (18/26)
E	33	62.8 (26-86) 13.82 (n=33)	32.0 (22.5-40.2) 5.3 (n=22)	67.9% (19/28)

[a]Due to the nature of the cohort, not all demographic information is available for all participants. The number of values on which the reported summary data for each characteristic is based is therefore provided.

FHL-1 and FHR1-5 levels in the control and NA cohorts (n=76, where age data were available). No significant associations were seen (Supplementary Figure 2B-H), confirming that the observed elevation in protein levels with more severe COVID-19 symptoms is disease, rather than age-driven. The cohort also shows some variability in sex in the experimental groups, although the critical comparisons of Control versus groups C, D and E are well aligned. Nevertheless, we also investigated the possibility of sex-associated differences for all protein levels in the control and NA cohorts. No such statistically significant association was found (Supplementary Figure 3).

Measurement of FH, FHL-1 and FHR1-5 in 28 day samples

For 77 SARS-CoV-2 positive individuals, we collected an additional sample at approximately 28 days after the first. Of these 77 samples, 58 were included in the baseline analysis, with a further 19 analysed only in this timecourse study. The demographic data for this subset is shown in Table 3. Notably, while most samples were collected between 25-31 days after the first sample, there are 2 cases in Group C (49 and 53 days), 4 in Group D (40, 44, 47 and 48 days) and one in Group E (46 days) where samples were collected over 40 days later. This does not cause a significant difference in sampling time between groups.

Later timepoint samples were batched alongside the baseline samples for each individual and randomly assigned to analysis batches for measurement of circulating FH, FHL-1 and FHR1-5 proteins. Similar cross-batch quality controls were employed as with the baseline study. Reproducibility across batches was excellent, with replicates of a standard samples run in all batches routinely measuring within 2 s.d. of the mean (Supplementary Figure 4), with replicates of an individual study sample analysed across consecutive batches FH = 11.2%, FHL-1 = 16.2%, FHR1 = 28.6%, FHR2 = 9.1%, FHR3 = 9.45%, FHR4 = 3.8% and FHR5 = 6.3% (1 d.p.).

This study contains a nested, independent replicate analysis of the baseline samples, albeit with an overlapping subset of samples. However, analysis of this subset confirms the finding from the first, larger study, in that statistically significant elevations of FHL-1 (p=0.047), FHR3 (p=0.045) and FHR5 (p=0.0071) proteins could be observed, in this case between Group A and Group E individuals, while FHR2 showed a significant increase between Groups B and C (p=0.048) and Groups B and D (p=0.041), implying that elevations in FHL-1 and FHRs are apparent upon replicate analysis, albeit this is a lower powered subset. Note that this analysis did not include healthy controls or SARS-CoV-2 negative patients where the largest differences were seen in the original baseline study.

Analysis of day 28 samples demonstrated that, although COVID-19 symptoms had largely resolved in most cases, with only 5 remaining in intensive care at this timepoint, there is still evidence of elevations of FHL-1 and FHR proteins at this time in the most severe cases (Figure 3), most notably FHL-1, FHR2 and FHR5.

Pairwise analysis of samples taken from the same individual across the two timepoints reveals how the levels of FH, FHL-1 and FHRs resolve over time. All comparisons for each protein separated by disease severity are shown in Supplementary Figure 4. As may be expected, there is a general decrease in levels of all proteins after 28 days in those individuals with asymptomatic, mild or moderate symptoms as in the majority of cases symptoms resolve. This is particularly evident for FHL-1 and FHR5. Notably, this is also the case for FH, implying that individuals do experience a slight elevation of FH level upon infection, although this is not detectable in a standard case-

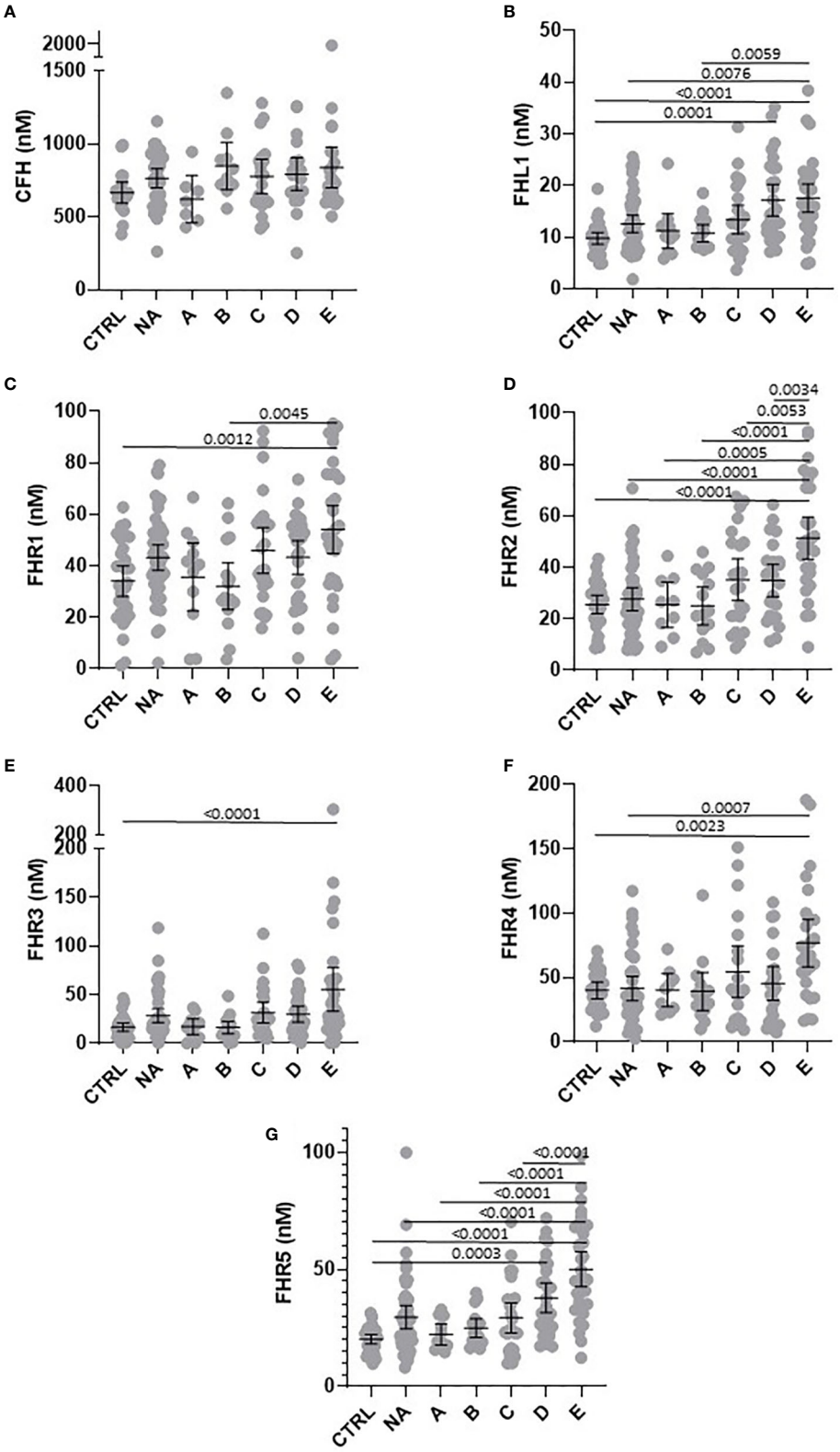

FIGURE 1
Circulating concentration of FHL-1 and FHR1 to FHR5 is elevated in COVID-19 patients. Scatter plots of FH **(A)**, FHL1 **(B)**, and FHR1 to FHR5 **(C–G)** represent the measured plasma protein concentration in nM. Pairwise adjusted p-values were obtained from a Tukey's multiple comparisons test (4 d.p.).

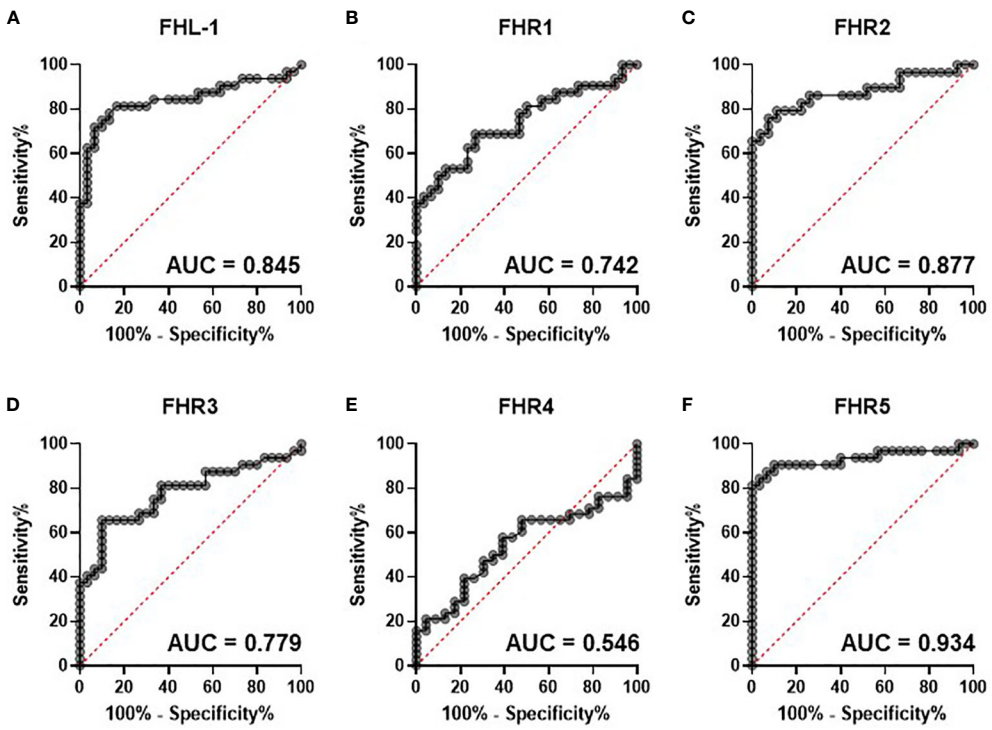

FIGURE 2
Circulating complement cofactors predict disease severity. Receiver Operating Characteristic (ROC) curves for control versus severe [group **(E)**] disease are shown for circulating FHL-1 **(A)** and FHRs 1-5 **(B-F)**. Area under the curve is provided to 3 d.p.

control design due to the background of between-patient variability (Figure 4A). In contrast, individuals who experienced severe COVID-19 symptoms demonstrate a further elevation in circulating FH, FHR1 and FHR2 levels 28 days after their initial diagnosis, on top of the higher levels of these proteins seen in these patients versus a healthy cohort in our baseline analysis. (Figure 4B). Strikingly, 9/12 (75%) of Group E samples showed a greater than 50% elevation in at least one of the FHRs after 28 days, compared to 14/65 (22.5%) in all other groups combined. However, this continued elevation was not correlated with length of stay in intensive care, or whether the patient was still in intensive care at this second timepoint, although we do not have data regarding other symptom severity at this time, e.g. non-ICU admission or continued requirement for oxygen at home. These data support the hypothesis that levels of circulating soluble complement regulators play a role in determining and/or driving disease severity in patients with COVID-19.

TABLE 3 Demographic data from patient subset used in time course analysis.

Patient Classification	Total	Age (yrs) Mean (range) s.d (n)[a]	BMI Mean (range) s.d (n)[a]	% Male[a]
A	11	37.7 (20 - 72) 15.9 (n = 11)	25.2 (20.9-31.8) 3.9 (n = 8)	18.2% (2/11)
B	23	39.0 (20 - 70) 13.9 (n = 23)	25.9 (19.6 - 43.4) 6.1 (n = 19)	13% (3/23)
C	14	59.8 (42 - 77) 11.0 (n = 13)	30.3 (21.1 - 42.9) 6.7 (n = 12)	53.9% (7/13)
D	17	63.1 (44 - 87) 12.0 (n = 17)	29.2 (20.8 - 36.2) 4.5 (n = 16)	64.7% (11/17)
E	12	62.3 (38 - 81) 12.4 (n = 12)	32.3 (22.5-40.2) 6.1 (n = 10)	75% (9/12)

[a]Due to the nature of the cohort, not all demographic information is available for all participants. The number of values on which the reported summary data for each characteristic is based is therefore provided.

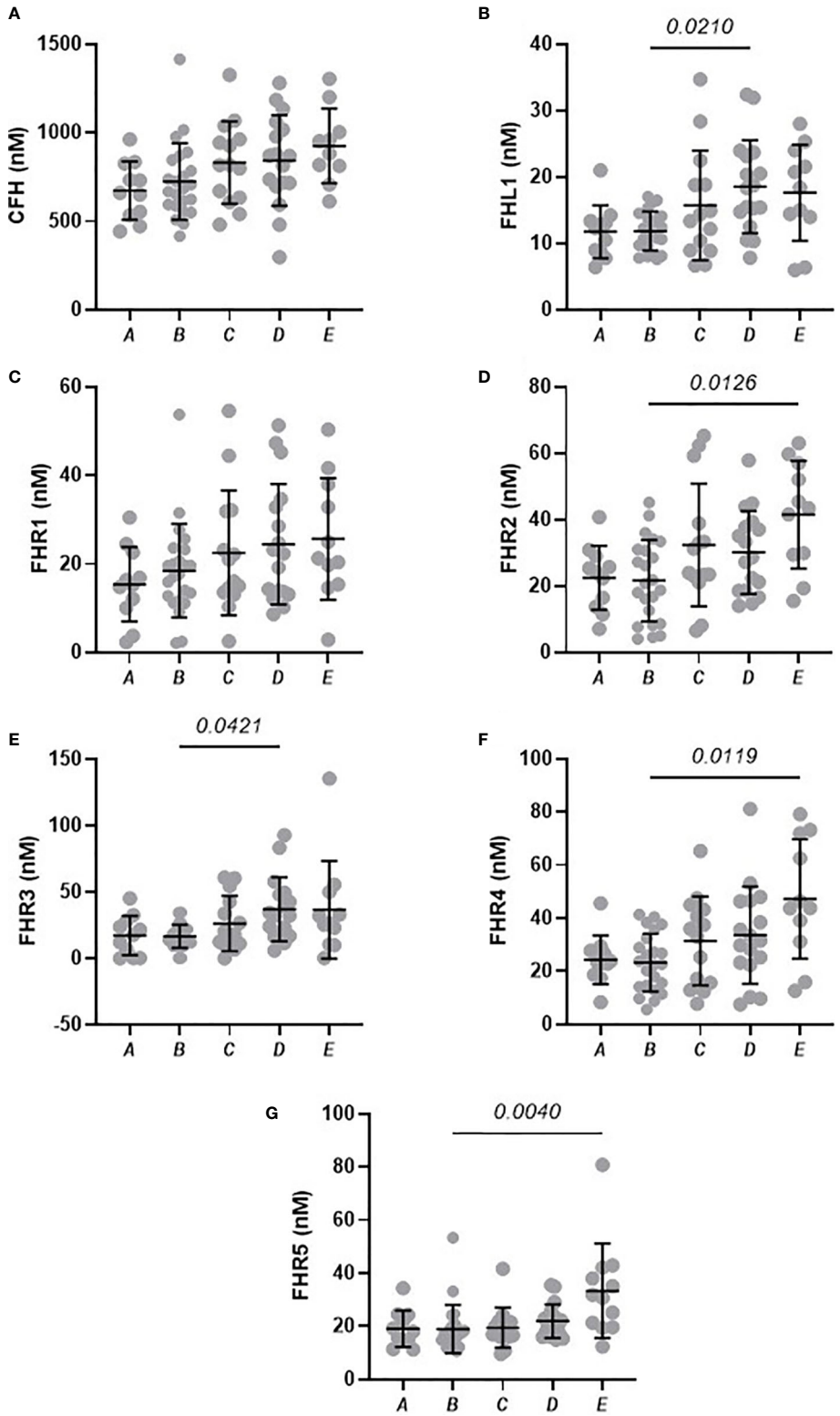

FIGURE 3
Circulating concentrations of FHL-1 and FHR1 to FHR5 in COVID-19 patients after 28 days. Scatter plots of FH **(A)**, FHL1 **(B)**, and FHR1 to FHR5 **(C–G)** represent the measured plasma protein concentration in nM. Pairwise adjusted p-values were obtained from a Tukey's multiple comparisons test (4 d.p.).

Discussion

Immune overactivation is established as a key driver of COVID-19 disease severity, although the mechanisms underpinning this overactivation are unclear. While much of the focus has been on the adaptive response, there is clearly a role for the activation of the complement system in driving, or contributing to this overactivation (17). In this study, we sought to uncover the role played by a key series of complement activation regulators, the Complement Factor H family. FH is a critical regulator of the complement amplification loop, as a co-factor for Factor I it is required for the degradation and inactivation of C3b. A splice variant of FH, FHL-1, has the same activity but is present at much lower circulating levels, while the FHR proteins, encoded by distinct genes at the same chromosomal location, retain C3b binding capability but lack co-factor activity, and so can compete with FH and in essence prevent C3b breakdown. We hypothesised that, given existing data on complement overactivation and the observation from global proteomics studies that members of the complement family are overactivated in severe disease, levels of this family of co-factors could play a role in predicting disease severity or outcome in SARS-Cov-2 positive patients.

To measure these proteins, we used a mass spectrometry-based assay. Because MS can accurately identify peptides based on their mass, it provides enhanced selectivity over antibody-based approaches, which is especially important in studies such as this where the target proteins share significant homology. While antibody assays have been published for some FHRs (28), no such assay has been developed to detect FHL-1, which is identical to the N-terminal part of FH with the exception of a 4 amino acid C-terminal tail (29). This approach has been used previously to study complement co-factors in age-related macular degeneration (24) and glioblastoma (30). A standard quality control regimen was used to ensure that all samples were randomised across analysis batches, and common samples included to ensure that data were comparable between batches

Our study was divided into two independent parts. The first was an analysis of samples collected at baseline (time of diagnosis) and included both a healthy control cohort and a cohort who were symptomatic and presented at hospital for a SARS-CoV-2 test but were found to be negative. The second was a time course analysis of SARS-CoV-2-positive individual approximately 28 days following initial diagnosis.

The baseline study identified that all measured proteins, with the exception of FH, were present at higher levels in more severe disease. Elevation of FHL-1, independent of FH, is particularly striking since FHL-1 is a spice variant and as such is driven from the same promoter as FH, implying an altered regulation of splicing, translation or degradation of this shorter isoform compared to its larger and more abundant counterpart, an observation that we have also made in age-related macular degeneration (24) and glioblastoma (30). While increases were seen in all FHR proteins, elevations were highest in FHR2 and FHR5, which increased between healthy controls and severe disease by 1.97-fold ($p<0.0001$) and 2.4-fold ($p<0.0001$) respectively. ROC curves constructed between severe COVID-19 vs healthy controls gave AUROC values of 0.877 and 0.934 suggesting a strong predictive relationship. ROC curves considering multiple proteins did not improve this prediction significantly, while ROC curves on all COVID-19 patients to predict hospitalisation yielded more modest AUROCs of 0.76.

While previous studies of the global proteome have incidentally detected elevation in FHR-5 correlated with more severe cases of COVID-19 (12), this study represents the first targeted analysis of these proteins and as such is the first observation of a global increase across the factor H family of proteins. These data compare favourably to other recent studies investigating COVID-19 severity biomarkers. For example, the recent work by Wang et al. (31) used a 30 protein panel to predict disease severity and using a machine learning approach achieved AUROC for severe disease (WHO outcome score 7) vs mild (WHO outcome score 3) of approximately 0.85. In our study a similar analysis for FHR5 only, between groups A+B vs Group D+E, gives a AUROC of 0.84 for similar sized cohorts. Intriguingly, FHR2, but not FHR5, was identified in that group's discovery proteomics effort (13) but was not included in the final panel of 30.

The second part of this study looked at how complement regulator levels change over time, with a subset of individuals providing a second sample at approximately 28 days post the baseline sample. Paired analysis of samples from individuals with symptomatic, mild or moderate disease (i.e. disease not requiring hospitalisation) demonstrated a reduction in levels of most FH-family proteins, including FH which we did not show to be elevated in our baseline study. This is possibly due to the magnitude of change being relatively small compared to between patient variability, so it is masked in a case-control design but is apparent in a time course where each individual acts as their own control. This supports our observation from the baseline study that SARS-CoV-2 infection results in elevation of circulating complement co-factors. However, in individuals with severe disease co-factor levels are actually increased on average 28 days following diagnosis. It is unclear whether this is a true reflection of severe disease i.e. that complement can become 'more dysregulated' over time in more severe cases, or simply a consequence of our study taking few timepoint samples. A higher resolution timecourse, perhaps weekly sampling and with a more reproducible sampling frequency than was achieved in this cohort, is required to confirm the trajectory of these proteins more accurately. We also recognise that there is a sampling bias in this study, as patients with the most severe disease who did not survive for 28 days after diagnosis are necessarily excluded. What these data do show is that the complement cascade response is not resolved at 28 days in severe cases.

This study does have limitations. Due to the nature of the pandemic at the time of collection, complete metadata is not available for all individuals in the cohort as it was not collected at

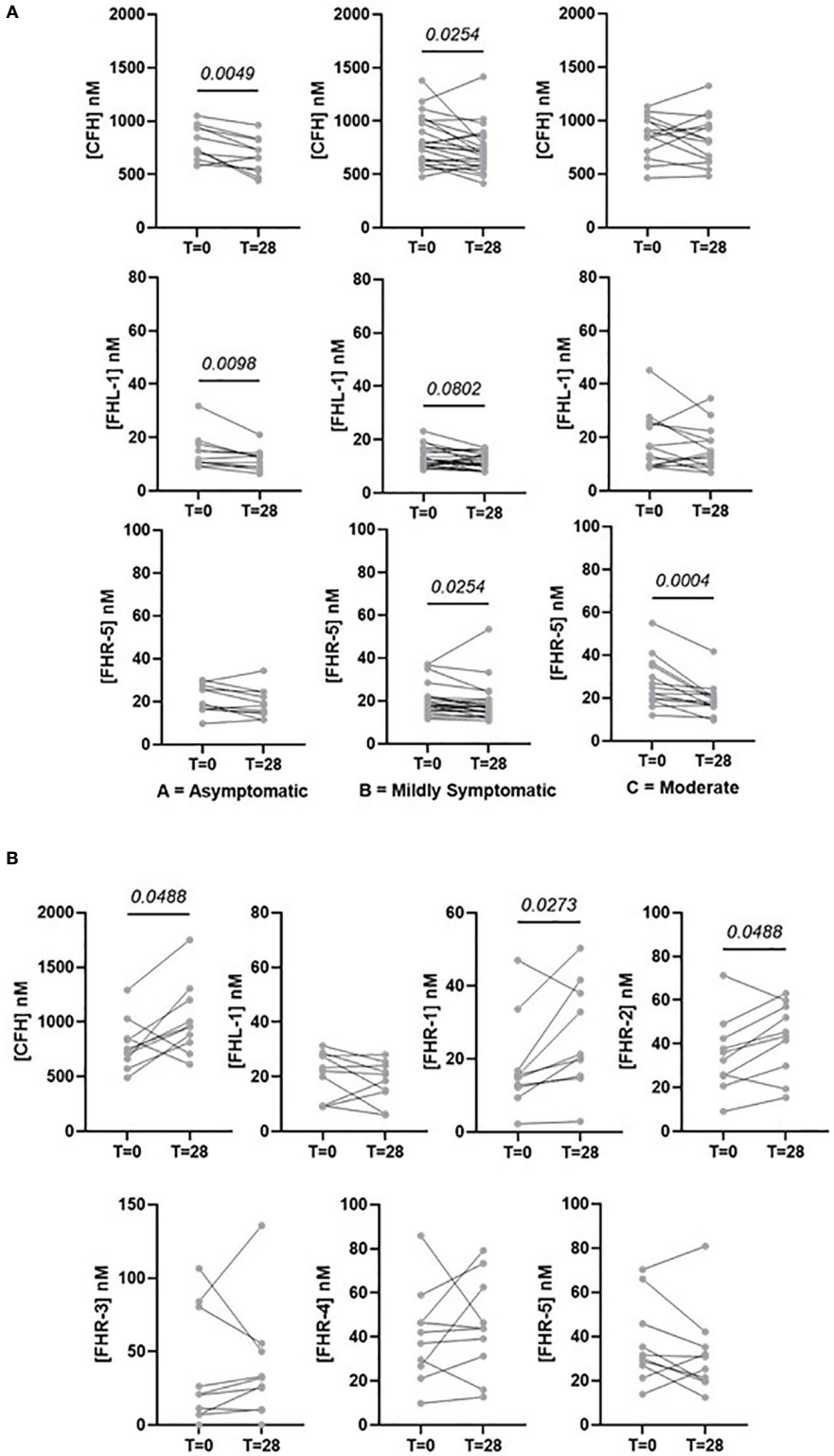

FIGURE 4
Selected pairwise comparisons of circulating concentrations of FHL-1 and FHR1 to FHR5 in COVID-19 patients after 28 days. **(A)** CFH, FHL-1 and FHR5 in asymptomatic to moderate symptomatic individuals. **(B)** CFH, FHL-1 and FHR1-5 in patients with critical (Group E) COVID-19.

the time and is now only obtainable by manual extraction from patient records. As such it is not possible for us to perform convincing multivariate analysis or to correlate our findings with co-morbidities and treatments, for example. However, in previous studies on larger cohorts we have shown no effect of age, sex or BMI on FH, FHL-1 or FHR1-5 levels (24) and so we do not anticipate that adding these variables would alter our conclusions. Samples were collected in wave 1 of the pandemic in the UK, driven primarily by the original wild-type variant of the SARS-CoV-2 virus. All samples were collected before the emergence of the delta variant which caused a more severe disease (32) and the current predominant omicron variant which is more transmissible but appears to result in a less severe phenotype that delta, albeit worse than the wild-type, even in unvaccinated individuals (33). As such we believe it would be valuable to reanalyse FHL-1 and FHR levels in samples from both the delta and omicron waves, and from better defined cohorts in terms of both numbers and clinical metadata to investigate whether levels of these proteins contribute to the more severe symptoms seen with these variants, along with correlation of FHR levels with other complement activation or inflammatory markers in these cohorts.

Increased FHR levels are predicted to decrease C3b turnover, and as such increase complement cascade activation. This agrees with observations in clinical samples around increase deposition of C5b-9 (16, 20) in more severe cases and supports the hypothesis that the complement cascade is a viable target for both prediction of COVID-19 prognosis in infected individuals, and supports therapeutic efforts for complement blockade as a means of treating or preventing severe COVID-19 outcomes.

Data availability statement

The raw data supporting the conclusions of this article will be made available by the authors, without undue reservation.

Ethics statement

The studies involving human participants were reviewed and approved by Cambridge Central Research Ethics Committee. The patients/participants provided their written informed consent to participate in this study.

Author contributions

RU and SC contributed to conception and design of the study. AT, WA, TS and RU acquired the data and performed initial analysis. KR-U analysed the clinical data. All authors interpreted the data. WA, TS and RU wrote the first draft of the manuscript. All authors contributed to the article and approved the submitted version.

Funding

Development of the FH, FHL-1 and FHR assay was funded by the Medical Research Council, UK (MR/P025838/1). The Stoller Biomarker Discovery Centre was established with an award from the MRC (MR/M008959/1). The work was funded by awards from NIHR to the NIHR BioResource (RG94028 & RG85445). SJC receives money and support from the Helmut Ecker Foundation.

Acknowledgments

We thank NIHR BioResource volunteers for their participation, and gratefully acknowledge NIHR BioResource centres, NHS Trusts and staff for their contribution. We thank the National Institute for Health and Care Research, NHS Blood and Transplant, and Health Data Research UK as part of the Digital Innovation Hub Programme. The views expressed are those of the author(s) and not necessarily those of the NHS, the NIHR or the Department of Health and Social Care. This work was facilitated by the Manchester NIHR Biomedical Research Centre and the Greater Manchester Comprehensive Local Research Network.

Conflict of interest

SC and RU are inventors named in patent applications that describe the use of complement inhibitors for therapeutic purposes and the use of circulating complement protein measurement for patient stratification, and are co-founders of and shareholders in Complement Therapeutics, a company which focuses on the development of complement targeted therapeutics, for chronic diseases focussed on Age-related Macular Degeneration.

The remaining authors declare that the research was conducted in the absence of any commercial or financial relationships that could be constructed as a potential conflict of interest.

Publisher's note

All claims expressed in this article are solely those of the authors and do not necessarily represent those of their affiliated organizations, or those of the publisher, the editors and the reviewers. Any product that may be evaluated in this article, or claim that may be made by its manufacturer, is not guaranteed or endorsed by the publisher.

Supplementary material

The Supplementary Material for this article can be found online at: https://www.frontiersin.org/articles/10.3389/fimmu.2022.1032331/full#supplementary-material

References

1. Brodin P. Immune determinants of COVID-19 disease presentation and severity. *Nat Med* (2021) 27:28–33. doi: 10.1038/s41591-020-01202-8

2. Kim JH, Marks F, Clemens JD. Looking beyond COVID-19 vaccine phase 3 trials. *Nat Med* (2021) 27:205–11. doi: 10.1038/s41591-021-01230-y

3. Horby P, Lim WS, Emberson JR, Mafham M, Bell JL, Linsell L, et al. Dexamethasone in hospitalized patients with covid-19. *New Engl J Med* (2021) 384:693–704. doi: 10.1056/NEJMoa2021436

4. Iacobucci G. Covid-19: How is vaccination affecting hospital admissions and deaths? *BMJ* (2021) 374:n2306. doi: 10.1136/bmj.n2306

5. Filbin MR, Mehta A, Schneider AM, Kays KR, Guess JR, Gentili M, et al. Longitudinal proteomic analysis of severe COVID-19 reveals survival-associated signatures, tissue-specific cell death, and cell-cell interactions. *Cell Rep Med* (2021) 2:100287. doi: 10.1016/j.xcrm.2021.100287

6. Ahsan N, Rao RSP, Wilson RS, Punyamurtula U, Salvato F, Petersen M, et al. Mass spectrometry-based proteomic platforms for better understanding of SARS-CoV-2 induced pathogenesis and potential diagnostic approaches. *Proteomics* (2021) 21:e2000279. doi: 10.1002/pmic.202000279

7. Suvarna K, Biswas D, Pai MGJ, Acharjee A, Bankar R, Palanivel V, et al. Proteomics and machine learning approaches reveal a set of prognostic markers for COVID-19 severity with drug repurposing potential. *Front Physiol* (2021) 12:652799. doi: 10.3389/fphys.2021.652799

8. Völlmy F, Toorn HVD, Zenezini Chiozzi R, Zucchetti O, Papi A, Volta CA, et al. A serum proteome signature to predict mortality in severe COVID-19 patients. *Life Sci alliance 4* (2021) 4:e202101099. doi: 10.26508/lsa.202101099

9. Geyer PE, Arend FM, Doll S, Louiset ML, Virreira Winter S, Müller-Reif JB, et al. High-resolution serum proteome trajectories in COVID-19 reveal patient-specific seroconversion. *EMBO Mol Med* (2021) 13:e14167. doi: 10.15252/emmm.202114167

10. D'Alessandro A, Thomas T, Dzieciatkowska M, Hill RC, Francis RO, Hudson KE, et al. Serum proteomics in COVID-19 patients: Altered coagulation and complement status as a function of IL-6 level. *J Proteome Res* (2020) 19:4417–27. doi: 10.1021/acs.jproteome.0c00365

11. Park J, Kim H, Kim SY, Kim Y, Lee JS, Dan K, et al. In-depth blood proteome profiling analysis revealed distinct functional characteristics of plasma proteins between severe and non-severe COVID-19 patients. *Sci Rep* (2020) 10:22418. doi: 10.1038/s41598-020-80120-8

12. Demichev V, Tober-Lau P, Lemke O, Nazarenko T, Thibeault C, Whitwell H, et al. A time-resolved proteomic and prognostic map of COVID-19. *Cell Syst* (2021) 12:780–94.e7. doi: 10.1016/j.cels.2021.05.005

13. Messner CB, Demichev V, Wendisch D, Michalick L, White M, Freiwald A, et al. Ultra-High-Throughput clinical proteomics reveals classifiers of COVID-19 infection. *Cell Syst* (2020) 11:11–24.e4. doi: 10.1016/j.cels.2020.05.012

14. Zilow G, Sturm JA, Rother U, Kirschfink M. Complement activation and the prognostic value of C3a in patients at risk of adult respiratory distress syndrome. *Clin Exp Immunol* (1990) 79:151–7. doi: 10.1111/j.1365-2249.1990.tb05171.x

15. Ramlall V, Thangaraj PM, Meydan C, Foox J, Butler D, Kim J, et al. Immune complement and coagulation dysfunction in adverse outcomes of SARS-CoV-2 infection. *Nat Med* (2020) 26:1609–15. doi: 10.1038/s41591-020-1021-2

16. Aiello S, Gastoldi S, Galbusera M, Ruggenenti P, Portalupi V, Rota S, et al. C5a and C5aR1 are key drivers of microvascular platelet aggregation in clinical entities spanning from aHUS to COVID-19. *Blood Adv* (2022) 6:866–81. doi: 10.1182/bloodadvances.2021005246

17. Afzali B, Noris M, Lambrecht BN, Kemper C. The state of complement in COVID-19. *Nat Rev Immunol* (2022) 22:77–84. doi: 10.1038/s41577-021-00665-1

18. Bumiller-Bini V, de Freitas Oliveira-Toré C, Carvalho TM, Kretzschmar GC, Gonçalves LB, Alencar NM, et al. MASPs at the crossroad between the complement and the coagulation cascades - the case for COVID-19. *Genet Mol Biol* (2021) 44:e20200199. doi: 10.1590/1678-4685-gmb-2020-0199

19. Lage SL, Rocco JM, Laidlaw E, Rupert A, Galindo F, Kellogg A, et al. Activation of complement components on circulating blood monocytes from COVID-19 patients. *Front Immunol* (2022) 13:815833. doi: 10.3389/fimmu.2022.815833

20. Niederreiter J, Eck C, Ries T, Hartmann A, Märkl B, Büttner-Herold M, et al. Complement activation *via* the lectin and alternative pathway in patients with severe COVID-19. *Front Immunol* (2022) 13:835156. doi: 10.3389/fimmu.2022.835156

21. Cserhalmi M, Papp A, Brandus B, Uzonyi B, Józsi M. Regulation of regulators: Role of the complement factor h-related proteins. *Semin Immunol* (2019) 45:101341. doi: 10.1016/j.smim.2019.101341

22. Xu B, Kang Y, Du Y, Guo W, Zhu L, Zhang H. Atypical hemolytic uremic syndrome-associated FHR1 isoform FHR1*B enhances complement activation and inflammation. *Front Immunol* (2022) 13:755694. doi: 10.3389/fimmu.2022.755694

23. Garam N, Cserhalmi M, Prohászka Z, Szilágyi Á., Veszeli N, Szabó E, et al. FHR-5 serum levels and CFHR5 genetic variations in patients with immune complex-mediated membranoproliferative glomerulonephritis and C3-glomerulopathy. *Front Immunol* (2021) 12:720183. doi: 10.3389/fimmu.2021.720183

24. Cipriani V, Tierney A, Griffiths JR, Zuber V, Sergouniotis PI, Yates JRW, et al. The impact of genetic-risk variants for age-related macular degeneration on circulating factor-h-like 1 and factor-h-related protein concentrations. *Am J Hum Genet* (2021) 108:1385–400. doi: 10.1016/j.ajhg.2021.05.015

25. Overmyer KA, Shishkova E, Miller IJ, Balnis J, Bernstein MN, Peters-Clarke TM, et al. Large-Scale multi-omic analysis of COVID-19 severity. *Cell Syst* (2021) 12:23–40.e7 doi: 10.1016/j.cels.2020.10.003.

26. WHO Working Group on the Clinical Characterisation and Management of COVID-19 infection. A minimal common outcome measure set for COVID-19 clinical research. *Lancet Infect Dis* (2020) 20:e192-e197 doi: 10.1016/S1473-3099(20)30483-7.

27. MacLean B, Tomazela DM, Shulman N, Chambers M, Finney GL, Frewen B, et al. Skyline: an open source document editor for creating and analyzing targeted proteomics experiments. *Bioinformatics* (2010) 26:966–8. doi: 10.1093/bioinformatics/btq054

28. Lorés-Motta L, van Beek AE, Willems E, Zandstra J, van Mierlo G, Einhaus A, et al. Common haplotypes at the CFH locus and low-frequency variants in CFHR2 and CFHR5 associate with systemic FHR concentrations and age-related macular degeneration. *Am J Hum Genet* (2021) 108:1367–84. doi: 10.1016/j.ajhg.2021.06.002

29. Ripoche J, Day AJ, Harris TJ, Sim RB. The complete amino acid sequence of human complement factor h. *Biochem J* (1988) 249:593–602. doi: 10.1042/bj2490593

30. Zhai L, Bell A, Ladomersky E, Lauing KL, Bollu L, Nguyen B, et al. Tumor cell IDO enhances immune suppression and decreases survival independent of tryptophan metabolism in glioblastoma. *Clin Cancer Res an Off J Am Assoc Cancer Res* (2021) 27:6514–28. doi: 10.1158/1078-0432.CCR-21-1392

31. Wang Z, Cryar A, Lemke O, Tober-Lau P, Ludwig D, Helbig ET, et al. A multiplex protein panel assay for severity prediction and outcome prognosis in patients with COVID-19: An observational multi-cohort study. *eClinicalMedicine* (2022) 49:101495. doi: 10.1016/j.eclinm.2022.101495

32. Hu Z, Huang X, Zhang J, Fu S, Ding D, Tao Z. Differences in clinical characteristics between delta variant and wild-type SARS-CoV-2 infected patients. *Front Med* (2021) 8:792135. doi: 10.3389/fmed.2021.792135

33. Sigal A, Milo R, Jassat W. Estimating disease severity of omicron and delta SARS-CoV-2 infections. *Nat Rev Immunol* (2022) 22:267–9. doi: 10.1038/s41577-022-00720-5

frontiers | Frontiers in Immunology

TYPE Systematic Review
PUBLISHED 18 October 2022
DOI 10.3389/fimmu.2022.1007102

Check for updates

OPEN ACCESS

EDITED BY
Christian Marcel Karsten,
University of Lübeck, Germany

REVIEWED BY
Michael Kirschfink,
Heidelberg University, Germany
Seyed Moein Moghimi,
Newcastle University, United Kingdom

*CORRESPONDENCE
Erik J. M. Toonen
e.toonen@hycultbiotech.com

†These authors contributed equally to this work

SPECIALTY SECTION
This article was submitted to Molecular Innate Immunity, a section of the journal Frontiers in Immunology

RECEIVED 29 July 2022
ACCEPTED 13 September 2022
PUBLISHED 18 October 2022

CITATION
Brandwijk RJMGE, Michels MAHM, van Rossum M, de Nooijer AH, Nilsson PH, de Bruin WCC and Toonen EJM (2022) Pitfalls in complement analysis: A systematic literature review of assessing complement activation. *Front. Immunol.* 13:1007102. doi: 10.3389/fimmu.2022.1007102

COPYRIGHT
© 2022 Brandwijk, Michels, van Rossum, de Nooijer, Nilsson, de Bruin and Toonen. This is an open-access article distributed under the terms of the Creative Commons Attribution License (CC BY). The use, distribution or reproduction in other forums is permitted, provided the original author(s) and the copyright owner(s) are credited and that the original publication in this journal is cited, in accordance with accepted academic practice. No use, distribution or reproduction is permitted which does not comply with these terms.

Pitfalls in complement analysis: A systematic literature review of assessing complement activation

Ricardo J. M. G. E. Brandwijk[1†], Marloes A. H. M. Michels[2], Mara van Rossum[1], Aline H. de Nooijer[3], Per H. Nilsson[4,5,6], Wieke C. C. de Bruin[1] and Erik J. M. Toonen[1*†]

[1]R&D Department, Hycult Biotechnology b.v., Uden, Netherlands, [2]Radboud Institute for Molecular Life Sciences, Department of Pediatric Nephrology, Amalia Children's Hospital, Radboud University Medical Center, Nijmegen, Netherlands, [3]Department of Internal Medicine and Radboud Center for Infectious Diseases, Radboud University Medical Center, Nijmegen, Netherlands, [4]Department of Immunology, University of Oslo and Oslo University Hospital Rikshospitalet, Oslo, Norway, [5]Linnaeus Centre for Biomaterials Chemistry, Linnaeus University, Kalmar, Sweden, [6]Department of Chemistry and Biomedical Sciences, Linnaeus University, Kalmar, Sweden

Background: The complement system is an essential component of our innate defense and plays a vital role in the pathogenesis of many diseases. Assessment of complement activation is critical in monitoring both disease progression and response to therapy. Complement analysis requires accurate and standardized sampling and assay procedures, which has proven to be challenging.

Objective: We performed a systematic analysis of the current methods used to assess complement components and reviewed whether the identified studies performed their complement measurements according to the recommended practice regarding pre-analytical sample handling and assay technique. Results are supplemented with own data regarding the assessment of key complement biomarkers to illustrate the importance of accurate sampling and measuring of complement components.

Methods: A literature search using the Pubmed/MEDLINE database was performed focusing on studies measuring the key complement components C3, C5 and/or their split products and/or the soluble variant of the terminal C5b-9 complement complex (sTCC) in human blood samples that were published between February 2017 and February 2022. The identified studies were reviewed whether they had used the correct sample type and techniques for their analyses.

Results: A total of 92 out of 376 studies were selected for full-text analysis. Forty-five studies (49%) were identified as using the correct sample type and techniques for their complement analyses, while 25 studies (27%) did not use the correct sample type or technique. For 22 studies (24%), it was not specified which sample type was used.

Conclusion: A substantial part of the reviewed studies did not use the appropriate sample type for assessing complement activation or did not

mention which sample type was used. This deviation from the standardized procedure can lead to misinterpretation of complement biomarker levels and hampers proper comparison of complement measurements between studies. Therefore, this study underlines the necessity of general guidelines for accurate and standardized complement analysis

KEYWORDS

complement system, complement diagnostics, systematic review, immunoassays, standardization of measurements, complement activation

Introduction

Complement is a key innate immune system and is part of the first line of defense against pathogens. It is recognized as being evolutionary among the oldest pathogen recognition systems, and not only has this system a critical role in killing microbes, it also bridges innate and adaptive immune responses. The realization that an increasing number of human diseases are, at least partly, complement-mediated has driven a renewed interest in complement. Accurate analysis of complement components and complement activation is of utmost importance for diagnosing disease and/or therapy monitoring (1–5). However, reliably determining the complement status of individual patients has proven to be challenging (1, 5). Measured concentrations of complement system proteins vary widely among different laboratories due to non-unified protocols for pre-analytical sample handling, including collection, processing, and storage. Also, laboratories do not always use the correct sample type for the method or assay used. Other reasons for inconsistencies in concentrations are the lack of uniform and recognized calibrators, the use of different techniques, reagents, and antibodies recognizing different epitopes in the antigen. This indicates the high need for standardization of techniques, assays and biomaterials in combination with proper pre-analytical sample handling and storage (2, 3).

This review aimed to provide an overview and general guidelines for measuring complement activation in a reliable and standardized way. We performed a systematic analysis of the literature regarding current methods used to assess complement C3, C5 and/or their split products and/or the soluble terminal complement complex (sTCC; also referred to as sC5b-9 or membrane attack complex, MAC) in human blood. We reviewed whether the identified studies performed their complement measurements according to the recommended practice regarding pre-analytical sample handling and assay technique. Results were supplemented with own data, not included in the systematic review, to illustrate the importance of using the correct biomaterials, methods, and techniques for the assessment of complement components.

Complement pathway activation

The complement system comprises of approximately 50 soluble and cell surface-bound proteins organized to eliminate structures recognized as dangerous. These danger signals include invading microorganisms, apoptotic and necrotic cells and immune complexes (6, 7). Furthermore, complement can link innate and adaptive immune responses by mediating regulation of T cell and B cell responses (8). More recently, several studies reported a role for intracellular complement (9–11).

The complement pathway is tightly regulated by a network of proteins to avoid uncontrolled activation (Figure 1) (12). The system is organized in three activation pathways: the classical pathway (CP), the lectin pathway (LP) and the alternative pathway (AP). Each pathway is activated by different molecules. The CP is activated by the binding of C1q to antigen-bound-IgM or -IgG hexamers forming immune complexes. The LP is activated by binding of one of the recognition molecules mannose-binding lectin (MBL), collectin 10, 11 or 12, or ficolin-1, -2, or -3 to microorganism-associated molecular patterns (MAMPs) or carbohydrate structures located on damaged cells. The AP is continuously activated at a low level as a result of spontaneous C3 hydrolysis allowing for activation on surfaces that lack proper complement regulation, typically non-host surfaces (12–15). Pathway activation results in the cleavage and activation of complement C3 and C5. Subsequently, this will lead to the generation of active fragments such as C3a, C3b, iC3b, C3dg, C4a, C4b and C5a and the formation of TCC (also known as MAC or C5b-9) (1). While TCC is inserted into pathogen cell membranes, resulting in cell death of sensitive cells, typically Gram-negative bacteria, the other activation fragments bind to their corresponding

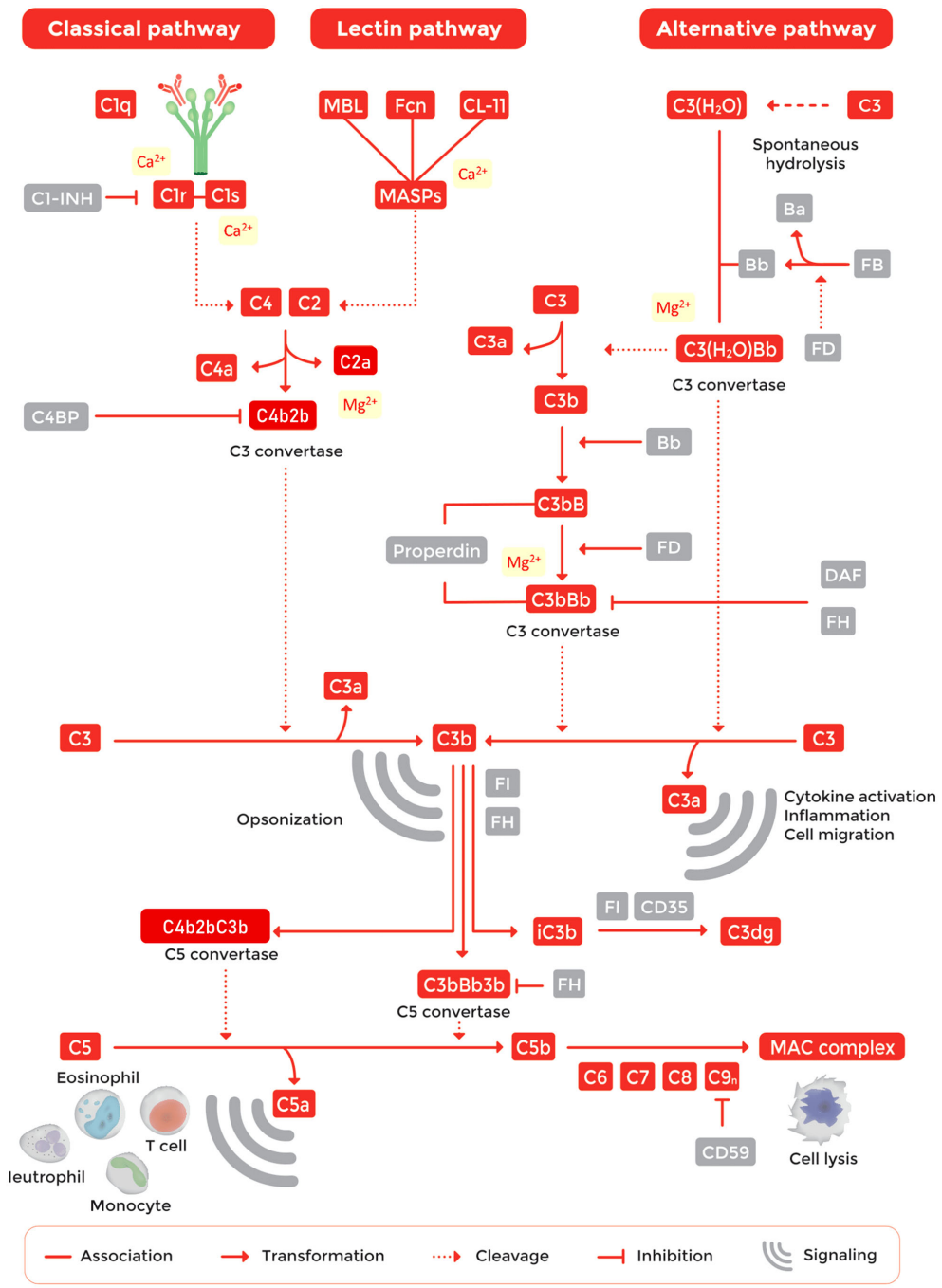

FIGURE 1
Overview of the complement pathway.

complement receptor expressed by various cell types. Binding of activation products to these receptors leads to a variety of biological responses such as phagocytosis, cell migration, chemotaxis, cytokine production, cell activation and modulation of pattern recognition receptor (PRR)-induced responses (Figure 1) (12, 13, 16–18).

Inadequate functioning of the complement system, e.g. by component deficiencies or exaggerated activation, has been linked to numerous diseases, both rare and common, and the list is growing continuously (Table 1) (13, 72–75). An imbalance in complement activation and regulation can lead to life-threatening conditions such as coagulation dysregulation,

TABLE 1 Overview of complement-related diseases.

Disease	Mechanism	Recommended analysis	Ref.
Age-related macular degeneration (AMD)	Genetic variants in complement genes *C3*, *CFB CFH*, and *CD46 (MCP)*.	Genetic analysis of the genes *C3, CFB, CFH, CD46*	(19)
Alzheimer disease (AD)	Local generation of C3a and C5a creating an inflammatory environment. Altered levels of C1q, FB, C4, C4a, TCC. Deposition of TCC on neuronal cells may be responsible for neuritic loss.	Analysis of complement components C1q, FB, C4, C4a and TCC	(20, 21)
Amyotrophic lateral sclerosis (ALS)	Dysregulation of complement, complement activation in the spinal cord, C5aR1-C5a signalling during progression suggests that the terminal complement pathway contributes to the pathogenesis of ALS.	Analysis of terminal pathway components, such as TCC	(22)
ANCA-associated vasculitis	Signalling through the C5a-C5a receptor, contributes to the immunopathology of ANCA-associated vasculitis	ELISA for C5a	(23, 24)
Anti-glomerular basement membrane (anti-GMB) disease	Autoantibodies- or immune complexes-induced complement activation	ELISA for anti-C1q antibodies	(25, 26)
Angioedema	Genetic variants in C1-INH (Hereditary angioedema; HAE), autoantibodies against C1-INH (acquired angioedema)	C1-INH, C4, C1q, anti-C1-INH autoantibodies, molecular analysis C1-INH.	(27)
Atypical haemolytic uremic syndrome (aHUS)	Genetic variants in *C3, CFB, CFH, CFI, CD46 (MCP)* genes.	CH50, AH50, functional ELISA for CP, AP, ELISA for C3, FB, C3a, C3d, TCC, FH, FI, anti-FH autoantibodies, molecular analysis *CFH, CFI, C3, CFB, CD46 (MCP)*	(28)
Cancer	Complement-induced inflammation leading to tumour growth and metastasis.	Analysis of terminal pathway components, such as TCC	(29)
Cold agglutinin disease	Cold agglutinin (CA) IgM immune complexes bind C1q and thereby initiates the classical complement pathway	CH50	(30)
Diabetes	Increased levels of complement activation in plasma.	Analysis of terminal pathway components, such as C3d and TCC	(31)
Epilepsy	Deposition of C1q, C3b and TCC in affected brain tissue.	Analysis of components such as C1q, C3, C5 and TCC	(32)
Glomerulopathies (C3G)	Genetic variants in *C3, CFB CFH, CFI* and *CFHR5*; presence of autoantibodies (C3NeF) preventing AP regulation.	CH50, AH50, functional ELISA for CP, AP, ELISA for C3, C4, C3a, C3d, TCC, FH, FI, C3 and C4 nephritic factor, autoantibodies to FH and FB, C3 convertase, molecular analysis of CFH, CFI, C3, FB, MCP (CD46)	(33–35)
Guillain–Barré Syndrome (GBS)	IgG anti-ganglioside antibodies that lead to GBS cause complement-mediated disruption of interactions between Schwann cells and axon. Terminal complement activation and TCC deposition on Schwann cell. Elevated levels C3a and C5a in the CSF of patients	ELISA for C3a, C5a, TCC. Measurement of anti-ganglioside antibodies	(36)
Henoch-Schoenlein purpura [Immunoglobulin A vasculitis (IgAV)]	Most common form of childhood vasculitis, characterized by IgA1-immune deposits, complement factors and neutrophil infiltration, which is accompanied with vascular inflammation. Autoantibodies- or immune complexes-induced complement activation *via* the alternative and lectin pathway. Levels of TCC in the urine might be a useful indicator of renal injury	Analysis of terminal pathway component TCC	(37, 38)

(Continued)

TABLE 1 Continued

Disease	Mechanism	Recommended analysis	Ref.
Hypocomplementemic Urticarial Vasculitis Syndrome (HUVS)	Exact pathophysiology unknown. Rare immune complex-mediated small vessel vasculitis characterized by urticaria, hypocomplementemia (low C1q, C3, and C4), and systemic manifestations, and it is also associated with circulating anti-C1q autoantibodies	ELISA for C1q, C3, C4, autoantibodies against C1q	(39, 40)
Huntington's disease	Autosomal dominant neurodegenerative disorder caused by a cytosine-adenine-guanine (CAG) trinucleotide repeat expansion in the huntingtin gene. Upregulation of complement components C7 and C9 in HD, increased levels of clusterin are associated with disease progression. Upregulation of C5a-C5aR axis.	ELISA for C5a, C7, C9, TCC	(36, 41)
Infection disorders	Pathogens trigger innate immune responses and activate the complement pathway either directly by pathogen-derived antigens or indirectly by molecules released by host cells binding to these antigens.	CH50, AH50, functional ELISA for CP, AP, LP. ELISA for C3, C4, C1q, C3a, C3d, TCC, C5-C9, Properdin, MBL	(42, 43)
Inflammatory bowel disease	Appropriate activation of the intestinal complement system seems to play an important role in the resolution of chronic intestinal inflammation, while over-activation and/or dysregulation may worsen intestinal inflammation. C3 and C4a are suggested as diagnostic markers	ELISA for C3 and C4a	(44, 45)
Kidney ischemia/ reperfusion (I/R) injury	Complement molecules influence function of factors such as free radicals, neutrophils, and the products of activated endothelium. Complement activation releases biologically active, proinflammatory products. C4a, C3a, and C5a can induce smooth muscle contraction, increase vascular permeability, and cause the release of histamine. C5a acts on neutrophils, promoting chemotaxis and activation and acts on neutrophils and endothelium to upregulate cell adhesion molecules such as CD11b/CD18 and the intercellular adhesion molecule (ICAM-1). C5b-9 inserts into the membrane of target cells, inducing cell injury and necrosis. C5b-9 also activates neutrophils and endothelium by upregulating adhesion molecules and promoting the release of cell stimulants such as hydrolytic enzymes, reactive oxygen species, arachidonic acid metabolites, and cytokines. In addition, C5b-9 can enhance the procoagulant properties of the endothelium	ELISA for C3/C3 split products, C4/C4 split products, C5/C5a split products, TCC, FH, properdin. C4d staining of kidney biopsies	(46–49)
Kidney transplant injury	Antibody-mediated renal injury; individuals with pre-existing circulating antibodies are at high risk to develop complement-dependent reaction against transplanted kidney; local synthesis of complement components together with loss of regulatory mechanisms for complement activation, especially of C3, C5 and TCC.	ELISA for C3/C3 split products, C4/C4 split products, C5/C5a split products, TCC, FH, properdin. C4d staining of kidney biopsies	(47, 49, 50)
Multiple sclerosis	Inflammatory, demyelinating disease of the central nervous system that leads to variable axonal and neuronal damage. Causes are largely unknown. Depositions of C1q, C3d, and C5b-9 in white matter lesions of MS. Complement proteins, activation products and inhibitors were found at MS plaques. Astrocyte-enriched extracellular vesicles derived from the plasma of MS patients contained high levels of C1q, C3, C3b, iC3b, C5, and C5a. C3a in CSF at baseline assessment of patients with clinically isolated syndrome and newly diagnosed relapsing-remitting MS could be a promising prognostic marker of disease activity Also genetic variants were identified, for instance in MASP1 and C2 to be associated with the disease.	ELISA for C3 and C3 activation products such as C3a	(32, 36)
Myasthenia gravis (MG)	MG is an antibody-mediated autoimmune disease of the postsynaptic neuromuscular junction presenting with a fluctuating degree of weakness in ocular, bulbar, limb, and respiratory muscles. Activation of complement *via* disease-specific autoantibodies to the acetylcholine receptor (AChR). Inhibition of C5 or TCC could be beneficial in refractory MG	ELISA for C5/C5a, TCC	(36, 51)
Myocardial infarction	Complement activation is an important factor for inflammation and injury of ischemic and infarcted myocardial tissue. Lectin pathway main driver in myocardial reperfusion injury. Complement-derived effector molecules as described above are involved in producing the inflammation, tissue injury, and necrosis of the heart tissue during reperfusion	Analysis of terminal pathway component C3/ C3 split products, C5/C5 split products and TCC	(52)
Neuromyelitis optica	Neuromyelitis optica spectrum disorder (NMOSD) is an autoimmune inflammatory disease of the central nervous system (CNS), characterized by pathogenic, complement-activating autoantibodies against the main water channel in the CNS, aquaporin 4 (AQP4)	Anti-AQP4 autoantibodies	(53)
Organ transplantation	C3 is activated during transplant and is associated with late allograft damage and rejection. C5a and C3a anaphylatoxins increase the inflammatory response. C5a fragment serves as a chemotactic agent for neutrophils and macrophages, there is also evidence that C3a induced chemotaxis of monocytes and mast cells. In Antibody-mediated rejection (AMR), donor-specific antibodies (DSAs) form immune complexes on the surface of (kidney) allograft endothelium bind C1q complement component, leading to the activation of the classical complement pathway. The C4d fragment formed following this activation, and deposited in the peritubular capillaries of the kidney allograft, is an important biomarker of antibody-mediated rejection	ELISA for C3/C3 split products, C4/C4 split products, C5/C5a split products, TCC, FH, properdin. C4d staining of kidney biopsies	(29, 47, 54)
Parkinson disease (PD)	PD is characterized by dopamine deficiency at the basal ganglia and deposition of a-synuclein that forms Lewy bodies. However, the exact neuropathologic mechanisms remain elusive. Studies regarding the role of complement in PD are controversial. Some reported the involvement of the classical complement pathway by recognizing anti C3d, C4d, C7 and C9 antibodies in substantia nigra or by the aggregation of iC3b and C9 in	ELISA for clusterin and C1r	(36, 55–58)

(Continued)

TABLE 1 Continued

Disease	Mechanism	Recommended analysis	Ref.
	Lewy bodies of PD patients. Other studies failed to correlate complement activation with cortical Lewy Bodies. Clusterin and complement C1r were decreased compared to controls and have been proposed as useful biomarkers of disease progression		
Paroxysmal nocturnal haemoglobinuria (PNH)	PNH is a rare disease that presents clinically with a variety of symptoms, the most prevalent of which are hemolytic anemia, hemoglobinuria, and somatic symptoms including fatigue and shortness of breath. In patients with PNH, CD55 and CD59 are lacking, and RBCs undergo excessive complement-mediated hemolysis leading to hemolytic anemia, thrombosis, renal dysfunction, and pulmonary hypertension	CD55, CD59, fluorescently labeled aerolysine (FLAER) test	(59)
Periodontitis	Inflammatory disease in tooth-supporting tissues, induced by bacteria growing in a biofilm on tooth surfaces. Components of the complement system are present in the periodontal tissue leading to local induced complement activation. C1q, factor B, factor Bb, C3, C3a, C3b, C3c, C3d, C4, C5, C5a, C5b and C9 have all been detected in diseased periodontal tissue	ELISA for C1q, factor B, factor Bb, C3, C3a, C3b, C3c, C3d, C4, C5, C5a, C5b and C9	(60)
Polytrauma	Evidence of systemically increased complement activation: C3a, C5a, high C3a/C3 ratio in case of organ dysfunction after trauma. Predominance of alternative pathway activation. C5a is seen to delay the fracture healing by delaying neutrophil apoptosis and delaying recruitment of osteoblast and osteoclast progenitors.	CH50, MBL, C3a, C5a, SC5b-9, C4BP total, C4BP-β, and factor I by ELISA	(61–63)
Refractory generalized myasthenia gravis (gMG). See also myasthenia gravis	gMG is a rare autoimmune disorder characterized by skeletal muscle weakness caused by disrupted neurotransmission at the neuromuscular junction. Autoantibodies attack acetylcholine receptors, which are essential in facilitating muscle contraction and movement.	ELISA for C5/C5a, TCC	(29, 36)
Rheumatoid arthritis	Evidence suggesting complement activation in synovial tissue. Increased levels of C2, C3 and C3a in RA patients	C2, C4b, C5a, FD, MBL, FI, C1q, C3,C3a, C3b C4, FB, FH, properdin, TCC	(64)
Schizophrenia	Genetic variant in *C4A* associated with increased risk. Increased copy number of *C4A*	Genetic variant analysis *C4A*	(65)
Sepsis/multi-organ dysfunction	Hyperinflammatory response after infection (cytokine storm). Increased levels of C3a, C5a and TCC. Excessive complement activation and consumption during septic shock.	ELISA for C3, C3a,C3c, C5, C5a, and TCC (sC5b-9), CH50	(66–68)
Skin diseases	Excessive complement activation, may be caused by autoantibody-induced cytotoxic effects of TCC on epidermal or vascular cells thereby causing inflammation.	Analysis of terminal pathway components, such as TCC	(69)
Systemic lupus erythematosus (SLE)	Genetic variants in *C1Q, C2, C4, CR2, CR3*; impairment of complement-mediated clearance of immune complexes and apoptotic cells. Autoantibodies against C1q.	CH50, functional ELISA for CP. ELISA for C4 (C4a/b), C1q, C3, C3a, C3d, TCC, anti-C1q autoantibodies	(39, 40)
Thrombotic thrombocytopenic purpura (TTP)	Excessive AP activation. Functional deficiency of ADAMTS13 plays a substantial role in the development of TTP. Increased complement activation, increased levels of complement activation markers C4d, C3bBbP and C3a.	C3, Factors H, I, B and total alternative pathway activity together with complement activation fragments (C3a) or complexes (C1rs-INH, C3bBbP, sC5b9) measured by ELISA or RID.	(70)
Trauma (see also polytrauma)	Evidence of systemically increased complement activation: C3a, C5a, high C3a/C3 ratio in case of organ dysfunction after trauma. Predominance of alternative pathway activation. C5a is seen to delay the fracture healing by delaying neutrophil apoptosis and delaying recruitment of osteoblast and osteoclast progenitors.	CH50, MBL, C3a, C5a, SC5b-9, C4BP total, C4BP-β, and factor I by ELISA	(61–63)
Urticarial vasculitis (see also Hypocomplementemic Urticarial Vasculitis Syndrome)	Exact pathophysiology unknown. Rare immune complex-mediated small vessel vasculitis characterized by urticaria, hypocomplementemia (low C1q, C3, and C4), and systemic manifestations, and it is also associated with circulating anti-C1q autoantibodies	ELISA for C1q, C3, C4, autoantibodies against C1q	(39, 40)
Uveitis	Inflammation of the uvea, the pigmented layer that lies between the inner retina and the outer fibrous layer composed of the sclera and cornea. Presence of autoantibodies activating complement.	Human C3a radioimmunoassay Immunoelectrophoresis (IEP)	(71)

systemic inflammation and failure of organs such as the eyes, kidneys, skin, brain and vascular system (75–77). Because of the large number of complement-mediated diseases, together with recent results from large-scale genomics and proteomic studies (78, 79), the interest in the complement system has renewed, especially as a promising target for therapeutic intervention. This was demonstrated more than a decade ago by the first complement-specific drug, eculizumab (Soliris, Alexion), targeting the key complement component C5 (29). In recent years, human complement studies have become very important in drug delivery, nanomedicine and biomaterial fields, as elegantly summarized by Moghimi and coworkers (80, 81). Interestingly, assessment of complement within these fields is often performed using incorrect or suboptimal assays and samples that were inappropriate handled regarding collection, storage and pre-analytical preparations (80). As complement is involved in an increasing number of human diseases, standardized measurement of complement components is essential (1–5, 82). However, accurate determination of the complement status of individual patients has proven still to be challenging and needs to be performed in a uniform way.

To provide insight into the current practice in complement measurements at individual labs, we conducted a systematic literature search in which we reviewed which sample type and techniques were used for the assessment of complement activation in the past five years. The studies were assessed for their quality based on the recommended guidelines for studying complement activation as described below.

Current guidelines for assessing complement activation

For accurate complement analysis, it is important that the complement activation is blocked at blood sampling since activation *ex-vivo* during sample processing may alter the results of interest (2, 12). Hence, appropriate pre-analytical sample handling is a necessity to avoid erroneous results. For complement analysis, samples may be assessed either for complement function or quantification of individual complement components (2, 3, 83). Both types of analysis require a specific approach regarding the sample type, pre-analytical sample handing and measurements.

Assessment of complement function

For assessing the ability of complement activation, serum samples should be used (84). Whole blood should be collected in serum tubes. These collection tubes are available either with or without a clot activator (e.g. silica). Note that some complement analyses may be affected by the type of collection tube, e.g. ficolin 2 is depleted in serum retrieved from tubes with silica, which should especially be taken into account when assessing the lectin pathway (80, 85, 86). Let blood coagulate for approximately 30 min at RT. Please be aware that blood coagulation kinetics are slightly slower in tubes without a clot activator, so ensure complete clot retraction. Optimize if needed. For both type of serum collection tubes, separate the serum fraction by centrifugation (2000*xg*, 10 min) at 4°C. Process serum within 1 h. Complement activation is temperature-dependent so always keep serum on ice to avoid *ex-vivo* complement activation (12, 80, 81, 87, 88). Store serum samples at -80°C since storage at higher temperatures such as -20°C will create a slow freezing rate that allows for complement activation. Mechanical stress (rigorous shaking or vortexing) and repeated cycles of freezing and thawing should be minimized as much as possible since every cycle may increase complement activation (2, 84) (Figure 2A). Next to serum, also Hirudin-plasma (or Lepirudin; recombinant Hirudin) can be used for the assessment of complement function as Hirudin blocks coagulation but allows complement activation (when used in low concentrations: 0.2 IU/mL and 2 IU/mL) (89). As complement is also activated by a low pH (<7.1), it is advised to monitor and control it (with appropriate buffers) to avoid erroneous measurements (90).

For studying complement function, it is of utmost importance that the appropriate buffers are used. For assessing CP and LP activation, buffers containing both Ca^{2+} and Mg^{2+} should be used. These cations are required in order to form protein complexes which initiate or mediate progression of complement activation. Ca^{2+} is essential for the activation of CP and LP protease complexes that cleave C4 and C2 (91, 92), whereas Mg^{2+} is needed for the binding of C2 to C4b to form CP/LP C3 convertases (93). For studying AP activation, CP and LP activity must be blocked by adding ethylene glycol tetraacetic acid (EGTA) to chelate Ca^{2+} (Figure 1). Additionally, an optimal concentration of Mg^{2+} is required since the binding of Factor B to C3b to form the AP C3 convertase is Mg^{2+}-dependent (3, 94). Traditional complement buffers like GVB++ (gelatin veronal buffer) contain 0.15 mM Ca^{2+} and 0.5 mM Mg^{2+}. Hirudin or lepirudin do not interfere with divalent cations.

For assessing complement function, several techniques and assays are available (Figure 2B). Traditionally, complement function of the CP and AP was assessed using respectively the CH50 and AH50 hemolytic assays. These assays detect reduction, absence and/or inactivity of several components of the complement pathway. The CH50 is based on the capacity of serum to activate complement *in-vitro* and subsequently lyse sheep erythrocytes opsonized with anti-sheep antibodies (usually rabbit IgG) *via* the CP. The AH50 is based on complement-dependent lysis of rabbit erythrocytes, which cannot recruit the soluble human complement regulator Factor H, thereby allowing for AP activation (95). If one or more complement components are absent (e.g. due to a genetic deficiency) or their levels decreased (e.g. due to overactivation leading to consumption), hemolytic activity is decreased. When both assays are performed side-by-side, they can indicate C3 and terminal pathway (TP) deficiencies (C5, C6, C7, C8, and C9; absence of hemolysis in both CH50 and AH50), CP deficiencies (C1, C2, C4; absence of lysis in CH50 only) and AP deficiencies

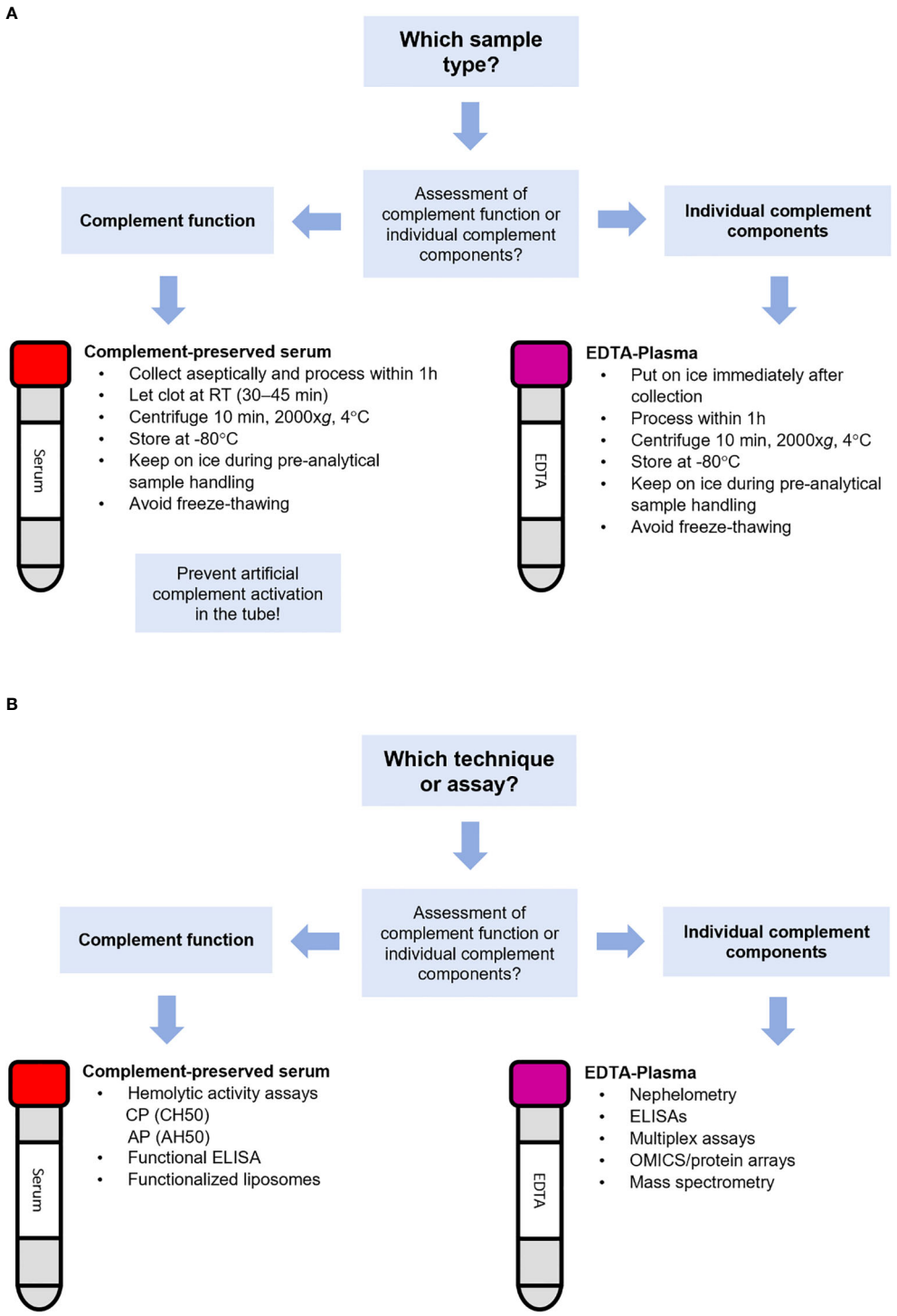

FIGURE 2
Flowchart for the selection of the appropriate sample type and technique for complement analysis. Flowchart for selection of **(A)** the appropriate sample type or **(B)** the appropriate technique for the assessment of complement.

(Factor B, D, H, I, properdin; absence of lysis in AH50 only). Factor H and Factor I deficiency can also result in C3 consumption as a result of uncontrolled AP activation, leading to low CH50.

Complement function can also be assessed using functionalized enzyme-linked immunosorbent assays (ELISA), which are considered more accurate and reproducible and are less prone to variation. This type of assays uses plates coated with either IgM, mannose or lipopolysaccharides (LPS) to examine CP, LP or AP activation respectively. In the presence of the appropriate buffers, complement is activated in the patient's serum sample (at 37°C). Next, pathway activation is assessed by the detection of C5b-9 in the terminal pathway using a specific conjugate antibody directed to a neo-epitope in C5b-9 (12, 96, 97). These assays require a relatively high sample dilution to prevent cross-pathway interference. However, using a sample dilution that is too high might lead to false negative results. When concentrations for critical complement components needed for complement activation are too low, the pathway will not be activated. As the window for the correct sample dilution is rather small, it is easily missed. Therefore, this high sample dilution may be considered as a drawback when these types of assays are used.

A third type of assay for assessing complement function is the liposome immunoassay. This type of assay consists of liposomes coated with antigens (for instance with dinitrophenyl (DNP)) and containing a reporter molecule (signal-producing molecules). When serum is mixed with the liposomes and an antibody-containing reagent (in this case anti-DNP), the formed immune complex will trigger complement activation resulting in disruption of the liposomes and release of the entrapped reporter molecule from the lysed vesicles. The degree of reporter release corresponds to the degree of complement activation and can easily be measured (98, 99).

Assessment of individual complement components

For analysis of individual complement components, EDTA-plasma should be used having at least a final concentration of 10 mM (82, 100), especially when measuring activation products. Using EDTA-plasma, any further activation of complement is minimized (but not completely excluded) since EDTA chelates Ca^{2+} and Mg^{2+} thereby blocking the function of the C1 complex and the C3 convertases (4, 83, 100–102). Of note, nafamostat mesylate (0.2 mg/mL) can be used in addition to EDTA to maximize inhibition of artificial complement activation (100). Heparin-plasma should be avoided as heparin interacts with many complement proteins and regulators such as C1, C1q, C1-INH, C2, C4, C4b, C4BP, MASP-1, MASP-2, C3, C3b, FB, FD, FH, properdin, C6, C8, C9 and vitronectin, thereby affecting complement function (84, 103). Low levels of heparin (<2 IU/mL) can activate complement whereas high levels (20 IU/mL) inhibit complement activation (89). If possible, we recommend to also avoid citrate-plasma for the assessment of complement components. Although differences in concentrations for markers such as C4d, Bb, C3a, C5a and sTCC are very small between freshly processed EDTA- and citrate-plasma samples, these markers are more stable in EDTA-plasma when stored longer at either RT or 4°C before processing. Citrate-plasma also tends to be more sensitive for freeze-thawing (83, 104). Serum cannot be used for the assessment of individual complement components, especially activation products. Due to the absence of complement inhibitors, artificial complement activation during collection, shipment, processing and/or pre-analytical sample handling will cause an increase of many complement components making reliable determination of these markers impossible (83, 104).

EDTA-whole blood should be kept on ice and centrifugated at 4°C within 60 minutes after collection. Keep transportation and logistics of samples from the patients to the lab as short as possible and handle samples with care (keep on ice, minimize mechanical stress). Isolated EDTA-plasma should be kept on ice and as soon as possible snap-frozen and placed in -80°C. Shipment of EDTA-plasma for complement analysis should always be done on dry ice. EDTA-plasma for complement marker analysis should be thawed and kept on ice and repeated freeze-thawing should be avoided. Different markers have various sensitivity to freeze-thawing (100). Note that EDTA-plasma should not be used for functional complement testing in the assays described above as these assays detect *in-vitro* complement activation which is inhibited by EDTA (1) (Figure 2A).

Several techniques for analysis of complement components are available (Figure 2B). In most clinical laboratories, analysis of individual complement components such as C3, C4 and sometimes C5 is performed by nephelometry or turbidimetry. These techniques are widely used in clinical laboratories because they are relatively easily automated and inexpensive. However, a major drawback of nephelometry and turbidimetry is that it cannot distinguish between the native non-activated complement protein and its activated split products. For instance, for C3 it will detect both the intact non-activated C3 and its activated proteolytic fragments C3a, C3b, iC3b, C3c and/or C3d (105). Another drawback of is that these methods use a relatively large sample volume. This is especially a challenge for complement analysis in young children, of whom often only small amounts of sample is available.

ELISA is a technique also widely used for quantification of individual complement components, its activated split products and complement regulators. When using well-defined antibodies, ELISA can quantify complement-derived split products next to the native intact protein, reflecting the actual state of complement activation (2, 3, 105). For measuring the specific complement activation products antibodies recognizing split-product-specific neoepitopes, i.e. neoepitopes that only

become exposed after cleavage of the native protein, should be used. In addition, detection of split products generated *via* complement-independent bypass routes is possible (106).

Next to ELISA, a more recent technique being developed for the quantification of individual complement components and their split products is (in most cases bead-based) multiplex assays. Such assay is, in principle, a combination of immunoassays thereby able to analyze multiple analytes at the same time. Next to the advantages of saving time and sample volume, these assays provide a comprehensive overview of the patient's complement activation status in a single run (107). Currently, the specificity of these commercial bead based multiplex complement assays is still under debate (107, 108) which argues thorough validation of its use in comparison to existing assay formats.

Methods

Systematic literature review

Our systematic review procedure was adopted from the Preferred Reporting Items for Systematic Reviews and Meta-Analyses (PRISMA) guidelines (109). Structured literature searches using the Pubmed/MEDLINE database were performed in February 2022. Search terms included the medical subject headings (MeSH) terms for: "Complement C3" OR "Complement C3a" OR "Complement C5" OR "Complement C5a" OR "Complement Membrane Attack Complex" AND "Complement activation" to retrieve all studies assessing these complement components. Supplementary Dataset 1 lists all keywords captured by the MeSH terms used. Next, titles and abstracts were screened by two independent researchers (ET and RB) to determine if the study met the inclusion criteria (see below). Studies potentially of interest were selected and full text papers were retrieved for in-depth review.

Inclusion criteria

All studies that assessed the complement components C3, C5 and/or their split products C3a and C5a and/or sTCC (MAC, sC5b-9) in human blood samples (serum and plasma) that were published in peer-reviewed journals between February 2017 and February 2022 were included.

Exclusion criteria

The following studies were excluded: not assessing complement components C3, C5 and/or their split products and/or sTCC in human blood samples, animal studies, *ex-vivo* stimulation studies, reviews or editorials, studies in languages other than English and no full text available. The selection process was performed by two authors (ET and RB), based on titles, abstracts, and subsequently full text papers.

Quality assessment

Subsequently, studies that passed the inclusion criteria were categorized according to sample type and techniques used for complement assessment. Studies that were identified as using the correct sample type for their complement measurements (according to the guidelines addressed above and in Figure 2) were scored regarding overall quality standards for performing research, using the following criteria (110):

1. Did the study provide sufficient information regarding the experimental design and methods (e.g. appropriate method/approach to investigate study aim, clear which analyses were performed in which experimental groups/samples)?
2. Were the baseline characteristics sex and age checked and matched in the control cohorts used for the study?
3. Was sample collection, storage and handling performed according to the requirements for assessment of complement components as outlined in this paper?
4. Were measurements performed in a blinded fashion?

Using these criteria, the nominated studies were awarded a score ranging from 0 to 4, 1 point per met criterion.

Assessment of C3, C5, their split products and sTCC in human samples to demonstrate the effect of (in)correct pre-analytical sample handling, antigenicity and selecting the appropriate technique

Three experiments were performed to illustrate the importance of correct pre-analytical sample handling and complement assessment.

In the first experiment, we tested the effect of artificial complement activation in the tube induced by inappropriate pre-analytical sample handling. The components C3c and sTCC were measured in complement-preserved serum samples (n=5) and in plasma samples anticoagulated either with citrate, heparin, EDTA 10 mM (normal EDTA blood collection tube, no extra EDTA added) and EDTA ≥20 mM (normal EDTA blood collection tube with extra EDTA added) (n=5 for each anticoagulant). All samples used for this experiment were derived from healthy controls (HC). Plasma samples were put on ice immediately after collection and processed within 1 h (centrifuged for 10 min., 2000x*g* at 4°C and stored at -80°C until further use). Complement-preserved serum samples from were collected aseptically and processed within 1 h (clotted at room RT 30-45 min., centrifuged for 10 min., 2000x*g* at 4°C and stored at -80°C until further use). Aliquots for all samples were thawed and incubated either at RT or on ice for 10 min, 1 h, 2 h and 16 h before measurements. Subsequently, C3c and sTCC levels were

measured by commercially available solid-phase ELISA assays according to the manufacturer's instructions (Cat# HK368 (C3c), HK328 (sTCC), Hycult Biotech, Uden, The Netherlands). Assays are specific for these markers and do not detect other activation products (e.g. C3b, iC3b, C3d) or components not integrated in the TCC. The levels measured in the samples incubated for 10 min were used as a baseline and were set to 100%. All other timepoints were compared to baseline.

Secondly, we assessed C3 concentrations in EDTA-plasma derived from HC (n=6) using two in-house assay designs. These assays did not differ from each other, except for the capture antibody to test the effect of (differences in) antigenicity between antibodies. Samples were collected and handled as described above. Samples were thawed on ice and kept on ice during pre-analytical sample handling. Two distinct capture antibodies were used, recognizing a different epitope in the C3 protein, i.e., the monoclonal antibody clone 3E7 (cat# HM2286) *versus* the monoclonal antibody 1H8 (cat# HM2287; Hycult biotech, Uden, The Netherlands). Antibody concentrations and all other reagents and buffers (HK355; Hycult biotech, Uden, The Netherlands), as well as the calibrator (human native C3; cat#113, Complement Technology, TX, USA) were the same between the two assay designs and assays were performed by the same operator on the same day. C3 concentrations were measured using both setups in parallel according to manufacturer instructions. Briefly, microtiter wells (Nunc maxisorp cat# 468667, Thermo Fisher Scientific, Waltham, MA, USA) were coated either with clone 3E7 or 1H8 at 4°C overnight (5 µg/ml) in 1x PBS. After blocking with 1x PBS, 1% BSA for 1 – 1.5 hours, wells were washed four times using 1x PBS, 0.05% Tween 20. Calibrator was added to the wells in a 2x serial dilution ranging from 500 to 7.8 ng/ml in dilution buffer (DB; 1x PBS, 0.1% BSA). EDTA-plasma samples were added to the wells in a serial dilution ranging from 1:500 to 1:64000, also in DB. Both calibrator and samples were incubated 1 h at RT. For both assays the same detection antibody was used (monoclonal antibody clone 474; cat# HM2073, biotinylated; Hycult biotech, Uden, The Netherlands). After washing, wells were incubated with detection antibody (0.1 µg/ml in DB) for 1 h at RT. Again, wells were washed and tetramethylbenzidine substrate (TMB; K-blue aqueous; Neogen, Scotland, UK) was added starting an enzymatic reaction that produced a colored product that can be measured. Reaction was stopped after 30 min. by adding oxalic acid and the absorbance at 450 nm was measured.

The third experiment focused on choosing the appropriate marker, accompanied by the correct technique and the added value of quantifying both native complement proteins and their split products in parallel in patients with a severe acute respiratory syndrome coronavirus-2 (SARS-CoV-2) infection. Results were adapted from a previously reported study (66). The complement markers C3, C3a, C3c, C5 and sTCC were assessed in EDTA-plasma samples from patients with PCR-proven or clinically presumed Corona Virus Disease 2019 (COVID-19) admitted to the intensive care unit (ICU) and in HC. Also here, EDTA-plasma samples were collected, processed, and handled as described above. Complement measurements were performed using commercially available solid-phase ELISA assays according to the manufacturer's instructions [Cat# HK355 (C3), HK354 (C3a), HK368 (C3c), HK390 (C5), HK328 (TCC), Hycult Biotech, Uden, The Netherlands].

Statistics

Continuous data were presented as the mean ± SEM following criteria for normal distribution. Data were analyzed using a (paired) student t-test, ANOVA or Mann-Whitney test where appropriate (Graphpad Prism 8.4.2, San Diego, CA, USA). A p-value <0.05 was considered significant.

Ethics statement

The study protocol was approved by the local ethics committee (CMO 2020 6344 and CMO 2016 2963) and performed in accordance with the latest version of the declaration of Helsinki and guidelines for good clinical practice (GCP).

Results

Systematic literature review

A systematic literature review was conducted to provide a comprehensive overview of the methods and sample types used for the assessment of complement markers during the period February 2017 – February 2022. Subsequently, we assessed whether the identified studies performed their complement analyses in a reliable manner regarding techniques and sample types. We focused on the key complement markers C3, C5 and their split products C3a and C5a, and sTCC.

In total, 441 records were identified through database searching using the indicated MeSH terms (Figure 3). After excluding non-English papers, animal studies, reviews/editorials and records of which no full text was available, 376 records remained (Supplementary Dataset 2). These remaining abstracts were screened based on whether levels of the complement components C3, C5 and/or their split products and/or TCC were assessed in human blood. Studies performing *ex-vivo* stimulation experiments, assessing complement deposition in

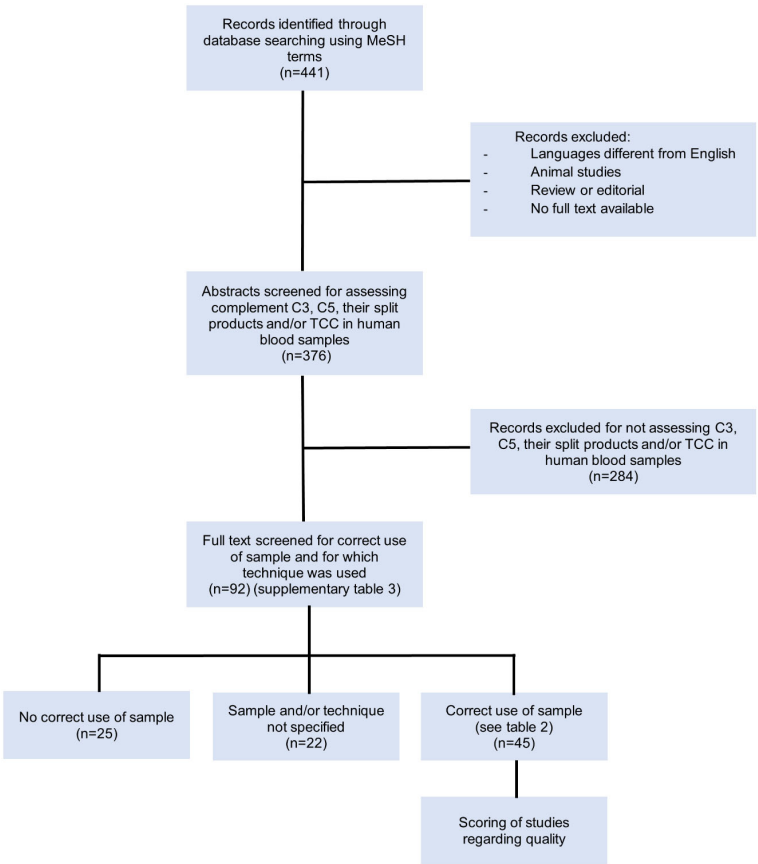

FIGURE 3
Flowchart of the systematic literature search selection process.

tissues or using cultured cells were excluded. A total of 92 articles were selected for full text analysis. Study characteristics such as aim of the study, experimental set-up and used techniques were recorded (Supplementary Table 1).

Regarding the techniques used for measuring complement components in these 92 studies, 69 studies used ELISA (75%), 12 studies (13%) used turbidimetry/nephelometry and three studies (3%) used mass spectrometry. Nine studies (10%) used other techniques and 11 studies (12%) did not specify the technique that was used (Figure 4). Several studies used more than one technique for their measurements, hence the number of performed analyses is higher than the total number of the identified studies.

These 92 identified studies were assessed on whether complement measurements were performed correctly and reliably concerning sample type, pre-analytical sample handling and techniques with regard to the complement components being investigated. This resulted in the identification of three distinct groups (Figure 4; Supplementary Table 1):

1. Studies identified as using the correct sample type for assessing complement activation products (mostly EDTA-plasma) (n=45; 49%) (Table 2).
2. Studies identified as not using the correct sample type (mostly serum) (n=25; 27%).
3. Studies that did not specify the sample matrix or the techniques used for measuring complement (n=22; 24%).

Studies identified as using the correct sample type for assessing complement activation products

For the 45 studies identified as using the correct sample type (mostly EDTA-plasma), ELISA was the method of choice (n=43; 96%), sometimes supplemented with other techniques such as nephelometry or rocket immuno-electrophoresis (n=6; 7%). In this first group, roughly two categories could be identified: studies investigating complement in health and disease (n=39;

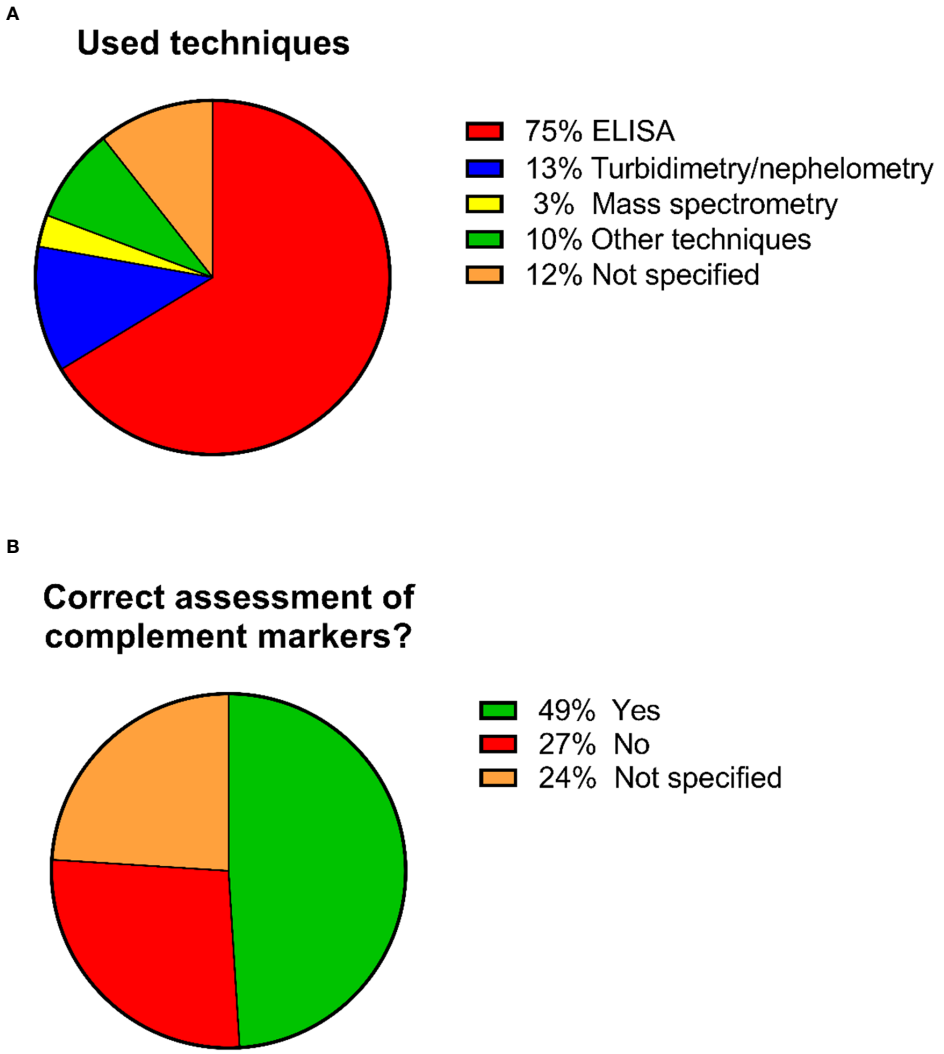

FIGURE 4
Pie charts showing the percentages regarding the used techniques and whether the correct sample types were used for complement assessment. A total of 92 studies were included in the analysis. **(A)** Percentages regarding the used techniques. Several studies used more than 1 technique for their measurements, hence the number of performed analyses is higher than the total number of the identified studies. **(B)** Percentages of studies that used/did not used the correct sample type for complement assessment.

87%) and studies with a technical aim such as development or improvement of new tools and assays (n=6; 13%). Regarding studies investigating complement in health and disease, 31 studies assessed complement markers in patients compared to controls in a wide range of infectious, autoimmune, inflammatory and inflammatory-associated diseases or conditions (66, 111–140). A total of 8 studies focused on complement regulation and activation after treatment in patients (141–148). Regarding the technical studies, 3 studies described the development of new tools or assays (149–151) and 3 studies focused on the development/improvement of new methods or procedures (152–154) (Table 2). Next, these 45 studies were scored regarding overall quality standards according to the criteria listed in the methods section. This resulted in a total score ranging from 0 to 4. All studies but one (score=2) reached a good score of 3, indicating that all the criteria were met except that analyses were not performed in a blinded fashion or that this was not mentioned (Table 2).

Studies identified as not using the correct sample type

A total of 25 studies (27%) were identified as not using the correct sample type for the complement measurements (Figure 4; Supplementary Table 1). Most of these studies used serum samples

TABLE 2 Overview of the 45 selected studies that assessed complement components *ex-vivo* in the past 5 years (2017-2022).

Author	PMID	Aim of the study	Groups analyzed	Complement markers	Sample matrix	Technique used for analysis	Scoring criteria 1	2	3	4	Total	Ref.
Witczak BJ	34759922	Investigate posttransplant complement activation in long-term kidney graft and survival in kidney transplant recipients	Kidney transplant recipients	TCC	EDTA-plasma	ELISA	1	1	1	–	3	(98)
Liu M	34671343	Investigate complement proteins as early-pregnancy predictors and potential diagnostic markers of preeclampsia	Healthy and preeclampsia pregnant women before delivery	C3a, C5a	EDTA-plasma	ELISA	1	1	1	–	3	(60)
Pache F	34464830	Investigate C3 and C4 levels in AQP4-IgG+ neuromyelitis optica spectrum disorder, myelin oligodendrocyte glycoprotein antibody-associated disease and multiple sclerosis patients	MOGAD, MS and HC	C3	EDTA-plasma	Immunoturbidimetry assay	1	1	1	–	3	(61)
Michels MAHM	34456924	Assess CP convertase activity in C3G and IC-MPGN (immune complex-mediated membranoproliferative glomerulonephritis) patients	C3G, IC-MPGN patients, HC	C5, TCC	EDTA-plasma	ELISA	1	1	1	–	3	(62)
Nilsson PH	34380648	Characterize human whole blood ex vivo model based on the GPRP peptide for anticoagulation. Examine its utility to assess the effect of thrombin on complement activation	GPRP- and lepirudin-anticoagulated plasma	C3, C5, C5a, TCC	GPRP- and lepirudin-anticoagulated plasma	ELISA	1	1	1	–	3	(102)
Prens LM	34252397	Evaluate systemic complement activation in patients with hidradenitis suppurativa (HS)	HS patients and HC	C3, C5a, TCC	EDTA-plasma	ELISA, Radial immunodiffusion technique	1	1	1	–	3	(63)
Chiu YL	34177889	Investigate alternative pathway activation and disease activity in IgA nephropathy (IgAN)	IgAN and HC	C5a	EDTA-plasma	ELISA	1	1	1	–	3	(64)
Dhooge PPA	34170959	Assess complement activation in Stargardt disease (STGD1) patients	STGD1 patients and controls	C3	EDTA-plasma	ELISA	1	1	1	–	3	(65)
Sinkovits G	33841446	Investigate complement activation in COVID-19	COVID-19 severity groups	C3a, TCC	EDTA-plasma	ELISA	1	1	1	–	3	(66)
Rognes IN	33832430	Describe complement activation in trauma patients from admission to 10 days after injury	Trauma patients	TCC	EDTA-plasma	ELISA	1	1	1	–	3	(67)
Milosevits G	33549818	Study role complement in infusion reactions (IRs) in pediatric patients treated with Abelcet	Pediatric patients treated with Abelcet	C3a	EDTA-plasma	ELISA	1	1	1	–	3	(93)
De Nooijer AH	33038254	Investigate complement activation in COVID-19	COVID-19 and Sepsis patient vs. controls	C3a, C3c, TCC	EDTA-plasma	ELISA	1	1	1	–	3	(59)
Mastellos DC	32961333	Compare eculizumab with compstatin-based C3-targeted drug candidate AMY-101 in COVID-19	COVID-19 patients treated with Eculizumab *vs.* AMY-101	C3, C3a, TCC	EDTA-plasma	ELISA, nephelometric after PEG precipitation (C3dg)	1	1	1	–	3	(92)
Troldborg A	32941885	Characterization of mAb for C3dg and development of time-resolved immunoassay	The SLE patients and controls	C3dg	EDTA-plasma	ELISA	1	1	1	–	3	(100)
Halkjær L	32431705	Establishing an assay for measuring complement activation at C3 level	SLE patients	C3dg	EDTA, citrate, heparin plasma, serum	ELISA	1	1	1	–	3	(99)

(Continued)

10.3389/fimmu.2022.1007102

TABLE 2 Continued

Author	PMID	Aim of the study	Groups analyzed	Complement markers	Sample matrix	Technique used for analysis	Scoring criteria 1	2	3	4	Total	Ref.
Denzinger M	32281172	Activation of complement at the interface of wound dressings	Healthy controls	TCC	EDTA-plasma	Not specified	–	1	1	–	2	(69)
Grinde D	32152940	Evaluate complement in DiGeorge syndrome	DiGeorge syndrome patients	TCC	EDTA-plasma	ELISA	1	1	1	–	3	(70)
Kristensen MK	32082310	Assess complement in necrotizing soft-tissue infection (NSTI) patients	NSTI patients vs. HC	C3, C3bc, TCC	EDTA-plasma	ELISA	1	1	1	–	3	(71)
Chauvet S	32034108	Investigate complement activation in children with acute postinfectious GN	Children with acute postinfectious GN vs. children with C3G and hypocomplementemia	C3, TCC	EDTA-plasma	ELISA	1	1	1	–	3	(72)
Abe T	31917735	Investigate complement in sepsis, including disseminated intravascular coagulation (DIC)	Sepsis patients with and without DIC.	TCC	EDTA-plasma	ELISA	1	1	1	–	3	(73)
Sartain S	31774252	Asses AP activation in Transplant-associated thrombotic microangiopathy (TA-TMA) after hematopoietic stem cell transplantation (HSCT)	HSCT patients with TA-TMA and without TA-TMA	C3a, C5a, TCC	EDTA-plasma	ELISA	1	1	1	–	3	(96)
Tjernberg AR	31691001	Explore complement response to Streptococcus pneumoniae in celiac disease (CD)	CD vs HC	C3a, TCC	EDTA-plasma	ELISA	1	1	1	–	3	(74)
Faria B	31497011	Investigate effect of intravenous iron on complement activation in-vivo	Non-dialysis vs. dialysis patients	TCC	EDTA-plasma	ELISA	1	1	1	–	3	(91)
Scambi C	31479579	Investigate complement activation in women with antiphospholipid syndrome (APS)	APS non-pregnant patients and pregnant APS women	C5a, TCC	Citrate-plasma	ELISA	1	1	1	–	3	(75)
Schein TN	31461782	Examine TCC levels in HIV patients with poor immune reconstitution	HIV-infected patients and HC	TCC	EDTA-plasma	ELISA	1	1	1	–	3	(76)
Zhang MF	31399080	Asses complement in patients with primary membranous nephropathy (pMN)	Patients with biopsy-proven pMN vs. HC	C3a, C5a, TCC	EDTA-plasma	ELISA	1	1	1	–	3	(77)
Vercauteren KOA	31379459	Assess preanalytical stability of widely used tests to screen complement.	HC	C3d, C3c	EDTA-plasma	ELISA, nephelometric and immunofixation after PEG precipitation	1	1	1	–	3	(104)
Gavriilaki E	31266080	Evaluate complement, endothelial damage, and activation of coagulation in patients with transplant-associated thrombotic microangiopathy (TA-TMA)	Patients with TA-TMA and control HCT recipients without TA-TMA	TCC	EDTA-plasma	ELISA	1	1	1	–	3	(78)
Lynch AM	31203676	Examine complement activation in patients with age-related macular degeneration (AMD), geographic atrophy, and neovascular AMD	AMD patients vs. cataract controls	C3a, TCC	EDTA-plasma	ELISA	1	1	1	–	3	(79)
Elvington M	31019515	Development of an ELISA to quantitate C3(H2O)	Inflammatory-driven diseases vs. HC	C3(H20)	Serum and plasma	ELISA	1	1	1	–	3	(101)
Høiland II	30920726	Investigate TCC and future risk of incident venous thromboembolism (VTE)	VTE patiens vs HC	TCC	EDTA-plasma	ELISA	1	1	1	–	3	(80)

(Continued)

10.3389/fimmu.2022.1007102

TABLE 2 Continued

Author	PMID	Aim of the study	Groups analyzed	Complement markers	Sample matrix	Technique used for analysis	Scoring criteria 1	2	3	4	Total	Ref.
Mansur S	30889724	Study the polyethersulphone (PES) membrane blended with polyurethane (PU) for blood purification applications	Plasma with and without PU	C3a	Citrate-plasma	ELISA	1	1	1	–	3	(103)
Burwick RM	30399106	Evaluate C5b-9 in blood and urine in preeclampsia	Women with preeclampsia with severe features vs. control	TCC	EDTA-plasma	ELISA	1	1	1	–	3	(81)
Rodríguez E	30380547	Investigate complement in AKI pathogenesis.	AKI patients vs. controls	TCC	EDTA-plasma	ELISA	1	1	1	–	3	(82)
Chauvet S	30333829	Investigate complement in patients with C3G with monoclonal immunoglobulin (MIg-C3G)	MIg-C3G patients	C3, TCC	EDTA-plasma	ELISA, nephelometry	1	1	1	–	3	(83)
Bavia L	29908956	Investigate C3d and sC5b9 as biomarkers for myocardial injury	Acute myocardial infarction (AMI) patients vs. controls	C3d, TCC	EDTA-plasma	Rocket immunoelectrophoresis and ELISA	1	1	1	–	3	(84)
Kanni T	29405257	Explore complement activation in hidradenitis suppurativa (HS)	HS patients vs. HC	C5a, TCC	Heparin-plasma	ELISA	1	1	1	–	3	(85)
Siljan WW	29171871	Examine TCC in community-acquired pneumonia (CAP).	CAP patients severity groups	TCC	EDTA-plasma	ELISA	1	1	1	–	3	(86)
Trendelenburg M	29064269	Explore role complement in long-term survival in acute heart failure (AHF)	Patients with AHF vs. HC	C3a, TCC	EDTA-plasma	ELISA	1	1	1	–	3	(87)
Qi J	28801815	Asses complement in thrombotic microangiopathy after allogeneic stem cell transplantation (Transplantation-associated thrombotic microangiopathy; TA-TMA)	TA-TMA patients and patients without TA-TMA)	C3b, TCC	EDTA-plasma	ELISA	1	1	1	–	3	(95)
Togarsimalemath SK	28729035	Describe genetic rearrangements involving multiple CFHR genes leading to a CFHR1-R5 hybrid protein	C3G patients	C3, TCC	EDTA-plasma	ELISA	1	1	1	–	3	(88)
Suffritti C	28707730	Evaluate complement activation in acute episode of congestive heart failure (CHF)	CHF patients	C3, TCC	EDTA-plasma	Radial immunodiffusion and ELISA	1	1	1	–	3	(89)
Grosso G	28669410	Investigate TAFI and TAFIa, complement activation, fibrin clot permeability and fibrinolytic function in antiphospholipid syndrome (APS)	APS patients vs. HC	C5a	Citrate-plasma	ELISA	1	1	1	–	3	(90)
Nilsson PH	28610663	Investigation of a C5a neoepitope exposed on C5 after binding to eculizumab *in-vivo*	Sample pre and post eculizumab treatment	C5a	EDTA-plasma	ELISA	1	1	1	–	3	(94)
Wehling C	27784126	Monitoring of complement activation and eculizumab in complement-mediated renal disorders	aHUS, C3G and ab-mediated renal graft rejection (AMR) patients treated with eculizumab	C3, C3d, C5a, TCC	EDTA-plasma	ELISA	1	1	1	–	3	(97)

10.3389/fimmu.2022.1007102

for measuring individual complement components and their split products. This group also showed a larger variety in techniques used for complement analysis when compared to the group using the correct sample type. ELISA was used in 13 studies (52%), turbidimetry/nephelometry in 7 studies (28%), mass spectrometry in 2 studies (8%) and 5 studies (20%) used other techniques. A total of 5 studies (20%) did not specify the used techniques. Once again, several studies used more than one technique for their measurements, hence the number of performed analyses is higher than the total number of the identified studies.

Studies that did not specify the sample matrix or the techniques used for measuring complement

The last group of 22 studies (24%) did not specify which sample type was used for their measurements. For 6 out of these 22 studies (27%), it is unclear whether serum or plasma was used. The remaining 16 studies (73%) used plasma samples for their measurements but did not specify which anticoagulant tubes were used. Regarding the techniques, 12 studies (55%) reported using ELISA, one study (5%), mass spectrometry and one study (5%) nephelometry. For the remaining eight studies (36%), it is unclear which technology was applied. In addition, little information was provided regarding pre-analytical sample handling and storage (Figure 4; Supplementary Table 1).

Overall, from the 92 selected studies for in-depth analyses, 45 studies (49%) were identified as using the correct sample type for their complement measurements. A total of 47 studies (51%) did not use the correct sample type or it was not clear which sample type was used.

Assessment of C3, C5, their split products and sTCC in human samples to demonstrate the effect of (in)correct pre-analytical sample handling, antigenicity and selecting the appropriate technique

To demonstrate the effect of artificial complement activation in the tube induced by inappropriate pre-analytical sample handling, we measured C3c and sTCC concentrations in complement-preserved serum samples and in plasma samples anticoagulated either with citrate, heparin, EDTA 10 mM and EDTA ≥20 mM. Samples were incubated at RT or on ice for 10 min, 1 h, 2 h and 16 h before measurements. C3c concentrations measured in all plasma samples at RT did not significantly differ from baseline concentrations (10 min) when measured after 1h and 2h. However, both C3c concentrations and the degree of variation between samples increased when plasma samples were measured after 16 h at RT (but this difference did not reach statistical significance due to large variation and low number of samples) (Figure 5A). In contrast, a strong increase in C3c concentrations was observed in complement-preserved serum measured after 1 h and 2 h at RT when compared to baseline and the difference reached statistical significance after 2 h (36342 ± 2685 ng/ml *versus* 15201 ± 2760 ng/ml; p=0.0005). Relative C3c values in serum increased 2.0 to 5.4-fold after 16 h when compared to baseline (Figure 5A). When plasma samples were kept on ice, no differences in C3c concentrations or much variation between samples was observed after 1 h, 2 h and 16 h (Figure 5B). Also for complement-preserved serum on ice, C3c concentrations did not differ at 1 h and 2 h but after 16 h relative C3c values ranged from 0.69 (decrease) to 4.3-fold when compared to baseline (Figure 5B). For sTCC, levels show the same pattern as observed for C3c. For plasma samples, sTCC concentrations at RT did not differ at 1 h and 2 h but after 16 h, both concentrations and degree of variation between samples increased (again this increase did not reach statistical significance due to large variation and low number of samples) (Figure 5C). Of note, sTCC concentrations in complement-preserved serum samples showed a different pattern as observed for C3c. Concentrations tended to be lower at 1 h, 2 h and 16 h at RT but this was not statistically significant (Figure 5C). When samples were kept on ice, all plasma samples showed no differences in sTCC concentrations at 1 h, 2 h and 16 h when compared to baseline (Figure 5D). Concentrations of sTCC in complement-preserved serum samples on ice tended to fluctuate between timepoints but this did not reach statistical significance (Figure 5D). Overall, EDTA-plasma samples showed most stable results regarding C3c and sTCC levels overtime for both RT and on ice. In addition, less variation in concentrations was observed between samples anticoagulated with 20 mM EDTA when compared to 10 mM EDTA (Figures 5A–D).

To illustrate the effect of antibodies that differ in antigenicity, we quantified C3 concentrations in EDTA-plasma samples from healthy controls using two ELISA setups capturing C3 at two different epitopes (Figures 6A, B). Mean C3 values were 2.7-fold higher in the assay in which HM2287 was used as capturing antibody compared to the assay in which HM2286 was used (1223 ± 120.9 µg/ml *versus* 449 ± 28.6 µg/ml; p<0.0001) (Figure 6B).

To demonstrate that choosing the correct technique/approach for assessing complement activation is of major importance for correct interpretation of results, we quantified C3, C3a, C3c, C5 and sTCC using ELISA in COVID-19 patients admitted to the ICU. This technique was chosen because of its ability to quantify and distinguish between native complement proteins and their complement-activated split products. Results show that the EDTA-plasma concentrations for the split/activation products C3a, C3c and sTCC were significantly (p<0.0001) increased in ICU patients when compared to HC. In contrast, C3 and C5 concentrations did not differ between these two groups (Figure 7) (66).

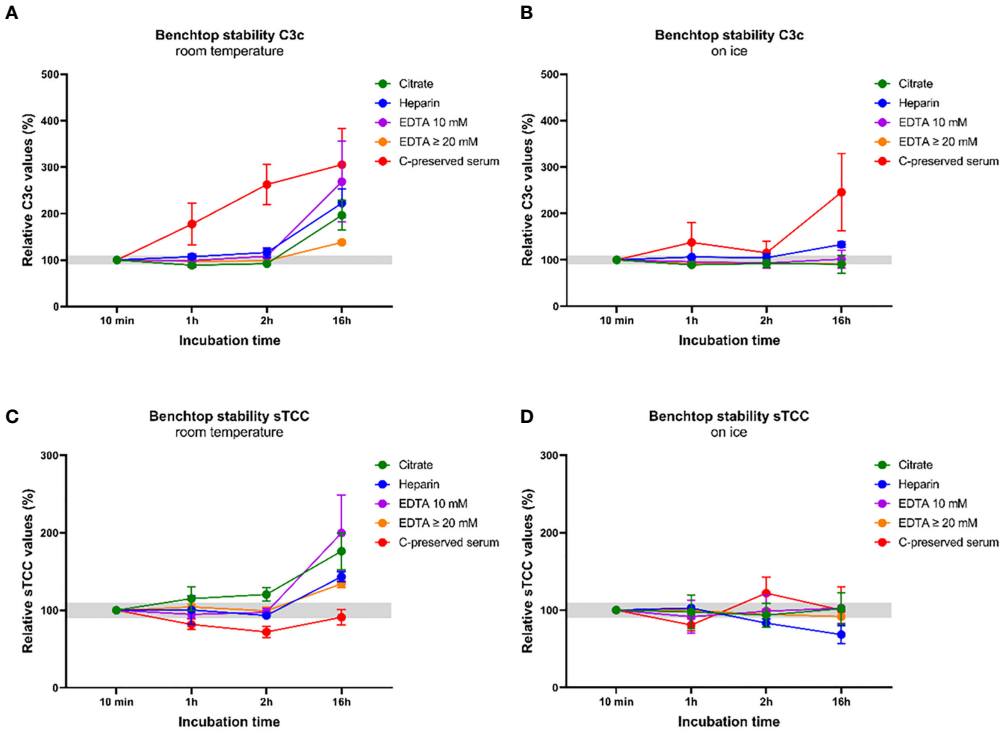

FIGURE 5
Benchtop stability of the components C3c and soluble TCC in serum samples and in plasma samples with different anticoagulants. C3c and sTCC levels were measured in complement-preserved serum samples (n=5) and in plasma samples anticoagulated either with citrate, heparin, EDTA 10 mM and EDTA ≥20 mM (n=5 for each anticoagulant). All samples were thawed and incubated at RT or on ice for 10 min, 1h, 2h and 16h before measurements. **(A)** C3c levels measured after incubation at RT and **(B)** on ice. **(C)** sTCC levels measured after incubation at RT and **(D)** on ice. Samples were analyzed using a serial dilution ranging from 1:50 to 1:400 and data are represented as mean ± SEM. Deviation from baseline ≤10% is highlighted in grey.

Discussion

In this review, we systematically reviewed the available literature in the period 2017-2022 regarding measurements for C3, C5 and/or their split products and/or sTCC in human blood samples and whether these measurements were performed correctly and reliably concerning sample type, pre-analytical sample handling and used techniques and assays.

Out of 376 records, a total of 92 studies were included. From those 92 studies, 45 studies (49%) were identified as using the correct sample type for their measurements. Using our scoring method to assess the overall quality of those 45 studies, most studies showed a total score of 3, indicating good quality. However, it is remarkable that performing a study in a blinded fashion is not standard procedure or is not mentioned. Although beyond the scope of this paper, we would like to stress the importance of basic guidelines and procedures for experiments to assure the quality and integrity of laboratory studies. For instance, ideally samples should be blinded for the operator performing the measurements and experimental groups should be randomly dispersed over the plates. If possible, run all samples on the same plate, especially when samples are paired. This is of course not always possible when the number of samples is too high. In that case, use assays/materials from the same batch to avoid batch-to-batch differences as much as possible. For each separate plate, QC samples with known values should be included on different spots throughout the plate to assess intra- and inter-variability. These procedures for conducting an experiment are often not mentioned.

Twenty-five (27%) studies did not use the correct sample type for their complement measurements. EDTA-plasma is the preferred sample type for measuring individual complement components and their activation products to minimize artificial complement activation. Most of these 25 studies chose serum for their analysis. This does not necessarily mean that the results presented in these 25 studies are unreliable and that these studies are invalid. However, complement components analyses in serum samples can be subjected to artificial complement activation during clotting leading to increased variation in concentrations between samples thereby introducing noise (155). In addition, the identified studies using serum samples did not mention exactly how serum was prepared and what type

of collection tubes (with or without clot activator) were used. As also mentioned above, different serum collection tubes may affect complement analyses of the lectin pathway (80, 85). It has been shown that the use of silica as clot activator results in lower ficolin-2 levels and increased ficolin-1 levels (85, 86). In contrast, ficolin-2 depletion does not occur in serum prepared using collection tubes without a clot activator, but the study of Geno and coworkers showed that ficolin-2 inhibitors arise in serum after long-time storage at -80°C (156). These aspects make accurate measurements and identification of differences in concentrations between experimental groups difficult, especially when these differences are subtle. Complement split products are particularly sensitive to false results and measuring them in serum is not valid.

The third group identified consisted of 22 studies (24%) that did not specify which sample type was used for their measurements. Often, these studies also did not report the technology used for their analyses. Also here, this does not necessarily mean that these studies are of lower quality regarding the assessment of complement. However, for these studies it is very difficult to objectively assess and value the results as it is not clear how these results were obtained. Providing information regarding samples, collection tubes, shipment conditions, pre-analytical sample handling and storage, used techniques and methods is key, not only for assessing complement activation but for performing research in general. Providing this information is not only the responsibility of the authors but also of the reviewers during the peer-review process.

Limitations of the systematic literature review

A systematic review is a powerful analytical tool to collect and analyze data in an objective and standardized way. However, as with all methods, there are limitations. One limitation of our study is that the research question did not include complement components other than the complement markers C3, C5, their split products and TCC. These markers were selected as these are key components of the complement system and, to date, the only approved complement-specific drug targets C5. Another drawback of our study is that systematic searches by using keywords is limited. If MeSH keywords do not match or are not mentioned in titles and/or abstracts, these studies are missed. Next to these 'practical' limitations, we are aware that our systematic search does not fully represent pre-analytical sample handling and complement assessment in a daily diagnostic setting. Complement measurements performed solely for diagnostic purposes are not reported in the Pubmed/MEDLINE database and are therefore missed.

Need for appropriate pre-analytical sample handling and standardized measurement of complement markers

As mentioned in the introduction, there is a high need for appropriate pre-analytical sample handling, storage of samples and standardization of complement testing to be able to compare results between studies and laboratories. Most of the twenty-five studies identified as not using not the correct sample type for their measurements, used serum samples to measure complement activation products.

To provide insight in the effect of artificial complement activation of serum samples in the tube, we measured C3c and sTCC levels in both serum and plasma samples incubated at RT or on ice for several hours. The results clearly show that in serum samples, both C3c levels and variation in levels between samples immediately increases when samples are 'left on the bench' at RT for a couple of hours. For plasma samples, this effect is completely absent for the first few hours and only after 16 h, also here some increase in variation and levels is observed. These effects in plasma after 16 h are expected as it is known that these anticoagulants minimize complement activation but not inhibit it completely (1). Incubating samples on ice most certainly slows down artificial complement activation, as the effects on C3c levels in serum are less pronounced when compared to RT. However, also here it is clear that levels and variation between samples changes over time, thereby obscuring the measurements. More or less the same effects were seen for the sTCC measurements, but it was not expected that levels would decrease in serum samples after incubation at RT. An explanation for this is currently lacking, although when also observing the serum sTCC levels incubated on ice, it is clear that levels varied a lot, making measurements difficult to interpret, especially with these low numbers. Regarding the different plasma samples analyzed in this experiment, results show that the concentrations for both C3c and sTCC remained stable for 2 h at RT and on ice in EDTA-plasma. Although concentrations and variations between samples shifted a little after 1 and 2 h in citrate and heparin plasma, they remained relatively stable when compared to baseline. However, it is well-known from literature that EDTA is more effective in inhibiting complement activation when compared to citrate and heparin (83, 157, 158). This holds true not only for benchtop stability but also after freeze-thawing of samples (83), although the magnitude of effects varies between the different complement components. Overall, these results re-confirm that EDTA-plasma is the most stable sample type for measuring complement activation products. Moreover, our results showed that levels in EDTA-plasma samples with extra EDTA (≥20 mM instead of 10 mM) were more stable when compared to plasma samples with no extra EDTA (normal EDTA collection tube). This might argue

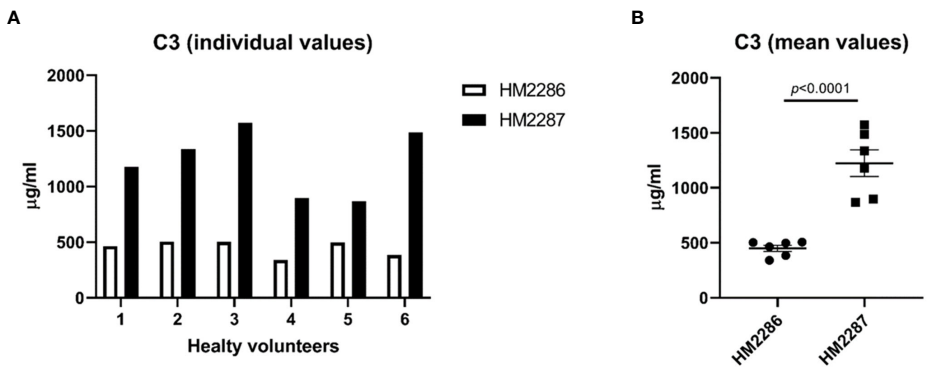

FIGURE 6
C3 EDTA-plasma concentrations in healthy individuals measured using two different assay designs. EDTA-plasma samples were analyzed in duplicates and data are represented as **(A)** individual values and **(B)** mean ± SEM.

for the need of adding extra EDTA when samples are collected for the measurement of complement activation products. However, a larger study is needed to confirm these initial results.

Of note, our guidelines for sample handling are more strict than the actual limits that we (and others) have measured in our experimental set-up with healthy control samples (83). However, importantly, conditions in clinical practice are less controlled than in planned experimental settings of blood collection, as was the case in this study. In addition, samples in which there is already (low-rate) complement activation, *in vitro* activation

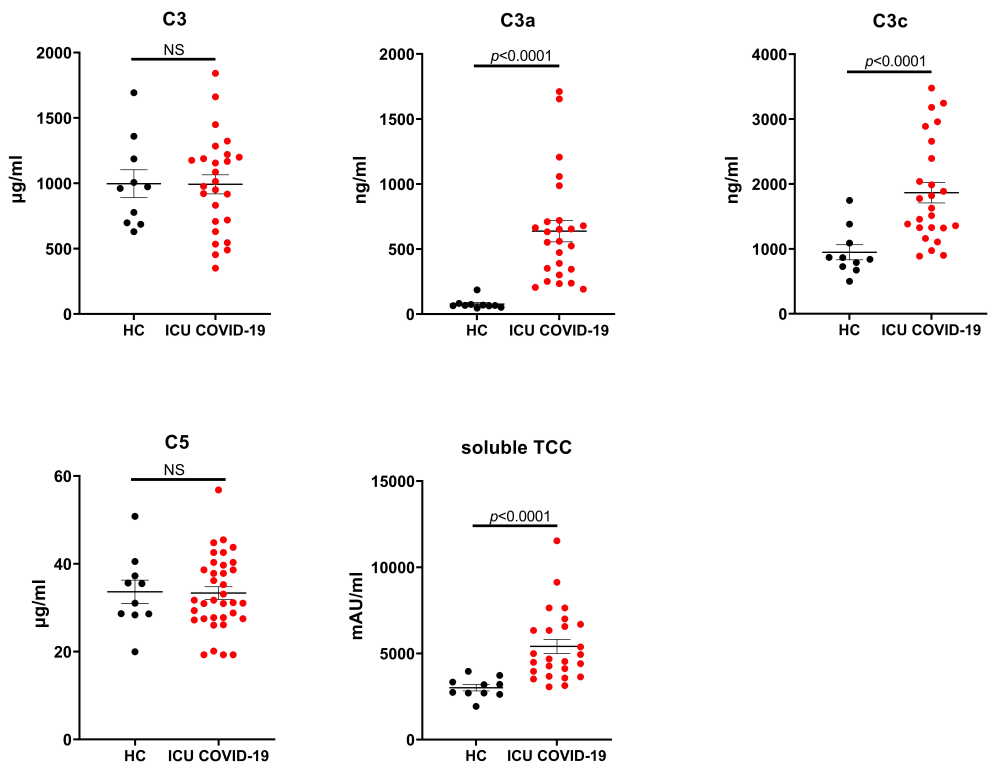

FIGURE 7
C3 and C5 consumption in COVID-19 patients. EDTA-plasma sample values for the markers C3, C3a, C3c, C5 and soluble TCC. Samples were analyzed using a serial dilution ranging from 1:500 to 1:64000 and data are represented as individual values and mean ± SEM. NS, non-significant; HC, healthy volunteers; ICU, intensive care unit; COVID-19, Corona Virus Disease 2019.

may have faster kinetics, making them even more prone to false results after inappropriate handling.

To illustrate the effect of poorly standardized testing, we measured C3 levels in ETDA-plasma from HCs using two assay setups. Both assays were exact the same except that two distinct capture antibodies were used, recognizing different epitopes in the C3 protein. Recognizing alternative epitopes also means that binding affinity for the C3 antigen differs between the two antibodies. Variation in binding affinity will result in different amounts of antigen that can be detected in an assay. Indeed, results showed a 2.7-fold change in mean C3 levels between the two assay setups in this small cohort of healthy individuals. These results show that using two distinct antibodies, recognizing different epitopes of C3, leads to difficulties in assessing and comparing data and may have consequences for interpretation. Differences can be explained by the conformational changes of C3 during activation (159). Together with accessibility, small changes in conformational epitopes can lead to changes in affinity and antibody kinetics when applied in assays. This indicates the need for assays using antibodies that recognize the same epitope within the antigen being measured, especially in the light that antibody-based assays are among the most-preferred methods for complement assessment. Next to that, assays need to be calibrated against uniform protein standards in order to produce results that can be compared between different testing facilities.

Furthermore, our results show that selecting the correct markers, accompanied by the appropriate technique, is of high importance for measuring complement, especially in a diagnostic setting. Our measurements in COVID-19 patients, using dedicated ELISAs for both the native proteins as well as the split products, clearly showed that complement is activated in COVID-19. Levels for the complement activation markers C3a, C3c and sTCC were increased in patients when compared to controls whereas no differences in levels for the native proteins C3 and C5 were detected. Measuring only C3 and C5 plasma concentrations (and not the split products), as performed in most peripheral hospitals handling routine protocols, would have led to the incorrect conclusion that complement is not activated in these COVID-19 patients. Using nephelometry to measure complement activation would, in this case, not suffice as this technique will not distinguish between native complement proteins and its split products and therefore measure a mixture of C3 and its activation products C3a, C3b, iC3b, C3c and C3d. This would have obscured the outcome. Also using ELISAs for only the unprocessed markers C3 and C5 would not suffice is this case. The combination of measurement of native and activated complement fragments would yield more and earlier insights in unexpected protein levels, deficiencies and could aid to predict the remaining complement-activating potential or aid in staging of complement during disease.

These inconsistencies indicate the high need for well-characterized and standardized assays. This need for standardization and well-defined and characterized assays is well-known within the field. It is therefore that in 2009, the Sub-Committee for the Standardization and Quality Assessment of Complement Measurements (the 'Complement EQA Group') was formally recognized and became part of the IUIS (International Union of Immunological Societies) Quality Assessment and Standardization Committee (https://iuis.org/committees/qas/) (2, 82). Next to that, the Complement EQA Group is a standing committee also of the International Complement Society (ICS). The purpose of the EQA group is to facilitate standardized diagnostic complement analysis by developing calibrator materials and test recommendations (2, 82). Initial steps have been made as a serum standard to be used as calibrator for quantitative and functional complement analysis in normal, non-activated human serum (Standard 1; ICS#1) was prepared and evaluated. Next to 'Standard 1', also a complement activated standard (Standard 2; ICS#2) was prepared to be used as calibrator in assays for quantifying complement activation products. Both calibrators, together with single patient pathological samples were sent around to participating complement diagnostics laboratories for quality assessment rounds (or ring trials); an inter-laboratory test that allows to evaluate the performance of testing laboratories. Using the calibrators ICS#1 and #2, several complement factors were quantified in parallel in all participating laboratories. The between-laboratory coefficient of variation (CV%) ranged between 0.07 and 0.99 (2, 3, 82). Creating such calibrators with defined amounts of the individual complement components for complement assessment in a diagnostic setting will most certainly improve the quality and consistency of the test results and much progress has been made regarding this. However, as also stated by the Complement EQA Group, other assay components should be used in a standardized matter. For instance, recommendations for sample matrices and advice/descriptions regarding the preferred epitopes in antibody-based assays would most likely improve standardized complement measurements. Next, the EQA Group could provide concentration ranges for complement markers within diseases to be used as reference values for laboratories. This will provide each testing facility the opportunity to set up its own assay without infringing reproducibility in test results between different laboratories.

Conclusions and future perspective

As the results of our systematic literature review have illustrated, 49% of the identified studies investigating complement activation uses the appropriate sample type for their analysis while 27% of the studies did not. For 24% of the studies, it was not clear what sample type or technique was used. Next, we provided examples that using inappropriate sample types and techniques might lead to misinterpretation of results.

Complement biology is an emerging field given the prominent pathogenic involvement in many diseases and its potential for tailored therapeutic intervention. As a result, assessment of complement activation and regulation will become more important in the near future for both research and the daily diagnostic setting. Therefore, it is of utmost importance that complement analysis is performed in a robust and reliable manner. This holds not only for the assessment itself, but also for sample collection, shipment, pre-analytical sample handling, and storage. We underline the importance of awareness regarding these matters and that they may influence the outcome of complement studies.

For the future, we recommend that a uniform protocol is used for standardized sample collection, shipment, pre-analytical handling and storage for both the assessment of complement function as the measurements of individual complement components. Next to that, a more detailed description of the study design is needed regarding used methods and materials (e.g., type of collection tubes). For functional testing, complement-preserved serum (prepared as indicated in Figure 2) should be used. To assess individual complement components, EDTA-plasma must be used to minimize artificial complement activation. A first set-up for this uniform protocol is outlined in Figure 2. The assessment itself should be performed using standardized assays to produce results that are robust and comparable between diagnostic laboratories. Regarding the assays, standardized calibrators and reagents must be used. Antibody-based assays should preferably use antibodies recognizing the same epitope to minimize the variation in kinetics of the antibodies for the antigen. Standardization of complement analysis is organized and coordinated by the Sub-Committee for the Standardization and Quality Assessment of Complement Measurements (the 'Complement EQA Group'). We believe that this group should be strongly embedded within and supported by the complement society so that they can have a leading role in providing clear directives for complement measurements.

Data availability statement

The original contributions presented in the study are included in the article/Supplementary Material. Further inquiries can be directed to the corresponding author.

Author contributions

ET, RB and WB designed and supervised the study. ET, MR and AN performed the experiments. ET analyzed the data and wrote the manuscript. RB, MM, AN, PN and WB critically reviewed the manuscript. All authors discussed and interpreted the results, critically read the article and approved the final version.

Funding

ET received funding from European Union's Horizon 2020 research and innovation programme under grant agreement No. 899163 "Screening of inFlammation to enable personalized Medicine" (SciFiMed, https://scifimed.eu/) and under grant agreement No. 860044 "COmplement Regulation and Variations in Opportunistic infectionS" (CORVOS; EU-H2020-MSCA-ITN-EJD; https://www.corvos.eu). RB received funding from the Dutch Kidney foundation (DKF) / Top Consortia for Knowledge and Innovation's (TKI) & Life Sciences & Health (LSH) joint project "Improved Risk Stratification prior to Kidney Transplantation by Discriminating Pathogenic from Clinically Irrelevant Donor Epitope Specific HLA antibodies in relation to complement activation" (STRIDE.COM) under grant agreement No. DKF PPS09 / TKI-LSH19014-H026.

Acknowledgments

We thank Alexander Hoischen for his help and advice during this study.

Conflict of interest

RB, MR, WB and ET are employees of Hycult Biotech b.v.

The remaining authors declare that the research was conducted in the absence of any commercial or financial relationships that could be construed as a potential conflict of interest.

Publisher's note

All claims expressed in this article are solely those of the authors and do not necessarily represent those of their affiliated organizations, or those of the publisher, the editors and the reviewers. Any product that may be evaluated in this article, or claim that may be made by its manufacturer, is not guaranteed or endorsed by the publisher.

Supplementary material

The Supplementary Material for this article can be found online at: https://www.frontiersin.org/articles/10.3389/fimmu.2022.1007102/full#supplementary-material

References

1. Nilsson B, Ekdahl KN. Complement diagnostics: Concepts, indications, and practical guidelines. *Clin Dev Immunol* (2012), 962702. doi: 10.1155/2012/962702

2. Prohaszka Z, Nilsson B, Frazer-Abel A, Kirschfink M, et al. Complement analysis 2016: Clinical indications, laboratory diagnostics and quality control. *Immunobiology* (2016) 221(11):1247–58. doi: 10.1016/j.imbio.2016.06.008

3. Prohaszka Z, Kirschfink M, Frazer-Abel A. Complement analysis in the era of targeted therapeutics. *Mol Immunol* (2018) 102:84–8. doi: 10.1016/j.molimm.2018.06.001

4. Kirschfink M, Mollnes TE. Modern complement analysis. *Clin Diagn Lab Immunol* (2003) 10(6):982–9. doi: 10.1128/CDLI.10.6.982-989.2003

5. Mohebnasab M, Eriksson O, Persson B, Sandholm K, Mohlin C, Huber-Lang M, et al. Current and future approaches for monitoring responses to anti-complement therapeutics. *Front Immunol* (2019) 10:2539. doi: 10.3389/fimmu.2019.02539

6. Walport MJ. Complement. Frst of two parts. *N Engl J Med* (2001) 344 (14):1058–66. doi: 10.1056/NEJM200104053441406

7. Walport MJ. Complement. Second of two parts. *N Engl J Med* (2001) 344 (15):1140–4. doi: 10.1056/NEJM200104123441506

8. Dempsey PW, Allison ME, Akkaraju S, Goodnow CC, Fearon DT. C3d of complement as a molecular adjuvant: Bridging innate and acquired immunity. *Science* (1996) 271(5247):348–50. doi: 10.1126/science.271.5247.348

9. Elvington M, Liszewski MK, Bertram P, Kulkarni HS, Atkinson JP. A C3 (H20) recycling pathway is a component of the intracellular complement system. *J Clin Invest* (2017) 127(3):970–81. doi: 10.1172/JCI89412

10. Liszewski MK, Kolev M, Le Friec G, Leung M, Bertram PG, Fara AF, et al. Intracellular complement activation sustains T cell homeostasis and mediates effector differentiation. *Immunity* (2013) 39(6):1143–57. doi: 10.1016/j.immuni.2013.10.018

11. Tam JC, Bidgood SR, McEwan WA, James LC. Intracellular sensing of complement C3 activates cell autonomous immunity. *Science* (2014) 345 (6201):1256070. doi: 10.1126/science.1256070

12. Ekdahl KN, Persson B, Mohlin C, Sandholm K, Skattum L, Nilsson B. Interpretation of serological complement biomarkers in disease. *Front Immunol* (2018) 9:2237. doi: 10.3389/fimmu.2018.02237

13. Luo S, Hu D, Wang M, Zipfel PF, Hu Y. Complement in hemolysis- and thrombosis- related diseases. *Front Immunol* (2020) 11:1212. doi: 10.3389/fimmu.2020.01212

14. Hajishengallis G, Reis ES, Mastellos DC, Ricklin D, Lambris JD. Novel mechanisms and functions of complement. *Nat Immunol* (2017) 18(12):1288–98. doi: 10.1038/ni.3858

15. Ricklin D, Reis ES, Mastellos DC, Gros P, Lambris JD. Complement component C3 - the "Swiss army knife" of innate immunity and host defense. *Immunol Rev* (2016) 274(1):33–58. doi: 10.1111/imr.12500

16. Lachmann PJ. Genetic deficiencies of the complement system. In: *Boll ist sieroter Milan* (Milano, Italy: Istituto Sieroterapico Milanese), vol. 53. (1974). p. suppl:195–207.

17. Ling M, Murali M. Analysis of the complement system in the clinical immunology laboratory. *Clin Lab Med* (2019) 39(4):579–90. doi: 10.1016/j.cll.2019.07.006

18. Ricklin D, Mastellos DC, Reis ES, Lambris JD. The renaissance of complement therapeutics. *Nat Rev Nephrol* (2018) 14(1):26–47. doi: 10.1038/nrneph.2017.156

19. Geerlings MJ, de Jong EK, den Hollander AI. The complement system in age-related macular degeneration: A review of rare genetic variants and implications for personalized treatment. *Mol Immunol* (2017) 84:65–76. doi: 10.1016/j.molimm.2016.11.016

20. Yang LB, Li R, Meri S, Rogers J, Shen Y. Deficiency of complement defense protein CD59 may contribute to neurodegeneration in alzheimer's disease. *J Neurosci* (2000) 20(20):7505–9. doi: 10.1523/JNEUROSCI.20-20-07505.2000

21. Krance SH, Wu CY, Zou Y, Mao H, Toufighi S, He X, et al. The complement cascade in alzheimer's disease: a systematic review and meta-analysis. *Mol Psychiatry* (2019) 26(10):5532–41. doi: 10.1038/s41380-019-0536-8

22. Woodruff TM, Costantini KJ, Crane JW, Atkin JD, Monk PN, Taylor SM, et al. The complement factor C5a contributes to pathology in a rat model of amyotrophic lateral sclerosis. *J Immunol* (2008) 181(12):8727–34. doi: 10.4049/jimmunol.181.12.8727

23. Kallenberg CG, Heeringa P. Complement system activation in ANCA vasculitis: A translational success story? *Mol Immunol* (2015) 68(1):53–6. doi: 10.1016/j.molimm.2015.06.005

24. Wester Trejo MAC, Trouw LA, Bajema IM. The role of complement in antineutrophil cytoplasmic antibody-associated vasculitis. *Curr Opin Rheumatol* (2019) 31(1):3–8. doi: 10.1097/BOR.0000000000000557

25. Ma R, Cui Z, Liao YH, Zhao MH. Complement activation contributes to the injury and outcome of kidney in human anti-glomerular basement membrane disease. *J Clin Immunol* (2013) 33(1):172–8. doi: 10.1007/s10875-012-9772-2

26. Hu SY, Jia XY, Yang XW, Yu F, Cui Z, Zhao MH. Glomerular C1q deposition and serum anti-C1q antibodies in anti-glomerular basement membrane disease. *BMC Immunol* (2013) 14:42. doi: 10.1186/1471-2172-14-42

27. Unsworth DJ. Complement deficiency and disease. *J Clin Pathol* (2008) 61 (9):1013–7. doi: 10.1136/jcp.2008.056317

28. Raina R, Krishnappa V, Blaha T, Kann T, Hein W, Burke L, et al. Atypical hemolytic-uremic syndrome: An update on pathophysiology, diagnosis, and treatment. *Ther Apher Dial* (2019) 23(1):4–21. doi: 10.1111/1744-9987.12763

29. Mastellos DC, Ricklin D, Lambris JD. Clinical promise of next-generation complement therapeutics. *Nat Rev Drug Discovery* (2019) 18(9):707–29. doi: 10.1038/s41573-019-0031-6

30. Berentsen S. Complement activation and inhibition in autoimmune hemolytic anemia: Focus on cold agglutinin disease. *Semin Hematol* (2018) 55 (3):141–9. doi: 10.1053/j.seminhematol.2018.04.002

31. Shim K, Begum R, Yang C, Wang H. Complement activation in obesity, insulin resistance, and type 2 diabetes mellitus. *World J Diabetes* (2020) 11(1):1–12. doi: 10.4239/wjd.v11.i1.1

32. Schartz ND, Tenner AJ. The good, the bad, and the opportunities of the complement system in neurodegenerative disease. *J Neuroinflamm* (2020) 17 (1):354. doi: 10.1186/s12974-020-02024-8

33. Michels M, van de Kar NCAJ, Okrój M, Blom AM, van Kraaij SAW, Volokhina EB, et al. Overactivity of alternative pathway convertases in patients with complement-mediated renal diseases. *Front Immunol* (2018) 9:612. doi: 10.3389/fimmu.2018.00612

34. Merinero HM, García SP, García-Fernández J, Arjona E, Tortajada A, Rodríguez de Córdoba S, et al. Complete functional characterization of disease-associated genetic variants in the complement factor h gene. *Kidney Int* (2018) 93 (2):470–81. doi: 10.1016/j.kint.2017.07.015

35. Medjeral-Thomas NR, Pickering MC, Cook HT. Complement and kidney disease, new insights. *Curr Opin Nephrol Hypertens* (2021) 30(3):310–6. doi: 10.1097/MNH.0000000000000705

36. Gavriilaki M, Kimiskidis VK, Gavriilaki E. Precision medicine in neurology: The inspirational paradigm of complement therapeutics. *Pharm (Basel)* (2020) 13 (11):341. doi: 10.3390/ph13110341

37. Lin Q, Min Y, Li Y, Zhu Y, Song X, Xu Q, et al. Henoch-schonlein purpura with hypocomplementemia. *Pediatr Nephrol* (2012) 27(5):801–6. doi: 10.1007/s00467-011-2070-z

38. Dumont C, Mérouani A, Ducruet T, Benoit G, Clermont MJ, Lapeyraque AL, et al. Clinical relevance of membrane attack complex deposition in children with IgA nephropathy and henoch-schonlein purpura. *Pediatr Nephrol* (2020) 35 (5):843–50. doi: 10.1007/s00467-019-04445-x

39. Buck A, Christensen J, McCarty M. Hypocomplementemic urticarial vasculitis syndrome: a case report and literature review. *J Clin Aesthet Dermatol* (2012) 5(1):36–46.

40. Bigler C, Schaller M, Perahud I, Osthoff M, Trendelenburg M. Autoantibodies against complement C1q specifically target C1q bound on early apoptotic cells. *J Immunol* (2009) 183(5):3512–21. doi: 10.4049/jimmunol.0803573

41. Woodruff TM, Crane JW, Proctor LM, Buller KM, Shek AB, de Vos K, et al. Therapeutic activity of C5a receptor antagonists in a rat model of neurodegeneration. *FASEB J* (2006) 20(9):1407–17. doi: 10.1096/fj.05-5814com

42. Torina A, Villari S, Blanda V, Vullo S, La Manna MP, Shekarkar Azgomi M, et al. Innate immune response to tick-borne pathogens: Cellular and molecular mechanisms induced in the hosts. *Int J Mol Sci* (2020) 21(15):5437. doi: 10.3390/ijms21155437

43. Ermert D, Ram S, Laabei M. The hijackers guide to escaping complement: Lessons learned from pathogens. *Mol Immunol* (2019) 114:49–61. doi: 10.1016/j.molimm.2019.07.018

44. Sina C, Kemper C, Derer S. The intestinal complement system in inflammatory bowel disease: Shaping intestinal barrier function. *Semin Immunol* (2018) 37:66–73. doi: 10.1016/j.smim.2018.02.008

45. Miao Z, Ding K, Jin S, Dai L, Dai C, Li X. Using serum peptidomics to discovery the diagnostic marker for different stage of ulcerative colitis. *J Pharm BioMed Anal* (2021) 193:113725. doi: 10.1016/j.jpba.2020.113725

46. Zhou W, Farrar CA, Abe K, Pratt JR, Marsh JE, Wang Y, et al. Predominant role for C5b-9 in renal ischemia/reperfusion injury. *J Clin Invest* (2000) 105 (10):1363–71. doi: 10.1172/JCI8621

47. Howard MC, Nauser CL, Farrar CA, Sacks SH. Complement in ischaemia-reperfusion injury and transplantation. *Semin Immunopathol* (2021) 43(6):789–97. doi: 10.1007/s00281-021-00896-3

48. Arias-Cabrales CE, Riera M, Pérez-Sáez MJ, Gimeno J, Benito D, Redondo D, et al. Activation of final complement components after kidney transplantation as a marker of delayed graft function severity. *Clin Kidney J* (2021) 14(4):1190–6. doi: 10.1093/ckj/sfaa147

49. Doreille A, Dieude M, Cardinal H. The determinants, biomarkers, and consequences of microvascular injury in kidney transplant recipients. *Am J Physiol Renal Physiol* (2019) 316(1):F9–F19. doi: 10.1152/ajprenal.00163.2018

50. Franzin R, Stasi A, Fiorentino M, Stallone G, Cantaluppi V, Gesualdo L, et al. Inflammaging and complement system: A link between acute kidney injury and chronic graft damage. *Front Immunol* (2020) 11:734. doi: 10.3389/fimmu.2020.00734

51. Howard JFJr. Myasthenia gravis: The role of complement at the neuromuscular junction. *Ann N Y Acad Sci* (2018) 1412(1):113–28. doi: 10.1111/nyas.13522

52. Vogel CW. The role of complement in myocardial infarction reperfusion injury: An underappreciated therapeutic target. *Front Cell Dev Biol* (2020) 8:606407. doi: 10.3389/fcell.2020.606407

53. Uzonyi B, Szabó Z, Trojnár E, Hyvärinen S, Uray K, Nielsen HH, et al. Autoantibodies against the complement regulator factor h in the serum of patients with neuromyelitis optica spectrum disorder. *Front Immunol* (2021) 12:660382. doi: 10.3389/fimmu.2021.660382

54. Kielar M, Gala-Błądzińska A, Dumnicka P, Ceranowicz P, Kapusta M, Naumnik B, et al. Complement components in the diagnosis and treatment after kidney transplantation-is there a missing link? *Biomolecules* (2021) 11(6). doi: 10.3390/biom11060773

55. Loeffler DA, Camp DM, Conant SB. Complement activation in the parkinson's disease substantia nigra: an immunocytochemical study. *J Neuroinflamm* (2006) 3:29. doi: 10.1186/1742-2094-3-29

56. Yamada T, McGeer PL, McGeer EG. Lewy bodies in parkinson's disease are recognized by antibodies to complement proteins. *Acta Neuropathol* (1992) 84 (1):100–4. doi: 10.1007/BF00427222

57. Rozemuller AJ, Eikelenboom P, Theeuwes JW, Jansen Steur EN, de Vos RA. Activated microglial cells and complement factors are unrelated to cortical lewy bodies. *Acta Neuropathol* (2000) 100(6):701–8. doi: 10.1007/s004010000225

58. Kitamura Y, Kojima M, Kurosawa T, Sasaki R, Ichihara S, Hiraku Y, et al. Proteomic profiling of exosomal proteins for blood-based biomarkers in parkinson's disease. *Neuroscience* (2018) 392:121–8. doi: 10.1016/j.neuroscience.2018.09.017

59. Shah N, Bhatt H. Paroxysmal nocturnal hemoglobinuria. In: *StatPearls*. FL: Treasure Island (2021).

60. Damgaard C, Holmstrup P, Van Dyke TE, Nielsen CH. The complement system and its role in the pathogenesis of periodontitis: Current concepts. *J Periodontal Res* (2015) 50(3):283–93. doi: 10.1111/jre.12209

61. Burk AM, Martin M, Flierl MA, Rittirsch D, Helm M, Lampl L, et al. Early complementopathy after multiple injuries in humans. *Shock* (2012) 37(4):348–54. doi: 10.1097/SHK.0b013e3182471795

62. Huber-Lang M, Kovtun A, Ignatius A. The role of complement in trauma and fracture healing. *Semin Immunol* (2013) 25(1):73–8. doi: 10.1016/j.smim.2013.05.006

63. Amara U, Flierl MA, Rittirsch D, Klos A, Chen H, Acker B, et al. Molecular intercommunication between the complement and coagulation systems. *J Immunol* (2010) 185(9):5628–36. doi: 10.4049/jimmunol.0903678

64. Bemis EA, Norris JM, Seifert J, Frazer-Abel A, Okamoto Y, Feser ML, et al. Complement and its environmental determinants in the progression of human rheumatoid arthritis. *Mol Immunol* (2019) 112:256–65. doi: 10.1016/j.molimm.2019.05.012

65. Nimgaonkar VL, Prasad KM, Chowdari KV, Severance EG, Yolken RH. The complement system: a gateway to gene-environment interactions in schizophrenia pathogenesis. *Mol Psychiatry* (2017) 22(11):1554–61. doi: 10.1038/mp.2017.151

66. de Nooijer AH, Grondman I, Janssen NAF, Netea MG, Willems L, van de Veerdonk FL, et al. Complement activation in the disease course of COVID-19 and its effects on clinical outcomes. *J Infect Dis* (2020) 223(2):214–24. doi: 10.1093/infdis/jiaa646.

67. Karasu E, Nilsson B, Köhl J, Lambris JD, Huber-Lang M. Targeting complement pathways in polytrauma- and sepsis-induced multiple-organ dysfunction. *Front Immunol* (2019) 10:543. doi: 10.3389/fimmu.2019.00543

68. Unnewehr H, Rittirsch D, Sarma JV, Zetoune F, Flierl MA, Perl M, et al. Changes and regulation of the C5a receptor on neutrophils during septic shock in humans. *J Immunol* (2013) 190(8):4215–25. doi: 10.4049/jimmunol.1200534

69. Panelius J, Meri S. Complement system in dermatological diseases - fire under the skin. *Front Med (Lausanne)* (2015) 2:3. doi: 10.3389/fmed.2015.00003

70. Reti M, Farkas P, Csuka D, Rázsó K, Schlammadinger Á, Udvardy ML, et al. Complement activation in thrombotic thrombocytopenic purpura. *J Thromb Haemost* (2012) 10(5):791–8. doi: 10.1111/j.1538-7836.2012.04674.x

71. Jha P, Bora PS, Bora NS. The role of complement system in ocular diseases including uveitis and macular degeneration. *Mol Immunol* (2007) 44(16):3901–8. doi: 10.1016/j.molimm.2007.06.145

72. Jodele S, Kohl J. Tackling COVID-19 infection through complement-targeted immunotherapy. *Br J Pharmacol* (2020) 178(14):2832–48. doi: 10.22541/au.158880110.01220133

73. Thurman JM. Complement and the kidney: An overview. *Adv Chronic Kidney Dis* (2020) 27(2):86–94. doi: 10.1053/j.ackd.2019.10.003

74. Reis ES, Mastellos DC, Ricklin D, Mantovani A, Lambris JD. Complement in cancer: untangling an intricate relationship. *Nat Rev Immunol* (2018) 18(1):5–18. doi: 10.1038/nri.2017.97

75. Reis ES, Mastellos DC, Hajishengallis G, Lambris JD. New insights into the immune functions of complement. *Nat Rev Immunol* (2019) 19(8):503–16. doi: 10.1038/s41577-019-0168-x

76. Ricklin D, Reis ES, Lambris JD. Complement in disease: A defence system turning offensive. *Nat Rev Nephrol* (2016) 12(7):383–401. doi: 10.1038/nrneph.2016.70

77. Cedzynski M, Thielens NM, Mollnes TE, Vorup-Jensen T. Editorial: The role of complement in health and disease. *Front Immunol* (2019) 10:1869. doi: 10.3389/fimmu.2019.01869

78. Montaldo C, Messina F, Abbate I, Antonioli M, Bordoni V, Aiello A, et al. Multi-omics approach to COVID-19: a domain-based literature review. *J Transl Med* (2021) 19(1):501. doi: 10.1186/s12967-021-03168-8

79. Yu L, Shen H, Ren X, Wang A, Zhu S, Zheng Y, et al. Multi-omics analysis reveals the interaction between the complement system and the coagulation cascade in the development of endometriosis. *Sci Rep* (2021) 11(1):11926. doi: 10.1038/s41598-021-90112-x

80. Moghimi SM, Dmitri S. Critical issues and pitfalls in serum and plasma handling for complement analysis in nanomedicine and bionanotechnology. *Nano Today* (2022) 44:101479. doi: 10.1016/j.nantod.2022.101479

81. Moghimi SM, Simberg D, Papini E, Farhangrazi ZS. Complement activation by drug carriers and particulate pharmaceuticals: Principles, challenges and opportunities. *Adv Drug Delivery Rev* (2020) 157:83–95. doi: 10.1016/j.addr.2020.04.012

82. Frazer-Abel A, Kirschfink M, Prohaszka Z. Expanding horizons in complement analysis and quality control. *Front Immunol* (2021) 12:697313. doi: 10.3389/fimmu.2021.697313

83. Mollnes TE, Garred P, Bergseth G. Effect of time, temperature and anticoagulants on in vitro complement activation: consequences for collection and preservation of samples to be examined for complement activation. *Clin Exp Immunol* (1988) 73(3):484–8.

84. Lachmann PJ. Preparing serum for functional complement assays. *J Immunol Methods* (2010) 352(1-2):195–7. doi: 10.1016/j.jim.2009.11.003

85. Hein E, Bay JT, Munthe-Fog L, Garred P. Ficolin-2 reveals different analytical and biological properties dependent on different sample handling procedures. *Mol Immunol* (2013) 56(4):406–12. doi: 10.1016/j.molimm.2013.05.233

86. Brady AM, Spencer BL, Falsey AR, Nahm MH. Blood collection tubes influence serum ficolin-1 and ficolin-2 levels. *Clin Vaccine Immunol* (2014) 21 (1):51–5. doi: 10.1128/CVI.00607-13

87. Ekdahl KN, Norberg D, Bengtsson AA, Sturfelt G, Nilsson UR, Nilsson B. Use of serum or buffer-changed EDTA-plasma in a rapid, inexpensive, and easy-to-perform hemolytic complement assay for differential diagnosis of systemic lupus erythematosus and monitoring of patients with the disease. *Clin Vaccine Immunol* (2007) 14(5):549–55. doi: 10.1128/CVI.00486-06

88. Moghimi SM, Simberg D, Skotland T, Yaghmur A, Hunter AC, et al. The interplay between blood proteins, complement, and macrophages on nanomedicine performance and responses. *J Pharmacol Exp Ther* (2019) 370 (3):581–92. doi: 10.1124/jpet.119.258012

89. Mollnes TE, Brekke OL, Fung M, Fure H, Christiansen D, Bergseth G, et al. Essential role of the C5a receptor in e coli-induced oxidative burst and phagocytosis revealed by a novel lepirudin-based human whole blood model of inflammation. *Blood* (2002) 100(5):1869–77.

90. Kenawy HI, Boral I, Bevington A. Complement-coagulation cross-talk: A potential mediator of the physiological activation of complement by low pH. *Front Immunol* (2015) 6:215. doi: 10.3389/fimmu.2015.00215

91. Almitairi JOM, Venkatraman Girija U, Furze CM, Simpson-Gray X, Badakshi F, Marshall JE, et al. Structure of the C1r-C1s interaction of the C1 complex of complement activation. *Proc Natl Acad Sci U.S.A.* (2018) 115(4):768–73. doi: 10.1073/pnas.1718709115

92. Wallis R, Mitchell DA, Schmid R, Schwaeble WJ, Keeble AH. Paths reunited: Initiation of the classical and lectin pathways of complement activation. *Immunobiology* (2010) 215(1):1–11. doi: 10.1016/j.imbio.2009.08.006

93. Mortensen S, Jensen JK, Andersen GR. Solution structures of complement C2 and its C4 complexes propose pathway-specific mechanisms for control and activation of the complement proconvertases. *J Biol Chem* (2016) 291(32):16494–507. doi: 10.1074/jbc.M116.722017

94. Nilsson UR, Nilsson B. Simplified assays of hemolytic activity of the classical and alternative complement pathways. *J Immunol Methods* (1984) 72(1):49–59. doi: 10.1016/0022-1759(84)90432-0

95. Platts-Mills TA, Ishizaka K. Activation of the alternate pathway of human complements by rabbit cells. *J Immunol* (1974) 113(1):348–58.

96. Gadjeva M, Thiel S, Jensenius JC. Assays for the mannan-binding lectin pathway. *Curr Protoc Immunol* (2004), 13 6. doi: 10.1002/0471142735.im1306s58

97. Seelen MA, Roos A, Wieslander J, Mollnes TE, Sjöholm AG, Wurzner R, et al. Functional analysis of the classical, alternative, and MBL pathways of the complement system: Standardization and validation of a simple ELISA. *J Immunol Methods* (2005) 296(1-2):187–98. doi: 10.1016/j.jim.2004.11.016

98. Hendrickson OD , Skopinskaya SN, Yarkov SP, Zherdev AV, Dzantiev BB. Development of liposome immune lysis assay for the herbicide atrazine. *J Immunoassay Immunochem* (2004) 25(3):279–94. doi: 10.1081/IAS-200028084

99. Jaskowski TD, Martins TB, Litwin CM, Hill HR. Comparison of three different methods for measuring classical pathway complement activity. *Clin Diagn Lab Immunol* (1999) 6(1):137–9. doi: 10.1128/CDLI.6.1.137-139.1999

100. Bergseth G, Ludviksen JK, Kirschfink M, Giclas PC, Nilsson B, Mollnes TE. An international serum standard for application in assays to detect human complement activation products. *Mol Immunol* (2013) 56(3):232–9. doi: 10.1016/j.molimm.2013.05.221

101. Levine L, Osler AG, Mayer MM. Studies on the role of ca++ and mg++ in complement fixation and immune hemolysis. III. the respective roles of ca++ and mg++ in immune hemolysis. *J Immunol* (1953) 71(5):374–9.

102. Levine L, Cowan KM, Osler AG, Mayer MM. Studies on the role of ca++ and mg++ in complement fixation and immune hemolysis. i. uptake of complement nitrogen by specific precipitates and its inhibition by ethylenediamine tetraacetate. *J Immunol* (1953) 71(5):359–66.

103. Zaferani A, Talsma D, Richter MK, Daha MR, Navis GJ, Seelen MA, et al. Heparin/heparan sulphate interactions with complement–a possible target for reduction of renal function loss? *Nephrol Dial Transplant* (2014) 29(3):515–22. doi: 10.1093/ndt/gft243

104. Yang S, McGookey M, Wang Y, Cataland SR, Wu HM. Effect of blood sampling, processing, and storage on the measurement of complement activation biomarkers. *Am J Clin Pathol* (2015) 143(4):558–65. doi: 10.1309/AJCPXPD7ZQXNTIAL

105. Mollnes TE, Kirschfink M. Complement analysis in clinic and research. *Adv Exp Med Biol* (2006) 586:361–80. doi: 10.1007/0-387-34134-X_24

106. Harboe M, Thorgersen EB, Mollnes TE. Advances in assay of complement function and activation. *Adv Drug Delivery Rev* (2011) 63(12):976–87. doi: 10.1016/j.addr.2011.05.010

107. Sandholm K, Garred P, Bergseth G.. Discrepancies in plasma levels of complement components measured by a newly introduced commercially available magnetic bead technique compared to presently available clinical reference intervals. *Scand J Immunol* (2020) 91(2):e12831. doi: 10.1111/sji.12831

108. Sandholm K, Persson B, Abdalla S, Mohlin C, Nilsson B, Ekdahl KN. Quantification of complement proteins with special reference to C1q: Multiplex versus ELISA versus rocket immunoelectrophoresis versus nephelometry. *Methods Mol Biol 2021* (2227) p:33–41. doi: 10.1007/978-1-0716-1016-9_3

109. Moher D, Liberati A, Tetzlaff J, Altman DG. Preferred reporting items for systematic reviews and meta-analyses: the PRISMA statement. In: *Ann Intern med*, vol. 151. (2009). p. 264–9, W64. doi: 10.7326/0003-4819-151-4-200908180-00135

110. Young JM, Solomon MJ. How to critically appraise an article. *Nat Clin Pract Gastroenterol Hepatol* (2009) 6(2):82–91. doi: 10.1038/ncpgasthep1331

111. Liu M, Luo X, Xu Q, Yu H, Gao L, Zhou R, Wang T, et al. Adipsin of the alternative complement pathway is a potential predictor for preeclampsia in early pregnancy. *Front Immunol* (2021) 12:702385. doi: 10.3389/fimmu.2021.702385

112. Pache F, Ringelstein M, Aktas O, Kleiter I, Jarius S, Siebert N, et al. C3 and C4 complement levels in AQP4-IgG-positive NMOSD and in MOGAD. *J Neuroimmunol* (2021) 360:577699. doi: 10.1016/j.jneuroim.2021.577699

113. Michels M, van de Kar NCAJ, van Kraaij SAW, Sarlea SA, Gracchi V, Engels FAPT, et al. Different aspects of classical pathway overactivation in patients with C3 glomerulopathy and immune complex-mediated membranoproliferative glomerulonephritis. *Front Immunol* (2021) 12:715704. doi: 10.3389/fimmu.2021.715704

114. Prens LM, Ardon CB, van Straalen KR, van der Zee HH, Seelen MAJ, Laman JD, et al. No evident systemic terminal complement pathway activation in hidradenitis suppurativa. *J Invest Dermatol* (2021), 2966–9, 141(12). doi: 10.1016/j.jid.2021.03.037

115. Chiu YL, Lin WC, Shu KH, Fang YW, Chang FC, Chou YH, et al. Alternative complement pathway is activated and associated with galactose-deficient IgA1 antibody in IgA nephropathy patients. *Front Immunol* (2021) 12:638309. doi: 10.3389/fimmu.2021.638309

116. Dhooge PPA, Runhart EH, Li CHZ, de Kat Angelino CM, Hoyng CB, van der Molen RG, et al. Systemic complement activation levels in stargardt disease. *PloS One* (2021) 16(6):e0253716. doi: 10.1371/journal.pone.0253716

117. Sinkovits G, Mező B, Réti M, Müller V, Iványi Z, Gál J, et al. Complement overactivation and consumption predicts in-hospital mortality in SARS-CoV-2 infection. *Front Immunol* (2021) 12:663187. doi: 10.3389/fimmu.2021.663187

118. Rognes IN, Pischke SE, Ottestad W, Røislien J, Berg JP, Johnson C, et al. Increased complement activation 3 to 6 h after trauma is a predictor of prolonged mechanical ventilation and multiple organ dysfunction syndrome: A prospective observational study. *Mol Med* (2021) 27(1):35. doi: 10.1186/s10020-021-00286-3

119. Denzinger M, Held M, Daigeler A, Krajewski S, Link A. Complement activation at the interface of wound dressings and blood does not influence keratinocyte migration/proliferation in vitro. *Wound Repair Regener* (2020) 28 (4):573–5. doi: 10.1111/wrr.12817

120. Grinde D, Øverland T, Lima K, Schjalm C, Mollnes TE, Abrahamsen TG. Complement activation in 22q11.2 deletion syndrome. *J Clin Immunol* (2020) 40 (3):515–23. doi: 10.1007/s10875-020-00766-x

121. Kristensen MK, Hansen MB, Madsen MB, Hansen CB, Pilely K, Hyldegaard O, et al. Complement activation is associated with mortality in patients with necrotizing soft-tissue infections-a prospective observational study. *Front Immunol* (2020) 11:17. doi: 10.3389/fimmu.2020.00017

122. Chauvet S, Berthaud R, Devriese M, Mignotet M, Vieira Martins P, Robe-Rybkine T, et al. Anti-factor b antibodies and acute postinfectious GN in children. *J Am Soc Nephrol* (2020) 31(4):829–40. doi: 10.1681/ASN.2019080851

123. Abe T, Kubo K, Izumoto S, Shimazu S, Goan A, Tanaka T, et al. Complement activation in human sepsis is related to sepsis-induced disseminated intravascular coagulation. *Shock* (2020) 54(2):198–204. doi: 10.1097/SHK.0000000000001504

124. Tjernberg AR, Woksepp H, Sandholm K, Johansson M, Dahle C, Ludvigsson JF, et al. Celiac disease and complement activation in response to streptococcus pneumoniae. *Eur J Pediatr* (2020) 179(1):133–40. doi: 10.1007/s00431-019-03490-w

125. Scambi C, Ugolini S, Tonello M, Bortolami O, De Franceschi L, Castagna A, et al. Complement activation in the plasma and placentas of women with different subsets of antiphospholipid syndrome. *Am J Reprod Immunol* (2019) 82 (6):e13185. doi: 10.1111/aji.13185

126. Schein TN, Blackburn TE, Heath SL, Barnum SR. Plasma levels of soluble membrane attack complex are elevated despite viral suppression in HIV patients with poor immune reconstitution. *Clin Exp Immunol* (2019) 198(3):359–66. doi: 10.1111/cei.13366

127. Zhang MF, Huang J, Zhang YM, Qu Z, Wang X, Wang F, et al. Complement activation products in the circulation and urine of primary membranous nephropathy. *BMC Nephrol* (2019) 20(1):313. doi: 10.1186/s12882-019-1509-5

128. Gavriilaki E, Chrysanthopoulou A, Sakellari I, Batsis I, Mallouri D, Touloumenidou T, et al. Linking complement activation, coagulation, and neutrophils in transplant-associated thrombotic microangiopathy. *Thromb Haemost* (2019) 119(9):1433–40. doi: 10.1055/s-0039-1692721

129. Lynch AM, Mandava N, Patnaik JL, Frazer-Abel AA, Wagner BD, Palestine AG, et al. Systemic activation of the complement system in patients with advanced age-related macular degeneration. *Eur J Ophthalmol* (2020) 30 (5):1061–8. doi: 10.1177/1120672119857896

130. Hoiland II, Liang RA, Braekkan SK, Pettersen K, Ludviksen JK, Latysheva N, et al. Complement activation assessed by the plasma terminal complement complex and future risk of venous thromboembolism. *J Thromb Haemost* (2019) 17 (6):934–43. doi: 10.1111/jth.14438

131. Burwick RM, Velásquez JA, Valencia CM, Gutiérrez-Marín J, Edna-Estrada F, Silva JL, et al. Terminal complement activation in preeclampsia. *Obstet Gynecol* (2018) 132(6):1477–85. doi: 10.1097/AOG.0000000000002980

132. Rodriguez E, Gimeno J, Arias-Cabrales C, Barrios C, Redondo-Pachón D, Soler MJ, et al. Membrane attack complex and factor h in humans with acute kidney injury. *Kidney Blood Press Res* (2018) 43(5):1655–65. doi: 10.1159/000494680

133. Chauvet S, Roumenina LT, Aucouturier P, Marinozzi MC, Dragon-Durey MA, Karras A, et al. Both monoclonal and polyclonal immunoglobulin contingents mediate complement activation in monoclonal gammopathy associated-C3 glomerulopathy. *Front Immunol* (2018) 9:2260. doi: 10.3389/fimmu.2018.02260

134. Bavia L, Lidani KCF, Andrade FA, Sobrinho MIAH, Nisihara RM, de Messias-Reason IJ. Complement activation in acute myocardial infarction: An early marker of inflammation and tissue injury? *Immunol Lett* (2018) 200:18–25. doi: 10.1016/j.imlet.2018.06.006

135. Kanni T, Zenker O, Habel M, Riedemann N, Giamarellos-Bourboulis EJ. Complement activation in hidradenitis suppurativa: A new pathway of pathogenesis? *Br J Dermatol* (2018) 179(2):413–9. doi: 10.1111/bjd.16428

136. Siljan WW, Holter JC, Nymo SH, Husebye E, Ueland T, Aukrust P. Cytokine responses, microbial aetiology and short-term outcome in community-acquired pneumonia. *Eur J Clin Invest* (2018) 48(1):e12865. doi: 10.1111/eci.12865

137. Trendelenburg M, Stallone F, Pershyna K, Eisenhut T, Twerenbold R, Wildi K, et al. Complement activation products in acute heart failure: Potential role in pathophysiology, responses to treatment and impacts on long-term survival. *Eur Heart J Acute Cardiovasc Care* (2018) 7(4):348–57. doi: 10.1177/2048872617694674

138. Togarsimalemath SK, Sethi SK, Duggal R, Le Quintrec M, Jha P, Daniel R, et al. A novel CFHR1-CFHR5 hybrid leads to a familial dominant C3 glomerulopathy. *Kidney Int* (2017) 92(4):876–87. doi: 10.1016/j.kint.2017.04.025

139. Suffritti C, Tobaldini E, Schiavon R, Strada S, Maggioni L, Mehta S, et al. Complement and contact system activation in acute congestive heart failure patients. *Clin Exp Immunol* (2017) 190(2):251–7. doi: 10.1111/cei.13011

140. Grosso G, Vikerfors A, Woodhams B, Adam M, Bremme K, Holmström M, et al. Thrombin activatable fibrinolysis inhibitor (TAFI) - a possible link between coagulation and complement activation in the antiphospholipid syndrome (APS). *Thromb Res* (2017) 158:168–73. doi: 10.1016/j.thromres.2017.06.028

141. Witczak BJ, Pischke SE, Reisæter AV, Midtvedt K, Ludviksen JK, Heldal K, et al. Elevated terminal C5b-9 complement complex 10 weeks post kidney transplantation was associated with reduced long-term patient and kidney graft survival. *Front Immunol* (2021) 12:738927. doi: 10.3389/fimmu.2021.738927

142. Milosevits G, Mészáros T, Őrfi E, Bakos T, Garami M, Kovács G. Complement-mediated hypersensitivity reactions to an amphotericin b-containing lipid complex (Abelcet) in pediatric patients and anesthetized rats: Benefits of slow infusion. *Nanomedicine* (2021) 34:102366. doi: 10.1016/j.nano.2021.102366

143. Mastellos DC, Pires da Silva BGP, Fonseca BAL, Fonseca NP, Auxiliadora-Martins M, Mastaglio S, et al. Complement C3 vs C5 inhibition in severe COVID-19: Early clinical findings reveal differential biological efficacy. *Clin Immunol* (2020) 220:108598. doi: 10.1016/j.clim.2020.108598

144. Sartain S, Shubert S, Wu MF, Wang T, Martinez C. The alternative complement pathway activation product ba as a marker for transplant-associated thrombotic microangiopathy. *Pediatr Blood Cancer* (2020) 67(3):e28070. doi: 10.1002/pbc.28070

145. Faria B, Gaya da Costa M, Poppelaars F, Franssen CFM, Pestana M, Berger SP, et al. Administration of intravenous iron formulations induces complement activation in-vivo. *Front Immunol* (2019) 10:1885. doi: 10.3389/fimmu.2019.01885

146. Qi J, Wang J, Chen J, Su J, Tang Y, Wu X, et al. Plasma levels of complement activation fragments C3b and sC5b-9 significantly increased in patients with thrombotic microangiopathy after allogeneic stem cell transplantation. *Ann Hematol* (2017) 96 (11):1849–55. doi: 10.1007/s00277-017-3092-9

147. Nilsson PH, Thomas AM, Bergseth G, Gustavsen A, Volokhina EB, van den Heuvel LP, et al. Eculizumab-C5 complexes express a C5a neoepitope in vivo: Consequences for interpretation of patient complement analyses. *Mol Immunol* (2017) 89:111–4. doi: 10.1016/j.molimm.2017.05.021

148. Wehling C, Amon O, Bommer M, Hoppe B, Kentouche K, Schalk G, et al. Monitoring of complement activation biomarkers and eculizumab in complement-mediated renal disorders. *Clin Exp Immunol* (2017) 187(2):304–15. doi: 10.1111/cei.12890

149. Troldborg A, Halkjær L, Pedersen H, Hansen A, Loft AG, Lindegaard H, et al. Complement activation in human autoimmune diseases and mouse models; employing a sandwich immunoassay specific for C3dg. *J Immunol Methods* (2020) 486:112866. doi: 10.1016/j.jim.2020.112866

150. Halkjaer L, Troldborg A, Pedersen H, Jensen L, Hansen AG, Hansen TK, et al. Complement receptor 2 based immunoassay measuring activation of the complement system at C3-level in plasma samples from mice and humans. *Front Immunol* (2020) 11:774. doi: 10.3389/fimmu.2020.00774

151. Elvington M, Liszewski MK, Liszewski AR, Kulkarni HS, Hachem RR, Mohanakumar T, et al. Development and optimization of an ELISA to quantitate C3(H 2 O) as a marker of human disease. *Front Immunol* (2019) 10:703. doi: 10.3389/fimmu.2019.00703

152. Nilsson PH, Johnson C, Quach QH, Macpherson A, Durrant O, Pischke SE, et al. A conformational change of complement C5 is required for thrombin-mediated cleavage, revealed by a novel ex vivo human whole blood model preserving full thrombin activity. *J Immunol* (2021) 207(6):1641–51. doi: 10.4049/jimmunol.2001471

153. Vercauteren KOA, Lambrecht S, Delanghe J. Preanalytical classical and alternative complement pathway activity loss. *Biochem Med (Zagreb)* (2019) 29 (3):030701. doi: 10.11613/BM.2019.030701

154. Mansur S, Othman MHD, Ismail AF, Kadir SHSA, Goh PS, Hasbullah H, et al. Synthesis and characterisation of composite sulphonated polyurethane/polyethersulphone membrane for blood purification application. *Mater Sci Eng C Mater Biol Appl* (2019) 99:491–504. doi: 10.1016/j.msec.2019.01.092

155. Hamad OA, Ekdahl KN, Nilsson PH, Andersson J, Magotti P, Lambris JD, et al. Complement activation triggered by chondroitin sulfate released by thrombin receptor-activated platelets. *J Thromb Haemost* (2008) 6(8):1413–21. doi: 10.1111/j.1538-7836.2008.03034.x

156. Geno KA, Kennedy RE, Sawyer P, Brown CJ, Nahm MH. Ficolin-2 inhibitors are present in sera after prolonged storage at -80 degrees c. *PeerJ* (2016) 4:e2705. doi: 10.7717/peerj.2705

157. Henno LT, Storjord E, Christiansen D, Bergseth G, Ludviksen JK, Fure H, et al. Effect of the anticoagulant, storage time and temperature of blood samples on the concentrations of 27 multiplex assayed cytokines - consequences for defining reference values in healthy humans. *Cytokine* (2017) 97:86–95. doi: 10.1016/j.cyto.2017.05.014

158. Strobel L, Johswich KO. Anticoagulants impact on innate immune responses and bacterial survival in whole blood models of neisseria meningitidis infection. *Sci Rep* (2018) 8(1):10225. doi: 10.1038/s41598-018-28583-8

159. Janssen BJ, Gros P. Structural insights into the central complement component C3. *Mol Immunol* (2007) 44(1-3):3–10. doi: 10.1016/j.molimm.2006.06.017

frontiers | Frontiers in Immunology

TYPE Original Research
PUBLISHED 04 November 2022
DOI 10.3389/fimmu.2022.1039765

Check for updates

OPEN ACCESS

EDITED BY
Peter F. Zipfel,
Leibniz Institute for Natural Product Research and Infection Biology, Germany

REVIEWED BY
Mohamed Daha,
Leiden University Medical Center (LUMC), Netherlands
Maciej Cedzynski,
Institute for Medical Biology (PAN), Poland

*CORRESPONDENCE
Zoltán Prohászka
prohaszka.zoltan@med.semmelweis-univ.hu

SPECIALTY SECTION
This article was submitted to Molecular Innate Immunity, a section of the journal Frontiers in Immunology

RECEIVED 08 September 2022
ACCEPTED 06 October 2022
PUBLISHED 04 November 2022

CITATION
Hurler L, Toonen EJM, Kajdácsi E, van Bree B, Brandwijk RJMGE, de Bruin W, Lyons PA, Bergamaschi L, Cambridge Institute of Therapeutic Immunology and Infectious Disease-National Institute of Health Research (CITIID-NIHR) COVID BioResource Collaboration, Sinkovits G, Cervenak L, Würzner R and Prohászka Z (2022) Distinction of early complement classical and lectin pathway activation *via* quantification of C1s/C1-INH and MASP-1/C1-INH complexes using novel ELISAs.
Front. Immunol. 13:1039765.
doi: 10.3389/fimmu.2022.1039765

Distinction of early complement classical and lectin pathway activation *via* quantification of C1s/C1-INH and MASP-1/C1-INH complexes using novel ELISAs

Lisa Hurler[1], Erik J. M. Toonen[2], Erika Kajdácsi[1], Bregje van Bree[2], Ricardo J. M. G. E. Brandwijk[2], Wieke de Bruin[2], Paul A. Lyons[3,4], Laura Bergamaschi[3,4], Cambridge Institute of Therapeutic Immunology and Infectious Disease-National Institute of Health Research (CITIID-NIHR) COVID BioResource Collaboration, György Sinkovits[1], László Cervenak[1], Reinhard Würzner[5] and Zoltán Prohászka[1,6]*

[1]Department of Internal Medicine and Haematology, Semmelweis University, Budapest, Hungary, [2]Research and Development Department, Hycult Biotech, Uden, Netherlands, [3]Cambridge Institute of Therapeutic Immunology and Infectious Disease, Jeffrey Cheah Biomedical Centre, University of Cambridge, Cambridge, United Kingdom, [4]Department of Medicine, University of Cambridge, Addenbrooke's Hospital, Cambridge, United Kingdom, [5]Institute of Hygiene and Medical Microbiology, Medical University of Innsbruck, Innsbruck, Austria, [6]Research Group for Immunology and Haematology, Semmelweis University – Eötvös Loránd Research Network (Office for Supported Research Groups), Budapest, Hungary

The most commonly used markers to assess complement activation are split products that are produced through activation of all three pathways and are located downstream of C3. In contrast, C4d derives from the cleavage of C4 and indicates either classical (CP) or lectin pathway (LP) activation. Although C4d is perfectly able to distinguish between CP/LP and alternative pathway (AP) activation, no well-established markers are available to differentiate between early CP and LP activation. Active enzymes of both pathways (C1s/C1r for the CP, MASP-1/MASP-2 for the LP) are regulated by C1 esterase inhibitor (C1-INH) through the formation of covalent complexes. Aim of this study was to develop validated immunoassays detecting C1s/C1-INH and MASP-1/C1-INH complex levels. Measurement of the complexes reveals information about the involvement of the respective pathways in complement-mediated diseases. Two sandwich ELISAs detecting C1s/C1-INH and MASP-1/C1-INH complex were developed and tested thoroughly, and it was investigated whether C1s/C1-INH and MASP-1/C1-INH complexes could serve as markers for either early CP or LP activation. In addition, a reference range for these complexes in healthy adults was defined, and the assays were clinically validated utilizing

samples of 414 COVID-19 patients and 96 healthy controls. The immunoassays can reliably measure C1s/C1-INH and MASP-1/C1-INH complex concentrations in EDTA plasma from healthy and diseased individuals. Both complex levels are increased in serum when activated with zymosan, making them suitable markers for early classical and early lectin pathway activation. Furthermore, measurements of C1-INH complexes in 96 healthy adults showed normally distributed C1s/C1-INH complex levels with a physiological concentration of 1846 ± 1060 ng/mL (mean ± 2SD) and right-skewed distribution of MASP-1/C1-INH complex levels with a median concentration of 36.9 (13.18 - 87.89) ng/mL (2.5-97.5 percentile range), while levels of both complexes were increased in COVID-19 patients ($p<0.0001$). The newly developed assays measure C1-INH complex levels in an accurate way. C1s/C1-INH and MASP-1/C1-INH complexes are suitable markers to assess early classical and lectin pathway activation. An initial reference range was set and first studies showed that these markers have added value for investigating and unraveling complement activation in human disease.

KEYWORDS

early complement activation, classical pathway activation, lectin pathway activation, C1-INH complexes, assay development and validation, C1s/C1-INH complex, MASP-1/C1-INH complex

Introduction

The complement system is a proteolysis-based activation cascade, consisting of more than 40 plasma proteins, which acts as a first line defense in the fight against microorganisms such as bacteria, viruses or fungi. Besides, the complement system also plays a role in the clearance of damaged or altered host cells (1), in enhancing the adaptive immune response (2), and in autoimmune diseases. It can be activated *via* three different pathways, the classical (CP), the lectin (LP), and the alternative pathway (AP). An overview of classical and lectin pathway activation as well as a proposed scheme of complex formation is demonstrated in Figure 1.

The classical pathway is activated by binding of the recognition protein C1q, part of the C1 complex ($C1qC1r_2C1s_2$), to circulating antibody-antigen complexes containing IgG or IgM. Activation can also occur in an immune complex-independent manner, through binding of C1q to acute phase proteins like the C-reactive protein or Pentraxin 3 (4, 5). Additionally, there is also the possibility of direct interaction between the initiator C1q and viral proteins, including surface proteins of HIV-1 and EBV (6), lipopolysaccharides such as on the surface of bacteria (7), and apoptotic cells (8). Upon binding of the C1 complex to an activating target surface, structural changes occur in the C1q, which trigger the associated zymogen C1r in the C1 complex to autoactivate. Auto-activated C1r can subsequently activate proenzyme C1s (9), which then allows proteolytic cleavage of C2 and C4, initiating the formation of the classical C3 convertase (C4b2b) and downstream complement activation. The lectin pathway is activated in a slightly different way. While classical pathway activation can only be initiated by C1q, the lectin pathway can be activated through several pattern recognition molecules: collectins, such as the mannan-binding lectin (MBL), collectin-10, and collectin-11; and the three ficolins, ficolin-1, ficolin-2 and ficolin-3 (10). Upon recognition of triggering carbohydrate structures or acetyl group patterns on pathogen surfaces, both the MBL-associated serine protease 1 (MASP-1) and -2 (MASP-2) are activated. While activated MASP-2 can cleave C4 and C2, MASP-1 can only cleave C2 as a central component of the complement cascade, and not C4 (11). However, MASP-1 can also cleave MASP-2, thereby additionally enhancing C4 and C2 cleavage (12, 13). Activation of the CP and LP and subsequent cleavage of C2 and C4 will lead to the formation of C3 and C5 convertases and downstream complement activation. Finally, this results in the formation of the terminal complement complex (TCC), also known as the membrane attack complex (MAC complex), when formed on the membrane of a target cell (14). After complement activation, the targeted cell will either be osmotically lysed or opsonized and eliminated by phagocytosis (15).

For assessing complement activation, several well-known and widely used biomarkers are available (see Figure 1). Most

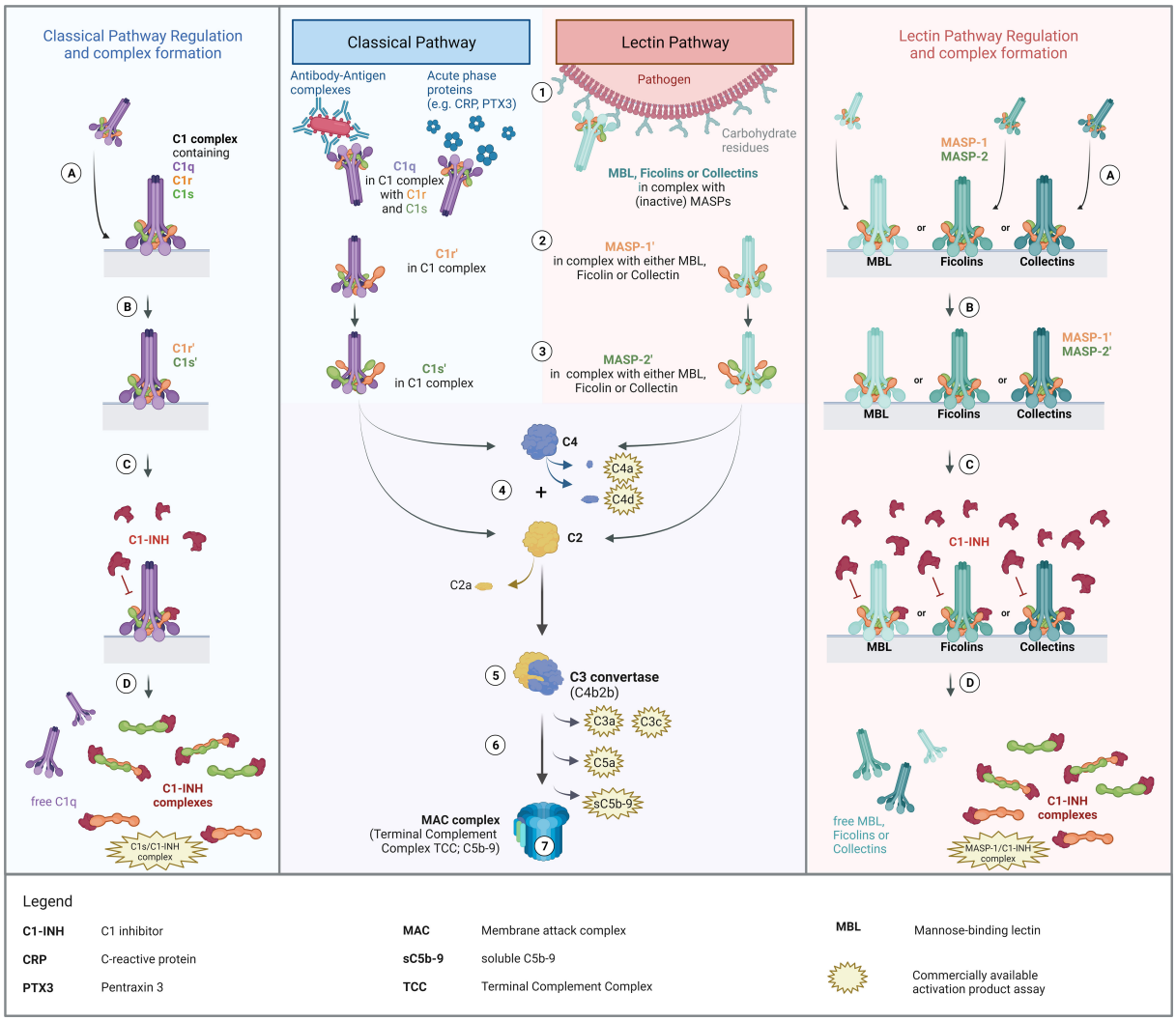

FIGURE 1
Overview of Classical and Lectin Pathway activation, regulation by C1-INH and proposed mechanism of complex formation. Middle panel: Activation of the classical and the lectin pathway (1). Recognition of triggering compound by the respective recognition molecules (C1q for classical pathway; MBL, ficolins or collectins for lectin pathway) and binding thereof to the activating compounds/structures. (2) Zymogen autoactivation of the first serine protease after structural changes of the associated recognition molecules upon binding to activating structures. (3) Catalytically activation of the second serine proteases by the activated first serine proteases. (4) Cleavage of C2 and C4 by activated serine proteases. (5) Formation of the classical C3 convertase, consisting of C4b and C2b [updated nomenclature according to (3)]. (6) Downstream complement activation going along with the release of several complement activation/split products. (7) Formation of the Terminal Complement Complex (TCC) or the Membrane Attack Complex (MAC complex), when formed on a membrane, and lysis or cell clearance. Left and right panel: Regulation of classical and lectin pathway activation by C1-INH and proposed theory of complex formation. (A) Binding of the pattern recognition molecule to an activating surface, resulting in conformational changes in the respective protein complexes. (B) Activation of serine proteases, allowing downstream complement activation. (C) Regulation of pathway activation by C1-INH through covalent binding to active sites of the serine proteases, blocking protease function and further activation of the respective pathways. (D) Dissociation of the complexes upon binding of C1-INH and release of C1-INH complexes as well as free pattern recognition molecules into the circulation. The figure was created with BioRender.com.

commonly used markers for measuring complement activation in human plasma are C3 split products (anaphylatoxin C3a, C3c and C3d), C4 split products C4a and C4d, the alternative pathway activation product Bb (not shown in Figure 1), the anaphylatoxin C5a and the terminal pathway activation product sC5b-9 (16). C3 split products, such as the anaphylatoxin C3a, C3c and C3d, as well as the terminal complement complex (TCC/sC5b-9) are produced as a result of activation of all three complement pathways. As an example, C3d is a robust marker for C3 activation, extensively studied in complement-mediated diseases such as age-related macular degeneration (AMD) or Systemic lupus erythematosus (SLE) (17, 18). In contrast, C4d is

derived from the cleavage of C4 and hence indicates both classical and lectin pathway but not alternative pathway activation. Besides that, many C3d and C4d assays are widely used in routine diagnostics and available commercially, especially investigation of C4d is mainly used for immunostaining in (kidney) biopsies (19–21). Although C4d is perfectly able to distinguish between CP/LP and AP activation, no well-established markers to measure early classical and early lectin pathway activation are available. Information thereof could provide further insights into - and better understanding of - the role of complement in health and disease. Next to that, it might have added value for the diagnosis of complement-mediated disease as well as for monitoring disease onset and severity. Additionally, knowledge about the early CP and LP activation state could help in the development and monitoring of complement inhibitors specifically targeting early components like C1s (22, 23).

Activation of complement *via* both the CP and LP is tightly regulated by C1 esterase inhibitor (C1-INH), a highly glycosylated protein encoded by the *SERPING1* gene, predominantly expressed in the liver (24). C1-INH is the only known regulator of the early classical and lectin pathways, while it also has a profound role in regulating the contact system, the fibrinolytic system as well as the coagulation system (25). With regard to the CP, it can covalently bind to activated C1r and C1s, blocking the serine protease function and hence inhibiting proteolytic cleavage of C4 and C2 and further CP activation (26). Upon binding of C1-INH, the C1 complex dissociates and releases free C1q as well as covalent C1r/C1-INH and C1s/C1-INH complexes (27). Those complexes are internalized and degraded by the low density lipoprotein receptor-related protein rapidly after release into the circulation (28). C1-INH also regulates the lectin pathway as it forms covalent complexes by directly binding activated MASP-1 and MASP-2, thereby downregulating pathway activation.

For both protein complexes, several studies have reported that levels in circulation are associated with human disease. Regarding C1s/C1-INH, levels were increased 2-3-fold in Hereditary angioedema (HAE) patients when compared to controls (29, 30). In addition, increased C1s complex levels were also reported for other diseases involving classical pathway activation, such as Systemic lupus erythematosus (SLE), glomerulonephritis, and rheumatoid arthritis (RA) (31, 32). Concerning MASP/C1-INH complexes, a given amount of both MASP-1/C1-INH and MASP-2/C1-INH naturally exists in the circulation (33). However, lower MASP-1/C1-INH complex levels were reported in HAE patients with decreased C1-INH activity (33), whereas type II HAE patients seem to have increased MASP-1/C1-INH levels when compared to healthy controls (30). These results suggest that C1s/C1-INH and MASP/C1-INH protein complexes are involved in the pathogenesis of several complement-mediated diseases and that they may have added value as biomarkers for diagnosis and disease- or treatment monitoring. While the specific function of the C1-INH complexes is not known yet and requires further research, complex formation of CP and LP serine proteases with C1-INH does require activation of the respective serine proteases (like C1s, C1r, MASP-1 or MASP-2), making the complexes promising biomarkers to distinguish between early classical and early lectin pathway activation. Higher levels of the C1-INH complexes in disease might indicate higher levels of complement regulation through C1-INH and hence also higher activation levels of the respective pathways.

So far, no commercially available assays exist in order to measure C1s/C1-INH complex and MASP-1/C1-INH complex concentrations in a reliable and standardized way, making it difficult to compare already published studies about C1-INH complexes. In this study, we aimed to develop two sensitive and specific immunoassays for quantifying C1s/C1-INH and MASP-1/C1-INH complexes in human blood samples (plasma and serum). In addition, we intended to show that C1-INH complex levels increase upon *in-vitro* activation of the respective pathways in human serum, making them suitable biomarkers for indirect measurement of ongoing activation of either the classical pathway (C1s/C1-INH complex) or the lectin pathway (MASP-1/C1-INH complex).

A further aim was to clinically validate these complexes also *in vivo*. Therefore, we investigated C1-INH complex levels in COVID-19 patients, where complement activation is known to play a role in the pathomechanism of the disease, and compared the results to C1-INH complex concentrations measured in healthy controls' samples.

Material and methods

Patient cohort

A total of 414 COVID-19 patients (34, 35) and 96 healthy controls (34, 36) were enrolled and sampled as described elsewhere. In brief, whole blood was collected into EDTA-treated tubes, before cells and plasma were separated by centrifugation. EDTA-plasma samples were stored in aliquots at -80°C until further usage.

Ethical approval was obtained from the East of England – Cambridge Central Research Ethics Committee ("NIHR BioResource" REC ref 17/EE/0025, and "Genetic variation AND Altered Leucocyte Function in health and disease – GANDALF" REC ref 08/H0308/176), the Hungarian Ethical Review Agency (ETT-TUKEB; No. 8361-1/2011-EKU and IV/4403-2/2020/EKU) and the Government Office of the Capital City Budapest (31110-7/2014/EKU (481/2014)), based on the position of the Medical Research Council. The studies were conducted in accordance with the Declaration of Helsinki. Written informed consent to participate in this study was provided by the participants or their closest relative available.

Biological samples

Matching sample sets, consisting of citrate plasma, heparin plasma, EDTA plasma and serum each, of ten healthy individuals were purchased from BioIVT (BioIVT, New York, USA), stored in aliquots at -80°C and included in measurements during the assay development. C1s/C1-INH complex and C1s enzyme were purchased from CompTech (Complement Technology Inc., Texas, USA), while C1q was purchased from Quidel (Quidel Corporation, San Diego, USA).

Recombinant serine proteases (C1r, C1s, MASP-1, MASP-2) and C1-INH were prepared and purified in-house as described elsewhere (30). Blood samples from animals were obtained from commercial sources. Murine, pig and dog sera were ordered from Innovative (Innovative Research Inc., Michigan, USA), while rat and horse sera were purchased from Harlan (Harlan Bioproducts for Science Inc., Maryland, USA). For complement activation experiments, complement-preserved normal human serum (NHS) was prepared freshly from a pool of 12 healthy individuals and stored in aliquots at -80°C until further usage.

Production of monoclonal antibodies against C1s, MASP-1 and C1-INH

C1-INH was further purified from human plasma C1-INH concentrate by ion-exchange chromatography and size exclusion chromatography (30). Recombinant CCP1-CCP2-SP fragments of C1s and MASP-1 were produced and purified as previously published (37, 38).

Eight-to-ten-week-old BALB/c mice were repeatedly immunized (100 µg antigen/mouse in complete Freund's adjuvant subcutaneously, 50 µg antigen/mouse in incomplete Freund's adjuvant subcutaneously, finally, 50 µg antigen/mouse in PBS intravenously). Mice with high serum antibody titer against C1s, MASP-1 or C1-INH were sacrificed, the spleens were removed and splenocytes were fused with Sp2/0-Ag14 myeloma cells in the presence of PEG solution (Hybri-Max, Sigma-Aldrich, Budapest, Hungary). Selection was performed by standard HAT supplemented DMEM (Sigma-Aldrich, Budapest, Hungary) (39). Clones were tested for specificity and cross-reactivity by direct antigen ELISA, and for isotype by sandwich ELISA (data not shown).

In silico analysis of amino acid sequence

Similarity of amino acid sequences of the complex components (C1s, MASP-1 and C1-INH) and other human proteins was tested *in silico* using *Homo sapiens* protein BLAST (https://blast.ncbi.nlm.nih.gov). More than 60% agreement in the amino acid sequence between the tested protein and any other protein sequence in the database was chosen as an arbitrary cut off for high similarity and did require experimental specificity testing of the developed antibodies in a direct ELISA setup.

Direct ELISA to test specificity of antibodies

The specificity of in-house produced antibodies for complement proteins was tested by direct ELISA. Relevant proteins of the respective pathways (either recombinant or commercial ones purified from human serum, dependent on availability) were immobilized at a concentration of 1 µg/mL in bicarbonate buffer (0.1 M bicarbonate, pH 9.6; 100 µL/well) on Nunc Maxisorp 96 well plates (Thermo Fisher Scientific, Waltham, USA) at 4°C over night. Wells were blocked with 2% BSA in PBS for 1.5 h at room temperature. After blocking, plates were washed with PBS-Tween. Primary monoclonal antibodies (anti C1-INH, anti C1s or anti MASP-1 used in the complex assays) were added at a concentration of 3 µg/mL in dilution buffer from the complex assays and incubated for 1h at room temperature. After washes (4x), HRP-conjugated goat anti-mouse antibody (Southern Biotech, Birmingham, USA) was added (1:4000 in dilution buffer of the complex assays) and incubated for 1 h at room temperature. Following washes, 50% TMB in H_2O was added, the plate was incubated for 5 min before the reaction was stopped using Oxalic acid and the absorbance was measured at 450 nm on a plate reader. Measurements were done in duplicate, while the experiment was performed in triplicate.

Preparation of in-house MASP-1/C1-INH complexes

MASP-1/C1-INH complexes were prepared in-house as described before (30). In short, recombinantly produced activated MASP-1 (CCP1-CCP2-SP domain) was incubated in a 1:1 molar ratio with ultra-pure C1-INH (purified by anion exchange chromatography) for 2 h at 37°C in PBS. After incubation, complex formation was validated using SDS page and complexes were stored in 1% BSA-PBS at -80°C until further usage, while repeated freeze-thawing was prevented through aliquoting.

Development of C1s/C1-INH and MASP-1/C1-INH complex assays and assay performance

Two novel immunoassay detecting levels of C1s/C1-INH (cat #HK399) and MASP-1/C1-INH (cat# HK3001) complex *in*

vitro were developed. Plasma samples (citrate, heparin and EDTA), serum samples and standards were incubated in wells coated with monoclonal antibodies recognizing either the serine proteases C1s or MASP-1 of the complex. After incubation and washing, wells were incubated with an HRP-labeled monoclonal antibody detecting bound C1-INH in the complexes. Addition of tetramethylbenzidine (TMB) substrate started an enzymatic reaction thereby producing a colored product. The reaction was stopped by adding oxalic acid and the absorbance at 450 nm (OD450 nm) was measured using a spectrophotometer. This protocol was used to evaluate several assay characteristics such as (but not limited to) sensitivity, specificity, parallelism between calibrator and samples, matrix effects, recovery, intra- and inter variability and stability of samples and calibrators. All assay development aspects were evaluated using the following general requirements:

- Max. optical density at 450 nm (OD450 nm) ≤ 3.0,
- OD450 nm highest concentration standard/calibrator (S1) 1.7<OD450 nm< 3.0,
- OD450 nm blank ≤ 0.2, signal to noise ratio (S/N) > 10.

Variation between samples or conditions was evaluated by calculating the coefficient of variation.

$$\%\,CV = \frac{standard\ \ deviation\ \ (SD)}{mean} x100$$

Recovery of C1-INH complexes in EDTA plasma

To evaluate recovery of C1-INH complexes in EDTA plasma, samples of three individuals with different, but previously determined, complex concentrations (low, middle, and high) were mixed in different percentages/ratios (100–0, 75–25, 50–50, 25–75, 0–100) and incubated for 30 min at room temperature. Next, C1s/C1-INH complex and MASP-1/C1-INH complex concentrations were measured in these mixed samples. Recovery was determined according to following equation in which the expected concentration was compared to the observed (measured) concentration:

$$recovery\ [\%] = \frac{measured\ \ concentration\ \ of\ \ mixed\ \ sample}{expected\ \ concentration\ \ [(percentage\ \ x\ \ value\ \ sample\ \ A) + (percentage\ \ x\ \ value\ \ sample\ \ B)]} x100$$

In general, requirements were met if recovery was between 80% - 120%.

Specificity of the assays

The specificity or cross-reactivity of the C1-INH complex assays was tested in two ways. Firstly, cross-reactivity with other proteins or family members and the uncomplexed complement components was investigated. Uncomplexed complement components (C1s and C1-INH for the C1s/C1-INH complex, and MASP-1 and C1-INH for the MASP-1/C1-INH complex) were diluted in dilution buffer and signals were measured in the C1-INH complex assays as described above. Secondly, it was also investigated whether the assays show cross reactivity with species other than human. Serum samples of animal origin (mouse, rat, pig, horse and dog) were measured 10x less diluted compared to dilutions used for human samples.

Inter- and intra-assay variation

Intra-assay variation (multiple determinations of single samples within a single test run) was tested by the measurement of three independent aliquots each of four different samples within one test run. The experiment was conducted separately by two different operators and means and coefficients of variation (%CV) were calculated from the aliquots tested. Inter-assay variation (multiple determinations of single samples in several assay runs) was determined by calculation of the means and %CVs between the test runs from both operators.

A coefficient of variation <10% indicates low variation for intra-assay variation, while a coefficient of variation <20% indicates low variation for inter-assay variation.

Stability testing of C1-INH complexes

During development, both benchtop and freeze-thaw stability in samples were evaluated. Benchtop stability of the C1-INH complexes was assessed by incubating undiluted samples for different time intervals at room temperature as well as on ice, before those samples were measured in the assays as described above. The measured complex concentration of a sample kept at the respective condition for 10 minutes served as a control. Freeze-thaw stability was evaluated by repeatedly freezing (-80°C) and thawing individual aliquots of the samples for up to 4 cycles and comparing the measured C1-INH complex concentrations to concentrations determined in an unthawed aliquot. When performing the freeze-thawing steps, samples were thawed at room temperature, kept on ice for 10 min and subsequently frozen at -80°C. Stability testing of

the complexes was done in EDTA plasma, citrate plasma as well as in purified form (commercially available C1s/C1-INH complex or in-house MASP-1/C1-INH complex). Changes of the complex concentration between 80-120% compared to the controls (10 min sample for the benchtop stability, unthawed sample for the freeze-thaw stability) were considered as acceptable.

Preparation of zymosan activated serum

Zymosan was boiled in PBS for 1 h, and subsequently washed 4 times in PBS. After washing, zymosan was mixed to a final concentration of 10 mg/mL with 2% complement-preserved normal human serum (NHS) in VBS^{++} buffer (veronal-buffered saline containing 0.15 mM Ca^{2+} and 1 mM Mg^{2+}), before tubes were incubated at 37°C on a shaker (250 RPM). Samples were taken directly after mixing and after incubation for 5 min, 10 min, 20 min, 30 min, 1 h, 2 h, 3 h and 5 h. Directly after sampling, each sample was supplemented with EDTA to a final concentration of 10 mM, in order to avoid further artificial complement activation. Remaining zymosan was removed by centrifugation and the supernatant was stored at -80°C until further usage. When measuring C1-INH complex concentrations, samples were diluted further (3x for the MASP-1/C1-INH complex assay and 30x for the C1s/C1-INH assay) to measure in the reliable range of the assays, and levels of C1s/C1-INH and MASP-1/C1-INH complex were determined as described above.

Several controls were included: Auto-activation of the classical and lectin pathway was measured in NHS without addition of either EDTA or zymosan, one control sample contained NHS and 10 mM EDTA as a negative control (NHS+EDTA) and another sample contained all three components (NHS +zymosan+EDTA).

Specific activation of CP or LP

For specific activation of either the classical or the lectin pathway, complement-preserved normal human serum (NHS) was activated in a final concentration of 2% on WIESLAB® Complement System Screen plates (SVAR Life Science; WIESLAB® Complement System Classical Pathway (COMPLCP310RUO) for specific CP activation, WIESLAB® Complement System MBL Pathway (COMPLMP320RUO) for specific LP activation). Samples were activated for 5 min, 10 min, 20 min, 30 min, 1 h, 2 h and 3 h. After activation, the samples were collected from the wells, stored at -80°C, and used for C1s/C1-INH and MASP-1/C1-INH complex measurements at a later time point. Both complexes were determined as described before.

Subsequently, the level of complement pathway activity (as measured by C9 neoepitope formation during activation) was determined according to the manufacturer's instructions. Results were expressed as percentages calculated by the OD values measured in positive and negative controls, as suggested by the SVAR kits protocol.

Statistical analysis

GraphPad Prism 9 was used for statistical analysis and for data visualization. Comparisons of C1-INH complex levels in two different groups were performed either using the Mann-Whitney U or the one sample t-test when appropriate. For the zymosan and CP/LP activation, influence of incubation time and added reagents (zymosan, EDTA or both) or coating (IgM or mannan) on C1-INH complex concentrations was tested by performing a two-way ANOVA. If not stated otherwise, concentrations are given as mean ± SD. Normal distribution of complex levels was tested using the D'Agostino& Pearson test. For normally distributed values, the reference range was calculated using mean ±2SD. For skewed distribution of values, the reference range was reported using median (2.5 percentile range - 97.5 percentile range).

In all statistical tests a p-value<0.05 was considered statistically significant (* $p<0.05$, ** $p<0.01$, *** $p<0.001$, **** $p<0.0001$).

Results

Development and characterization of sandwich ELISAs measuring C1s/C1-INH complex and MASP-1/C1-INH complex

Two new immunoassays have been developed, measuring either C1s/C1-INH or MASP-1/C1-INH complex levels, both formed during complement regulation by binding of C1-INH to activated serine proteases.

The new assays are sandwich ELISAs that use murine monoclonal antibodies specifically recognizing either C1s (C1s/C1-INH assay) or MASP-1 (MASP-1/C1-INH assay), and C1-INH, ensuring that only C1-INH complexes are detected. While the initial assay setup was established using purified C1s/C1-INH and MASP-1/C1-INH complexes as a standard, minimally different curve progressions are obtained when the complexes are measured in EDTA plasma (Figures 2A, B). Hence, an EDTA plasma pool with known C1-INH complex concentrations was chosen as a calibrator for both assays, while exemplary standard curves are shown in Figures 2C, D. For the C1s/C1-INH assay, the curve progression was linear between 1.6-100.0 ng/mL (LLoQ: 0.2

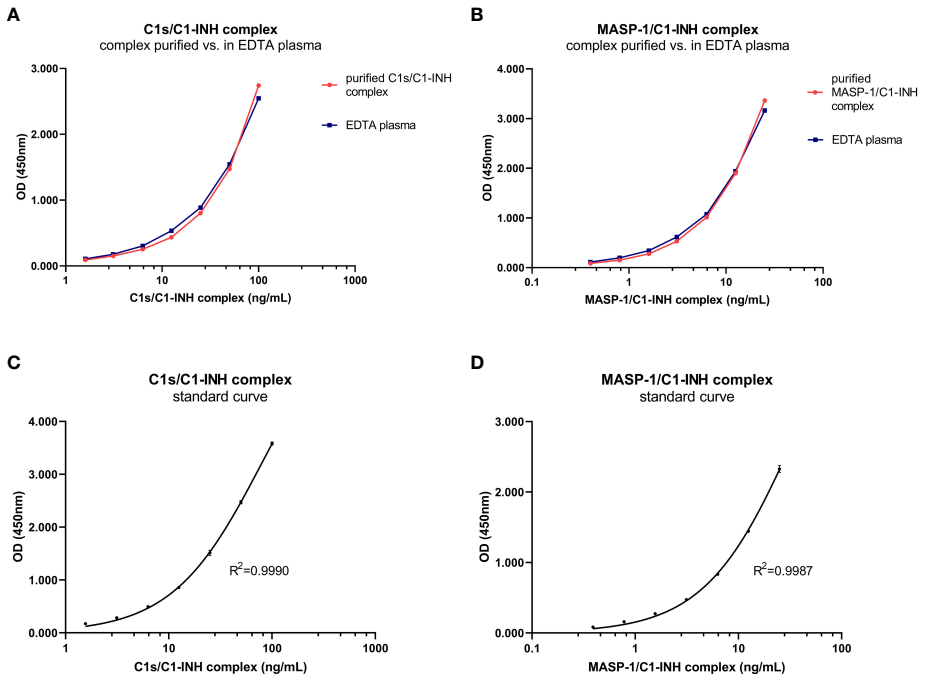

FIGURE 2
C1-INH complex standards purified in buffer and in EDTA plasma and exemplary standard curves. Parallelism of the C1-INH complexes is shown either purified in buffer (red) or in EDTA plasma (blue) for concentrations ranging from 1.6-100 ng/mL C1s/C1-INH complex **(A)** and 0.4-25 ng/mL MASP-1/C1-INH complex **(B)**. Representative results of a C1s/C1-INH complex standard curve **(C)**, ranging from 0 to 100 ng/mL; and a MASP-1/C1-INH complex standard curve **(D)**, ranging from 0 to 25 ng/mL. The coefficient of determination was obtained using non-linear regression (One-site binding, Hyperbola). OD, optical density; R^2, coefficient of determination; nm, nanometer; EDTA, Ethylenediaminetetraacetic acid.

ng/mL, ULoQ: 100.0 ng/mL) and resulted in a coefficient of determination of R^2 = 0.9990 between measured optical density (OD) values at 450nm and C1s/C1-INH complex concentration. For the MASP-1/C1-INH assay, the curve progression was linear between 0.4-25.0 ng/mL (LLoQ: 0.06 ng/mL, ULoQ: 50 ng/mL), resulting in R^2 = 0.9987. Non-linear regression (one-site binding, Hyperbola) was chosen for curve fitting. When levels of the respective C1-INH complexes are higher than the highest concentrations of the standard curves, a matrix effect and saturation of the standard curve can be observed (data not shown). Such interactions can be avoided by measuring samples at increased dilutions.

Matrix effects can occur when a target analyte interacts with matrix components in plasma or serum samples, and this might result in erroneous sample readings. In order to investigate whether matrix effects occur and to evaluate which matrices are suitable for reliable measurements of C1-INH complexes using these new immunoassays, serially diluted citrate plasma, heparin plasma, EDTA plasma and serum samples derived from the same individual were analyzed (Figure 3). Calculated concentrations and coefficients of variation (%CVs) for these matrices are listed in Table 1. While C1-INH complex concentrations could be measured in all four matrices, the resulting values vary depending on the sample type. C1s/C1-INH complex levels were similar in EDTA and citrate plasma, while higher levels were observed in heparin plasma and serum. Therefore, the latter sample types need to be diluted more during measurements in the ELISA. For the MASP-1/C1-INH complex, highest levels were measured in serum and lower complex levels in all plasma types tested. Coefficients of variation for serum samples were slightly higher compared to plasma samples for both complexes, but all %CVs were below 10% and hence in an acceptable range.

Although *in silico* amino acid searches did not identify any proteins with >60% similarity to the antigens used for antibody development, cross-reactivity of the individual antibodies was tested in a direct ELISA using either purified or recombinant proteins of the respective pathways, depending on availability. The anti C1-INH monoclonal antibody showed a strong signal for purified C1-INH, while very weak signals could also be observed detecting purified C1q or C1s (OD450nm<0.1 for both proteins, and hence below the background threshold of OD450nm<0.2 and neglectable) (Figure 4A). The antibody did not bind to any of the recombinant proteins tested. The anti C1s antibody showed strong signals for both, recombinant and purified C1s, but not for any other protein tested, while the anti MASP-1 monoclonal antibody only showed signals for recombinant MASP-1 (Figure 4B).

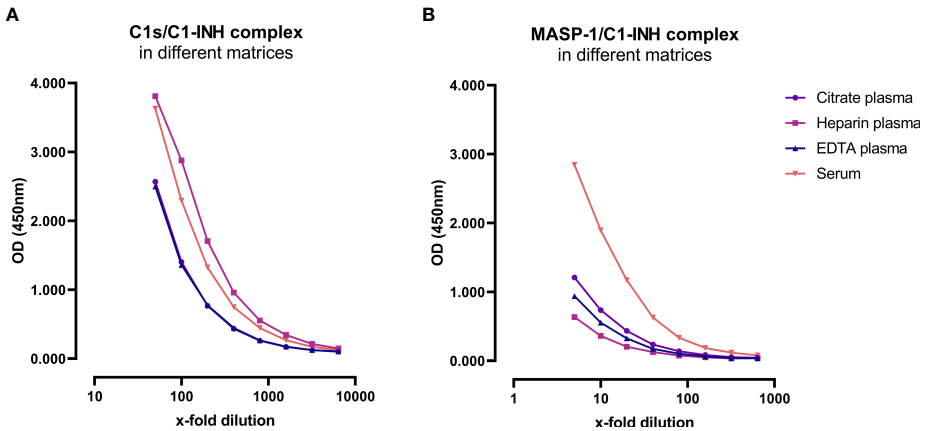

FIGURE 3
C1-INH complex concentrations in different matrices. Exemplary results of Citrate plasma (purple), Heparin plasma (pink), EDTA plasma (blue) and serum samples (red) from a single individual are plotted in a dilution range from 50x-6400x for the C1s/C1-INH complex **(A)** and in a dilution range from 5x-640x for the MASP-1/C1-INH complex **(B)**. Influence of matrices on C1-INH complex concentrations was investigated in two individuals, while results of one individual each are shown here as an example. OD, optical density; EDTA, Ethylenediaminetetraacetic acid; nm, nanometer.

After the sandwich ELISA protocol was established, cross-reactivity of the assays was investigated using uncomplexed complement components. When applying both the uncomplexed proteins and the C1-INH complexes (standard curve) to the assays, in concentrations 4x higher compared to the standard curve, only the C1-INH complexes are showing specific signals (Figures 4C, D).

Cross-reactivity of the complex assays with other species was tested using blood samples from animal origin. When measuring blood samples from animals (mouse, rat, horse, pig, dog) in the immunoassays, only murine samples (n=3) showed strong cross-reactivity in the C1s/C1-INH assay, while no signals were observed using blood from other animals tested (Figure 4E). None of the animal sera tested showed a strong signal in the MASP-1/C1-INH assay (Figure 4F).

In order to assess the accuracy of the assays, inter-assay variation (variation of multiple measurements of single samples in a single test run) and intra-assay variation (variation of multiple determinations of a single sample in several test runs performed by different operators) were investigated. Both assays showed inter- and intra-assay coefficients of variation<10%, indicating only low variation between multiple runs as well as between different operators (Table 2).

Recovery of the C1-INH complexes was analyzed in EDTA plasma by mixing of samples with varying complex concentrations in different ratios. An average recovery >90% was seen for both immunoassays (Table 3). In general, a recovery between 80-120% was accepted in the experiment, indicating high accuracy. The expected concentrations of the single samples are plotted against the measured concentrations in Figure 5. In both cases expected vs. measured concentration correlated significantly ($p<0.0001$), with correlation coefficients of R=1.000 for the C1s/C1-INH complex and R=0.999 for the MASP-1/C1-INH complex.

In summary, the tests performed during assay development and optimization showed that both assays are able to measure the C1-INH complexes in an accurate, specific and reliable manner. Described assay characteristics are summarized in Table 4.

TABLE 1 Analysis of different matrices.

	C1s/C1-INH complex				MASP-1/C1-INH complex			
Matrix	**Citrate**	**Heparin**	**EDTA**	**Serum**	**Citrate**	**Heparin**	**EDTA**	**Serum**
mean concentration(ng/mL)	2270	6215	2348	4612	37.5	16.6	26.5	121.7
SD (ng/mL)	81	279	93	251	1.8	0.8	1.6	10.6
CV (%)	3.6	4.5	4.0	5.4	4.7	4.7	5.9	8.7

Representative results of a single individual are listed, while influence of matrices on C1-INH complex concentrations was investigated in two individuals each. Samples were 2-fold serially diluted to establish best dilution ranges over at least three dilution steps for each matrix tested. %CV was calculated to determine the variability for each serial dilution and a %CV ≤20 was considered as minimal matrix effect. SD, standard deviation; %CV, coefficient of variation; EDTA, ethylenediaminetetraacetic acid.

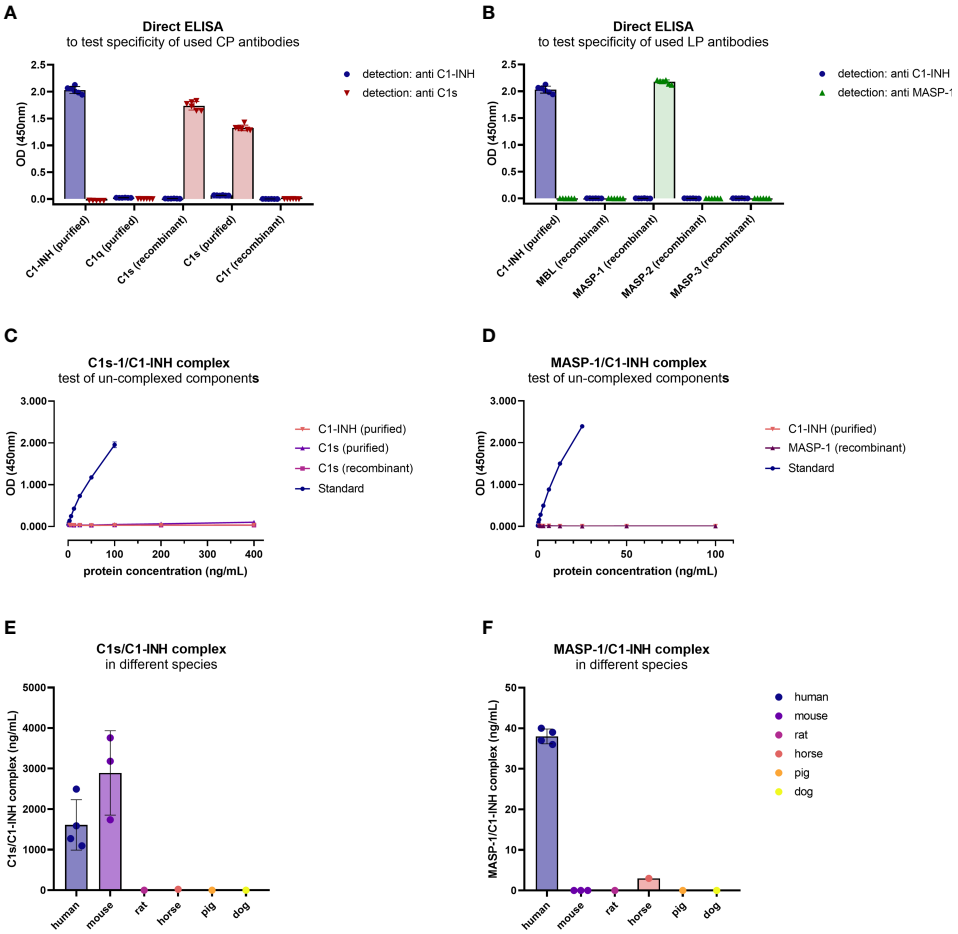

FIGURE 4
Cross-reactivity of antibodies and new immunoassays. **(A, B)** Binding of antibodies to proteins of the respective pathways was tested in a direct ELISA. For classical pathway proteins, detection was done with either the C1-INH or C1s antibody, while for lectin pathway proteins detection was done with the C1-INH and MASP-1 antibodies also used during assay development. Conditions were tested in duplicates, while the experiment was performed in triplicates. **(C, D)** Cross-reactivity of un-complexed complement components was tested using either purified or recombinant proteins of the complex, dependent on availability. While C1s (purified and recombinant) and C1-INH (purified) were tested in the C1s/C1-INH complex assay **(C)**, MASP-1 (recombinant) and C1-INH (purified) were measured in the MASP-1/C1-INH assay **(D)**. **(E, F)** Cross-reactivity of serum samples from animal origin was investigated in the assays using human EDTA plasma samples (n=4) as a reference, murine serum (n=3), rat serum (n=1), horse serum (n=1), pig serum (n=1) and dog serum (n=1) (**E**: C1s/C1-INH complex, **F**: MASP-1/C1-INH complex). Animal samples were measured 10x less diluted compared to human samples. OD, optical density; nm, nanometer.

Validation of C1-INH complexes as markers for early complement activation markers

In order to validate the C1-INH complexes as markers for early classical and early lectin pathway activation, normal human serum (complement-preserved) was activated by zymosan and changes of C1s/C1-INH complex and MASP-1/C1-INH complex levels over time were measured after activation using the newly developed immunoassays. The results showed a strong increase in the complex concentrations for both C1-INH complexes investigated, while the concentrations at time zero (T0) were comparable for all four approaches tested, with mean concentrations of 2829 ± 138 ng/mL C1s/C1-INH complex and 111.4 ± 3.5 ng/mL MASP-1/C1-INH complex (Figures 6A, B).

For the C1s/C1-INH complex, complex levels in the NHS+zymosan sample increased reaching a plateau of around 16000 ng/mL after 5 h of activation, a 5.7-fold increase compared to the starting concentration (Figure 6A). Complex concentrations in the NHS sample without any additions also increased up to a level of 14000 ng/mL C1s/C1-INH within 5 h, indicating strong auto-activation of the classical pathway when no EDTA is present. Both controls with EDTA were stable for up to 2 h, while in the NHS+EDTA sample an increase in C1s/C1-INH complexes up to 5000 ng/mL was measured when incubating for more than 2 hours at 37°C.

10.3389/fimmu.2022.1039765

TABLE 2 Inter- and Intra-assay variation of C1-INH complex assays.

C1s/C1-INH complex		sample 1	sample 2	sample 3	sample 4
Intra-assay variation					
Operator 1	mean aliquot 1-3 (ng/mL)	1161	1967	1595	1285
	SD (ng/mL)	90	121	49	63
	CV (%)	7.8	6.2	3.1	4.9
Operator 2	mean aliquot 1-3 (ng/mL)	1245	2135	1868	1399
	SD (ng/mL)	47	166	99	43
	CV (%)	3.8	7.8	5.3	3.1
Inter-assay variation					
	mean Operator 1 and 2 (ng/mL)	1203	2051	1731	1342
	SD (ng/mL)	79	159	165	79
	CV (%)	6.6	7.8	9.5	5.9
MASP-1/C1-INH complex		**sample 1**	**sample 2**	**sample 3**	**sample 4**
Intra-assay variation					
Operator 1	mean aliquot 1-3 (ng/mL)	273.2	115.5	57.3	35.5
	SD (ng/mL)	6.6	0.7	3.6	0.5
	CV (%)	2.4	0.6	6.2	1.5
Operator 2	mean aliquot 1-3 (ng/mL)	259.0	108.3	52.4	34.7
	SD (ng/mL)	8.1	2.4	1.2	0.6
	CV (%)	3.1	2.2	2.4	1.8
Inter-assay variation					
	mean Operator 1 and 2 (ng/mL)	266.1	111.9	54.9	35.1
	SD (ng/mL)	10.2	4.3	3.6	0.7
	CV (%)	3.8	3.8	6.6	1.9

Intra-assay variation (multiple determinations of single samples within a single test run) and inter-assay variation (multiple determinations of single samples in several assay runs) was determined for both complex assays by calculation of mean concentrations and %CV using 3 independent aliquots of 4 different samples in 2 test runs (performed by 2 different operators). A %CV ≤10 indicates low variation for the intra-assay variation, while a CV% ≤20 indicates low inter-assay variation. %CV, coefficient of variation.

Formation of the MASP-1/C1-INH complex seems to reach its maximum more rapid, with the highest rate of C1-INH complex formation again being observed in the NHS sample activated with zymosan (Figure 6B). Here the complex concentration doubled to 224 ng/mL within one hour, while the concentration did not increase further when activation is continued out to 5 h. In contrast to the C1s/C1-INH complex, no significant increase in MASP-1/C1-INH complex was seen in the normal human serum without activator (zymosan) or in the samples additionally containing EDTA (NHS+EDTA and NSH+zymosan+EDTA).

A two-way ANOVA showed highly significant effects of the added compounds (EDTA or zymosan) as well as the incubation time for both complexes, when compared to the control samples (results in legend of Figure 6).

In addition, formation of C1-INH complexes was also investigated in conditions where only one of the two pathways were specifically activated. When only activating the classical pathway using IgM coating, concentrations of C1s/C1-INH complex did increase in accordance with CP activity, measured by the formation of C9 neoepitope within the same samples, while MASP-1/C1-INH complex levels did not change markedly (Figures 6C, D). During CP activation, C1s/C1-INH complex levels already show a significant increase within 5 min ($p=0.0101$), and this increase stayed highly significant when activating for 10 minutes or longer, when compared to baseline ($p>0.0001$). Vice versa, when specifically activating the lectin pathway *via* mannan coating, there is a significant increase in MASP-1/C1-INH complex levels (60 min activation: $p=0.0140$; >60 min activation: $p<0.0001$) as well as of the LP activity (again measured by C9 neoepitope formation) over time, whereas C1s/C1-INH complex concentrations remained unchanged when compared to baseline values (Figure 6D). Only when activating the LP for more than 2h at room temperature, C1s/C1-INH complex levels also differ significantly from baseline ($p=0.0456$), which can be explained by auto-activation of the classical pathway. Those findings further confirm the potential of C1-INH complexes as specific markers for early classical and early lectin pathway activation.

Since increasing C1-INH complex levels were also observed without the addition of zymosan, the rate of auto-activation of the respective complement pathways was investigated in EDTA plasma and citrate plasma by incubating several samples for up to 16 h at room temperature and on ice. While incubation on ice for up to 16

10.3389/fimmu.2022.1039765

TABLE 3 Recovery of C1s/C1-INH and MASP-1/C1-INH complexes in EDTA plasma.

	Sample composition (%)				
	100 + 0	**75 + 25**	**50 + 50**	**25 + 75**	**0 + 100**
	mixture of sample 1 (high) and sample 2 (medium)				
C1s/C1-INH (ng/mL)	12086	10517	7014	5160	2476
Recovery (%)	–	109	96	106	–
	mixture of sample 1 (high) and sample 3 (low)				
C1s/C1-INH (ng/mL)	11728	9436	6002	3325	1135
Recovery (%)	–	104	93	88	–
	mixture of sample 2 (medium) and sample 3 (low)				
C1s/C1-INH (ng/mL)	2736	2013	1712	1386	1136
Recovery (%)	–	86	88	90	–
	mixture of sample 1 (high) and sample 2 (medium)				
MASP-1/C1-INH (ng/mL)	271	201	152	90	58
Recovery (%)	–	92	93	81	–
	mixture of sample 1 (high) and sample 3 (low)				
MASP-1/C1-INH (ng/mL)	256	184	140	71	30
Recovery (%)	–	92	97	82	–
	mixture of sample 2 (medium) and sample 3 (low)				
MASP-1/C1-INH (ng/mL)	56	47	41	34	30
Recovery (%)	–	95	96	94	–

Recovery of the C1s/C1-INH complex (upper part) and MASP-1/C1-INH complex (lower part) was investigated by mixing EDTA plasma samples of three individuals with low, middle and high complex concentration in different ratios (100 + 0, 75 + 25, 50 + 50, 25 + 75, 0 + 100). After 30min. of incubation, C1-INH complex concentrations were determined in the respective assays and recovery (difference between expected and observed C1-INH complex concentration) was calculated according to the equation stated in the Material and Methods section. EDTA, ethylenediaminetetraacetic acid; min, minutes.

h does not strongly affect C1-INH complex concentrations in EDTA plasma, an increase is seen when samples are kept at room temperature for more than four hours (Figures 7A–D). Especially for the C1s/C1-INH complex, additional complex formation is observed even in EDTA plasma at room temperature when incubating for more than two hours (Figure 7A).

Citrate plasma showed additional complex formation if samples are kept at room temperature for more than 1 h

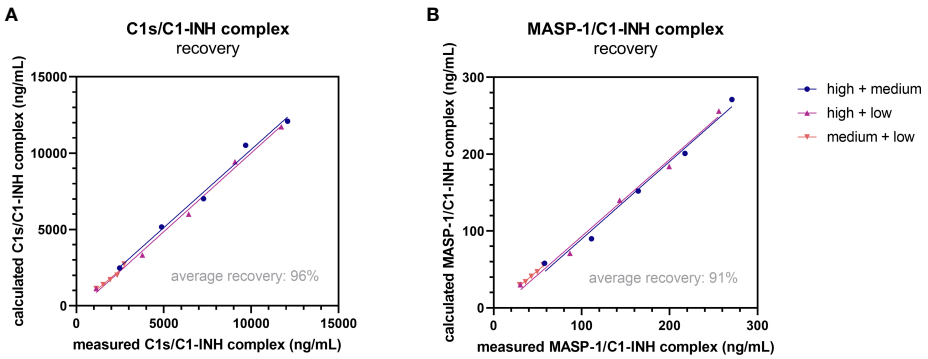

FIGURE 5
Recovery of complexes in EDTA plasma. Recovery of the C1s/C1-INH complex **(A)** and MASP-1/C1-INH complex **(B)** was investigated by mixing EDTA plasma samples of three individuals with low, middle and high complex concentration in different ratios (100 + 0, 75 + 25, 50 + 50, 25 + 75, 0 + 100). After 30 min of incubation, C1-INH complex concentrations were determined in the respective assays and recovery (difference between expected and observed C1-INH complex concentration) was calculated according to the equation stated in the Material and Methods section. EDTA, ethylenediaminetetraacetic acid; min, minutes.

TABLE 4 Summarized characteristics of newly developed C1-INH complex assays.

	C1s/C1-INH complex assay	MASP-1/C1-INH complex assay
Standard range	100.0 – 1.6 ng/mL	25.0 – 0.4 ng/mL
Limit of quantification **ULoQ** **LLoQ**	100.0 ng/mL 0.2 ng/mL	50 ng/mL 0.06 ng/mL
cross-reactivity with uncomplexed components	no	no
cross-reactivity with animal serum (mouse, rat, horse, pig, dog)	mouse	no
Inter-assay variation	< 10%	< 10%
Intra-assay variation	< 10%	< 10%
Matrices to be used (minimal required dilution)	EDTA plasma (100x) Citrate plasma (100x) Heparin plasma (200x) Serum (200x)	EDTA plasma (5x) Citrate plasma (5x) Heparin plasma (5x) Serum (10x)
Measured complex concentration in healthy individuals, n=96	1846 ± 1060 ng/mL [mean ± 2SD]	40.5 (13.8-87.9) ng/mL [median (2.5-97.5 percentile range)]

EDTA, ethylenediaminetetraacetic acid; ULoQ, upper limit of quantification; LLoQ, lower limit of quantification; SD, standard deviation.

(Figures 7C, D), while concentrations are more than double the initial levels after 16 h at room temperature. When incubating on ice, the formation of new C1-INH complexes occurs more slowly, but again at a higher rate than when compared to EDTA plasma.

Those findings indicate the importance of sample handling and the usage of EDTA plasma when investigating complement activation products in general, but more specifically C1-INH complexes.

To obtain more information about appropriate sample handling, we also investigated freeze-thaw stability of the C1-INH complexes in EDTA plasma samples as well as in purified form (commercially available C1s/C1-INH complex and in-house MASP-1/C1-INH complex). Exposure of the samples to up to four freeze-thaw cycles revealed that both complexes are relatively stable in EDTA plasma for multiple rounds of freezing and thawing. However, the purified C1s/C1-INH complex seems to be more prone to degradation with an increasing number of freeze-thaw cycles compared to the MASP-1/C1-INH complex (Figures 7E, F).

Clinical validation of the novel immunoassays in healthy controls and COVID-19

The newly developed assays were used to measure C1s/C1-INH complex and MASP-1/C1-INH complex levels in healthy individuals (n=96) as well as in a total of 414 COVID-19 patients.

In healthy individuals, measurement of C1-INH complexes resulted in a mean physiological concentration of 1846 ± 1060 ng/mL C1s/C1-INH complex (mean ± 2SD) and in 36.9 (13.18 - 87.89) ng/mL MASP-1/C1-INH complex [median (2.5 percentile range – 97.5 percentile range)]. Distribution of the concentration levels measured in healthy adults are shown in Figures 8A, B. While physiological C1s/C1-INH complex concentrations are normally distributed within the observed concentration range (p=0.0974), MASP-1/C1-INH complex levels are right-skewed (p<0.0001).

Besides that, no significant differences in C1-INH complex levels between healthy males (n=50) and females (n=46) were observed (Figures 8C, D). Additionally, no correlation is present between the C1-INH complex levels and the age of healthy adults (Figures 8E, F).

In order to perform a proof-of-concept study including diseased samples, the new immunoassays were utilized to measure C1-INH complex concentrations in a cohort of 414 COVID-19 patients (median delay between symptom onset or positive PCR test and sampling: 10.0 days (IQR 6.0 – 27.8)).

Measurements showed increased C1-INH complex levels in COVID-19 patients when compared to healthy controls, with a mean concentration of 2407 ± 1283 ng/mL C1s/C1-INH complex (Mann-Whitney U test: p<0.0001, Figure 9A) and 51.5 (33.5-76.1) ng/mL MASP-1/C1-INH complex (Mann-Whitney U test: p<0.0001, Figure 9B).

Discussion

Although complement dysregulation and overactivation underlies many pathological conditions (40–42), its precise role is often not clear. To understand how complement is dysregulated in a certain type of disease, it is important to unravel which pathway (either the CP, LP or AP) is (over) activated and to what extent. Here we propose that C1-INH complexes might be suitable markers to monitor early classical or lectin pathway activation. However, as tools for accurately

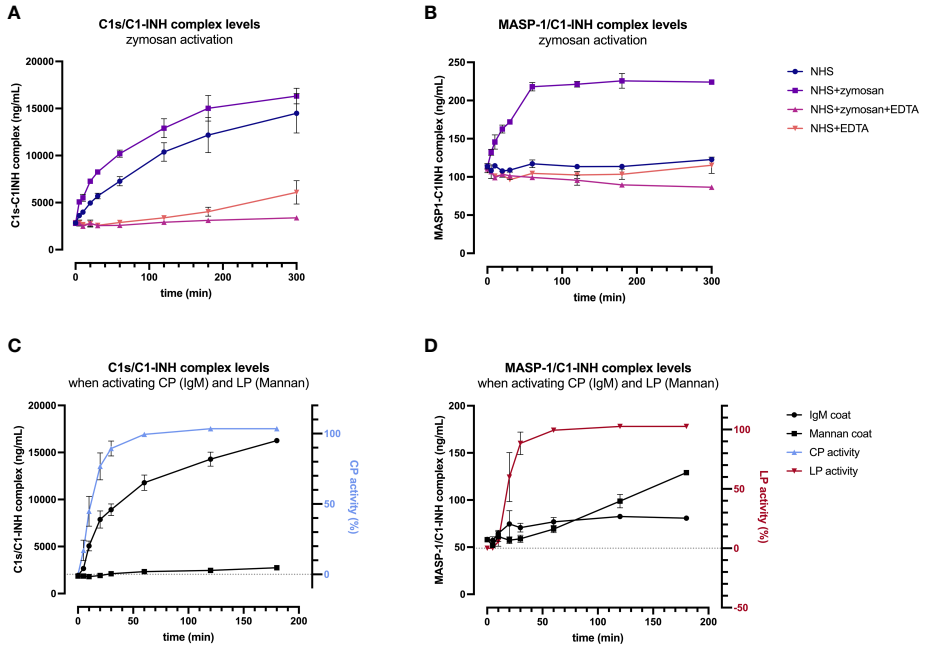

FIGURE 6
Validation of C1-INH complexes as activation markers: zymosan-initiated **(A, B)** and pathway-specific **(C, D)** complex formation over time. For zymosan-activation **(A, B)**, normal human serum was incubated either alone or with zymosan, EDTA, or a mix thereof, for up to 5 hours at 37 °C. Samples were taken at several time points and concentrations of C1s/C1-INH complex **(A)** and MASP-1/C1-INH complex **(B)** were determined using the new immunoassays. Plotted values show C1-INH complex concentrations (mean ± SD) of two independent activation experiments performed in duplicates each, while effects of added compounds (zymosan, EDTA) and incubation time on C1-INH complex levels were analyzed with a two-way ANOVA with Tukey's multiple comparisons test. For the C1s/C1-INH complex, a statistically significant effect was seen for the zymosan-treated sample for both, the incubation time ($p<0.0001$) as well as the treatment (NHS+zymosan vs. NHS: $p=0.0399$, NHS+zymosan vs. NHS+zymosan+EDTA: $p<0.0001$, NHS +zymosan vs. NHS+EDTA: $p<0.0001$). For the MASP-1/C1-INH complex, the zymosan-treated sample did also show statistically significant effects for the incubation time ($p<0.0001$) as well as the treatment (NHS+zymosan vs. all other treatments tested: $p<0.0001$). For pathway-specific activation **(C, D)**, normal human serum was incubated on wells coated with either IgM (CP) or mannan (LP), for up to 3 hours at 37 °C. After incubation, C1-INH complex levels were determined in the supernatant (**C**: C1s/C1-INH complex; **D**: MASP-1/C1-INH complex), while C9 neoepitope formation was measured on the respective wells (WIESLAB® Complement System kits). Plotted values show mean concentrations of C1-INH complexes (mean ± SD) and normalized CP and LP activity (as measured by C9 neoepitope formation using positive and negative controls provided in the kits) of three independent experiments. NHS, normal human serum; EDTA, ethylenediaminetetraaceticacid; SD, standard deviation; min, minutes; IgM, immunoglobulin M; TCC, terminal complement complex.

measuring these markers are currently lacking, we aimed to develop novel immunoassays that are able to assess these complexes in human samples. We successfully developed two sandwich enzyme-linked immunosorbent assay that allow the quantification of C1s/C1-INH and MASP-1/C1-INH complex levels in a comparable manner in human plasma and serum samples. In addition, we define a reference range in healthy controls for both complexes. Beyond that, we show that measurement of ongoing complement activation is possible through the determination of C1-INH complex levels, where C1s/C1-INH levels indicate early classical pathway activation and MASP-1/C1-INH complex levels serve as a marker for early lectin pathway activation.

The newly developed immunoassays show low inter- and intra assay variation as well as high recovery, indicating that the complexes can be quantified in a reliable and robust manner. The monoclonal antibodies used for both assays are highly specific as no or only very weak cross-reactivity was observed for the un-complexed proteins (C1s, MASP-1 and C1-INH) and related proteins (C1q, C1r, MBL, MASP-2 and -3) in both a direct or sandwich ELISA setup. Although the weak signals for both the un-complexed as well as the related proteins are probably due to a non-specific background signal, it cannot be excluded that some of these signals are caused by contamination from the complexes themselves. When available, we used proteins purified from human blood (C1q, C1s, C1-INH). It is possible that these purified proteins contain traces of the complexes in addition to the individual proteins as purification methods are never 100% successful. Indeed, for the purified proteins that were commercially available, the suppliers only guarantee a purity of ≥90%. Also cross-reactivity with species other than human was tested and the C1s/C1-INH complex assay strongly cross-reacted with murine samples, although not fully validated yet, making it also a

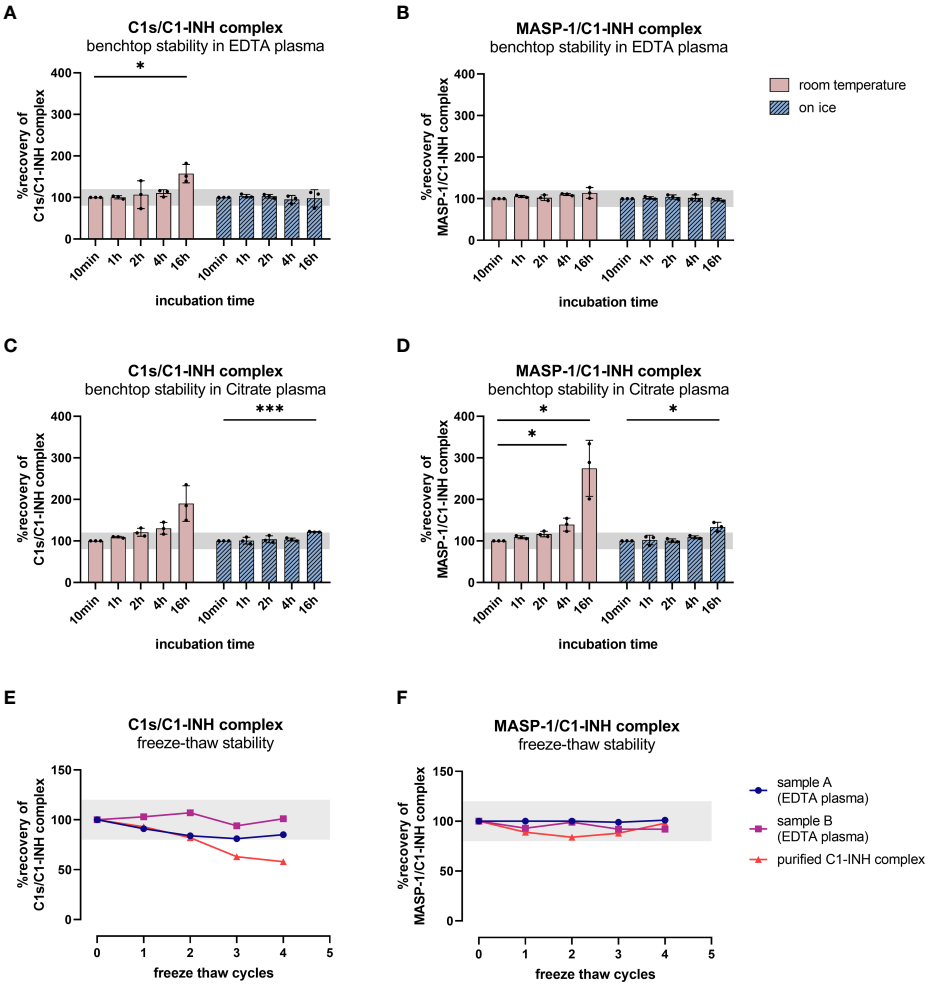

FIGURE 7
Benchtop stability of C1-INH complexes in EDTA plasma and Citrate plasma **(A–D)** and freeze-thaw stability of complexes in EDTA plasma and in purified form **(E, F)**. For benchtop testing (panels **A–D**), samples were stored at room temperature (red graphs) or on ice (blue graphs) for different time intervals (10 min-16 h). Afterwards concentrations of either C1s/C1-INH complex (**A**: EDTA plasma, **C**: Citrate plasma) or MASP-1/C1-INH complex (**B**: EDTA plasma, **D**: Citrate plasma) were measured in the samples. C1-INH concentrations of the 10 min samples were set as 100% and the amount of complexes at other time points was calculated in relation to the 10 min sample. Differences to the 10 min sample were calculated using one sample t-test (* $p<0.05$, *** $p<0.001$, non-significant results are not marked). Due to natural variation in biomarker measurements, acceptable concentrations ranged from 80-120% compared to the concentration in the respective 10 min sample. For analysis of freeze-thaw stability (panels **E, F**), aliquots of either purified C1-INH complex (plotted in red) or two independent EDTA plasma samples (plotted in blue and pink) were exposed to 0 to 4 freeze-thaw cycles and concentrations of C1s/C1-INH complex **(E)** and MASP-1/C1-INH complex **(F)** were determined in the respective sandwich ELISAs. Due to natural variation when measuring biomarkers, acceptable complex concentrations ranged from 80-120% of the original concentration (0 freeze thaw cycles) and the accepted range is marked in grey on the figures. min, minutes; h, hours; EDTA, ethylenediaminetetraacetic acid.

potential tool for researchers investigating classical pathway activation or CP related diseases in mice. The MASP-1/C1-INH complex assay did not show strong signals when using samples of animal origin.

Robust immunoassays are particularly important within the complement field, as it has been shown that measuring complement components in a reliable way is challenging. Large variation exists in complement measurements between different laboratories, partly caused by a lack of standardized assays and reagents (43). As well known for other complement measurements (44, 45), sample type and handling is crucial when determining C1-INH complex levels. The assays described here can be used for all human plasma types and serum, while dilutions might have to be adopted depending on the matrix used. However, heparinized plasma should be avoided when measuring C1-INH complexes as low signals for the MASP-1/C1-INH complex were observed when using heparin plasma. This effect might be caused by the fact that MASP-1, in the

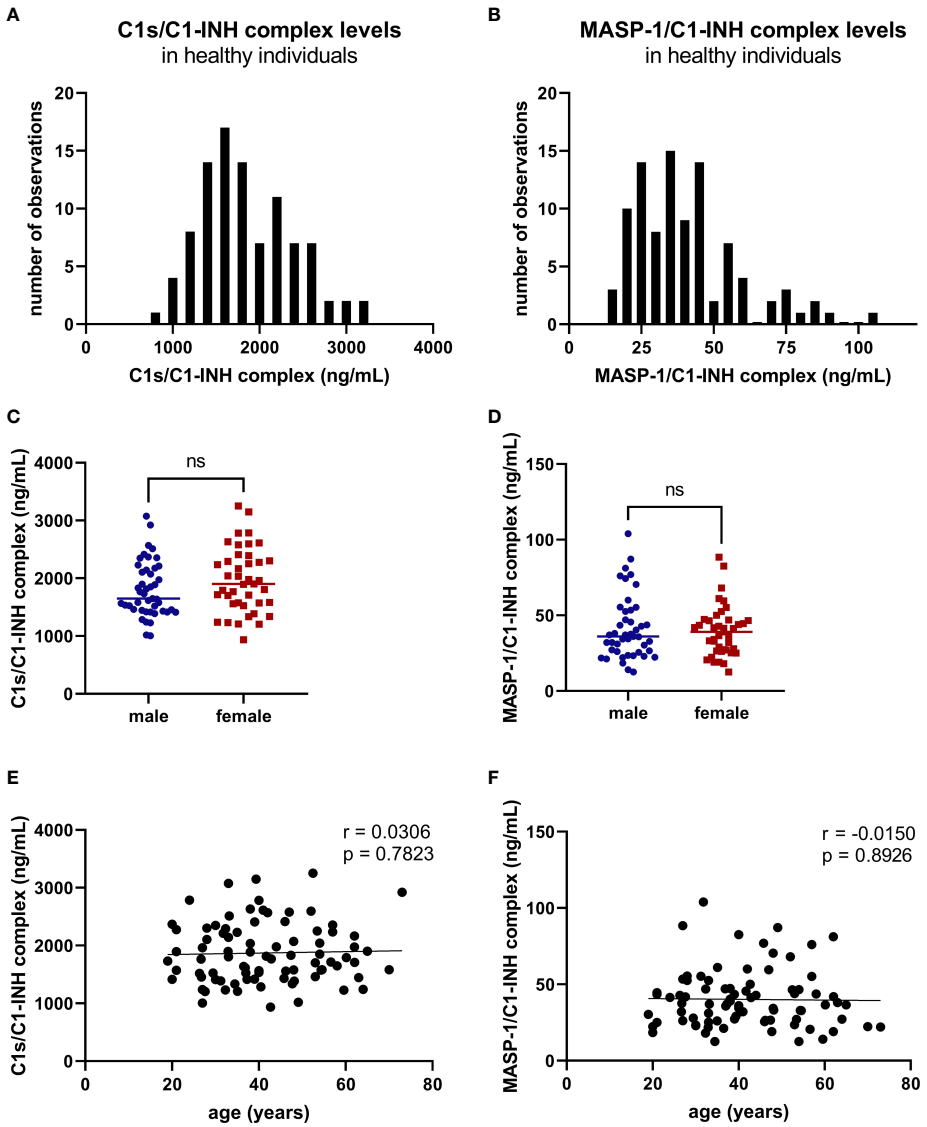

FIGURE 8
C1-INH complex levels in healthy adult individuals. C1-INH complex concentrations were measured in 96 healthy adult individuals, using the new immunoassays. Distributions of C1s/C1-INH complex **(A)** and MASP-1/C1-INH complex concentrations **(B)** are shown in histograms. Concentrations in healthy adults were furthermore stratified according to gender (**C**: C1s/C1-INH complex, **D**: MASP-1/C1-INH complex) and age (**E**: C1s/C1-INH complex, **F**: MASP-1/C1-INH complex). No significant differences between males (n=50) and females (n=46) were observed when comparing the groups using Mann-Whitney test. ns, not significant; r, correlation coefficient.

presence of heparin, is more likely to form complexes with antithrombin than with C1-INH (46, 47). Due to increased complex formation between MASP-1 and antithrombin, the MASP-1/C1-INH complex formation might be diminished. In contrast, C1s/C1-INH complex levels were highest in heparin plasma in our experiments. A possible explanation is that heparin is able to enhance the rate of inhibition of active C1s by C1-INH (48), leading to artificial complex formation.

Additional complex formation can also occur in serum samples, which is especially true for the C1s/C1-INH complex. In general, it is recommended to use EDTA plasma samples when the activation state of complement pathways at a given time-point is investigated. EDTA chelates both Ca^{2+} and Mg^{2+} and thereby blocks the function of the complement by destabilizing the pattern-recognition complexes (49–51). Our results show that an EDTA concentration ≥10 mM was able to effectively minimize *in vitro* complement activation for either 4 h at room temperature or 16 h on ice, also shown by Yang and co-workers in the past (52). Typically, EDTA plasma should be used when investigating C1-INH complex levels, samples should be

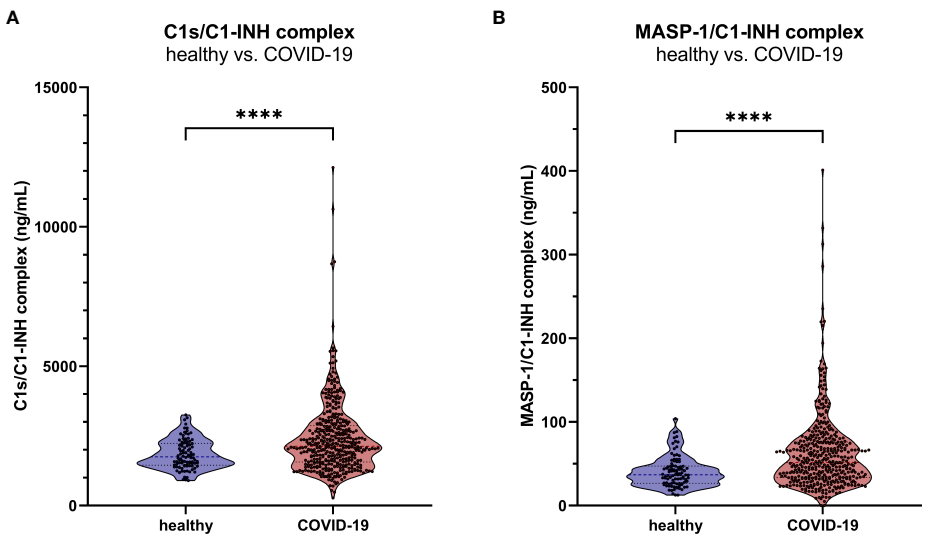

FIGURE 9
C1-INH complex levels in adult COVID-19 patients. The new immunoassays were clinically validated by the measurement of C1s/C1-INH complex **(A)** and MASP-1/C1-INH complex levels **(B)** in 414 COVID-19 patients as well as in 96 healthy controls. P values for the pair-wise group comparisons (healthy vs. COVID-19) were calculated by the Mann-Whitney test (**** p<0.0001).

stored at -80°C until further usage and kept on ice after thawing until the measurements in order to avoid *de novo* formation of C1-INH complexes *ex vivo*. When sample handling is not appropriate, particularly the classical pathway can be activated (53). This spontaneous CP activation without addition of activating reagents such as zymosan can be caused by naturally circulating immune complexes or by Ig aggregation during incubation *ex vivo* (53, 54). The MASP-1/C1-INH complex seems to be less prone to sample handling. As expected, no increase of MASP-1/C1-INH complex levels was observed when incubating NHS without zymosan, since no substance specifically activating the lectin pathway is present in serum under physiological conditions.

During assay development, the stability of the complexes was also investigated after freeze-thawing. C1-INH complexes in purified form are more at risk of degradation than in plasma during repeated freeze-thawing, as we observed that complex concentrations in EDTA plasma remain relatively stable and do not decrease much after up to four freeze-thaw cycles. Similar findings were made earlier for C1rs/C1-INH and other complement activation products (55), allowing reliable determination of C1-INH complexes also in samples that have been thawed before, provided that sample handling in between freezing is appropriate.

After establishing a first prototype assay for both complexes, we further investigated whether these complexes indeed could serve as biomarkers for assessing early CP and/or LP activation. For this, Zymosan A, a carbohydrate polymer prepared from *Saccharomyces cerevisiae* cell walls was used. It is mainly known for AP activation through enhancement of alternative pathway C3 convertase assembly and stability (56), but can also induce LP and CP activation (57, 58). Therefore, Zymosan A was chosen to monitor *in vitro* CP and LP activation. When complement-preserved serum samples were incubated with zymosan, both C1-INH complexes showed an increase in concentration over time. Besides that, specific activation of the classical pathway led to a strong increase only in the levels of C1s/C1-INH complex as well as the formation of C9 neoepitope, while selective activation of the lectin pathway only resulted in formation of MASP-1/C1-INH complexes (Figure 6). These results provide evidence that the complexes may specifically differentiate between activation of the early classical or lectin pathway, and are potentially suitable markers for assessing and monitoring early CP and/or LP activation in various *in vitro* and *in vivo* conditions.

So far, the only way to investigate CP and LP activity in general are either hemolytic assays or functional ELISAs. The former are based on hemolysis of antibody-sensitized erythrocytes of animal origin by complement components of the added samples (59), while the latter are determining activity of the different pathways by measuring a neo-epitope generated by the MAC formation following activation (60, 61). Both require complement-preserved serum of the specimen to be tested and do not give an indication about ongoing activation of the respective pathways at a given time-point. Availability of complement-preserved serum is often a problem, especially when it comes to investigations of big cohorts. Measurement of the C1-INH complexes as described here does not require complement-preserved samples and can also be done in a more standardized way compared to hemolytic assays relying on fresh animal blood cells for every experiment.

The reference range of C1s/C1-INH complex in healthy adults was found to be 1846 ± 1060 ng/mL (mean ± 2SD), and hence is in line with concentrations already published in the literature utilizing in-house immunoassays. C1s/C1-INH complex concentrations previously reported were 1.0 ± 0.2 mg/L in plasma and 2.1 ± 0.8 mg/L in serum of nine healthy individuals (62), or 25.04 (13.9-36.9) nM in EDTA plasma of six healthy controls (30). While the C1s/C1-INH complex concentration was normally distributed, MASP-1/C1-INH complex levels were slightly right-skewed in healthy adults and the distribution did not pass normality testing. This indicates that other factors may have an effect on MASP-1/C1-INH complex levels, like involvement of the respective proteins in other physiological processes or influence of the genetic background of the individuals (63). However, further investigations are necessary in order to confirm potential causes of the observed right-skewed distribution. Due to a missing normally distribution, the 2.5 - 97.5 percentile range was used to define a reference range for the new lectin pathway activation marker, resulting in a physiological concentration of 36.9 (13.18 -87.89) ng/mL MASP-1/C1-INH complex. Although differences in some complement protein levels are reported to be significantly influenced by gender and age (64), no significant changes in C1-INH complex levels between males and females were observed in our study, which is in line with previous investigations of several complement activation products, also including C1rs/C1-INH (55). Besides that, the complex levels did not correlate with age in healthy adults, so probably no correction for age or gender is necessary in future studies investigating C1-INH complex levels. Additional studies in other cohorts are needed to determine whether these ranges are broadly applicable.

Finally, we showed increased C1-INH complex levels in patients with COVID-19 when compared to healthy controls. In COVID-19, complement is known to be activated *via* all three pathways. While lectin pathway activation occurs through direct binding of MBL to viral envelope particles (65, 66), the classical pathway is activated later through recognition of circulating SARS-CoV-2 specific antibodies by C1q (67, 68) or through immune complexes with IgG bound to proteins of the virus (69). Besides the positive feedback loop function of the alternative pathway upon CP and LP activation, competition of SARS-CoV-2 with factor H for binding sites at heparan sulfate can further increase AP activation (67, 70). Since complement is known to be activated in COVID-19 (34, 35), this cohort was chosen as a technical cohort to see whether C1-INH complex levels differ between healthy and diseased individuals. Measurement of C1-INH complexes confirms significantly higher complex levels in COVID-19 compared to healthy controls, indicating ongoing early activation of both, the classical and lectin pathway [median delay between symptom onset or positive PCR test and sampling: 10.0 days (IQR 6.0 – 27.8)]. Further investigations in this direction are necessary, especially when it comes to different severity groups or disease outcome, correlations with other complement components or potential triggers of the respective pathways, such as associations between C1s/C1-INH levels and anti SARS-CoV-2 antibody concentrations or MASP-1/C1-INH complex concentrations and lectin pathway pattern recognition molecule levels.

However, the findings are in line with measurements using in-house methods for C1-INH complex determinations in other conditions where complement is involved in the disease course. As an example, Füst et al. investigated C1rs/C1-INH complex levels in a cohort of HIV patients as a measure of classical pathway activation. In this study, 1.5 times higher complex levels were measured in HIV seropositive patients compared to seronegative patients and healthy controls (71). Besides that, increased C1-INH complex concentrations were also found in previous publications investigating C1s/C1-INH complex levels as an indicator for classical pathway activation in RA and SLE patients (32) or $(C1\text{-}INH)_2$ C1r-C1s complexes to indicate C1 activation in glomerulonephritis (31). So far, there are no publications discussing the MASP-1/C1-INH complex as a potential marker for early lectin pathway activation in disease, but our results show that the levels thereof indeed indicate lectin pathway activation, which of course needs to be validated in larger studies in the future.

In upcoming studies the function of C1s/C1-INH and MASP-1/C1-INH complexes should be investigated more in detail. When the complexes are formed during regulation of CP and LP activation *via* binding of C1-INH, spontaneous activation of the respective pathways and therefore consumption of C4 and C2 is limited. If the complexes also have other functions in between their release into the circulation and degradation (28) awaits further research. Besides that, C1s and MASP-1 are not the only serine proteases regulated by C1-INH. Within the complement system, C1-INH can furthermore inhibit C1r and MASP-2, also leading to the formation of covalent complexes (72, 73). Additionally, C1-INH also plays a role in other systems, such as the contact system, the fibrinolytic system as well as the coagulation system *via* binding to kallikrein, Factor XII (FXII) and Factor XI (FXI) (25). Especially the complement and the coagulation system closely interact with each other. MASP-1 for example can activate coagulation factors and thereby promote the formation of clots (74), while FXIIa/C1-INH complexes were shown to be decreased in vascular disease in SLE patients (75). If the here described C1-INH complexes might also shed light on the regulation of coagulation and thromboinflammation or if altering complex levels are indicative for a higher risk of thrombotic events still needs further research.

In summary, we have developed and validated two new sandwich immunoassays measuring C1s/C1-INH and MASP-1/C1-INH complexes in a reliable and accurate way. The new assays allow us to monitor early classical pathway activation, measured by C1s/C1-INH complexes, and early lectin pathway

activation, indicated by MASP-1/C1-INH complex concentrations. For future studies, we recommend using EDTA plasma samples when measuring C1-INH complex levels in order to obtain the most reliable results. Samples should be kept on ice before the measurement and experiments should be performed within one hour after thawing to avoid additional *ex vivo* complex formation. To prevent matrix effects, samples should be diluted at least 100 times for measuring C1s/C1-INH complex levels and at least 5 times for quantification of MASP-1/C1-INH complex levels, but it is highly recommended that pilot studies are performed to determine the optimal dilution before larger sample sets are being investigated. We have set reference ranges for future applications, and our first proof-of-concept study showed that levels of both markers are increased in COVID-19, suggesting that C1-INH complex measurements might have added value for investigating and unravelling early CP and LP activation in other human diseases where complement is involved, such as SLE, HAE, Sepsis as well as other viral, bacterial and fungal infections.

Group members of Cambridge Institute of Therapeutic Immunology and Infectious Disease-National Institute of Health Research (CITIID-NIHR) COVID BioResource Collaboration

Stephen Baker, John R. Bradley, Patrick F. Chinnery, Daniel J. Cooper, Gordon Dougan, Ian G. Goodfellow, Ravindra K. Gupta, Nathalie Kingston, Paul J. Lehner, Paul A. Lyons, Nicholas J. Matheson, Caroline Saunders, Kenneth G. C. Smith, Charlotte Summers, James Thaventhiran, M. Estee Torok, Mark R. Toshner, Michael P. Weekes, Gisele Alvio, Sharon Baker, Areti Bermperi, Karen Brookes, AshleaBucke, Jo Calder, Laura Canna, Cherry Crucusio, Isabel Cruz, Rnalie de Jesus, Katie Dempsey, Giovanni Di Stephano, Jason Domingo, Anne Elmer, Julie Harris, Sarah Hewitt, Heather Jones, Sherly Jose, Jane Kennet, Yvonne King, Jenny Kourampa, Emily Li, Caroline McMahon, Anne Meadows, Vivien Mendoza, Criona O'Brien, Charmain Ocaya, Ciro Pascuale, Marlyn Perales, Jane Price, Rebecca Rastall, Carla Ribeiro, Jane Rowlands, Valentina Ruffolo, Hugo Tordesillas, Phoebe Vargas, Bensi Vergese, Laura Watson, Jieniean Worsley, Julie-Ann Zerrudo, Laura Bergamaschi, Ariana Betancourt, Georgie Bower, Ben Bullman, Chiara Cossetti, Aloka De Sa, Benjamin J. Dunore, Maddie Epping, Stuart Fawke, Stefan Gräf, Richard Grenfell, Andrew Hinch, Josh Hodgson, Christopher Huang, Oisin Huhn, Kelvin Hunter, Isobel Jarvis, Emma Jones, Maša Josipović, Ekaterina Legchenko, Daniel Lewis, Joe Marsden, Jennifer Martin, Federica Mescia, Francesca Nice, Ciara O'Donnell, Ommar Omarjee, Marianne Perera, Linda Pointon, Nicole Pond, Nathan Richoz, Nika Romashova, Natalia Savoinykh, Rahul Sharma, Joy Shih, Mateusz Strezlecki, Rachel Sutcliffe, Tobias Tilly, Zhen Tong, Carmen Treacy, Lori Turner, Jennifer Wood, Marta Wylot, John Allison, Heather Biggs, Helen Butcher, Daniela Caputo, Debbie Clapham-Riley, Eleanor Dewhurst, Christian Fernandez, Anita Furlong, Barbara Graves, Jennifer Gray, Tasmin Ivers, Emma Le Gresley, Rachel Linger, Mary Kasanicki, Sarah Meloy, Francesca Muldoon, Nigel Ovington, Sofia Papadia, Christopher J. Penkett, Isabel Phelan, Venkatesh Ranganath, Jennifer Sambrook, Katherine Schon, Hannah Stark, Kathleen E. Stirrups, Paul Townsend, Julie von Ziegenweidt, Jennifer Webster, Ali Asaripour, Lucy Mwaura, Caroline Patterson, Gary Polwarth, Katherine Bunclark, Michael Mackay, Alice Michael, Sabrina Rossi, Mayurun Selvan, Sarah Spencer, Cissy Yong, Petra Polgarova.

Data availability statement

The raw data supporting the conclusions of this article will be made available by the authors, without undue reservation.

Ethics statement

The studies involving human participants were reviewed and approved by The East of England – Cambridge Central Research Ethics Committee ("NIHR BioResource" REC ref 17/EE/0025, and "Genetic variation AND Altered Leucocyte Function in health and disease - GANDALF" REC ref 08/H0308/176), The Hungarian Ethical Review Agency (ETT-TUKEB; No. 8361-1/2011-EKU and IV/4403-2/2020/EKU), and The Government Office of the Capital City Budapest (31110-7/2014/EKU (481/2014)), based on the position of the Medical Research Council. The studies were conducted in accordance with the Declaration of Helsinki. The patients/participants provided their written informed consent to participate in this study.

Author contributions

ZP and ET designed and supervised the study. LH, BB and EK performed the experiments and analyzed the data. ZP, GS, PL and LB were involved in recruitment and sampling of healthy controls and patients. ET and LH wrote the first draft of the manuscript. ZP, EK, BB, RB, WB, PL, LC, and RW critically reviewed the manuscript. All authors contributed to the article and approved the submitted version.

Funding

The research was financed by the Higher Education Institutional Excellence Programme of the Ministry of Human Capacities in Hungary, within the framework of the molecular

biology thematic program of the Semmelweis University, "MOLORKIV"(TKP2021-EGA-24) to ZP. ZP, RW and LH are supported by funds of the EU MSCA project CORVOS 860044. The research was further funded by the Austrian Science Fund (FWF), HOROS W-1253.

Acknowledgments

We acknowledge the technical assistance of Márta Kókai, Éva Zsuzsanna Szendrei, Lászlóné Kertész, Edina Szabó and Beáta Takács, and the help of Veronika Makó during development of monoclonal antibodies with many thanks. We further thank Dorottya Csuka for the help with creating the figure using BioRender. Parts of the work were presented at the 28th International Complement Virtual Workshop (ICW2021) and the 18th European Meeting on Complement in Human Disease (EMCHD2022).

Conflict of interest

ET, BB, RB and WB are employees of Hycult Biotech.

The remaining authors declare that the research was conducted in the absence of any commercial or financial relationships that could be construed as a potential conflict of interest.

Publisher's note

All claims expressed in this article are solely those of the authors and do not necessarily represent those of their affiliated organizations, or those of the publisher, the editors and the reviewers. Any product that may be evaluated in this article, or claim that may be made by its manufacturer, is not guaranteed or endorsed by the publisher.

References

1. Flierman R, Daha MR. The clearance of apoptotic cells by complement. *Immunobiology* (2007) 212(4-5):363–70. doi: 10.1016/j.imbio.2006.11.005

2. Dunkelberger JR, Song WC. Complement and its role in innate and adaptive immune responses. *Cell Res* (2010) 20(1):34–50. doi: 10.1038/cr.2009.139

3. Bohlson SS, Garred P, Kemper C, Tenner AJ. Complement nomenclature-deconvoluted. *Front Immunol* (2019) 10:1308. doi: 10.3389/fimmu.2019.01308

4. McGrath FD, Brouwer MC, Arlaud GJ, Daha MR, Hack CE, Roos A. Evidence that complement protein C1q interacts with c-reactive protein through its globular head region. *J Immunol* (2006) 176(5):2950–7. doi: 10.4049/jimmunol.176.5.2950

5. Roy N, Ohtani K, Hidaka Y, Amano Y, Matsuda Y, Mori K, et al. Three pentraxins c-reactive protein, serum amyloid p component and pentraxin 3 mediate complement activation using collectin CL-P1. *Biochim Biophys Acta Gen Subj.* (2017) 1861(2):1–14. doi: 10.1016/j.bbagen.2016.11.023

6. Thielens NM, Tacnet-Delorme P, Arlaud GJ. Interaction of C1q and mannan-binding lectin with viruses. *Immunobiology* (2002) 205(4-5):563–74. doi: 10.1078/0171-2985-00155

7. Roumenina LT, Popov KT, Bureeva SV, Kojouharova M, Gadjeva M, Rabheru S, et al. Interaction of the globular domain of human C1q with salmonella typhimurium lipopolysaccharide. *Biochim Biophys Acta* (2008) 1784 (9):1271–6. doi: 10.1016/j.bbapap.2008.04.029

8. Nauta AJ, Trouw LA, Daha MR, Tijsma O, Nieuwland R, Schwaeble WJ, et al. Direct binding of C1q to apoptotic cells and cell blebs induces complement activation. *Eur J Immunol* (2002) 32(6):1726–36. doi: 10.1002/1521-4141(200206)32:6<1726::AID-IMMU1726>3.0.CO;2-R

9. Ziccardi RJ, Cooper NR. Activation of C1r by proteolytic cleavage. *J Immunol* (1976) 116(2):504–9.

10. Kjaer TR, Thiel S, Andersen GR. Toward a structure-based comprehension of the lectin pathway of complement. *Mol Immunol* (2013) 56(3):222–31. doi: 10.1016/j.molimm.2013.05.220

11. Rossi V, Cseh S, Bally I, Thielens NM, Jensenius JC, Arlaud GJ. Substrate specificities of recombinant mannan-binding lectin-associated serine proteases-1 and -2. *J Biol Chem* (2001) 276(44):40880–7. doi: 10.1074/jbc.M105934200

12. Takahashi M, Iwaki D, Kanno K, Ishida Y, Xiong J, Matsushita M, et al. Mannose-binding lectin (MBL)-associated serine protease (MASP)-1 contributes to activation of the lectin complement pathway. *J Immunol* (2008) 180(9):6132–8. doi: 10.4049/jimmunol.180.9.6132

13. Héja D, Kocsis A, Dobó J, Szilágyi K, Szász R, Závodszky P, et al. Revised mechanism of complement lectin-pathway activation revealing the role of serine protease MASP-1 as the exclusive activator of MASP-2. *Proc Natl Acad Sci U.S.A.* (2012) 109(26):10498–503. doi: 10.1073/pnas.1202588109

14. Merle NS, Church SE, Fremeaux-Bacchi V, Roumenina LT. Complement system part I - molecular mechanisms of activation and regulation. *Front Immunol* (2015) 6:262. doi: 10.3389/fimmu.2015.00262

15. Müller-Eberhard HJ. The killer molecule of complement. *J Invest Dermatol* (1985) 85(1 Suppl):47s–52s. doi: 10.1111/1523-1747.ep12275445

16. Ekdahl KN, Persson B, Mohlin C, Sandholm K, Skattum L, Nilsson B. Interpretation of serological complement biomarkers in disease. *Front Immunol* (2018) 9:2237. doi: 10.3389/fimmu.2018.02237

17. Troldborg A, Jensen L, Deleuran B, Stengaard-Pedersen K, Thiel S, Jensenius JC. The C3dg fragment of complement is superior to conventional C3 as a diagnostic biomarker in systemic lupus erythematosus. *Front Immunol* (2018) 9:581. doi: 10.3389/fimmu.2018.00581

18. Heesterbeek TJ, Lechanteur YTE, Lorés-Motta L, Schick T, Daha MR, Altay L, et al. Complement activation levels are related to disease stage in AMD. *Invest Ophthalmol Vis Sci* (2020) 61(3):18. doi: 10.1167/iovs.61.3.18

19. Martin M, Trattner R, Nilsson SC, Björk A, Zickert A, Blom AM, et al. Plasma C4d correlates with C4d deposition in kidneys and with treatment response in lupus nephritis patients. *Front Immunol* (2020) 11:582737. doi: 10.3389/fimmu.2020.582737

20. Yang X, Yuan Y, Shao X, Pang H, Che X, Cao L, et al. C4d as a screening tool and an independent predictor of clinical outcomes in lupus nephritis and IgA nephropathy. *Front Med (Lausanne).* (2022) 9:832998. doi: 10.3389/fmed.2022.832998

21. Ding Y, Yu X, Wu L, Tan Y, Qu Z, Yu F. The spectrum of C4d deposition in renal biopsies of lupus nephritis patients. *Front Immunol* (2021) 12:654652. doi: 10.3389/fimmu.2021.654652

22. Röth A, Barcellini W, D'Sa S, Miyakawa Y, Broome CM, Michel M, et al. Sutimlimab in cold agglutinin disease. *N Engl J Med* (2021) 384(14):1323–34. doi: 10.1056/NEJMoa2027760

23. Roth A, Barcellini W, D'Sa S, Miyakawa Y, Broome CM, Michel M, et al. Complement C1s inhibition with sutimlimab results in durable response in cold agglutinin disease: CARDINAL study 1-year interim follow-up results. *Haematologica* (2022) 107(7):1698–702. doi: 10.3324/haematol.2021.279812

24. Stavenhagen K, Kayili HM, Holst S, Koeleman CAM, Engel R, Wouters D, et al. N- and O-glycosylation analysis of human C1-inhibitor reveals extensive mucin-type O-glycosylation. *Mol Cell Proteomics.* (2018) 17(6):1225–38. doi: 10.1074/mcp.RA117.000240

25. Zeerleder S. C1-inhibitor: more than a serine protease inhibitor. *Semin Thromb Hemost.* (2011) 37(4):362–74. doi: 10.1055/s-0031-1276585

26. Reboul A, Arlaud GJ, Sim RB, Colomb MG. A simplified procedure for the purification of C1-inactivator from human plasma. *Interaction complement*

subcomponents C1r C1s. FEBS Lett (1977) 79(1):45–50. doi: 10.1016/0014-5793(77)80347-5

27. Sim RB, Arlaud GJ, Colomb MG. C1 inhibitor-dependent dissociation of human complement component C1 bound to immune complexes. *Biochem J* (1979) 179(3):449–57. doi: 10.1042/bj1790449a

28. Storm D, Herz J, Trinder P, Loos M. C1 inhibitor-C1s complexes are internalized and degraded by the low density lipoprotein receptor-related protein. *J Biol Chem* (1997) 272(49):31043–50. doi: 10.1074/jbc.272.49.31043

29. Nielsen EW, Johansen HT, Gaudesen O, Osterud B, Olsen JO, Høgåsen K, et al. C3 is activated in hereditary angioedema, and C1/C1-inhibitor complexes rise during physical stress in untreated patients. *Scand J Immunol* (1995) 42(6):679–85. doi: 10.1111/j.1365-3083.1995.tb03711.x

30. Kajdácsi E, Jandrasics Z, Veszeli N, Makó V, Koncz A, Gulyás D, et al. Patterns of C1-Inhibitor/Plasma serine protease complexes in healthy humans and in hereditary angioedema patients. *Front Immunol* (2020) 11:794. doi: 10.3389/fimmu.2020.00794

31. Waldo FB, West CD. Quantitation of (C1INH)2 C1r-C1s complexes in glomerulonephritis as an indicator of C1 activation. *Clin Immunol Immunopathol* (1987) 42(2):239–49. doi: 10.1016/0090-1229(87)90011-0

32. Auda G, Holme ER, Davidson JE, Zoma A, Veitch J, Whaley K. Measurement of complement activation products in patients with chronic rheumatic diseases. *Rheumatol Int* (1990) 10(5):185–9. doi: 10.1007/BF02274831

33. Hansen CB, Csuka D, Munthe-Fog L, Varga L, Farkas H, Hansen KM, et al. The levels of the lectin pathway serine protease MASP-1 and its complex formation with C1 inhibitor are linked to the severity of hereditary angioedema. *J Immunol* (2015) 195(8):3596–604. doi: 10.4049/jimmunol.1402838

34. Bergamaschi L, Mescia F, Turner L, Hanson AL, Kotagiri P, Dunmore BJ, et al. Longitudinal analysis reveals that delayed bystander CD8+ T cell activation and early immune pathology distinguish severe COVID-19 from mild disease. *Immunity* (2021) 54(6):1257–75.e8. doi: 10.1016/j.immuni.2021.05.010

35. Sinkovits G, Mező B, Réti M, Müller V, Iványi Z, Gál J, et al. Complement overactivation and consumption predicts in-hospital mortality in SARS-CoV-2 infection. *Front Immunol* (2021) 12:663187. doi: 10.3389/fimmu.2021.663187

36. Trojnar E, Józsi M, Szabó Z, Réti M, Farkas P, Kelen K, et al. Elevated systemic pentraxin-3 is associated with complement consumption in the acute phase of thrombotic microangiopathies. *Front Immunol* (2019) 10:240. doi: 10.3389/fimmu.2019.00240

37. Gál P, Závodszky P. Structure and function of the serine-protease subcomponents of C1: protein engineering studies. *Immunobiology* (1998) 199 (2):317–26. doi: 10.1016/S0171-2985(98)80036-3

38. Ambrus G, Gál P, Kojima M, Szilágyi K, Balczer J, Antal J, et al. Natural substrates and inhibitors of mannan-binding lectin-associated serine protease-1 and -2: A study on recombinant catalytic fragments. *J Immunol* (2003) 170 (3):1374–82. doi: 10.4049/jimmunol.170.3.1374

39. Schneider Z, Cervenak J, Baranyi M, Papp K, Prechl J, László G, et al. Transgenic expression of bovine neonatal fc receptor in mice boosts immune response and improves hybridoma production efficiency without any sign of autoimmunity. *Immunol Lett* (2011) 137(1-2):62–9. doi: 10.1016/j.imlet.2011.02.018

40. Ricklin D, Hajishengallis G, Yang K, Lambris JD. Complement: a key system for immune surveillance and homeostasis. *Nat Immunol* (2010) 11(9):785–97. doi: 10.1038/ni.1923

41. Morgan BP, Harris CL. Complement, a target for therapy in inflammatory and degenerative diseases. *Nat Rev Drug Discovery* (2015) 14(12):857–77. doi: 10.1038/nrd4657

42. Carroll MV, Sim RB. Complement in health and disease. *Adv Drug Delivery Rev* (2011) 63(12):965–75. doi: 10.1016/j.addr.2011.06.005

43. Prohászka Z, Nilsson B, Frazer-Abel A, Kirschfink M. Complement analysis 2016: Clinical indications, laboratory diagnostics and quality control. *Immunobiology* (2016) 221(11):1247–58. doi: 10.1016/j.imbio.2016.06.008

44. Sinosich MJ, Teisner B, Brandslund I, Fisher M, Grudzinskas JG. Influence of time, temperature and coagulation on the measurement of C3, C3 split products and C4. *J Immunol Methods* (1982) 55(1):107–14. doi: 10.1016/0022-1759(82)90083-7

45. Vercauteren KOA, Lambrecht S, Delanghe J. Preanalytical classical and alternative complement pathway activity loss. *Biochem Med (Zagreb).* (2019) 29 (3):030701. doi: 10.11613/BM.2019.030701

46. Dobó J, Harmat V, Beinrohr L, Sebestyén E, Závodszky P, Gál P. MASP-1, a promiscuous complement protease: structure of its catalytic region reveals the basis of its broad specificity. *J Immunol* (2009) 183(2):1207–14. doi: 10.4049/jimmunol.0901141

47. Paréj K, Dobó J, Závodszky P, Gál P. The control of the complement lectin pathway activation revisited: both C1-inhibitor and antithrombin are likely physiological inhibitors, while α2-macroglobulin is not. *Mol Immunol* (2013) 54 (3-4):415–22. doi: 10.1016/j.molimm.2013.01.009

48. Sim RB, Arlaud GJ, Colomb MG. Kinetics of reaction of human C1-inhibitor with the human complement system proteases C1r and C1s. *Biochim Biophys Acta* (1980) 612(2):433–49. doi: 10.1016/0005-2744(80)90126-6

49. Villiers CL, Arlaud GJ, Painter RH, Colomb MG. Calcium binding properties of the C1 subcomponents C1q, C1r and C1s. *FEBS Lett* (1980) 117 (1):289–94. doi: 10.1016/0014-5793(80)80964-1

50. Pfeifer PH, Kawahara MS, Hugli TE. Possible mechanism for in vitro complement activation in blood and plasma samples: futhan/EDTA controls *in vitro* complement activation. *Clin Chem* (1999) 45(8 Pt 1):1190–9. doi: 10.1093/clinchem/45.8.1190

51. Gingras AR, Girija UV, Keeble AH, Panchal R, Mitchell DA, Moody PC, et al. Structural basis of mannan-binding lectin recognition by its associated serine protease MASP-1: Implications for complement activation. *Structure* (2011) 19 (11):1635–43. doi: 10.1016/j.str.2011.08.014

52. Yang S, McGookey M, Wang Y, Cataland SR, Wu HM. Effect of blood sampling, processing, and storage on the measurement of complement activation biomarkers. *Am J Clin Pathol* (2015) 143(4):558–65. doi: 10.1309/AJCPXPD7ZQXNTIAL

53. Manderson AP, Pickering MC, Botto M, Walport MJ, Parish CR. Continual low-level activation of the classical complement pathway. *J Exp Med* (2001) 194 (6):747–56. doi: 10.1084/jem.194.6.747

54. Schifferli JA, Taylor RP. Physiological and pathological aspects of circulating immune complexes. *Kidney Int* (1989) 35(4):993–1003. doi: 10.1038/ki.1989.83

55. Bergseth G, Ludviksen JK, Kirschfink M, Giclas PC, Nilsson B, Mollnes TE. An international serum standard for application in assays to detect human complement activation products. *Mol Immunol* (2013) 56(3):232–9. doi: 10.1016/j.molimm.2013.05.221

56. Fearon DT, Austen KF. Activation of the alternative complement pathway due to resistance of zymosan-bound amplification convertase to endogenous regulatory mechanisms. *Proc Natl Acad Sci U.S.A.* (1977) 74(4):1683–7. doi: 10.1073/pnas.74.4.1683

57. Super M, Levinsky RJ, Turner MW. The level of mannan-binding protein regulates the binding of complement-derived opsonins to mannan and zymosan at low serum concentrations. *Clin Exp Immunol* (1990) 79(2):144–50. doi: 10.1111/j.1365-2249.1990.tb05170.x

58. Schenkein HA, Ruddy S. The role of immunoglobulins in alternative complement pathway activation by zymosan. i. human IgG with specificity for zymosan enhances alternative pathway activation by zymosan. *J Immunol* (1981) 126(1):7–10.

59. Nilsson UR, Nilsson B. Simplified assays of hemolytic activity of the classical and alternative complement pathways. *J Immunol Methods* (1984) 72(1):49–59. doi: 10.1016/0022-1759(84)90432-0

60. Seelen MA, Roos A, Wieslander J, Mollnes TE, Sjöholm AG, Wurzner R, et al. Functional analysis of the classical, alternative, and MBL pathways of the complement system: standardization and validation of a simple ELISA. *J Immunol Methods* (2005) 296(1-2):187–98. doi: 10.1016/j.jim.2004.11.016

61. Roos A, Bouwman LH, Munoz J, Zuiverloon T, Faber-Krol MC, Fallaux-van den Houten FC, et al. Functional characterization of the lectin pathway of complement in human serum. *Mol Immunol* (2003) 39(11):655–68. doi: 10.1016/S0161-5890(02)00254-7

62. Nilsson T, Bäck O. Determination of C1s-C1 inhibitor complexes in plasma by means of an enzyme linked immunosorbent assay. *Clin Exp Immunol* (1985) 60 (1):178–82.

63. Adamek M, Heyder J, Heinold A, Fiedler G, Opelz G, Tran TH. Characterization of mannose-binding lectin (MBL) variants by allele-specific sequencing of MBL2 and determination of serum MBL protein levels. *Tissue Antigens* (2013) 82(6):410–5. doi: 10.1111/tan.12232

64. Gaya da Costa M, Poppelaars F, van Kooten C, Mollnes TE, Tedesco F, Würzner R, et al. Age and sex-associated changes of complement activity and complement levels in a healthy Caucasian population. *Front Immunol* (2018) 9:2664. doi: 10.3389/fimmu.2018.02664

65. Ali YM, Ferrari M, Lynch NJ, Yaseen S, Dudler T, Gragerov S, et al. Lectin pathway mediates complement activation by SARS-CoV-2 proteins. *Front Immunol* (2021) 12:714511. doi: 10.3389/fimmu.2021.714511

66. Stravalaci M, Pagani I, Paraboschi EM, Pedotti M, Doni A, Scavello F, et al. Recognition and inhibition of SARS-CoV-2 by humoral innate immunity pattern recognition molecules. *Nat Immunol* (2022) 23(2):275–86. doi: 10.1038/s41590-021-01114-w

67. Satyam A, Tsokos MG, Brook OR, Hecht JL, Moulton VR, Tsokos GC. Activation of classical and alternative complement pathways in the pathogenesis of lung injury in COVID-19. *Clin Immunol* (2021) 226:108716. doi: 10.1016/j.clim.2021.108716

68. Holter JC, Pischke SE, de Boer E, Lind A, Jenum S, Holten AR, et al. Systemic complement activation is associated with respiratory failure in COVID-19 hospitalized patients. *Proc Natl Acad Sci U.S.A.* (2020) 117(40):25018–25. doi: 10.1073/pnas.2010540117

69. Felsenstein S, Herbert JA, McNamara PS, Hedrich CM. COVID-19: Immunology and treatment options. *Clin Immunol* (2020) 215:108448. doi: 10.1016/j.clim.2020.108448

70. Yu J, Gerber GF, Chen H, Yuan X, Chaturvedi S, Braunstein EM, et al. Complement dysregulation is associated with severe COVID-19 illness. *Haematologica* (2022) 107(5):1095–105. doi: 10.3324/haematol.2021.279155

71. Füst G, Ujhelyi E, Hidvégi T, Pálóczi K, Mihalik R, Hollán S, et al. The complement system in HIV disease. *Immunol Invest.* (1991) 20(2):231–41. doi: 10.3109/08820139109050792

72. Sim RB, Reboul A, Arlaud GJ, Villiers CL, Colomb MG. Interaction of 125I-labelled complement subcomponents c-1r and c-1s with protease inhibitors in plasma. *FEBS Lett* (1979) 97(1):111–5. doi: 10.1016/0014-5793(79)80063-0

73. Wong NK, Kojima M, Dobó J, Ambrus G, Sim RB. Activities of the MBL-associated serine proteases (MASPs) and their regulation by natural inhibitors. *Mol Immunol* (1999) 36(13-14):853–61. doi: 10.1016/S0161-5890(99)00106-6

74. Jenny L, Dobó J, Gál P, Pál G, Lam WA, Schroeder V. MASP-1 of the complement system enhances clot formation in a microvascular whole blood flow model. *PloS One* (2018) 13(1):e0191292. doi: 10.1371/journal.pone.0191292

75. Bäck J, Lood C, Bengtsson AA, Ekdahl KN, Nilsson B. Contact activation products are new potential biomarkers to evaluate the risk of thrombotic events in systemic lupus erythematosus. *Arthritis Res Ther* (2013) 15(6):R206. doi: 10.1186/ar4399

COPYRIGHT

© 2022 Hurler, Toonen, Kajdácsi, van Bree, Brandwijk, de Bruin, Lyons, Bergamaschi, Cambridge Institute of Therapeutic Immunology and Infectious Disease-National Institute of Health Research (CITIID-NIHR) COVID BioResource Collaboration, Sinkovits, Cervenak, Würzner and Prohászka. This is an open-access article distributed under the terms of the Creative Commons Attribution License (CC BY). The use, distribution or reproduction in other forums is permitted, provided the original author(s) and the copyright owner(s) are credited and that the original publication in this journal is cited, in accordance with accepted academic practice. No use, distribution or reproduction is permitted which does not comply with these terms.

frontiers | Frontiers in Immunology

TYPE Review
PUBLISHED 14 November 2022
DOI 10.3389/fimmu.2022.1036136

Check for updates

OPEN ACCESS

EDITED BY
Lillemor Skattum,
Lund University, Sweden

REVIEWED BY
Yuzhou Zhang,
The University of Iowa, United States
Jiaxuan Chen,
Affiliated Hospital of Guangdong Medical University, China

*CORRESPONDENCE
Marloes A. H. M. Michels
marloes.michels@radboudumc.nl

SPECIALTY SECTION
This article was submitted to Molecular Innate Immunity, a section of the journal Frontiers in Immunology

RECEIVED 04 September 2022
ACCEPTED 12 October 2022
PUBLISHED 14 November 2022

CITATION
Michels MAHM, Volokhina EB, van de Kar NCAJ and van den Heuvel LPWJ (2022) Challenges in diagnostic testing of nephritic factors.
Front. Immunol. 13:1036136.
doi: 10.3389/fimmu.2022.1036136

COPYRIGHT
© 2022 Michels, Volokhina, van de Kar and van den Heuvel. This is an open-access article distributed under the terms of the Creative Commons Attribution License (CC BY). The use, distribution or reproduction in other forums is permitted, provided the original author(s) and the copyright owner(s) are credited and that the original publication in this journal is cited, in accordance with accepted academic practice. No use, distribution or reproduction is permitted which does not comply with these terms.

Challenges in diagnostic testing of nephritic factors

Marloes A. H. M. Michels[1]*, Elena B. Volokhina[1,2], Nicole C. A. J. van de Kar[1], Lambertus P.W. J. van den Heuvel[1,3,4,5] and on behalf of the COMBAT consortium

[1]Department of Pediatric Nephrology, Amalia Children's Hospital, Radboud University Medical Center, Nijmegen, Netherlands, [2]Innatoss Laboratories, Oss, Netherlands, [3]Department of Laboratory Medicine, Radboud University Medical Center, Nijmegen, Netherlands, [4]Department of Pediatrics/Pediatric Nephrology, University Hospitals Leuven, Leuven, Belgium, [5]Department of Development and Regeneration, University Hospitals Leuven, Leuven, Belgium

Nephritic factors (NeFs) are autoantibodies promoting the activity of the central enzymes of the complement cascade, an important first line of defense of our innate immune system. NeFs stabilize the complement convertase complexes and prevent their natural and regulator-mediated decay. They are mostly associated with rare complement-mediated kidney disorders, in particular with C3 glomerulopathy and related diseases. Although these autoantibodies were already described more than 50 years ago, measuring NeFs for diagnostic purposes remains difficult, and this also complicates our understanding of their clinical associations. In this review, we address the multifactorial challenges of NeF diagnostics. We describe the diseases NeFs are associated with, the heterogenic mechanisms of action of different NeF types, the different methods available in laboratories used for their detection, and efforts for standardization. Finally, we discuss the importance of proper NeF diagnostics for understanding the clinical impact of these autoantibodies in disease pathophysiology and for considering future complement-directed therapy.

KEYWORDS

nephritic factor, complement system, complement dysregulation, complement alternative pathway, assay standardization, C3 glomerulopathy, immune complex-mediated glomerulonephritis

1 Introduction

With the enhanced understanding of the role of the complement system (Figure 1) in the pathogenesis of many diseases (1), the characterization and diagnosis of patients with complement-mediated disorders has gained a novel dimension. In-depth characterization of the complement dysregulation has become an important part of standard patient laboratory tests. More importantly, the acknowledgment of the role of complement has provided us with novel strategies to target complement-mediated

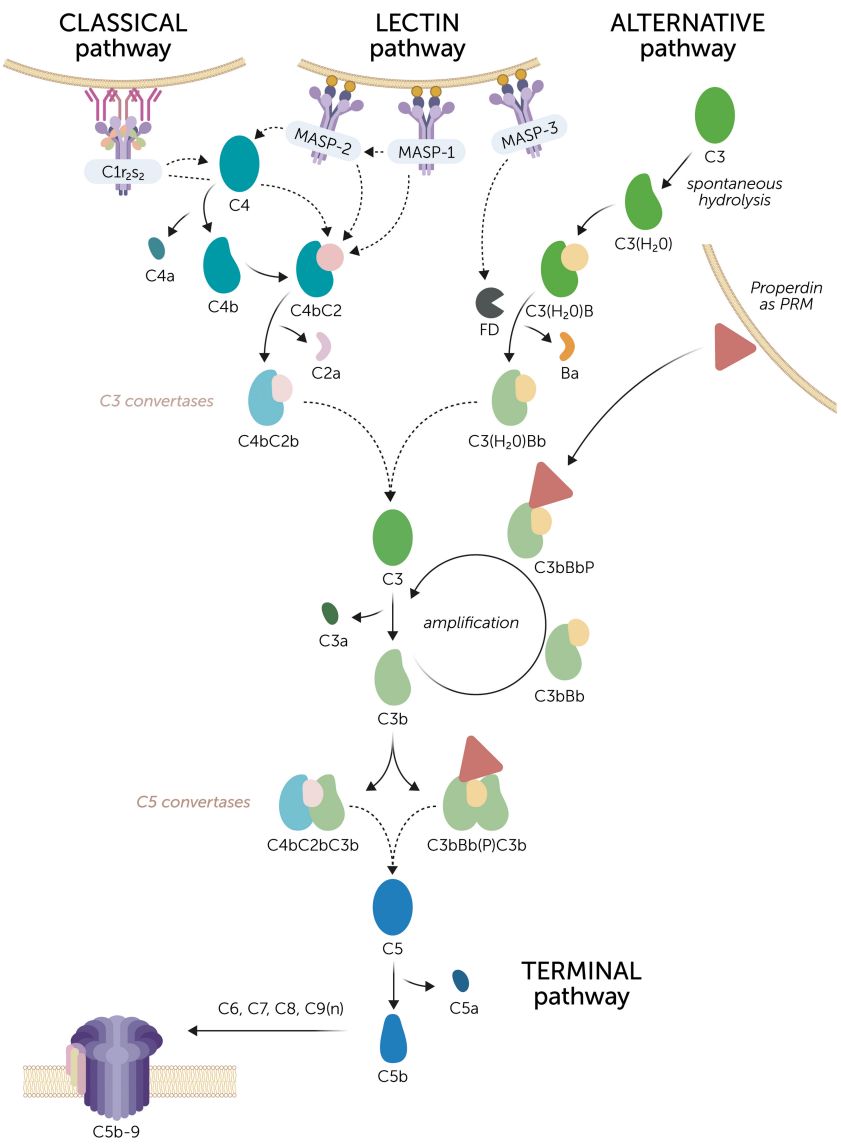

FIGURE 1
The complement system. Three routes can initiate complement activation. The classical pathway is activated by C1q coupled to the C1r2s2 proteases, together known as the C1 complex that recognizes, for example, antigen-antibody complexes. The lectin pathway is initiated by mannose-binding lectin (MBL), ficolins, or lectins, which recognize specific carbohydrate patterns on foreign surfaces. These pattern recognition molecules (PRMs) are coupled to the MBL-associated serine proteases (MASPs) MASP-1 or MASP-2. MASP-1 is autoactivated and is required to activate MASP-2. Activation of the classical and lectin pathway results in the cleavage of C4 and C2 by the C1r2s2 proteases and MASPs to form the C3 convertase C4bC2b. The alternative pathway is constantly active at a low rate due to the spontaneous hydrolysis of C3. Factor D (FD), which is activated by MASP-3, cleaves factor B to enable the formation of the initial C3 convertase C3(H_2O)Bb. The C3 convertases convert C3 into C3a and C3b. Subsequently, the complement activation can be amplified *via* the alternative pathway. C3b can form new C3 convertase complexes that are stabilized by properdin (C3bBbP). Of note, properdin can also act as a PRM on certain surfaces to initiate alternative pathway activation. Upon continued C3 cleavage and C3b formation, C5 convertase complexes are formed, denoted as C4bC2bC3b and C3bBb(P)C3b, although their exact composition is unknown. C5 convertases cleave C5 into C5a and C5b, after which C5b recruits C6, C7, C8, and multiple copies of C9 to form the C5b-9 complex. This is the terminal complement complex that forms a pore and disrupts the membrane of the target cell. Dashed arrows indicate cleaving interactions.

diseases. After the success story of the complement inhibitor eculizumab in the treatment of atypical hemolytic uremic syndrome (2–4), great efforts have been made to achieve similar successes for the treatment of other diseases. Numerous new complement-directed therapeutics are currently in the drug development pipeline (5, 6). To keep up with the advances in drug development, it is crucial to have accurate and reliable assays available to characterize the

complement activation status and complement-dysregulating factors in each patient.

One of the most challenging assays in the field of complement diagnostics is the detection of nephritic factors (NeFs). NeFs are stabilizing autoantibodies directed against the central enzymes of the complement system: the convertase complexes. By prolonging their activity and preventing their normal regulation, NeFs can contribute to an overactive complement system. Especially in the kidney disease C3 glomerulopathy (C3G), NeFs targeting the complement alternative pathway (AP) C3 convertase, i.e. C3NeFs, are considered the main driver of disease in many patients. However, robust and reliable standardized assays for C3NeF are lacking and this is hampering C3NeF research. According to the External Quality Assessment (EQA) rounds, organized by INSTAND e.V., the average success rate for C3NeF detection in the past five years (2016-2020) was 48% among the participating laboratories (7). This indicates that only half of all laboratories were able to correctly identify the presence or absence of C3NeFs in the reference samples sent around. Similar challenges apply for NeFs stabilizing the convertases of the complement classical pathway (CP), i.e. C4NeFs. Thus, important hurdles are still to be overcome in this field.

In this review, we provide an overview of the challenges in NeF testing and discuss the implications this has on our understanding of their role in disease. The two main factors complicating NeF analysis are the intrinsic heterogeneity of NeFs regarding their function and the large variety of methodologies used by different laboratories. Differences in NeF findings therefore hamper the research to their association with disease and/or disease activity. This underlines the need of standardization to aid research and diagnostics of NeFs and the diseases they are involved in.

2 C3 nephritic factor and C4 nephritic factor

In 1969, the term C3NeF was ascribed to a factor present in the serum of a hypocomplementemic membranoproliferative glomerulonephritis (MPGN) patient that specifically and very efficiently cleaved C3 when the serum was mixed with normal human serum (8). Later studies found that this C3NeF activity was mediated by stabilization of the AP convertase (9) and that C3NeFs had a heterogeneous immunoglobulin nature, mainly IgG (10–13). Therefore, nowadays, the term C3NeF is used to describe autoantibodies directed to neoepitopes of the AP C3 convertase that prolong the enzyme's half-life, thereby resulting in enhanced cleavage of C3 (Figure 2).

Analogous to C3NeFs, in 1980 autoantibodies directed against the convertases shared by the CP and lectin pathway (LP) were reported (14, 15). These autoantibodies later became known as C4NeFs due to their capacity to stabilize the C4bC2b convertase complex (Figure 2). In many aspects, C4NeFs are functionally similar to C3NeFs, except for their specificity for convertases in another complement pathway. C4NeFs are IgGs recognizing neoepitopes in the CP/LP convertases to prolong their half-life and increase their ability to cleave C3.

3 Diseases associated with nephritic factors

C3NeFs are best described in the rare but severe kidney disease C3G. C3G is characterized by AP dysregulation leading to the deposition of C3 breakdown fragments in the glomeruli (16) (Figure 2). To establish the C3G diagnosis a kidney biopsy is required. The defining feature is a dominant staining for C3 visualized by immunofluorescence microscopy, i.e., a staining intensity of at least two orders of magnitude greater than staining for any other immune reactant (e.g., IgG, IgM, IgA, and C1q) (16–18). C3G can be subdivided into dense deposit disease (DDD) and C3 glomerulonephritis (C3GN) based on the glomerular complement deposition pattern visualized by electron microscopy. C3GN also encompasses CFHR5 nephropathy, which is a genetically driven familial form of C3G. The majority of the C3G patients show clear signs of AP activation in their blood. This includes increased markers of complement activation, e.g. C3 breakdown products and soluble (s)C5b-9, and low serum C3 levels, indicative of complement consumption due to excessive activation (19–22). C3NeFs are found in approximately 50% of the C3G cases, but the C3NeF prevalence among cohorts varies within a range of 26-75% (Table 1) (20–36). The large differences in these findings may not only be due to the different compositions of the patient cohorts, e.g. age of the patients and number of patients with DDD or C3GN, but also due to the heterogeneity of C3NeFs (see *section 4*) and the ability of the different assays used to detect all C3NeFs (see *section 5*).

C3NeFs are also found in a substantial number of patients with idiopathic (primary) immune complex-mediated MPGN (IC-MPGN). The prevalence in patient cohorts is reported between 23% and 54% (22, 26, 29, 34–36). The pattern of glomerular injury in IC-MPGN resembles the injury in C3G, but IC-MPGN is distinguished from C3G by the substantial presence of immunoglobulin deposits, which can cause CP activation in the glomerulus. However, the finding that genetic and acquired abnormalities of the AP, including C3NeFs, are found in both diseases suggests they may share a disease spectrum (37). This is also supported by cases in which the IC-MPGN pattern evolves to a C3G pattern in subsequent biopsies or vice versa.

Next to these glomerular kidney diseases, C3NeFs are common in patients with acquired partial lipodystrophy

(APL). APL is an extremely rare disorder characterized by fat loss in the upper half of the body, usually occurring during childhood or adolescence (38). Most patients have C3 hypocomplementemia and in approximately 70-80% of the cases C3NeFs are found, especially in those with low serum C3 levels (38–40). Supposedly as a result of the C3NeF presence, approximately 20% of the patients develop C3G (38, 41, 42).

Lastly, C3NeFs have been described, although much less frequently, in patients with meningococcal infections and disease (43–45), in patients with systemic lupus erythematosus (SLE), who often also showed presence of APL and/or C3G (46–48), and in post-infectious glomerulonephritis (49–51).

C4NeFs have been reported in several diseases as well. The first reports from 1980 identified C4NeFs in a patient with acute post-infectious glomerulonephritis (15) and in patients with SLE (14). Later studies have described C4NeFs in more patients with SLE (52, 53), in patients with MPGN (52, 54, 55), in patients with Sjögren syndrome (52), and in a patient with sepsis caused by an *N. meningitidis* infection (56). More recently, the focus of C4NeF research has been on C3G and IC-MPGN. C4NeFs have been reported in two C3G cohorts with an incidence of 3% (30) and 8% (57) and in mixed C3G/IC-MPGN cohorts with an incidence of 6% (58) and 14% (59). Interestingly, in a substantial proportion of these patients both C4NeFs and C3NeFs are found (30, 52, 54, 55, 58, 59).

4 Nephritic factor heterogeneity

C3NeFs form a heterogeneous group of immunoglobulins that likely bind to different epitopes of the AP convertase. First, they differ in the extent to which they prolong the half-life of the

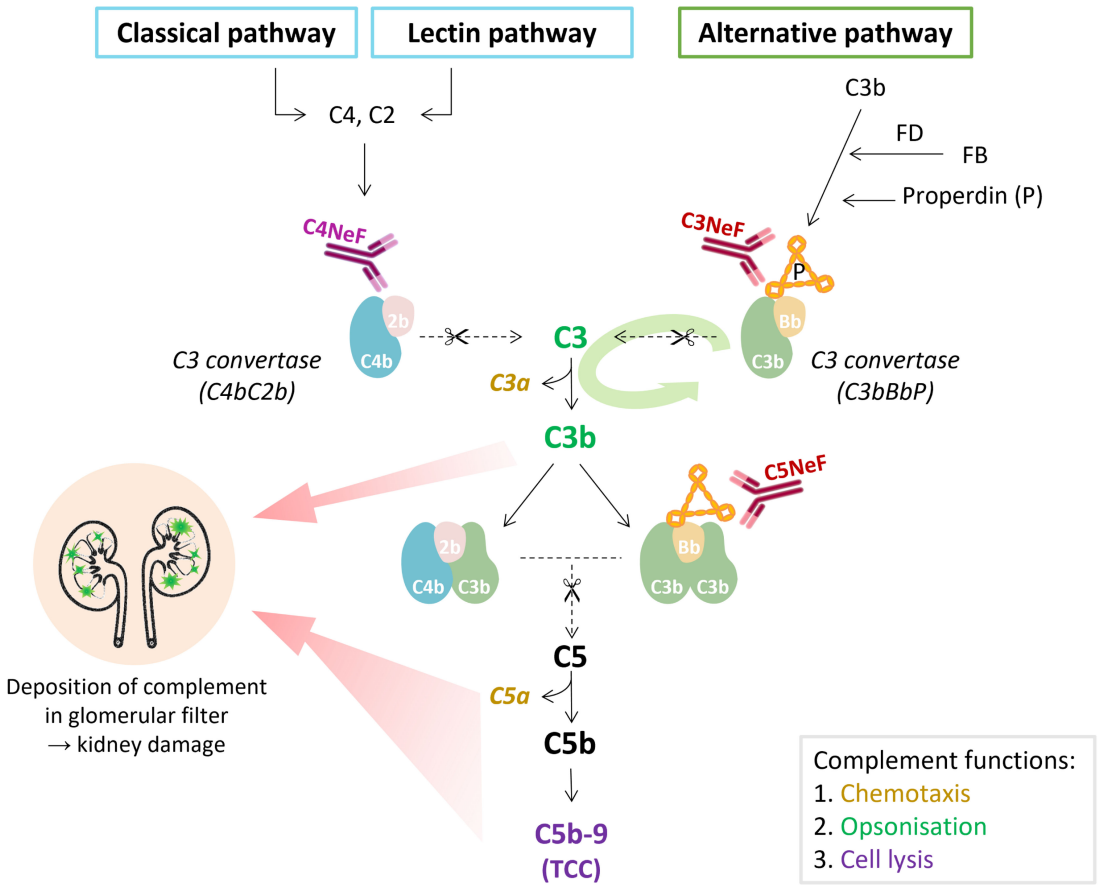

FIGURE 2
The place of nephritic factors in the complement system. C3 nephritic factors (C3NeF) stabilize the alternative pathway convertase complexes, whereas C4 nephritic factors (C4NeF) stabilize the convertases shared by the classical and lectin pathways. The term C5 nephritic factor (C5NeF) has been proposed for NeFs stabilizing alternative pathway C5 convertases. The green oval arrow illustrates the amplification loop of the alternative pathway. The colors of the complement components correspond to their function as indicated in the gray box. Overactivation of the complement system, mediated by NeFs, may result in the deposition of complement (breakdown) proteins in the glomerulus, inflammatory responses, and kidney injury. In C3 glomerulopathy, C3 degradation products are most abundant in the glomeruli, though terminal pathway proteins are also found. TCC, terminal complement complex.

TABLE 1 Prevalence of C3 nephritic factor (C3NeF) in C3 glomerulopathy (C3G) cohorts.

Study	Year	Country	Total C3G cohort (n)	Pediatric onset[a] (% of total)	Tested for C3NeF (n)	C3G (% C3NeF)	DDD (% C3NeF)	C3GN (% C3NeF)
Nasr et al. (23)	2009	USA	32	44%[b]	9		78%	
Sethi et al. (24)	2012	USA	12	17%[c]	10			50%
Zhang et al. (25)	2012	USA	32	71%[c]	32		78%	
Servais et al. (26)	2012	France	85	36%[b]	75	57%	86%	45%
Rabasco et al. (27)	2015	Spain	60	n.r.	23			48%
Corvillo et al. (28)	2016	Spain	80	n.r.	49	35%	70%	10%
Iatropoulos et al.[d] (29)	2016	Italy	73	n.r.	n.r.	54%	78%	44%
Zhang et al. (30)	2017	USA	168	n.r.	168	52%	72%	38%
Marinozzi et al. (20)	2017	France	127	45%[c]	101	75%		
Bomback et al. (31)	2018	USA	111	32%[c]	51	27%	11%	31%
Ravindran et al. (32)	2018	USA	114	n.r.	69	43%	30%	46%
Iatropoulos et al.[d] (22)	2018	Italy	93	68%[c]	85	49%	78%	38%
Michels et al. (33)	2018	NL	27	n.r.	27	59%	67%	57%
Garam et al. (34)	2020	Europe[e]	48	n.r.	47	26%	45%	19%
Levine et al. (35)	2020	UK	61	n.r.	41	44%	59%	33%
Wong et al. (36)	2021	UK	39	100%	36	39%	62%	26%
Michels et al. (21)	2022	NL	29	100%	28	71%	67%	80%

USA, United States of America; NL, The Netherlands; UK, United Kingdom; DDD, dense deposit disease; C3GN, C3 glomerulonephritis; n.r., not reported.
[a]Age at time of investigation may be different in some studies.
[b]<16 years at onset.
[c]<18 years at onset.
[d]Additional collaborations with centers in Israel, Portugal, France, Switzerland, Russia, and Turkey.
[e]34 centers in Central and Eastern Europe.

C3 convertase (20, 25, 60), ranging from tens of minutes to even hours. Second, C3NeFs confer the convertase with varying resistance against the various complement regulatory proteins. C3NeFs may interfere with Factor H (FH) (60–65), complement receptor 1 (CR1) (60, 66), and decay-accelerating factor (DAF) (60, 67), although the efficiency (for each regulator) differs between NeFs of different patients. Few C3NeFs were found that did not or hardly interfere with any of these regulators of extrinsic decay (60). Third, C3NeFs differ in their dependence on the convertase-stabilizing protein properdin. Some C3NeFs are only active in the presence of properdin, i.e. properdin-dependent NeFs, whereas other C3NeFs also, or only (20), act on convertases without properdin, i.e. properdin-independent NeFs (20, 25, 60, 62, 68–70). Finally, it has been shown that NeFs can differ in their ability to affect C5 convertase activity and C5 conversion, sometimes referred to as C5NeF activity (20, 60–62, 71) (Figure 2). It is this marked heterogeneity that has complicated our understanding of C3NeFs since their discovery until today.

Although less studied, C4NeFs also form a heterogeneous group. Convertase stabilization through interference with complement regulator-mediated extrinsic decay has been described for C4 binding protein (C4BP) (30, 56, 72, 73), CR1 (30, 56, 74), and DAF (57, 67). Some studies have shown the specific ability of C4NeFs to also stabilize the C5 convertase complex C4bC2bC3b (56, 73), suggesting also C4NeFs may recognize different epitopes in different patients. However, it is important to note that research on the stabilization of CP/LP and especially AP C5 convertases by NeFs is hampered by the unknown exact structure of the C5 convertase complex and the transient nature between convertase complexes that cleave C3 and C5.

5 Nephritic factor detection methods

A major bottleneck in NeF research, related to the heterogeneous nature of NeFs, is the difficulty and diversity of detection methods, which are often only available in specialized laboratories. Many different assays are being used for NeF identification and tests differ in sensitivity and specificity. C4NeF testing is available in even fewer laboratories than C3NeF testing, so here we focus on the methods described for C3NeF detection, which often have a parallel version for detecting C4NeFs. NeF assays can generally be divided into three groups (Figure 3): [1] binding assays that detect the binding of the NeF to the convertase complex, [2] functional

assays that measure the C3 activation products, and [3] functional assays that detect the stabilization of the convertase. C3NeFs can be variably positive in these different assays, hence some laboratories use a combination of them for C3NeF detection (25, 60).

5.1 C3NeF binding assays

C3NeF binding assays (Figure 3A) are usually enzyme-linked immunosorbent assay (ELISA)-based methods aimed to detect the interaction of the C3NeF antibody with its target, i.e.

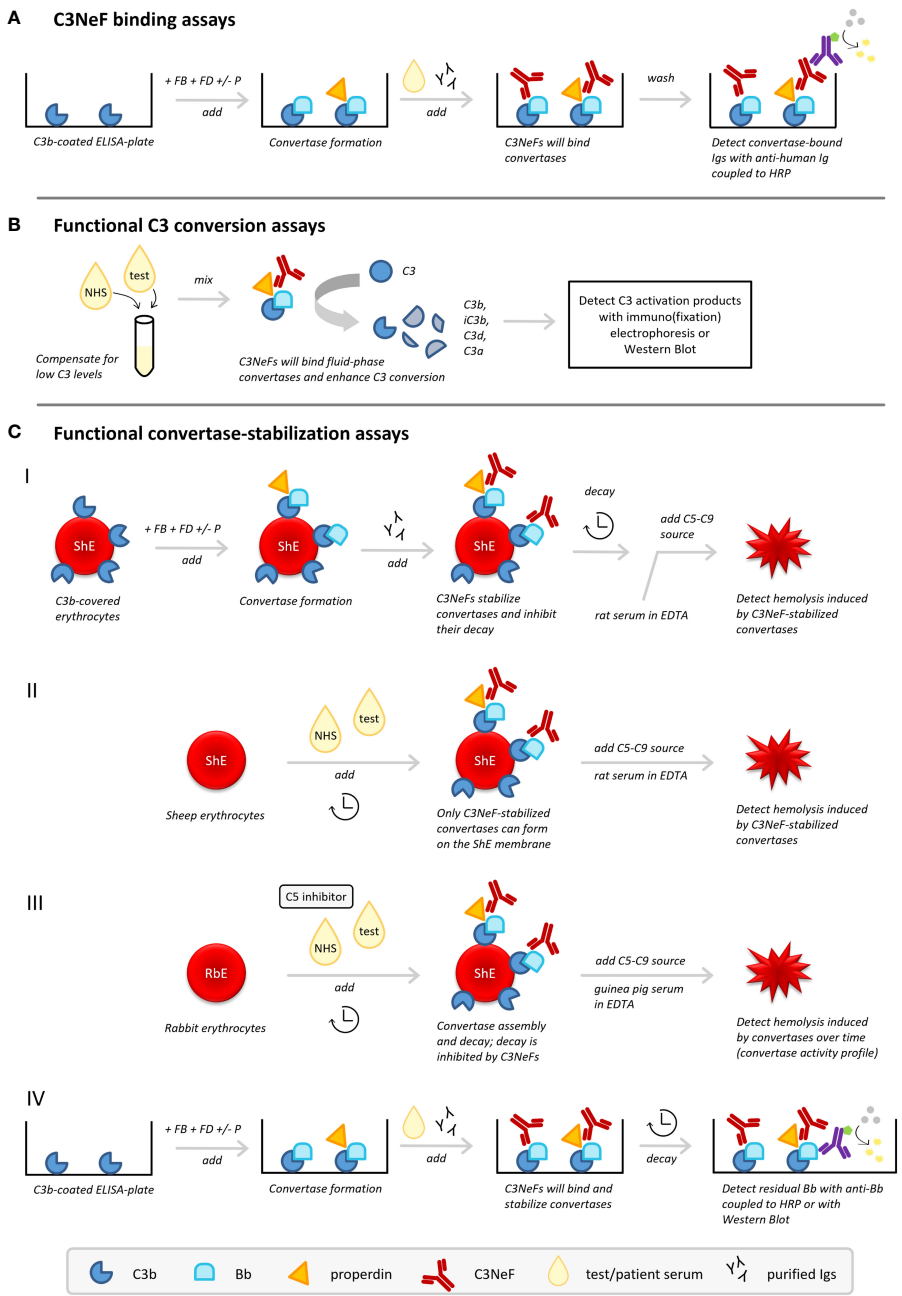

FIGURE 3
C3 nephritic factor (C3NeF) detection methods. Three types of methods to detect C3NeFs can be distinguished: **(A)** assays detecting NeF binding to the convertase, **(B)** functional assays measuring C3 conversion influenced by NeFs, and **(C)** functional assays measuring convertase stabilization by NeFs. ELISA, enzyme-linked immunosorbent assay; FB, Factor B; FD, Factor D; HRP, horseradish peroxidase; Igs, immunoglobulins; NHS, normal human serum; P, properdin; RbE, rabbit erythrocytes; ShE, sheep erythrocytes.

plate-bound AP convertases formed from purified complement components (25, 60, 61, 75). Typically, plates are coated with C3b; then Factor B (FB) and Factor D (FD), in presence or absence of properdin, are added to allow formation of AP convertase complexes. After washing, or simultaneous with the addition of purified AP components, the test sample is added, i.e. purified patient immunoglobulins or patient sera. If C3NeFs are present, their binding can be detected *via* horseradish peroxidase-conjugated anti-human immunoglobulin antibodies supporting substrate conversion. Importantly, a C3b-only well should be used as a blank control in these methods.

In general, binding assays are easy to implement in laboratories and directly identify the immunoglobulin nature of the factor interacting with the enzyme complex. However, these assays are not functional assays, so they may detect a binding interaction that might not influence enzyme function. Besides this chance on false-positive results, the assay may also give false-negative results, as the convertases formed on microtiter plates can adopt artificial conformations that may not be recognized by all NeFs (Table 2).

5.2 Functional C3NeF assays measuring C3 activation products

Functional assays measuring the activation products of C3 (Figure 3B) were the first assays described for measuring C3NeF activity (8, 76). These tests measure the release of C3 breakdown products after mixing the test sample with control serum by immunoelectrophoresis or western blotting (25, 60). Many patients with C3G and other diseases related to C3NeF have low serum levels of C3 as a result of consumption. Hence, mixing with control serum to supply uncleaved C3 is essential to allow formation of fluid phase AP convertases to be stabilized by the NeFs from the test sample. C3NeF positivity will then result in increased C3 conversion.

The advantage of these assays is that they are detecting a functional enzyme effect. However, increased C3 breakdown may also be caused by other factors, so a positive outcome does not have to be specific for presence of C3NeFs (Table 2).

Zhao et al. recently described a variant on this assay. Fluid phase C3 convertases were assembled with purified components, which were then mixed with patient immunoglobulins and additional C3 (61). C3 conversion was measured by the release of C3a detected by ELISA.

5.3 Functional C3NeF assays measuring convertase stabilization

Functional assays measuring the convertase-stabilizing function of C3NeFs were developed later, mostly in the form of hemolytic assays (9) (Figure 3C). These assays have supplemented or replaced many of the previous assays and are frequently used today. Although there are variations in the exact procedures, AP hemolytic C3NeF assays generally follow the same principle: to measure the activity of C3NeF-stabilized convertases on the erythrocyte membrane *via* C5b-9-induced hemolysis. Hemolysis provides the easy readout of released hemoglobin that can be detected spectrophotometrically.

TABLE 2 Advantages and limitations of the different nephritic factor (NeF) detection assays.

Assay type	Advantages	Limitations
C3NeF binding assays	• Easy to implement (ELISA) • Directly identify immunoglobulin nature	• Detect binding, not function • Artificial conformations of convertases possible
Functional C3NeF assays measuring C3 cleavage	• Detect a functional effect	• Non-specific[a]
Functional C3NeF assays measuring convertase stabilization	• Detect a functional effect	
ShE with purified complement components	• *Physiological conformations of convertases on a membrane* • *Directly identify immunoglobulin nature*	• *Require expertise*[b] • *Time-consuming*
ShE with whole serum	• *Physiological conformations of convertases on a membrane* • *Physiological conditions of convertase assembly and decay*	• *Require expertise*[b] • *Lysis may occur in step 1*
RbE with whole serum	• *Physiological conformations of convertases on a membrane* • *Physiological conditions of convertase assembly and decay*	• *Require expertise*[b] • *Additional approaches required to identify immunoglobulin nature*
ELISA-based	• *Easy to implement (ELISA)*	• *Artificial conformations of convertases possible*

ELISA, enzyme-linked immunosorbent assay; ShE, sheep erythrocytes; RbE, rabbit erythrocytes.
[a]The assay described by Zhao et al. (61) has increased specificity compared to the original assays.
[b]Hemolytic assays are dependent on the availability of (fresh) erythrocytes and are prone to batch-to-batch variability of erythrocytes.

5.3.1 Sheep erythrocyte hemolytic assays with convertases formed from purified components

In the first variant, sheep erythrocytes are used as the platform for formation of AP convertases with purified complement components (Figure 3C.I). Since sheep erythrocytes are rich in sialic acids and therefore naturally protected against human complement attack by recruiting the major AP regulator FH (77, 78), specific approaches need to be applied to cover the sheep erythrocytes with initial C3b. C3b can be deposited on the sensitized, i.e. anti-sheep antibody-treated, sheep erythrocyte membrane *via* CP convertase intermediates (79, 80) or on unsensitized sheep erythrocytes by using FB-partially inactivated/FH-depleted serum (25). Subsequently, AP convertases are built from purified components (FB and FD, with or without properdin) followed by the addition of patient immunoglobulin fractions as a potential source of C3NeFs. Importantly, convertases are then left to decay for a set time period. After this incubation, the residual activity of convertases is examined by the addition of rat serum diluted in ethylenediaminetetraacetic acid (EDTA) as a heterologous source of C5-C9. This allows stabilized convertases to cleave C5 and induce C5b-9-mediated hemolysis. Rat serum, as well as guinea pig serum, is compatible with human complement and more potent in generating C5b-9; the EDTA prevents *de novo* convertase formation from these sera. If no C3NeFs are present in the test sample, the convertases are broken down after a certain decay time and no hemolysis is observed. However, if hemolysis is observed, it indicates that convertases have been stabilized by C3NeFs present in the test sample, allowing them to induce C5b-9 formation (20, 25, 81).

5.3.2 Sheep erythrocyte hemolytic assays with convertases formed from whole serum

Another widely applied hemolytic C3NeF assay combines unsensitized sheep erythrocytes with a mix of control serum and test serum (82–84) (Figure 3C.II). This method exploits the ability of C3NeFs to form and stabilize convertase complexes on the surface of the naturally non-activating sheep erythrocyte by overcoming the negative regulation; an action that cannot be fulfilled by serum in the absence of C3NeFs (83). A limited time frame is used to restrict the complement activation by the test sample to convertase assembly and to prevent lysis. Hemolysis is only induced in a standardized second step by addition of rat serum in EDTA-buffer. If no hemolysis is seen, no C3NeFs were present and no convertases could be formed on the sheep erythrocyte membrane. Although this time-dependent separation of convertase assembly and hemolysis will apply for most samples, it should be noted that some patient samples *are* able to cause (unwanted) hemolysis in the convertase formation step of those assays (85) (Table 2).

5.3.3 Rabbit erythrocyte hemolytic assays with convertases formed from whole serum

Recently, an adapted variant of this assay using rabbit erythrocytes (86, 87) was optimized for C3NeF diagnostics (33) (Figure 3C.III). Rabbit erythrocytes have a low sialic acid content and are therefore potent AP activators. When mixed with control serum and test serum, AP convertases will spontaneously assemble on their membrane. Importantly, a C5 inhibitor, e.g. eculizumab, is added here to strictly prevent hemolysis during this first step and to separate convertase assembly from hemolysis readout. After washing of the erythrocytes, guinea pig serum in EDTA is added to allow preformed convertases to cleave C5 and induce C5b-9-mediated hemolysis. In contrast to previous assays, the full convertase activity profile with convertase assembly and decay is visualized by using different incubation periods for the test serum incubation. Compared to control serum showing a profile with convertase assembly and clear convertase breakdown, serum containing C3NeFs will show a prolonged convertase activity profile with persistently high levels of lysis over time, indicative of stabilized convertases.

Of note, both this assay and the assay described in *section 5.3.2* do not directly identify C3NeFs, since the immunoglobulin nature of the convertase-stabilizing factor in serum is not confirmed. Mixing control serum with patient immunoglobulin fractions as an extra test overcomes this limitation and will specify if the convertase-stabilizing factor is an autoantibody (33). On the other hand, assessing the kinetics of convertase assembly and decay in complete serum offers the advantage of the physiological environment. All complement regulators and other serum factors that may influence convertase activity are present, so this maximizes the chance of detecting functionally relevant pathogenic factors (Table 2).

5.3.4 ELISA-based convertase stabilization assays

The principles of convertase stabilization by NeFs in the hemolytic assays above, especially the one described in *section 5.3.1*, have also been translated to assays analyzing the kinetics of convertase dissociation on a microtiter plate (Figure 3C.IV). AP convertases are built from purified components on a C3b-coated microtiter plate after which serum or patient immunoglobulin fractions are added. Instead of hemolysis, residual plate-bound Bb fragments detected after a certain time of decay are used as a measure of intact convertases stabilized by C3NeFs (60, 61). Recently, also a variant of this ELISA-based assay was described that combined convertase formation and decay on microtiter plates with residual Bb analysis on western blot (62).

Of note, these assays do not assess the C3/C5 cleaving capacities of the C3NeF-stabilized convertases. Furthermore, in hemolytic assays, convertases are formed on a membrane surface in their natural orientation *via* the reactive thioester of C3, whereas convertases formed on microtiter plates may adopt

artificial configurations. Nonetheless, the availability of erythrocytes and batch-to-batch variability are a major challenge of hemolytic assays, making these assays often only available in specialized labs. In contrast, ELISA techniques are much more easy to implement (Table 2).

6 Efforts for assay standardization

As stated before, C3NeF detection in general is problematic, with the EQA rounds from 2016-2020 reporting success rates for identifying the reference samples between 31% (2020) and 75% (2016) (7). Thus, if results of a sample are compared between laboratories, or even between different tests within one laboratory, variable outcomes are obtained. At the moment, a golden standard is lacking and there is a high need for standardization. The same holds true for C4NeF assays.

First, it is important to note that properdin-dependent C3NeFs are missed in assays that study the stability of C3bBb convertases formed from purified components without properdin. In line with this, previous reports describing panels with multiple C3NeF assays have shown that additional NeFs could be identified when properdin was incorporated in the test settings (20, 25, 60, 62). Marinozzi et al. also identified a group of C3NeFs that was only detected in absence of properdin (20), and this is supported by our own unpublished observations. However, it remains to be investigated what the physiological relevance of these NeFs is, as in physiological conditions properdin is always present in the circulation.

Recently, a *CFB* construct based on the gain-of-function variant p.Lys323Glu was proposed as a standardized positive control for C3NeF assays (88). This genetic variation is associated with atypical hemolytic uremic syndrome and has previously been shown to result in a stabilized convertase complex that is more resistant to negative regulation (89). The construct caused prolonged convertase activity reminiscent of that of patients with C3NeF activity (33, 88). Therefore, this might be a good alternative for patient serum or patient immunoglobulins, of which material is limited. For C4NeF assays, a similar approach could be followed, as recently also *C2* gain-of-function variants resulting in stabilized CP convertase complexes were identified (90).

Furthermore, surfaces other than erythrocytes have been described for convertase analysis, namely magnetic beads and liposomes (91, 92). These platforms may be more suitable for standardization due to lower batch-to-batch variability. However, these setups have not yet been validated for C3NeF or C4NeF detection. Besides, magnetic beads are a less physiological model than erythrocytes. The optimal platform for the detection of functionally relevant NeFs should still be determined. Thus, future research may not only focus on improved standardization but also on further assay optimization with different (cellular) targets for convertase assembly.

7 Clinical implications

Assay standardization may also lead to a better understanding of the role of C3NeFs and C4NeFs in disease. For a long time, it has been difficult to relate C3NeF presence with complement (activity) markers and clinical parameters, such as disease activity and outcome. Nonetheless, increased interest in this field of research has led to major progresses during the last decade. Here, we will discuss some of the main findings of the clinical associations of NeFs, with a focus on C3G/IC-MPGN.

7.1 Clinical associations of C3NeFs

By stabilizing AP convertases, C3NeFs increase the potential of C3 conversion, which may lead to consumption of C3. Indeed, previous studies have associated the lowered C3 levels in patients with C3G with the presence of C3NeFs (20, 26, 29, 93). Recently, two studies on pediatric C3G cohorts showed that although C3 levels at presentation did not differ between patients with or without C3NeFs, the last measured C3 levels during follow-up were significantly lower in the patients that had tested positive for C3NeF (21, 36). This indicates the presence of C3NeF was associated with a higher likelihood of continued C3 consumption. In line with this, a previous report showed permanently low C3 during follow-up in 67% (12/18) of the C3NeF-positive children with C3G (94).

In a subset of patients with C3G, the complement system is dysregulated up to the level of the terminal pathway as seen by elevated sC5b-9 levels. This implies that there is also enhanced activation of the C5 convertases in those patients, and it was already hypothesized in 1986 that different NeF types may lie at the basis of this difference (71). Several studies have related properdin-dependent C3NeFs to (stronger) terminal pathway activation and to the C3GN phenotype (20, 62, 68, 69). On itself, C3GN is also associated with more pronounced terminal pathway activation (e.g. higher sC5b-9 and lower C5 and properdin) compared to the DDD subtype (19, 21). In 2017, the term C5 nephritic factor (C5NeF) was coined for NeFs that stabilize the AP C5 convertase. This was based on the finding that these NeFs stabilized convertases formed from purified proteins with properdin (C3bBbP) and were correlated with increased sC5b-9 levels (20). Some patients with C5NeFs were also C3NeF positive, i.e. they also tested positive when the stability of convertases formed without properdin (C3bBb) was assayed. In this regard, single C5NeF positive patients as described by this study correspond to the patients with properdin-dependent C3NeFs, and C3NeF/C5NeF double-positive patients correspond to patients with properdin-independent C3NeFs. Importantly, the exact composition and conformation of AP C5 convertases (and CP/LP C5 convertases) remain unknown. Furthermore, some patients with presumed C5NeFs (isolated or in combination with C3NeFs) do not show

C5 convertase dysregulation, i.e. increased sC5b-9 levels, and conversely, some patients without C5NeFs do have increased sC5b-9 levels (20, 62). Moreover, complement markers are not always available. Therefore, the application of C5NeF terminology may be confusing, as it is unclear whether the C5NeF terminology is directly interchangeable with the properdin-dependency of NeFs and whether it may be used regardless of C5 convertase dysregulation. This is why it may be preferable to classify the NeF types based on their dependence on properdin for recognizing the convertase and to refrain from implications on the specific stabilization of the C5 convertase complex.

Even though C3NeFs are the most commonly found AP aberrations in C3G, not much is known about their behavior over time in the course of the disease and their relation to clinical outcome. While some patients have been shown to maintain their C3NeF activity for more than 10 years (58), C3NeF findings may also fluctuate over time, with some patients eventually losing their C3NeFs (26, 33, 93, 94). The longitudinal follow-up of C3NeFs is often not part of standard patient investigations. Moreover, many studies did not find correlations between C3NeF activity and clinical parameters (93, 94), although some studies have shown that patients with C3NeFs were more likely to have a better outcome (20, 29).

7.2 Clinical associations of C4NeFs

Lately, C4NeF research has also mostly focused on C3G and IC-MPGN. One of the most important questions here is how and to what extent a CP-dysregulating factor can contribute to AP-driven disease. In many patients with C3G, the disease is preceded by an infectious trigger, which exposes C4NeF epitopes. C3G shows many clinical similarities with post-infectious glomerulonephritis, such as low serum C3 levels, but in contrast to C3G, the C3 consumption and disease generally resolve within weeks or months (95, 96). However, some (atypical) cases evolve to C3G, indicating that an initial CP-mediated response may evolve to a primarily AP-driven pathology, likely *via* the AP amplification loop. Possibly, C4NeFs elicit such a similar mechanism in C3G and IC-MPGN.

The majority of C3G/IC-MPGN patients with C4NeFs are characterized by strong complement activation up to the level of the terminal pathway, especially patients positive for both C4NeFs and C3NeFs (30, 54, 58, 59). This double positivity for both C4NeF and C3NeF occurs in many cases and makes it difficult to determine the individual contribution of both NeFs to the disease. Furthermore, C4NeFs may persist over the disease course and during partial remission up to 70 months (58).

Studies on the relationship between C4NeF activity and clinical markers are scarce and often lack power due to the low number of positive patients. Besides, the scarce literature shows conflicting results. In a cohort with 100 hypocomplementemic MPGN patients described in 1994, nephrotic syndrome and poor prognosis occurred more frequently in C3NeF/C4NeF double-positive patients compared to single C3NeF or single C4NeF-positive patients (54). A recent study with 119 IC-MPGN/C3G patients showed that C4NeF-positive and C3NeF/C4NeF double-positive patients less frequently had a lowered eGFR at presentation and that, during the follow-up, none of the 17 patients reached kidney failure requiring kidney replacement therapy (in contrast to 17/92 C4NeF-negative patients) (59). In a study of our group, we did not observe an abnormal clinical presentation or disease course compared to C3G/IC-MPGN patients without C4NeFs (58).

8 Conclusions and future directions

With the increase in complement therapeutics, laboratory analysis of the complement system has become increasingly important (97). For example, it can be key in monitoring complement-directed therapy, as has been shown for the C5 inhibitor eculizumab in atypical hemolytic uremic syndrome (98, 99). It is well-known that accurate NeF analysis is challenging. This is due to the heterogenic nature of NeF autoantibodies, including differences in properdin-dependency, and due to inconsistent outcomes of samples tested in different assays between laboratories or even between different assays within one laboratory. As outlined in this review, each assay has its own advantages and disadvantages. There is a high need for comparison of NeF findings between groups. The considerable inconsistency between cohort findings now complicates the interpretation of the results of the NeF associations with complement biomarkers and/or disease parameters. Assay standardization, in combination with longitudinal analysis of NeFs and all relevant complement and clinical parameters in patients, may help to reveal different pathophysiological mechanisms of complement dysregulation in different patient groups. It may even provide more insight in disease outcome. Iatropoulos et al. showed that disease outcome was better predicted when patients were divided in groups based on cluster analysis, including not only pathology findings but also complement (e.g. NeF presence) and clinical findings, than based on the traditional subdivision into C3GN, DDD, and IC-MPGN (22). Moreover, our group showed *in vitro* proof that properdin inhibition may be a potential novel therapeutic approach for patients with properdin-dependent NeFs, likely regardless of disease classification (70). Thus, accurate and reliable NeF diagnostics are essential to better understand disease, to characterize patient (sub)groups and to move forward towards more specific complement-directed therapy in different patient groups.

Author contributions

MM wrote the manuscript. EV, NK, and LH critically reviewed the manuscript. All authors listed have made a substantial, direct and intellectual contribution to the work, and approved it for publication.

Funding

This work was supported by the Dutch Kidney Foundation (13OCA27 COMBAT Consortium and 20OK021 PERSPECTIV).

Acknowledgments

This study was performed on behalf of the COMBAT Consortium. This is an interuniversity collaboration in the Netherlands that is formed to study basic mechanisms, assay development, and therapeutic translation of complement-mediated renal diseases. Principal investigators are (in alphabetical order): S. Berger (Department of Internal Medicine-Nephrology, University Medical Center Groningen, Groningen, Netherlands), J. van den Born (Department of Internal Medicine-Nephrology, University Medical Center Groningen, Groningen, Netherlands), P. Gros (Department of Chemistry, Utrecht University, Utrecht, Netherlands), L. van den Heuvel (Department of Pediatric Nephrology, Radboud University Medical Center, Nijmegen, Netherlands), N. van de Kar (Department of Pediatric Nephrology, Radboud University Medical Center, Nijmegen, Netherlands), C. van Kooten (Department of Internal Medicine-Nephrology, Leiden University Medical Center, Leiden, Netherlands), M. Seelen (Department of Internal Medicine-Nephrology, University Medical Center Groningen, Groningen, Netherlands), A. de Vries (Department of Internal Medicine-Nephrology, Leiden University Medical Center, Leiden, Netherlands). NK and BH and are members of the European Reference Network for Rare Kidney Diseases (ERKNet)-Project No 739532.

Conflict of interest

The authors declare that the research was conducted in the absence of any commercial or financial relationships that could be construed as a potential conflict of interest.

Publisher's note

All claims expressed in this article are solely those of the authors and do not necessarily represent those of their affiliated organizations, or those of the publisher, the editors and the reviewers. Any product that may be evaluated in this article, or claim that may be made by its manufacturer, is not guaranteed or endorsed by the publisher.

References

1. Pouw RB, Ricklin D. Tipping the balance: Intricate roles of the complement system in disease and therapy. *Semin Immunopathol* (2021) 43(6):757–71. doi: 10.1007/s00281-021-00892-7

2. Legendre CM, Licht C, Muus P, Greenbaum LA, Babu S, Bedrosian C, et al. Terminal complement inhibitor eculizumab in atypical hemolytic-uremic syndrome. *N Eng J Med* (2013) 368(23):2169–81. doi: 10.1056/NEJMoa1208981

3. Menne J, Delmas Y, Fakhouri F, Licht C, Lommelé Å, Minetti EE, et al. Outcomes in patients with atypical hemolytic uremic syndrome treated with eculizumab in a long-term observational study. *BMC Nephrol* (2019) 20(1):125. doi: 10.1186/s12882-019-1314-1

4. Dmytrijuk A, Robie-Suh K, Cohen MH, Rieves D, Weiss K, Pazdur R. FDA Report: Eculizumab (Soliris) for the treatment of patients with paroxysmal nocturnal hemoglobinuria. *Oncologist* (2008) 13(9):993–1000. doi: 10.1634/theoncologist.2008-0086

5. Mastellos DC, Ricklin D, Lambris JD. Clinical promise of next-generation complement therapeutics. *Nat Rev Drug Discov* (2019) 18(9):707–29. doi: 10.1038/s41573-019-0031-6

6. Zelek WM, Xie L, Morgan BP, Harris CL. Compendium of current complement therapeutics. *Mol Immunol* (2019) 114:341–52. doi: 10.1016/j.molimm.2019.07.030

7. Frazer-Abel A, Kirschfink M, Prohászka Z. Expanding horizons in complement analysis and quality control. *Front Immunol* (2021) 12:697313. doi: 10.3389/fimmu.2021.697313

8. Spitzer RE, Vallota EH, Forristal J, Sudora E, Stitzel A, Davis NC, et al. Serum C'3 lytic system in patients with glomerulonephritis. *Science* (1969) 164(3878):436–7. doi: 10.1126/science.164.3878.436

9. Daha MR, Fearon DT, Austen KF. C3 nephritic factor (C3NeF): Stabilization of fluid phase and cell-bound alternative pathway convertase. *J Immunol* (1976) 116(1):1–7.

10. Daha MR, Austen KF, Fearon DT. Heterogeneity, polypeptide chain composition and antigenic reactivity of C3 nephritic factor. *J Immunol* (1978) 120(4):1389–94.

11. Daha MR, van Es LA. Further evidence for the antibody nature of C3 nephritic factor (C3NeF). *J Immunol* (1979) 123(2):755–8.

12. Davis AE3rd, Ziegler JB, Gelfand EW, Rosen FS, Alper CA. Heterogeneity of nephritic factor and its identification as an immunoglobulin. *Proc Natl Acad Sci USA* (1977) 74(9):3980–3. doi: 10.1073/pnas.74.9.3980

13. Scott DM, Amos N, Sissons JG, Lachmann PJ, Peters DK. The immunogloblin nature of nephritic factor (NeF). *Clin Exp Immunol* (1978) 32 (1):12–24.

14. Daha MR, Hazevoet HM, Vanes LA, Cats A. Stabilization of the classical pathway C3 convertase C42, by a factor F-42, isolated from serum of patients with systemic lupus erythematosus. *Immunology* (1980) 40(3):417–24.

15. Halbwachs L, Leveillé M, Lesavre P, Wattel S, Leibowitch J. Nephritic factor of the classical pathway of complement: Immunoglobulin G autoantibody directed against the classical pathway C3 convertase enzyme. *J Clin Invest* (1980) 65 (6):1249–56. doi: 10.1172/jci109787

16. Pickering MC, D'Agati VD, Nester CM, Smith RJ, Haas M, Appel GB, et al. C3 glomerulopathy: Consensus report. *Kidney Int* (2013) 84(6):1079–89. doi: 10.1038/ki.2013.377

17. Goodship TH, Cook HT, Fakhouri F, Fervenza FC, Frémeaux-Bacchi V, Kavanagh D, et al. Atypical hemolytic uremic syndrome and C3 glomerulopathy: Conclusions from a "Kidney disease: Improving global outcomes" (KDIGO)

controversies conference. *Kidney Int* (2017) 91(3):539–51. doi: 10.1016/j.kint.2016.10.005

18. Hou J, Markowitz GS, Bomback AS, Appel GB, Herlitz LC, Barry Stokes M, et al. Toward a working definition of C3 glomerulopathy by immunofluorescence. *Kidney Int* (2014) 85(2):450–6. doi: 10.1038/ki.2013.340

19. Zhang Y, Nester CM, Martin B, Skjoedt MO, Meyer NC, Shao D, et al. Defining the complement biomarker profile of C3 glomerulopathy. *Clin J Am Soc Nephrol* (2014) 9(11):1876–82. doi: 10.2215/cjn.01820214

20. Marinozzi MC, Chauvet S, Le Quintrec M, Mignotet M, Petitprez F, Legendre C, et al. C5 nephritic factors drive the biological phenotype of C3 glomerulopathies. *Kidney Int* (2017) 92(5):1232–41. doi: 10.1016/j.kint.2017.04.017

21. Michels MAHM, Wijnsma KL, Kurvers RAJ, Westra D, Schreuder MF, van Wijk JAE, et al. Long-term follow-up including extensive complement analysis of a pediatric C3 glomerulopathy cohort. *Pediatr Nephrol* (2022) 37(3):601–12. doi: 10.1007/s00467-021-05221-6

22. Iatropoulos P, Daina E, Curreri M, Piras R, Valoti E, Mele C, et al. Cluster analysis identifies distinct pathogenetic patterns in C3 glomerulopathies/immune complex-mediated membranoproliferative GN. *J Am Soc Nephrol* (2018) 29 (1):283–94. doi: 10.1681/asn.2017030258

23. Nasr SH, Valeri AM, Appel GB, Sherwinter J, Stokes MB, Said SM, et al. Dense deposit disease: Clinicopathologic study of 32 pediatric and adult patients. *Clin J Am Soc Nephrol* (2009) 4(1):22–32. doi: 10.2215/cjn.03480708

24. Sethi S, Fervenza FC, Zhang Y, Zand L, Vrana JA, Nasr SH, et al. C3 glomerulonephritis: Clinicopathological findings, complement abnormalities, glomerular proteomic profile, treatment, and follow-up. *Kidney Int* (2012) 82 (4):465–73. doi: 10.1038/ki.2012.212

25. Zhang Y, Meyer NC, Wang K, Nishimura C, Frees K, Jones M, et al. Causes of alternative pathway dysregulation in dense deposit disease. *Clin J Am Soc Nephrol* (2012) 7(2):265–74. doi: 10.2215/cjn.07900811

26. Servais A, Noel LH, Roumenina LT, Le Quintrec M, Ngo S, Dragon-Durey MA, et al. Acquired and genetic complement abnormalities play a critical role in dense deposit disease and other C3 glomerulopathies. *Kidney Int* (2012) 82(4):454–64. doi: 10.1038/ki.2012.63

27. Rabasco C, Cavero T, Roman E, Rojas-Rivera J, Olea T, Espinosa M, et al. Effectiveness of mycophenolate mofetil in C3 glomerulonephritis. *Kidney Int* (2015) 88(5):1153–60. doi: 10.1038/ki.2015.227

28. Corvillo F, Bravo Garcia-Morato M, Nozal P, Garrido S, Tortajada A, Rodriguez de Cordoba S, et al. Serum properdin consumption as a biomarker of C5 convertase dysregulation in C3 glomerulopathy. *Clin Exp Immunol* (2016) 184 (1):118–25. doi: 10.1111/cei.12754

29. Iatropoulos P, Noris M, Mele C, Piras R, Valoti E, Bresin E, et al. Complement gene variants determine the risk of immunoglobulin-associated MPGN and C3 glomerulopathy and predict long-term renal outcome. *Mol Immunol* (2016) 71:131–42. doi: 10.1016/j.molimm.2016.01.010

30. Zhang Y, Meyer NC, Fervenza FC, Lau W, Keenan A, Cara-Fuentes G, et al. C4 nephritic factors in C3 glomerulopathy: A case series. *Am J Kidney Dis* (2017) 70(6):834–43. doi: 10.1053/j.ajkd.2017.07.004

31. Bomback AS, Santoriello D, Avasare RS, Regunathan-Shenk R, Canetta PA, Ahn W, et al. C3 glomerulonephritis and dense deposit disease share a similar disease course in a large United States cohort of patients with C3 glomerulopathy. *Kidney Int* (2018) 93(4):977–85. doi: 10.1016/j.kint.2017.10.022

32. Ravindran A, Fervenza FC, Smith RJH, De Vriese AS, Sethi S. C3 glomerulopathy: Ten years' experience at Mayo clinic. *Mayo Clin Proc* (2018) 93 (8):991–1008. doi: 10.1016/j.mayocp.2018.05.019

33. Michels MAHM, van de Kar NCAJ, Okrój M, Blom AM, van Kraaij SAW, Volokhina EB, et al. Overactivity of alternative pathway convertases in patients with complement-mediated renal diseases. *Front Immunol* (2018) 9:612. doi: 10.3389/fimmu.2018.00612

34. Garam N, Prohászka Z, Szilágyi Á, Aigner C, Schmidt A, Gaggl M, et al. Validation of distinct pathogenic patterns in a cohort of membranoproliferative glomerulonephritis patients by cluster analysis. *Clin Kidney J* (2020) 13(2):225–34. doi: 10.1093/ckj/sfz073

35. Levine AP, Chan MMY, Sadeghi-Alavijeh O, Wong EKS, Cook HT, Ashford S, et al. Large-scale whole-genome sequencing reveals the genetic architecture of primary membranoproliferative GN and C3 glomerulopathy. *J Am Soc Nephrol* (2020) 31(2):365–73. doi: 10.1681/asn.2019040433

36. Wong EKS, Marchbank KJ, Lomax-Browne H, Pappworth IY, Denton H, Cooke K, et al. C3 glomerulopathy and related disorders in children: Etiology-phenotype correlation and outcomes. *Clin J Am Soc Nephrol* (2021) 16(11):1639–51. doi: 10.2215/cjn.00320121

37. Noris M, Daina E, Remuzzi G. Membranoproliferative glomerulonephritis: No longer the same disease and may need very different treatment. *Nephrol Dial Transplant* (2021) Epub ahead of print.. doi: 10.1093/ndt/gfab281

38. Misra A, Peethambaram A, Garg A. Clinical features and metabolic and autoimmune derangements in acquired partial lipodystrophy: Report of 35 cases and review of the literature. *Med (Baltimore)* (2004) 83(1):18–34. doi: 10.1097/01.md.0000111061.69212.59

39. Corvillo F, Ceccarini G, Nozal P, Magno S, Pelosini C, Garrido S, et al. Immunological features of patients affected by Barraquer-Simons syndrome. *Orphanet J Rare Dis* (2020) 15(1):9. doi: 10.1186/s13023-019-1292-1

40. Corvillo F, Okrój M, Nozal P, Melgosa M, Sánchez-Corral P, López-Trascasa M. Nephritic factors: An overview of classification, diagnostic tools and clinical associations. *Front Immunol* (2019) 10:886. doi: 10.3389/fimmu.2019.00886

41. Corvillo F, López-Trascasa M. Acquired partial lipodystrophy and C3 glomerulopathy: Dysregulation of the complement system as a common pathogenic mechanism. *Nefrol (Engl Ed)* (2018) 38(3):258–66. doi: 10.1016/j.nefro.2017.10.002

42. Garg A. Acquired and inherited lipodystrophies. *N Eng J Med* (2004) 350 (12):1220–34. doi: 10.1056/NEJMra025261

43. Teisner B, Elling P, Svehag SE, Poulsen L, Lamm LU, Sjöholm A. C3 nephritic factor in a patient with recurrent Neisseria meningitidis infections. *Acta Pathol Microbiol Immunol Scand C* (1984) 92(6):341–9. doi: 10.1111/j.1699-0463.1984.tb00098.x

44. Fijen CA, Kuijper EJ, te Bulte MT, Daha MR, Dankert J. Assessment of complement deficiency in patients with meningococcal disease in the Netherlands. *Clin Infect Dis* (1999) 28(1):98–105. doi: 10.1086/515075

45. Thompson RA, Yap PL, Brettle RB, Dunmow RE, Chapel H. Meningococcal meningitis associated with persistent hypocomplementaemia due to circulating C3 nephritic factor. *Clin Exp Immunol* (1983) 52(1):153–6.

46. Walport MJ, Davies KA, Botto M, Naughton MA, Isenberg DA, Biasi D, et al. C3 nephritic factor and SLE: Report of four cases and review of the literature. *QJM* (1994) 87(10):609–15.

47. Cronin CC, Higgins TJ, Molloy M. Lupus, C3 nephritic factor and partial lipodystrophy. *QJM* (1995) 88(4):298–9.

48. Hristova MH, Stoyanova VS. Autoantibodies against complement components in systemic lupus erythematosus - role in the pathogenesis and clinical manifestations. *Lupus* (2017) 26(14):1550–5. doi: 10.1177/0961203317709347

49. Davis CA, McAdams AJ, Wyatt RJ, Forristal J, McEnery PT, West CD. Idiopathic rapidly progressive glomerulonephritis with C3 nephritic factor and hypocomplementemia. *J Pediatr* (1979) 94(4):559–63. doi: 10.1016/s0022-3476(79)80010-4

50. Frémeaux-Bacchi V, Weiss L, Demouchy C, May A, Palomera S, Kazatchkine MD. Hypocomplementaemia of poststreptococcal acute glomerulonephritis is associated with C3 nephritic factor (C3NeF) IgG autoantibody activity. *Nephrol Dial Transplant* (1994) 9(12):1747–50.

51. Chauvet S, Berthaud R, Devriese M, Mignotet M, Vieira Martins P, Robe-Rybkine T, et al. Anti-factor B antibodies and acute postinfectious GN in children. *J Am Soc Nephrol* (2020) 31(4):829–40. doi: 10.1681/asn.2019080851

52. Arakawa M, Seino J, Kinoshita Y, Fukuda K, Saito T, Furuyama T. Nephritic factor (NeF) of alternate pathway (NeFA) and of classical pathway (NeFc). *Tohoku J Exp Med* (1982) 138(4):401–9. doi: 10.1620/tjem.138.401

53. Daha MR, Hazevoet HM, van Es LA. Heterogeneity, polypeptide chain composition and antigenic reactivity of autoantibodies (F-42) that are directed against the classical pathway C3 convertase of complement and isolated from sera of patients with systemic lupus erythematosus. *Clin Exp Immunol* (1984) 56(3):614–20.

54. Ohi H, Yasugi T. Occurrence of C3 nephritic factor and C4 nephritic factor in membranoproliferative glomerulonephritis (MPGN). *Clin Exp Immunol* (1994) 95(2):316–21.

55. Tanuma Y, Ohi H, Watanabe S, Seki M, Hatano M. C3 nephritic factor and C4 nephritic factor in the serum of two patients with hypocomplementaemic membranoproliferative glomerulonephritis. *Clin Exp Immunol* (1989) 76(1):82–5.

56. Miller EC, Chase NM, Densen P, Hintermeyer MK, Casper JT, Atkinson JP. Autoantibody stabilization of the classical pathway C3 convertase leading to C3 deficiency and neisserial sepsis: C4 nephritic factor revisited. *Clin Immunol* (2012) 145(3):241–50. doi: 10.1016/j.clim.2012.09.007

57. Blom AM, Corvillo F, Magda M, Stasilojc G, Nozal P, Perez-Valdivia MA, et al. Testing the activity of complement convertases in serum/plasma for diagnosis of C4NeF-mediated C3 glomerulonephritis. *J Clin Immunol* (2016) 36(5):517–27. doi: 10.1007/s10875-016-0290-5

58. Michels MAHM, van de Kar NCAJ, van Kraaij SAW, Sarlea SA, Gracchi V, Engels F, et al. Different aspects of classical pathway overactivation in patients with C3 glomerulopathy and immune complex-mediated membranoproliferative glomerulonephritis. *Front Immunol* (2021) 12:715704. doi: 10.3389/fimmu.2021.715704

59. Garam N, Prohaszka Z, Szilagyi A, Aigner C, Schmidt A, Gaggl M, et al. C4 nephritic factor in patients with immune-complex-mediated membranoproliferative glomerulonephritis and C3-glomerulopathy. *Orphanet J Rare Dis* (2019) 14(1):247. doi: 10.1186/s13023-019-1237-8

60. Paixao-Cavalcante D, Lopez-Trascasa M, Skattum L, Giclas PC, Goodship TH, de Cordoba SR, et al. Sensitive and specific assays for C3 nephritic factors clarify mechanisms underlying complement dysregulation. *Kidney Int* (2012) 82 (10):1084–92. doi: 10.1038/ki.2012.250

61. Zhao F, Afonso S, Lindner S, Hartmann A, Löschmann I, Nilsson B, et al. C3-glomerulopathy autoantibodies mediate distinct effects on complement C3- and C5-convertases. *Front Immunol* (2019) 10:1030. doi: 10.3389/fimmu.2019.01030

62. Donadelli R, Pulieri P, Piras R, Iatropoulos P, Valoti E, Benigni A, et al. Unraveling the molecular mechanisms underlying complement dysregulation by nephritic factors in C3G and IC-MPGN. *Front Immunol* (2018) 9:2329. doi: 10.3389/fimmu.2018.02329

63. Jelezarova E, Schlumberger M, Sadallah S, Späth PJ, Schifferli JA, Lutz HU. A C3 convertase assay for nephritic factor functional activity. *J Immunol Methods* (2001) 251(1-2):45–52. doi: 10.1016/s0022-1759(01)00295-2

64. Ohi H, Watanabe S, Fujita T, Yasugi T. Significance of C3 nephritic factor (C3NeF) in non-hypocomplementaemic serum with membranoproliferative glomerulonephritis (MPGN). *Clin Exp Immunol* (1992) 89(3):479–84. doi: 10.1111/j.1365-2249.1992.tb06984.x

65. Weiler JM, Daha MR, Austen KF, Fearon DT. Control of the amplification convertase of complement by the plasma protein beta1H. *Proc Natl Acad Sci U.S.A.* (1976) 73(9):3268–72. doi: 10.1073/pnas.73.9.3268

66. Daha MR, Kok DJ, Van Es LA. Regulation of the C3 nephritic factor stabilized C3/C5 convertase of complement by purified human erythrocyte C3b receptor. *Clin Exp Immunol* (1982) 50(1):209–14.

67. Ito S, Tamura N, Fujita T. Effect of decay-accelerating factor on the assembly of the classical and alternative pathway C3 convertases in the presence of C4 or C3 nephritic factor. *Immunology* (1989) 68(4):449–52.

68. Clardy CW, Forristal J, Strife CF, West CD. A properdin dependent nephritic factor slowly activating C3, C5, and C9 in membranoproliferative glomerulonephritis, types I and III. *Clin Immunol Immunopathol* (1989) 50 (3):333–47. doi: 10.1016/0090-1229(89)90141-4

69. Tanuma Y, Ohi H, Hatano M. Two types of C3 nephritic factor: Properdin-dependent C3NeF and properdin-independent C3NeF. *Clin Immunol Immunopathol* (1990) 56(2):226–38. doi: 10.1016/0090-1229(89)90141-4

70. Michels MAHM, van de Kar NCAJ, van den Bos RM, van der Velden TJAM, van Kraaij SAW, Sarlea SA, et al. Novel assays to distinguish between properdin-dependent and properdin-independent C3 nephritic factors provide insight into properdin-inhibiting therapy. *Front Immunol* (2019) 10:1350. doi: 10.3389/fimmu.2019.01350

71. Mollnes TE, Ng YC, Peters DK, Lea T, Tschopp J, Harboe M. Effect of nephritic factor on C3 and on the terminal pathway of complement *in vivo* and *in vitro*. *Clin Exp Immunol* (1986) 65(1):73–9.

72. Daha MR, van Es LA. Relative resistance of the F-42-stabilized classical pathway C3 convertase to inactivation by C4-binding protein. *J Immunol* (1980) 125(5):2051–4.

73. Gigli I, Sorvillo J, Mecarelli-Halbwachs L, Leibowitch J. Mechanism of action of the C4 nephritic factor. Deregulation of the classical pathway of C3 convertase. *J Exp Med* (1981) 154(1):1–12. doi: 10.1084/jem.154.1.1

74. Fischer E, Kazatchkine MD, Mecarelli-Halbwachs L. Protection of the classical and alternative complement pathway C3 convertases, stabilized by nephritic factors, from decay by the human C3b receptor. *Eur J Immunol* (1984) 14(12):1111–4. doi: 10.1002/eji.1830141209

75. Skattum L. Analysis of C3 nephritic factors by ELISA. *Methods Mol Biol* (2019) 1901:177–82. doi: 10.1007/978-1-4939-8949-2_13

76. Peters DK, Martin A, Weinstein A, Cameron JS, Barratt TM, Ogg CS, et al. Complement studies in membrano-proliferative glomerulonephritis. *Clin Exp Immunol* (1972) 11(3):311–20.

77. Kazatchkine MD, Fearon DT, Austen KF. Human alternative complement pathway: Membrane-associated sialic acid regulates the competition between B and beta1 H for cell-bound C3b. *J Immunol* (1979) 122(1):75–81.

78. Ferreira VP, Pangburn MK, Cortés C. Complement control protein Factor H: The good, the bad, and the inadequate. *Mol Immunol* (2010) 47(13):2187–97. doi: 10.1016/j.molimm.2010.05.007

79. Chabannes M, Bordereau P, Martins PV, Dragon-Durey MA. Sheep erythrocyte preparation for hemolytic tests exploring complement functional activities. *Methods Mol Biol* (2021) 2227:61–7. doi: 10.1007/978-1-0716-1016-9_6

80. Ohi H, Watanabe S, Fujita T, Seki M, Hatano M. Detection of C3bBb-stabilizing activity (C3 nephritic factor) in the serum from patients with membranoproliferative glomerulonephritis. *J Immunol Methods* (1990) 131 (1):71–6. doi: 10.1016/0022-1759(90)90234-m

81. Chabannes M, Frémeaux-Bacchi V, Chauvet S. Detection of C3 nephritic factor by hemolytic assay. *Methods Mol Biol* (2021) 2227:147–58. doi: 10.1007/978-1-0716-1016-9_15

82. West CD. A hemolytic method for the measurement of nephritic factor. *J Immunol Methods* (2008) 335(1-2):1–7. doi: 10.1016/j.jim.2007.12.001

83. Rother U. A new screening test for C3 nephritis factor based on a stable cell bound convertase on sheep erythrocytes. *J Immunol Methods* (1982) 51(1):101–7. doi: 10.1016/0022-1759(82)90386-6

84. López-Trascasa M, Marín MA, Fontán G. C3 nephritic factor determination. A comparison between two methods. *J Immunol Methods* (1987) 98(1):77–82. doi: 10.1016/0022-1759(87)90438-8

85. Skattum L, Mårtensson U, Sjöholm AG. Hypocomplementaemia caused by C3 nephritic factors (C3 NeF): Clinical findings and the coincidence of C3 NeF type II with anti-C1q autoantibodies. *J Intern Med* (1997) 242(6):455–64. doi: 10.1111/j.1365-2796.1997.tb00018.x

86. Blom AM, Volokhina EB, Fransson V, Strömberg P, Berghard L, Viktorelius M, et al. A novel method for direct measurement of complement convertases activity in human serum. *Clin Exp Immunol* (2014) 178(1):142–53. doi: 10.1111/cei.12388

87. Okroj M, Holmquist E, King BC, Blom AM. Functional analyses of complement convertases using C3 and C5-depleted sera. *PLoS One* (2012) 7(10): e47245. doi: 10.1371/journal.pone.0047245

88. Urban A, Borowska A, Felberg A, van den Heuvel L, Stasilojc G, Volokhina E, et al. Gain of function mutant of complement factor b K323E mimics pathogenic C3NeF autoantibodies in convertase assays. *Autoimmunity* (2018) 51(1):18–24. doi: 10.1080/08916934.2017.1423286

89. Goicoechea de Jorge E, Harris CL, Esparza-Gordillo J, Carreras L, Arranz EA, Garrido CA, et al. Gain-of-function mutations in complement factor B are associated with atypical hemolytic uremic syndrome. *Proc Natl Acad Sci USA* (2007) 104(1):240–5. doi: 10.1073/pnas.0603420103

90. Urban A, Volokhina E, Felberg A, Stasiłojć G, Blom AM, Jongerius I, et al. Gain-of-function mutation in complement C2 protein identified in a patient with aHUS. *J Allergy Clin Immunol* (2020) 146(4):916–9.e11. doi: 10.1016/j.jaci.2020.02.014

91. Yorulmaz Avsar S, Jackman JA, Kim MC, Yoon BK, Hunziker W, Cho NJ. Immobilization strategies for functional complement convertase assembly at lipid membrane interfaces. *Langmuir* (2017) 33(29):7332–42. doi: 10.1021/acs.langmuir.7b01465

92. Zwarthoff SA, Berends ETM, Mol S, Ruyken M, Aerts PC, Józsi M, et al. Functional characterization of alternative and classical pathway C3/C5 convertase activity and inhibition using purified models. *Front Immunol* (2018) 9:1691. doi: 10.1034/j.1399-3038.2001.012003166.x.

93. Schwertz R, Rother U, Anders D, Gretz N, Scharer K, Kirschfink M. Complement analysis in children with idiopathic membranoproliferative glomerulonephritis: A long-term follow-up. *Pediatr Allergy Immunol* (2001) 12 (3):166–72.

94. Nicolas C, Vuiblet V, Baudouin V, Macher MA, Vrillon I, Biebuyck-Gouge N, et al. C3 nephritic factor associated with C3 glomerulopathy in children. *Pediatr Nephrol* (2014) 29(1):85–94. doi: 10.1007/s00467-013-2605-6

95. Al-Ghaithi B, Chanchlani R, Riedl M, Thorner P, Licht C. C3 glomerulopathy and post-infectious glomerulonephritis define a disease spectrum. *Pediatr Nephrol* (2016) 31(11):2079–86. doi: 10.1007/s00467-015-3311-3

96. Sethi S, Fervenza FC, Zhang Y, Zand L, Meyer NC, Borsa N, et al. Atypical postinfectious glomerulonephritis is associated with abnormalities in the alternative pathway of complement. *Kidney Int* (2013) 83(2):293–9. doi: 10.1038/ki.2012.384

97. Prohászka Z, Kirschfink M, Frazer-Abel A. Complement analysis in the era of targeted therapeutics. *Mol Immunol* (2018) 102:84–8. doi: 10.1016/j.molimm.2018.06.001

98. Volokhina E, Wijnsma K, van der Molen R, Roeleveld N, van der Velden T, Goertz J, et al. Eculizumab dosing regimen in atypical HUS: Possibilities for individualized treatment. *Clin Pharmacol Ther* (2017) 102(4):671–8. doi: 10.1002/cpt.686

99. Wijnsma KL, Ter Heine R, Moes D, Langemeijer S, Schols SEM, Volokhina EB, et al. Pharmacology, pharmacokinetics and pharmacodynamics of eculizumab, and possibilities for an individualized approach to eculizumab. *Clin Pharmacokinet* (2019) 58(7):859–74. doi: 10.1007/s40262-019-00742-8

frontiers | Frontiers in Immunology

TYPE Case Report
PUBLISHED 14 November 2022
DOI 10.3389/fimmu.2022.1008294

Check for updates

OPEN ACCESS

EDITED BY
Erik J. M. Toonen,
Hycult Biotech, Netherlands

REVIEWED BY
Jean-François Subra,
Nephrologie Dialyse Transplantation
chu angers, France
Ondrej Viklicky,
Institute for Clinical and Experimental
Medicine (IKEM), Czechiaf

*CORRESPONDENCE
Peter F. Zipfel
peter.zipfel@leibniz-hki.de

SPECIALTY SECTION
This article was submitted to
Molecular Innate Immunity,
a section of the journal
Frontiers in Immunology

RECEIVED 31 July 2022
ACCEPTED 22 September 2022
PUBLISHED 14 November 2022

CITATION
Stea ED, Skerka C, Accetturo M,
Pesce F, Wiech T, Hartman A,
Pontrelli P, Conserva F, Castellano G,
Zipfel PF and Gesualdo L (2022) Case
report: Novel FHR2 variants in atypical
Hemolytic Uremic Syndrome: A case
study of a translational medicine
approach in renal transplantation.
Front. Immunol. 13:1008294.
doi: 10.3389/fimmu.2022.1008294

COPYRIGHT
© 2022 Stea, Skerka, Accetturo, Pesce,
Wiech, Hartman, Pontrelli, Conserva,
Castellano, Zipfel and Gesualdo. This is
an open-access article distributed under
the terms of the Creative Commons
Attribution License (CC BY). The use,
distribution or reproduction in other
forums is permitted, provided the
original author(s) and the copyright
owner(s) are credited and that the
original publication in this journal is
cited, in accordance with accepted
academic practice. No use,
distribution or reproduction is
permitted which does not comply with
these terms.

Case report: Novel FHR2 variants in atypical Hemolytic Uremic Syndrome: A case study of a translational medicine approach in renal transplantation

Emma Diletta Stea[1], Christine Skerka[2], Matteo Accetturo[1], Francesco Pesce[1], Thorsten Wiech[3], Andrea Hartman[2], Paola Pontrelli[1], Francesca Conserva[1], Giuseppe Castellano[1], Peter F. Zipfel[2,4]* and Loreto Gesualdo[1]

[1]Department of Emergency and Organ Transplantation, Nephrology and Urology Units, University of Bari Aldo Moro, Bari, Italy, [2]Department of Infection Biology, Leibniz Institute for Natural Product Research and Infection Biology, Jena, Germany, [3]Section of Nephropathology, Institute of Pathology, University Hospital Hamburg-Eppendorf, Hamburg, Germany, [4]Institute of Microbiology, Friedrich-Schiller-University, Jena, Germany

Atypical hemolytic–uremic syndrome (aHUS) is a severe thrombotic microangiopathy in which kidney involvement is common. aHUS can be due to either genetic or acquired abnormalities, with most abnormalities affecting the alternative complement pathway. Several genetic factors/alterations can drive the clinical presentation, therapeutic response, and risk of recurrence, especially recurrence following kidney transplantation. We report here the case of a 22-year-old man who developed a severe form of aHUS. Renal biopsy revealed thrombotic microangiopathy and features of chronic renal damage. Despite two eculizumab infusions, the patient remained dialysis dependent. Two novel rare variants, c.109G>A (p.E37K) and c.159 C>A (p.Y53*), were identified in the factor H-related 2 (*FHR2*) gene, and western blot analysis revealed a significant reduction in the level of FHR2 protein in the patient's serum. Although FHR2 involvement in complement 3 glomerulopathy has been reported previously, a role for FRH2 as a complement modulator has not yet been definitively shown. In addition, no cases of aHUS in individuals with *FHR2* variants have been reported. Given the role of FHRs in the complement system and the fact that this patient was a candidate for a kidney transplant, we studied the relevance of low FHR2 plasma levels through a set of functional *in vitro* assays. The aim of our work was to determine if low FHR2 plasma levels could influence complement control at the endothelial surface with a view to identifying a therapeutic approach tailored to this specific patient. Interestingly, we observed that low FHR2 levels in the patient's serum could induce complement activation, as well as C5b–9 deposition on human endothelial cells, and affected cell morphology. As C5b–9 deposition is a prerequisite for endothelial cell damage, these results suggest that extremely low FHR2 plasma levels increase the risk of aHUS. Given their ability to reduce

C5b–9 deposition, recombinant FHR2 and eculizumab were tested *in vitro* and found to inhibit hemolysis and endothelial cell surface damage. Both molecules showed effective and comparable profiles. Based on these results, the patient underwent a kidney transplant, and received eculizumab as induction and maintenance therapy. Five years after transplantation, the patient remains in good general health, with stable graft function and no evidence of disease recurrence. To our knowledge, this is first reported case of an aHUS patient carrying *FHR2* mutations and provides an example of a translational therapeutic approach in kidney transplantation.

KEYWORDS

complement associated kidney diseases, complement inhibition, Factor H related proteins, thrombotic microangiopathy, aHUS

Introduction

Atypical hemolytic–uremic syndrome (aHUS) is a systemic endotheliosis that is characterized by severe microangiopathy and renal failure, leading to uncontrolled activation of the alternative complement pathway (1, 2). The causes of this severe kidney disease are genetic abnormalities, mostly of complement genes, and acquired factors (autoantibodies), most of which affect the binding affinity of the central regulator, factor H, to the cellular surface. The imbalance between complement activators and regulators leads to enhanced lytic complement complex (C5b–9) deposition in the vasculature, primarily in glomerular blood vessels. Vascular damage drives kidney dysfunction (1–3) and, therefore, blockade of distal complement and of lytic C5b–9 is the major goal of current therapeutic approaches, for example with eculizumab or ravulizumab.

The specific or individual genetic background of patients with aHUS influences the subtle effects of complement action, thus affecting therapeutic responses, recurrence rates, and prognosis throughout the entire process of renal transplantation (4, 5). In transplant settings, some environmental triggers, such as ischemia–reperfusion injury, acute rejection, and immunosuppressive drugs, induce activation of the complement system and contribute to disease recurrence and graft loss (6).

The risk of aHUS recurrence on the allograft ranges from less than 20% to more than 90% depending on the patient's genetic background and the therapeutic strategy. Recipients with mutations in the genes encoding circulating complement factors [i.e., C3 (C3), factor H, factor I, factor B] have a higher risk of recurrence than patients with genetic variants encoding membrane and local modulators of the complement system, such as cluster of differentiation 46 (CD46) (6–8).

Zuber et al. (8, 9) suggested that patients with aHUS can be divided into three different categories according to the risk of post-transplant disease recurrence. Mutations in factor H, rearrangement in factor H/factor H-related (*FHR*) genes, gain of function mutations in C3 and complement factor B, and a previous history of aHUS recurrence were found to be associated with a high recurrence risk, and this was confirmed Kidney Disease Improving Global Outcomes (KDIGO) working group, which recommends the prophylactic use of eculizumab on the day of transplantation to prevent overactivation of the complement system (10). In these puzzle-like scenarios, the discovery of novel genes and of novel risk variants associated to aHUS is of high interest and significance. To determine the most appropriate therapeutic interventions in an individual patient, especially in a transplant setting, investigation of the exact genetic background, gene risk haplotypes, and autoimmune factors is extremely helpful, as the prophylactic use of eculizumab, ravulizumab, or plasma therapy remains at clinicians' discretion (10).

Here, we present the first case of a patient with aHUS carrying two novel *FHR2* gene variants and with severely reduced plasma levels of FHR2. Eberhardt et al. (11–13) have shown that FHR2, a novel complement modulator and inhibitor, inhibits C3 convertase and blocks C5b–9 assembly. However, the exact role of FHR2 in complement modulation, in particular how it interacts with other FHRs (i.e., multimer formation with FHR1 and FHR5) and with complement components, such as C3, the cleavage products C3b and C3d, and its involvement in aHUS pathogenesis are still unclear.

Faced with a patient who was a candidate for a kidney transplant, we performed a set of functional assays *in vitro* to determine if extremely low FHR2 plasma levels can influence complement activation and C5b–9 deposition on endothelial cellular surfaces, and, if so, whether or not these effects could be reversed by restoring FHR2 levels or by eculizumab. We then used the results of the *in vitro* assays to inform and formulate the best therapeutic approach for this specific patient. The *in vitro*

tests showed that extremely low plasma FHR2 levels can induce complement activation and enhance C5b–9 deposition on endothelial cells, suggesting that low FHR2 levels can form the basis for aHUS onset. Moreover, both recombinant FHR2 and eculizumab were able to control complement action in the patient's plasma, and to reduce endothelial C5b–9 deposition to a similar degree. Collectively, these findings allowed us to tailor induction therapy and maintenance therapy following kidney transplant. This translational approach, based on genetic testing, circulating complement profiling, and functional *in vitro* experiments, provides a novel framework that is useful to optimize the targeted treatment of complement dysfunction in the clinical setting.

Case report

A 24-year-old Caucasian man was referred to the nephrology unit for a pre-transplantation kidney evaluation. At the age of 22 years, the patient had been admitted to hospital following the sudden development of swelling of the face and legs, epistaxis, postural instability, chest pain, purpuric rush on both arms, and high blood pressure (180/90 mmHg). The patient reported flu-like symptoms without fever during the previous 2 weeks. Laboratory analysis revealed hemolytic anemia (i.e., hemoglobin 7.2 g/dl; schistocytes 10%, lactate dehydrogenase 1,724 U/l, haptoglobin < 0.08 g/l), thrombocytopenia (100×10^3/µl), severe kidney failure (creatinine 16.85 mg/dl), and low C3 plasma levels (0.5 g/l; normal range = 0.8–1.8 g/l) (Supplementary Table 1). ADAMTS13 (a disintegrin and metalloprotease with thrombospondin type 1 motifs 13) activity was more than 5% and the verocytotoxin-producing *Escherichia coli* test was negative. Kidney measurements on ultrasound were close to the lower limits of the reference values (i.e., right kidney longitudinal axis: 10.5 cm; left kidney length: 11 cm), with a normal cortical thickness. Of note was that the patient had no family history of thrombotic microangiopathy (TMA) or other kidney diseases, and reported good health. Laboratory analyses carried out before the onset of aHUS, when the patient was aged 6 years, showed normal kidney function and no urinary abnormalities.

Kidney biopsy revealed glomerular sclerosis, diffuse interstitial fibrosis (90%), tubular atrophy, and the vascular lesions typically associated with TMA. aHUS was diagnosed. Despite blood transfusions, hemodialysis, steroid treatment, and the administration of two doses of eculizumab (900 mg/week × 2 weeks) starting 1 month after hospitalization, the patient rapidly progressed to end-stage renal disease. Given the findings of kidney biopsy, eculizumab administration was discontinued and the patient remained dialysis dependent.

Genetics, western blot analysis, and complement assays

The screening of complement genes associated with aHUS was performed with next-generation sequencing using an in-house genetic panel, and confirmed by Sanger sequencing (see Supplementary Material). Significantly, the patient showed two novel variants in the *FHR2* gene: 1) a novel missense variant, c.109G>A, resulting in the exchange of E37 to K37; and, 2) a nonsense variant, c.159 C>A, which introduces a premature stop codon at position 53 (Figure 1B). Both c.109G>A and c.159 C>A affect the short consensus repeat domain (SCR) 1; neither is present in the Exome Variation Data Bank and neither was detected in a cohort of 60 healthy control subjects. No hybrid *FHR* genes or genomic deletions were detected by multiplex ligation-dependent probe amplification (MLPA) Supplementary Material.

Family studies revealed that the c.159 C>A variant introducing the stop codon was inherited from the patient's healthy father (the patient's healthy mother showed wild-type *FHR2*) and that the p.E37K exchange was a *de novo* variant (Figure 1B). These genetic variations affect FHR2 plasma levels. Western blot analysis revealed the absence of FHR2 in the patient's serum, in contrast to a normal human serum (NHS), and normal intensity and mobility of factor H (Figure 1A). On longer blot exposure, however, the two FHR2 bands could be identified in the patient's sample. Densitometry scan analysis revealed that FHR2 levels in the patient's plasma were about 5% of those in NHS (Figure 1A). FHR1, FHR3, FHR4, and FHR5 levels were comparable to those of NHS (data not shown).

Functional *in vitro* tests

Considering the possibility of a kidney transplant, we then performed a set of functional assays *in vitro* to investigate the impact of FHR2 variations on catabolite activator protein Complement Alternative Pathway (CAP) modulation and to define the specific therapeutic approach for our patient.

High levels of the complement activation fragments C3a, Ba, and sC5b–9 were detected in the patient's serum, suggesting CAP activation (Supplementary Material and Supplementary Figures 1A–C). To investigate this further, we used a guinea pig model to measure the degree of hemolysis induced by adding different concentrations (i.e. 2.5%, 5%, 7.5%, and 10%) of fresh patient serum (HS#2337) or NHS to guinea pig blood *in vitro* (methods described in Supplementary Material). The patient's serum induced more erythrocyte lysis (33%, 39%, 41%, and 56%) than NHS (11%, 22%, 24%, and 30%), confirming CAP activation. The effect was dose dependent, and differences at

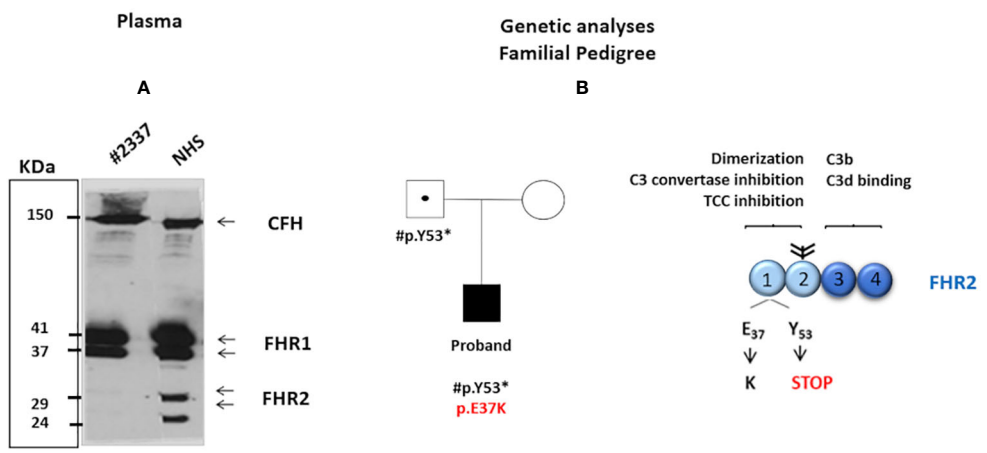

FIGURE 1
(A) Western blot analysis was carried out under non-reducing conditions with polyclonal anti-complement factor H-related protein 1 (FHR1). The intensity of FHR2 was much lower (around 5%) in the patient's serum than in NHS = 100%. The positions of the two FHR2 isoform are indicated. In contrast, the intensity of complement factor H and of FHR1 appears similar in both the patient's serum and NHS. **(B)** The patient's family pedigree. The proband (filled symbol) carries two rare novel variants in the SCR1 of FHR2: a *de novo*p.E37K missense variant (shown in red) and p.Y53* (inherited from the patient's father). The father is a healthy carrier of p.Y53* (dotted symbol). The patient's mother presents no variants in FHR2 (open symbol). The structure of the FHR2 protein is shown. FHR2 is composed of four SCRs. SCRs 1 and 2 (light blue) are involved in dimer formation, C3 convertase inhibition, and terminal complement component blocking. In contrast, SCRs 3 and 4 (dark blue) bind C3b and the C3d. Two FHR2 molecules form a dimer through their N-terminal SCRs. Attached carbohydrates are indicated in black.

serum concentrations of 2.5%, 5%, and 10% were statistically significant (Figure 2A).

Next we investigated the role of a low plasma level of FHR2 in the modulation of the alternative pathway, testing whether the addition of FHR2 to active HS#2337 restores the hemolytic effect. The hemolytic assay was repeated, incubating 5% patient serum with increasing amounts of recombinant FHR2 (from 0 to 280 ng). The negative control was 5% NHS. When recombinant FHR2 was

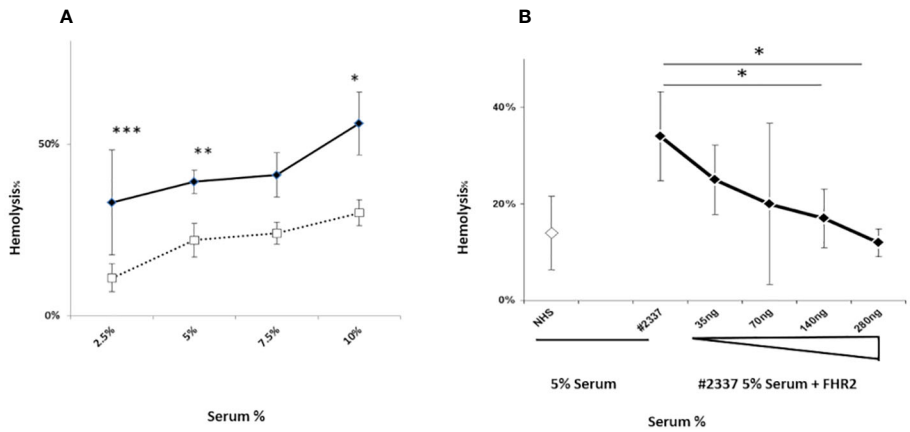

FIGURE 2
A FHR2 defect results in activation the complement alternative pathway. **(A)** Lysis of guinea pig erythrocytes. Guinea pig erythrocytes were incubated with increasing concentrations (2.5%, 5%, 7.5%, or 10%) of patient serum HR#2337 (filled rhombus) or NHS (open square). Lysis was determined by measuring the absorbance of released hemoglobin at 414 nm. The patient's serum induced more erythrocyte lysis (33%, 39%, 41%, and 56%) than NHS (11%, 22%, 24%, and 30%). The difference was statistically significant at serum concentrations of 2.5%, 5%, and 10%. The results are mean ± standard deviation (SD) of three independent experiments. $*p < 0.05$, $**p < 0.01$, $***p < 0.001$. **(B)** Guinea pig erythrocytes were incubated with 5% NHS (open rhombus) or 5% HR#2337 serum (filled rhombus) alone or enriched with increasing amounts (35 ng, 70 ng, 140 ng, or 280 ng) of recombinant FHR2. The addition of recombinant FHR2 reduced erythrocyte lysis from 34% to 12%. The results are mean ± SD of three independent experiments. $*p < 0.05$.

added to the HS#2337, erythrocytes lysis was reduced from 34% to 12%, suggesting a role for FHR2 as a surface regulator of the alternative pathway (Figure 2B). The effect was dose dependent, and the lytic activity of the patient's serum was fully restored by the addition of 140–280 ng of FHR2. As the systemic endotheliosis induced by a high level of C5b–9 cell deposition represents a milestone in the pathogenesis of aHUS, we evaluated C5b–9 deposition using human umbilical vein endothelial cells (HUVECs) incubated with patient serum and with NHS, using confocal microscopy and flow cytometry (methods described in Supplementary Material).

As shown in Figure 3A, C5b–9 fluorescence was intense and diffuse on endothelial cells exposed to HS#2337, was minimal on cells incubated with NHS, and was absent on cells incubated with phosphate-buffered saline. Moreover, HUVECs incubated with 30% HS#2337 presented a loss of the typical shape, and their usual morphology was lost (Figure 3D).

The results were confirmed by flow cytometry. Endothelial cells exposed to 30% patient's serum showed a C5b–9 signal 2-fold higher than that observed when incubating the cells with NHS [mean fluorescence intensity (MFI) express in percentage: HS#2337, 554; NHS, 208] (Figures 3B, C). The difference was statistically significant ($p \leq 0.05$). As low FHR2 levels reduce complement regulation, causing more C5b–9 deposition, we carried out an assay to determine whether or not recombinant FHR2 was able to reverse the strong C5b–9 deposition induced by HS#2337. To this end, HUVECs were incubated with 30% patient serum to which increasing amounts of recombinant FHR2 (from 0 to 280 ng) were added, and C5b–9 signaling was evaluated by flow cytometry. *In vitro* addition of FHR2 to HS#2337 reduced HUVECs C5b-9 deposition in a dose-dependent manner. When FHR2 was used at a concentration of 280ng, C5b-9 signaling on HUVECs was completely lost (MFI: HS#2337, 1017; HS#2337 + 280 ng FHR2, 442) (Figures 4A, B). Thus, adding FHR2 to the patient's serum restored the complement modulation *in vitro*, re-establishing the physiological state.

Considering the poor response to eculizumab during aHUS onset, we also assayed whether or not the C5-blocking complement inhibitor can also effectively reduce the high C5b–9 levels observed in the patient's serum. Therefore, an increasing amount of eculizumab (increasing from 0 to 52 ng) was added *in vitro* to 20% HS#2337. C5b–9 levels were then measured by ELISA. *In vitro*, the drug blocked the C5b–9 generation in the plasma of our patient in a dose-dependent manner, confirming its efficacy in this unique scenario (Figure 4D).

Finally, we compared FHR2 and eculizumab efficacy in regulating HS#2337-induced C5b–9 deposition. HUVECs were incubated with HS#2337, with HS#2337 plus FHR2 (280 ng), and with HS#2337 plus eculizumab (35 ng). C5b–9 signaling was then evaluated by confocal microscopy (Figure 4C). Interestingly, eculizumab and FHR2 reduced C5b–9 deposition on endothelial cells in a similar manner (Figure 4C), thus offering potential future therapeutic opportunities.

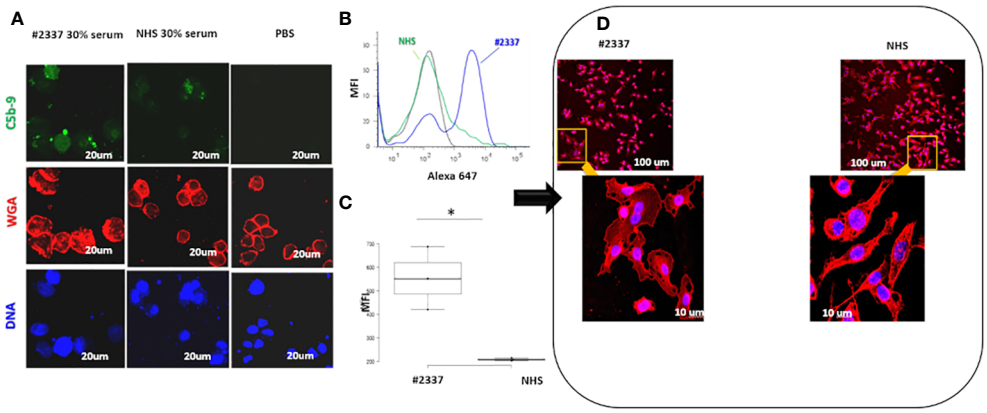

FIGURE 3
Low serum FHR2 levels result in enhanced C5b–9 deposition on HUVECs, modifying cell morphology. **(A)** HUVECs incubated with 30% HS#2337 (Laser Scanning Microscopy, LSM) showed greater deposition of C5b–9 (green fluorescence) than cells that were incubated with 30% NHS. Nuclei were stained with 4′,6-diamidino-2-phenylindole (DAPI) (blue fluorescence). The intact membrane was stained with wheat germ agglutinin Texas Red (WGA) (red fluorescence). Scale bar, 20um. A result representative of three independent experiments is shown. **(B)** Fluorescence-activated cell sorting (FACS) confirmed the results obtained with LSM. HUVECs incubated with 30% patient serum lacking FHR2 showed greater C5b–9 deposition than HUVECs incubated with NHS. MFI, mean fluorescence intensity. **(C)** The boxplot displays the Mean Fluorescence Intensity (MFI) of HUVEC incubated with either the patient's serum (white) or NHS serum (grey). Data for the triplicate experiments is shown. *$p < 0.05$. **(D)** HUVECs were incubated with HS#2337 or NHS. Cell morphology was determined by examination of WGA fluorescence using Laser scanning microscopy. Cells exposed to HS#2337 are retracted, losing their typical extended shape, and have more intracellular inclusions. Scale bar 100 µm and 10 µm.

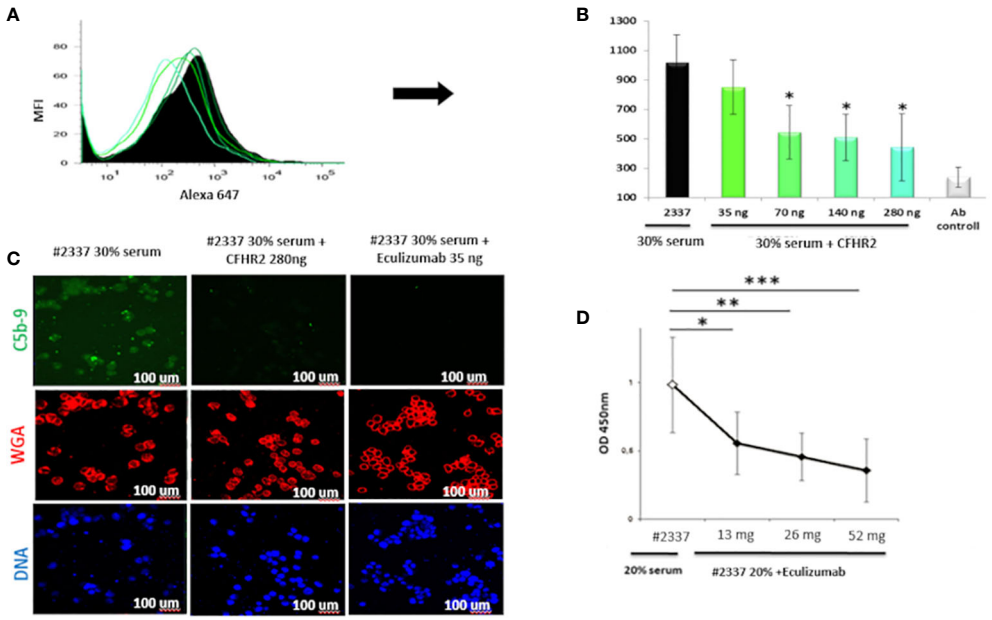

FIGURE 4
Recombinant FHR2 and eculizumab block C5b−9 deposition by HS#2337. **(A, B)** Endothelial cells were incubated with HS#2337 (30%) for 30 minutes. An increasing amount of recombinant FHR2 was added to HS#2337 serum and C5b−9 signaling was examined by flow cytometry. Antibody (Ab) control represents no interaction. The recombinant FHR2 reduced, in a dose-dependent manner, C5b−9 deposition on HUVECs, and this reduction was statistically significant at 70 ng, 140 ng, and 280 ng of FHR2. MFI, mean fluorescence intensity. The results are mean ± standard deviation (SD) of three independent experiments. **(C)** The effects of eculizumab and FHR2 on C5b−9 deposition was compared by laser scanning microscopy. HUVECs were incubated with 30% HS#2337serum, with 30% HS#2337serum premixed with 280 ng of FHR2 and with 30% HS#2337 serum premixed with eculizumab (35 ng). C5b−9 deposition was evaluated using the monoclonal C5b−9 antibody. **(D)** Increasing amounts of eculizumab (from 0 to 52ng) were added to 20% HS#2337, and the effect on C5b−9 generation was evaluated by ELISA. Eculizumab significantly reduced C5b−9 generation. The effect is dose dependent. Results represent mean ± SD of three independent experiments (see Supplementary Material for more details). Eculizumab and FHR2 reduced C5b−9 deposition (green fluorescence) on endothelial cells to a similar degree. Nuclei were stained with 4′,6-diamidino-2-phenylindole (DAPI) (blue fluorescence). Intact membrane was stained with wheat germ agglutinin Texas Red (WGA) (red fluorescence). Scale bar, 100 µm. The result is representative of three independent experiments. *$p < 0.05$, **$p < 0.01$, ***$p < 0.001$.

Personalized treatment strategy and patient outcome

Following 23 months of hemodialysis, the patient underwent a kidney transplant at the University Hospital of Bari (Italy), receiving a cadaveric graft from a standard criteria donor. Two (A11, B18) of six antigens were mismatched, four (A24, B35, DR11, DR14) of six human leucocyte antigens were matched, no donor-specific antibodies were detected, and the panel-reactive antibody positivity was 0% (Supplementary Table 1).

Based on the patient's clinical history and genetic background, and the results of the *in vitro* assays, we defined a tailor-made therapeutic strategy. Before surgery, the patient received a single plasma exchange, thymoglobulin infusion, steroids, and one dose of eculizumab (900 mg) to confer a high level of graft protection. During the post-transplant phase, steroids were gradually reduced, and plasma exchange was replaced by plasma infusion, which was administered as thymoglobulin for 6 days. This therapeutic scheme allowed the introduction of calcineurin inhibitors (i.e., tacrolimus 0.1 mg/kg) 4 days after the transplant, attenuating the endothelial damage, coupled with mycophenolate (Supplementary Figure 2). Complement analysis of the patient's serum (on the 10th day post transplant) showed low levels of activation of fragments C3a, Ba, and sC5b–9, confirming the *in vivo* efficacy of this therapeutic approach (Supplementary Figure 3). Eculizumab was administered weekly for 3 weeks, and then every 2 weeks for 2 months. Given the early graft function, the absence of organ rejection, and the absence aHUS recurrence, the administration of eculizumab was suspended 2 months after transplantation, and the patient was closely monitored with regular follow-up visits. During the 5 years of follow-up, no signs of hemolysis, kidney graft dysfunction, or proteinuria were detected (Supplementary Table 2).

Discussion

Kidney transplantation in patients with aHUS is associated with poor outcomes due to high recurrence rates and graft loss. The genetic background has a strong influence on the natural

history of the disease (6–8). The KDIGO working group recommends the prophylactic use of eculizumab in the management of patients with aHUS who receive a kidney transplant and carry pathogenic or gain-of-function gene mutations (10). However, the graft outcome in transplanted patients with aHUS carrying novel variants, especially in emerging genes, is unpredictable, thus hampering our ability to optimize immunosuppressive therapy.

Our patient developed a severe form of aHUS after an upper respiratory infection, which is hypothesized to be the disease trigger. Unfortunately, eculizumab was administered 1 month following disease onset and, thus, therapy initiation was significantly delayed. Moreover, owing to the chronicity aspect of kidney chronocity, clinicians decided to administer only two doses of eculizumab.

Unusually, the patient described in this study carries two novel rare variants of the *FHR2* gene, and these were associated with a reduction in plasma concentration of the protein. FHR2 is a dimeric plasma protein that is composed of four SCRs, with high sequence similarity to FH, FHR1, and FHR5 (14). Eberhardt et al. (11) showed that FHR2 inhibits C3 convertase and blocks C5b–9 assembly through its N-terminal domain (SCR 1–2), which is also involved in dimer formation. Despite these findings, the exact role of FHR2 in complement modulation and aHUS pathogenesis is still under investigation, presenting an open challenge for scientists and clinicians. Our patient presented a heterozygous *de novo* missense FHR2 variant, inherited from his father, which results in amino acids exchanges in SCR1 (i.e., E37 to K37) and the introduction of a premature stop codon (c.159C> G; p.Y53*) in SCR1. These variants are located within the N-terminal domain, which mediates FHR2 dimerization and inhibition of C5b–9 assembly, suggesting an important impact on protein function (11). Moreover, p.Y53*, which corresponds to p.Y35* in the protein nomenclature without signal peptide, is located in the highly conserved first N-terminal domain of FHR2, between the residues Tyr34 and Ser36, with the nearby residue Tyr39 being critical in dimer stability (15).

The macroscopic gene rearrangement of *FHR2* with FHR1 and FHR5 has been linked to C3 glomerulopathy in three familial cases because of the expression of aberrant hybrid plasma proteins able to overactivate the CAP (16–18). In our patient with aHUS, MLPA excluded the presence of copy number variations in the *FHR2* and in the *FHR*s gene family. In addition, western blot analysis did not reveal the presence of hybrid proteins, but only a level for FHR2, suggesting the possibility of a different pathogenic scenario.

The patient also exhibited overactivation of the initial and final step of the CAP pathway, shown by low C3 plasma levels and increased serum amounts of complement activation fragments Ba, C3a, and sC5b–9. The functional impact of this FHR2 defect on CAP activation was studied using both the patient's serum and the FHR2 recombinant protein. FHR2 serum deficiency is linked to high CAP activation, and this was revealed by a higher degree of erythrocytes lysis in the patient's sample than in NHS. Moreover, the addition of increasing amounts of recombinant FHR2 to the patient serum gradually restored the complement control, suggesting a role of FHR2 in CAP modulation, especially on the cell surface.

It is well known that complement deregulation in endothelial cells plays a crucial role in aHUS pathogenesis. Large amounts of the terminal product of the complement cascade (C5b–9) on endothelial cells cause cell death and unmask prothrombotic agents, favoring TMA development (19). In our study, the patient's FHR2-deficient serum induced a higher level of C5b–9 deposition on HUVECs than did NHS, leading to morphological changes in the cells. The addition of CFHR2 to the serum of our patient significantly reduced C5b–9 deposition on HUVECs in a dose-dependent manner, re-establishing complement control. Indeed, FHR2 acts a complement surface regulator, possibly supporting CFH inhibitory role during complement activation.

When it became apparent that our patient would need to undergo kidney transplantation, we evaluated the opportunity to administer a C5b-blocking complement inhibitor. Thus, we investigated the effect of eculizumab on C5b–9 serum levels and deposition of C5b–9 on cells. Through a series of different *in vitro* assays, we demonstrated that eculizumab was effective in reducing C5b–9 signaling in this specific patient with FHR2 deficiency, as demonstrated through ELISAs and observation of HUVECs incubated with the patient's serum. Interestingly, eculizumab and the recombinant FHR2 showed a comparable effect on controlling the complement system, indicating their potential benefits for the treatment of these patients.

Based on the results of these biological tests, we decided to prophylactically administer eculizumab plus plasma therapy before the transplant surgery (20). The prophylactic use of combined eculizumab plus plasma therapy has been reported in a small number of transplant patients with severe aHUS with a severe phenotype, but further studies in larger cohorts are needed to confirm its utility in preventing disease recurrence and graft loss in this group of patients (10, 21).

Plasma therapy was administered for 6 days after transplantation, whereas eculizumab was used for 2 months to confer a higher protection from complement activation. The discontinuation of eculizumab is debated, and depends on genetic variants, clinical history, and laboratory tests (22). Although two trials have recently shown the usefulness of eculizumab administration for 2 years in patients with aHUS (23), there is no clear evidence on the best timing for discontinuation, especially after kidney transplantation. The time frame for aHUS post-transplant recurrence ranges from 3 days to 6 years, with a median of 2 months. Here, we successfully discontinued eculizumab therapy 2 months after transplantation. At 5 years' follow-up, the patient showed normal graft function and no signs of disease recurrence

(Supplementary Table 2). Short-term preventive eculizumab therapy with plasma infusions was administered based on the results of specific laboratory tests, described above, and these tests (not available routinely) allowed us to set up a tailor-made treatment protocol in a patient carrying an unknown gene variant.

In summary, we reported the first case of aHUS in a patient with a genetic defect within FHR2 that seems associated with very low plasma level of this protein. We successfully transplanted the patient using personalized induction and maintenance therapy. Moreover, the analyses carried out in this index clinical case allowed us to investigate in depth the role of the FHR2 surface complement regulator, and to demonstrate that loss of/reduction in this factor may contribute to the pathogenesis of aHUS. This unique patient provides an example of the application of a translational medicine framework that could be useful in managing patients with aHUS carrying novel genetic variants of unknown significance, with the aim of defining the best therapeutic strategy in those undergoing kidney transplantation.

Data availability statement

The original contributions presented in the study are included in the article/Supplementary Material. Further inquiries can be directed to the corresponding author.

Ethics statement

Ethics review and approval were not required for the study on human participants in accordance with the local legislation and institutional requirements. The patients/participants provided their written informed consent to participate in this study. Written informed consent was obtained from the individual(s) for the publication of any potentially identifiable images or data included in this article.

Author contributions

ES collected the data, created the figures, and drafted the manuscript with PFZ and CS. ES carried out the experiments with support from AH. MA, PP, FC and GC supported the genetic analysis and the collection of clinical and biological materials. FC provided linguistic and scientific support during revision. TW provided the kidney biopsy and supported the experimental project design. FP revised all statistical analyses and helped draft the manuscript. PFZ and LG supervised the project. All authors discussed the results and contributed to the final manuscript. LG, GC, and ES defined the therapeutic strategy for patient #2337 during the kidney transplantation. All authors contributed to the article and approved the submitted version.

Funding

PFZ and TW received funding by the Collaborative Reserch Center CRC 1192, by the Deutsche Forschungsgemeinschaft. PFZ received support from KIDNEEDS Iowa, USA. ES was supported by a scholarship from the Società Italiana di Nefrologia (Rome, Italy).

Acknowledgments

We thank the patient and his family for participating in the study and for contributing valuable specimens. We thank Monika von der Heide, Hans-Martin Dahse, and Ina Löschmann (Department of Infection Biology, Leibniz Institute for Natural Product Research and Infection Biology, Jena, Germany) for excellent technical support.

Conflict of interest

The authors declare that the research was conducted in the absence of any commercial or financial relationships that could be construed as a potential conflict of interest.

Publisher's note

All claims expressed in this article are solely those of the authors and do not necessarily represent those of their affiliated organizations, or those of the publisher, the editors and the reviewers. Any product that may be evaluated in this article, or claim that may be made by its manufacturer, is not guaranteed or endorsed by the publisher.

Supplementary material

The Supplementary Material for this article can be found online at: https://www.frontiersin.org/articles/10.3389/fimmu.2022.1008294/full#supplementary-material

References

1. Noris M, Remuzzi G. Glomerular diseases dependent on complement activation, including atypical hemolytic uremic syndrome, membranoproliferative glomerulonephritis, and C3 glomerulopathy: Core curriculum. *Am J Kidney Dis* (2015) 66(2):359–75. doi: 10.1053/j.ajkd.2015.03.040

2. Nester CM, Barbour T, De Cordoba SR, Dragon-Durey MA, Fremeaux-Bacchi V, Goodship TH, et al. Atypical aHUS: State of the art. *Mol Immunol* (2015) 67(1):31–42. doi: 10.1016/j.molimm.2015.03.246

3. Kerr H, Richards A. Complement-mediated injury and protection of endothelium: lessons from atypical haemolytic uraemic syndrome. *Immunobiology* (2012) 217(2):195–203. doi: 10.1016/j.imbio.2011.07.028

4. Noris M, Capriolo J, Bresin E, Mossali C, Pianetti G, Gamba S, et al. Relative role of genetic complement abnormalities in sporadic and familial aHUS and their impact on clinical phenotype. *Clin J Am Soc Nephrol* (2010) 5(10):1844–59. doi: 10.2215/CJN.02210310

5. Wong EKS, Goodship THJ, Kavanagh D. Complement therapy in atypical haemolytic uraemic syndrome (aHUS). *Mol Immunol* (2013) 56(3):199–212. doi: 10.1016/j.molimm.2013.05.224

6. Bresin E, Daina E, Noris M, Castelletti F, Stefanov R, Hill P, et al. International registry of recurrent and familial HUS/TTP. outcome of renal transplantation in patients with non-shiga-toxin-associated hemolytic uremic syndrome: Prognostic significance of genetic background. *Clin J Am Soc Nephrol* (2006) 1:88–99. doi: 10.2215/CJN.00050505

7. Duineveld C, Verhave JC, Berger SP. Living donor kidney transplantation in atypical hemolytic uremic syndrome: A case series. *Am J Kidney Dis* (2017) 70:770–7. doi: 10.1053/j.ajkd.2017.06.024

8. Zuber J, Le Quentrec M, Krid S, Bertoye C, Gueutin V, Lahoche A, et al. Eculizumab for atypical hemolytic uremic syndrome recurrence in renal transplantation. *Am J Transplant* (2012) 12:3337–54. doi: 10.1111/j.1600-6143.2012.04252.x

9. Zuber J, Fakhouri F, Roumenina LT. Use of eculizumab for atypical haemolytic uraemic syndrome and C3 glomerulopathies. *Nat Rev Nephrol* (2012) 8:643–57. doi: 10.1038/nrneph.2012.214

10. Goodship TH, Cook HT, Fakhouri F, Fervenza FC, Frémeaux-Bacchi V, Kavanagh D, et al. Atypical hemolytic uremic syndrome and C3 glomerulopathy: Conclusions from a "Kidney disease: Improving global outcomes" (KDIGO) controversies conference. *Kidney Int* (2017) 91:539–51. doi: 10.1016/j.kint.2016.10.005

11. Eberhardt HU, Buhlmann D, Hortschansky P, Chen Q, Böhm S, Kemper MJ, et al. Human factor h-related protein 2 (CFHR2) regulates complement activation. *PloS One* (2013) 8(11):e78617. doi: 10.1371/journal.pone.0078617

12. Skerka C, Moulds JM, Taillon-Miller P. The human factor h-related gene 2 (FHR2): structure and linkage to the coagulation factor XIIIb gene. *Immunogenetics* (1995) 42(4):268–74. doi: 10.1007/bf00176444

13. Skerka C, Chen Q, Fremeaux-Bacchi V. Complement factor h related proteins (CFHRs). *Mol Immunol* (2013) 56(3):170–80. doi: 10.1016/j.molimm.2016.07.007

14. Zipfel PF, Wiech T, Stea ED. CFHR gene variations provide insights in the pathogenesis of the kidney diseases atypical hemolytic uremic syndrome and C3 glomerulopathy. *J Am Soc Nephrol* (2020) 31(2):241–56. doi: 10.1681/asn.2019050515

15. Goicoechea de Jorge E, Caesar JJE, Malik TH, Patel M, Colledge M, Johnson S, et al. Dimerization of complement factor h-related proteins modulates complement activation. *Vivo Proc Natl Acad Sci U S A*. (2013) 110(12):4685–90. doi: 10.1073/pnas.1219260110

16. Xiao X, Ghossein C, Tortajada A, Zhang Y, Meyer N, Jones M, et al. Familial C3 glomerulonephritis caused by a novel CFHR5-CFHR2 fusion gene. *Mol Immunol* (2016) 77:89–96. doi: 10.1016/j.molimm.2016.07.007

17. Sugawara Y, Kato H, Yoshida Y, Fujisawa M, Kokame K, Miyata T, et al. Novel CFHR2-CFHR1 hybrid in C3 glomerulopathy identified by genomic structural variation analysis. *Kidney Int Rep* (2019) 4(12):1759–62. doi: 10.1016%2Fj.ekir.2019.09.008

18. Chen Q, Wiesener M, Eberhardt HU, Hartmann A, Uzonyi B, Kirschfink M, et al. Complement factor h-related hybrid protein deregulates complement in dense deposit disease. *J Clin Invest* (2014) 124(1):145–55. doi: 10.1172/jci71866

19. Noris M, Galbusera M, Gastoldi S, Macor P, Banterla F, Bresin E, et al. Dynamics of complement activation in aHUS and how to monitor eculizumab therapy. *Blood* (2014) 124(11):1715–26. doi: 10.1182/blood-2014-02-558296

20. Gonzalez Suarez ML, Thongprayoon C, Mao MA. Outcomes of kidney transplant patients with atypical hemolytic uremic syndrome treated with eculizumab: A systematic review and meta-analysis. *J Clin Med* (2019) 8:919. doi: 10.3390/jcm8070919

21. Siedlecki AM, Isbel M, Walle V. Eculizumab use for kidney transplantation in patients with a diagnosis of atypical hemolytic uremic syndrome. *Kidney Int Rep* (2019) 4:434–46. doi: 10.1016/j.ekir.2018.11.010

22. Sethi S, Fervenza FC. Membranoproliferative glomerulonephritis–a new look at an old entity. *New Engl J Med* (2012) 366:1119–31. doi: 10.1056/NEJMra1108178

23. Laurence J. Defining treatment duration in atypical hemolytic uremic syndrome in adults: A clinical and pathological approach. *Clin Adv Hematol Oncol* (2020) 18(4):221–30.

frontiers | Frontiers in Physiology

TYPE Review
PUBLISHED 17 November 2022
DOI 10.3389/fphys.2022.1012112

Check for updates

OPEN ACCESS

EDITED BY
David Sebastián,
Institute for Research in Biomedicine,
Spain

REVIEWED BY
Juliana Camacho-Pereira,
Federal University of Rio de Janeiro,
Brazil
Sergio Rius-Pérez,
University of Valencia, Spain

*CORRESPONDENCE
Junnian Zheng,
jnzheng@xzhmu.edu.cn
Hui Tian,
huitian@xzhmu.edu.cn

†These authors have contributed equally to this work

SPECIALTY SECTION
This article was submitted to Mitochondrial Research, a section of the journal Frontiers in Physiology

RECEIVED 15 August 2022
ACCEPTED 02 November 2022
PUBLISHED 17 November 2022

CITATION
Wang Q, Chai D, Sobhani N, Sun N, Neeli P, Zheng J and Tian H (2022), C1QBP regulates mitochondrial plasticity to impact tumor progression and antitumor immune response. *Front. Physiol.* 13:1012112. doi: 10.3389/fphys.2022.1012112

COPYRIGHT
© 2022 Wang, Chai, Sobhani, Sun, Neeli, Zheng and Tian. This is an open-access article distributed under the terms of the Creative Commons Attribution License (CC BY). The use, distribution or reproduction in other forums is permitted, provided the original author(s) and the copyright owner(s) are credited and that the original publication in this journal is cited, in accordance with accepted academic practice. No use, distribution or reproduction is permitted which does not comply with these terms.

C1QBP regulates mitochondrial plasticity to impact tumor progression and antitumor immune response

Qiping Wang[1†], Dafei Chai[2†], Navid Sobhani[2], Nan Sun[3,4,5], Praveen Neeli[2], Junnian Zheng[4,5]* and Hui Tian[3,4,5]*

[1]Jiangyin Clinical Medical College, Jiangsu University, Jiangyin, Jiangsu, China, [2]Department of Medicine, Baylor College of Medicine, Houston, TX, United States, [3]Cancer Institute, Xuzhou Medical University, Xuzhou, Jiangsu, China, [4]Center of Clinical Oncology, Affiliated Hospital of Xuzhou Medical University, Xuzhou, Jiangsu, China, [5]Jiangsu Center for the Collaboration and Innovation of Cancer Biotherapy, Cancer Institute, Xuzhou Medical University, Xuzhou, Jiangsu, China

Mitochondrial plasticity including mitochondrial dynamics, metabolic flexibility, and mitochondrial quality control, impact tumor cells' progression and determine immune cells' fate. Complement C1q binding protein (C1QBP) plays an indispensable role through regulating mitochondrial morphology, metabolism, and autophagy. C1QBP promotes mitochondrial plasticity to impact tumor metastasis and their therapeutic response. At the same time, C1QBP is involved in regulating immune cells' maturation, differentiation, and effector function through the enhancement of mitochondrial function. In this regard, manipulation of C1QBP has been shown to adjust the competitive balance between tumor cells and immune cells. In the course of evolution, mitochondrial plasticity has endowed numerous advantages against the relentless microenvironment of tumors. In this current review, we summarize the current knowledge of the mechanism of C1QBP regulation of cancer and immunity. We explain this process in vision of potentially new anticancer therapies.

KEYWORDS

C1QBP, mitochondrial plasticity, metabolic flexibility, tumor progression, antitumor immune response, immunotherapy

Introduction

Mitochondria can rapidly sense energy availability and generate precursors necessary for the biosynthesis of amino acids, lipids, and nucleotides to meet cellular requirements or respond to adverse cellular stimulation (Mishra and Chan, 2016; Ahola et al., 2019). Most importantly, mitochondria function as the hub of numerous signal pathways, including the tricarboxylic acid (TCA) cycle, oxidative phosphorylation (OXPHOS), and fatty acid oxidation (FAO), which endow cells with the considerable adaptation to face a variety of challenging stresses (Vyas et al., 2016; Schvartzman et al., 2018).

Complement C1q binding protein (C1QBP), also known as p32 or hyaluronic acid-binding protein (HABP1), is a multicompartmental protein. In other words, C1QBP exists in multiple subcellular compartments, including the nucleus, endoplasmic reticulum, Golgi, and on the cell surface (Ghebrehiwet et al., 2001; Fogal et al., 2008). For example, C1QBP located on the cell surface interacts with tumor homing peptide, Lyp-1, which specifically recognizes an epitope in tumor cells (Fogal et al., 2008). Moreover, it binds with the pre-mRNA splicing factor (SF2/ASF) in the nucleus, which controls RNA splicing by sequestering an essential RNA splicing factor into an inhibitory complex (Petersen-Mahrt et al., 1999). However, increasing evidence has demonstrated that C1QBP predominantly resides in the mitochondria through its 33-residue N-terminal mitochondria-targeting signal (MTS) sequence and is essential for embryonic development, which is dependent on mitochondrial translation and OXPHOS (Muta et al., 1997; Fogal et al., 2010; Yagi et al., 2012; Zhai et al., 2021). It has been reported that *C1qbp* deletion induces embryos' mid-gestation lethality and triggers severe dysfunction of the mitochondrial respiratory chain due to failure of mitochondrial protein synthesis. The association of C1QBP with mitochondrial RNA and mitochondrial ribosomes is required for some mitochondrial protein translation. Besides, C1QBP is also involved in mitochondrial autophagy to remove the dysfunctional mitochondria to maintain healthy cellular homeostasis (Jiao et al., 2015; Jiao and You, 2016). Consequently, C1QBP is integral to mitochondrial fitness, cell metabolism, and survival.

Given that tumor cells and T cells share the metabolic similarities of proliferation, expansion as well as activation, manipulation of mitochondrial plasticity would impact the metabolic competition between tumor cells and T cells in the context of the tumor microenvironment (TME). Tumor cells depend on C1QBP for progression and therapeutic resistance, while immune cells also depend on it for a persistent and powerful antitumor response. This review discusses the dual roles of C1QBP for mitochondrial function in tumor malignancy and immune cells. Finally, we give our expert opinion on potential new mitochondrial-dependent immune stimulation mechanism based-therapies targeting C1QBP.

Complement C1q binding protein modulation of mitochondrial plasticity

Mitochondria are highly dynamic organelles constantly undergoing fission and fusion. When they are too damaged, they go through mitophagy, which is the selective degradation of mitochondria by autophagy. It has been elucidated that C1QBP plays a vital role in maintaining mitochondrial homeostasis through regulating mitochondrial morphology, metabolism, and mitophagy. Thereby this protein is fundamental for modulating mitochondrial plasticity and fitness.

Complement C1q binding protein regulates mitochondrial morphology

Mitochondria undergo constant fission and fusion cycles according to the cellular bioenergetic situation. This fine-tuning of mitochondria is vital to give cells the optimal energy supply and survival. The mitochondrial architecture principally consists of optical atrophy 1 (OPA1), mitofusin 1/2 (Mfn1/2), the mitochondrial fission controlled by dynamin-related protein 1 (Drp1), and its mitochondrial adaptor fission protein 1 (Fis1) (Santel and Fuller, 2001; Chen and Chan, 2005; Loson et al., 2013).

C1QBP modulates mitochondrial morphology and integrity. *C1qbp* silencing not only promoted mitochondrial fragmentation but also repressed mitochondrial fusion (Fogal et al., 2010; Li et al., 2011; Hu et al., 2013; Noh et al., 2020). For example, Solhee Noh et al. found that genetic ablation of *C1QBP* activates the overlapping activity with m-AAA protease (OMA1) to cleave OPA1, which leads to mitochondrial fragmentation and swelling (Noh et al., 2020). C1QBP regulated mitochondrial morphology by regulating OMA1-dependent proteolytic processing of OPA1. On the other hand, MengJie Hu et al. revealed that overexpression of C1QBP increased mitochondrial fibrils (Hu et al., 2013). At the same time, C1QBP siRNA-treated cells contained predominantly small spherical mitochondria compared with the mainly normal elongated mitochondria in control cells. To further explore the underlying mechanism, they examined the expression of *Mfn1, Mfn2,* and mitochondrial *Drp-1* and found that the C1QBP siRNA treatment resulted in a detectable loss of *Mfn1* and *Mfn2* and decreased Drp-1 levels. Here, siRNA-mediated *C1qbp* knockdown induced a more punctate mitochondrial morphology, which was associated with the reduction of the mitochondrial fusion mediator proteins, a sign of potential subsequent degradation.

Complement C1q binding protein is involved in mitochondrial metabolism

Some tumor cells significantly depend on mitochondrial-mediated oxidative phosphorylation (Funes et al., 2007; Moreno-Sanchez et al., 2007). Since oxidative metabolism may recycle lactate, mitochondrial metabolism is advantageous for tumor cells that are highly glycolytic (Sonveaux et al., 2008). Moreover, glycolytic pathway oncogenes may upregulate some genes encoding mitochondrial proteins or those involved in mitochondrial biogenesis (Li et al., 2005). Additionally, mitochondria regulate cellular bioenergetic and biosynthetic processes of important cancer signaling pathways, such as

proliferation, metastasis and self-renewal (Viale et al., 2014; Liu and Shi, 2020). Collectively, these findings suggest that oncogene-driven glycolytic metabolism should be balanced, at least in part, by concomitant changes to mitochondria. Mitochondrial metabolism may potentiate cellular plasticity and metabolic flexibility to deal with the relentless microenvironment.

C1QBP plays an indispensable role in mitochondrial function and metabolic regulation. For example, *C1qbp*-deficient mouse embryonic fibroblasts (MEFs) cells exhibit reduced OXPHOS function (Yagi et al., 2012). A mutation of *C1qbp* has also been suggested as a cause of mitochondrial respiratory chain disorder. In this regard, C1QBP is a crucial regulator of mitochondria-mediated OXPHOS.

Complement C1q binding protein is responsible for mitochondrial quality control

A functional mitochondrial network responding to physiological adaptations and stress conditions is critical for a healthy cellular condition. Given that mitochondria are exposed to high levels of reactive oxygen species, they have evolved multiple systems of quality control to ensure that the requisite number of functional mitochondria are present to meet cellular demands. Mitochondria eliminate the damaged mitochondrial proteins through autophagy. Thus, understanding how C1QBP orchestrates mitophagy to maintain mitochondrial homeostasis could provide critical insights.

Jiao et al. (2015) reported that C1QBP controlled mitochondrial autophagy to help cells adapt better to the challenging microenvironment (Jiao and You, 2016). Serine/threonine kinase Unc-51-like kinase-1 (ULK1) is crucial in inducing mitophagy. This protein is susceptible to proteasome-mediated degradation. C1QBP regulates ULK1 stability by forming a protein complex with ULK1. The interaction between ULK1 and C1QBP is indispensable to maintaining steady-state levels of ULK1, thereby preventing its polyubiquitylation. Moreover, it has been shown that mitophagy defects can be recovered by re-introducing ULK1 into C1QBP-deficient cells, which suggested that C1QBP protected mitophagy through the prevention of ULK1 degradation. Considering that mitochondrial homeostasis and oxidative phosphorylation might be mutually beneficial (Wrighton, 2013), mitochondrial quality control may serve as an important mechanism for maintaining cellular energy homeostasis. Therefore, C1QBP exerts a protective effect under starvation conditions by both inducing Ulk1-dependent autophagy and maintaining oxidative phosphorylation. In this regard, C1QBP-Ulk1-mitophagy axis may provide a survival advantage when nutrients are scarce, which ultimately promotes tumorigenesis.

Taken together, mitochondrial plasticity including mitochondrial dynamics, metabolism, and autophagy is tightly linked to mitochondrial structure, function and homeostasis. C1QBP overexpression promotes mitochondrial plasticity to endow tumor cells with proliferation and malignant progression. On the contrast, *C1qbp* knocking down dampens mitochondrial adaptation and metabolic flexibility, which is responsible for tumor repression.

Complement C1q binding protein is implicated in tumor progression

C1QBP is expressed at high levels in a significant number of tumor types, including melanoma, colon, ovarian, gastric, prostate, brain, and breast, compared with their nonmalignant counterparts (Chen et al., 2009; Amamoto et al., 2011; Yu et al., 2013; Niu et al., 2015; Wang et al., 2015; Gao et al., 2016; Rousso-Noori et al., 2021; Sinha et al., 2021). Various studies involving patients have revealed that C1QBP is positively linked to the tumor stage and poor prognosis, as shown in Table 1.

As expected, high expression levels of C1QBP are inversely correlated with tumor patients' prognosis, making C1QBP a valuable independent prognostic marker of outcomes in tumor patients. For example, upregulation of *C1qbp* mRNA has been detected in low and high-grade gliomas, especially recurrent glioblastoma (GBM) (Rousso-Noori et al., 2021). This protein significantly is associated with the extent of the disease progression. It might also serve as a tumor-associated antigen (TAA) in gliomas.

Furthermore, C1QBP modulates tumor proliferation and metastasis. Its expression level in breast cancer was closely linked with distant metastasis and tumor node metastasis (TNM) stages (Wang et al., 2015). X Zhang et al. (2013) reported that during metastasis, the C1QBP up-modulation was confined to metastatic islands, which could have significant implications if further experiments could show it can regulate tumor metastasis. On this note, the authors showed that C1QBP held the activity of protein kinase C and modulated EGF-induced cancer cell chemotaxis, which thus impacted tumor cell migration. In contrast, C1QBP silencing attenuated tumor progression and metastasis *in vivo* by modulating the tumor microenvironment through inhibiting tumor angiogenesis and macrophage infiltration (Sinha et al., 2021). Based on such premises, C1QBP can be a target of a novel therapeutic approaches in the regulation of tumor progression and metastasis. Additionally, C1QBP has been observed to adhere to the cell surface and interact with integrin αvβ3, a regulatory molecule of cell migration. C1QBP-integrin interaction results in transcriptional upregulation of MT1-MMP expression and finally MMP-2 activation, leading to enhanced tumorigenicity and cell migration in B16F10 melanoma cell line (Prakash et al., 2011). Besides,

TABLE 1 C1QBP overexpressed in a variety of tumor cells is implicated in tumor malignant progression and tumor therapeutic treatment.

C1QBP as a tumor biomarker	C1QBP and tumor progression	Tumor therapies targeting C1QBP
C1QBP as a prognostic marker is related to metastasis and poor prognosis in cancer patients (Chen et al., 2009; Niu et al., 2015; Wang et al., 2015)	C1QBP interacts with PKC to modulate in cancer cell chemotaxis (Zhang et al., 2013)	C1QBP as a new target can be utilized for precise delivery of imaging or therapeutic agents to tumors (Sanchez-Martin et al., 2011)
C1QBP as a tumor biomarker is tightly associated with the lymph node and peritoneal metastasis in epithelial ovarian cancer patients (Yu et al., 2013)	C1QBP is involved in tumor invasion and migration (Prakash et al., 2011)	C1QBP antibody inhibits growth factor stimulated lamellipodia formation, cell migration and focal adhesion kinase activation as well as prevents even angiogenesis (Kim et al., 2016)
C1QBP as a critical regulator for tumor progression of prostate cancer is positively correlated with pathological stage and relapse of the disease (Amamoto et al., 2011)	C1QBP promotes tumor metastasis by targeting EMT markers, and modulating TME (Sinha et al., 2021)	C1QBP as the receptor of a nanoparticle drug, CGKRK nanoworms, has been found to be effective in orthotopic glioblastoma and breast cancer (Agemy et al., 2013)
C1QBP as a tumor diagnostic marker is correlated with progression and poor prognosis of the gastric cancer patients (Gao et al., 2016)	C1QBP shifts tumor metabolism to OXPHOS leading to the enhanced tumorigenicity (Fogal et al., 2010)	A C1QBP binding peptide displays improved tumor penetration and increased efficacy in suppressing breast tumor growth *in vivo* (Hunt et al., 2017)
C1QBP as a tumor associated antigen (TAA) is overexpressed in clinic low- and high-grade gliomas (Rousso-Noori et al., 2021)	C1QBP impacts the lamellipodia formation and a concomitant decrease in FAK kinase, thus promoting tumor migration and tumorigenesis (Kim et al., 2011)	C1QBP-specific CAR T cells recognize and specifically eliminate C1QBP expressing glioma cells and tumor derived endothelial cells (Rousso-Noori et al., 2021)

C1qbp knocking down exhibits the disruption of lamellipodia formation and a concomitant decrease in focal adhesion kinase (FAK) kinase and receptor kinase, inhibiting cellular migration and tumorigenesis (Kim et al., 2011).

On the other hand, increasing evidence has shown that C1QBP-mediated tumorigenesis is tightly associated with mitochondrial metabolism maintenance. Fogal et al. (2010) found that knocking down C1QBP expression in human cancer cells strongly shifted their metabolism from oxidative OXPHOS to glycolysis. C1QBP deficiency resulted in less *in vivo* tumorigenicity, probably due to the reduced synthesis of the mitochondrial-DNA-encoded OXPHOS polypeptides. Thus, C1QBP is implicated in mitochondrial protein translation and affects several electron transport complexes' functions. On the other hand, recovering C1QBP reestablished their animal tumorigenicity in these knockdown cells.

Notably, C1QBP was also reported to be involved in glutamine oxidation (Fogal et al., 2015). It is commonly known that glutamine is essential for mammalian cell proliferation. It is therefore associated with tumor progression of any type of cancer. Higher glutamine oxidation positively correlates with a higher degree of tumor progression *in vivo*. Myc can upregulate *C1qbp* transcription, resulting in the regulation of glutamine metabolism, which suggest that a high level of Myc in malignant brain cancers is accompanied by increased expression of C1QBP. On the other hand, attenuation of C1QBP expression stunted glioma cells' growth. C1QBP silencing in glutamine-addicted glioma cells induced resistance to glutamine deprivation. In other words, C1QBP is involved in mitochondrial metabolism and plays an integral role in Myc-induced glutamine addiction in cancer cells.

Additionally, C1QBP has been shown implicated in mitochondrial-dependent apoptosis of tumor cells. Hu et al. reported that siRNA-mediated *C1qbp* knockdown enhanced mitochondrial fragmentation, which was accompanied by a loss of detectable levels of the mitochondrial fusion mediator proteins Mfn 1/2. Furthermore, siRNA-mediated C1QBP knockdown enhanced tumor cell death in response to cisplatin treatment (Hu et al., 2013).

Overall, C1QBP regulates mitochondrial metabolism and dynamics to potentiate mitochondrial plasticity, thereby endowing tumor cells with a bioenergetic advantage for proliferation, metastasis, and resistance to therapies, as shown in Figure 1.

Complement C1q binding protein regulates immune cells maturation, differentiation and antitumor immune function

Warburg hypothesized that the shift to aerobic glycolysis was a cause of cancer. Aerobic glycolysis supports macromolecule synthesis, rapid proliferation and heightened ATP demand, which are necessary for tumor rapid progression. However, even though tumor cells have high rates of glucose consumption *via* glycolysis, mitochondrial function was later found to be essential in several types of tumor (Wallace, 2012; Ward and Thompson, 2012). A significant proportion of their ATP is still produced *via* OXPHOS, again suggesting that at least some mitochondrial function is preserved in tumor cells. Similar to tumor cells, immune cells always shift to glycolysis to support their rapid growth and production of biosynthetic factors for

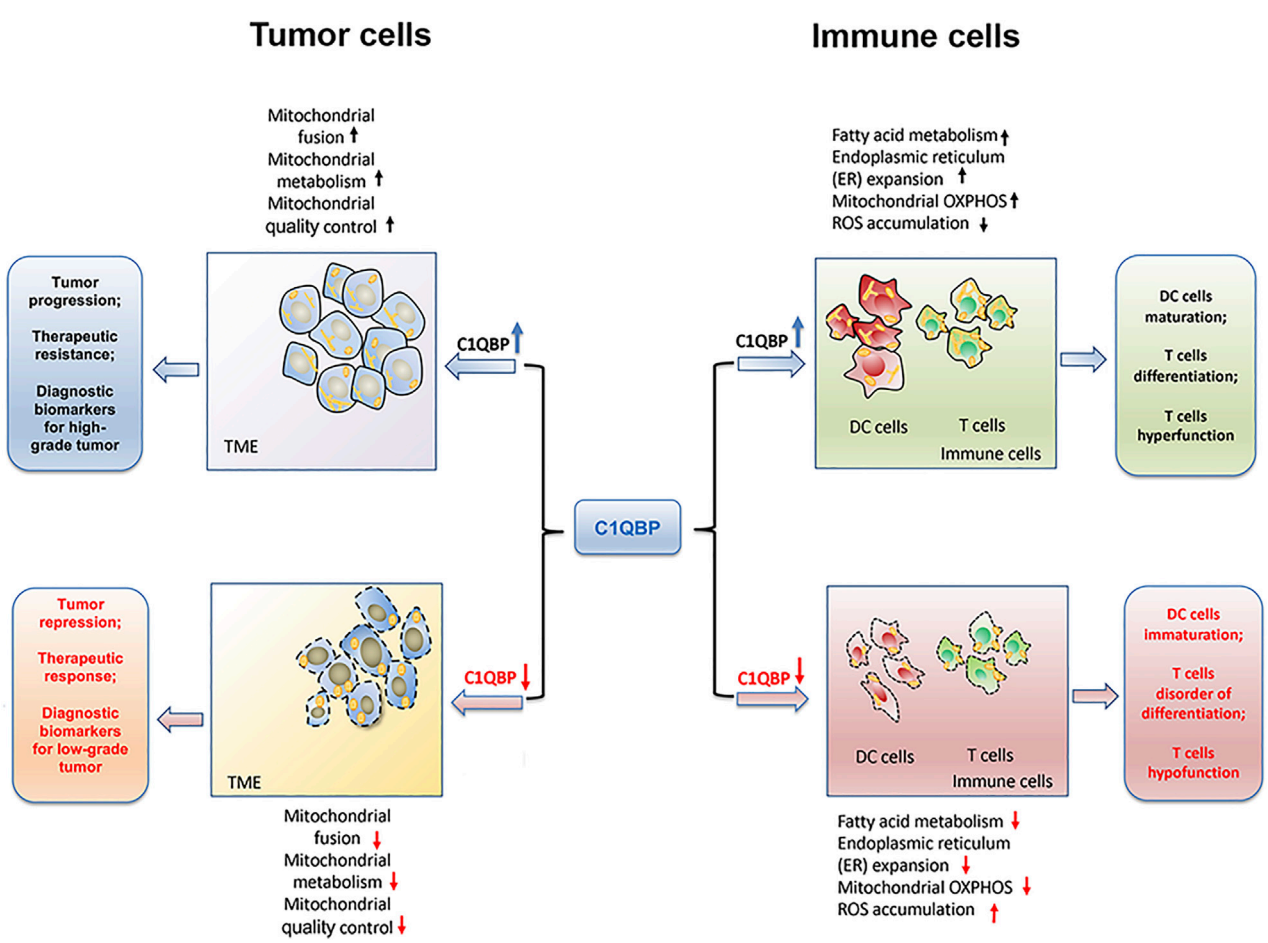

FIGURE 1
C1QBP regulation of mitochondrial plasticity to impact tumor progression and antitumor immunity. C1QBP regulates mitochondrial fusion, mitochondrial OXPHOS, and mitochondrial quality control to impact tumor malignant progression and therapeutic response. On the other hand, C1QBP also changes fatty acid metabolism, ER expansion, and ROS accumulation, thus modulating DCs' maturation as well as T cells' differentiation and their effector function.

differentiation into effector cells (Kouidhi et al., 2017). However, mitochondria generate metabolic intermediates that are important for their growth and proliferation as well as for their cytotoxicity and cytokine production. Several mitochondrial energy metabolism pathways have been implicated in shaping T-cells function and differentiation (Sena et al., 2013). Besides, memory $CD8^+$ T cells require mitochondria-mediated FAO to support their long-term survival (Araki et al., 2009). Therefore, it is evident that mitochondrial function not only affects tumor onset, progression and distant metastasis but also controls immune cells' maturation, differentiation, and long-term maintenance. A body of literature indicates that C1QBP plays a vital role in mitochondrial-dependent metabolic flexibility of critical immune cells of the immune systems (Gotoh et al., 2018; Zhai et al., 2021; Tian et al., 2022).

Complement C1q binding protein impacts dendritic cells' maturation

Dendritic cells (DCs) have different functions, and among them are the following ones: 1) constitute the most potent antigen-presenting cells; 2) induce primary immune responses; 3) capture antigens in peripheral tissues; 4) recognize pathogen-associated molecular patterns of invading microbes post-Toll-like receptors (TLRs) ligation, which leads to cellular activation and changes in gene expression and cellular metabolism in DCs (Banchereau et al., 2000; Kawai and Akira, 2011). Gotoh et al. (2018) reported that C1QBP was indispensable in DCs metabolism and maturation. Their study found that mitochondrial C1QBP and pyruvate dehydrogenase (PDH) activity are necessary for DC maturation both *in vitro* and *in vivo*. Although pyruvate and lactate were similarly produced by

both W.T. and *C1qbp*$^{-/-}$ DCs, after lipopolysaccharide (LPS) stimulation, LPS-induced citrate production was impaired *C1qbp*$^{-/-}$ DCs. Generally, glucose is processed by the cytosolic glycolytic pathway to generate pyruvate. Acetyl-coenzyme A (acetyl-CoA) is produced from pyruvate by the PDH complex and subsequently reacts with oxaloacetate to form citrate in mitochondria. Given that after LPS stimulation, the upstream metabolites of citrate in wild type (WT) and *C1qbp*$^{-/-}$ DCs were produced at similar levels, the authors focused on the activity of PDH in both DCs types. They revealed that C1QBP could bind to PDH-E2 in DCs by immunoprecipitation experiments. Furthermore, the PDH activity in WT was significantly higher than that in *C1qbp*$^{-/-}$ DCs at the basal condition, which means C1QBP may control PDH activity by binding to PDH-E2 to regulate citrate production and further support DC. maturation. Notably, PDH-mediated citrate production from pyruvate is involved in fat acid synthesis (FAS). This mechanism impacts the endoplasmic reticulum (ER) expansion. Interestingly, ER expansion was observed in WT DCs but not in *C1qbp*$^{-/-}$ DCs after LPS stimulation.

Therefore, C1QBP bound to PDH-E2 promoted the activity of PDH, facilitating citrate production and enhancing FAS and ER expansion. In this regard, C1QBP involvement in regulating DCs maturation by controlling mitochondrial metabolism other than the electron transport chain (ETC) has many consequences to help fine-tune mitochondria expression, and alterations could lead to the decreased immune function of DCs.

Complement C1q binding protein is involved in T cells differentiation

Besides DCs maturation, C1QBP was also reported to be implicated in the regulation of T cells differentiation. Zhai et al. (2021) revealed that C1QBP was involved in the modulation of effector CD8$^+$ T cells differentiation to affect their antiviral and antitumor immune responses further. Firstly, *C1qbp* deficiency in T cells intrinsically impaired the differentiation of effector CD8$^+$ T cells, which is attributed to a failure to increase their mitochondrial respiratory capacities. They found that activated CD8$^+$ T cells had greater glycolytic and OXPHOS requirements than activated CD4$^+$ T cells and were more sensitive to OXPHOS impairment. In other words, C1QBP-mediated augmentation of OXPHOS was necessary for the differentiation of effector CD8$^+$ T cells. Moreover, C1QBP promoted the epigenetic and transcriptional programs of effector CD8$^+$ T cells. It achieved it by controlling the production of metabolites, including acetyl-CoA, fumarate, and 2-HG. Their study revealed that *C1qbp* deficiency mediated OXPHOS impairment. This, in turn, capitulated in decreased acetyl-CoA but increased fumarate and 2-HG. Moreover, downregulation of acetyl-CoA subsequently dampens histone protein H3K27 acetylation, which enhances CpG methylation to reduce some genes expression encoding several master transcription factors that drive effector CD8$^+$ T cell differentiation such as *Id2, Prdm1,* and *Tbx21*.

Consequently, CD8$^+$ T cell differentiation becomes retarded. C1QBP facilitates the epigenetic and transcriptional programs of effector CD8$^+$ T cells differentiation by controlling metabolites coupled to OXPHOS. In this regard, they provide a mechanistic association between mitochondrial metabolism and CD8$^+$ T cell differentiation, which means these metabolite supplementations or targeting OXPHOS may have significant application in T cell therapies for cancer.

Complement C1q binding protein regulates T cells exhaustion, proliferation and anti-apoptosis

Tumor-infiltrating T cells encounter not only persistent tumor antigen but also experience metabolic stress from the tumor microenvironment such as glucose competition, metabolite accumulation, and hypoxia (Vardhana et al., 2020; Yu et al., 2020). Scharping et al. (2016) revealed that continuous antigen stimulation, coordinated with hypoxia, impaired mitochondrial functions to drive T cells terminal exhaustion. Although hypoxia alone cannot induce T cells dysfunction, its association with persistent antigen stimulation plays a fundamental role in T cells exhaustion. While on the one hand, the tumor microenvironment makes tumor-infiltrating T cells with dysfunctional mitochondria have a lower mass and activity (measured as spare respiratory capacity), driving T cells' metabolic insufficiency. On the other hand, the continuous activation of tumor-infiltrating cells further increases mitochondrial reactive oxygen species (ROS) to exacerbate the exhausted phenotype of tumor-specific T cells. Of note, mitigating hypoxia effectively alleviates these tumor-infiltrating T cells exhaustion. Mitochondria has a fundamental role in modulating T cells' development, fate, and function. Fine-tuning mitochondria is critical for altering the different metabolic preferences and activities within cells. Recently it was shown that impaired ATP production and accumulation of mitochondrial ROS in dysfunctional T cells within the suppressive tumor microenvironment aggravated T cells exhaustion (Li et al., 2020; Vardhana et al., 2020). However, the relationship between metabolic stress and T cell exhaustion remains still unclear.

The question of whether the mitochondrial protein C1QBP is implicated with T cells exhaustion is interesting. Our previous study found that *C1qbp* knockdown modulated T cells with the accumulation of ROS and the loss of mitochondrial membrane potential, thus impairing T cell mitochondrial fitness (Tian et al., 2022). At the same time, C1QBP insufficiency aggravated exhausted T cells. We assessed exhaustion markers, such as PD-1, Tim-3, and LAG-3 in these tumor-specific T cells. We

found that these inhibitory receptors exhibited higher expression levels in tumor-infiltrating *C1qbp*$^{+/-}$ T cells than the corresponding WT cells. In this regard, *C1qbp* knocking down exacerbated the tumor-infiltrating T cells exhaustion, leading to a reduced antitumor immune response.

Chronic antigen stimulation drives the defective oxidative phosphorylation and promotes ROS generation in activated T cells, so *C1qbp* could dampen T cells proliferation while remaining susceptible to cellular apoptosis. To detect the underlying molecular mechanism, we noticed AKT/mTOR proliferation signaling pathway and Bcl-2 anti-apoptotic signaling pathway. Our previous results demonstrated that *C1qbp* insufficiency inhibited the AKT/mTOR signaling pathway, which conferred T cells with relatively weaker proliferation capacity (Tian et al., 2022). At the same time, *C1qbp* knocking down reduced the anti-apoptotic proteins recruitment, such as Bcl-2 and Bcl-XL, but aggravated caspase-3 activation and poly (ADP-ribose) polymerase (PARP) cleavage, which thus accelerated T cells apoptotic process. Therefore, *C1qbp* knockdown induces T cells exhaustion and pre-apoptosis but retarded their proliferation as well as antitumor immune function.

Overall, the potentiation of immune cells' mitochondrial plasticity through C1QBP promotes fatty acid metabolism, ER expansion, and mitochondrial OXPHOS, but relieves the accumulation of ROS, which could further enhance the DCs maturation, T cells differentiation as well as the tumor-infiltration T cells durability (Figure 1).

Manipulation of complement C1q binding protein impacts the competitive balance between tumor cells and immune cells

Targeting complement C1q binding protein ameliorates tumor progression

C1QBP is involved in tumor progression and metastasis, making it an attractive, actionable target against cancer, bringing to the development of monoclonal antibodies (mAbs). Such therapies were successful in inhibiting tumor growth and migration (Sanchez-Martin et al., 2011). The unique upregulation of C1QBP in certain tumors, and targeting it, in various ways, in such tumors could be a valuable strategy (Yenugonda et al., 2017; Rousso-Noori et al., 2021). C1QBP can also be found at the cell surface of angiogenic endothelial cells besides tumor cells. In nature, C1QBP acts as a receptor bound by the CGKRK peptide. Based on such premises, Agemy *et al.* devised a tumor-targeted nanosystem, through which CGKRK pentapeptide delivers a proapoptotic peptide into the mitochondria of tumor blood vessel endothelial cells and tumor cells (Agemy et al., 2013). The treatment was highly effective, especially in the refractory glioblastoma mouse models, compared to other antiangiogenic therapies.

Moreover, another tumor-homing peptide, LyP-1 (CGNKRTRGC), capable of targeting the cell surface of localized C1QBP, has been used to deliver nanoparticles to breast tumors overexpressing C1QBP and has shown efficacy *in vivo* (Luo et al., 2010). However, both the anti-C1QBP antibody and the LyP-1 peptide targeted the C1QBP subset that was exposed on the cell surface. Yenugonda et al. (2017) developed C1QBP-directed therapeutics to inhibit the protein in all subcellular compartments, including mitochondria. A primary screening assay employing a glutamine-addicted glioma cell line identified a hit compound called M36, which could bind and inhibit C1QBP located on the cellular membrane and in the mitochondria. In addition, they further demonstrated that M36 impedes the growth of glioma cells and patient-derived glioma stem cells in culture due to C1QBP genetic knockdown.

In addition, antibody neutralization of C1QBP inhibits lamellipodia formation, cell migration and focal adhesion kinase activation (Kim et al., 2016). At the same time, this antigen-antibody reaction inactivates receptor tyrosine kinases (RTKs) activation in various cancer cells and prevents even angiogenesis, resulting in the decreased tumorigenesis *in vivo*. Notably, A novel tumor penetrating peptide, linTT1 (AKRGARSTA), as a tumor targeting ligand for nanoparticles (Sharma et al., 2017). C1QBP as the primary homing receptor for linTT1, is expressed on the cell surface of peritoneal carcinoma cell lines (Paasonen et al., 2016). Iron oxide nanoworms (NWs) functionalized with the linTT1 peptide in tandem with a pro-apoptotic peptide showed C1QBP-dependent cytotoxicity (Hunt et al., 2017). At the same time, the linTT1-NWs predominantly accumulates in CD31-positive blood vessels, in LYVE-1-positive lymphatic structures, and in CD11b-positive tumor macrophages, thus resulting in significant reduction of weight of peritoneal tumors and significant decrease in the number of metastatic tumor nodules. In this regard, C1QBP-directed intraperitoneal targeting of other anticancer agents may represent a potential strategy to improve their therapeutic index.

Enhancement of complement C1q binding protein optimizes the antitumor function of immune cells

Considering that C1QBP is be specifically expressed on the surface of glioma cells, it is regarded as a suitable tumor associated antigen (TAA) for redirected chimeric antigen receptor (CAR) T cell therapy. Rousso-Noori et al. (2021) reported that C1QBP-specific CAR T cells exerted a dual antitumor and antiangiogenic therapeutic benefit in gliomas. Their study focused on designing CAR T cells targeting C1QBP positive glioma cells. They found that the CAR T cells targeting C1QBP reduced tumor vascularization and extended

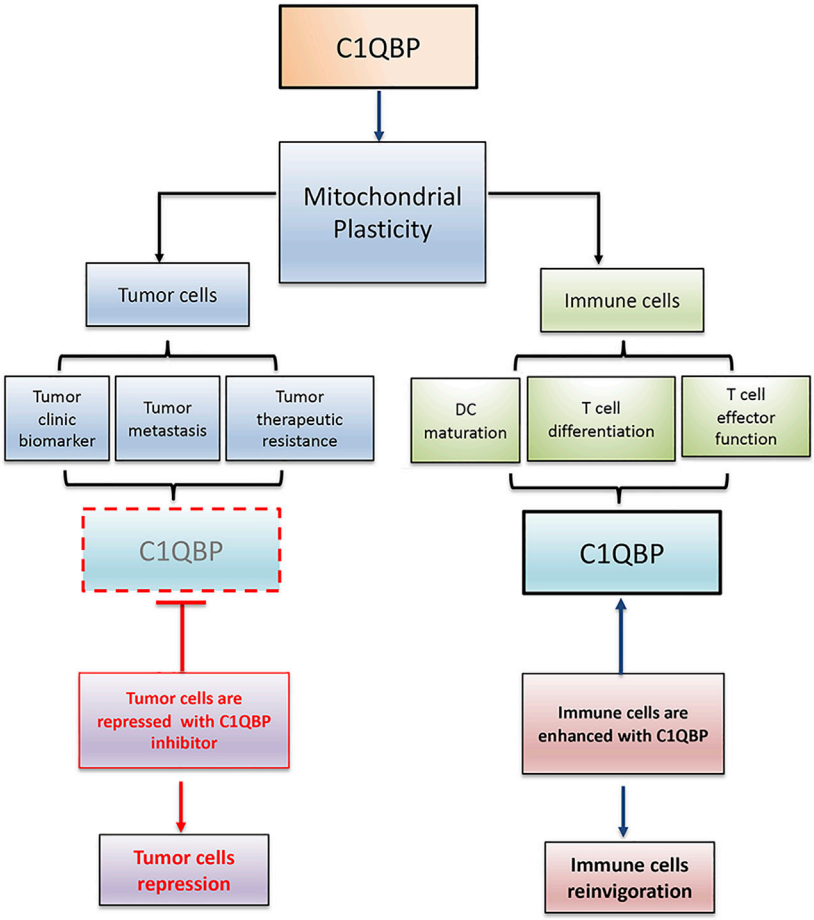

FIGURE 2
C1QBP regulation of mitochondrial plasticity alters the competitive balance between tumor cells and immune cells. Tumor cells disarmed from C1QBP exhibit reduced tumor proliferation, metastasis, and therapeutic resistance, while immune cells potentiated with C1QBP perform the active and durable antitumor immunity. In this regard, strategic manipulation of C1QBP would repress tumor progression but optimize antitumor immune function.

the overall survival of mice bearing gliomas, thus providing proof-of-principle evidence that C1QBP-CAR T cells can recognize and eliminate not only glioma cells but also tumor endothelial cells. Thus, CAR T cells targeting C1QBP may serve as a therapeutic option for glioblastoma patients through specifically recognizing and eliminating C1QBP expressing glioma cells and tumor derived endothelial cells, finally controlling tumor growth in orthotopic syngeneic and xenograft mouse models.

On the other hand, upregulation of mitochondrial plasticity may effectively reinvigorate T cell's robust and persistent immune function. This could alter the metabolic competition between tumor cells and immune systems. Thus, it is worth noting that C1QBP modified CAR T cells' immune function and their long-term maintenance. Our previous study demonstrated that *C1qbp* knockdown attenuated CAR T cells' antitumor immune response (Tian et al., 2022). Specifically, we constructed the $C1qbp^{+/-}$ and $C1qbp^{+/+}$ CAR T cells targeting B7-H3. We found that *C1qbp* knocking down reduced CAR T cells' release of IFN-γ and TNF-α cytokines, which reduced the corresponding immunotherapeutic efficacy of CAR T cells *in vivo*. In contrast, sufficient *C1qbp* potentiated CAR T cells' mitochondrial adaptation to the relentless TME by ameliorating their exhaustion, thereby improving their durable antitumor immune function.

Since the mitochondrial function and metabolic flexibility imply the fate and function of immune cells, metabolic interventions manipulating immunity are rare. Using new proteins to achieve this purpose represents a great opportunity that remains untapped. Therefore, developing strategies for potentiation of mitochondrial-dependent metabolic flexibility could improve the efficacy of current immune-based anticancer therapy.

Future direction

Mitochondrial plasticity endows cells with superior adaptation to the relentless microenvironment. This adaptation is regulated spatially and temporally by regulating gene expression and metabolic signatures, associated mitochondrial dynamics, metabolism, and quality control.

On the one hand, for tumor cells to survive, they are forced to remodel their signaling pathways by altering transcription, translation, and post-translational modifications to acquire phenotypic heterogeneity. Such heterogeneity, in turn, determines whether tumor cells resist environmental stress, enter dormancy or metastasize. Notably, it is imperative to know that mitochondrial plasticity plays a critical role in aiding cancer cells in acquiring metastatic traits under adverse environmental conditions. Cancer stem cells (CSCs) as a population of cells with stem cell-like properties are considered to be the root cause of tumor heterogeneity, which is also responsible for metastatic dissemination and therapeutic resistance (Clevers, 2011; Pattabiraman and Weinberg, 2014). CSCs are characterized by the increased mitochondrial mass and the elevated mitochondrial biogenesis (Luo and Wicha, 2015; Song et al., 2015; Peiris-Pages et al., 2016). In this scenario, mitochondrial biogenesis accompanied with increased membrane potential, and higher generation of mitochondria-derived ROS, has recently been regarded as a regulatory instigator of tumor stemness. Thus, the question whether C1QBP would regulate mitochondrial biogenesis to further impact tumor stemness will be of interest.

On the other hand, we must also stress that potentiation of immune cells, through enhancement of mitochondrial plasticity, contributes to preventing immune exhaustion and durable antitumor immunity. Improving T cells' mitochondrial fitness can result in persistent immune function. It can cope with a stressful microenvironment. Consequently, in our opinion, an enhancement of mitochondrial function could be a promising strategy for tumor immunotherapy that could be used in combination with the current checkpoint blockade therapies available, such as anti-PD-L1, PD-1, and CTLA-4. Besides, a successful immune response depends on the ability of T cells not only to proliferate extensively and attain effector functions but also to generate long-lived memory T cells. FAO engagement is critical for the generation of memory T cells (Raud et al., 2018). C1QBP was reported to be involved in regulation of lipid metabolism and homeostasis (Liu et al., 2017; Liu et al., 2018). Therefore, the question whether metabolic reprogramming such as FAO through modulation of C1QBP would probably impact the generation of long-lived memory T cells requires further evaluation.

In conclusion, C1QBP is vital in maintaining mitochondrial plasticity. Therefore, inhibition of C1QBP in tumor cells and promotion of C1QBP in immune cells would beneficially adjust the competitive balance between tumor and immune cells, providing a very reasonable therapeutic opportunity by finding a way to correctly fine-tune mitochondrial-based metabolic flexibility (Figure 2).

Author contributions

Conception and Writing: QW, DC, JZ, and HT; Revision of the manuscript: NSo, NSu, PN, and HT. All authors read and approved the final manuscript.

Funding

This work was supported by the National Natural Science Foundation of China (Nos. 82073012, 81871869, and 32200124), Jiangsu Universtiy Clinical Medicine Technology Development Fund, Jiangsu Young Medical Talents Project, Jiangsu Provincial Key Medical Discipline, the Project of Invigorating Health Care through Science, Technology and Education (No. ZDXKA2016014).

Conflict of interest

The authors declare that the research was conducted in the absence of any commercial or financial relationships that could be construed as a potential conflict of interest.

Publisher's note

All claims expressed in this article are solely those of the authors and do not necessarily represent those of their affiliated organizations, or those of the publisher, the editors and the reviewers. Any product that may be evaluated in this article, or claim that may be made by its manufacturer, is not guaranteed or endorsed by the publisher.

References

Agemy, L., Kotamraju, V. R., Friedmann-Morvinski, D., Sharma, S., Sugahara, K. N., and Ruoslahti, E. (2013). Proapoptotic peptide-mediated cancer therapy targeted to cell surface p32. *Mol. Ther.* 21 (12), 2195–2204. doi:10.1038/mt.2013.191

Ahola, S., Langer, T., and MacVicar, T. (2019). Mitochondrial proteolysis and metabolic control. *Cold Spring Harb. Perspect. Biol.* 11 (7), a033936. doi:10.1101/cshperspect.a033936

Amamoto, R., Yagi, M., Song, Y., Oda, Y., Tsuneyoshi, M., Naito, S., et al. (2011). Mitochondrial p32/C1QBP is highly expressed in prostate cancer and is associated with shorter prostate-specific antigen relapse time after radical prostatectomy. *Cancer Sci.* 102 (3), 639–647. doi:10.1111/j.1349-7006.2010.01828.x

Araki, K., Turner, A. P., Shaffer, V. O., Gangappa, S., Keller, S. A., Bachmann, M. F., et al. (2009). mTOR regulates memory CD8 T-cell differentiation. *Nature* 460 (7251), 108–112. doi:10.1038/nature08155

Banchereau, J., Briere, F., Caux, C., Davoust, J., Lebecque, S., Liu, Y. J., et al. (2000). Immunobiology of dendritic cells. *Annu. Rev. Immunol.* 18, 767–811. doi:10.1146/annurev.immunol.18.1.767

Chen, H., and Chan, D. C. (2005). Emerging functions of mammalian mitochondrial fusion and fission. *Hum. Mol. Genet.* 142, R283–R289. doi:10.1093/hmg/ddi270

Chen, Y. B., Jiang, C. T., Zhang, G. Q., Wang, J. S., and Pang, D. (2009). Increased expression of hyaluronic acid binding protein 1 is correlated with poor prognosis in patients with breast cancer. *J. Surg. Oncol.* 100 (5), 382–386. doi:10.1002/jso.21329

Clevers, H. (2011). The cancer stem cell: Premises, promises and challenges. *Nat. Med.* 17 (3), 313–319. doi:10.1038/nm.2304

Fogal, V., Babic, I., Chao, Y., Pastorino, S., Mukthavaram, R., Jiang, P., et al. (2015). Mitochondrial p32 is upregulated in Myc expressing brain cancers and mediates glutamine addiction. *Oncotarget* 6 (2), 1157–1170. doi:10.18632/oncotarget.2708

Fogal, V., Richardson, A. D., Karmali, P. P., Scheffler, I. E., Smith, J. W., and Ruoslahti, E. (2010). Mitochondrial p32 protein is a critical regulator of tumor metabolism via maintenance of oxidative phosphorylation. *Mol. Cell. Biol.* 30 (6), 1303–1318. doi:10.1128/MCB.01101-09

Fogal, V., Zhang, L., Krajewski, S., and Ruoslahti, E. (2008). Mitochondrial/cell-surface protein p32/gC1qR as a molecular target in tumor cells and tumor stroma. *Cancer Res.* 68 (17), 7210–7218. doi:10.1158/0008-5472.CAN-07-6752

Funes, J. M., Quintero, M., Henderson, S., Martinez, D., Qureshi, U., Westwood, C., et al. (2007). Transformation of human mesenchymal stem cells increases their dependency on oxidative phosphorylation for energy production. *Proc. Natl. Acad. Sci. U. S. A.* 104 (15), 6223–6228. doi:10.1073/pnas.0700690104

Gao, H., Yao, Q., Lan, X., Li, S., Wu, J., Zeng, G., et al. (2016). Elevated HABP1 protein expression correlates with progression and poor survival in patients with gastric cancer. *Onco. Targets. Ther.* 9, 6711–6718. doi:10.2147/OTT.S114756

Ghebrehiwet, B., Lim, B. L., Kumar, R., Feng, X., and Peerschke, E. I. (2001). gC1q-R/p33, a member of a new class of multifunctional and multicompartmental cellular proteins, is involved in inflammation and infection. *Immunol. Rev.* 180, 65–77. doi:10.1034/j.1600-065x.2001.1800106.x

Gotoh, K., Morisaki, T., Setoyama, D., Sasaki, K., Yagi, M., Igami, K., et al. (2018). Mitochondrial p32/C1qbp is a critical regulator of dendritic cell metabolism and maturation. *Cell Rep.* 25 (7), 1800–1815. doi:10.1016/j.celrep.2018.10.057

Hu, M., Crawford, S. A., Henstridge, D. C., Ng, I. H., Boey, E. J., Xu, Y., et al. (2013). p32 protein levels are integral to mitochondrial and endoplasmic reticulum morphology, cell metabolism and survival. *Biochem. J.* 453 (3), 381–391. doi:10.1042/BJ20121829

Hunt, H., Simon-Gracia, L., Tobi, A., Kotamraju, V. R., Sharma, S., Nigul, M., et al. (2017). Targeting of p32 in peritoneal carcinomatosis with intraperitoneal linTT1 peptide-guided pro-apoptotic nanoparticles. *J. Control. Release* 260, 142–153. doi:10.1016/j.jconrel.2017.06.005

Jiao, H., Su, G. Q., Dong, W., Zhang, L., Xie, W., Yao, L. M., et al. (2015). Chaperone-like protein p32 regulates ULK1 stability and autophagy. *Cell Death Differ.* 22 (11), 1812–1823. doi:10.1038/cdd.2015.34

Jiao, H., and You, H. (2016). p32: A new player in autophagy. *Mol. Cell. Oncol.* 3 (3), e1061097. doi:10.1080/23723556.2015.1061097

Kawai, T., and Akira, S. (2011). Toll-like receptors and their crosstalk with other innate receptors in infection and immunity. *Immunity* 34 (5), 637–650. doi:10.1016/j.immuni.2011.05.006

Kim, B. C., Hwang, H. J., An, H. T., Lee, H., Park, J. S., Hong, J., et al. (2016). Antibody neutralization of cell-surface gC1qR/HABP1/SF2-p32 prevents lamellipodia formation and tumorigenesis. *Oncotarget* 7 (31), 49972–49985. doi:10.18632/oncotarget.10267

Kim, K. B., Yi, J. S., Nguyen, N., Lee, J. H., Kwon, Y. C., Ahn, B. Y., et al. (2011). Cell-surface receptor for complement component C1q (gC1qR) is a key regulator for lamellipodia formation and cancer metastasis. *J. Biol. Chem.* 286 (26), 23093–23101. doi:10.1074/jbc.M111.233304

Kouidhi, S., Elgaaied, A. B., and Chouaib, S. (2017). Impact of metabolism on T-cell differentiation and function and cross talk with tumor microenvironment. *Front. Immunol.* 8, 270. doi:10.3389/fimmu.2017.00270

Li, F., Wang, Y., Zeller, K. I., Potter, J. J., Wonsey, D. R., O'Donnell, K. A., et al. (2005). Myc stimulates nuclearly encoded mitochondrial genes and mitochondrial biogenesis. *Mol. Cell. Biol.* 25 (14), 6225–6234. doi:10.1128/MCB.25.14.6225-6234.2005

Li, W., Cheng, H., Li, G., and Zhang, L. (2020). Mitochondrial damage and the road to exhaustion. *Cell Metab.* 32 (6), 905–907. doi:10.1016/j.cmet.2020.11.004

Li, Y., Wan, O. W., Xie, W., and Chung, K. K. (2011). p32 regulates mitochondrial morphology and dynamics through parkin. *Neuroscience* 199, 346–358. doi:10.1016/j.neuroscience.2011.10.003

Liu, Y., Leslie, P. L., Jin, A., Itahana, K., Graves, L. M., and Zhang, Y. (2017). p32 heterozygosity protects against age- and diet-induced obesity by increasing energy expenditure. *Sci. Rep.* 7 (1), 5754. doi:10.1038/s41598-017-06209-9

Liu, Y., Leslie, P. L., Jin, A., Itahana, K., Graves, L. M., and Zhang, Y. (2018). p32 regulates ER stress and lipid homeostasis by down-regulating GCS1 expression. *FASEB J.* 32 (7), 3892–3902. doi:10.1096/fj.201701004RR

Liu, Y., and Shi, Y. (2020). Mitochondria as a target in cancer treatment. *MedComm* 1 (2), 129–139. doi:10.1002/mco2.16

Loson, O. C., Song, Z., Chen, H., and Chan, D. C. (2013). Fis1, mff, MiD49, and MiD51 mediate Drp1 recruitment in mitochondrial fission. *Mol. Biol. Cell* 24 (5), 659–667. doi:10.1091/mbc.E12-10-0721

Luo, G., Yu, X., Jin, C., Yang, F., Fu, D., Long, J., et al. (2010). LyP-1-conjugated nanoparticles for targeting drug delivery to lymphatic metastatic tumors. *Int. J. Pharm.* 385 (1-2), 150–156. doi:10.1016/j.ijpharm.2009.10.014

Luo, M., and Wicha, M. S. (2015). Metabolic plasticity of cancer stem cells. *Oncotarget* 6 (34), 35141–35142. doi:10.18632/oncotarget.6177

Mishra, P., and Chan, D. C. (2016). Metabolic regulation of mitochondrial dynamics. *J. Cell Biol.* 212 (4), 379–387. doi:10.1083/jcb.201511036

Moreno-Sanchez, R., Rodriguez-Enriquez, S., Marin-Hernandez, A., and Saavedra, E. (2007). Energy metabolism in tumor cells. *FEBS J.* 274 (6), 1393–1418. doi:10.1111/j.1742-4658.2007.05686.x

Muta, T., Kang, D., Kitajima, S., Fujiwara, T., and Hamasaki, N. (1997). p32 protein, a splicing factor 2-associated protein, is localized in mitochondrial matrix and is functionally important in maintaining oxidative phosphorylation. *J. Biol. Chem.* 272 (39), 24363–24370. doi:10.1074/jbc.272.39.24363

Niu, M., Sun, S., Zhang, G., Zhao, Y., Pang, D., and Chen, Y. (2015). Elevated expression of HABP1 is correlated with metastasis and poor survival in breast cancer patients. *Am. J. Cancer Res.* 5 (3), 1190–1198.

Noh, S., Phorl, S., Naskar, R., Oeum, K., Seo, Y., Kim, E., et al. (2020). p32/C1QBP regulates OMA1-dependent proteolytic processing of OPA1 to maintain mitochondrial connectivity related to mitochondrial dysfunction and apoptosis. *Sci. Rep.* 10 (1), 10618. doi:10.1038/s41598-020-67457-w

Paasonen, L., Sharma, S., Braun, G. B., Kotamraju, V. R., Chung, T. D., She, Z. G., et al. (2016). New p32/gC1qR ligands for targeted tumor drug delivery. *Chembiochem* 17 (7), 570–575. doi:10.1002/cbic.201500564

Pattabiraman, D. R., and Weinberg, R. A. (2014). Tackling the cancer stem cells - what challenges do they pose? *Nat. Rev. Drug Discov.* 13 (7), 497–512. doi:10.1038/nrd4253

Peiris-Pages, M., Martinez-Outschoorn, U. E., Pestell, R. G., Sotgia, F., and Lisanti, M. P. (2016). Cancer stem cell metabolism. *Breast Cancer Res.* 18 (1), 55. doi:10.1186/s13058-016-0712-6

Petersen-Mahrt, S. K., Estmer, C., Ohrmalm, C., Matthews, D. A., Russell, W. C., and Akusjarvi, G. (1999). The splicing factor-associated protein, p32, regulates RNA splicing by inhibiting ASF/SF2 RNA binding and phosphorylation. *EMBO J.* 18 (4), 1014–1024. doi:10.1093/emboj/18.4.1014

Prakash, M., Kale, S., Ghosh, I., Kundu, G. C., and Datta, K. (2011). Hyaluronan-binding protein 1 (HABP1/p32/gC1qR) induces melanoma cell migration and tumor growth by NF-kappa B dependent MMP-2 activation through integrin α(v)β(3) interaction. *Cell. Signal.* 23 (10), 1563–1577. doi:10.1016/j.cellsig.2011.04.009

Raud, B., McGuire, P. J., Jones, R. G., Sparwasser, T., and Berod, L. (2018). Fatty acid metabolism in CD8(+) T cell memory: Challenging current concepts. *Immunol. Rev.* 283 (1), 213–231. doi:10.1111/imr.12655

Rousso-Noori, L., Mastandrea, I., Talmor, S., Waks, T., Globerson Levin, A., Haugas, M., et al. (2021). P32-specific CAR T cells with dual antitumor and antiangiogenic therapeutic potential in gliomas. *Nat. Commun.* 12 (1), 3615. doi:10.1038/s41467-021-23817-2

Sanchez-Martin, D., Cuesta, A. M., Fogal, V., Ruoslahti, E., and Alvarez-Vallina, L. (2011). The multicompartmental p32/gClqR as a new target for antibody-based tumor targeting strategies. *J. Biol. Chem.* 286 (7), 5197–5203. doi:10.1074/jbc.M110.161927

Santel, A., and Fuller, M. T. (2001). Control of mitochondrial morphology by a human mitofusin. *J. Cell Sci.* 114 (5), 867–874. doi:10.1242/jcs.114.5.867

Scharping, N. E., Menk, A. V., Moreci, R. S., Whetstone, R. D., Dadey, R. E., Watkins, S. C., et al. (2016). The tumor microenvironment represses T cell mitochondrial biogenesis to drive intratumoral T cell metabolic insufficiency and dysfunction. *Immunity* 45 (2), 374–388. doi:10.1016/j.immuni.2016.07.009

Schvartzman, J. M., Thompson, C. B., and Finley, L. W. S. (2018). Metabolic regulation of chromatin modifications and gene expression. *J. Cell Biol.* 217 (7), 2247–2259. doi:10.1083/jcb.201803061

Sena, L. A., Li, S., Jairaman, A., Prakriya, M., Ezponda, T., Hildeman, D. A., et al. (2013). Mitochondria are required for antigen-specific T cell activation through reactive oxygen species signaling. *Immunity* 38 (2), 225–236. doi:10.1016/j.immuni.2012.10.020

Sharma, S., Kotamraju, V. R., Molder, T., Tobi, A., Teesalu, T., and Ruoslahti, E. (2017). Tumor-penetrating nanosystem strongly suppresses breast tumor growth. *Nano Lett.* 17 (3), 1356–1364. doi:10.1021/acs.nanolett.6b03815

Sinha, S., Singh, S. K., Jangde, N., Ray, R., and Rai, V. (2021). p32 promotes melanoma progression and metastasis by targeting EMT markers, Akt/PKB pathway, and tumor microenvironment. *Cell Death Dis.* 12 (11), 1012. doi:10.1038/s41419-021-04311-5

Song, I. S., Jeong, J. Y., Jeong, S. H., Kim, H. K., Ko, K. S., Rhee, B. D., et al. (2015). Mitochondria as therapeutic targets for cancer stem cells. *World J. Stem Cells* 7 (2), 418–427. doi:10.4252/wjsc.v7.i2.418

Sonveaux, P., Vegran, F., Schroeder, T., Wergin, M. C., Verrax, J., Rabbani, Z. N., et al. (2008). Targeting lactate-fueled respiration selectively kills hypoxic tumor cells in mice. *J. Clin. Invest.* 118 (12), 3930–3942. doi:10.1172/JCI36843

Tian, H., Wang, G., Wang, Q., Zhang, B., Jiang, G., Li, H., et al. (2022). Complement C1q binding protein regulates T cells' mitochondrial fitness to affect their survival, proliferation, and anti-tumor immune function. *Cancer Sci.* 113 (3), 875–890. doi:10.1111/cas.15261

Vardhana, S. A., Hwee, M. A., Berisa, M., Wells, D. K., Yost, K. E., King, B., et al. (2020). Impaired mitochondrial oxidative phosphorylation limits the self-renewal of T cells exposed to persistent antigen. *Nat. Immunol.* 21 (9), 1022–1033. doi:10.1038/s41590-020-0725-2

Viale, A., Pettazzoni, P., Lyssiotis, C. A., Ying, H., Sanchez, N., Marchesini, M., et al. (2014). Oncogene ablation-resistant pancreatic cancer cells depend on mitochondrial function. *Nature* 514 (7524), 628–632. doi:10.1038/nature13611

Vyas, S., Zaganjor, E., and Haigis, M. C. (2016). Mitochondria and cancer. *Cell* 166 (3), 555–566. doi:10.1016/j.cell.2016.07.002

Wallace, D. C. (2012). Mitochondria and cancer. *Nat. Rev. Cancer* 12 (10), 685–698. doi:10.1038/nrc3365

Wang, J., Song, Y., Liu, T., Shi, Q., Zhong, Z., Wei, W., et al. (2015). Elevated expression of HABP1 is a novel prognostic indicator in triple-negative breast cancers. *Tumour Biol.* 36 (6), 4793–4799. doi:10.1007/s13277-015-3131-x

Ward, P. S., and Thompson, C. B. (2012). Metabolic reprogramming: A cancer hallmark even warburg did not anticipate. *Cancer Cell* 21 (3), 297–308. doi:10.1016/j.ccr.2012.02.014

Wrighton, K. H. (2013). Metabolism: Putting energy into mitophagy. *Nat. Rev. Mol. Cell Biol.* 14 (6), 324. doi:10.1038/nrm3586

Yagi, M., Uchiumi, T., Takazaki, S., Okuno, B., Nomura, M., Yoshida, S., et al. (2012). p32/gC1qR is indispensable for fetal development and mitochondrial translation: importance of its RNA-binding ability. *Nucleic Acids Res.* 40 (19), 9717–9737. doi:10.1093/nar/gks774

Yenugonda, V., Nomura, N., Kouznetsova, V., Tsigelny, I., Fogal, V., Nurmemmedov, E., et al. (2017). A novel small molecule inhibitor of p32 mitochondrial protein overexpressed in glioma. *J. Transl. Med.* 15 (1), 210. doi:10.1186/s12967-017-1312-7

Yu, H., Liu, Q., Xin, T., Xing, L., Dong, G., Jiang, Q., et al. (2013). Elevated expression of hyaluronic acid binding protein 1 (HABP1)/P32/C1QBP is a novel indicator for lymph node and peritoneal metastasis of epithelial ovarian cancer patients. *Tumour Biol.* 34 (6), 3981–3987. doi:10.1007/s13277-013-0986-6

Yu, Y. R., Imrichova, H., Wang, H., Chao, T., Xiao, Z., Gao, M., et al. (2020). Disturbed mitochondrial dynamics in CD8(+) TILs reinforce T cell exhaustion. *Nat. Immunol.* 21 (12), 1540–1551. doi:10.1038/s41590-020-0793-3

Zhai, X., Liu, K., Fang, H., Zhang, Q., Gao, X., Liu, F., et al. (2021). Mitochondrial C1qbp promotes differentiation of effector CD8(+) T cells via metabolic-epigenetic reprogramming. *Sci. Adv.* 7 (49), eabk0490. doi:10.1126/sciadv.abk0490

Zhang, X., Zhang, F., Guo, L., Wang, Y., Zhang, P., Wang, R., et al. (2013). Interactome analysis reveals that C1QBP (complement component 1, q subcomponent binding protein) is associated with cancer cell chemotaxis and metastasis. *Mol. Cell. Proteomics* 12 (11), 3199–3209. doi:10.1074/mcp.M113.029413

frontiers | Frontiers in Immunology

TYPE Original Research
PUBLISHED 23 December 2022
DOI 10.3389/fimmu.2022.1080388

Check for updates

OPEN ACCESS

EDITED BY
Erik J.M. Toonen,
Hycult Biotech, Netherlands

REVIEWED BY
Ben King,
Lund University, Sweden
Solaleh Emamgholipour,
Tehran University of Medical Sciences,
Iran

*CORRESPONDENCE
M. Bjerre
mette.bjerre@clin.au.dk

†These authors share first authorship

SPECIALTY SECTION
This article was submitted to
Molecular Innate Immunity,
a section of the journal
Frontiers in Immunology

RECEIVED 26 October 2022
ACCEPTED 09 December 2022
PUBLISHED 23 December 2022

CITATION
Dørflinger GH, Høyem PH,
Laugesen E, Østergaard JA, Funck KL,
Steffensen R, Poulsen PL, Hansen TK
and Bjerre M (2022) High MBL-
expressing genotypes are associated
with deterioration in renal function in
type 2 diabetes.
Front. Immunol. 13:1080388.
doi: 10.3389/fimmu.2022.1080388

COPYRIGHT
© 2022 Dørflinger, Høyem, Laugesen,
Østergaard, Funck, Steffensen, Poulsen,
Hansen and Bjerre. This is an open-
access article distributed under the
terms of the Creative Commons
Attribution License (CC BY). The use,
distribution or reproduction in other
forums is permitted, provided the
original author(s) and the copyright
owner(s) are credited and that the
original publication in this journal is
cited, in accordance with accepted
academic practice. No use,
distribution or reproduction is
permitted which does not comply with
these terms.

High MBL-expressing genotypes are associated with deterioration in renal function in type 2 diabetes

G. H. Dørflinger[1,2†], P. H. Høyem[3†], E. Laugesen[3], J. A. Østergaard[3,4], K. L. Funck[3,4], R. Steffensen[5], P. L. Poulsen[4,5], T. K. Hansen[4] and M. Bjerre[1*]

[1]Medical/Steno Aarhus Research Laboratory, Aarhus University, Aarhus, Denmark, [2]Department of Internal Medicine, Regional Hospital Gødstrup, Gødstrup, Denmark, [3]Department of Endocrinology and Internal Medicine, Aarhus University Hospital, Aarhus, Denmark, [4]Steno Diabetes Center Aarhus, Aarhus University Hospital, Aarhus, Denmark, [5]Regional Centre for Blood Transfusion and Clinical Immunology, Aalborg University Hospital, Aalborg, Denmark

Introduction: Accumulating evidence support that mannan-binding lectin (MBL) is a promising prognostic biomarker for risk-stratification of diabetic micro- and macrovascular complications. Serum MBL levels are predominately genetically determined and depend on MBL genotype. However, Type 1 diabetes (T1D) is associated with higher MBL serum levels for a given MBL genotype, but it remains unknown if this is also the case for patients with T2D. In this study, we evaluated the impact of MBL genotypes on renal function trajectories serum MBL levels and compared MBL genotypes in newly diagnosed patients with T2D with age- and sex-matched healthy individuals. Furthermore, we evaluated differences in parameters of insulin resistance within MBL genotypes.

Methods: In a cross-sectional study, we included 100 patients who were recently diagnosed with T2D and 100 age- and sex-matched individuals. We measured serum MBL levels, MBL genotype, standard biochemistry, and DEXA, in all participants. A 5-year clinical follow-up study was conducted, followed by 12-year data on follow-up biochemistry and clinical status for the progression to micro- or macroalbuminuria for the patients with T2D.

Results: We found similar serum MBL levels and distribution of MBL genotypes between T2D patients and healthy individuals. The serum MBL level for a given MBL genotype did not differ between the groups neither at study entry nor at 5-year follow-up. We found that plasma creatinine increased more rapidly in patients with T2D with the high MBL expression genotype than with the medium/low MBL expression genotype over the 12-year follow-up period ($p = 0.029$). Serum MBL levels did not correlate with diabetes duration nor with HbA1c. Interestingly, serum MBL was inversely correlated with body fat

percentage in individuals with high MBL expression genotypes both at study entry (p=0.0005) and 5-years follow-up (p=0.002).

Discussion: Contrary to T1D, T2D is not *per se* associated with increased MBL serum level for a given MBL genotype or with diabetes duration. Serum MBL was inversely correlated with body fat percentage, and T2D patients with the high MBL expression genotype presented with deterioration of renal function.

KEYWORDS

diabetes duration, mannan-binding lectin, MBL genotypes, albuminuria, T2D

Introduction

Increasing evidence supports that activation of the complement system plays an important role in developing diabetes-related micro- and macrovascular complications (1, 2). Mannan-binding lectin (MBL) is a serum protein primarily produced in the liver with the ability to distinguish between self and non-self-cells based on carbohydrate pattern recognition. MBL-binding to carbohydrate patterns initiates the lectin pathway, which leads to inflammatory cell recruitment, opsonization, and membrane attack complex formation (3). Hyperglycemia is associated with altered carbohydrate patterns present on the self-cell surface (4). Thus, MBL may cause inexpedient complement activation and tissue injury through binding to glycated self-tissue.

Serum MBL levels are largely determined genetically by six common single nucleotide polymorphisms (SNPs) in the *MBL2* gene, resulting in large inter-individual serum levels of MBL (5–7). The six SNPs in the *MBL2* gene are divided into three MBL expression genotypes; low MBL expression (O/O) with serum MBL levels below (≤100 µg/L), medium MBL expression (A/O) with serum MBL levels (101–1,000 µg/L), and high expression MBL (A/A) with serum MBL (>1,000 µg/L) (5, 8).

We and others have shown that high expression MBL genotypes and high MBL serum levels are associated with an increased risk of both micro- and macrovascular complications in patients with diabetes (9–12). Additionally, we observed a significantly increased mortality in patients with T1D and the high MBL expression genotype as compared with the patients with a "non-high-expression" MBL genotype (13). High MBL level has been reported as an independent marker of diabetic nephropathy and cardiovascular disease both in patients with T1D (9, 14) and T2D (15, 16). To our knowledge, no longitudinal studies have been performed in regard to MBL levels and development in renal function.

Several studies have found associations between serum MBL levels and insulin resistance (17, 18), though in nondiabetic settings low serum MBL levels were associated with insulin resistance. A study of weight loss and changes in insulin resistance and serum MBL levels showed that weight loss-induced changes in serum MBL concentration were positively associated with the increase in insulin sensitivity (18). This indicates that MBL levels are influenced by the degree of insulin resistance.

We have previously found significantly higher serum MBL levels among patients with T1D compared to healthy subjects (9, 12). However, the distribution of MBL genotypes did not differ between the groups (12) and therefore did not explain the phenotypic differences. These findings are supported by significantly higher serum MBL in patients with new-onset juvenile T1D as compared with their non-diabetic siblings matched for high-expression MBL genotype (19) as well as in animal studies (20).

It remains unknown if T2D *per se* is associated with altered MBL serum levels for a given MBL genotype. We have previously found comparable serum MBL levels in T2D and healthy individuals, but the relation to MBL genotype distribution was not clarified (21).

The current study aimed to investigate MBL serum level and MBL genotype in newly diagnosed T2D patients compared to age- and sex-matched healthy individuals. Additionally, we examined the relationship between MBL and renal decline as well as diabetes duration and insulin resistance.

Methods

Participants

100 patients with type 2 diabetes (T2D) were consecutively recruited from the outpatient clinic and 100 healthy subjects (controls) matched for age and sex were included in the study as previously described (22). Inclusion criteria at study entry were >18 years of age and, for patients, <5 years duration since

diagnosis of diabetes. The diabetes-related treatment for all patients with type 2 diabetes was managed by their general practitioner according to the normal guidelines including insulin-treatment, other antihyperglycemic treatments than insulin, and non-pharmacological treatment such as guidance in a lifestyle intervention. The healthy subjects were recruited by advertising in the local press, and excluded if diabetes was diagnosed by fasting glucose and oral glucose tolerance tests. General exclusion criteria were: acute or chronic infectious disease, end-stage renal failure, pregnancy or lactation, prior or present cancer, and contraindications to MRI scanning (claustrophobia, magnetic material in the body, and body weight > 120 kg). Three T2D patients and one healthy individual were excluded from the study due to missing genotype, no serum MBL sample, or withdrawal of consent.

The participants were invited for a 5-year follow-up visit and 63 patients with T2D and 72 healthy controls attended (23). In total, 37 T2D patients dropped out during follow-up for the following reasons: follow-up invitation rejected (n=24), no contact (n=6), GAD-positive (n=2), deaths (n=5). Twenty-eight participants from the control group dropped out during follow-up for the following reasons: follow-up invitation rejected (n=22), no contact (n=2), death (n=4). For this study, we obtained a dual-energy x-ray absorptiometry (DEXA), blood, and urine sampling, and the medical history of the participants was obtained by a questionnaire at both visits. A 12-year follow-up on clinical diabetes status was also performed: HbA1c, UACR, creatinine, and CRP were obtained from the medical records for the patients with T2D (n = 54).

The study was conducted according to the Declaration of Helsinki and was approved by the local Ethical Committee (1-10-72-349-13) and by the Danish Data Protection Agency (1-16-02-505-13), Denmark. All participants gave their written, informed consent to participate.

Blood analyses

Fasting blood samples were obtained from the antecubital vein. The serum was separated and stored at -80°C until further analysis. Serum MBL levels were measured using an in-house time-resolved immune-fluorometric assay with a lower detection level of 10 µg/L, as described previously by (24). The intra- and inter-assay variations (%CV) were below 10%. High-sensitive C-reactive protein (hsCRP) levels were quantified by an in-house assay as previously described by (25). The limit of detection was 0.005 µg/L. The intra- and inter-assay variations (%CV) were below 5 and 6%, respectively.

All other blood and urine samples were analyzed with accredited methods at the Department of Clinical Biochemistry at Aarhus University Hospital.

MBL expression genotypes

Genomic DNA was extracted from whole blood using the Maxwell 16 System Blood DNA Purification Kit (Promega, Madison, WI, USA) according to the manufacturer's protocol. Genotyping for six SNPs (single-nucleotide polymorphism) in the *MBL2* gene was performed using a real-time polymerase chain reaction with TaqMan SNP Genotyping Assays (Applied Biosystems, Foster City, CA, USA) as previously described by (26). Three SNPs are located within the promoter region of the *MBL2 gene* (rs11003125, rs7096206, rs12780112)]) and three SNPs (rs1800450, rs5030737, rs1800451) are located in exon 1 of the *MBL2 gene.* Because of linkage disequilibrium, the six SNPs give rise to seven major haplotypes: HYPA, LYQA, LYPA, LXPA, LYPB, LYQC, and HYPD that were further categorized into three MBL expression genotypes; low (O/O), medium (A/O), and high (A/A) as previously described (5, 7). These MBL expression genotypes has previously been shown to be correlated with serum MBL levels below (≤100 µg/L), (101–1,000 µg/L), and (>1,000 µg/L), respectively (8).

Blood pressure

Ambulatory blood pressure (BP) was measured at 20-min intervals for 24 h using Spacelab 90217 (Spacelabs Healthcare, Issaquah, Washington, USA) in between study days. Office BP was measured on the right arm with an appropriately sized cuff, and mean SBP and DBP were calculated as the average of three measurements obtained by an oscillometric BP monitor (Riester Champion N; Riester GmbH; Jungingen, Germany) after more than 5 min of rest in the seated position. Mean arterial BP (MAP) was calculated as DBP + 0.4 × pulse pressure (PP).

Body composition

A dual-energy radiograph absorptiometry scan (DEXA Discovery System; Hologic, Marlborough, Massachusetts, USA) was performed to estimate lean and fat body mass.

Urinary albumin-to-creatine ratio and estimated glomerular filtration rate

Urinary albumin excretion (UAE) was evaluated by albumin-to-creatinine ratios (ACR) in three morning urine samples. Patients were classified as microalbuminuric when at least two of three samples had urinary albumin-to-creatine ratios of 2.5:25 mg/mmol (men) and 3.5:35 mg/mmol (women) or above. The estimated glomerular filtration rate (eGRF) was

calculated from the MDRD study equation from serum creatinine (27).

Statistics

Data are presented as mean (± SD) if normally distributed and median (IQR) if non-normally distributed. Given the exploratory aims of the cohort study, power calculations were not carried out. MBL measurements below assay detection limit was set to 10 µg/L. Comparisons between groups were performed using an unpaired t-test for normally distributed data and Mann-Whitney's U-test for non-normally distributed data. Comparisons of paired data points were achieved with the Wilcoxon signed Rank sum test. Multiple linear regression (Generalized Linear Model) was used to allow adjustment for confounders. The Chi-square test tested the difference in distribution between non-continuous variables. Spearman's correlation analysis was used to estimate the strength of the association between non-normally distributed variables. P-values were considered significant if <0.05. To characterize the effect of MBL expression genotype on different biomarkers mixed model ANOVA was performed, where data passed the normality test. All calculations were performed in R.

Results

Clinical characteristics of the T2D patients and their age- and sex-matched healthy individuals are shown in Table 1. The diabetes duration at study entry was 1.9 years (IQR: 0.7;3.2). All the participants had well-adjusted treatment, regarding glycemia, blood lipids, and blood pressure. The T2D patients had a higher

TABLE 1 Characteristics of the participants at study entry. Data are mean ± SD unless other indicated.

	T2D Patients (n=100)	Healthy controls (n=100)	P-value
Sex (male/female) (%)	52/48	52/48	
Age (years)	58 (± 9.8)	58 (± 9.7)	0.892
Diabetes duration at study entry (years) (median (IQR))	1.9 (2.4)	–	–
Body Mass Index (kg/m^2)	30 (± 4.7)	26 (± 4.0)	<0.001
Fat percent (%)	32.8 (± 8.4)	28.8 (± 8.2)	0.001
HbA1c (mmol/mol)	48.0 (± 7.0)	37.9 ±(± 3.8)	<0.001
Total-cholesterol (mmol/L)	4.4 (± 0.8)	5.7 (± 1.0)	<0.001
LDL-cholesterol (mmol/L)	2.3 (± 0.7)	3.4 (± 1.0)	<0.001
HDL-cholesterol (mmol/L)	1.4 (± 0.3)	1.7 (± 0.6)	<0.001
Triglycerides (mmol/L)	1.6 (± 0.7)	1.4 (± 0.7)	0.036
Urine-albumin/creatinine ratio (mg/mmol) (median (IQR))	2.76 (4.23)	2.01 (2.13)	0.001
Estimated glomerular filtration rate (eGFR) (ml/min/1.73m^2) (median (IQR))	87.4 (22.5)	81.6 (16.2)	0.01
High sensitive CRP (mg/L) (median (IQR))	1.83 (2.68)	0.79 (1.01)	<0.001
24-h ABPM systolic BP (mmHg)	126 (± 18.8)	125 (± 12.5)	0.625
24-h ABPM diastolic BP (mmHg)	74 (± 7.4)	76 (± 7.7)	0.186
Smoking (present/previous/never) (%)	21/36/42	21/33/46	0.732
Diabetes treatment (insulin or insulin+other antihyperglycemic/other antihyperglycemic other/ lifestyle intervention) (%)	8/65/27	–	–
Statin treatment (%)	76	18	<0.001
Antihypertensive treatment (n %)	63	25	<0.001
Mannan binding Lectin (MBL) (median (IQR))			
Total group (µg/L)	643 (1152.5)	798 (1394)	0.274
Low MBL expression genotype (O/O), (µg/L)	15 (15.5), (n=15)	24 (30), (n=13)	0.527
Medium MBL expression genotype (A/O),(µg/L)	421 (412), (n=41)	402 (557.5), (n=43)	0.564
High MBL expression genotype (A/A), (µg/L)	1522 (1259), (n=42)	1691 (1255), (n=43)	0.384

body fat percentage, HbA1c, albumin/creatinine ratio (ACR), and hsCRP as compared to the healthy individuals. A significantly higher proportion of the T2D group was treated with statins, which may explain their significantly lower total- and LDL-cholesterol levels compared to the control group. Similarly, the T2D group was more often treated with one or more anti-hypertensive medications, which was probably the reason for T2D patients not having higher blood pressure than the control group. Data from 63 patients with T2D and 72 controls were available for 5-year follow-up (Table 2) and the baseline characteristics for the paired group have previously been described (28).

Distribution of MBL genotype (low-, medium- and high -expression) in the T2D group was 14,4%, 42,3% and 43,3%, respectively, which was similar to the control group, 13%, 43% and 43% (p=0.78). Serum MBL levels (regardless of genotype) did not differ between the T2D group and the control group (643 µg/L (IQR 251;1404) vs. 798 µg/L (IQR 266.5;1660.5), respectively, (p=0.274)) at study entry (Figure 1A) or after 5-years follow up (Figure 1B). Serum MBL levels remained similar in the two groups after adjustment for HbA1c, urine-albumin/creatinine ratio, antihypertensive treatment, and statin treatment in a multiple linear regression analysis.

Change in MBL level over time:

MBL levels in paired samples, for T2D patients with high MBL expression genotype, was 1949 µg/L (IQR 1200;2231) at study entry and 1548 µg/L (1051;2063) at the 5-year follow-up visit (p= 0.143) (Figure 2A). Analyzing the MBL ratio in a multiple linear regression model diabetes status (p= 0.01) and a high MBL expressing genotype (p= 0.005) seems to influence the outcome. MBL levels decreased significantly in the high MBL expression healthy control group over the 5 years from 1950 µg/L (IQR 1168;2526) at study

TABLE 2 Characteristics of the participants at 5-year follow-up. Data are mean ± SD unless other indicated.

	T2D Patients (n=63)	Healthy controls (n=72)	P-value
Sex (male/female) (n)	33/30	36/36	0.784
Age (years)	65.4 (± 9.6)	63.2 (± 10)	0.200
Diabetes duration at study entry (years) (median (IQR))	7.7 (2.5)		
Body Mass Index (kg/m^2)	30.2 (± 5.5)	26.8 (± 4.1)	<0.001
Fat percent (%)	34.7 (± 8.3)	31.2 (± 8.0)	0.016
HbA1c (%)	52.8 (± 11.6)	38.2 (± 3.4)	<0.001
Total-cholesterol (mmol/L)	3.98 (± 1.03)	5.3 (± 1.1)	<0.001
LDL-cholesterol (mmol/L)	1.9 (± 0.84)	3.1 (± 1.02)	<0.001
HDL-cholesterol (mmol/L)	1.3 (± 0.41)	1.6 (± 0.6)	<0.001
Triglycerides (mmol/L)	1.84 (± 1.8)	1.13 (± 0.9)	0.006
Urine-albumin/creatinine ratio (mg/mmol) (median (IQR))	3.3 (± 8)	0.6 (± 3.3)	0.012
High sensitive CRP (mg/L) (median (IQR))	1.8 (2.7)	1.1 (2.35)	0.39
24-h ABPM systolic BP (mmHg)	127.8 (± 13.5)	129.3 (± 12.4)	0.49
24-h ABPM diastolic BP (mmHg)	74.4 (± 7.3)	78.9 (± 7.8)	0.001
Smoking (present/previous/never) (%)	27/9/27	22/12/38	0.161
Diabetes treatment (insulin or insulin+other antihyperglycemic/other antihyperglycemic/lifestyle intervention) (%)	11/45/44		
Statin treatment (n)	53	16	<0.001
Antihypertensive treatment (n)	48	26	0.001
Mannan binding Lectin (MBL) (median (IQR))			
Total group (µg/L)	337 (1154)	584 (1215)	0.108
Low MBL expression genotype (O/O), (µg/L)	10 (0.50), (n=11)	16 (18), (n=10)	0.025
Medium MBL expression genotype (A/O), (µg/L)	295 (205), (n=27)	316 (231), (n=27)	0.426
High MBL expression genotype (A/A), (µg/L)	1548 (1012), (n=24)	1585 (1273), (n=32)	0.682

entry and to 1514 µg/L (IQR 1087;2022) after 5 years of follow-up, p=0.005 (Figure 2A). A similar decrease in serum MBL levels was found in the medium MBL expressing genotypes, where MBL levels decreased over the 5-year follow-up from 417 µg/L (IQR 265;518) to 295 µg/L (IQR: 147;352) for patients with T2D (p<0.001) and 347 µg/L (IQR 234;545) to 316 (IQR 197;427) in the healthy control subjects (p=0.003) (Figure 2B).

MBL was reduced in the low MBL expression genotype of patients with T2D, 15 µg/L (IQR 11;21) at study entry versus 10 µg/L (IQR 10;11) p=0.025 and in the control group, 24 µg/L (IQR: 10;30) to 16 µg/L (IQR: 11;29) p=0.4. However, due to the low sample size and values near the assay detection limit, the statistic should be interpreted cautiously in this subgroup. Adjustments for HbA1c, ACR, antihypertensive treatment, and statin treatment respectively did not change the results, neither in the total cohort nor after subdividing by MBL expressing genotype.

MBL difference between sex:

Men had higher serum MBL levels compared to women in the entire study group (991 µg/L (IQR 299;1831) vs. 460 µg/L (IQR 186; 1024), p= 0.004. This was also the case with men in the control group who had significantly higher serum MBL levels compared to women (1107 µg/L (IQR 318; 1950) vs. 442 µg/L (IQR 207; 1148), p= 0.03). However, the serum MBL levels was

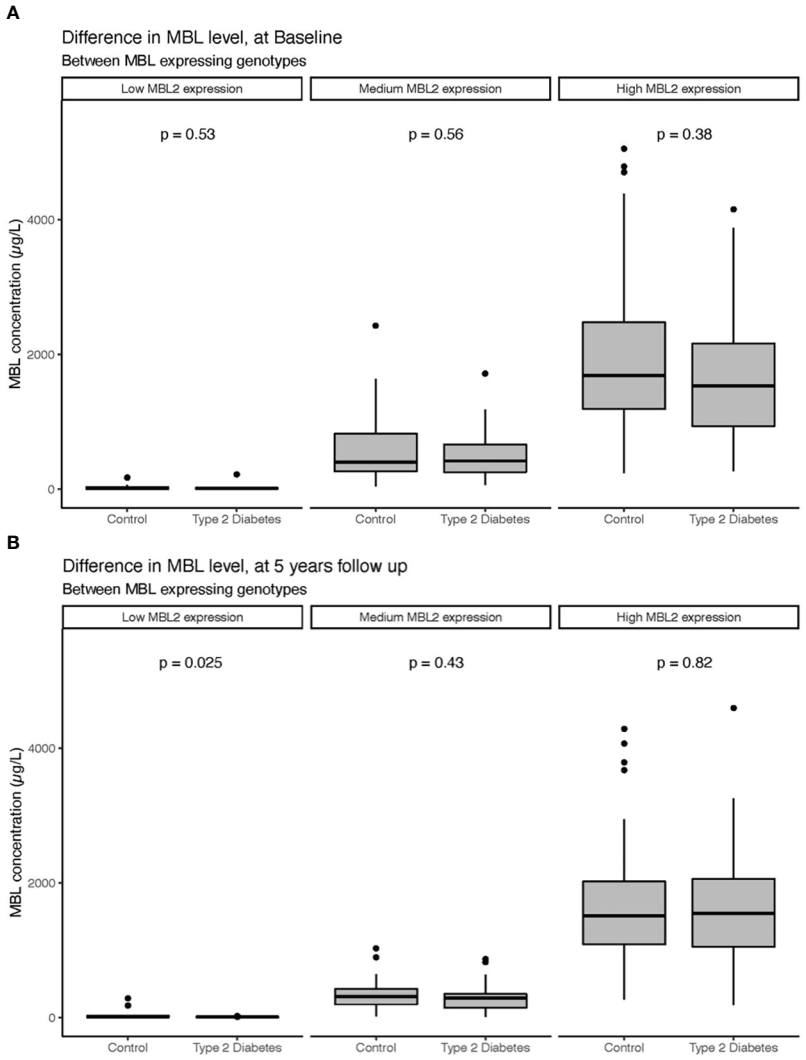

FIGURE 1
Serum levels of MBL at study entry **(A)** and 5-year follow-up **(B)** in patients with T2D and healthy controls divided according to MBL expressing genotypes. Bars represent medians, and boxes indicate IQRs. P-values are calculated with the Mann-Whitney U-test for differences between groups.

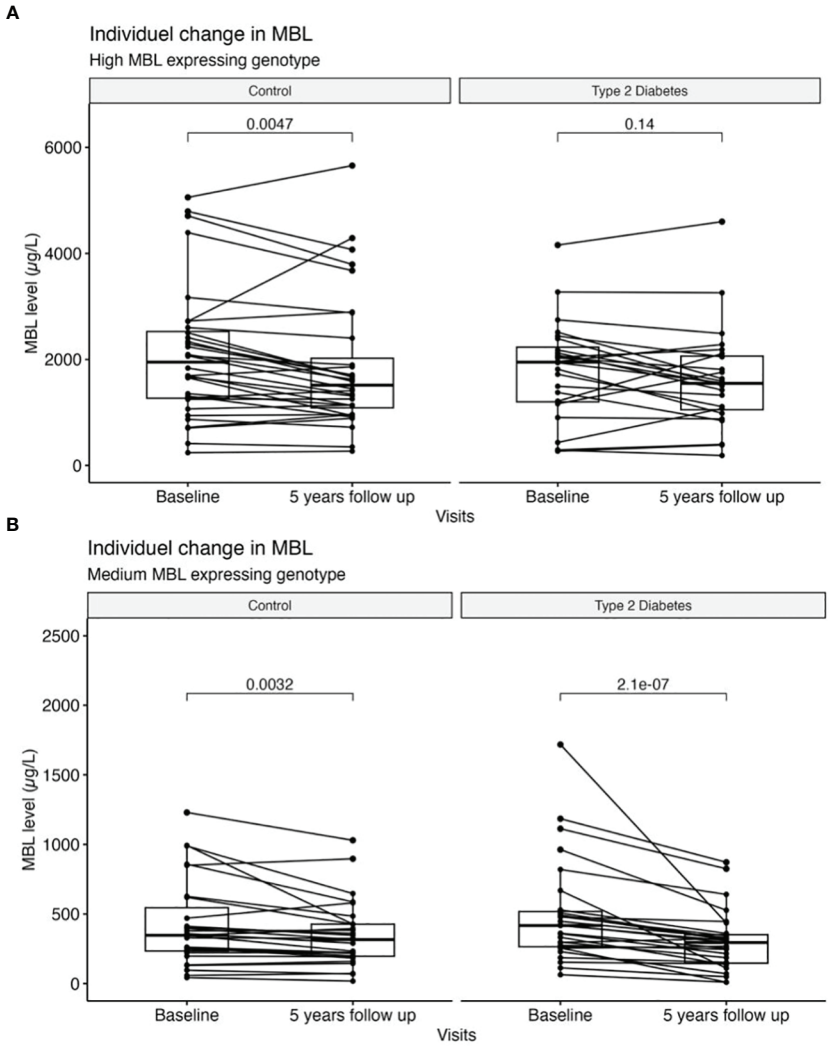

FIGURE 2
Individual change in serum levels of MBL between baseline and 5-year follow-up. **(A)** High MBL expressing genotypes and **(B)** medium MBL expressing genotypes are divided according to diabetes status. Bars represent medians, and boxes indicate IQRs. P-values are calculated with the Wilcoxon signed-rank test for differences between groups.

barely significantly higher in men with T2D compared to women (820 µg/L (IQR 296;1767) vs. 478 µg/L (IQR 192;933), p= 0.054). Unequal distribution of MBL genotypes between men and women in either group did not explain the difference.

Correlations between MBL, body fat %, and insulin resistance:

A weak inverse correlation between serum MBL level and body fat percentage was present in the entire group (ρ=-0.21, p=0.003). The outcome was not influenced by either HbA1c, antihypertensive treatment, statin treatment, or diabetes status when analyzing data in a multiple linear regression analysis. However, MBL expressing genotype significantly influenced the correlation between MBL and body fat percentage (p< 0.001). Subdividing by MBL genotype, a negative correlation with fat percentage was present for the high MBL expression genotype (ρ= -0.51, p=0.0005) (Figure 3). No correlations were found in medium or low MBL expression genotypes, which might be due to the low sample size. At the 5-year follow-up, these correlations were still present in the total cohort (ρ= -0.268, p=0.002).

No correlations were found between MBL and HOMA-β or HOMA-IR and no significant differences in MBL serum levels were found in T2D patients treated with insulin compared to those treated with other anti-diabetic medication or with lifestyle

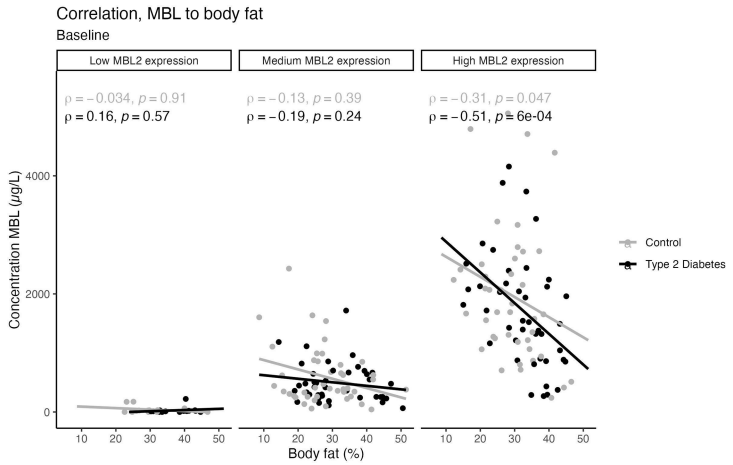

FIGURE 3
Scatter plots with trend lines showing a possible linear relationship between body fat percentage and Serum MBL levels, divided by MBL expressing genotype. Grey dots represent healthy individuals and the black dots represent participants with T2D. Spearman's correlation analysis was used to generate the correlation coefficients and associated p-value.

TABLE 3 An overview of Spearman's correlation analysis (r) and p-value for serum MBL levels and different variables according to diabetes status.

	MBL			
	T2D		Healthy controls	
Variables	ρ	p-value	ρ	p-value
Diabetes duration (years)	0.106	0.299	–	–
HbA1c (mmol/mol)	-0.181	0.075	0.071	0.487
UACR (mg/mmol)	-0.052	0.612	0.001	0.992
eGFR (ml/min/1.73m^2)	-0.184	0.070	-0.19	0.061
CRP (mg/L)	-0.133	0.191	0.051	0.615
BMI (kg/m^2)	-0.358	<0.001	-0.049	0.633
Fat percent	-0.271	0.007	-0.130	0.201

intervention alone. Also, no significant correlations were found between serum MBL level and HbA1c, hsCRP, total-, LDL- or HDL-cholesterol respectively at either study entry or 5-year follow-up (Table 3). Statin treatment or any antihypertensive treatment was not significantly associated with altered MBL serum levels.

The difference in biomarkers for nephropathy 12-year follow-up:

In participants with T2D, both eGFR and plasma creatinine differed significantly between high and medium/low expressing genotypes after 12 years of follow-up. The median for eGFR was 70.0 ml/min/1.73m^2 (IQR 55.5;85.5) in the high MBL expression genotype and 76.9 ml/min/1.73m^2 (IQR 80.9; 90.0) in the medium/low MBL expression genotype, (p= 0.012). Plasma creatinine was significantly higher in the high MBL expression genotype (76.7 µmol/L (IQR 68.6;98.2)) as compared to 70.0 µmol/L (IQR 68.6;98.2) in the medium/low MBL expression genotype (p= 0.02). A mixed model ANOVA was performed to compare the effect of the MBL genotype on the development of plasma creatinine. For patients with T2D, we found that plasma creatinine increased more rapidly in the high MBL expression genotype than in the medium/low MBL expression genotype (Figure 4), $F(2, 100) = 4.09$, $p = 0.029$. Statistical testing of hsCRP, HbA1c and the ACR did not uncover any significant differences after 12-years of follow-up.

Data from 54 patients with were available for our final analysis (Baseline characteristics of participants attending versus those not attending the follow-up visit are listed in Table S1). Participants lost to follow-up were significantly

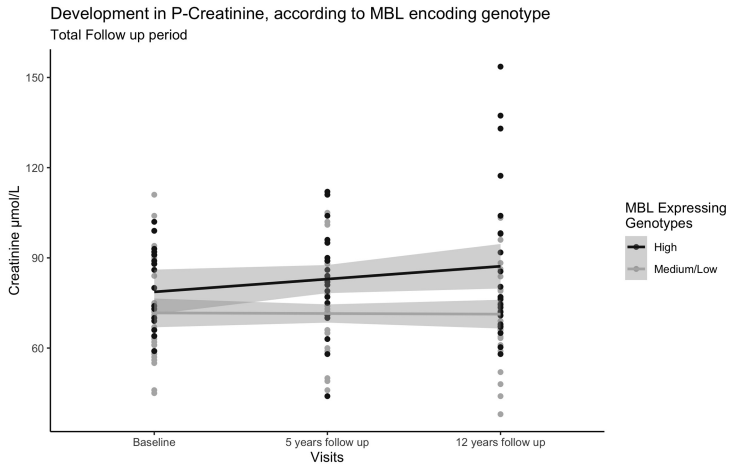

FIGURE 4
Dot plot with trend lines showing development in plasma creatinine in participants with T2D over the 12-year follow-up period. Black points represent participants with the high MBL expressing genotype (n=22) and the grey points represent participants with medium/low MBL expression genotypes (n=30). A mixed model ANOVA was performed to compare the effect of the MBL genotype on the development of plasma creatinine.

younger (p= 0.036) and had lower levels of low-density lipoprotein cholesterol (p= 0.012).

Discussion

We showed a similar distribution of MBL genotypes in newly diagnosed T2D patients as in age- and sex-matched healthy individuals. The distribution of MBL expression genotype in healthy individuals has previously been reported in a large Danish population study (n=9245) (29). They showed an MBL expression genotype frequency of 58% for high (A/A), 37% for the middle (A/O), and 5% for low (or MBL deficient O/O). We have recently shown a frequency slightly shifted towards MBL deficiency (A/A 54.5%, A/O 30.8%, and O/O 14.7%) in a group (n=3043) of newly diagnosed T2D patients (16). This distribution is similar to the distribution found in the present study.

Here we showed that serum MBL levels for a given MBL expression genotype were not altered in patients with recently diagnosed T2D as opposed to what has previously been observed in patients with T1D. In a group of patients with T2D and suspected acute myocardial infarction (30), the distribution of MBL genotypes was comparable to the background population, however, as a group, the T2D patients with AMI had higher serum MBL levels than previously reported in the background population of T2D patients, which may be related to vascular stress (30). Although serum MBL levels are known to be determined largely by polymorphisms in the *MBL2* gene, differences in circulating MBL levels of up to 10-fold can be found between individuals despite identical genotypes (6).

Portal hypoinsulinemia is present when the portal system is bypassed in subcutaneous insulin administration, as opposed to the pancreas-secreted insulin. The increased serum MBL level for a given genotype seen in T1D patients (9) has generated the hypothesis that the portal hypoinsulinemia characteristic of T1D may increase hepatic MBL synthesis. T2D, on the other hand, is characterized by insulin resistance, including hepatic insulin resistance. Thus, it seems plausible that T2D patients may also have high MBL serum levels for a given MBL genotype because of hepatic insulin resistance. However, the current study did not find evidence of this mechanism. A possible explanation for the lack of stimulation could be that hepatic insulin resistance is counteracted by increased endogenous insulin secretion, and as a net result does not affect MBL levels in T2D or the fact that the patients with T2D were not significantly more insulin resistant than the control group. The inclusion criteria included a maximum diabetes duration of 5 years. *In vitro* studies with human hepatocytes supported clinical observations of hormonal influence on MBL synthesis, with a significant increase in MBL expression after incubation with thyroid hormones and growth hormone (31), whereas insulin and IGF-1 had no effect. Interestingly, we found that MBL levels decreased after 5-years of follow-up, in healthy individuals with the high MBL expression genotype and remained unchanged in patients with T2D and was not explained by weight gain or change in fat percent.

We found a highly significant inverse correlation between MBL and fat percentage, determined by a whole-body DEXA scan, a very precise expression for obesity. This finding is supported by other studies. In women with polycystic ovary syndrome, obesity was associated with lower MBL levels (17). Among non-diabetic men,

MBL serum level was significantly lower in obese subjects than in lean subjects. Further, MBL was significantly correlated with insulin sensitivity as assessed by euglycemic-hyperinsulinemic clamp (18). In a study of nine morbidly obese women, MBL levels also correlated with insulin sensitivity (32). An alternative explanation for the inverse associations between MBL levels and insulin sensitivity, suggests that MBL acts as an anti-inflammatory protein by promoting phagocytic clearance of various inflammatory agents, which would in turn cause subjects with low MBL levels to develop chronic low-grade inflammation, and ensuing insulin resistance or obesity. However, we have shown that MBL levels are unaffected by significant weight loss in obese subjects (33). In the current study, we found no correlation between MBL and hsCRP, an accepted marker of low-grade inflammation. We, therefore, find the hypothesis of MBL as an anti-inflammatory protein less plausible and inclined to the view that MBL secretion is under the regulation of insulin.

It seems somehow contradictive though, that fat percent (followed by insulin resistance) is inversely correlated with MBL levels, whereas T2D patients (insulin resistant) overall have similar MBL levels to age- and sex-matched healthy individuals. We speculate that in obese, non-diabetic individuals, insulin resistance is overcome by increased endogenous insulin secretion, making their net insulin action in the liver able to suppress MBL production. At the time when endogenous insulin secretion can no longer counteract insulin resistance (at the debut of T2D) the net insulin action in the liver is lower and does not overall suppress MBL, although, within the group of T2D, there is still an increasing suppression of MBL with increasing fat percent and obesity.

We found that MBL serum levels were inversely associated with fat percent and triglycerides in the group of T2D patients at study entry and also after 5 years of diabetes duration for the fat percent. A common pathway in the form of peroxisome proliferator-activated receptor-α (PPARα) for regulating MBL levels and triglycerides has been suggested by (34). PPARs are ligand-activated transcription factors known to regulate glucose, fatty acid and lipoprotein metabolism, energy balance, and inflammation, among others (35). Along with the regulation of lipid and glucose metabolism, PPARα is an attractive candidate gene for the risk of metabolic syndrome and T2D. Hepatic *MBL2* gene expression and circulating MBL levels are reported to be stimulated by PPARα and fenofibrate in humans, linking PPAR to the regulation of innate immunity and complement activation in humans thus suggesting a possible role of MBL in lipid metabolism (34).

The present study shows an increasing plasma creatinine concentration over the 12-years follow-up period in the T2D patients with the high MBL expression genotype as compared to the medium/low MBL expression genotype. This corresponds with our previous findings, that the high MBL expression genotype was more frequent in T1D patients with diabetic nephropathy than in those with normal urinary albumin excretion (10) and that the presence of high MBL genotypes was associated with a 1.5-fold increased risk of developing nephropathy compared to patients with a 'low expression' MBL genotype (9) in patients with T1D. Also, serum MBL concentrations were significantly higher in patients with macroalbuminuria as compared to patients with normal albumin excretion rate, which persisted in the group of patients with high MBL expression genotypes (10), however, no SNPs in the *MBL2* gene were reported to confer risk of T1D or diabetic nephropathy. Cai et al. showed that serum and urine MBL levels were higher in patients with T2D and diabetic nephropathy who were prone to develop end-stage renal failure (36), and several studies have reported an association between high plasma MBL levels and the development of diabetic nephropathy in patients with T2D (15, 37, 38). In contrast, Adrian et al. showed that the MBL genotype was not associated with long-term clinical effects in patients with end-stage renal disease, however, only 8% of the patients in the study had diabetes (39). We have recently shown a U-shaped association between serum MBL, high MBL expression genotypes, and risk of cardiovascular events in a large group of patients newly diagnosed with T2D but not with all-cause mortality, supporting the role of MBL in vascular complications (16).

Limitations

The group of T2D patients is newly diagnosed, and well-regulated and may therefore not be representative of T2D patients in general. Unfortunately, only 63% (T2D) and 72% (healthy controls) of the individuals were able or willing to participate in the 5-years follow-up study and we were only able to receive 12-year follow-up biochemistry from patients with T2D but no data from the healthy control group.

Conclusion

In conclusion, we found similar MBL serum levels for any given MBL genotype between T2D patients and matched healthy control subjects. Furthermore, we found a significant inverse correlation between fat percentage and serum MBL levels in the high MBL expression genotype, but the mechanism for this finding needs to be further investigated. We show deterioration of renal function, illustrated by lower eGFR and increased serum creatinine in T2D patients with the high MBL expression genotype.

Data availability statement

The original contributions presented in the study are included in the article/Supplementary Material. Further inquiries can be directed to the corresponding authors.

Ethics statement

The studies involving human participants were reviewed and approved by the Central Denmark Region Committees on

Health Research Ethics (1-10-72-349-13) and by the Danish Data Protection Agency (1-16-02-505-13), Denmark. The patients/participants provided their written informed consent to participate in this study.

Author contributions

Conception and study design: GD, JØ, TH and MB. Patient recruitment and collection of clinical samples: PH, EL, KF, PP and TH. Methods and data analysis: GD, RS and MB. Manuscript drafts: GD and MB. All authors interpreted the data. All authors contributed to the article and approved the submitted version.

Funding

The study was funded by the A.P. Møller Foundation and Steno Diabetes Center Aarhus.

Acknowledgments

The authors thank the laboratory staff at the Medical/Steno Aarhus Research lab, for invaluable technical assistance.

Conflict of interest

The authors declare that the research was conducted in the absence of any commercial or financial relationships that could be construed as a potential conflict of interest.

Publisher's note

All claims expressed in this article are solely those of the authors and do not necessarily represent those of their affiliated organizations, or those of the publisher, the editors and the reviewers. Any product that may be evaluated in this article, or claim that may be made by its manufacturer, is not guaranteed or endorsed by the publisher.

Supplementary material

The Supplementary Material for this article can be found online at: https://www.frontiersin.org/articles/10.3389/fimmu.2022.1080388/full#supplementary-material

SUPPLEMENTARY TABLE 1
Baseline characteristics in participants included and not included in the 12 years follow-up data-analysis

References

1. Hansen TK. Mannose-binding lectin (MBL) and vascular complications in diabetes. *Horm Metab Res* (2005) 37 Suppl 1:95–8. doi: 10.1055/s-2005-861372

2. Flyvbjerg A. Diabetic angiopathy, the complement system and the tumor necrosis factor superfamily. *Nat Rev Endocrinol* (2010) 6(2):94–101. doi: 10.1038/nrendo.2009.266

3. Thiel S, Vorup-Jensen T, Stover CM, Schwaeble W, Laursen SB, Poulsen K, et al. A second serine protease associated with mannan-binding lectin that activates complement. *Nature* (1997) 386(6624):506–10. doi: 10.1038/386506a0

4. Fortpied J, Vertommen D, Van Schaftingen E. Binding of mannose-binding lectin to fructosamines: a potential link between hyperglycaemia and complement activation in diabetes. *Diabetes Metab Res Rev* (2010) 26(4):254–60. doi: 10.1002/dmrr.1079

5. Garred P, Larsen F, Seyfarth J, Fujita R, Madsen HO. Mannose-binding lectin and its genetic variants. *Genes Immun* (2006) 7(2):85–94. doi: 10.1038/sj.gene.6364283

6. Steffensen R, Thiel S, Varming K, Jersild C, Jensenius JC. Detection of structural gene mutations and promoter polymorphisms in the mannan-binding lectin (MBL) gene by polymerase chain reaction with sequence-specific primers. *J Immunol Methods* (2000) 241(1-2):33–42. doi: 10.1016/S0022-1759(00)00198-8

7. Madsen HO, Garred P, Thiel S, Kurtzhals JA, Lamm LU, Ryder LP, et al. Interplay between promoter and structural gene variants control basal serum level of mannan-binding protein. *J Immunol* (1995) 155(6):3013–20. doi: 10.4049/jimmunol.155.6.3013

8. Gadjeva M, Takahashi K, Thiel S. Mannan-binding lectin–a soluble pattern recognition molecule. *Mol Immunol* (2004) 41(2-3):113–21. doi: 10.1016/j.molimm.2004.03.015

9. Hansen TK, Tarnow L, Thiel S, Steffensen R, Stehouwer CD, Schalkwijk CG, et al. Association between mannose-binding lectin and vascular complications in type 1 diabetes. *Diabetes* (2004) 53(6):1570–6. doi: 10.2337/diabetes.53.6.1570

10. Kaunisto MA, Sjolind L, Sallinen R, Pettersson-Fernholm K, Saraheimo M, Frojdo S, et al. Elevated MBL concentrations are not an indication of association between the MBL2 gene and type 1 diabetes or diabetic nephropathy. *Diabetes* (2009) 58(7):1710–4. doi: 10.2337/db08-1495

11. Saraheimo M, Forsblom C, Hansen TK, Teppo AM, Fagerudd J, Pettersson-Fernholm K, et al. Increased levels of mannan-binding lectin in type 1 diabetic patients with incipient and overt nephropathy. *Diabetologia* (2005) 48(1):198–202. doi: 10.1007/s00125-004-1594-1

12. Hansen TK, Thiel S, Knudsen ST, Gravholt CH, Christiansen JS, Mogensen CE, et al. Elevated levels of mannan-binding lectin in patients with type 1 diabetes. *J Clin Endocrinol Metab* (2003) 88(10):4857–61. doi: 10.1210/jc.2003-030742

13. Ostergaard JA, Thiel S, Lajer M, Steffensen R, Parving HH, Flyvbjerg A, et al. Increased all-cause mortality in patients with type 1 diabetes and high-expression mannan-binding lectin genotypes: a 12-year follow-up study. *Diabetes Care* (2015) 38(10):1898–903. doi: 10.2337/dc15-0851

14. Zhao SQ, Hu Z. Mannose-binding lectin and diabetic nephropathy in type 1 diabetes. *J Clin Lab Anal* (2016) 30(4):345–50. doi: 10.1002/jcla.21861

15. Guan LZ, Tong Q, Xu J. Elevated serum levels of mannose-binding lectin and diabetic nephropathy in type 2 diabetes. *PloS One* (2015) 10(3):e0119699. doi: 10.1371/journal.pone.0119699

16. Gedebjerg A, Bjerre M, Kjaergaard AD, Steffensen R, Nielsen JS, Rungby J, et al. Mannose-binding lectin and risk of cardiovascular events and mortality in type 2 diabetes: A Danish cohort study. *Diabetes Care* (2020) 43(9):2190–8. doi: 10.2337/dc20-0345

17. Kowalska I, Fernandez-Real JM, Straczkowski M, Kozlowska A, Adamska A, Ortega F, et al. Insulin resistance is associated with decreased circulating mannan-binding lectin concentrations in women with polycystic ovary syndrome. *Diabetes Care* (2008) 31(4):e20. doi: 10.2337/dc07-1872

18. Fernandez-Real JM, Straczkowski M, Vendrell J, Soriguer F, Perez Del Pulgar S, Gallart L, et al. Protection from inflammatory disease in insulin resistance: the role of mannan-binding lectin. *Diabetologia* (2006) 49(10):2402–11. doi: 10.1007/s00125-006-0381-6

19. Bouwman LH, Eerligh P, Terpstra OT, Daha MR, de Knijff P, Ballieux BE, et al. Elevated levels of mannose-binding lectin at clinical manifestation of type 1

diabetes in juveniles. *Diabetes* (2005) 54(10):3002–6. doi: 10.2337/diabetes.54.10.3002

20. Ostergaard JA, Bjerre M, Dagnaes-Hansen F, Hansen TK, Thiel S, Flyvbjerg A. Diabetes-induced changes in mannan-binding lectin levels and complement activation in a mouse model of type 1 diabetes. *Scand J Immunol* (2013) 77(3):187–94. doi: 10.1111/sji.12027

21. Hansen TK, Gall MA, Tarnow L, Thiel S, Stehouwer CD, Schalkwijk CG, et al. Mannose-binding lectin and mortality in type 2 diabetes. *Arch Intern Med* (2006) 166(18):2007–13. doi: 10.1001/archinte.166.18.2007

22. Laugesen E, Hoyem P, Stausbol-Gron B, Mikkelsen A, Thrysoe S, Erlandsen M, et al. Carotid-femoral pulse wave velocity is associated with cerebral white matter lesions in type 2 diabetes. *Diabetes Care* (2013) 36(3):722–8. doi: 10.2337/dc12-0942

23. Funck KL, Laugesen E, Ovrehus K, Jensen JM, Norgaard BL, Dey D, et al. Increased high-risk coronary plaque burden is associated with arterial stiffness in patients with type 2 diabetes without clinical signs of coronary artery disease: a computed tomography angiographystudy.*JHypertens*(2017)35(6):1235–43.doi:10.1097/HJH.0000000000001308

24. Thiel S, Moller-Kristensen M, Jensen L, Jensenius JC. Assays for the functional activity of the mannan-binding lectin pathway of complement activation. *Immunobiology* (2002) 205(4-5):446–54. doi: 10.1078/0171-2985-00145

25. Holt CB, Ostergaard JA, Thiel S, Hansen TK, Mellbin L, Sorensson P, et al. Circulating lectin pathway proteins do not predict short-term cardiac outcomes after myocardial infarction. *Clin Exp Immunol* (2019) 198(1):94–100. doi: 10.1111/cei.13315

26. Klostergaard A, Steffensen R, Moller JK, Peterslund N, Juhl-Christensen C, Molle I. Sepsis in acute myeloid leukaemia patients receiving high-dose chemotherapy: no impact of chitotriosidase and mannose-binding lectin polymorphisms. *Eur J Haematol* (2010) 85(1):58–64. doi: 10.1111/j.1600-0609.2010.01443.x

27. Levey AS, Coresh J, Balk E, Kausz AT, Levin A, Steffes MW, et al. National kidney foundation practice guidelines for chronic kidney disease: evaluation, classification, and stratification. *Ann Internal Med* (2003) 139(2):137–47. doi: 10.7326/0003-4819-139-2-200307150-00013

28. Funck KL, Laugesen E, Hoyem P, Stausbol-Gron B, Kim WY, Ostergaard L, et al. Arterial stiffness and progression of cerebral white matter hyperintensities in patients with type 2 diabetes and matched controls: a 5-year cohort study. *Diabetol Metab Syndr* (2021) 13(1):71. doi: 10.1186/s13098-021-00691-y

29. Dahl M, Tybjaerg-Hansen A, Schnohr P, Nordestgaard BG. A population-based study of morbidity and mortality in mannose-binding lectin deficiency. *J Exp Med* (2004) 199(10):1391–9. doi: 10.1084/jem.20040111

30. Mellbin LG, Hamsten A, Malmberg K, Steffensen R, Ryden L, Ohrvik J, et al. Mannose-binding lectin genotype and phenotype in patients with type 2 diabetes and myocardial infarction: a report from the DIGAMI 2 trial. *Diabetes Care* (2010) 33(11):2451–6. doi: 10.2337/dc10-0903

31. Sorensen CM, Hansen TK, Steffensen R, Jensenius JC, Thiel S. Hormonal regulation of mannan-binding lectin synthesis in hepatocytes. *Clin Exp Immunol* (2006) 145(1):173–82. doi: 10.1111/j.1365-2249.2006.03101.x

32. Manco M, Fernandez-Real JM, Equitani F, Vendrell J, Valera Mora ME, Nanni G, et al. Effect of massive weight loss on inflammatory adipocytokines and the innate immune system in morbidly obese women. *J Clin Endocrinol Metab* (2007) 92(2):483–90. doi: 10.1210/jc.2006-0960

33. Hoyem PH, Bruun JM, Pedersen SB, Thiel S, Richelsen B, Christiansen JS, et al. The effect of weight loss on serum mannose-binding lectin levels. *Clin Dev Immunol* (2012) 2012:354894. doi: 10.1155/2012/354894

34. Rakhshandehroo M, Stienstra R, de Wit NJ, Bragt MC, Haluzik M, Mensink RP, et al. Plasma mannose-binding lectin is stimulated by PPARalpha in humans. *Am J Physiol Endocrinol Metab* (2012) 302(5):E595–602. doi: 10.1152/ajpendo.00299.2011

35. Grygiel-Gorniak B. Peroxisome proliferator-activated receptors and their ligands: nutritional and clinical implications–a review. *Nutr J* (2014) 13:17. doi: 10.1186/1475-2891-13-17

36. Cai K, Ma Y, Wang J, Nie W, Guo J, Zhang M, et al. Mannose-binding lectin activation is associated with the progression of diabetic nephropathy in type 2 diabetes mellitus patients. *Ann Transl Med* (2020) 8(21):1399. doi: 10.1186/s12967-020-02310-2

37. Zheng JM, Ren XG, Jiang ZH, Chen DJ, Zhao WJ, Li LJ. Lectin-induced renal local complement activation is involved in tubular interstitial injury in diabetic nephropathy. *Clin Chim Acta* (2018) 482:65–73. doi: 10.1016/j.cca.2018.03.033

38. Li XQ, Chang DY, Chen M, Zhao MH. Complement activation in patients with diabetic nephropathy. *Diabetes Metab* (2019) 45(3):248–53. doi: 10.1016/j.diabet.2018.04.001

39. Adrian T, Hornum M, Eriksson F, Hansen JM, Pilely K, Garred P, et al. Mannose-binding lectin genotypes and outcome in end-stage renal disease: a prospective cohort study. *Nephrol Dial Transplant* (2018) 33(11):1991–7. doi: 10.1093/ndt/gfy034

frontiers | Frontiers in Immunology

TYPE Original Research
PUBLISHED 17 January 2023
DOI 10.3389/fimmu.2023.1107063

Check for updates

OPEN ACCESS

EDITED BY
Erik J.M. Toonen,
Hycult Biotech, Netherlands

REVIEWED BY
Moon H. Nahm,
University of Alabama at Birmingham,
United States
Shanmuga Priyaa Madhukaran,
University of Texas Southwestern Medical
Center, United States

*CORRESPONDENCE
Anna S. Świerzko
aswierzko@cbm.pan.pl

†These authors have contributed
equally to this work and share
first authorship

SPECIALTY SECTION
This article was submitted to
Molecular Innate Immunity,
a section of the journal
Frontiers in Immunology

RECEIVED 24 November 2022
ACCEPTED 02 January 2023
PUBLISHED 17 January 2023

CITATION
Gajek G, Świerzko AS, Jarych D, Mikulski D, Kobiela P, Chojnacka K, Kufelnicka-Babout M, Szala-Poździej A, Chrzanowski J, Sobczuk K, Fendler W, Matsushita M, Domżalska-Popadiuk I, Mazela J, Kalinka J, Sekine H and Cedzyński M (2023) Association of low ficolin-2 concentration in cord serum with respiratory distress syndrome in preterm newborns.
Front. Immunol. 14:1107063.
doi: 10.3389/fimmu.2023.1107063

COPYRIGHT
© 2023 Gajek, Świerzko, Jarych, Mikulski, Kobiela, Chojnacka, Kufelnicka-Babout, Szala-Poździej, Chrzanowski, Sobczuk, Fendler, Matsushita, Domżalska-Popadiuk, Mazela, Kalinka, Sekine and Cedzyński. This is an open-access article distributed under the terms of the Creative Commons Attribution License (CC BY). The use, distribution or reproduction in other forums is permitted, provided the original author(s) and the copyright owner(s) are credited and that the original publication in this journal is cited, in accordance with accepted academic practice. No use, distribution or reproduction is permitted which does not comply with these terms.

Association of low ficolin-2 concentration in cord serum with respiratory distress syndrome in preterm newborns

Gabriela Gajek[1†], Anna S. Świerzko[1*†], Dariusz Jarych[1], Damian Mikulski[2†], Paulina Kobiela[3], Karolina Chojnacka[4], Maja Kufelnicka-Babout[5], Agnieszka Szala-Poździej[1], Jędrzej Chrzanowski[2], Katarzyna Sobczuk[5], Wojciech Fendler[2], Misao Matsushita[6], Iwona Domżalska-Popadiuk[3], Jan Mazela[7], Jarosław Kalinka[5], Hideharu Sekine[8] and Maciej Cedzyński[1]

[1]Laboratory of Immunobiology of Infections, Institute of Medical Biology, Polish Academy of Sciences, Łódź, Poland, [2]Department of Biostatistics and Translational Medicine, Medical University of Łódź, Łódź, Poland, [3]Department of Neonatology, Medical University of Gdańsk, Gdańsk, Poland, [4]II Department of Neonatology, Poznań University of Medical Sciences, Poznań, Poland, [5]Department of Perinatology, First Chair of Gynecology and Obstetrics, Medical University of Łódź, Łódź, Poland, [6]Department of Applied Biochemistry, Tokai University, Hiratsuka, Kanagawa, Japan, [7]Department of Neonatology, Poznań University of Medical Sciences, Poznań, Poland, [8]Department of Immunology, Fukushima Medical University, Fukushima, Japan

Introduction: Ficolin-2 is a serum pattern recognition molecule, involved in complement activation *via* the lectin pathway. This study aimed to investigate the association of ficolin-2 concentration in cord blood serum with complications related to premature birth.

Methods: 546 premature neonates were included. The concentration of ficolin-2 in cord blood serum was determined by a sandwich TRIFMA method. *FCN2* genetic variants were analysed with RFLP-PCR, allele-specific PCR, Sanger sequencing or allelic discrimination using TaqMan probes method.

Findings: Cord blood serum ficolin-2 concentration correlated positively with Apgar score and inversely with the length of hospitalisation and stay at Neonatal Intensive Care Unit (NICU). Multivariate logistic regression analysis indicated that low ficolin-2 increased the possibility of respiratory distress syndrome (RDS) diagnosis [OR=2.05, 95% CI (1.24-3.37), p=0.005]. Median ficolin-2 concentration was significantly lower in neonates with RDS than in premature babies without this complication, irrespective of *FCN2* gene polymorphisms localised to promoter and 3'untranslated regions: for patients born <33 GA: 1471 ng/ml *vs.* 2115 ng/ml (p=0.0003), and for patients born ≥33 GA 1610 ng/ml *vs.* 2081 ng/ml (p=0.012). Ficolin-2 level was also significantly lower in neonates requiring intubation in the delivery room (1461 ng/ml *vs.* 1938 ng/ml, p=0.023) and inversely correlated weakly with the duration of respiratory support (R=-0.154, p<0.001). Interestingly, in the neonates born at GA <33, ficolin-2 concentration permitted differentiation of those with/without RDS [AUC=0.712, 95% CI (0.612-0.817), p<0.001] and effective separation of babies with mild RDS from those with

moderate/severe form of the disease [AUC=0.807, 95% CI (0.644-0.97), p=0.0002].

Conclusion: Low cord serum ficolin-2 concentration (especially in neonates born at GA <33 weeks) is associated with a higher risk of developing moderate/severe RDS, requiring respiratory support and intensive care.

KEYWORDS

FCN2, ficolin-2, newborn, prematurity, preterm, respiratory distress syndrome (RDS)

1 Introduction

Preterm birth is often associated with multiple pregnancies, infections and gestational diabetes, however most (even >60%) cases are unexplained (1). Common prematurity-associated complications include neonatal sepsis, necrotizing enterocolitis (NEC), intraventricular haemorrhage, patent ductus arteriosus (PDA) and retinopathy. Due to smaller surface area for gas exchange, thicker blood-gas barrier and fewer type II alveolar epithelial cells, respiratory problems are more common in preterm than in term infants (2) and are the main reasons for morbidity and mortality in premature babies. If not recognised and managed quickly, respiratory disease can escalate to respiratory failure and cardiopulmonary arrest (3). The similarities in clinical signs for common causes of respiratory distress like pneumonia, transient tachypnea of neonates (TTN), respiratory distress syndrome (RDS) and meconium aspiration syndrome (MAS) make it difficult to distinguish between them (4).

Human lung development begins between the 4th and 7th weeks of pregnancy and the formation of alveoli continues until early postnatal life (5). RDS is a multifactorial and complex disease associated with inadequate pulmonary surfactant production by immature lungs, resulting in microatelectasis, severe hypoxia, and acidosis (3, 6). The development of RDS may be caused by inadequate clearance of fetal lung liquid as well (7). Genetic susceptibility to RDS in preterm infants has also been demonstrated (8). RDS long-term complications include bronchopulmonary dysplasia (BPD) and asthma. In term and post-mature neonates, respiratory distress may be associated with meconium aspiration syndrome (MAS), and with a higher incidence of asthma in later life.

The complement system is a crucial mediator of the immune response to infection. It interacts with other innate mechanisms as well as acquired immunity, and engages in cross-talk with other endogenous cascades, like the coagulation network (9). It also contributes to cell homeostasis (10), tissue development and repair (11, 12), and reproduction (13). Low activity of classical, lectin or alternative routes of complement in sera of premature babies may enhance their vulnerability to infections due to impaired clearance of pathogens *via* opsonophagocytosis or direct lysis of pathogens. The lectin pathway (LP) of complement activated by microbial glycoconjugates may play a crucial role in the protection of neonates from infections due to their poor response to T-independent polysaccharide antigens and limited transplacental transfer of maternal antibodies [reviewed in (14)].

Knowledge concerning associations of LP with complications related to prematurity is still limited. Several reports have documented correlations of LP-specific factors in serum with gestational age [reviewed in (14)]. One of the pattern-recognition molecules initiating the lectin pathway of complement is ficolin-2. In a large cohort of neonates (recruited consecutively, including approx. 18% preterms), relative ficolin-2 insufficiency was shown to be associated with prematurity, low birthweight and perinatal infections (15). Ficolin-2 was also demonstrated to contribute to the clearance of serotype III group B streptococci – a common cause of neonatal sepsis (16), often clinically and radiographically indistinguishable from RDS (17). In women diagnosed with pre-eclampsia, serum ficolin-2 concentration was significantly lower in comparison with uncomplicated pregnancies (18, 19). Moreover, deposition of ficolin-2 on apoptotic trophoblasts in preeclampsia was observed (18).

So far, published reports have not demonstrated a strong relationship between prematurity-associated complications and the frequency of promoter or exon 8 *FCN2* gene variants, known to markedly influence ficolin-2 level/activity (20). Recently we analysed 15 polymorphisms localised to the *FCN2* 3'untranslated region (3'UTR) in a large group of preterm babies. Our data revealed that reconstructed diplotypes, including both the G variant at rs4521835 and the C variant at rs73664188 (classified into proposed group VI) were associated with a significantly lower ficolin-2 concentration in cord serum (21).

Ficolin-2 is considered to be an important factor of innate immunity. Several reports suggested its association not only with infections but also with non-infectious diseases and its potential application as a prognostic marker (22–24). In this study, we examined ficolin-2 levels in cord-blood serum of preterm neonates in the context of prematurity-associated complications and its possible usefulness for their diagnosis. Moreover, the genetically determined origin of the differences in ficolin-2 levels observed was verified *via* analysis of *FCN2* gene polymorphisms.

2 Material and methods

2.1 Subjects

Cord blood samples from 546 Polish preterm neonates, including 118 born at gestational age (GA) <33rd weeks (range 24-32 weeks), and 428 born between 33rd and 37th weeks of pregnancy were

obtained from the Department of Newborns' Infectious Diseases (Poznań University of Medical Sciences, Poland), Department of Neonatology (Medical University of Gdańsk, Poland) and Department of Perinatology (Medical University of Łódź, Poland). This cohort included 504 subjects investigated previously (21).

The basic clinical data are presented in Table 1. The clinical data for neonates separated into the subgroups born at GA <33 and GA ≥33 are presented in Supplementary Table 1. The study was approved by the corresponding local ethics committees (Bioethics Committee of The Karol Marcinkowski Poznań University of Medical Sciences, Independent Bioethics Committee for Scientific Research at Medical University of Gdańsk, Bioethics Committee of The Medical University of Łódź). Written informed parental consent was obtained. This work conforms to the provisions of the Declaration of Helsinki.

Cord samples were taken at birth into sodium citrate (for DNA isolation) and clot activator (for serum) containing tubes. Isolated serum was kept at -80°C. DNA was isolated using GeneMATRIX Quick Blood Purification Kit (EURx Ltd. Gdańsk, Poland), according to the manufacturer's protocol.

TABLE 1 Clinical data of preterm neonates included into the study (n=546).

Variable	N (%)
Sex	M: 285 (52.2) F: 261 (47.8)
GA <33 GA ≥33	118 (21.6%) 428 (78.4%)
Birthweight <1500 g	62 (11.4)
Multiple pregnancy	106 (19.4)
Gestational diabetes mellitus (GDM)	90 (16.5)
Hypertension in mother	70 (12.8)
Pre-eclampsia	25 (4.6)
Preterm premature rupture of membranes (pPROM)[1]	99 (18.1)
Antenatal corticosteroid therapy[2]	221 (40.4)
Caesarean section	349 (63.9)
Early-onset infection (EOI)[3]	81 (14.8)
Respiratory distress syndrome (RDS)[4]	140 (25.6)
Patent ductus arteriosus (PDA)	14 (2.6)
Tachycardia[5]	36 (6.6)
Necrotizing enterocolitis (NEC)	17 (3.1)
Perinatal hypoxia[6]	20 (3.7)
Respiratory support[7]	163 (29.9)
Delivery room intubation	31 (5.7)
Mean length of hospitalisation (days)[8]	15.3
Mean length of stay at NICU (days)[8]	5.0

[1]-more than 24 h before delivery, [2]- at least one course, [3]- caused by variety of agents (including *staphylococci, E. coli, Klebsiella* sp. and GBS; in majority of cases however, agents were not identified and infection was diagnosed basing on clinical symptoms), [4]- respiratory distress with an oxygen requirement to maintain oxygen saturations of ≥90%, accompanied by a characteristic chest radiograph, [5]- >160 per min, [6]- pH ≤7.0 or BE ≤12 mM/ml in umbilical artery or within 1h of life, [7]- mechanical ventilation, continuous positive airway pressure (CPAP) or both, [8]- after excluding three cases of death

2.2 Determination of ficolin-2 concentration in cord sera

Ficolin-2 concentrations in 481 cord blood serum samples were determined by TRIFMA, as described by Świerzko et al. (25). Briefly, anti-ficolin-2 mAb (ABS 005-16, BioPorto Diagnostics, Denmark) for 384 HB Optiplate coating, whereas biotinylated mAb (GN4, Hycult Biotech, The Netherlands) and Eu^{3+}-labelled streptavidin (Perkin Elmer, USA) for protein detection were used. The 25th percentile (determined for the whole group or for subgroups of neonates born at GA <33 and at GA ≥33) was taken as an indicator of low ficolin-2 concentration. Although the influence of tubes used for blood collection on concentration of ficolin-2 determined in serum was evidenced (26, 27), tubes of the same type were used in all three clinics collecting samples what makes all data fully comparable.

2.3 Determination of *FCN2* polymorphisms

The differences in ficolin-2 levels were analysed in the context of the *FCN2* gene promoter haplotype GGCA [corresponding to single nucleotide polymorphisms at positions: -986 (rs3124952); -602 (rs3124953); -64 (rs7865453); -4 (rs17514136)] (28) and 3'UTR group VI diplotype (21), both associated with low ficolin-2 concentration.

Briefly, promoter polymorphisms at positions -986 and -602 were investigated by PCR-RFLP analysis in 503 DNA samples, according to the procedures published by Metzger et al. (29). SNP at positions -64 and -4 were determined using allele-specific PCR or PCR-RFLP, respectively, as described by Szala et al. (30), with minor modifications. Polymorphisms in the *FCN2* 3'UTR were determined *via* Sanger sequencing or allelic discrimination using TaqMan probes (21). Haplotypes and diplotypes were created using Haploview 4.2 and PHASE software.

2.4 Statistical analysis

To determine whether continuous variables had a normal distribution, the Shapiro–Wilk test was conducted. The ficolin-2 concentrations were compared using Mann-Whitney *U* test or Kruskal-Wallis test with *post-hoc* Dunn test, depending on the number of compared groups. Spearman's rank correlation test assessed the correlations. The frequencies of genotypes/clinical complications were compared by Fischer's exact or χ^2 test when appropriate. Odds ratios were calculated using online MedCalc software (https://www.medcalc.org). Clinical associations of low ficolin-2 concentration were verified using multiple logistic regression analysis. The predictive power of ficolin-2 was evaluated by receiver operating characteristics (ROC) curves and area under the curve (AUC) analysis. The Statistica (version 13.3, TIBCO Software) and SigmaPlot (version 12, Systat Software) software were used for data management and statistical calculations. P values <0.05 were considered statistically significant.

3 Results

3.1 Low ficolin-2 levels in the context of basic clinical characteristics and outcomes

Median ficolin-2 concentrations differed markedly between neonates born before the 33rd week of gestation and those born at GA ≥33 (median 1639 ng/ml *vs* 2036 ng/ml, p=0.0024) (Supplementary Figure 1A). Moreover, in neonates with very low birthweight (VLBW, <1500 g), ficolin-2 was significantly lower than in babies with higher birthweight (median 1496 ng/ml *vs* 2018 ng/ml, p=0.0001) (Supplementary Figure 1B).

Weak but significant correlations of ficolin-2 concentration with Apgar 1' and Apgar 5' scores were observed (R=0.18, p=0.0002 and R=0.24, p<0.0001, respectively). The median ficolin-2 level for babies with Apgar 1' score <7 (1559 ng/ml) was lower than that for those with Apgar 1' score ≥7 (2014 ng/ml, p=0.01) (Supplementary Figure 1C). In the case of Apgar 5', medians were 1409 ng/ml and 2042 ng/ml, respectively (p=0.0098) (Supplementary Figure 1D).

Moreover, ficolin-2 inversely correlated with the length of hospitalisation (R=-0,2, p<0,0001) and the length of stay at the neonatal intensive care unit (NICU) (R=-0.13, p=0.007). In neonates who stayed in the hospital for >2 weeks, the median ficolin-2 concentration was significantly lower (1646 ng/ml) than in babies, who stayed in the hospital for a shorter time (2094 ng/ml, p=0.0001) (Supplementary Figure 1E). In the group of neonates with ficolin-2 levels below 1295 ng/ml (<25th percentile), the length of stay at the neonatal ward was generally longer (mean 18 days, range 2-78 days) than in those with higher ficolin-2 (mean 14 days, range 1-91 days, p=0.02). Furthermore, ficolin-2 concentration was significantly lower (1749 ng/ml) in neonates who stayed at least 5 days at NICU in comparison with babies who stayed there for up to 4 days or did not need intensive care (2018 ng/ml, p=0.022) (Supplementary Figure 1F). It is worth noting that all neonates with ficolin-2 concentration <25th percentile and born at GA <33 required hospitalisation at NICU and their stay was generally longer than that of newborns with the same GA but with higher ficolin-2 levels [22.8 days (range 4-61 days) *vs.* 14.9 days (range 0-84 days), p=0.002].

3.2 Low ficolin-2 levels in the context of complications associated with prematurity

The data concerning relationships between low (<25th percentile) ficolin-2 concentration in the cord blood and selected prenatal clinical complications of prematurity in the whole cohort are presented in Table 2. Additionally, *FCN2* gene promoter haplotype GGCA and 3'UTR diplotype group VI were included in the analysis. Corresponding analyses between subgroups depending on gestational age (<33 weeks and ≥33 weeks, in the context of a wider panel of complications) are presented in Supplementary Table 2.

Logistic univariate regression analysis revealed associations of low ficolin-2 with VLBW, *FCN2* promoter GGCA haplotype and group VI 3'UTR diplotype (Table 2). In contrast, premature rupture of membranes (pPROM) was associated with higher ficolin-2 concentrations. Multivariate analysis confirmed that low birthweight [OR=2.14, 95%CI (1.14-4.02), p=0.018] and GGCA haplotype [OR=2.57, 95%CI (1.26-5.26), p=0.0098], (but not the group VI 3'UTR diplotype) independently predicted low ficolin-2 concentration (Table 2).

3.3 Low ficolin-2 levels in the context of respiratory distress syndrome

Next, the univariate and multivariate logistic regression analysis for RDS as the dependent variable was performed (Table 3). According to the final model, the likelihood of RDS development was increased in neonates with low ficolin-2 cord blood serum concentration [OR=2.05, 95% CI (1.24-3.37), p=0.0051]. It was also associated with shorter GA [OR=7.64, 95% CI: (4.34-13.43), p<0.0001], very low birthweight [OR=3.2, 95% CI (1.46-7.03), p=0.0037], and PDA [OR=11.04, 95% CI (1.87-65.02), p=0.008].

Median ficolin-2 concentration was significantly lower in newborns diagnosed with RDS compared with neonates without this complication (for patients born <33 GA: 1471 *vs.* 2115 ng/ml, p=0.0003; for patients born ≥33 GA: 1610 *vs.* 2081 ng/ml; p=0.012) (Figure 1A). For thirty-eight neonates with RDS born at GA <33, data about disease severity were available. Kruskal-Wallis test revealed a significant difference in ficolin-2 levels among groups of babies with no RDS, those with mild and more advanced RDS (p=0.015) (medians: 2115 ng/ml, 2002 ng/ml and 1275 ng/ml, respectively). The *post-hoc* analysis showed significantly lower ficolin-2 in cord blood serum in neonates diagnosed with more advanced compared with those with mild RDS (p=0.0017) or without this complication (p=0.0084) (Figure 1B).

The management of RDS includes exogenous surfactant therapy (by intubation in the delivery room) as well as assisted ventilation. Ficolin-2 concentrations were lower in babies requiring intubation in the delivery room than in those who did not require it (1461 *vs.* 1938 ng/ml, p=0.023) (Figure 2A). The duration of respiratory support (mechanical ventilation and/or continuous positive airway pressure, CPAP) inversely correlated with ficolin-2 concentration in cord serum (R=-0.154, p<0.001).

Furthermore, Kruskal-Wallis analysis showed a statistically significant difference in the level of ficolin-2 across three groups: without respiratory support, with respiratory support duration <10 days and with respiratory support ≥10 days (p=0.001) (Figure 2B). Patients who did not require respiratory support had higher median ficolin-2 concentration (median 2089 ng/ml) compared with patients requiring ≥10 days of respiratory support (median 1447 ng/ml, *post-hoc* Dunn test p=0.0017) but compared with neonates on <10 days of respiratory support the difference was not statistically significant (median 1782 ng/ml, p=0.208).

The potential of ficolin-2 to discriminate between patients with and without RDS was also tested. When all samples were analysed, the selective power of ficolin-2 appeared rather low [AUC=0.643, 95% CI (0.588-0.699), p<0.0001] (Figure 3A). When analysis was performed for neonates born at GA <33 only, it increased to AUC=0.712 [95% CI (0.612-0.817), p=0.0003] (Figure 3B). Then, we developed a simple logistic regression model with GA and birthweight (≥/<1500 g) as independent variables. This model yielded AUC of 0.75 [95% CI

10.3389/fimmu.2023.1107063

TABLE 2 Univariate and multivariate[1] regression analysis of potential factors for low ficolin-2 concentration (below 25th percentile)[2] in the whole cohort.

Variable	Univariate analysis			Multivariate analysis		
	OR	95%CI	*p*	OR	95%CI	*p*
GA <33 weeks	1.33	0.82-2.15	0.2478	-	-	-
Birthweight <1500 g	**2.12**	**1.17-3.84**	**0.0126**	**2.14**	**1.14-4.02**	**0.0177**
Promoter GGCA haplotype	**3.63**	**2.06-6.40**	**<0.0001**	**2.57**	**1.26-5.26**	**0.0098**
3'UTR diplotype group VI	**2.46**	**1.54-3.93**	**0.0002**	1.51	0.85-2.70	0.1641
Sex (Male)	1.31	0.86-2.01	0.2107	–	–	–
GDM	1.01	0.58-1.79	0.9634	–	–	–
pPROM	**0.55**	**0.31-0.99**	**0.0460**	0.55	0.29-1.05	0.0685
Fetal growth restriction (FGR)	1.55	0.83-2.88	0.1698	–	–	–
Intrauterine hypoxia	0.81	0.22-2.96	0.7512	–	–	–
Hypertension in pregnancy	1.17	0.63-2.17	0.6134	–	–	–

[1]- multivariate analysis data are shown when p<0.1 in univariate analysis; [1]- 1295 ng/ml. The values are marked in bold when statistically significant.

(0.70-0.81, p<0.001] with a sensitivity 59.5% and specificity 88.0%. Ficolin-2 level incorporation into the model significantly increased its performance up to AUC 0.80 [95% CI (0.74-0.85), p=0.011) (Figure 3C). Importantly, sensitivity of this model reached 69.1% with preserved specificity (79.8%). Furthermore, ficolin-2 concentration could better differentiate between mild and moderate/severe RDS in newborns born at GA <33 [AUC=0.807, 95% CI (0.644-0.97), p=0.0002] with sensitivity of 75% and specificity of 91% at cut off 1469 ng/ml (Figure 3D). It should however be remembered that the number of samples with corresponding data concerning disease severity was rather small.

4 Discussion

The main goal of this work was to investigate the association of ficolin-2 concentration at birth with the risk of complications related to prematurity. We demonstrated that low (<25th percentile) ficolin-2

TABLE 3 Univariate and multivariate logistic regression analysis[1] of potential factors for RDS development.

Variable	Univariate analysis			Multivariate analysis		
	OR	95%CI	*p*	OR	95%CI	*p*
GA <33 weeks	**11.41**	**7.14-18.23**	**<0.0001**	**7.64**	**4.34-13.43**	**<0.0001**
Birthweight <1500 g	**9.75**	**5.39-17.63**	**<0.0001**	**3.20**	**1.46-7.03**	**0.0037**
Low ficolin-2	**2.51**	**1.64-3.85**	**<0.0001**	**2.05**	**1.24-3.37**	**0.0051**
Promoter GGCA haplotype	1.33	0.75-2.35	0.326	–	–	–
3'UTR diplotype group VI	1.31	0.82-2.07	0.255	–	–	–
Sex (Male)	1.24	0.84-1.84	0.273	–	–	–
Caesarean section	1.45	0.95-2.20	0.081	1.36	0.81-2.30	0.247
GDM	1.37	0.84-2.25	0.207	–	–	–
Preeclampsia	1.66	0.72-3.85	0.236	–	–	–
pPROM	1.11	0.68-1.82	0.667	–	–	–
Fetal growth restriction (FGR)	0.98	0.54-1.80	0.956	–	–	–
NEC	**13.65**	**3.83-48.66**	**0.0001**	3.90	0.86-17.57	0.0767
PDA	**18.80**	**4.15-85.1**	**0.0001**	**11.04**	**1.87-65.02**	**0.008**
Tachycardia	1.23	0.57-2.65	0.59	–	–	–
Hypertension in pregnancy	1.01	0.57-1.80	0.966	–	–	–

[1]- multivariate analysis data are shown when p<0.1 in univariate analysis. The values are marked in bold when statistically significant.

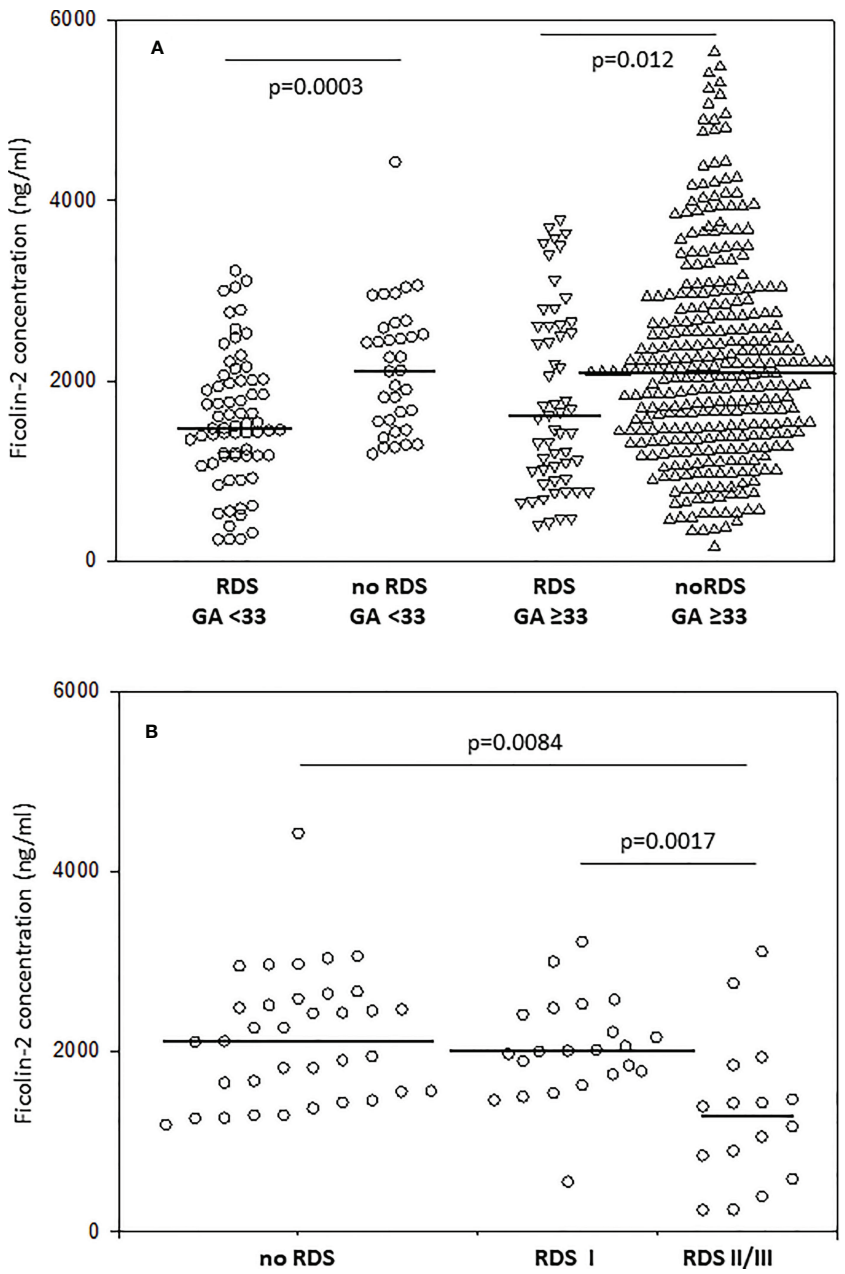

FIGURE 1
The comparison of ficolin-2 cord blood serum concentration in preterm neonates with and without respiratory distress syndrome (RDS), depending on gestational age **(A)** and disease severity in neonates delivered at GA <33 **(B)**. The horizontal lines mark median values. Medians were compared with the use of Mann-Whitney *U* test **(A)** and Kruskal-Wallis test (p=0.015) with *post-hoc* Dunn test **(B)**.

is associated with a lower Apgar score, prolonged hospitalisation and stay at NICU. Moreover, a strong relationship with increased probability of RDS was found (Table 3). Therefore, immediately after birth preterms with low ficolin-2 levels are generally in poorer condition than those with higher concentrations of this protein.

RDS was originally described as hyaline membrane disease-(HMD)-associated vascular disruption leading to the leakage of plasma into the alveolar spaces and layering of fibrin and necrotic cells arising from type II pneumocytes along the alveolar ductus (6). It develops at or within 24 h after birth, and causes hypoxia in association with a lack of surfactant. Untreated disease leads to severe hypoxia resulting in multiple organ failure and even death.

Lung injury and progression to pulmonary edema are also suspected to be consequences of the activation of complement and its cross-talk with the coagulation system (31, 32). Several reports have described lower concentrations of complement factors and higher levels of complement activation products in neonates with RDS, especially in the subgroup poorly responding to surfactant treatment compared with good responders (33). Elevated C3a was also proposed to differentiate RDS from RDS accompanied by perinatal asphyxia (34). Knowledge concerning the role of lectin pathway factors in RDS is limited to a single report by Dogan et al. (35), showing significantly higher frequency of *MBL2* genotypes associated with low concentration of MBL in affected neonates. Our

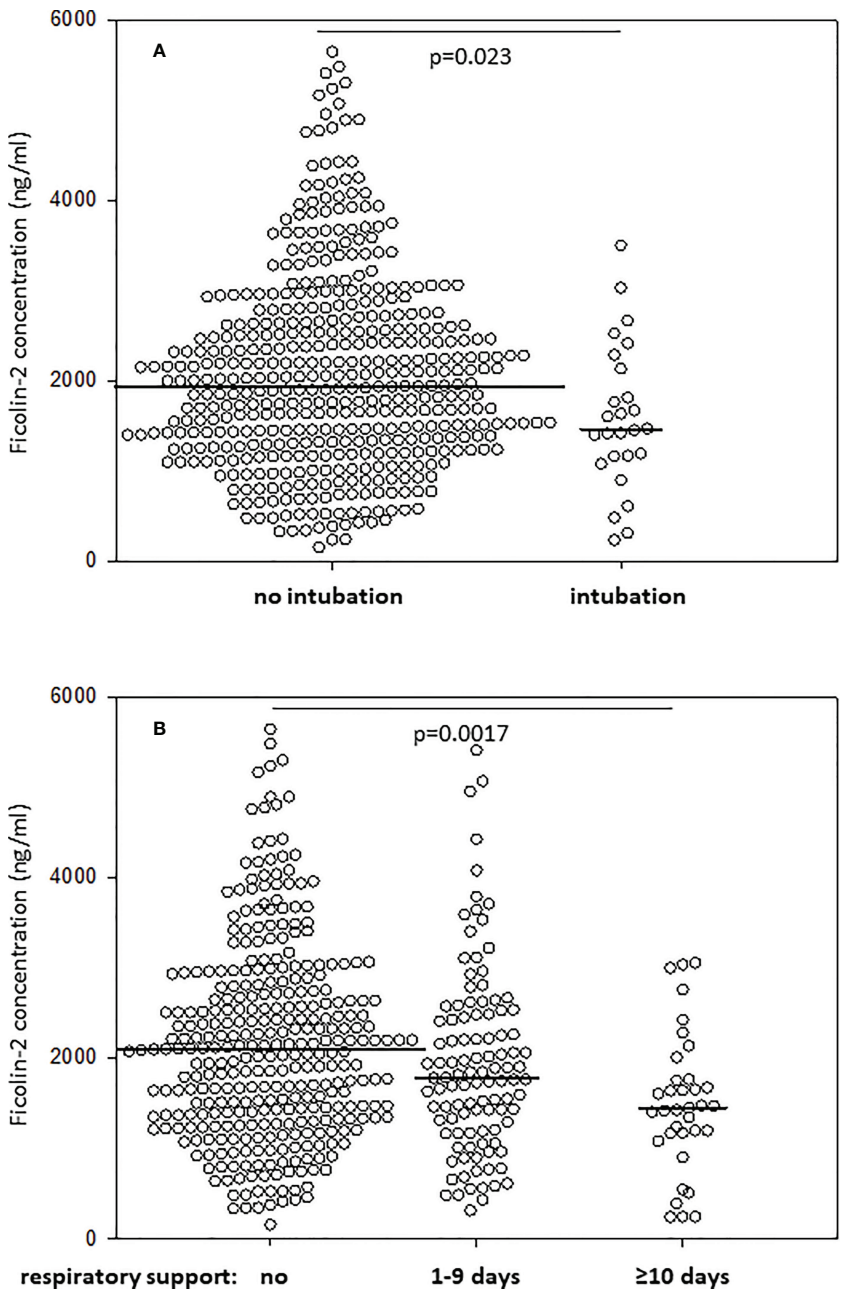

FIGURE 2
Comparison of ficolin-2 concentration in neonates requiring and not requiring intubation at delivery room **(A)** and/or respiratory support (mechanical ventilation, CPAP, or both) **(B)**. The horizontal lines mark median values. Medians were compared with the use of Mann-Whitney *U* test **(A)** and Kruskal-Wallis test (p=0.001) with *post-hoc* Dunn test **(B)**.

results showing increased probability of development of RDS in preterms with low ficolin-2 confirm an association of the complement system with this complication. Interestingly, we found no significant relationship between *FCN2* gene polymorphisms and RDS.

Respiratory distress syndrome may be prevented by corticosteroid administration and its treatment usually requires mechanical or non-invasive ventilation and transbronchial exogenous surfactant application. However, it may still result in the development of neonatal chronic lung disease and possibly severe long-term lung damage. Selection of specific and sensitive markers of RDS could be helpful in the diagnostic process and in choosing appropriate treatment. Despite intensive studies, so far no such marker is available. Our results may be helpful in this context since they suggest that ficolin-2 insufficiency has the potential to differentiate between preterms with and without RDS as well as those with mild or more severe disease, at least in the subgroup born at GA<33 (Figure 3). Moreover, we reported that low ficolin-2 in cord blood may predict a need for intubation in the delivery room as well as a requirement for intensive respiratory support.

Several reports evidenced association of low ficolin-2 concentration with diseases of the respiratory system. For example, relative ficolin-2 deficiency was shown to predispose to the development of bronchiectasis (36) and to predict disease

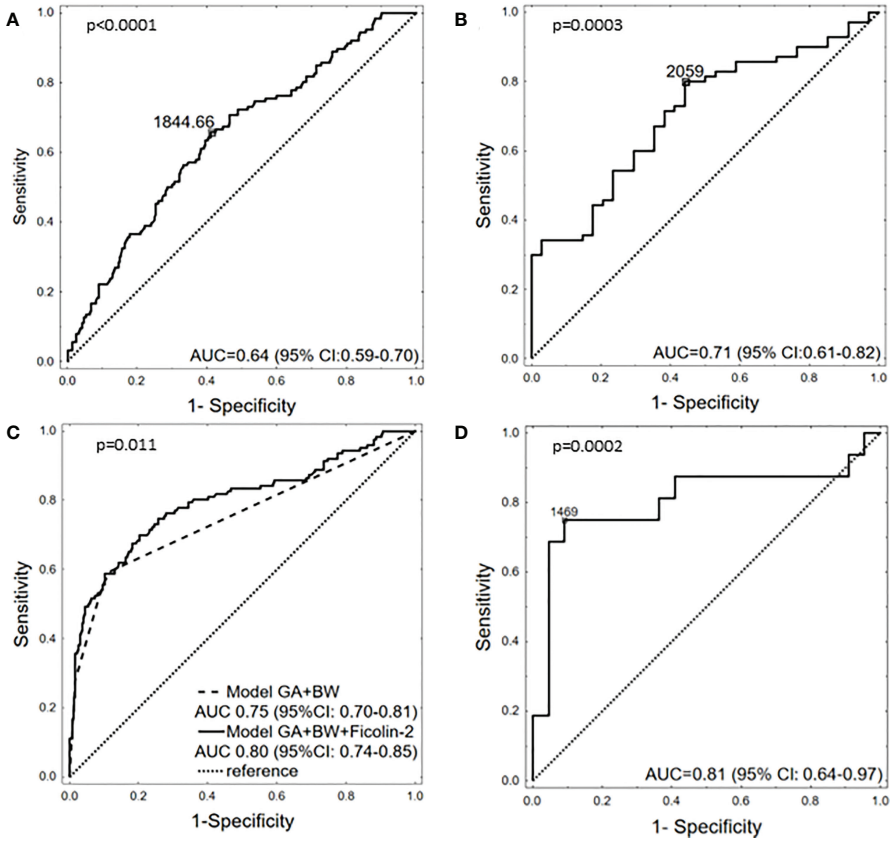

FIGURE 3
The potency of ficolin-2 to differentiate between babies with and without RDS in whole cohort **(A)**, between neonates with and without RDS, born at GA <33 **(B)**, between neonates with and without RDS, depending on GA (<33 *vs.* ≥33) and BW (<1500g *vs.* ≥1500g) **(C)** and between babies born at GA <33 with mild **(I)** and moderate/severe (II+III) RDS **(D)**.

progression in patients with idiopathic pulmonary fibrosis (37). Although, no association of ficolin-2 with susceptibility to community-acquired pneumonia was shown (38), its low concentration may increase the risk of infection with *Mycobacterium tuberculosis* or *M. avium* complex (39, 40). Median ficolin-2 level was also demonstrated to be significantly lower in paediatric patients with asthma and/or allergic rhinitis suffering from recurrent respiratory infections than in controls (41). Interestingly, Schaubel et al. (42) reported that neonatal RDS (with and without BPD) significantly enhances the risk of asthma in pre-school-aged children. Although ficolin-2 is synthesised by hepatocytes and secreted into the circulation, it can be present in the lung as well (43, 44). Interestingly, very low *FCN2* mRNA was found in the fetal lung (45).

Low circulating ficolin-2 in RDS patients may be inborn or be a consequence of its consumption or leakage into the air space due to impaired function of the alveolar-capillary barrier. It may lead not only to complement activation, but also to activation of the coagulation system, *via* complexed MASP (MBL-associated serine proteases). Purified ficolin-2-MASP complexes were shown to release fibrinopeptides from fibrinogen, activate factor XIII and in consequence, to form a clot (46). It is also possible that ficolin-2 interacts with lung surfactant components like cholesterol crystals which constitute up to 8% of native lung surfactant. Ficolin-2-MASP complex deposition, followed by complement C4 activation on cholesterol crystals was documented by Pilely et al. (47). On the other hand, cholesterol is a major component of meconium - involved also in respiratory distress pathology and mentioned among factors responsible for surfactant inactivation (48).

Apoptosis was proposed to contribute to the pathogenesis of RDS, since numerous apoptotic cells were detected mainly in the respiratory epithelium in lungs of affected infants (49). Late apoptotic/necrotic cells may be also a target for ficolin-2/ficolin-2-MASP complexes resulting in complement activation and enhanced phagocytosis (50, 51).

Our data confirmed association of the *FCN2* gene promoter polymorphisms and ficolin-2 concentration, published previously by others and ourselves (20, 28, 52). We previously reported also the relationship of 3'UTR diplotypes (group VI) with low ficolin-2 (21). That was confirmed here in univariate analysis, however lost statistical significance after multivariate logistic regression. It has to be remembered as well that prenatal steroid administration might affect ficolin-2 concentration in cord serum. We found a difference between babies born at GA ≥33 to mothers treated with steroids *vs.* those of mothers who were not receiving such a treatment, which however was not confirmed in multivariate regression analysis (Supplementary Table 2B).

We report here for the first time possible involvement of ficolin-2 insufficiency in neonatal RDS development. However, it is not clear whether low concentration in cord blood is a cause or consequence of

disease progression. It can be assumed that cord blood ficolin-2 <1500 ng/ml may enhance the probability of moderate/severe RDS and the need for surfactant therapy and assisted ventilation. Determination of ficolin-2 concentration in cord serum may be considered a new early prognostic factor in RDS development, helpful to distinguish RDS from other prematurity-associated respiratory disorders and thus facilitating the choice of appropriate treatment. That, however, should be confirmed by an independent study, ideally taking into account responsiveness to treatment and changes of ficolin-2 levels during the course of RDS.

Data availability statement

The raw data supporting the conclusions of this article will be made available by the authors, without undue reservation.

Ethics statement

The studies involving human participants were reviewed and approved by Bioethics Committee of The Karol Marcinkowski Poznań University of Medical Sciences, Independent Bioethics Committee for Scientific Research at Medical University of Gdańsk, Bioethics Committee of The Medical University of Łódź. Written informed consent to participate in this study was provided by the participants' legal guardian/next of kin.

Author contributions

GG and AŚ determined ficolin-2 concentrations; AS-P, GG, AŚ, and DJ determined *FCN2* gene promoter polymorphisms. AŚ coordinated project realisation, designed the study, planned and supervised experimental work; DJ sequenced *FCN2* gene 3'UTR; PK, KC, MK-B, and KS were responsible for patients' qualification, taking and collecting samples as well as collecting clinical data; ID-P, JM, and JK supervised qualification and recruitment of patients and analysis of clinical data; MM and HS provided anti-ficolin-2 mAbs for initial experiments, contributed to modification of the procedure and discussed corresponding data; DM, JC, WF, and MC performed statistical analysis; MC contributed to the study design, supervision of experimental work and analysed promoter haplotypes. The draft manuscript was written by AŚ and MC, discussed, corrected and finally approved by all authors. All authors contributed to the article and approved the submitted version.

Funding

This work was funded by National Science Centre, Poland, grant 2015/17/B/NZ6/04250 and Institute of Medical Biology, Polish Academy of Sciences.

Acknowledgments

The authors are very grateful to David C. Kilpatrick for reviewing and editing the first draft of the article.

Conflict of interest

The authors declare that the research was conducted in the absence of any commercial or financial relationships that could be construed as a potential conflict of interest.

Publisher's note

All claims expressed in this article are solely those of the authors and do not necessarily represent those of their affiliated organizations, or those of the publisher, the editors and the reviewers. Any product that may be evaluated in this article, or claim that may be made by its manufacturer, is not guaranteed or endorsed by the publisher.

Supplementary material

The Supplementary Material for this article can be found online at: https://www.frontiersin.org/articles/10.3389/fimmu.2023.1107063/full#supplementary-material

References

1. Vogel JP, Chawanpaiboon S, Moller AB, Watananirun K, Bonet M, Lumbiganon P. The global epidemiology of preterm birth. *Best Pract Res Clin Obstet Gynaecol* (2018) 52:3–12. doi: 10.1016/j.bpobgyn.2018.04.003

2. Moss TJM, Westover AJ. Inflammation-induced lung maturation: lessons from animal experimentation. *Paediatr Respir Rev* (2017) 23:72–7. doi: 10.1016/j.prrv.2016.10.004

3. Reuter S, Moser C, Baack M. Respiratory distress in the newborn. *Pediatr Rev* (2014) 35:417–28. doi: 10.1542/pir.35.10.417

4. Sweet LR, Keech C, Klein NP, Marshall HS, Tagbo BN, Quine D, et al. Respiratory distress in the neonate: Case definition & guidelines for data collection, analysis, and presentation of maternal immunization safety data. *Vaccine* (2017) 35:6506–17. doi: 10.1016/j.vaccine.2017.01.046

5. Gao Y, Cornfield DN, Stenmark KR, Thebaud B, Abman SH, Raj JU. Unique aspects of the developing lung circulation: Structural development and regulation of vasomotor tone. *Pulm Circ* (2016) 6:407–25. doi: 10.1086/688890

6. Locci G, Fanos V, Gerosa C, Faa G. Hyaline membrane disease (HMD): the role of the perinatal pathologist. *J Pediatr Neonatal Ind Med* (2014) 3:e030255. doi: 10.7363/030255

7. O'Brodovich H. Fluid clearance from the lungs of newborns, infants and children. *Paediatr Respir Rev* (2006) 7(suppl. 1):S62–3. doi: 10.1016/j.prrv.2006.04.173

8. Levit O, Jiang Y, Bizzarro MJ, Hussain N, Buhimschi C, Gruen JR, et al. The genetic susceptibility to respiratory distress syndrome. *Pediatr Res* (2009) 66:693–7. doi: 10.1203/PDR.0b013e3181bbce86

9. Dzik S. Complement and coagulation: cross talk trough time. *Transfus Med Rev* (2019) 33:199–206. doi: 10.1016/j.tmrv.2019.08.004

10. Hahjishengallis G, Reis ES, Mastellos DC, Ricklin D, Lambris JD. Novel mechanisms and functions of complement. *Nat Immunol* (2017) 18:1288–98. doi: 10.1038/ni.3858

11. Mastellos D, Gemenis AE, Lambris JD. Complement: and inflammatory pathway fulfilling multiple roles at the interface of innate immunity and development. *Curr Drug Targets Inflamm Allergy* (2005) 4:125–7. doi: 10.2174/1568010053622993

12. DeAngelis RA, Markiewski MM, Kourtzelis I, Rafail S, Syriga M, Sandor A, et al. A complement – IL-4 regulatory circuits controls liver regeneration. *J Immunol* (2012) 188:641–8. doi: 10.4049/jimmunol.1101925

13. Riley-Vargas RC, Lanzendorf S, Atkinson JP. Targeted and restricted complement activation on acrosome-reacted spermatozoa. *J Clin Invest* (2005) 115:1241–9. doi: 10.1172/JCI23213

14. Cedzyński M , Świerzko A.St., Kilpatrick DC. Factors of the lectin pathway of complement activation and their clinical associations in neonates. *J Biomed Biotechnol* (2012) 2012:363246. doi: 10.1155/2012/363246

15. Swierzko AS, Atkinson APM, Cedzynski M, Macdonald SL, Szala A, Domzalska-Popadiuk I, et al. Two factors of the lectin pathway of complement, l-ficolin and mannan-binding lectin, and their association with prematurity, low birthweight and infections in a large cohort of polish neonates. *Mol Immunol* (2009) 46:551–8. doi: 10.1016/j.molimm.2008.07.025

16. Aoyagi Y, Adderson EE, Min JG, Matsushita M, Fujita T, Takahashi S, et al. Role of l-ficolin/mannose-binding lectin-associated serine protease complexes in the oposonophagocytosis of type III group b streptococci. *J Immunol* (2005) 174:418–25. doi: 10.4049/jimmunol.174.1.418

17. Yadav S, Lee B, Kamity R. Neonatal respiratory distress syndrome. In: *StatPearls*. Treasure Island (FL: StatPearls Publishing (2022).

18. Wang CC, Yim KW, Poon TCW, Choy KW, Chu CY, Lui WT, et al. Innate immune response by ficolin binding in apoptotic placenta is associated with the clinical syndrome of preeclampsia. *Clin Chem* (2007) 53:42–52. doi: 10.1373/clinchem.2007.074401

19. Halmos A, Rigo J, Szijarto J, Fust G, Prohaszka Z, Molvares A. Circulating ficolin-2 and ficolin-3 in normal pregnancy and pre-eclampsia. *Clin Exp Immunol* (2012) 169:49–56. doi: 10.1111/j.1365-2249.2012.04590.x

20. Kilpatrick DC, Swierzko A, Matsushita M, Domzalska-Popadiuk I, Borkowska-Kłos M, Szczapa J, et al. The relationship between *FCN2* genotypes and serum ficolin-2 (L-ficolin) proteins concentrations from a large cohort of neonates. *Hum Immunol* (2013) 74:867–71. doi: 10.1016/j.humimm.2013.04.011

21. Świerzko AS, Jarych D, Gajek G, Chojnacka K, Kobiela P, Kufelnicka-Babout M, et al. Polymorphisms of the *FCN2* gene 3'UTR region and their associations in preterm newborns., front. *Immunol* (2021) 12:741140. doi: 10.3389/fimmu.2021.741140

22. Carbone F, Valente A, Perego C, Bertolotto M, Pane B, Spienella G, et al. Ficolin-2 serum levels predict the occurrence of acute coronary syndrome in patients with severe carotid artery stenosis. *Pharmacol Res* (2021) 166:1054462. doi: 10.1016/j.phrs.2021.105462

23. Giraudi PJ, Salvoza N, Bonazza D, Saitta C, Lombardo D, Casagranda B, et al. Ficolin-2 plasma level assesses liver fibrosis in non-alcoholic fatty liver disease. *Int J Mol Sci* (2022) 23:2813. doi: 10.3390/ijms23052813

24. Turek-Jakubowska A, Dębski J, Jakubowski M, Szahidewicz-Krupska E, Gawryś J, Gawryś K, et al. New candidates for biomarkers and drug targets of ischemic stroke-a first dynamic LC-MS human serum proteomic study. *J Clin Med* (2022) 11:339. doi: 10.3390/jcm11020339

25. Świerzko AS, Michalski M, Sokołowska A, Nowicki M, Szala-Poździej A, Eppa Ł, et al. Associations of ficolins with haematological malignancies in patients receiving high-dose chemotherapy and autologous hematopoietic stem cell transplantations. *Front Immunol* (2020) 10:3097. doi: 10.3389/fimmu.2019.03097

26. Hein E, Bay JT, Munthe-Fog L, Garred P. Ficolin-2 reveals different analytical and biological properties dependent on different sample handling procedures. *Mol Immunol* (2013) 56:406–12. doi: 10.1016/j.molimm.2013.05.233

27. Brady AM, Spencer BL, Falsey AR, Nahm MH. Blood collection tubes influence serum ficolin-1 and ficolin-2 levels. *Clin Vaccine Immunol* (2014) 21:51–5. doi: 10.1128/CVI.00607-13

28. Szala-Poździej A, Świerzko AS, Gajek G, Kufelnicka-Babout M, Chojnacka K, Kobiela P, et al. Association of the *FCN2* gene promoter region polymorphisms with very low birthweight in preterm neonates. *Int J Mol Sci* (2022) 23:15336. doi: 10.3390/ijms232315336

29. Metzger ML, Michelfelder I, Goldacker S, Mekaoui K, Liztman J, Guzman D, et al. Low ficolin-2 levels in common variable immunodeficiency patients with bronchiectasis. *Clin Exp Immunol* (2015) 179:256–64. doi: 10.1111/cei.12459

30. Szala A, Swierzko A, Cedzynski M. Cost-effective procedures for genotyping of human *FCN2* gene single nucleotide polymorphisms. *Immunogenetics* (2013) 65:439–46. doi: 10.1007/s00251-013-0696-7

31. Jeffries AL, Coates G, O'Brodovich H. Pulmonary epithelial permeability in hyaline membrane disease. *N Engl J Med* (1984) 311:1075–80. doi: 10.1056/NEJM198410253111703

32. Yurdakok M, Korkmaz A, Kirazli S, Aygun C, Yigit S. Global fibrinolytic capacity in early respiratory distress syndrome: A pilot study. *Am J Hematol* (2002) 69:255–7. doi: 10.1002/ajh.10060

33. Wagner MH, Sonntag J, Strauss E, Obladen M. Complement and contact activation related to surfactant response in respiratory distress syndrome. *Pediatr Res* (1999) 45:14–8. doi: 10.1203/00006450-199901000-00004

34. Schrod L, Frauendienst-Egger G, von Stockhausen HB, Kirschfink M. Complement fragment C3a in plasma of asphyxiated neonates. *Eur J Pediatr* (1992) 151:688–92. doi: 10.1007/BF01957575

35. Dogan P, Ozkan H, Koksal N, Oral HB, Bagci O, Varal IG. Mannose-binding lectin gene polymorphism and its effect on short term outcomes in preterm infants. *J Pediatr (Rio J)* (2020) 96:520–6. doi: 10.1016/j.jped.2019.03.001

36. Kilpatrick DC, Chalmers JD, MacDonald SL, Murray M, Ali M, Hart SP, et al. Stable bronchiesctasis is associated with low serum l-ficolin concentrations. *Clin Respir J* (2009) 3:29–33. doi: 10.1111/j.1752-699X.2008.00105.x

37. Ashley SL, Xia M, Murray S, O'Dwyer DN, Grant E, White ES, et al. Six-SOMAmer index relating to immune, protease and angiogenic functions predicts progression in IPF. *PloS One* (2016) 11:e0159878. doi: 10.1371/journal.pone.0159878

38. Chalmers JD, Fleming GB, Rutherford J, Matsushita M, Kilpatrick DC, Hill AT. Serum ficolin-2 in hospitalized patients with community-acquired pneumonia. *Inflammation* (2014) 37:1635–41. doi: 10.1007/s10753-014-9891-4

39. Luo F, Sun X, Wang Y, Wang Q, Wu Y, Pan Q, et al. Ficolin-2 defends against virulent *Mycobacterium tuberculosis* infection *in vivo*, and its insufficiency is associated with infections in humans. *PloS One* (2013) 8:e73859. doi: 10.1371/journal.pone.0073859

40. Kobayashi T, Kuronuma K, Saito A, Ikeda K, Ariki S, Saitou A, et al. Insufficient serum l-ficolin is associated with disease presence and extent of pulmonary *Mycobacterium avium* complex disease. *Resp Res* (2019) 20:224. doi: 10.1186/s12931-019-1185-9

41. Cedzynski M, Atkinson APM, Swierzko A, MacDonald SL, Szala A, Zeman K, et al. L-ficolin (ficolin-2) insufficiency is associated with combined allergic and infectious respiratory disease in children. *Mol Immunol* (2009) 47:415–9. doi: 10.1016/j.molimm.2009.08.028

42. Schaubel D, Johansen H, Dutta M, Desmeules M, Becker A, Mao Y. Neonatal characteristics as risk factors for preschool asthma. *J Asthma* (1996) 33:255–64. doi: 10.3109/02770909609055366

43. Bidula S, Sexton DW, Abdolrasouli A, Shah A, Reed A, Armstrong-Jones D, et al. The serum opsonin l-ficolin is detected in lungs of human transplant recipients following fungal infections and modulates inflammation and killing of *Aspergillus fumigatus*. J. *Infect Dis* (2015) 212:234–46. doi: 10.1093/infdis/jiv027

44. Vogt S, Trendelenburg M, Tamm M, Stolz D, Hostettker KE, Osthoff M. Local and systemic recognition receptors of the lectin pathway of complement in a cohort of patients with interstitial lung diseases. *Front Immunol* (2020) 11:562564. doi: 10.3389/fimmu.2020.562564

45. Hummelshoj T, Munthe Fog L, Madsen HO, Sim RB, Garred P. Comparative study of the human ficolins reveals unique features of ficolin-3 (Hakata antigen). *Mol Immunol* (2008) 45:1623–32. doi: 10.1016/j.molimm.2007.10.006

46. Gulla K, Gupta K, Krarup A, Gal P, Schwaeble WJ, Sim RB, et al. Activation of mannan-binding lectin-associated serine proteases leads to generation of a fibrin clot. *Immunology* (2010) 129:482–95. doi: 10.1111/j.1365-2567.2009.03200.x

47. Pilely K, Rosbjerg A, Genster N, Gal P, Pal G, Halvorsen B, et al. Cholesterol crystals activate the lectin complement pathway *via* ficolin-2 and mannose-binding lectin: implications for the progression of atherosclerosis. *J Immunol* (2016) 196:5064–74. doi: 10.4049/jimmunol.1502595

48. Krafft MP. Overcoming inactivation of the lung surfactant by serum proteins: a potential role of fluorocarbons. *Soft Matter* (2015) 11:5982–94. doi: 10.1039/C5SM00926J

49. Jensen ML, Honore C, Hummelshoj T, Hansen BE, Madsen HO, Garred P. Ficolin-2 recognizes DNA and participates in the clearance of dying host cells. *Mol Immunol* (2007) 44:856–65. doi: 10.1016/j.molimm.2006.04.002

50. Lukkarinen HP, Laine J, Kaapa PO. Lung epithelial cells undergo apoptosis in neonatal respiratory distress syndrome. *Pediatr Res* (2003) 53:254–9. doi: 10.1203/00006450-200302000-00009

51. Kuraya M, Ming Z, Liu X, Matsushita M, Fujita T. Specific binding of l-ficolin and h-ficolin to apoptotic cells leads to complement activation. *Immunobiology* (2005) 209:689–97. doi: 10.1016/j.imbio.2004.11.001

52. Munthe-Fog L, Hummelshoj T, Hansen BE, Koch C, Madsen HO, Skjodt K, et al. The impact of *FCN2* polymorphisms and haplotypes on the ficolin-2 serum levels. *Mol Immunol* (2007) 65:383–92. doi: 10.1111/j.1365-3083.2007.01915.x

frontiers | Frontiers in Immunology

TYPE Review
PUBLISHED 20 January 2023
DOI 10.3389/fimmu.2022.1055050

Check for updates

OPEN ACCESS

EDITED BY
Lillemor Skattum,
Lund University, Sweden

REVIEWED BY
Svetlana Hakobyan,
Cardiff University, United Kingdom
Mariya Hristova,
University College London,
United Kingdom

*CORRESPONDENCE
Roosmarijn E. Vandenbroucke
Roosmarijn.Vandenbroucke@irc.VIB-UGent.be

†These authors share senior authorship

SPECIALTY SECTION
This article was submitted to Molecular Innate Immunity, a section of the journal Frontiers in Immunology

RECEIVED 27 September 2022
ACCEPTED 07 December 2022
PUBLISHED 20 January 2023

CITATION
Burgelman M, Dujardin P, Vandendriessche C and Vandenbroucke RE (2023) Free complement and complement containing extracellular vesicles as potential biomarkers for neuroinflammatory and neurodegenerative disorders. *Front. Immunol.* 13:1055050. doi: 10.3389/fimmu.2022.1055050

COPYRIGHT
© 2023 Burgelman, Dujardin, Vandendriessche and Vandenbroucke. This is an open-access article distributed under the terms of the Creative Commons Attribution License (CC BY). The use, distribution or reproduction in other forums is permitted, provided the original author(s) and the copyright owner(s) are credited and that the original publication in this journal is cited, in accordance with accepted academic practice. No use, distribution or reproduction is permitted which does not comply with these terms.

Free complement and complement containing extracellular vesicles as potential biomarkers for neuroinflammatory and neurodegenerative disorders

Marlies Burgelman[1,2], Pieter Dujardin[1,2], Charysse Vandendriessche[1,2†] and Roosmarijn E. Vandenbroucke[1,2*†]

[1]VIB Center for Inflammation Research, VIB, Ghent, Belgium, [2]Department of Biomedical Molecular Biology, Ghent University, Ghent, Belgium

The complement system is implicated in a broad range of neuroinflammatory disorders such as Alzheimer's disease (AD) and multiple sclerosis (MS). Consequently, measuring complement levels in biofluids could serve as a potential biomarker for these diseases. Indeed, complement levels are shown to be altered in patients compared to controls, and some studies reported a correlation between the level of free complement in biofluids and disease progression, severity or the response to therapeutics. Overall, they are not (yet) suitable as a diagnostic tool due to heterogeneity of reported results. Moreover, measurement of free complement proteins has the disadvantage that information on their origin is lost, which might be of value in a multi-parameter approach for disease prediction and stratification. In light of this, extracellular vesicles (EVs) could provide a platform to improve the diagnostic power of complement proteins. EVs are nanosized double membrane particles that are secreted by essentially every cell type and resemble the (status of the) cell of origin. Interestingly, EVs can contain complement proteins, while the cellular origin can still be determined by the presence of EV surface markers. In this review, we summarize the current knowledge and future opportunities on the use of free and EV-associated complement proteins as biomarkers for neuroinflammatory and neurodegenerative disorders.

KEYWORDS

complement, extracellular vesicle (EV), biomarker, neuroinflammation, Alzheimer's disease, multiple sclerosis

1 Introduction

The diagnosis for disorders of the central nervous system (CNS), including neurodegenerative and neuroinflammatory diseases, is still challenging (1). Because of their rising prevalence, high heterogeneity and the urge for early and accurate disease detection, the need for reliable biomarkers for diagnosis, prognosis or treatment response is high. Since dysregulation of the complement system is a common pathologic feature in several CNS diseases (2–7), a lot of research has been conducted to investigate its biomarker potential. Complement proteins are indispensable during development of the nervous system, more specifically during synaptic pruning and axonal growth (8–12). However, several studies have shown that a broad list of CNS diseases, including Alzheimer's disease (AD) and multiple sclerosis (MS), are associated with aberrant, complement-mediated synapse elimination (5, 10, 11). Furthermore, expression and activation of complement proteins is often observed in disease-associated CNS lesions including AD and MS plaques (2, 13–16). Most importantly, in regard to biomarker research, the level of several complement proteins in biofluids is often found to be altered in CNS disease patients compared to (healthy) controls. In this review, we will discuss the potential and the limitations of complements proteins as biomarkers in neuroinflammatory and neurodegenerative diseases, focusing on AD and MS.

2 The complement system

As an essential part of the innate immune system, the complement system ensures rapid recognition and clearance of pathogens or danger-associated signals (5, 17, 18). In addition, the system also coordinates adaptive immune functions (3, 18). The complement system comprises more than 40 proteins and embodies a complex set of interactions (5, 18). Overall, complement activation can be achieved *via* three pathways, which are summarized in Figure 1 and are extensively reviewed by others (3, 5, 19, 20). The classical and lectin pathways show a similar course, however their way of activation differs (3, 5, 19). The classical pathway is triggered *via* binding of the C1 complex to the Fc domain of antibodies present in pathogen-immune complexes, or *via* its interaction with apoptotic cells or polyanionic molecules such as phosphorylated tau or amyloid-beta (Aβ) fibrils (3, 5, 19). In the lectin pathway, activation happens *via* the recognition of microbial carbohydrates by pattern binding proteins, including mannose-binding lectin (MBL), resulting in the activation of mannan-binding lectin serine protease 1 (MASP1) and MASP2 (3, 5, 19). After activation, both the classical and lectin pathway mediate C4 and C2 conversion into C4a/C4b and C2a/C2b, respectively. Subsequently, C2a and C4b complex together form the C3 convertase (C4b2a). In contrast, the alternative pathway acts differently, as hydrolyzed C3 ($C3_{H2O}$) and factor B (fB) are cleaved by factor D (fD) and form a solvent-based C3 convertase ($C3_{H2O}Bb$) (3, 19). The latter pathway is constantly active at low level to scan cells for alerting signals (19). Eventually, all complement activation pathways lead to the cleavage of the central complement protein C3, resulting in C3a/C3b formation (3, 5, 19). Since C3b also forms a C3 convertase together with cleaved factor B (C3bBb), a vicious cycle of C3 cleavage is formed that efficiently amplifies the response (3, 19). Subsequently, an additional C3b binds to the C3 convertase (C4b2a3b or C3bBb3b) to form C5 convertase, by which C5 is converted into C5a/C5b. These effector molecules are classified as opsonins (C3b, C5b) and anaphylatoxins (C3a, C5a) (3, 5, 19). On the one hand, opsonins will mediate efficient target elimination *via* the formation of the C5b-C9 complex, also known as the membrane attack complex (MAC) or the terminal complement complex (TCC), to mediate target lysis. On the other hand, opsonins tag the target to enhance phagocytosis. Additionally, anaphylatoxins induce leukocyte chemotaxis.

3 The potential of free complement proteins as biomarkers

3.1 Free complement as biomarker in AD

The early diagnosis of AD patients is crucial for better patient care, the timely administration of potential treatments and enrolment in clinical trials. The present reliance on clinical cognitive and behavioral testing, brain scans and medical history does not fulfill this necessity, with definitive diagnosis only possible postmortem. Unfortunately, the identification of early biomarkers is an arduous task as brain changes are estimated to already occur twenty years before symptoms arise (21, 22) together with a large individual variability in starting age, symptoms, and the speed of disease progression. It is thus of great importance to further unravel the early molecular changes to identify novel diagnostic tools. Currently, the most predictive AD biomarker is the combination of lowered levels of amyloid-beta 42 ($A\beta_{42}$) with increased total tau (tTau) and phosphorylated tau (pTau) levels in the cerebrospinal fluid (CSF). Although promising, their levels stagnate after disease onset and do not allow staging from mild cognitive impairment (MCI) to AD dementia (23, 24). Furthermore, CSF collection by lumbar puncture is invasive and not frequently performed for AD diagnosis as is the case for MS as discussed further. As opposed to CSF, plasma AD biomarkers are less established, and the availability is still limited. Hence, additional biomarkers to

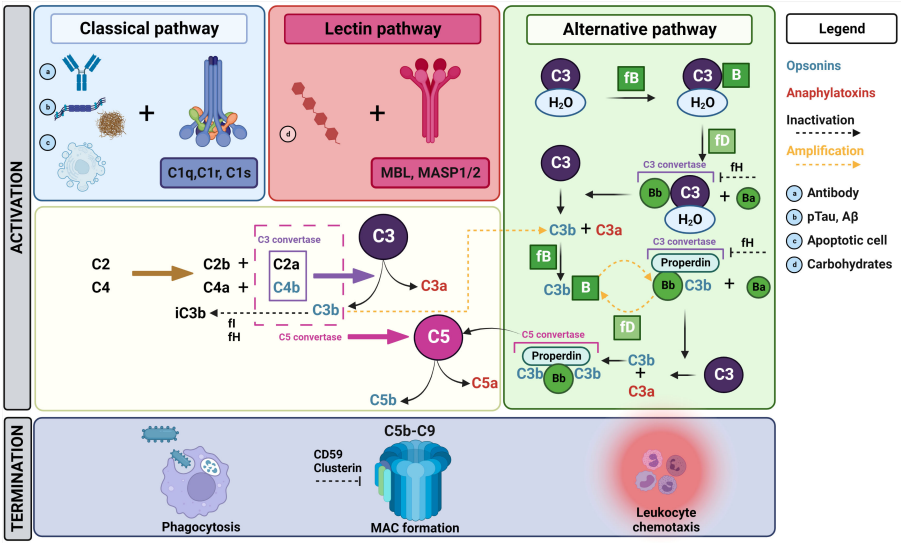

FIGURE 1
Overview of the complement cascade. The complement cascade can be activated *via* three different pathways. In the classical pathway, the C1 complex (C1r, C1s, C1q) recognizes antibody complexes **(A)** bound to pathogens, polyanionic molecules such as pTau and Aβ **(B)** or damage-associated patterns on apoptotic cells **(C)**. Following C1 activation, C2 and C4 will be converted to C2a/b and C4a/b, respectively. C2a and C4b complex together and form a C3 convertase, which will cleave C3 to create C3a and C3b. Subsequently, C3b will complex with C2aC4b to form C5 convertase, which will lead to the conversion of C5 into C5a and C5b. Finally, C5b will initiate the formation of the MAC complex by recruiting C6, C7, C8 and C9, ultimately resulting into target lysis. Several other activation products (C3b, C4b) formed during the complement pathway enhance phagocytosis *via* opsonizing the target. The lectin pathway is activated *via* the recognition of microbial carbohydrates **(D)** including MBL, resulting in the activation of MASP1/2. Thereafter, the same cascade steps as described above for C3 and C5 conversion are initiated. On the contrary, the alternative pathway is constitutively active at low level for constant scanning of cells. Here, a limited number of C3 molecules is hydrolyzed, which exposes a new binding site for fB. Subsequently, fD will cleave fB-bound C3 resulting in Bb-bound hydrolyzed C3, which functions as a C3 convertase resulting in C3a/C3b production. Thereafter, C3b will again react with fB and properdin. The resulting complex consisting of properdin, C3b and Bb also functions as a C3 convertase, which will again cleave C3 into C3b and C3a. Eventually, properdin and Bb will capture two C3b molecules to form a C5 convertase. By this, C5 can be cleaved, resulting in MAC formation as described above. As indicated in this figure, several amplification loops are present within the complement pathways. There are also different regulating factors that influence or inhibit certain parts of the cascade. For example, fH acts as inhibitor for the C3 convertases in the alternative pathway and acts as a cofactor for fI, which is in turn a regulator for the degradation of several activation products including the inactivation of C3b into iC3b. Additionally, clusterin acts as an inhibitor of MAC formation. mannan-binding lectin serine protease 1/2 (MASP1/2), mannose binding lectin (MBL), phosphorylated tau (pTau), amyloid-β (Aβ), factor I (fI), factor H (fH), factor B (fB), membrane attack complex (MAC). Figure created in Biorender and content in accordance with Dalakas et al. (3), Ricklin et al. (19) and Schartz et al. (5).

improve preclinical diagnosis, staging and prognosis are necessary. The growing evidence on the involvement of the complement system in AD has brought attention on its use as such a biomarker. For example, polymorphisms in multiple complement genes are associated with increased AD risk (25–29). Furthermore, C1q is activated by Aβ and reciprocally promotes Aβ aggregation (30–33). Similarly, C1q is activated by tau and induces microglial engulfment of excitatory synapses (34, 35). A broad range of preclinical studies making use of complement inhibitors and/or knock-out (KO) mouse models also indicate that complement dysregulation is not a secondary reaction to pathology but a disease-driving force (2), for instance by mediating aberrant synaptic pruning (12, 36, 37). Consequently, complement proteins could have early biomarker potential, and numerous efforts have been made to measure and compare their levels in CSF and plasma in MCI and AD patients and/or different control groups.

3.1.1 Complement proteins levels in CSF and their biomarker potential

Studies on CSF complement levels are generally consistent with either increased or unchanged levels in AD (Table 1). More specifically, an increase in the CSF levels of C1s (38), C1q (38), C4 (45), clusterin (39, 48, 49), complement receptor 1 (CR1) (45) and factor H (fH) (41) has been reported in AD patients compared to healthy controls (HC) and/or MCI. Conversely, unchanged levels were shown for C1q (39, 40), clusterin (50) and fH (39, 44, 46). For the central complement protein C3, the outcomes in case-control studies are most inconsistent. On one hand, we found four studies reporting elevated C3 levels in the CSF of AD patients compared to HC (41–43) or MCI (45). On the other hand, C3 concentration was unaltered in two other studies (44, 46), in which the cohort sizes were two to three times larger than in the discussed studies showing increased levels. Notably, a recent meta-

TABLE 1 Overview of changes and biomarker potential of complement proteins in the cerebrospinal fluid (CSF) of mild cognitive impairment (MCI) and Alzheimer's disease (AD) patients compared to a control group.

Cerebrospinal fluid			
Protein	Comparison	Change	Ref.
C1s	AD *vs* HC	↑	(38)
C1q	AD *vs* HC	=	(39, 40)
		↑	(38)
	MCI *vs* HC	=	(40)
	NA	+ correlation with tTau	(40)
C3	AD *vs* HC	↑	(39, 41–43)
		+ correlation with cognitive impairment (MMSE) in AD	(41, 42)
	AD *vs* MCI	=	(44)
		↑	(45)
	AD *vs* MCI *vs* HC	= - correlation with cognitive decline progression (ADAS-Cog) in MCI	(46)
		+ interaction between C3 levels and APOE E4 alleles on CSF amyloid and tau	(47)
	AD *vs* MCI	↑	(45)
C4	AD *vs* HC	↑	(45)
	AD *vs* MCI	(↑)	(45)
Clusterin	AD *vs* HC	↑	(39, 48, 49)
	AD *vs* MCI *vs* HC	= + correlation with Tau and pTau	(50)
	NA	+ correlation with Aβ-associated atrophy in non-demented elderly	(51)
CR1	AD/MCI-AD *vs* MCI/HC	↑	(45)
Factor H	AD *vs* HC	=	(39)
		↑	(41)
		+ correlation with cognitive impairment (MMSE) in AD	(41)
	AD *vs* MCI	=	(44)
	AD *vs* MCI *vs* HC	= - correlation with cognitive decline progression (ADAS-Cog) and lateral ventricular volume in MCI	(46)

The characteristics of the patient groups that were compared are indicated in the 'comparison' column. The 'change' column indicates which level alteration was observed for the respective complement component. Symbols: ↑ significant increase, (↑) increased, unsignificant trend, = unchanged. Amyloid-beta (Aβ), Alzheimer's disease (AD), Alzheimer's Disease Assessment Scale-Cognitive Subscale (ADAS-Cog), healthy control (HC), mild cognitive impairment (MCI), mini-mental state examination (MMSE), not applicable (NA), total tau (tTau).

analysis combining clinical data from peer-reviewed articles in close to three thousand records demonstrated increased C3 CSF levels (39) supporting the positive studies. However, the two cited studies showing unchanged C3 levels were not included in this meta-analysis, which may have skewed the comparison. Next, one study reported significantly elevated CSF C4 levels in AD patients compared to HC, and an increased trend compared to MCI (45). To our knowledge, no studies reported a decrease in complement levels in the CSF of AD/MCI patients.

Although significant differences in multiple CSF complement components were found between diagnostic groups, none was reported to show adequate capability for classifying AD *versus* MCI/HC patients. More specifically, Daborg et al. showed that adding the complement proteins CR1, C3 and C4 to a multivariate constructed receiver operating characteristic (ROC) curve for the core biomarkers tTau, pTau and $A\beta_{42}$ did not improve the area under the curve (AUC) (45). In the study of Toledo et al. the addition of C3, fH or C3:fH ratios did not improve the performance of tTau:$A\beta_{42}$ in

classifying AD subjects or MCI subjects *versus* HC (AUC 0.84 regardless of C3 and/or fH inclusion) (46). Similarly, Wang et al. showed that none of the ROC calculations using C3 or fH alone yielded acceptable sensitivity and/or specificity (41). The only exception was when the value of C3:Aβ_{42} and fH:Aβ_{42} ratios was also evaluated for AD *versus* control, where high sensitivity and specificity were achieved (C3:Aβ42, sensitivity 92.1% and specificity 76.9%; fH:Aβ_{42}, sensitivity 92.1% and specificity 80.2%). Finally, Brosserson et al. indicated that CSF C1q levels in AD patients *versus* HC are not diagnostic with a discriminative power (equally weighted sensitivity and specificity) around 60% (40).

Taken together, CSF complement levels seem unsuitable as diagnostic AD biomarkers. Nevertheless, they could have potential as predictor for disease severity. A longitudinal analysis of MCI patients indicated a negative correlation between C3 and fH levels and cognitive decline progression (46) but this was not reflected by lower levels in AD/MCI patients in cross-sectional analyses. In addition, lower fH levels were also shown to correlate with increased lateral ventricular volume in MCI patients, which represents a marker of disease progression (52). As opposed to the inverse correlation between complement levels and cognitive impairment in MCI, a positive correlation is observed in AD patients. Indeed, in a cohort of AD patients with CSF hemoglobin concentration less than 200 ng/ml, a significant correlation between lower mini-mental state examination (MMSE) score and increased concentrations of CSF C3 and fH was reported (41). In addition, another study mentions that CSF C3 was positively correlated with cognitive impairment in their AD cohort, but it should be noted that the data and analysis could not be found in the report (42). Finally, it has been reported that C1q, C3 and clusterin are also associated with higher tTau levels (40, 47, 50) and that clusterin correlates with Aβ-associated atrophy in non-demented elderly (51).

3.1.2 Complement proteins levels in the blood and their biomarker potential

Because of the accessibility of plasma- over CSF-based biomarkers, their identification and potential use has been explored extensively (Table 2). However, since the blood is not

TABLE 2 Overview of changes and biomarker potential of complement proteins in the plasma of Alzheimer's disease (AD) and mild cognitive impairment (MCI) patients compared to a control group.

Plasma			
Protein	Comparison	Change	Ref.
C1q	AD *vs* HC	(↑)	(39)
C1R	AD *vs* HC	(↑)	(53)
C1s	AD *vs* HC	=	(54)
	MCI convertors *vs* MCI non-convertors	=	(54)
C3	AD *vs* HC	=	(39)
		trend for + correlation with cognitive decline (MMSE) in combined group of AD and MCI	(55)
		↑	(55–57)
		(↑)	(53)
	aMC *vs* NC	↑	(58)
	MCI *vs* HC	↑	(57, 59)
	sMC *vs* NC	↑	(58)
	AD *vs* MCI	↓	(59)
	NA	- correlation with AD risk. Risk amplified in APOE ϵ44 carriers	(60)
iC3b	AD *vs* HC	=	(54)
	MCI convertors *vs* MCI non-convertors	=	(54)
C4	AD *vs* HC	=	(39, 53)
		↑	(56, 59)

(Continued)

TABLE 2 Continued

Plasma			
Protein	Comparison	Change	Ref.
C4a	AD *vs* HC	↑	(61)
		(↑)	(39)
C4d	AD *vs* HC	=	(54)
	MCI convertors *vs* MCI non-convertors	=	(54)
	aMC *vs* NC	↑	(58)
	sMC *vs* NC	↑	(58)
C6	aMC *vs* NC	↓	(58)
	sMC *vs* NC	↓	(58)
C9	AD *vs* HC	=	(54)
		(↑)	(39)
	MCI convertors *vs* MCI non-convertors	=	(54)
TCC	AD *vs* HC	=	(54)
	MCI convertors *vs* MCI non-convertors	↓	(54)
C1 inhibitor	AD *vs* HC	↓	(53)
	NA	- correlation with rosiglitazone drug efficacy in AD patients as defined by change in ADAS-Cog score	(62)
Clusterin	AD *vs* HC	=	(39, 48, 50, 63)
		↑	(54, 56)
	AD *vs* HC *vs* LBD *vs* depr *vs* FTD *vs* VD *vs* PD	=	(64)
	MCI convertors *vs* MCI non-convertors	↑	(54)
	MCI *vs* HC	↑	(50)
	NA	- correlation with cognitive decline rate in AD (MMSE)	(50)
		+ correlation with severity of AD (MMSE)	(63, 65)
		+ correlation with entorhinal cortex atrophy, disease severity (MMSE) and rapid clinical progression in AD	(66)
		+ correlation with cognitive decline rate in MCI (MMSE)	(50)
		+ correlation with decreased brain atrophy rate in MCI	(67)
		↑ AD risk	(65)
		↓AD risk in younger old persons (59–61, 63, 68–73) ↑ AD risk in older persons (74–83)	(72)
		↑ risk for progression from MCI to AD	(50)
CR1	AD *vs* HC	↓	(59)
Factor B	AD *vs* HC	=	(53)
		(↓)	(39)
Factor Bb	AD *vs* HC	=	(54)
	MCI convertors *vs* MCI non-convertors	=	(54)

(Continued)

TABLE 2 Continued

Plasma			
Protein	Comparison	Change	Ref.
Factor H	AD *vs* HC	=	(39, 53, 54, 70)
		↑	(56, 71)
	MCI convertors *vs* MCI non-convertors	=	(54)
	MCI *vs* HC	↑	(57, 59)
	NA	- correlation with rosiglitazone drug efficacy in AD patients (ADAS-Cog)	(62)
		+ correlation with disease severity (MMSE)	(71)
Factor I	AD *vs* HC	=	(54)
	AD *vs* MCI	↑	(59)
	MCI convertors *vs* MCI non-convertors	↓	(54)

The characteristics of the patient groups that were compared are indicated in the 'comparison' column. The 'change' column indicates which level alteration was observed for the respective complement component. Symbols: ↑ significant increase, (↑) increased, unsignificant trend, ↓ significant decrease, = unchanged. Alzheimer's disease (AD), Alzheimer's Disease Assessment Scale-Cognitive Subscale (ADAS-Cog), depression (depr), frontotemporal dementia (FTD), asymptomatic mutation carrier (aMC), healthy control (HC), Lewy Body dementia (DLB), mild cognitive impairment (MCI), mini-mental state examination (MMSE), not applicable (NA), Parkinson's disease (PD), symptomatic mutation carrier (sMC), vascular dementia (VD).

in direct contact with the diseased brain as is the case for CSF, combined with its complexity and heterogeneity, the identification of reproducible plasma biomarkers is challenging. Moreover, the majority of soluble complement proteins originate from the liver (84) which could mask brain-derived complement perturbations. Accordingly, AD plasma biomarker studies are more heterogenous and conflicting in comparison to CSF studies.

For the three classical complement activator proteins C1q, C1r and C1s, strong evidence for altered levels is lacking, with a trend for increased levels in AD plasma in C1q and C1r (39, 53) while no differences are reported related to C1s (54). Analyses on the plasma concentrations of the alternative complement pathway component fB or its cleaved form Bb also consistently found no differences (39, 53, 54). Similarly, no significant differences were observed in the terminal pathway proteins (39, 54) in AD patients compared to HC. To our knowledge, no evidence for the involvement or increased levels of lectin pathway components in AD has been published. Presumably, it seems that the focal point of changes in AD plasma complement levels is the central axis of the complement system, and not the activator and terminal pathways. Indeed, several studies reported a significant increase in C3 levels in the plasma of AD patients (53, 55–58). Notably, one study reported elevated plasma C3 levels in MCI patients compared to HC, but also compared to AD patients (59). Together, these studies indicate that plasma C3 levels are increased in AD, with a more pronounced increase in the earlier MCI phase. Surprisingly, a meta-analysis by Krance et al. did not endorse these results, underlying the heterogeneity in plasma measurements (39). Substantial variability was indeed detected in the plasma meta-analysis, but the source of the C3 heterogeneity could not be identified. Moreover, a larger scale population study indicated that low baseline levels of plasma C3 are associated with higher AD risk, which was amplified in APOE ϵ44 highly susceptible individuals (60). Case-control comparisons on plasma C4 levels are less consistent. Increased C4 concentrations in AD patients have been reported compared to HC (56, 58, 59, 61). In contrast, other studies did not replicate the increased C4 levels (39, 53, 54). Remarkably, a recent study detected elevated C4 in the saliva of AD patients, albeit without diagnostic utility (68).

For the complement regulators C1 inhibitor, CR1, fH, factor I (fI) and clusterin, case-control studies also indicated changes in their plasma levels. Firstly, one study indicated lower C1 inhibitor levels in AD plasma (53) and another group showed the same for CR1 (59). Interestingly, polymorphisms in the CR1 gene are a well-known AD risk factor replicated in multiple datasets (25–27, 29, 69). Secondly, studies measuring fH levels are divided between unaltered (39, 53, 54, 70) and increased (56, 71) concentrations in the plasma of AD patients compared to HC. Two studies also reported significantly higher fH in MCI subjects *versus* HC (57, 59) while no difference was observed between MCI patients converting to AD compared to non-convertors (54), arguing against the use of plasma fH as a prognostic AD biomarker. Next, reports on the C3b/C4b protease fI are contradicting, with a study showing unchanged levels between AD and HC (54), another study reporting increased levels in AD plasma compared to MCI (59) and a comparison between MCI convertors and non-convertors indicating a decreased fI plasma concentration (54). Finally, levels of the terminal pathway inhibitor clusterin have been

shown to be increased in AD (54, 56) and MCI (50) patients, although this observation has been refuted in other reports (39, 48, 50, 63). Of note, AD-related alterations in clusterin levels could be age-dependent, as it has been shown that higher concentrations are associated with increased dementia risk among elderly persons, as opposed to a decreased risk younger elderly people (72).

Despite the overarching trend of altered complement plasma levels in AD, especially in central axis complement proteins and complement regulators, most studies agree regarding their limited suitability as diagnostic biomarkers. For instance, Cheng et al. reported an accuracy of 64.3% of C4 to distinguishing AD from HC, with 64.3% sensitivity and 64.4% specificity (56). Cutler et al. reported that C1 inhibitor gave a sensitivity and specificity of both 58%, and a sensitivity of only 30.2% when the specificity was set at 80% (53). In addition, setting specificity at 80% gave a sensitivity value of 40% for fH in a ROC analysis by Hye et al. (71). Based on the complexity of AD, combinations of complement proteins with each other or with other variables might hold more potential. In a model by Hakobyan et al. combining clusterin with co-variables associated with AD, the predicted specificity was 75% at 70% sensitivity (54). In the same study, a model combining clusterin, TCC and fI with APOE status was predictive of MCI conversion with an AUC of 0.85 (79% predicted specificity at 80% sensitivity). Furthermore, a model from Wang et al. containing C3 and fH together with four other protein markers (ApoeE1, ApoCIII, ApoE, A2 macroglobulin) and age, sex, genotype, and education level covariates could differentiate MCI and AD from HC with an AUC of 0.743 and 0.837 respectively (41). Finally, a model combining fB and fH with age could moderately predict MCI progression to AD (AUC of 0.71) (59).

Similar to CSF, plasma complement levels have also been analyzed as predictor for disease severity. Thambisetty et al. observed a trend (p-value 0.07) for association between plasma C3 and MMSE score in a combined group of AD and MCI subjects (55). Moreover, another study showed the same association for fH, with increased plasma concentrations correlating with increased cognitive decline (decreased MMSE scores) (71). However, the authors made use of semiquantitative immunoblotting, so a validation study with alternative quantitative assays is necessary. The complement-associated protein clusterin is most associated with AD severity. Importantly, clusterin is a multifunctional protein, so this association could also stem from other mechanism than inhibition of the terminal complement pathway. For example, clusterin is also involved in Aβ aggregation and clearance, cholesterol and lipid regulation, and apoptosis (73, 85). Nevertheless, it is recognized as a robust marker of disease severity in both MCI and AD, as its association with cognitive decline (50, 63, 65, 66) and atrophy (50, 66, 67) has been replicated across studies in using different assay platforms. Finally, one study explored the use of complement levels as potential marker for drug efficacy, in which the plasma levels of C1 inhibitor and fH were negatively correlated with the efficacy of the PPARγ agonist rosiglitazone in AD patients (62).

3.2 Free complement as biomarker in MS

MS is an inflammatory, autoimmune-mediated disease of the CNS which is characterized by the formation of inflammatory demyelinating lesions and neurodegeneration (86, 87). The exact etiological basis for this disease is still unknown, although it is clear that both genetics and environmental triggers are involved. Nowadays, magnetic resonance imaging (MRI) is still the most important tool for MS diagnosis, disease activity and treatment response (88, 89). In general, at least two demyelinating lesions disseminated in space and time must be identified for diagnosing MS. Additionally, identification of oligoclonal bands and IgG into the CSF of patients is commonly used but is very labor intensive and costly (88, 89).

Also in MS pathology, several reports indicate the link with the complement system. For example, many complement proteins are detected in both white and grey matter lesions (13–16). More specifically, immunohistochemical analysis of MS plaques of patients with progressive MS revealed the presence of several complement proteins (C3, fB, C1q), activation products (C3b, iC3b, C4d, TCC) as well as regulators (fH, C1 inhibitor, clusterin) (13). Regarding the cellular source, reactive astrocytes and microglia are often proposed as primary sources of complement (13, 14). Complement-mediated demyelination is believed to be dominated by the classical pathway, as C1q is highly present in MS plaques and C3 as well as MAC activation is observed in white matter lesions (3, 13). Next to its role in demyelination, complement has been suggested to be implicated in mediating synaptic alterations by being involved in aberrant synaptic pruning. Mainly based on animal studies, C3-mediated synaptic loss is claimed to be linked with microglial activation and phagocytosis (74–76, 90). Finally, several complement KO mouse models illustrate the involvement of complements in MS pathology. For example, a study with C3 KO mice indicates the requirement of C3 for development of maximal experimental autoimmune encephalomyelitis (EAE) disease (77). Also, inhibition of the alternative complement pathway *via* monoclonal antibody-mediated fB inhibition, attenuated chronic EAE but did not prevent disease development (78).

Over the past decades, several studies explored the presence of complement components in the blood and CSF to evaluate their potential as biomarkers for MS diagnosis, disease severity and prognosis. In these studies, the levels of a broad variety of complement components were measured in biofluids from MS patients and compared with HC or non-inflammatory other neurological disease patients (NI-ONDC), or comparing different MS patient subgroups (Tables 3, 4). In the following

TABLE 3 Overview and biomarker potential of complement components evaluated in the cerebrospinal fluid (CSF) of multiple sclerosis (MS) patients compared to a control group.

Cerebrospinal fluid					
Protein	Change	Comparison	Ref.	Biomarker potential	Ref.
C1q	↑	MS (RR, CIS) *vs* HC rMS *vs* HC MS (RR, SP) *vs* NI-ONDC	(79, 91)	Positive correlation with neuroinflammatory and neurodegenerative marker levels	(79)
C1s	(↑)	MS (RR, SP, PP) *vs* HC	(92)	NA	
C1 inhibitor	(↑)	MS (RR, SP, PP) *vs* NIDC	(93)	NA	
C3	↑	MS (NS) *vs* HC rMS *vs* HC MS (PP, SP, RR) *vs* NI-ONDC	(79, 83, 94, 95)	Positive correlation with EDSS score ↑ associated with MRI lesion number (≥9), nerve injury (NFL)	(95)
	↓	RRMS *vs* controls (with low back pain, no white matter abnormalities)	(96)		
	=	MS (NS) *vs* HC MS (NS) *vs* ONDC pMS *vs* controls (NS) CIS *vs* RRMS	(82, 97, 98)		
C3a	↑	MS (RR, CIS) with new T2 lesions during follow-up (4y) vs absence of new T2 lesions EDA-3 vs NEDA-3 scored MS patients (RR, CIS) follow up (1y)	(79)	Positive correlation with neuroinflammatory and neurodegenerative marker levels, T2 and GAD+ MRI lesions at baseline and during follow up.	(79)
	=	MS (RR, CIS) *vs* HC rMS *vs* ONDC	(79, 99)		
iC3b	↑	CIS *vs* NIDC	(93)	NA	
C4	(↑)	MS (RR, SP, PP) *vs* NIDC	(93)	NA	
	↓	pMS *vs* controls (NS)	(98)		
	=	MS (NS) *vs* HC MS (NS) *vs* ONDC MS (RR, SP) *vs* controls (low back pain, no white matter abnormalities) CIS *vs* RRMS	(82, 83, 96, 97)		
C4a	↑	MS (RR, SP, PP) *vs* HC	(80)	NA	
	=	rMS *vs* ONDC	(99)		
C4b	↑	active RRMS *vs* NI-ONDC	(94)	NA	
C5a	=	MS *vs* ONDC	(99)	NA	
TCC (C5b-9)	↑	MS (RR, NS) *vs* NI-ONDC RRMS *vs* ON-MS with ON CIS *vs* NIDC	(93, 100, 101)	Positive correlation with EDSS	(101)
	(↑)	MS (RR, SP, PP) *vs* HC	(92, 102)		
	=	MS (RR, CIS) *vs* HC	(79)		
C9	↓	rMS/pMS *vs* ONDC	(103, 104)	NA	
	(↓)	MS (RR, SP, PP) *vs*. HC	(92)		
	=	MS (NS) *vs* ONDC	(105, 106)		

(Continued)

TABLE 3 Continued

Cerebrospinal fluid					
Protein	Change	Comparison	Ref.	Biomarker potential	Ref.
Factor H	↓	MS *vs* HC active RRMS *vs* NI-ONDC	(94, 107)	NA	
	(↑)	MS (RRMS, pMS) *vs* ONDC	(108)		
Factor B	↓	MS *vs* HC	(107)	NA	
	(↓)	MS (RR, SP, PP) *vs* HC	(92)		
Factor I	↑	CIS *vs* NIDC	(93)	NA	
	=	MS (RR, SP, PP) *vs* HC	(92)		
MASP-2	=	MS (SP, PP) *vs* controls (NS, non-MS)	(81)	NA	
FHR125	↑	CIS *vs* NIDC	(93)	NA	
sCR2	↑	MS (SP, RR) *vs* NI-ONDC	(91)	Positive correlation with MSSS	(91)
Clusterin	(↑)	MS (RR, SP, PP) *vs* HC	(92)	NA	

The characteristics of the patient groups that were compared are indicated in the 'comparison' column. The 'change' column represents the observed level alteration for the respective complement component between patient populations as represented in the 'comparison' column. The 'biomarker potential' column includes the studies that indicate a positive correlation between the level of the respective complement component and a measure as assessment of ongoing disease activity or severity, disease progression, patient stratification and/or response to treatment. To cover as much as research as possible, we did not set restrictions concerning the publication date of the references that were retrieved for this review. Symbols: ↑: significant increase; (↑): increased, unsignificant trend; ↓: significant decrease; =: unchanged. clinically isolated syndrome (CIS), evidence of disease activity (EDA), expanded disability status scale (EDSS), Factor H-related (FHR), gadolinium positive (GAD+), healthy controls (HC), magnetic resonance imaging (MRI), mannose-binding lectin-associated serine protease (MASP-2), multiple sclerosis (MS), MS severity score (MSSS), neurofilament light chain (NFL), no evidence of disease activity (NEDA), non-inflammatory other neurological disease controls (NI-ONDC), not applicable (NA), not specified (NS), optic neuritis (ON), primary progressive (PP), relapsing-remitting (RR), relapsing-remitting multiple sclerosis (RRMS), relapsing MS (rMS), secondary progressive (SP), progressive MS (pMS), terminal complement complex (TCC).

TABLE 4 Overview and biomarker potential of complement components evaluated in plasma or serum of multiple sclerosis (MS) patients compared to a control group.

Plasma/serum					
Protein	Change	Comparison	Ref.	Biomarker potential	Ref.
C1s	↑	NMO *vs* RRMS	(109)	NA	
	↓	RRMS *vs* HC	(109)		
	=	MS (RR, SP, PP) *vs* HC	(92)		
C1 inhibitor	↑	MS (RR, SP, PP) *vs* HC NMO *vs* RRMS	(92, 109)	↑ 3 months IFNA treatment (RRMS) *vs* baseline	(110)
	↓	RRMS *vs* HC	(109)		
C3	↑	MS (RR, SP, PP) *vs* HC MS (RR, CIS) *vs* HC rMS *vs* HC	(79, 92)	Positive correlation with EDSS	(111)
	↓	MS (RR, SP) *vs* controls (low back pain, no white matter abnormalities) NMO *vs* RRMS	(96, 109)		
	=	pMS *vs* controls (NS)	(98)		
iC3b	↓	RRMS *vs* HC	(109)	NA	
C3a	↑	MS (RR, PP, SP) *vs* HC	(112)	NA	
	=	MS (RRMS, CIS) *vs* HC early relapse onset MS *vs*(NI-) ONDC rMS vs ONDC	(79, 99, 113)		

(Continued)

TABLE 4 Continued

Plasma/serum					
Protein	Change	Comparison	Ref.	Biomarker potential	Ref.
C3bc	NA	NA	NA	↑ 3 months IFNA treatment (RRMS) *vs* baseline	(114)
C4	↑	MS (RR, SP, PP) *vs* HC RRMS *vs* HC relapse RRMS *vs* remission RRMS NMO *vs* MS	(92, 111, 115)	Positive correlation with EDSS	(111)
	(↑)	MS (RR, SP, PP) *vs* HC	(80)		
	=	MS (RR, SP) *vs* controls (low back pain, no white matter abnormalities)	(96)		
C4a	↑	MS (RR, SP, PP) *vs* HC Acute/active RRMS *vs* HC pMS vs controls (NS) active RRMS *vs* stable RRMS	(80, 92, 98)	NA	
	↓	MS (RR, SP, PP) *vs* HC NMO *vs* MS (RR, SP, PP)	(112)		
	=	rMS *vs* ONDC early relapse onset MS *vs*(NI-) ONDC	(99, 113)		
C4d	↑	NMO *vs* RRMS	(109)	NA	
C5	↑	NMO *vs* RRMS	(109)	NA	
	=	early relapse onset MS *vs*(NI-) ONDC	(113)		
C5a	↑	NMO *vs* RRMS	(109)	NA	
	=	rMS *vs* ONDC	(99)		
TCC (MAC or C5b-9)	↑	MS (RR, SP, PP) *vs* HC NMO *vs* RRMS	(109, 112)	↑ three and six months IFNA treatment (RRMS) vs baseline	(114)
	↓	RRMS *vs*. HC	(109)		
	=	early relapse onset MS *vs*(NI-) ONDC MS (RRMS, CIS) *vs* HC	(79, 113)		
C9	↑	acute RRMS *vs* stable RRMS	(92)	NA	
	↓	MS (RR, SP, PP) *vs* HC	(92)		
	=	pMS/rMS *vs* ONDC	(103)		
Factor H	↑	MS (RR, SP, PP) *vs* HC Acute/relapse RRMS *vs* stable/ remission RRMS pMS (PPMS, SPMS) *vs* RRMS transition rMS to pMS NMO *vs* RRMS	(92, 108, 109, 116)	Positive correlation with EDSS Distinguishing SPMS from RRMS (89.41%, distinction, 69.47% specificity positive predictive value of 72.38%, test cut-off value 4237 mg/l)	(108)
	↓	remission RRMS patients on *vs* off treatment	(108)		
	=	early relapse onset MS *vs*(NI-) ONDC	(113)		
Factor B	=	MS (RR, SP, PP) *vs* HC acute RRMS *vs* stable RRMS	(92)	NA	
Factor Ba	=	early relapse onset MS *vs*(NI-) ONDC	(113)	NA	
Factor Bb	↑	NMO *vs* RRMS	(109)	NA	
	↓	RRMS *vs* HC	(109)		

(Continued)

TABLE 4 Continued

Plasma/serum					
Protein	Change	Comparison	Ref.	Biomarker potential	Ref.
	=	MS (RR, SP, PP) *vs* HC	(92)		
Factor I	=	MS (RR, SP, PP) *vs* HC early relapse onset MS *vs*(NI-) ONDC	(92, 113)	NA	
MASP-2	↑	MS (SP, PP) *vs* controls (NS, non-MS)	(81)	NA	
Clusterin	=	MS (RR, SP, PP) *vs* HC	(92)	NA	

The characteristics of the patient groups that were compared are indicated in the 'comparison' column. The 'change' column represents the observed level alteration for the respective complement component between patient populations as represented in the 'comparison' column. The 'biomarker potential' column includes the studies that indicate a positive correlation between the level of the respective complement component and a measure as assessment of ongoing disease activity or severity, disease progression, patient stratification and/or response to treatment. To cover as much as research as possible, we did not set restrictions concerning the publication date of the references that were retrieved for this review. Symbols: ↑: significant increase; (↑): increased, unsignificant trend; ↓: significant decrease; =: unchanged. clinically isolated syndrome (CIS), expanded disability status scale (EDSS), healthy controls (HC), Glatiramer acetate (GA), interferon alpha (IFNA), mannose-binding lectin-associated serine protease (MASP-2), MS severity score (MSSS), multiple sclerosis (MS), neuromyelitis optica (NMO), non-inflammatory other neurological disease controls (NI-ONDC), not applicable (NA), not specified (NS), optic neuritis (ON), progressive MS (pMS), primary progressive (PP), secondary progressive (SP), relapsing MS (rMS), relapsing-remitting (RR), relapsing-remitting multiple sclerosis (RRMS), Response Gene To Complement 32 (RGC-32), terminal complement complex (TCC).

sections, we describe the overall alterations in complement levels in CSF and blood and discuss which correlations could be established between complement levels and measures for MS severity, progression, patient stratification and treatment response.

3.2.1 Complement proteins levels in CSF and their biomarker potential

CSF is a biofluid that is frequently collected by lumbar punction as part of the MS diagnosis process to test oligoclonal banding as a sign of intrathecal antibody synthesis (86). Table 3 represents an overview of complement components that were examined in the CSF of MS patients compared to a control group. In general, the alterations of complement components in the CSF of MS patients compared to a certain control group are quite cohesive between studies. Most studies indicate that the amount of complement factors is significantly increased (C1q, C4a) or unchanged (C3a, C4, MASP-2, fI) in the CSF of MS patients compared to HC (79–83, 92). Exceptions are fH and fB, which showed a significant decrease in CSF of MS patients compared to HC (94, 107). For complement C3, research outcomes are conflicting, as two studies indicate a significant increase (79, 83) while one study did not observe a difference in CSF C3 levels (82) in MS patients compared to HC. Only two studies evaluated CSF TCC levels in MS patients *versus* HC (79, 102). Mollnes et al. reported increased TCC levels in 30% of the MS patients (102), while Håkansson et al. reported that there was no difference in TCC levels between MS patients and HC (79). Instead of HC, a lot of studies included (NI-)ONDC patients as control group. Here, the majority of investigated complement factors was elevated (C1q, C1 inhibitor, iC3b, C4b, fI, fH, TCC, FHR125, soluble Complement Receptor 2 (sCR2)) or unchanged (C3a, C4, C4a, C5a) in CSF of MS patients compared to NI-ONDC patients (82, 91, 93–96, 99–101, 108). Of the examined complement factors, fH was unanimously decreased (94, 103, 104). For C3, two studies reported a significantly increased amount in MS patients *versus* NI-ONDC (94, 95). In contrast, one study could not detect a difference in C3 levels (82) and another study described decreased C3 levels in MS patient compared to a control group with low back pain (without white matter abnormalities) (96). The same was true for terminal factor C9, for which two studies indicated a significant decrease in MS *versus* ONDC (103, 104), while two other studies could not detect differences between MS and ONDC (105, 106). Also for C4, CSF levels were increased in one study (93) while unchanged in another study (82). A few studies also investigated whether CSF complement levels were different between specific subgroups of MS patients. For example, comparing clinically isolated syndrome (CIS) patients with relapsing-remitting (RR) MS patients did not show any changes in C3 or C4 levels (97). Interestingly, C3a levels in the CSF of RRMS and CIS patients were significantly elevated when they encountered new T2 MRI lesions during a follow-up period of 4 years compared to RRMS and CIS patients that did not develop new MRI lesions during the same follow-up period (79). Moreover, C3a levels were also significantly increased in patients that received evidence of disease activity (EDA)-3 scoring compared to no evidence of disease activity (NEDA)-3 scoring patients during a follow-up time of one year (79).

Although investigated by a limited number of studies, some correlations were discovered between the level of a single complement factor and a measure for ongoing disease activity or severity, disease progression and patient stratification (Table 3). Most of the significant correlations could link a complement level to a measure for disease severity or progression. For example, a positive correlation was observed between CSF C3 levels and expanded disability status scale (EDSS) score (95), CSF TCC levels and EDSS score (101) and CSF sCR2 levels and MS severity score (MSSS) score (91). Furthermore, C1q levels and C3a levels were

both positively correlated with the level of neuroinflammatory and neurodegenerative markers in the CSF (79). Remarkably, C3a levels were positively correlated with the amount of gadolinium-positive and T2 MRI lesions present at baseline and after follow-up (79).

Some studies also aimed to determine the source of complement factors in the CSF by measuring CSF:blood ratios of certain complement factors. An increased CSF:blood ratio suggests that elevated CSF complement levels are either a consequence of peripheral leakage due to dysfunctional brain barrier function or intrathecal complement synthesis. To clarify this, researchers studied whether a correlation exists between an increased CSF:blood ratio for complement proteins and an increased CSF:blood ratio for albumin and/or a raised IgG index, which are considered as two measures for MS disease activity (117–119). One study recorded significantly increased CSF:serum ratios for fH in MS patients compared to ONDC, which was strongly correlated with CSF:serum albumin ratio (Pearson's correlation = 0.83, $P < 0.001$), suggesting influx of fH from periphery to CSF due to brain barrier dysfunction (108). Also for complement proteins C1s and clusterin, the CSF:plasma ratio correlated with CSF:serum albumin ratio (92). On the other hand, CSF:serum ratio for C4a was increased in MS patients compared to HC, but CSF C4a levels showed moderate correlation with CSF IgG ($r = 0.53$, $p = 0.01$) while not with CSF albumin, suggesting C4a CSF was more likely the result of intrathecal synthesis (80). For C9 and fB, CSF:plasma ratio correlated with both CSF:serum albumin ratio and IgG index (92).

3.2.2 Complement protein levels in the blood and their biomarker potential

Over the years, a broad variety of complement components present in the blood was studied in MS patients *versus* different control groups. As discussed above, blood is a more accessible biofluid than CSF, but it is also more prone to non-disease specific influences such as general inflammation. Therefore, it is not surprising that studies regarding complement level alterations in the blood show more variable results compared to CSF analyses. An overview of complement components that were examined in the blood of MS patients compared to controls is shown in Table 4.

In the blood, several studies reported upregulated C3, C4 and fH levels in MS patients compared to HC (79, 80, 92, 108, 112, 115, 116). However, in case of C3 this increase rendered insignificant when an adjustment for high-sensitivity C-reactive protein (hsCRP) levels was performed *via* covariance analysis, meaning that C3 levels in the plasma were affected by hsCRP as a result of systemic inflammation rather than MS disease itself (79). For fB, fI and clusterin, no difference in blood levels between MS patients and HC could be detected (79, 92), while iC3b and C9 were described to be decreased in MS compared to HC (92, 109). Several studies also reported alterations in MS *versus* HC for C1s, C1 inhibitor, C3a, C4a, TCC and factor Bb but the results of these studies were conflicting. Blood levels of C1 inhibitor and C4a were increased (80, 92) or decreased (109, 112) in MS *versus* HC. C1s and factor Bb levels were shown to stay unchanged (92) or decreased (109). In contrast, C3a was reported to stay unchanged (79) or increased (112). Also for TCC, the results of the different studies are variable, as it was reported to be increased (112), decreased (109) or unchanged (79) when MS was compared with HC. Most studies that implemented (NI-)ONDC patients as control group concluded there was no difference with the blood levels of the investigated complement factor (*i.e.*, C3a, C4, C4a, C5, C5a, C9, fH, factor Ba) compared to (NI-)ONDC patients (96, 99, 103, 113), except one study which reported decreased C3 levels in serum of MS patients *versus* control patients with low back pain (96). Some complement factors were also found to differ between certain MS patients groups or between MS patients and other demyelinating diseases such as neuromyelitis optica (NMO). For example, increased levels of C1s, C1 inhibitor, C4d, C5, C5a, fH, factor Bb and TCC and decreased levels of C3 were detected in the blood of NMO patients *versus* MS patients (109). Within MS patient populations, acute or active RRMS patients showed increased levels of C4a, C9 and fH compared to stable RRMS patients (80, 92, 108).

Regarding the biomarker potential of blood detected complement components, a positive correlation between the level of C3, C4 and fH and EDSS score as a measure for disease activity or severity was described (108, 111). Furthermore, fH also positively correlated with MSSS scores and was a valuable marker for distinguishing secondary progressive (SP) MS from RRMS, with a positive prediction value of 72,4%. fH is therefore an interesting biomarker candidate as indicator of disease progression and disease course (108). To our knowledge, no study found a real correlation between complement levels and response to therapy. However, it was reported that after three months interferon alpha (IFNA) treatment, C1 inhibitor and TCC levels were elevated in RRMS patients compared to their baseline levels (110, 114). For TCC, blood levels were also increased six months of IFNA treatment compared to baseline levels (114). Instead of complement factors themselves, the expression of a gene induced by complement activation, namely Responsive Gene to Complement 32 (RGC-32), could have remarkable biomarker potential for the prediction of both relapse and responsiveness to Glatiramer acetate (GA) therapy (120). Kruszewski et al. investigated the expression level of RGC-32 in peripheral blood mononuclear cells and could show decreased expression of RGC-32 in peripheral blood mononuclear cells (PBMCs) of RRMS patients in acute disease state compared to RRMS patients in remission (120). On the contrary, GA responders showed upregulation of RGC-32 expression compared to GA non-responders (120). By implementing ROC analysis, they could claim that RCG-32 expression levels could predict the probability for relapse and GA responsiveness with 90% and 85% probability, respectively (120).

3.2.3 Biomarker potential of combined complement factors in MS

As summarized in Tables 3, 4, few correlations are described between the level of one single complement component and a measure for ongoing disease activity or severity, disease progression, patient stratification and/or response to treatment. However, the combination of multiple complement factor could be a stronger tool to create predictive models. Indeed, a few studies reported logistic regression (LR) models encompassing a set of complement factors together with other clinical patient characteristics to be valuable as a predictive tool. Combining C9 plasma levels, disease duration and age resulted in a LR model to predict for clinical relapse within a group of RRMS patients (AUC 0.73) (92). In the same research, another LR model combining C3, C9, C1 inhibitor and fH plasma levels could predict the probability of MS compared to HC (AUC 0.97) (92). Another study created a LR model comprising plasma levels of C1 inhibitor and TCC, which was effective to distinguish NMO from MS patients (AUC 0.98) (109). Furthermore, a model which combined CSF levels of C3, C9, fB, C1q, fI and properdin with patient age was also valuable for distinguishing NMO from MS (AUC 0.81) (93). In a study with relatively small patient groups, the CSF levels of C3, C4, IgM, mononuclear cells, neuron-specific enolase, S100 and lactate, as well as CSF:blood albumin ratio and IgM index were taken into account to calculate a score that could successfully discriminate between RRMS and SPMS patients (121).

3.3 Free complement as biomarker in other neurological diseases

The involvement of the complement system in the pathology of other neurodegenerative and neuroinflammatory diseases such as Parkinson's disease (122), ischemic stroke (122, 123), glioblastoma multiforme (124), is extensively reviewed by others. Compared to AD and MS, the applicability of free complement as biomarker was less extensively studied in these other pathologies. Therefore, the biomarker potential of free complement in other neurological diseases will not be addressed in this review.

4 The biomarker potential of complement-containing extracellular vesicles

As discussed previously, complement proteins are involved in the pathology of several neuroinflammatory and neurodegenerative diseases. Even though the level of free complement proteins in both blood and CSF has been thoroughly studied (Tables 1–4), there is no clear consensus for implementation of complement proteins as biomarkers until today. However, the consideration of shifting to complement-containing extracellular vesicles (EVs) as interesting biomarkers instead of free complement proteins has gained progressive attention during the past five years.

4.1 Extracellular vesicles

EVs are nanosized double membrane particles which are released by a broad variety of cell types (125, 126). They carry a lot of biological information (*i.e.*, proteins, nucleic acids, metabolites, lipids) which typically resembles the state of their cell of origin. This biological information packed within EVs can be transferred to other nearby or distant cells, which categorizes EVs as an important form of intercellular communication (127). Dependent on their way of biogenesis, EVs can be further divided into subclasses. Exosomes are formed as intraluminal vesicles (ILVs) within multivesicular bodies as a part of the endosomal pathway (127). Subsequently, MVBs fuse with the plasma membrane to release the ILVs as exosomes (127). The second EV subtype are ectosomes or microvesicles, which are formed by direct outwards budding of the plasma membrane (127, 128). A third group of EVs, the apoptotic bodies, are specifically formed during apoptotic cell death *via* random blebbing of the plasma membrane (127). Despite the description of these different EV subtypes, discriminatory subtype-specific markers are lacking (125, 129). For this reason, we will collectively use the term EV in this review.

EV research, especially in the context of biomarker studies, needs to fulfill the requirements for high standardized isolation and quality control. Therefore, the Minimal Information for Studies of EVs (MISEV) guidelines were developed and are continuously updated (129). EV sample preparation procedures as well as EV source information must be accurately described. This includes a description of the volume of fluid, and/or cell number, and/or tissue mass from which EVs were extracted, as well as the quantification of EV amount per volume of initial fluid or per number of producing cells/mass of tissue by implementing two distinct methods such as assessing protein amount, particle number and lipid amount. Additionally, EV nature are recommended to be verified by checking the presence of at least three protein markers. More specifically, analysis of at least one transmembrane or glycosylphosphatidylinositol (GPI)-anchored protein associated with the plasma membrane and/or endosomes (general or cell-/tissue-specific), one cytosolic or periplasmic protein marker and one non-EV co-isolated structure is required to prove the presence and purity of the EV preparations. Additionally, researchers can only claim the nature of small EVs by evaluating an extra set of markers, which comprises proteins that are situated in/on intracellular cellular compartments, including the Golgi apparatus, mitochondria, autophagosomes, peroxisomes and the endoplasmic reticulum. Proteins associated with these intracellular compartments are normally not enriched in smaller EVs (<200 nm diameter) (129).

4.2 Why EVs are interesting in the context of biomarker studies

The consideration of shifting from free protein levels to EV-associated protein levels in biomarker research stems from the fact that EVs have multiple characteristics regarding biomarker potential, which could overcome some of the limitations of free proteins. Firstly, the membranous nature of EVs makes them stable carriers that can protect their cargo from degradation (130). Secondly, it is possible to unravel the cellular source of EVs *via* analyzing the presence of cell-specific markers (131). In the context of disease, it can be an advantage to focus on EVs carrying the protein of interest originating from a cell type that is specifically engaged in the pathology to narrow down off-target, non-specific sources. For CNS diseases, it is a major advantage that brain-derived EVs can cross brain barriers and can thereby be isolated from peripheral biofluids (132). These peripheral liquid biopsies are more easy to collect compared to CSF and are a less expensive alternative to imaging (132). For example, astrocyte EVs are often defined by the presence of L-Glutamate/L-Aspartate Transporter (GLAST), while L1 cell adhesion molecule (L1CAM) is an extensively studied marker to enrich for neuronal EVs (131, 132). Thirdly, EVs carry disease specific signatures as they mimic the status of their cell of origin (130, 132). Knowledge about cellular EV origin can not only be an advantage for diagnostic purposes, but also allows to gain more insights into the underlying disease mechanisms itself (130, 133, 134). Finally, analysis of EVs can improve measurement sensitivity and signal-to-noise ratio, specifically when enriched for a certain cell type-specific EV population (132, 135). The improved sensitivity can be illustrated by the fact that alterations in plasma EVs are often absent in complete plasma (132). Since most EVs present in the blood do not originate from the CNS, the choice to enrich for EVs produced by neurons or glial cells can improve signal-to-noise ratio (132).

In the following sections, we will describe the findings of studies on the complement content of EVs in different neurological pathologies, which illustrates their growing importance in the field of biomarker identification. The most important conclusions regarding EV-associated complement, as well as EV characterization and EV quality control conducted by the studies discussed in this review are summarized in Table 5.

4.3 Complement-containing EVs in dementia

Among the different CNS diseases, complement-associated EVs have been investigated most intensively in the context of dementia, more particularly in AD. Moreover, most of the AD-focused studies aim to specifically investigate astrocyte-derived EVs (AEVs), because astrocytes play an important role during AD pathology. While astrocytes have highly important neuronal supportive functions during homeostatic conditions (156, 157), they transform to a proinflammatory (A1) phenotype during neurodegenerative diseases, mediating neurotoxicity *via* a mechanism that is currently not completely elucidated (158–160). Importantly, pro-inflammatory A1 astrocytes are shown to highly upregulate the expression of complement protein C3 in brain tissue samples of AD patients and AD mouse models (161–163). The involvement of astrocyte-related complement upregulation in relation to the astrocyte-mediated neurotoxicity has been proposed, but the question remains whether astrocytes are the main complement source in AD (37, 159, 161).

Analysis of complement content of plasma-derived AEVs from AD patients *versus* age- and gender- matched HC indicated significantly increased factors of the classical and alternative pathways (C1q, C4b, C3d, C3b, fB, fD, fBb, and TCC), while mannose-binding lectin levels were unchanged (138, 139). A similar set of increased complement components (C1q, C4b, fD, fBb, C5b, C3b, and TCC) was observed in patients with MCI that converted to dementia within 3 years (MCIC) compared to stable MCI patients (MCIS) (139). The observation that the mean complement levels in AEVs were higher in patients with moderate AD compared to preclinical AD was further confirmed in a longitudinal study where AD patients were tracked over a period of 5 to 12 years (138). Furthermore, AEV levels of complement regulatory proteins (CD46, CD59, CR1, decay accelerating factor) were decreased in AD *versus* HC (138) and MCIC *versus* MCIS (139). On top of the complement enrichment, these AEVs were also characterized by an elevated inflammatory content as their IL-6, IL-1β and TNF loading was higher in AD patients compared to HC (138). Remarkably, when comparing complement levels in AEVs and neuron-derived EVs (NEVs), the level of investigated complement components in NEVs is 6- to 50- fold lower than in AEVs (138). These findings therefore support the hypothesis that these complement-enriched, inflammatory AEVs are contributing as astrocyte-produced factors that are conceivably neurotoxic during the late inflammatory phase of AD (138). This hypothesis is strengthened by another study that reported the ability of AD patient plasma-derived AEVs to induce MAC deposition on neurons, accompanied with disruption of neuronal membrane integrity, reduction of neurite density and the reduction of neuronal viability (137). On top of this, these results indicate that AEV-associated complement proteins may be implemented as predictive biomarkers for MCI to AD conversion (138, 139). Next to AEVs, microglial-EVs (MEVs) and NEVs are also studied in the context of AD. Regarding microglial-derived EVs (MEVs), one study isolated MEVs from human cortex tissue and reported elevated MEV-associated C4 levels, as well as upregulated complement regulator CD59 in AD *versus* HC (140). In contrast to AD, EV-associated complement in frontotemporal lobar degeneration (FTLD) was only investigated once, in which sporadic as well as genetic forms

TABLE 5 Minimal Information for Studies of EVs (MISEV) guidelines related information about EV isolation and characterization in the studies discussed in this review, investigating human- and mouse-derived EVs.

Patient studies									
Patient info (disease/controls)			Biofluid/ tissue as EV source	EV cellular source (marker)	Complement content EVs	EV isolation	EV characterization		Ref.
							Global quantification	Protein marker detection	
Dementia	FTLD (genetic GRN/C9orf72, sporadic)	HC	Plasma	Bulk	↑ C1q, C3, C4 cargo per EV in FTLD ↓ C4 cargo in GRN+(homo) *vs* GRN+(het) and sporadic ↑ C4 cargo in sporadic *vs* GRN+(het) ↑ C4 EV/plasma ratio in sporadic *vs* GRN+ FTLD ↓ C4 EV/plasma ratio in GRN+ (homo) *vs* HC and other FTLD groups ↑ C3 EV/plasma ratio in sporadic *vs* HC and other FTLD groups	Total Exosome Isolation kit	☐ A ☒ B (NTA) ☐ C ☐ D ☐ E	☒ 1 (CD9) ☒ 2 (TSG101) ☐ 3 ☒ 4 (Calnexin)	(136)
	AD, FTLD	A/G HC	Plasma	Bulk (CD81+) Astrocytes (GLAST+) Neurons (L1CAM+)	AEVs and NEVs of AD patients are neurotoxic (induction Membrane Attack Complex (MAC) expression, membrane disruption, reduced neurite density, decreased cell viability)	ExoQuick + IP	☒ A (0,5 ml) ☒ B (NTA) ☒ C (Bradford) ☐ D ☒ E	☒ 1 (CD81, CD9, CD63) ☒ 2 (ALIX) ☒ 3 (ApoA1) ☒ 4 (GM130)	(137)
	AD (mild) AD (moderate)	A/G HC Pre-clinical AD	Plasma	Astrocytes (GLAST+)	↑ C1q, C4b, C3d, factor B, factor D, fBb, C3b and TCC (C5b-C9) in AEVs of mild AD *vs* HC. Mean complement levels higher in moderate AD *vs* preclinical AD.	ExoQuick + IP	☒ A (250 µl) ☐ B ☐ C ☐ D ☐ E	☒ 1 (CD81, CD59, CD55) ☐ 2 ☐ 3 ☐ 4	(138)
	MCIC AD (mild, moderate)	MCIS A/G HC	Plasma	Astrocytes (GLAST+)	↑ C1q, C4b, fD, fragment Bb, C5b, C3b, C5b-C9 in AEVs of MCIC *vs* MCIS. ↓ CD46, CD59, and type 1 complement receptor in AEVs in MCIC *vs* MCIS.	ExoQuick + IP	☒ A (250 µl) ☐ B ☐ C ☐ D ☐ E	☒ 1 (CD81, CD59, CD55) ☐ 2 ☐ 3 ☐ 4	(139)
	AD Braak stage V-VI	A/G HC	Brain tissue (parietal cortex)	Microglia (CD11b+)	Proteomic EV analysis ↑ C4, CD59 in MEVs from AD *vs* HC	GentleMACS tissue dissociation Sucrose density gradient UC + IP	☐ A ☒ B (TRPS) ☐ C ☒ D (lipidomics) ☒ E	☒ 1 (CD9, CD81, CD63, CD11b) ☒ 2 (syntenin-1) ☒ 3 ☒ 4 (GM130, Calnexin)	(140)

(Continued)

10.3389/fimmu.2022.1055050

TABLE 5 Continued

Patient studies									
Patient info (disease/controls)			Biofluid/ tissue as EV source	EV cellular source (marker)	Complement content EVs	EV isolation	EV characterization		Ref.
							Global quantification	Protein marker detection	
Parkinson's disease	PD HY stages II and III	HC	Plasma	Bulk	Proteomic EV analysis ↓ Clusterin, C1r in PD *vs* HC	SEC (EV-Second)	☒ A (200 µl) ☐ B ☒ C (Bradford) ☐ D ☒ E	☒ 1 (CD81, CD9) ☐ 2 ☐ 3 ☐ 4	(141)
	PD Mild and severe	HC	Serum	Bulk	Proteomic EV analysis ↓ C1q in PD *vs* HC ↑ Clusterin, C1r in progression from mild to severe PD ↓ C1q in progression from mild to severe PD	DUC	☒ A (5 ml) ☐ B ☒ C (BCA) ☐ D ☐ E	☐ 1 ☐ 2 ☐ 3 ☐ 4	(142)
Multiple sclerosis	RRMS, pMS	HC	Plasma	Astrocytes (GLAST+)	↑ C1q, C3b/iC3b, C5, C5a, fH (pMS vs. HC) ↑ C1q, C3, C3b/iC3b, C5, C5a, fH (RRMS *vs* HC) No difference: C4, C9, fB (MS vs. HC)	ExoQuick + IP	☒ A (0,5 ml) ☒ B (NTA) ☐ C ☐ D ☐ E	☐ 1 ☐ 2 ☐ 3 ☐ 4	(143)
	RRMS	IIH	CSF	Bulk	Proteomics on CSF-EVs C3b, C4, C6, fB, fH uniquely enriched in RRMS-EVs *vs* RRMS-CSF, while not enriched in IIH.	Precipitation + SEC (ExoSpin)	☒ A (5 ml) ☒ B (NTA) ☒ C (NanoDrop) ☐ D ☒ E	☒ 1 (CD81, CD9) ☒ 2 (TSG101) ☒ 3 (HSA) ☐ 4	(144)
	MS	NA	CSF	NA	MAC-containing "vesicles"	NA	☐ A ☐ B ☐ C ☐ D ☐ E	☐ 1 ☐ 2 ☐ 3 ☐ 4	(145)
Ischemic stroke	Symptomatic IS	HC	Serum	Bulk	Proteomic EV analysis ↑ C1qB, C1r in IS *vs* HC	ExoTrap	☒ A (500 µl) ☐ B ☒ C (BCA) ☐ D ☐ E	☒ 1 (CD9, CD81) ☒ 2 (TSG101) ☐ 3 ☒ 4 (Calnexin)	(146)
	IS (CS, CSC)	HC	Serum	Bulk Neurons (L1CAM+)	Proteomic EV analysis C1qA: unique for serum EVs and NEVs from CSC-IS patients.	ExoQuick Ultra (Bulk)	☐ A ☒ B (NTA) ☐ C	☒ 1 (CD63, CD81) ☒ 2 (ALIX)	(147)

(Continued)

10.3389/fimmu.2022.1055050

TABLE 5 Continued

Patient studies									
Patient info (disease/controls)			Biofluid/ tissue as EV source	EV cellular source (marker)	Complement content EVs	EV isolation	EV characterization		Ref.
							Global quantification	Protein marker detection	
					C3 abundant in IS (CSC and CS) and HC in serum EVs and NEVs.	SmartSEC + IP (NEVs)	☐ D ☒ E	☒ 3 (Albumin) ☐ 4	
Brain tumor	GBM	HC	Plasma	Bulk	Proteomic EV analysis ↑ C3, C5, C1q, fH in GBM *vs* HC	DUC	☒ A (5 ml) ☒ B (NTA) ☒ C (MicroBCA) ☐ D ☒ E	☒ 1 (CD81, CD9, CD63, CD41a) ☒ 2 (HSP70) ☐ 3 ☒ 4 (GM130)	(148)
	GBM	HC	Plasma	Bulk	Proteomic EV analysis ↑ C3, C4b in GBM *vs* HC	DUC	☒ A (15 ml blood) ☒ B (NTA) ☐ C ☐ D ☒ E	☒ 1 (CD9, CD63) ☒ 2 (TSG101) ☐ 3 ☐ 4	(149)
	GBM Grade II-IV	MEN HC	Plasma	Bulk	Proteomic EV analysis ↑ C3 in GBM *vs* controls	SEC (qEV, Izon)	☒ A (0.5 ml) ☒ B (NTA) ☐ C ☐ D ☒ E	☒ 1 (CD9, ITGA2B, ITGA6, PDCD6IP) ☒ 2 (ANXA1/2/6, FLOT1, HSP90A1B, GAPDH, HIST1H4A) ☐ 3 ☒ 4	(150)
Mouse studies/primary culture studies									
Mouse model Cell culture			Biofluid/ tissue as EV source	EV cellular source (marker)	Complement content EVs	EV isolation	EV characterization		Ref.
							Global quantification	Protein marker detection	
Dementia	AβO CPE primary culture	Scram-bled CPE primary culture	Culture medium	CPE cells	Proteomic EV analysis ↑ C3 in AβO-stimulated CPE *vs* scrambled	SEC (qEV)	☒ A (500 µl) ☒ B (NTA) ☐ C ☐ D ☒ E	☒ 1 (CD81, CD9) ☒ 2 (TSG101) ☐ 3 ☒ 4 (Calnexin)	(151)

(Continued)

10.3389/fimmu.2022.1055050

TABLE 5 Continued

Mouse studies/primary culture studies									
Mouse model Cell culture			Biofluid/ tissue as EV source	EV cellular source (marker)	Complement content EVs	EV isolation	EV characterization		Ref.
							Global quantification	Protein marker detection	
	2xTg-AD 5xFAD 3xTg-AD	WT	Plasma	Neuron (L1CAM+) Astrocyte (GLAST+)	↑ AEV C1q in 3xTg-AD *vs* WT	IP (ExoSORT)	☐ A ☒ B (NTA) ☒ C (Bradford) ☐ D ☐ E	☒ 1 (CD81, CD9, CD63) ☒ 2 (FLOT1) ☒ 3 (APOA, albumin) ☒ 4 (Calnexin)	(152)
	CAST.APP/PS1	CAST WT HC	Brain tissue	Bulk	Proteomic EV analysis C1qa, C1qc increased in EVs from CAST APP/PS1 *vs* WT, but not significant	DUC + sucrose gradient	☒ A (0.4g) ☒ B (NTA) ☒ C (BCA) ☐ D ☒ E	☒ 1 (CD9, CD81, CD63, ITGA) ☒ 2 (ANXA5) ☐ 3 ☒ 4 (GM130, CYC1)	(153)
Brain tumor	GBM mouse model Longitudinal samplings (baseline, T1, T2)	NA	Serum	Bulk	Proteomic EV analysis Complements among group of deregulated proteins in EVs C1ra and C1sa deregulated in EVs between T2 and T1 stages.	Precipitation (Total Exosome Isolation reagent) or SEC	☒ A (50µl) ☒ B (DLS) ☐ C ☐ D ☒ E	☒ 1 (CD9, ITGA) ☒ 2 (ANXA4, ANXA5, ANXA7) ☐ 3 ☐ 4	(154)
	GBM mouse model Longitudinal samplings (baseline, pre-symptomatic T1, symptomatic T2)	NA	Serum	Bulk	Proteomic EV analysis ↓ C4b in T1 *vs* baseline ↑ C1qa, C1ra, C1s1 in T1 and T2 *vs* baseline	SEC (qEV – 70nm)	☒ A (50µl) ☐ B ☒ C (MicroBCA) ☐ D ☐ E	☒ 1 (ITGB1) ☒ 2 (HSPA8, ACT) ☒ 3 (Albumin) ☐ 4	(155)

For global EV quantification requirements, consult checkboxes A-E. Checkbox A) Cell number/fluid volume/tissue mass from which EVs were isolated. Checkbox B) Analysis of particle number. Checkbox C) Analysis of protein amount. Checkbox D) Analysis of lipid amount. Checkbox E) Analysis by electron microscopy. For information regarding EV protein marker detection that has been conducted by the indicated studies, consult checkboxes 1-4. Checkbox 1) Transmembrane or Glycosylphosphatidylinositol (GPI)-anchored protein(s) localized in cells at plasma membrane or endosomes. Checkbox 2) Cytosolic protein(s) with membrane-binding or -association capacity. Checkbox 3) Assessment of presence/absence of expected contaminants. Checkbox 4) For small EVs <200nm: verifying protein(s) associated with compartments other than plasma membrane or endosomes. extracellular vesicles (EVs), astrocyte-EV (AEV), neuronal-EV (NEV), microglial-EV (MEV), not described (ND), not applicable (NA), idiopathic intracranial hypertension (IIH); multiple sclerosis (MS), relapsing-remitting MS, progressive MS (pMS), Alzheimer's disease (AD), Fronto-Temporal Lobar Degeneration (FTLD), Parkinson's disease (PD), Glioblastoma multiforme (GBM), meningioma (MEN), ischemic stroke (IS), subcortical (SC), cortical-subcortical (CSC), mild cognitive impairment (MCI), MCI stable (MCIS), MCI converting to dementia (MCIC), Hoehn and Yahr (HY), healthy controls (HC), age-gender matched healthy controls (A/G HC), homozygous (hom), heterozygous (het), Nanoparticle Tracking Analysis (NTA), Bicinchoninic Acid Assay (BCA) Bradford assay (BA), mass spectrometry (MS), differential ultracentrifugation (DUC), ultracentrifugation (UC), Annexin A5 (ANXA5), flow cytometry (FC), transmission electron microscopy (TEM), size exclusion chromatography (SEC), high sensitivity flow cytometry (hsFC), immunoprecipitation (IP), Tunable Resistive Pulse Sensing (TRPS), factor H (fH), factor B (fB), factor D (fD), terminal complement complex (TCC), human serum albumin (HSA), heat-shock protein (HSP), A-beta oligomers (AβO), choroid plexus epithelial cells (CPE), wildtype (WT).

10.3389/fimmu.2022.1055050

of FTLD (heterozygous/homozygous GRN mutation carriers, intermediate/pathological C9orf72 expansion carriers) were included. Although the concentration of plasma EVs was lower in sporadic and genetic FTLD patients, the C1q, C3 and C4 cargo per EV was higher in FTLD compared to EVs from HC (136). Additionally, EV-complement related differences between different subgroups of FTLD were also detected. For example, C4 cargo was decreased in GRN+ homozygous genetic FTLD *versus* heterozygous GRN+ and pathological C9orf72 genetic FTLD, while EV-associated C4 increased in sporadic FTLD compared to heterozygous GRN+ FTLD (136). C1q, C3 and C4 EV:plasma ratios were also compared between the different groups. Compared to HC, C3 EV:plasma ratios were elevated in sporadic FTLD while C4 EV:plasma ratios were decreased in homozygous GRN+ FTLD (136). Moreover, C4 EV:plasma ratios were increased in sporadic FTLD *versus* GRN+ genetic FTLD but decreased in homozygous GRN+ FTLD *versus* all other FLTD groups (136). For C1q, no differences in EV:plasma ratios could be detected amongst all groups investigated (136).

Next to patient studies, there is a limited amount of EV research on animal models for AD, in which complement components were found into EVs. C1q levels were shown to be increased in plasma-derived AEVs from 3xTg-AD mice compared to WT mice (152). Moreover, C1q levels in plasma-derived AEV were positively correlated with C1q levels in the hippocampus and cortex, which implies that C1q levels in AEVs can reflect C1 levels in the indicated brain regions (152). Another study showed an insignificant increase in C1qa and C1qc levels in CAST APP/PS1 mice brain derived EVs compared to EVs from WT control mice (153). Moreover, we previously reported an increased release of C3-containing EVs by choroid plexus epithelial (CPE) cells that were stimulated with amyloid-beta oligomers (AβO), identifying a novel source of complement-containing EVs that might potentially be detected in the CSF as biomarker for AD (151).

4.4 Complement-containing EVs in Parkinson's disease

For PD, two small-sized proteomic studies on blood-derived EVs from sporadic PD patients in different progression stages compared to HC revealed alterations in the level of EV-associated complement proteins (141, 142). Both studies aimed to identify potential EV-associated biomarkers for PD diagnosis and PD progression. A pilot study with 16 PD patients, stratified *via* the stage of PD progression according to the Hoehn and Yahr (HY) stages (HY stages II and III), observed a significant decrease of complement proteins clusterin and C1r, as well as apolipoprotein A1 (ApoA1) in plasma EVs from PD patients *versus* HC (141). Therefore, these three EV-enriched proteins may be proposed as potential biomarker candidates for PD diagnosis (141). However, only ApoA1 present in the EV fractions could be correlated with PD progression, as ApoA1-EV levels were decreased in PD patients with HY stage III *versus* HY stage II, while plasma protein levels of ApoA1 remained unchanged (141). However, we want to remark that ApoA1 has been indicated as a contaminant that often co-isolates with EVs during EV preparations according to the MISEV guidelines (129). On the contrary, the second proteomic study on serum EVs, including 20 PD patients subdivided according to the HY scale into mild (HY < 3) and severe (HY > 3), could identify complement proteins that were significantly altered during PD disease progression (142). Here, increased EV levels of clusterin and C1r were detected in PD patients with progression from mild to severe disease, whereas decreased levels of EV-associated C1q were detected in PD patients *versus* HC as well as during progression from mild to severe PD (142). These results indicate a potential for clusterin, C1r and C1q as EV biomarkers for PD progression (142). In conclusion, when comparing both PD studies, both C1r and clusterin might be interesting biomarkers for PD diagnosis and/or progression, but validation with larger patient cohorts is essential.

4.5 Complement-containing EVs in MS

The first observation of complement-associated vesicles in MS was made over 30 years ago by Scolding et al., who discovered the presence of MAC-containing vesicles in the CSF of MS patients (145). These MAC-containing vesicles were also found to be produced by oligodendrocytes as a response to complement activation (145). More recently, two patient studies report altered complement EV content in biofluid samples of MS patients. One proteomic analysis of EVs isolated from the CSF of RRMS patients revealed a unique enrichment of several complement proteins (C3b, C4, C6, fB, fH) in EVs compared to CSF levels, while these were not enriched in CSF-EV samples of idiopathic intracranial hypertension control patients (144). We found one study that investigated the biomarker potential of complement-containing EVs in MS. In this study, the potential of circulating NEVs and AEVs as biomarkers for complement-mediated synaptic loss during MS was examined (143). Therefore, synaptic proteins were analyzed in NEVs while a wide spectrum of complement components (C1q, C3, C3b/iC3b, C4, C5, C5a, C9, fB, fH) was measured in AEVs (143). Interestingly, decreased levels of synaptic proteins synaptopodin and synaptophysin in NEVs were strongly correlated with increased levels of complement proteins (C1q, C3b/iC3b, C5, C5a, fH) in AEVs in MS plasma samples compared to HC (143). Importantly, the increase in complement proteins within EVs was only present in AEVs, while total plasma EVs or neat plasma was not showing differences between MS and HC (143).

4.6 Complement-containing EVs in glioblastoma multiforme

Also in the cancer field, circulating EVs may carry potential biomarkers that could be highly valuable to accelerate and further improve the diagnosis and follow-up process for specific malignancies. In this review, we particularly focus on GBM brain tumors, the most prevalent, highly malignant glial tumor in the CNS which is frequently diagnosed only in later disease stages and is associated with a poor prognosis (164). Also in this neurological pathology, the intercommunicative role of EVs has been described in the bidirectional crosstalk between the GBM tumor and its microenvironment (165–167). The involvement of the complement system in GBM pathology is also illustrated by multiple reports and is reviewed by others (124, 168). In general, the complement system seems to play a role in several aspects of GB tumorigenesis, such as the maintenance and migration of glioma stem-like tumor niche cells, GB tumor angiogenesis and immune cell cross talk (124). Other key findings include the presence of complement deposits (C1q, C3, TCC, fB) in tumor tissue (169) and altered complement (C1q, fB) levels in serum (169).

For plasma EVs isolated from GBM patients, three independent proteomic analyses all indicated the enrichment for complement protein C3 compared to HC (148–150). Additionally, also enrichment for C1q, C4b and fH were reported in one of the indicated EV proteome studies (148, 149). Next to complement components, enrichment for other inflammatory and coagulation proteins characterize the overall inflammatory signature of GBM-plasma EVs across studies (148, 149). Strikingly, this inflammatory EV phenotype disappeared after tumor resection, which highlights the potential to use this signature to distinguish GBM tumor bearing patients from HC (149). Findings from GBM mouse model studies further support the growing potential of EV-associated complement components in GBM biomarker research. In a longitudinal study, serum samples for EV analysis were collected to monitor disease progression and therapeutic interventions (154). Here, complement proteins (C1rs, C1ra) were present within the list of deregulated proteins in both GBM 12 days after tumor induction (T1) and GBM 21 days after GL261 implantation (T2) (154). A second longitudinal study with a similar set-up, which analyzed the proteome of EVs from serum collected at baseline, pre-symptomatic (T1) and symptomatic stages (T2), detected upregulated levels of C1qa, C1s1 and C1ra in T1 and T2 stages *versus* baseline, while C4b was downregulated during T1 stage compared to baseline (155).

4.7 Complement-containing EVs in ischemic stroke

Besides neurodegenerative and neuroinflammatory diseases, complement proteins are also shown to play a role in the pathogenesis of (neuro)vascular disorders such as atherosclerosis and IS (123, 170). On the one hand, the lectin and alternative complement pathways as well as C3a and C5a binding to their receptors, are implicated in secondary brain tissue injury (123, 170). For example, after a cerebral ischemic event, C3aR and C5aR expression was activated on endothelial cells, glial cells and leukocytes, which may promote inflammatory and/or repair processes at ischemic sites by regulating glial cell activation and chemotaxis (171, 172). Also, the therapeutic potential of modulated complement activation has been illustrated by the fact that modulation or inhibition of complement activation can effectively reduce ischemic brain injury (173, 174). Also, increased levels of C1q and the C1r-C1s-C1inhibitor complex are associated with poor cardiovascular outcomes (175, 176). On the other hand, complement factors including C3a and C5a are also important mediators of neurogenesis and neural plasticity during cerebral ischemia (177, 178). For further extensive reading about the involvement of complement in IS, we refer to reviews written by others (123, 170). In literature, the role of EVs in IS and their potential to transfer information about post-IS processes involving tissue damage and repair have been extensively reviewed as well (179–181). Therefore, linking EVs and complement proteins is an interesting strategy for EV-biomarker identification in IS.

For IS, two proteomic studies on blood-derived EVs were conducted (146, 147). In the first Japanese study with small sample size, four proteins among which C1q subunit B and C1r subunit were significantly enriched in serum EVs from patients who developed symptomatic stroke compared to the HC (146). An important remark here is that the serum samples for EV-proteome analysis obtained in this study were collected during regular health check-ups and not nearby the moment of IS itself, and the diagnosis of IS was based on questionnaires which may imply measurement errors. The second study investigated EV proteome profiles of a larger cohort of IS patients, subdivided in subcortical (SC) and cortical-subcortical (CSC) IS patients, in which serum samples were collected within the first 24h post-IS (147). Here, it was discovered that the C1q A chain protein was specifically present in serum EVs as well as serum-derived NEVs from CSC-IS patients (147). Remarkably, C3 was abundantly present in serum EVs and serum-derived NEVs of CSC- and SC-IS patients as well as HC (147).

5 Discussion

Despite the high number of studies investigating complement proteins in the blood and CSF of AD and MS patients, there is currently no clear consensus on their clinical applicability as biomarker. Possible explanations for the high variability across studies include small patient cohorts, different patient inclusion/exclusion criteria or diagnostic parameters and the use of various methods to analyze complement content. Indeed, different complement analysis tools with variable sensitivity and specificity are implemented across biomarker studies to measure complement proteins, including western blot, ELISA, proteomics and multi-array immunoassays. Even when the same detection method for complement components was implemented, variation still arises due to the usage of different complement antibodies or the way samples were prepared for analysis. Moreover, sample collection and analysis should be further standardized for biomarker research and application. Overall, a limited number of studies could show a statistically significant correlation between the level of (a) certain complement protein(s) and disease parameter(s), but the concerning correlations are only described by single studies. In the future, it is required to repeat these studies with bigger patient cohorts to confirm these correlations. However, complement dysregulation is definitely not restricted to one particular CNS disease and almost all complement proteins seem to be affected. Therefore, it is unlikely that free complement components alone will be valuable as biomarkers to distinguish between CNS diseases. Nevertheless, they can still be valuable for supporting the diagnostic process, for example by representing a part of the biomarkers that change within a certain disease instead of considering them as secluded biomarkers for disease diagnosis, progression and response to treatment.

Proteins captured inside or at the surface of EVs as biomarkers have several advantages over free proteins. For example, EVs are stable and protect their cargo from degradation. Interestingly, the cellular source of EVs can be determined by detection of cell-specific markers present on or inside EVs. Finally, EVs are carriers of disease specific signatures because they mimic the status of their cell of origin. This is not only an advantage for diagnostic purposes, but also allows to gain more insights into the underlying disease mechanisms. For example, AD biomarkers are difficult to analyze in peripheral biofluids, while brain-derived EVs can be isolated from peripheral sources by making use of EV enrichment *via* cell type specific markers on EVs (*e.g.*, GLAST, L1CAM). However, before being able to implement EVs as clinical biomarker platform, EV isolation and quality control procedures should be further standardized. Moreover, the knowledge about complement-containing EVs is still limited and until today, no effective correlation studies to link complement-EV levels with disease characteristics have been conducted yet. Notably, as most research on complement EV content is based on proteomic analyses, complement proteins can be detected inside EVs. However, it is possible that the measured complement proteins are only associated with the EVs at their outside instead of being a real part of their cargo. In conclusion, shifting the focus to complement-containing EVs as potential biomarkers for neuroinflammatory and neurodegenerative diseases seems very promising, but further research is still needed to reveal its true value.

Author contributions

All authors contributed to the article and approved the submitted version.

Funding

All sources of funding received for the research being submitted. FWO: 1295223N, 1157621N, 1195021N Charcot Foundation: 2020-023 Stichting Alzheimer Onderzoek (SAO-FRA): 2019-0028.

Conflict of interest

The authors declare that the research was conducted in the absence of any commercial or financial relationships that could be construed as a potential conflict of interest.

Publisher's note

All claims expressed in this article are solely those of the authors and do not necessarily represent those of their affiliated organizations, or those of the publisher, the editors and the reviewers. Any product that may be evaluated in this article, or claim that may be made by its manufacturer, is not guaranteed or endorsed by the publisher.

References

1. Hansson O. Biomarkers for neurodegenerative diseases. *Nat Med* (2021) 27 (6):954–63. doi: 10.1038/s41591-021-01382-x

2. Dujardin P, Vandenbroucke RE, Van Hoecke L. Fighting fire with fire: The immune system might be key in our fight against alzheimer's disease. *Drug Discovery Today* (2022) 27(5):1261–83. doi: 10.1016/j.drudis.2022.01.004

3. Dalakas MC, Alexopoulos H, Spaeth PJ. Complement in neurological disorders and emerging complement-targeted therapeutics. *Nat Rev Neurol* (2020) 16(11):601–17. doi: 10.1038/s41582-020-0400-0

4. Zelek WM, Morgan BP. Targeting complement in neurodegeneration: challenges, risks, and strategies. *Trends Pharmacol Sci*(2022) 43(8):615–28. doi: 10.1016/j.tips.2022.02.006

5. Schartz ND, Tenner AJ. The good, the bad, and the opportunities of the complement system in neurodegenerative disease. *J Neuroinflamm*(2020) 17(1). doi: 10.1186/s12974-020-02024-8

6. Tatomir A, Talpos-Caia A, Anselmo F, Kruszewski AM, Boodhoo D, Rus V, et al. The complement system as a biomarker of disease activity and response to treatment in multiple sclerosis. *Immunol Res*(2017) 65(6):1103–9. doi: 10.1007/s12026-017-8961-8

7. Morgan BP, Gommerman JL, Ramaglia V. An "Outside-in" and "Inside-out" consideration of complement in the multiple sclerosis brain: Lessons from development and neurodegenerative diseases. *Front Cell Neurosci*(2021) 14. doi: 10.3389/fncel.2020.600656

8. Warwick CA, Keyes AL, Woodruff TM, Usachev YM. The complement cascade in the regulation of neuroinflammation, nociceptive sensitization, and pain. *J Biol Chem*(2021) 297(3):101085. doi: 10.1016/j.jbc.2021.101085

9. Woodruff TM, Ager RR, Tenner AJ, Noakes PG, Taylor SM. The role of the complement system and the activation fragment C5a in the central nervous system. *Neuromol Med*(2010) 12(2):179–92. doi: 10.1007/s12017-009-8085-y

10. Lee JD, Coulthard LG, Woodruff TM. Complement dysregulation in the central nervous system during development and disease. *Semin Immunol*(2019) 45. doi: 10.1016/j.smim.2019.101340

11. Stephan AH, Barres BA, Stevens B. The complement system: an unexpected role in synaptic pruning during development and disease. *Annu Rev Neurosci* (2012) 35:369–89. doi: 10.1146/annurev-neuro-061010-113810

12. Stevens B, Allen NJ, Vazquez LE, Howell GR, Christopherson KS, Nouri N, et al. The classical complement cascade mediates CNS synapse elimination. *Cell.*(2007) 131(6):1164–78. doi: 10.1016/j.cell.2007.10.036

13. Ingram G, Loveless S, Howell OW, Hakobyan S, Dancey B, Harris CL, et al. Complement activation in multiple sclerosis plaques: an immunohistochemical analysis. *Acta Neuropathol Commun* (2014) 2:53. doi: 10.1186/2051-5960-2-53

14. Watkins LM, Neal JW, Loveless S, Michailidou I, Ramaglia V, Rees MI, et al. Complement is activated in progressive multiple sclerosis cortical grey matter lesions. *J Neuroinflamm*(2016) 13. doi: 10.1186/s12974-016-0611-x

15. Barnett MH, Parratt JD, Cho ES, Prineas JW. Immunoglobulins and complement in postmortem multiple sclerosis tissue. *Ann Neurol* (2009) 65 (1):32–46. doi: 10.1002/ana.21524

16. Lucchinetti C, Bruck W, Parisi J, Scheithauer B, Rodriguez M, Lassmann H. Heterogeneity of multiple sclerosis lesions: implications for the pathogenesis of demyelination. *Ann Neurol* (2000) 47(6):707–17. doi: 10.1002/1531-8249(200006)47:6<707::AID-ANA3>3.0.CO;2-Q

17. Reis ES, Mastellos DC, Hajishengallis G, Lambris JD. New insights into the immune functions of complement. *Nat Rev Immunol*(2019) 19(8):503–16. doi: 10.1038/s41577-019-0168-x

18. Lo MW, Woodruff TM. Complement: Bridging the innate and adaptive immune systems in sterile inflammation. *J Leukoc Biol*(2020) 108(1):339–51. doi: 10.1002/JLB.3MIR0220-270R

19. Ricklin D, Hajishengallis G, Yang K, Lambris JD. Complement: a key system for immune surveillance and homeostasis. *Nat Immunol*(2010) 11(9):785–97. doi: 10.1038/ni.1923

20. Merle NS, Church SE, Fremeaux-Bacchi V, Roumenina LT. Complement system part I - molecular mechanisms of activation and regulation. *Front Immunol* (2015) 6. doi: 10.3389/fimmu.2015.00262

21. Vermunt L, Sikkes SAM, van den Hout A, Handels R, Bos I, van der Flier WM, et al. Duration of preclinical, prodromal, and dementia stages of alzheimer's disease in relation to age, sex, and APOE genotype. *Alzheimers Dement*(2019) 15 (7):888–98. doi: 10.1016/j.jalz.2019.04.001

22. Villemagne VL, Burnham S, Bourgeat P, Brown B, Ellis KA, Salvado O, et al. Amyloid beta deposition, neurodegeneration, and cognitive decline in sporadic alzheimer's disease: a prospective cohort study. *Lancet Neurol*(2013) 12(4):357–67. doi: 10.1016/S1474-4422(13)70044-9

23. Buchhave P, Stomrud E, Blennow K, Zetterberg H, Londos E, Minthon L, et al. Longitudinal study of CSF biomarkers in patients with alzheimer's disease. *Eur J Neurol*(2009) 16:337–. doi: 10.1371/journal.pone.0006294

24. Zetterberg H, Pedersen M, Lind K, Svensson M, Rolstad S, Eckerstrom C, et al. Intra-individual stability of CSF biomarkers for alzheimer's disease over two years. *J Alzheimers Dis*(2007) 12(3):255–60. doi: 10.3233/JAD-2007-12307

25. Lambert JC, Heath S, Even G, Campion D, Sleegers K, Hiltunen M, et al. Genome-wide association study identifies variants at CLU and CR1 associated with alzheimer's disease. *Nat Genet*(2009) 41(10):1094–U68. doi: 10.1038/ng.439

26. Harold D, Abraham R, Hollingworth P, Sims R, Gerrish A, Hamshere ML, et al. Genome-wide association study identifies variants at CLU and PICALM associated with alzheimer's disease. *Nat Genet*(2009) 41(10):1088–U61. doi: 10.1038/ng.440

27. Chibnik LB, Shulman JM, Leurgans SE, Schneider JA, Wilson RS, Tran D, et al. CR1 is associated with amyloid plaque burden and age-related cognitive decline. *Ann Neurol*(2011) 69(3):560–9. doi: 10.1002/ana.22277

28. Naj AC, Jun G, Beecham GW, Wang LS, Vardarajan BN, Buros J, et al. Common variants at MS4A4/MS4A6E, CD2AP, CD33 and EPHA1 are associated with late-onset alzheimer's disease. *Nat Genet*(2011) 43(5):436. doi: 10.1038/ng.801

29. Brouwers N, Van Cauwenberghe C, Engelborghs S, Lambert JC, Bettens K, Le Bastard N, et al. Alzheimer Risk associated with a copy number variation in the complement receptor 1 increasing C3b/C4b binding sites. *Mol Psychiatr*(2012) 17 (2):223–33. doi: 10.1038/mp.2011.24

30. Rogers J, Cooper NR, Webster S, Schultz J, Mcgeer PL, Styren SD, et al. Complement activation by beta-amyloid in Alzheimer-disease. *P Natl Acad Sci USA*(1992) 89(21):10016–20. doi: 10.1073/pnas.89.21.10016

31. Webster S, Glabe C, Rogers J. Multivalent binding of complement protein C1Q to the amyloid beta-peptide (A beta) promotes the nucleation phase of a beta aggregation. *Biochem Bioph Res Co*(1995) 217(3):869–75. doi: 10.1006/bbrc.1995.2852

32. Webster S, Bonnell B, Rogers J. Charge-based binding of complement component C1q to the Alzheimer amyloid beta-peptide. *Am J Pathol*(1997) 150 (5):1531–6.

33. Boyett KW, DiCarlo G, Jantzen PT, Jackson J, O'Leary C, Wilcock D, et al. Increased fibrillar beta-amyloid in response to human C1q injections into hippocampus and cortex of APP+PS1 transgenic mice. *Neurochem Res*(2003) 28 (1):83–93. doi: 10.1023/A:1021600212829

34. Shen Y, Lue LF, Yang LB, Roher A, Kuo YM, Strohmeyer R, et al. Complement activation by neurofibrillary tangles in alzheimer's disease. *Neurosci Lett*(2001) 305(3):165–8. doi: 10.1016/S0304-3940(01)01842-0

35. Dejanovic B, Huntley MA, De Maziere A, Meilandt WJ, Wu T, Srinivasan K, et al. Changes in the synaptic proteome in tauopathy and rescue of tau-induced synapse loss by C1q antibodies. *Neuron*(2018) 100(6):1322. doi: 10.1016/j.neuron.2018.10.014

36. Shi QQ, Colodner KJ, Matousek SB, Merry K, Hong SY, Kenison JE, et al. Complement C3-deficient mice fail to display age-related hippocampal decline. *J Neurosci*(2015) 35(38):13029–42. doi: 10.1523/JNEUROSCI.1698-15.2015

37. Hong S, Beja-Glasser VF, Nfonoyim BM, Frouin A, Li S, Ramakrishnan S, et al. Complement and microglia mediate early synapse loss in Alzheimer mouse models. *Science.*(2016) 352(6286):712–6. doi: 10.1126/science.aad8373

38. Khoonsari PE, Haggmark A, Lonnberg M, Mikus M, Kilander L, Lannfelt L, et al. Analysis of the cerebrospinal fluid proteome in alzheimer's disease. *PLos One* (2016) 11(3). doi: 10.1371/journal.pone.0150672

39. Krance SH, Wu CY, Zou Y, Mao HY, Toufighi S, He XY, et al. The complement cascade in alzheimer's disease: a systematic review and meta-analysis. *Mol Psychiatr*(2021) 26(10):5532–41. doi: 10.1038/s41380-019-0536-8

40. Brosseron F, Traschutz A, Widmann CN, Kummer MP, Tacik P, Santarelli F, et al. Characterization and clinical use of inflammatory cerebrospinal fluid protein markers in alzheimer's disease. *Alzheimers Res Ther*(2018) 10. doi: 10.1186/s13195-018-0353-3

41. Wang Y, Hancock AM, Bradner J, Chung KA, Quinn JF, Peskind ER, et al. Complement 3 and factor h in human cerebrospinal fluid in parkinson's disease, alzheimer's disease, and multiple-system atrophy. *Am J Pathol*(2011) 178(4):1509–16. doi: 10.1016/j.ajpath.2011.01.006

42. Hu WT, Chen-Plotkin A, Arnold SE, Grossman M, Clark CM, Shaw LM, et al. Novel CSF biomarkers for alzheimer's disease and mild cognitive impairment. *Acta Neuropathologica.*(2010) 119(6):669–78. doi: 10.1007/s00401-010-0667-0

43. Wu T, Dejanovic B, Gandham VD, Gogineni A, Edmonds R, Schauer S, et al. Complement C3 is activated in human AD brain and is required for neurodegeneration in mouse models of amyloidosis and tauopathy. *Cell Rep* (2019) 28(8):2111. doi: 10.1016/j.celrep.2019.07.060

44. Hu WT, Watts KD, Tailor P, Nguyen TP, Howell JC, Lee RC, et al. CSF complement 3 and factor h are staging biomarkers in alzheimer's disease. *Acta Neuropathol Com* (2016) 4. doi: 10.1186/s40478-016-0277-8

45. Daborg J, Andreasson U, Pekna M, Lautner R, Hanse E, Minthon L, et al. Cerebrospinal fluid levels of complement proteins C3, C4 and CR1 in alzheimer's disease. *J Neural Transm*(2012) 119(7):789–97. doi: 10.1007/s00702-012-0797-8

46. Toledo JB, Korff A, Shaw LM, Trojanowski JQ, Zhang J. Neuroimaging AsD. low levels of cerebrospinal fluid complement 3 and factor h predict faster cognitive decline in mild cognitive impairment. *Alzheimers Res Ther* (2014) 6(3). doi: 10.1186/alzrt266

47. Bonham LW, Desikan RS, Yokoyama JSInIti AsDN. The relationship between complement factor C3, APOE epsilon 4, amyloid and tau in alzheimer's disease. *Acta Neuropathol Com* (2016) 4. doi: 10.1186/s40478-016-0339-y

48. Deming Y, Xia J, Cai YF, Lord J, Holmans P, Bertelsen S, et al. A potential endophenotype for alzheimer's disease: cerebrospinal fluid clusterin. *Neurobiol Aging* (2016) 37. doi: 10.1016/j.neurobiolaging.2015.09.009

49. Nilselid AM, Davidsson P, Nagga K, Andreasen N, Fredman P, Blennow K. Clusterin in cerebrospinal fluid: Analysis of carbohydrates and quantification of native and glycosylated forms. *Neurochem Int* (2006) 48(8):718–28. doi: 10.1016/j.neuint.2005.12.005

50. Jongbloed W, van Dijk KD, Mulder SD, van de Berg WDJ, Blankenstein MA, van der Flier W, et al. Clusterin levels in plasma predict cognitive decline and progression to alzheimer's disease. *J Alzheimers Dis* (2015) 46(4):1103–10. doi: 10.3233/JAD-150036

51. Desikan RS, Thompson WK, Holland D, Hess CP, Brewer JB, Zetterberg H, et al. The role of clusterin in amyloid-beta-Associated neurodegeneration. *JAMA Neurol* (2014) 71(2):180–7. doi: 10.1001/jamaneurol.2013.4560

52. Nestor SM, Rupsingh R, Borrie M, Smith M, Accomazzi V, Wells JL, et al. Ventricular enlargement as a possible measure of alzheimers disease progression validated using the alzheimers disease neuroimaging initiative database. *Brain.* (2008) 131:2443–54. doi: 10.1093/brain/awn146

53. Cutler P, Akuffo EL, Bodnar WM, Briggs DM, Davis JB, Debouck CM, et al. Proteomic identification and early validation of complement 1 inhibitor and pigment epithelium -derived factor: Two novel biomarkers of alzheimer's disease in human plasma. *Proteom Clin Appl* (2008) 2(4):467–77. doi: 10.1002/prca.200780101

54. Hakobyan S, Harding K, Aiyaz M, Hye A, Dobson R, Baird A, et al. Complement biomarkers as predictors of disease progression in alzheimer's disease. *J Alzheimers Dis* (2016) 54(2):707–16. doi: 10.3233/JAD-160420

55. Thambisetty M, Simmons A, Hye A, Campbell J, Westman E, Zhang Y, et al. Plasma biomarkers of brain atrophy in alzheimer's disease. *PLos One* (2011) 6(12). doi: 10.1371/journal.pone.0028527

56. Cheng ZH, Yin JJ, Yuan HW, Jin CH, Zhang FQ, Wang ZQ, et al. Blood-derived plasma protein biomarkers for alzheimer's disease in han Chinese. *Front Aging Neurosci* (2018) 10. doi: 10.3389/fnagi.2018.00414

57. Wang T, Wang XN, Yao YX, Zhao CS, Yang CX, Han Y, et al. Association of plasma apolipoproteins and levels of inflammation-related factors with different stages of alzheimer's disease: a cross-sectional study. *BMJ Open* (2022) 12(4). doi: 10.1136/bmjopen-2021-054347

58. Muenchhoff J, Poljak A, Thalamuthu A, Gupta VB, Chatterjee P, Raftery M, et al. Changes in the plasma proteome at asymptomatic and symptomatic stages of autosomal dominant alzheimer's disease. *Sci Rep-Uk* (2016) 6. doi: 10.1038/srep29078

59. Morgan AR, Touchard S, Leckey C, O'Hagan C, Nevado-Holgado AJ, Barkhof F, et al. Inflammatory biomarkers in alzheimer's disease plasma. *Alzheimers Dement* (2019) 15(6):776–87. doi: 10.1016/j.jalz.2019.03.007

60. Rasmussen KL, Nordestgaard BG, Frikke-Schmidt R, Nielsen SF. An updated Alzheimer hypothesis: Complement C3 and risk of alzheimer's disease-a cohort study of 95,442 individuals. *Alzheimers Dement* (2018) 14(12):1589–601. doi: 10.1016/j.jalz.2018.07.223

61. Bennett S, Grant M, Creese AJ, Mangialasche F, Cecchetti R, Cooper HJ, et al. Plasma levels of complement 4a protein are increased in alzheimer's disease. *Alz Dis Assoc Dis* (2012) 26(4):329–34. doi: 10.1097/WAD.0b013e318239dcbd

62. Akuffo EL, Davis JB, Fox SM, Gloger IS, Hosford D, Kinsey EE, et al. The discovery and early validation of novel plasma biomarkers in mild-to-moderate alzheimer's disease patients responding to treatment with rosiglitazone. *Biomarkers.* (2008) 13(6):618–36. doi: 10.1080/13547500802445199

63. Hsu JL, Lee WJ, Liao YC, Wang SJ, Fuh JL. The clinical significance of plasma clusterin and a beta in the longitudinal follow-up of patients with alzheimer's disease. *Alzheimers Res Ther* (2017) 9. doi: 10.1186/s13195-017-0319-x

64. Silajdzic E, Minthon L, Bjorkqvist M, Hansson O. No diagnostic value of plasma clusterin in alzheimer's disease. *PLos One* (2012) 7(11). doi: 10.1371/journal.pone.0050237

65. Schrijvers EMC, Koudstaal PJ, Hofman A, Breteler MMB. Plasma clusterin and the risk of Alzheimer disease. *Jama-J Am Med Assoc* (2011) 305(13):1322–6. doi: 10.1001/jama.2011.381

66. Thambisetty M, Simmons A, Velayudhan L, Hye A, Campbell J, Zhang Y, et al. Association of plasma clusterin concentration with severity, pathology, and progression in Alzheimer disease. *Arch Gen Psychiat* (2010) 67(7):739–48. doi: 10.1001/archgenpsychiatry.2010.78

67. Thambisetty M, An Y, Kinsey A, Koka D, Saleem M, Guntert A, et al. Plasma clusterin concentration is associated with longitudinal brain atrophy in mild cognitive impairment. *Neuroimage.*(2012) 59 (1):212–7. doi: 10.1016/j.neuroimage.2011.07.056

68. Tvarijonaviciute A, Zamora C, Ceron JJ, Bravo-Cantero AF, Pardo-Marin L, Valverde S, et al. Salivary biomarkers in alzheimer's disease. *Clin Oral Invest* (2020) 24(10):3437–44. doi: 10.1007/s00784-020-03214-7

69. Hazrati LN, Van Cauwenberghe C, Brooks PL, Brouwers N, Ghani M, Sato C, et al. Genetic association of CR1 with alzheimer's disease: A tentative disease mechanism. *Neurobiol Aging* (2012) 33(12). doi: 10.1016/j.neurobiolaging.2012.07.001

70. Williams MA, Haughton D, Stevenson M, Craig D, Passmore AP, Silvestri G. Plasma complement factor h in alzheimer's disease. *J Alzheimers Dis* (2015) 45 (2):369–72. doi: 10.3233/JAD-142742

71. Hye A, Lynham S, Thambisetty M, Causevic M, Campbell J, Byers HL, et al. Proteome-based plasma biomarkers for alzheimer's disease. *Brain.* (2006) 129:3042–50. doi: 10.1093/brain/awl279

72. Weinstein G, Beiser AS, Preis SR, Courchesne P, Chouraki V, Levy D, et al. Plasma clusterin levels and risk of dementia, alzheimer's disease, and stroke. *Alzheimers Dement (Amst)*(2016) 3:103–9. doi: 10.1016/j.dadm.2016.06.005

73. Nuutinen T, Suuronen T, Kauppinen A, Salminen A. Clusterin: A forgotten player in alzheimer's disease. *Brain Res Rev* (2009) 61(2):89–104. doi: 10.1016/j.brainresrev.2009.05.007

74. Hammond JW, Bellizzi MJ, Ware C, Qiu WQ, Saminathan P, Li H, et al. Complement-dependent synapse loss and microgliosis in a mouse model of multiple sclerosis. *Brain Behav Immun* (2020) 87:739–50. doi: 10.1016/j.bbi.2020.03.004

75. Ramaglia V, Hughes TR, Donev RM, Ruseva MM, Wu X, Huitinga I, et al. C3-dependent mechanism of microglial priming relevant to multiple sclerosis. *Proc Natl Acad Sci U S A.* (2012) 109(3):965–70. doi: 10.1073/pnas.1111924109

76. Werneburg S, Jung J, Kunjamma RB, Ha SK, Luciano NJ, Willis CM, et al. Targeted complement inhibition at synapses prevents microglial synaptic engulfment and synapse loss in demyelinating disease. *Immunity* (2020) 52 (1):167. doi: 10.1016/j.immuni.2019.12.004

77. Szalai AJ, Hu XZ, Adams JE, Barnum SR. Complement in experimental autoimmune encephalomyelitis revisited: C3 is required for development of maximal disease. *Mol Immunol* (2007) 44(12):3132–6. doi: 10.1016/j.molimm.2007.02.002

78. Hu X, Holers VM, Thurman JM, Schoeb TR, Ramos TN, Barnum SR. Therapeutic inhibition of the alternative complement pathway attenuates chronic EAE. *Mol Immunol* (2013) 54(3-4):302–8. doi: 10.1016/j.molimm.2012.12.018

79. Hakansson I, Ernerudh J, Vrethem M, Dahle C, Ekdahl KN. Complement activation in cerebrospinal fluid in clinically isolated syndrome and early stages of relapsing remitting multiple sclerosis. *J Neuroimmunol* (2020) 340. doi: 10.1016/j.jneuroim.2020.577147

80. Ingram G, Hakobyan S, Robertson NP, Morgan BP. Elevated plasma C4a levels in multiple sclerosis correlate with disease activity. *J Neuroimmunol* (2010) 223(1-2):124–7. doi: 10.1016/j.jneuroim.2010.03.014

81. Kwok JY, Vaida F, Augst RM, Yu DY, Singh KK. Mannose binding lectin mediated complement pathway in multiple sclerosis. *J Neuroimmunol* (2011) 239 (1-2):98–100. doi: 10.1016/j.jneuroim.2011.08.018

82. Link H. Complement factors in multiple-sclerosis. *Acta Neurologica Scandinavica* (1972) 48(5):521. doi: 10.1111/j.1600-0404.1972.tb07572.x

83. Yam P, Petz LD, Tourtellotte WW, Ma BI. Measurement of complement components in cerebral spinal-fluid by radioimmunoassay in patients with multiple-sclerosis. *Clin Immunol Immunop.* (1980) 17(4):492–505. doi: 10.1016/0090-1229(80)90145-2

84. Lubbers R, van Essen MF, van Kooten C, Trouw LA. Production of complement components by cells of the immune system. *Clin Exp Immunol* (2017) 188(2):183–94. doi: 10.1111/cei.12952

85. Yu JT, Tan L. The role of clusterin in alzheimer's disease: Pathways, pathogenesis, and therapy. *Mol Neurobiol* (2012) 45(2):314–26. doi: 10.1007/s12035-012-8237-1

86. McGinley MP, Goldschmidt CH, Rae-Grant AD. Diagnosis and treatment of multiple sclerosis: A review. *JAMA.* (2021) 325(8):765–79. doi: 10.1001/jama.2020.26858

87. Reich DS, Lucchinetti CF, Calabresi PA. Multiple sclerosis. *N Engl J Med* (2018) 378(2):169–80. doi: 10.1056/NEJMra1401483

88. Paul A, Comabella M, Gandhi R. Biomarkers in multiple sclerosis. *Cold Spring Harb Perspect Med* (2019) 9(3). doi: 10.1101/cshperspect.a029058

89. Ziemssen T, Akgun K, Bruck W. Molecular biomarkers in multiple sclerosis. *J Neuroinflamm*(2019) 16 (1):272. doi: 10.1186/s12974-019-1674-2

90. Bourel J, Planche V, Dubourdieu N, Oliveira A, Sere A, Ducourneau EG, et al. Complement C3 mediates early hippocampal neurodegeneration and memory impairment in experimental multiple sclerosis. *Neurobiol Dis* (2021) 160:105533. doi: 10.1016/j.nbd.2021.105533

91. Lindblom RP, Aeinehband S, Strom M, Al Nimer F, Sandholm K, Khademi M, et al. Complement receptor 2 is increased in cerebrospinal fluid of multiple sclerosis patients and regulates C3 function. *Clin Immunol* (2016) 166-167:89–95. doi: 10.1016/j.clim.2016.04.003

92. Ingram G, Hakobyan S, Hirst CL, Harris CL, Loveless S, Mitchell JP, et al. Systemic complement profiling in multiple sclerosis as a biomarker of disease state. *Mult Scler* (2012) 18(10):1401–11. doi: 10.1177/1352458512438238

93. Zelek WM, Fathalla D, Morgan A, Touchard S, Loveless S, Tallantyre E, et al. Cerebrospinal fluid complement system biomarkers in demyelinating disease. *Mult Scler J* (2020) 26(14):1929–37. doi: 10.1177/1352458519887905

94. Li Y, Qin Z, Yang M, Qin Y, Lin C, Liu S. Differential expression of complement proteins in cerebrospinal fluid from active multiple sclerosis patients. *J Cell Biochem* (2011) 112(7):1930–7. doi: 10.1002/jcb.23113

95. Aeinehband S, Lindblom RP, Al Nimer F, Vijayaraghavan S, Sandholm K, Khademi M, et al. Complement component C3 and butyrylcholinesterase activity are associated with neurodegeneration and clinical disability in multiple sclerosis. *PLos One* (2015) 10(4):e0122048. doi: 10.1371/journal.pone.0122048

96. Jongen PJ, Doesburg WH, Ibrahim-Stappers JL, Lemmens WA, Hommes OR, Lamers KJ. Cerebrospinal fluid C3 and C4 indexes in immunological disorders of the central nervous system. *Acta Neurol Scand*(2000) 101(2):116–21. doi: 10.1034/j.1600-0404.2000.101002116.x

97. Sladkova V, Mares J, Lubenova B, Zapletalova J, Stejskal D, Hlustik P, et al. Degenerative and inflammatory markers in the cerebrospinal fluid of multiple sclerosis patients with relapsing-remitting course of disease and after clinical isolated syndrome. *Neurol Res* (2011) 33(4):415–20. doi: 10.1179/016164110X12816242542535

98. Jans H, Heltberg A, Zeeberg I, Kristensen JH, Fog T, Raun NE. Immune-complexes and the complement factor-C4 and factor-C3 in cerebrospinal-fluid and serum from patients with chronic progressive multiple-sclerosis. *Acta Neurologica Scandinavica* (1984) 69(1):34–8. doi: 10.1111/j.1600-0404.1984.tb07777.x

99. Kuroda H, Fujihara K, Takano R, Takai Y, Takahashi T, Misu T, et al. Increase of complement fragment C5a in cerebrospinal fluid during exacerbation of neuromyelitis optica. *J Neuroimmunol* (2013) 254(1-2):178–82. doi: 10.1016/j.jneuroim.2012.09.002

100. Sanders ME, Koski CL, Robbins D, Shin ML, Frank MM, Joiner KA. Activated terminal complement in cerebrospinal-fluid in Guillain-Barre-Syndrome and multiple-sclerosis. *J Immunol* (1986) 136(12):4456–9.

101. Sellebjerg F, Jaliashvili I, Christiansen M, Garred P. Intrathecal activation of the complement system and disability in multiple sclerosis. *J Neurol Sci*(1998) 157(2):168–74. doi: 10.1016/S0022-510X(98)00086-0

102. Mollnes TE, Vandvik B, Lea T, Vartdal F. Intrathecal complement activation in neurological diseases evaluated by analysis of the terminal complement complex. *J Neurological Sci* (1987) 78(1):17–28. doi: 10.1016/0022-510X(87)90074-8

103. Morgan BP, Campbell AK, Compston DAS. Terminal component of complement (C9) in cerebrospinal-fluid of patients with multiple-sclerosis. *Lancet.* (1984) 2(8397):251–5. doi: 10.1016/S0140-6736(84)90298-8

104. Compston DAS, Morgan BP, Oleesky D, Fifield R, Campbell AK. Cerebrospinal-fluid C9 in demyelinating disease. *Neurology.* (1986) 36(11):1503–6. doi: 10.1212/WNL.36.11.1503

105. Rodriguez M, Wynn DR, Kimlinger TK, Katzmann JA. Terminal component of complement (C9) in the cerebrospinal-fluid of patients with multiple-sclerosis and neurologic controls. *Neurology.* (1990) 40(5):855–7. doi: 10.1212/WNL.40.5.855

106. Halawa I, Lolli F, Link H. Terminal component of complement C9 in csf and plasma of patients with Ms and aseptic-meningitis. *Acta Neurologica Scandinavica* (1989) 80(2):130–5. doi: 10.1111/j.1600-0404.1989.tb03854.x

107. Finehout EJ, Franck Z, Lee KH. Complement protein isoforms in CSF as possible biomarkers for neurodegenerative disease. *Dis Markers* (2005) 21(2):93–101. doi: 10.1155/2005/806573

108. Ingram G, Hakobyan S, Hirst CL, Harris CL, Pickersgill TP, Cossburn MD, et al. Complement regulator factor h as a serum biomarker of multiple sclerosis disease state. *Brain* (2010) 133(Pt 6):1602–11. doi: 10.1093/brain/awq085

109. Hakobyan S, Luppe S, Evans DR, Harding K, Loveless S, Robertson NP, et al. Plasma complement biomarkers distinguish multiple sclerosis and neuromyelitis optica spectrum disorder. *Mult Scler* (2017) 23(7):946–55. doi: 10.1177/1352458516669002

110. Ulvestad E, Aarseth JH, Vedeler C, Nyland H, Myhr KM. The effects of interferon-alpha 2a on concentrations of immunoglobulins, complement and lymphocytes in patients with multiple sclerosis. *Scand J Immunol* (2004) 59 (1):103–8. doi: 10.1111/j.0300-9475.2004.01360.x

111. Zhang B, Jiang Y, Yang Y, Peng FH, Hu XQ. Correlation between serum thyroxine and complements in patients with multiple sclerosis and neuromyelitis optica. *Neuroendocrinol Lett* (2008) 29(2):256–60.

112. Nytrova P, Potlukova E, Kemlink D, Woodhall M, Horakova D, Waters P, et al. Complement activation in patients with neuromyelitis optica. *J Neuroimmunol* (2014) 274(1-2):185–91. doi: 10.1016/j.jneuroim.2014.07.001

113. Keller CW, Oechtering J, Wiendl H, Kappos L, Kuhle J, Lunemann JD. Impact of complement activation on clinical outcomes in multiple sclerosis. *Ann Clin Transl Neurol* (2021) 8(4):944–50. doi: 10.1002/acn3.51334

114. Myhr KM, Sadallah S, Mollnes TE, Meri S, Nyland HI, Schifferli J, et al. Interferon-alpha 2a effects on complement activation and regulation in MS patients. *Acta Neurologica Scandinavica* (2000) 101(1):30–5. doi: 10.1034/j.1600-0404.2000.00013.x

115. Sawai S, Umemura H, Mori M, Satoh M, Hayakawa S, Kodera Y, et al. Serum levels of complement C4 fragments correlate with disease activity in multiple sclerosis: proteomic analysis. *J Neuroimmunol* (2010) 218(1-2):112–5. doi: 10.1016/j.jneuroim.2009.10.019

116. Rasol HAA, Helmy H, Aziz MA. Serum complement factor h and Tyr4O2 his gene polymorphism among egyptians with multiple sclerosis. *Neurological Res* (2015) 37(10):845–52. doi: 10.1179/1743132815Y.0000000075

117. LeVine SM. Albumin and multiple sclerosis. *BMC Neurol* (2016) 16:47. doi: 10.1186/s12883-016-0564-9

118. Freedman MS, Thompson EJ, Deisenhammer F, Giovannoni G, Grimsley G, Keir G, et al. Recommended standard of cerebrospinal fluid analysis in the diagnosis of multiple sclerosis: a consensus statement. *Arch Neurol* (2005) 62 (6):865–70. doi: 10.1001/archneur.62.6.865

119. Zheng Y, Zhang YX, Yang F, Ding MP. IgG index for multiple sclerosis diagnosis: old test do the trick. *Neurology.* (2020) 94(15).

120. Kruszewski AM, Rao G, Tatomir A, Hewes D, Tegla CA, Cudrici CD, et al. RGC-32 as a potential biomarker of relapse and response to treatment with glatiramer acetate in multiple sclerosis. *Exp Mol Pathol* (2015) 99(3):498–505. doi: 10.1016/j.yexmp.2015.09.007

121. Jongen PJ, Lamers KJ, Doesburg WH, Lemmens WA, Hommes OR. Cerebrospinal fluid analysis differentiates between relapsing-remitting and secondary progressive multiple sclerosis. *J Neurol Neurosurg Psychiatry* (1997) 63(4):446–51. doi: 10.1136/jnnp.63.4.446

122. Ziabska K, Ziemka-Nalecz M, Pawelec P, Sypecka J, Zalewska T. Aberrant complement system activation in neurological disorders. *Int J Mol Sci* (2021) 22(9). doi: 10.3390/ijms22094675

123. Ma Y, Liu Y, Zhang Z, Yang GY. Significance of complement system in ischemic stroke: A comprehensive review. *Aging Dis* (2019) 10(2):429–62. doi: 10.14336/AD.2019.0119

124. Bouwens van der Vlis TAM, Kros JM, Mustafa DAM, van Wijck RTA, Ackermans L, van Hagen PM, et al. The complement system in glioblastoma multiforme. *Acta Neuropathol Commun* (2018) 6(1):91. doi: 10.1186/s40478-018-0591-4

125. Burgelman M, Vandendriessche C, Vandenbroucke RE. Extracellular vesicles: A double-edged sword in sepsis. *Pharm (Basel)*(2021) 14(8). doi: 10.3390/ph14080829

126. Pauwels MJ, Vandendriessche C, Vandenbroucke RE. Special delEVery: Extracellular vesicles as promising delivery platform to the brain. *Biomedicines.* (2021) 9(11). doi: 10.3390/biomedicines9111734

127. van Niel G, D'Angelo G, Raposo G. Shedding light on the cell biology of extracellular vesicles. *Nat Rev Mol Cell Biol* (2018) 19(4):213–28. doi: 10.1038/nrm.2017.125

128. Cocucci E, Meldolesi J. Ectosomes and exosomes: shedding the confusion between extracellular vesicles. *Trends Cell Biol* (2015) 25(6):364–72. doi: 10.1016/j.tcb.2015.01.004

129. Thery C, Witwer KW, Aikawa E, Alcaraz MJ, Anderson JD, Andriantsitohaina R, et al. Minimal information for studies of extracellular vesicles 2018 (MISEV2018): A position statement of the international society for extracellular vesicles and update of the MISEV2014 guidelines. *J Extracell Vesicles* (2018) 7(1):1535750. doi: 10.1080/20013078.2018.1535750

130. Boukouris S, Mathivanan S. Exosomes in bodily fluids are a highly stable resource of disease biomarkers. *Proteomics Clin Appl*(2015) 9(3-4):358–67. doi: 10.1002/prca.201400114

131. Huo L, Du X, Li X, Liu S, Xu Y. The emerging role of neural cell-derived exosomes in intercellular communication in health and neurodegenerative diseases. *Front Neurosci* (2021) 15:738442. doi: 10.3389/fnins.2021.738442

132. Vandendriessche C, Kapogiannis D, Vandenbroucke RE. Biomarker and therapeutic potential of peripheral extracellular vesicles in alzheimer's disease. *Adv Drug Delivery Rev* (2022) 114486. doi: 10.1016/j.addr.2022.114486

133. Jan AT, Malik MA, Rahman S, Yeo HR, Lee EJ, Abdullah TS, et al. Perspective insights of exosomes in neurodegenerative diseases: A critical appraisal. *Front Aging Neurosci* (2017) 9:317. doi: 10.3389/fnagi.2017.00317

134. Ciferri MC, Quarto R, Tasso R. Extracellular vesicles as biomarkers and therapeutic tools: From pre-clinical to clinical applications. *Biol (Basel)* (2021) 10 (5). doi: 10.3390/biology10050359

135. Mustapic M, Eitan E, Werner JKJr., Berkowitz ST, Lazaropoulos MP, Tran J, et al. Plasma extracellular vesicles enriched for neuronal origin: A potential window into brain pathologic processes. *Front Neurosci* (2017) 11:278. doi: 10.3389/fnins.2017.00278

136. Bellini S, Saraceno C, Benussi L, Squitti R, Cimini S, Ricci M, et al. Plasma small extracellular vesicles with complement alterations in GRN/C9orf72 and sporadic frontotemporal lobar degeneration. *Cells*(2022) 11(3). doi: 10.3390/cells11030488

137. Nogueras-Ortiz CJ, Mahairaki V, Delgado-Peraza F, Das D, Avgerinos K, Eren E, et al. Astrocyte- and neuron-derived extracellular vesicles from alzheimer's disease patients effect complement-mediated neurotoxicity. *Cells* (2020) 9(7). doi: 10.3390/cells9071618

138. Goetzl EJ, Schwartz JB, Abner EL, Jicha GA, Kapogiannis D. High complement levels in astrocyte-derived exosomes of Alzheimer disease. *Ann Neurol* (2018) 83(3):544–52. doi: 10.1002/ana.25172

139. Winston CN, Goetzl EJ, Schwartz JB, Elahi FM, Rissman RA. Complement protein levels in plasma astrocyte-derived exosomes are abnormal in conversion from mild cognitive impairment to alzheimer's disease dementia. *Alzheimers Dement (Amst)* (2019) 11:61–6. doi: 10.1016/j.dadm.2018.11.002

140. Cohn W, Melnik M, Huang C, Teter B, Chandra S, Zhu C, et al. Multi-omics analysis of microglial extracellular vesicles from human alzheimer's disease brain tissue reveals disease-associated signatures. *Front Pharmacol* (2021) 12:766082. doi: 10.3389/fphar.2021.766082

141. Kitamura Y, Kojima M, Kurosawa T, Sasaki R, Ichihara S, Hiraku Y, et al. Proteomic profiling of exosomal proteins for blood-based biomarkers in parkinson's disease. *Neuroscience.* (2018) 392:121–8. doi: 10.1016/j.neuroscience.2018.09.017

142. Jiang R, Rong C, Ke R, Meng S, Yan X, Ke H, et al. Differential proteomic analysis of serum exosomes reveals alterations in progression of Parkinson disease. *Med (Baltimore)* (2019) 98(41):e17478. doi: 10.1097/MD.0000000000017478

143. Bhargava P, Nogueras-Ortiz C, Kim S, Delgado-Peraza F, Calabresi PA, Kapogiannis D. Synaptic and complement markers in extracellular vesicles in multiple sclerosis. *Mult Scler* (2021) 27(4):509–18. doi: 10.1177/1352458520924590

144. Welton JL, Loveless S, Stone T, von Ruhland C, Robertson NP, Clayton A. Cerebrospinal fluid extracellular vesicle enrichment for protein biomarker discovery in neurological disease; multiple sclerosis. *J Extracell Vesicles* (2017) 6 (1):1369805. doi: 10.1080/20013078.2017.1369805

145. Scolding NJ, Morgan BP, Houston WA, Linington C, Campbell AK, Compston DA. Vesicular removal by oligodendrocytes of membrane attack complexes formed by activated complement. *Nature.* (1989) 339(6226):620–2. doi: 10.1038/339620a0

146. Mitaki S, Wada Y, Sheikh AM, Yamaguchi S, Nagai A. Proteomic analysis of extracellular vesicles enriched serum associated with future ischemic stroke. *Sci Rep* (2021) 11(1):24024. doi: 10.1038/s41598-021-03497-0

147. Otero-Ortega L, Alonso-Lopez E, Perez-Mato M, Laso-Garcia F, Gomez-de Frutos MC, Diekhorst L, et al. Circulating extracellular vesicle proteins and MicroRNA profiles in subcortical and cortical-subcortical ischaemic stroke. *Biomedicines* (2021) 9(7). doi: 10.3390/biomedicines9070786

148. Cilibrasi C, Simon T, Vintu M, Tolias C, Samuels M, Mazarakis NK, et al. Definition of an inflammatory biomarker signature in plasma-derived extracellular vesicles of glioblastoma patients. *Biomedicines* (2022) 10(1). doi: 10.3390/biomedicines10010125

149. Osti D, Del Bene M, Rappa G, Santos M, Matafora V, Richichi C, et al. Clinical significance of extracellular vesicles in plasma from glioblastoma patients. *Clin Cancer Res* (2019) 25(1):266–76. doi: 10.1158/1078-0432.CCR-18-1941

150. Hallal S, Azimi A, Wei H, Ho N, Lee MYT, Sim HW, et al. A comprehensive proteomic SWATH-MS workflow for profiling blood extracellular vesicles: A new avenue for glioma tumour surveillance. *Int J Mol Sci* (2020) 21(13). doi: 10.3390/ijms21134754

151. Vandendriessche C, Balusu S, Van Cauwenberghe C, Brkic M, Pauwels M, Plehiers N, et al. Importance of extracellular vesicle secretion at the blood-cerebrospinal fluid interface in the pathogenesis of alzheimer's disease. *Acta Neuropathol Commun* (2021) 9(1):143. doi: 10.1186/s40478-021-01245-z

152. Delgado-Peraza F, Nogueras-Ortiz CJ, Volpert O, Liu D, Goetzl EJ, Mattson MP, et al. Neuronal and astrocytic extracellular vesicle biomarkers in blood reflect brain pathology in mouse models of alzheimer's disease. *Cells* (2021) 10(5). doi: 10.3390/cells10050993

153. Muraoka S, Jedrychowski MP, Iwahara N, Abdullah M, Onos KD, Keezer KJ, et al. Enrichment of neurodegenerative microglia signature in brain-derived extracellular vesicles isolated from alzheimer's disease mouse models. *J Proteome Res* (2021) 20(3):1733–43. doi: 10.1021/acs.jproteome.0c00934

154. Anastasi F, Greco F, Dilillo M, Vannini E, Cappello V, Baroncelli L, et al. Proteomics analysis of serum small extracellular vesicles for the longitudinal study of a glioblastoma multiforme mouse model. *Sci Rep* (2020) 10(1):20498. doi: 10.1038/s41598-020-77535-8

155. Greco F, Anastasi F, Pardini LF, Dilillo M, Vannini E, Baroncelli L, et al. Longitudinal bottom-up proteomics of serum, serum extracellular vesicles, and cerebrospinal fluid reveals candidate biomarkers for early detection of glioblastoma in a murine model. *Molecules* (2021) 26(19). doi: 10.3390/molecules26195992

156. Sofroniew MV, Vinters HV. Astrocytes: biology and pathology. *Acta Neuropathol* (2010) 119(1):7–35. doi: 10.1007/s00401-009-0619-8

157. Verkhratsky A, Nedergaard M. The homeostatic astroglia emerges from evolutionary specialization of neural cells. *Philos Trans R Soc Lond B Biol Sci* (2016) 371(1700). doi: 10.1098/rstb.2015.0428

158. Liddelow SA, Barres BA. Reactive astrocytes: Production, function, and therapeutic potential. *Immunity.* (2017) 46(6):957–67. doi: 10.1016/j.immuni.2017.06.006

159. Ben Haim L, Carrillo-de Sauvage MA, Ceyzeriat K, Escartin C. Elusive roles for reactive astrocytes in neurodegenerative diseases. *Front Cell Neurosci* (2015) 9:278. doi: 10.3389/fncel.2015.00278

160. Goetzl EJ, Miller BL. Multicellular hypothesis for the pathogenesis of alzheimer's disease. *FASEB J*(2017) 31(5):1792–5. doi: 10.1096/fj.201601221R

161. Lian H, Yang L, Cole A, Sun L, Chiang AC, Fowler SW, et al. NFkappaB-activated astroglial release of complement C3 compromises neuronal morphology and function associated with alzheimer's disease. *Neuron.* (2015) 85(1):101–15. doi: 10.1016/j.neuron.2014.11.018

162. Orre M, Kamphuis W, Osborn LM, Jansen AHP, Kooijman L, Bossers K, et al. Isolation of glia from alzheimer's mice reveals inflammation and dysfunction. *Neurobiol Aging* (2014) 35(12):2746–60. doi: 10.1016/j.neurobiolaging.2014.06.004

163. Liddelow SA, Guttenplan KA, Clarke LE, Bennett FC, Bohlen CJ, Schirmer L, et al. Neurotoxic reactive astrocytes are induced by activated microglia. *Nature* .(2017) 541(7638):481–7. doi: 10.1038/nature21029

164. Louis DN, Perry A, Reifenberger G, von Deimling A, Figarella-Branger D, Cavenee WK, et al. The 2016 world health organization classification of tumors of the central nervous system: a summary. *Acta Neuropathol* (2016) 131 (6):803–20. doi: 10.1007/s00401-016-1545-1

165. Simon T, Jackson E, Giamas G. Breaking through the glioblastoma micro-environment *via* extracellular vesicles. *Oncogene.* (2020) 39(23):4477–90. doi: 10.1038/s41388-020-1308-2

166. Hallal S, Mallawaaratchy DM, Wei H, Ebrahimkhani S, Stringer BW, Day BW, et al. Extracellular vesicles released by glioblastoma cells stimulate normal astrocytes to acquire a tumor-supportive phenotype *Via* p53 and MYC signaling pathways. *Mol Neurobiol* (2019) 56(6):4566–81. doi: 10.1007/s12035-018-1385-1

167. Zhang Z, Xu J, Chen Z, Wang H, Xue H, Yang C, et al. Transfer of MicroRNA *via* macrophage-derived extracellular vesicles promotes proneural-to-Mesenchymal transition in glioma stem cells. *Cancer Immunol Res* (2020) 8 (7):966–81. doi: 10.1158/2326-6066.CIR-19-0759

168. Zhu H, Yu X, Zhang S, Shu K. Targeting the complement pathway in malignant glioma microenvironments. *Front Cell Dev Biol* (2021) 9:657472. doi: 10.3389/fcell.2021.657472

169. Bouwens TAM, Trouw LA, Veerhuis R, Dirven CMF, Lamfers MLM, Al-Khawaja H. Complement activation in glioblastoma multiforme pathophysiology: Evidence from serum levels and presence of complement activation products in tumor tissue. *J Neuroimmunol* (2015) 278:271–6. doi: 10.1016/j.jneuroim.2014.11.016

170. Clarke AR, Christophe BR, Khahera A, Sim JL, Connolly ESJr. Therapeutic modulation of the complement cascade in stroke. *Front Immunol* (2019) 10:1723. doi: 10.3389/fimmu.2019.01723

171. Van Beek J, Bernaudin M, Petit E, Gasque P, Nouvelot A, MacKenzie ET, et al. Expression of receptors for complement anaphylatoxins C3a and C5a following permanent focal cerebral ischemia in the mouse. *Exp Neurol* (2000) 161(1):373–82. doi: 10.1006/exnr.1999.7273

172. Barnum SR, Ames RS, Maycox PR, Hadingham SJ, Meakin J, Harrison D, et al. Expression of the complement C3a and C5a receptors after permanent focal ischemia: An alternative interpretation. *Glia.* (2002) 38(2):169–73. doi: 10.1002/glia.10069

173. Alawieh A, Tomlinson S. Injury site-specific targeting of complement inhibitors for treating stroke. *Immunol Rev* (2016) 274(1):270–80. doi: 10.1111/imr.12470

174. Arumugam TV, Magnus T, Woodruff TM, Proctor LM, Shiels IA, Taylor SM. Complement mediators in ischemia-reperfusion injury. *Clin Chim Acta* (2006) 374(1-2):33–45. doi: 10.1016/j.cca.2006.06.010

175. Hertle E, Arts ICW, van der Kallen CJH, Feskens EJM, Schalkwijk CG, Stehouwer CDA, et al. Classical pathway of complement activation: Longitudinal associations of C1q and C1-INH with cardiovascular outcomes: The CODAM study (Cohort on diabetes and atherosclerosis maastricht)-brief report. *Arterioscler Thromb Vasc Biol* (2018) 38(5):1242–4. doi: 10.1161/ATVBAHA.118.310806

176. Horvath Z, Csuka D, Vargova K, Kovacs A, Molnar AA, Gulacsi-Bardos P, et al. Elevated C1rC1sC1inh levels independently predict atherosclerotic coronary heart disease. *Mol Immunol* (2013) 54(1):8–13. doi: 10.1016/j.molimm.2012.10.033

177. Rahpeymai Y, Hietala MA, Wilhelmsson U, Fotheringham A, Davies I, Nilsson AK, et al. Complement: a novel factor in basal and ischemia-induced neurogenesis. *EMBO J* (2006) 25(6):1364–74. doi: 10.1038/sj.emboj.7601004

178. Stokowska A, Atkins AL, Moran J, Pekny T, Bulmer L, Pascoe MC, et al. Complement peptide C3a stimulates neural plasticity after experimental brain ischaemia. *Brain.*(2017) 140(2):353–69. doi: 10.1093/brain/aww314

179. Jafarzadeh-Esfehani R, Soudyab M, Parizadeh SM, Jaripoor ME, Nejad PS, Shariati M, et al. Circulating exosomes and their role in stroke. *Curr Drug Targets* (2020) 21(1):89–95. doi: 10.2174/1389450120666190821153557

180. Wang MM, Feng YS, Tan ZX, Xing Y, Dong F, Zhang F. The role of exosomes in stroke. *Mol Biol Rep* (2020) 47(8):6217–28. doi: 10.1007/s11033-020-05569-2

181. Zheng X, Hermann DM, Bahr M, Doeppner TR. The role of small extracellular vesicles in cerebral and myocardial ischemia-molecular signals, treatment targets, and future clinical translation. *Stem Cells* (2021) 39(4):403–13. doi: 10.1002/stem.3329

frontiers | Frontiers in Immunology

TYPE Original Research
PUBLISHED 24 January 2023
DOI 10.3389/fimmu.2023.1081793

Check for updates

OPEN ACCESS

EDITED BY
Per Nilsson,
Linnaeus University, Sweden

REVIEWED BY
Huy Quach,
Mayo Clinic, United States
Christine Gaboriaud,
UMR5075 Institut de Biologie Structurale (IBS), France
Tiancai Liu,
Southern Medical University, China

*CORRESPONDENCE
Sheng Xia
xiasheng1519@163.com
Li Zhu
tzheartchina@126.com

SPECIALTY SECTION
This article was submitted to Molecular Innate Immunity, a section of the journal Frontiers in Immunology

RECEIVED 27 October 2022
ACCEPTED 04 January 2023
PUBLISHED 24 January 2023

CITATION
Ye J, Xu J, Zhang C, Zhu L and Xia S (2023) Quantitative fluorescence resonance energy transfer-based immunoassay for activated complement C1s.
Front. Immunol. 14:1081793.
doi: 10.3389/fimmu.2023.1081793

COPYRIGHT
© 2023 Ye, Xu, Zhang, Zhu and Xia. This is an open-access article distributed under the terms of the Creative Commons Attribution License (CC BY). The use, distribution or reproduction in other forums is permitted, provided the original author(s) and the copyright owner(s) are credited and that the original publication in this journal is cited, in accordance with accepted academic practice. No use, distribution or reproduction is permitted which does not comply with these terms.

Quantitative fluorescence resonance energy transfer-based immunoassay for activated complement C1s

Jun Ye[1,2], Jie Xu[2], Chuanmeng Zhang[2], Li Zhu[2*] and Sheng Xia[1*]

[1]Department of Immunology, School of Medicine, Jiangsu University, Zhenjiang, Jiangsu, China, [2]The Center for Translational Medicine, The Affiliated Taizhou People's Hospital of Nanjing Medical University, Taizhou, Jiangsu, China

Objectives: C1s activation is associated with the pathogenesis of various diseases, indicating the potential value of C1s activation detection in clinic. Here we aimed to establish fluorescence resonance energy transfer (FRET)-based immunoassay for the quantitative detection of activated C1s in serum.

Methods: FRET-based fluorogenic peptides, sensitive to the enzymatic activity of activated C1s, were prepared and labeled with the fluorophore ortho-aminobenzoic acid (Abz) and quencher 2,4-dinitrophenyl (Dnp), and then were further selected depending on its Kcat/Km value. C1s in the samples was captured and separated using anti-C1s-conjugated magnetic microbeads. Next, enzymatic activity of activated C1s in samples and standards was examined using fluorescent quenched substrate assays. Limit of detection (LOD), accuracy, precision, and specificity of FRET-based immunoassay were also investigated.

Results: This method presented a linear quantification range for the enzymatic activity of activated C1s up to 10 μmol min^{-1} mL^{-1} and LOD of 0.096 μmol·min^{-1}·mL^{-1} for serum samples. The recovery of the method was in the range of 90% ~ 110%. All CV values of the intra-analysis and inter-analysis of three levels in samples were less than 10%. The cross-reaction rates with C1r enzyme, MASP1, and MASP2 were less than 0.5%. No significant interferences were found with bilirubin (0.2 mg mL^{-1}), Chyle (2000 FTU), and haemoglobin (5 mg mL^{-1}), but anticoagulants (EDTA, citrate and heparin) inhibited the enzymatic ability of activated C1s. Thus, this established method can be used for the determination of active C1s in human serum samples in the concentration interval of 0.096-10.000 μmol min^{-1} mL^{-1}.

Conclusions: One anti-C1s-based FRET immunoassay for activated C1s detection in serum samples were established, and it will be useful to explore the role of C1s activation in the pathogenesis, diagnosis and treatment in complement-related diseases.

KEYWORDS

complement, C1s, FRET, C4, C2, immunoassay

1 Introduction

Complements are natural immune molecules that serve as the first line-of-defence in the immune response (1–3). In the physiological state, complement molecules are quiescent. In the adaptive and innate immune states, complement molecules are sequentially activated, which then further promote the immune response. For decades, studies have shown that the activation of the complement system is associated with the onset, progression, and prognosis of various diseases, such as novel coronavirus infection, tumours, and autoimmune diseases (1–4). Up to now, three complement activation pathways have been identified, including the classical pathway, alternative pathway, and mannose-binding lectin pathway. Activation of the complement pathways requires soluble complement molecules, cell membrane receptors, or regulatory molecules. Complement-related biomarkers can be monitored to predict disease progression.

C1 is a multimolecular protease that triggers the activation of the classical pathway, which functions in antimicrobial host defence, immune tolerance, and recognition of abnormal structures. The C1 complex is a Ca^{2+}-dependent tetramer, which comprises two copies of two proteases, C1r and C1s, and a recognition protein, C1q ($C1qr_2s_2$) (5). C1q mediates the binding of C1 to the target molecule, thereby inducing the activation of C1r, which converts the proenzyme C1s specifically to cleave C2 and C4 (6). The function of the classical complement system largely depends on the activation of the subcomponent C1s (7). Therefore, quantitative detection of active C1s can help to understand the exact role of classical pathway activation in the pathogenesis of complement-associated diseases.

Indeed, C1s play important roles in maintaining homeostasis and onset of certain diseases. In particular, C1s mutations are associated with rare genetic diseases, infectious susceptibility and autoimmune disorders. Ongoing studies also have indicated that the aberrant activation of C1s contributes to the onset of autoimmune and infectious diseases, and even cancers (8, 9). In recent years, inhibitors and monoclonal antibodies against C1s have been explored in several clinical trials. It is noteworthy that the FDA have approved the C1s monoclonal antibody Sutimlimab (sutimlimab-jome; ENJAYMO™) for the treatment of cold lectin disease (CAD) in February 2022 (10). Therefore, clinical evaluation of C1s activation may serve as a novel potential clinic biomarker especially for diagnosis, prognosis evaluation, and even for the selection of individualized therapies against activated C1s in diseases (11). For the detection of C1s, various methods have been established, including immunohistochemical analysis, immunoblotting (12), immunofluorescence staining (13), bilateral diffusion (14), gelatin zymography (15), LC-MS/MS (16) and ELISA (17). These methods can detect both natural and active complement molecules, but can not effectively distinguish whether C1s are in an active or inactive state. As the complement system is only functional when activated in cascade, it is particularly important to detect whether these complement components are activated or not.

Fluorescence resonance energy transfer (FRET)-based immunoassays exploit the distance-dependent transfer of resonance energy from an excited donor fluorophore to a proximal ground-state acceptor fluorophore (18, 19). The spectral properties of the FRET donor-acceptor complex enable direct detection of the acceptor emission without a separation step from the unbound partners (18, 19). The development of homogeneous FRET-based immunoassays contributes to quick and highly specific on-site detection of protein biomarkers for clinical molecular diagnostics of cancers (20, 21) and autoimmune diseases (22). Based on the specific cleavage of C2 and C4 proteins by the active C1s (23), we currently designed the FRET-based peptide that could be cleaved by the active C1s, which conjugated with magnetic microbeads. This study aimed to establish a quantitative immunoassay for the detection of active C1s in serum samples (Figure 1).

2 Materials and methods

2.1 Materials

2.1.1 Reagents and instruments

Buffer solution used in this study included phosphate-buffered saline (PBS) (0.137 M NaCl, 0.0027 M KCl, 0.01 M Na_2HPO_4, 0.002 M KH_2PO_4, pH 7.4); Tris buffer (0.05 M Tris, 0.15 M NaCl, 0. 2% (w/v)

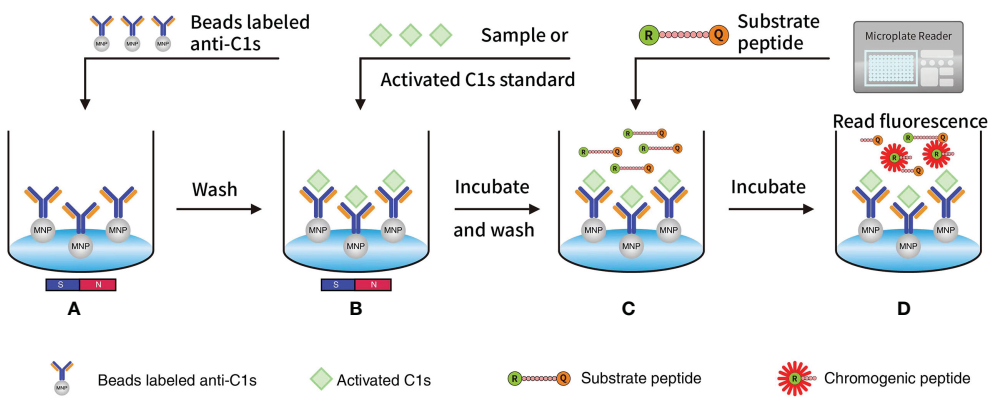

FIGURE 1
Quantitative FRET immunoassay of the activated C1s based on the capture of anti-C1s antibody: **(A)** MNP or Beads were precoated with antibody against activated C1s and then added into wells; **(B)** Activated C1s standard or samples were added and then specifically combined with MNP-labelled anti-C1s antibody; **(C)** Substrate peptide was added and then cleaved by activated C1s; **(D)** Fluorescence intensity from Abz on the substrate fragment was monitored by a microplate reader, and the enzymatic ability of activated C1s was quantitatively analysed. Abz, ortho-aminobenzoic acid; MNP, magnetic nanoparticles; FRET, fluorescence resonance energy transfer.

10.3389/fimmu.2023.1081793

PEG 8000); assay buffer (50 mM Tris, 250 mM NaCl, pH 8.0); binding buffer (0.1 M MES buffer, pH 5.0); washing buffer (TBS with 0.05% Tween 20); and blocking buffer (0.05 M Tris with 1.0% BSA and 0.05% Tween 20). In addition, Tris buffer with 0.05% Tween 20 and BSA was used as the desired buffer. A Synergy HT Multifunction Microplate Reader was purchased from BioTek (Winooski, VT, USA).

Carboxyl-coated magnetic beads (1 μm) were purchased from Merck (Whitehouse Station, NJ, USA). C1s enzyme (A104, activated C1s, double-chain C1s) and C1r enzyme (A102, activated C1r, double-chain C1r) were purchased from CompTech (Tyler, TX, USA). MASP1 (H00005648) and MASP2 (H00010747) were purchased from Abnova (Taipei City, Taiwan, China). C1r, MASP1, and MASP2 were diluted in PBS with concentrations of 660 $\mu g \cdot mL^{-1}$, 5000 $\mu g \cdot mL^{-1}$, and 5000 $\mu g \cdot mL^{-1}$, respectively.

Interference Check A Plus A Kit (ZG0501) was obtained from Sysmex (Kobe, Japan). C1s ELISA assay kit was purchased from RapidBio Systems (Catalog NO: 6141000964; Calabasas, CA, USA). Anti-C1s antibody was screened in-house developed, and then sequenced and genetically engineered with CHO system by Biointron (Taizhou, China). N-Carbobenzyloxy-Lys-thiobenzyl ester (Z-K-SBzl) (M-1300) was purchased from Bachem (Bubendorf, Switzerland). 5,5'-dithio-(bis-2-nitrobenzoic acid) (DTNB) (D-8130) was purchased from Sigma-Aldrich. 1-Ethyl-3-[3-dimethylaminopropyl] carbidedimide hydrochloride (EDC) (22980) was purchased from Thermo Fisher Scientific (Cleveland, OH, USA).

2.1.2 Patients enrolment and sample collection

Total 20 patients with primary diagnosis of rheumatoid arthritis (RA) and 20 healthy individuals matched for sex and age (± 10 years) were enrolled. The diagnosis of RA was in accordance with the 2010 American College of Rheumatology (ACR)-European League Against Rheumatism (EULAR) classification criteria for rheumatoid arthritis.

Venous blood was collected by antecubital venepuncture from participants. Serum and plasma samples treated with different anticoagulants (citrate, EDTA, or heparin) were collected and stored at -80°C before use. This study is complied with all relevant national regulations and institutional policies, and is in accordance with the tenets of the Helsinki Declaration (as revised in 2013). This study has been approved by the Ethics Committee of Taizhou People's Hospital (KY2020-184-01). Informed consent was obtained from each subject.

2.2 Design and preparation of peptide substrates

Substrate candidates were designed based on that active C1s cleave complement components C2 and C4 (24, 25). Three peptide substrates, namely, peptide 1 (GLQRALEI), peptide 2 (SLGRKIQI) and peptide 3 (GYLGRSYKVG) were finally selected for further optimization as previously described (25). The substrate library peptides were synthesized with a purity of greater than 97.43% by Scipeptide (Shanghai, China). Next, FRET-based fluorogenic peptides were prepared with the fluorophore ortho-aminobenzoic acid (Abz) and quencher 2,4-dinitrophenyl (Dnp).

The activity of active C1s on the fluorogenic peptides was firstly studied. Here, 2.5 μL of active C1s (100 μg/mL) (A104, CompTech. Tyler, TX, USA) was added to each well containing the individual peptides with different concentrations (0, 4.72, 9.44, 18.88, 37.75, 75.5, 150, and 300 μM). The reaction system was supplemented with Tris buffer in a volume of 100 μL. Fluorescent intensity was monitored using a microplate reader (BioTek, Winooski, VT, USA) every 5 mins for 2 h at 37°C. The activity of C1s on the individual substrate was monitored based on the alterations of the fluorescence of Abz at excitation wavelength of 360/40 nm and emission wavelength of 460/40 nm. Subsequently, the relationship between the substrate concentration and reactivity was fitted by the Michaelis-Menten equation. V_{max} and K_m values of the samples were calculated. Then, K_{cat} was calculated using the formula $K_{cat} = V_{max}$/molecular weight. The peptide with the highest K_{cat}/K_m value was selected as the candidate substrate for further experiments.

2.3 Preparation of anti-C1s antibody-conjugated magnetic microbeads

Firstly, the quality of anti-C1s was characterized by using polyacrylamide gel electrophoresis and size exclusion chromatography-high performance liquid chromatography (SEC-HPLC) (Supplementary Figure 1). Moreover, the binding capacities of anti-C1s with active C1s, C1(C1q2C1r2C1s) and C1s zymogen were analyzed using ELISA. The data showed that Anti-C1s had capability to bind all three C1s forms, but it had stronger binding with active C1s than C1 and C1s zymogen. There no difference between C1 and C1s zymoger to bind with anti-C1s(Supplementary Figure 2). Next, anti C1s-conjugated magnetic microbeads were prepared using carboxyl-coated magnetic beads and anti-C1s antibody according to the manufacturer's instructions. Approximately 10 mg magnetic microbeads were washed in binding buffer three times before using. The recombinant anti-C1s monoclonal antibody (200 μg) was mixed with the magnetic microbeads, followed by gentle agitation and incubation for 15 min. Then, 1-ethyl-3-(3-dimethylaminopropyl)-carbodiimide (EDC) was used as the couplant. In detail, 500 μg of the couplant was added into 50 mg microbeads, mixed gently *via* vortexing, and incubated for 1 h. The mixture was next added with 1 mL of binding buffer, and further incubated at room temperature. Next, the beads were washed three times 3 h after the incubation, followed by resuspending in 1 mL of Tris buffer with the desired buffer and storing at 4°C. Before use in the assay, microbeads were washed, magnetically separated and aspirated.

2.4 Enzymatic hydrolysis of colorimetric peptide substrates by C1s

The activity of recombinant human complement C1s protein was measured using N-carbobenzyloxy-Lys-thiobenzyl ester (Z-Lys-SBzl) in the presence of 5,5'-dithio-bis(2-nitrobenzoic acid) (DTNB) as described previously (26). The specific enzymatic activity of C1s was calculated as follows:

$$\text{Specific Activity } (pmol/\min/\mu g) = \frac{\text{Adjusted Vmax}\diamond(\text{OD}/\min) \times \text{well volume(L)} \times 10^{12}\text{pmol/mol}}{\text{ext.coeff}^{\square}(M^{-1}cm^{-1}) \times \text{path corr.}^{\triangle}(cm) \times \text{amount of enzyme } (\mu g)}$$

where ◇ represented adjusted for the substrate blank; □ represented an extinction coefficient of 13260 M_{-1}·cm_{-1}; and △ represented a path correction of 0.320 cm, respectively.

Our prior data showed that the activity of 1 μg of the C1s standard used in the experiments was 0.0534 μmol/min. Bound with anti-C1s had no obviously negative effects on the enzymatic capacity of active C1s (Supplementary Figure 3).

2.5 Serum and plasma C1s measured by ELISA

C1s levels in serum and plasma samples were detected using an ELISA kit according to the manufacturer's instructions. Serum and plasma samples were diluted in dilution buffer. Briefly, 50 μL of human complement C1s standard or diluted samples were added into each well and incubated with 100 μL of horseradish peroxidase (HRP)-labelled C1s antibody. The plate was sealed and incubated at 37°C for 1 h. The microplate was washed three times with wash buffer manually. Then, 100 μL of a mixture of chromogen solution A and solution B was added to each well, and then the plate was incubated at 37°C for 15 min in the dark. The absorbance of each well was read at a wavelength of 450 nm within 15 min after 50 μL of stop solution was added to each well and gently mixed. A standard curve was generated by plotting the absorbance of standards on the X-axis against the concentrations of C1s (0, 5, 10, 20, 40, and 80 μg/mL) on the Y-axis. Then the concentrations of C1s in serum and plasma samples were calculated according to the standard curve.

2.6 Fluorescent quenched substrate assays for C1s activity on chromogenic peptides

The enzymatic activity of C1s in the samples was measured. Activated C1s standards or samples were sequentially diluted 10-fold into PBS. then added to the wells (100 μL per well) of a 96-well microtiter plate. A constant amount of anti-C1s antibody-conjugated magnetic microbeads (10 mg/mL, 30 μL per well) were added to each well of the microtiter plate and agitated at room temperature for 10 minutes. The beads were washed with 200 μL of PBS for three times, magnetically separated, and resuspended in 90 μL of Tris buffer. Next, 10 μL of chromogenic peptide (1 μg/mL) was added to each well and mixed adequately. The fluorescence of each well was determined immediately.

2.7 Optimal reaction time and standard curve

To determine the optimal reaction time, the reaction was performed with 10 μL of chromogenic peptide 3 (1 μg/mL) and activated C1s with different concentrations (0.625, 1.25, 2.5, 5, and 10 μmol·min^{-1}·mL^{-1}). The standard curve was prepared with the activated C1s standards (10, 5, 2.5, 1.25, 0.625, and 0 μmol min^{-1} mL^{-1}). The activity of the C1s standards was set on the X-axis, and the detected fluorescence intensities were set on the Y-axis. The linear least square method was used to fit these log data to prepare the standard curve, which was used to calculate the C1s enzymatic activity in the samples.

2.8 Limit of detection, accuracy, precision, and specificity

To confirm LOD, the reaction was carried out under optimal conditions. The fluorescence intensity was repeatedly examined in the absence of activated C1s. For the accuracy of the optimal method, the relative recoveries were examined. Human serum samples were spiked with activated C1s standard solutions (2.671, 2.671, and 5.342 μmol·min^{-1}·mL^{-1}) with a volume ratio of 1:1. The relative recovery rate was calculated. The intraday repeatability and interday reproducibility were examined, and the coefficients of variation (CVs) were calculated. For clinical samples, complement analogues in serum, such as C1r, MASP1, and MASP2 may interfere with the detection of C1s activity. Therefore, C1r, MASP1, and MASP2 were assayed for cross reactivity. Then, the cross-reaction rates were calculated using the following formula: the cross-reactivity (%) = (measured concentration/original concentration) × 100%.

2.9 Statistical analysis

GraphPad Prism 5.0 (GraphPad Software, La Jolla, CA, USA) was used to analyze the relationship between the substrate concentration and reactivity based on the Michaelis-Menten equation. SigmaPlot 12.0 software was used for the statistical analyses (Systat Software Inc., San Jose, CA). A paired t-test was used to analyse the samples of the two groups, and one-way ANOVA was used to test for differences among at least three groups. $P < 0.05$ was considered statistically significant.

3 Results

3.1 Optimization of peptide substrates

To select the optimal peptide substrate of active C1s for fluorescent quenched substrate assay, the kinetic parameters for C1s-mediated cleavage of the three candidate peptides were detected. Michaelis-Menten curves were generated, where initial velocity (V_0) was plotted against substrate peptide 1 (Figure 2A), peptide 2 (Figure 2B), and peptide 3 (Figure 2C). The specificity for cleavage of substrate peptide 1, peptide 2, and peptide 3 by activated C1s were shown in Figure 2D. Kcat/Km value of peptide 3 was obviously higher than that of peptide 1 and peptide 2 ($P < 0.001$). However, Kcat/Km values were not significantly different between peptide 1 and peptide 2 ($P = 0.846$). Thus, peptide 3 was selected as the candidate substrate peptide for developing FRET-based fluorescent substrate peptide.

3.2 Determination of optimal reaction time and generation of standard curve

For determination of optimal reaction time, fluorescence intensity was recorded within 0-90 min (Figure 3A). Fluorescence intensity increased with the reaction time extended. Simultaneously, the fluorescence intensity was strongly increased by activated C1s with high enzyme activity. The correlation was preserved within 20-80 min by quadratic regression analysis. The R^2 values of four reaction times were 0.984 ± 0.0114

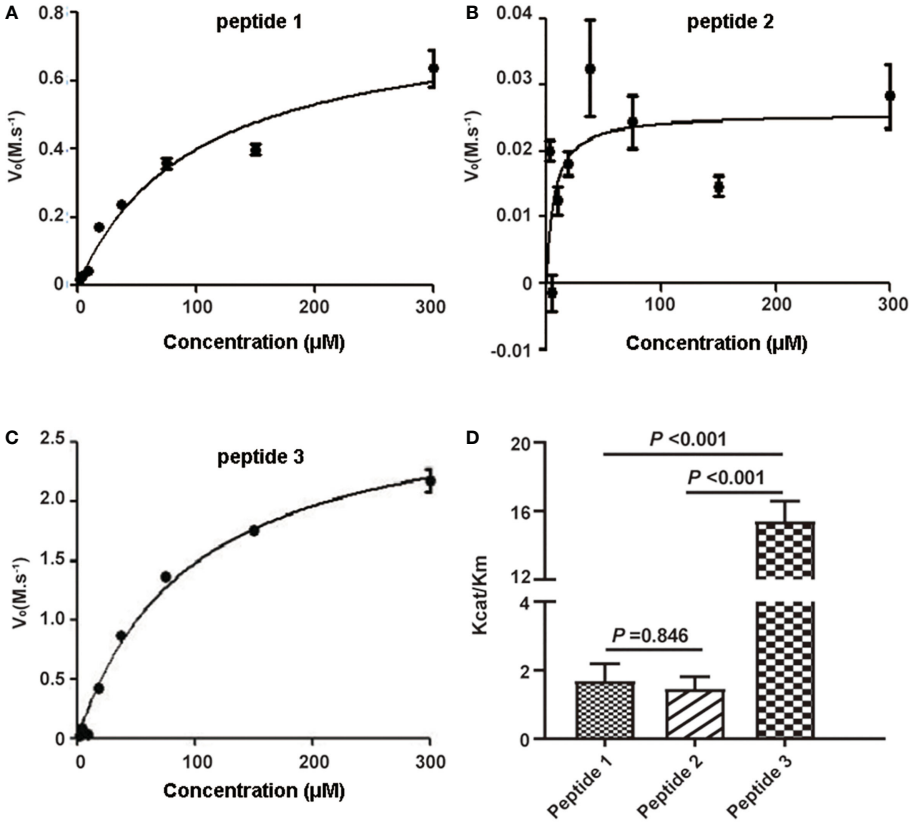

FIGURE 2
Kinetic analysis of human active C1s on cleavage of synthetic peptide substrates. Michaelis-Menten curves were generated where velocity (v_o) was plotted against the concentrations of **(A)** peptide 1, **(B)** peptide 2, and **(C)** peptide 3; **(D)** K_{cat}/K_m values of the proteolytic activity of C1s on three peptide substrates. Data are presented as the means ± standard deviation (n = 3). *P*-values were calculated by one-way ANOVA.

(20 min), 0.993 ± 0.005 (40 min), 0.996 ± 0.003 (60 min), and 0.983 ± 0.005 (80 min), respectively (Table 1). As the R^2 value at 60 minutes was closer to 1, this time was finally set as the optimal reaction endpoint. The standard curve of fluorescence and C1s activity was generated (Figure 3B). The following equation was obtained: $Y = 49.418X^2 + 1120.4X - 42.3$ (R^2 = 0.9985). Figure 3B showed that the fluorescence intensity increased with increasing C1s activity up to 10 μmol·min^{-1}·mL^{-1}.

3.3 Determination of LOD

LOD was determined under optimal condition. The fluorescence intensity was repeatedly detected 20 mins for the reaction after the magnetic microbeads-labelled anti-C1s antibody was added with substrate peptide 3 in the absence of activated C1s. The LOD for activated C1s was 0.096 μmol·min^{-1}·mL^{-1} in this immunoassay.

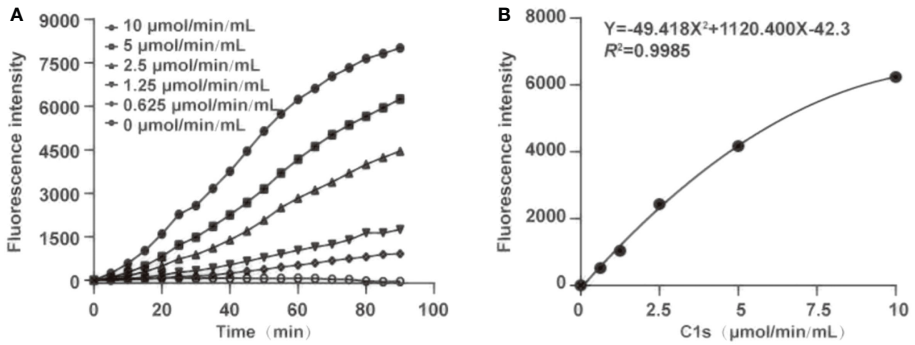

FIGURE 3
Optimization of the reaction time and generation of standard curve. **(A)** The optimum reaction time was ascertained in the presence of chromogenic peptide 3 (10 μL, 1 μg/mL). Fluorescence intensity was recorded at the indicated time; **(B)** Plot of standard curves were generated against activated C1s with different concentrations (0.625, 1.25, 2.5, 5, and 10 μmol·min^{-1}·mL^{-1}).

3.4 Accuracy and precision

Accuracy and precision of the method were then evaluated through recovery and repeatability. Prior to spiking, the activity of activated C1s in human serum samples was 0.246, 1.985, and 1.966 μmol·min^{-1}·mL^{-1}, respectively. Table 2 showed that the recovery rates were 90.38%, 104.87%, and 90.34%, which was acceptable for the potential application of method in C1s detection in clinical samples. The intraday repeatability and interday reproducibility were examined. The results of intraday and interday assays were shown in Table 3. The CVs of repeatability and reproducibility were less than 10%, which clearly indicated an acceptable precision.

3.5 Specificity

The cross-reaction rates of the C1r enzyme, MASP1 and MASP2 were all less than 0.5% with a rate of 0.15%, 0.04%, and 0.04%, respectively (Table 4). The cross-reaction with C1r enzyme, MASP1, and MASP2 was not significant, suggesting that the assay can specifically measure activated C1s in serum samples with high specificity. Cross-reactivity has been checked for C1r, MASP-1, MASP-2 (Table 4). The cross-reactivity measured for C1r seems quite high as compared to the others. This may be due to certain C1s contaminant in the C1r sample, which would contribute to the immunocapture and measured activity. Moreover, bilirubin, chyle, and haemoglobin in the clinical samples may potentially interfere with the assay for C1s activity. Therefore, the interference tests were further performed with activated C1s standard solutions at low, medium and high concentrations and interference substances including bilirubin (0, 0.06, 0.14, and 0.20 mg·mL^{-1}), chyle (0, 600, 1400, and 2000 FTU), and haemoglobin (0, 1.5, 3.5, and 5 mg·mL^{-1}). None of these interferents significantly affected the assay of C1s activity (Table 5).

3.6 Effects of anticoagulants on activated C1s detection

Anticoagulants are required for blood collection and isolation to inhibit blood clotting. It is unclear whether anticoagulants used during blood collection interfere with the cleavage of substrate peptide by activated C1s. Figure 4A showed that the enzymatic activities of complement C1s were significantly decreased after EDTA ($P < 0.0001$) or heparin ($P < 0.01$) treatment. Although the p values between citrate and serum was less significant ($P > 0.05$), citrate treatment also showed some degree suppressive effects on the cleavage of C1s in plasma samples. The total protein levels of C1s were also detected by ELISA, and the data in Figure 4B showed that no significant differences in C1s contents between serum and three anticoagulants-treated groups ($P > 0.05$). Next, to confirm the effects of anticoagulants on the enzymatic activities of activated C1s, the activated C1s standard solutions (25 pmol·min^{-1}·μg^{-1}) were treated with EDTA (1.5 mg·mL^{-1}), citrate (109 mmol·L^{-1}), and heparin (15 IU·mL^{-1}). The data in Figure 4C showed that the enzymatic abilities of C1s were suppressed by EDTA (26.54%) ($P < 0.001$), citrate (55.27%) ($P < 0.01$), and heparin (36.4%) ($P < 0.01$). Thus, these data demonstrated that the assayed anticoagulants, especially EDTA, significantly suppressed the enzymatic activity of activated C1s in the clinical samples.

TABLE 1 The R^2 value at various reaction times (n = 4).

	Reaction time			
	20 min	40 min	60 min	80 min
R^2	0.984 ± 0.0114	0.993 ± 0.005	0.996 ± 0.003	0.983 ± 0.005

TABLE 2 Relative recovery of C1s obtained from human serum samples spiked with C1s of different activities.

Sample	C1s base-line (μmol min^{-1} mL^{-1})	C1s spiked (μmol min^{-1} mL^{-1})	C1s detected (μmol min^{-1} mL^{-1})	Recovery (%)
Sample 1	0.246	2.671	1.330	90.38
Sample 2	1.985	2.671	2.393	104.87
Sample 3	1.966	5.342	3.301	90.34

3.7 Determination of activated C1s in clinical serum samples

Next, we investigated the reference activity range of activated C1s in the healthy individuals by the established FRET-based immunoassay. A total of 306 healthy individuals were included in the analysis, and the corresponding serum samples were collected for the quantitative analysis of C1s activity. The obtained results were shown in Figure 5 and Table 6. The minimum and maximum values of the C1s activity in the detected samples were 0.165 and 2.547 μmol·min^{-1}·mL^{-1}. The mean value and standard deviation were 1.023 μmol·min^{-1}·mL^{-1} and 0.422 μmol·min^{-1}·mL^{-1}. The central 94.77% healthy individuals (290/306) were detected with activated C1s in the range of 0.26 and 1.90 μmol·min^{-1}·mL^{-1}, indicating that the reference range of activated C1s assayed by FRET-based immunoassay was 0.26-1.90 μmol·min^{-1}·mL^{-1}. However, this reference range was obtained based on a small sample cohort. In future studies, the sample size will be expanded and the significance of the established FRET-based immunoassay will be explored in a variety of diseases.

3.8 Determination of active C1s in serum samples from patients with RA

The serum samples of 20 patients with RA and 20 healthy participants were measured. The results showed that the active C1s in the serum samples from patients with RA was significantly increased compared to that of the control group ($P < 0.05$) (Figure 6).

4 Discussion

The detection methods for C1s reported include bilateral diffusion (14), ELISA, gelatin zymography (15) and LC-MS/MS (16). However,

TABLE 3 Precision tests of C1s activity assay.

Samples	Intra-assay (n = 10)			Inter-assay (n = 10)		
	Means	SD	CV (%)	Means	SD	CV (%)
Low conc. (μmol·min^{-1}·mL^{-1})	0.314	0.028	8.91	0.298	0.028	9.40
Med conc. (μmol·min^{-1}·mL^{-1})	1.588	0.097	6.11	1.666	0.156	9.36
High conc.(μmol·min^{-1}·mL^{-1})	4.567	0.305	6.68	4.412	0.374	8.48

TABLE 4 Cross-reactivity of C1s activity assay.

Interfering substances	C1s activity	Interference concentration	Cross-reactivity rate (%)
C1r enzyme	0.053 μmol·min^{-1}·mL^{-1} (1 μg·mL^{-1})	660 μg·mL^{-1}	0.15
MASP1	0.107 μmol·min^{-1}·mL^{-1} (2 μg·mL^{-1})	5000 μg·mL^{-1}	0.04
MASP2	0.096 μmol·min^{-1}·mL^{-1} (1.8 μg·mL^{-1})	5000 μg·mL^{-1}	0.04

TABLE 5 Interference of C1s activity assay by bilirubin, chyle and hemoglobin (n = 4).

	Low conc. (μmol·min^{-1}·mL^{-1})	Med conc. (μmol·min^{-1}·mL^{-1})	High conc. (μmol·min^{-1}·mL^{-1})
Bilirubin conc. (mg·mL^{-1})			
0	0.323 ± 0.019	1.748 ± 0.166	3.322 ± 0.156
0.06	0.343 ± 0.019	1.822 ± 0.136	3.346 ± 0.269
0.14	0.335 ± 0.015	1.808 ± 0.077	3.258 ± 0.264
0.20	0.329 ± 0.025	1.581 ± 0.123	3.279 ± 0.185
Chyle conc. (FTU)			
0	0.339 ± 0.033	1.890 ± 0.130	3.321 ± 0.123
600	0.345 ± 0.018	1.942 ± 0.191	3.285 ± 0.135
1400	0.333 ± 0.040	1.739 ± 0.093	3.182 ± 0.317
2000	0.325 ± 0.056	1.992 ± 0.165	3.250 ± 0.323
Hb conc. (mg·mL^{-1})			
0	0.366 ± 0.025	1.800 ± 0.170	3.406 ± 0.241
1.5	0.352 ± 0.035	1.730 ± 0.068	3.555 ± 0.215
3.5	0.364 ± 0.033	1.653 ± 0.157	3.301 ± 0.269
5	0.374 ± 0.030	1.657 ± 0.085	3.493 ± 0.301

FTU, formazine turbidity unit; Hb, haemoglobin.

bilateral diffusion, gelatin zymography, and LC-MS/MS techniques only enable qualitative or semi-quantitative analysis. The accuracy of the results is poor and the CV values are highly variable as the ELISA plate need to be repeatedly cleaned during the assay. More notably, these methods only measure the level of C1s protein and are unable to distinguish between C1s being in the active or inactive state. C1s are normally presented *in vivo* as zymogens and exert enzymatic activity when activated by C1r. Therefore, accurate determination of activated C1 activity is particularly important for understanding the exact role of C1 in physiological and pathological conditions in humans and mammals.

A previous study had determined the active status of C1s exploiting the characteristic of C1s cleaved into C2 and C4 (23). Unfortunately, the procedure of this method is cumbersome to perform. Additionally, this method shows limited specificity as the targets C4 and C2 molecules can also be cleaved by MASP2. In certain cases, DTNB was employed to measure the activity of recombinant C1s (27). Unfortunately, DTNB also serves as a substrate for granzyme H (26). Thus, DTNB are not suitable for measuring C1s activity in a specific manner. The assessment of complement function has been designed based on the regulatory effects of C1 inhibitor on the proteases of the C1 complex (C1r and C1s) (28). However, this

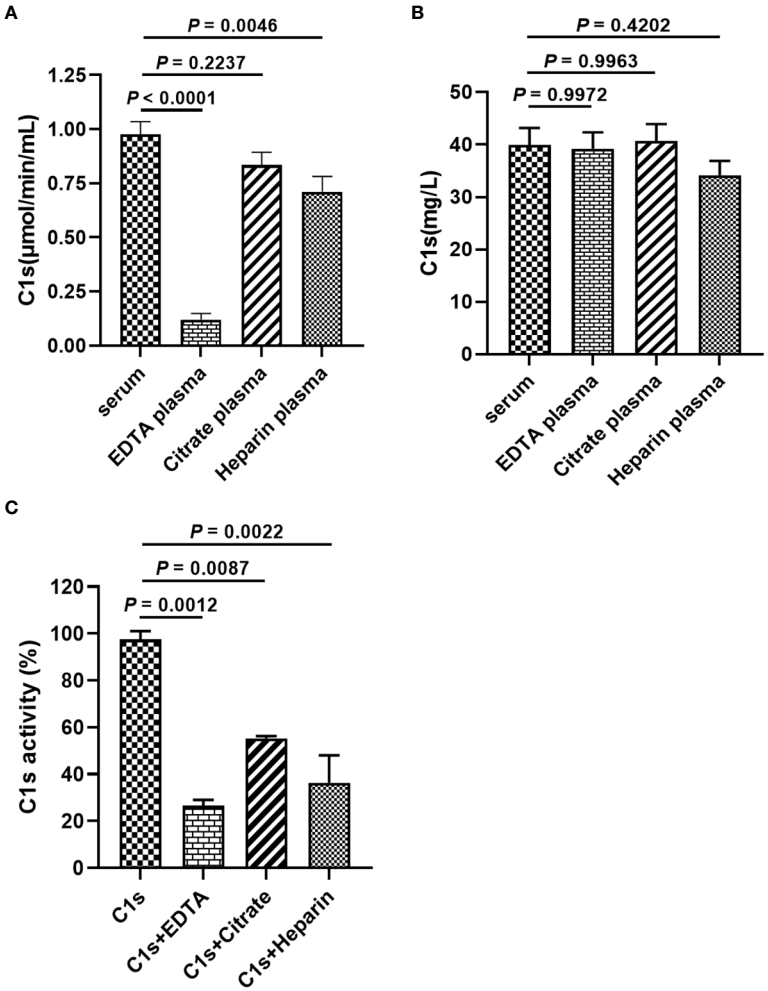

FIGURE 4
Effects of anticoagulants on FRET-based immunoassay for activated complement C1s detection. **(A)** Enzyme activity of complement C1s in serum and plasma samples by FRET-based immunoassay; **(B)** Protein contents of C1s in serum and plasma samples by ELISA; Human blood samples (n = 18) were collected with EDTA, citrate and heparin as anti-agglutinins. **(C)** Activated C1s standard solutions assayed by FRET-based immunoassay after treatment with EDTA, citrate and heparin; Data are presented as the means ± standard deviation (n = 3). ns, P>0.05; **P<0.01; ***P<0.001; P<0.0001. *P*-values were calculated by one-way ANOVA.

method is not sufficient because it not only relies on the convenient spectrophotometric measurement of the active C1s, but also the activated C1r. Thus, it could be used for C1INH detection, but it is not available for active C1s assay due to lack of specificity.

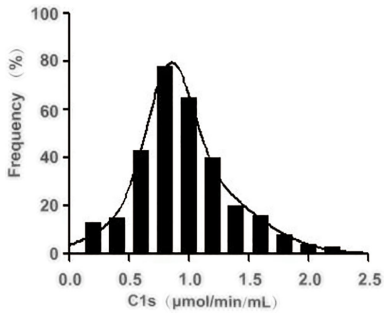

FIGURE 5
Distribution of the activated complement C1s activity in serum from healthy individuals. The activity of C1s was analysed by FRET-based immunoassay. n = 306.

The subcomponent C1s in the serum acts as the pro-enzymic form and is responsible for the activation of components C2 and C4 (29–31). Based on this functional mechanism, the unique serine protease activity of activated C1s, which can specifically cleave the target proteins C2 and C4, was combined with FRET technology to detect C1s activity. Here, specific peptides were designed considering that active C1s catalyzes the cleavage of C2 between R243 and K244 (peptide 1), and C4 between R756 and A757 (peptide 2) (24, 25). Next, FRET-based fluorogenic peptides 3 were synthesized, and the activity of active C1s was indicated by calculating the Kcat/Km value. The results showed that the Kcat/Km values of peptide 3 were significantly higher than the values of peptide 1 and peptide 2. FRET-based peptide 3 was selected as a candidate substrate for the detection of active C1s in serum samples. The active C1s in the system cleave the substrate peptides, and then Abz would no longer be quenched by Dnp. Consequently, chromogenic peptide could emit detectable fluorescence signals. However, if active C1s are absent in

10.3389/fimmu.2023.1081793

TABLE 6 Reference interval of activated C1s in healthy individuals (n=306).

	Activated C1s (μmol·min^{-1}·mL^{-1})					
	< 0.260	0.261-0.670	0.671-1.080	1.081-1.490	1.491-1.900	> 1.900
Samples	8	55	144	65	26	8
Percentage (%)	2.61	17.97	47.06	21.24	8.50	2.61
Total (%)	2.61	20.59	67.65	88.89	97.39	100

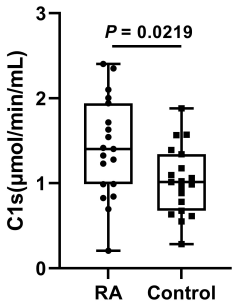

FIGURE 6
The levels of active C1s in serum of patients with RA. Data are presented as the means ± standard deviation (each group: n = 20). *P* = 0.0219 by *t* test.

the system, the substrate peptides remain intact and the distance between Abz and Dnp is 10-100 angstroms (Å). Therefore, Dnp quenches the fluorescence emitted by Abz, and the fluorescence could not be detected. The fluorescence intensity based on FRET is strongly related to the activity of active C1s (Figure 1).

It is noteworthy that MASP-2 is another key enzyme that can cleave C4 and C2 to assemble C3 convertase (C4b2a), which may interrupt the specificity in clinical samples (32). Also within the realm of possibility is the fact that the selected substrate peptide 3 can be cleaved by other protease. Hence, in this study, magnetic microbeads were conjugated with recombinant C1s-specific antibody that could specifically capture active C1s, and this complex can be magnetically separated from the interfering mediums. Subsequently, we established a FRET-based immunoassay to detect active C1s, which showed low detection limits, good correlation, wide linearity range and acceptable recoveries (Figures 1, 2). In particular, this assay method we developed is effective in avoiding interference from bilirubin, chyle and haemoglobin. As for the intra-assay CV, it has been indicated that the intra-assay CV for assaying the activity of the classical pathway, alternative pathway, and mannose-binding lectin ranged between 35% and 99%, while the CVs of the two controls for C1INH activity were 43% and 28%, respectively (33). These results indicate that there are uncertain influences in the current assays for complement activity and single complement component. In the present study, we controlled the CVs of repeatability and reproducibility of active C1s within 10%.

The C1 complex is a calcium-dependent complex composed of three distinct subcomponents (34). Both EDTA and citrate can bind calcium ions, and little is known about the effects of these anticoagulants on the activity of classic complement pathway initiated by the C1 complex. In our study, we observed that heparin, EDTA, and citrate significantly reduce the activity of classical, alternative and mannose-binding lectin pathways, with only about 50% of classic complement pathway activity in plasma treated with anticoagulants (heparin, EDTA, and citrate) compared to complement activity in serum (Figure 4). Another study showed that C1 hemolytic activity was significantly reduced in a dose-dependent manner in both EDTA- and citrate-treated samples. Subsequent hemolytic activity of C1 could not be restored even after recalcification (35). Ca^{2+} binding is the premise of C1s activation, which indicates that Ca^{2+} also plays an important role in regulating C1s function. Actually, C1s zymogen and active C1s with catalytic ability have comparable binding valence to Ca^{2+} and similar affinity. This binding causes the generation of a dimeric molecule of 6.0s from a 4.5s monomer, which is a dimerization reaction that appears to primarily involve the chain of each monomer, presumably with these two Ca^{2+} binding sites located on the A chain of the C1s dimer (34). Heparin is another anticoagulant frequently available in clinical practice, which has been proved to affect C1s activity by binding to the SP domain of C1s and facilitating C1s biding to C1IHN (36, 37). Recently, our preliminary data showed that heparin or EDTA can significantly inhibit C1s activity in plasma compared to serum. Furthermore, no differences in C1 protein levels were observed in samples treated with heparin, EDTA or citrate, respectively.

RA is an autoimmune disease. It has been shown that the activation of the classical pathway is present in the serum of patients with RA (38). Moreover, serum samples from RA showed significantly elevated levels of C5b6789 (39). Assayed with our established method, active C1s in the serum samples is significantly elevated, suggesting activation of the classical pathway in patients with RA (Figure 6).

In summary, we established a FRET-based immunoassay to detect active C1s. This method is suitable for the detection of active C1s in serum samples within the reference range. In complement-related diseases, the levels of active C1s in serum are fundamental information for the diagnosis and treatment of diseases as well as for the study of its pathogenesis.

Data availability statement

The original contributions presented in the study are included in the article/Supplementary Material. Further inquiries can be directed to the corresponding authors.

Ethics statement

The studies involving human participants were reviewed and approved by the Ethics Committee of Taizhou People's Hospital (KY2020-184-01). The patients/participants provided their written informed consent to participate in this study.

Author contributions

SX and LZ contributed to conception and design of the study. JY and JX organized the database. JY and CZ performed the statistical analysis. JY wrote the first draft of the manuscript. JX, CZ, LZ and SX wrote and revised the manuscript. All authors contributed to the article and approved the submitted version.

Funding

This work was supported by the 2022 Taizhou Scientific Project (TS202211); the 2020 Taizhou People's Hospital Mandatory Project (No. ZL202022); and the National Natural Science Foundation of China (No. 81871234, 82172763).

Conflict of interest

The authors declare that the research was conducted in the absence of any commercial or financial relationships that could be construed as a potential conflict of interest.

Publisher's note

All claims expressed in this article are solely those of the authors and do not necessarily represent those of their affiliated organizations, or those of the publisher, the editors and the reviewers. Any product that may be evaluated in this article, or claim that may be made by its manufacturer, is not guaranteed or endorsed by the publisher.

Supplementary material

The Supplementary Material for this article can be found online at: https://www.frontiersin.org/articles/10.3389/fimmu.2023.1081793/full#supplementary-material

References

1. Ramlall V, Thangaraj PM, Meydan C, Foox J, Butler D, Kim J, et al. Immune complement and coagulation dysfunction in adverse outcomes of SARS-CoV-2 infection. *Nat Med* (2020) 26(10):1609–15. doi: 10.1038/s41591-020-1021-2

2. Lintner KE, Wu YL, Yang Y, Spencer CH, Hauptmann G, Hebert LA, et al. Early components of the complement classical activation pathway in human systemic autoimmune diseases. *Front Immunol* (2016) 7:36. doi: 10.3389/fimmu.2016.00036

3. Riihilä P, Viiklepp K, Nissinen L, Farshchian M, Kallajoki M, Kivisaari A, et al. Tumour-cell-derived complement components C1r and C1s promote growth of cutaneous squamous cell carcinoma. *Br J Dermatol* (2020) 182(3):658–70. doi: 10.1111/bjd.18095

4. Defendi F, Thielens MN, Clavarino G, Cesbron JY, Dumestre-Pérard C. The immunopathology of complement proteins and innate immunity in autoimmune disease. *Clin Rev Allergy Immunol* (2020) 58(2):229–51. doi: 10.1007/s12016-019-08774-5

5. Almitairi JOM, Girija UV, Furze CM, Simpson-Gray X, Badakshi F, Marshall JE, et al. Structure of the C1r-C1s interaction of the C1 complex of complement activation. *Proc Natl Acad Sci U.S.A.* (2018) 115(4):768–73. doi: 10.1073/pnas.1718709115

6. Rossi V, Bally I, Lacroix M, Arlaud GJ, Thielens NM. Classical complement pathway components C1r and C1s: Purification from human serum and in recombinant form and functional characterization. *Methods Mol Biol 2014* (1100) p:43–60. doi: 10.1007/978-1-62703-724-2_4

7. Lu J, Kishore U. C1 complex: An adaptable proteolytic module for complement and non-complement functions. *Front Immunol* (2017) 8:592. doi: 10.3389/fimmu.2017.00592

8. Jäger U, D'Sa S, chörgenhofer C, Bartko J, Derhaschnig U, Sillaber C, et al. Inhibition of complement C1s improves severe hemolytic anemia in cold agglutinin disease: A first-in-human trial. *Blood* (2019) 133(9):893–901. doi: 10.1182/blood-2018-06-856930

9. Peerschke EI, Panicker S, Bussel J. Classical complement pathway activation in immune thrombocytopenia purpura: inhibition by a novel C1s inhibitor. *Br J Haematol* (2016) 173(6):942–5. doi: 10.1111/bjh.13648

10. Dhillon S. Sutimlimab: First approval. *Drugs* (2022) 82(7):817–23. doi: 10.1007/s40265-022-01711-5

11. Ye J, Yang P, Yang Y, Xia S. Complement C1s as a diagnostic marker and therapeutic target: Progress and propective. *Front Immunol* (2022) 13:1015128. doi: 10.3389/fimmu.2022.1015128

12. Nakagawa K, Sakiyama H, Tsuchida T, Yamaguchi K, Toyoguchi T, Masuda R, et al. Complement C1s activation in degenerating articular cartilage of rheumatoid arthritis patients: Immunohistochemical studies with an active form specific antibody. *Ann Rheum Dis* (1999) 58(3):175–81. doi: 10.1136/ard.58.3.175

13. Loos M, Storz R, Müller W, Lemmel EM. Immunofluorescence studies on the subcomponents of the first component of complement (C1): detection of C1q and C1s in different cells of biopsy material and on human as well as on guinea pig peritoneal macrophages. *Immunobiology* (1981) 158(3):213–24. doi: 10.1016/S0171-2985(81)80071-X

14. Ziccardi RJ, Cooper NR. Demonstration and quantitation of activation of the first component of complement in human serum. *J Exp Med* (1978) 147(2):385–95. doi: 10.1084/jem.147.2.385

15. Ugarte-Berzal E, Martens E, Boon L, Vandooren J, Blockmans D, Proost P, et al. EDTA/gelatin zymography method to identify C1s versus activated MMP-9 in plasma and immune complexes of patients with systemic lupus erythematosus. *J Cell Mol Med* (2019) 23(1):576–85. doi: 10.1111/jcmm.13962

16. Kodeboyina SK, Lee TJ, Bollinger K, Ulrich L, Bogorad D, Estes A, et al. Aqueous humor proteomic alterations associated with visual field index parameters in glaucoma patients: A pilot study. *J Clin Med* (2021) 10(6):1180. doi: 10.3390/jcm10061180

17. Daugan MV, Revel M, Russick J, Dragon-Durey M, Gaboriaud C, Robe-Rybkine T, et al. Complement C1s and C4d as prognostic biomarkers in renal cancer: Emergence of noncanonical functions of C1s. *Cancer Immunol Res* (2021) 9(8):891–908. doi: 10.1158/2326-6066.CIR-20-0532

18. Takkinen K, Žvirblienė A. Recent advances in homogenous immunoassays based on resonance energy transfer. *Curr Opin Biotechnol* (2019) 55:16–22. doi: 10.1016/j.copbio.2018.07.003

19. Qiu X, Hildebrandt N. A clinical role for förster resonance energy transfer in molecular diagnostics of disease. *Expert Rev Mol Diagn* (2019) 19(9):767–71. doi: 10.1080/14737159.2019.1649144

20. Chen M, Wu Y, Lin G, Hou J, Li M, Liu T. Quantum-dot-based homogeneous time-resolved fluoroimmunoassay of alpha-fetoprotein. *Anal Chim Acta* (2012) 741:100–5. doi: 10.1016/j.aca.2012.06.042

21. Wegner KD, Jin Z, Lindén S, Jennings TL, Hildebrandt N. Quantum-dot-basedFörster resonance energy transfer immunoassay for sensitive clinical diagnostics of low-volume serum samples. *ACS Nano* (2013) 7(8):7411–9. doi: 10.1021/nn403253y

22. Rusanen J. New applications for TR-FRET-based homogeneous immunoassays in diagnosis of infectious and autoimmune diseases. (2022).

23. Matsumoto M, Toivonen A, Hepojoki J, Hepojoki S, Arikoski P, Heikkinen M, et al. Probing the C4-binding site on C1s with monoclonal antibodies. evidence for a C4/C4b-binding site on the gamma-domain. *J Immunol* (1989) 142(8):2743–50. doi: 10.1371/journal.pone.0225851

24. O'Brien G, Quinsey NS, Whisstock JC, Pike RN. Importance of the prime subsites of the C1s protease of the classical complement pathway for recognition of substrates. *Biochemistry* (2003) 42(50):14939–45. doi: 10.1021/bi035507b

25. Kerr FK, O'Brien G, Quinsey NS, Whisstock JC, Boyd S, Banda MG, et al. Elucidation of the substrate specificity of the C1s protease of the classical complement pathway. *J Biol Chem* (2005) 280(47):39510–4. doi: 10.1074/jbc.M506131200

26. Edwards KM, Kam CM, Powers JC, Trapani JA. The human cytotoxic T cell granule serine protease granzyme h has chymotrypsin-like (chymase) activity and is taken up into cytoplasmic vesicles reminiscent of granzyme b-containing endosomes. *J Biol Chem* (1999) 274(43):30468–73. doi: 10.1074/jbc.274.43.30468

27. Keizer MP, Pouw RB, Kamp AM, Patiwael S, Marsman G, Hart MH, et al. TFPI inhibits lectin pathway of complement activation by direct interaction with MASP-2. *Eur J Immunol* (2015) 45(2):544–50. doi: 10.1002/eji.201445070

28. Nilsson T, Wiman B. Kinetics of the reaction between human C1-esterase inhibitor and C1r or C1s. *Eur J Biochem* (1983) 129(3):663–7. doi: 10.1111/j.1432-1033.1983.tb07100.x

29. Gaboriaud C, Rossi V, Bally I, Arlaud GJ, JFontecilla-Camps JC. Crystal structure of the catalytic domain of human complement c1s: a serine protease with a handle. *EMBO J* (2000) 19(8):1755–65. doi: 10.1093/emboj/19.8.1755

30. Gál P, Ambrus G, Závodszky P. C1s, the protease messenger of C1. Structure, function and physiological significance. *Immunobiology* (2002) 205(4-5):383–94. doi: 10.1078/0171-2985-00140

31. Gaboriaud C, Thielens NM, Gregory LA, Rossi V, Fontecilla-Camps JC, Arlaud GJ, et al. Structure and activation of the C1 complex of complement: unraveling the puzzle. *Trends Immunol* (2004) 25(7):368–73. doi: 10.1016/j.it.2004.04.008

32. Thiel S, Vorup-Jensen T, Stover CM, Schwaeble W, Laursen SB, Poulsen K, et al. A second serine protease associated with mannan-binding lectin that activates complement. *Nature* (1997) 386(6624):506–10. doi: 10.1038/386506a0

33. Prohászka Z, Nilsson B, Frazer-Abel A, Kirschfink M. Complement analysis 2016: Clinical indications, laboratory diagnostics and quality control. *Immunobiology* (2016) 221(11):1247–58. doi: 10.1016/j.imbio.2016.06.008

34. Villiers CL, Arlaud GJ, Painter RH, Colomb MG. Calcium binding properties of the C1 subcomponents C1q, C1r and C1s. *FEBS Lett* (1980) 117(1):289–94. doi: 10.1016/0014-5793(80)80964-1

35. Zapf S, Loos M. Effect of EDTA and citrate on the functional activity of the first component of complement, C1, and the C1q subcomponent. *Immunobiology* (1985) 170 (3):123–32. doi: 10.1016/S0171-2985(85)80085-1

36. Rossi V, Bally I, Ancelet S, Xu Y, Frémeaux-Bacchi V, Vivès RR, et al. Functional characterization of the recombinant human C1 inhibitor serpin domain: insights into heparin binding. *J Immunol* (2010) 184(9):4982–9. doi: 10.4049/jimmunol.0902016

37. Hor L, Pan J, Whisstock JC, Pike RN, Wijeyewickrema LC. Mapping the binding site of C1-inhibitor for polyanion cofactors. *Mol Immunol* (2020) 126:8–13. doi: 10.1016/j.molimm.2020.06.018

38. Trouw LA, Haisma EM, Levarht EWN, van der Woude D, Ioan-Facsinay A, Daha MR, et al. Anti-cyclic citrullinated peptide antibodies from rheumatoid arthritis patients activate complement via both the classical and alternative pathways. *Arthritis Rheum* (2009) 60(7):1923–31. doi: 10.1002/art.24622

39. Bemis EA, Norris JM, Seifert J, Frazer-Abel A, Okamoto Y, Feser ML, et al. Complement and its environmental determinants in the progression of human rheumatoid arthritis. *Mol Immunol* (2019) 112:256–65. doi: 10.1016/j.molimm.2019.05.012

frontiers | Frontiers in Immunology

TYPE Original Research
PUBLISHED 02 February 2023
DOI 10.3389/fimmu.2023.1114509

Check for updates

OPEN ACCESS

EDITED BY
Lillemor Skattum,
Lund University, Sweden

REVIEWED BY
Marina Noris,
Mario Negri Institute for Pharmacological Research (IRCCS), Italy
Alberto Lopez Lera,
Centro de Investigación Biomédica en Red de Enfermedades Raras (CIBERER), Spain

*CORRESPONDENCE
Thilo Bartolmäs
thilo.bartolmaes@charite.de

SPECIALTY SECTION
This article was submitted to Molecular Innate Immunity, a section of the journal Frontiers in Immunology

RECEIVED 02 December 2022
ACCEPTED 23 January 2023
PUBLISHED 02 February 2023

CITATION
Bartolmäs T, Pruß A and Mayer B (2023) Three different pathways of IgM-antibody-dependent hemolysis are mainly regulated by complement.
Front. Immunol. 14:1114509.
doi: 10.3389/fimmu.2023.1114509

COPYRIGHT
© 2023 Bartolmäs, Pruß and Mayer. This is an open-access article distributed under the terms of the Creative Commons Attribution License (CC BY). The use, distribution or reproduction in other forums is permitted, provided the original author(s) and the copyright owner(s) are credited and that the original publication in this journal is cited, in accordance with accepted academic practice. No use, distribution or reproduction is permitted which does not comply with these terms.

Three different pathways of IgM-antibody-dependent hemolysis are mainly regulated by complement

Thilo Bartolmäs*, Axel Pruß and Beate Mayer

Institute of Transfusion Medicine, Charité-Universitätsmedizin Berlin, Corporate Member of Freie Universität Berlin, Humboldt-Universität zu Berlin, and Berlin Institute of Health, Berlin, Germany

Antibodies to red blood cells (RBCs) may hemolyze erythrocytes *via* Fc-mediated phagocytosis or complement-dependent. Complement activation on RBCs can be detected by C3d-direct antiglobulin test (DAT), which is the only test in immune hematology that directly targets complement. However, a positive DAT with anti-C3d cannot distinguish between C3b-mediated extravascular hemolysis, C5b-C9-mediated intravascular hemolysis and C5b-C8-mediated eryptosis. Furthermore, DAT is not suitable to estimate the strength of hemolysis. Autoimmune hemolytic anemia (AIHA) is a rare disease that is caused by autoantibodies to red blood cells that is divided in warm AIHA and in cold agglutinin disease (CAD). The causative antibodies in CAD and sometimes in warm AIHA are from the IgM class. Depending on strength of complement activation they can induce extravascular hemolysis, intravascular hemolysis and eryptosis. We studied the three types of hemolysis by use of sera from patients with CAD under various conditions. We found that additionally to the routinely applied C3d-DAT, indirect tests for complement activity (free hemoglobin and Annexin V-binding to phosphatidylserine-exposing RBCs) should be used to determine the portion of extravascular, intravascular and eryptotic hemolysis. Eryptotic hemolysis may have a significant share in clinical relevant CAD or IgM warm AIHA, which should be considered for successful treatment.

KEYWORDS

eryptosis, AIHA, complement, DAT, cold agglutinin, hemolysis

Introduction

The complement system is part of the innate immune system that serves mainly the clearance of apoptotic cells and the pathogen elimination. It can be launched *via* three distinct pathways, named classical, lectin and alternative pathway (1) that converge on the formation of an enzyme complex capable to convert complement component C3 into active products C3a and C3b (2). C3b binds to the C3 convertase to form C5 convertase which

cleaves C5 into C5a and C5b. C5b recruits complement components C6, C7, C8 and C9 which ultimately form the membrane-attack complex (MAC) (1).

The alternative pathway is permanently activated by spontaneous hydrolysis that converts C3 finally into C3a and C3b (tick-over). RBCs are susceptible to complement attacks. Complement activation on RBC surface is regulated by two GPI-anchored proteins: CD55 (decay accelerating factor, DAF) that increases the removal of the complement complex C3 convertase, and CD59 (membrane inhibitor of reactive lysis, MIRL) that inhibits C9 binding to C5b, C6, C7 and C8, hence inhibiting the formation of the MAC. Due to a mutation in the X-linked phosphatidylinositol glycan class A (PIG-A) gene and subsequent deficiency in glycosylphosphatidylinositol (GPI) anchor, these GPI-linked proteins are absent or minimally expressed on paroxysmal nocturnal hemoglobinuria (PNH) blood cells (3).

Antibodies to red blood cells (RBCs) may be either allogeneic or autologous. They usually belong either to the IgG class (e.g. anti-D, warm autoantibodies) or IgM class (isoagglutinins: Anti-A, Anti-B or cold autoantibodies). Most antibodies are capable to activate complement (IgM, IgG1, IgG3) *via* the classical pathway, however, strength of activation is different with hexameric IgM > pentameric IgM >> IgG3 > IgG1 >> IgG2. Some antibody (sub)classes do not activate complement *via* the classical pathway (IgG4, IgA) (4).

Autoimmune hemolytic anemias (AIHA) are rare diseases caused by autoantibodies (aabs) against RBCs. These disorders are diagnosed on the basis of evidence of hemolysis in combination with characteristic serological findings, especially the direct antiglobulin test (DAT). This test is used to detect antibodies on RBCs and to identify their immunoglobulin class. The majority of cases of AIHA are mediated by warm-reactive autoantibodies, i.e., antibodies displaying optimal reactivity with human RBC at 37°C and which are usually of the IgG immunoglobulin class (5). In contrast, autoantibodies in cold agglutinin disease (CAD) are usually from IgM class directed typically against I/i carbohydrate antigens. Their thermal amplitude, i.e. the highest temperature they agglutinate RBCs, is usually below 32°C and their maximal reactivity is at 4°C (6). AIHAs can be either idiopathic or secondary due to a variety of diseases like leukemia, systemic lupus erythematosus, lymphoproliferative disorders, infections (7).

The pathogenic role of autoantibodies depends on their immunoglobulin class, subclass, thermal amplitude, as well as affinity and efficiency in activating complement (8).

IgG aabs in warm AIHA usually activate complement to C3b, leading to Fc-mediated phagocytosis (mostly in spleen) or C3b-mediated phagocytosis (mostly in the liver). Complement degradation also plays a key role in complement regulation. C3b is converted into iC3b within 1 min and in about 10 min further degraded into C3d, which no longer fixes complement, nor does it serve as an opsonin (2). C3d is fixed stably to RBCs by a molecular binding and is thus a marker of earlier complement activation.

In contrast to the aforementioned so-called extravascular hemolysis, intravascular hemolysis requires complete complement activation until the membrane attack complex. This can usually only be achieved with IgM antibodies, although there are reports of IgG-mediated intravascular hemolysis.

A single IgM molecule is capable of activating C1q (9). C1 can be activated already below 15°C, however, C4 needs temperatures above 18°C for activation (10). The C2/C4 complex, which is important for C3 activation, is unstable at elevated temperatures. Additionally, a large number of activated C3 and C5 (about 90000 molecules) are required for lysis (10). This explains why most patients with CAD have only a chronic mild (extravascular) hemolysis, since the thermal amplitude of IgM aabs is often below 20°C and the complement system is not fully activated. On the other hand, CAD patients with thermal amplitudes above 30°C or patients with warm IgM-AIHA may have severe or even fatal intravascular hemolysis (11).

Whereas intravascular and extravascular hemolysis have been known for a long time a third form of hemolysis, eryptosis, has only recently been considered to be a significant contributor to AIHA when IgM is involved (12). Eryptosis, the suicidal death of RBCs, resembling the apoptosis of nucleated cells has been described to occur in a variety of diseases (13, 14). Its hallmark is the breakdown of phosphatidylserine (PS) -asymmetry upon Ca^{2+} influx into RBCs. Phosphatidylserine- exposure can be easily accessed by annexin V-binding (15). We gave evidence of eryptosis in 7 of 13 patients with IgM warm AIHA and all patients with significant CAD (12). We could further show that IgM-mediated eryptosis requires complement (16). Incubation with fresh serum from CAD patients can induce eryptosis in donor O RBCs. This can be abolished by serum heat inactivation (i.a.) or EDTA addition prior to incubation with O RBCs. Furthermore, eryptosis is also suppressed strongly by adding anti-C5 (Eculizumab ®) or partially with anti-C8 but is increased with anti-C9. Incubation of O RBCs with heat-inactivated patients serum and single complement factor-deficient sera (C5, C6, C7, C8 or C9-deficient) revealed that eryptosis (exposure of PS at the surface of RBCs) is increased gradually in the sublytic terminal complexes to reach a maximum at the C5b-8 stage (16). The significance of eryptosis to AIHA is not yet clear, since eryptotic cells are quickly removed from circulation by phagocytosis (15). Thus, eryptotic RBCs mostly have the same fate as C3b-opsonized RBCs, all these cells undergo extracellular hemolysis. However, since classical IgG- or C3b-mediated extravascular hemolysis or eryptosis require different therapies, a more thorough differentiation may be beneficial. Therefore, we used sera from three different patients with clinically relevant CAD to further investigate the influence of IgM aab on donor RBCs under different conditions (temperature, titer, complement concentration) looking for signs of intravascular hemolysis (free hemoglobin), eryptosis (Annexin V-binding to externalized PS) and extravascular hemolysis (using C3d as a surrogate for C3b). All three hemolysis pathways usually run in parallel under physiological conditions, but to different extents depending on titer, temperature and complement factor concentration.

Materials and methods

Samples and reagents

Serum and EDTA samples were from three patients with clinically relevant AIHA of cold type (12). Fresh O RBCs and serum from healthy blood donors were used in the incubation experiments and as controls and source of complement, respectively. To diminish individual variability, fresh serum from three donors were pooled before use. This study was approved by the local Ethics Committee with registration number EA2/058/12.

Direct antiglobulin test (DAT), eluates, antibody titers and thermal amplitude

Routine diagnostic tests were performed with EDTA samples in our immunohematological reference laboratory as described before for monospecific DAT, eluates and thermal amplitude (17, 18). Antibody titers were performed at 4°C.

Hemolysis experiments

A typical experiment was performed by incubation of 20 µl donor RBCs (blood group O) with a total of 400 µl of a 1:10 mixture of patient's serum with fresh donor serum as a source of complement or, if applicable, heat-inactivated donor serum, as indicated. The proportion of patient's serum to donor serum was 1:10 to insure similar complement concentrations in parallel experiments. Incubation time and temperature was generally 48 hours at 20°C. 48 h was found to be the optimal time for measuring eryptosis after induction with patients serum (12). In thermal amplitude experiments, cells were incubated 4 hours at the indicated temperature, reaction was stopped by addition of EDTA and samples stored 48 hours at 4°C. The supernatant was then separated for determination of free hemoglobin and cells were washed carefully three times at 37°C to avoid sheer stress as a cause of RBC damage.

Free hemoglobin

300 µl of supernatant from the hemolysis experiment were mixed with 1,2 ml hemoglobin buffer (Hämoglobinreagenz, Bioanalytic GmbH, Freiburg Germany) according to the manufacturers recommendation. After 5 min. incubation at room temperature cyanohemoglobin was measured in a Hitachi photometer (wavelength 671 nm).

Complement factor C3d on donor RBCs (C3d-DAT)

Twenty-five µl of anti-C3d (diluted 1:40, from DAKO, Agilent Technologies, St. Clara, USA) were added to 50 µl of warm washed O RBCs from hemolysis experiments and examined for agglutination using the buffered gel card (ID-card "NaCl, Enzyme Test and Cold Agglutinins" Bio-Rad, Cressier sur Morat, Switzerland) (18). As a control for autoagglutination RBCs were centrifuged without anti-C3d.

Flow cytometry

Eryptosis was measured as previously described (12). Annexin V-binding to extracellular exposed PS was used as a marker of eryptosis. Briefly, 5 µl of washed RBCs from hemolysis experiments were diluted in 200 µl Annexin V-binding buffer (BD Biosciences, Heidelberg, Germany). Therefrom 5 µl of RBCs were added to 5 µl of PE-(phycoerythrin) Annexin V in 45 µl of Annexin V-binding buffer (BD Biosciences, Heidelberg, Germany). After incubation at room temperature for 15 min, the mixture was diluted with 450 µl of Annexin V-binding buffer and analysed by flow cytometry (MACSQuant® Flow Cytometer, Miltenyi Biotech, Germany). At least 20 000 events were collected for each sample. Data were analyzed using the FlowJo® software (FlowJo, LLC; USA) and the percentage of PE-Annexin V positive cells compared to the negative controls were calculated. A positive control was generated by incubation of 5 µL RBCs in 200 µL of a HEPES-buffered Ringer's solution with the Ca^{2+} ionophore ionomycin (1 µmol L^{-1}).

Statistics

For each data point 2-5 experiments were performed. Data are expressed as arithmetic means ± standard error of the mean (SEM) and statistical analysis was performed using IBM SSPS statistics software v24. Significance between two groups (patient vs. negative control) was determined using unpaired student's T test with probabilities of $P < 0.05$ considered statistically significant.

Results

DAT, eluates, antibody-titers and thermal amplitude

All three patients had a typical serological picture of a cold agglutinin disease. Monospecific DAT was strongly positive only with anti-C3d; with anti-IgM, anti-IgG, anti-IgA it was negative. Eluates were negative. In the serum, cold agglutinins with I-specificity were found with a thermal amplitude of 35° (P1), 28° (P2) and 22°C (P3), respectively. The aabs-titers found at 4°C were 1024 in P1 and P2, and 512 in P3.

Intravascular hemolysis, extravascular hemolysis and eryptosis occur simultaneously

Initially, patients' sera were diluted with fresh donor serum (1:10), as a source of complement and added to donor cells at 20°C for 48 h. As a control RBCs were treated with donor serum. Experiments were performed in triplicate (Figure 1). RBCs treated with serum of either patient showed a strong C3d-load (positive C3d-DAT). Since C3d results from a quick degradation of C3b within approximately 11 minutes (2), it may be considered as a substitute for potential C3b-mediated extravascular hemolysis. However, it is not clear how large the share of ingested C3b-RBCs compared to C3d-RBCs is, since it may depend heavily on patients' macrophage count and activity. C3d was not found on RBCs from control experiments. Similarly, free hemoglobin (fHb) was detectable in the supernatant of all experiments with patient sera, giving evidence of intravascular hemolysis. Serum of patient 3 generated less free hemoglobin, which corresponds to its lower thermal amplitude. Annexin V-binding to externalized phosphatidylserine (PS+ RBCs) as a marker

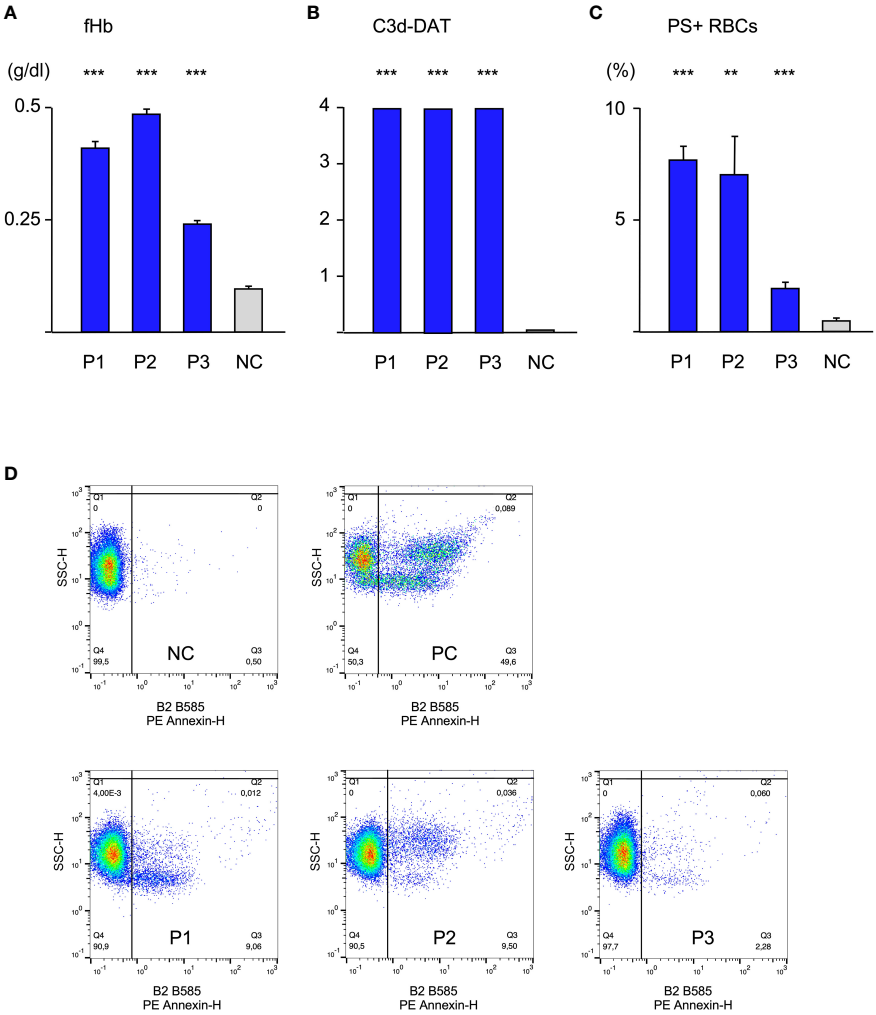

FIGURE 1
Hemolysis parameter from incubation of O RBCs with patients' sera (dilution 1:10 with fresh AB serum, 48 hours at 20°C), **(A)** free Hemoglobin (fHb), **(B)** direct antiglobulin test with anti-C3d (C3d-DAT, reaction strength: 0 no agglutination, 1 weak, 2 moderate, 3 strong, 4 very strong), **(C)** Annexin V-binding to phosphatidylserine- exposing RBCs (PS+RBCs); arithmetic means ± SEM. Five replicate experiments have been performed. *** statistically highly significant ($p < 0{,}001$), ** very significant ($p < 0{,}01$) vs negative control. **(D)** Scatter plots showing PE Annexin V-binding to O RBCs after incubation with serum from Patients P1-P3, NC negative control (AB serum), PC positive control (incubation of RBCs with ionomycine).

for eryptosis was elevated in all patients' experiments and again sera from patient 1 and 2 produced stronger eryptosis than serum from patient 3. These results show that all three forms of hemolysis occur simultaneously and the thermal amplitude may play a significant role for intravascular hemolysis and eryptosis.

Thermal amplitude is of main significance for the type of hemolysis

To further elucidate the role of the thermal amplitude, we performed experiments at different temperatures (Figure 2A). Free hemoglobin was strongly increased at 20°C and 26°C in all cases but at 32°C it could only be detected to a much lesser extent with sera of patients 1 and of patient 2. Free hemoglobin was not elevated with serum from patient 3 at this temperature. Annexin V-binding was found to be highest in all cases at 20°C; at 26°C it was substantially lower but still elevated. At 32°C, eryptosis was only strongly detectable in experiment with serum from patient 1. C3d was bound strongly at all temperatures.

Variation of the antibody concentration

In the next experiments, patients' serum was used at different dilutions ranging from 1:10 to 1:1000 for incubation with O RBCs at room temperature (Figure 2B). Sera of all patients induced hemolysis, eryptosis and complement deposition at RBCs at a titer of 10. At a dilution of 1:100, free hemoglobin and Annexin V-binding were detected only with patients' sera 1 and 2. At a dilution of 1:1000 only C3d-deposition was detected after incubation with all patients' sera, indicating that at this dilution only extravascular hemolysis may take place.

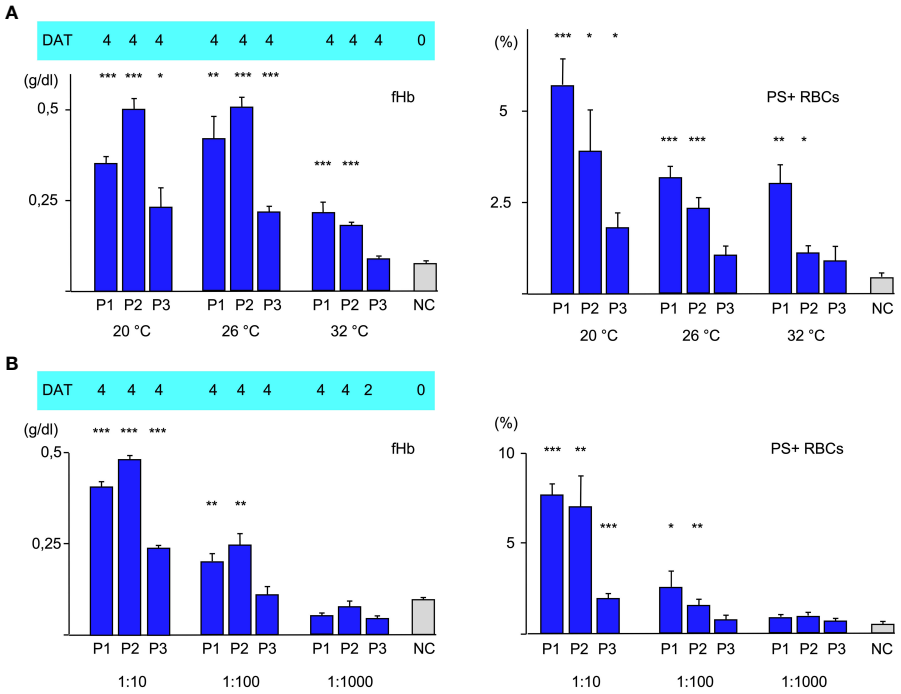

FIGURE 2
(A) Hemolysis parameter from incubation of O RBCs with patients' sera (dilution 1:10 with fresh AB serum, 4 hours at different temperatures): top C3d-DAT (reaction strength: 0 no agglutination, 1 weak, 2 moderate, 3 strong, 4 very strong), left free Hemoglobin (fHb), right Annexin V-binding to phosphatidylserine-exposing RBCs (PS+RBCs). Three replicate experiments have been performed. *** statistically highly significant ($p < 0,001$), ** very significant ($p < 0,01$), * significant ($p < 0,05$) vs negative control. **(B)** Hemolysis parameter from incubation of O RBCs with patients' sera (at different dilutions 1:10, 1:100, 1:1000 with fresh AB serum, 48 hours at 20°C): top C3d-DAT (reaction strength: 0 no agglutination, 1 weak, 2 moderate, 3 strong, 4 very strong), left free Hemoglobin (fHb), right Annexin V-binding to phosphatidylserine- exposing RBCs (PS+RBCs). Three replicate experiments have been performed.

Complement variation

To analyze the effect of disposable complement on the three types of hemolysis, fresh serum as a source of complement was mixed with heat-inactivated serum at different ratios, added to patients' serum 10:1 and used for incubation with O RBCs for 48 h at 20°C. As expected, free hemoglobin and Annexin V-binding to RBCs decreased with lower concentration of fresh serum, indicating decreasing intravascular hemolysis and eryptosis. C3d-binding was strong as shown by DAT. Unexpectedly, using more than 90% heat-inactivated serum with aab from P1, but not P2 and P3 led to a very strong agglutination of O RBCs and made measurement of PE-Annexin V in flow cytometry impossible, since it was difficult to separate the RBCs without damaging them to much.

Discussion

Intravascular hemolysis and extravascular hemolysis due to alloantibodies or autoantibodies (aab) to RBCs are known since many years. Whereas the first is caused by the membrane attack complex (C5b-C8) induced mostly by IgM antibodies, the latter is either elicited by IgG antibodies alone or by complement component C3b that is bound to RBCs following antibody (IgG/IgM) contact. In contrast, eryptosis as a cause of aab-mediated hemolysis has been shown first a few years ago by our group (12). Lately, we found that sublytic terminal component complexes (especially C5b-C8) are responsible for IgM-mediated eryptosis (16). Interestingly, more than 40 years ago, independent groups found a C5b-C8 or C8-mediated hemolysis that differed in its mechanism from the already known intravascular hemolysis (19, 20). They found that C5b-C8 or C8-mediated hemolysis (like the later found eryptosis) was delayed for several hours, whereas intravascular hemolysis occurred instantaneously. In this work, we measured all three types of hemolysis during experiments *in vitro* using IgM-aab from patients with cold agglutinin disease.

Though our data is relatively small, due to the rarity of this disease, it still suggests that all three types of hemolysis may occur simultaneously. This is an important finding, since eryptotic cells are either rapidly removed from circulation by macrophages (extravascular hemolysis) or undergo membrane blebbing, cell shrinkage, membrane fragility and finally intravascular hemolysis (14). Thus, eryptotic cells in circulation are usually underestimated. In our *in vitro* experiments, eryptotic cells represent up to more than 10% of the O RBCs with patients' sera diluted tenfold. However, since eryptosis may require specific therapy, as we have already shown by use of erythropoietin (12), it is recommendable to determine eryptotic cells in IgM warm autoimmune hemolytic anemia (AIHA) or cold agglutinin disease (CAD).

Moreover, our data confirm that thermal amplitude is the pivotal feature in patients with CAD as can be seen in Figure 2A in the difference between Patients 1 and 2 vs. 3. In case of patients 2 and 3, free hemoglobin as a marker of intravascular hemolysis and Annexin V-binding as a marker of eryptosis were detectable even above the

thermal amplitude that was measured by agglutination. Patient 1 had a thermal amplitude of more than 32°C, therefore we cannot make a statement about this case. Another noticeable point is the fact that free hemoglobin remained pretty much unchanged comparing 20°C and 26°C, whereas eryptosis was substantially lower. This may be explained by the fact that the strength of complement system is dependent from temperature. A more activated complement system may promote intravascular hemolysis (C5b-C9, MAC) at the expense of eryptosis (C5b-C8) as long as the IgM aab are sufficiently bound. Agglutination of CAD is weakening with rising temperatures, therefore there is an oppositional effect of complement activation and antibody binding to RBCs. Likewise, the similar amount of PS-exposing RBCs at 26°C and 32°C in the experiment with serum from P1 may be explained by stronger complement activation compensating weaker aab binding. The C3d-load of RBCs did not change with temperature. The fact that IgM aab bind at least for a short time even at core-temperature (37°) has been shown before and was used as an explanation for the mild hemolysis that occurred in some patients even in hot summer months (21).

In the next set of experiments, we compared different antibody dilutions (Figure 2B). As expected, both, fHb and PS+RBCs declined with dilution of the aab. At a dilution of 1:1000 only C3d could be detected on the O RBCs. At this titer only very few IgM aab may attach to the RBCs, however it was shown before that one IgM molecule is suffient to bind one C1 molecule (9).

What seems more interesting, is that even in a 100 fold dilution of aab there is still a remarkable intravascular hemolysis and eryptosis detectable by using sera from patient 1 and 2. This may explain why even when the beneficial effect of rituximab (anti-CD20) has been shown in two recent prospective trials, the partial response rate was about 50% and only few complete remissions could be seen (22).

In a final experiment, the amount of fresh donor serum as a source of complement was varied (Figure 3). A replacement of 50% fresh serum with heat-inactivated serum seems to have a rather huge effect on free hemoglobin (intravascular hemolysis) and Annexin V-binding (eryptosis). This result hints to complement inhibition as an effective therapeutic option in clinical relevant CAD/AIHA as is currently done with the newly emerged C1s-antibody (sutimlimab®) (23). At 33% fresh serum complement (by dilution with heat-inactivated serum 1:2) or below only a C3d-positive DAT (extravascular hemolysis) is detectable.

As a conclusion, all three forms of hemolysis are detectable together in patients with clinically relevant cold agglutinin disease. In patients with a low thermal amplitude of 4°C only some extravascular hemolysis may occur, but the general importance of the thermal amplitude could be clearly shown, especially the fact that strong complement activation to sublytical complement complexes or the membrane attack complex can be seen above the thermal amplitude determined by agglutination. Therefore avoidance of exposure to the cold is the main therapeutic approach in these patients. Medical treatment is difficult, which is also shown in this work, by demonstrating a remarkable residual fHb and eryptosis at substantially lowered aab titers and substitutive effects of intravascular hemolysis by eryptosis in case of lowered complement factors.

However, an accommodating combination of rituximab, erythropoietin or C1s-antibody (sutimlimab® (23) and in cases of

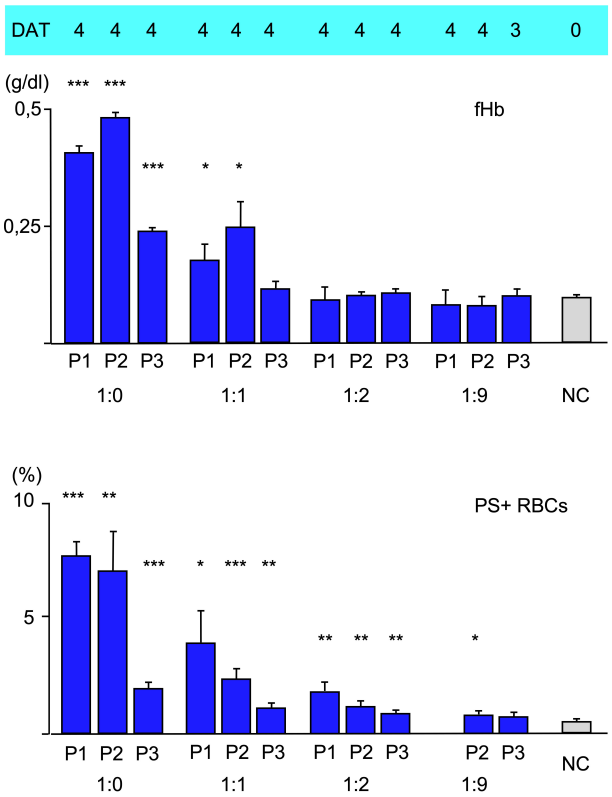

FIGURE 3
Hemolysis parameter from incubation of O RBCs with patients' sera (dilution 1:10) with a mixture of fresh AB serum and heat-inactivated (i.a.) AB serum, 48 hours at 20°C): 1:0 only fresh AB-serum, 1:1 50% fresh, 50% i.a. AB serum, 1:2 34% fresh, 66% i.a. AB serum, 1:9 10% fresh, 90% i.a. AB serum. top C3d-DAT (reaction strength: 0 no agglutination, 1 weak, 2 moderate, 3 strong, 4 very strong), middle free Hemoglobin (fHb), bottom Annexin V-binding to phosphatidylserine-exposing RBCs (PS+RBCs). Three replicate experiments have been performed (with mixture 1:2 and 1:9: two replicate experiments). *** statistically highly significant (p < 0,001), ** very significant (p < 0,01), * significant (p < 0,05) vs negative control.

severe life-threatening hemolysis C5-antibody (eculizumab®) may be beneficial in patients with difficult to control CAD.

Routine diagnosis in clinical relevant patients with cold agglutinin disease may be incomplete as it is done today. A positive C3d-DAT is valuable information to suspect IgM aab, however in patients with CAD as well as in our experiments reaction strength is mostly very high, without correlation to the clinical picture. Thermal amplitude may be the best routine parameter to estimate clinical relevance of cold agglutinins (21). Hemolysis parameter (lactat dehydrogenase, haptoglobin, bilirubin, hemoglobin) are mandatory and serum complement C3 and C4 levels may be helpful to assess a clinical picture (24). However, to get a better insight of IgM aab-induced complement activity and its caused types of hemolysis, our data indicate that free hemoglobin and eryptosis should be determined additionally.

Our findings on the three different types of immune hemolysis may apply beyond CAD, since eryptosis has been shown also for IgM-warm autoantibodies (12). In addition, we recently found strong eryptosis and intravascular hemolyis in a patient with sickle cell disease due to an irregular IgM alloantibody directed against the Lewis-Antigen Le(b) (unpublished data).

Data availability statement

The raw data supporting the conclusions of this article will be made available by the authors, without undue reservation.

Ethics statement

The studies involving human participants were reviewed and approved by Ethikkommission der Charité, Charitéplatz 1, 10117 Berlin, Vote No. EA2/058/12. Written informed consent for participation was not required for this study in accordance with the national legislation and the institutional requirements.

Author contributions

TB designed and performed the experiments. BM treated the patients. TB, BM and AP analyzed the data. TB wrote the paper with input from all other authors. All authors contributed to the article and approved the submitted version.

Acknowledgments

We acknowledge financial support from the Open Access Publication Fund of Charité – Universitätsmedizin Berlin and the German Research Foundation (DFG).

Conflict of interest

The authors declare that the research was conducted in the absence of any commercial or financial relationships that could be construed as a potential conflict of interest.

Publisher's note

All claims expressed in this article are solely those of the authors and do not necessarily represent those of their affiliated organizations, or those of the publisher, the editors and the reviewers. Any product that may be evaluated in this article, or claim that may be made by its manufacturer, is not guaranteed or endorsed by the publisher.

References

1. Merle NS, Church SE, Fremeaux-Bacchi V, Roumenina LT. Complement system part I - molecular mechanisms of activation and regulation. *Front Immunol* (2015) 6:262. doi: 10.3389/fimmu.2015.00262

2. Stowell SR, Winkler AM, Maier CL, Arthur CM, Smith NH, Girard-Pierce KR, et al. Initiation and regulation of complement during hemolytic transfusion reactions. *Clin Dev Immunol* (2012) 2012:307093. doi: 10.1155/2012/307093

3. Rachidi S, Musallam KM, Taher AT. A closer look at paroxysmal nocturnal hemoglobinuria. *Eur J Intern Med* (2010) 21(4):260–7. doi: 10.1016/j.ejim.2010.04.002

4. Berentsen S. Role of complement in autoimmune hemolytic anemia. *Transfusion Med hemother* (2015) 42(5):303–10. doi: 10.1159/000438964

5. Petz LD, Garratty G. *Immune hemolytic anemias. 2. ed.* Philadephia, Pa: Churchill Livingstone (2004). p. 591.

6. Swiecicki PL, Hegerova LT, Gertz MA. Cold agglutinin disease. *Blood* (2013) 122 (7):1114–21. doi: 10.1182/blood-2013-02-474437

7. Petz LD. Cold antibody autoimmune hemolytic anemias. *Blood Rev* (2008) 22(1):1–15. doi: 10.1016/j.blre.2007.08.002

8. Barcellini W. New insights in the pathogenesis of autoimmune hemolytic anemia. *Transfusion Med hemother* (2015) 42(5):287–93. doi: 10.1159/000439002

9. Rosse WF, Sherwood JB. Cold-reacting antibodies: Differences in the reaction of anti-I antibodies with adult and cord red blood cells. *Blood* (1970) 36(1):28–42. doi: 10.1182/blood.V36.1.28.28

10. Rosse WF, Adams J, Logue G. Hemolysis by complement and cold-reacting antibodies: Time and temperature requirements. *Am J Hematol* (1977) 2(3):259–70. doi: 10.1002/ajh.2830020308

11. Garratty G. Immune hemolytic anemia associated with negative routine serology. *Semin Hematol* (2005) 42(3):156–64. doi: 10.1053/j.seminhematol.2005.04.005

12. Bartolmas T, Mayer B, Balola AH, Salama A. Eryptosis in autoimmune haemolytic anaemia. *Eur J haematol* (2018) 100(1):36–44. doi: 10.1111/ejh.12976

13. Lang E, Lang F. Triggers, inhibitors, mechanisms, and significance of eryptosis: The suicidal erythrocyte death. *BioMed Res Int* (2015) 2015:513518. doi: 10.1155/2015/513518

14. Pretorius E, du Plooy JN, Bester J. A comprehensive review on eryptosis. *Cell Physiol Biochem* (2016) 39(5):1977–2000. doi: 10.1159/000447895

15. Lang E, Qadri SM, Lang F. Killing me softly - suicidal erythrocyte death. *Int J Biochem Cell Biol* (2012) 44(8):1236–43. doi: 10.1016/j.biocel.2012.04.019

16. Balola AHA, Mayer B, Bartolmas T, Salama A. Sublytic terminal complement components induce eryptosis in autoimmune haemolytic anaemia related to igm autoantibodies. *Cell Physiol Biochem* (2019) 53(3):453–64. doi: 10.33594/000000150

17. Mayer B, Yurek S, Kiesewetter H, Salama A. Mixed-type autoimmune hemolytic anemia: Differential diagnosis and a critical review of reported cases. *Transfusion* (2008) 48(10):2229–34. doi: 10.1111/j.1537-2995.2008.01805.x

18. Bartolmas T, Mayer B, Yurek S, Genth R, Salama A. Paradoxical findings in direct antiglobulin test and classification of agglutinating autoantibodies using eluates and monospecific anti-human globulin sera. *Vox sanguinis* (2015) 108(1):58–63. doi: 10.1111/vox.12187

19. Gee AP, Boyle MD, Borsos T. Distinction between C8-mediated and C8/C9-mediated hemolysis on the basis of independent 86rb and hemoglobin release. *J Immunol* (1980) 124(4):1905–10. doi: 10.4049/jimmunol.124.4.1905

20. Morgan BP, Imagawa DK, Dankert JR, Ramm LE. Complement lysis of U937, a nucleated mammalian cell line in the absence of C9: Effect of C9 on C5b-8 mediated cell lysis. *J Immunol* (1986) 136(9):3402–6. doi: 10.4049/jimmunol.136.9.3402

21. Bartolmas T, Yurek S, Balola AH, Mayer B, Salama A. Evidence suggesting complement activation and haemolysis at core temperature in patients with cold autoimmune haemolytic anaemia. *Transfusion Med hemother* (2015) 42(5):328–32. doi: 10.1159/000437200

22. Berentsen S. How I treat cold agglutinin disease. *Blood* (2021) 137(10):1295–303. doi: 10.1182/blood.2019003809

23. Berentsen S, Barcellini W, D'Sa S, Jilma B. Sutimlimab for treatment of cold agglutinin disease: Why, how and for whom? *Immunotherapy* (2022) 14(15):1191–204. doi: 10.2217/imt-2022-0085

24. Wang Z, Bo L, Xu Y, Liu H, Zhao Y. Features of serum complement C3 and C4 levels in autoimmune hemolytic anemia patients. *Int J Lab Hematol* (2021) 43(5):1154–8. doi: 10.1111/ijlh.13469

frontiers | Frontiers in Immunology

TYPE Original Research
PUBLISHED 09 February 2023
DOI 10.3389/fimmu.2023.1112257

Check for updates

OPEN ACCESS

EDITED BY
Erik J. M. Toonen,
Hycult Biotech, Netherlands

REVIEWED BY
Mathieu Lemaire,
University of Toronto, Canada
Marcin Okrój,
Intercollegiate Faculty of Biotechnology of University of Gdańsk and Medical University of Gdańsk, Poland

*CORRESPONDENCE
Marina Noris
marina.noris@marionegri.it

SPECIALTY SECTION
This article was submitted to Molecular Innate Immunity, a section of the journal Frontiers in Immunology

RECEIVED 30 November 2022
ACCEPTED 20 January 2023
PUBLISHED 09 February 2023

CITATION
Gastoldi S, Aiello S, Galbusera M, Breno M, Alberti M, Bresin E, Mele C, Piras R, Liguori L, Santarsiero D, Benigni A, Remuzzi G and Noris M (2023) An *ex vivo* test to investigate genetic factors conferring susceptibility to atypical haemolytic uremic syndrome. *Front. Immunol.* 14:1112257. doi: 10.3389/fimmu.2023.1112257

COPYRIGHT
© 2023 Gastoldi, Aiello, Galbusera, Breno, Alberti, Bresin, Mele, Piras, Liguori, Santarsiero, Benigni, Remuzzi and Noris. This is an open-access article distributed under the terms of the Creative Commons Attribution License (CC BY). The use, distribution or reproduction in other forums is permitted, provided the original author(s) and the copyright owner(s) are credited and that the original publication in this journal is cited, in accordance with accepted academic practice. No use, distribution or reproduction is permitted which does not comply with these terms.

An *ex vivo* test to investigate genetic factors conferring susceptibility to atypical haemolytic uremic syndrome

Sara Gastoldi, Sistiana Aiello, Miriam Galbusera, Matteo Breno, Marta Alberti, Elena Bresin, Caterina Mele, Rossella Piras, Lucia Liguori, Donata Santarsiero, Ariela Benigni, Giuseppe Remuzzi and Marina Noris*

Clinical Research Center for Rare Diseases Aldo e Cele Daccò and Centro Anna Maria Astori, Science and Technology Park Kilometro Rosso, Istituto di Ricerche Farmacologiche Mario Negri IRCCS, Bergamo, Italy

Introduction: Comprehensive genetic analysis is essential to clinical care of patients with atypical haemolytic uremic syndrome (aHUS) to reinforce diagnosis, and to guide treatment. However, the characterization of complement gene variants remains challenging owing to the complexity of functional studies with mutant proteins. This study was designed: 1) To identify a tool for rapid functional determination of complement gene variants; 2) To uncover inherited complement dysregulation in aHUS patients who do not carry identified gene variants.

Methods: To address the above goals, we employed an ex-vivo assay of serum-induced C5b-9 formation on ADP-activated endothelial cells in 223 subjects from 60 aHUS pedigrees (66 patients and 157 unaffected relatives).

Results: Sera taken from all aHUS patients in remission induced more C5b-9 deposition than control sera, independently from the presence of complement gene abnormalities. To avoid the possible confounding effects of chronic complement dysregulation related to aHUS status, and considering the incomplete penetrance for all aHUS-associated genes, we used serum from unaffected relatives. In control studies, 92.7% of unaffected relatives with known pathogenic variants exhibited positive serum-induced C5b-9 formation test, documenting a high sensitivity of the assay to identify functional variants. The test was also specific, indeed it was negative in all non-carrier relatives and in relatives with variants non-segregating with aHUS. All but one variants in aHUS-associated genes predicted in-silico as likely pathogenic or of uncertain significance (VUS) or likely benign resulted as pathogenic in the C5b-9 assay. At variance, variants in putative candidate genes did not exhibit a functional effect, with the exception of a *CFHR5* variant. The C5b-9 assay in relatives was helpful in defining the relative functional effect of rare variants in 6 pedigrees in which the proband carried more than one genetic abnormality. Finally, for 12 patients without

identified rare variants, the C5b-9 test in parents unmasked a genetic liability inherited from an unaffected parent.

Discussion: In conclusion, the serum-induced C5b-9 formation test in unaffected relatives of aHUS patients may be a tool for rapid functional evaluation of rare complement gene variants. When combined with exome sequencing the assay might be of help in variant selection, to identify new aHUS-associated genetic factors.

KEYWORDS

rare variants, aHUS, complement, endothelial cells, endothelial C5b-9 formation

Introduction

Atypical haemolytic uremic syndrome (aHUS) is a rare but usually severe form of HUS which in the past resulted in end-stage kidney disease (ESKD) in up to two thirds of affected patients (1).

Mutations in genes that encode complement factor H (FH), factor I (FI), and factor B (FB), membrane-cofactor protein (MCP), C3 and thrombomodulin (THBD), and anti-FH antibodies have been found in 50-60% of patients with primary aHUS, documenting the crucial role of uncontrolled complement activation in the pathogenesis of the disease (2). Penetrance is incomplete for all aHUS-associated genes as documented by finding within pedigrees of several unaffected carriers (2).

The introduction of anti-complement therapy has dramatically improved the outcome of aHUS patients (3, 4). Eculizumab is a humanised anti-C5 antibody that blocks C5 cleavage into C5a and C5b. The latter participates in the assembly of the terminal C5b-9 membrane attack complex (MAC). Eculizumab inhibits the common final step of all complement pathways, while preserving upstream complement functions, such as opsonisation.

Ever since therapeutic complement inhibition was approved, speedy recognition of complement-dependent aHUS has become a major diagnostic issue. However, at present, the differential diagnosis of aHUS from other thrombotic microangiopathies (TMA) is essentially made after ruling out severe ADAMTS13 deficiency (thrombotic thrombocytopenic purpura, TTP), infection with Shiga-like toxin producing bacteria (STEC-HUS), or coexisting conditions assumed to be the etiologic disease factor (secondary HUS) (5). In addition, the duration and optimal dose of treatment are often debated, particularly given the extremely high costs of the drug (6). Results from a prospective multicentre study of eculizumab discontinuation in adult and paediatric aHUS patients (7) showed that carriers of a rare complement gene variant had an increased risk of relapse, and proposed that complement genetics could help selecting patients who will undergo eculizumab discontinuation.

Thus, a comprehensive genetic analysis is essential to clinical care for aHUS patients in order to confirm the diagnosis and guide treatment (8, 9). However, genetic testing still takes too long and fails to identify an underlying complement genetic abnormality in 40% of patients. In addition, the definition of the identified variants in complement genes as pathogenic or benign remains challenging and time-consuming, given the complexity of functional studies with recombinant or plasma purified mutants (9). As a result, a high number of variants are defined as variants of uncertain significance (VUS). The interpretation of aHUS-associated gene variants is further complicated by the fact that penetrance is largely incomplete; indeed, in over 90% of cases the variant is inherited from an unaffected parent and may be present in other unaffected relatives.

This study was designed based on two objectives: 1) To identify a tool for rapid functional determination of rare complement gene variants; 2) To find genetic forms of aHUS among patients without an identified gene variant in known disease-associated genes.

In order to address the above goals, we used a published ex vivo assay based on ADP-activated confluent human microvascular endothelial cells (HMEC-1) that are exposed to serum from carriers of aHUS-associated complement gene variants (10). This assay reproduces the 2-hit model of aHUS, according to which one or more gene abnormalities predispose to aHUS, but a trigger that perturbs endothelial cells is required for terminal complement activation on cell surface, and aHUS to occur (10).

We hypothesised that if a complement gene variant causes a genetic liability to complement dysregulation, this can be unmasked by measuring C5b-9 formation on endothelium incubated with serum from unaffected relatives who carry the gene variant. The latter will provide the advantage versus their proband of not having confounding complement-activating factors that are associated with the chronic aHUS status in their circulation. Carriers of variants with pathogenic significance will exhibit higher-than-normal serum-induced C5b-9 formation, whereas carriers of variants with no functional impact will have a negative test result.

Methods

Study participants

Participants were patients with primary aHUS and their available relatives, recruited from those included in the International Registry of Recurrent and Familial Haemolytic Uremic Syndrome/Thrombotic Thrombocytopenic Purpura (HUS/TTP) between 2008 and 2021. The

Registry was established in 1996 at the Aldo e Cele Daccò Clinical Research Center for Rare Diseases (Ranica, Bergamo) (villacamozzi.marionegri.it/seu).

For this retrospective study we analysed all available samples from pedigrees with primary aHUS (n=60) for whom genetic data and serum samples were available, both from the probands and from the relatives. Sixty-six patients who met the inclusion criteria (probands, n=60; affected relatives, n=6) and 157 healthy relatives for a total of 223 subjects were studied. Among the probands, 14 have a familial history of the disease (Figure 1A and Supplementary Table 1).

Patients were studied at different time points: 1) during the acute phase before any treatment (n=16); 2) while in remission, without treatment for >6 months (n=50); 3) in remission under standard eculizumab treatment for the patients (n=4) for whom only samples taken during eculizumab treatment were available. Four patients were studied both during the acute phase and while in remission (Supplementary Table 1). The samples used for this study were stored at Centro Risorse Biologiche (CRB) "Mario Negri", Biobank "Malattie Rare e Malattie Renali".

Diagnosis of HUS was made in patients who have had one or more episodes of microangiopathic haemolytic anaemia and thrombocytopenia, with haematocrit (Ht) <30%, haemoglobin (Hb) <10 g/dL, serum lactate dehydrogenase (LDH) >500 IU/L, undetectable haptoglobin, fragmented erythrocytes in the peripheral blood smear, and platelet count <150,000/µL, associated with acute renal failure (serum creatinine >1.3 mg/dL for adults, >0.5 mg/dL for children below 5 years of age and >0.8 mg/dL for children aged 5-10, and/or urinary protein/creatinine ratio >200 mg/g; or an increase in serum creatinine or the urinary protein/creatinine ratio >15% compared to baseline levels) (11). TTP was ruled out on the basis of ADAMTS13 activity >10% and no anti-ADAMTS13 antibodies.

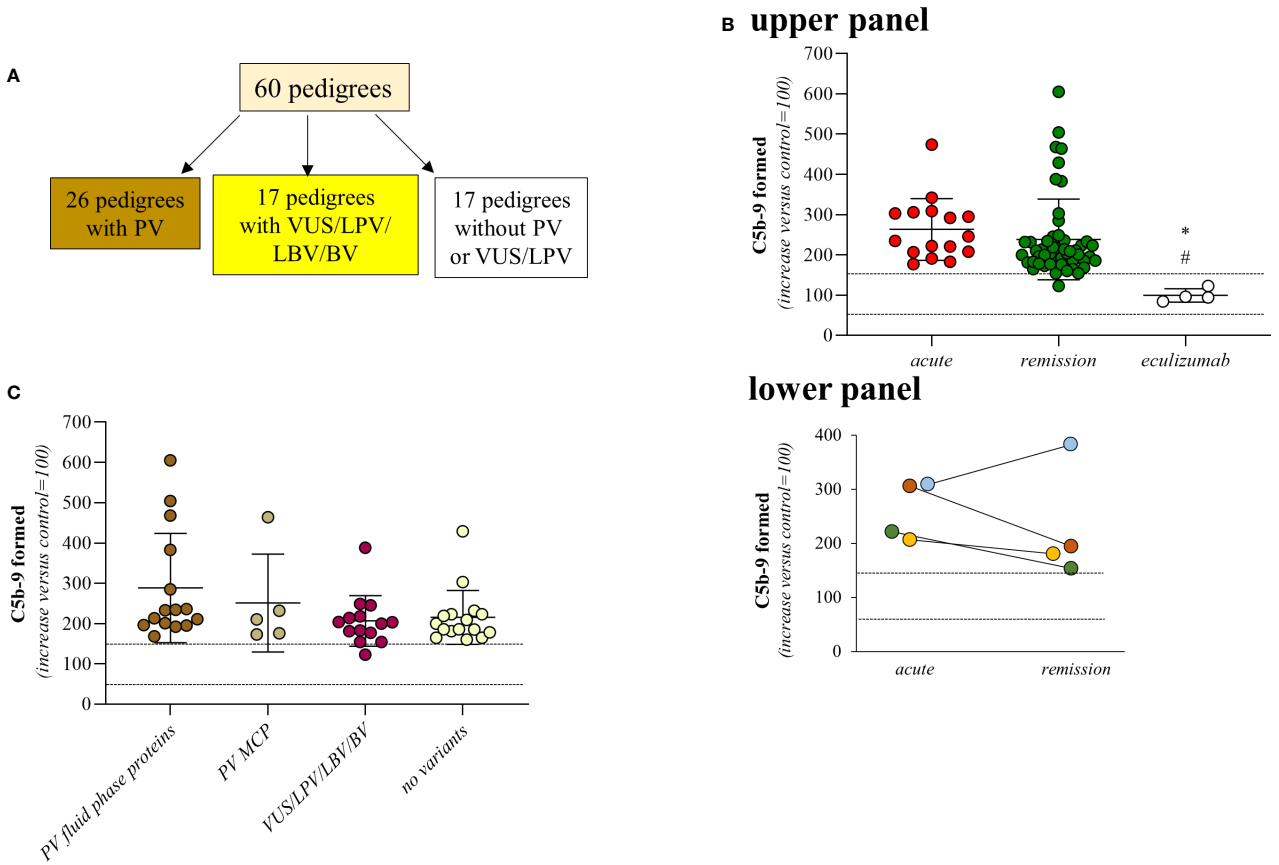

FIGURE 1
Serum from aHUS patients induces higher-than-normal C5b-9 formation on activated HMEC-1. **(A)** Distribution of rare complement gene variants among the 60 pedigrees. **(B)** Upper Panel, Endothelial surface area covered by C5b-9 staining after 2h incubation of ADP-activated HMEC-1 with serum (diluted 1:2 in test medium) from aHUS patients. Serum from aHUS patients was collected during the acute phase of the disease (n=16), or during remission (n=50), or during eculizumab treatment (n=4). Dotted lines are upper and lower limits of normal range. **Lower Panel,** Endothelial surface area covered by C5b-9 staining after 2h incubation of ADP-activated HMEC-1 with serum (diluted 1:2 in test medium) from aHUS patients. Serum from aHUS patients (n=4) was collected both during the acute phase of the disease and during the remission. Dotted lines are upper and lower limits of normal range. **(C)** Endothelial surface area covered by C5b-9 staining after 2h incubation of ADP-activated HMEC-1 with serum (diluted 1:2 in test medium) from aHUS patients who were in remission. aHUS patients were subdivided into carriers of pathogenetic variants (PV) in genes encoding fluid phase complement proteins (n=15), or pathogenetic variants (PV) in the *MCP* gene only (n=5), or VUS/LPV/LBV/BV (n=14) or non-carrier of rare variants (n=16). Dotted lines are upper and lower limits of normal range. The results are shown as the fold increase of stained surface area after incubation with aHUS serum versus control pool of sera run in parallel. Points represent fold increase values of single subjects. Horizontal bars are mean ± SD values. *P<0.01 vs aHUS patients in acute phase, #P<0.05 vs aHUS in remission. PV, pathogenic variant; LPV, likely pathogenic variant; VUS, variant of uncertain significance; LBV/BV, likely benign/benign variant.

Primary aHUS was diagnosed in HUS patients after ruling out both secondary underlying conditions and infections with Stx-*E.Coli*.

Stx-*E.Coli* infection was defined as the presence of *stx* and *eae* genes (by PCR) or Shiga-toxin (Vero cell assay) in the stool and/or antibodies anti Shiga-toxin (ELISA) and/or LPS O157, O26, O111, or O145 (ELISA) in serum. For patients, the Stx-*E.Coli* tests were processed centrally by the Food Safety, Nutrition and Veterinary Public Health Department, Istituto Superiore di Sanità, Rome, Italy.

Secondary aHUS was diagnosed in patients with underlying malignant hypertension, autoimmune diseases, other glomerulopathies, haematopoietic stem cell or solid organ transplantation, and cancer.

Full remission was defined as the normalisation of both haematological parameters (Ht >30% and Hb >10 g/dL and LDH <500 IU/L and platelets >150,000/µL) and renal function (serum creatinine <1.3 mg/dL for adults, <0.5 mg/dL for children below 5 years of age and <0.8 mg/dL for children aged 5-10; urinary protein/creatinine ratio <200 mg/g). Haematological remission in patients was defined as the normalisation of haematological parameters but with renal dysfunction.

The protocol was approved by the Ethical Committee of the Azienda Sanitaria Locale Bergamo, Italy. Participants or their legal guardians provided written informed consent.

Complement genetic abnormalities and anti-CFH autoantibodies

The screening of coding sequences of aHUS-associated genes (*CFH, CFHR1, MCP, CFI, CFB, C3, THBD* and *DGKE*) and candidate genes (*CFHR2, CFHR3, CFHR4, CFHR5*, and *C5*) was performed using amplicon-based next-generation sequencing (12). Rare functional variants (missense, nonsense, indel, or splicing variants) with minor allele frequency (MAF) <0.01 in Genome Aggregation Database (gnomAD, https://gnomad.broadinstitute.org/) were selected. Stop-gain, frameshift and splicing variants, and missense variants with published functional studies, were categorized as pathogenic variants (PV). The other variants were categorized as likely pathogenic (LPV), variants of uncertain significance (VUS), likely benign or benign, using guidelines from the American College of Medical Genetics and Genomics (ACMG) and from the KDIGO conference on aHUS and C3G (5, 13, 14). We also used the Combined Annotation Dependent depletion (CADD) version 1.6, which is a tool for scoring the deleteriousness of single nucleotide variants as well as insertion/deletion variants, which integrates multiple annotations into one metric (https://cadd.gs.washington.edu/info) (14, 15). We selected the PHRED-scaled C-score ranking; variants with CADD scores >10 were defined "potentially pathogenetic". The search for genomic abnormalities that affect *CFH* and *CFHR* genes (16, 17) was undertaken using multiplex ligation-dependent probe amplification as reported (18). We also genotyped the *CFH* single-nucleotide polymorphisms (SNPs) (c.1-331C>T, rs3753394; c.184G>A, p.V62I, rs800292; c.1204C>T, p.H402Y, rs1061170; c.2016A>G, p.Q672Q, rs3753396; c.2237-543G>A, rs1410996; c.2808G>T, p.E936D, rs1065489) that define the disease risk haplotype CFH_{TGTGGT} (known as *CFH*–H3 haplotype) and one SNP in *MCP* (rs7144, c.∗897T>C) that tags the risk MCP_{GGAAC} haplotype (11, 19–21). Anti-FH autoantibodies were measured in plasma using ELISA (22).

Serum-induced C5b-9 deposition on HMEC-1

The assay was performed as described previously (6, 10), with minor modifications. The human microvascular endothelial cells (HMEC-1 cell line) were a gift from Dr Edwin Ades and Francisco J. Candal of CDC and Dr Thomas Lawley of Emory University, Atlanta, GA. As growth medium we used MCDB 131 (Gibco, Grand Island, NY) supplemented with 10% foetal bovine serum (Gibco), 10 µg/mL hydrocortisone, 100 U/mL penicillin, 100 µg/mL streptomycin, 2 mM glutamine (Gibco), and 50 µg/mL endothelial cell growth factor. For each experiment the procedure was standardized by plating the same number of cells (75.000) that were cultured for 96 hours and left in serum-free medium for 24 hours. Thereafter the integrity and confluence of the cell monolayer was checked at phase-contrast microscope. If a slide did not full-fill the criteria, it was discarded. Cells were washed 3 times with test medium (HBSS: 137 mM NaCl, 5.4 mM KCl, 0.7 mM Na_2HPO_4, 0.73 mM KH_2PO_4, 1.9 mM $CaCl_2$, 0.8 mM $MgSO_4$, 28 mM Trizma base pH 7.3, 0.1% dextrose; with 0.5% BSA) and activated with 10 µM ADP (Sigma) for 10 minutes. Thereafter cells were exposed for 2 hours to serum from patients or healthy relatives or healthy controls, 50% in test medium (HBSS with 0.5% BSA). HMEC-1 were then fixed in 3% paraformaldehyde, blocked with PBS with 2% BSA and stained with rabbit anti-human complement C5b-9 complex antibody (Calbiochem, catalog number 204903, 1h at room temperature, 1/200 final dilution) followed by FITC-conjugated secondary antibody (Jackson Immuno Research Laboratories, catalog number 111-095-144, 1h at room temperature, 1/50 final dilution). We have previously validated the rabbit anti-human C5b-9 antibody using the mouse monoclonal anti-human C9 antibody (W13-15, Hycult Biotech, 1h at room temperature, 1/50 final dilution) that recognizes human C9 neoantigen. Results of C5b-9 formation on ADP-activated HMEC-1 exposed to aHUS serum with the rabbit anti-human C5b-9 were comparable to those with the anti-human C9 antibody (23).

Sera from 10 different healthy blood donors were pooled and the pool was run in each experiment as a reference (100%) for C5b-9 staining. We also analysed single sera from additional controls (n=35), tested separately as independent samples. The 35 donors did not overlap with the 10 donors of the pool. For each of them we calculated the percentages of C5b-9 deposits vs. control serum pool to set the normal range (mean ± 2SD of the percentage of C5b-9 deposits of the single control sera vs. control serum pool: ADP-activated HMEC-1, 60-149%) (Supplementary Figure 1).

In addition, in each experiment, we added the serum from an aHUS patient that had shown a strong positivity on ADP-activated HMEC-1 in previous experiments, as positive control. As negative control, in random experiments we added sCR1 (an inhibitor of the classical, alternative and lectin pathway of complement activation, 150 µg/ml, R&D System) to the tested serum (Supplementary Figure 2).

We verified the integrity of the cell monolayer after exposure to serum samples in parallel slides in which cells were stained with May-Grunwald Giemsa.

The fluorescent staining on the endothelial cell surface was acquired using the Apotome Axio Imager Z2 (Zeiss) microscope. Fifteen fields, which were systematically digitised along the surface

were acquired using a computer-based image analysis system. The nuclear staining with DAPI (4',6-diamidino-2-phenylindole, Sigma-Aldrich) was used as guide to determine if a fluorescent area was on HMEC-1 surface. The operator discarded the fields where cell confluence was missing. The exposure time was constant. The area occupied by the fluorescent staining was evaluated with automatic edge detection using the built-in specific functions of the software Image J (NIH, Bethesda, MD), and calculated as pixel^2 per field analysed (10). For each sample, 15 fields were analysed; the highest and the lowest values were discarded and the mean of pixel^2 the other 13 fields was calculated. We expressed the results as the percentage of the staining compared to the pixel^2 of the control serum pool (used as denominator), run in parallel (10). All the images were acquired, and the staining was calculated by the same operator (S.G.), who during the analysis was blinded about the nature of the samples. The results were confirmed by a second blinded operator (M.G.).

We previously documented (10) the good reproducibility of the assay at the concordance correlation test, by testing twice in different experiments the samples from several patients (10). As further check of good reproducibility of the assay, in the present study we performed biological replicates by analysing samples collected at 2 different time points in remission from 6 aHUS patients. As shown in Supplementary Figure 3, elevated C5b-9 formation on activated endothelial cells was confirmed in biological replicates.

Serum C3 and plasma sC5b-9 evaluation

For patients from which enough samples were available, we evaluated serum C3 and plasma sC5b-9 levels. Complement C3 was measured in serum by nephelometry. Normal ranges (defined as mean ± 2SD) for C3: 83-180 mg/dL, n=50. SC5b-9 levels were evaluated in EDTA plasma by MicroVue sC5b-9 Plus EIA (SC5b-9 Plus; Quidel). Normal range of plasma sC5b-9 in our laboratory: 127-400 ng/mL; n=50.

Statistical analysis

Comparisons of groups were performed with one-way analysis of variance (ANOVA).

Sensitivity of serum-induced C5b-9 formation (positive test: staining in pixel^2 significantly higher in the test sample than in the control sample, run in parallel) was calculated as: number of test samples with positive test/samples with positive results + false negatives.

The GraphPad Prism 8.3.0 software was used for statistical analysis unless otherwise stated. P values of less than 0.05 were considered to be statistically significant.

Results

Serum from aHUS patients caused higher-than-normal C5b-9 formation on activated endothelial cells

A total of 66 patients with primary aHUS from 60 pedigrees (60 probands and 6 affected relatives Figure 1A) were analysed with the serum-induced C5b-9 formation test on ADP-activated HMEC-1. Consistent with previously published data (6, 10), sera from all patients with acute aHUS studied before therapy (plasma or eculizumab) (n=16) and sera from all but one patient studied while in remission without therapy for >6 months (n=50), induced higher-than-normal (263 ± 77%, and 238 ± 101%, respectively, >149% of normal human serum pool) C5b-9 formation on ADP-activated HMEC-1 (Figure 1B, upper panel). As shown in Figure 1B lower panel, results obtained with serum from patients studied both during acute phase and in remission (n=4) showed similarly elevated C5b-9 formation on activated endothelial cells.

In agreement with our previous work (10), only a fraction of patients showed circulating markers of complement activation, such as reduced serum C3 and increased plasma sC5b-9, both during the acute phase (reduced C3: 10/16; increased sC5b-9: 3/6) or during remission (reduced C3: 20/47; increased sC5b-9: 6/14) (Supplementary Table 1). These results are in line with the cell surface restricted complement activation that characterizes aHUS. Of note, no correlations were found between C3 serum levels and C5b-9 formation on HMEC-1 (Spearman's coefficient of rank correlation: P=0.2095), and between sC5b-9 levels and C5b-9 formation on HMEC-1 (Spearman's coefficient of rank correlation: P=0.2750).

C5b-9 formation on endothelial cells exposed to sera from the four aHUS patients on eculizumab treatment was in the control range (99 ± 17%) (Figure 1B, upper panel).

We then divided the 50 patients who were in remission and out of treatment, on the basis of their genetic background. We did not observe any significant difference in serum-induced C5b-9 formation among the following subgroups: 1) patients with known rare pathogenic variants (PV) that affect fluid phase proteins (288 ± 136%, n=15); 2) patients with only PV that affect the cell surface protein MCP (251 ± 122%, n=5); 3) patients with variants of uncertain significance/likely pathogenic/likely benign/benign variants (VUS/LPV/LBV/BV) (207 ± 63%, n=14); 4) patients without identified genetic or acquired complement abnormalities (215 ± 67%, n=16) (Figure 1C; Tables 1, 2A). None of the studied patients had anti-FH antibodies.

Four out of 5 patients in remission with only *MCP* PVs also had one or two risk haplotypes in circulating complement factors, such as *CFH* (H3) and or *CFHR1**B (Supplementary Table 1), which could contribute to complement dysregulation (20, 24).

Altogether, the above findings show that the test for C5b-9 formation on ADP-activated HMEC-1 with aHUS serum cannot provide enough information about the impact (if any) of the underlying genetic abnormalities on complement dysregulation on the cell surface.

Serum from unaffected relative carriers of complement pathogenic variants induces C5b-9 formation on activated endothelial cells

Among the 26 pedigrees with PV, we identified 14 PV in genes that encode circulating complement proteins or regulators (*CFH*, n=7; *CFI*, n=1; *C3*, n=1; *CFHR1/CFH* gene conversion, n=1; hybrid

10.3389/fimmu.2023.1112257

TABLE 1 List of known rare pathogenic variants (PV) identified in aHUS patients.

family code	gene	nucleotide change	aminoacid change	variant effect	gnomAD frequency	classification	Dam/ Pred	CADD (versione1.3)	references (Doi)
#020, #856	*CFH*	c.3628C>T	p.R1210C	missense	0.0001451	pathogenic	1/11	11.77	10.1086/344515
#101	*CFH*	c.232A>G	p.R78G	missense	–	pathogenic	6/11	15.77	10.1074/ jbc.M110.211839
#267, #120, #265	*CFH*	c.3572C>T	p.S1191L	missense	–	pathogenic	4/11	18.67	10.1002/humu.9408
#45	*CFH*	c.3547T>A	p.W1183R	missense	–	pathogenic	–	23.9	10.1086/344515
#251	*CFH*	c.3572C>T + c.3590T>C	p.S1191L + p.V1197A	*CFH/ CFHR1* gene conversion	- 0.0000071	pathogenic	4/11- 7/11	18.67-19.52	10.1002/humu.9408
#52, #210	*CFH*	c.3590T>C	p.V1197A	missense	0.0000071	pathogenic	7/11	19.52	10.1002/humu.9408
#603, #81	*CFH*	c.3514G>T	p.E1172X	stop gained	0.000012	pathogenic	–	39	10.1172/JCI16651
#390	*CFH*	c.3493+1G>A	–	splice donor	0.000004	pathogenic	2/2	23.6	10.1016/ j.kint.2017.07.015
#192	*CFI*	c.1446_1450delTTCAC	p.L484Vfs3X	frameshift	0.0000279	pathogenic	–	27.9	10.1016/ j.molimm.2007.05.004
#563, #158	*C3*	c.1774C>T	p.R592W	missense	0.000004	pathogenic	7/12	34	10.4049/ jimmunol.1701695; 10.1182/blood-2008-01-133702
#380, #551	*CFHR1/ CFH hybrid*	reverse hybrid *CFHR1 1-5 – CFH 23*	–	hybrid	–	pathogenic	–	–	10.1681/ ASN.2013121339
#1245	*CFHR1/ CFH hybrid*	reverse hybrid *CFHR1 1-4 – CFH 22-23*	–	hybrid	–	pathogenic	–	–	10.1681/ ASN.2017050518
#316	*CFHR1*	c.869T>C + c.887C>T	p.L290S + p.A296V	*CFHR1/ CFH* gene conversion	0.0000264 – 0.000034	pathogenic	0/11	0.002 – 0.392	10.1681/ ASN.2017050518
#176	*CFH/ CFHR1 hybrid*	hybrid *CFH 1-21 – CFHR1 5-6*	–	hybrid	–	pathogenic	–	–	10.1002/humu.9408
#1065 #646, #782	*MCP*	c.286+2T>G	–	splice donor	0.0000521	pathogenic	2/2	14.54	10.1016/ j.molimm.2006.07.004
#458	*MCP*	c.760delT + c.770_772delATA	p.F254Lfs43X	frameshift	–	pathogenic	–	27.6	–
#192	*MCP*	c.287-2A>G	–	splice acceptor	0.0000251	pathogenic	2/2	20.1	10.1182/blood-2005-10-007252
#2816	*MCP*	c.282dupT	p.Y95Lfs2X	frameshift	–	pathogenic	0/0	23.3	–

genes n=3, *CFH/CFHR1* gene conversion n=1, Tables 1, 3) (25, 26). To evaluate the sensitivity of the ex vivo endothelial test to identify subjects carrying functional complement gene variants, we analysed serum from 41 healthy relatives who carried (from here on, unaffected relative carriers) the above PV, used as positive controls. Thirty-eight out of 41 carriers exhibited a higher-than-normal range (>149% of normal human serum pool) of serum-induced C5b-9 formation on ADP-activated HMEC-1 (208 ± 70%, n=41; Figure 2A) resulting in 92.7% sensitivity to identify carriers of a PV. In the same pedigrees, we were able to analyse 28 relatives who do not carry the above PV, who were used as negative controls. Serum from all of these subjects induced normal C5b-9 formation on endothelial cells (healthy relatives non-carrier of PV, 102 ± 20%, n=28; Figure 2A). We repeated the assay with serum from a subgroup of unaffected carriers (PV, n=3) or non-carriers (n=7) on unstimulated HMEC-1, and results showed normal C5b-9 formation with all sera

TABLE 2A List of rare likely pathogenetic variants (LPV), variants of uncertain significance (VUS) and benign and likely benign variants in genes encoding soluble proteins and identified in aHUS patients.

family code	gene	nucleotide change	aminoacid change	variant effect	gnomAD frequency	Dam/Pred n*	CADD	classification	references (Doi)
#2880^	***CFH***	**c.2957-7A>G**	**-**	**intronic/ splice region**	**0.0002**	**0/0**	**0.267**	**likely benign**	**-**
#155	***CFH***	**c.2908A>G**	**p.I970V**	**missense**	**0.00000796**	**1/3**	**0.010**	**VUS°**	**10.1182/blood-2005-10-007252; 10.4049/jimmunol.1701695**
#194	***CFH***	**c.3544_3545insGGTGGACAGCCAAACAGAAGCTTTATTCGAGAACAG**	**p.R1182delinsRWTAKQKLYSRTG**	**insertion**	**-**	**0/0**	**-**	**LPV**	**-**
#2813	***CFH***	**c.127C>A**	**p.P43T**	**missense**	**0.00000398**	**3/11**	**20.9**	**VUS**	**-**
#390	***CFH***	**c.1548T>A**	**p.N516K**	**missense**	**0.0003049**	**8/11**	**16.62**	**VUS°**	**10.4049/jimmunol.1701695; 10.1111/j.1600-6143.2008.02297.x; 10.1182/blood.2021012037**
#181	***CFH***	**c.2686_2700delAAATTGAGTTATACT**	**p.896_900delKLSYT**	**deletion**	**-**	**-**	**16.8**	**LPV°**	**10.4049/jimmunol.1701695**
#52	***CFH***	**c.2932T>C**	**p.W978R**	**missense**	**-**	**11/11**	**25.6**	**LPV**	**-**
#736	***CFH***	**c.2171C>A**	**p.T724K**	**missense**	**0.00009201**	**6/11**	**24.1**	**VUS**	**-**
#265	*CFI*	c.1661A>T	p.E554V	missense	0.00001415	4/4	25.4	VUS°	10.1681/ASN.2012090884; 10.2215/CJN.02210310; 10.1093/hmg/ddv091; 10.4049/jimmunol.1701695
#646	*CFI*	c.1322A>G	p.K441R	missense	0.003575	2/12	0.002	likely benign°	10.4049/jimmunol.1701695
#593	***CFI***	**c.560G>A**	**p.R187Q**	**missense**	**0.00007780**	**2/12**	**17.91**	**VUS°**	**10.4049/jimmunol.1701695**
#380	*C3*	c.2284G>A	p.V762I	missense	0.00001193	0/12	0.254	VUS	10.2215/CJN.02210310
#2169	***C3***	**c.181G>A**	**p.D61N**	**missense**	**0.00001988**	**6/12**	**19.03**	**LPV**	**-**
#2880^	***C3***	**c.962G>T**	**p.G321V**	**missense**	**-**	**8/12**	**26.3**	**LPV**	**-**
#1485^	***C3***	**c.74+1delG**	**-**	**intronic/ splice region**	**-**	**0/0**	**23.6**	**VUS**	**-**
#1077	***C3***	**c.1898A>G**	**p.K633R**	**missense**	**0.0004565**	**1/12**	**0.043**	**VUS°**	**10.4049/jimmunol.1701695; 10.1182/blood-2009-05-221549**
#4	***C3***	**c.485C>G**	**p.T162R**	**missense**	**-**	**4/12**	**14.34**	**VUS°**	**10.4049/jimmunol.1701695; 10.2215/CJN.02210310**
#856	*CFB*	c.1778+8C>T	-	intronic/ splice region	0.00005677	0/0	7.153	VUS°	10.4049/jimmunol.1701695

(Continued)

10.3389/fimmu.2023.1112257

TABLE 2A Continued

family code	gene	nucleotide change	aminoacid change	variant effect	gnomAD frequency	Dam/ Pred n*	CADD	classification	references (Doi)
#1485^	***CFB***	**c.1018A>T**	**p.N340Y**	**missense**	**-**	**6/12**	**13.56**	**VUS**	**-**
#267, #623	***C5***	**c.1060C>A**	**p.L354M**	**missense**	**0.005561**	**6/11**	**25**	**benign+**	**-**
#2071	***C5***	**c.4924T>G**	**p.L1642V**	**missense**	**0.00006765**	**0/12**	**14.44**	**VUS+**	**-**
#1683	*C5*	c.3029C>T	p.A1010V	missense	0.0007	5/12	23.9	VUS	-
#412^	***CFHR2***	**c.325A>G**	**p.T109A**	**missense**	**0.0058**	**3/11**	**14.5**	**benign**	**-**
#20	***CFHR4***	**c.758delG**	**p.C253Lfs15X**	**frameshift**	**-**	**-**	**25.0**	**VUS**	**-**
#1279	***CFHR4***	**CFHR1-CFHR4 duplication**	**-**	**-**	**-**	**-**	**-**	**VUS**	**10.1159/000497823**
#101	*CFHR4*	c.799+3A>C	-	intronic/ splice region	0.00098	0/0	2.578	likely benign	-
#1494	***CFHR4***	**c.1058T>A**	**p.I106N**	**-**	**-**	**-**	**12.97**	**VUS**	**-**
#563	*CFHR4*	c.1207A>T	p.N156Y	missense	-	-	22.7	VUS	-
#267	*CFHR5*	c.1412G>A	p.G471E	missense	0.0006083	6/11	22.3	VUS	10.4049/jimmunol.1701695
#412^	***CFHR5***	**c.485_486dupAA**	**p.E163Kfs10X**	**frameshift**	**0.0063**	**0/0**	**22.7**	**LPV°**	**-**

° databases of complement gene mutation (https://www.complement-db.org/home.php).
* Dam/Pre n: number of damaging predictions/total number of predictions. Variants carried by at least one unaffected relative are in bold characters.
^ Pedigrees with combined variants.
+: ClinVar; https://www.ncbi.nlm.nih.gov/clinvar.

TABLE 2B List of rare complement gene variants identified in unaffected aHUS relatives but not in probands.

family code	gene	nucleotidechange	aminoacidchange	varianteffect	gnomAD allele frequency	CADD	*references (Doi)*
#623	*CFI*	c.1044+9G>A	–	intronic/spliceregion	0.00001989	2.153	-
#1650	*CFI*	c.1642G>C	p.E548Q	missense	0.0008207	29.1	10.4049/jimmumol.1701695°
#155	*CFB*	c.1037-10C>G	-	intronicregion	0.00073	7.632	-
#603	*CFB*	c.1270+6T>C	-	intronicregion/spliceregion	-	15.8	-
#623	*C5*	c.130G>T	p.Y44D	missense	-	24.4	-
#265	*CFHR2*	c.212C>T	p.T71M	missense	0.00398	18.04	
#1998	*CFHR4*	c.643C>G	p.P215A	missense	-	12.83	-

° database of complement gene mutation (https://www.complement-db.org/home.php).

10.3389/fimmu.2023.1112257

10.3389/fimmu.2023.1112257

TABLE 3 Results of C5b-9 test in unaffected family members who carry PV in genes encoding fluid phase proteins that segregate with the disease.

gene	nucleotide change	aminoacid change	C5b-9 formed *(% increase versus control=100)*	n° carriers positive C5b-9 test *(>149%)*
CFH	c.3628C>T	p.R1210C	171%	6/7
			281%	
			144%	
			175%	
			454%	
			204%	
			186%	
CFH	c.232A>G	p.R78G	199%	2/2
			240%	
CFH	c.3572C>T	p.S1191L	284%	10/10
			478%	
			201%	
			155%	
			168%	
			151%	
			168%	
			187%	
			167%	
			196%	
CFH	reverse hybrid *CFHR1* $_{1\text{-}5}$ – *CFH*$_{23}$	Hybrid	208%	2/2
			216%	
CFH	hybrid *CFH* $_{1\text{-}21}$ – *CFH*$_{5\text{-}6}$	Hybrid	184%	1/1
CFH	reverse hybrid *CFHR1* $_{1\text{-}4}$ – *CFH*$_{22\text{-}23}$	Hybrid	307%	2/3
			166%	
			143%	
CFH	c.3547T>C	p.W1183R	157%	1/1
CFH	c.3514G>T	p.E1172X	209%	2/2
			252%	
CFH	c.3590T>C	p.V1197A	205%	3/3
			167%	
			217%	
CFH	c.3493+1G>A	–	194%	1/1
CFH	*CFH/CFHR1* gene conversion c.3572C>T + c.3590T/C*	p.S1191L + p.V1197A	216%	1/1
CFI	c.1446_1450delTTCAC	p.L484Vfs3X	190%	1/1
C3	c.1774C>T	p.R592W	155%	5/6
			148%	
			237%	
			151%	

(Continued)

10.3389/fimmu.2023.1112257

TABLE 3 Continued

gene	nucleotide change	aminoacid change	C5b-9 formed *(% increase versus control=100)*	n° carriers positive C5b-9 test *(>149%)*
			223%	
			207%	
CFHR1	*CFHR1/CFH* gene conversion c.869T>C + c.887C>T	p.L290S + p.A296V	189%	1/1
Overall				38/41

* doi: 10.1002/humu.9408.

(Supplementary Figure 4), confirming that the ex vivo assay can reproduce the "two hit" model of aHUS.

Results for 2 representative pedigrees are shown in Figure 2B (#267) and Figure 2C (#1245). The detailed clinical and family history of the 2 pedigrees are reported in the Supplementary Material.

In contrast, all but one unaffected relative carriers of PV only in the surface complement regulator MCP exhibited C5b-9 formation on ADP-activated HMEC-1 in the normal range (114 ± 27%, n=8 from 6 pedigrees) (Figure 2A and Table 4). Notably, the only unaffected MCP carrier showing higher than normal serum-

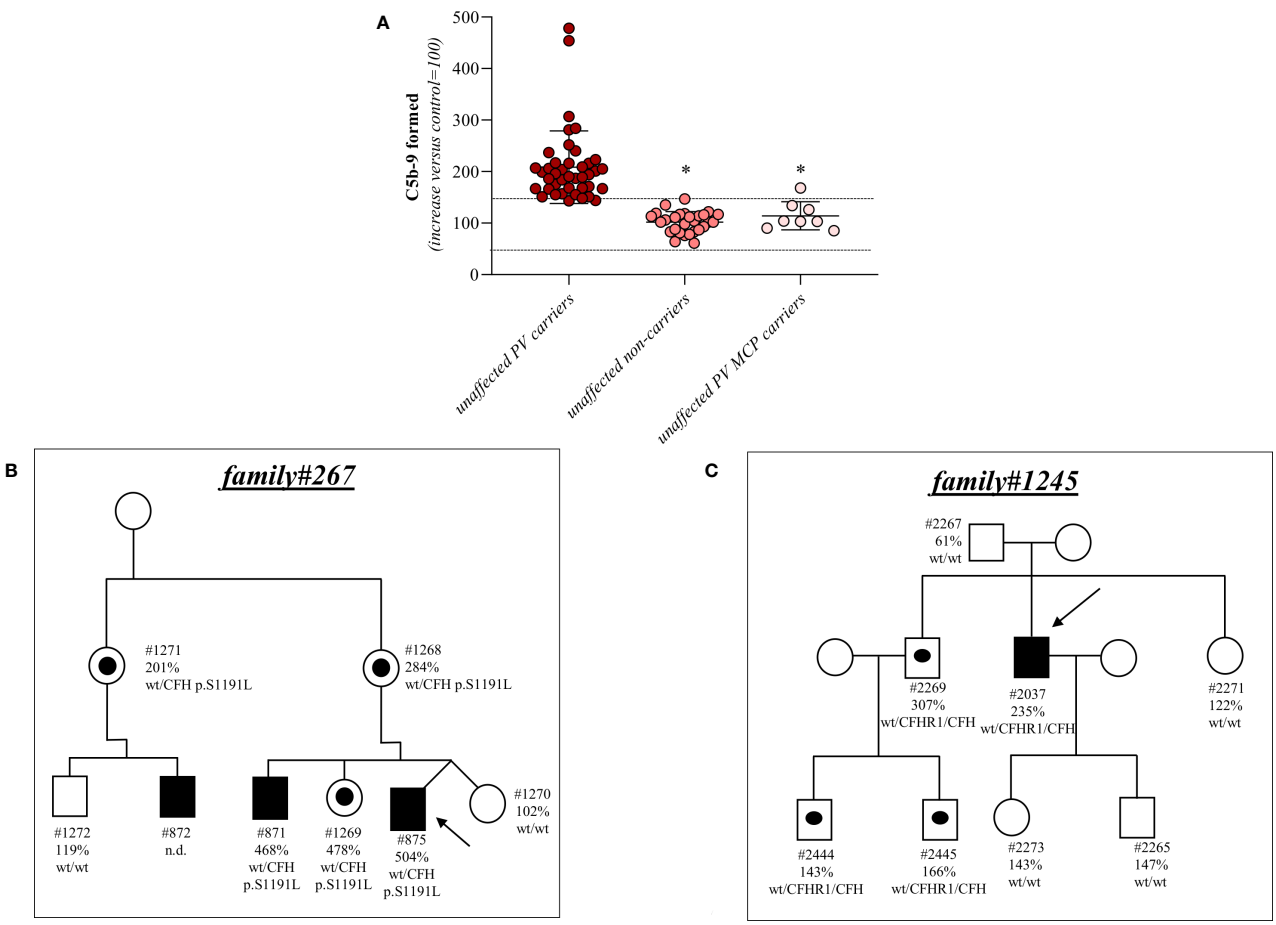

FIGURE 2
Serum from unaffected relative carriers of PV induces higher than normal C5b-9 formation on HMEC-1. **(A)** Endothelial surface area covered by C5b-9 staining after 2h incubation of ADP-activated HMEC-1 with serum (diluted 1:2 in test medium) from either unaffected carriers of PV in genes encoding for fluid phase complement proteins (n=41), or from unaffected non-carriers of PV (n=28) or from unaffected carriers of PV in the *MCP* gene only (n=8). The results are shown as the fold increase of stained surface area after incubation with serum from unaffected carriers versus control pool of sera run in parallel. Points represent fold increase values of single subjects. Horizontal bars are mean ± SD values. Dotted lines are upper and lower limits of normal range. *P<0.0001 vs. unaffected carriers of PV. **(B)** Pedigree #267 of aHUS proband #875 (indicated by the arrow) with a PV in CFH p.S1191L. The same PV was found in his brother (affected, #871), his mother (#1268), his sister (#1269), his uncle (#1271) and his cousin (affected, #872). **(C)** Pedigree #1245 of aHUS proband #2037 (indicated by the arrow) with a pathogenic *CFHR1/CFH* hybrid gene ($CFHR1_{1-4}$-CFH_{22-23}). The same hybrid was also found in his brother (#2269) and his nephews (#2444 and #2445). In each pedigree, the affected subjects are in black, healthy carriers of PV are identified with a black dot. The circles indicate females and the squares indicate males.

induced C5b-9 formation also had the H3 haplotype, indicating a possible contribution of this haplotype in complement dysregulation, as we observed in affected MCP carriers.

Serum-induced C5b-9 formation test in unaffected carriers helps with the functional characterisation of gene variants

Based on the results of the serum-induced C5b-9 formation test that we found with the carriers of PV, we used the same approach to characterise rare variants predicted to be LPV or VUS, or likely benign or benign in silico. In the probands from 28 pedigrees, we identified 30 rare variants – classified as LPV, VUS, likely benign, or benign – in aHUS-associated genes that encode soluble proteins (*CFH, CFI, C3, CFB* and *CFHR1*, Table 2A) or in candidate complement genes (*C5, CFHR2, CFHR4* and *CFHR5*, Table 2A). For 22 variants we found at least one unaffected carrier relative, for a total of 27 relatives.

We found excessive C5b-9 formation on ADP-activated HMEC-1 in 18 of 27 relatives, indicating that they may have a genetic liability to complement dysregulation on the cell surface (Figure 3A; Table 5).

Specifically, the test was positive in 7 out of 8 (87.5%), 10 out of 16 (62.5%), 1 out of 1 and 0 out of 2 subjects with LPV, VUS, likely benign or benign variants, respectively. Notably, among subjects with VUS, all the 6 that exhibited a negative C5b-9 test had variants only in putative candidate genes (*C5* and *CFHR4*). As observed with carriers of PV, when the assay with sera from unaffected carriers of LPV/VUS was repeated on unstimulated HMEC-1 (n=7), results showed normal C5b-9 formation for all subjects (Supplementary Figure 4).

Finally, in a few pedigrees with carriers of LPV (n=3) or VUS (n=4) that showed a positive test we could analyse sera from at least one non-carrier relative (Supplementary Table 2), all of which formed normal amount of C5b-9 on activated HMEC-1. To summarise, the results showed that all but one variants in aHUS-associated genes that were predicted in silico to be LPV, or VUS as well as a likely benign variant, were experimentally shown to be pathogenic. At variance, variants in putative candidate genes did not exhibit a functional effect in the C5b-9 test, with the only exception of a LPV in the *CFHR5* gene that showed a positive test (Figure 3A).

We further predicted variant pathogenicity computationally using CADD, adjusting the CADD score threshold for pathogenicity to >10. As shown in Figure 3B, 10 of 14 variants in disease-associated genes exhibited concordance between CADD and the results of the C5b-9 test, in contrast with only 1 of 6 variants in putative candidate genes (Figure 3C).

Among the 60 studied pedigrees we identified 7 rare variants that did not segregate with the disease (Table 2B), since they were present in unaffected relatives (n=10) but not in the probands. The C5b-9 test was negative in all of these subjects (Figure 3D), independently of their classification and CADD values (Table 6), supporting the potential of the test to differentiate between variants that do or do not have functional consequences on complement activation on the cell surface.

Finally, in 6 pedigrees the probands exhibited combined PV/LPV (family #52, Figure 4), or PV/VUS (family #390, and family #265, Figure 4), or combined VUS (family #1485, Figure 4), or combined LPV/likely benign variants (family #2880, Figure 4) or combined LPV/benign variants (family #412, Figure 4). The test was positive in unaffected carriers of the PV *CFH* p.V1197A and *CFH* c.3493+1G>A (Figure 4). The results of the C5b-9 test in unaffected carrier relatives indicated a functional pathogenic role for the *CFH* p.W978R LPV (CADD 25.6), the *CFH* p.N516K VUS (CADD 16.62), the *C3* c.74 +1delG>- VUS (CADD 23.6), the *CFB* p.N340Y VUS (CADD 13.6), the *CFH* c.2957-7A>G likely benign (CADD 26.3) and the *CFHR5* p.E163Kfs10x LPV (CADD 22.7) (Figure 4). As for the *CFI* p.E554V VUS (CADD 25.4) in pedigree #265, the test was non-informative because we did not find an unaffected relative who carried this variant alone. However, it is likely non-functional since it did not segregate with the disease in this family because it was present in only one of the two affected subjects (Figure 4). The detailed clinical and family histories of the 6 pedigrees are reported in the Supplementary Material.

Serum-induced C5b-9 formation test in trios of patients without variants in known genes may identify new genetic forms of aHUS

In 17 pedigrees we did not identify rare variants in disease-associated or candidate complement genes in the probands. To

TABLE 4 Results of C5b-9 test in unaffected family members who carry PV in MCP segregating with the disease.

gene	nucleotide change	aminoacid change	C5b-9 formed *(% increase versus control=100)*	n° carriers positive C5b-9 test *(>149%)*
MCP	c.286+2T>G	-	85%	0/5
			90%	
			104%	
			103%	
			103%	
MCP	c.760delT	-	134%	0/1
MCP	c.282dupT	p.Y95Lfs2X	168%	1/1
MCP	c.287-2A>G	-	126%	0/1
Overall				1/8

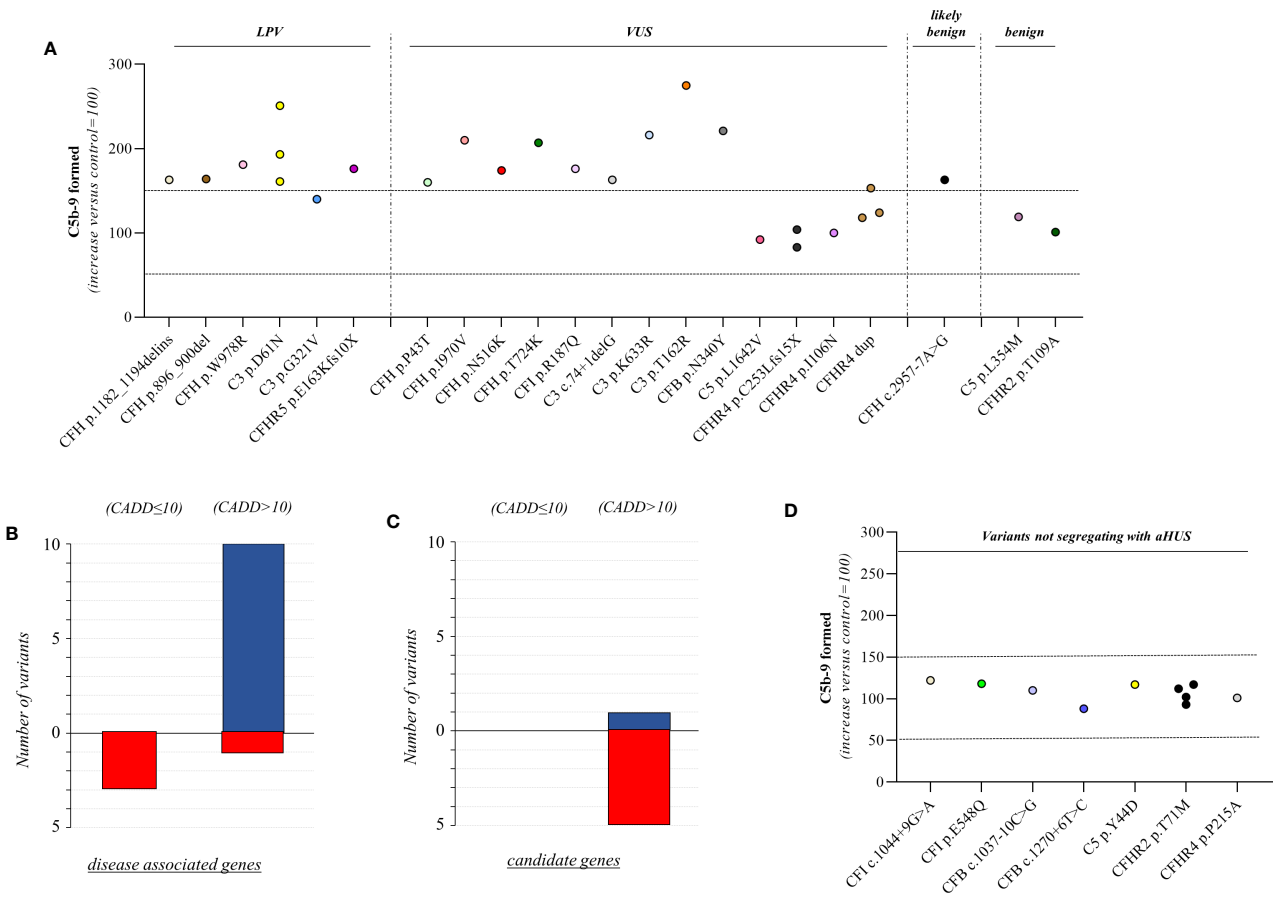

FIGURE 3
C5b-9 formation on HMEC-1 exposed to serum from unaffected relative carriers of rare complement gene variants. **(A)** Endothelial surface area covered by C5b-9 staining after 2h incubation of ADP-activated HMEC-1 with serum (diluted 1:2 in test medium) from carriers of variants likely pathogenic (LPV, n=8), of uncertain significance (VUS, n=16), likely benign (n=1), or benign (n=2). Results are shown as fold increase of stained surface area after incubation with serum from unaffected carriers versus control pool of sera run in parallel. Points represent fold increase values for single subjects. Dotted lines are upper and lower limits of normal range. **(B)** Breakdown of CADD computational predictions using a default score value cutoff >10 in disease-associated genes. (CADD ≤ 10: benign prediction; CADD > 10: pathogenic prediction) **(C)** Breakdown of CADD computational predictions using a default score value cutoff >10 in candidate genes. Red columns indicate variants with incorrect prediction; Blue columns indicate variants with correct predictions. **(D)** Endothelial surface area covered by C5b-9 staining after 2h incubation of ADP-activated HMEC-1 with serum (diluted 1:2 in test medium) from carriers of rare variants that do not segregate with aHUS (n=10). Results are shown as fold increase of stained surface area after incubation with serum from carriers of rare variants not segregating with aHUS versus control pool of sera run in parallel. Points represent fold increase values of single subjects. Dotted lines are upper and lower limits of normal range.

evaluate whether any of the above probands had inherited, from the unaffected parent, an unknown genetic abnormality predisposing to complement activation on the endothelial surface, we analysed C5b-9 formation in the probands and their parents (trios).

In 8 trios we found higher-than-normal range serum-induced C5b-9 formation, both in the probands (remission, n=8) and in their fathers (proband: 194 ± 26%; father: 197 ± 60%, Figure 5A). In contrast, the serum samples from the mothers caused normal C5b-9 formation on endothelial cells (117 ± 19%, Figure 5A). These results suggest that the probands inherited a genetic defect from the father. A representative trio is shown in Figure 5D (see clinical history in Supplementary Material).

In 4 trios the sera from both the probands (remission, n=3; acute, n=1) and their mothers induced excessive C5b-9 formation on HMEC-1 (patient: 229 ± 51%; mother: 181 ± 22%; Figure 5B) indicating a genetic abnormality inherited from the mother. Consistent with this, in these trios the serum from the fathers induced normal C5b-9 formation on endothelial cells (94 ± 19%; Figure 5B). A representative trio is shown in Figure 5E (see clinical history in Supplementary Material).

Finally, in 5 trios both parents exhibited normal C5b-9 formation on ADP-activated HMEC-1, whereas the test was positive in all probands (remission, n=5) (patient: 237 ± 110%; father: 116 ± 15%; mother: 134 ± 12%, Figure 5C). For these trios, the results of the test did not allow us to determine whether the disease was associated with a *de novo* genetic abnormality, a recessive inheritance, or whether it was not genetically determined.

Discussion

By studying 223 subjects who belong to 60 aHUS pedigrees, here we show that the ex vivo assay based on serum-induced C5b-9 formation on activated HMEC-1 may represent a potential tool for a rapid evaluation of the functional impact of rare complement gene variants. In addition, we provide evidence that this assay could also be

TABLE 5 Results of C5b-9 formation test in family members who carry VUS/LPV/LBV or benign variants.

gene	nucleotide change	aminoacid change	classification	gnomAD frequency	CADD	C5b-9 formed *(% increase vs control=100)*	n° carriers positive C5b-9 test *(>149%)*
CFH	c.127C>A	p.P43T	VUS	0.000003983	20.9	160%	1/1
CFH	c.2957-7A>G	-	likely benign	0.0002	0.267	163%	1/1
CFH	c.2908A>G	p.I970V	VUS	0.000007955	0.010	210%	1/1
CFH	c.3544_3545insGGTGGACAGCCAAACAGAAGCTTTATTCGAGAACAG	p.R1182delinsRWTAKQKLYSRTG	LPV	-	0.006	163%	1/1
CFH	c.1548T>A	p.N516K	VUS	0.0003049	16.62	174%	1/1
CFH	c.2686_2700delAAATTGAGTTATACT	p.896_900delKLSYT	LPV	-	16.80	164%	1/1
CFH	c.2932T>C	p.W978R	LPV	-	25.6	181%	1/1
CFH	c.2171C>A	p.T724K	VUS	0.00009201	24.1	207%	1/1
CFI	c.560G>A	p.R187Q	VUS	0.00007780	17.91	176%	1/1
C3	c.181G>A	p.D61N	LPV	0.00001988	19.03	161% 251% 193%	3/3
C3	c.962C>T	p.G321V	LPV	-	26.3	140%	0/1
C3	c.74+1delG	-	VUS	-	23.6	163%	1/1
C3	c.1898A>G	p.K633R	VUS	0.0004565	0.043	216%	1/1
C3	c.485C>G	p.T162R	VUS	-	14.34	275%	1/1
CFB	c.1018A>T	p.N340Y	VUS	-	13.56	221%	1/1
C5	c.4924C>G	p.L1642V	VUS	0.00006765	14.44	92%	0/1
C5	c.1060A>C	p.L354M	benign	0.005561	25	119%	0/1
CFHR2	c.325A>G	p.T109A	benign	0.0058	14.5	101%	0/1
CFHR4	c.758delG	p.C253Lfs15X	VUS	-	25	104% 83%	0/2
CFHR4	c.1058T>A	p.I106N	VUS	-	12.97	100%	0/1
CFHR4	*CFHR1-CFHR4* dup	-	VUS	-	-	153% 133% 124%	1/3
CFHR5	c.485_486dupAA	p.E163Kfs10X	LPV	0.0063	22.7	176%	1/1
Overall							18/27

10.3389/fimmu.2023.1112257

10.3389/fimmu.2023.1112257

TABLE 6 Results of C5b-9 formation test in family members who carry variants not segregating with the disease.

gene	nucleotide change	aminoacid change	gnomAD allele frequency	CADD	C5b-9 formed *(% increase versus control=100)*	n° carriers positive C5b-9 test *(>149%)*
CFI	c.1044+9G>A	-	0.00001989	2.153	122%	0/1
CFI	c.1642G>C	p.E548Q	0.0008207	29.1	118%	0/1
CFB	c.1037-10C>G	-	0.00073	7.632	110%	0/1
CFB	c.1270+6T>C	-	-	15.8	88%	0/1
C5	c.130G>T	p.Y44D	-	24.4	117%	0/1
CFHR2	c.212C>T	p.T71M	0.00398	18.04	112%	0/4
					102%	
					117%	
					93%	
CFHR4	c.643C>G	p.P215A	-	12.83	101%	0/1
Overall						0/10

useful for uncovering inherited complement dysregulation in aHUS patients who do not carry variants in known disease-associated genes.

Genetic analysis using next-generation sequencing makes it possible to search for nucleotide variants in the whole complement gene set quickly and inexpensively. Nevertheless, some particularities of complement genes should be considered, including the high sequence homology between *CFH* and *CFHRs* genes (9), and additional techniques, such as MLPA, are often required to correctly identify the generation of structural variations in the Regulators of Complement Activation (RCA) gene cluster (27).

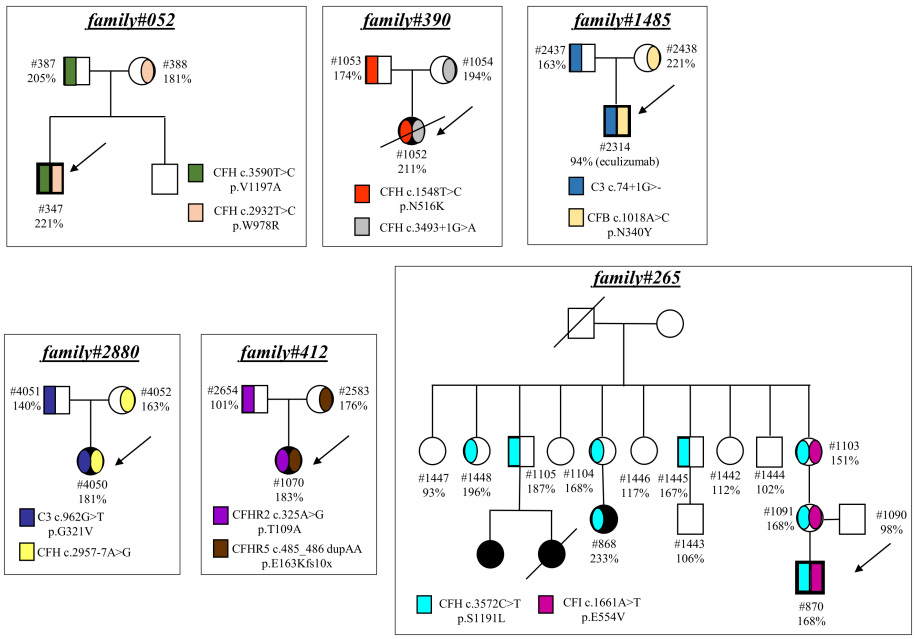

FIGURE 4
Pedigrees with combined variants. Pedigree #052 of the proband #347. Genetic analysis revealed a pathogenic variant in *CFH* (p.V1197A) inherited from the father (#387, green) and also a LPV in *CFH* (p.W978R) inherited from the mother (#388, pink). Pedigree #390 of the aHUS proband #1052. Genetic analysis revealed a pathogenic variant in *CFH* (c.3493+1G>A) inherited from the mother (#1054, grey) and a rare VUS in *CFH* (p.N516K) inherited from the father (#1053, red). Pedigree #265 of proband #870 carrying a pathogenic variant in *CFH* (p.S1191L, light blue) inherited from the mother and also present in the maternal affected relative (#868). Genetic analysis in the proband also found a VUS in *CFI* (p.E554V, purple) inherited from the mother but absent in the maternal affected relative. Pedigree #1485 of proband #2314. Genetic analysis revealed a VUS in *C3* (c.74+1delG) inherited from the father (#2437, blue) and a VUS in *CFB* (p.N340Y) inherited from the mother (#2438, orange). Arrows indicate probands, affected subjects are in black. Pedigree #2880 of the proband #4050. Genetic analysis revealed a LPV in *C3* (p.G321V) inherited from the father (#4051, deep blue) and a likely benign variant in *CFH* (c.2957-7A>G) inherited from the mother (#4052, yellow). Pedigree #412 of the proband #1070. Genetic analysis revealed a benign variant in *CFHR2* (p.T109A) inherited from the father (#2654, purple) and a LPV in *CFHR5* (p.E163Kfs10x) inherited from the mother (#2583, brown). Arrows indicate probands, affected subjects are in black. The circles are used for female subjects and squares for male subjects.

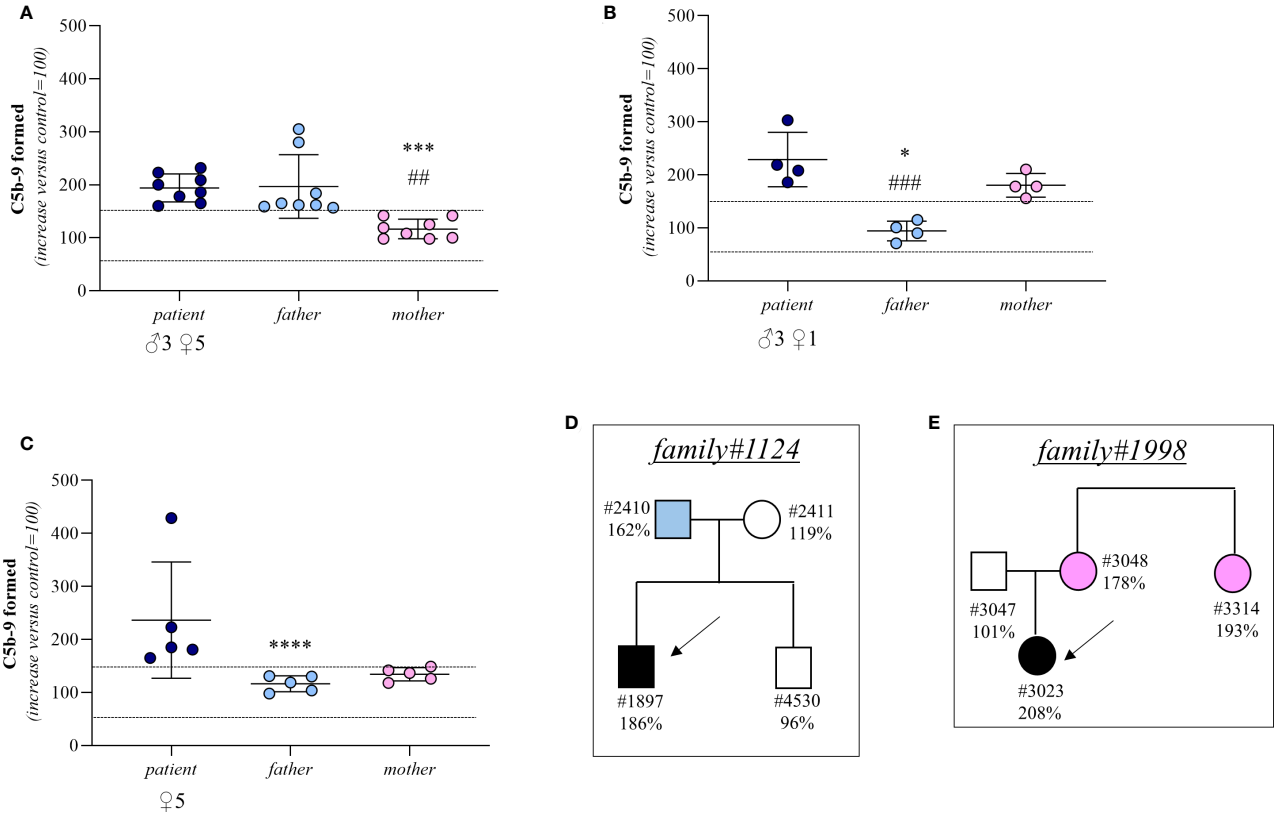

FIGURE 5
C5b-9 formation on activated HMEC-1 induced by serum from aHUS patients without identified mutations and from their parents. **(A–C)** Endothelial surface area covered by C5b-9 staining after 2h incubation of ADP-activated HMEC-1 with serum (diluted 1:2 in test medium) from aHUS patients without identified mutations (remission, n=16; acute, n=1) and their parents. Dotted lines are upper and lower limits of normal range. Results are shown as fold increase of stained surface area after incubation with serum from aHUS patients and their parents versus control pool of sera run in parallel. Points represent fold increase values of single subjects. Horizontal bars are mean ± SD values. *P<0.001, ***P<0.01, ****P<0.05 vs patient; ##P<0.01, ###P<0.05 vs other parent. **(D)** Pedigree #1124 of patient #1897 without identified mutations. **(E)** Pedigree #1998 of patient #3023 without identified mutations. Arrows indicate probands, affected individuals are in black. The circles indicate female subjects and the squares male subjects.

Among the variants identified through genetic analyses in aHUS patients, only a subgroup can be defined as pathogenic with certainty, based on either published functional studies or a clear-cut effect on transcription/translation (9, 28). But we do not know the functional significance of a large majority of variants. This is an important issue, because knowing the real functional impact of gene variants is crucial to better understanding the pathogenesis of aHUS in each patient and can help confirm a diagnosis, guide patient management, inform prognosis, and reduce the need for invasive procedures (8, 9, 28, 29).

It is not easy to determine the functional meaning of a gene variant. In line with published guidelines (13) (https://www.acgs.uk.com/media/11631/uk-practice-guidelines-for-variant-classification-v4-01-2020.pdf), rare gene variants can be categorised – as pathogenic, likely pathogenic, variants of uncertain significance, likely benign and benign – based on criteria that include prevalence in healthy individuals (MAF), localisation within the gene and segregation with the disease, as well as in silico estimation of the influence of the variant on protein structure or function.

Recently, the capacity of in silico predictions to really establish whether or not a variant may be pathogenetic has been doubted, and this limitation applies particularly to gain-of-function variants in *C3* and *CFB* genes (30, 31). Even the CADD tool, which scores the predicted deleteriousness of variants by integrating multiple annotations into one metric, often fails. In this regard, a study by Merinero et al. (32) described the functional characterisation of 28 new *CFH* gene variants. All 17 variants that were classified as pathogenic in silico were confirmed to be pathogenic in functional studies. However, among the 11 variants categorised as benign or VUS, 7 were found to be pathogenetic by functional studies, leading the authors to conclude that with the current algorithms' prediction is unreliable, mainly in the case of variants categorised as benign or VUS. In a subsequent paper the same group further demonstrated the limitations of algorithms in predicting the pathogenicity of 105 *CFH* variants, concluding that functional studies are necessary (29).

Functional studies are complicated and time-consuming. In addition, each complement factor and regulator carriers out multiple and complex activities and several functional tests should be performed to obtain a clear picture of the impact of a given variant. In this regard, only 29 of the 79 VUS studied by Merinero et al. (29) turned out to alter FH expression or function as observed in 4 different functional *in vitro* tests. However, one cannot rule out the possibility that for any of the remaining variants, additional functional tests would have revealed a pathogenic impact on FH function.

With the goal of overcoming the above obstacles, here we decided to use the ex vivo serum-induced C5b-9 formation test on activated

endothelium (10). Consistent with our published results (6, 10) the assay was always positive with serum from aHUS patients who were in remission, and it could not discriminate in patients between carriers and non-carriers of complement gene variants.

This finding may be related both to the presence of additional predisposing factors (such as the CFH H3 haplotypes) and to subclinical chronic disease activity associated with the presence in aHUS serum of heme, extracellular vesicles, ROS, or inflammatory cytokines that may favour the formation of C5b-9 on an activated endothelium (33–35).

We therefore changed our approach, based on two considerations. First, penetrance of aHUS is incomplete, as documented by the finding in aHUS families of numerous asymptomatic relatives who carry the same gene abnormality as the proband (24). In addition, the large majority of aHUS disease-associated variants are inherited from an unaffected parent (2, 36). Second, by studying a small number of relatives of aHUS patients, we previously found that sera from unaffected relatives carrying the same pathogenic variant as the proband caused higher-than-normal C5b-9 formation on endothelium (10), whereas sera from non-carrier relatives did not.

With these concepts in mind, and to overcome the confounding effect of aHUS status, here we performed the C5b-9 formation test in several aHUS pedigrees with at least one unaffected relative who shared with the proband a published functionally characterised variant. We found that almost 93% of unaffected relatives with pathogenic variants in circulating complement factors exhibited a positive serum-induced C5b-9 formation test, evidence of the test's high sensitivity in identifying functional variants. The test in relatives showed that all non-carriers exhibited a negative C5b-9 formation test. In addition, all the unaffected relatives with rare complement gene variants that did not segregate with aHUS exhibited a negative serum-induced C5b-9 formation, indicating that the test was specific for identifying disease-relevant gene abnormalities. Based on the above results we then investigated whether the ex vivo C5b-9 formation test could be useful for better and more quickly characterising LPV, VUS and likely benign/benign variants.

Sera from all relatives but one who carry LPV in known disease-associated genes induced higher-than-normal C5b-9 formation. The *CFH* p.1182delins LPV was described previously in a family (37). Although no functional studies were performed, the variant may have profound effects on FH activity, since it causes the insertion of 12 extra amino acids in the SCR20, a domain that encompasses binding sites for C3b and polyanionic carbohydrates and is important for complement regulation on host surfaces (38–40). The *CFH* p.896_900 del and the p.W978R variants are located in SCR15 and SCR16, respectively, which belong to the central segment of the protein whose function is still poorly characterised (41, 42). As for the LPVs in C3 gene, the functional C5b-9 test was positive in carriers of the p.D61N. This is in line with its location in the MG1 domain, which participates in the formation of a key ring and may be crucial for the C3 structure–function relationships (43). The finding that serum from the unaffected carrier of the *C3* p.G321V did not induce excessive C5b-9 formation on HMEC-1 suggested that this LPV does not have a functional effect.

The results from serum of the carrier of the LPV in the putative candidate *CFHR5* gene may help to clarify the involvement of FHR5 in aHUS. Several authors have described potentially pathogenic *CFHR5* variants in aHUS patients (44–48). On the other hand, Osborne et al. (30) failed to find a significant association between rare variants in *CFHR5* and aHUS. Among the FHR proteins, only FHR5, like FH, has FI-dependent cofactor activity, leading to C3b inactivation, and C3 convertase decay accelerating activity (48), but these activities have been observed in the fluid phase only at higher than physiological concentrations (49, 50). On the other hand, FHR5 has been shown to specifically interact with C3b, heparin and other cellular and extracellular ligands through its central SCR3-7, suggesting it may carry out local cell and tissue activity (48). The present data showing that serum from the subject carrying the *CFHR5* p.E163Kfs10x variant – which causes protein truncation in SCR3 – induced excessive C5b-9 formation on the endothelial cell surface, supports the hypothesis that FHR5 might regulate complement at the endothelial cell surface.

Notably, all relatives with VUS in aHUS-associated genes had a positive C5b-9 formation test, whereas the assay was negative for carriers of VUS only in putative candidate genes (*CFHR4*, and *C5)*. The latter results do not support the hypothesis that VUS we found in candidate genes play a role in inducing complement dysregulation on endothelium. However, other functional studies should be performed before completely ruling out the possibility that these VUS have a role in aHUS pathogenesis.

Consistent with the previous report by Merinero et al. (32) that documented the pathogenicity of 4 *CFH* variants categorised as benign, the unaffected relative from our cohort who carries a likely benign *CFH* variant was positive in the C5b-9 formation test. Altogether, the present results and other published data (29, 32) confirm that in silico predictions might be unreliable in the case of benign or likely benign variants.

The C5b-9 assay in parents was particularly helpful in defining the relative functional effect of rare variants in pedigrees in which the proband carried more than one genetic abnormality. Thus, in two pedigrees both variants that the proband inherited from either parent were associated with ex vivo complement activation on the endothelium, whereas in two other pedigrees only one variant appeared to be functional. Notably, in one of the latter pedigrees the proband inherited a *C3* LPV from the father and a likely benign variant in *CFH* from the mother. The test reversed the in silico prediction; indeed, serum from the mother was positive in the C5b-9 test, while a negative result was found with serum from the father with the LPV.

Finally, the C5b-9 test allowed us to unmask in a few patients without rare variants – either in disease-associated or in candidate genes – a genetic liability inherited from unaffected parents. This applied to pedigrees in which either the father or the mother had a positive test, revealing the presence of a genetic abnormality predisposing to complement dysregulation. In one pedigree, the maternal inheritance of the unknown genetic factor was confirmed by the positive test in the maternal aunt.

Exome sequencing has proven to be a rapid and cost-effective way of discovering causative genes and has been useful in identifying mutations involved in rare Mendelian diseases (51). However, pitfalls and hurdles remain, including the difficulty of selecting from among a huge number of rare, potentially causative variants in several genes. This issue is further amplified by the oligogenic nature and incomplete penetrance of aHUS, particularly in non-familial cases.

Combining exome sequencing with results from C5b-9 tests in parents as well as in informative, unaffected relatives could help researchers select variants and possibly identify new genetic factors that predispose to aHUS.

The C5b-9 formation test in unaffected relatives described here has some limitations that should be considered. First, while the assay catches abnormalities in soluble complement proteins that are present in serum, it is not informative regarding the functional effects of rare variants in complement regulatory proteins expressed on the cell membrane, such MCP or THBD, since HMEC-1 cells express the wild-type proteins. To overcome this limitation, we are working to obtain endothelial cells from iPSC derived from PBMC from patients and unaffected relatives with *MCP* or *THBD* variants that will be used as target cells in the C5b-9 formation test. In addition, the test was not conclusive in pedigrees without identified variants with negative C5b-9 results in both parents. In these cases, the question of whether the disease in the proband was associated with a *de novo* genetic abnormality or a recessive inheritance or was not genetically determined remained open.

In conclusion, the results of this study provide evidence that the serum-induced C5b-9 formation test performed in unaffected relatives of aHUS patients may be a tool for rapidly obtaining important information about the functional consequences of rare complement gene variants. When combined with exome sequencing the assay might be of help in guiding variant selection, to identify new aHUS-associated genetic factors. Genetic studies in rare diseases are often complicated by incomplete penetrance. In addition, the progressive decrease of average size of families, at least in Europe and Western countries, lowers the probability to find familial cases. The approach of using disease-relevant assays in relatives to extend the number of informative subjects, could be applied to other rare diseases to help variant selection and characterization, while limiting the hurdle of recruiting large cohorts of patients.

Data availability statement

The original contributions presented in the study are included in the article/Supplementary Materials. Further inquiries can be directed to the corresponding author.

Ethics statement

The studies involving human participants were reviewed and approved by Ethical Committee of the Azienda Sanitaria Locale Bergamo, Italy. Written informed consent to participate in this study was provided by the participants' legal guardian/next of kin.

Author contributions

SG, MG, MB, SA, and MN designed the research, interpreted the data, and wrote the paper; SG, RP, MA, LL, CM, MB, and DS performed the research and analysed the data; EB provided detailed clinical information on patients and wrote family histories; MN, SA, AB, and GR critically revised the manuscript. All authors contributed to the article and approved the submitted version.

Funding

RP and MB are recipients of a research contract from Progetto DDD Onlus-Associazione per la lotta alla DDD (Milan, Italy). CM is the recipient of a grant from Fondazione Regionale per la Ricerca Biomedica (FRRB; UNEARTH project 1745126). LL is the recipient of a fellowship from Fondazione Aiuti per la Ricerca sulle Malattie Rare ARMR ONLUS (Bergamo, Italy). This work was partially supported by UNEARTH project 1745126. The funding sources had no role in study design, nor in the collection, analysis or interpretation of data, nor in the writing of the report or in the decision to submit the paper for publication.

Acknowledgments

We would like to acknowledge the contributions of Silvia Prandini, Veruscka Lecchi, Diana Cadè, Sara Gamba, and Erica Daina in sample and clinical data collection. The authors thank all clinicians from the other centres, and patients for their membership in and support of the International Registry of HUS/TTP. The authors also are grateful to Kerstin Mierke for editing the manuscript.

Conflict of interest

MN has received honoraria from Alexion Pharmaceuticals for giving lectures, and for participating in advisory boards, and she has received research grants from Omeros, Gemini, Novartis and BioCryst Pharmaceuticals. AB has received honoraria from Alexion Pharmaceuticals and BioCryst Pharmaceuticals. GR has consultancy agreements with AbbVie, Alexion Pharmaceuticals, Novartis Pharma and BioCryst Pharmaceuticals.

The remaining authors declare that the research was conducted in the absence of any commercial or financial relationships that could be construed as a potential conflict of interest.

Publisher's note

All claims expressed in this article are solely those of the authors and do not necessarily represent those of their affiliated organizations, or those of the publisher, the editors and the reviewers. Any product that may be evaluated in this article, or claim that may be made by its manufacturer, is not guaranteed or endorsed by the publisher.

Supplementary material

The Supplementary Material for this article can be found online at: https://www.frontiersin.org/articles/10.3389/fimmu.2023.1112257/full#supplementary-material

References

1. Noris M, Remuzzi G. Atypical hemolytic-uremic syndrome. *N Engl J Med* (2009) 361:1676–87. doi: 10.1056/NEJMra0902814

2. Noris M, Caprioli J, Bresin E, Mossali C, Pianetti G, Gamba S, et al. Relative role of genetic complement abnormalities in sporadic and familial aHUS and their impact on clinical phenotype. *Clin J Am Soc Nephrol* (2010) 5:1844–59. doi: 10.2215/CJN.02210310

3. Fakhouri F, Frémeaux-Bacchi V, Loirat C. Atypical hemolytic uremic syndrome: From the rediscovery of complement to targeted therapy. *Eur J Intern Med* (2013) 24:492–5. doi: 10.1016/j.ejim.2013.05.008

4. Legendre CM, Licht C, Muus P, Greenbaum LA, Babu S, Bedrosian C, et al. Terminal complement inhibitor eculizumab in atypical hemolytic-uremic syndrome. *N Engl J Med* (2013) 368:2169–81. doi: 10.1056/NEJMoa1208981

5. Goodship THJ, Cook HT, Fakhouri F, Fervenza FC, Frémeaux-Bacchi V, Kavanagh D, et al. Atypical hemolytic uremic syndrome and C3 glomerulopathy: Conclusions from a "Kidney disease: Improving global outcomes" (KDIGO) controversies conference. *Kidney Int* (2017) 91:539–51. doi: 10.1016/j.kint.2016.10.005

6. Galbusera M, Noris M, Gastoldi S, Bresin E, Mele C, Breno M, et al. An ex vivo test of complement activation on endothelium for individualized eculizumab therapy in hemolytic uremic syndrome. *Am J Kidney Dis Off J Natl Kidney Found* (2019) 74:56–72. doi: 10.1053/j.ajkd.2018.11.012

7. Fakhouri F, Fila M, Hummel A, Ribes D, Sellier-Leclerc A-L, Ville S, et al. Eculizumab discontinuation in children and adults with atypical hemolytic-uremic syndrome: A prospective multicenter study. *Blood* (2021) 137:2438–49. doi: 10.1182/blood.2020009280

8. Fakhouri F, Frémeaux-Bacchi V. Thrombotic microangiopathy in aHUS and beyond: Clinical clues from complement genetics. *Nat Rev Nephrol* (2021) 17:543–53. doi: 10.1038/s41581-021-00424-4

9. Rodríguez de Córdoba S. Genetic variability shapes the alternative pathway complement activity and predisposition to complement-related diseases. *Immunol Rev* (2023) 313:71–90. doi: 10.1111/imr.13131

10. Noris M, Galbusera M, Gastoldi S, Macor P, Banterla F, Bresin E, et al. Dynamics of complement activation in aHUS and how to monitor eculizumab therapy. *Blood* (2014) 124:1715–26. doi: 10.1182/blood-2014-02-558296

11. Piras R, Iatropoulos P, Bresin E, Todeschini M, Gastoldi S, Valoti E, et al. Molecular studies and an ex vivo complement assay on endothelium highlight the genetic complexity of atypical hemolytic uremic syndrome: The case of a pedigree with a null CD46 variant. *Front Med* (2020) 7:579418. doi: 10.3389/fmed.2020.579418

12. Iatropoulos P, Noris M, Mele C, Piras R, Valoti E, Bresin E, et al. Complement gene variants determine the risk of immunoglobulin-associated MPGN and C3 glomerulopathy and predict long-term renal outcome. *Mol Immunol* (2016) 71:131–42. doi: 10.1016/j.molimm.2016.01.010

13. Richards S, Aziz N, Bale S, Bick D, Das S, Gastier-Foster J, et al. Standards and guidelines for the interpretation of sequence variants: A joint consensus recommendation of the American college of medical genetics and genomics and the association for molecular pathology. *Genet Med Off J Am Coll Med Genet* (2015) 17:405–24. doi: 10.1038/gim.2015.30

14. Kircher M, Witten DM, Jain P, O'Roak BJ, Cooper GM, Shendure J. A general framework for estimating the relative pathogenicity of human genetic variants. *Nat Genet* (2014) 46:310–5. doi: 10.1038/ng.2892

15. Rentzsch P, Witten D, Cooper GM, Shendure J, Kircher M. CADD: predicting the deleteriousness of variants throughout the human genome. *Nucleic Acids Res* (2019) 47: D886–94. doi: 10.1093/nar/gky1016

16. Valoti E, Alberti M, Tortajada A, Garcia-Fernandez J, Gastoldi S, Besso L, et al. A novel atypical hemolytic uremic syndrome-associated hybrid CFHR1/CFH gene encoding a fusion protein that antagonizes factor h-dependent complement regulation. *J Am Soc Nephrol* (2015) 26:209–19. doi: 10.1681/ASN.2013121339

17. Venables JP, Strain L, Routledge D, Bourn D, Powell HM, Warwicker P, et al. Atypical haemolytic uraemic syndrome associated with a hybrid complement gene. *PloS Med* (2006) 3:e431. doi: 10.1371/journal.pmed.0030431

18. Piras R, Breno M, Valoti E, Alberti M, Iatropoulos P, Mele C, et al. CFH and CFHR copy number variations in C3 glomerulopathy and immune complex-mediated membranoproliferative glomerulonephritis. *Front Genet* (2021) 12:670727. doi: 10.3389/fgene.2021.670727

19. Caprioli J, Castelletti F, Bucchioni S, Bettinaglio P, Bresin E, Pianetti G, et al. Complement factor h mutations and gene polymorphisms in haemolytic uraemic syndrome: The c-257T, the A2089G and the G2881T polymorphisms are strongly associated with the disease. *Hum Mol Genet* (2003) 12:3385–95. doi: 10.1093/hmg/ddg363

20. Bresin E, Rurali E, Caprioli J, Sanchez-Corral P, Fremeaux-Bacchi V, Rodriguez de Cordoba S, et al. Combined complement gene mutations in atypical hemolytic uremic syndrome influence clinical phenotype. *J Am Soc Nephrol JASN* (2013) 24:475–86. doi: 10.1681/ASN.2012090884

21. Esparza-Gordillo J, Goicoechea de Jorge E, Buil A, Carreras Berges L, López-Trascasa M, Sánchez-Corral P, et al. Predisposition to atypical hemolytic uremic syndrome involves the concurrence of different susceptibility alleles in the regulators of complement activation gene cluster in 1q32. *Hum Mol Genet* (2005) 14:703–12. doi: 10.1093/hmg/ddi066

22. Valoti E, Alberti M, Iatropoulos P, Piras R, Mele C, Breno M, et al. Rare functional variants in complement genes and anti-FH autoantibodies-associated aHUS. *Front Immunol* (2019) 10:853. doi: 10.3389/fimmu.2019.00853

23. Aiello S, Gastoldi S, Galbusera M, Ruggenenti P, Portalupi V, Rota S, et al. C5a and C5aR1 are key drivers of microvascular platelet aggregation in clinical entities spanning from aHUS to COVID-19. *Blood Adv* (2022) 6(3):866–81. doi: 10.1182/bloodadvances.2022007722

24. Arjona E, Huerta A, Goicoechea de Jorge E, Rodríguez de Córdoba S. Familial risk of developing atypical hemolytic-uremic syndrome. *Blood* (2020) 136:1558–61. doi: 10.1182/blood.2020006931

25. Heinen S, Sanchez-Corral P, Jackson MS, Strain L, Goodship JA, Kemp EJ, et al. *De novo* gene conversion in the RCA gene cluster (1q32) causes mutations in complement factor h associated with atypical hemolytic uremic syndrome. *Hum Mutat* (2006) 27:292–3. doi: 10.1002/humu.9408

26. Goicoechea de Jorge E, Tortajada A, García SP, Gastoldi S, Merinero HM, García-Fernández J, et al. Factor h competitor generated by gene conversion events associates with atypical hemolytic uremic syndrome. *J Am Soc Nephrol* (2018) 29:240–9. doi: 10.1681/ASN.2017050518

27. Garcia-Fernandez J, Vilches-Arroyo S, Olavarrieta L, Perez-Perez J, Rodriquez de Cordoba S. Detection of genetic rearrangements in the regulators of complement activation RCA cluster by high-throughput sequencing and MLPA. *Methods Mol Biol Clifton NJ* (2021) 2227:159–178. doi: 10.1007/978-1-0716-1016-9_16

28. Thurman JM, Fremeaux-Bacchi V. Alternative pathway diagnostics. *Immunol Rev* (2023) 313: 225–238. doi: 10.1111/imr.13156

29. Martín Merinero H, Zhang Y, Arjona E, Del Angel G, Goodfellow R, Gomez-Rubio E, et al. Functional characterization of 105 factor h variants associated with aHUS: Lessons for variant classification. *Blood* (2021) 138:2185–201. doi: 10.1182/blood.2021012037

30. Osborne AJ, Breno M, Borsa NG, Bu F, Frémeaux-Bacchi V, Gale DP, et al. Statistical validation of rare complement variants provides insights into the molecular basis of atypical hemolytic uremic syndrome and C3 glomerulopathy. *J Immunol Baltim Md 1950* (2018) 200:2464–78. doi: 10.4049/jimmunol.1701695

31. Marinozzi MC, Vergoz L, Rybkine T, Ngo S, Bettoni S, Pashov A, et al. Complement factor b mutations in atypical hemolytic uremic syndrome-disease-relevant or benign? *J Am Soc Nephrol* (2014) 25:2053–65. doi: 10.1681/ASN.2013070796

32. Merinero HM, García SP, García-Fernández J, Arjona E, Tortajada A, Rodríguez de Córdoba S. Complete functional characterization of disease-associated genetic variants in the complement factor h gene. *Kidney Int* (2018) 93:470–81. doi: 10.1016/j.kint.2017.07.015

33. Roumenina LT, Rayes J, Frimat M, Fremeaux-Bacchi V. Endothelial cells: Source, barrier, and target of defensive mediators. *Immunol Rev* (2016) 274:307–29. doi: 10.1111/imr.12479

34. Frimat M, Tabarin F, Dimitrov JD, Poitou C, Halbwachs-Mecarelli L, Fremeaux-Bacchi V, et al. Complement activation by heme as a secondary hit for atypical hemolytic uremic syndrome. *Blood* (2013) 122:282–92. doi: 10.1182/blood-2013-03-489245

35. Frimat M, Boudhabhay I, Roumenina LT. Hemolysis derived products toxicity and endothelium: Model of the second hit. *Toxins* (2019) 11:660. doi: 10.3390/toxins11110660

36. Ardissino G, Longhi S, Porcaro L, Pintarelli G, Strumbo B, Capone V, et al. Risk of atypical HUS among family members of patients carrying complement regulatory gene abnormality. *Kidney Int Rep* (2021) 6:1614–21. doi: 10.1016/j.ekir.2021.03.885

37. Filler G, Radhakrishnan S, Strain L, Hill A, Knoll G, Goodship TH. Challenges in the management of infantile factor h associated hemolytic uremic syndrome. *Pediatr Nephrol Berl Ger* (2004) 19:908–11. doi: 10.1007/s00467-004-1526-9

38. Sánchez-Corral P, Pérez-Caballero D, Huarte O, Simckes AM, Goicoechea E, López-Trascasa M, et al. Structural and functional characterization of factor h mutations associated with atypical hemolytic uremic syndrome. *Am J Hum Genet* (2002) 71:1285–95. doi: 10.1086/344515

39. Manuelian T, Hellwage J, Meri S, Caprioli J, Noris M, Heinen S, et al. Mutations in factor h reduce binding affinity to C3b and heparin and surface attachment to endothelial cells in hemolytic uremic syndrome. *J Clin Invest* (2003) 111:1181–90. doi: 10.1172/JCI16651

40. Pangburn MK. Cutting edge: localization of the host recognition functions of complement factor h at the carboxyl-terminal: Implications for hemolytic uremic syndrome. *J Immunol Baltim Md 1950* (2002) 169:4702–6. doi: 10.4049/jimmunol.169.9.4702

41. Schmidt CQ, Herbert AP, Mertens HDT, Guariento M, Soares DC, Uhrin D, et al. The central portion of factor h (modules 10-15) is compact and contains a structurally deviant CCP module. *J Mol Biol* (2010) 395:105–22. doi: 10.1016/j.jmb.2009.10.010

42. Makou E, Mertens HDT, Maciejewski M, Soares DC, Matis I, Schmidt CQ, et al. Solution structure of CCP modules 10-12 illuminates functional architecture of the complement regulator, factor h. *J Mol Biol* (2012) 424:295–312. doi: 10.1016/j.jmb.2012.09.013

43. Janssen BJC, Huizinga EG, Raaijmakers HCA, Roos A, Daha MR, Nilsson-Ekdahl K, et al. Structures of complement component C3 provide insights into the function and evolution of immunity. *Nature* (2005) 437:505–11. doi: 10.1038/nature04005

44. Monteferrante G, Brioschi S, Caprioli J, Pianetti G, Bettinaglio P, Bresin E, et al. Genetic analysis of the complement factor h related 5 gene in haemolytic uraemic syndrome. *Mol Immunol* (2007) 44:1704–8. doi: 10.1016/j.molimm.2006.08.004

45. Maga TK, Nishimura CJ, Weaver AE, Frees KL, Smith RJH. Mutations in alternative pathway complement proteins in American patients with atypical hemolytic uremic syndrome. *Hum Mutat* (2010) 31:E1445–1460. doi: 10.1002/humu.21256

46. Tseng M-H, Tsai J-D, Tsai I-J, Huang S-M, Huang J-L, Fan W-L, et al. Whole-exome sequencing detects mutations in pediatric patients with atypical hemolytic uremic syndrome in Taiwan. *Clin Chim Acta Int J Clin Chem* (2019) 494:143–50. doi: 10.1016/j.cca.2019.03.1623

47. Bu F, Borsa NG, Jones MB, Takanami E, Nishimura C, Hauer JJ, et al. High-throughput genetic testing for thrombotic microangiopathies and C3 glomerulopathies. *J Am Soc Nephrol* (2016) 27:1245–53. doi: 10.1681/ASN.2015040385

48. Westra D, Vernon KA, Volokhina EB, Pickering MC, van de Kar NCAJ, van den Heuvel LP. Atypical hemolytic uremic syndrome and genetic aberrations in the complement factor h-related 5 gene. *J Hum Genet* (2012) 57:459–64. doi: 10.1038/jhg.2012.57

49. Lucientes-Continente L, Márquez-Tirado B, Goicoechea de Jorge E. The factor h protein family: The switchers of the complement alternative pathway. *Immunol Rev* (2023) 313: 25–45. doi: 10.1111/imr.13166

50. McRae JL, Duthy TG, Griggs KM, Ormsby RJ, Cowan PJ, Cromer BA, et al. Human factor h-related protein 5 has cofactor activity, inhibits C3 convertase activity, binds heparin and c-reactive protein, and associates with lipoprotein. *J Immunol Baltim Md 1950* (2005) 174:6250–6. doi: 10.4049/jimmunol.174.10.6250

51. Knoers N, Antignac C, Bergmann C, Dahan K, Giglio S, Heidet L, et al. Genetic testing in the diagnosis of chronic kidney disease: Recommendations for clinical practice. *Nephrol Dial Transplant* (2022) 37:239–54. doi: 10.1093/ndt/gfab218

frontiers | Frontiers in Immunology

TYPE Original Research
PUBLISHED 16 February 2023
DOI 10.3389/fimmu.2023.1107295

Check for updates

OPEN ACCESS

EDITED BY
Erik J. M. Toonen,
Hycult Biotech, Netherlands

REVIEWED BY
Svetlana Hakobyan,
Cardiff University, United Kingdom
Patric Turowski,
University College London,
United Kingdom

*CORRESPONDENCE
Alberto Paradela
alberto.paradela@cnb.csic.es
Cândida T. Tomaz
ctomaz@ubi.pt

SPECIALTY SECTION
This article was submitted to Molecular Innate Immunity, a section of the journal Frontiers in Immunology

RECEIVED 24 November 2022
ACCEPTED 01 February 2023
PUBLISHED 16 February 2023

CITATION
Santos FM, Ciordia S, Mesquita J, Cruz C, Sousa JPC, Passarinha LA, Tomaz CT and Paradela A (2023) Proteomics profiling of vitreous humor reveals complement and coagulation components, adhesion factors, and neurodegeneration markers as discriminatory biomarkers of vitreoretinal eye diseases.
Front. Immunol. 14:1107295.
doi: 10.3389/fimmu.2023.1107295

COPYRIGHT
© 2023 Santos, Ciordia, Mesquita, Cruz, Sousa, Passarinha, Tomaz and Paradela. This is an open-access article distributed under the terms of the Creative Commons Attribution License (CC BY). The use, distribution or reproduction in other forums is permitted, provided the original author(s) and the copyright owner(s) are credited and that the original publication in this journal is cited, in accordance with accepted academic practice. No use, distribution or reproduction is permitted which does not comply with these terms.

Proteomics profiling of vitreous humor reveals complement and coagulation components, adhesion factors, and neurodegeneration markers as discriminatory biomarkers of vitreoretinal eye diseases

Fátima M. Santos [1,2], Sergio Ciordia [2], Joana Mesquita [1], Carla Cruz [1,3], João Paulo Castro e Sousa [1,4], Luís A. Passarinha [1,5,6,7], Cândida T. Tomaz [1,3*] and Alberto Paradela [2*]

[1]CICS-UBI – Health Sciences Research Centre, University of Beira Interior, Covilhã, Portugal, [2]Functional Proteomics Laboratory, Centro Nacional de Biotecnología, CSIC, Madrid, Spain, [3]Chemistry Department, Faculty of Sciences, University of Beira Interior, Covilhã, Portugal, [4]Department of Ophthalmology, Centro Hospitalar de Leiria, Leiria, Portugal, [5]Associate Laboratory i4HB - Institute for Health and Bioeconomy, Faculdade de Ciências e Tecnologia, Universidade NOVA, Caparica, Portugal, [6]UCIBIO–Applied Molecular Biosciences Unit, Departamento de Química/Departamento Ciências da Vida, Faculdade de Ciências e Tecnologia, Universidade NOVA de Lisboa, Caparica, Portugal, [7]Laboratório de Fármaco-Toxicologia, UBIMedical, Universidade da Beira Interior, Covilhã, Portugal

Introduction: Diabetic retinopathy (DR) and age-related macular degeneration (AMD) are leading causes of visual impairment and blindness in people aged 50 years or older in middle-income and industrialized countries. Anti-VEGF therapies have improved the management of neovascular AMD (nAMD) and proliferative DR (PDR), no treatment options exist for the highly prevalent dry form of AMD.

Methods: To unravel the biological processes underlying these pathologies and to find new potential biomarkers, a label-free quantitative (LFQ) method was applied to analyze the vitreous proteome in PDR (n=4), AMD (n=4) compared to idiopathic epiretinal membranes (ERM) (n=4).

Results and discussion: Post-hoc tests revealed 96 proteins capable of differentiating among the different groups, whereas 118 proteins were found differentially regulated in PDR compared to ERM and 95 proteins in PDR compared to dry AMD. Pathway analysis indicates that mediators of complement, coagulation cascades and acute phase responses are enriched in PDR vitreous, whilst proteins highly correlated to the extracellular matrix (ECM) organization, platelet degranulation, lysosomal degradation, cell adhesion, and central nervous system development were found underexpressed. According to these results, 35 proteins were selected and monitored by MRM (multiple reaction monitoring) in a larger cohort of patients with ERM (n=21), DR/PDR (n=20), AMD (n=11), and retinal detachment (n=13). Of these, 26 proteins could differentiate

between these vitreoretinal diseases. Based on Partial least squares discriminant and multivariate exploratory receiver operating characteristic (ROC) analyses, a panel of 15 discriminatory biomarkers was defined, which includes complement and coagulation components (complement C2 and prothrombin), acute-phase mediators (alpha-1-antichymotrypsin), adhesion molecules (e.g., myocilin, galectin-3-binding protein), ECM components (opticin), and neurodegeneration biomarkers (beta-amyloid, amyloid-like protein 2).

KEYWORDS

age-related macular degeneration, biomarkers, complement and coagulation cascades, extracellular matrix, neurodegeneration, proliferative diabetic retinopathy, retinal detachment, vitreous proteomics

Introduction

Despite improvements in the prevention and control of ocular diseases in the past 30 years, the public health burden associated to visual impairment and blindness is expected to increase due to the growth and aging of the world population and the increase in the prevalence of chronic diseases such as diabetes mellitus (1, 2). Diabetic retinopathy (DR) and age-related macular degeneration (AMD) are leading causes of visual impairment and blindness in middle-income and industrialized countries and, therefore, they are considered priority eye diseases by World Health Organization (3). DR is a microvascular complication that develops in patients with diabetes (4). In the non-proliferative stage, microvascular changes such as microaneurysms, basement membrane thickening, and loss of pericytes occur in response to hyperglycemia, but increasing evidence suggests that microvascular changes may be preceded by neuroglial degeneration. Proliferative diabetic retinopathy (PDR) is led by retinal ischemia, which combined with an imbalance in the levels of inflammatory and pro-angiogenic cytokines can trigger intra-retinal and intravitreal neovascularization (NV) (1, 4, 5). AMD is a multifactorial disease characterized by the loss of central vision due to the degeneration of photoreceptors and retinal pigment epithelium (RPE) (6, 7). In an early phase, AMD is characterized by the accumulation of yellowish deposits (drusen) underneath the retina but it can further progress to late AMD, recognized either by progressive atrophy of RPE (Dry AMD), non-neovascular intraretinal exudation, or macular neovascularization (MNV) (6, 8). Approximately 10-15% of all AMD patients develop neovascular AMD (nAMD) (9, 10), which includes type 1 macular NV (occult choroidal NV), type 2MNV (classic choroidal NV), and type 3 macular NV (11, 12).

Vascular Endothelial Growth Factor (VEGF) signaling plays a key role in vascular development and stimulation of ocular angiogenesis (13, 14). For this reason, anti-VEGF drugs, which include ranibizumab, aflibercept, bevacizumab, brolucizumab, and the recently FDA-approved faricimab (15), were established as first-line therapy for the management of diabetic macular edema (16), PDR (17, 18) and nAMD (19, 20). Nevertheless, anti-VEGF therapy requires frequent and costly intravitreal injections and has been associated with local side effects (e.g., endophthalmitis, cataracts, retinal detachment, vitreous hemorrhage, and increased ocular pressure) (1, 21). Furthermore, some patients exhibit only a moderate to poor response after continued intensive anti-VEGF treatment (22, 23). Although several therapeutic strategies have shown significant potential in preclinical studies and clinical trials (24–26), therapies for dry AMD are still commercially unavailable and its management relies on regular follow-up evaluation, the prevention of risk factors, and increased intake of vitamins and antioxidants (8, 24). Therefore, a better knowledge of the pathological mechanisms underlying the disease onset or progression could be helpful to explore effective therapeutic alternatives for the management of these proliferative eye diseases.

So far, the characterization of the proteome of the vitreous humor in DR/PDR has contributed extensively to the identification of target pathways and candidate biomarkers for its diagnosis and treatment (27–30). However, the validation of these potential biomarkers in a larger number of samples, essential for assessing their relevance in clinical practice, is frequently unaccomplished (31). On the other hand, few studies have focused on the characterization of vitreous proteomics in AMD (32–34). To elucidate the underlying pathological mechanisms, we have applied a label-free quantitative (LFQ) proteomics approach for the understanding of the vitreous proteome in PDR and AMD compared to idiopathic epiretinal membranes (ERM) samples. A scheduled multiple reaction monitoring (MRM) method was designed for potential biomarker verification in a larger cohort of human vitreous samples.

Material and methods

Collection of vitreous samples by pars plana vitrectomy

Vitreous samples were collected at the Ophthalmology Service of Leiria-Pombal Hospital, Portugal, as previously described (35), according to a protocol approved by the hospital ethics committee (Code: CHL-15481). All patients included in this study gave their informed consent, which adhered to the tenets of the Declaration of Helsinki. Vitreous samples were collected in sterile cryogenic vials at the beginning of pars plana vitrectomy by aspiration into a 2 mL

10.3389/fimmu.2023.1107295

syringe attached to the vitreous cutter. Upon collection, vitreous samples were placed immediately on ice and frozen at -80°C until further analysis. The medical history of the patients was assessed to confirm the diagnosis, baseline characteristics, and associated diseases. Demographic characteristics, including age and gender, and the description of corresponding vitreous samples are summarized in Table 1 (more details in Supplementary Table 1). Samples from patients subjected to intraocular surgeries or intravitreal drug treatments in the previous 3 months were excluded from the study. Most patients underwent surgery for ERM removal due to the marked decrease in visual acuity. For label-free proteomic analysis, 12 patients (7 women and 5 men) diagnosed with PDR (n=4), dry AMD (n=4), and ERM (n=4) were selected. Older patients or with other serious illnesses associated (e.g., neoplasia) were removed from the study. For MRM, a larger cohort (n=65) was used, including some of the samples previously analyzed in the LFQ experiment. MRM experiments were performed on vitreous samples from patients with ERM (n=21), DR/PDR (n=20), AMD (n=11), and rhegmatogenous retinal detachment (RRD) with and without proliferative vitreoretinopathy (PVR) (n=13). Finally, 27 patients were selected for Western Blot (WB) analysis, including patients with ERM (n=5), PDR (n=9), AMD (n=6), and RRD (n=7), from which 3 patients have PVR.

Preparation of vitreous samples

Vitreous samples were centrifuged at 18400 x g for 15 min at 4°C and supernatant protein concentration was determined using Pierce 660 nm protein assay (Thermo Fisher Scientific, Massachusetts, USA; RRID : SCR_008452), according to manufacturer's instructions. For the removal of high-abundant proteins, High Select™ Top14 Abundant Protein Depletion Mini Spin Columns (Thermo Fischer Scientific, Massachusetts, USA; RRID : SCR_008452) were used. Briefly, 300 µl of sample (400 µg of protein) was homogeneously mixed with the resin and incubated for 10 min at room temperature. Depleted vitreous samples were recovered by centrifugation at 1000 x g for 2 min and concentrated using Nanosep® Centrifugal Devices 10K (Pall, Madrid, Spain). Then, samples were solubilized with loading sample buffer, denaturized at 60 °C for 10 min, loaded, and concentrated in a 12% SDS-PAGE gel. After Quick Coomassie staining, protein bands were manually excised, cut into cubes (1 mm2), and placed in 96-well plates. In-gel tryptic digestion was performed automatically in a Proteineer DP robot (Bruker Daltonics, Bremen, Germany), as previously described (36). Tryptic peptides were extracted by adding 1% formic acid in 50% acetonitrile, collected from wells, dried by speed-vacuum centrifugation, and frozen at -20°C until further processing.

LC-MS/MS quantitative analysis

LC-MS/MS analyses were performed using a nanoLC Ultra 1D plus (Eksigent Technologies, AB SCIEX, Foster City, CA) coupled to a SCIEX TripleTOF 5600 Mass Spectrometer System (RRID : SCR_018053) *via* a Nanospray III source. Tryptic peptides were solubilized using solvent A (2% acetonitrile [ACN] in water, 0.1% FA) and the concentration was determined using Thermo Fisher Qubit fluorimeter (RRID : SCR_018095), according to manufacturer's instructions. Tryptic peptides (1 µg) were loaded on a C18 Acclaim PepMap™ 100 trapping column (Thermo Scientific, 100 µm I.D. × 2 cm, 5 µm particle diameter, 100 Å) using solvent A at 2 µL/min and, after desalting, switched online with an Acquity UPLC® M-Class Peptide BEH C18 analytical Column (Waters, 75 µm × 15 cm, 1.7 µm, 130 Å). Peptides were fractionated at a flow rate of 250 nL/min in a 250 min gradient with increasing concentrations of ACN (2% to 90%). TripleTOF 5600 system was operated in positive ion mode as follows: ion spray voltage 2300 V, curtain gas (CUR) 35, interface heater temperature (IHT) 150°C, ion source gas 1 (GS1) of 25, and declustering potential (DP) of 100 V. Data were acquired in information-dependent acquisition (IDA) mode with Analyst®TF 1.7 Software (SCIEX, USA; RRID : SCR_015785). IDA parameters

TABLE 1 Demographic characteristics of patients involved in the study and description of corresponding vitreous samples collected *via* pars plana vitrectomy.

		ERM[1] (n=25)	DR/PDR[1] (n=21)	AMD[1] (n=12)	RRD/PVR[1] (n=14)
Demographic characteristics	Gender[2]	F=6 M=19	F=7 M=14	F=7 M=5	F=5 M=9
	Age (Mean ± SD)	73± 15	60 ± 16	78 ± 6	70 ± 13
	Age (range)	9-88	22-79	70-92	41-94
	Eye Submitted to PPV[3]	LE=10 RE=15	LE=10 RE=11	LE=6 RE=6	LE=8 RE=6
Characterization of vitreous samples	Protein concentration (µg/µl, MD ± SD)	0.99 ± 0.92	2.15 ± 2.10	1.12 ± 1.05	1.32 ± 1.46
Experiments	Label-free quantitation	n=4	n=4	n=4	____
	Verification by MRM	n=21	n=20	n=11	n=13
	Western blot analyses	n=5	n=9	n=6	n=7

[1]ERM, Epiretinal membranes; DR/PDR, Diabetic retinoaphy/Proliferative diabetic retinopathy; AMD, Age-related macular degeneration; RRD/PVR, Rhegmatogenous retinal detachment/ Proliferative vitreoretinopathy. [2] F, Female; M, Male. [3] PPV, Pars plana vitrectomy; RE, right eye; LE, left eye.

were: survey scan in the mass range of 350–1250 m/z, accumulation time 250 ms, followed by MS2 spectrum accumulation for 100 ms (100–1800 m/z) in a cycle of 4.04 sec. MS/MS fragmentation criteria were: ions in the 350-1250 m/z range with a charge state of 2–5 and an abundance threshold greater than 90 counts. Dynamic exclusion was set to 15s. IDA rolling collision energy (CE) parameter script was used to control the CE.

Bioinformatics and statistical analysis

MaxQuant 1.6.5.0 (RRID : SCR_014485) was used to generate peak lists from raw files, peptide and protein identification after database search, and for LFQ intensity-based absolute quantification (iBAQ). Andromeda search engine was used to search the acquired MS/MS spectra against the UniProtKB Homo sapiens database (20418 reviewed protein sequences). Search parameters were set as follows: carbamidomethyl (C) as a fixed modification, oxidation (M), acetyl (Protein N-term), Gln→pyro-Glu and, Glu→pyro-Glu as variable modifications, trypsin/P as protease allowing up to 2 missed cleavages. Precursor mass tolerances were set at 20 ppm and the fragment mass tolerance at 0.01 Da. Proteins identified only with modified peptides ("only by site"), reversed sequences, and potential contaminants were removed. For LFQ, multiplicity was set at 1, LFQ min ratio counts at 2, and the options "iBAQ" and "match between runs" (time window of 0.7 min and alignment of 20 min) were selected. False discovery rate (FDR) of peptides and proteins was set at 1%. Additionally, mgf. files were generated using PeakView® Software (AB SCIEX, RRID : SCR_015786) and searched using Mascot v.2.2.04 (RRID : SCR_014322) against the homo sapiens UniProtKB reviewed database, as described above. Search parameters were identical to those previously described but peptide mass tolerance and MS/MS fragment tolerance were set to 25 ppm and 0.05 Da, respectively. FDR of ≤1% at the peptide level was assessed by applying a target-Decoy approach. Decoy sequence database contained reversed shuffled peptide sequences (37).

The protein normalized intensity lists of the 12 vitreous samples from PDR (n=4), nAMD (n=4), and ERM (n=4) groups were processed using Perseus 1.6.10.0 (RRID : SCR_015753). The normalized intensity was calculated by dividing the intensity of each protein by the sum of the intensity of all proteins detected in that sample and multiplying it by the median of the sum of the intensity of all proteins detected in vitreous samples. Depleted proteins, potential contaminants, reversed and proteins only identified by site were removed. Data were logarithmized (Log2), filtered by valid values (min 70% of valid values), and missing values were imputed with random numbers from a normal distribution (width=0.3, shift=1.8). Multi-scatter plots and histograms were applied to evaluate data quality. *Post-hoc* tests, hierarchical clustering, principal component analysis (PCA), and two-sample t-tests were performed for differentiating the three groups in terms of protein expression based on intensity differences. A permutation-based method was used to correct for multiple hypothesis testing with the number of randomizations set to 250 and an FDR<5%. Differentially expressed proteins were analyzed using DAVID (RRID : SCR_001881) (38), and ClueGO 2.5.7 (RRID : SCR_005748) (39) for functional enrichment based on gene ontology (GO) analyses and pathways/reactions (KEGG (RRID : SCR_012773) and Reactome (RRID : SCR_003485)). Protein-protein association networks were assessed using the online tool STRING 11 (RRID : SCR_005223), with high confidence (0.75), based on the molecular action (40).

Verification by multiple reaction monitoring

Proteotypic peptide transitions for MRM-based targeted proteomics analysis were selected using Skyline v. 19.1.0.193 (RRID : SCR_014080). MRM assays were performed in an Eksigent nanoLC Ultra 1D plus system (AB SCIEX, Foster City, CA) coupled to a SCIEX 5500 QTRAP 5500 Mass Spectrometer (RRID : SCR_020517)via a Nanospray III source. A scheduled method was designed for the relative quantitation of 35 proteins, using 2-3 proteotypic peptides per protein and 3-4 transitions per peptide (332 transitions in total). The Homo sapiens UniProtKB reviewed database was used as background proteome. The selected enzyme was trypsin/P [KR |-] and peptide parameters were set to: a length range of 8 to 25 amino acids, 2+ and 3+ charged, no missed cleavages, and potentially modified residues such as methionine (Met, M) and cysteine (Cys, C). When possible, peptides were selected to cover distinct regions of the protein sequence. As described above, 10 µg of non-depleted vitreous samples were loaded on an SDS-PAGE gel and in-gel digested. Peptide concentration was determined using Thermo Fisher Qubit fluorimeter (RRID : SCR_018095), according to manufacturer's instructions, and 1 µg of tryptic peptides was loaded onto a C18 Acclaim PepMapTM 100 column (Thermo Scientific, 300 µm I.D. × 5 cm, 5 µm particle diameter, 100 Å) using solvent A (2%B ACN, 0.1% formic acid in water) at 2 µL/min. After desalting, the trap column was switched online with a C18 BioSphere column (Nano-separations, 75 µm I.D. × 15 cm, 3 µm particle diameter, 120 Å) and peptides were fractionated in a 30 min gradient (4 to 90% of 100% ACN, 0.1% formic acid) at 300 nL/min, followed by 15 min of equilibration to initial conditions. The 5500 QTRAP system was operated in positive polarity and MRM scan mode, with an ion spray voltage of 2800 V, IHT of 150 °C, CUR of 20, GS1 of 25, medium collision gas, and DP of 80 V. Scheduled mode was enabled and detection window set at 300 sec. Collision energy and expected retention time for each transition were defined in Skyline. Beta-galactosidase standards and a pool of vitreous samples were injected alternately with the vitreous samples to monitor oscillations in the MS signal and in the retention time. Raw MS data were imported into Skyline and the automatically selected transition peaks were manually revised considering the retention time and the intensity distribution of the selected transitions. The total area of each protein was calculated by summing the area of the respective peptides (calculated as the sum of all peptide transitions). To correct the fluctuations in MS signal over time, the calculated total area of each protein was normalized by dividing it by the total area of digested beta-galactosidase (injected between each batch) and multiplying by the median. Statistical analysis by one-way ANOVA (Tukey's HSD) and *post-hoc* tests and multivariate statistical analyses were performed using Metaboanalyst v5.0 (RRID : SCR_015539) (41). Partial least squares discriminant analysis (PLS-DA) was used to build a predictive model to define a panel of discriminatory biomarkers of vitreoretinal diseases. The predictive ability (Q2), R-Squared (R2), and accuracy of the model were calculated *via* cross-validation to define the optimal number of components for classification. Classical univariate and

multivariate exploratory receiver operating characteristic (ROC) analyses were performed to evaluate the diagnostic potential of discriminatory proteins between the disease groups. ROC curves were generated in multivariate exploratory analyses by Monte-Carlo cross-validation using balanced sub-sampling, in which two-thirds of the samples are used to evaluate the feature importance. For model building, PLS-DA was defined as classification method and PLS-DA built-in as the feature ranking method, while the number of latent variables was defined to 2.

Western blotting assays

For western blot analysis, equal amounts of proteins (15 µg) were separated by SDS-PAGE and transferred to a PVDF membrane using the Trans-Blot Turbo™ Transfer System (Bio-Rad Laboratories, Hercules, CA, USA). After blocking with 5% of powdered milk in 0.1% Tween-20, membranes were incubated overnight at 4°C with distinct antibodies in 5% of BSA. These included 1:3000-diluted polyclonal rabbit anti-human chromogranin-A (CHGA) antibody (Agilent Cat# A0430, RRID : AB_2847855), 1:500-diluted polyclonal rabbit anti-tissue inhibitor of metalloproteinase inhibitor 2 (TIMP2) antibody (Abcam Cat# ab74216, RRID : AB_1271228), 1:1000-diluted monoclonal mouse anti-β-Amyloid (APP) antibody (Sigma-Aldrich Cat# A5213, RRID : AB_476742), and 1:500-diluted monoclonal mouse anti-cystatin C (CYTC) antibody (sc-515732; Santa Cruz Biotechnology). Thereafter, PVDF membranes were incubated with a 1:10000 dilution of anti-mouse IgG (Fab specific)–Peroxidase antibody (Sigma-Aldrich Cat# A3682, RRID : AB_258100) or anti-Rabbit IgG (whole molecule)–Peroxidase antibody (Sigma-Aldrich Cat# A0545, RRID : AB_257896). Protein bands were visualized using the Clarity Western ECL Substrate (Biorad, Hercules, CA, USA). Band detection and relative quantification were performed using Image lab 5.0 software (Biorad, Hercules, CA, USA, RRID : SCR_014210). Statistical analyses (Kruskal-Wallis tests, q-value<0.05) were performed using GraphPad Prism (RRID : SCR_002798).

Results

Vitreous proteome in diabetic retinopathy and age-related macular degeneration

For the discovery phase, LFQ quantitative proteomics was applied to analyze the proteome of vitreous collected from patients with DR (n=4), dry AMD (n=4), and ERM (n=4). Using two different strategies for protein database search, a total of 680 proteins were identified, of which 586 proteins were identified by MASCOT and 580 proteins by MaxQuant (corresponding to 474 protein groups) (Supplementary Table 2). The mass spectrometry proteomics data have been deposited to the ProteomeXchange Consortium *via* the PRIDE (42) partner repository with the dataset identifier PXD038285. An average of 366 ± 31 protein groups was identified in control ERM vitreous, 361 ± 46 protein groups in dry AMD, and 310 ± 14 protein groups in PDR. A total number of 195 protein groups were detected in all the samples. Multiple scatter plots (Supplementary Figure 1) were applied to assess data reproducibility and correlation within and between disease groups and showed high data reproducibility. The best correlation values between replicates and within groups was found for PDR samples (average 0.89 ± 0.02), but samples from dry AMD and ERM groups also showed good correlation values within groups (average 0.87 ± 0.05). Sample correlation was higher within than between groups, except for the dry AMD group. One of the samples collected from a patient with dry AMD (VH 219) showed a poorer correlation (< 0.8) with other dry AMD samples and a higher correlation with samples from the PDR group (> 0.87). For this reason, this sample was removed from quantitative analysis, improving within-group Pearson correlation values from an average of 0.84 ± 0.06 to 0.90 ± 0.01 (Supplementary Figure 1).

Subsequently, *post-hoc* tests and hierarchical clustering were performed to differentiate the three groups in terms of protein expression based on intensity differences. *Post-hoc* tests revealed that 96 proteins are differentially expressed among the three disease groups. Specifically, 83 and 79 proteins differed between PDR and ERM or between PDR and dry AMD groups, respectively (Supplementary Table 3). Hierarchical clustering analysis of these 96 proteins is represented in a heatmap based on their intensities normalized to log base 2 (Figure 1A). Figure 1A reveals that most of these proteins are downregulated in PDR compared to ERM and dry AMD groups (blue cluster), except for a small cluster (orange cluster) composed mainly of complement (C5, C2, CFH) and coagulation factors such as prothrombin (THRB), among other proteins. Only inter-alpha-trypsin inhibitor heavy chain H3 (ITIH3) differentiates the dry AMD from ERM control samples in hierarchical clustering, as represented in a pink cluster (Figure 1A). These proteins were compared with those found differentially expressed in vitreous from DR and AMD in previous proteomics studies (Supplementary Table 3). Furthermore, multiple t-tests with an FDR cutoff of 5% were performed to identify differentially expressed proteins in PDR versus dry AMD and PDR versus ERM (Figures 1B, C and Supplementary Table 3). We found 118 significantly regulated proteins (17 up- and 101 down-) and 95 proteins (10 up- and 85 down-) in PDR relative to the ERM and dry AMD groups, respectively. Most of the proteins (5 up- and 76 down-regulated proteins) differentiated between PDR and either of the two other diseases, but 14 and 37 proteins were unique to the comparison with the dry AMD and ERM groups, respectively. Fetuin-B, keratin, type II cytoskeletal 2 epidermal, and serum amyloid P-component showed the highest levels of expression in PDR (FDR<0.001), while the more significant down-regulated proteins were protein CREG1, neural cadherin (CADH2), galectin-3-binding protein (LGALS3BP), Putative phospholipase B-like 2, and CYTC. LGALS3BP and CYTC were also significantly downregulated in PDR versus dry AMD, as well as cathepsin Z (CATZ), spondin-1 (SPON1), and tenascin-R (TNR). Complement C2 (C2) showed the most statistically significant change in the PDR group compared to dry AMD with an FDR lower than 0.001 (Figure 1C). Other complement factors (e.g., CFB, C8B), acute-phase response proteins (e.g., alpha-2-antiplasmin), and proteins related to lysosomal degradation (e.g., alpha-N-acetylgalactosaminidase, Prosaposin, Cathepsin L1) and ECM organization (metalloproteinase inhibitor 1 [TIMP1]) showed differential expression only in PDR compared to ERM. Although

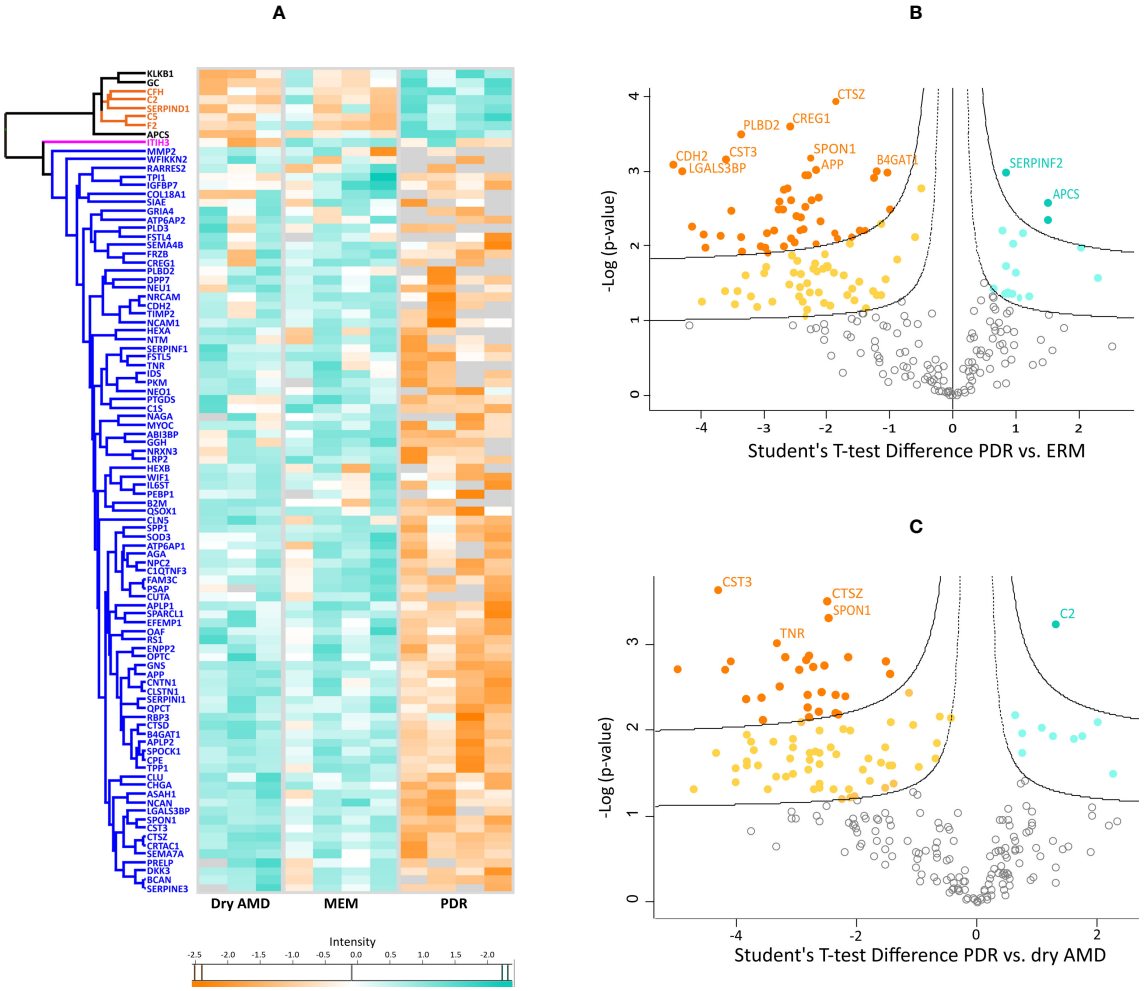

FIGURE 1
(A) Heatmap representing the intensities normalized to log base 2 and analyzed by hierarchical clustering of 96 proteins found differentially expressed among the three disease groups in posthoc tests. Hawaii plots display the proteins found up-regulated (blue-green) and down-regulated (orange) in proliferative diabetic retinopathy (PDR) compared to patients with **(B)** epiretinal membranes (ERM) and with **(C)** dry age-related macular degeneration (dry AMD).

some proteins such as ProSAAS, neurosecretory protein VGF, or phosphoglycerate mutase 1 were exclusively detected in dry AMD samples, no differential proteins were found compared to ERM controls with an FDR<5%.

Functional enrichment of differentially expressed proteins

To gain insights into the biological roles and pathways of the differentially expressed proteins, these were analyzed using bioinformatics tools such as DAVID, ClueGo (Cytoscape app), and STRING. Functional enrichment indicates that proteins underexpressed in PDR are highly correlated and share common biological processes/pathways such as extracellular matrix (ECM) disassembly and organization, platelet degranulation, lysosomal degradation, cell adhesion, and central nervous system development (e.g., regulation of axon regeneration) (Figures 2A, B and Supplementary Table 4). Some of these underexpressed proteins, including beta-hexosaminidase (HEXA, HEXB) and N-acetylglucosamine-6-sulfatase (GNS), are involved in chondroitin sulfate and keratan sulfate catabolic processes (Figure 2C). Furthermore, some of the proteins involved in these processes also participate in cell adhesion and ECM organization (e.g, brevican core protein [BCAN] and neurocan core protein [NCAN]) or are themselves ECM components such as prolargin. In turn, proteins related to acute-phase responses and fibrin clot formation are only found upregulated in PDR compared to ERM, whereas complement and coagulation proteins are up-regulated in PDR in both comparisons. According to GO classification for molecular function (Figure 2D), both up- and downregulated proteins in PDR have serine-type endopeptidase activity (7.0- and 6.0-fold enrichment), serine-type endopeptidase (18.5- and 17.6-fold) and metalloendopeptidase inhibitor activities (46.7- and 35.6-fold), or binding function (e.g., heparin and calcium). On the other hand, down-regulated proteins have serine-type carboxypeptidase activity (32.0- and 54.2-fold) and/or binding functions or are ECM structural constituents (13.4- and 14.2-fold). According to GO classification for cellular components (Figure 2E), most of the differentially expressed proteins are localized extracellularly and, notoriously, many of them are associated with extracellular exosomes (87 proteins). A significant part of downregulated proteins in PDR compared to ERM and dry AMD are in

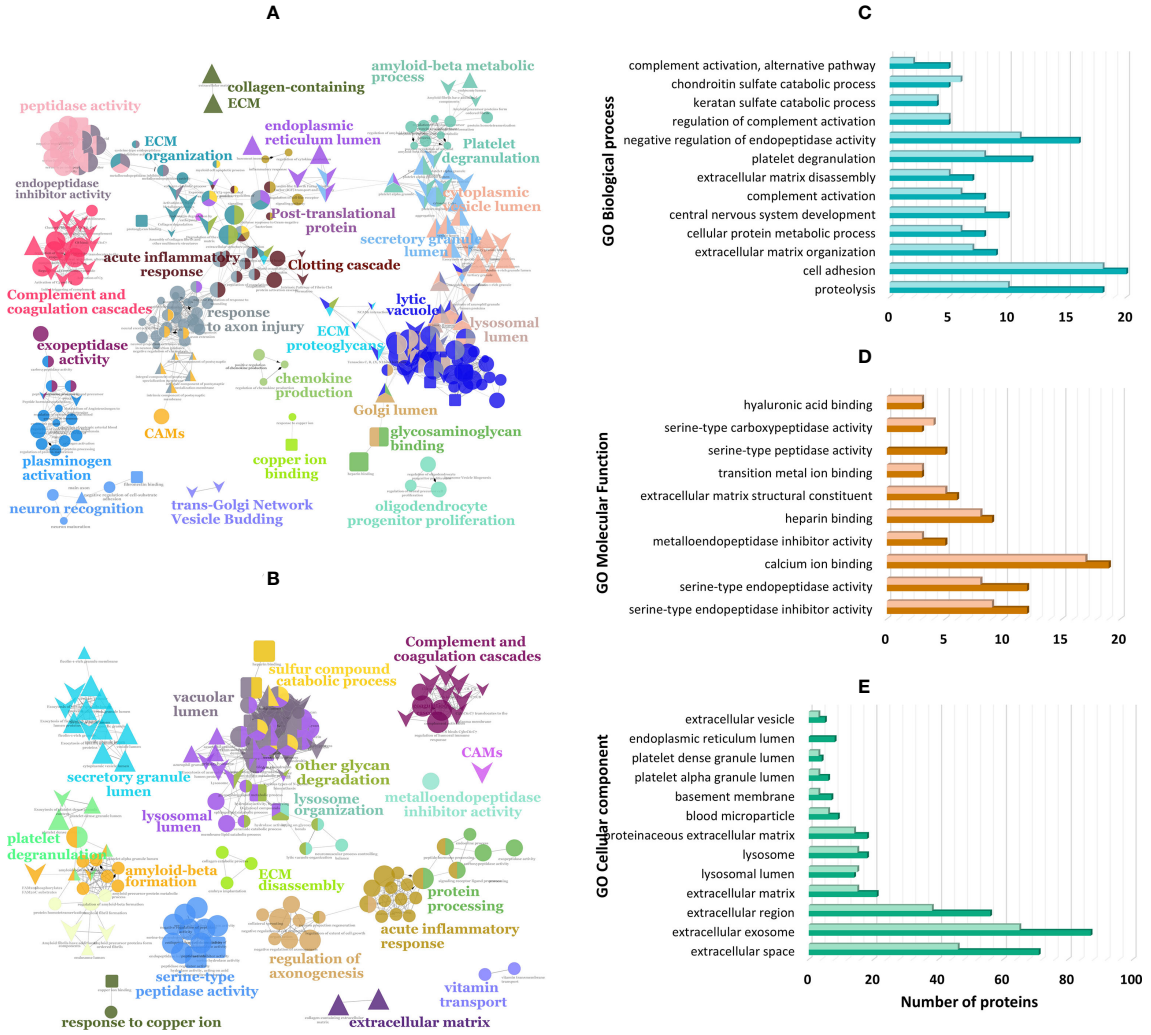

FIGURE 2
Functionally grouped network of enriched categories generated in ClueGO (Cytoscape app) for the proteins found differentially expressed in proliferative diabetic retinopathy (PDR) compared to patients with **(A)** epiretinal membranes (ERM) and with **(B)** dry age-related macular degeneration (dry AMD). These proteins were also classified according to gene ontology (GO) terms using DAVID Bioinformatics tool and ClueGo for **(C)** biological process, **(D)** molecular function, and **(E)** cellular component with the darkest colors representing proteins differentially expressed in PDR versus ERM, and lightest colors representing proteins differentially expressed in PDR versus dry AMD.

the basement membrane (13.7- and 7.3-fold enrichment), the lysosomal lumen (25.4- and 33.9-fold enrichment), and secretory vesicles, such as platelet dense granule (44.1 and 41.1-fold enrichment), whereas overexpressed proteins are mainly blood microparticles. Many of the proteins found underexpressed in PDR compared to ERM and dry AMD are related to ECM with fold enrichment of 11.0 and 9.7, respectively. Although less significant, many underregulated proteins are localized in the neuronal cell body, axons, node of Ranvier, perineuronal nets, and postsynaptic membranes.

Differentially expressed proteins were collated using the DAVID bioinformatics tool (Supplementary Table 4). Proteins involved in pathways such as complement and coagulation cascades, lysosomal degradation, ECM organization, and regulation of inflammatory response, were found associated with type 2 diabetes and macular edema, whereas the pigment epithelium-derived factor (PEDF) and serine protease HTRA1 were found specifically related to DR. These two proteins, as well as complement components (e.g., CFH, C2), regulators of complement cascades (clusterin (CLU)) and amyloidosis proteins (amyloid-beta precursor protein [APP], CYTC3) are also associated to macular degeneration and pathological processes, such as choroidal neovascularization, geographic atrophy, and retinal drusen.

In addition, STRING was used to generate high-confidence (0.70) protein-protein interaction networks between the 118 and 95 differentially expressed proteins in PDR versus ERM (Figure 3A) and PDR versus dry AMD, respectively (Figure 3B). Some biological processes/pathways stand out in both analyses, including multicellular organism and nervous system development, myeloid leukocyte activation, regulation of proteolysis, and cell adhesion, as well as proteins associated with lysosomes. These data reinforce that ECM organization, complement and coagulation cascades, and inflammatory responses are relevant in these diseases. Specific pathways/terms such as regulation of insulin-like growth factor (IGFs) transport and uptake by insulin-like growth factor binding proteins (IGFBPs), amyloidosis, neurodegeneration, metabolism of angiotensinogen to angiotensin, post-translational modifications (e.g.,

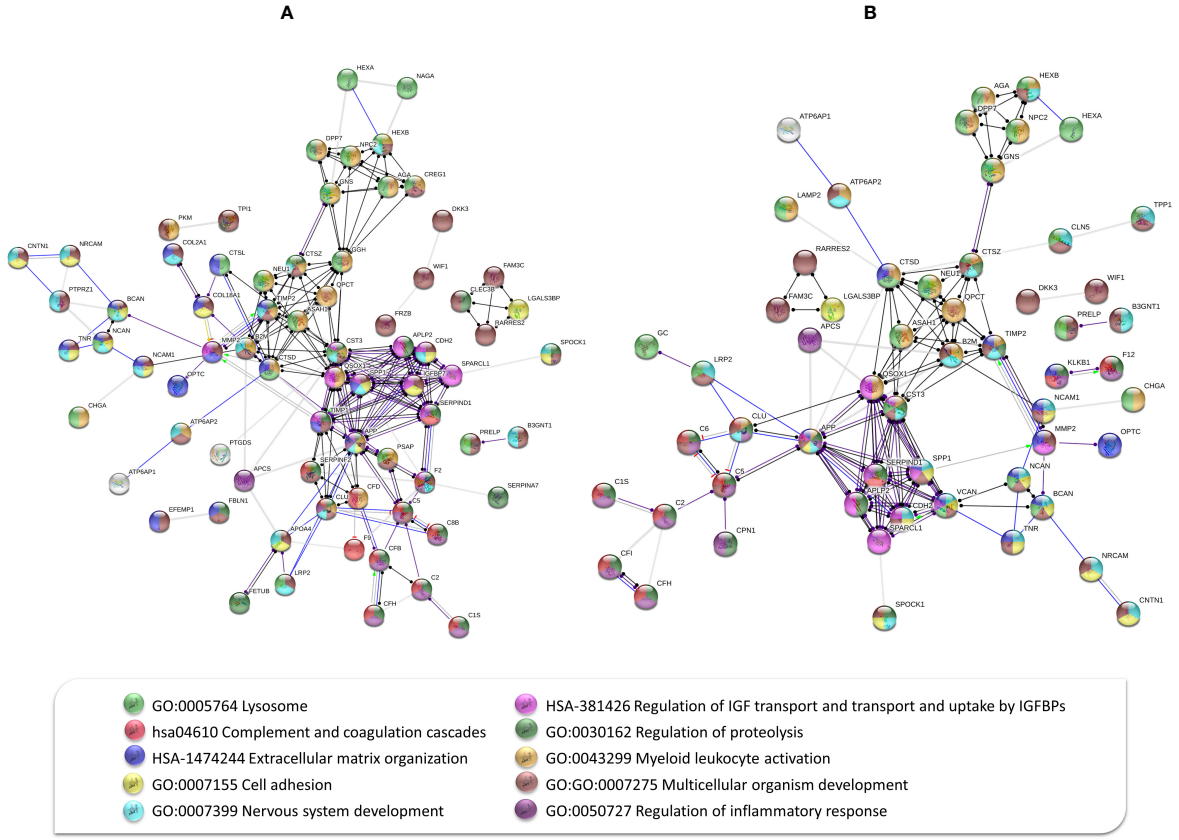

FIGURE 3
Protein-protein interaction network between **(A)** 118 differentially expressed proteins in proliferative diabetic retinopathy (PDR) versus epiretinal membranes (ERM), and **(B)** 95 differentially expressed proteins in PDR versus dry age-related macular degeneration based on molecular action with high confidence (0.70). Some biological processes/pathways stand out in both interaction networks, including complement and coagulation cascades, lysosomal degradation, cell adhesion, extracellular matrix organization, multicellular organism, and nervous system development, among others, as represented by colored nodes.

phosphorylation), and regulation of Wnt signaling and MAPK cascades were also found associated to differentially expressed proteins. Remarkably, several proteins, including APP, CLU, CYTC, CATZ, osteopontin (OSTP), TIMP2, and lecticans (e.g., NCAN and BCAN), play key roles in multiple pathways, as seen in Figure 3.

Selection of potential biomarkers for verification by multiple reaction monitoring

Several potential biomarkers were selected for further verification by targeted proteomics (MRM). Selection was performed according to their statistically significant differential expression levels found in the discovery phase (LFQ experiment), their interaction with other proteins as described in STRING interaction network, and the pathways in which they are involved. Among the selected biomarkers there are proteins involved in complement and coagulation cascades, amyloidosis, ECM organization, cell adhesion, and lysosomal enzymes, among others (Supplementary Table 5.1). Selection criteria considered the number of unique (specific) peptides detected for each protein and the signal-noise ratio in the fragmentation spectrum to increase the probability to detect the proteins by MRM in non-depleted vitreous samples. Some of the biomarkers reported in previously published proteomics studies, such as alpha-1-antitrypsin (A1AT), were also considered. A1AT, which was depleted in the discovery phase, is an acute-phase protein highly abundant in vitreous that was selected as a potential biomarker according to previous studies performed in AMD (32), RD/PVR (43–45), and DR/PDR (43, 46–50). Some of the biomarkers selected from proteins found differentially expressed here were reported in our previous study (51), including retinoschisin (XLRS1) and LGALS3BP. Both were found upregulated in rhegmatogenous retinal detachment (RRD) compared to ERM, while coagulation factor IX (F9) and complement components C8 chain (C8) and C2 were found down-regulated. Alpha-1-antichymotrypsin (AACT) and complement component C9 (C9), non-reported as differential in the present study, were also considered for verification. Therefore, a group of patients with RRD, without and with PVR, were included in this verification. MRM experiments were performed on vitreous samples from patients with ERM (n=21), DR/PDR (n=20), AMD (n=11), and RRD/PVR (n=13). The final scheduled MRM method including the list of potential biomarkers and the corresponding peptides and transitions monitored, as well as other parameters, is detailed in the Supplementary Table 5.1.

Of the 35 proteins analyzed, MRM results for TIMP2 and CHGA were not considered for quantitation due to the poor-quality quantitative data. CHGA was undetected in many samples, whereas in the case of TIMP2 only a peptide could be detected with few

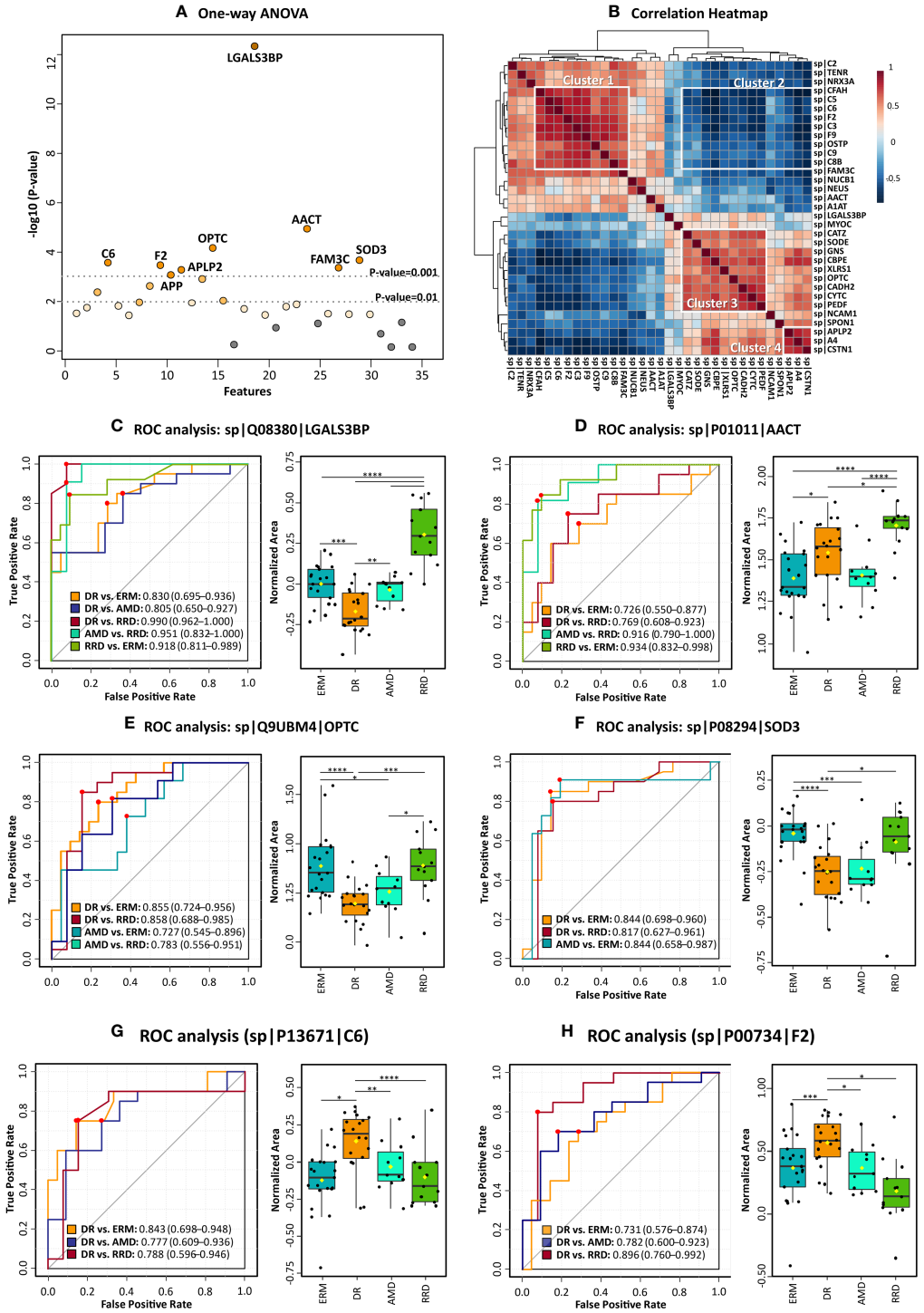

FIGURE 4
Statistical analysis of candidate vitreous biomarkers analyzed by multiple reaction monitoring was performed by MetaboAnalyst5.0 **(A)** One-way ANOVA plot with the more statistically relevant biomarkers highlighted with different orange grades (stronger colors represent more significant p-values). **(B)** Heatmap showing the correlation between different candidate biomarkers. **(C–H)** Results of univariate biomarker analysis of the top six candidate biomarkers in one-way ANOVA analysis, including the ROC curves for statistically significant comparisons between groups and respective box plots. Data is presented in the box plots as median ± SD and the statistical analysis was performed by two-sample t-tests, with the symbol asterisk determining the statistical significance. *p-value<0.05, ** p-value<0.01, ***q-value<0.001, and ****q-value≤ 0.0001.

10.3389/fimmu.2023.1107295

transitions. However, these proteins were analyzed by WB analysis (Supplementary Figure 3). CHGA was found downregulated by LFQ in patients with PDR compared to dry AMD and ERM, but this result could not be confirmed by WB analysis. In opposition to the LFQ results, MRM analysis showed that TIMP2 levels are increased in PDR compared to ERM and AMD groups. Additionally, TIMP2 levels are significantly lower in RRD/PVR group, and it was not even detected in two samples (HV 500 and HV 785).

Evaluation of discriminatory biomarkers of vitreoretinal diseases

One-way ANOVA, *post-hoc* tests, and classical univariate ROC curve analyses were performed in MetaboAnalyst to evaluate the potential of the candidate biomarkers to discriminate between the different vitreoretinal diseases understudy (Supplementary Table 5, Figure 4A). One-way ANOVA and *post-hoc* tests showed that 26 out of the 35 analyzed proteins were verified as differential between the different groups. ROC analysis of PEDF, A1AT, and NUCB1 showed that these biomarkers also have the power to discriminate between groups accordingly, but they show more modest area under the curve (AUC) values compared to other biomarkers (0.7<AUC<0.8, p-value<0.05). Furthermore, correlation analysis showed that there is a strong correlation between the levels of these candidate biomarkers, standing out of 4 correlation clusters (Supplementary Table 5.5; Figure 4B).

Among all quantified proteins, LGALS3BP, AACT, and OPTC showed the highest potential to differentiate between groups with AUC>0.85 (ANOVA p-value<0.0001), as seen in Figures 4C–E. The high levels of LGALS3BP found in RRD groups by MRM analysis confirms our previous data (51). Therefore, this biomarker candidate could distinguish proficiently RRD patients from the other disease groups (0.8>AUC>0.99, p-value< 5,00E-03). The LGALS3BP downregulation in DR compared to ERM and AMD has also been confirmed, allowing this candidate biomarker to distinguish this disease from ERM (AUC=0.83, p-value=1.02E-04) and AMD (AUC=0. 80, p-value=4.61E-03). AACT was found to be upregulated in RRD compared to ERM, in contrast with our previous iTRAQ results (51). The highest levels of AACT were found in the RRD group, discriminating this group from the others with high efficiency, especially from ERM (AUC=0.93, p-value=6.94E-06) and AMD (AUC=0.92, p-value=4.55E-05). The downregulation of OPTC in DR compared to both AMD and ERM was also verified. OPTC allowed to efficiently differentiate DR (AUC≥0.85, p-value ≤ 1.23E-04) and less efficiently AMD (AUC≥0.73, p-value ≤ 0.05) from ERM/RRD. Furthermore, the correlation heatmap (Figure 4B) shows that OPTC levels correlate inversely with coagulation and complement components (cluster 2). However, OPTC correlated directly with other proteins that were also verified as downregulated in DR (cluster 3). The last ones include carboxypeptidase E (CBPE), CYTC, and the extracellular superoxide dismutase [Cu-Zn] (SOD3), as well as vitreous antiangiogenic factors (PEDF), lysosomal enzymes (GNS), and cell adhesion factors (CADH2, XLRS1, and CSTN1). All these proteins were capable of differentiating DR from ERMs (AUC≥0.71, p-value ≤ 0.05), whereas PEDF, CYTC, XLRS1, and SOD3 also can discriminate patients with DR from RRD (AUC≥0.75, p-value ≤ 2.15E-02). Indeed, SOD3 showed to be one of the more efficient biomarkers in distinguishing DR from ERM/RRD groups (0.82≤AUC ≤ 0.84; p-value ≤ 1.41E-02) and one of the few biomarkers to differentiate AMD from ERM (AUC=0.84, p-value=9.33E-04).

Also related to cluster 3, the downregulation of several adhesion molecules in PDR compared to ERM/AMD was confirmed by MRM, except for neurexin-3 (NRX3A), whose PDR levels were higher than in ERM (Supplementary Table 5.2). NRX3A, along with SOD3 and OPTC, is unique in its ability to differentiate between AMD and ERM groups (AUC=0.75, p-value=1.51E-02). Several adhesion molecules are capable to discriminate between DR and ERM (Supplementary Table 5.4) but CDH2, calsyntenin-1 (CSTN1), and LGALS3BP showed better efficacy with AUCs higher than 0.76 (p-value<1.00E-02). In turn, CSTN1 and LGALS3BP showed a great potential to differentiate between DR and AMD with AUC of 0.81 (p-value=1.16E-03) and 0.80 (p-value=1.57E-03), respectively. In turn, the lowest SPON1 levels were detected in the RRD group, confirming this protein as a good discriminatory biomarker when compared to AMD (AUC=0.81, p-value=6.46E-03) and ERM groups (AUC=0.80, p-value=7.65E-03), but not from DR. MRM analysis could not confirm the downregulation of OSTP in DR, but distinguished RRD from DR very efficiently (AUC=0.87, p-value=1.63E-04).

The upregulation of several complement and coagulation components was confirmed in DR versus ERM and AMD, which allows differentiate DR from the other disease groups with high sensitivity and specificity (AUC≥0.69, p-value<0.05). Furthermore, the levels of these components correlated positively (cluster 1, Figure 4B). However, correlation was negative (correlation value<-0.7, p-value<1.00E-04) with CSTN1, CBPE, GNS, and A4 levels (cluster 2, Figure 4B). In fact, these factors can only distinguish between RD and other pathologies. C6, CFH, and C5 showed more efficiency to differentiate between DR and ERM, with AUC≥0.83 (p-value ≤ 1.00E-03), but CFH was not capable to differentiate DR from the other groups. On the other hand, we could not confirm the previously reported downregulation of C8B, C9, and F9 in RRD (51) in comparison to ERM/AMD, but these differences are significant when compared to DR, allowing to differentiate them (AUC≥0.75, p-value<0.05). THRB discriminated very efficiently patients with DR from RRD (AUC=0.90, p-value=3.75E-05), whilst coagulation factor IX (F9) distinguished reliably patients with DR from AMD (AUC=0.87, p-value=5.64E-04) and RRD (AUC=0.80, p-value= 1,35E-03). Although the levels of most of the complement and coagulation components are very similar in these two pathologies, DR and AMD groups could be distinguished with AUC≥0.76 (p-value≤ 0.05) by several proteins, including F9, THRB, C5, and C3.

Another small cluster is related to proteins associated with amyloidosis (Figure 4). Downregulation of CYTC, APP, and amyloid-like protein 2 (APLP2) was confirmed by MRM (Supplementary Table 5, Figure 5). Noticeably, changes in expression levels of APP and APLP2 are quite similar, showing a high correlation value (Pearson correlation=0.80). The highest levels were found in AMD, and this difference is highly significant when compared with DR and RRD groups, where the levels are the lowest. The analysis of CYTC by MRM confirmed its statistically significant downregulation in DR samples compared to ERM and AMD groups, as well as to RRD. APP, CYTC, and APLP2 discriminate efficiently

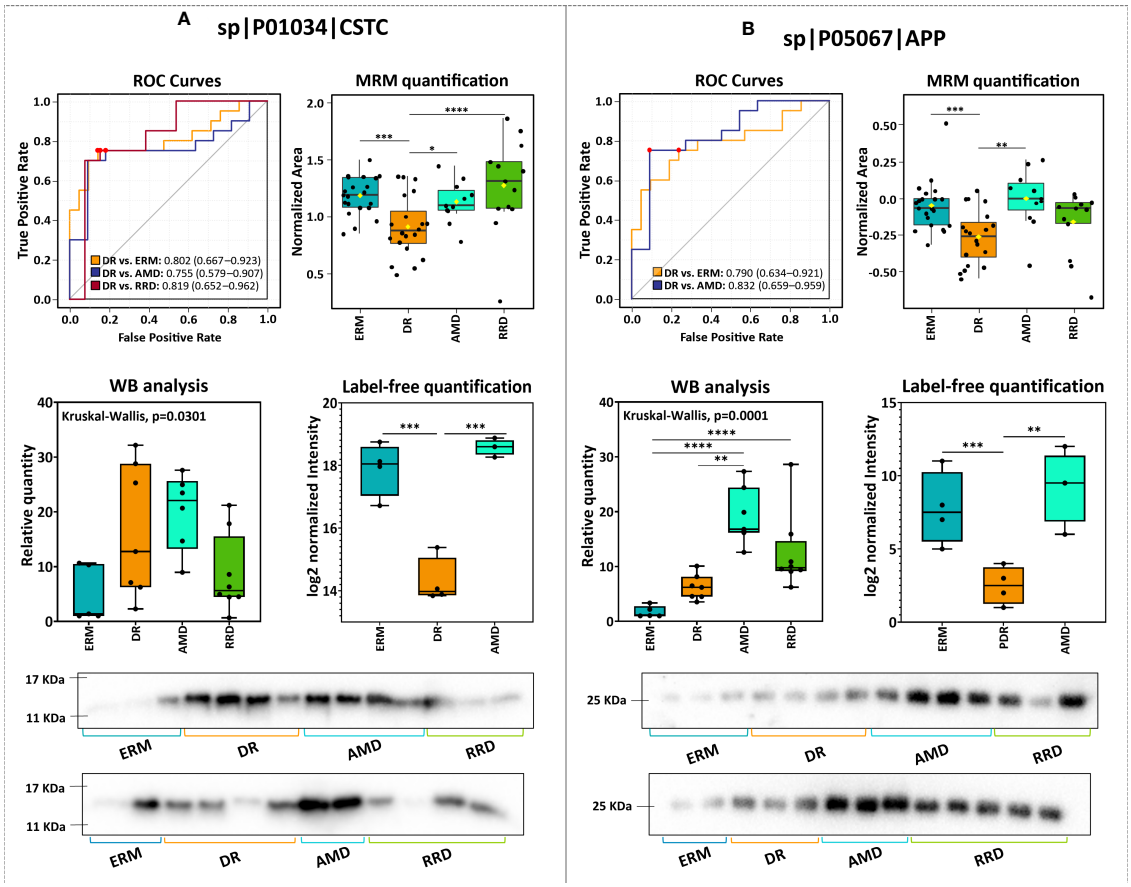

FIGURE 5
Comparison of the results of the analysis of **(A)** cystatin-C (CST3) and amyloid-beta (APP) by label-free quantitation (LFQ), multiple reaction monitoring (MRM), and western blot (WB), and respective ROC curves.

DR from ERM (AUC≥0.78, p-value<1.00E-03) and AMD (AUC≥0.75, p-value<0.05). CYTC is capable to differentiate RRD from DR (AUC=0.82, p-value=4.53E-03), whereas APLP2 differentiated this group from ERM (AUC=0.72, p-value=7.16E-03) and AMD samples (AUC=0.84, p-value=1.36E-02). APP and CYTC expression levels were also confirmed by WB analysis (Figure 5 and Supplementary Figures 3), showing the downregulation of both proteins in PDR compared to AMD, but not to ERM controls. Interestingly, the APP precursor was not detected in WB analysis but two bands corresponding to APP fragments, a strong band at 25 kDa (APP fragment), and a faint band between 48 kDa and 63 kDa (Supplementary Figure 3.1).

Considering these results, partial least squares discriminant analysis (PLS-DA) was used to build a predictive model to define a panel of discriminatory biomarkers of vitreoretinal diseases. Using this strategy, a panel of fifteen candidate biomarkers was defined (Figure 6A). PLS-DA model showed high predictive ability (Q2) and accuracy (Figure 6C). According to 3D PCA, this biomarker panel is capable to separate all vitreoretinal conditions, although this separation is more evident for RRD group (Figure 6B). Furthermore, multivariate Exploratory ROC analysis were performed to assess the sensitivity/specificity of this panel of biomarkers (Figure 6D). In all comparisons between groups, the use of all 15 proteins from the panel provides the best predictive accuracy, although this value (>90%) is better when RRD group is compared with the other (Supplementary Figures 4). Multivariate ROC curves showed a very good sensitivity/specificity for all comparisons but the best results were obtained for RRD group compared with ERM (AUC=0.996), DR (AUC=0.97), and AMD (AUC=0.968) (Figure 6D).

Discussion

The study of the vitreous proteome has gained increasing interest to understand the pathophysiological mechanisms underlying eye diseases. Many researchers have contributed to the characterization of the human vitreous proteome in diverse pathologies, such as DR (27–30), AMD (32–34), RRD (51–55), PVR (44, 45, 56, 57), and ERM (58–62). Although the study of the vitreous proteome promises to elucidate some of the pathogenic mechanisms underlying vitreoretinal diseases, the demand for reliable vitreous biomarkers has not yet been met (63, 64). Therefore, the validation of the proposed biomarkers in a large number of samples could be decisive to assess their relevance in clinical practice (31). In this work, an LFQ-based method was applied first in the discovery phase to compare the vitreous proteome in patients affected with PDR, dry AMD, and ERM with the aim of unraveling the pathophysiological mechanisms of these diseases. This approach allowed us to identify 118 proteins differentially expressed (17 up- and 101 down-) in PDR compared to ERM patients, whereas 95 proteins (10 up- and 85 down-) were found differentially expressed in PDR compared to

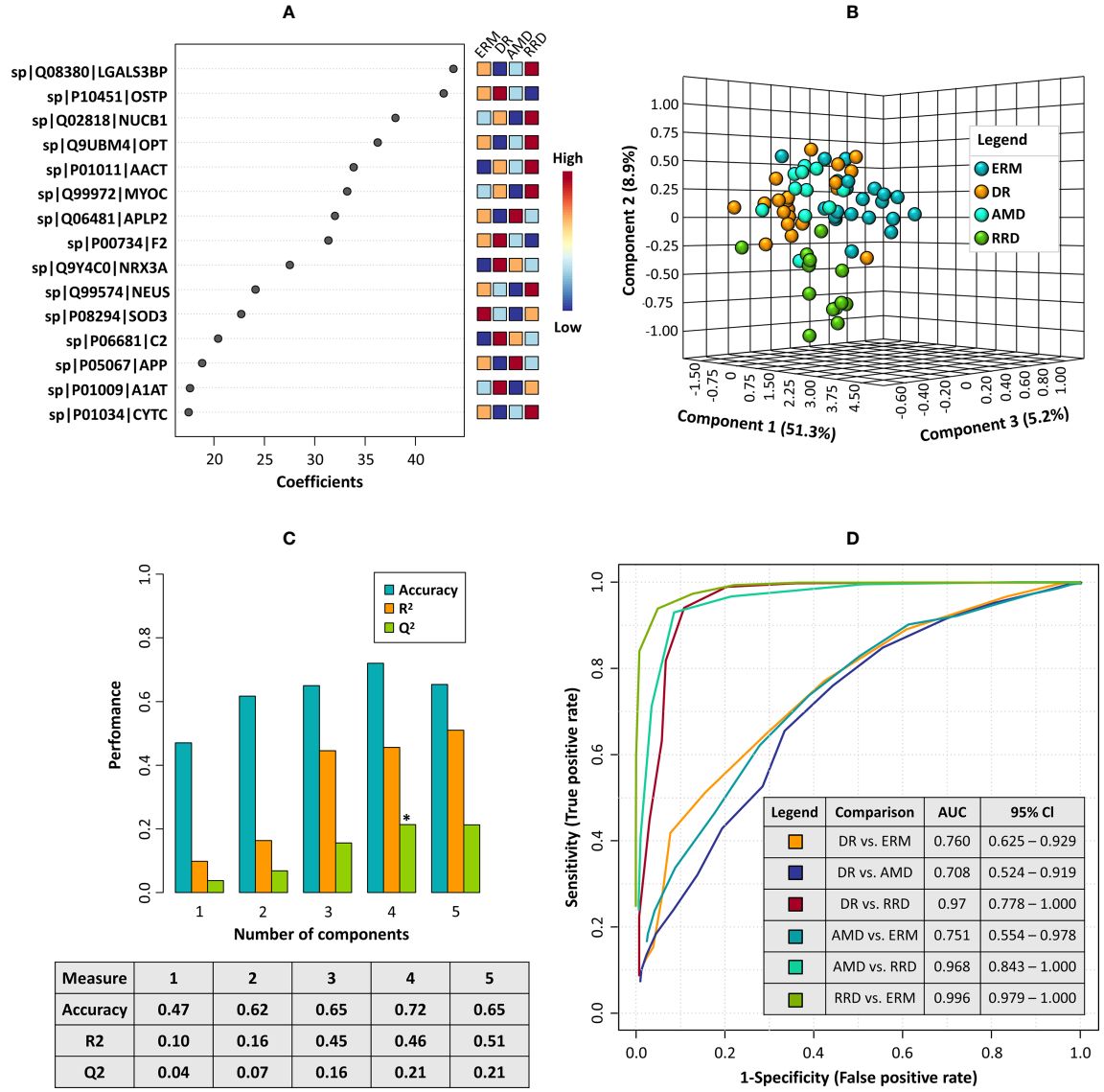

Measure	1	2	3	4	5
Accuracy	0.47	0.62	0.65	0.72	0.65
R2	0.10	0.16	0.45	0.46	0.51
Q2	0.04	0.07	0.16	0.21	0.21

FIGURE 6
(A) The plot of the top fifteen candidate biomarkers according to the partial least squares discriminant analysis (PLS-DA) model. **(B)** 3D principal component analysis (PCA) plot shows the separation between disease groups based on the top fifteen candidate biomarkers panel **(C)** Barplot representing the values of predictive ability (Q2), R-Squared (R2), and accuracy calculated for the PLS-DA model in the cross-validation analysis. **(D)** Combined ROC curves showing the results of multivariate receiver operating characteristics for the panel of 15 candidate biomarkers, including the area under the curve (AUC) and the confidence intervals (95% CI) for each comparison between different disease groups.

nAMD patients. Functional enrichment analyses suggested that proteins up-regulated in PDR are mainly associated with immune system biological processes such as complement, coagulation cascades, and acute-phase responses. On the contrary, the analysis of downregulated proteins shows that vitreous from ERM and nAMD compared to PDR patients are enriched in adhesion and neuronal proteins, lysosomal proteases, and other proteolytic enzymes, as well as in ECM components. In turn, no significant differences were observed comparing the vitreous of patients with AMD and ERM (only ITIH3 differentiates these diseases), suggesting that these diseases share common pathophysiological mechanisms. Moreover, one of the dry AMD samples correlated more strongly with PDR samples rather than with samples of its own pathological group. This suggests that, at an earlier stage, AMD pathogenesis could share common molecular mechanisms with ERM, but after progressing to a proliferative etiology, it partially resembles PDR. Our assumption is that differences found in the vitreous proteome could be considered as a source of potential biomarkers for better stratification of eye diseases. Consequently, we selected several candidate biomarkers for further verification by MRM-based targeted proteomics. From the initial list of 35 candidate biomarkers, MRM verified 26 proteins involved in diverse biological processes and with the potential to differentiate between the disease groups.

The low levels of complement and coagulation cascades in the eye are characteristic of its immune-privileged status, contributing to retinal homeostasis and integrity (65–67). Chronic activation of complement and coagulation pathways has been implicated in a variety of pathophysiological features, including increased vascular permeability (68, 69), loss and activation of choriocapillaris endothelial cells (70, 71), inflammation (71, 72), and loss of

photoreceptors (66). From the first experiments using quantitative proteomics techniques, several complement components have been reported to be upregulated in DR/PDR (Supplementary Table 3.3) (34, 47, 48, 73–75). Although the exact role of complement and coagulation cascades in DR remains unclear, some studies have suggested that there is dysregulation and activation of the alternative pathway (76, 77). Likewise, the activation of the complement was reported in RD/PVR (44, 45, 52, 78, 79), as well as its involvement in pathological processes, such as increased vascular permeability, endothelial cell proliferation, migration, RPE atrophy, reactive gliosis, and loss of photoreceptor outer segments (45, 66). On the other hand, genetic studies strongly support the association between complement components (e.g., CO3, CFH, and CFB) and the risk for AMD (80–82). Therefore, modulation of the complement system could represent a therapeutic alternative to target ocular inflammation in AMD disease (83). However, few quantitative studies in nAMD vitreous have reported changes in complement-specific factors (34). We show here that several complement and coagulation components are significantly up-regulated in DR/PDR and AMD, reinforcing their role in these diseases. Our LFQ approach showed that complement factors such as C2 and CFH are up-regulated in PDR compared to AMD in the LFQ experiment, but this difference could not be confirmed when a larger set of samples were analysed by MRM. Schori and co-workers also reported the enrichment of complement cascade components in PDR vitreous but found reduced levels of CFH in nAMD (34). These results suggest that these complement factors increase gradually in vitreous as the disease progresses from a non-proliferative to a proliferative etiology. Indeed, higher levels of complement and coagulation factors were detected in severe forms of DR and AMD associated with neovascularization, fibrovascular proliferation, vitreous-macular traction syndrome, macular edema, and vitreous hemorrhage. In contrast, complement C1s subcomponent was found to be downregulated in PDR compared to ERM/dry AMD in LFQ, as well as lower levels of complement factor D (previously reported to be up-regulated in DR/PDR (34, 48, 74)) and complement factor I were found in PDR compared to ERM and dry AMD, respectively. Some complement and coagulation proteins had been already detected as downregulated in RRD/PVR compared to other pathologies under study as described by our group (51) and other research groups (52, 54). It has been suggested that the intravitreal levels of complement and coagulation factors increase in RRD as the disease progresses to PVR (51) due to the increased influx of plasma proteins into the retina and vitreous cavity as a result of the breakdown of the blood-retinal barrier (84, 85). Although the number of samples is insufficient to assess the statistical differences between vitreous from RRD and PVR patients, the highest levels of complement and coagulation components were found in a patient with re-detachment associated with PVR. Therefore, the increase of these proteins in vitreous is non-specific for a particular disease but could be a suitable predictor of its progression to a proliferative etiology.

However, the role of complement and coagulation cascades in vitreoretinal diseases could be more complex, as they may be involved in pathological processes shared by DR/PDR, AMD, and RRD/PVR, as recently reviewed by our group (86). In healthy neurosensory tissues, activated complement components can act as neurotrophic and anti-inflammatory factors, promoting cell survival and tissue remodeling. Nonetheless, unrestricted activation of complement cascades may cause direct damage to retinal tissue, as well as the recruitment of immune cells, thus contributing to inflammation and neurodegeneration (87). In this work, we report a significant number of adhesion molecules, nervous system development proteins, and ECM components up-regulated in dry AMD and ERM (cluster 3, Figure 4B), reinforcing the well-known neurodegenerative nature of these pathologies (33, 59, 61, 62), Interestingly, many of them were found to be inversely correlated with coagulation and complement components (cluster 2, Figure 4B). OPTC was one of the ECM components found downregulated in PDR and validated by MRM and it differentiated very efficiently DR and AMD from ERM/RRD. This glycoprotein is highly abundant in vitreous where it exerts its anti-angiogenic activity by regulating the adhesion characteristics of ECM components through its competitive binding to collagen, inhibiting endothelial cell interactions, and preventing the strong adhesions required for pro-angiogenic signalling (88). The downregulation of OPTC had already been reported in PDR in comparison to healthy and surrogate controls (50, 75, 89). Similarly, lower levels of OPTC were observed in patients with nAMD, with levels being lower in patients with more advanced degrees of CNV (33). The decrease of the levels of OPTC in vitreous, which was verified both in PDR and AMD groups, might conduce to an angiogenic environment in the eye. This hypothesis was reinforced by the downregulation of PEDF, whose levels were closely related to those of OPTC, in PDR compared to ERM and AMD, although we only confirmed this result in DR *vs* ERM. PEDF is mainly secreted by the RPE and is a potent inhibitor of angiogenesis, although it participates in other processes such as neuronal differentiation in retinoblastoma cells, inhibits retinal inflammation, and protects retinal neurons from light-induced damages, oxidative stress, and glutamate excitotoxicity (90, 91). PEDF levels in the vitreous of patients are controversial as they are not consistent across studies in PDR (47, 49, 50, 73, 89, 92–94) and nAMD (33, 95, 96). Nevertheless, the antiangiogenic and neurotrophic activities of PEDF are not only controlled by its expression levels, but also by changes in the phosphorylation levels (97, 98), which could explain these discrepancies. Another protein found positively correlated with the levels of OPTC and PEDF is SOD3, an enzyme with antioxidant activity. It was found downregulated both in the discovery phase and MRM verification in all disease groups compared to ERM controls, but these changes were more significant when we compared DR/PDR and ERM. It has been suggested that SOD3 is locally sequestered in vitreous ECM through binding to heparan sulfate proteoglycans (e.g., heparin), in areas of oxidative stress to protect retina and neighboring structures from superoxide radical-induced damages (99). Impaired redox balance in vitreous has been implicated in DR, AMD, and PVR, as reviewed recently by our group (100). Although SOD3 exerts its protective effect by removal of superoxide radicals, it has been suggested that it also promotes the survival of starving photoreceptor cells by enhancing glucose availability (101), stabilizing the retinal vasculature and reducing vessel leakage through the stabilization of hypoxia-inducible factors (102). Other proteins that belong to cluster 3 are cell adhesion factors. Our MRM results confirmed the up-regulation in AMD and ERM of proteins involved in neuronal cell adhesion (CSTN1, CDH2, SPON1), retinal cell-cell adhesion (XLRS1), and integrin-mediated cell adhesion (LGALS3BP),

suggesting that these proteins are potential biomarkers to discriminate between DR and the other disease groups. In particular, LGALS3BP differentiated very efficiently all the disease groups, with the highest levels found in RRD/PVR and the lowest in PDR, as previously reported (44, 51, 75). Cell adhesion molecules participate in a wide number of biological processes in central nervous system development and retina, including neurogenesis, neuronal cell migration, and differentiation, formation and regeneration of axons, and formation of synapses and complex of glial networks synapse (103, 104). The role of adhesion molecules is supported by ECM that provides a scaffolding *via* ECM–integrin-binding for cell migration (105). Besides controlling basic cellular activities (106, 107), ECM remodeling modulates pathological features of vitreoretinal diseases like neovascularization (108, 109), inflammation (110, 111), and fibrosis (112, 113). ECM degradation mediated by metalloproteinases (MMPs) provides scaffolding areas that enable cell adhesion and migration, but also promotes changes in the bioavailability of factors sequestered in ECM, including growth factors, chemoattractant, and other signaling molecules (106, 108, 109). We found both MMP2 and TIMP2 downregulated in PDR compared to ERM and dry AMD. In turn, TIMP1 was found downregulated in PDR with respect to ERM, but not with dry AMD. In the most extreme cases, some of these molecules were not even detected in several PDR vitreous samples. However, western blot analysis could detect higher levels of TIMP2 in DR/PDR and AMD groups. It has been suggested that TIMP2 is constitutively expressed in the human retina in physiological conditions, but its expression levels change in response to a pathological stimulus (114). Zou and co-workers have reported that TIMP2 is downregulated in PDR but treatment with ranibizumab increases its expression levels, confirming its relevance as an inhibitor of angiogenesis (75). OSTP is a matricellular protein, acting both as a soluble cytokine or as an immobilized ECM compound that mediates cell migration, cell-matrix adhesion, and survival of many cell types, inflammatory responses, angiogenesis, and tissue remodeling (115, 116). OSTP was found downregulated in PDR in the discovery phase, in agreement with previous reports (34, 75, 89). However, these results were only partially confirmed by MRM, where the levels were only found downregulated in DRR/PVR group. Higher intravitreal levels of OSTP have been reported in PDR compared to RD, especially in patients with active PDR, suggesting a role of these proteins in angiogenesis (117).

Another small cluster of proteins (cluster 4, Figure 4B) that suggest the role of neurodegeneration in these retinal diseases are APP and related proteins (e.g., CYTC, CLSTN1, SPP1, APLP2). They form a cluster of interacting proteins that integrate multiple pathways, both in the protein-protein interaction network (Figure 3) and correlation heatmap (Figure 4B). APP is a membrane glycoprotein produced by retinal ganglion cells and the RPE that is important for neurite growth, neuronal adhesion, and axonogenesis. APP processing results in the accumulation of amyloid fragments in the eye, in particular in drusen, which have been associated with neurodegeneration in retinal diseases such as AMD and glaucoma (118–120). The increased phagocytic capacity of microglia and the expression of APP degrading enzymes have been suggested to contribute to the amyloid-beta clearance in physiological conditions. Notwithstanding, the neurotoxicity associated with the generation of APP peptides seems to be mediated by its intralysosomal accumulation through macroautophagy, and consequent lysosomal membrane permeabilization, promoting the neuroinflammation by the induction of pro-inflammatory cytokines and NLRP3 inflammasome (121–123). Furthermore, APP peptides can induce mitochondrial dysfunction, oxidative stress, the activation of the complement cascade, and changes in the vascular endothelium in the retina (120, 124). In this work, APP and APP-like proteins (e.g., APLP2) were found upregulated in AMD in comparison to DR/PDR, PDR, and RRD/PVR, and the results were verified by MRM. Several authors reported the underexpression of these proteins in PDR (34, 47, 48, 75), whereas Yu and co-workers detected them in moderate but not in severe PVR or healthy controls (44), confirming our data. Considering that APP is an integral membrane protein, we suggest that these quantitative results might correspond to APP fragments. This hypothesis was confirmed by WB analysis. Two bands corresponding to putative APP fragments were detected, a faint band between 48 kDa and 63 kDa and an intense band at 25 kDa that might correspond, respectively, to amyloid fragments such as Aβ40 and Aβ42 (125) and c-terminal fragments from APP resultant from proteolytic processing (126). This APP fragment (25 KDa) was highly abundant in vitreous from AMD patients, pointing to a potential biomarker of neurodegenerative vitreoretinal diseases. Associated with amyloidosis, CST3 was also found upregulated in AMD compared to DR, but higher levels were found in RRD. CST3 is a potent inhibitor of lysosomal and extracellular cysteine proteinases ubiquitously expressed by all mammalian tissues and present in all body fluids. In the eye, it is particularly abundant in RPE (127). Mutations in CST3 genes were associated with an increased risk of developing nAMD (128) and hereditary cerebral haemorrhage with amyloidosis (129). Mutant variants of CST3 form deposits with APP peptides in senile plaques and arteriolar walls in the brain of AD patients, suggesting a role in amyloidosis (127, 128). On the other hand, it has been suggested the involvement of CST3 in several neuroprotective mechanisms by inhibition of cysteine proteases and induction of autophagy, induction of neurogenesis, and inhibition of oligomerization and amyloid fibril formation (130). Another interesting outcome from our study was the high levels of CST3 found in DRR/PVR, which was previously reported by Yu and co-workers (44). To our knowledge, there are no studies regarding the role of CST3 in RRD/PVR, but some evidence indicates that it inhibits the epithelial-mesenchymal transition, a clinical feature of PVR that occurs in RPE cells, in mammary epithelial cells (131).

Conclusion

The characterization of the vitreous humor proteome is essential for the elucidation of the molecular mechanisms underlying ocular pathologies. Nevertheless, most potential biomarkers described to date have not been validated in a large cohort, limiting their utility in clinical practice. We have applied an LFQ-based method to analyze the vitreous proteome in PDR and AMD compared to ERM. Our findings agree with previous results and reinforce the involvement of complement and coagulation cascades in the pathogenesis of PDR and nAMD. However, our findings suggest that these proteins are not specific biomarkers of any of these pathologies, but suitable predictors

instead of their progression to a proliferative etiology. In addition, a significant number of adhesion molecules, nervous system development proteins, lysosomal proteins, and ECM components were found up-regulated in dry AMD and ERM, reinforcing the neurodegenerative nature of these pathologies. This indicates that the use of vitreous from patients with ERM (or other pathologies such as macular holes) as surrogate control should be taken carefully. Although functional analysis did not highlight proteins related to angiogenesis, the downregulation of anti-angiogenic factors such as OPTC and PEDF in PDR and AMD might suggest that the vitreous humor in these pathologies could be being transformed in an environment prone to angiogenic processes. An interesting outcome of our results is the central role of APP in neurodegeneration as it integrates multiple pathways, emphasizing the multifactorial nature of these diseases. Our analysis provided a list of biomarkers with the potential to discriminate between several vitreoretinal diseases, including DR/PDR, AMD, DDR/PVR, and ERM. According to ROC curves, complement and coagulation components (C2 and prothrombin), acute-phase mediators (AACT), adhesion molecules (e.g., myocilin, LGALS3BP), ECM component (OPTC), and neurodegeneration biomarkers (APP and amyloid-like protein 2) are the most efficient discriminators between different disease groups. In conclusion, our study illuminates some of the mechanisms underlying PDR and AMD and provides potential biomarkers in vitreous. These proteins could be assessed in samples obtained as part of the clinical routine for the prognosis of the disease and the response to treatment. In addition, they could be potential target candidates for the development of new pharmaceutical drugs.

Data availability statement

The datasets presented in this study can be found in online repositories. The names of the repository/repositories and accession number(s) can be found in the article/Supplementary Material.

Ethics statement

The studies involving human participants were reviewed and approved by Affiliation: Ophthalmology Service of Leiria-Pombal Hospital, Portugal. Code of protocol approved by the hospital ethics committee: CHL-15481. The patients/participants provided their written informed consent to participate in this study.

Author contributions

The experiments were conceptualized and designed by FS, SC, CT, and AP. JS performed pars plana vitrectomy and assisted JM in the storage of vitreous samples and collection of information about the patients. FS, SC, CC, and AP conduct the experiments and analyzed the data. FS and SC were responsible for data curation. FS prepared the original draft and SC, JM, LP, CT, and AP reviewed the manuscript. This worked was supervised by LP, CT, and AP. All authors contributed to the article and approved the submitted version.

Funding

FS acknowledges a doctoral fellowship [SFRH/BD/112526/2015] from FCT. This project was supported by the University of Beira Interior— Health Sciences Research Centre (CICS-UBI) supported by FEDER funds through the POCI—COMPETE 2020—Operational Programme Competitiveness and Internationalisation in Axis I—Strengthening research, technological development, and innovation Project (POCI-01- 0145-FEDER-007491) and by CICS-UBI projects UIDB/00709/2020 and UIDP/00709/2020, financed by national funds through the Portuguese Foundation for Science and Technology/ MCTES. This work was also supported by the Applied Molecular Biosciences Unit-UCIBIO which is financed by national funds from FCT/MCTES (UID/ Multi/04378/2019). CNB-CSIC proteomics lab is a member of Proteored, PRB2-ISCIII and is supported by grant PT13/ 0001, of the PE I +D+i 2013–2016, funded by ISCIII and FEDER.

Acknowledgments

The authors acknowledge CICS-UBI researchers Daniela Talhada, Catarina Ferreira, Telma Quintela, Catarina Duarte, and Elisa Cairrão for providing some of the antibodies used in the validation of biomarkers by western blot.

Conflict of interest

The authors declare that the research was conducted in the absence of any commercial or financial relationships that could be construed as a potential conflict of interest.

Publisher's note

All claims expressed in this article are solely those of the authors and do not necessarily represent those of their affiliated organizations, or those of the publisher, the editors and the reviewers. Any product that may be evaluated in this article, or claim that may be made by its manufacturer, is not guaranteed or endorsed by the publisher.

Supplementary material

The Supplementary Material for this article can be found online at: https://www.frontiersin.org/articles/10.3389/fimmu.2023.1107295/full#supplementary-material

References

1. Duh EJ, Sun JK, Stitt AW. Diabetic retinopathy: current understanding, mechanisms, and treatment strategies. *JCI Insight* (2017) 2:1–13. doi: 10.1172/jci.insight.93751

2. Wong WL, Su X, Li X, Cheung CMG, Klein R, Cheng CY, et al. Global prevalence of age-related macular degeneration and disease burden projection for 2020 and 2040: A systematic review and meta-analysis. *Lancet Glob Heal* (2014) 2:e106–16. doi: 10.1016/S2214-109X(13)70145-1

3. Yoshida S, Nakama T, Ishikawa K, Nakao S, Sonoda K, Ishibashi T. Periostin in vitreoretinal diseases. *Cell Mol Life Sci* (2017) 74:4329–37. doi: 10.1007/s00018-017-2651-5

4. Wang W, Lo ACY. Diabetic retinopathy: Pathophysiology and treatments. *Int J Mol Sci* (2018) 19:1–14. doi: 10.3390/ijms19061816

5. Kusuhara S, Fukushima Y, Ogura S, Inoue N, Uemura A. Pathophysiology of diabetic retinopathy: The old and the new. *Diabetes Metab J* (2018) 42:364–76. doi: 10.4093/dmj.2018.0182

6. Ardeljan D, Chan CC. Aging is not a disease: Distinguishing age-related macular degeneration from aging. *Prog Retin Eye Res* (2013) 37:68–89. doi: 10.1016/j.preteyeres.2013.07.003

7. Lim LS, Mitchell P, Seddon JM, Holz FG, Wong TY. Age-related macular degeneration. *Lancet* (2012) 379:1728–38. doi: 10.1016/S0140-6736(12)60282-7

8. Apte RS. Age-related macular degeneration. *N Engl J Med* (2021) 385:539–47. doi: 10.1056/NEJMcp2102061

9. Gehrs KM, Anderson DH, Johnson LV, Hageman GS. Age-related macular degeneration - emerging pathogenetic and therapeutic concepts. *Ann Med* (2006) 38:450–71. doi: 10.1080/07853890600946724

10. Jager RD, Mieler WF, Miller JW. Age-related macular degeneration. *N Engl J Med* (2008) 358:2606–17. doi: 10.1056/NEJMra0801537

11. Spaide RF, Jaffe GJ, Sarraf D, Freund KB, Sadda SR, Staurenghi G, et al. Consensus nomenclature for reporting neovascular age-related macular degeneration data: Consensus on neovascular age-related macular degeneration nomenclature study group. *Ophthalmology* (2020) 127:616–36. doi: 10.1016/j.ophtha.2019.11.004

12. Sharma A, Parachuri N, Kumar N, Bandello F, Kuppermann BD, Loewenstein A, et al. Terms non-exudative and non-neovascular: awaiting entry at the doors of AMD reclassification. *Graefe's Arch Clin Exp Ophthalmol* (2021) 259:1381–3. doi: 10.1007/s00417-021-05164-6

13. Amadio M, Govoni S, Pascale A. Targeting VEGF in eye neovascularization: What's new?: a comprehensive review on current therapies and oligonucleotide-based interventions under development. *Pharmacol Res* (2016) 103:253–69. doi: 10.1016/j.phrs.2015.11.027

14. Mesquita J, Castro-de-Sousa JP, Vaz-Pereira S, Neves A, Passarinha LA, Tomaz CT. Vascular endothelial growth factors and placenta growth factor in retinal vasculopathies: Current research and future perspectives. *Cytokine Growth Factor Rev* (2018) 39:102–15. doi: 10.1016/j.cytogfr.2017.11.005

15. Heier JS, Khanani AM, Quezada Ruiz C, Basu K, Ferrone PJ, Brittain C, et al. Efficacy, durability, and safety of intravitreal faricimab up to every 16 weeks for neovascular age-related macular degeneration (TENAYA and LUCERNE): two randomised, double-masked, phase 3, non-inferiority trials. *Lancet* (2022) 399:729–40. doi: 10.1016/S0140-6736(22)00010-1

16. Zhang W, Qu X, Chen B, Snyder M, Li B, Tang Y, et al. Aflibercept, bevacizumab, or ranibizumab for diabetic macular edema: Two-year results from a comparative effectiveness randomized clinical trial. *Ophthalmology* (2016) 133:48–61. doi: 10.1161/CIRCULATIONAHA.115.017472.Critical

17. Zhao Y, Singh RP. The role of anti-vascular endothelial growth factor (anti-VEGF) in the management of proliferative diabetic retinopathy. *Drugs Context* (2018) 7:1–10. doi: 10.7573/dic.212532

18. Arrigo A, Aragona E, Bandello F. VEGF-targeting drugs for the treatment of retinal neovascularization in diabetic retinopathy. *Ann Med* (2022) 54:1089–111. doi: 10.1080/07853890.2022.2064541

19. Schmidt-Erfurth U, Kaiser PK, Korobelnik J-F, Brown DM, Chong V, Nguyen QD, et al. Intravitreal aflibercept injection for neovascular age-related macular degeneration. *Ophthalmology* (2014) 121:193–201. doi: 10.1016/j.ophtha.2013.08.011

20. Tadayoni R, Sararols L, Weissgerber G, Verma R, Clemens A, Holz FG. Brolucizumab: A newly developed anti-VEGF molecule for the treatment of neovascular age-related macular degeneration. *Ophthalmologica* (2021) 244:93–101. doi: 10.1159/000513048

21. Bressler SB, Almukhtar T, Bhorade A, Bressler NM, Glassman AR, Huang SS, et al. Repeated intravitreous ranibizumab injections for diabetic macular edema and the risk of sustained elevation of intraocular pressure OR the need for ocular hypotensive treatment. *JAMA Ophthalmol* (2015) 133:589–97. doi: 10.1001/jamaophthalmol.2015.186

22. Gonzalez VH, Campbell J, Holekamp NM, Kiss S, Loewenstein A, Augustin AJ, et al. Early and long-term responses to anti–vascular endothelial growth factor therapy in diabetic macular edema: Analysis of protocol I data. *Am J Ophthalmol* (2016) 172:72–9. doi: 10.1016/j.ajo.2016.09.012

23. Wykoff CC, Brown DM, Maldonado ME, Croft DE. Aflibercept treatment for patients with exudative age-related macular degeneration who were incomplete responders to multiple ranibizumab injections (TURF trial). *Br J Ophthalmol* (2014) 98:951–5. doi: 10.1136/bjophthalmol-2013-304736

24. Cabral De Guimaraes TA, Daich Varela M, Georgiou M, Michaelides M. Treatments for dry age-related macular degeneration: Therapeutic avenues, clinical trials and future directions. *Br J Ophthalmol* (2022) 106:297–304. doi: 10.1136/bjophthalmol-2020-318452

25. Samanta A, Aziz AA, Jhingan M, Singh SR, Khanani AM, Chhablani J. Emerging therapies in nonexudative age-related macular degeneration in 2020. *Asia-Pacific J Ophthalmol* (2021) 10:408–16. doi: 10.1097/APO.0000000000000355

26. Thomas CN, Sim DA, Lee WH, Alfahad N, Dick AD, Denniston AK, et al. Emerging therapies and their delivery for treating age-related macular degeneration. *Br J Pharmacol* (2022) 179:1908–37. doi: 10.1111/bph.15459

27. Nawaz IM, Rezzola S, Cancarini A, Russo A, Costagliola C, Semeraro F, et al. Human vitreous in proliferative diabetic retinopathy: Characterization and translational implications. *Prog Retin Eye Res* (2019) 109:110–9. doi: 10.1016/j.preteyeres.2019.03.002

28. Csősz É, Deák E, Kalló G, Csutak A, Tőzsér J. Diabetic retinopathy: Proteomic approaches to help the differential diagnosis and to understand the underlying molecular mechanisms. *J Proteomics* (2017) 150:351–8. doi: 10.1016/j.jprot.2016.06.034

29. Weber SR, Zhao Y, Gates C, Ma J, da Veiga Leprevost F, Basrur V, et al. Proteomic analyses of vitreous in proliferative diabetic retinopathy: Prior studies and future outlook. *J Clin Med* (2021) 10:2309. doi: 10.3390/jcm10112309

30. Youngblood H, Robinson R, Sharma A, Sharma S. Proteomic biomarkers of retinal inflammation in diabetic retinopathy. *Int J Mol Sci* (2019) 20:4755. doi: 10.3390/ijms20194755

31. Monteiro JP, Santos FM, Rocha AS, Castro-de-Sousa JP, Queiroz JA, Passarinha LA, et al. Vitreous humor in the pathologic scope: Insights from proteomic approaches. *Proteomics - Clin Appl* (2015) 9:187–202. doi: 10.1002/prca.201400133

32. Koss MJ, Hoffmann J, Nguyen N, Pfister M, Mischak H, Mullen W, et al. Proteomics of vitreous humor of patients with exudative age-related macular degeneration. *PLos One* (2014) 9:1–11. doi: 10.1371/journal.pone.0096895

33. Nobl M, Reich M, Dacheva I, Siwy J, Mullen W, Schanstra JP, et al. Proteomics of vitreous in neovascular age-related macular degeneration. *Exp Eye Res* (2016) 146:107–17. doi: 10.1016/j.exer.2016.01.001

34. Schori C, Trachsel C, Grossmann J, Zygoula I, Barthelmes D, Grimm C. The proteomic landscape in the vitreous of patients with age-related and diabetic retinal disease. *Invest Ophthalmol Vis Sci* (2018) 59:31–40. doi: 10.1167/iovs.18-24122

35. Mesquita J, Castro de Sousa J, Vaz-Pereira S, Neves A, Tavares-Ratado P, M. Santos F, et al. VEGF-b levels in the vitreous of diabetic and non-diabetic patients with ocular diseases and its correlation with structural parameters. *Med Sci* (2017) 5:17. doi: 10.3390/medsci5030017

36. Sorokin DY, Messina E, Smedile F, Roman P, Damsté JSSS, Ciordia S, et al. Discovery of anaerobic lithoheterotrophic haloarchaea, ubiquitous in hypersaline habitats. *ISME J* (2017) 11:1245–60. doi: 10.1038/ismej.2016.203

37. Käll L, Storey JD, MacCoss MJ, Noble WS. Assigning significance to peptides identified by tandem mass spectrometry using decoy databases. *J Proteome Res* (2008) 7:29–34. doi: 10.1021/pr700600n

38. Jiao X, Sherman BT, Huang DW, Stephens R, Baseler MW, Lane HC, et al. DAVID-WS: A stateful web service to facilitate gene/protein list analysis. *Bioinformatics* (2012) 28:1805–6. doi: 10.1093/bioinformatics/bts251

39. Bindea G, Mlecnik B, Hackl H, Charoentong P, Tosolini M, Kirilovsky A, et al. ClueGO: A cytoscape plug-in to decipher functionally grouped gene ontology and pathway annotation networks. *Bioinformatics* (2009) 25:1091–3. doi: 10.1093/bioinformatics/btp101

40. Szklarczyk D, Gable AL, Lyon D, Junge A, Wyder S, Huerta-Cepas J, et al. STRING v11: Protein-protein association networks with increased coverage, supporting functional discovery in genome-wide experimental datasets. *Nucleic Acids Res* (2019) 47:607–13. doi: 10.1093/nar/gky1131

41. Pang Z, Zhou G, Ewald J, Chang L, Hacariz O, Basu N, et al. Using MetaboAnalyst 5.0 for LC–HRMS spectra processing, multi-omics integration and covariate adjustment of global metabolomics data. *Nat Protoc* (2022) 17:1735–61. doi: 10.1038/s41596-022-00710-w

42. Perez-Riverol Y, Bai J, Bandla C, García-Seisdedos D, Hewapathirana S, Kamatchinathan S, et al. The PRIDE database resources in 2022: a hub for mass spectrometry-based proteomics evidences. *Nucleic Acids Res* (2022) 50:D543–52. doi: 10.1093/nar/gkab1038

43. Shitama T, Hayashi H, Noge S, Uchio E, Oshima K, Haniu H, et al. Proteome profiling of vitreoretinal diseases by cluster analysis. *Proteomics - Clin Appl* (2008) 2:1265–80. doi: 10.1002/prca.200800017

44. Yu J, Liu F, Cui SJ, Liu Y, Song ZY, Cao H, et al. Vitreous proteomic analysis of proliferative vitreoretinopathy. *Proteomics* (2008) 8:3667–78. doi: 10.1002/pmic.200700824

45. Yu J, Peng R, Chen H, Cui C, Ba J. Elucidation of the pathogenic mechanism of rhegmatogenous retinal detachment with proliferative vitreoretinopathy by proteomic analysis. *Investig Ophthalmol Vis Sci* (2012) 53:8146–53. doi: 10.1167/iovs.12-10079

46. Nakanishi T, Koyama R, Ikeda T, Shimizu A. Catalogue of soluble proteins in the human vitreous humor: Comparison between diabetic retinopathy and macular hole. *J Chromatogr B Anal Technol BioMed Life Sci* (2002) 776:89–100. doi: 10.1016/S1570-0232(02)00078-8

47. Gao B-B, Chen X, Timothy N, Aiello LP, Feener EP. Characterization of the vitreous proteome in diabetes without diabetic retinopathy and diabetes with proliferative diabetic retinopathy. *J Proteome Res* (2008) 7:2516–25. doi: 10.1021/pr800112g

48. Loukovaara S, Nurkkala H, Tamene F, Gucciardo E, Liu X, Repo P, et al. Quantitative proteomics analysis of vitreous humor from diabetic retinopathy patients. *J Proteome Res* (2015) 14:5131–43. doi: 10.1021/acs.jproteome.5b00900

49. Kim SJ, Kim SJ, Park J, Lee HK, Park KS, Yu HG, et al. Differential expression of vitreous proteins in proliferative diabetic retinopathy. *Curr Eye Res* (2006) 31:231–40. doi: 10.1080/02713680600557030

50. Wang H, Feng L, Hu J, Xie C, Wang F. Differentiating vitreous proteomes in proliferative diabetic retinopathy using high-performance liquid chromatography coupled to tandem mass spectrometry. *Exp Eye Res* (2013) 108:110–9. doi: 10.1016/j.exer.2012.11.023

51. Santos F, Gaspar L, Ciordia S, Rocha A, Castro e Sousa J, Paradela A, et al. iTRAQ quantitative proteomic analysis of vitreous from patients with retinal detachment. *Int J Mol Sci* (2018) 19:1–22. doi: 10.3390/ijms19041157

52. Wu Z, Ding N, Yu M, Wang K, Luo S, Zou W, et al. Identification of potential biomarkers for rhegmatogenous retinal detachment associated with choroidal detachment by vitreous iTRAQ-based proteomic profiling. *Int J Mol Sci* (2016) 17:1–17. doi: 10.3390/ijms17122052

53. Gaspar LM, Santos FM, Albuquerque T, Castro-de-Sousa JP, Passarinha LA, Tomaz CT. Proteome analysis of vitreous humor in retinal detachment using two different flow-charts for protein fractionation. *J Chromatogr B* (2017) 1061–1062:334–41. doi: 10.1016/j.jchromb.2017.07.049

54. Öhman T, Gawriyski L, Miettinen S, Varjosalo M, Loukovaara S. Molecular pathogenesis of rhegmatogenous retinal detachment. *Sci Rep* (2021) 11:1–15. doi: 10.1038/s41598-020-80005-w

55. Luo S, Xu H, Yang L, Gong X, Shen J, Chen X, et al. Quantitative proteomics analysis of human vitreous in rhegmatogenous retinal detachment associated with choroidal detachment by data-independent acquisition mass spectrometry. *Mol Cell Biochem* (2022) 477:1849–63. doi: 10.1007/s11010-022-04409-0

56. Roybal CN, Velez G, Toral MA, Tsang SH, Bassuk AG, Mahajan VB. Personalized proteomics in proliferative vitreoretinopathy implicate hematopoietic cell recruitment and mTOR as a therapeutic target. *Am J Ophthalmol* (2018) 186:152–63. doi: 10.1016/j.ajo.2017.11.025

57. Yu J, Peng R, Chen H, Cui C, Ba J, Wang F. Kininogen 1 and insulin-like growth factor binding protein 6: Candidate serum biomarkers of proliferative vitreoretinopathy. *Clin Exp Optom* (2014) 97:72–9. doi: 10.1111/cxo.12088

58. Mandal N, Kofod M, Vorum H, Villumsen J, Eriksen J, Heegaard S, et al. Proteomic analysis of human vitreous associated with idiopathic epiretinal membrane. *Acta Ophthalmol* (2013) 91:333–4. doi: 10.1111/aos.12075

59. Pollreisz A, Funk M, Breitwieser FP, Parapatics K, Sacu S, Georgopoulos M, et al. Quantitative proteomics of aqueous and vitreous fluid from patients with idiopathic epiretinal membranes. *Exp Eye Res* (2013) 108:48–58. doi: 10.1016/j.exer.2012.11.010

60. Yu J, Feng L, Wu Y, Wang H, Ba J, Zhu W, et al. Vitreous proteomic analysis of idiopathic epiretinal membranes. *Mol Biosyst* (2014) 10:2558–66. doi: 10.1039/c4mb00240g

61. Öhman T, Tamene F, Göös H, Loukovaara S, Varjosalo M. Systems pathology analysis identifies neurodegenerative nature of age-related vitreoretinal interface diseases. *Aging Cell* (2018) 17:e12809. doi: 10.1111/acel.12809

62. Sun C, Zou H, Yang Z, Yang M, Chen X, Huang Y, et al. Proteomics and phosphoproteomics analysis of vitreous in idiopathic epiretinal membrane patients. *Proteomics – Clin Appl* (2022) 16:2100128. doi: 10.1002/prca.202100128

63. Rocha AS, Santos FM, Monteiro JP, Castro-de-Sousa JP, Queiroz JA, Tomaz CT, et al. Trends in proteomic analysis of human vitreous humor samples. *Electrophoresis* (2014) 35:2495–508. doi: 10.1002/elps.201400049

64. Angi M, Kalirai H, Coupland SE, Damato BE, Semeraro F, Romano MR. Proteomic analyses of the vitreous humour. *Mediators Inflammation* (2012) 2012:1–7. doi: 10.1155/2012/148039

65. Mukai R, Okunuki Y, Husain D, Kim CB, Lambris JD, Connor KM. The complement system is critical in maintaining retinal integrity during aging. *Front Aging Neurosci* (2018) 10:15. doi: 10.3389/fnagi.2018.00015

66. Sweigard JH, Matsumoto H, Smith KE, Kim LA, Paschalis EI, Okonuki Y, et al. Inhibition of the alternative complement pathway preserves photoreceptors after retinal injury. *Sci Transl Med* (2015) 7:21–4. doi: 10.1126/scitranslmed.aab1482

67. Clark SJ, Bishop PN. The eye as a complement dysregulation hotspot. *Semin Immunopathol* (2018) 40:65–74. doi: 10.1007/s00281-017-0649-6

68. Gao BB, Clermont A, Rook S, Fonda SJ, Srinivasan VJ, Wojtkowski M, et al. Extracellular carbonic anhydrase mediates hemorrhagic retinal and cerebral vascular permeability through prekallikrein activation. *Nat Med* (2007) 13:181–8. doi: 10.1038/nm1534

69. Abdulaal M, Haddad NMN, Sun JK, Silva PS. The role of plasma kallikrein-kinin pathway in the development of diabetic retinopathy: Pathophysiology and therapeutic approaches. *Semin Ophthalmol* (2016) 31:19–24. doi: 10.3109/08820538.2015.1114829

70. Whitmore SS, Sohn EH, Chirco KR, Drack AV, Stone EM, Tucker BA, et al. Complement activation and choriocapillaris loss in early AMD: Implications for pathophysiology and therapy. *Prog Retin Eye Res* (2015) 45:1–29. doi: 10.1016/j.preteyeres.2014.11.005

71. Skei JM, Fingert JH, Russell SR, Stone EM, Mullins RF. Complement component C5a activates ICAM-1expression on human choroidal endothelial cells. *Investig Ophthalmol Vis Sci* (2010) 51:5336–42. doi: 10.1167/iovs.10-5322

72. Bastiaans J, Van Meurs JC, Van Holten-Neelen C, Nijenhuis MSTe, Kolijn-Couwenberg MJ, Van Hagen PM, et al. Factor xa and thrombin stimulate proinflammatory and profibrotic mediator production by retinal pigment epithelial cells: A role in vitreoretinal disorders? *Graefe's Arch Clin Exp Ophthalmol* (2013) 251:1723–33. doi: 10.1007/s00417-013-2335-2

73. García-Ramírez M, Canals F, Hernández C, Colomé N, Ferrer C, Carrasco E, et al. Proteomic analysis of human vitreous fluid by fluorescence-based difference gel electrophoresis (DIGE): a new strategy for identifying potential candidates in the pathogenesis of proliferative diabetic retinopathy. *Diabetologia* (2007) 50:1294–303. doi: 10.1007/s00125-007-0627-y

74. Minamoto A, Yamane K, Yokoyama T. Proteomics of vitreous fluid. In: Thongboonkerd V, editor. *Proteomics of human body fluids*. Totowa, NJ, New Jersey: Humana Press (2007). p. 495–507. doi: 10.1007/978-1-59745-432-2_23

75. Zou C, Han C, Zhao M, Yu J, Bai L, Yao Y, et al. Change of ranibizumab-induced human vitreous protein profile in patients with proliferative diabetic retinopathy based on proteomics analysis. *Clin Proteomics* (2018) 15:1–10. doi: 10.1186/s12014-018-9187-z

76. Mandava N, Tirado-Gonzalez V, Geiger MD, Patnaik JL, Frazer-Abel A, Lynch AM, et al. Complement activation in the vitreous of patients with proliferative diabetic retinopathy. *Investig Opthalmology Vis Sci* (2020) 61:39. doi: 10.1167/iovs.61.11.39

77. Shahulhameed S, Vishwakarma S, Chhablani J, Tyagi M, Pappuru RR, Jakati S, et al. A systematic investigation on complement pathway activation in diabetic retinopathy. *Front Immunol* (2020) 11:154. doi: 10.3389/fimmu.2020.00154

78. Luo S, Chen Y, Yang L, Gong X, Wu Z. The complement system in retinal detachment with choroidal detachment. *Curr Eye Res* (2022) 47:809–12. doi: 10.1080/02713683.2022.2038634

79. Chen G, Li T, Zheng Q, Hou J, Tang S, Li W. Differential expression and significance of complement C4b and transthyretin in proliferative vitreoretinopathy. *Chin J Ophthalmol* (2011) 47:726–31.

80. Toomey CB, Johnson LV, Bowes Rickman C. Complement factor h in AMD: Bridging genetic associations and pathobiology. *Prog Retin Eye Res* (2018) 62:38–57. doi: 10.1016/j.preteyeres.2017.09.001

81. Loyet KM, DeForge LE, Katschke KJ, Diehl L, Graham RR, Pao L, et al. Activation of the alternative complement pathway in vitreous is controlled by genetics in age-related macular degeneration. *Investig Ophthalmol Vis Sci* (2012) 53:6628–37. doi: 10.1167/iovs.12-9587

82. de Jong S, Gagliardi G, Garanto A, de Breuk A, Lechanteur YTE, Katti S, et al. Implications of genetic variation in the complement system in age-related macular degeneration. *Prog Retin Eye Res* (2021) 84:100952. doi: 10.1016/j.preteyeres.2021.100952

83. Park DH, Connor KM, Lambris JD. The challenges and promise of complement therapeutics for ocular diseases. *Front Immunol* (2019) 10:1007. doi: 10.3389/fimmu.2019.01007

84. Cunha-Vaz J. The blood–retinal barrier in retinal disease. *Eur Ophthalmic Rev* (2009) 03:105. doi: 10.17925/eor.2009.03.02.105

85. Campochiaro PA, Bryan JA, Conway BP, Jaccoma EH. Intravitreal chemotactic and mitogenic activity: Implication of blood-retinal barrier breakdown. *Arch Ophthalmol* (1986) 104:1685–7. doi: 10.1001/archopht.1986.01050230123046

86. dos Santos FM, Ciordia S, Mesquita J, de Sousa JPC, Paradela A, Tomaz CT, et al. Vitreous humor proteome: unraveling the molecular mechanisms underlying proliferative and neovascular vitreoretinal diseases. *Cell Mol Life Sci* (2023) 80.1:1–28. doi: 10.1007/s00018-022-04670-y

87. Kawa MP, Machalinska A, Roginska D, Machalinski B. Complement system in pathogenesis of AMD: Dual player in degeneration and protection of retinal tissue. *J Immunol Res* (2014) 2014:1–12. doi: 10.1155/2014/483960

88. Le Goff MM, Sutton MJ, Slevin M, Latif A, Humphries MJ, Bishop PN. Opticin exerts its anti-angiogenic activity by regulating extracellular matrix adhesiveness. *J Biol Chem* (2012) 287:28027–36. doi: 10.1074/jbc.M111.331157

89. Balaiya S, Zhou Z, Chalam KV. Characterization of vitreous and aqueous proteome in humans with proliferative diabetic retinopathy and its clinical correlation. *Proteomics Insights* (2017) 8:1–10. doi: 10.1177/1178641816686078

90. Park K, Jin J, Hu Y, Zhou K, Ma J-XX. Overexpression of pigment epithelium-derived factor inhibits retinal inflammation and neovascularization. *AJPA* (2011) 178:688–98. doi: 10.1016/j.ajpath.2010.10.014

91. Barnstable CJ, Tombran-Tink J. Neuroprotective and antiangiogenic actions of PEDF in the eye: Molecular targets and therapeutic potential. *Prog Retin Eye Res* (2004) 23:561–77. doi: 10.1016/j.preteyeres.2004.05.002

92. Simó R, Higuera M, García-Ramírez M, Canals F, García-Arumí J, Hernández C. Elevation of apolipoprotein a-I and apolipoprotein h levels in the vitreous fluid and overexpression in the retina of diabetic patients. *Arch Ophthalmol* (2008) 126:1076–81. doi: 10.1001/archopht.126.8.1076

93. Wang H, Feng L, Hu J, Xie C, Wang F. Characterisation of the vitreous proteome in proliferative diabetic retinopathy. *Proteome Sci* (2012) 10:1–11. doi: 10.1186/1477-5956-10-15

94. Duh EJ, Yang HS, Haller JA, De Juan E, Humayun MS, Gehlbach P, et al. Vitreous levels of pigment epithelium-derived factor and vascular endothelial growth factor: Implications for ocular angiogenesis. *Am J Ophthalmol* (2004) 137:668–74. doi: 10.1016/j.ajo.2003.11.015

95. Huber M, Wachtlin J. Vitreous levels of proteins implicated in angiogenesis are modulated in patients with retinal or choroidal neovascularization. *Ophthalmologica* (2012) 228:188–93. doi: 10.1159/000339952

96. Holekamp NM, Bouck N, Volpert O. Pigment epithelium-derived factor is deficient in the vitreous of patients with choroidal neovascularization due to age-related macular degeneration. *Am J Ophthalmol* (2002) 134:220–7. doi: 10.1016/S0002-9394(02)01549-0

97. Maik-Rachline G, Seger R. Variable phosphorylation states of pigment-epithelium-derived factor differentially regulate its function. *Blood* (2006) 107:2745–52. doi: 10.1182/blood-2005-06-2547

98. Maik-Rachline G, Shaltiel S, Seger R. Extracellular phosphorylation converts pigment epithelium-derived factor from a neurotrophic to an antiangiogenic factor. *Blood* (2005) 105:670–8. doi: 10.1182/blood-2004-04-1569

99. Wert KJ, Velez G, Cross MR, Wagner BA, Teoh-Fitzgerald ML, Buettner GR, et al. Extracellular superoxide dismutase (SOD3) regulates oxidative stress at the vitreoretinal interface. *Free Radic Biol Med* (2018) 124:408–19. doi: 10.1016/J.FREERADBIOMED.2018.06.024

100. Santos FM, Mesquita J, Castro-de-Sousa JP, Ciordia S, Paradela A, Tomaz CT. Vitreous humor proteome: Targeting oxidative stress, inflammation, and neurodegeneration in vitreoretinal diseases. *Antioxidants* (2022) 11:505. doi: 10.3390/antiox11030505

101. Brown EE, DeWeerd AJ, Ildefonso CJ, Lewin AS, Ash JD. Mitochondrial oxidative stress in the retinal pigment epithelium (RPE) led to metabolic dysfunction in both the RPE and retinal photoreceptors. *Redox Biol* (2019) 24:1–11. doi: 10.1016/j.redox.2019.101201

102. Mira E, Carmona-Rodríguez L, Pérez-Villamil B, Casas J, Fernández-Aceñero MJ, Martínez-Rey D, et al. SOD3 improves the tumor response to chemotherapy by stabilizing endothelial HIF-2α. *Nat Commun* (2018) 9:575. doi: 10.1038/s41467-018-03079-1

103. Togashi H, Sakisaka T, Takai Y. Cell adhesion molecules in the central nervous system. *Cell Adhes Migr* (2009) 3:29–35. doi: 10.4161/cam.3.1.6773

104. Missaire M, Hindges R. The role of cell adhesion molecules in visual circuit formation: From neurite outgrowth to maps and synaptic specificity. *Dev Neurobiol* (2015) 75:569–83. doi: 10.1002/dneu.22267

105. Ridley AJ, Schwartz MA, Burridge K, Firtel RA, Ginsberg MH, Borisy G, et al. Cell migration: Integrating signals from front to back. *Sci (80-)* (2003) 302:1704–9. doi: 10.1126/science.1092053

106. Lu P, Takai K, Weaver VM, Werb Z. Extracellular matrix degradation and remodeling in development and disease. *Cold Spring Harb Perspect Biol* (2011) 3: a005058–a005058. doi: 10.1101/cshperspect.a005058

107. Frantz C, Stewart KM, Weaver VM. The extracellular matrix at a glance. *J Cell Sci* (2010) 123:4195–200. doi: 10.1242/jcs.023820

108. Sottile J. Regulation of angiogenesis by extracellular matrix. *Biochim Biophys Acta - Rev Cancer* (2004) 1654:13–22. doi: 10.1016/j.bbcan.2003.07.002

109. Bishop PN. The role of extracellular matrix in retinal vascular development and preretinal neovascularization. *Exp Eye Res* (2015) 133:30–6. doi: 10.1016/j.exer.2014.10.021

110. Sorokin L. The impact of the extracellular matrix on inflammation. *Nat Rev Immunol* (2010) 10:712–23. doi: 10.1038/nri2852

111. Singh M, Tyagi SC. Metalloproteinases as mediators of inflammation and the eyes: Molecular genetic underpinnings governing ocular pathophysiology. *Int J Ophthalmol* (2017) 10:1308–18. doi: 10.18240/ijo.2017.08.20

112. Chaudhary R, Scott RAH, Wallace G, Berry M, Logan A, Blanch RJ. Inflammatory and fibrogenic factors in proliferative vitreoretinopathy development. *Transl Vis Sci Technol* (2020) 9:1–17. doi: 10.1167/tvst.9.3.23

113. Wynn TA. Common and unique mechanisms regulate fibrosis in various fibroproliferative diseases. *J Clin Invest* (2007) 117:524–9. doi: 10.1172/JCI31487

114. Das A, Navaratna D, McGuire PG. Beyond VEGF – other factors important in retinal neovascularization: Potential targets in proliferative diabetic retinopathy. In: *Diabetic retinopathy*. Totowa, NJ: Humana Press (2008). p. 375–98. doi: 10.1007/978-1-59745-563-3_16

115. Chowdhury UR, Jea SY, Oh DJ, Rhee DJ, Fautsch MP. Expression profile of the matricellular protein osteopontin in primary open-angle glaucoma and the normal human eye. *Investig Ophthalmol Vis Sci* (2011) 52:6443–51. doi: 10.1167/iovs.11-7409

116. Lund SA, Giachelli CM, Scatena M. The role of osteopontin in inflammatory processes. *J Cell Commun Signal* (2009) 3:311–22. doi: 10.1007/s12079-009-0068-0

117. Abu El-Asrar AM, Imtiaz Nawaz M, Kangave D, Siddiquei MM, Geboes K. Osteopontin and other regulators of angiogenesis and fibrogenesis in the vitreous from patients with proliferative vitreoretinal disorders. *Mediators Inflammation* (2012) 2012:1–8. doi: 10.1155/2012/493043

118. Ratnayaka JA, Serpell LC, Lotery AJ. Dementia of the eye: the role of amyloid beta in retinal degeneration. *Eye* (2015) 29:1013–26. doi: 10.1038/eye.2015.100

119. Luibl V, Isas JM, Kayed R, Glabe CG, Langen R, Chen J. Drusen deposits associated with aging and age-related macular degeneration contain nonfibrillar amyloid oligomers. *J Clin Invest* (2006) 116:378–85. doi: 10.1172/JCI25843

120. Gupta VBV, Gupta VBV, Chitranshi N, Gangoda S, Vander Wall R, Abbasi M, et al. One protein, multiple pathologies: multifaceted involvement of amyloid β in neurodegenerative disorders of the brain and retina. *Cell Mol Life Sci* (2016) 73:4279–97. doi: 10.1007/s00018-016-2295-x

121. Gold M, El Khoury J. β-amyloid, microglia, and the inflammasome in alzheimer's disease. *Semin Immunopathol* (2015) 37:607–11. doi: 10.1007/s00281-015-0518-0

122. Cuenca N, Fernández-Sánchez L, Campello L, Maneu V, de la Villa P, Lax P, et al. Cellular responses following retinal injuries and therapeutic approaches for neurodegenerative diseases. *Prog Retin Eye Res* (2014) 43:17–75. doi: 10.1016/j.preteyeres.2014.07.001

123. Zheng L, Kågedal K, Dehvari N, Benedikz E, Cowburn R, Marcusson J, et al. Oxidative stress induces macroautophagy of amyloid β-protein and ensuing apoptosis. *Free Radic Biol Med* (2009) 46:422–9. doi: 10.1016/j.freeradbiomed.2008.10.043

124. Salminen A, Ojala J, Kauppinen A, Kaarniranta K, Suuronen T. Inflammation in alzheimer's disease: Amyloid-β oligomers trigger innate immunity defence *via* pattern recognition receptors. *Prog Neurobiol* (2009) 87:181–94. doi: 10.1016/j.pneurobio.2009.01.001

125. Prakasam A, Muthuswamy A, Ablonczy Z, Greig NH, Fauq A, Rao KJ, et al. Differential accumulation of secreted AβPP metabolites in ocular fluids. *J Alzheimer's Dis* (2010) 20:1243–53. doi: 10.3233/JAD-2010-100210

126. García-Ayllón MS, Lopez-Font I, Boix CP, Fortea J, Sánchez-Valle R, Lleó A, et al. C-terminal fragments of the amyloid precursor protein in cerebrospinal fluid as potential biomarkers for Alzheimer disease. *Sci Rep* (2017) 7:1–7. doi: 10.1038/s41598-017-02841-7

127. Paraoan L, Hiscott P, Gosden C, Grierson I. Cystatin c in macular and neuronal degenerations: Implications for mechanism(s) of age-related macular degeneration. *Vision Res* (2010) 50:737–42. doi: 10.1016/j.visres.2009.10.022

128. Zurdel J. CST3 genotype associated with exudative age related macular degeneration. *Br J Ophthalmol* (2002) 86:214–9. doi: 10.1136/bjo.86.2.214

129. Palsdottir A, Snorradottir AO, Thorsteinsson L. Hereditary cystatin c amyloid angiopathy: Genetic, clinical, and pathological aspects. *Brain Pathol* (2006) 16:55–9. doi: 10.1111/j.1750-3639.2006.tb00561.x

130. Gauthier S, Kaur G, Mi W, Tizon B, Levy E. Protective mechanisms by cystatin c in neurodegenerative diseases. *Front Biosci - Sch* (2011) 3 S:541–54. doi: 10.2741/s170

131. Sokol JP, Neil JR, Schiemann BJ, Schiemann WP. The use of cystatin c to inhibit epithelial–mesenchymal transition and morphological transformation stimulated by transforming growth factor-β. *Breast Cancer Res* (2005) 7:R844. doi: 10.1186/bcr1312

Glossary

A1AT	Alpha-1-antitrypsin
AACT	Alpha-1-antichymotrypsin
AMD	Age-Related Macular Degeneration
APLP2	Amyloid-like protein 2
APP	Beta-Amyloid
BCAN	Brevican core protein
CADH2	neural cadherin
CATZ	Cathepsin Z
CE	Collision energy
CFH	Complement factor H
CHGA	Chromogranin-A
CLU	Clusterin
C2	Complement C2
C5	Complement C5
C6	Complement C6
C8B	Component C8 beta chain
C9	Complement C9
CSTC	Cystatin-C
CSTN1	Calsyntenin-1
DP	Declustering Potential
DR	Diabetic Retinopathy
ECM	Extracellular Matrix
ERM	Epiretinal Membranes
F2	Prothrombin
F9	Coagulation Factor IX
GNS	N-acetylglucosamine-6-sulfatase
IDA	Information-dependent acquisition
IGFBPs	Insulin-like Growth Factor Binding Proteins
IGFs	Insulin-like Growth Factor
IHT	Interface heater temperature
ITIH3	Inter-alpha-trypsin Inhibitor Heavy Chain H3
LGALS3BP	Galectin-3-binding Protein
MNV	Macular neovascularization
MRM	Multiple Reaction Monitoring
nAMD	“Wet” or Neovascular AMD
NCAN	Neurocan core protein
NRX3A	Neurexin-3
OPTC	Opticin
OSTP	Osteopontin
PDR	Proliferative Diabetic Retinopathy

(Continued)

Continued

PEDF	Pigment Epithelium-Derived Factor
PVR	Proliferative Vitreoretinopathy
ROC	Receiver Operating Characteristic
RRD	Rhegmatogenous Retinal Detachment
SOD3	Extracellular Superoxide Dismutase [Cu-Zn]
SPON1	Spondin-1
TIMP1	Metalloproteinase Inhibitor 1
TIMP2	Metalloproteinase Inhibitor 2
TNR	Tenascin-R
VEGF	Vascular Endothelial Growth Factor
XLRS1	Retinoschisin

frontiers | Frontiers in Immunology

TYPE Original Research
PUBLISHED 20 February 2023
DOI 10.3389/fimmu.2023.1113015

Check for updates

OPEN ACCESS

EDITED BY
Lillemor Skattum,
Lund University, Sweden

REVIEWED BY
Maciej Cedzynski,
Institute for Medical Biology, Polish Academy of Sciences, Poland
Rafael Bayarri-Olmos,
Rigshospitalet, Denmark

*CORRESPONDENCE
Mihály Józsi
mihaly.jozsi@ttk.elte.hu

†These authors have contributed equally to this work and share last authorship

SPECIALTY SECTION
This article was submitted to Molecular Innate Immunity, a section of the journal Frontiers in Immunology

RECEIVED 30 November 2022
ACCEPTED 23 January 2023
PUBLISHED 20 February 2023

CITATION
Matola AT, Fülöp A, Rojkovich B, Nagy G, Sármay G, Józsi M and Uzonyi B (2023) Autoantibodies against complement factor B in rheumatoid arthritis.
Front. Immunol. 14:1113015.
doi: 10.3389/fimmu.2023.1113015

COPYRIGHT
© 2023 Matola, Fülöp, Rojkovich, Nagy, Sármay, Józsi and Uzonyi. This is an open-access article distributed under the terms of the Creative Commons Attribution License (CC BY). The use, distribution or reproduction in other forums is permitted, provided the original author(s) and the copyright owner(s) are credited and that the original publication in this journal is cited, in accordance with accepted academic practice. No use, distribution or reproduction is permitted which does not comply with these terms.

Autoantibodies against complement factor B in rheumatoid arthritis

Alexandra T. Matola[1,2], Angéla Fülöp[3], Bernadette Rojkovich[3], György Nagy[4,5,6,7], Gabriella Sármay[1], Mihály Józsi[1,2*†] and Barbara Uzonyi[1,2†]

[1]Department of Immunology, ELTE Eötvös Loránd University, Budapest, Hungary, [2]MTA-ELTE Complement Research Group, Eötvös Loránd Research Network (ELKH) at the Department of Immunology, ELTE Eötvös Loránd University, Budapest, Hungary, [3]Buda Hospital of the Hospitaller Order of Saint John of God, Budapest, Hungary, [4]Department of Rheumatology and Clinical Immunology, Semmelweis University, Budapest, Hungary, [5]Department of Internal Medicine and Oncology, Semmelweis University, Budapest, Hungary, [6]Heart and Vascular Center, Faculty of Medicine, Semmelweis University, Budapest, Hungary, [7]Department of Genetics, Cell- and Immunobiology, Faculty of Medicine, Semmelweis University, Budapest, Hungary

Rheumatoid arthritis (RA) is a chronic inflammatory autoimmune disorder affecting the joints. Many patients carry anti-citrullinated protein autoantibodies (ACPA). Overactivation of the complement system seems to be part of the pathogenesis of RA, and autoantibodies against the pathway initiators C1q and MBL, and the regulator of the complement alternative pathway, factor H (FH), were previously reported. Our aim was to analyze the presence and role of autoantibodies against complement proteins in a Hungarian RA cohort. To this end, serum samples of 97 ACPA-positive RA patients and 117 healthy controls were analyzed for autoantibodies against FH, factor B (FB), C3b, C3-convertase (C3bBbP), C1q, MBL and factor I. In this cohort, we did not detect any patient with FH autoantibodies but detected C1q autoantibodies in four patients, MBL autoantibodies in two patients and FB autoantibodies in five patients. Since the latter autoantibodies were previously reported in patients with kidney diseases but not in RA, we set out to further characterize such FB autoantibodies. The isotypes of the analyzed autoantibodies were IgG2, IgG3, IgGκ, IgGλ and their binding site was localized in the Bb part of FB. We detected *in vivo* formed FB–autoanti-FB complexes by Western blot. The effect of the autoantibodies on the formation, activity and FH-mediated decay of the C3 convertase in solid phase convertase assays was determined. In order to investigate the effect of the autoantibodies on complement functions, hemolysis assays and fluid phase complement activation assays were performed. The autoantibodies partially inhibited the complement-mediated hemolysis of rabbit red blood cells, inhibited the activity of the solid phase C3-convertase and C3 and C5b-9 deposition on complement activating surfaces. In summary, in ACPA-positive RA patients we identified FB autoantibodies. The characterized FB autoantibodies did not enhance complement activation, rather, they had inhibitory effect on complement. These results support the involvement of the complement system in the pathomechanism

of RA and raise the possibility that protective autoantibodies may be generated in some patients against the alternative pathway C3 convertase. However, further analyses are needed to assess the exact role of such autoantibodies.

KEYWORDS

complement, alternative pathway, C3 convertase, autoantibody, rheumatoid arthritis, factor B (FB)

Introduction

Rheumatoid arthritis (RA) is a chronic inflammatory autoimmune disorder targeting typically the peripheral joints of the hands and feet, leading to persistent inflammation. With time it may cause the formation of a new tissue with infiltrating inflammatory immune cells called pannus and the destruction of the bones and cartilage which may give rise to deformities (1, 2). RA affects approximately 0.5-1% of the population (3) with slightly different frequencies between geographical regions and populations (4–6). RA affects mainly women with rising prevalence with age (7, 8). Though the cause of RA is unknown, several predisposing factors may play a role in disease development: environmental exposures such as smoking (9), infection and genetic factors (3, 10, 11). Presumably, hormonal factors also play a role in the mechanism causing the overrepresentation of women in the disease (8, 12).

Most of the patients develop rheumatoid factor or anti-modified protein antibodies. The classical serological marker of RA was rheumatoid factor, an autoantibody targeting the Fc region of IgG. It has relatively low specificity as it can be found in other pathological conditions and healthy individuals (8, 13, 14). By contrast, autoantibodies against modified (e.g., carbamylated, citrullinated, acetylated) self-proteins are more specific for RA and can be detected in patients before clinical onset, in the subclinical stage (8, 15). The most frequently detected anti-citrullinated protein antibody (ACPA) is a diagnostic criterion of RA (16) and the presence of ACPA can predict the development of the disease (17–19).

The above-mentioned autoantibodies can form immune complexes with self-antigens in the patients and activate complement, which plays a remarkable role in the pathogenesis of RA (20). The complement system as part of the innate immune system has a crucial role in host defense including elimination of microbes, apoptotic and necrotic cells, and the clearance of immune complexes (21). The activation trigger defines by which of the three pathways will complement be activated. The classical pathway is initiated by the binding of its pattern recognition molecule C1q to IgG- or IgM-containing immune complexes. The lectin pathway is induced by sensing microbial carbohydrate structures, and the alternative pathway is constantly activated on a low level (C3 tick over mechanism) due to the spontaneous hydrolysis of the thioester group of the central C3 molecule (C3(H_2O)). Thus, factor B (FB) bound to C3(H_2O) and cleaved by factor D (FD), forms the fluid phase C3 convertase of the alternative pathway, C3(H_2O)Bb. This in turn cleaves C3, generating C3b which can covalently bind to target surfaces and together with FB (again, cleaved by FD) and the stabilizing properdin forms the C3 convertase of the alternative pathway C3bBbP. The activation of the cascades leads to the generation of small anaphylatoxins (e.g., C3a, C5a) and larger fragments which opsonize the target (20–23). To avoid activation on host surfaces, complement is tightly regulated at several points by membrane-bound and fluid-phase regulators (24). In case of mutations or presence of autoantibodies against complement components and/or regulators, the system turns defective, and plays an important role in the pathomechanism of several autoimmune diseases (20, 25).

The involvement of the complement system in RA has long been studied. Decreased levels of C3 and C4 proteins (26) and elevated levels of complement activation products C3a, C5a, Bb and soluble C5b-9 (sC5b-9) in the synovial fluid of patients suggested the overactivation of the complement system (27–29). Elevated levels of sC5b-9 in patients' plasma (30, 31) indicate that the complement activation in RA is not limited to the joints but may affect other organs and tissues. Furthermore, treatment with anti-rheumatic drugs can decrease the elevated sC5b-9 levels (31). Autoantibodies against complement components were found in RA patients, including C1q (32, 33), factor H (FH) (34) and mannose binding lectin (MBL) (35), further confirming the involvement of the three complement pathways in the pathomechanism of RA, although the functions and relevance of these autoantibodies were not investigated and are still unknown.

To assess the role of anti-complement autoantibodies in RA, the aim of this study was to investigate whether the previously reported autoantibodies can be detected and/or other, novel autoantibodies can be found in a Hungarian cohort of RA patients. Here, we report the identification and characterization of FB autoantibodies in RA.

Materials and methods

Proteins and antibodies

Complement proteins FH (#341274), FB (#341262), C3b (#204860), C3 (#204885), factor I (FI) (#341280), C1q (#204876), goat anti-FB (#341272) and goat anti-FH (#341276) antiserum were obtained from Merck (Darmstadt, Germany; obtained *via* Merck Life Science Kft., Budapest, Hungary). FD (#A409), properdin (#A412), mouse anti-C5b-9 (#A239), anti-FB (Bb) (#A227), anti-FB (Ba) (#A225) and C3a EIA kit (#A032) were from Quidel (obtained *via* Biomedica, Budapest, Hungary). Purified human IgG (#I2511), human serum albumin (#A3782), human alpha-1 antitrypsin

(#SRP6312), antibodies against C1q (#234390), human IgG (#A6029), IgM (#A0420), IgA (#A0295), IgG1 (clone HP-6001, #I9388), IgG2 (clone HP-6002, #I9513), IgG3 (clone HP-6050, #I7260), IgG4 (clone HP-6025, #I7385), IgGκ (clone KP-53, #K4377), IgGλ (clone HP-6054, #L6522), and avidin-HRP (#A7419) were purchased from Merck. Mouse IgG1 (clone MOPC-21, #BZ-400101) was obtained from BioLegend (San Diego, CA). MBL (#9086-MB) and biotin-conjugated goat anti-MBL (#BAF2307) were from R&D Systems (Minneapolis, MN), HRP-conjugated goat anti-mouse (#P0447), rabbit anti-goat (#P0449) and swine anti-rabbit (#P0217) antibodies were from DAKO (Hamburg, Germany). Goat anti-C3 $F(ab')_2$ (#55062) and HRP-conjugated goat anti-C3 $F(ab')_2$ (#55237) were from MP Biomedicals (Solon, OH).

Serum samples

Serum samples were collected from Hungarian rheumatoid arthritis patients (n=97) and from healthy individuals (n=117) after informed consent in accordance with the Declaration of Helsinki. The study was approved by the National Ethical Committee (33986-1/2018 EKU). Characteristics of the patients and healthy donors are shown in Table 1.

Autoantibody detection

Autoantibodies were detected using ELISA method, as described by Józsi and Uzonyi (36). Briefly, FH, FB, C3b, FI in 5 µg/ml, MBL and C1q in 2 µg/ml and HSA or alpha-1 antitrypsin as negative controls were immobilized on microtiter plates. After blocking with 5% BSA in DPBS-0.1% Tween-20, serum samples were added in DPBS-0.1% Tween-20 at a dilution of 1:50 for 1 hour at RT. To detect autoantibodies against solid phase C3 convertase of the alternative pathway (C3bBbP), the convertase was built up (see below) and incubated with serum samples diluted 1:50. The bound autoantibodies were detected with HRP-conjugated goat anti-human IgG, anti-human IgA or anti-human IgM. Color reaction was developed by adding TMB solution (BioLegend). After stopping with H_2SO_4, absorbance was measured at 450 nm and at 620 nm as reference wavelength. To detect anti-MBL autoantibodies, serum samples were diluted in DPBS containing 10 mM EDTA. In the case of detecting anti-C1q autoantibodies, serum samples were diluted in DPBS containing 1 M NaCl to avoid interaction of C1q globular heads with IgG Fc parts. Samples were accepted as positive if the mean OD value for the investigated protein was at least two-fold greater than the mean OD value for the negative control protein alpha-1 antitrypsin. The isotypes of the autoantibodies were determined using monoclonal antibodies specific for IgG1, IgG2, IgG3, IgG4, IgGκ and IgGλ.

IgG isolation

IgG fraction of the serum samples were isolated by Protein G column (GE Healthcare) according to the manufacturer's instructions. For functional analyses, the *in vivo* formed FB–FB-autoantibody complexes were removed. To this end, FB-specific antibodies isolated by Protein G column from goat anti-FB antiserum were immobilized on NHS column (GE Healthcare). The patient's and control's IgG fractions were loaded onto the anti-FB column, the flow-through fraction was collected and tested for the presence of FB.

Western blot

To analyze FHR1- and/or FHR3-deficiency, serum samples at a dilution of 1:50 were separated on 10% SDS-PAGE under non-reducing conditions and transferred to nitrocellulose membrane (BioRad). After blocking with 1% BSA, 4% non-fat milk powder in DPBS-0.05% Tween-20, FHR3 and FHR1 were detected with rabbit anti-FHR3 (kindly provided by Dr. Ilse Jongerius, Sanquin Health Solutions, Amsterdam, the Netherlands) and goat anti-FH antisera and the corresponding HRP-conjugated secondary antibodies, respectively. The blots were developed with the ECL detection kit (Merck).

To detect *in vivo* formed immune complexes, IgG fractions of the autoanti-FB positive patient and healthy controls were separated on 10% SDS-PAGE under non-reducing conditions and blotted onto nitrocellulose membrane. After blocking with 1% BSA, 4% non-fat milk powder in DPBS-0.05% Tween-20, the membranes were incubated with goat anti-FB antiserum and HRP-conjugated rabbit anti-goat antibodies. These immune complexes were removed before further experiments to prevent their interference with the assays.

Convertase assays

The solid phase AP C3 convertase was built up as described by Hourcade et al. in 2002 (37) with modifications. C3b was immobilized

TABLE 1 Characteristics of patients with RA and healthy controls.

Characteristics		RA (N=97)	Healthy control (N=117)
Sex	Female (%)	79 (81.4%)	73 (62.4%)
	Male (%)	18 (18.6%)	44 (37.6%)
Age	Average (years)	62.5	31.2
	Median (years)	64	25
	Min-Max (years)	24-87	21-81

10.3389/fimmu.2023.1113015

at 5 μg/ml on microplate wells (Maxisorp, NUNC). After washing, 2 μg/ml FB, 4 μg/ml properdin and 0.1 μg/ml FD were added in convertase buffer (DPBS containing 4% BSA, 2 mM $NiCl_2$, 0.1% Tween-20) for 1 hour at 37°C. Convertase formation was detected with goat anti-FB and HRP-conjugated rabbit anti-goat antibodies. Convertase activity was determined by adding 10 μg/ml C3 for 1 hour at 37°C. The generated C3a was measured by the C3a EIA kit (Quidel). In some assays, patient's or control IgG was added together with convertase components to analyze their effect on convertase formation. Convertase decay was determined after incubation of the formed convertase with the isolated IgG fractions alone or in the presence of 1 μg/ml FH for 1 hour at 37°C. Remaining convertase was detected with goat anti-FB antiserum.

Complement activation assay

LPS (#L4524, Merck) was immobilized at 10 μg/ml on Maxisorp microplate wells. Wells were washed with DPBS and blocked with 2% BSA. 10% complement active normal human serum (Quidel) was preincubated with the FB-free autoantibodies or with 5×10^6 rabbit red blood cells (RRBC, Culex Bt.) as positive control for 15 min at 37°C. The serum was then added to the LPS-coated wells for 1 h at 37°C to determine the remaining complement activity. Complement deposition was measured with HRP-conjugated goat anti-C3 or mouse anti-C5b-9 and HRP-conjugated goat anti-mouse IgG.

Hemolysis assay

5×10^6 RRBC were incubated with 7% complement active normal human serum (Quidel) in HEPES buffer (20 mM HEPES, 7 mM $MgCl_2$, 10 mM EGTA, 144 mM NaCl, 1% BSA, pH 7.4) with serial dilutions of purified IgG for 30 min at 37°C. After centrifugation, optical density of the supernatants was measured at 414 nm.

Statistical analysis

Statistical analyses were performed with GraphPad Prism version 6.01 for Windows (GraphPad Software, San Diego, CA). A p value < 0.05 was considered statistically significant. Comparison of gender distribution between RA patients and healthy controls were determined by χ^2 test. To compare continuous variables (age), Mann–Whitney U test was performed. Comparison of FHR1- and/or FHR3-deficiency distribution between RA patients and healthy donors were performed by χ^2 test. For comparison of the effects of IgG isolated from RA547 or healthy controls, one-way ANOVA was used with Dunnett's multiple comparison test.

Results

Screening for anti-complement autoantibodies

To investigate the presence and role of complement-specific autoantibodies in RA, we screened a Hungarian RA cohort for autoantibodies against FH, as well as C1q and MBL which were described as autoantibody targets in RA (33–35). In addition, we looked for autoantibodies against FB, FI, C3b and the solid phase C3 convertase C3bBbP, and analyzed the cohort for deficiency of the complement proteins FHR1 and FHR3. Serum samples of RA patients and healthy controls were tested for IgG and IgM antibodies against the above-mentioned complement components in ELISA.

Healthy control samples were negative for all tested antibodies, and we did not detect autoantibodies against FH, FI, C3b or the C3bBbP convertase in this RA cohort (Supplementary Figures 1C, D and data not shown). Four patients (RA240, RA268, RA557, RA587) were positive for autoantibodies against C1q (Figure 1A; Supplementary Figure 1A), two patients were positive for autoantibodies against MBL (RA277, RA348) (Figure 1B; Supplementary Figure 1B) and five patients (RA223, RA243,

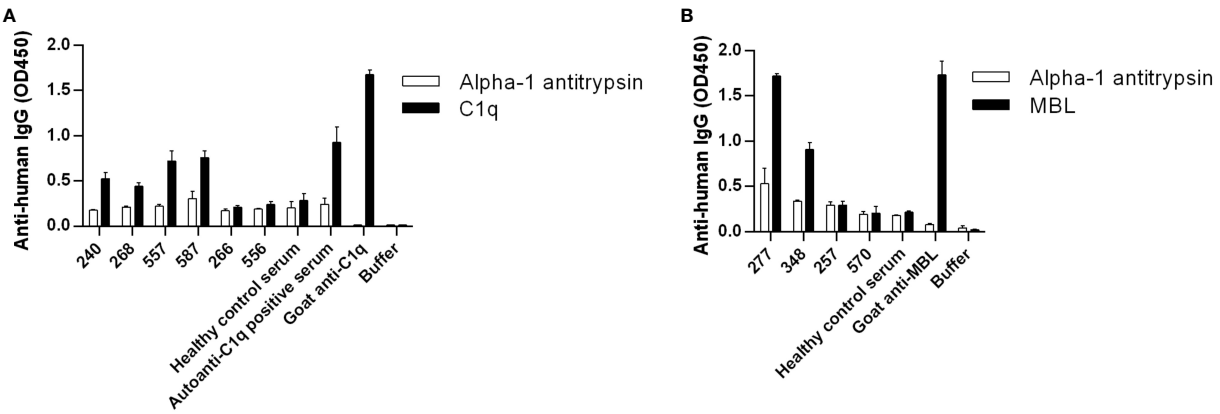

FIGURE 1
Detection of autoantibodies against C1q and MBL in RA patients. **(A)** C1q, **(B)** MBL, and alpha-1 antitrypsin as negative control were immobilized on microtiter plate wells. After blocking, serum samples diluted 1:50 were added. In the case of C1q, high salt concentration buffer was used and in the case of MBL 10 mM EDTA was used to exclude unspecific binding, as described in Materials and methods. Bound IgG was detected by HRP-conjugated anti-human IgG. Selected samples are shown: positive patient samples, some negative patient samples and controls. For full datasets please refer to Supplementary Figure 1. Data are mean ± SEM of two experiments.

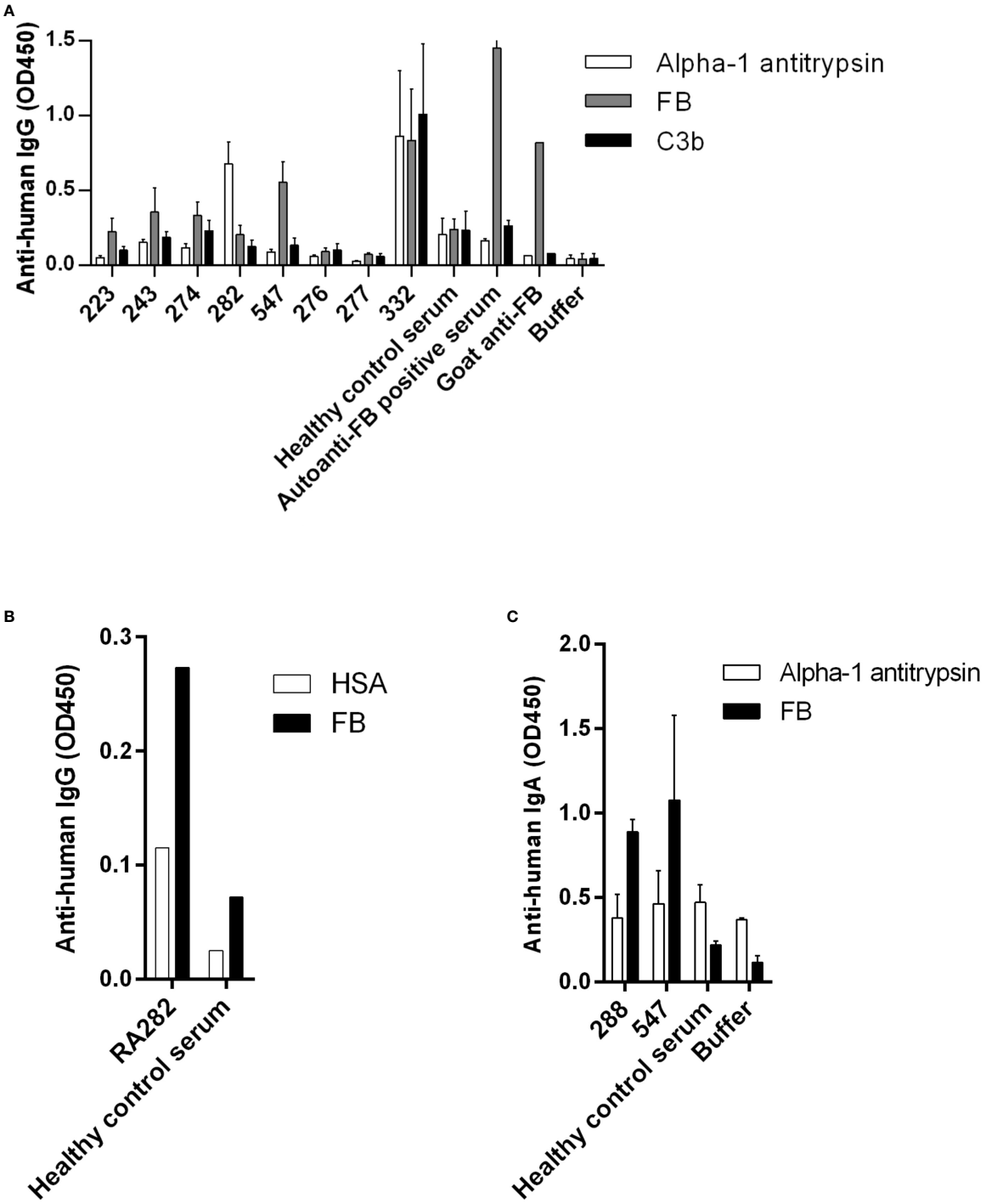

FIGURE 2
Autoanti-FB in RA patients. **(A)** FB, C3b and alpha-1 antitrypsin as negative control were immobilized on microtiter plate wells. After blocking, serum samples diluted 1:50 were added. Bound IgG was detected by HRP-conjugated anti-human IgG. Data are mean ± SEM of three experiments. **(B)** RA282 autoanti-FB was analyzed and confirmed using another negative control protein, human serum albumin (HSA). Data from a single experiment are shown. **(C)** IgA autoantibodies against FB were detected using HRP-conjugated anti-human IgA. Data are mean ± SD of two experiments. In all three panels selected samples are shown: positive patient samples, some negative patient samples and controls. For full datasets please refer to Supplementary Figure 1.

RA274, RA282, RA547) were positive for autoanti-FB IgG (Figure 2A; Supplementary Figure 1C). The serum of patient RA282 showed high signal on alpha-1 antitrypsin, and it turned out that this patient had autoantibodies against alpha-1 antitrypsin. Positivity for FB-autoantibodies was determined using other inert proteins as negative controls (Figure 2B). In two patients (RA288, RA547) autoanti-FB IgA was detected (Figure 2C). Characteristics of the autoantibody positive patients are shown in Table 2. The titer and isotype were determined for all the five autoanti-FB IgG positive samples. We could detect in all samples both light chains and various

10.3389/fimmu.2023.1113015

TABLE 2 Characteristics of the autoantibody positive patients.

Patient ID	Age at onset (years)	Sex	CRP (mg/l)	RF (U/ml)	Anti-CCP (U/ml)	DAS index	Treatment	Detected autoantibody
223	57	male	16	71	749	6.9	Methotrexat, Metilprednizolon, Sulfasalazine	anti-FB IgG
240	52	female			128.47	2.27		anti-C1q IgG
243	75	male		360.9	2403.87	0.84	Tocilizumab	anti-FB IgG
268	67	female				6.59		anti-C1q IgG
274	32	female		40	373	6.54	Methotrexat	anti-FB IgG
277	52	female		120	452.76	5.25	Leflunomide	anti-MBL IgG
282	80	male			497.89	3.09	Certolizumab pegol	anti-FB IgG
288	73	female		249	399	0.91	Tocilizumab	anti-FB IgA
348	73	female			617.34			anti-MBL IgG
547	41	female				3.0	Certolizumab pegol	anti-FB IgG, IgA
557	64	female			290	5.4		anti-C1q IgG
587	45	male			61			anti-C1q IgG

Reference ranges:
RF (rheumatoid factor): >20 U/ml positive.
Anti-CCP (cyclic citrullinated peptide): <20 non-RA, >20 RA.
DAS index (disease activity score): <2.6 remission, 2.6-3.1 low disease activity, 3.1-5.1 moderate disease activity, >5.1 high disease activity.

combinations of heavy chains, pointing to an oligoclonal origin of the autoantibodies (Table 3). Based on the amount of serum available, RA547 sample was selected and further characterized in detail.

IgG of RA547 and that of healthy controls was isolated from serum by Protein G column. IgG-depleted serum of RA547 did not show binding to FB (Figure 3A) while the isolated IgG fraction showed dose-dependent binding to FB (Figure 3B), and the antibody also bound to FB as part of the solid phase C3 convertase (C3bBbP) (Figure 3C). To test whether the antibody binds FB in its native form *in vivo*, the isolated IgG fraction was analyzed by Western blot. A strong band corresponding to FB was detected in the RA547 sample, indicating the formation of FB–anti-FB immune complexes *in vivo*. (Figure 3D).

RA547 autoanti-FB characterization

Characteristics as titer, isotype, and binding site of the autoanti-FB in RA547 were determined in ELISA-based assays (Table 3 and Figure 4). The titer and isotype were determined in the third available sample (Figures 4B, C). The presence of anti-FB autoantibodies was monitored in serial samples; over time, probably due to therapy, the anti-FB autoantibody levels decreased, and in the last sample it was not detectable anymore (Figure 4A). To determine the binding site of autoantibodies on FB, immobilized FB was preincubated with monoclonal antibodies specific for either the Ba or Bb part of FB, as well as with anti-FB antiserum. The anti-Bb and the polyclonal anti-FB reduced the binding of the autoantibodies to FB, while anti-Ba did not significantly influence the binding, suggesting that the autoantibody binding site is on the enzymatically active Bb part of FB (Figure 4D). Functional effects of the antibodies were analyzed in further assays.

FB autoantibodies influence the activation of the alternative pathway and affect the terminal pathway

To measure the effect of the purified, patient-derived anti-FB autoantibodies on the activation of the alternative pathway, rabbit red

TABLE 3 Titer and isotype of the autoanti-FB IgG antibodies.

Sample ID	Titer	Isotype
RA223	1/800	IgG3, IgG4, IgGκ, IgGλ
RA243	1/200	IgG4, IgGκ, IgGλ
RA274	1/400	IgG2, IgG3, IgG4, IgGκ, IgGλ
RA282	1/50	IgG2, IgG4, IgGκ, IgGλ
RA547	1/800	IgG2, IgG3, IgGκ, IgGλ

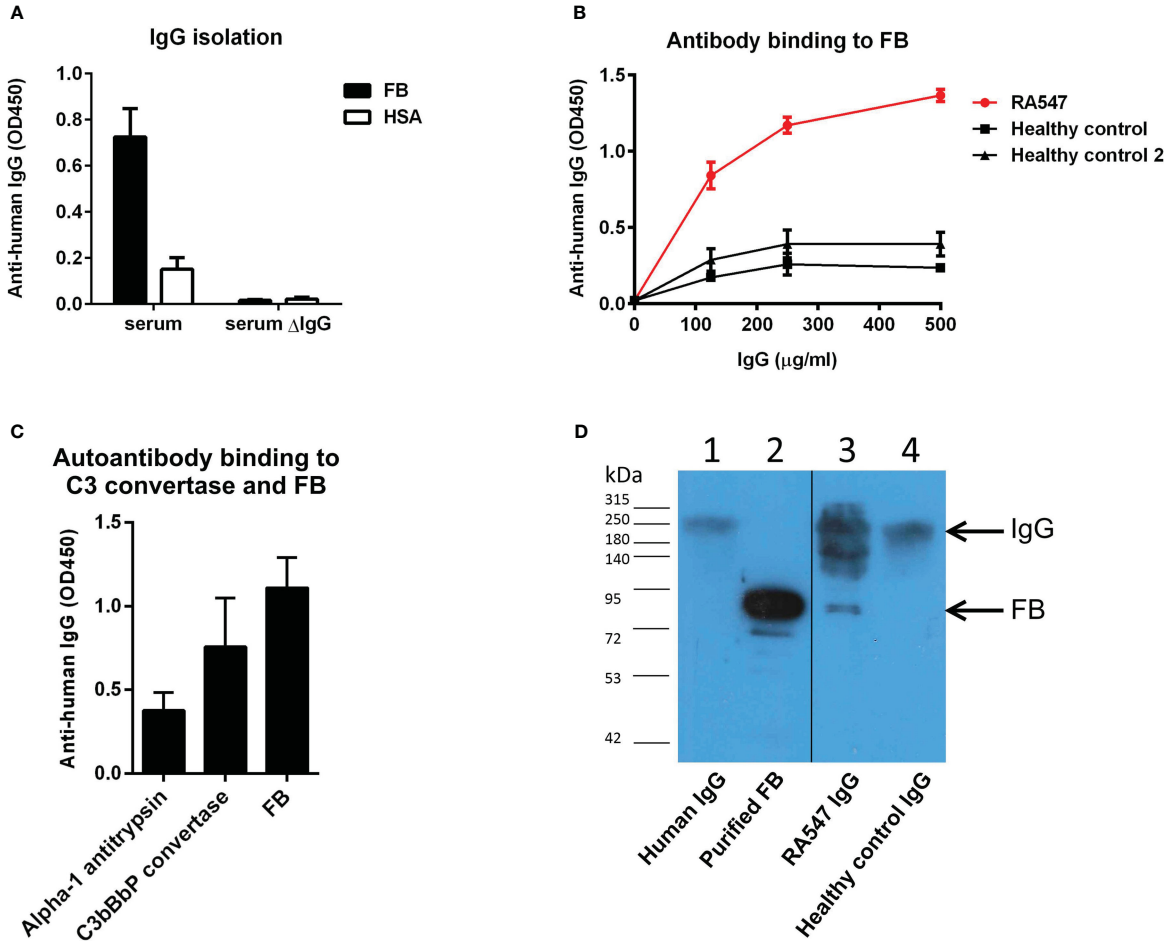

FIGURE 3
Anti-FB autoantibody characterization. **(A)** IgG was isolated with Protein G column from RA547 patient's serum and healthy controls' sera. The IgG depleted serum lost its ability to bind FB. **(B)** Serial dilutions from RA patient's IgG showed dose-dependent binding to FB in contrast to healthy control IgG. Data are mean ± SD from three independent experiments. **(C)** Autoanti-FB bound to FB as part of the C3 convertase of the alternative pathway (C3bBbP). **(D)** *In vivo* formed IgG-FB complexes were detected in the patient's IgG fraction with polyclonal anti-FB antibody in Western blot. Lanes: 1: purified IgG, 2: purified FB, 3: RA547 IgG, 4: Healthy control IgG. 25 μg isolated IgG was run on SDS-PAGE, blotted onto nitrocellulose membrane, and developed by anti-FB antibody. Blot is representative of three experiments.

blood cells (RRBCs), which are sensitive to lysis in normal human serum, were used. RRBCs were mixed with normal human serum in a buffer containing Mg^{2+}-EGTA, which allows only the activation of the alternative pathway, and supplemented with serial dilutions of IgG isolated from the serum of the patient or healthy controls. After incubation, lysis was determined by measuring the OD of released hemoglobin in the supernatant. Compared to the control IgGs, patient IgG inhibited the hemolysis in a dose-dependent manner (Figure 5).

Next, we investigated how the autoantibodies influence complement activation in serum in the fluid phase as described by Zhao et al. (38). To this end, normal human serum was mixed and incubated with IgG from RA547 or healthy controls and with RRBC as positive control. After incubation, the residual complement activity was measured on LPS-coated surface in the form of C3- and C5b-9-deposition (Figure 6). Serum alone retains its complement activity and when added to LPS, C3- and C5b-9-depostion can be detected. RRBC depletes complement during incubation, so no complement deposition can be measured on LPS, similar to the EDTA-treated serum sample. Incubation of the serum with IgG generally led to activity loss to some extent, probably due to activation *via* immune complexes present in the IgG preparations. However, compared to the IgG of healthy individuals, the autoanti-FB-containing patient IgG further decreased both C3- and C5b-9-deposition, presumably *via* inhibitory effects of the anti-FB autoantibodies (Figure 6).

FB-autoantibodies impair the activity of the solid phase C3 convertase of the alternative pathway

To decipher the mechanism behind the inhibitory effects measured using whole serum, next we analyzed the effect of the autoantibodies on the C3 convertase. C3bBbP was generated on microplates using purified proteins as described by Hourcade et al. (37) and Strobel et al. (39) with modifications. Convertase formation was detected with polyclonal goat anti-FB, while convertase activity was determined by adding C3 and measuring the generated C3a (Figure 7A).

First, we investigated the effects of autoantibodies on convertase formation. IgG from the patient and healthy controls were added to

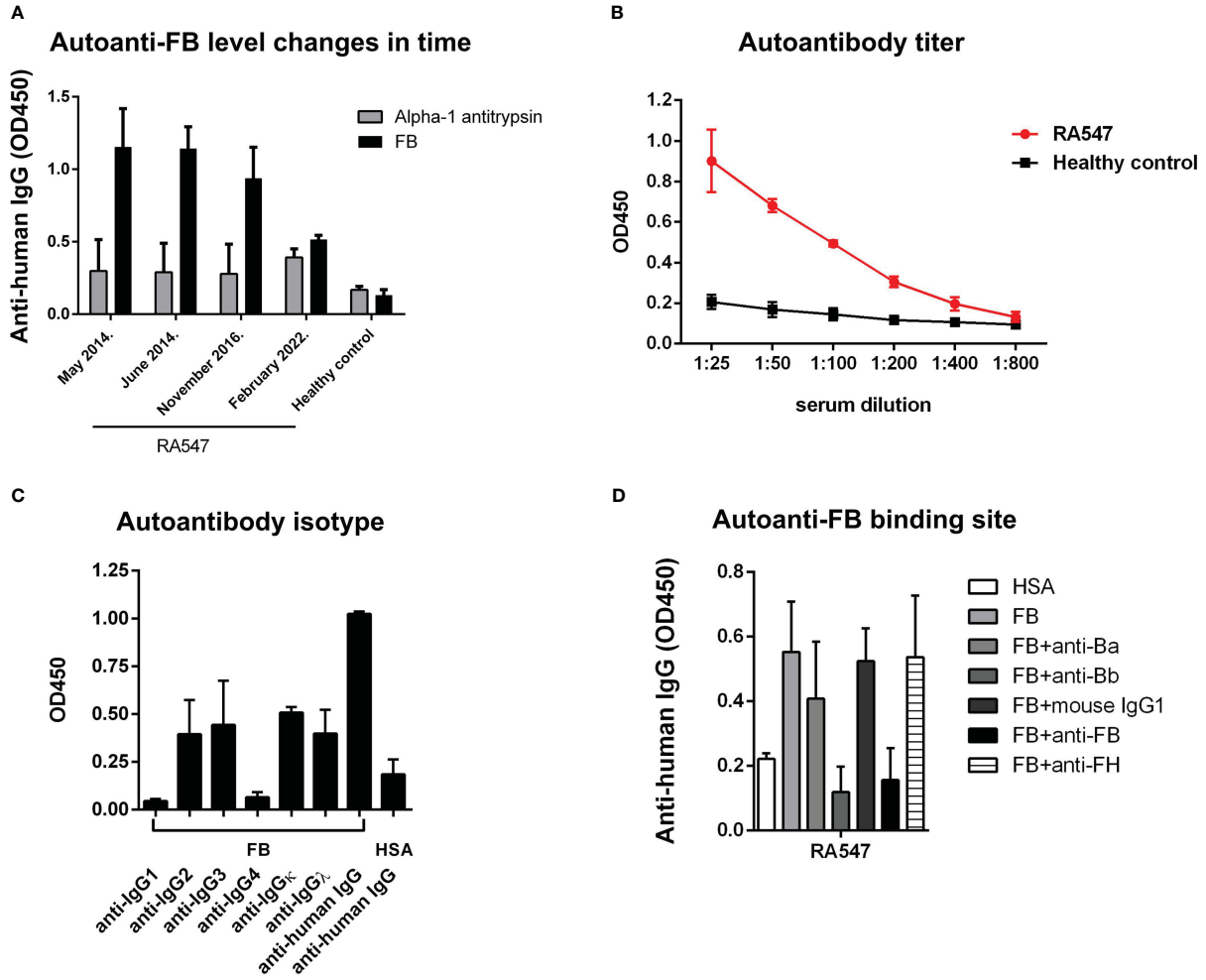

FIGURE 4
Autoantibody characterization. **(A)** We had serum samples from four time points to analyze the presence of autoanti-FB in RA547. Data are results ± SD of two experiments. **(B)** Titer of autoanti-FB was determined in ELISA, with serial dilutions of the patient's serum. **(C)** Autoantibodies were added to immobilized FB, and the isotypes were determined with monoclonal antibodies against the IgG subclasses. Data are mean ± SD from two independent experiments. Values obtained with an autoantibody negative healthy control as a background were subtracted from the values obtained with RA547 before plotting. **(D)** Autoantibody binding to immobilized FB was decreased by the preincubation of FB with monoclonal anti-Bb antibody and with polyclonal anti-FB antiserum. Data are mean ± SEM from three independent experiments. Values obtained with an autoantibody negative healthy control as a background were subtracted from the values obtained with RA547.

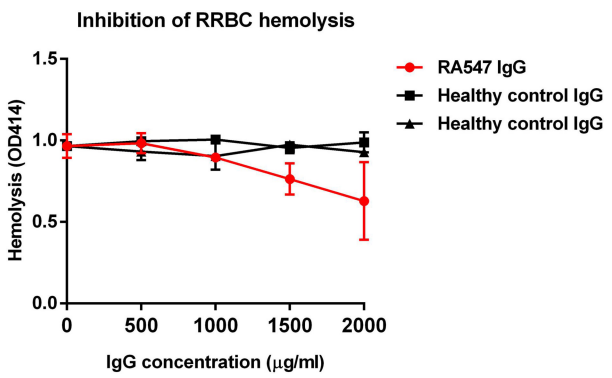

FIGURE 5
RA547 patient's IgG dose-dependently inhibited RRBC hemolysis. Complement active normal human serum was mixed with RRBCs and IgG from patient or healthy controls, then incubated for 30 min at 37°C. Samples were centrifuged, and the OD of the supernatant was measured at 414 nm. Data are mean ± SD from two independent experiments.

immobilized C3b together with the components of the convertase and, after incubation, convertase formation was measured. The anti-FB autoantibodies did not influence the assembly of the C3bBbP convertase (Figure 7B).

Next, we measured the effects of the autoantibodies on the FH-mediated decay of the convertase. The generated convertase was preincubated with IgG from the patient or healthy controls, then FH was added without removing the antibodies. After incubation, the remaining convertase was detected with goat anti-FB. The anti-FB autoantibodies had no effect in this assay; they did not protect the convertase from FH-mediated decay (Figure 7C).

Lastly, the effect of autoantibodies on convertase activity was measured. The generated convertase was preincubated with IgG from the patient and healthy controls, then C3 was added and the released C3a was measured from the supernatant. When added to the convertase, IgG of healthy controls had no effect, whereas, anti-FB autoantibodies significantly reduced the amount of generated C3a, similarly to that observed with the polyclonal anti-FB, used as positive control (Figure 7D).

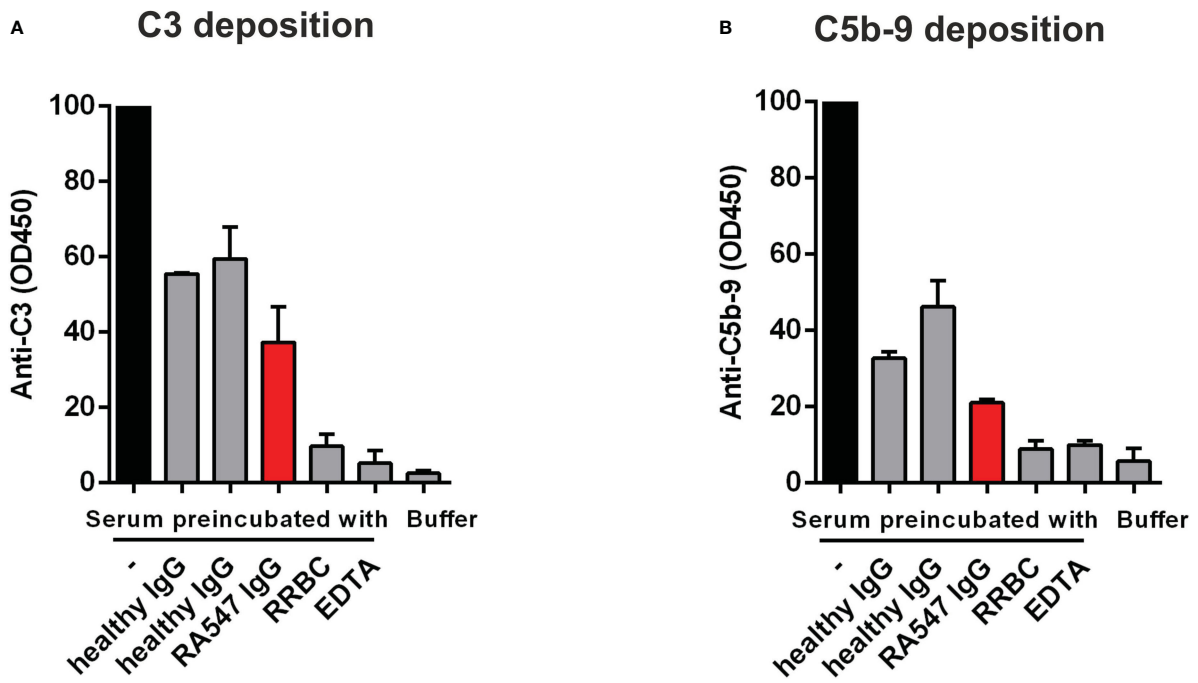

FIGURE 6
Anti-FB autoantibodies decrease complement activation-derived deposition of C3 and C5b-9 on LPS-coated surface. Normal human serum was preincubated with PBS, patient- or healthy control-derived IgG, and RRBC as a positive control, then added to LPS-coated wells. EDTA was used to inhibit complement activation on LPS. The deposition of **(A)** C3 and **(B)** C5b-9 was detected with anti-C3 and anti-C5b-9 antibodies, respectively. Data are mean ± SD from two independent experiments. RRBC: Rabbit Red Blood Cell.

FHR1 and FHR3 deficiency

Deficiency of FHR1 and/or FHR3 is associated with various conditions, it can be both a protective and a predisposing factor depending on the disease (22, 40). We investigated the frequency of FHR1 and FHR3 deficiency in this RA cohort. Genomic DNA was not available; therefore, serum samples were screened for the presence of the FHR1 and FHR3 proteins by Western blot. To our knowledge, none of the patients or controls received plasmapheresis or fresh frozen plasma, thus the detected proteins have no *ex vivo* origin. We found individuals lacking only FHR1, only FHR3 or both proteins, both among the RA patients and the healthy controls, and the differences between the two groups were not significant (Table 4; Supplementary Figure 2).

Discussion

In this study we analyzed the presence of autoantibodies against complement components in a Hungarian RA cohort. We found anti-C1q and anti-MBL autoantibodies (Figure 1.), in accordance with previous reports (32, 33, 35). No antibodies against FH, FI, C3b and the alternative pathway C3 convertase (C3bBbP) were detected in these samples. In the case of FH, our results contradict the findings of Foltyn Zadura et al., who found FH-autoantibodies in 16.5% and 9.2% of the analyzed samples (34). While high IgG signals on FH-coated wells in 6.9% of samples were detected in our assays, these serum samples gave high signal on inert control protein as well, thus we considered them false positives. In addition to anti-C1q and anti-MBL autoantibodies, we found anti-FB autoantibodies in 5 patients, which have not been described in RA so far. The anti-FB IgG titer varied between patients; however, the presence of both light chains and various heavy chains (Table 3) was a common feature, suggesting an oligoclonal origin of the antibodies in all cases. Since the RA group and the healthy control group significantly differed regarding age and gender in our study, we cannot state that the identified autoantibodies are RA-specific. However, to our knowledge, no anti-FB autoantibodies have been described in healthy people at any age.

The analyzed anti-FB autoantibodies bind FB both in its native form and as part of the C3 convertase (Figure 3C). In contrast to C3Nefs that bind to and stabilize the C3 convertase, increase its activity and enhance terminal pathway activity (41), the analyzed anti-FB autoantibody did not influence solid-phase C3 convertase stability but impaired its activity (Figure 7). This is also different from the characteristics of the anti-FB autoantibody described in dense deposit disease (DDD) by Strobel et al. that stabilized the C3 convertase, increased its activity but inhibited the C5 convertase (39). FB autoantibodies described by Chen et al. in DDD and Marinozzi et al. in C3G also appeared pathogenic by enhancing C3 turnover (42, 43). Here, the anti-FB autoantibody binding site was mapped to the enzymatically active Bb part on FB (Figure 4D). Presumably, the autoantibody binding to Bb in the C3 convertase leads to impairment of C3 convertase activity measured in ELISA and in hemolysis assay (Figures 7D, 5).

Since our Western blot analysis demonstrated the presence of FB within the isolated patient IgG fraction (Figure 3D), we conclude that the autoanti-FB antibodies formed immune complexes in the patient *in vivo*. We observed impaired complement activation in the form of reduced C3 and C5b-9 deposition on LPS-coated surface after preincubation of the serum with purified patient IgG, containing the FB–autoanti-FB immune complexes (Figure 6). This could be explained by activation of the classical pathway by the immune complexes and/or by the inhibitory effect of the anti-FB autoantibodies on C3 convertases formed on the LPS surface.

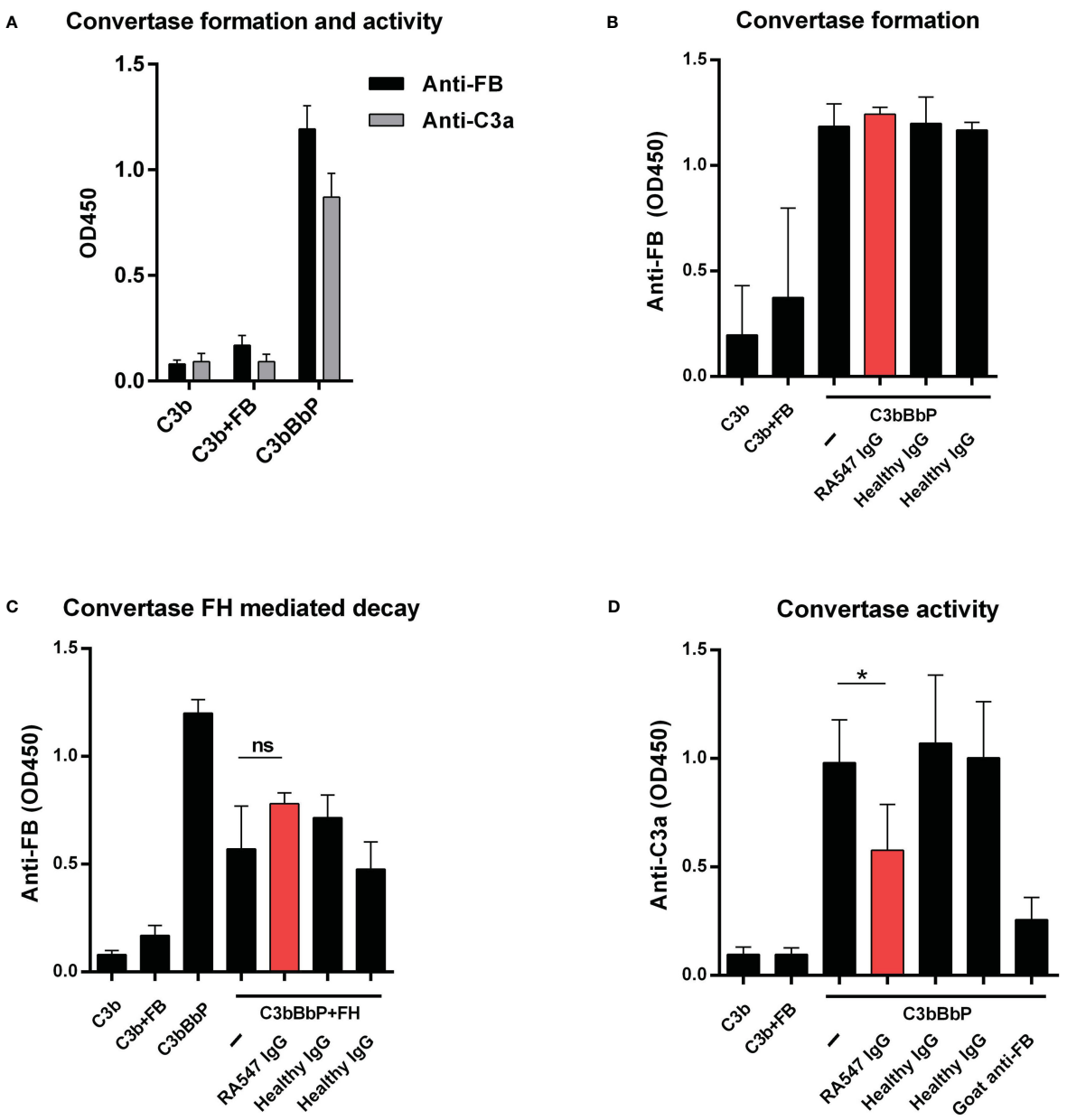

FIGURE 7
Effect of the patient's IgG on alternative pathway C3 convertase. **(A)** Generation of solid phase C3 convertase in microplate wells. We added FB, FD and properdin together to the immobilized C3b and, after incubation, detected the convertase formation by polyclonal anti-FB. To confirm the activity of the convertase, C3 was added in the fluid phase, and we measured the released C3a from the supernatant with commercially available C3a EIA (Quidel). **(B)** To test the autoantibodies' effect on convertase formation, we added the patient's or healthy controls' IgG together with FB, FD and properdin to immobilized C3b. The assembly of the convertase was detected with polyclonal goat anti-FB antibody. **(C)** Autoantibodies had no effect on the FH mediated decay of the C3 convertase. The convertase was incubated with IgG and FH and the remaining convertase was detected with polyclonal anti-FB antibody. **(D)** To investigate the effect of the patient's autoantibodies on the activity of the convertase, the convertase was incubated with purified IgG and, after washing, C3 was added. Supernatants were collected and the C3 cleavage product C3a was measured using C3a EIA. Data are mean ± SD of three **(A, C, D)** or two **(B)** independent experiments. *$p<0.05$, One-Way ANOVA.

The production of such autoantibodies may be triggered by the prolonged presence of the complement protein activation products and complexes due to overactivation of the system. Our data demonstrate that not all the complement specific autoantibodies are pathogenic and contribute to complement activation in RA. Autoantibodies may be beneficial for patients, as it was shown for autoantibodies against FH in non-small cell lung cancer where anti-FH blocked FH activity at tumor cells (44) or in lupus patients (45). The autoanti-FB in RA reported here also demonstrates that some autoantibodies could hold back the overwhelming complement activation which may be beneficial for the patients. This suggests that the generation of such non-activating autoantibodies is part of a protective response and contributes to the prevention of the tissue damage caused by excessive complement activation.

The data also highlight that the presence/level of autoanti-FB in RA can be transient (Figure 4A) probably depending on the actual state of the disease (remission, or active phase), and the received treatment. In patient RA547 the autoanti-FB levels were mostly constant between May 2014 and November 2016, during which the patient had anti-TNFα therapy (certolizumab pegol). Later the therapy was changed (from 2020) to

TABLE 4 Overview of FHR1- and FHR3-deficiency in the RA patients and healthy controls.

Sample	N	FHR3 deficient	FHR1 deficient	FHR3/FHR1 deficient
RA	94	4 (4.25%)	1 (1.06%)	5 (5.31%)
Healthy control	117	2 (1.71%)	3 (2.56%)	4 (3.42%)

adalimumab which is another kind of anti-TNFα treatment. In the most recent serum sample of the patient (February 2022) autoanti-FB was not detectable, presumably due to the change in therapy or disease activity.

Autoantibodies against the components of the convertase can disturb the balance of complement activation, contributing to autoimmune diseases (39, 46). In many cases, autoantibodies have diagnostic and prognostic value, therefore their detection is coming to fore (47). Though in RA autoantibodies against the early components of the complement system (32, 33, 35) as well as autoantibodies against the complement regulator FH (34) were described years ago, their role in disease mechanism has not been investigated. Our results further support that the pathophysiology of RA implies the complement system and its dysfunction. These data also draw attention to the importance of characterization and functional analysis of autoantibodies, because simply detecting autoantibodies can be misleading and reporting their presence may misinform physicians. FB autoantibodies may be pathogenic in certain conditions, such as likely in DDD, but may be non-pathogenic or even protective in other diseases.

Data availability statement

The original contributions presented in the study are included in the article/Supplementary Material. Further inquiries can be directed to the corresponding author.

Ethics statement

The studies involving human participants were reviewed and approved by National Ethical Committee (33986-1/2018 EKU). The patients/participants provided their written informed consent to participate in this study.

Author contributions

ATM and BU performed experiments, analyzed the data, prepared the figures. AF, BR, GN took care of the patients and provided serum samples. GS, MJ and BU initiated the study, supervised the research. ATM, BU and MJ wrote the manuscript with help of the other authors. All authors read and approved the manuscript. All authors contributed to the article and approved the submitted version.

Funding

The work of the authors was supported in part by the National Research, Development and Innovation Fund of Hungary (grant K 125219), the Institutional Excellence Program to ELTE (NKFIH-1157/8/2019, D11206), the Eötvös Loránd Research Network and the Hungarian Academy of Sciences (0106307), and by project no. FIEK_16-1-2016-0005, implemented with the support provided from the National Research, Development and Innovation Fund of Hungary, financed under the FIEK_16 funding scheme.

Acknowledgments

We thank Dr. Ilse Jongerius (Sanquin Health Solutions, Amsterdam, the Netherlands) for providing the rabbit anti-FHR3 antiserum.

Conflict of interest

The authors declare that the research was conducted in the absence of any commercial or financial relationships that could be construed as a potential conflict of interest.

Publisher's note

All claims expressed in this article are solely those of the authors and do not necessarily represent those of their affiliated organizations, or those of the publisher, the editors and the reviewers. Any product that may be evaluated in this article, or claim that may be made by its manufacturer, is not guaranteed or endorsed by the publisher.

Supplementary material

The Supplementary Material for this article can be found online at: https://www.frontiersin.org/articles/10.3389/fimmu.2023.1113015/full#supplementary-material

References

1. Okroj M, Heinegård D, Holmdahl R, Blom AM. Rheumatoid arthritis and the complement system. *Ann Med* (2007) 39(7):517–30. doi: 10.1080/07853890701477546

2. Firestein GS. Evolving concepts of rheumatoid arthritis. *Nature* (2003) 423 (6937):356–61. doi: 10.1038/nature01661

3. Silman AJ, Pearson JE. Epidemiology and genetics of rheumatoid arthritis. *Arthritis Res* (2002) 4(Suppl 3):S265–72. doi: 10.1186/ar578

4. Bernatsky S, Dekis A, Hudson M, Pineau CA, Boire G, Fortin PR, et al. Rheumatoid arthritis prevalence in Quebec. *BMC Res Notes.* (2014) 7:937. doi: 10.1186/1756-0500-7-937

5. Kuo CF, Luo SF, See LC, Chou IJ, Chang HC, Yu KH. Rheumatoid arthritis prevalence, incidence, and mortality rates: A nationwide population study in Taiwan. *Rheumatol Int* (2013) 33(2):355–60. doi: 10.1007/s00296-012-2411-7

6. Arima H, Koirala S, Nema K, Nakano M, Ito H, Poudel KM, et al. High prevalence of rheumatoid arthritis and its risk factors among Tibetan highlanders living in tsarang, mustang district of Nepal. *J Physiol Anthropol.* (2022) 41(1):12. doi: 10.1186/s40101-022-00283-3

7. Scott DL, Wolfe F, Huizinga TWJ. Rheumatoid arthritis. *Lancet* (2010) 376 (9746):1094–108. doi: 10.1016/S0140-6736(10)60826-4

8. van Delft MAM, Huizinga TWJ. An overview of autoantibodies in rheumatoid arthritis. *J Autoimmunity.* (2020) 110:102392. doi: 10.1016/j.jaut.2019.102392

9. Di Giuseppe D, Discacciati A, Orsini N, Wolk A. Cigarette smoking and risk of rheumatoid arthritis: A dose-response meta-analysis. *Arthritis Res Ther* (2014) 16(2):R61. doi: 10.1186/ar4498

10. Chen HH, Huang N, Chen YM, Chen TJ, Chou P, Lee YL, et al. Association between a history of periodontitis and the risk of rheumatoid arthritis: A nationwide, population-based, case–control study. *Ann Rheum Dis* (2013) 72(7):1206–11. doi: 10.1136/annrheumdis-2012-201593

11. Busch R, Kollnberger S, Mellins ED. HLA associations in inflammatory arthritis: Emerging mechanisms and clinical implications. *Nat Rev Rheumatol* (2019) 15(6):364–81. doi: 10.1038/s41584-019-0219-5

12. Alpízar-Rodríguez D, Pluchino N, Canny G, Gabay C, Finckh A. The role of female hormonal factors in the development of rheumatoid arthritis. *Rheumatology* (2017) 56 (8):1254–63. doi: 10.1093/rheumatology/kew318

13. Sokolova MV, Schett G, Steffen U. Autoantibodies in rheumatoid arthritis: Historical background and novel findings. *Clin Rev Allergy Immunol* (2022) 63(2):138–51. doi: 10.1007/s12016-021-08890-1

14. Newkirk MM. Rheumatoid factors: Host resistance or autoimmunity? *Clin Immunol* (2002) 104(1):1–13. doi: 10.1006/clim.2002.5210

15. Kwon EJ, Ju JH. Impact of posttranslational modification in pathogenesis of rheumatoid arthritis: Focusing on citrullination, carbamylation, and acetylation. *Int J Mol Sci* (2021) 22(19):10576. doi: 10.3390/ijms221910576

16. Aletaha D, Neogi T, Silman AJ, Funovits J, Felson DT, Bingham CO, et al. 2010 Rheumatoid arthritis classification criteria: An American college of Rheumatology/European league against rheumatism collaborative initiative. *Arthritis Rheum* (2010) 62 (9):2569–81. doi: 10.1002/art.27584

17. Hensvold AH, Frisell T, Magnusson PKE, Holmdahl R, Askling J, Catrina AI. How well do ACPA discriminate and predict RA in the general population: A study based on 12 590 population-representative Swedish twins. *Ann Rheum Dis* (2017) 76(1):119–25. doi: 10.1136/annrheumdis-2015-208980

18. Seri A, Mohamed HKA, Essa MEA, Elagib EM, Eltahirm NIA, Mansour SMA, et al. Analysis of serum immune markers in seropositive and seronegative rheumatoid arthritis among sudanese patients and the relation between the serotype and joint involvement: A cohort study. *Open Access Rheumatol* (2021) 13:325–32. doi: 10.2147/OARRR.S339134

19. Carbonell-Bobadilla N, Soto-Fajardo C, Amezcua-Guerra LM, Batres-Marroquín AB, Vargas T, Hernández-Diazcouder A, et al. Patients with seronegative rheumatoid arthritis have a different phenotype than seropositive patients: A clinical and ultrasound study. *Front Med (Lausanne)* (2022) 9:978351. doi: 10.3389/fmed.2022.978351

20. Galindo-Izquierdo M, Pablos Alvarez JL. Complement as a therapeutic target in systemic autoimmune diseases. *Cells* (2021) 10(1):148. doi: 10.3390/cells10010148

21. Ricklin D, Hajishengallis G, Yang K, Lambris JD. Complement: A key system for immune surveillance and homeostasis. *Nat Immunol* (2010) 11(9):785–97. doi: 10.1038/ni.1923

22. Cserhalmi M, Papp A, Brandus B, Uzonyi B, Józsi M. Regulation of regulators: Role of the complement factor H-related proteins. *Semin Immunol* (2019) 45:101341. doi: 10.1016/j.smim.2019.101341

23. Ricklin D, Reis ES, Mastellos DC, Gros P, Lambris JD. Complement component C3 – the "Swiss army knife" of innate immunity and host defense. *Immunol Rev* (2016) 274 (1):33–58. doi: 10.1111/imr.12500

24. Schmidt CQ, Lambris JD, Ricklin D. Protection of host cells by complement regulators. *Immunol Rev* (2016) 274(1):152–71. doi: 10.1111/imr.12475

25. Matola AT, Józsi M, Uzonyi B. Overview on the role of complement-specific autoantibodies in diseases. *Mol Immunol* (2022) 151:52–60. doi: 10.1016/j.molimm.2022.08.011

26. Swaak AJG, van Rooyen A, Planten O, Han H, Hattink O, Hack E. An analysis of the levels of complement components in the synovial fluid in rheumatic diseases. *Clin Rheumatol* (1987) 6(3):350–7. doi: 10.1007/BF02206833

27. Moxley G, Ruddy S. Elevated C3 anaphylatoxin levels in synovial fluids from patients with rheumatoid arthritis. *Arthritis Rheumatol* (1985) 28(10):1089–95. doi: 10.1002/art.1780281003

28. Hornum L, Hansen AJ, Tornehave D, Fjording MS, Colmenero P, Wätjen IF, et al. C5a and C5aR are elevated in joints of rheumatoid and psoriatic arthritis patients, and C5aR blockade attenuates leukocyte migration to synovial fluid. *PloS One* (2017) 12(12): e0189017. doi: 10.1371/journal.pone.0189017

29. Brodeur JP, Ruddy S, Schwartz LB, Moxley G. Synovial fluid levels of complement SC5b-9 and fragment bb are elevated in patients with rheumatoid arthritis. *Arthritis Rheumatol* (1991) 34(12):1531–7. doi: 10.1002/art.1780341209

30. Corallini F, Bossi F, Gonelli A, Tripodo C, Castellino G, Mollnes TE, et al. The soluble terminal complement complex (SC5b-9) up-regulates osteoprotegerin expression and release by endothelial cells: Implications in rheumatoid arthritis. *Rheumatology* (2008) 48(3):293–8. doi: 10.1093/rheumatology/ken495

31. Nguyen THP, Hokstad I, Fagerland MW, Mollnes TE, Hollan I, Feinberg MW, et al. Antirheumatic therapy is associated with reduced complement activation in rheumatoid arthritis. *PloS One* (2022) 17(2):e0264628. doi: 10.1371/journal.pone.0264628

32. Siegert CE, Daha MR, Halma C, van der Voort EA, Breedveld FC. IgG and IgA autoantibodies to C1q in systemic and renal diseases. *Clin Exp Rheumatol* (1992) 10 (1):19–23.

33. Liaskos C, Rentouli S, Simopoulou T, Gkoutzourelas A, Norman GL, Brotis A, et al. Anti-C1q autoantibodies are frequently detected in patients with systemic sclerosis associated with pulmonary fibrosis. *Br J Dermatol* (2019) 181(1):138–46. doi: 10.1111/bjd.17886

34. Foltyn Zadura A, Zipfel PF, Bokarewa MI, Sturfelt G, Jönsen A, Nilsson SC, et al. Factor h autoantibodies and deletion of complement factor h-related protein-1 in rheumatic diseases in comparison to atypical hemolytic uremic syndrome. *Arthritis Res Ther* (2012) 14(4):R185. doi: 10.1186/ar4016

35. Gupta B, Raghav SK, Agrawal C, Chaturvedi VP, Das RH, Das HR. Anti-MBL autoantibodies in patients with rheumatoid arthritis: Prevalence and clinical significance. *J Autoimmun* (2006) 27(2):125–33. doi: 10.1016/j.jaut.2006.07.002

36. Józsi M, Uzonyi B. Detection of complement factor b autoantibodies by ELISA. *Methods Mol Biol* (2021) 2227:141–5. doi: 10.1007/978-1-0716-1016-9_14

37. Hourcade DE, Mitchell L, Kuttner-Kondo LA, Atkinson JP, Medof ME. Decay-accelerating factor (DAF), complement receptor 1 (CR1), and factor h dissociate the complement AP C3 convertase (C3bBb) *via* sites on the type a domain of bb. *J Biol Chem* (2002) 277(2):1107–12. doi: 10.1074/jbc.M109322200

38. Zhao F, Afonso S, Lindner S, Hartmann A, Löschmann I, Nilsson B, et al. C3-glomerulopathy autoantibodies mediate distinct effects on complement C3- and C5-convertases. *Front Immunol* (2019) 10:1030. doi: 10.3389/fimmu.2019.01030

39. Strobel S, Zimmering M, Papp K, Prechl J, Józsi M. Anti-factor b autoantibody in dense deposit disease. *Mol Immunol* (2010) 47(7–8):1476–83. doi: 10.1016/j.molimm.2010.02.002

40. Medjeral-Thomas N, Pickering MC. The complement factor h-related proteins. *Immunol Rev* (2016) 274(1):191–201. doi: 10.1111/imr.12477

41. Corvillo F, Okrój M, Nozal P, Melgosa M, Sánchez-Corral P, López-Trascasa M. Nephritic factors: An overview of classification, diagnostic tools and clinical associations. *Front Immunol* (2019) 10:886. doi: 10.3389/fimmu.2019.00886

42. Marinozzi MC, Roumenina LT, Chauvet S, Hertig A, Bertrand D, Olagne J, et al. Anti-factor b and anti-C3b autoantibodies in C3 glomerulopathy and ig-associated membranoproliferative GN. *J Am Soc Nephrol* (2017) 28(5):1603–13. doi: 10.1681/ASN.2016030343

43. Chen Q, Müller D, Rudolph B, Hartmann A, Kuwertz-Bröking E, Wu K, et al. Combined C3b and factor b autoantibodies and MPGN type II. *New Engl J Med* (2011) 365(24):2340–2. doi: 10.1056/NEJMc1107484

44. Campa MJ, Gottlin EB, Bushey RT, Patz EF. Complement factor h antibodies from lung cancer patients induce complement-dependent lysis of tumor cells, suggesting a novel immunotherapeutic strategy. *Cancer Immunol Res* (2015) 3(12):1325–32. doi: 10.1158/2326-6066.CIR-15-0122

45. Li LL, Tan Y, Song D, Li YZ, Yu F, Chen M, et al. Anti-complement factor h autoantibodies may be protective in lupus nephritis. *Clinica Chimica Acta* (2020) 508:1–8. doi: 10.1016/j.cca.2020.05.005

46. Chauvet S, Berthaud R, Devriese M, Mignotet M, Vieira Martins P, Robe-Rybkine T, et al. Anti-factor b antibodies and acute postinfectious GN in children. *J Am Soc Nephrology.* (2020) 31(4):829–40. doi: 10.1681/ASN.2019080851

47. Leslie D, Lipsky P, Notkins AL. Autoantibodies as predictors of disease. *J Clin Invest* (2001) 108(10):1417–22. doi: 10.1172/JCI14452

frontiers | Frontiers in Immunology

TYPE Original Research
PUBLISHED 21 February 2023
DOI 10.3389/fimmu.2023.1112188

Check for updates

OPEN ACCESS

EDITED BY
Erik J. M. Toonen,
Hycult Biotech (Netherlands), Netherlands

REVIEWED BY
Arunika Mukhopadhaya,
Indian Institute of Science Education and Research Mohali, India
Ka-Yee Grace Choi,
University of British Columbia, Canada

*CORRESPONDENCE
Jessica Bertrand
Jessica.bertrand@med.ovgu.de

SPECIALTY SECTION
This article was submitted to Molecular Innate Immunity, a section of the journal Frontiers in Immunology

RECEIVED 30 November 2022
ACCEPTED 01 February 2023
PUBLISHED 21 February 2023

CITATION
Meinshausen A-K, Färber J, Illiger S, Macor P, Lohmann CH and Bertrand J (2023) C9 immunostaining as a tissue biomarker for periprosthetic joint infection diagnosis.
Front. Immunol. 14:1112188.
doi: 10.3389/fimmu.2023.1112188

COPYRIGHT
© 2023 Meinshausen, Färber, Illiger, Macor, Lohmann and Bertrand. This is an open-access article distributed under the terms of the Creative Commons Attribution License (CC BY). The use, distribution or reproduction in other forums is permitted, provided the original author(s) and the copyright owner(s) are credited and that the original publication in this journal is cited, in accordance with accepted academic practice. No use, distribution or reproduction is permitted which does not comply with these terms.

C9 immunostaining as a tissue biomarker for periprosthetic joint infection diagnosis

Ann-Kathrin Meinshausen[1], Jacqueline Färber[2], Sebastian Illiger[1], Paolo Macor[3], Christoph H. Lohmann[1,4] and Jessica Bertrand[1,4]*

[1]Department of Orthopaedic Surgery, Otto-von-Guericke University Magdeburg, Magdeburg, Germany, [2]Institute of Medical Microbiology, Infection Control and Prevention, Otto-von-Guericke University Magdeburg, Magdeburg, Germany, [3]Department of Life Sciences, University of Trieste, Trieste, Italy, [4]Health Campus Immunology, Infectiology and Inflammation, Otto-von-Guericke University Magdeburg, Magdeburg, Germany

Background: Culture-negative periprosthetic joint infections (PJI) are often false diagnosed as aseptic implant failure leading to unnecessary revision surgeries due to repeated infections. A marker to increase the security of e PJI diagnosis is therefore of great importance. The aim of this study was to test C9 immunostaining of periprosthetic tissue as a novel tissue-biomarker for a more reliable identification of PJI, as well as potential cross-reactivity.

Method: We included 98 patients in this study undergoing septic or aseptic revision surgeries. Standard microbiological diagnosis was performed in all cases for classification of patients. Serum parameters including C-reactive protein (CRP) serum levels and white blood cell (WBC) count were included, and the periprosthetic tissue was immunostained for C9 presence. The amount of C9 tissue staining was evaluated in septic versus aseptic tissue and the amount of C9 staining was correlated with the different pathogens causing the infection. To exclude cross-reactions between C9 immunostaining and other inflammatory joint conditions, we included tissue samples of a separate cohort with rheumatoid arthritis, wear particles and chondrocalcinosis.

Results: The microbiological diagnosis detected PJI in 58 patients; the remaining 40 patients were classified as aseptic. Serum CRP values were significantly increased in the PJI cohort. Serum WBC was not different between septic and aseptic cases. We found a significant increase in C9 immunostaining in the PJI periprosthetic tissue. To test the predictive value of C9 as biomarker for PJI we performed a ROC analyses. According to the Youden's criteria C9 is a very good biomarker for PJI detection with a sensitivity of 89% and a specificity of 75% and an AUC of 0.84. We did not observe a correlation of C9 staining with the pathogen causing the PJI. However, we observed a cross reactivity with the inflammatory joint disease like rheumatoid arthritis and different metal wear types. In addition, we did not observe a cross reactivity with chondrocalcinosis.

Conclusion: Our study identifies C9 as a potential tissue-biomarker for the identification of PJI using immunohistological staining of tissue biopsies. The use of C9 staining could help to reduce the number of false negative diagnoses of PJI.

KEYWORDS

periprosthetic joint infection, diagnostic biomarker, C9, inflammatory joint disease, complement pathway

Introduction

The complement pathway is one of the important mechanisms of the innate immune system to fight infections (1). The complement signaling pathway can be activated in three different ways, the classical, the lectin and the alternative signaling pathway (2, 3), all activating the enzymatic C3-convertase (4, 5). The cleavage of C3 starts a protein cascade, which generates the membrane attack complex (MAC) (6, 7). The MAC complex kills bacteria by destroying the bacterial membrane (8–11). In a study from 2018, it was shown that the activation of the terminal complement pathway during periprosthetic joint infections (PJI) can be used as a marker for the detection of PJI. In this study, C9 showed the most promising results (12).

A PJI is a serious complication after implantation of an endoprosthesis. The incidence is about 1% in all implanted hip and 2% in all implanted knee endoprosthesis. During the revision surgery, the probability of a PJI increases, as well as after a previous infection of the respective joint. Some comorbidities also influence the predisposition of the patient to develop a PJI (13). Typical signs of PJI are pain, swelling and warming of the skin around the joint, as well as fever (14–17), increased serum C-reactive protein (CRP) and in some cases serum leucocyte count (WBC) (18).

A wide range of pathogens can cause PJI. The most frequent pathogens found in PJI are from the *Staphylococcus* genus, especially *Staphylococcus aureus* and *Staphylococcus epidermidis* (19–21). *Streptococcus* spp. or *Enterococcus* are also common pathogens in PJI (20–22). Less frequently, gram-negative bacteria such as *Escherichia coli*, *Enterobacter* spp., *Klebsiella* spp. or *Pseudomonas* spp. can be found in PJI (23). The bacteria can occur in a monomicrobial infection or in combinations in a polymicrobial infection (24).

Early identification of PJIs is important to prevent sepsis and severe tissue damage. Currently, the standard of diagnostic is based on the evaluation of clinical symptoms, analysis of radiolucent lines in an X-ray and the microbiological diagnosis of tissue and fluid samples according to the MSIS criteria (25). There is currently no standard biomarker for PJI identification, but serum inflammation markers are considered as indicators. However, especially for the identification of low-grade infections, serum inflammation markers are not reliable (26). Some PJIs are not detected as infections and diagnosed as aseptic implant failure in case of culture negative PJIs (CN-PJI). The current rate of CN-PJI is about 1- 42% (26–31). Therefore, there is a need for biomarkers to facilitate a more secure identification of PJIs. Some biomarkers for more secure identification of PJIs have been proposed such as synovial fluid alpha-defensin (32, 33) or synovial fluid CRP (34, 35) concentration. CRP belongs to the acute-phase proteins and various clinical studies have already investigated the use of synovial fluid CRP levels as a biomarker for the detection of infections (36–44). Póvoa et al. described that the synovial fluid CRP concentration can be significantly increased during infections. However, some non-infected patients showed also increased synovial fluid CRP-levels, suggesting a possible interference of other inflammatory processes (40). Therefore, CRP can serve as a general indicator of inflammation, but cannot clearly distinguish between aseptic and septic inflammation and thereby facilitate identification of infections.

Another proposed biomarker for PJI is the synovial fluid alpha-defensin concentration. Alpha-defensin is an antimicrobial peptide mainly released by neutrophils (45–47). The synovial fluid alpha-defensin immunoassay has been described to identify PJI with a specificity of 95% and sensitivity of 100% (32, 48–50). However, the synovial fluid alpha-defensin concentration can also be elevated in the presence of wear particles or metallosis (12, 32, 51, 52) and in the presence of crystal deposits (53). Furthermore, the high costs of this detection method together with the cross reactivity in case of wear induced implant loosening (54) result in a demand for alternative biomarkers to secure the diagnosis of PJIs.

We have previously shown that C9 could be a potential indicator for PJI in periprosthetic tissue using immunohistochemical staining (12). The main limitation of the study was the low patient number included in this study and the restriction to shoulder implants. Therefore, in this study we aim to validate the immunostaining for C9 in the periprosthetic tissue for PJI identification using a larger cohort and periprosthetic tissue from knee and hip revisions, as well as testing the cross-reactivity with other inflammatory joint diseases.

Material and methods

Patients

98 patients undergoing a revision surgery on the total hip (THA) or the knee joint arthroplasty (TKA) were included in the present study. Ethical approval for this study was provided by the Institutional Review Board of the Medical School (No 207/17). Informed consent was obtained by the patients prior to inclusion into the study.

The surgeries were performed in the Department of Orthopaedic Surgery. The demographic data (patient age at the date of surgery, implantation time, sex, implant type, previous surgery) where recorded. The implantation time describes the time from the installation of the prosthesis to the removal of the prosthesis due to aseptic or septic reasons. As previous surgery is the number of previous operations on the affected joint described, excluding the implantation of the first implant in this joint.

All patients in this study were treated according to the in-house algorithm for identifying a PJI. This identification is based on the MSIS criteria (55). Infections were identified if the major criteria applied: at least two positive cultures of the same organism in tissue cultures or the minor criteria were increased. The minor criteria included:

- Medical history was suggestive of infection
- Serum c-reactive protein level was above the threshold of 5 mg/L
- Serum white blood cell count was above the threshold of 10 Gpt/l
- Histology showed typical inflammatory signs e.g. neutrophils

Based on the available microbiological, histopathological, and clinical findings, patients were classified as septic (PJI present) and

aseptic (PJI absent). Exclusion criteria were the presence of inflammatory joint diseases, such as rheumatoid arthritis, gout, chondrocalcinosis or severe metallosis.

To test for cross reactivity of C9 antibody staining wit inflammatory joint diseases, we included another control cohort of chondrocalcinosis (N=14) and rheumatoid arthritis (N= 11) patients coming for primary endoprosthesis implantation, and patients with aseptic implant loosening and an extensive amount of wear particles (N=33) The patients with aseptic implant loosening due to wear particles were further separated in patients with CoCr wear (N= 10), with Ti/Pe wear (N=16) and ceramic on ceramic (N=7) The samples for chondrocalcinosis (CC), rheumatoid arthritis (RA) and wear particles were declared as aseptic as no pathogen was identified in the microbiological diagnostic.

Microbiological diagnostic testing

Periprosthetic tissue samples were minced into pieces and homogenized in an Ultra-Turrax Drive control disperser (IKA®-Werke GmbH & Co. KG, Germany) at 6,000 rpm for 2 min in interval direction change. Briefly, the homogenized samples were inoculated on agar plates: Columbia agar with 5% sheep blood (Becton Dickinson, Heidelberg, Germany), chocolate agar and Schaedler agar (Oxoid, Munich, Germany) under aerobic conditions with 5% CO_2 and anaerobically at 35± 1°C. Additionally, the samples were inoculated in thioglycolate and Schaedler broth (bioMérieux, Marcy L'Etoile, France) at 35 ± 1°C for 14 days. The identification of pathogens was performed by MALDI-TOF MS (VITEK® MS, bioMérieux, Marcy L'Etoile, France).

Immunohistochemically staining

The periprosthetic tissues were fixed overnight in 4% paraformaldehyde. The tissue was embedded in paraffin and cut into 4-µm sections. The immunofluorescent staining was performed using a C9-antibody (Abcam, Cambridge, England). The corresponding IgG antibody was used as isotype control for the staining. The demasking of the epitopes was performed 0.25 mg/ml pepsin for 45 min at 37°C. The dilution of the antibody was performed in 4% BSA, for the C9-antibody a dilution of 1:500 and for the IgG isotype control a dilution of 1:1000 was used. As secondary antibody an Alexa Fluor®555 anti-rabbit (Abcam, Cambridge, England) (1:200 in PBS). The area of red immunofluorescence was calculated as the percentage of the total tissue area in 400x magnification pictures. The average of 3 representative pictures for each sample was calculated using ImageJ (version 1.5; National Institutes of Health, Bethesda, MA, USA). The amount of fluorescence staining was adjusted to the IgG control for the whole cohort and residual staining of the IgG controls for each picture were subtracted to ensure the reliability of evaluated C9-antibody staining.

Statistical analysis

Statistical analysis was performed using GraphPad Prism (version 8; GraphPad Software, San Diego, CA, USA). Normality and log normality tests were performed to calculate the normal distribution; in the case of a nonparametric distribution, the mean ± SEM using descriptive statistics were calculated. Kruskal-Wallis test and Mann-Whitney test were used to test statistical significance. The ROC curve was performed using the statistical program for ROC curves in Prism. Youden's criteria were applied to calculate the threshold for the biomarker.

Results

Serum CRP and WBC count are indicators for periprosthetic joint infection

We included 98 patients in the PJI versus aseptic cohort in this study. The patients were divided into septic and aseptic according to the described classification based on the MSIS criteria (56). We included 40 aseptic and 58 septic samples. The reasons for aseptic revision were wear induced loosening, malpositioning or luxation of the implant. The periprosthetic tissues of hip arthroplasty (THA) and total knee arthroplasty (TKA) revisions from male and female patients were included. The average age was comparable in both groups (Table 1). In the septic group, we included 36 cases of septic THA and 22 septic TKA. In the aseptic group, we included 18 THA and 22 TKA revisions. The implantation time was lower in the septic in comparison to the aseptic group. The number of previous surgeries at the respective joint is indicated in (Table 1). Both groups included patients with several previous surgeries at the site of implantation. (Table 2) summarizes the comorbidities of the included patients. PJI patients had more often diabetes (21/58), renal insufficiency (11/58), COPD (6/58) and heart insufficiency (6/58) compared to the aseptic cohort.

The bacterial spectrum identified by the microbiological diagnostic showed that *Staphylococcus* spp. infections occurred most frequently (37/58), followed by *Streptococcus* spp. (5/58), anaerobic bacteria (5/58), polymicrobial infections (5/58) and *Enterococcus* spp. (3/58) (Figure 1A). The CRP serum level was significantly increased in the septic group compared to the aseptic

TABLE 1 Demographic data.

Cohort	Patients	Sex	Age [yr]	Location	Implant. time [m]	No. of previous revisions
Septic	58	♂ 36	72 ± 9	TKA: 22	38 ± 63	1 (21/53); 2 (19/53); 3
		♀ 22		THA: 36		(8/53); 4 (4/53); 7 (1;53)
Aseptic	40	♂ 18	71 ± 10	TKA: 22	95 ± 76	1 (18/35); 2 (10/35); 3
		♀ 22		THA: 18		(4/35); 4 (2/35); 10 (1/35)

10.3389/fimmu.2023.1112188

TABLE 2 Comorbidities.

	Septic (N=58)	Aseptic (N=40)
Diabetes	**21**	**17**
Osteoporosis	2	1
Renal insufficiency	**11**	**6**
COPD	**6**	**1**
Heart insufficiency	**6**	**1**
Asthma	1	4
Other	11	5

The bold values belong to the relevant comorbidities.

cohort (Figure 1B) ($p < 0.0001$). However, not all patients within the septic (42.40 ± 12.66 mg/l) cohort showed a pathological CRP value of more than 5 mg/l. Importantly, 12 out of 40 aseptic (3.3 ± 2.61 mg/l) patients also exhibited an increased CRP value. The serum WBC count was not significantly ($p = 0.2373$) changed between the aseptic (7.84 ± 0.37 Gpt/l) and the septic (8 ± 1.76 Gpt/l) (Figure 1C).

C9 immunostaining of periprosthetic tissue could serve as potential biomarker for PJI identification

C9 immunostaining has been proposed to be a reliable marker for the identification of PJI using tissue biopsies (12). To validate this observation we stained the periprosthetic tissue of hip and knee endoprosthesis revision surgeries due to PJI or aseptic implant loosening or malpositioning for C9. We observed significantly more C9 immunostaining in the septic tissue (mean ± SEM: 2.74% ± 0.65%) (Figure 2A) compared to the aseptic cohort (mean ± SEM: 0.34% ± 0.22%) ($p<0.0001$).

To investigate the predictive value of C9 staining, a receiver operating curve (ROC) curve analysis using the respective C9 immunostained area for each sample, was performed (Figure 2B). Here, we plotted the percentage of C9 positive area in the septic tissues (sensitivity) against the percentage of C9 positive area in the aseptic tissue (100%-specificity). The area under the curve (AUC) of the ROC analysis is 0.84. Using the Youden's criteria the threshold for the sensitivity and the specificity (red dashed line) was calculated. The sensitivity for the C9 staining was at 89% (95% of Cl: 78.83% to 96.11%), while the specificity was at 75% (95% of Cl: 58.80% to 87.31%).

To investigate whether there is a pathogen-dependent increase of C9 tissue staining we divided the PJI samples according to the identified pathogen into Staphylococcus spp. (N= 37, 1.75% ± 0.49%), *Enterococcus* spp. (N= 6, 9.69% ± 4.27%), *Streptococcus* spp. (N= 3, 5.1% ± 3.13%), Anaerobia (N= 5, 1.86% ± 0.68%) and Polymicrobial infections (N= 5, 4.9% ± 4.15%) and depicted the C9 stained tissue area for each sample. The statistical analysis of C9 immunostaining showed no difference in the amount of C9 tissue staining with regard to the different pathogens detected by the microbiological diagnostic. (Supplementary Figure 1D). Next we co compare the amount of C9 immunofluorescent staining with the aseptic cohort. We observed a significant difference for all pathogens compared to the aseptic tissue, indicating that C9 could be a universal biomarker (Figure 2C).

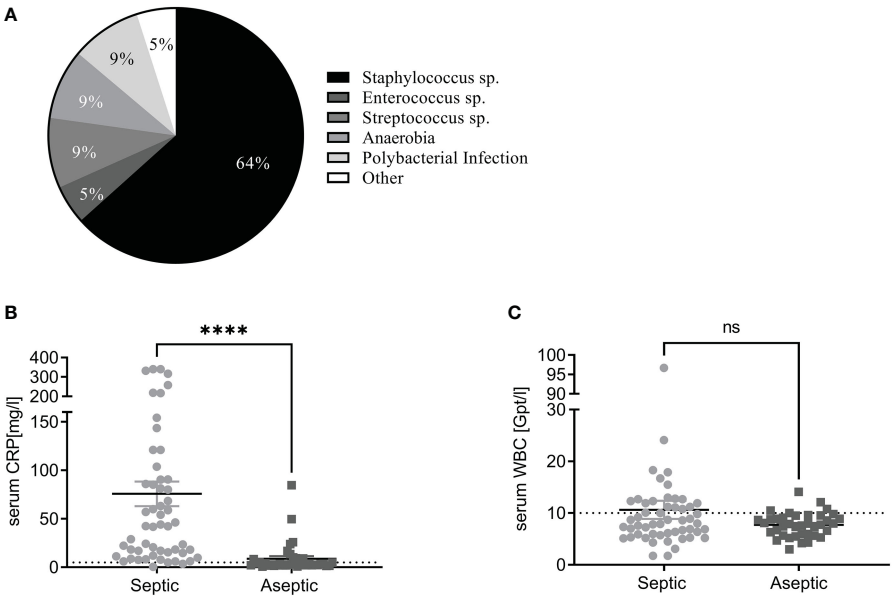

FIGURE 1
Serum CRP and WBC count are indicators for periprosthetic joint infection **(A)** Pie chart of the identified pathogen spectrum. *Staphylococcus* spp. was the major pathogen that was identified by the microbiological diagnostic. Other bacteria were less frequently detected. **(B)** Serum C-reactive protein (CRP) values (mg/l) in septic (light grey) and aseptic (dark grey) groups. The serum CRP value of the septic cohort was significantly increased in the septic compared with the aseptic cohort (Mann-Whitney test: $p<0.0001$). The pathologic threshold is 5mg/L is indicated as a black dashed line. **(C)** The mean value of the serum white blood cell (WBC) count (Gpt/l) was not different between both cohorts (Mann-Whitney test: $p= 0.237$). Most patients exhibited a WBC count below the pathological threshold of 10 Gpt/l (black dashed line) for all tested groups. ****$P < 0.0001$, ns, not significant.

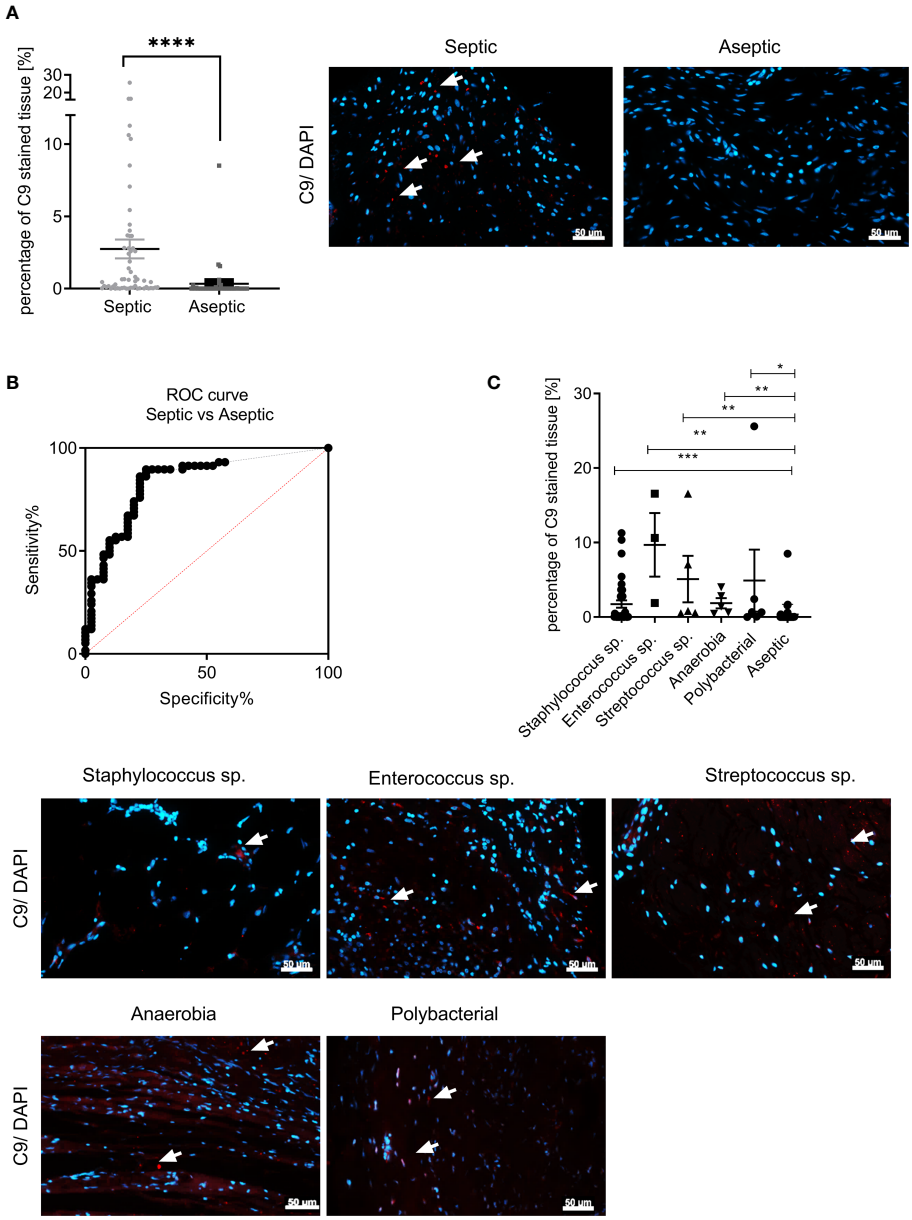

FIGURE 2
C9 immunostaining of periprosthetic tissue could serve as potential biomarker for PJI identification. **(A)** The statistical analysis of the percentage of red fluorescence within the total tissue area (C9 immunostaining) of the aseptic (dark grey, N = 40; n = 120) and septic (light grey, N = 58, n = 174) cohort can be seen as a scatter dot plot. The values indicate the percentage of C9 immunostaining. Three images for each patient sample were analyzed (Mann-Whitney test: $p < 0.0001$). A representative picture for a septic (left) and an aseptic (right) sample are depicted. (nuclei: blue, anti-C9 immunostaining: red). White arrows indicate C9 stained tissue area. The scale bar (white bars) indicates 50 µm and pictures were taken at 400x magnification. **(B)** The ROC-curve for individual percentages of C9 stained tissue area for septic and aseptic samples. The area under the curve is 0.84. The sensitivity of 89% (95% of CI: 78.83% to 96.11%) and the specificity of 75% (95% of CI: 58.80% to 87.31%) were calculated using the Youden's criteria (red dashed line). **(C)** Representative immunohistochemical staining of C9-antibody (red) in periprosthetic tissue of patients with an PJI caused by *staphylococcus* sp., *streptococcus* sp., *enterococcus* sp., anaerobia and polymicrobial infections compared to the aseptic cohort. The values indicate the percentage of C9 immunostaining. Three images for each patient sample were analyzed (*staphylococcus*: N = 37; n = 111, *enterococcus* N = 3; n = 9; *streptococcus*: N = 5; n = 15; *anaerobia*: N = 5; n = 15; polymicrobial infection: N = 6; n = 18; aseptic: N = 58, n = 174). White arrows indicate C9 stained tissue area. The scale bar (white bars) indicates 50 µm and pictures were taken at 400x magnification. No pathogen dependent influence on the percentage of C9 immunostained tissue was observed (Kruskal-Wallis test with Dunn's *post hoc* test: $p<0.0001$). *$p < 0.05$, **$p < 0.01$, ***$p < 0.001$, **** $p < 0.0001$; n, total number of measurements; N, number of samples, ns, not significant.

Anti-C9 immunostaining showed no cross reactivity with chondrocalcinosis and most wear particle types

Since other proposed biomarkers for PJI, such as alpha-defensin, showed cross-reactions with tissue residues of hemorrhaging or abrasive wear, we investigated the cross reactivity of C9 with different inflammatory joint conditions. We included periprosthetic tissue samples from patients with chondrocalcinosis (CC) (14 samples), rheumatoid arthritis (RA) (11 samples) and different types of wear particles (33 samples) (Table 3). The wear particles resulted from the bearing coupling and therefore, the

samples were divided into patients with cobalt-chromium (CoCr) (11 samples), titanium-plastic (Ti+Pe) (15 samples) and ceramic (CoC) wear (7 samples). The average age the CC cohort was 65 ± 10, RA had an average age of 61 ± 14 and the wear particle cohort had an average age of 65 ± 11. In the CC cohort 5 samples were from male patients while 9 samples were from females. All periprosthetic tissue sections were collected from the knee. Three samples were from male patients in the RA cohort, while 7 samples were from female patients. In the cohort of the wear particle cohort 17 samples were used from male patients, while 16 samples were used from female patients. The periprosthetic tissue was collected from the hip and the knee (Table 3).

We stained the periprosthetic tissue from the different cohorts for C9 and depicted the amount of C9 stained tissue area in the diagram. Patients with CC showed a C9 tissue staining of mean ± SEM: 0.2% ± 0.18%, RA mean ± SEM: 2.83% ± 0.96%, and wear particles had a mean ± SEM: 1.98% ± 1.1% (Figure 3A). The amount of C9 immunostaining was significantly higher in the infected periprosthetic tissue compared to CC synovial tissue ($p < 0.0001$). C9 staining was also significantly increased in case of wear particles in the periprosthetic tissue compared to septic ($p < 0.0001$). However, no significant difference in the amount of C9 staining in septic tissue compared to RA synovial tissue was observed ($p > 0.9999$).

To test the predictive value of C9 as biomarker in case of the above-mentioned inflammatory joint diseases, we performed a ROC analyses for C9 tissue staining for each condition. The discrimination between CC and septic using C9 staining showed a good predictive value (AUC: 0.88) (Figure 3B). The separation of the amount in C9 staining between septic and RA was lower and showed a lower predictive value. The separation between septic and wear particle containing tissue using C9 staining, however, exhibited an AUC: 0.78.

Since we observed marked differences in the percentage of C9 stained tissue area in the presence of wear particles, we investigated whether the abrasion type had an influence on the amount of C9 stained tissue area (Figure 3C). When comparing the C9 stained area in the septic samples with Ti+ PE (mean ± SEM: 0.45% ± 0.32%, $p < 0.0001$), and Ceramic on Ceramic (CoC) (mean ± SEM: 0.22% ± 0.18%, $p = 0.0156$) a clear separation was observed. In the presence of CoCr (mean ± SEM: 5.66% ± 3.57%, $p = 0.4095$), however, no statistical significance was determined, indicating a cross-reaction between the C9 antibody staining with CoCr wear particles in tissues (Figure 3C).

Discussion

The current study investigated the use of C9 immunostaining of periprosthetic tissues as a biomarker for PJI using patients undergoing THA or TKA revision due to septic or aseptic implant revision. As expected, patients with more than two previous surgeries at the respective joint exhibited more frequently septic (Table 1) (57–59). Comorbidities such as congestive heart failure, diabetes, depression, anemia, chronic lung disease, obesity, rheumatologic disease, kidney disease, and pulmonary circulatory disorders were established as typical risk factors for developing a PJI (60–62). These observations were corroborated in our septic patient cohort (Table 2). The patients in the septic cohort exhibited more often comorbidities compared to the patients in the aseptic cohort. Especially diabetes, renal insufficiency, heart failure, and COPD were more common in the septic group than in the aseptic group.

PJI has been associated with an increase in systemic inflammatory serum markers (14). We observed an increased serum CRP level in most patients in the septic cohort (Figure 1B). However, the discrimination was not clear, as also some aseptic patients exhibited an increased CRP value, as well as not all septic patients exhibited a pathological serum CRP level. Other studies already showed that the predictive value of the serum CRP level for identification of PJI is low (63, 64). The serum WBC count did not show a significant difference between the septic and aseptic cohort in our study. This observation has already been described in another study (65).

In our cohort, we mostly identified pathogens from the *Staphylococcus* genus in the septic samples (64%) (Figure 1A). This is consistent with other studies, showing that *S. aureus* and *S. epidermidis* occur most frequently in PJIs (19, 21, 66). PJIs caused by *Streptococcus* spp. and *Enterococcus*, as well as polymicrobial infection and anaerobic pathogens were detected with lower frequency. This is also corroborated by others, as Enterococcus spp. and Streptococcus spp. occur less common in PJIs (66) as well as anaerobia (67, 68).

The MSIS criteria (25) describe that one major factor for the identification of a PJI are two tissue cultures positive for the same pathogen. However, contamination during sampling, the presence of a biofilm on the implant or pre-treatment with antibiotics affects the detection of pathogens using the routine microbiological diagnostic methods (69–72). These influencing factors increase the risk of culture negative (CN)-PJI, leading to an inadequate treatment of the patient (26, 27). Therefore, minor factors such as serum CRP, synovial fluid WBC or histopathology of tissue samples are used for

TABLE 3 Patient characteristics of septic, CC, RA and wear particles cohort.

Cohort	Number	Sex	Age [yr]	Location	CRP [mg/l]	WBC [Gpt/l]
Septic	58	♂ 36 ♀ 22	72 ± 9	TKA: 22 THA: 36	38 ± 63	1 (21/53); 2 (19/53); 3
CC	19	♂ 15 ♀ 4	67 ± 11	TKA: 19 THA: 0	(8/53); 4 (4/53); 7 (1;53)	(8/53); 4 (4/53); 7 (1;53)
RA	17	♂ 2 ♀ 15	66 ± 18	TTK: 22 TsA: 36	95 ± 76	1 (18/35); 2 (10/35); 3
				TTK: 2 TSA: 2		
Wear particles	16	♂ 5 ♀ 11	70 ± 13	TKA:4 THA:12	13 ± 34.93	7 ± 1,34

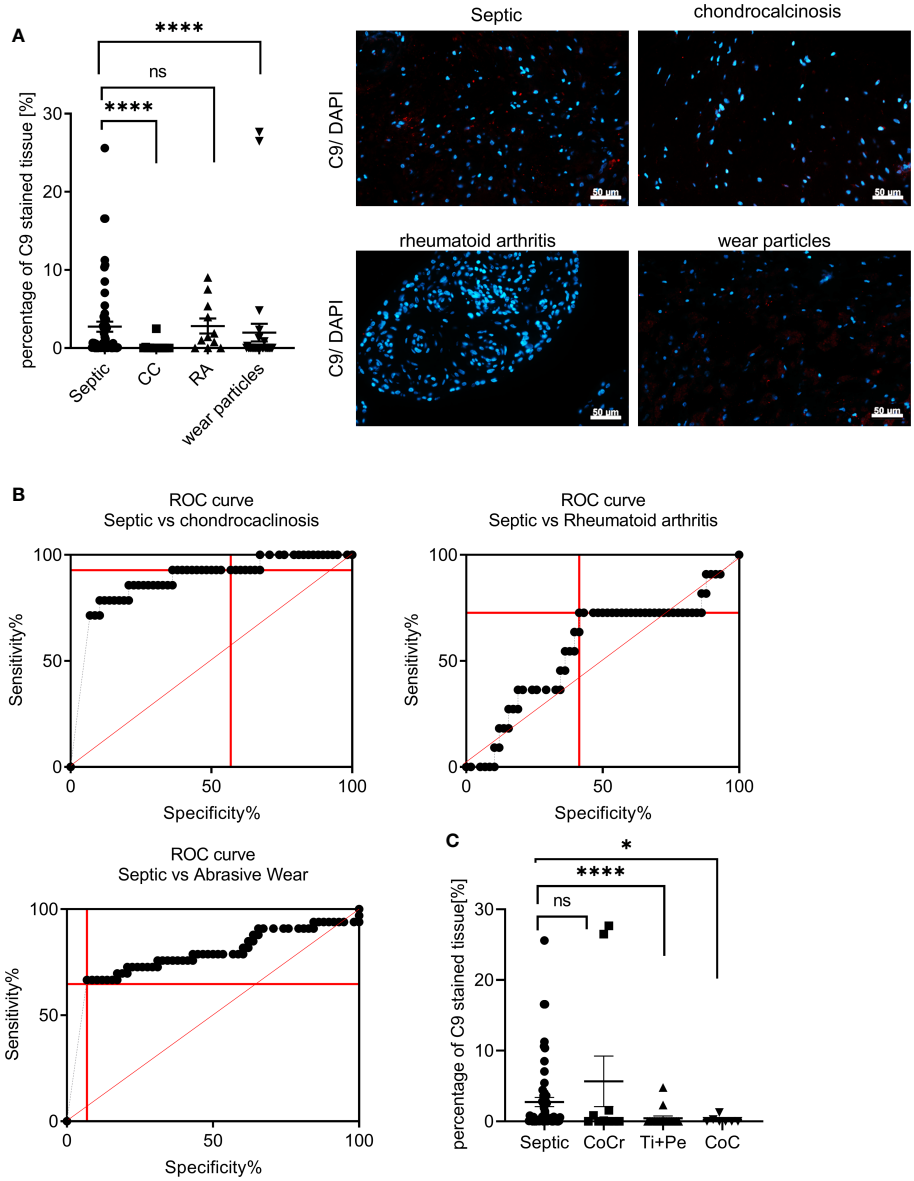

FIGURE 3
Anti-C9 immunostaining showed no cross reactivity with chondrocalcinosis and most wear particle types **(A)** Representative immunohistochemical stainings of periprosthetic tissue of patients with PJI (septic), chondrocalcinosis, rheumatoid arthritis and wear particles with the C9-antibody (red) are shown. The values indicate the percentage of C9 stained tissue area. Three images for each patient sample were analyzed (septic: N = 58; chondrocalcinosis: N = 14; rheumatoid arthritis: N = 11; wear particles: N = 33). White arrows indicate C9 stained tissue area. The scale bar (white bar) indicates 50 µm and pictures were taken at 400x magnification. (ANOVA: *post hoc*, septic vs CC ($p < 0.0001$), septic vs wear particles ($p < 0.0001$), septic vs RA ($p > 0.999$). **(B)** The ROC-curve for individual percentages of C9 stained tissue area for septic and aseptic samples. Using the Youden's criteria the best ratio of sensitivity to specificity was selected for each condition (red dashed line). The ROC-curve for septic versus CC group showed an area under the curve of 0.88. The sensitivity was 92.86% (95% of CI: 66.13% to 99.82%) while the specificity was 56.90% (95% of CI: 43.23% to 69.84%).The ROC-curve for septic versus RA group showed an area under the curve of 0.56. Using the Youden's criteria the best ratio of sensitivity to specificity was selected (red dashed line). The sensitivity was 72.73% (95% of CI: 39.03% to 93.98%while the specificity was 58.62% (95% of CI: 44.93% to 71.40%). The ROC-curve for septic versus wear particles had an AUC of 0.77. Using the Youden's criteria the best ratio of sensitivity to specificity was selected (red dashed line). The sensitivity was 64.71% (95% of CI: 46.49% to 80.25%while the specificity was 93.1% (95% of CI: 83,27% to 98,09%). **(C)** Representative immunohistochemical staining of the C9-antibody (red) in periprosthetic tissue of patients with PJI (septic) or various wear types can be seen. The values indicate the percentage of C9 stained tissue (septic: N = 58; CoCr: N = 10; Ti+PE: N = 16; CoC: N = 7). Three images for each patient sample were analyzed. White arrows indicate C9 stained tissue area. The scale bar (white bars) indicates 50 µm and pictures were taken at 400 x magnification. (ANOVA: *post hoc*). *$p < 0.05$, ****$p < 0.0001$;.

the verification of the diagnosis. Our data indicate that the serum CRP and the serum WBC count in our cohort was of low predictive value for septic identification. The serum CRP, as well as the serum WBC count, can be increased during other acute inflammatory disease, making both parameters unreliable indicators for PJI (65, 73, 74). The prevalence of CN-PJI is about 1- 42% (28–31) raising the need for a biomarker to decrease the number of CN-PJIs.

The complement pathway is an important mechanisms of the innate immune system to fight infections (1). It was shown that previously that C3, C5 and C9 were detectable by immunostaining in

the periprosthetic tissue in a cohort of shoulder PJI patients (12). Here, C9 immunostaining of the tissue showed the highest sensitivity and specificity to discriminate between the septic and the aseptic cohort. Therefore, the authors suggested that C9 immunostaining could be used as a possible biomarker for the identification of PJI (12). We observed again a significant increase in C9 immunostaining of the periprosthetic tissue of PJI patients, compared to aseptic loosening (Figure 2A). The ROC curve for percentage C9 immunostaining in the tissue comparing aseptic tissues with septic tissues resulted in an AUC value of 0.84. The Youden's index indicated a sensitivity of 89.66% and specificity of 75% for C9 as biomarker for PJI. Therefore, according to the classification of biomarkers (75), C9 immunostaining of periprosthetic tissue could be an excellent biomarker for identification of PJI. However, the synovial fluid alpha-defensin ELISA has been described to exhibit a sensitivity of 100% and specificity of 95% for identifying PJI (32, 48–50). It is suggested, that synovial fluid alpha-defensin detection should be used as a supplementary diagnostic method in cases in which PJI cannot be diagnosed clearly, that are nevertheless suspected to be septic (54).

C9 immunostaining exhibited a sensitivity of 89.6%, indicating that not all septic tissues showed C9 immunostaining. A reason might be that the complement pathway is mainly activated in the early phase of infection (76) and that C9 is not present in later stages of infection. However, we did not find a significant correlation when comparing the implantation time with the percentage of C9 stained periprosthetic tissue (Supplementary Figure 1B, $p = 0.9985$)). In addition, we did not observe a statistical significance for the percentage of C9 stained tissue within the septic cohort, when we divided the PJI cases into early (<3 months after implantation), delayed (3 – 12 months after implantation) and late (>12 months after implantation) infections (Supplementary Figure 1). Therefore, we think that the phase of infection is not the reason for some septic samples being negative for C9 immunostaining.

Next, we tested if the percentage of C9 immunostaining might be dependent on the pathogen causing the PJI (Figure 2C). Here, we divided the septic cohort based on the bacteria causing the PJI into *Staphylococcus* spp. (66), *Streptococcus* spp., *Enterococcus* spp. (66). and *Anaerobia* (67, 68) as well as polymicrobial PJI (15). No significant difference in the percentage of C9 immunostaining of the periprosthetic tissue was observed between the tested pathogens, indicating that the amount of C9 immunostaining is not pathogen dependent. This finding indicates, that C9 as a potential biomarker can be used independently from factors such as stage of infection, implantation time and pathogen causing the PJI.

Besides not all septic samples being positive for C9 immunostaining, also some aseptic samples were positive for C9 staining, explaining the specificity of 75% for C9 as a biomarker.

As synovial fluid alpha-defensin showed a cross-reactivity in the presence of crystal deposits (53, 77) and abrasive wear (52), we wanted to investigate if the C9 immunostaining in the tissue showed similar cross-reactivity with other inflammatory joint conditions such as chondrocalcinosis (CC), rheumatoid arthritis (RA) and wear particles. We observed no cross-reactivity of C9 immunostaining in the tissue CC and most types of wear particles, while C9 was not able to distinguish between RA and septic. Thurman et al. proposed that some autoantibodies, such as they are present in rheumatoid arthritis (RA), could also activate the terminal complement pathway (78–80). This fact could explain why C9 was also detectable in tissue of RA patients.

Metal particles are known to induce an inflammatory tissue responses (81), therefore it was investigated whether the different wear particle types could also influence the detection of C9 in the periprosthetic tissue (Figure 3C). We found that in the presence of titanium and PE particles (Ti+Pe) and ceramic particles (CoC) C9 was mainly present in the septic cohort, but not in the tissue of the respective bearing couplings. In contrast, periprosthetic tissue from patients with CoCr implants showed a similar C9 immunostaining compared to the septic cohort. A study showed that an immune response was elicited in the presence of cobalt, chromium, and nickel, while no increase was detected with titanium particles (82). CoCr particles were shown to exhibit a sever inflammatory response in a mouse model (81), indicating a difference in the inflammatory capacity of different wear partciles and making CoCr particles more inflammatory than others. This observation could explain why only CoCr wear particles showed a cross-reactivity with C9 immunostaining.

As the synovial fluid alpha-defensin immunoassay is not suggested as stand-alone technique for the routine diagnostic, but should rather be applied in cases where the diagnosis of PJI was unclear (54), we propose that C9 immunostaining should be applied to help the decision making in unclear cases of PJI.

One limitation of our study is that the location of the collected periprosthetic tissue was not clearly defined and standardized throughout the cohort. Due to the unclear sampling area, some samples could be closer to the infection site than other samples, explaining the variety in the percentage of C9 immunostaining in the tissue samples. As in this septic cohort more gram-positive bacteria were causing the PJI, it would be interesting include more samples of other pathogens to clearly show whether there might be a pathogen dependent difference in the C9 detection. Furthermore, we did not analyze specifically if low-grade infections could be identified more clearly with the help of C9 staining, to help identify PJI in unclear cases. Further experiments will be needed to validate the possible use of C9 immunostaining for a more reliably detection of CN-PJIs and low-grade infections.

Conclusion

In this study, we shown that C9 immunostaining is a very good tissue-biomarker for the identification of PJI with biopsy specimens. Due to the high AUC value as well as the high sensitivity and specificity of C9 immunostaining, we propose the use of C9 immunostaining in cases of unclear diagnosis of PJI to secure the treatment suggestion.

Data availability statement

The raw data supporting the conclusions of this article will be made available by the authors, without undue reservation.

Ethics statement

The studies involving human participants were reviewed and approved by Institutional Review Board of the Medical School Magdeburg (No 207/17). The patients/participants provided their written informed consent to participate in this study.

Author contributions

A-KM performed the histological stainings and evaluation of data. JF performed the microbiological diagnostic. SI identified the relevant patients and provided the patient history as well as performed the sampling. PM developed the C9 antibody and discussed data and helped interpreting the results. CL helped writing the manuscript and discussing and interpreting the data. JB made the conceptualization and supervision for the project and wrote the manuscript. All authors contributed to the article and approved the submitted version.

Funding

The project was funded by the federal state Saxony-Anhalt and European Structural and Investment Funds (ESF, 2014-2020; project No. ZS/2016/08/80645).

Acknowledgments

The authors acknowledge the excellent technical assistance of Carolin Schneider, Anja Schröder and Mandy Könnecke.

Conflict of interest

The authors declare that the research was conducted in the absence of any commercial or financial relationships that could be construed as a potential conflict of interest.

Publisher's note

All claims expressed in this article are solely those of the authors and do not necessarily represent those of their affiliated organizations, or those of the publisher, the editors and the reviewers. Any product that may be evaluated in this article, or claim that may be made by its manufacturer, is not guaranteed or endorsed by the publisher.

Author disclaimer

The project was funded by the federal state Saxony-Anhalt and European Structural and Investment Funds (ESF, 2014-2020; project No. ZS/2016/08/80645). The authors, their immediate families, and any research foundations with which they are affiliated have not received any financial payments or other benefits from any commercial entity related to the subject of this article.

Supplementary material

The Supplementary Material for this article can be found online at: https://www.frontiersin.org/articles/10.3389/fimmu.2023.1112188/full#supplementary-material

SUPPLEMENTARY FIGURE 1

No correlation between the percentages of C9 stained tissue area with the serum CRP level, implantation time, and stage of infection **(A)** In order to test a potential correlation between the percentage of C9 tissue staining and the serum CRP value of the respective patient. No correlation was observed for the septic and aseptic cohort (Linear regression septic r^2 = 0.01; 95% CI = -0.01 to 0.02, p = 0.41; N = 54; aseptic r^2 = 0.004; 95% CI = -0.02 to 0.04, p = 0.07; N = 37). **(B)** A potential correlation between the percentage of C9 tissue staining and the implantation time in month the septic and aseptic cohort were compared. No correlation was found for the septic and aseptic cohort (Linear regression: septic r^2 = 7.08e-008, 95% CI = -0.02 to 0.02, p = 0.09; N = 53, aseptic septic r^2 = 0.04, 95% CI = -0.01 to 0.003, p = 0.26; N = 37). **(C)** Potential influence of infection type (early: <3 months after implantation;, delayed: 3 – 12 months after implantation, months after implantation) on the percentage of C9 tissue staining (early: N = 12, delayed: N = 14, late: N = 27, One-Way-ANOVA with Tukey *post hoc* test F (2, 50) = 1.26, p=0.29). **(D)** Representative immunohistochemical staining of C9-antibody (red) in periprosthetic tissue of patients with an PJI caused by staphylococcus sp., streptococcus sp., enterococcus sp., anaerobia and polymicrobial infections. The values indicate the percentage of C9 immunostaining. Three images for each patient sample were analyzed (staphylococcus: N = 37; n = 111, enterococcus N = 3; n = 9; streptococcus: N = 5; n = 15; anaerobia: N = 5; n = 15; polymicrobial infection: N = 6; n = 18). White arrows indicate C9 stained tissue area. The scale bar (white bars) indicates 50 µm and pictures were taken at 400x magnification. No pathogen dependent influence on the percentage of C9 immunostained tissue was observed (One-way ANOVA with Tukey *post hoc* test: F (4, 51) = 2.682, p=0.0417, which resulted in no significant difference after multiple comparisons between the different groups).

References

1. Dunkelberger JR, Song WC. Complement and its role in innate and adaptive immune responses. *Cell Res* (2010) 20(1):34–50. doi: 10.1038/cr.2009.139

2. Walport MJ. Complement. first of two parts. *N Engl J Med* (2001) 344(14):1058–66. doi: 10.1056/NEJM200104053441406

3. Walport MJ. Complement. second of two parts. *N Engl J Med* (2001) 344(15):1140–4. doi: 10.1056/NEJM200104123441506

4. Gros P, Milder FJ, Janssen BJC. Complement driven by conformational changes. *Nat Rev Immunol* (2008) 8(1):48–58. doi: 10.1038/nri2231

5. Janssen BJ, Huizinga EG, Raaijmakers HC, Roos A, Daha MR, Nilsson-Ekdahl K, et al. Structures of complement component C3 provide insights into the function and evolution of immunity. *Nature* (2005) 437(7058):505–11. doi: 10.1038/nature04005

6. Mold C. Role of complement in host defense against bacterial infection. *Microbes Infect* (1999) 1(8):633–8. doi: 10.1016/S1286-4579(99)80063-X

7. Sjöholm AG, Jönsson G, Braconier JH, Sturfelt G, Truedsson L. Complement deficiency and disease: An update. *Mol Immunol* (2006) 43(1-2):78–85. doi: 10.1016/j.molimm.2005.06.025

8. Ram S, Mackinnon FG, Gulati S, McQuillen DP, Vogel U, Frosch M, et al. The contrasting mechanisms of serum resistance of neisseria gonorrhoeae and group b *neisseria meningitidis*. *Mol Immunol* (1999) 36(13-14):915–28. doi: 10.1016/S0161-5890(99)00114-5

9. Taylor PW. Complement-mediated killing of susceptible gram-negative bacteria: an elusive mechanism. *Exp Clin Immunogenet* (1992) 9(1):48–56.

10. Berends ET, Mohan S, Miellet WR, Ruyken M, Rooijakkers SH. Contribution of the complement membrane attack complex to the bactericidal activity of human serum. *Mol Immunol* (2015) 65(2):328–35. doi: 10.1016/j.molimm.2015.01.020

11. Adler Sørensen C, Rosbjerg A, Hebbelstrup Jensen B, Krogfelt KA, Garred P. The lectin complement pathway is involved in protection against enteroaggregative *escherichia coli* infection. *Front Immunol* (2018) 9:1153. doi: 10.3389/fimmu.2018.01153

12. Meinshausen AK, Martens N, Berth A, Farber J, Awiszus F, Macor P, et al. The terminal complement pathway is activated in septic but not in aseptic shoulder revision arthroplasties. *J Shoulder Elbow Surg* (2018) 27(10):1837–44. doi: 10.1016/j.jse.2018.06.037

13. Andrej Trampuz M, Werner Zimmerli MD. Diagnosis and treatment of implant-associated septic arthritis and osteomyelitis. *Curr Infect Dis Rep* (2008) 10:394–403. doi: 10.1007/s11908-008-0064-1

14. Tsaras G, Osmon DR, Mabry T, Lahr B, Sauveur JS, Yawn B, et al. Incidence, secular trends, and outcomes of prosthetic joint infection: A population-based study, Olmsted county, Minnesota, 1969–2007. *Infection Control Hosp Epidemiol* (2015) 33(12):1207–12. doi: 10.1086/668421

15. Peel TN, Cheng AC, Buising KL, Choong PFM. Microbiological aetiology, epidemiology, and clinical profile of prosthetic joint infections: Are current antibiotic prophylaxis guidelines effective? *Antimicrobial Agents Chemotherapy* (2012) 56(5):2386–91. doi: 10.1128/AAC.06246-11

16. Duff GP, Lachiewicz PF, Kelley SS. Aspiration of the knee joint before revision arthroplasty. *Clin Orthop Relat Res* (1996) 331:132–9. doi: 10.1097/00003086-199610000-00018

17. Sendi P, Banderet F, Graber P, Zimmerli W. Clinical comparison between exogenous and haematogenous periprosthetic joint infections caused by staphylococcus aureus. *Clin Microbiol Infection* (2011) 17(7):1098–100. doi: 10.1111/j.1469-0691.2011.03510.x

18. Osmon DR, Berbari EF, Berendt AR, Lew D, Zimmerli W, Steckelberg JM, et al. Diagnosis and management of prosthetic joint infection: Clinical practice guidelines by the infectious diseases society of americaa. *Clin Infect Dis* (2012) 56(1):e1–e25. doi: 10.1093/cid/cis966

19. Barrett L, Atkins B. The clinical presentation of prosthetic joint infection. *J Antimicrobial Chemotherapy* (2014) 69(suppl_1):i25–7. doi: 10.1093/jac/dku250

20. Nair PK, Bhat VG, Vaz MS. Prosthetic joint infections – a clinico-microbiological perspective: Review article. *Clin Infect Dis* (2014) 4:9–15. doi: 10.5495/wjcid.v4.i3.9

21. Zimmerli W, Sendi P. Pathogenesis of implant-associated infection: The role of the host. *Semin Immunopathology* (2011) 33(3):295–306. doi: 10.1007/s00281-011-0275-7

22. Lamagni T. Epidemiology and burden of prosthetic joint infections. *J Antimicrobial Chemotherapy* (2014) 69(suppl_1):i5–i10. doi: 10.1093/jac/dku247

23. Esposito S, Leone S. Prosthetic joint infections: Microbiology, diagnosis, management and prevention. *Int J Antimicrob Agents* (2008) 32(4):287–93. doi: 10.1016/j.ijantimicag.2008.03.010

24. Peel TN, Buising KL, Choong PFM. Diagnosis and management of prosthetic joint infection. *Curr Opin Infect Dis* (2012) 25:670–6. doi: 10.1097/QCO.0b013e32835915db

25. Parvizi J, Tan TL, Goswami K, Higuera C, Della Valle C, Chen AF, et al. The 2018 definition of periprosthetic hip and knee infection: An evidence-based and validated criteria. *J Arthroplasty* (2018) 33(5):1309–1314.e2. doi: 10.1016/j.arth.2018.02.078

26. Zappe B, Graf S, Ochsner PE, Zimmerli W, Sendi P. Propionibacterium spp. in prosthetic joint infections: A diagnostic challenge. *Arch Orthopaedic Trauma Surg* (2008) 128(10):1039–46. doi: 10.1007/s00402-007-0454-0

27. Millett PJ, Yen Y-M, Price CS, Horan MP, van der Meijden OA, Elser F F, et al. Propionibacterium acnes infection as an occult cause of postoperative shoulder pain: A case series. *Clin orthopaedics related Res* (2011) 469(10):2824–30. doi: 10.1007/s11999-011-1767-4

28. Berbari EF, Marculescu C, Sia I, Lahr BD, Hanssen AD, Steckelberg JM, et al. Culture-negative prosthetic joint infection. *Clin Infect Dis* (2007) 45(9):1113–9. doi: 10.1086/522184

29. Parvizi J, Ghanem E, Menashe S, Barrack RL, Bauer TW. Periprosthetic infection: What are the diagnostic challenges? *J Bone Joint Surg Am* (2006) 88 Supplementary 4:138–47. doi: 10.2106/JBJS.F.00609

30. Ghanem E, Parvizi J, Clohisy J, Burnett S, Sharkey PF, Barrack R. Perioperative antibiotics should not be withheld in proven cases of periprosthetic infection. *Clin Orthop Relat Res* (2007) 461:44–7. doi: 10.1097/BLO.0b013e318065b780

31. Bejon P, Berendt A, Atkins BL, Green N, Parry H, Masters S, et al. Two-stage revision for prosthetic joint infection: Predictors of outcome and the role of reimplantation microbiology. *J Antimicrob Chemother* (2010) 65(3):569–75. doi: 10.1093/jac/dkp469

32. Deirmengian C, Kardos K, Kilmartin P, Cameron A, Schiller K, Parvizi J. Combined measurement of synovial fluid α-defensin and c-reactive protein levels: Highly accurate for diagnosing periprosthetic joint infection. *J Bone Joint Surg Am* (2014) 96(17):1439–45. doi: 10.2106/JBJS.M.01316

33. Sigmund IK, Holinka J, Gamper J, Staats K, Böhler C, Kubista B, et al. Qualitative α-defensin test *(Synovasure)* for the diagnosis of periprosthetic infection in revision total joint arthroplasty. *Bone Joint J* (2017) 99-b(1):66–72. doi: 10.1302/0301-620X.99B1.BJJ-2016-0295.R1

34. Omar M, Ettinger M, Reichling M, Petri M, Guenther D, Gehrke T, et al. Synovial c-reactive protein as a marker for chronic periprosthetic infection in total hip arthroplasty. *Bone Joint J* (2015) 97-b(2):173–6. doi: 10.1302/0301-620X.97B2.34550

35. Tetreault MW, Wetters NG, Moric M, Gross CE, Della Valle CJ. Is synovial c-reactive protein a useful marker for periprosthetic joint infection? *Clin Orthop Relat Res* (2014) 472(12):3997–4003. doi: 10.1007/s11999-014-3828-y

36. Póvoa P, Almeida E, Moreira P, Fernandes A, Mealha R, Aragão A, et al. C-reactive protein as an indicator of sepsis. *Intensive Care Med* (1998) 24(10):1052–6. doi: 10.1007/s001340050715

37. Sierra R, Rello J, Bailén MA, Benítez E, Gordillo A, León C, et al. C-reactive protein used as an early indicator of infection in patients with systemic inflammatory response syndrome. *Intensive Care Med* (2004) 30(11):2038–45. doi: 10.1007/s00134-004-2434-y

38. Lobo SM, Lobo FR, Bota DP, Lopes-Ferreira F, Soliman HM, Mélot C, et al. C-reactive protein levels correlate with mortality and organ failure in critically ill patients. *Chest* (2003) 123(6):2043–9. doi: 10.1378/chest.123.6.2043

39. Póvoa P, Teixeira-Pinto AM, Carneiro AH. C-reactive protein, an early marker of community-acquired sepsis resolution: A multi-center prospective observational study. *Crit Care* (2011) 15(4):R169. doi: 10.1186/cc10313

40. Póvoa P, Coelho L, Almeida E, Fernandes A, Mealha R, Moreira P, et al. C-reactive protein as a marker of infection in critically ill patients. *Clin Microbiol Infect* (2005) 11(2):101–8. doi: 10.1111/j.1469-0691.2004.01044.x

41. Fraunberger P, Wang Y, Holler E, Parhofer KG, Nagel D, Walli AK, et al. Prognostic value of interleukin 6, procalcitonin, and c-reactive protein levels in intensive care unit patients during first increase of fever. *Shock* (2006) 26(1):10–2. doi: 10.1097/01.shk.0000215319.06866.bd

42. Lee CC, Chen SY, Tsai CL, Wu SC, Chiang WC, Wang JL, et al. Prognostic value of mortality in emergency department sepsis score, procalcitonin, and c-reactive protein in patients with sepsis at the emergency department. *Shock* (2008) 29(3):322–7. doi: 10.1097/SHK.0b013e31815077ca

43. Bjerk SM, Baker JV, Emery S, Neuhaus J, Angus B, Gordin FM, et al. Biomarkers and bacterial pneumonia risk in patients with treated HIV infection: A case-control study. *PloS One* (2013) 8(2):e56249. doi: 10.1371/journal.pone.0056249

44. Schmit X, Vincent JL. The time course of blood c-reactive protein concentrations in relation to the response to initial antimicrobial therapy in patients with sepsis. *Infection* (2008) 36(3):213–9. doi: 10.1007/s15010-007-7077-9

45. Gollwitzer H, Dombrowski Y, Prodinger PM, Peric M, Summer B, Hapfelmeier A, et al. Antimicrobial peptides and proinflammatory cytokines in periprosthetic joint infection. *JBJS* (2013) 95(7):644–51. doi: 10.2106/JBJS.L.00205

46. Ganz T, Selsted ME, Szklarek D, Harwig SS, Daher K, Bainton DF, et al. Defensins. natural peptide antibiotics of human neutrophils. *J Clin Invest* (1985) 76(4):1427–35. doi: 10.1172/JCI112120

47. Chalifour A, Jeannin P, Gauchat J-F, Blaecke A, Malissard M, N'Guyen T, et al. Direct bacterial protein PAMP recognition by human NK cells involves TLRs and triggers α-defensin production. *Blood* (2004) 104(6):1778–83. doi: 10.1182/blood-2003-08-2820

48. Deirmengian C, Hallab N, Tarabishy A, Della Valle C, Jacobs JJ, Lonner J, et al. Synovial fluid biomarkers for periprosthetic infection. *Clin Orthop Relat Res* (2010) 468(8):2017–23. doi: 10.1007/s11999-010-1298-4

49. Deirmengian C, Kardos K, Kilmartin P, Cameron A, Schiller K, Booth RE Jr, et al. The alpha-defensin test for periprosthetic joint infection outperforms the leukocyte esterase test strip. *Clin Orthop Relat Res* (2015) 473(1):198–203. doi: 10.1007/s11999-014-3722-7

50. Deirmengian C, Kardos K, Kilmartin P, Cameron A, Schiller K, Parvizi J. Diagnosing periprosthetic joint infection: Has the era of the biomarker arrived? *Clin Orthop Relat Res* (2014) 472(11):3254–62. doi: 10.1007/s11999-014-3543-8

51. Bingham J, Clarke H, Spangehl M, Schwartz A, Beauchamp C, Goldberg B. The alpha defensin-1 biomarker assay can be used to evaluate the potentially infected total joint arthroplasty. *Clin Orthop Relat Res* (2014) 472(12):4006–9. doi: 10.1007/s11999-014-3900-7

52. Bonanzinga T, Zahar A, Dütsch M, Lausmann C, Kendoff D, Gehrke T. How reliable is the alpha-defensin immunoassay test for diagnosing periprosthetic joint infection? a prospective study. *Clin Orthop Relat Res* (2017) 475(2):408–15. doi: 10.1007/s11999-016-4906-0

53. Plate A, Stadler L, Sutter R, Anagnostopoulos A, Frustaci D, Zbinden R, et al. Inflammatory disorders mimicking periprosthetic joint infections may result in false-positive α-defensin. *Clin Microbiol Infection* (2018) 24(11):1212.e1–1212.e6. doi: 10.1016/j.cmi.2018.02.019

54. Amanatullah DF, Cheng RZ, Jih III, Maloney WJ, Finlay AK, Kappagoda S, et al. The routine use of synovial alpha-defensin is not necessary. *Bone Joint J* (2020) 102-B(5):593–9. doi: 10.1302/0301-620X.102B5.BJJ-2019-0473.R3

55. Tarabichi M, Shohat N, Goswami K, Alvand A, Silibovsky R, Belden K, et al. Diagnosis of periprosthetic joint infection: The potential of next-generation sequencing. *J Bone Joint Surg Am* (2018) 100(2):147–54. doi: 10.2106/JBJS.17.00434

56. Tan TL, Kheir MM, Shohat N, Tan DD, Kheir M, Chen C, et al. Culture-negative periprosthetic joint infection: An update on what to expect. *JB JS Open Access* (2018) 3(3):e0060. doi: 10.2106/JBJS.OA.17.00060

57. Goldberg AL, Kettelhut IC, Furuno J, Fagan JM, Baracos V. Activation of protein breakdown and prostaglandin E2 production in rat skeletal muscle in fever is signaled by a macrophage product distinct from interleukin 1 or other known monokines. *J Clin Invest* (1988) 81(5):1378–1383). doi: 10.1172/JCI113466

58. Smucny M, Menendez ME, Ring D, Feeley BT, Zhang AL. Inpatient surgical site infection after shoulder arthroplasty. *J Shoulder Elbow Surg* (2015) 24(5):747–53. doi: 10.1016/j.jse.2014.12.024

59. Fehring TK, Odum S, Calton TF, Mason JB. Articulating versus static spacers in revision total knee arthroplasty for sepsis. *Ranawat Award Clin Orthop Relat Res* (2000) 380):9–16. doi: 10.1097/00003086-200011000-00003

60. Baek S-H. Identification and preoperative optimization of risk factors to prevent periprosthetic joint infection. *World J orthopedics* (2014) 5(3):362–7. doi: 10.5312/wjo.v5.i3.362

61. Bozic KJ, Lau E, Kurtz S, Ong K, Berry DJ. Patient-related risk factors for postoperative mortality and periprosthetic joint infection in medicare patients undergoing TKA. *Clin Orthop Relat Res* (2012) 470(1):130–7. doi: 10.1007/s11999-011-2043-3

62. Bozic KJ, Lau E, Kurtz S, Ong K, Rubash H, Vail TP, et al. Patient-related risk factors for periprosthetic joint infection and postoperative mortality following total hip arthroplasty in Medicare patients. *JBJS* (2012) 94(9):794–800. doi: 10.2106/JBJS.K.00072

63. Pohlig F, Mühlhofer HML, Lenze U, Lenze FW, Suren C, Harrasser N, et al. Diagnostic accuracy of arthroscopic biopsy in periprosthetic infections of the hip. *Eur J Med Res* (2017) 22(1):6. doi: 10.1186/s40001-017-0246-0

64. Sanzén L, Sundberg M. Periprosthetic low-grade hip infections erythrocyte sedimentation rate and c-reactive protein in 23 cases. *Acta Orthopaedica Scandinavica* (1997) 68(5):461–5. doi: 10.3109/17453679708996263

65. Parvizi J, Gehrke T. Definition of periprosthetic joint infection. *J Arthroplasty* (2014) 29(7):1331. doi: 10.1016/j.arth.2014.03.009

66. Nair P, Bhat V, Vaz MS. Prosthetic joint infections-a clinico-microbiological perspective: Review article. *World J Clin Infect Dis* (2014) 4(3):9–15. doi: 10.5495/wjcid.v4.i3.9

67. Tande AJ, Patel R. Prosthetic joint infection. *Clin Microbiol Rev* (2014) 27(2):302–45. doi: 10.1128/CMR.00111-13

68. Shah NB, Tande AJ, Patel R, Berbari EF. Anaerobic prosthetic joint infection. *Anaerobe* (2015) 36:1–8. doi: 10.1016/j.anaerobe.2015.08.003

69. Trampuz A, Piper KE, Hanssen AD, Osmon DR, Cockerill FR, Steckelberg JM, et al. Sonication of explanted prosthetic components in bags for diagnosis of prosthetic joint infection is associated with risk of contamination. *J Clin Microbiol* (2006) 44(2):628–31. doi: 10.1128/JCM.44.2.628-631.2006

70. Holinka J, Bauer L, Hirschl AM, Graninger W, Windhager R, Presterl E. Sonication cultures of explanted components as an add-on test to routinely conducted microbiological diagnostics improve pathogen detection. *J Orthop Res* (2011) 29 (4):617–22. doi: 10.1002/jor.21286

71. Trampuz A, Osmon DR, Hanssen AD, Steckelberg JM, Patel R. Molecular and antibiofilm approaches to prosthetic joint infection. *Clin Orthop Relat Res* (2003) 414):69–88. doi: 10.1097/01.blo.0000087324.60612.93

72. Cremniter J, Slassi A, Quincampoix JC, Sivadon-Tardy V, Bauer T, Porcher R, et al. Decreased susceptibility to teicoplanin and vancomycin in coagulase-negative staphylococci isolated from orthopedic-device-associated infections. *J Clin Microbiol* (2010) 48(4):1428–31. doi: 10.1128/JCM.02098-09

73. Ghanem E, Antoci V Jr, Pulido L, Joshi A, Hozack W, Parvizi J. The use of receiver operating characteristics analysis in determining erythrocyte sedimentation rate and c-reactive protein levels in diagnosing periprosthetic infection prior to revision total hip arthroplasty. *Int J Infect Dis* (2009) 13(6):e444–9. doi: 10.1016/j.ijid.2009.02.017

74. Berbari E, Mabry T, Tsaras G, Spangehl M, Erwin PJ, Murad MH, et al. Inflammatory blood laboratory levels as markers of prosthetic joint infection: A systematic review and meta-analysis. *J Bone Joint Surg Am* (2010) 92(11):2102–9. doi: 10.2106/JBJS.I.01199

75. Turabieh H, Mafarja M, Li X. Iterated feature selection algorithms with layered recurrent neural network for software fault prediction. *Expert Syst Appl* (2019) 122:27–42. doi: 10.1016/j.eswa.2018.12.033

76. Janeway CA Jr, Walport M, Li X. *Immunobiology: The immune system in health and disease. 5th edition*. New York: Garland Science (2001).

77. Han X, Xie K, Jiang X, Wang L, Wu H, Qu X, et al. Synovial fluid α-defensin in the diagnosis of periprosthetic joint infection: The lateral flow test is an effective intraoperative detection method. *J Orthopaedic Surg Res* (2019) 14(1):274. doi: 10.1186/s13018-019-1320-9

78. Heinen S, Pluthero FG, van Eimeren VF, Quaggin SE, Licht C. Monitoring and modeling treatment of atypical hemolytic uremic syndrome. *Mol Immunol* (2013) 54 (1):84–8. doi: 10.1016/j.molimm.2012.10.044

79. Lintner KE, Wu YL, Yang Y, Spencer CH, Hauptmann G, Hebert LA, et al. Early components of the complement classical activation pathway in human systemic autoimmune diseases. *Front Immunol* (2016) 7(36). doi: 10.3389/fimmu.2016.00036

80. Thurman JM, Yapa R. Complement therapeutics in autoimmune disease. *Front Immunol* (2019) 10(672). doi: 10.3389/fimmu.2019.00672

81. Baldwin L, Hunt JA. Host inflammatory response to NiCr, CoCr, and Ti in a soft tissue implantation model. *J Orthop Surg Res* (2006) 79A(3):574–81. doi: 10.1002/jbm.a.30856

82. Hallab NJ, et al. Immune responses correlate with serum-metal in metal-on-metal hip arthroplasty. *J Arthroplasty* (2004) 19(8 Supplementary 3):88–93. doi: 10.1016/j.arth.2004.09.012

frontiers | Frontiers in Immunology

TYPE Original Research
PUBLISHED 12 April 2023
DOI 10.3389/fimmu.2023.1107334

Check for updates

OPEN ACCESS

EDITED BY
Lillemor Skattum,
Department of Laboratory Medicine, Lund University, Sweden

REVIEWED BY
Christian Drouet,
U1016 Institut Cochin (INSERM), France
Hadida Yasmin,
Cooch Behar Panchanan Barma University, India

*CORRESPONDENCE
Małgorzata Karbownik-Lewińska
malgorzata.karbownik-lewinska@umed.lodz.pl

SPECIALTY SECTION
This article was submitted to Molecular Innate Immunity, a section of the journal Frontiers in Immunology

RECEIVED 24 November 2022
ACCEPTED 21 March 2023
PUBLISHED 12 April 2023

CITATION
Matusiak AE, Stępniak J, Lewiński A and Karbownik-Lewińska M (2023) Decreased mannan-binding lectin level in adults with hypopituitarism; dependence on appropriate hormone replacement therapies.
Front. Immunol. 14:1107334.
doi: 10.3389/fimmu.2023.1107334

COPYRIGHT
© 2023 Matusiak, Stępniak, Lewiński and Karbownik-Lewińska. This is an open-access article distributed under the terms of the Creative Commons Attribution License (CC BY). The use, distribution or reproduction in other forums is permitted, provided the original author(s) and the copyright owner(s) are credited and that the original publication in this journal is cited, in accordance with accepted academic practice. No use, distribution or reproduction is permitted which does not comply with these terms.

Decreased mannan-binding lectin level in adults with hypopituitarism; dependence on appropriate hormone replacement therapies

Aleksandra E. Matusiak[1], Jan Stępniak[2], Andrzej Lewiński[1,3] and Małgorzata Karbownik-Lewińska[1,2]*

[1]Department of Endocrinology and Metabolic Diseases, Polish Mother's Memorial Hospital – Research Institute, Lodz, Poland, [2]Department of Oncological Endocrinology, Medical University of Lodz, Lodz, Poland, [3]Department of Endocrinology and Metabolic Diseases, Medical University of Lodz, Lodz, Poland

Background: Mannan-binding lectin (MBL) is a main component of the lectin pathway of the complement system. Although there are some studies showing links between endocrine and immune systems, the ones concerning hypopituitarism are limited. The aim of this study was to check whether there is any association between blood MBL level and pituitary hormone deficiencies and whether this relationship is affected by appropriate hormone replacement therapies.

Methods: One hundred and twenty (120) inpatients, aged 18-92, were divided into two main groups, *i.e.* control individuals (21/120) and patients with pituitary diseases (99/120). The latter were diagnosed either with hypopituitarism (n=42) or with other pituitary diseases (not causing hypopituitarism) (n=57). Additionally, hypopituitary patients on appropriate replacement therapies (compensated hypopituitarism) were compared to patients on inappropriate replacement therapies (non-compensated hypopituitarism). Several parameters in blood serum were measured, including MBL level, pituitary and peripheral hormones and different biochemical parameters.

Results: Serum MBL level was significantly lower in patients with hypopituitarism comparing to controls (1358.97 ± 244.68 vs. 3199.30 ± 508.46, $p<0.001$) and comparing to other pituitary diseases (1358.97 ± 244.68 vs. 2388.12 ± 294.99, $p=0.015$) and this association was confirmed by univariate regression analysis. We evaluated the distribution of patients with relation to MBL level; there was a clear difference in this distribution between control individuals (among whom no subjects had MBL level <500 ng/mL) and patients with hypopituitarism (among whom 43% of patients had MBL level <500 ng/mL). Moreover, patients with non-compensated hypopituitarism had lower mean and median MBL levels comparing to patients with compensated hypopituitarism (1055.38 ± 245.73 vs. 2300.09 ± 579.93, $p=0.027$; 488.51 vs. 1951.89, $p=0.009$, respectively) and this association was confirmed in univariate regression analysis. However, mean and median MBL levels in patients with compensated hypopituitarism vs. controls

did not differ significantly (2300.09 ± 579.93 vs. 3199.30 ± 508.46, p=0.294; 1951.90 vs. 2329.16; p=0.301, respectively).

Conclusion: Hypopituitarism in adults is associated with a decreased blood concentration of mannan-binding lectin, a phenomenon which does not exist in hypopituitary patients on the appropriate hormone replacement therapies. Therefore measurement of mannan-binding lectin level in patients with hypopituitarism may be considered as a parameter contributing to adjust optimal doses of hormone replacement therapies.

KEYWORDS

mannan-binding lectin (MBL), complement system, lectin pathway, hypopituitarism, endocrine disorders

1 Introduction

The complement system is an important effector arm of innate immunity and plays a crucial role in the defense against common pathogens. Effective defense and maintenance of homeostasis requires a perfect balance between complement activation and control.

Mannan-binding lectin (MBL, also referred to as mannose-binding lectin), which constitutes a main component of the lectin pathway of the complement system, is an immune defense plasma protein synthesized in the liver and its basal concentration in human plasma is primarily genetically determined (1, 2). MBL plays a crucial role in the immune response (2).

Although the concentration of MBL is genetically determined, there are some other factors affecting MBL level such as bacterial infection, for example caused by *Streptococcus pneumoniae* (3) or viral infection resulting in hepatitis C (4) or COVID-19 (5).

There are studies showing the existence of casual links between the endocrine and the immune system. MBL is one possible connection between these fields. Of great importance are findings showing association of MBL level with thyroid dysfunction. Increased MBL blood concentrations were found in hyperthyroid, while decreased MBL levels were found in hypothyroid (6, 7) patients. Even high-normal TSH (>2.5 mIU/L) in women of childbearing age, which is commonly considered to be just abnormal in this specific population, was associated with lower MBL concentrations (8). Clinical findings also indicate that growth hormone (GH) influences the concentration of MBL in blood plasma (9, 10). Baseline concentrations of MBL were found to be lower in GH deficient patients and higher in patients with acromegaly (9). Moreover, treatment with rhGH significantly increased MBL concentrations in healthy and GH-deficient subjects (9). Expectedly, the treatment with pegvisomant (GH receptor antagonist) or with octreotide (somatostatin analog) in acromegalic patients decreased MBL level (9). Also stimulatory effects of growth hormone and thyroid hormones on MBL synthesis in the human hepatocyte cell line were documented (11). According to our knowledge there are no published data regarding effects of other pituitary tropic hormones (or their deficiencies) on complement lectin pathway. Therefore published evidence on connections between endocrine system and lectin pathway is rather poor and our study does constitute a next step to broaden this field.

The aim of the present study was to investigate whether pituitary hormone deficiencies (hypopituitarism) influence MBL blood level and whether MBL concentration may be changed in response to appropriate hormone replacement therapies in patients with hypopituitarism. Also a possible relationship between MBL and other laboratory parameters, which may be affected by pituitary dysfunction, was examined.

2 Materials and methods

The Ethical Committee of the Polish Mother's Memorial Hospital - Research Institute, Lodz, Poland approved all the procedures applied in the present study, and fully informed written consent was obtained from all patients (No. 47/2019, 87/2022).

One hundred and twenty (120) inpatients (89 females, 74%), aged 18-92, who were admitted to the hospital because any pituitary disease was suspected, were enrolled to the study in the years 2019-2022. All participants were patients of the Department of Endocrinology and Metabolic Diseases, Polish Mother's Memorial Hospital - Research Institute, Lodz, Poland. Individuals were not randomized into groups and blinding was not performed because our study is not a randomized controlled trial (and individuals simply could not ethically be randomized and blinded).

The patients were divided into two main groups:

– Controls – twenty one out of 120 subjects (21/120; 17.5%) with non-secreting pituitary microadenomas, Empty Sella Syndrome and pituitary cysts [the two latter not causing

pituitary dysfunction] and with no other endocrine diseases; therefore no therapeutical intervention was required and these patients were treated as healthy individuals;

– Patients with pituitary diseases – ninety nine out of 120 subjects (99/120; 82.5%). All these patients required any endocrine treatment.

The second group of 99 patients was further divided into two following groups:

- forty two (42) out of 120 subjects (42/120; 35%) diagnosed with hypopituitarism of different degree, *i.e.* with different number of pituitary deficiencies;
- fifty seven (57) out of 120 subjects (57/120; 47.5%) with other pituitary diseases (not causing hypopituitarism of any degree) such as secreting microadenomas or non-secreting and secreting macroadenomas; patients after pituitary surgery or after radiotherapy (but without pituitary insufficiency); two patients with *PROP-1* gene mutation; one patient with Schaaf-Yang syndrome; also patients with non-secreting microadenomas or Empty Sella Syndrome and with coexisting primary hypothyroidism.

Patients with hypopituitarism (n=42) were divided into two following groups:

- patients who were on appropriate hormone replacement therapies (compensated hypopituitarism; n=10)
- patients who were not on appropriate hormone replacement therapies (non-compensated hypopituitarism; n=32).

We evaluated the accuracy of hormone replacement therapies by checking if levels of the individual end-organ hormones are in target ranges, according to the current guidelines (12).

Patients with hypopituitarism (n=42) had the following pituitary deficiencies:

1. one pituitary deficiency (n=9); compensated (n=5) vs. non-compensated (n=4):

- isolated GH deficiency (Shaaf-Yang Syndrome), 1 patient; non-compensated
- isolated LH/FSH deficiency (hypogonadotropic hypogonadism due to macroprolactinoma), 1 patient; non-compensated
- isolated TSH deficiency (one patient with pituitary apoplexy being secondary to abrupt hemorrhage or infarction of pituitary adenoma and two idiopathic cases confirmed in thyrotropin-releasing hormone (TRH) stimulation test), 3 patients; compensated
- isolated ACTH deficiency (two cases after surgery due to Cushing disease and two cases of the empty sella syndrome), 4 patients; compensated (n=2) vs. non-compensated (n=2)

2. two pituitary deficiencies (n=7); compensated (n=1) vs. non-compensated (n=6):

- LH/FSH and GH deficiency (2 patients); non-compensated
- LH/FSH and TSH deficiency (3 patients); compensated (n=1) vs. non-compensated (n=2)
- TSH and ACTH deficiency (2 patients); non-compensated

3. three pituitary deficiencies (n=9); compensated (n=2) vs. non-compensated (n=7):

- GH, LH/FSH and TSH (3 patients); non-compensated
- GH, LH/FSH and ACTH deficiency (3 patients); compensated (n=1) vs. non-compensated (n=2)
- GH, TSH and ACTH deficiency (1 patient); non-compensated
- LH/FSH, TSH and ACTH deficiency (2 patients); compensated (n=1) vs. non-compensated (n=1);

4. four pituitary (GH, LH/FSH, TSH, ACTH) deficiencies (n=12); compensated (n=2) vs. non-compensated (n=10)
5. five pituitary (GH, LH/FSH, TSH, ACTH, Prl) deficiencies (panhypopituitarism) (n=5); non-compensated.

Study design diagram is presented in Figure 1.

Exclusion criteria constituted: malignant diseases and severe acute/chronic diseases other than pituitary or thyroid diseases.

Body mass and body height were measured to calculate BMI.

Blood samples were collected after an overnight fast at 7 a.m. and all laboratory parameters were measured either in the whole

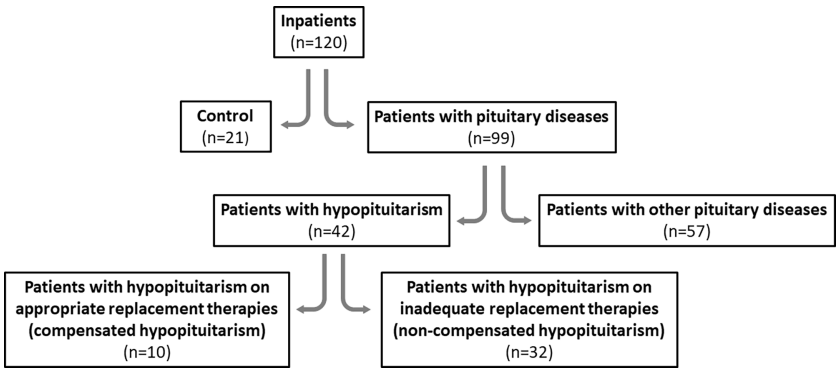

FIGURE 1
Study design diagram.

blood or blood serum for diagnostic purposes. Additionally, blood sample (1 mL) was centrifuged (3000 x g, 10 min, 4°C) in order to obtain serum, and stored at -80°C until appropriate assay to measure MBL level.

2.1 Parameters measured in blood serum

The concentrations of hormones (thyroid-stimulating hormone, TSH; free triiodothyronine, FT3; free thyroxine, FT4; luteinizing hormone, LH; follicle-stimulating hormone, FSH; adrenocorticotropic hormone; ACTH; cortisol; growth hormone, GH; prolactin, Prl; parathyroid hormone, PTH), of thyroid antibodies (thyroid peroxidase antibody, TPOAb; thyroglobulin antibody, TgAb; TSH receptor antibody, TSHRAb) and of vitamin D were measured in blood serum with immunochemiluminescent method (Cobas e-601; Roche Diagnostics). Other laboratory parameters (insulin-like growth factor I, IGF-I; total cholesterol, TChol; HDL cholesterol, HDLC; LDL cholesterol, LDLC; triglycerides, TGs; glucose; aspartate aminotransferase, ASPAT; alanine aminotransferase, ALAT; bilirubin; sodium, Na; potassium, K; chlorides, Cl; calcium, Ca; urea; creatinine; C-reactive protein, CRP) were measured in blood serum with standard methods (Vitros 4600/Vitros 5.1; Johnson&Johnson). Complete blood count, *i.e.*, red blood cells, RBC; hemoglobin, Hgb; white blood cells, WBC; hematocrit, HCT; platelets; neutrophils; lymphocytes; eosinophils; basophils; and monocytes were measured with Sysmex XN-2000 Hematology System.

Anthropometric measurements included body height and body mass, which were used to calculate Body Mass Index (BMI).

2.2 Assay to measure MBL

Serum concentration of MBL was measured by an enzyme-linked immunoabsorbant assay (ELISA) using a commercial *Homo sapiens (Human) MBL ELISA KIT* (Cloud-Clone Corp, USA, no. SEB480Hu), with a detection threshold of 0.156-10 ng/mL. The kit is a sandwich enzyme immunoassay for *in vitro* quantitative measurement of MBL. The protocol for the ELISA was performed following the manufacturer's guidelines. The absorbance was measured with the use of multifunctional microplate reader (VICTOR X4, Perkin Elmer, USA) with a wavelength of 450 ± 10 nm. Each sample was measured twice. The concentration of the tested factor in the analyzed sample was determined on the basis of a calibration curve created with the use of Four Parameter Logistic (4PL) Regression. WorkOut 2.5 software was used for the analysis.

2.3 Statistical analyses

The Student's unpaired *t* test or Mann-Whitney U test were used to compare differences between independent groups; the results are presented as means ± SEM or median ± SEM, respectively. To evaluate correlations between MBL level and all other linear parameters, Pearson's correlation coefficient was applied.

Univariate followed by multivariate regression analyses were performed to determine which linear (continuous) variables might have been associated with considered dichotomized variables (patients with hypopituitarism vs. patients without hypopituitarism, compensated vs. non-compensated hypopituitarism).

The 2-sided ratio comparison test was used to determine the probability (frequency) of events.

Distribution of number/percentage of patients with different MBL concentrations is presented on histograms.

Statistical analysis was performed using SigmaPlot version 11.0 (RRID : SCR_003210) (Systat Software, Inc., San Jose, CA, USA). Statistical significance has been determined at the level of $p<0.05$.

Experimental individuals were not randomized into groups because this was deemed irrelevant to this study. Blinding was unnecessary as this is not a randomized controlled trial (and individuals simply could not ethically be blinded).

3 Results

All linear laboratory parameters in control individuals (n=21) were compared to those obtained in patients with hypopituitarism (n=42), in patients with other pituitary diseases (n=57) and also in patients with pituitary diseases (n=42+57) (Table 1). Patients with hypopituitarism and also all patients with pituitary diseases were, unfortunately, older than control individuals. The groups did not differ regarding body mass and BMI. Expectedly concentrations of some pituitary hormones or hormones released by their target peripheral glands were lower in

TABLE 1 Clinical/laboratory parameters in control individuals (n=21) vs. patients with hypopituitarism (n=42), vs. patients with other pituitary diseases (n=57) and vs. all patients with pituitary diseases (n=99).

	Control (n=21)	Patients with hypopituitarism (n=42)	Patients with other pituitary diseases (n=57)	Patients with pituitary diseases (n=99)
Age [years]	37.92 ± 3.77 n=21	50.26 ± 2.79 n=42 p=0.012	45.47 ± 2.21 n=57 p=0.084	47.50 ± 1.75 n=99 p=0.024
Body mass [kg]	75.94 ± 7.66 n=18	79.21 ± 3.05 n=42 p=0.640	79.45 ± 2.42 n=50 p=0.567	79.35 ± 7.66 n=84 p=0.527
Height [cm]	167.64 ± 2.25 n=18	162.71 ± 4.28 n=42 p=0.425	167.68 ± 1.19 n=50 p=0.986	165.68 ± 1.85 n=84 p=0.639

(Continued)

TABLE 1 Continued

	Control (n=21)	Patients with hypopituitarism (n=42)	Patients with other pituitary diseases (n=57)	Patients with pituitary diseases (n=99)
BMI [kg/m^2]	26.83 ± 2.53 n=18	27.70 ± 0.79 n=34 *p*=0.682	28.24 ± 0.82 n=18 *p*=0.489	28.02 ± 0.58 n=84 *p*=0.485
ACTH [pg/mL]	44.81 ± 5.51 n=16	26.98 ± 4.33 n=34 *p*=0.019	30.87 ± 2.68 n=53 *p*=0.018	29.35 ± 2.35 n=87 *p*=0.011
LH [IU/L]	14.00 ± 3.11 n=20	4.19 ± 0.89 n=37 *p*<0.001	13.40 ± 1.62 n=53 *p*=0.854	9.51 ± 1.12 n= 91 *p*=0.111
FSH [IU/L]	15.47 ± 4.66 n=20	7.18 ± 1.81 n=36 *p*=0.054	22.28 ± 3.38 n=54 *p*=0.279	16.06 ± 2.26 n=91 *p*=0.912
Prl [ng/mL]	14.33 ± 1.88 n=21	305.44 ± 226.75 n=39 *p*=0.352	40.06 ± 10.50 n=53 *p*=0.130	152.56 ± 96.58 n=92 *p*=0.497
IGF-I [ng/mL]	190.04 ± 19.17 n=18	114.85 ± 19.03 n=40 *p*=0.019*	184.41 ± 20.93 n=51 *p*=0.880	153.84 ± 14.9 n=91 *p*=0.295
Cortisol [µg/L] (µg/dL)	157.8 ± 11.9 (15.78 ± 1.19) n=20	78.8 ± 10.6 (7.88 ± 1.06) n=42 *p*<0.001	134.2 ± 5.2 (13.42 ± 0.52) n=56 *p*=0.040	110.4 ± 6.1 (11.04 ± 0.61) n=98 *p*=0.001
TSH [mIU/L]	2.39 ± 0.21 n=21	1.20 ± 0.21 n=40 *p*<0.001	1.77 ± 0.14 n=57 *p*=0.022	1.54 ± 0.12 n=99 *p*=0.003
FT3 [pg/mL]	3.16 ± 0.11 n=21	2.43 ± 0.08 n=42 *p*<0.001	2.69 ± 0.05 n=57 *p*<0.001	2.58 ± 0.05 n=99 *p*<0.001
FT4 [ng/L] (ng/dL)	12.4 ± 0.4 (1.24 ± 0.04) n=21	11.6 ± 0.6 (1.16 ± 0.06) n=42 *p*=0.399	12.3 ± 0.2 (1.23 ± 0.02) n=57 *p*=0.811	12.0 ± 0.3 (1.20 ± 0.03) n=99 *p*=0.560
TPOAb [IU/mL]	42.69 ± 29.87 n=18	31.30 ± 10.12 n=27 *p*=0.678	43.06 ± 12.81 n=40 *p*=0.990	38.32 ± 8.64 n= 67 *p*=0.847
TgAb [IU/mL]	57.61 ± 29.59 n=18	23.73 ± 6.09 n=25 *p*=0.200	156.77 ± 91.07 n=39 *p*=0.470	101.93 ± 54.19 n= 66 *p*=0.675
TSHRAb [IU/L	0.84 ± 0.09 n=18	0.86 ± 0.07 n=24 *p*=0.832	0.68 ± 0.06 n=39 *p*=0.155	0.74 ± 0.04 n= 65 *p*=0.325
TChol [mg/L] (mg/dL)	1713.3 ± 72.1 (171.33 ± 7.21) n=21	1960.2 ± 76.2 (196.02 ± 7.62) n=42 *p*=0.043	1814.6 ± 57.2 (181.46 ± 5.72) n=57 *p*=0.334	1876.4 ± 46.5 (187.64 ± 4.65) n=99 *p*=0.128
HDLC [mg/L] (mg/dL)	501.9 ± 28.1 (50.19 ± 2.81) n=21	521.4 ± 24.0 (52.14 ± 2.40) n=42 *p*=0.622	514.6 ± 20.6 (51.46 ± 2.06) n=57 *p*=0.741	517.5 ± 15.6 (51.75 ± 1.56) n=99 *p*=0.668
LDLC [mg/L] (mg/dL)	953.8 ± 52.2 (95.38 ± 5.22) n=21	1071.4 ± 59.7 (107.14 ± 5.97) n=42 *p*=0.208	1054.9 ± 42.9 (105.49 ± 4.29) n=57 *p*=0.196	1061.9 ± 35.2 (106.19 ± 3.52) n=99 *p*=0.181
HDLC/T.Chol.	0.295 ± 0.02 n=21	0.284 ± 0.02 n=42 *p*=0.696	0.29 ± 0.01 n=56 *p*=0.964	0.29 ± 0.01 n=98 *p*=0.873
TGs [mg/L] (mg/dL)	1425.7 ± 197.9 (142.57 ± 19.79) n=21	1549.5 ± 141.4 (154.95 ± 14.14) n=42 *p*=0.624	1367.5 ± 97.6 (136.75 ± 9.76) n=57 *p*=0.772	1443.2 ± 82.3 (144.32 ± 8.23) n=99 *p*=0.930
Glucose [mg/L] (mg/dL)	891.9 ± 32.4 (89.19 ± 3.24) n=21	909 ± 40.5 (90.90 ± 4.05) n=42 *p*=0.783	897.4 ± 19.1 (89.74 ± 1.91) n=57 *p*=0.883	902.3 ± 20.3 (90.23 ± 2.03) n=99 *p*=0.824
RBC [10^{12}/L]	4.59 ± 0.12 n=21	4.37 ± 0.08 n=42 *p*=0.133	4.44 ± 0.06 n=57 *p*=0.254	4.41 ± 0.05 n=99 *p*=0.151

(Continued)

TABLE 1 Continued

	Control (n=21)	Patients with hypopituitarism (n=42)	Patients with other pituitary diseases (n=57)	Patients with pituitary diseases (n=99)
Hgb [g/L] [g/dL]	138.2 ± 4.2 (13.82 ± 0.42) n=21	128.5 ± 3.6 (12.85 ± 0.36) n=42 p=0.107	130.6 ± 1.9 (13.06 ± 0.19) n=57 p=0.059	129.7 ± 1.9 (12.97 ± 0.19) n=99 p=0.061
WBC [10^9/L]	6.39 ± 0.36 n=21	7.21 ± 0.31 n=42 p=0.114	6.63 ± 0.29 n=57 p=0.655	6.87 ± 0.21 n=99 p=0.330
HCT [vol%]	40.30 ± 1.14 n=21	38.15 ± 0.60 n=42 p=0.071	38.12 ± 0.58 n= 57 p=0.068	38.13 ± 0.42 n=99 p=0.041
Platelets[10^9/L]	220.91 ± 8.73 n=21	227.29 ± 8.72 n=42 p=0.646	241.33 ± 8.08 n=57 p=0.159	235.37 ± 5.96 n=99 p=0.288
Neutrophils [10^9/L]	3.43 ± 0.30 n=21	3.33 ± 0.21 n=42 p=0.788	3.49 ± 0.19 n=57 p=0.866	3.42 ± 0.14 n=99 p=0.984
Lymphocytes [10^9/L]	2.241 ± 0.12 n=21	2.87 ± 0.19 n=42 p=0.035	2.32 ± 0.12 n=57 p=0.693	2.55 ± 0.11 n=99 p=0.207
Eosinophils [10^9/L]	0.178 ± 0.02 n=21	0.247 ± 0.05 n=42 p=0.354	0.21 ± 0.02 n=57 p=0.396	0.22 ± 0.02 n=99 p=0.389
Basophils [10^9/L]	0.040 ± 0.003 n=21	0.051 ± 0.007 n=42 p=0.317	0.040 ± 0.003 n=57 p=0.993	0.045 ± 0.004 n= 99 p=0.569
Monocytes [10^9/L]	0.507 ± 0.03 n=21	0.617 ± 0.052 n=42 p=0.163	0.59 ± 0.03 n=57 p=0.173	0.60 ± 0.03 n=99 p=0.155
ASPAT [U/L]	31.09 ± 2.31 n=21	27.83 ± 1.92 n=41 p=0.305	24.29 ± 0.93 n=57 p=0.002	25.78 ± 0.98 n=98 p=0.027
ALAT [U/L]	30.60 ± 3.96 n=20	25.72 ± 1.92 n=40 p=0.216	22.11 ± 1.48 n=56 p=0.015	23.61 ± 1.19 n=96 p=0.029
Bilirubin [mg/L] (mg/dL])	8.42 ± 1.1 (0.842 ± 0.11) n=17	7.7 ± 0.8 (0.77 ± 0.08) n=38 p=0.593	7.2 ± 0.4 (0.72 ± 0.04) n=53 p=0.234	7.4 ± 0.4 (0.74 ± 0.04) n=91 p=0.347
Na [mmol/L]	139.90 ± 0.43 n=21	139.67 ± 0.46 n=42 p=0.742	139.72 ± 0.29 n=57 p=0.737	139.70 ± 0.26 n=99 p=0.727
K [mmol/L]	4.27 ± 0.06 n=21	5.19 ± 0.92 n=42 p=0.483	4.23 ± 0.04 n=57 p=0.630	4.64 ± 0.39 n=99 p=0.667
Cl [mmol/L]	104.62 ± 0.66 n=21	104.14 ± 0.59 n=41 p=0.623	105.61 ± 0.36 n=57 p=0.164	105.00 ± 0.33 n=98 p=0.624
Ca [mmol/L]	2.31 ± 0.03 n=19	2.29 ± 0.021 n=36 p=0.559	2.27 ± 0.02 n=50 p=0.251	2.28 ± 0.01 n=86 p=0.331
Urea [mg/L] (mg/dL)	311.9 ± 25.8 (31.19 ± 2.58) n=16	330.3 ± 15.1 (33.03 ± 1.51) n=39 p=0.526	317.1 ± 17.3 (31.71 ± 1.73) n=49 p=0.876	322.9 ± 11.7 (32.29 ± 1.17) n=88 p=0.708
Creatinine [mg/L] (mg/dL)	7.53 ± 0.3 (0.753 ± 0.03) n=20	8.34 ± 0.3 (0.834 ± 0.03) n=42 p=0.105	7.4 ± 0.3 (0.74 ± 0.03) n=56 p=0.761	7.8 ± 0.2 (0.78 ± 0.02) n=98 p=0.626
GFR [mL/(min×1.72 m²)]	97.52 ± 4.32 n=20	89.70 ± 6.58 n=42 p=0.438	99.56 ± 3.81 n=56 p=0.768	95.33 ± 3.58 n=98 p=0.790
Vit D [ng/mL]	25.70 ± 2.41 n=16	29.92 ± 2.18 n=33 p=0.242	26.86 ± 2.04 n=39 p=0.745	28.26 ± 1.49 n=72 p=0.448
PTH [pg/mL]	35.16 ± 3.92 n=16	42.72 ± 3.27 n=35 p=0.177	53.94 ± 11.49 n=44 p=0.335	48.97 ± 6.56 n=79 p=0.351

Comparison between subgroups was performed by Student's unpaired t-test. Statistical significance was determined at the level of $p<0.05$. *p=0.019 vs. Control and vs. patients with other pituitary diseases. Statistically significant differences are shaded.

patients with hypopituitarism (and also in patients with other pituitary diseases or in all patients with pituitary diseases) than in control individuals and these differences relate to ACTH, LH, FSH (of borderline significance), TSH and, regarding peripheral hormones, to cortisol and FT3. Of importance is the finding that IGF-I concentration was significantly lower in patients with hypopituitarism comparing to healthy individuals as well as comparing to patients with other pituitary diseases (p=0.019 in case of both comparisons). Regarding lipid profile, total cholesterol was higher in patients with hypopituitarism than in controls (p=0.043).

Because MBL level can be affected by inflammation, we have checked the prevalence of the increased C reactive protein (CRP) concentrations in particular groups and we did not find statistically significant differences between any groups, *i.e.* control (1/15, 7%) vs. patients with hypopituitarism (7/33, 21%), p=0.233; control (1/15, 7%) vs. patients with other pituitary diseases (6/45, 13%), p=0.531; patients with hypopituitarism (7/33, 21%) vs. patients with other pituitary diseases (6/45, 13%), p=0.349. In control individuals only one patient had slightly increased CRP level, *i.e.* 14.8 mg/L (1.48 mg/dL), comparing to the upper normal range being 10 mg/L (1 mg/dL). In hypopituitary patients and in patients with other pituitary diseases the highest CRP levels were 14.2 mg/L (1.42 mg/dL) and 14.9 mg/L (1.49 mg/dL), respectively (data not shown).

The concentration of MBL in blood serum was significantly lower in patients with pituitary diseases (n=99) than in control individuals (Figure 2 left). When patients with hypopituitarism (n=42) and patients with other pituitary diseases (n=57) were considered separately, the lowest MBL level was found in patients with hypopituitarism – comparing to control individuals, as well as comparing to patients with other pituitary diseases (Figure 2 right).

We evaluated the distribution of patients (number of patients – Figure 3 left graphs; percentage of patients – Figure 3 right graphs) with relation to MBL level. There is a clear difference in this distribution between control individuals, in whom no subjects had MBL level below 500 ng/mL and most subjects, i.e. 19/21 (90.5%), had MBL level above 1000 ng/mL, *versus* hypopituitary patients, in whom as many as 18/42 patients (42.9%) had MBL level below 500 ng/mL and 18/42 patients (42.9%) had MBL level above 1000 ng/mL. Histogram presenting patients with other pituitary diseases is something in between the two, with only 8/57 patients (14%) having MBL concentration below 500 ng/mL, and with as many as 39/57 patients (68.4%) who had MBL level above 1000 ng/mL.

In the group of patients with hypopituitarism (n=42) we have checked if patients with the lowest levels of MBL (<500 ng/mL) differ from patients with higher levels of MBL (>500 ng/mL) regarding their age. The mean age of patients with MBL levels <500 ng/mL (n=18) was 49.39± 4.44 whereas of those with MBL levels above this cut-off point (n=24) the mean age was 50.92 ± 3.65 and this difference was not statistically significant (p=0.790). Similarly, no differences regarding mean age of patients with lower levels of MBL (<500 ng/mL) (n=13) *versus* higher levels of MBL (>500 ng/mL) (n=44) were found when the group of patients with other pituitary diseases (n=57) was considered (48.38 ± 4.11 vs. 44.61 ± 2.60, p=0.479).

We compared mean and median values of MBL level in a group of patients with hypopituitarism who were on appropriate replacement therapies (compensated hypopituitarism) *versus* patients being on inadequate replacement therapies (non-compensated hypopituitarism) (Figure 4). Patients with non-compensated hypopituitarism did have lower mean MBL level (Figure 4 left graph) and lower median MBL level (Figure 4 right graph) comparing to patients with compensated hypopituitarism. Patients with non-compensated hypopituitarism obviously had lower mean MBL level (Figure 4 left graph) and lower median MBL level (Figure 4 right graph) comparing to control individuals. However, mean and median MBL levels in patients with compensated hypopituitarism *versus* controls did not differ significantly (Figure 4, 2300.09 ± 579.93 vs. 3199.30 ± 508.46, p=0.294; 1951.90 vs. 2329.16; p=0.301, respectively).

Additionally, MBL level was compared between patients with compensated *versus* non-compensated hypopituitarism depending on how many pituitary axes were involved, *i.e.* on the number of pituitary deficiencies (Table 2). Although no statistically significant differences were found (due to low numbers of individuals and to very high standard error of the mean, SEM) mean MBL levels tend to be higher in patients with compensated hypopituitarism in most of subgroups considered. Of importance is the finding that among patients with non-compensated hypopituitarism a tendency is seen for lower mean (Figure 5 left) and median (Figure 5 right) MBL levels in patients with higher numbers of pituitary deficiencies; the lowest MBL level was found in patients with panhypopituitarism. Unfortunately, these differences did not reach statistical significance (Table 2 and Figure 5).

Possible correlations between MBL level and all other linear parameters were evaluated in control individuals, in patients with hypopituitarism, in patients with other pituitary diseases, and it the whole group of individuals (Table 3). Of great importance with relation to the findings of the present study is the observation that MBL level did not correlate with age in any of the groups considered. The most prominent result does constitute the positive correlation between MBL level and insulin-like growth factor I (IGF-I) level in patients with hypopituitarism and in patients with other pituitary diseases and also in the whole group of individuals. Positive correlation between MBL level and glucose concentration was found in patients with hypopituitarism. MBL level also correlated with FT3 concentration in the whole group examined. Apart from patients with hypopituitarism, in all other groups MBL level correlated with hematocrit (HCT) as well as with red blood cells (RBC) (the latter with borderline significance). Other correlations such as between MBL level and TgAb concentration or hemoglobin (Hgb) in controls or between MBL level and bilirubin concentration in patients with hypopituitarism or between MBL level and potassium concentration (negative correlation) in patients with other pituitary diseases can be neglected and therefore they will be not discussed in this paper.

We evaluated the percentage of abnormal lipid profile in control individuals *versus* unhealthy patients (Table 4). The increased total cholesterol was found more frequently in patients with hypopituitarism (Table 4 above) or in patients with pituitary diseases (Table 4 below) than in control individuals.

The univariate/multivariate logistic regression analyses were performed to determine which linear variables are associated with

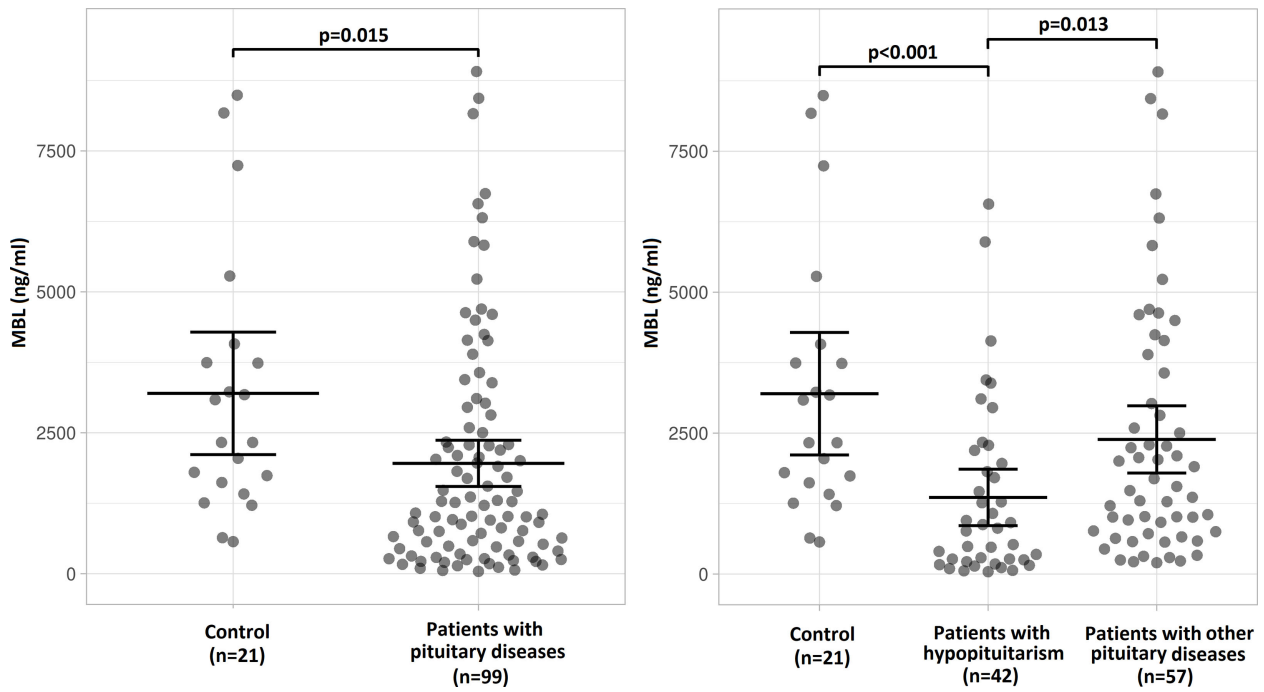

FIGURE 2
Mean (± SEM) values of mannan-binding lectin (MBL) level in control individuals (n=21) and in patients with pituitary diseases (n=99) (left) or mean (± SEM) values of MBL level in control individuals (n=21), in patients with hypopituitarism (n=42) and in patients with other pituitary diseases (n=57) (right). Statistical evaluation was performed by an unpaired Student's *t*-test. The statistical differences are marked in the graphics.

hypopituitarism (Table 5). In the univariate analysis conducted in a group of 63 subjects (control individuals plus patients with hypopituitarism; n=21+42) the following three determinants, *i.e.* age, total cholesterol (TChol) concentration and lymphocyte concentration, were positively associated with hypopituitarism, whereas MBL level, TSH concentration, FT3 concentration, LH, ACTH and IGF-I were negatively associated with hypopituitarism. Unfortunately, all these determinants lost their statistical significance in multivariate logistic regression analysis (Table 5 above).

When univariate regression analysis was performed in the whole group of individuals (n=120) the same relationships were found as described above for the group of 63 patients. Additionally, FSH was negatively, whereas creatinine was positively, associated with hypopituitarism. In multivariate regression analysis the only determinant positively associated with hypopituitarism was, unexpectedly, TChol concentration (Table 5 below).

Another univariate logistic regression analysis was performed only in the group of patients with hypopituitarism to determine which linear variables are associated with inadequate hormone replacement therapies (non-compensated hypopituitarism) (Table 6). Three determinants, *i.e.* FT3, LH and MBL levels were negatively associated with inadequate replacement therapies (non-compensated hypopituitarism). In multivariate regression analysis these three determinants lost their statistical significance.

Because vitamin D deficiency affects the immune system we have checked if the percentages of patients with decreased vitamin D differ between Control and unhealthy individuals and if MBL levels differ between individuals with vitamin D deficiency and with vitamin D sufficiency (Table 7). Regarding the first comparison (made with the two-sided ratio comparison test), severe vitamin D deficiency occurred less commonly in patients with hypopituitarism vs. Controls (5/33, 15% vs. 6/16, 37%, p=0.087) as well as less commonly in the group of all patients with pituitary diseases (n=99) vs. Control (16/72, 22% vs. 6/16, 37%, p=0.211), however these differences did not reach statistical significance (data not presented). Regarding the other comparison, the evaluation was done in the group of patients with hypopituitarism as well as in the whole group examined. Severe vitamin D deficiency <20 ng/mL was characterized, unexpectedly, by higher MBL levels when the evaluation was done in patients with hypopituitarism as well as in the whole group examined, however these differences were of borderline significance (Table 7 below). The cut-off vitamin D level of 30 ng/mL was not associated with any substantial differences (Table 7 above).

Because the level of thyroid antibodies express thyroid autoimmunity resulting from the disturbed efficiency of the immune system we checked the prevalence of the increased concentrations of thyroid antibodies (positive thyroid antibodies) in our population sample and mean MBL levels in individuals with positive *versus* negative thyroid antibodies. In the whole group examined (n=120), in patients with hypopituitarism (n=42), in patients with other pituitary diseases (n=57) and in control individuals (n=21), positive thyroid antibodies were found with the following frequencies: 16/85 (18.82%), 4/27 (14.81%), 9/40 (22.50%), and 3/21 (14.29%), respectively (data not presented). As evaluated by the ratio comparison test, the prevalence of positive thyroid antibodies did not differ statistically between the following groups: control vs. hypopituitary patients, p=0.923; control vs. other

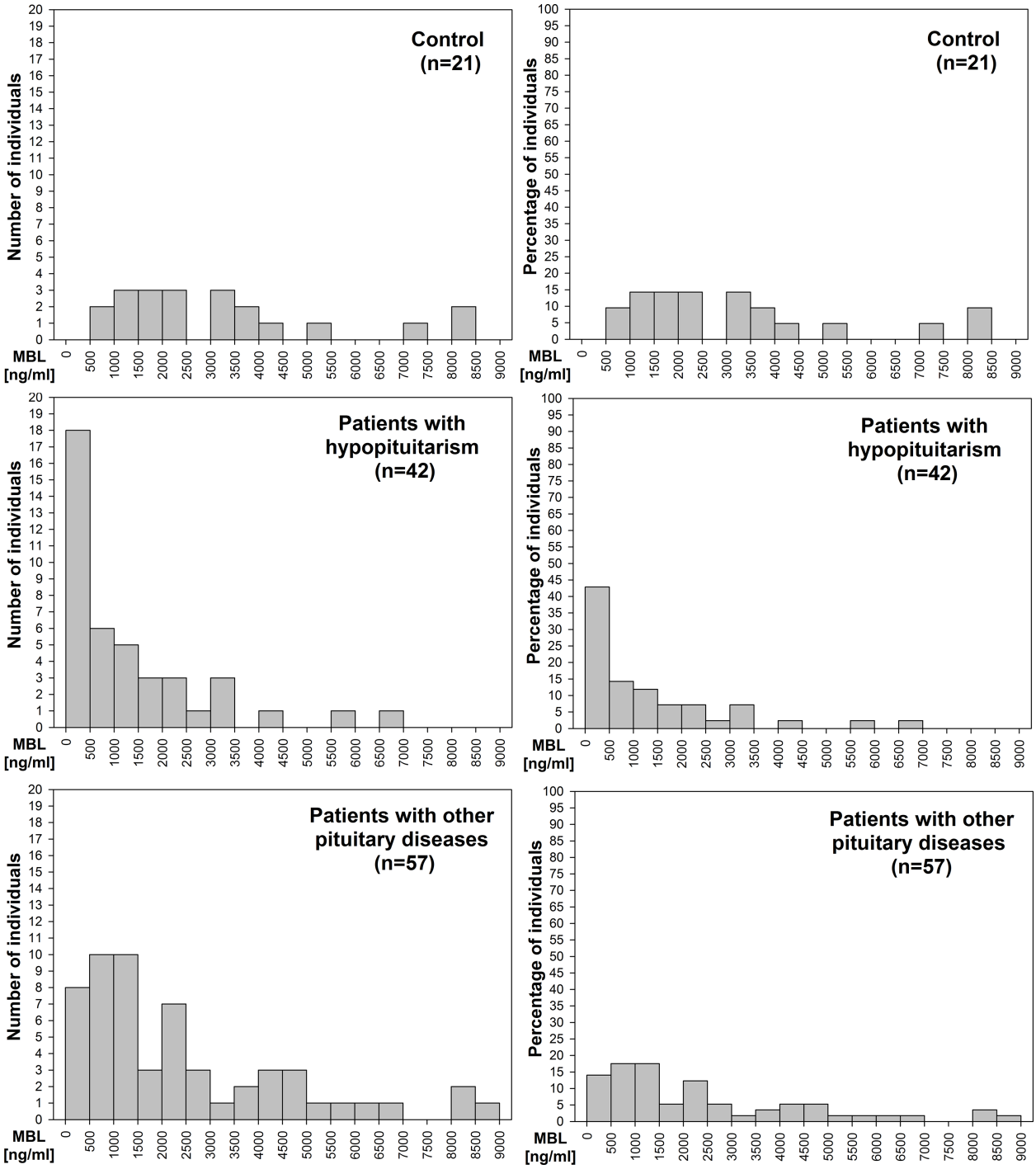

FIGURE 3
Histograms of the distribution of number of patients (left graphs) or percentage of patients (right graphs) with relation to mannan-binding lectin (MBL) level in control individuals (n=21), in patients with hypopituitarism (n=42), and in patients with other pituitary diseases (n=57).

pituitary diseases, p=0.454; hypopituitary patients vs. patients with other pituitary diseases, p=0.478.

Thereafter, we compared MBL levels between subgroups with positive and negative thyroid antibodies. MBL concentrations did not differ statistically between individuals with positive *versus* negative thyroid antibodies when the statistical comparison was made in the whole group of individuals or in patients with hypopituitarism or in patients with other pituitary diseases or in control individuals; Respective comparisons of MBL levels are as follows: 2231.13 ± 605.94 ng/mL vs. 2134.04 ± 259.46 ng/mL, p=0.874; 613.70 ± 223.04 ng/mL vs.1399.36 ± 312.80 ng/mL, p=0.315; 1820.67 ± 604.92 ng/mL vs. 2386.34 ± 433.09 ng/mL, p=0.520; 5619.05 ng/mL ± 1568.53 ng/mL vs. 2739.16 ng/mL ± 585.68 ng/mL, p=0.068 (data not presented).

Summarizing the issue on the possible contribution of positive thyroid antibodies to MBL level it should be stated on the basis of

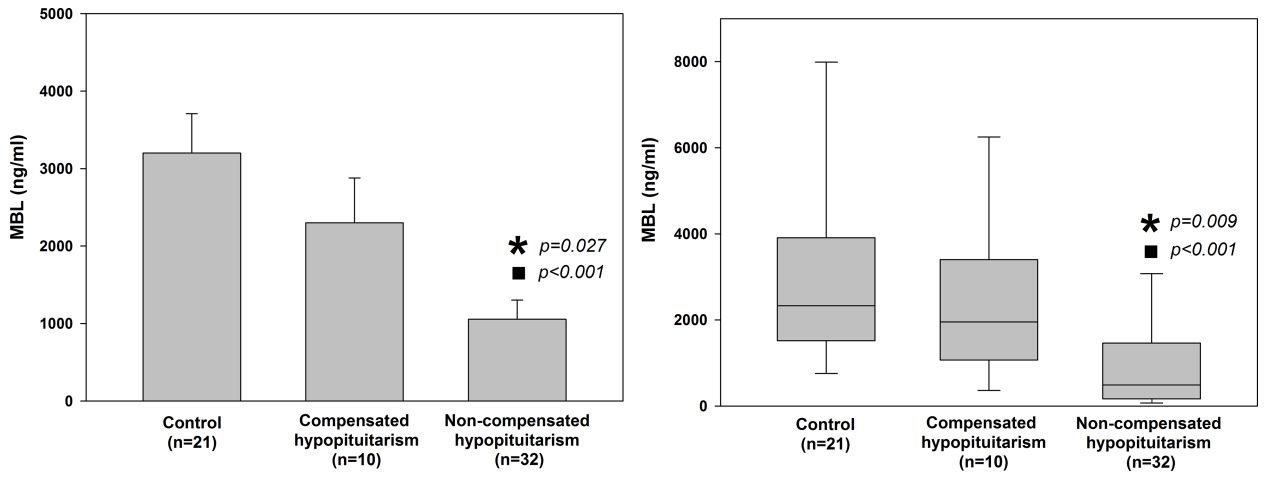

FIGURE 4
Bar chart of mean (± SEM) (left graph) and box plot of median (± SEM) (right graph) values of mannan-binding lectin (MBL) level in control individuals (n=21) and patients with hypopituitarism (n=42) who are on appropriate replacement therapies (compensated hypopituitarism, n=10) vs. inadequate replacement therapies (non-compensated hypopituitarism, n=32). Central line of each box denotes the median, the top and bottom edges of the box show the 25% and 75% percentile, with the 10% and 90% percentiles shown by the upper and lower whiskers. Statistical evaluation was performed by an unpaired Student's *t*-test or Mann-Whitney U test respectively. *$p<0.05$ vs. compensated hypopituitarism, ■$p<0.05$ vs control individuals.

the current results that MBL concentration, in any of groups considered, is not statistically affected by thyroid autoimmunity.

4 Discussion

It is well known that patients with hypopituitarism have impaired general health (13, 14). It is highly probable that the immune response might be disturbed, at least or especially *via* secondary adrenal insufficiency (15). That is why it can be hypothesized that certain abnormalities of the lectin pathway of the complement system are already present under conditions of pituitary hormone insufficiency.

Patients with hypopituitarism considered in our study suffered from hypopituitarism of different degree, *i.e.* they had from one to all five pituitary deficiencies. Therefore we discuss shortly particular pituitary deficiencies with relation to our study. Regarding GH deficiency, that one was not confirmed in our patients with the use of insulin tolerance test, being still a gold standard. The reason being is that just till recently we did not have in Poland the reimbursement for the treatment with recombinant human GH (rhGH); however, it has just been confirmed in 2018 (16). It should be recalled that in most cases hypopituitarism develops gradually with GH deficiency being usually the first one, followed by LH/FSH deficiency, TSH deficiency, ACTH deficiency and prolactin deficiency (12, 17). Therefore, it is highly probable that most of our patients with different diagnosed pituitary deficiencies had also GH deficiency (with exception of patients with isolated deficiencies) and that was confirmed indirectly by lower IGF-I levels in patients with hypopituitarism (Table 1) and by the observation that lower IGF-I concentrations, similarly to pituitary tropic hormones (*i.e.*

TABLE 2 Mean (± SEM) values of mannan-binding lectin (MBL) level in patients with hypopituitarism (n=42) who are on appropriate replacement therapies (compensated hypopituitarism, n=10) vs. inadequate replacement therapies (non-compensated hypopituitarism, n=32) presented in particular subgroups of individuals depending on how many pituitary axes are involved.

	Compensated hypopituitarism (n=10)	Non-compensated hypopituitarism (n=32)
One pituitary deficiency (n=9)	1662.73 ± 581.48 n=5	1494.68 ± 660.73 n=4
Two pituitary deficiencies (n=7)	6562.51 n=1	1042.48 ± 509.37 n=6
Three pituitary deficiencies (n=9)	1736.58 ± 456.18 n=2	1335.99 ± 773.59 n=7
Four pituitary deficiencies (n=12)	2325.82 ± 1061.62 n=2	955.13 ± 439.57 n=10
Five pituitary deficiencies (n=5)	- n=0	507.02 ± 246.51 n=5

Statistical evaluation was performed by Mann-Whitney U test. No statistically significant differences were found.

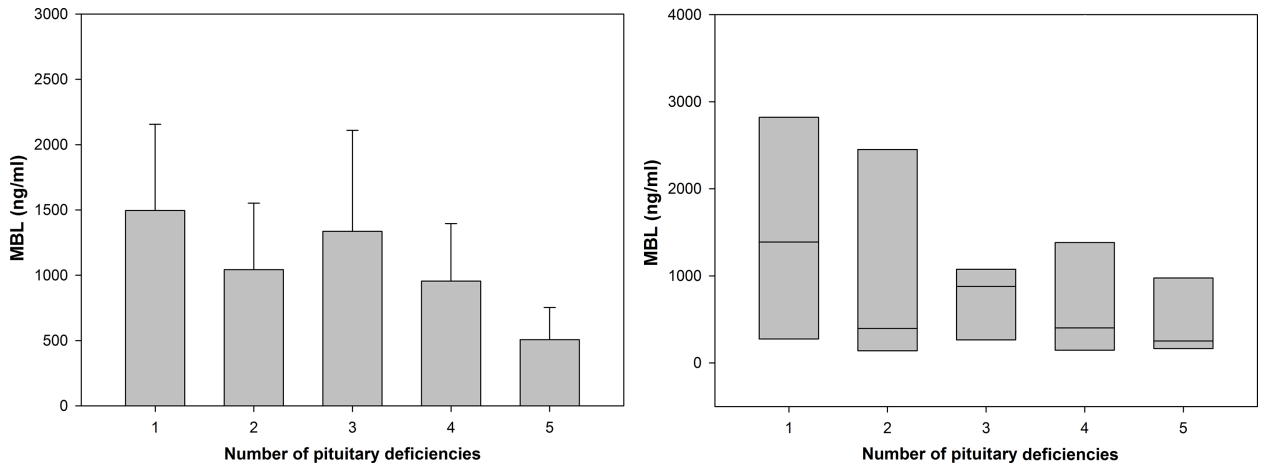

FIGURE 5
Bar chart of mean (± SEM) (left graph) and box plot of median (± SEM) (right graph) values of mannan-binding lectin (MBL) level in patients with hypopituitarism who are on inadequate replacement therapies (non-compensated hypopituitarism) presented in particular subgroups of individuals depending on how many pituitary axes are involved. Central line of each box denotes the median, the top and bottom edges of the box show the 25% and 75% percentile. No statistically significant differences were found.

TSH, LH and ACTH), were associated with hypopituitarism in the univariate regression analysis (Table 5).

The main observation from our study is that MBL level is lower in patients with hypopituitarism comparing to healthy individuals and even to patients with other pituitary diseases (Figure 2) and the former relationship was also confirmed by univariate regression analysis (Table 5). When the distribution of patients with relation to MBL level was evaluated, no healthy individuals had MBL level below 500 ng/mL whereas almost half of hypopituitary subjects had MBL below this cut-off level.

TABLE 3 Correlations between mannan-binding lectin (MBL) level and clinical/laboratory parameters in 4 groups considered: Control individuals (n=21), patients with hypopituitarism (n=42), patients with other pituitary diseases (n=57), and the whole group of individuals (n=120).

	MBL [ng/mL] r; *p*-value; n			
	Control individuals (n=21)	Patients with hypopituitarism (n=42)	Patients with other pituitary diseases (n=57)	The whole group of individuals (n=120)
Age [years]	0.0149 *p*=0.949 n=21	-0.1050 *p*=0.512 n=42	-0.0404 *p*=0.765 n=57	-0.115 *p*=0.213 n=120
Body mass [kg]	-0.0740 *p*=0.770 n=18	0.1010 *p*=0.576 n=33	-0.0142 *p*=0.922 n=50	-0.0192 *p*=0.849 n=101
Height [cm]	0.305 *p*=0.219 n=18	-0.297 *p*=0.0932 n=33	-0.0505 *p*=0.728 n=50	-0.0271 *p*=0.788 n=101
BMI [kg/m^2]	-0.163 *p*=0.519 n=18	0.0802 *p*=0.657 n=33	0.0121 *p*=0.934 n=50	-0.0381 *p*=0.706 n=101
ACTH [pg/mL]	-0.142 *p*=0.599 n=16	-0.0887 *p*=0.618 n=34	-0.124 *p*=0.375 n=53	-0.0373 *p*=0.709 n=103
LH [IU/L]	0.0287 *p*=0.904 n=20	0.0260 *p*=0.880 n=36	0.102 *p*=0.467 n=53	0.121 *p*=0.207 n=110
FSH [IU/L]	-0.0815 *p*=0.733 n=20	0.0036 *p*=0.983 n=36	-0.0922 *p*=0.503 n=55	-0.0159 *p*=0.869 n=111
Prl [ng/mL]	0.161 *p*=0.485 n=21	-0.0805 *p*=0.631 n=38	-0.0174 *p*=0.902 n=53	-0.0821 *p*=0.390 n=112
IGF-I [ng/mL]	0.220 *p*=0.381 n=18	0.4410 *p*=0.0049 n=40	0.429 *p*=0.002 n=51	0.434 *p*<0.001 n=108

(Continued)

TABLE 3 Continued

	MBL [ng/mL] r; *p*-value; n			
	Control individuals (n=21)	Patients with hypopituitarism (n=42)	Patients with other pituitary diseases (n=57)	The whole group of individuals (n=120)
Cortisol [μg/L]	0.120 *p*=0.614 n=20	0.0788 *p*=0.620 n=40	-0.173 *p*=0.203 n=56	0.141 *p*=0.127 n=116
TSH [mIU/L]	0.132 *p*=0.569 n=21	0.1630 *p*=0.320 n=39	-0.0464 *p*=0.732 n=57	0.144 *p*=0.122 n=117
FT3 [pg/mL]	0.122 *p*=0.599 n=21	0.2920 *p*=0.0639 n=42	0.149 *p*=0.268 n=57	0.294 *p*=0.0012 n=120
FT4 [ng/L]	0.223 *p*=0.332 n=21	-0.190 *p*=0.235 n=42	-0.133 *p*=0.324 n=57	-0.0562 *p*=0.543 n=120
TPOAb [IU/mL]	0.190 *p*=0.450 n=18	-0.200 *p*=0.317 n=27	-0.193 *p*=0.234 n=40	-0.0305 *p*=0.782 n=85
TgAb [IU/mL]	0.560 *p*=0.0156 n=18	-0.0758 *p*=0.707 n=27	-0.160 *p*=0.332 n=39	-0.0487 *p*=0.660 n=84
TSHRAb [IU/L	-0.289 *p*=0.246 n=18	0.1960 *p*=0.337 n=26	0.202 *p*=0.217 n=39	0.0581 *p*=0.602 n=83
TChol [mg/L]	-0.209 *p*=0.363 n=21	-0.0858 *p*=0.594 n=42	0.135 *p*=0.316 n=57	-0.0441 *p*=0.634 n=120
HDLC [mg/L]	-0.0313 *p*=0.893 n=21	-0.2720 *p*=0.0854 n=42	0.0268 *p*=0.843 n=57	-0.0768 *p*=0.407 n=120
LDLC [mg/L]	-0.191 *p*=0.408 n=21	-0.0236 *p*=0.884 n=42	0.132 *p*=0.326 n=57	0.00642 *p*=0.945 n=120
HDLC/TChol	-0.0077 *p*=0.973 n=21	-0.2060 *p*=0.196 n=42	-0.138 *p*=0.312 n=56	-0.111 *p*=0.229 n=118
TGs [mg/L]	-0.143 *p*=0.535 n=21	-0.1680 *p*=0.292 n=42	-0.160 *p*=0.332 n=39	-0.0309 *p*=0.739 n=120
Glucose [mg/L]	-0.00914 *p*=0.694 n=21	0.3670 *p*=0.0182 n=42	0.207 *p*=0.122 n=57	0.177 *p*=0.0537 n=120
RBC [10^{12}/L]	0.425 *p*=0.054 n=21	-0.1550 *p*=0.332 n=42	0.248 *p*=0.0633 n=57	0.204 *p*=0.0264 n=119
Hgb [g/L]	0.575 *p*=0.006 n=21	-0.0836 *p*=0.603 n=42	0.203 *p*=0.130 n=57	0.0793 *p*=0.391 n=120
WBC [10^9/L]	-0.259 *p*=0.257 n=21	-0.2860 *p*=0.0698 n=42	0.0616 *p*=0.649 n=57	-0.124 *p*=0.179 n=120
HCT [vol%]	0.500 *p*=0.0209 n=21	-0.0961 *p*=0.550 n=42	0.263 *p*=0.0481 n=57	0.259 *p*=0.004 n=120
Platelets [10^9/L]	-0.315 *p*= 0.165 n=21	-0.2920 *p*= 0.0638 n=42	-0.0641 *p*=0.636 n=57	-0.149 *p*=0.107 n=120
Neutrophils [10^9/L]	-0.255 *p*= 0.264 n=21	-0.2480 *p*= 0.118 n=42	0.0788 *p*=0.560 n=57	-0.0564 *p*=0.542 n=120
Lymphocytes [10^9/L]	-0.155 *p*= 0.502 n=21	-0.0877 *p*= 0.586 n=42	0.0137 *p*=0.919 n=57	-0.113 *p*=0.222 n=120
Eosinophils [10^9/L]	0.183 *p*= 0.426 n=21	-0.0633 *p*= 0.694 n=42	0.0377 *p*=0.780 n=57	-0.0293 *p*=0.751 n=120

(Continued)

TABLE 3 Continued

	MBL [ng/mL] r; *p*-value; n			
	Control individuals (n=21)	Patients with hypopituitarism (n=42)	Patients with other pituitary diseases (n=57)	The whole group of individuals (n=120)
Basophils [10^9/L]	-0.0394 *p*= 0.865 n=21	-0.1180 *p*= 0.462 n=42	-0.00193 *p*=0.989 n=57	-0.0893 *p*=0.334 n=120
Monocytes [10^9/L]	-0.0722 *p*=0.756 n=21	-0.0812 *p*=0.614 n=42	0.104 *p*=0.440 n=57	-0.0214 *p*=0.818 n=120
ASPAT [U/L]	0.0158 *p*= 0.946 n=21	-0.0176 *p*= 0.914 n=40	-0.113 *p*=0.402 n=57	-0.0302 *p*=0.746 n=118
ALAT [U/L]	-0.0484 *p*= 0.840 n=20	0.0336 *p*= 0.839 n=39	-0.129 *p*=0.342 n=56	-0.0437 *p*=0.643 n=115
Bilirubin [mg/L]	0.196 *p*= 0.451 n=17	0.3960 *p*= 0.0154 n=37	-0.0748 *p*=0.594 n=53	0.129 *p*=0.184 n=107
Na [mmol/L]	0.411 *p*= 0.064 n=21	0.0700 *p*= 0.664 n=42	-0.0952 *p*=0.481 n=57	0.0481 *p*=0.603 n=120
K [mmol/L]	0.363 *p*=0.106 n=21	-0.0645 *p*=0.689 n=42	-0.268 *p*=0.044 n=57	-0.070 *p*=0.449 n=120
Cl [mmol/L]	0.290 *p*=0.203 n=21	-0.0422 *p*=0.796 n=41	0.0192 *p*=0.887 n=57	0.0898 *p*=0.334 n=118
Ca [mmol/L]	0.158 *p*=0.518 n=19	-0.2630 *p*=0.127 n=35	-0.182 *p*=0.207 n=50	-0.121 *p*=0.220 n=104
Urea [mg/L]	0.114 *p*=0.673 n=16	-0.1900 *p*=0.254 n=38	0.0355 *p*=0.809 n=49	-0.0304 *p*=0.761 n=103
Creatinine [mg/L]	0.378 *p*=0.100 n=20	-0.1970 *p*=0.217 n=42	0.0394 *p*=0.773 n=56	-0.0272 *p*=0.771 n=117
GFR [mL/(min×1.72 m^2)]	-0.216 *p*=0.360 n=20	0.2320 *p*=0.144 n=42	0.107 *p*=0.431 n=56	0.131 *p*=0.159 n=118
Vit D [ng/mL]	0.335 *p*=0.204 n=16	-0.1410 *p*=0.440 n=32	-0.124 *p*=0.453 n=39	-0.0579 *p*=0.597 n=86
PTH [pg/mL]	-0.208 *p*=0.440 n=16	-0.1540 *p*=0.383 n=34	-0.152 *p*=0.324 n=44	-0.124 *p*=0.232 n=94

Statistical evaluation was performed by the Pearson's correlation test. r - Pearson's correlation coefficient. Statistical significance was determined at the level of $p<0.05$. Statistically significant differences are shaded.

Such studies have not been performed before. There were only studies concerning relationship between MBL and GH deficiency or excess (9, 10), as it has been already mentioned in the Introduction section. Although IGF-I is the main mediator of GH action on numerous processes, such as linear bone growth and metabolic processes (18), probably it does not mediate GH action on the lectin pathway, because IGF-I treatment did not change MBL level in healthy and GH deficient individuals (9). However, positive correlation between IGF-I and MBL found in our study (Table 3) is not in contradiction with the above (9), but simply indicates that low IGF-I level expresses GH deficiency. After all it would be very difficult to confirm the possible correlation between MBL and GH levels due to short half-life of GH making its blood concentration unstable (19).

Not only pituitary tropic hormones, but also peripheral hormones produced by target endocrine glands, contribute to appropriate functioning of the immune system (20–23) and, at the same time, probably also to proper formation of MBL. Such an assumption can be confirmed by results from the present study showing that patients with hypopituitarism being on appropriate replacement therapies (patients with compensated hypopituitarism) had higher MBL levels comparing to those on inadequate replacement therapies (patients with non-compensated hypopituitarism, Figure 4 and Table 6).

Positive correlation found between MBL and glucose concentration in patients with hypopituitarism may be associated with the fact that glucose concentration is positively regulated by two pituitary hormones, *i.e.* GH and ACTH (*via* cortisol). In turn, positive correlation noted between MBL and FT3 in the whole group examined

TABLE 4 Percentage of abnormal lipid profile in control individuals (n=21) vs. patients with hypopituitarism (n=42) (above), and in control individuals (n=21) vs. patients with pituitary diseases (n=99) (below).

	Control n=21	Patients with hypopituitarism n=42	*p*
TChol ≥2000 mg/L (≥200 mg/dL)	n=3 14%	n=18 43%	0.025
HDLC <400 mg/L (<40 mg/dL)	n=5 24%	n=7 17%	0.509
LDLC >1000 mg/L (>100 mg/dL)	n=10 48%	n=23 55%	0.601
TGs >1500 mg/L (>150 mg/dL)	n=7 33%	n=19 45%	0.364
HDLC/TChol <0.2	n=1 5%	n=3 7%	0.759
	Control n=21	Patients with pituitary diseases n=99	*p*
TChol ≥2000 mg/L (≥200 mg/dL)	n=3 14%	n=38 38%	0.037
HDLC <400 mg/L (<40 mg/dL)	n=5 24%	n=17 40%	0.170
LDLC >1000 mg/L (>100 mg/dL)	n=10 48%	n=54 56%	0.504
TGs >1500 mg/L (>150 mg/dL)	n=7 33%	n=40 40%	0.551
HDLC/TChol <0.2	n=1 5%	n=5 5%	1.000

Statistical evaluation was performed by the two-sided ratio comparison test. Statistical significance was determined at the level of $p<0.05$. Statistically significant differences are shaded.

may result from stimulatory effects of thyroid hormones on complement system and MBL level, as it was already mentioned in the Introduction section (6–8). Consistently, the finding that lower FT3 concentrations in patients with hypopituitarism are associated with inadequate replacement therapy, as was documented by univariate regression analysis (Table 6), is expected and may result directly from the lack of L-thyroxine therapy in patients with secondary hypopituitarism.

Regarding abnormal lipid profile, the increased total cholesterol was observed more frequently in patients with pituitary diseases, especially in hypopituitary patients, comparing to healthy individuals (Table 4), and total cholesterol concentration was found to be the only independent factor associated with hypopituitarism (Table 5). Such relationships may result mostly from two pituitary deficiencies, namely GH deficiency (24, 25) and TSH deficiency (causing secondary hypothyroidism) (26). Regarding the latter, such findings are in agreement with what is commonly observed in patients with primary hypothyroidism (26, 27). Even high normal TSH (8, 27, 28) and isolated hypothyroxinemia (29) were associated with abnormal lipid profile in women of childbearing age.

Because a proper supply of vitamin D contributes to appropriate functioning of the immune system (30–32), we checked to what extent vitamin D deficiency changes MBL level. Our patients with hypopituitarism (and also the whole group examined) who had severe vitamin D deficiency were characterized by higher MBL levels than those with recommended vitamin D concentrations (Table 7). Therefore such results exclude the possibility that lower MBL level found in our hypopituitary patients may result from vitamin D deficiency. At the same time such results make our observation that low MBL level is directly associated with hypopituitarism much stronger. In turn, rarer occurrence of severe vitamin D deficiency in our hypopituitary patients may possibly result from the assumption that patients who were treated properly with peripheral hormones due to hypopituitarism, did take adequate dose of vitamin D either. It can be mentioned that our observation is in apparent contradiction with

TABLE 5 Univariate and multivariate logistic regression analyses of hypopituitarism determinants (linear variables) performed in the following groups: Control plus patients with hypopituitarism (n=21+42) (above), and the whole group of individuals (n=120) (below).

Variable	Control plus patients with hypopituitarism (n=21+42)					
	Univariate regression			Multivariate regression		
	OR	95%CI	*p*	OR	95%CI	*p*
Age [years]	1.042	1.01-1.08	*0.017*	*0.922*	*0.62-1.38*	*0.693*
MBL [ng/mL]	0.999	0.99-1.00	*0.004*	*0.997*	*0.99-1.01*	*0.519*
TSH [mIU/L]	0.455	0.28-0.75	*0.002*	*0.164*	*0.01-26.72*	*0.487*
FT3 [pg/mL]	0.043	0.01-0.23	*<0.001*	*<0.001*	*1.53-3.09*	*0.541*
TChol [mg/L]	1.013	1.00-1.03	*0.049*	*1.110*	*0.79-1.55*	*0.541*
LH [IU/L]	0.878	0.79-0.96	*0.007*	*0.895*	*0.63-1.26*	*0.528*
ACTH [pg/mL]	0.970	0.94-0.99	*0.045*	*0.856*	*0.63-1.15*	*0.308*
IGF-I [ng/mL]	0.994	0.98-1.00	*0.041*	*1.020*	*0.97-1.07*	*0.441*
Lymphocytes [10^9/L]	1.877	1.01-3.48	*0.046*	*17.272*	*0.04-7195.24*	*0.355*
Variable	Whole group of individuals (n=120)					
	Univariate regression			Multivariate regression		
	OR	95%CI	*p*	OR	95%CI	*p*
Age [years]	1.023	1.00-1.04	*0.046*	1.031	0.98-1.08	*0.209*
MBL [ng/mL]	1.001	0.99-1.00	*0.005*	1.001	0.99-1.00	*0.119*
TSH [mIU/L]	0.558	0.38-0.81	*0.002*	0.780	0.45-1.35	*0.377*
FT3 [pg/mL]	0.186	0.075-0.46	*<0.001*	0.640	0.13-3.07	*0.577*
TChol [mg/L]	1.009	1.00-1.018	*0.045*	1.018	1.00-1.03	*0.019*
LH [IU/L]	0.849	0.78-0.93	*<0.001*	0.841	0.68-1.04	*0.115*
FSH [IU/L]	0.949	0.91-0.987	*0.008*	1.003	0.91-1.10	*0.952*
ACTH [pg/mL]	0.970	0.94-0.99	*0.004*	0.982	0.95-1.01	*0.241*
IGF-I [ng/mL]	0.992	0.99-1.00	*0.004*	1.002	0.99-1.01	*0.483*
Lymphocytes [10^9/L]	1.732	1.16-2.58	*0.007*	1.221	0.62-2.41	*0.564*
Creatinine [mg/L]	9.108	1.32-62.93	*0.025*	3.227	0.17-59.98	*0.432*

Only statistically significant determinants are presented in the univariate analysis. Statistical significance was determined at the level of $p<0.05$. Statistically significant differences are shaded.

TABLE 6 Univariate logistic regression analysis of non-compensated hypopituitarism (inadequate hormone replacement therapies) determinants (linear variables) performed in patients with hypopituitarism (n=42).

Variable	Patients with hypopituitarism (n=42)					
	Univariate regression			Multivariate regression		
	OR	95%CI	*p*	OR	95%CI	*p*
FT3 [pg/mL]	0.120	0.02-0.2	*0.020*	0.144	0.017-1.18	*0.071*
LH [IU/L]	0.814	0.68-0.97	*0.024*	0.800	0.64-0.99	*0.073*
MBL [ng/mL]	0.999	0.99-1.00	*0.048*	0.999	0.99-1.00	*0.127*

Only statistically significant determinants are presented in the univariate analysis. Statistical significance was determined at the level of $p<0.05$. Statistically significant differences are shaded.

TABLE 7 Mean MBL concentration in patients with/without Vit. D deficiency (<30 ng/mL/≥30 ng/mL) (above) or severe vitamin D deficiency (<20 ng/mL/≥20 ng/mL) (below) evaluated in control individuals (n=21) and in the whole group of individuals (n=120).

	MBL [ng/mL]		*p*
	Vit D <30 ng/mL	Vit D >30 ng/mL	
Group of 42 patients	1528.93 ± 391.49 n=17	1398.11 ± 430.46 n=16	*0.824*
Group of 120 patients	2085.88 ± 277.38 n=31	2168.46 ± 415.46 n=57	*0.865*
	MBL [ng/mL]		*p*
	Vit D <20 ng/mL	Vit D >20 ng/mL	
Group of 42 patients	2709.24 ± 918.59 n=5	1232.82 ± 280.72 n=27	*0.060*
Group of 120 patients	2855.11 ± 513.16 n=21	1911.19 ± 252.19 n=66	*0.080*

Comparison between subgroups was performed by Student's unpaired *t*-test. Statistical significance was determined at the level of $p<0.05$.

results showing that growth hormone deficiency (non-compensated) is associated with vitamin D deficiency (33).

Results obtained in the present study suggest that the degree to which MBL is decreased in patients with hypopituitarism depends on whether the patients were on appropriate replacement therapies and on how many pituitary axes were involved (Figures 4, 5 and Table 2). Regarding the first point (*i.e.* appropriate vs. inappropriate hormone replacement therapies) it has been statistically confirmed (Figure 4) that patients with compensated hypopituitarism have higher mean and median MBL levels when compared to patients with non-compensated hypopituitarism. Because MBL level in compensated patients did not differ statistically from healthy individuals we can state that appropriate hormone replacement therapies improved substantially the functioning of the lectin pathway. In other words, hypopituitary patients on appropriate replacement therapies have the same (or being very close) functioning of the lectin pathway as healthy individuals.

The other mentioned above component which affects MBL level in our hypopituitary patients is the number of pituitary deficiencies. Although no statistically significant differences were found between MBL levels with relation to numbers of pituitary deficiencies, a tendency is seen to the decreased MBL levels with higher numbers of pituitary axes involved. The observation showing that MBL level decreases in patients with four pituitary deficiencies, being especially low in patients with panhypopituitarism, suggests that ACTH deficiency (usually being the fourth deficiency in gradually developing hypopituitarism) resulting in secondary adrenal insufficiency contributes strongly to weakening of the lectin pathway. It should also be mentioned that extremely low MBL level of 96.2 ng/mL was found in our patient with one isolated ACTH deficiency. In this context it can be recalled that the hypothalamic-pituitary-adrenal (HPA) axis is stimulated during the course of certain immune processes (21) and that glucocorticoids, secreted from the adrenal cortex, have pleiotropic (both immunoenhancing and immunosuppressive) effects on the immune system (34, 35), playing also a role in the immune system development (36). In turn, in large prospective study of hypopituitary patients significant increase in the mortality from respiratory infections was reported (13); It is not excluded that the lectin pathway is involved in this last phenomenon because low MBL levels were found to be associated with increased susceptibility to infections (37). Regarding the fifth deficiency, *i.e.* prolactin deficiency, the low efficiency of the lectin pathway (resulting in low MBL level) could be rather associated with severity of the disease such as panhypopituitarism than with low concentration of prolactin by itself. It should be recalled that physiological role of prolactin, except pregnancy and lactation, is not of great significance comparing to other pituitary hormones. However, it is worth mentioning that prolactin participates in the pathogenesis and activity of several autoimmune disorders (38), such as for example systemic lupus erythematosus (39). It should be also mentioned that the single highest values of MBL levels found in our patients with non-compensated hypopituitarism did relate to an individual with three pituitary deficiencies (5891.87 ng/mL) and to another individual with four pituitary deficiencies (4135.07 ng/mL), which is not easy to explain. One should realize that not only low MBL levels but also its higher concentrations may be associated with some pathological conditions as it was confirmed for example in acromegalic patients (9). It can be concluded that due to low number of our patients with particular pituitary deficiencies the current results do constitute the basis for future studies with larger population samples to confirm that high numbers of pituitary deficiencies contribute to lower effectiveness of the lectin pathway.

Because positive thyroid antibodies (similarly to other kind of antibodies) result from the weakening of the immune system and because the association was found between MBL gene polymorphisms and susceptibility to autoimmune thyroid diseases (40) we checked whether the prevalence of positive thyroid antibodies differs between particular groups and whether mean MBL levels differ in individuals with positive *versus* negative thyroid

antibodies. The prevalence of positive thyroid antibodies was relatively high, *i.e.* from 14.29% to 22.50%, which can be explained by relatively high age of individuals (41). However, it did not differ between subgroups; It should be especially stressed that very similar percentages of positive thyroid antibodies were found in control and hypopituitary individuals (14.29% vs. 14.81%). Regarding MBL level, no statistically significant differences were found between individuals with positive *versus* negative antibodies independent of the group considered. Both these observations suggest that the thyroid autoimmunity was not the leading causative factor of the decreased MBL level in our patients with hypopituitarism.

Although patients with hypopituitarism were older than control individuals, we did not find any correlation between MBL level and age in any group considered (Table 2). Additionally regarding the group of hypopituitary patients and also of patients with other pituitary diseases, mean age of patients with lowest concentrations of MBL (<500 ng/mL) did not differ (was very similar) from mean age of patients with higher levels of MBL (>500 ng/mL) (49.34 ± 4.44 vs. 50.92 ± 3.65 years). Concerning published studies, it is not documented that MBL level is associated with age (42). The only exception is our previous study in which negative correlation was observed between MBL level and age in a specific group of individuals *i.e.* women of reproductive age (8).

The current study has, of course, some limitations. The first one is that the groups considered were not well matched in terms of age, however we confirmed statistically that MBL level was not associated with age in any group considered and, what is of great importance, patients with MBL <500 ng/mL were not older than those with MBL >500 ng/mL. Also in the earlier mentioned study, the group of GH deficient patients and healthy individuals were unmatched (9). The next limitation is that the population sample was relatively small (*i.e.* 120 individuals with 42 patients diagnosed with hypopituitarism). However in studies published so far population samples examined were similarly not very large, comprising 30 healthy individuals, 25 GH-deficient patients, 23 acromegalic patients (9) or four different studies with total group of 108 patients with Turner syndrome and 99 control individuals (10). Another limitation relates to the fact that our patients were not diagnosed with the insulin tolerance test (being a gold standard) to confirm GH deficiency and that they were not treated with rhGH. At last it should be stressed that the only measured parameter of the lectin pathway was MBL concentration so we do not know if decreased MBL level in hypopituitary patients results from decreased formation of this component or its increased consumption. It is also unknown to what extent MBL concentrations are associated with MBL genotypes in particular individuals; as in humans MBL2 genotype is the most important factor affecting circulating MBL concentration (43), it would be valuable to analyze polymorphisms in the MBL2 gene in our patients. Unfortunately, we do not possess appropriate fractions such as the whole blood or frozen clotted blood samples to extract genomic DNA. Therefore at this moment it is impossible to check if MBL concentrations and MBL2 genotypes are distributed in a similar way in the particular groups that are compared, which does constitute a separate limitation.

Taking into account results published so far, MBL level can serve especially as a diagnostic marker (6–8, 44–46). Regarding the application of our current findings, the measurement of MBL level in patients with pituitary hormone deficiencies may be helpful in adjusting optimal doses of appropriate hormone replacement therapies.

According to our knowledge our study is the first one to demonstrate lower MBL level in adults with hypopituitarism of different degree when comparing not only to healthy individuals, but also to hypopituitary patients being on appropriate hormonal replacement therapies. Whether the decreased MBL level in hypopituitary patients reverses alongside replacement treatment remains to be confirmed in longitudinal studies. Additionally, to confirm that high numbers of pituitary deficiencies contribute to lower effectiveness of the lectin pathway larger population samples should be examined. Therefore further studies should be performed to explain direct association between lectin pathway of the complement system with particular pituitary deficiencies and with appropriate hormonal treatment.

Summarizing, hypopituitarism in adults is associated with impaired lectin pathway of the complement system as documented by lower mannan-binding lectin levels. As this phenomenon does not exist in patients with compensated hypopituitarism, it is highly probable that the decreased concentrations of mannan-binding lectin return to normal with the appropriate hormone replacement therapies. Therefore measurement of mannan-binding lectin level in patients with hypopituitarism may be considered as an additional factor helpful to optimize hormone replacement therapies. Additionally, if changes of other components of the lectin pathway are confirmed in hypopituitary patients this will further clarify immune mechanisms of unfavorable consequences of pituitary hormone deficiencies and, consequently, will broaden the knowledge in the field of a relationship between immune and endocrine systems.

Data availability statement

The raw data supporting the conclusions of this article will be made available by the authors, without undue reservation.

Ethics statement

The studies involving human participants were reviewed and approved by Ethical Committee of the Polish Mother's Memorial Hospital - Research Institute, Lodz, Poland (No. 47/2019, 87/2022). The patients/participants provided their written informed consent to participate in this study.

Author contributions

Conceptualization: MK-L and AEM; methodology: MK-L and AL; software: JS; validation: MK-L; formal analysis: AEM, JS; investigation: AEM; writing—original draft preparation: AEM; writing—review and

editing: MK-L; visualization: JS; supervision: MK-L and AL. All authors contributed to the article and approved the submitted version.

Funding

This study was financially supported by statutory funds from the Medical University of Lodz, Lodz, Poland (Project No. 503/1-168-01/503-11-001-19-00 and 503/1-107-03/503-11-001-19-00).

Acknowledgments

The part of the studies, i.e. MBL measurements, was carried out at the Research Laboratory CoreLab of the Medical University of Lodz.

Conflict of interest

The authors declare that the research was conducted in the absence of any commercial or financial relationships that could be construed as a potential conflict of interest.

Publisher's note

All claims expressed in this article are solely those of the authors and do not necessarily represent those of their affiliated organizations, or those of the publisher, the editors and the reviewers. Any product that may be evaluated in this article, or claim that may be made by its manufacturer, is not guaranteed or endorsed by the publisher.

References

1. Turner MW. The role of mannose-binding lectin in health and disease. *Mol Immunol* (2003) 40:423–9. doi: 10.1016/S0161-5890(03)00155-X

2. Garred P, Genster N, Pilely K, Bayarri-Olmos R, Rosbjerg A, Ma YJ, et al. A journey through the lectin pathway of complement-MBL and beyond. *Immunol Rev* (2016) 274:74–97. doi: 10.1111/imr.12468

3. Gil E, Noursadeghi M, Brown JS. Streptococcus pneumoniae interactions with the complement system. *Front Cell Infect Microbiol* (2022) 12:929483. doi: 10.3389/fcimb.2022.929483

4. Zhang J, Chen N, Chen Z, Liu Y, Zheng K, Qiu Y, et al. Low mannose binding lectin, but not l-ficolin, is associated with spontaneous clearance of hepatitis c virus after infection. *Front Immunol* (2020) 11:587669. doi: 10.3389/fimmu.2020.587669

5. Devalaraja-Narashimha K, Ehmann PJ, Huang C, Ruan Q, Wipperman MF, Kaplan T, et al. Association of complement pathways with COVID-19 severity and outcomes. *Microbes Infect* (2022) 6:105081. doi: 10.1016/j.micinf.2022.105081

6. Potlukova E, Jiskra J, Freiberger T, Limanova Z, Zivorova D, Malickova K, et al. The production of mannan-binding lectin is dependent upon thyroid hormones regardless of the genotype: a cohort study of 95 patients with autoimmune thyroid disorders. *Clin Immunol* (2010) 136:123–9. doi: 10.1016/j.clim.2010.02.015

7. Riis AL, Hansen TK, Thiel S, Gravholt CH, Gjedde S, Gormsen LC, et al. Thyroid hormone increases mannan-binding lectin levels. *Eur J Endocrinol* (2005) 153:643–9. doi: 10.1530/eje.1.02013

8. Karbownik-Lewinska M, Stepniak J, Marcinkowska M, Krygier A, Lewinski A. High normal TSH is associated with lower mannan-binding lectin in women of childbearing age. *BMC Endocr Disord* (2020) 20:1. doi: 10.1186/s12902-019-0484-y

9. Hansen TK, Thiel S, Dall R, Rosenfalck AM, Trainer P, Flyvbjerg A, et al. GH strongly affects serum concentrations of mannan-binding lectin: evidence for a new IGF-I independent immunomodulatory effect of GH. *J Clin Endocrinol Metab* (2001) 86:5383–8. doi: 10.1210/jcem.86.11.8009

10. Gravholt CH, Leth-Larsen R, Lauridsen AL, Thiel S, Hansen TK, Holmskov U, et al. The effects of GH and hormone replacement therapy on serum concentrations of mannan-binding lectin, surfactant protein d and vitamin d binding protein in turner syndrome. *Eur J Endocrinol* (2004) 150:355–62. doi: 10.1530/eje.0.1500355

11. Sørensen CM, Hansen TK, Steffensen R, Jensenius JC, Thiel S. Hormonal regulation of mannan-binding lectin synthesis in hepatocytes. *Clin Exp Immunol* (2006) 145:173–82. doi: 10.1111/j.1365-2249.2006.03101.x

12. Fleseriu M, Hashim IA, Karavitaki N, Melmed S, Murad MH, Salvatori R. Samuels MH hormonal replacement in hypopituitarism in adults: an endocrine society clinical practice guideline. *J Clin Endocrinol Metab* (2016) 101:3888–921. doi: 10.1210/jc.2016-2118

13. Tomlinson JW, Holden N, Hills RK, Wheatley K, Clayton RN, Bates AS, et al. Association between premature mortality and hypopituitarism. West Midlands prospective hypopituitary study group. *Lancet* (2001) 357:425–31. doi: 10.1016/S0140-6736(00)04006-X

14. Jasim S, Alahdab F, Ahmed AT, Tamhane S, Prokop LJ, Nippoldt TB, et al. Mortality in adults with hypopituitarism: a systematic review and meta-analysis. *Endocrine* (2017) 56:33–42. doi: 10.1007/s12020-016-1159-3

15. Dineen R, Martin-Grace J, Thompson CJ, Sherlock M. The management of glucocorticoid deficiency: current and future perspectives. *Clin Chim Acta* (2020) 505:148–59. doi: 10.1016/j.cca.2020.03.006

16. Lewiński A, Smyczyńska J, Stawerska R, Hilczer M, Stasiak M, Bednarczuk T, et al. National program of severe growth hormone deficiency treatment in adults and adolescents after completion of growth promoting therapy. *Endokrynol Pol* (2018) 69:468–524. doi: 10.5603/EP.a2018.0054

17. Kim SY. Diagnosis and treatment of hypopituitarism. *Endocrinol Metab (Seoul)* (2015) 30:443–55. doi: 10.3803/EnM.2015.30.4.443

18. Giustina A, Mazziotti G, Canalis E. Growth hormone, insulin-like growth factors, and the skeleton. *Endocr Rev* (2008) 29:535–59. doi: 10.1210/er.2007-0036

19. Bidlingmaier M, Strasburger CJ. Growth hormone. *Handb Exp Pharmacol* (2010) 195:187–200. doi: 10.1007/978-3-540-79088-4_8

20. Averyanova M, Vishnyakova P, Yureneva S, Yakushevskaya O, Fatkhudinov T, Elchaninov A, et al. Sex hormones and immune system: menopausal hormone therapy in the context of COVID-19 pandemic. *Front Immunol* (2022) 13:928171. doi: 10.3389/fimmu.2022.928171

21. Besedovsky HO, del Rey A, Klusman I, Furukawa H, Monge Arditi G, Kabiersch A. Cytokines as modulators of the hypothalamus-pituitary-adrenal axis. *J Steroid Biochem Mol Biol* (1991) 40:613–8. doi: 10.1016/0960-0760(91)90284-C

22. Valentino R, Savastano S, Tommaselli AP, Riccio A, Mariniello P, Pronesti G, et al. Hormonal pattern in women affected by rheumatoid arthritis. *J Endocrinol Invest* (1993) 16:619–24. doi: 10.1007/BF03347683

23. Rey AD, Mahuad CV, Bozza VV, Bogue C, Farroni MA, Bay ML, et al. Endocrine and cytokine responses in humans with pulmonary tuberculosis. *Brain Behav Immun* (2007) 21:171–9. doi: 10.1016/j.bbi.2006.06.005

24. Karbownik-Lewinska M, Kokoszko A, Lewandowski KC, Shalet SM, Lewinski A. GH replacement reduces increased lipid peroxidation in GH-deficient adults. *Clin Endocrinol (Oxf)* (2008) 68:957–64. doi: 10.1111/j.1365-2265.2007.03142.x

25. Giovannini L, Tirabassi G, Muscogiuri G, Di Somma C, Colao A, Balercia G. Impact of adult growth hormone deficiency on metabolic profile and cardiovascular risk [Review]. *Endocr J* (2015) 62:1037–48. doi: 10.1507/endocrj.EJ15-0337

26. O'Brien T, Dinneen SF, O'Brien PC, Palumbo PJ. Hyperlipidemia in patients with primary and secondary hypothyroidism. *Mayo Clin Proc* (1993) 68:860–6. doi: 10.1016/S0025-6196(12)60694-6

27. Karbownik-Lewińska M, Stępniak J, Żurawska A, Lewiński A. Less favorable lipid profile and higher prevalence of thyroid antibodies in women of reproductive age with high-normal TSH-retrospective study. *Int J Environ Res Public Health* (2020) 17:2122. doi: 10.3390/ijerph17062122

28. Karbownik-Lewinska M, Marcinkowska M, Stepniak J, Lewinski A. TSH ≥2.5 mIU/l is associated with the increased oxidative damage to membrane lipids in women of childbearing age with normal thyroid tests. *Horm Metab Res* (2017) 49:321–6. doi: 10.1055/s-0042-120712

29. Karbownik-Lewińska M, Stępniak J, Lewiński A. Potential risk factors for isolated hypothyroxinemia in women of childbearing age-results from retrospective analysis. *J Clin Med* (2021) 10:5384. doi: 10.3390/jcm10225384

30. Zhao R, Zhang W, Ma C, Zhao Y, Xiong R, Wang H, et al. Immunomodulatory function of vitamin d and its role in autoimmune thyroid disease. *Front Immunol* (2021) 12:574967. doi: 10.3389/fimmu.2021.574967

31. Durrant LR, Bucca G, Hesketh A, Möller-Levet C, Tripkovic L, Wu H, et al. Vitamins D2 and D3 have overlapping but different effects on the human immune system revealed through analysis of the blood transcriptome. *Front Immunol* (2022) 13:790444. doi: 10.3389/fimmu.2022.790444

32. Ismailova A, White JH. Vitamin d, infections and immunity. *Rev Endocr Metab Disord* (2022) 23:265–77. doi: 10.1007/s11154-021-09679-5

33. Savanelli MC, Scarano E, Muscogiuri G, Barrea L, Vuolo L, Rubino M, et al. Cardiovascular risk in adult hypopituitaric patients with growth hormone deficiency: is there a role for vitamin d? *Endocrine* (2016) 52:111–9. doi: 10.1007/s12020-015-0779-3

34. Cain DW, Cidlowski JA. Immune regulation by glucocorticoids. *Nat Rev Immunol* (2017) 17:233–47. doi: 10.1038/nri.2017.1

35. Shimba A, Ejima A, Ikuta K. Pleiotropic effects of glucocorticoids on the immune system in circadian rhythm and stress. *Front Immunol* (2021) 12:706951. doi: 10.3389/fimmu.2021.706951

36. Quatrini L, Ricci B, Ciancaglini C, Tumino N, Moretta L. Regulation of the immune system development by glucocorticoids and sex hormones. *Front Immunol* (2021) 12:672853. doi: 10.3389/fimmu.2021.672853

37. Dommett RM, Klein N, Turner MW. Mannose-binding lectin in innate immunity: past, present and future. *Tissue Antigens* (2006) 68:193–209. doi: 10.1111/j.1399-0039.2006.00649.x

38. Borba VV, Zandman-Goddard G, Shoenfeld Y. Prolactin and autoimmunity. *Front Immunol* (2018) 9:73. doi: 10.3389/fimmu.2018.00073

39. Carreón-Talavera R, Santana-Sánchez P, Fuentes-Pananá EM, Legorreta-Haquet MV, Chávez-Sánchez L, Gorocica-Rosete PS, et al. Prolactin promotes proliferation of germinal center b cells, formation of plasma cells, and elevated levels of IgG3 anti-dsDNA autoantibodies. *Front Immunol* (2022) 13:1017115. doi: 10.3389/fimmu.2022.1017115

40. Xu J, Suo L, Zhao J, Cai T, Mei N, Du P, et al. MBL2 polymorphism may be a protective factor of autoimmune thyroid disease susceptibility. *Mol Genet Genomics* (2022) 298:95–105. doi: 10.1007/s00438-022-01960-9

41. Pinchera A, Mariotti S, Barbesino G, Bechi R, Sansoni P, Fagiolo U, et al. Thyroid autoimmunity and ageing. *Horm Res* (1995) 43:64–8. doi: 10.1159/000184239

42. Barton JC, Barton JC, Bertoli LF. Clinical and laboratory associations of mannose-binding lectin in 219 adults with IgG subclass deficiency. *BMC Immunol* (2019) 20:15. doi: 10.1186/s12865-019-0296-x

43. Garred P, Larsen F, Seyfarth J, Fujita R, Madsen HO. Mannose-binding lectin and its genetic variants. *Genes Immun* (2006) 7:85–94. doi: 10.1038/sj.gene.6364283

44. Rizk DV, Maillard N, Julian BA, Knoppova B, Green TJ, Novak J, et al. The emerging role of complement proteins as a target for therapy of IgA nephropathy. *Front Immunol* (2019) 10:504. doi: 10.3389/fimmu.2019.00504

45. So BYF, Chan GCW, Yap DYH, Chan TM. The role of the complement system in primary membranous nephropathy: a narrative review in the era of new therapeutic targets. *Front Immunol* (2022) 13:1009864. doi: 10.3389/fimmu.2022.1009864

46. Belmonte B, Mangogna A, Gulino A, Cancila V, Morello G, Agostinis C, et al. Distinct roles of classical and lectin pathways of complement in preeclamptic placentae. *Front Immunol* (2022) 13:882298. doi: 10.3389/fimmu.2022.882298

frontiers | Frontiers in Immunology

TYPE Original Research
PUBLISHED 25 October 2023
DOI 10.3389/fimmu.2023.1206409

Check for updates

OPEN ACCESS

EDITED BY
Erik J. M. Toonen,
Hycult Biotech, Netherlands

REVIEWED BY
Agnes Szilagyi,
Semmelweis University, Hungary
Christoph Licht,
University of Toronto, Canada

*CORRESPONDENCE
Lambertus P. van den Heuvel
bert.vandenheuvel@radboudumc.nl

†These authors have contributed equally to this work and share last authorship

RECEIVED 15 April 2023
ACCEPTED 03 October 2023
PUBLISHED 25 October 2023

CITATION
Stevens KH, Baas LM, van der Velden TJAM, Bouwmeester RN, van Dillen N, Dorresteijn EM, van Zuilen AD, Wetzels JFM, Michels MAHM, van de Kar NCAJ and van den Heuvel LP (2023) Modeling complement activation on human glomerular microvascular endothelial cells. *Front. Immunol.* 14:1206409. doi: 10.3389/fimmu.2023.1206409

COPYRIGHT
© 2023 Stevens, Baas, van der Velden, Bouwmeester, van Dillen, Dorresteijn, van Zuilen, Wetzels, Michels, van de Kar and van den Heuvel. This is an open-access article distributed under the terms of the Creative Commons Attribution License (CC BY). The use, distribution or reproduction in other forums is permitted, provided the original author(s) and the copyright owner(s) are credited and that the original publication in this journal is cited, in accordance with accepted academic practice. No use, distribution or reproduction is permitted which does not comply with these terms.

Modeling complement activation on human glomerular microvascular endothelial cells

Kes H. Stevens[1], Laura M. Baas[1], Thea J. A. M. van der Velden[1], Romy N. Bouwmeester[1], Niels van Dillen[1], Eiske M. Dorresteijn[2], Arjan D. van Zuilen[3], Jack F. M. Wetzels[4], Marloes A. H. M. Michels[1,5], Nicole C. A. J. van de Kar[1†] and Lambertus P. van den Heuvel[1,5,6,7*†]

[1]Department of Pediatric Nephrology, Amalia Children's Hospital, Radboud University Medical Center, Nijmegen, Netherlands, [2]Department of Pediatric Nephrology, Sophia Children's Hospital, Erasmus Medical Center, Rotterdam, Netherlands, [3]Department of Nephrology and Hypertension, University Medical Center Utrecht, Utrecht, Netherlands, [4]Department of Nephrology, Radboud University Medical Center, Nijmegen, Netherlands, [5]Department of Laboratory Medicine, Radboud University Medical Center, Nijmegen, Netherlands, [6]Department of Pediatrics/Pediatric Nephrology, University Hospitals Leuven, Leuven, Belgium, [7]Department of Development and Regeneration, University Hospitals Leuven, Leuven, Belgium

Introduction: Atypical hemolytic uremic syndrome (aHUS) is a rare kidney disease caused by dysregulation of the complement alternative pathway. The complement dysregulation specifically leads to damage to the glomerular endothelium. To further understand aHUS pathophysiology, we validated an *ex vivo* model for measuring complement deposition on both control and patient human glomerular microvascular endothelial cells (GMVECs).

Methods: Endothelial cells were incubated with human test sera and stained with an anti-C5b-9 antibody to visualize and quantify complement depositions on the cells with immunofluorescence microscopy.

Results: First, we showed that zymosan-activated sera resulted in increased endothelial C5b-9 depositions compared to normal human serum (NHS). The levels of C5b-9 depositions were similar between conditionally immortalized (ci) GMVECs and primary control GMVECs. The protocol with ciGMVECs was further validated and we additionally generated ciGMVECs from an aHUS patient. The increased C5b-9 deposition on control ciGMVECs by zymosan-activated serum could be dose-dependently inhibited by adding the C5 inhibitor eculizumab. Next, sera from five aHUS patients were tested on control ciGMVECs. Sera from acute disease phases of all patients showed increased endothelial C5b-9 deposition levels compared to NHS. The remission samples showed normalized C5b-9 depositions, whether remission was reached with or without complement blockage by eculizumab. We also monitored the glomerular endothelial complement deposition of an aHUS patient with a hybrid *complement factor H (CFH)/CFH-related 1* gene during follow-up. This patient had already chronic kidney failure and an ongoing deterioration of kidney function despite absence of markers indicating an aHUS flare. Increased C5b-9 depositions on ciGMVECs were observed in all samples obtained throughout different diseases phases, except for the samples with eculizumab levels above

target. We then tested the samples on the patient's own ciGMVECs. The C5b-9 deposition pattern was comparable and these aHUS patient ciGMVECs also responded similar to NHS as control ciGMVECs.

Discussion: In conclusion, we demonstrate a robust and reliable model to adequately measure C5b-9-based complement deposition on human control and patient ciGMVECs. This model can be used to study the pathophysiological mechanisms of aHUS or other diseases associated with endothelial complement activation *ex vivo*.

KEYWORDS

alternative pathway, atypical hemolytic uremic syndrome, C5b-9, complement system, eculizumab, glomerular endothelium

1 Introduction

Atypical hemolytic uremic syndrome (aHUS) is a rare but severe kidney disease belonging to the group of thrombotic microangiopathies (TMA) and is characterized by mechanical hemolytic anemia, thrombocytopenia and acute kidney injury (AKI) (1, 2). The damage to the glomerular endothelium is caused by a dysregulation of the alternative pathway (AP) of the complement system. Before the introduction of the complement inhibitor eculizumab, around 50% of the aHUS patients progressed into end-stage kidney failure, and mortality rates up to 25% in the acute phase were reported (3–8). With eculizumab, a humanized monoclonal antibody targeting C5, morbidity and mortality rates have significantly improved (9, 10).

The complement system is a powerful tool of the innate immune system to eliminate pathogens and apoptotic/necrotic host cells. The system can be initiated via three different pathways: the classical pathway, lectin pathway, and AP (11–13). In contrast to the classical and lectin pathway, the AP is constitutively active at a low level by a process called 'tick-over'. This results in low levels of active C3, able to form C3 convertases that cleave C3 into C3a and C3b. C3b is an important opsonin, but also supports subsequent formation of C5 convertases that cleave C5 into C5a and C5b. C5a is a powerful chemoattractant, and C5b supports formation of the C5b-9 complex, also known as the membrane attack complex. C5b-9 formation on the cell leads to impaired membrane integrity and serious cell damage (14). Therefore, the complement system, and especially the AP, is strictly regulated in physiological state to prevent host cell damage.

In up to 75% of the aHUS patients, genetic variants in genes encoding complement components are found (15–18). The most common are loss-of-function mutations in genes encoding for the complement regulatory proteins factor H (FH), factor I and membrane-cofactor protein (MCP), and gain-of-function mutations in complement C3 and factor B. In addition, genomic rearrangements in the *complement FH (CFH)* and *CFH related (CFHR) 1-5* region have been described, resulting in hybrid FH-FHR proteins which may interfere with normal complement regulation (19, 20). Furthermore, autoantibodies against FH may impair the homeostatic complement regulation and lead to aHUS (21). The disease penetrance of aHUS in mutation carriers is incomplete. Various triggering factors, such as infections, pregnancy, and/or certain medications, can elicit the development of aHUS (17, 22, 23).

Especially the kidneys are vulnerable for complement deposition and the subsequent TMA-mediated injury (24, 25). The glomerular microvascular endothelial cells (GMVECs) are the primary target of AP activation in aHUS, but the exact mechanisms behind this high susceptibility of GMVECs to complement deposition remains unknown. A possible explanation might be their morphological (fenestration) and functional (filtration) difference compared to other endothelial cells (25, 26).

Nonetheless, in the last decade, other endothelial cell types than GMVECs have frequently been used to study complement activation and deposition in patients with complement-mediated kidney diseases. For example, human dermal microvascular endothelial cells 1 (HMECs-1) (27–31) and human umbilical vein endothelial cells (HUVECs) (32–34) have been described as cell models for aHUS. However, these cells might not optimally reflect the *in vivo* situation, given the specific glomerular cell vulnerability in aHUS. Therefore, the aim of this study was to model complement activation in aHUS patients *ex vivo*, by measuring complement deposition on human conditionally immortalized GMVECs (ciGMVECs). Moreover, by having the unique possibility to

Abbreviations: aHUS, atypical hemolytic uremic syndrome; AKI, acute kidney injury; AP, alternative pathway; BSA, bovine serum albumin; *CFH, complement factor H*; *CFHR, complement factor H related*; ci, conditionally immortalized; DAPI, 4', 6-diamidino-2-phenylindole; ELISA, enzyme-linked immunosorbent assay; FCS, fetal calf serum; GMVECs, glomerular microvascular endothelial cells; FH, factor H; HBSS++, Hanks' Balanced Salt solution containing calcium and magnesium; HI-NHS, heat inactivated normal human serum; HMECs-1, Human dermal microvascular endothelial cells; HUVECs, human umbilical vein endothelial cells; LDH, lactate dehydrogenase; MCP, membrane-cofactor protein; NHS, normal human serum; PBS, phosphate buffered saline; TMA, thrombotic microangiopathy; UPCR, urine protein-to-creatinine ratio.

create a ciGMVEC line derived from an aHUS patient, we could model the complement activation in samples of an aHUS patient on patient's own endothelial cells.

2 Materials and methods

2.1 Ethics

Written informed consent was obtained from all aHUS patients or their legal guardians, and from all healthy controls of whom blood samples were used in this study. Informed consent was also obtained for isolating GMVECs from an aHUS patient (P1) who had bilateral nephrectomy in preparation to kidney transplantation. The study was performed in accordance with the appropriate version of the Declaration of Helsinki.

2.2 aHUS patients

Six patients diagnosed with aHUS were included in this study and were genetically characterized (Table 1). P1 was identified with a heterozygous deletion of *CFH* exon 22, *CFHR3* and *CFHR1* exon 1-5, indicating a genomic rearrangement resulting in a *CFH/CFHR1* hybrid gene (35). This rearrangement has been described to lead to a severe aHUS phenotype (36). P2 and P4-P6 carried a pathogenic *C3* variant, i.e. c.481C>T (p.Arg161Trp), resulting in decreased binding to FH and MCP, and increased binding to complement factor B, leading to a C3 convertase with increased activity (34, 37, 38). In P3, a homozygous *CFHR3-1* deletion was found in combination with autoantibodies against FH (39–41). P3 (P4 in Bouwmeester et al.), P4 (P12 in Bouwmeester et al.), and P5 (P18 in Bouwmeester et al.) were described in the CUREiHUS study (18). All patients were treated according to a restrictive eculizumab protocol, as described in the CUREiHUS study (18, 43).

P1 is known with aHUS from the age of 5 months and treated until the age of 11 years with chronic plasma therapy. He then was successfully switched to treatment with eculizumab. At the age of 15 years a further deterioration of his kidney function was observed without any signs of recurrence of aHUS. His radiographic examinations revealed an acquired glomerulocystic disease, a reduced left kidney function, and an abnormal venous system of unknown origin. A bilateral nephrectomy was performed to minimize the risk for aHUS recurrence after kidney transplantation. The blood taken at the age of 15 years and used in this study was marked as day 0 (d0). The medical history of this aHUS patient (P1) was in depth studied and reported previously (36).

TMA was defined by ≥2 of the following criteria: thrombocytopenia (platelet count <150 $\times 10^9$/l), lactate dehydrogenase (LDH) above the upper limit of normal (>250 U/l) and low/undetectable haptoglobin (<0.3 mg/l). AKI was defined as an increase in serum creatinine of ≥26.53 µmol/l (0.3 mg/dl) in 48 hours or ≥1.5 times baseline in <7 days.

2.3 Cell culture

GMVECs of P1 were isolated from kidney tissue obtained after nephrectomy and subsequently conditionally immortalized as described by Satchell et al. (44). Control ciGMVECs (obtained from Satchell et al. (44)) and P1 ciGMVECs were allowed to proliferate by culturing them at 33°C with 5% (v/v) CO_2 on 96-well plates (655090, Greiner, Cellstar®) coated with gelatin (48720, FLUKA). When confluent, cells were transferred to 37°C with 5% (v/v) CO_2 to induce growth arrest. After 7-8 days, cells were used for experiments. The growth medium, later referred to as endothelial medium, consisted of M199 medium (22340, Gibco) supplemented with 10% (v/v) heat-inactivated (HI) human serum (ISER, Innovative research), 10% (v/v) HI newborn calf serum (26010, Gibco), 2 mM L-glutamine (25030, Gibco), 100 U/ml penicillin, 100 mg/ml streptomycin (15140, Gibco), 5 U/ml heparin (Leo Pharmaceuticals), and 150 µg/ml bovine endothelial growth factor made according to the protocol described by Maciag et al. (45).

Primary GMVECs from human origin were obtained from kidney tissue after nephrectomy and cultured as previously described (46). Primary GMVECs were cultured at 37°C with 5% (v/v) CO_2 on gelatin-coated 96-well plates with endothelial medium until confluent.

TABLE 1 Genetics of atypical hemolytic uremic syndrome (aHUS) patients.

Patient	Gene	cDNA change	Protein change	Zygosity	Class[a]	FH autoantibodies	References
P1	*CFH-CFHR1* hybrid[b]			Heterozygous		Negative	(35, 36)
P2	*C3*	c.481C>T	p.Arg161Trp	Heterozygous	5	Negative	(34, 37, 38)
P3	*CFHR3-1* deletion			Homozygous	2	Positive	(39–41)
P4	*C3*	c.481C>T	p.Arg161Trp	Heterozygous	5	Negative	(34, 37, 38)
P5	*C3*	c.481C>T	p.Arg161Trp	Heterozygous	5	Negative	(34, 37, 38)
P6	*C3*	c.481C>T	p.Arg161Trp	Heterozygous	5	Negative	(34, 37, 38)

[a]Classification based on guidelines of the American College of Medical and Genomics (42) as benign (class 1), likely benign (class 2), uncertain significance (class 3), likely pathogenic (class 4), and pathogenic (class 5).
[b]Genomic analysis using multiplex ligation-dependent probe amplification identified a heterozygous deletion of *CFH* (LRG_47t1) exon 22, complete *CFHR3* (LRG_175t1) and CFHR1 (LRG_149t1) exon 1-5, indicating a genomic rearrangement resulting in a *CFH/CFHR1* hybrid gene (NC_000001.10: g.(196715167_196716320)_(196799888_196801005)del).
CFH, complement factor H; CFHR, complement factor H related.

HMECs-1 (ATCC® CRL3243™) were cultured at 37°C with 5% (v/v) CO_2 on uncoated 96-well plates with MCDB 131 medium (10372, Gibco) supplemented with 50 µg/ml bovine endothelial growth factor, 10% (v/v) fetal calf serum (FCS; 10270, Gibco), 2 mM L-glutamine, 1 µg/ml hydrocortisone (H0888, Sigma-Aldrich), 100 U/ml penicillin, and 100 mg/ml streptomycin.

2.4 Sample collection and sample preparation

Blood samples of aHUS patients and healthy individuals were collected and processed as described previously (47). Pooled normal human serum (NHS) was obtained by pooling 10 or 14 healthy individual samples. To obtain HI-NHS, NHS was incubated for 30 minutes at 56°C. Samples were aliquoted and stored at -80°C until use.

Serum samples were thawed on ice and diluted to the desired serum concentration in Hanks' balanced salt solution containing calcium and magnesium (HBSS++, 14025; Gibco) supplemented with 0.5% (w/v) bovine serum albumin (BSA; 820451, Millipore), later referred to as test medium. Where indicated, sera were pre-incubated for 5-10 minutes at room temperature with 300 µg/ml of the C5 blocker eculizumab (Soliris®, Alexion Pharmaceuticals) and/or 0.3 mg/ml zymosan (Z4250, Sigma-Aldrich). Zymosan was pre-diluted in magnesium-ethylene glycol tetra acetic acid buffer (Mg-EGTA; 2.03 mM veronal buffer, pH 7.4, 10 mM EGTA, 7 mM $MgCl_2$, 0.083% gelatin, 115 D-glucose, and 60 mM NaCl). Eculizumab and zymosan concentrations are indicated per volume of undiluted serum.

2.5 Complement deposition and immunofluorescence staining

Cells cultured on 96-well plates were washed twice with test medium and pre-incubated with test medium for 15 minutes at 37°C with 5% (v/v) CO_2. Next, cells were incubated with 33.3% serum in test medium with a final volume of 140 µl at 37°C with 5% (v/v) CO_2 for 2 hours, unless stated otherwise. After incubation, cells were washed twice with HBSS++, fixed with 3% paraformaldehyde/phosphate buffered saline (PBS; 10010, Gibco) for 10 minutes, and washed twice with PBS.

For immunofluorescence staining, cells were first blocked with 2% (w/v) BSA/PBS for 1 hour. Then, cells were stained with mouse anti-CD31 (1:100, 555444, BD Pharmingen) and/or rabbit anti-C5b-9 (1:200; 204903, Calbiochem), diluted in 1% (w/v) BSA/PBS with 10% (v/v) goat serum (ab7481, Abcam), for 1 hour. After washing three times, cells were incubated with the secondary antibodies (1:1000 in 1% BSA/PBS) Alexa488-conjugated goat anti-rabbit (A11008, Invitrogen), Alexa568-conjugated goat anti-mouse (ab175473, Abcam), and/or FITC-conjugated rabbit anti-C3c (1:20; F0201, Dako; recognizes the C3c part of C3, C3b and iC3b), for 1 hour. Cell nuclei were additionally stained with 5 µg/ml 4', 6-diamidino-2-phenylindole (DAPI; D1306, Invitrogen) for 5 minutes. All steps were performed with static conditions at room temperature. Images were captured with Zeiss Axio Observer 7 with artificial intelligence sample finder in combination with ZEN imaging software (Zeiss).

2.6 Quantification of C5b-9 deposition

For the quantification of C5b-9 depositions, an area of 4 mm^2 of each well was visualized, with focusing on DAPI and with equal visualization settings for all experiments. Fluorescence images were analyzed utilizing Fiji 1.51n software with a custom-made ImageJ macro to quantify C5b-9 (48).

2.7 Flow cytometry

Control ciGMVECs in 24-well plates (3524, Costar®, Corning Incorporated) were washed twice with test medium and subsequently incubated with 10% (v/v) serum in test medium with a final volume of 280 µl at 37°C with 5% (v/v) CO_2 for 1 hour. Next, cells were washed twice with HBSS++ and fixed with 0.5% paraformaldehyde/PBS for 15 minutes. After fixation, cells were stained with rabbit anti-C5b-9 (1:100) in 0.1% (v/v) BSA/PBS at 4°C for 30 minutes. After three washes with PBS, cells were incubated with Alexa488-conjugated goat anti-rabbit (1:100) at 4°C for 30 minutes. Cells were detached with 0.05% trypsin-ethylenediamine tetra acetic acid (25300, Gibco) and dissolved in 10% (v/v) FCS/PBS. Cells were spun down and resuspended in 0.1% (v/v) BSA/PBS. C5b-9 deposition was quantified using a CytoFLEX flow cytometer (Beckman Coulter) and results were analyzed with Kaluza 2.1.3 software (Beckman Coulter).

2.8 Collection of clinical data and standard laboratory measurement

Clinical and standard laboratory data were obtained from patients' electronic medical records. Serum C5 levels were measured with enzyme-linked immunosorbent assay (ELISA) as described previously (49). Patients were tested for autoantibodies against FH using an in-house ELISA (50).

2.9 Statistical analysis

Data are expressed as mean ± standard deviation. All statistical analyses were performed with GraphPad Prism version 9.0.0 for Windows (GraphPad Software, San Diego, California, USA). Data were analyzed by unpaired t-test, one-way ANOVA, or two-way ANOVA, followed by *post-hoc* analysis as indicated in figure legends. A p-value (P) of <0.05 was considered as statistically significant.

3 Results

3.1 Comparing complement C5b-9 deposition on glomerular endothelial cells

Human endothelial cell types from different origin have been used previously to model complement deposition *ex vivo*. We focused on studying complement activation on glomerular endothelial cells as these are the primary target in aHUS. Therefore, we first compared the performance of primary GMVECs with ciGMVECs as cellular models for complement activation *ex vivo*, by investigating the endothelial C5b-9 deposition upon incubation with NHS and zymosan-stimulated NHS. A baseline level of C5b-9 deposition was observed for both primary control GMVECs and control ciGMVECs upon incubation with NHS (Figures 1A, B). The amount of depositions significantly increased when the cells were incubated with NHS supplemented with zymosan to simulate an activated complement system (Figures 1A, B). Similar results were seen for the HMECs-1 (Supplementary Figures 1A, B), which is the most frequently described cellular model for aHUS (27–31), thereby further validating our results on the glomerular endothelial cell model.

To determine the discriminatory power between baseline C5b-9 deposition (NHS) and the C5b-9 level after incubation with activated complement (NHS-zymosan), the fold change of NHS-zymosan to NHS was calculated for primary GMVECs and ciGMVECs (Figure 1C). No significant difference was measured. We continued with validating ciGMVECs as a model for complement activation on the glomerular endothelial surface.

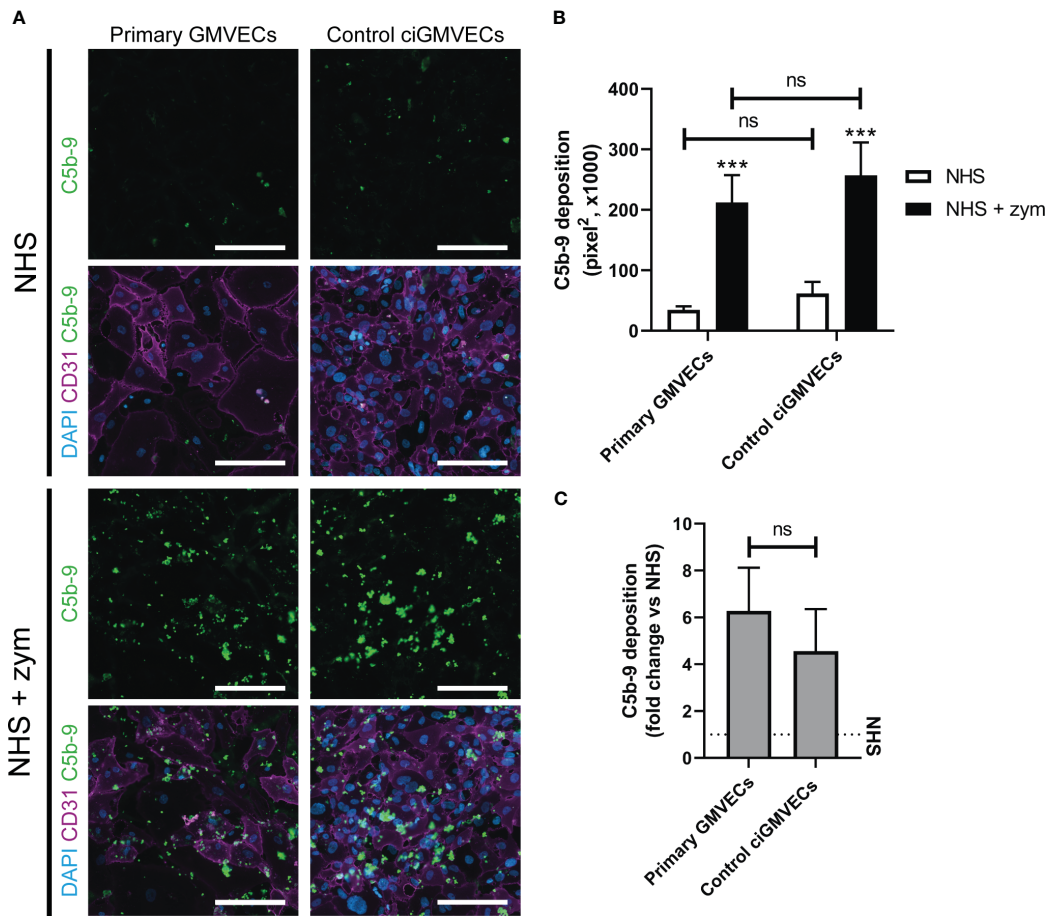

FIGURE 1
Serum-induced C5b-9 deposition on primary glomerular microvascular endothelial cells (GMVECs) and conditionally immortalized GMVECs (ciGMVECs). **(A-C)** Primary GMVECs and control ciGMVECs, from human origin, after incubation with 33.3% serum in test medium for 2 hours. **(A)** Representative immunofluorescence images of C5b-9 (green), CD31 (purple) and cell nuclei with 4', 6-diamidino-2-phenylindole (DAPI; blue) after incubation with normal human serum (NHS) and NHS-zymosan (zym). Scale bar: 200 µm. **(B, C)** Quantification of C5b-9 deposition in pixel^2 after serum incubation with NHS and NHS-zym **(B)** and as fold change of NHS-zym versus NHS **(C)**. Data are presented as mean ± standard deviation of three donors for primary GMVECs and nine independent experiments for control ciGMVECs. Experiments were performed with at least two replicates per condition. **(B)** Not significant (ns), ***P < 0.001, using two-way ANOVA followed by Tukey's multiple comparisons test. **(C)** Not significant (ns), using unpaired t-test.

10.3389/fimmu.2023.1206409

3.2 Human ciGMVECs as a model to adequately measure complement-mediated C5b-9 deposition

To determine if we could adequately and reliably measure complement-mediated C5b-9 deposition on the ciGMVECs, we visualized and quantified C5b-9 on the ciGMVECs upon incubation with different test sera in which complement was activated or blocked.

First, we showed that incubation of ciGMVECs with either HI-NHS or NHS supplemented with eculizumab resulted in decreased C5b-9 depositions compared to NHS (Figures 2A, B). The increase in C5b-9 deposition after incubation with NHS-zymosan could also be inhibited when serum was first treated with eculizumab (Figures 2A, B). With flow cytometry as an alternative method for C5b-9 quantification we further confirmed our microscope imaging findings for ciGMVECs (Supplementary Figure 2). In line with the C5b-9 deposition, we showed that the deposition of C3 was increased upon incubation with NHS-zymosan (Supplementary Figure 3). Together, these results indicate that the generation of C5b-9 on the endothelial surface was complement-mediated. Incubation of ciGMVECs with serum of aHUS P1 resulted in increased C5b-9 deposition compared to NHS (Figures 2A, B). No significant differences in the C5b-9 deposition levels were observed between 1-, 2- or 3-hour serum incubations (Supplementary Figure 4). Two-hour incubation with serum was used as the standard method for further experiments.

Next, we titrated eculizumab in NHS-zymosan to assess how the cellular model reflects *in vivo* (fluid-phase) complement inhibition by eculizumab. The target serum level of eculizumab for aHUS patients for adequate blockage of complement is above 50-100 µg/ml (51, 52). In line with this, we observed maximal blockage of C5b-9 depositions on ciGMVECs with concentrations of 100 µg/ml and higher, and partial inhibition of C5b-9 formation with 50 µg/ml eculizumab (Figure 2C). Concentrations of 20 µg/ml and lower did not affect the C5b-9 depositions induced by activated serum.

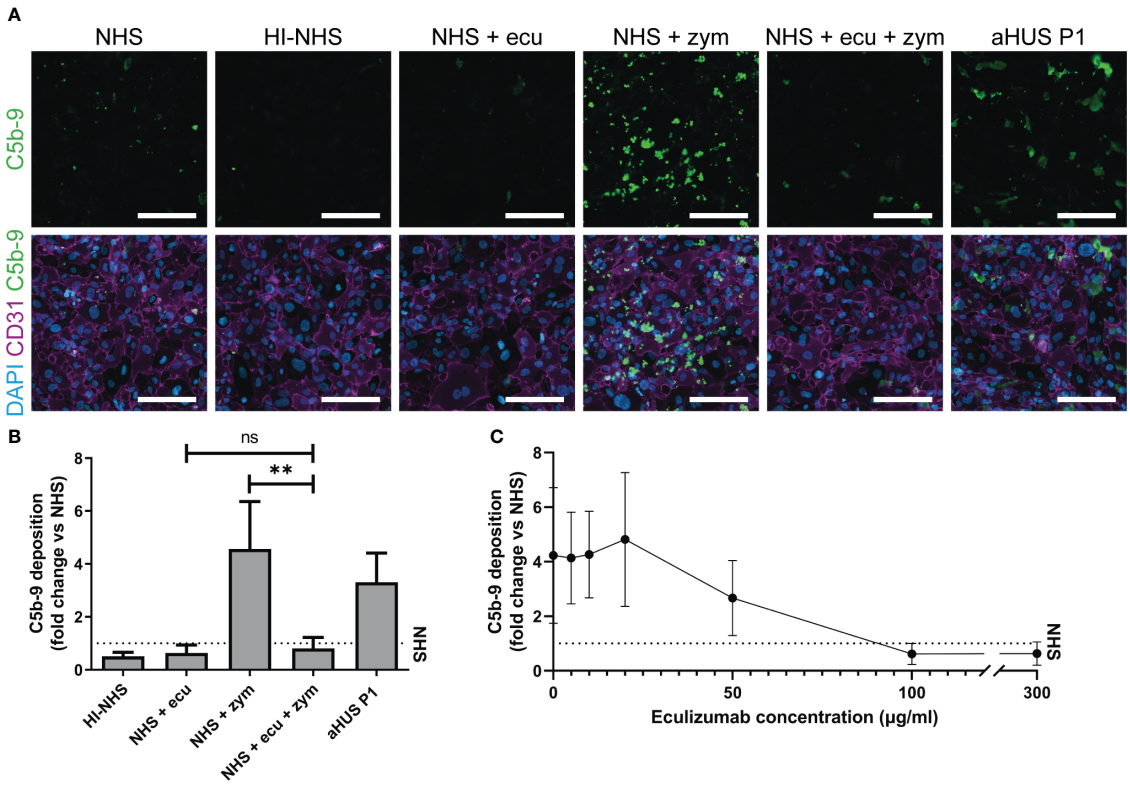

FIGURE 2
Human control conditionally immortalized glomerular microvascular endothelial cells (ciGMVECs) as model for complement deposition. **(A-C)** Control ciGMVECs were incubated with 33.3% serum in test medium for 2 hours. **(A)** Representative immunofluorescence images of C5b-9 (green), CD31 (purple) and cell nuclei with 4', 6-diamidino-2-phenylindole (DAPI; blue). Incubation with normal human serum (NHS), heat-inactivated NHS (HI-NHS), NHS supplemented with 300 µg/ml eculizumab (ecu), NHS with zymosan (zym), NHS + ecu + zym and aHUS P1 serum. Scale bars: 200 µm. **(B)** Quantification of serum-induced C5b-9 deposition on control ciGMVECs. Data are presented as mean ± standard deviation of the fold change to NHS (dotted line) run in parallel of nine independent experiments, except for aHUS P1 (three independent experiments). Experiments were performed with at least two replicates per condition (single measurements for aHUS P1 serum). Not significant (ns), **P < 0.01, using one-way ANOVA followed by Bonferroni's multiple comparisons test (aHUS P1 excluded for statistical analysis). **(C)** Eculizumab titration in NHS-zym. Data are presented as the mean ± standard deviation of the fold change to NHS (dotted line) run in parallel of three independent experiments performed with at least two replicates per condition.

3.3 C5b-9 deposition on human ciGMVECs in acute phase and remission

After validating ciGMVECs as a model to specifically measure complement-mediated C5b-9 depositions, we explored their usage for modeling aHUS by comparing aHUS patient samples obtained from different disease phases. Incubation of ciGMVECs with sera from P2, P3, P4, P5, and P6 obtained in the acute phase resulted in increased C5b-9 deposition levels, ranging from 1.37-7.69 fold the levels generated by NHS (Table 2; Supplementary Figure 5). In all serum samples, eculizumab levels were below the detection limit of 8 µg/ml.

Surprisingly, the sample of P4 obtained during evident hematological TMA and AKI (d10; Table 2) showed only slightly increased C5b-9 deposition compared to NHS. On the contrary, a second acute phase sample (d211; Table 2), showed higher C5b-9 deposition, despite the clinically less pronounced TMA. Of note, both relapses were triggered by a viral infection.

The remission samples of P2 and P5 with an eculizumab level above the therapeutic target suggesting adequate complement blockage, showed normalized C5b-9 depositions (Table 2; Supplementary Figure 5). The remission sera from P3 and P4, obtained while in remission after eculizumab withdrawal, also resulted in normalized endothelial C5b-9 deposition levels (Table 2; Supplementary Figure 2).

3.4 Monitoring C5b-9 deposition in an aHUS patient during eculizumab treatment on control and patient ciGMVECs

P1 developed a severe form of aHUS from the age of 5 months, which is described in detail in the materials and methods and by Bouwmeester et al. (36). We thoroughly monitored P1 during his chronic kidney failure and eculizumab treatment with various complement (activation) and TMA markers in the blood and studied if these parameters correlated with endothelial C5b-9 depositions. Interestingly, all samples of P1 in which the eculizumab concentrations were below the therapeutic target (<50 µg/ml) showed increased C5b-9 deposition on ciGMVECs (Figure 3A), irrespective of the clinical disease phase the samples were taken from. Thus, also samples taken when the patient did not show active signs of TMA showed increased cellular C5b-9 deposition. During adequate complement blockage, indicated by serum eculizumab levels above 50-100 µg/ml and a CH50 <10%, C5b-9 deposition was comparable or below NHS level (Figure 3A).

As this patient was not a "typical" aHUS patient because of ongoing decline in kidney function (described by Bouwmeester et al. (36)) and high C5b-9 deposition levels despite "quiescent" TMA markers, we hypothesized the glomerular endothelium of this patient might be more susceptible to complement activation and/or complement-mediated damage. When this patient received a kidney transplant, we were able to isolate GMVECs from the tissue of the removed native kidney from this patient to test this hypothesis. Incubation of the same series of serum samples obtained during follow-up with the patient's own ciGMVECs (P1 ciGMVECs) resulted in C5b-9 deposition that was similar to the deposition on control ciGMVECs (Figure 3A). Also, the patient cells were similarly susceptible to C5b-9 deposition induced by NHS (Figure 3B). The C5b-9 levels were not higher for P1 ciGMVECs compared to control ciGMVECs based on the fold change compared to NHS after incubation with different test sera (Supplementary Figure 6).

TABLE 2 Complement C5b-9 deposition of atypical hemolytic uremic syndrome (aHUS) patient samples on human control conditionally immortalized glomerular microvascular endothelial cells (ciGMVECs).

Patient	Day of sampling	Eculizumab target >50-100 µg/ml	Disease phase	C5b-9 deposition (fold change vs NHS run in parallel)[d]
P2	0	<8	Acute phase (TMA + AKI)	2.84[e]
	13	206	Remission phase[a]	0.30
P3	0	<8	Acute phase (TMA + AKI)	3.97
	307	<8	Remission phase	0.76
P4	0	<8	Pre-relapse	0.68
	10	<8	Acute phase (TMA + AKI)[b]	1.37
	211	<8	Acute phase (TMA + AKI)[c]	7.69
	344	<8	Remission phase	0.43
P5	0	<8	Acute phase (TMA + AKI)	2.17
	15	134	Remission phase[a]	0.59
P6	0	<8	Acute phase (TMA + AKI)	5.85

[a]Eculizumab level was above therapeutic target, suggesting adequate complement blockage.
[b]Lactate dehydrogenase (LDH) 1450 U/l, thrombocytes 21×10^9/l, urine protein-to-creatinine ratio (UPCR) 1.18 g/10mmol, and serum creatinine 130 µmol/l.
[c]LDH 612 U/l, thrombocytes 65×10^9/l, UPCR 0.37 g/10mmol, and serum creatinine 128 µmol/l.
[d]Patient samples: mean of two replicates of a single experiment. NHS: mean of at least three replicates of a single experiment.
[e]No duplicate.
AKI: acute kidney injury, NHS: normal human serum, TMA: thrombotic microangiopathy.

10.3389/fimmu.2023.1206409

4 Discussion

aHUS is a complex disease characterized by dysregulation of the AP, primarily caused by genetic variants in genes encoding complement components and/or by autoantibodies. Uncontrolled complement activity in aHUS causes AP activation and C5b-9 deposition on the GMVECs in the glomerulus. This contributes to endothelial cell activation and endothelial damage as well as a prothrombotic phenotype, leading to decreased kidney function. In this study, we showed that human control ciGMVECs and aHUS patient ciGMVECs can be used to adequately measure and model complement C5b-9 deposition on endothelial cells by different test sera and aHUS patient sera. Furthermore, aHUS patient ciGMVECs were incubated with patient's own serum samples.

The glomerulus is the main target of the complement-mediated damage in aHUS, suggesting a specific susceptibility of these cells to complement activation (24, 25, 53). Endothelial cells from different origin have different expression profiles of complement regulators and complement proteins, which may lead to different susceptibility for complement activation (in resting or activated state) (24, 25, 54, 55). Furthermore, glomerular endothelial cells may have different adaptive mechanisms for certain TMA triggers such as heme. For example, May et al. (56) showed a higher susceptibility for complement deposition of glomerular endothelial cells compared to other cell types upon heme stimulation. Thus, to reflect the physiological context as close as possible, glomerular endothelial cells were chosen as the preferred cell type for modeling aHUS *ex vivo*.

First, we showed that no significant differences were observed between primary GMVECs and control ciGMVECs with respect to their susceptibility for C5b-9 deposition by NHS and NHS-zymosan. Even though human primary GMVECs might reflect the *in vivo* situation better than ciGMVECs, primary GMVECs have several limitations (also reviewed in Meuleman et al. (53)). First, human primary GMVECs have limited availability and their isolation and culture is labor-intensive and requires great expertise. Second, these cells have a limited lifespan. Thus, multiple individual donors are needed resulting in differences in genetic background, and thereby inter-experimental variability. ciGMVECs do not have these practical limitations and are more suitable for standardized testing.

We showed that human ciGMVECs are a reliable and robust model for complement-mediated C5b-9 deposition, visualized and quantified with immunofluorescence microscopy. NHS-zymosan, which simulates an overactive complement system, resulted in increased C5b-9 deposition compared to NHS. On the other hand, inhibition of the complement system in NHS with eculizumab resulted in a dose-dependent decrease in C5b-9 deposition. Our results were in line with the recommended treatment target of eculizumab *in vivo*. Zymosan is obtained out of the cell wall of *Saccharomyces cerevisiae* and activates the complement system in serum via the AP by promoting rapid C3 cleavage (57, 58). However, zymosan might also activate endothelial cells as it is recognized by Toll-like receptors (59, 60). We could not identify to what extent cellular activation may have contributed to increased C5b-9 deposition.

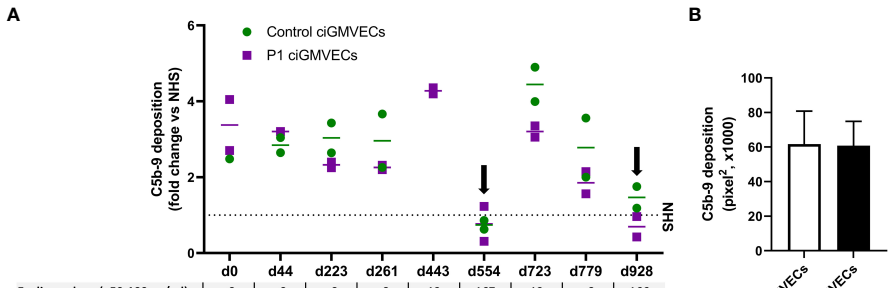

		d0	d44	d223	d261	d443	d554	d723	d779	d928
Eculizumab	(>50-100 µg/ml)	<8	<8	<8	<8	12	167	12	<8	166
CH50	(67-149%)	94	94	106	ND	69	<10	84	130	<10
AP50	(67-133%)	113	106	100	ND	ND	27	ND	143	ND
C3	(700-1500 mg/l)	927	796	825	1077	831	1018	801	ND	960
C3d	(<8.3 mg/l)	7.7	6.4	8.1	12	7.7	8.8	8.1	ND	14.6
C3d/C3 ratio	(<8.1)	8.3	8.0	9.8	11.1	9.3	8.7	10.1	ND	15.2
C5	(42-93 µg/ml)	108	107	114	137	118	127	137	157	119
Hemoglobin	(8.4-10.8 mmol/l)	7.0	6.9	6.6	6.3	7.5	7.4	6.4	5.4	7.1
LDH	(<250 U/l)	273	213	251	346	224	269	205	332	228
Thrombocytes	(150-400 x10⁹/l)	182	160	178	136	278	236	233	116	195
Creatinine	(<110 µmol/l)	141	172	188	359	226	282	242	551	777
Haptoglobin	(0.3-1.6 g/l)	0.86	0.48	0.55	0.52	0.93	0.84	1.32	0.26	1.46

FIGURE 3
Monitoring C5b-9 deposition by aHUS P1 during follow-up on control conditionally immortalized glomerular microvascular endothelial cells (ciGMVECs) and P1 ciGMVECs. **(A, B)** ciGMVECs derived from a control (green) or aHUS P1 (purple) were incubated with 33.3% serum in test medium for 2 hours. aHUS P1 sera were obtained during follow-up, indicated by days (d). **(A)** Data are presented as mean of two measurements (bars) or single measurements (squares and circles), all expressed in fold change compared to normal human serum (NHS) run in parallel (dotted line) performed in a single experiment for each cell line. The table inset shows the corresponding laboratory parameters for complement activation and TMA per test sample. Reference values of laboratory parameters are indicated between parentheses. Target values for adequate complement blockage by eculizumab are eculizumab >50 µg/ml, CH50 <10%, and AP50 <30%. Samples with adequate serum eculizumab levels are indicated with an arrow. LDH: lactate dehydrogenase, ND: not determined. **(B)** C5b-9 deposition on control ciGMVECs and P1 ciGMVECs after incubation with NHS. Data are presented as mean ± standard deviation of seven independent experiments for P1 ciGMVECs and nine independent experiments for control ciGMVECs. Not significant, using unpaired t-test. Experiments were performed with at least two replicates per condition.

In all acute phase samples of aHUS patients, increased C5b-9 deposition was observed compared to pooled NHS on (unstimulated) ciGMVECs. However, the most evident relapse for P4 (d10) did not show the highest C5b-9 deposition level in the assay compared to the other relapse (d211), which might indicate that the amount of C5b-9 deposition may not exactly reflect the disease state or that there may be a delay between clinical presentation and the complement effect on the endothelium. The assay detected normalized endothelial C5b-9 deposition levels in patients samples (P2-P5) in remission (either with or without adequate complement blockage by eculizumab).

Interestingly, all sera of P1, except the samples with eculizumab levels above target, induced elevated endothelial C5b-9 depositions, even though samples were obtained from disease phases without clinical or laboratory signs of TMA or complement activation present. The same effect was seen when the samples were tested on the patient's own ciGMVECs. This suggests that even though P1 showed a highly active complement deposition profile and ongoing decline in kidney function, the cells were not intrinsically, in resting state, more susceptible to complement activation (neither by patient serum nor by NHS). The cause of the high C5b-9 depositions in this patient with chronic kidney failure remains therefore unknown. Further studies are required to identify if patients with chronic kidney failure, either with or without aHUS, have increased complement activation.

Roumenina et al. (34, 61) and Frimat et al. (33) were the first to describe complement deposition on human glomerular endothelial cells (ciGMVECs). The authors described C3 deposition as mean readout for complement activation, which was primarily quantified with flow cytometry. Frimat et al. observed increased complement deposition in several aHUS patients versus control samples on resting cells, but for identifying all aHUS patient samples stimulation of the cells with heme was required (33). In Roumenina et al. (34), TNFα/IFNγ activation was used to discriminate healthy controls from aHUS patients with a C3 mutation. The authors did not describe or compare the disease phases of the aHUS patients. We did not need to pre-activate our cells to distinguish increased complement deposition in aHUS patients from controls. Thereby, our results are in line with groups working with HMECs-1 showing that the aHUS samples in the acute phase can be identified on resting cells (27, 31). This assay was first described by Noris et al. (27) and followed-up by Galbusera et al. (31) as an assay with the diagnostic aim of monitoring and individualizing eculizumab therapy and predicting relapses. Timmermans et al. (28) used the assay for showing complement depositions in hypertension-associated TMA, and Palomo et al. (29) published an adapted methodology with activated plasma samples and analyzed pre-eclampsia and HELLP (a pregnancy complication characterized by hemolysis, elevated liver enzymes, and low platelet count) patient samples in addition to aHUS samples. Some of these groups also showed increased C5b-9 deposition on activated cells after incubation with serum from unaffected mutation carriers and/or patients in the remission phase (27, 28, 34). We did not test such conditions as this was beyond the scope of our study.

To our knowledge, we are the first to show that unique aHUS patient GMVECs can be obtained, conditionally immortalized, and used as a cell line for experimental testing. This approach offers great promise for further research into the pathophysiology of aHUS, since it is now possible to align the endothelial cells of a patient with its own serum samples. In our case, the aHUS patient had a *CFH-CFHR1* hybrid gene, but it will also be very valuable to use this tool to generate cell lines from aHUS patients with mutations in membrane-bound regulators or from patients without confirmed complement mutations. This allows to investigate the effect of differences in endothelial cell characteristics on complement activation and susceptibility. After all, it remains unknown why some complement mutation carriers develop aHUS and others do not and if there are endothelial susceptibility factors contributing to aHUS in patients without proven genetic aberrations.

Our imaging strategy allows visualization of large areas of the well in one time in a reliable and fast way, even though the resolution may be lower compared to traditional confocal microscopy. In this study, the number of aHUS patients was still limited. Testing more aHUS patients with different genetic background during follow-up (and treatment) will help us to further understand aHUS pathophysiology. Nonetheless, it is important to emphasize that the *ex vivo* complement activity on endothelial cells cannot fully reflect the *in vivo* situation. For example, it has been suggested that the vascular heterogeneity of the glycomatrix is involved in glomerular diseases (24, 62). In addition, FH and properdin can interact with glycosaminoglycan heparan sulfate produced by endothelial cells (63). As these static 2D models do not fully reflect the glomerular organization, 3D models involving multiple cell types combined with flow conditions might be of potential to mimic the *in vivo* situation more closely.

In conclusion, we showed that human control ciGMVECs and aHUS patient ciGMVECs can be used to study and quantify endothelial C5b-9 complement deposition after serum incubation. Furthermore, by using human ciGMVECs, the described protocol is a promising tool to study complement pathophysiological mechanisms in the kidney, in particular the pathophysiology of aHUS. In addition, the model may be used for *in vitro* testing of novel complement therapeutics. The use of aHUS patient-derived (genetically altered) ciGMVECs might be of help to further explore the susceptibility of the endothelium to the disease under various circumstances.

Data availability statement

The original contributions presented in the study are included in the article/Supplementary Material. Further inquiries can be directed to the corresponding author.

Ethics statement

The studies involving humans were approved by Ethics Committee of Oost-Nederland (registration number of the CUREiHUS study: NL52817.091.15). The studies were conducted in accordance with the local legislation and institutional

requirements. Written informed consent for participation in this study was provided by the participants' legal guardians/next of kin. Written informed consent was obtained from the individual(s), and minor(s)' legal guardian/next of kin, for the publication of any potentially identifiable images or data included in this article.

Author contributions

Concept of the study: NK and LH; Design of the experiments: KS, LB, TV, NK, and LH; Experimental work: KS, LB, TV, and ND; Data interpretation: KS, LB, ND, MM, RB, NK, and LH; Collection and characterization of clinical samples: KS, LB, RB, JW, ED, AZ NK, and LH; Resources: NK and LH; Supervision: LB, MM, NK, and LH; Project administration: LH; Manuscript writing – original draft: KS; Manuscript writing – reviewing and editing: LB, MM, JW, ED, AZ, NK, LH, and RB. All authors contributed to the article and approved the submitted version.

Funding

This work was derived from work supported by research grants from the Netherlands Organization for Health Research and Development (ZonMw), "Goed Gebruik Geneesmiddelen" (projectnumber: 836031008), the Dutch Board of Health Insurance Companies (Zorgverzekeraars Nederland), and the Dutch Kidney Foundation (13OCA27 COMBAT Consortium and 20OK021 PERSPECTIV). They did not have any role in data collection, analysis or submission of this manuscript.

Acknowledgments

We would like to thank the Radboudumc Technology Center for microscopy for their support. The authors are very grateful to all patients for their willingness to participate in this study. We thank Joop Göertz and Monique Gerritsen-Otten for performing laboratory analysis.

Conflict of interest

NK, LH, AZ, ED, and JW are members of the European Reference Network for Rare Kidney Diseases (ERKNet)-Project No 739532. NK received consultancy fees from Roche Pharmaceuticals, Alexion and Novartis and is sub-investigator in APL2-C3G trial, Apellis. JW received grants from Alexion, Novartis and consultancy fees from Morphosys, Novartis, Otsuka, and Travere.

The remaining authors declare that the research was conducted in the absence of any commercial or financial relationships that could be construed as a potential conflict of interest.

The reviewer CL has declared a past authorship/collaboration with the author LvdH to the handling editor.

Publisher's note

All claims expressed in this article are solely those of the authors and do not necessarily represent those of their affiliated organizations, or those of the publisher, the editors and the reviewers. Any product that may be evaluated in this article, or claim that may be made by its manufacturer, is not guaranteed or endorsed by the publisher.

Supplementary material

The Supplementary Material for this article can be found online at: https://www.frontiersin.org/articles/10.3389/fimmu.2023.1206409/full#supplementary-material

References

1. Fakhouri F, Zuber J, Frémeaux-Bacchi V, Loirat C. Haemolytic uraemic syndrome. *Lancet* (2017) 390:681–96. doi: 10.1016/s0140-6736(17)30062-4

2. Westra D, Wetzels JF, Volokhina EB, van den Heuvel LP, van de Kar NC. A new era in the diagnosis and treatment of atypical haemolytic uraemic syndrome. *Neth J Med* (2012) 70(3):121–9.

3. Johnson S, Stojanovic J, Ariceta G, Bitzan M, Besbas N, Frieling M, et al. An audit analysis of a guideline for the investigation and initial therapy of diarrhea negative (atypical) hemolytic uremic syndrome. *Pediatr Nephrol* (2014) 29(10):1967–78. doi: 10.1007/s00467-014-2817-4

4. Fremeaux-Bacchi V, Fakhouri F, Garnier A, Bienaimé F, Dragon-Durey MA, Ngo S, et al. Genetics and outcome of atypical hemolytic uremic syndrome: A nationwide French series comparing children and adults. *Clin J Am Soc Nephrol* (2013) 8(4):554–62. doi: 10.2215/cjn.04760512

5. Kaplan BS, Meyers KE, Schulman SL. The pathogenesis and treatment of hemolytic uremic syndrome. *J Am Soc Nephrol* (1998) 9(6):1126–33. doi: 10.1681/asn.V961126

6. Taylor CM, Chua C, Howie AJ, Risdon RA. Clinico-pathological findings in diarrhoea-negative haemolytic uraemic syndrome. *Pediatr Nephrol* (2004) 19(4):419–25. doi: 10.1007/s00467-003-1385-9

7. Noris M, Remuzzi G. Atypical hemolytic-uremic syndrome. *N Engl J Med* (2009) 361(17):1676–87. doi: 10.1056/NEJMra0902814

8. Schieppati A, Ruggenenti P, Cornejo RP, Ferrario F, Gregorini G, Zucchelli P, et al. Renal function at hospital admission as a prognostic factor in adult hemolytic uremic syndrome. The Italian registry of haemolytic uremic syndrome. *J Am Soc Nephrol* (1992) 2(11):1640–4. doi: 10.1681/asn.V2111640

9. Legendre CM, Licht C, Muus P, Greenbaum LA, Babu S, Bedrosian C, et al. Terminal complement inhibitor eculizumab in atypical hemolytic-uremic syndrome. *N Engl J Med* (2013) 368(23):2169–81. doi: 10.1056/NEJMoa1208981

10. Greenbaum LA, Fila M, Ardissino G, Al-Akash SI, Evans J, Henning P, et al. Eculizumab is a safe and effective treatment in pediatric patients with atypical hemolytic uremic syndrome. *Kidney Int* (2016) 89(3):701–11. doi: 10.1016/j.kint.2015.11.026

11. Noris M, Remuzzi G. Overview of complement activation and regulation. *Semin Nephrol* (2013) 33(6):479–92. doi: 10.1016/j.semnephrol.2013.08.001

12. Merle NS, Church SE, Fremeaux-Bacchi V, Roumenina LT. Complement system part I - molecular mechanisms of activation and regulation. *Front Immunol* (2015) 6:262. doi: 10.3389/fimmu.2015.00262

13. Ricklin D, Hajishengallis G, Yang K, Lambris JD. Complement: A key system for immune surveillance and homeostasis. *Nat Immunol* (2010) 11(9):785–97. doi: 10.1038/ni.1923

14. Morgan BP. The membrane attack complex as an inflammatory trigger. *Immunobiology* (2016) 221(6):747–51. doi: 10.1016/j.imbio.2015.04.006

15. Malina M, Roumenina LT, Seeman T, Le Quintrec M, Dragon-Durey MA, Schaefer F, et al. Genetics of hemolytic uremic syndromes. *Presse Med* (2012) 41(3 Pt 2):e105-14. doi: 10.1016/j.lpm.2011.10.028

16. Bresin E, Rurali E, Caprioli J, Sanchez-Corral P, Fremeaux-Bacchi V, Rodriguez de Cordoba S, et al. Combined complement gene mutations in atypical hemolytic uremic syndrome influence clinical phenotype. *J Am Soc Nephrol* (2013) 24(3):475–86. doi: 10.1681/asn.2012090884

17. Loirat C, Fakhouri F, Ariceta G, Besbas N, Bitzan M, Bjerre A, et al. An international consensus approach to the management of atypical hemolytic uremic syndrome in children. *Pediatr Nephrol* (2016) 31(1):15–39. doi: 10.1007/s00467-015-3076-8

18. Bouwmeester RN, Duineveld C, Wijnsma KL, Bemelman FJ, van der Heijden JW, van Wijk JAE, et al. Early eculizumab withdrawal in patients with atypical hemolytic uremic syndrome in native kidneys is safe and cost-effective: Results of the CUREiHUS study. *Kidney Int Rep* (2023) 8(1):91–102. doi: 10.1016/j.ekir.2022.10.013

19. Feitz WJC, van de Kar N, Orth-Höller D, van den Heuvel L, Licht C. The genetics of atypical hemolytic uremic syndrome. *Med Genet* (2018) 30(4):400–9. doi: 10.1007/s11825-018-0216-0

20. Piras R, Valoti E, Alberti M, Bresin E, Mele C, Breno M, et al. CFH and CFHR structural variants in atypical hemolytic uremic syndrome: Prevalence, genomic characterization and impact on outcome. *Front Immunol* (2022) 13:1011580. doi: 10.3389/fimmu.2022.1011580

21. Iorember F, Nayak A. Deficiency of CFHR plasma proteins and autoantibody positive hemolytic uremic syndrome: Treatment rationale, outcomes, and monitoring. *Pediatr Nephrol* (2021) 36(6):1365–75. doi: 10.1007/s00467-020-04652-x

22. Geerdink LM, Westra D, van Wijk JA, Dorresteijn EM, Lilien MR, Davin JC, et al. Atypical hemolytic uremic syndrome in children: Complement mutations and clinical characteristics. *Pediatr Nephrol* (2012) 27(8):1283–91. doi: 10.1007/s00467-012-2131-y

23. Nester CM, Barbour T, de Cordoba SR, Dragon-Durey MA, Fremeaux-Bacchi V, Goodship TH, et al. Atypical aHUS: State of the art. *Mol Immunol* (2015) 67(1):31–42. doi: 10.1016/j.molimm.2015.03.246

24. Roumenina LT, Rayes J, Frimat M, Fremeaux-Bacchi V. Endothelial cells: Source, barrier, and target of defensive mediators. *Immunol Rev* (2016) 274(1):307–29. doi: 10.1111/imr.12479

25. Thurman JM, Harrison RA. The susceptibility of the kidney to alternative pathway activation-a hypothesis. *Immunol Rev* (2023) 313(1):327–38. doi: 10.1111/imr.13168

26. Ricklin D, Reis ES, Lambris JD. Complement in disease: A defence system turning offensive. *Nat Rev Nephrol* (2016) 12(7):383–401. doi: 10.1038/nrneph.2016.70

27. Noris M, Galbusera M, Gastoldi S, Macor P, Banterla F, Bresin E, et al. Dynamics of complement activation in aHUS and how to monitor eculizumab therapy. *Blood* (2014) 124(11):1715–26. doi: 10.1182/blood-2014-02-558296

28. Timmermans SAMEG, Abdul-Hamid MA, Potjewijd J, Theunissen ROMFIH, Damoiseaux JGMC, Reutelingsperger CP, et al. C5b9 formation on endothelial cells reflects complement defects among patients with renal thrombotic microangiopathy and severe hypertension. *J Am Soc Nephrol* (2018) 29(8):2234–43. doi: 10.1681/asn.2018020184

29. Palomo M, Blasco M, Molina P, Lozano M, Praga M, Torramade-Moix S, et al. Complement activation and thrombotic microangiopathies. *Clin J Am Soc Nephrol* (2019) 14(12):1719–32. doi: 10.2215/cjn.05830519

30. Bettoni S, Galbusera M, Gastoldi S, Donadelli R, Tentori C, Spartà G, et al. Interaction between multimeric von Willebrand factor and complement: A fresh look to the pathophysiology of microvascular thrombosis. *J Immunol* (2017) 199(3):1021–40. doi: 10.4049/jimmunol.1601121

31. Galbusera M, Noris M, Gastoldi S, Bresin E, Mele C, Breno M, et al. An ex vivo test of complement activation on endothelium for individualized eculizumab therapy in hemolytic uremic syndrome. *Am J Kidney Dis* (2019) 74(1):56–72. doi: 10.1053/j.ajkd.2018.11.012

32. Pouw RB, Brouwer MC, de Gast M, van Beek AE, van den Heuvel LP, Schmidt CQ, et al. Potentiation of complement regulator factor H protects human endothelial cells from complement attack in ahus sera. *Blood Adv* (2019) 3(4):621–32. doi: 10.1182/bloodadvances.2018025692

33. Frimat M, Tabarin F, Dimitrov JD, Poitou C, Halbwachs-Mecarelli L, Fremeaux-Bacchi V, et al. Complement activation by heme as a secondary hit for atypical hemolytic uremic syndrome. *Blood* (2013) 122(2):282–92. doi: 10.1182/blood-2013-03-489245

34. Roumenina LT, Frimat M, Miller EC, Provot F, Dragon-Durey MA, Bordereau P, et al. A prevalent C3 mutation in ahus patients causes a direct C3 convertase gain of function. *Blood* (2012) 119(18):4182–91. doi: 10.1182/blood-2011-10-383281

35. Venables JP, Strain L, Routledge D, Bourn D, Powell HM, Warwicker P, et al. Atypical haemolytic uraemic syndrome associated with a hybrid complement gene. *PloS Med* (2006) 3(10):e431. doi: 10.1371/journal.pmed.0030431

36. Bouwmeester RN, Ter Avest M, Wijnsma KL, Duineveld C, Ter Heine R, Volokhina EB, et al. Case report: Variable pharmacokinetic profile of eculizumab in an aHUS patient. *Front Immunol* (2021) 11:612706. doi: 10.3389/fimmu.2020.612706

37. Volokhina E, Westra D, Xue X, Gros P, van de Kar N, van den Heuvel L. Novel C3 mutation p.Lys65Gln in ahus affects complement factor h binding. *Pediatr Nephrol* (2012) 27(9):1519–24. doi: 10.1007/s00467-012-2183-z

38. Martínez-Barricarte R, Heurich M, López-Perrote A, Tortajada A, Pinto S, López-Trascasa M, et al. The molecular and structural bases for the association of complement C3 mutations with atypical hemolytic uremic syndrome. *Mol Immunol* (2015) 66(2):263–73. doi: 10.1016/j.molimm.2015.03.248

39. Zipfel PF, Edey M, Heinen S, Józsi M, Richter H, Misselwitz J, et al. Deletion of complement factor H-related genes CFHR1 and CFHR3 is associated with atypical hemolytic uremic syndrome. *PloS Genet* (2007) 3(3):e41. doi: 10.1371/journal.pgen.0030041

40. Lee BH, Kwak SH, Shin JI, Lee SH, Choi HJ, Kang HG, et al. Atypical hemolytic uremic syndrome associated with complement factor H autoantibodies and CFHR1/CFHR3 deficiency. *Pediatr Res* (2009) 66(3):336–40. doi: 10.1203/PDR.0b013e3181b1bd4a

41. Moore I, Strain L, Pappworth I, Kavanagh D, Barlow PN, Herbert AP, et al. Association of factor H autoantibodies with deletions of CFHR1, CFHR3, CFHR4, and with mutations in CFH, CFI, CD46, and C3 in patients with atypical hemolytic uremic syndrome. *Blood* (2010) 115(2):379–87. doi: 10.1182/blood-2009-05-221549

42. Richards S, Aziz N, Bale S, Bick D, Das S, Gastier-Foster J, et al. Standards and guidelines for the interpretation of sequence variants: A joint consensus recommendation of the American college of medical genetics and genomics and the association for molecular pathology. *Genet Med* (2015) 17(5):405–24. doi: 10.1038/gim.2015.30

43. Wijnsma KL, Duineveld C, Wetzels JFM, van de Kar N. Eculizumab in atypical hemolytic uremic syndrome: Strategies toward restrictive use. *Pediatr Nephrol* (2019) 34(11):2261–77. doi: 10.1007/s00467-018-4091-3

44. Satchell SC, Tasman CH, Singh A, Ni L, Geelen J, von Ruhland CJ, et al. Conditionally immortalized human glomerular endothelial cells expressing fenestrations in response to VEGF. *Kidney Int* (2006) 69(9):1633–40. doi: 10.1038/sj.ki.5000277

45. Maciag T, Cerundolo J, Ilsley S, Kelley PR, Forand R. An endothelial cell growth factor from bovine hypothalamus: Identification and partial characterization. *Proc Natl Acad Sci U.S.A.* (1979) 76(11):5674–8. doi: 10.1073/pnas.76.11.5674

46. van Setten PA, van Hinsbergh VW, van der Velden TJ, van de Kar NC, Vermeer M, Mahan JD, et al. Effects of RNF alpha on verocytotoxin cytotoxicity in purified human glomerular microvascular endothelial cells. *Kidney Int* (1997) 51(4):1245–56. doi: 10.1038/ki.1997.170

47. Michels M, van de Kar N, Okrój M, Blom AM, van Kraaij SAW, Volokhina EB, et al. Overactivity of alternative pathway convertases in patients with complement-mediated renal diseases. *Front Immunol* (2018) 9:612. doi: 10.3389/fimmu.2018.00612

48. Schindelin J, Arganda-Carreras I, Frise E, Kaynig V, Longair M, Pietzsch T, et al. Fiji: An open-source platform for biological-image analysis. *Nat Methods* (2012) 9(7):676–82. doi: 10.1038/nmeth.2019

49. van den Heuvel LP, van de Kar N, Duineveld C, Sarlea A, van der Velden T, Liebrand WTB, et al. The complement component C5 is not responsible for the alternative pathway activity in rabbit erythrocyte hemolytic assays during eculizumab treatment. *Cell Mol Immunol* (2020) 17(6):653–5. doi: 10.1038/s41423-020-0406-y

50. Dragon-Durey MA, Sethi SK, Bagga A, Blanc C, Blouin J, Ranchin B, et al. Clinical features of anti-factor H autoantibody-associated hemolytic uremic syndrome. *J Am Soc Nephrol* (2010) 21(12):2180–7. doi: 10.1681/asn.2010030315

51. Wijnsma KL, Ter Heine R, Moes D, Langemeijer S, Schols SEM, Volokhina EB, et al. Pharmacology, pharmacokinetics and pharmacodynamics of eculizumab, and possibilities for an individualized approach to eculizumab. *Clin Pharmacokinet* (2019) 58(7):859–74. doi: 10.1007/s40262-019-00742-8

52. Willrich MAV, Andreguetto BD, Sridharan M, Fervenza FC, Tostrud LJ, Ladwig PM, et al. The impact of eculizumab on routine complement assays. *J Immunol Methods* (2018) 460:63–71. doi: 10.1016/j.jim.2018.06.010

53. Meuleman M-S, Duval A, Fremeaux-Bacchi V, Roumenina LT, Chauvet S. Ex vivo test for measuring complement attack on endothelial cells: From research to bedside. *Front Immunol* (2022) 13:860689. doi: 10.3389/fimmu.2022.860689

54. Bongrazio M, Pries AR, Zakrzewicz A. The endothelium as physiological source of properdin: Role of wall shear stress. *Mol Immunol* (2003) 39(11):669–75. doi: 10.1016/s0161-5890(02)00215-8

55. Sartain SE, Turner NA, Moake JL. TNF regulates essential alternative complement pathway components and impairs activation of protein C in human glomerular endothelial cells. *J Immunol* (2016) 196(2):832–45. doi: 10.4049/jimmunol.1500960

56. May O, Merle NS, Grunenwald A, Gnemmi V, Leon J, Payet C, et al. Heme drives susceptibility of glomerular endothelium to complement overactivation due to inefficient upregulation of heme oxygenase-1. *Front Immunol* (2018) 9:3008. doi: 10.3389/fimmu.2018.03008

57. Fearon DT, Austen KF. Activation of the alternative complement pathway due to resistance of zymosan-bound amplification convertase to endogenous regulatory mechanisms. *Proc Natl Acad Sci U.S.A.* (1977) 74(4):1683–7. doi: 10.1073/pnas.74.4.1683

58. Rawal N, Pangburn MK. Formation of high-affinity C5 convertases of the alternative pathway of complement. *J Immunol* (2001) 166(4):2635–42. doi: 10.4049/jimmunol.166.4.2635

59. Salvador B, Arranz A, Francisco S, Córdoba L, Punzón C, Llamas MÁ, et al. Modulation of endothelial function by Toll like receptors. *Pharmacol Res* (2016) 108:46–56. doi: 10.1016/j.phrs.2016.03.038

60. Sato M, Sano H, Iwaki D, Kudo K, Konishi M, Takahashi H, et al. Direct binding of Toll-like receptor 2 to zymosan, and zymosan-induced NF-kappa B activation and tnf-alpha secretion are down-regulated by lung collectin surfactant protein A. *J Immunol* (2003) 171(1):417–25. doi: 10.4049/jimmunol.171.1.417

61. Roumenina LT, Jablonski M, Hue C, Blouin J, Dimitrov JD, Dragon-Durey MA, et al. Hyperfunctional C3 convertase leads to complement deposition on endothelial cells and contributes to atypical hemolytic uremic syndrome. *Blood* (2009) 114 (13):2837–45. doi: 10.1182/blood-2009-01-197640

62. Langford-Smith A, Day AJ, Bishop PN, Clark SJ. Complementing the sugar code: Role of GAGs and sialic acid in complement regulation. *Front Immunol* (2015) 6:25. doi: 10.3389/fimmu.2015.00025

63. Boels MG, Lee DH, van den Berg BM, Dane MJ, van der Vlag J, Rabelink TJ. The endothelial glycocalyx as a potential modifier of the hemolytic uremic syndrome. *Eur J Intern Med* (2013) 24(6):503–9. doi: 10.1016/j.ejim.2012.12.016

frontiers | Frontiers in Immunology

TYPE Original Research
PUBLISHED 26 October 2023
DOI 10.3389/fimmu.2023.1279612

Check for updates

OPEN ACCESS

EDITED BY
Mihály Józsi,
Eötvös Loránd University, Hungary

REVIEWED BY
Kevin James Marchbank,
Newcastle University, United Kingdom
Talat Malik,
Imperial College London, United Kingdom
Pilar Sánchez-Corral,
University Hospital La Paz Research Institute (IdiPAZ), Spain

*CORRESPONDENCE
Lambertus P. van den Heuvel
Bert.vandenheuvel@radboudumc.nl

†These authors have contributed equally to this work

RECEIVED 18 August 2023
ACCEPTED 16 October 2023
PUBLISHED 26 October 2023

CITATION
Gerogianni A, Baas LM, Sjöström DJ, van de Kar NCAJ, Pullen M, van de Peppel SJ, Nilsson PH and van den Heuvel LP (2023) Functional evaluation of complement factor I variants by immunoassays and SDS-PAGE. *Front. Immunol.* 14:1279612. doi: 10.3389/fimmu.2023.1279612

COPYRIGHT
© 2023 Gerogianni, Baas, Sjöström, van de Kar, Pullen, van de Peppel, Nilsson and van den Heuvel. This is an open-access article distributed under the terms of the Creative Commons Attribution License (CC BY). The use, distribution or reproduction in other forums is permitted, provided the original author(s) and the copyright owner(s) are credited and that the original publication in this journal is cited, in accordance with accepted academic practice. No use, distribution or reproduction is permitted which does not comply with these terms.

Functional evaluation of complement factor I variants by immunoassays and SDS-PAGE

Alexandra Gerogianni[1,2†], Laura M. Baas[3†], Dick J. Sjöström[1,2], Nicole C. A. J. van de Kar[3], Marit Pullen[4], Siem J. van de Peppel[3], Per H. Nilsson[1,2†] and Lambertus P. van den Heuvel[3,4,5,6*†]

[1]Linnaeus Centre for Biomaterials Chemistry, Linnaeus University, Kalmar, Sweden, [2]Department of Chemistry and Biomedicine, Linnaeus University, Kalmar, Sweden, [3]Department of Pediatric Nephrology, Radboud University Medical Center, Amalia Children's Hospital, Nijmegen, Netherlands, [4]Department of Genetics, Radboud University Medical Center, Nijmegen, Netherlands, [5]Department of Pediatrics/Pediatric Nephrology, University Hospitals Leuven, Leuven, Belgium, [6]Department of Development and Regeneration, University Hospitals Leuven, Leuven, Belgium

Factor I (FI) is an essential regulator of the complement system. Together with co-factors, FI degrades C3b, which inhibits further complement activation. Genetic mutations in FI are associated with pathological conditions like age-related macular degeneration and atypical hemolytic uremic syndome. Here, we evaluated eight recombinant FI genetic variants found in patients. We assessed FI's co-factor activity in the presence of two co-factors; Factor H and soluble CR1. Different analytical assays were employed; SDS-PAGE to evaluate the degradation of C3b, ELISA to measure the generation of fluid phase iC3b and the degradation of surface-bound C3b using a novel Luminex bead-based assay. We demonstrate that mutations in the FIMAC and SP domains of FI led to significantly reduced protease activity, whereas the two analyzed mutations in the LDLRA2 domain did not result in any profound changes in FI's function. The different assays employed displayed a strong positive correlation, but differences in the activity of the genetic variants Ile55Phe and Gly261Asp could only be observed by combining different methods and co-factors for evaluating FI activity. In conclusion, our results provide a new perspective regarding available diagnostic tools for assessing the impact of mutations in FI.

KEYWORDS

factor I, co-factor activity, functional assay, complement regulation, factor H, complement receptor I

Introduction

The complement system is an essential part of innate immunity and consists of around 50 plasma- and membrane proteins for host surveillance, including recognition and elimination of pathogens and cell debris (1). Complement activation can arise through three different routes; the classical, lectin, and the alternative pathways. All pathways result in the

proteolytical activation of zymogens, including cleavage of the central complement components C3 to C3a and C3b, and C5 to C5a and C5b, which leads to effector functions, including C3b-opsonization, generation of C3a- and C5a-anaphylatoxins and formation of the terminal C5b-9 complement pathway (2). The alternative pathway, activated by surface-deposited C3b or the fluid phase analog C3 (H_2O), acts as an intrinsic amplification loop for all pathways. Therefore, tight regulation of the alternative pathway on host cells is critical, as insufficient inhibition of C3b can lead to uncontrolled complement activation and excessive inflammation (3, 4).

Factor I (FI) is a key negative regulator of complement activation. In the presence of its co-factors, factor H (FH), factor H-like protein 1 (FHL-1), complement receptor 1 (CR1; CD35), and membrane co-factor protein (MCP; CD46), FI can cleave the α´-chain of C3b into iC3b, and in the presence of CR1, FI can further degrade iC3b into C3dg and C3c (2, 5–7). FI circulates in a zymogen-like state until the C3b/co-factor complex is engaged (8, 9). Then, FI is conformationally changed and able to cleave C3b (10). FI is a heterodimer with a molecular weight of 88 kDa (9). The non-catalytic heavy chain consists of a FI membrane attack complex (FIMAC) domain; a scavenger receptor cysteine-rich (SRCR) domain; two class A low-density lipoprotein receptor domains (LDLRA1 and LDLRA2); and a C-terminal region of unknown function, while the catalytic light chain has a chymotrypsin-like serine protease (SP) domain (7, 8).

Mutations in FI can impair its secretion or enzymatic function, which can lead to tissue damage and disease (11–13), including age-related macular degeneration (AMD) and atypical uremic syndrome (aHUS) (9, 10, 14). In both diseases, insufficient complement regulation drives the disease pathogenesis (15, 16).

Carriers of rare *CFI* variants were reported with younger age of AMD symptom onset (17), and loss of function FI variants are reported to have the greatest impact on the risk of developing the disease (18). It was demonstrated that rare variants in the SP domain of the *CFI* gene were associated with AMD (19). Furthermore, mutations in the FIMAC domain seem to interfere with FI-mediated C3b degradation (20). Mutations in the *CFI* gene are found in a relatively low incidence (<5%) in aHUS patients. However, the risk of recurrence was higher after kidney transplantation in carriers of pathogenic *CFI* variants (21–23).

The functional consequence for the majority of the *CFI* gene variants has not been examined yet, highlighting the need for functional characterization of genetic variants. Next to this, functional characterization of *CFI* genetic variants is done differently across laboratories, and standardization is lacking. The co-factor activity of FI may occur on either surface-bound C3b, or C3b in the fluid phase and to date, no comparisons between surface-bound and fluid-phase C3b degradation by FI have been reported.

To further investigate the pathophysiological consequences of carriers of rare *CFI* variants, we evaluated the functionality of eight recombinantly expressed FI-variants by both surface-bound and fluid phase C3b using three different methods (SDS-PAGE, ELISA and Luminex technology) with both FH and sCR1 as co-factor. Finally, we evaluated the correlation of these three functional readouts for FI activity and the usage of the two different co-factors.

Materials and methods

Reagents

Human complement proteins FH and FI were bought from CompTech (Tyler, TX). Human C3 was purified as described by Hammer et al. (24). Human C3b was produced by trypsin digestion of C3. C3 was incubated for five minutes at 22°C with 1% (w/w) trypsin from bovine pancreas (Merck; Kenilworth, NJ) and isolated with gel filtration on Sephadex G100 (GE Healthcare, Chicago, IL) followed by equilibration with 10 mM phosphate buffer, pH 7.4, and 0.145 M saline (PBS). C3b was also purchased from CompTech. Soluble CR1 (sCR1) was obtained from T Cell Sciences Inc. (Cambridge, MA).

CFI mutants

The *CFI* mutations were identified in the cohorts of aHUS and AMD patients at the Radboudumc Genetics department (Nijmegen, Netherlands). *CFI* variants are presented in Table 1 and their distribution throughout FI is shown in Figure 1.

Generation of recombinant FI

In vitro mutagenesis was performed on a pcDNA3 vector (ThermoFisher; Waltham, MA) containing the full-length wild-type *CFI* cDNA (ACCN NM_000204.4; GRCh37) using the Q5® Site-Directed Mutagenesis Kit (New England Biolabs; Ipswich, MA) with specific primers to introduce each variant into the wild-type gene (for primer sequences see Supplementary Methods, Table 1). After PCR, samples were digested with DpnI (ThermoFisher) for one hour at 37°C. Obtained plasmids were transformed into the *E.coli* DH5-α strain with heat pulse, after which the bacteria were selected on LB plates containing 50 μg/mL carbenicillin. DNA samples were purified using the PureYield™ Plasmid miniprep and midiprep kit (Promega; Madison, WI) according to the manufacturer's instructions. Fidelity of the clones was confirmed by PacBio sequencing. For the expression of recombinant protein, Human Embryonic Kidney 293T (HEK293T) cells were maintained in DMEM (ThermoFisher) supplemented with 10% FCS (ThermoFisher), 2 mM L-glutamine (ThermoFisher), 1% MEM non-essential amino acids solution (ThermoFisher), 1 nM sodium pyruvate (Merck), and 100 units/mL penicillin-streptomycin (ThermoFisher) and were seeded onto culture vessels pre-coated with 20 μg/mL collagen I (Merck). When the HEK293T cells reached 70-90% confluency, transfection was performed using lipofectamine 2000 transfection reagent (ThermoFisher). Forty hours post-transfection, the cells were washed twice with PBS, after which Opti-MEM (ThermoFisher) was added to the culture vessel. Supernatants were collected 55 hours post-transfection and subsequently concentrated with Amicon® Ultra 10kDa (Merck) following manufacturers' instructions.

TABLE 1 Overview of FI genetic variants and recombinant proteins.

cDNA change	Protein change	rs-number	Domain	GenomAD frequency (ALL)	Classification	Clinical phenotype
148C>G	Pro50Ala	rs144082872	FIMAC	0.01%	3	AMD and aHUS
163A>T	Ile55Phe	N/A	FIMAC	–	3	AMD
782G>A	Gly261Asp	rs112534524	LDLRA2	0.13%	2	AMD and aHUS
898G>A	Ala300Thr	rs11098044	LDLRA2	1.1%	1	AMD
1019T>C	Ile340Thr	rs769419740	SP	0.0073%	4	AMD and aHUS
1195T>C	Trp399Arg	rs778871974	SP	0.002%	2	AMD and aHUS
1204C>T	Pro402Ser	rs1416762682	SP	–	3	aHUS
1429G>C	Asp477His	rs754972981	SP	0.002%	3	AMD

Classification of the variants was done according to previously described guidelines (25) as benign (Class 1), likely benign (Class 2), uncertain significance (Class 3), likely pathogenic (Class 4) and pathogenic (Class 5). cDNA and protein changes were determined using transcript NM_000204.4.

Evaluation of FI recombinant proteins

Protein concentration: FI protein concentration in the concentrated supernatants was determined by ELISA as described previously (12, 26). In summary, a 96-wells high-binding plate (Greiner; Kremsmünster, Austria) was coated with a sheep anti-human FI antibody (LabNed; Edison, NJ) diluted 1:1000 in carbonate buffer pH 9.6 (15 mM $Na_2CO_3 \cdot 10H_2O$, 34.5mM $NaHCO_3$) and incubated overnight at 4°C. The plate was blocked for 30 minutes with superblock (ThermoFisher) and subsequently with PBS supplemented with 1% bovine serum albumin (BSA) for 1 hour at room temperature (RT). Following incubation, the plate was washed with PBS 0.05% v/v Tween-20 after blocking and between each of the following steps. Samples and the standard (serum-purified FI, CompTech) were diluted in PBS containing 0.05% v/v Tween-20 and 0.2% BSA and afterwards incubated for two hours at RT. After applying the samples, FI was detected with a mouse anti-human FI antibody (OX-21, ProSci; Fort Collins, CO) diluted 1:1000 in PBST-0.2% BSA and incubated for two hours at RT. After incubation, the secondary goat anti-mouse HRP antibody (Dako; Glostrup, Denmark) was diluted 1:2500 in PBST-0.2% BSA and incubated for 1 hour at RT. Detection was executed using o-phenylenediamine dihydrochloride substrate (OPD; Merck) diluted according to the manufacturer's instructions and incubated for 30 minutes at RT after which the reaction was stopped with the addition of 1 M H_2SO_4. Absorbance was measured at 492 nm by Tecan Spark 10M multi-mode microplate reader (Männedorf, Switzerland). All samples were measured in duplicates.

Protein identification: The recombinant proteins were diluted in Laemmli sample buffer enriched with 1:20 β-mercaptoethanol and incubated for 5 minutes at 95°C. Samples were separated on a 4-15% Mini-PROTEAN® TGX™ gel (Bio-Rad; Hercules, CA) for one hour at 120 V. Separated proteins were transferred to a 0.45 µm polyvinylidene fluoride (PVDF) membrane (Bio-Rad) for 7 minutes using the Trans-Blot® Turbo™ Transfer System (Bio-Rad), after which the membrane was blocked with PBS containing 5% milk for one hour at RT. The membrane was incubated overnight at 4°C with a goat anti-human FI antibody (Quidel, San Diego, CA) diluted 1:500 in PBS containing 5% milk. The membrane was

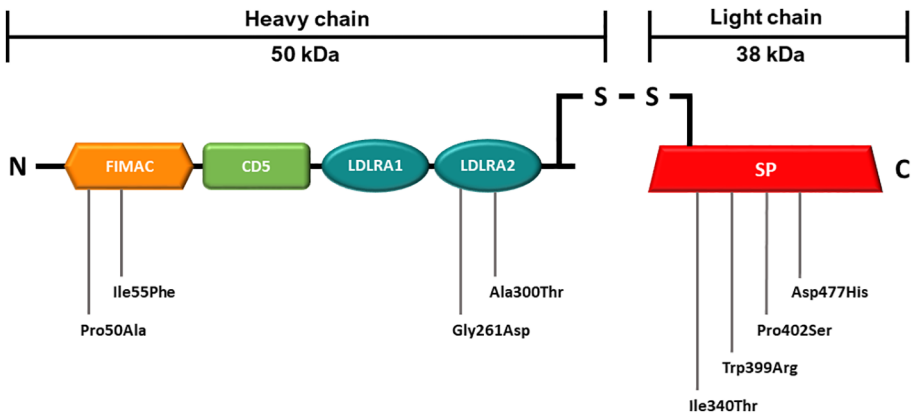

FIGURE 1
Schematic representation of the mature FI protein with mutations analyzed in this study. The 50 kDa heavy chain consists of four domains which are are shown in orange (FIMAC), green (CD5) and blue (LDRA1 and LDRA2). The 38 kDa light chain consists of one domain which is shown in red (SP). Details on the genetic variants are summarized in Table 1. FIMAC, Factor I-Membrane Attack Complex; CD5, scavenger receptor cysteine-rich domain; LDLRA1 and LDLRA2, Low density lipoprotein receptor domains 1 and 2; SP, Serine Protease domain.

washed three times for 5 minutes with PBS 0.05% Tween-20 on a rocking platform and incubated with the secondary donkey anti-goat HRP antibody (Dako) diluted 1:2000 in PBST containing 5% milk. After incubation, the membrane was washed three times for 5 minutes with PBS 0.05% Tween-20, and chemiluminescence was detected using the SuperSignal™ West Femto Maximum Sensitivity Substrate (Thermo Fischer).

SDS-PAGE

C3b (10 µg) was mixed with recombinant FI (0.1 µg) together with its co-factors (0.1 µg) FH or sCR1 and incubated in PBS for 60 minutes. Samples that contained C3b, FH, or sCR1 with and without FI (CompTech) were used as positive and negative controls, respectively. The total reaction volume was 10 µL, and the incubations were performed in 1.8 mL Nunc-cryotubes (Nunc; Roskilde, Denmark) at 37°C. After incubation, 5x SDS-PAGE reduced sample buffer (Bio-Rad) was added, and the samples were heated for 10 minutes at 95°C. The samples were applied on 12-wells 4 – 15% Tris-glycine gels and applied to SDS-PAGE with a molecular marker (Bio-Rad). The gels were stained with SYPRO Ruby protein stain (Bio-Rad) and evaluated using Chemi Doc Imaging System (Bio-Rad).

iC3b ELISA

FI recombinant proteins and the plasma purified FI positive control (CompTech) were diluted to 2 µg/mL in Tris-buffered saline pH 7.4 (TBS, 50 mM TrisHCl, 150 mM NaCl). C3b (15 µg/mL) and FH (3 µg/mL) were added to each sample and the reaction mixture was incubated for three hours at 37°C. C3b degradation was analyzed by detecting iC3b concentrations with ELISA. A high-binding microtiter plate (Greiner) was coated with mouse anti-iC3b (Quidel), diluted 1:2500 in a 50 mM carbonate buffer pH 9,6), by overnight incubation at 4°C and subsequently blocked with PBS 1% BSA for one hour at RT. The plate was washed with PBS 0.05% Tween-20 (PBST) after coating, blocking and between each of the following steps. Samples were diluted in PBST and incubated for 1 hour at RT. iC3b was detected with a rabbit anti-human C3c (Siemens; Erlangen, Germany) diluted 1:2000 in PBST with 0.2% BSA and incubated for 1 hour at RT followed by the secondary goat anti-rabbit HRP antibody (Dako) diluted 1:2000 in PBST with 0.2% BSA and incubated for one hour at RT. O-phenylenediamine dihydrochloride (OPD) (Sigma) was added as a substrate for the HRP and incubated for 30 minutes at RT after which the reaction was stopped with the addition of 1 M H_2SO_4. All samples were measured in duplicates. Absorbance was measured at 492 nm by Tecan Spark 10M multi-mode microplate reader (Männedorf, Switzerland).

Luminex assay

Conjugation of magnetic beads with C3b: C3b was conjugated to magnetic beads as described previously (27). Briefly, cystamine sulfate hydrate (6 µg, Merck) was coupled to Bio-Plex Pro™ magnetic COOH beads (Bio-Rad) with the use of the amine coupling kit (Bio-Rad) following the manufacturer's instructions. The beads were then incubated with dithiothreitol (DTT; Roche Diagnostics, Rotkreuz, Switzerland) at 6 µM final concentration for 20 minutes at 22°C to reduce the internal disulfide bond of cystamine. After thorough washing with 10 mM phosphate buffer and 0.145 M saline (PBS) at pH 7.4, C3 (15 µg) and trypsin (1 µg, Merck) were added to the beads and were incubated for 10 minutes at 37°C to induce C3 degradation resulting in C3b linkage to the beads via the thioester. After the incubation, the beads were washed thoroughly with PBS to end the reaction.

Assay: C3b magnetic beads were added to a black flat-bottom 96-well plate (Bio-Rad) containing 3000 beads/well with PBS with 0.1% Tween 20 and 0.05% BSA. After aspiration, recombinant FI (0.4 µg) and sCR1 (0.4 µg) were added to the wells to a total volume of 50 µL. C3b beads incubated with trypsin (140 µg/mL) and PBS were used as positive and negative control, respectively. All samples were incubated for one hour at 37°C on agitation (800 rpm). The reaction was stopped by washing three times with PBS 0.05% Tween-20. C3b degradation was evaluated by detecting the loss of the C3c-signal derived from bead-bound C3b and iC3b by using a biotinylated polyclonal rabbit anti-human C3c antibody (4 µg/mL, Dako) followed by washing and addition of streptavidin-PE (1:100, Bio-Rad). In both steps, the microplate was incubated for 30 minutes at room temperature. All reagents were diluted with PBS with 0.1% Tween 20 and 0.05% BSA. Mean fluorescent intensity (MFI) was determined using Bio-Plex MAGPIX Multiplex reader.

Data analysis and statistics

The SDS-PAGE data were analyzed by Image J (US National Institutes of Health, https://imagej.nih.gov/ij). Data visualization, absorbance spectroscopy calculations, and statistical analysis were performed using GraphPad Prism version 8.0.1 for Windows or MAC (San Diego, CA). Comparisons between multiple columns were analyzed with the one-way ANOVA with Dunnett's multiple comparison test. Pearson correlation coefficient was computed for the comparison of two variables.

Ethics statement

This study met the criteria of the Declaration of Helsinki (28).

Results

Degradation of fluid phase C3b (SDS-PAGE)

SDS-PAGE was applied to evaluate FI-mediated cleavage of the C3b α′-chain in the fluid phase in the presence of co-factors FH (Figures 2A, C) and sCR1 (Figures 2B, D). The eight recombinantly expressed FI-variants and the recombinantly expressed wild-type FI

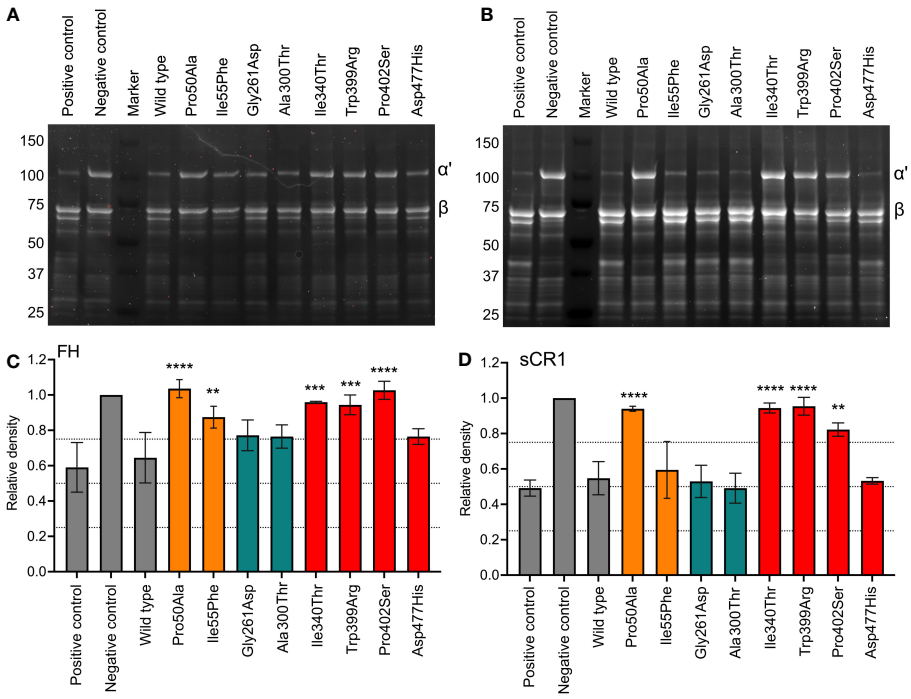

FIGURE 2
Functional analysis of recombinant FI proteins with SDS-PAGE. FI recombinant proteins (0.1 µg) were incubated with C3b (10 µg) and **(A, C)** FH (0.1 µg) or **(B, D)** sCR1 (0.1 µg) for 60 minutes at 37°C. The samples were reduced and applied onto a 12-well 4-15% SDS-PAGE. The gels were stained with SYPRO Ruby protein stain. Gels displayed **(A, B)** are representative of three independent experiments. Degradation of C3b was measured by densitometry and shown as the relative density of the intact C3b α´-chain (101 kDa) in relation to the β-chain (75 kDa). Positive and negative control samples, and wild-type (WT) are indicated in grey, FI protein domains are color coded according to: FIMAC domain in orange, LDLRA2 domain in blue and SP domain in red. The values are shown as mean +/- standard deviation of n=3. **p <0.01, ***p <0.001, and **** p <0.0001.

(Supplementary Figure 1) were evaluated in parallel to FI purified from human plasma. With FH as a co-factor, most FI mutants showed attenuated C3b degradation in comparison to both the recombinantly expressed wild type and the FI purified from plasma (Figures 2A, C). Mutations in the FIMAC domain, Pro50Ala and Ile55Phe, resulted in significantly less C3b α´-chain cleavage (p<0.0001 and p<0.01, respectively) compared to the WT. All of the mutations of the SP domain, apart from Asp477His, resulted in reduced C3b-degradation when compared to the WT; Ile340Thr and Trp399Arg (both p<0.001), and Pro402Ser (p<0.0001). No significant difference was observed for the analyzed mutations in the LDLRA2 domain. The degradation pattern of C3b with sCR1 was similar to that of FH (Figures 2B, D). Pro50Ala, Ile340Thr, Trp399Arg and Pro402Ser showed significantly less C3b-degradation than the control (p<0.05-p<0.0001). However, the two mutants in the LDLRA2 domain, Asp477His in the SP domain and Ile55Phe of the SP domain were similar to the WT and positive control.

Generation of iC3b (ELISA)

An ELISA specifically detecting a neoepitope in iC3b was employed to measure the percentage of iC3b generation as a result of C3b cleavage in the presence of FI with FH as co-factor (Figure 3). Variant Ala300Thr (LDLRA2 domain) showed similar degradation efficiency as the WT, whereas all other mutants showed significant reduction (p<0.01 or p<0.0001) in the formation of iC3b. Mutations in the SP domain displayed higher reduction in FI-activity than the ones located in the FIMAC domain; Ile340Thr, Trp399Arg and Pro402Ser resulted in the formation of approximately 80-90% less iC3b in comparison to the WT, while Pro50Ala and Ile55Phe resulted in the formation of 30% less iC3b than the WT.

Degradation of surface-bound C3b by Luminex technology

We have established a method to study the degradation of surface-bound C3b by incubating FI with sCR1 as a co-factor and detecting loss of C3c with Luminex technology. The two FIMAC mutations that were tested; Pro50Ala and Ile55Phe showed significantly reduced degradation of C3b (p<0.0001 and p<0.01, respectively) (Figure 4). Furthermore, the mutations in the LDLRA2 domain (Gly261Asp and Ala300Thr) showed C3b-cleavage comparable to the WT. Three mutations in the SP domain (Il340Thr, Trp399Arg, and Pro402Ser) had significantly less degradation of C3b (p<0.0001 for all); while the Asp477His mutation showed no significant change in degradation compared to the wild type.

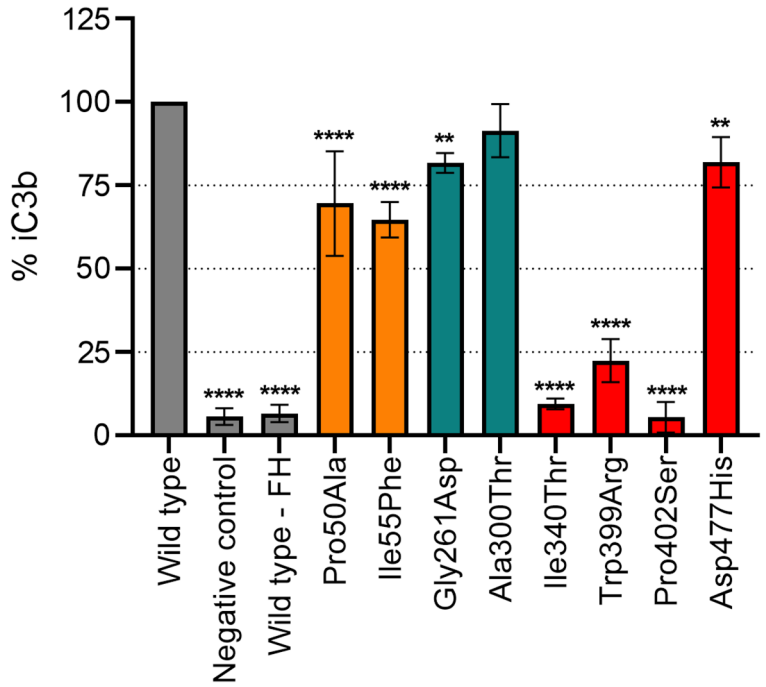

FIGURE 3
Functional analysis of recombinant FI proteins with iC3b-ELISA. Formation of iC3b was evaluated as C3b (75 µg/mL) degradation by recombinant FI variants (2 µg/mL) with FH (15 µg/mL) as a co-factor in TBS pH 7.4. The data as % iC3b is shown normalized for the recombinant wild-type (WT). Control samples are indicated in grey (WT and negative control), FI protein domains are indicated by color according to the following: FIMAC domain in orange, LDLRA2 domain in blue and SP domain in red. Samples were compared to the WT using one-way ANOVA followed by Dunnett's multiple comparison test. The values are shown as mean +/- standard deviation of n=3. **p <0.01, and ****p <0.0001.

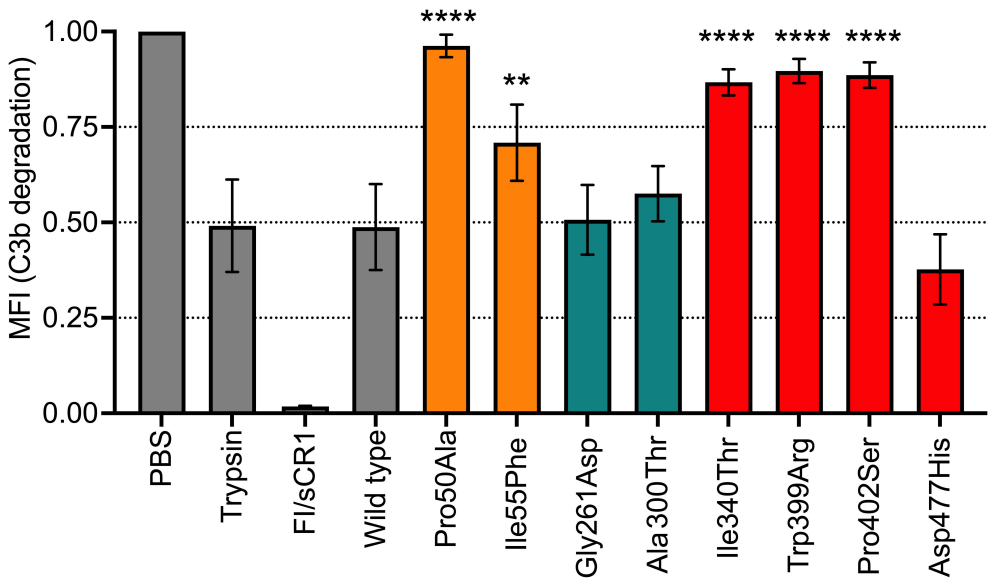

FIGURE 4
Functional analysis of recombinant FI proteins with Luminex technology. C3b was covalently bound to magnetic beads and incubated with FI recombinant proteins (0.4 µg) and sCR1 (0.4 µg) at 37°C for 60 minutes in PBS pH 7.4. C3b beads in PBS were used as the negative control sample, while C3b beads with either trypsin or purified FI and sCR1 were used as positive controls. All control samples, including wild-type (WT) control, are indicated in grey. The degradation of C3b/iC3b to C3c and C3dg was evaluated as C3c loss from the beads using a polyclonal antibody that detects C3c by measuring MFI. FI protein domains are color coded according to: FIMAC domain in orange, LDLRA2 domain in blue and SP domain in red. The values are normalized and shown as mean +/- standard deviation of n=3. **p <0.01, and ****p <0.0001.

Comparison of functional tests

To evaluate the coherence between the assays, the percentage of each variants' activity in comparison to the wild type for each assay was summarized in Table 2. Subsequently, each variants' activity was analyzed with the use of Pearson test (Figure 5). The iC3b ELISA and the SDS-PAGE showed a positive correlation (r=0.78, p<0.05), when using FH as a co-factor (Figure 5A). Similar results were found for the following variants in the LDLRA2 and SP domains; Ile340Thr, Trp399, Pro402Ser (low activity), and Gly261Asp, Ala300Thr and Asp477His (normal activity). The most profound difference was observed in regard to the FIMAC domain mutant Pro50Ala. Both assays showed significantly decreased C3b degradation for the variant, but the levels differed, where the iC3b ELISA still detected a substantial degree of iC3b formation. A comparison between the Luminex assay and the SDS-PAGE showed a strong positive correlation (r=0.91, p<0.01), when sCR1 was used as a co-factor (Figure 5B). Finally, the correlation between the two co-factors; FH and sCR1 in the SDS-PAGE was analyzed (Figure 5C). There was a strong positive correlation (r= 0.92, p=0.05). A similar degradation pattern was observed in most variants. The only variant that somewhat differed was Ile55Phe, which significantly attenuated degradation with FH, but not with sCR1.

Discussion

FI is a key regulator of the complement cascade and functional analysis of FI is of high clinical importance to understand disease pathophysiology related to uncontrolled complement activation, such as in AMD and aHUS (29, 30). In this study, we compared three FI functional assays to investigate the activity of eight genetic variants in FI compared to a recombinant wild-type control. We found that all mutations located in the FIMAC and the mutations within the SP domain, except Asp477His, resulted in impaired- or complete activity loss. The two mutations within the LDLRA2 domain did not impair activity. Overall, there was a large coherence between the three assays.

To elucidate whether the different FI-variants were dependent on the co-factor added for the degradation of fluid phase C3b, we performed assays using either FH or sCR1. As summarized in a recent review, recombinant FI-variants with mutations in the SP domain have been mainly associated with reduced iC3b generation and C3b co-factor activity, while mutations in the FIMAC domain tend to lead to decreased iC3b in serum. However, a great number of recombinantly expressed FI-variants has not been evaluated (31). In our experiments, the majority of the mutations occurring in the catalytic SP domain resulted in complete loss of activity of FI, with both FH and sCR1 as co-factors. The Pro50Ala mutant in the FIMAC domain, a domain important for binding to C3b (20, 32), showed significantly reduced activity in the presence of both co-factors in the fluid phase, as previously shown (12). This site is sterically close to the proposed binding site of heme, which interferes with FI's regulatory function (27). The mutant Ile55Phe, found in both aHUS and AMD patients, resulted in impaired activity in the presence of FH, which was also confirmed by decreased iC3b levels measured with ELISA. However, with sCR1, substantial degradation of C3b was seen by the SDS-PAGE analysis, where the activity was not significantly different from the wild-type control. The SDS-PAGE analysis is based on 60-minute incubation, and with sCR1 as a co-factor, we saw a trend toward a higher C3b consumption, *i.e.*, substrate depletion and thus a lower resolution for the variants that showed some activity. Additional methods, such as real-time visualization of the formation of C3b:co-factor:FI-complex could possibly reveal whether the difference observed for Ile55Phe is a true co-factor-dependent difference (33).

To analyze whether the mutations have a different effect when FI-mediated C3b-degradation takes place on a surface in comparison to the fluid phase, we used a novel assay that allows us to quantify C3b linked to magnetic beads. In this experimental set-up, we used only sCR1 as a co-factor, as it allows degradation of iC3b to C3dg for the loss of C3c into the fluid phase. Overall, the

TABLE 2 Overview of functional analysis of FI variants.

cDNA change	Protein change	SDS-PAGE		ELISA	Luminex	Classification (this study)
		FH	sCR1	FH	sCR1	
148C>G	Pro50Ala	**0** (5.1)	**12** (1.4)	**70** (15.7)	**2** (3.0)	Pathogenic
163A>T	Ile55Phe	**35** (6.2)	80 (16.1)	**65** (5.3)	**57** (10.0)	Pathogenic
782G>A	Gly261Asp	64 (8.7)	93 (9.1)	**82** (3.0)	96 (9.2)	Benign
898G>A	Ala300Thr	66 (6.6)	100 (8.5)	92 (8.0)	83 (7.2)	Benign
1019T>C	Ile340Thr	**11** (0.5)	**11** (2.8)	**10** (1.6)	**26** (3.4)	Pathogenic
1195T>C	Trp399Arg	**16** (5.6)	**9** (5.0)	**23** (6.4)	**21** (3.2)	Pathogenic
1204C>T	Pro402Ser	**0** (5.1)	**35** (3.8)	**6** (5.0)	**22** (3.4)	Pathogenic
1429G>C	Asp477His	66 (4.4)	92 (1.8)	**82** (7.5)	122 (9.2)	Benign

Summary of the results of the functional analysis of FI variants using three different functional assays and two cofactors (sCR1 and FH) shown in Figures 2–4. Statistically significant mean values are shown in bold type, standard deviation (+/-) is shown in brackets. Values of the ELISA, SDS-PAGE and Luminex assays are depicted in % of efficiency in comparison to the wild type FI measurement.

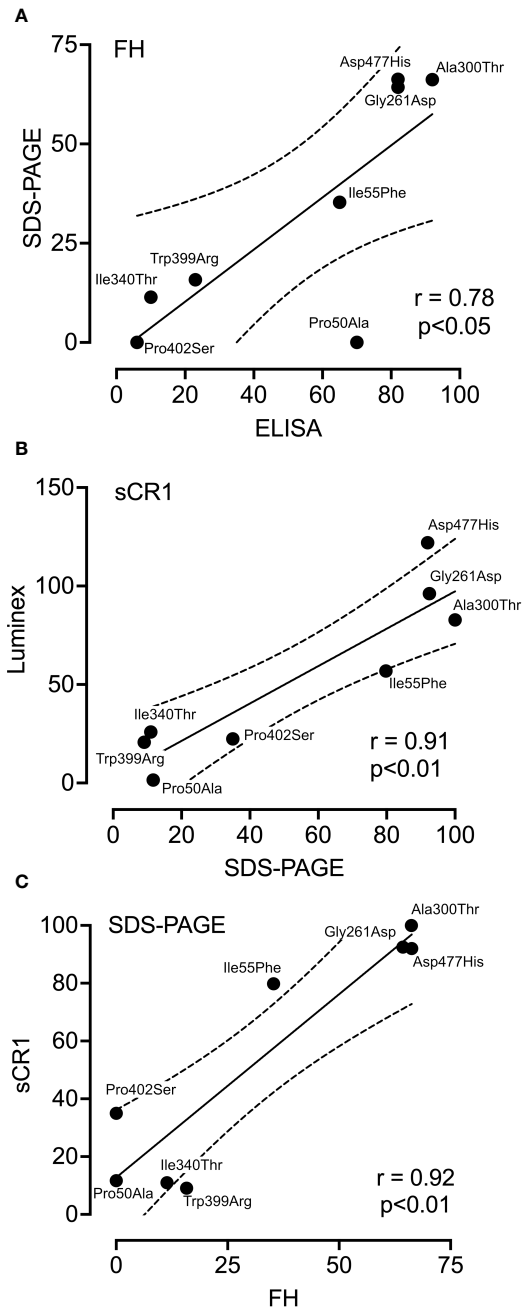

FIGURE 5
Correlation between the different co-factor activity assays. Pearson correlation analysis was performed to compare data obtained from three different functional assays; SDS-PAGE, ELISA and Luminex technology. The following pairs were analyzed; SDS-PAGE and ELISA when FH was used as a co-factor **(A)**, SDS-PAGE and luminex when sCR1 was used as a co-factor **(B)**, and SDS-PAGE in the presence of either FH or sCR1 **(C)**. r was calculated and used for the evaluation of the relationships of the variables.

C3b-degradation data from the Luminex assay corresponded well to what was seen by the degradation of fluid phase C3b with sCR1. The mutants in both SP and FIMAC domains, apart from Asp477His, showed strongly impaired activity. Ile340Thr and Asp477His in the SP domain were, among other genetic variants, recently evaluated in a corresponding study by de Jong et al. (12), whose data well correspond to what we found for these two variants. The mutation Ile55Phe in the FIMAC domain and Pro402Ser in the SP domain led to decreased degradation of surface-bound C3b in relation to soluble C3b. As the Ile55Phe mutation affects the contact surface with C3, this result could be explained due to reduced binding to C3b. It is reported that the enzymatic activity of FI variants is generally dependent on the binding capacity of FI to its co-factors (34). Furthermore, the Pro50Ala mutation also resulted in impaired ability of FI to degrade C3b deposited on sheep erythrocytes (34). The authors mention that substituting proline with alanine could interfere with the stability of the domain and, therefore, affect ligands that interact with surface-bound C3b.

In the last decades, the first complement inhibitors have been approved for clinical application in patients (35, 36). Understanding the functional consequence and significance of sequence variants for patient care will be essential for dedicated personalized medicine. This study provides novel information and methods concerning functional genomics for sequence variants observed in *CFI* and could assist in the interpretation of variants found in patients and improve the available tools for their diagnosis.

To summarize, we show that mutations located in the FIMAC, and SP domains impaired FI activity in various functional assays. In contrast, the two analyzed mutations in the LDLRA2 domain did not affect the function of FI to the same extent. While we demonstrated that the mutations affected the activity of FI in a similar manner independently of most of our experimental set-ups, some differences could only be detected by employing different methods or co-factors. For instance, attenuated activity for the Gly261Asp could only be detected in the iC3b ELISA, which shows the value of combining methods in the diagnostic testing. However, further functional studies with a larger number of variants in different domains of *CFI* are needed to further investigate the effect of the use of different cofactors on C3b degradation activity, and the impact on degradation of surface bound and fluid phase C3b by FI.

Data availability statement

The original contributions presented in the study are included in the article/Supplementary Material. Further inquiries can be directed to the corresponding author.

Ethics statement

Ethical approval was not required for the studies on humans in accordance with the local legislation and institutional requirements because only commercially available established cell lines were used.

Author contributions

LB: Writing – original draft, Investigation, Methodology. AG: Investigation, Methodology, Writing – original draft. DS: Writing – review & editing, Methodology. NK: Writing – review & editing, Funding acquisition, Resources. MP: Investigation, Writing –

review & editing, Methodology. SP: Investigation, Writing – review & editing. PN: Writing – review & editing, Conceptualization, Project administration, Supervision, Resources. LH: Project administration, Supervision, Writing – review & editing, Conceptualization, Resources.

Funding

The author(s) declare financial support was received for the research, authorship, and/or publication of this article. This work was supported by the Swedish Research Council (Project 2018-04087), the Crafoord Foundation (Project 20210961 and 20190890) and the Netherlands Organization for Health Research and Development (ZonMw), "Goed Gebruik Geneesmiddelen" (projectnumber: 836031008).

Acknowledgments

The authors are very grateful to Myrthe Blom for her technical assistance and to Elena Volokhina and Omar Tutakhel for the valuable scientific discussions.

Conflict of interest

The authors declare that the research was conducted in the absence of any commercial or financial relationships that could be construed as a potential conflict of interest.

Publisher's note

All claims expressed in this article are solely those of the authors and do not necessarily represent those of their affiliated organizations, or those of the publisher, the editors and the reviewers. Any product that may be evaluated in this article, or claim that may be made by its manufacturer, is not guaranteed or endorsed by the publisher.

Supplementary material

The Supplementary Material for this article can be found online at: https://www.frontiersin.org/articles/10.3389/fimmu.2023.1279612/full#supplementary-material

References

1. Dunkelberger JR, Song WC. Complement and its role in innate and adaptive immune responses. *Cell Res* (2010) 20(1):34–50. doi: 10.1038/cr.2009.139

2. Stowell SR, Winkler AM, Maier CL, Arthur CM, Smith NH, Girard-Pierce KR, et al. Initiation and regulation of complement during hemolytic transfusion reactions. *Clin Dev Immunol* (2012) 2012:307093. doi: 10.1155/2012/307093

3. Zipfel PF, Skerka C. Complement regulators and inhibitory proteins. *Nat Rev Immunol* (2009) 9(10):729–40. doi: 10.1038/nri2620

4. Harboe M, Ulvund G, Vien L, Fung M, Mollnes TE. The quantitative role of alternative pathway amplification in classical pathway induced terminal complement activation. *Clin Exp Immunol* (2004) 138(3):439–46. doi: 10.1111/j.1365-2249.2004.02627.x

5. Merle NS, Church SE, Fremeaux-Bacchi V, Roumenina LT. Complement system part I - molecular mechanisms of activation and regulation. *Front Immunol* (2015) 6:262. doi: 10.3389/fimmu.2015.00262

6. Sim E, Wood AB, Hsiung LM, Sim RB. Pattern of degradation of human complement fragment, C3b. *FEBS Lett* (1981) 132(1):55–60. doi: 10.1016/0014-5793(81)80426-7

7. Lachmann PJ. The story of complement factor I. *Immunobiology* (2019) 224(4):511–7. doi: 10.1016/j.imbio.2019.05.003

8. Roversi P, Johnson S, Caesar JJ, McLean F, Leath KJ, Tsiftsoglou SA, et al. Structural basis for complement factor I control and its disease-associated sequence polymorphisms. *Proc Natl Acad Sci U.S.A.* (2011) 108(31):12839–44. doi: 10.1073/pnas.1102167108

9. Kavanagh D, Richards A, Noris M, Hauhart R, Liszewski MK, Karpman D, et al. Characterization of mutations in complement factor I (CFI) associated with hemolytic uremic syndrome. *Mol Immunol* (2008) 45(1):95–105. doi: 10.1016/j.molimm.2007.05.004

10. Tzoumas N, Kavanagh D, Cordell HJ, Lotery AJ, Patel PJ, Steel DH. Rare complement factor I variants associated with reduced macular thickness and age-related macular degeneration in the UK biobank. *Hum Mol Genet* (2022) 31(16):2678–92. doi: 10.1093/hmg/ddac060

11. Wong EKS, Kavanagh D. Diseases of complement dysregulation-an overview. *Semin Immunopathol* (2018) 40(1):49–64. doi: 10.1007/s00281-017-0663-8

12. de Jong S, de Breuk A, Bakker B, Katti S, Hoyng CB, Nilsson SC, et al. Functional analysis of variants in complement factor I identified in age-related macular degeneration and atypical hemolytic uremic syndrome. *Front Immunol* (2021) 12:789897. doi: 10.3389/fimmu.2021.789897

13. Alba-Dominguez M, Lopez-Lera A, Garrido S, Nozal P, Gonzalez-Granado I, Melero J, et al. Complement factor I deficiency: A not so rare immune defect: Characterization of new mutations and the first large gene deletion. *Orphanet J Rare Dis* (2012) 7:42. doi: 10.1186/1750-1172-7-42

14. Sadallah S, Gudat F, Laissue JA, Spath PJ, Schifferli JA. Glomerulonephritis in a patient with complement factor I deficiency. *Am J Kidney Dis* (1999) 33(6):1153–7. doi: 10.1016/S0272-6386(99)70155-1

15. Bajwa R, DePalma JA, Khan T, Cheema A, Kalathil SA, Hossain MA, et al. C3 glomerulopathy and atypical hemolytic uremic syndrome: Two important manifestations of complement system dysfunction. *Case Rep Nephrol Dial* (2018) 8(1):25–34. doi: 10.1159/000486848

16. Zipfel PF, Lauer N, Skerka C. The role of complement in AMD. *Adv Exp Med Biol* (2010) 703:9–24. doi: 10.1007/978-1-4419-5635-4_2

17. Saksens NT, Geerlings MJ, Bakker B, Schick T, Daha MR, Fauser S, et al. Rare genetic variants associated with development of age-related macular degeneration. *JAMA Ophthalmol* (2016) 134(3):287–93. doi: 10.1001/jamaophthalmol.2015.5592

18. Seddon JM, Yu Y, Miller EC, Reynolds R, Tan PL, Gowrisankar S, et al. Rare variants in CFI, C3 and C9 are associated with high risk of advanced age-related macular degeneration. *Nat Genet* (2013) 45(11):1366–70. doi: 10.1038/ng.2741

19. den Hollander AI, de Jong EK. Highly penetrant alleles in age-related macular degeneration. *Cold Spring Harb Perspect Med* (2014) 5(3):a017202. doi: 10.1101/cshperspect.a017202

20. Nilsson SC, Nita I, Mansson L, Groeneveld TW, Trouw LA, Villoutreix BO, et al. Analysis of binding sites on complement factor I that are required for its activity. *J Biol Chem* (2010) 285(9):6235–45. doi: 10.1074/jbc.M109.097212

21. Noris M, Remuzzi G. Thrombotic microangiopathy after kidney transplantation. *Am J Transplant* (2010) 10(7):1517–23. doi: 10.1111/j.1600-6143.2010.03156.x

22. Sellier-Leclerc AL, Fremeaux-Bacchi V, Dragon-Durey MA, Macher MA, Niaudet P, Guest G, et al. Differential impact of complement mutations on clinical characteristics in atypical hemolytic uremic syndrome. *J Am Soc Nephrol* (2007) 18(8):2392–400. doi: 10.1681/ASN.2006080811

23. Esparza-Gordillo J, Jorge EG, Garrido CA, Carreras L, Lopez-Trascasa M, Sanchez-Corral P, et al. Insights into hemolytic uremic syndrome: Segregation of three independent predisposition factors in a large, multiple affected pedigree. *Mol Immunol* (2006) 43(11):1769–75. doi: 10.1016/j.molimm.2005.11.008

24. Hammer CH, Wirtz GH, Renfer L, Gresham HD, Tack BF. Large scale isolation of functionally active components of the human complement system. *J Biol Chem* (1981) 256(8):3995–4006. doi: 10.1016/S0021-9258(19)69557-8

25. Richards S, Aziz N, Bale S, Bick D, Das S, Gastier-Foster J, et al. Standards and guidelines for the interpretation of sequence variants: A joint consensus recommendation of the american college of medical genetics and genomics and the association for molecular pathology. *Genet Med* (2015) 17(5):405–24. doi: 10.1038/gim.2015.30

26. de Jong S, Volokhina EB, de Breuk A, Nilsson SC, de Jong EK, van der Kar N, et al. Effect of rare coding variants in the CFI gene on factor I expression levels. *Hum Mol Genet* (2020) 29(14):2313–24. doi: 10.1093/hmg/ddaa114

27. Gerogianni A, Dimitrov JD, Zarantonello A, Poillerat V, Chonat S, Sandholm K, et al. Heme interferes with complement factor I-dependent regulation by enhancing alternative pathway activation. *Front Immunol* (2022) 13:901876. doi: 10.3389/fimmu.2022.901876

28. World Medical A. World medical association declaration of helsinki: Ethical principles for medical research involving human subjects. *JAMA* (2013) 310(20):2191–4. doi: 10.1001/jama.2013.281053

29. Kavanagh D, Yu Y, Schramm EC, Triebwasser M, Wagner EK, Raychaudhuri S, et al. Rare genetic variants in the CFI gene are associated with advanced age-related macular degeneration and commonly result in reduced serum factor I levels. *Hum Mol Genet* (2015) 24(13):3861–70. doi: 10.1093/hmg/ddv091

30. Rodriguez de Cordoba S, Hidalgo MS, Pinto S, Tortajada A. Genetics of atypical hemolytic uremic syndrome (ahus). *Semin Thromb Hemost* (2014) 40(4):422–30. doi: 10.1055/s-0034-1375296

31. Hallam TM, Sharp SJ, Andreadi A, Kavanagh D. Complement factor I: Regulatory nexus, driver of immunopathology, and therapeutic. *Immunobiology* (2023) 228(5):152410. doi: 10.1016/j.imbio.2023.152410

32. Xue X, Wu J, Ricklin D, Forneris F, Di Crescenzio P, Schmidt CQ, et al. Regulator-dependent mechanisms of C3b processing by factor I allow differentiation of immune responses. *Nat Struct Mol Biol* (2017) 24(8):643–51. doi: 10.1038/nsmb.3427

33. Hallam TM, Cox TE, Smith-Jackson K, Brocklebank V, Baral AJ, Tzoumas N, et al. A novel method for real-time analysis of the complement C3b:FH:FI complex reveals dominant negative CFI variants in age-related macular degeneration. *Front Immunol* (2022) 13:1028760. doi: 10.3389/fimmu.2022.1028760

34. Nilsson SC, Kalchishkova N, Trouw LA, Fremeaux-Bacchi V, Villoutreix BO, Blom AM. Mutations in complement factor I as found in atypical hemolytic uremic syndrome lead to either altered secretion or altered function of factor i. *Eur J Immunol* (2010) 40(1):172–85. doi: 10.1002/eji.200939280

35. Zipfel PF, Wiech T, Rudnick R, Afonso S, Person F, Skerka C. Complement inhibitors in clinical trials for glomerular diseases. *Front Immunol* (2019) 10:2166. doi: 10.3389/fimmu.2019.02166

36. Fakhouri F, Schwotzer N, Golshayan D, Fremeaux-Bacchi V. The rational use of complement inhibitors in kidney diseases. *Kidney Int Rep* (2022) 7(6):1165–78. doi: 10.1016/j.ekir.2022.02.021

Frontiers in Immunology

Explores novel approaches and diagnoses to treat immune disorders.

The official journal of the International Union of Immunological Societies (IUIS) and the most cited in its field, leading the way for research across basic, translational and clinical immunology.

Discover the latest Research Topics

See more →

Frontiers

Avenue du Tribunal-Fédéral 34
1005 Lausanne, Switzerland
frontiersin.org

Contact us

+41 (0)21 510 17 00
frontiersin.org/about/contact